Thin Plates and Shells

Theory, Analysis, and Applications

Eduard Ventsel
Theodor Krauthammer

The Pennsylvania State University
University Park, Pennsylvania

MARCEL DEKKER, INC. NEW YORK • BASEL

ISBN: 0-8247-0575-0

This book is printed on acid-free paper.

Headquarters
Marcel Dekker, Inc.
270 Madison Avenue, New York, NY 10016
tel: 212-696-9000; fax: 212-685-4540

Eastern Hemisphere Distribution
Marcel Dekker AG
Hutgasse 4, Postfach 812, CH-4001 Basel, Switzerland
tel: 41-61-261-8482; fax: 41-61-261-8896

World Wide Web
http://www.dekker.com

The publisher offers discounts on this book when ordered in bulk quantities. For more information, write to Special Sales/Professional Marketing at the headquarters address above.

Current printing (last digit):
10 9 8 7 6 5 4 3 2 1

PRINTED IN THE UNITED STATES OF AMERICA

To:
Liliya, Irina, and Masha
and
Nina, Yoaav, Adi, and Alon

Preface

Thin-walled structures in the form of plates and shells are encountered in many branches of technology, such as civil, mechanical, aeronautical, marine, and chemical engineering. Such a widespread use of plate and shell structures arises from their intrinsic properties. When suitably designed, even very thin plates, and especially shells, can support large loads. Thus, they are utilized in structures such as aerospace vehicles in which light weight is essential.

In preparing this book, we had three main objectives: first, to offer a comprehensive and methodical presentation of the fundamentals of thin plate and shell theories, based on a strong foundation of mathematics and mechanics with emphasis on engineering aspects. Second, we wanted to acquaint readers with the most useful and contemporary analytical and numerical methods for solving linear and nonlinear plate and shell problems. Our third goal was to apply the theories and methods developed in the book to the analysis and design of thin plate-shell structures in engineering. This book is intended as a text for graduate and postgraduate students in civil, architectural, mechanical, chemical, aeronautical, aerospace, and ocean engineering, and engineering mechanics. It can also serve as a reference book for practicing engineers, designers, and stress analysts who are involved in the analysis and design of thin-walled structures.

As a textbook, it contains enough materal for a two-semester senior or graduate course on the theory and applications of thin plates and shells. Also, a special effort has been made to have the chapters as independent from one another as possible, so that a course can be taught in one semester by selecting appropriate chapters, or through equivalent self-study.

The textbook is divided into two parts. Part I (Chapters 1–9) presents plate bending theory and its application and Part II (Chapters 10–20) covers the theory, analysis, and principles of shell structures.

The book is organized in the following manner. First, the general linear theories of thin elastic plates and shells of an arbitrary geometry are developed by using the basic classical assumptions. Deriving the general relationships and equations of the linear shell theory requires some familiarity with topics of advanced mathematics, including vector calculus, theory of differential equations, and theory of surfaces. We tried to keep a necessary rigorous treatment of shell theory and its principles and, at the same time, to make the book more readable for graduate students and engineers. Therefore, we presented the fundamental kinematic and static relationships, and elements of the theory of surfaces, which are necessary for constructing the shell theory, without proof and verification. The detailed derivation and proof of the above relationships and equations are given in Appendices A–E so that the interested reader can refer to them.

Later on, governing differential equations of the linear general theory are applied to plates and shells of particular geometrical forms. In doing so, various approximate engineering shell theories are presented by introducing some supplementary assumptions to the general shell theory. The mathematical formulation of the above shell theories leads, as a rule, to a system of partial differential equations. A solution of these equations is the focus of attention of the book. Emphasis is given to computer-oriented methods, such as the finite difference and finite element methods, boundary element and boundary collocation methods, and to their application to plate and shell problems. Nevertheless, the emphasis placed on numerical methods is not intended to deny the merit of classical analytical methods that are also presented in the book, for example, the Galerkin and Ritz methods.

A great attempt has been made to emphasize the physical meanings of engineering shell theories, mathematical relationships, and adapted basic and supplementary assumptions. The accuracy of numerical results obtained with the use of the above theories, and possible areas of their application, are discussed. The main goal is to help the reader to understand how plate and shell structures resist the applied loads and to express this understanding in the language of physical rather than purely mathematical aspects. To this end, the basic ideas of the considered plate and shell models are demonstrated by comparisons with more simple models such as beams and arches, for which the main ideas are understandable for readers familiar with strength of materials. We believe that understanding the behavior of plate and shell structures enables designers or stress analysts to verify the accuracy of numerical structural analysis results for such structures obtained by available computer code, and to interpret these results correctly.

Postgraduate students, stress analysts, and engineers will be interested in the advanced topics on plate and shell structures, including the refined theory of thin plates, orthotropic and multilayered plates and shells, sandwich plate and shell structures, geometrically nonlinear plate, and shell theories. Much attention is also given to orthotropic and stiffened plates and shells, as well as to multishell structures that are commonly encountered in engineering applications. The peculiarities of the behavior and states of stress of the above thin-walled structures are analyzed in detail.

Since the failure of thin-walled structures is more often caused by buckling, the issue of the linear and nonlinear buckling analysis of plates and shells is given much attention in the book. Particular emphasis is placed on the formulation of elastic stability criteria and on the analysis of peculiarities of the buckling process for thin

shells. Buckling analysis of orthtropic, stiffened, and sandwich plates and shells is presented. The important issues of postbuckling behavior of plates and shells—in paticular, the load-carrying capacity of stiffened plates and shells—are discussed in detail. Some considerations of design stability analysis for thin shell structures is also provided in the book.

An introduction to the vibration of plates and shells is given in condensed form and the fundamental concepts of dynamic analysis for free and forced vibrations of unstiffened and stiffened plate and shell structures are discussed. The book emphasizes the understanding of basic phenomena in shell and plate vibrations. We hope that this materal will be useful for engineers in preventing failures and for acousticians in controlling noise.

Each chapter contains fully worked out examples and homework problems that are primarily drawn from engineering practice. The sample problems serve a double purpose: to help readers understand the basic principles and methods used in plate and shell theories and to show application of the above theories and methods to engineering design.

The selection, arrangement, and presentation of the material have been made with the greatest care, based on lecture notes for a course taught by the first author at The Pennsylvania State University for many years and also earlier at the Kharkov Technical University of Civil Engineering, Ukraine. The research, practical design, and consulting experiences of both authors have also contributed to the presented material.

The first author wishes to express his gratitude to Dr. R. McNitt for his encouragement, unwavering support, and valuable advice in bringing this book to its final form. Thanks are also due to the many graduate students who offered constructive suggestions when drafts of this book were used as a text. A special thanks is extended to Dr. I. Ginsburg for spending long hours reviewing and critiquing the manuscript. We thank Ms. J. Fennema for her excellence in sketching the numerous figures. Finally, we thank Marcel Dekker, Inc., and especially, Mr. B. J. Clark, for extraordinary dedication and assistance in the preparation of this book.

Eduard Ventsel
Theodor Krauthammer

Contents

Part I

Thin Plates

1

Introduction

1.1 GENERAL

Thin plates are initially flat structural members bounded by two parallel planes, called *faces*, and a cylindrical surface, called an *edge* or *boundary*. The generators of the cylindrical surface are perpendicular to the plane faces. The distance between the plane faces is called the *thickness* (h) of the plate. It will be assumed that the plate thickness is small compared with other characteristic dimensions of the faces (length, width, diameter, etc.). Geometrically, plates are bounded either by straight or curved boundaries (Fig. 1.1). The static or dynamic loads carried by plates are predominantly perpendicular to the plate faces.

The load-carrying action of a plate is similar, to a certain extent, to that of beams or cables; thus, plates can be approximated by a gridwork of an infinite number of beams or by a network of an infinite number of cables, depending on the flexural rigidity of the structures. This two-dimensional structural action of plates results in lighter structures, and therefore offers numerous economic advantages. The plate, being originally flat, develops shear forces, bending and twisting moments to resist transverse loads. Because the loads are generally carried in both directions and because the twisting rigidity in isotropic plates is quite significant, a plate is considerably stiffer than a beam of comparable span and thickness. So, thin plates combine light weight and a form efficiency with high load-carrying capacity, economy, and technological effectiveness.

Because of the distinct advantages discussed above, thin plates are extensively used in all fields of engineering. Plates are used in architectural structures, bridges, hydraulic structures, pavements, containers, airplanes, missiles, ships, instruments, machine parts, etc. (Fig. 1.2).

We consider a plate, for which it is common to divide the thickness h into equal halves by a plane parallel to its faces. This plane is called the *middle plane* (or simply,

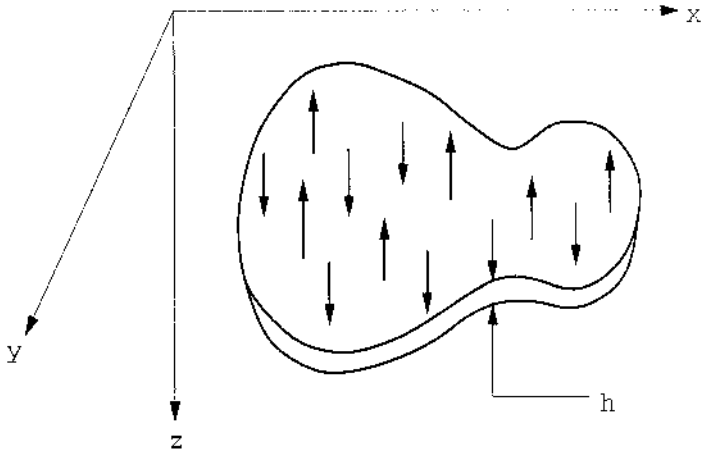

Fig. 1.1

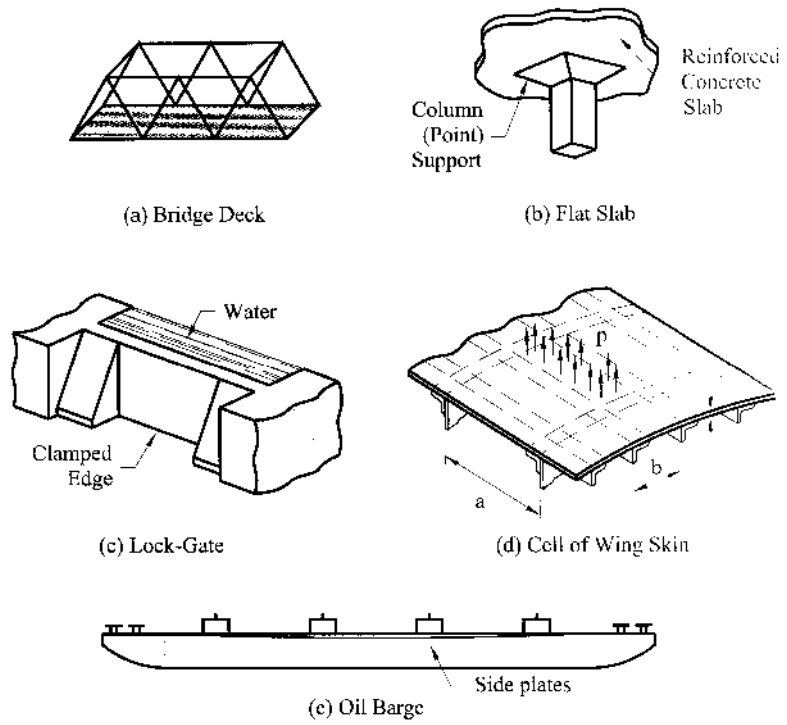

Fig. 1.2

the *midplane*) of the plate (Fig. 1.3). Being subjected to transverse loads, an initially flat plate deforms and the midplane passes into some curvilinear surface, which is referred to as the *middle surface*. With the exception of Secs 3.8 and 4.8, we will consider only plates of constant thickness. For such plates, the shape of a plate is adequately defined by describing the geometry of its middle plane. Depending on the shape of this midplane, we will distinguish between rectangular, circular, elliptic, etc., plates.

A plate resists transverse loads by means of bending, exclusively. The flexural properties of a plate depend greatly upon its thickness in comparison with other dimensions. Plates may be classified into three groups according to the ratio a/h, where a is a typical dimension of a plate in a plane and h is a plate thickness. These groups are

1. The first group is presented by *thick plates* having ratios $a/h \leq 8 \ldots 10$. The analysis of such bodies includes all the components of stresses, strains, and displacements as for solid bodies using the general equations of three-dimensional elasticity.
2. The second group refers to plates with ratios $a/h \geq 80 \ldots 100$. These plates are referred to as *membranes* and they are devoid of flexural rigidity. Membranes carry the lateral loads by axial tensile forces N (and shear forces) acting in the plate middle surface as shown in Fig. 1.7. These forces are called *membrane forces*; they produce projection on a vertical axis and thus balance a lateral load applied to the plate-membrane.
3. The most extensive group represents an intermediate type of plate, so-called *thin plate* with $8 \ldots 10 \leq a/h \leq 80 \ldots 100$. Depending on the value of the ratio w/h, the ratio of the maximum deflection of the plate to its thickness, the part of flexural and membrane forces here may be different. Therefore, this group, in turn, may also be subdivided into two different classes.

a. *Stiff plates*. A plate can be classified as a stiff plate if $w/h \leq 0.2$. Stiff plates are flexurally rigid thin plates. They carry loads two dimensionally, mostly by internal bending and twisting moments and by transverse shear forces. The middle plane deformations and the membrane forces are negligible. In engineering practice, the term plate is understood to mean a stiff plate, unless otherwise specified. The concept of stiff plates introduces serious simplifications that are discussed later. A funda-

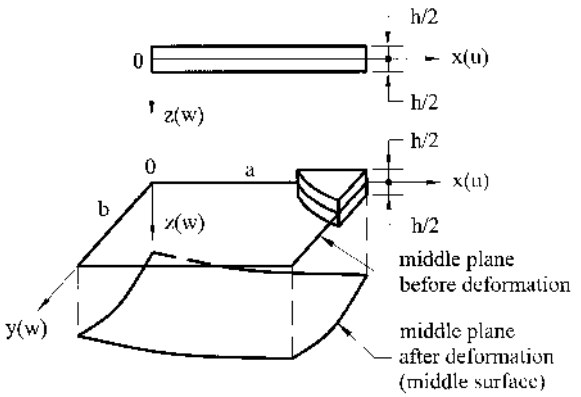

Fig. 1.3

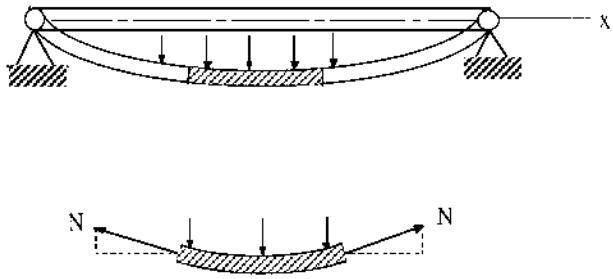

Fig. 1.4

mental feature of stiff plates is that the equations of static equilibrium for a plate element may be set up for an original (undeformed) configuration of the plate.

b. *Flexible plates*. If the plate deflections are beyond a certain level, $w/h \geq 0.3$, then, the lateral deflections will be accompanied by stretching of the middle surface. Such plates are referred to as flexible plates. These plates represent a combination of stiff plates and membranes and carry external loads by the combined action of internal moments, shear forces, and membrane (axial) forces. Such plates, because of their favorable weight-to-load ratio, are widely used by the aerospace industry. When the magnitude of the maximum deflection is considerably greater than the plate thickness, the membrane action predominates. So, if $w/h > 5$, the flexural stress can be neglected compared with the membrane stress. Consequently, the load-carrying mechanism of such plates becomes of the membrane type, i.e., the stress is uniformly distributed over the plate thickness.

The above classification is, of course, conditional because the reference of the plate to one or another group depends on the accuracy of analysis, type of loading, boundary conditions, etc.

With the exception of Sec. 7.4, we consider only small deflections of thin plates, a simplification consistent with the magnitude of deformation commonly found in plate structures.

1.2 HISTORY OF PLATE THEORY DEVELOPMENT

The first impetus to a mathematical statement of plate problems, was probably done by Euler, who in 1776 performed a free vibration analysis of plate problems [1].

Chladni, a German physicist, discovered the various modes of free vibrations [2]. In experiments on horizontal plates, he used evenly distributed powder, which formed regular patterns after induction of vibration. The powder accumulated along the nodal lines, where no vertical displacements occurred. J. Bernoulli [3] attempted to justify theoretically the results of these acoustic experiments. Bernoulli's solution was based on the previous work resulting in the Euler–D.Bernoulli's bending beam theory. J. Bernoulli presented a plate as a system of mutually perpendicular strips at right angles to one another, each strip regarded as functioning as a beam. But the governing differential equation, as distinct from current approaches, did not contain the middle term.

The French mathematician Germain developed a plate differential equation that lacked the warping term [4]; by the way, she was awarded a prize by the Parisian Academy in 1816 for this work. Lagrange, being one of the reviewers of this work, corrected Germain's results (1813) by adding the missing term [5]; thus, he was the first person to present the general plate equation properly.

Cauchy [6] and Poisson [7] were first to formulate the problem of plate bending on the basis of general equations of theory of elasticity. Expanding all the characteristic quantities into series in powers of distance from a middle surface, they retained only terms of the first order of smallness. In such a way they obtained the governing differential equation for deflections that coincides completely with the well-known Germain–Lagrange equation. In 1829 Poisson expanded successfully the Germain–Lagrange plate equation to the solution of a plate under static loading. In this solution, however, the plate flexural rigidity D was set equal to a constant term. Poisson also suggested setting up three boundary conditions for any point on a free boundary. The boundary conditions derived by Poisson and a question about the number and nature of these conditions had been the subject of much controversy and were the subject of further investigations.

The first satisfactory theory of bending of plates is associated with Navier [8], who considered the plate thickness in the general plate equation as a function of rigidity D. He also introduced an "exact" method which transformed the differential equation into algebraic expressions by use of Fourier trigonometric series.

In 1850 Kirchhoff published an important thesis on the theory of thin plates [9]. In this thesis, Kirchhoff stated two independent basic assumptions that are now widely accepted in the plate-bending theory and are known as "Kirchhoff's hypotheses." Using these assumptions, Kirchhoff simplified the energy functional of 3D elasticity theory for bent plates. By requiring that it be stationary he obtained the Germain-Lagrange equation as the Euler equation. He also pointed out that there exist only two boundary conditions on a plate edge. Kirchhoff's other significant contributions are the discovery of the frequency equation of plates and the introduction of virtual displacement methods in the solution of plate problems. Kirchhoff's theory contributed to the physical clarity of the plate bending theory and promoted its widespread use in practice.

Lord Kelvin (Thomson) and Tait [10] provided an additional insight relative to the condition of boundary equations by converting twisting moments along the edge of a plate into shearing forces. Thus, the edges are subject to only two forces: shear and moment.

Kirchhoff's book was translated by Clebsh [11]. That translation contains numerous valuable comments by de Saint-Venant: the most important being the extension of Kirchhoff's differential equation of thin plates, which considered, in a mathematically correct manner, the combined action of bending and stretching. Saint-Venant also pointed out that the series proposed by Cauchy and Poissons as a rule, are divergent.

The solution of rectangular plates, with two parallel simple supports and the other two supports arbitrary, was successfully solved by Levy [12] in the late 19th century.

At the end of the 19th and the beginning of the 20th centuries, shipbuilders changed their construction methods by replacing wood with structural steel. This change in structural materials was extremely fruitful in the development of various

plate theories. Russian scientists made a significant contribution to naval architecture by being the first to replace the ancient trade traditions with solid mathematical theories. In particular, Krylov [13] and his student Bubnov [14] contributed extensively to the theory of thin plates with flexural and extensional rigidities. Bubnov laid the groundwork for the theory of flexible plates and he was the first to introduce a modern plate classification. Bubnov proposed a new method of integration of differential equations of elasticity and he composed tables of maximum deflections and maximum bending moments for plates of various properties. Then, Galerkin developed this method and applied it to plate bending analysis. Galerkin collected numerous bending problems for plates of arbitrary shape in a monograph [15].

Timoshenko made a significant contribution to the theory and application of plate bending analysis. Among Timoshenko's numerous important contributions are solutions of circular plates considering large deflections and the formulation of elastic stability problems [16,17]. Timoshenko and Woinowsky-Krieger published a fundamental monograph [18] that represented a profound analysis of various plate bending problems.

Extensive studies in the area of plate bending theory and its various applications were carried out by such outstanding scientists as Hencky [19], Huber [20], von Karman [21,22], Nadai [23], Föppl [24].

Hencky [19] made a contribution to the theory of large deformations and the general theory of elastic stability of thin plates. Nadai made extensive theoretical and experimental investigations associated with a check of the accuracy of Kirchhoff's plate theory. He treated different types of singularities in plates due to a concentrated force application, point support effects, etc. The general equations for the large deflections of very thin plates were simplified by Föppl who used the stress function acting in the middle plane of the plate. The final form of the differential equation of the large-deflection theory, however, was developed by von Karman. He also investigated the postbuckling behavior of plates.

Huber, developed an approximate theory of orthotropic plates and solved plates subjected to nonsymmetrical distributed loads and edge moments. The bases of the general theory of anisotropic plates were developed by Gehring [25] and Boussinesq [26]. Lekhnitskii [27] made an essential contribution to the development of the theory and application of anisotropic linear and nonlinear plate analysis. He also developed the method of complex variables as applied to the analysis of anisotropic plates.

The development of the modern aircraft industry provided another strong impetus toward more rigorous analytical investigations of plate problems. Plates subjected to in-plane forces, postbuckling behavior, and vibration problems (flutter), stiffened plates, etc., were analyzed by various scientists and engineers.

E. Reissner [28] developed a rigorous plate theory which considers the deformations caused by the transverse shear forces. In the former Soviet Union the works of Volmir [29] and Panov [30] were devoted mostly to solution of nonlinear plate bending problems.

The governing equation for a thin rectangular plate subjected to direct compressive forces N_x was first derived by Navier [8]. The buckling problem for a simply supported plate subjected to the direct, constant compressive forces acting in one and two directions was first solved by Bryan [31] using the energy method. Cox [32], Hartmann [33], etc., presented solutions of various buckling problems for thin

rectangular plates in compression, while Dinnik [34], Nadai [35], Meissner [36], etc., completed the buckling problem for circular compressed plates. An effect of the direct shear forces on the buckling of a rectangular simply supported plate was first studied by Southwell and Skan [37]. The buckling behavior of a rectangular plate under nonuniform direct compressive forces was studied by Timoshenko and Gere [38] and Bubnov [14]. The postbuckling behavior of plates of various shapes was analyzed by Karman *et al*. [39], Levy [40], Marguerre [41], etc. A comprehensive analysis of linear and nonlinear buckling problems for thin plates of various shapes under various types of loads, as well as a considerable presentation of available results for critical forces and buckling modes, which can be used in engineering design, were presented by Timoshenko and Gere [38], Gerard and Becker [42], Volmir [43], Cox [44], etc.

A differential equation of motion of thin plates may be obtained by applying either the D'Alambert principle or work formulation based on the conservation of energy. The first exact solution of the free vibration problem for rectangular plates, whose two opposite sides are simply supported, was achieved by Voight [45]. Ritz [46] used the problem of free vibration of a rectangular plate with free edges to demonstrate his famous method for extending the Rayleigh principle for obtaining upper bounds on vibration frequencies. Poisson [7] analyzed the free vibration equation for circular plates. The monographs by Timoshenko and Young [47], Den Hartog [48], Thompson [49], etc., contain a comprehensive analysis and design considerations of free and forced vibrations of plates of various shapes. A reference book by Leissa [50] presents a considerable set of available results for the frequencies and mode shapes of free vibrations of plates could be provided for the design and for a researcher in the field of plate vibrations.

The recent trend in the development of plate theories is characterized by a heavy reliance on modern high-speed computers and the development of the most complete computer-oriented numerical methods, as well as by introduction of more rigorous theories with regard to various physical effects, types of loading, etc.

The above summary is a very brief survey of the historical background of the plate bending theory and its application. The interested reader is referred to special monographs [51,52] where this historical development of plates is presented in detail.

1.3 GENERAL BEHAVIOR OF PLATES

Consider a load-free plate, shown in Fig.1.3, in which the xy plane coincides with the plate's midplane and the z coordinate is perpendicular to it and is directed downwards. The fundamental assumptions of the linear, elastic, small-deflection theory of bending for thin plates may be stated as follows:

1. The material of the plate is elastic, homogeneous, and isotropic.
2. The plate is initially flat.
3. The deflection (the normal component of the displacement vector) of the midplane is small compared with the thickness of the plate. The slope of the deflected surface is therefore very small and the square of the slope is a negligible quantity in comparison with unity.
4. The straight lines, initially normal to the middle plane before bending, remain straight and normal to the middle surface during the deformation,

and the length of such elements is not altered. This means that the vertical shear strains γ_{xz} and γ_{yz} are negligible and the normal strain ε_z may also be omitted. This assumption is referred to as the "*hypothesis of straight normals*."

5. The stress normal to the middle plane, σ_z, is small compared with the other stress components and may be neglected in the stress–strain relations.
6. Since the displacements of a plate are small, it is assumed that the middle surface remains unstrained after bending.

Many of these assumptions, known as *Kirchhoff's hypotheses*, are analogous to those associated with the simple bending theory of beams. These assumptions result in the reduction of a three-dimensional plate problem to a two-dimensional one. Consequently, the governing plate equation can be derived in a concise and straightforward manner. The plate bending theory based on the above assumptions is referred to as the *classical* or *Kirchhoff's plate theory*. Unless otherwise stated, the validity of the Kirchhoff plate theory is assumed throughout this book.

1.4 SURVEY OF ELASTICITY THEORY

The classical theories of plates and shells are an important application of the theory of elasticity, which deals with relationships of forces, displacements, stresses, and strains in an elastic body. When a solid body is subjected to external forces, it deforms, producing internal strains and stresses. The deformation depends on the geometrical configuration of the body, on applied loading, and on the mechanical properties of its material. In the theory of elasticity we restrict our attention to *linear elastic materials*; i.e., the relationships between stress and strain are linear, and the deformations and stresses disappear when the external forces are removed. The classical theory of elasticity assumes the material is *homogeneous* and *isotropic*, i.e., its mechanical properties are the same in all directions and at all points.

The present section contains only a brief survey of the elasticity theory that will be useful for the development of the plate theory. All equations and relations will be given without derivation. The reader who desires to review details is urged to refer to any book on elasticity theory – for example [53–55].

1.4.1 Stress at a point: stress tensor

Consider an elastic body of any general shape subjected to external loads which are in equilibrium. Then, consider a material point anywhere in the interior of the body. If we assign a Cartesian coordinate frame with axes x, y, and z, as shown in Fig. 1.5, it is convenient to assign an infinitesimal element in the form of parallelepiped $(\mathrm{d}x, \mathrm{d}y, \mathrm{d}z)$, with faces parallel to the coordinate planes. Stresses acting on the faces of this element describe the intensity of the internal forces at a point on a particular face. These stresses can be broken down into a normal component (*normal stress*) and tangent component (*shear stress*) to the particular face. As a result, the three stress components, denoted by $\sigma_{xx}, \tau_{xy}, \tau_{xz}, \ldots$, will act on each face of the element. The subscript notation for the stress components is interpreted as follows: the first subscript indicates the direction of an outer normal to the face on which the stress component acts; the second subscript relates to the direction of the stress itself.

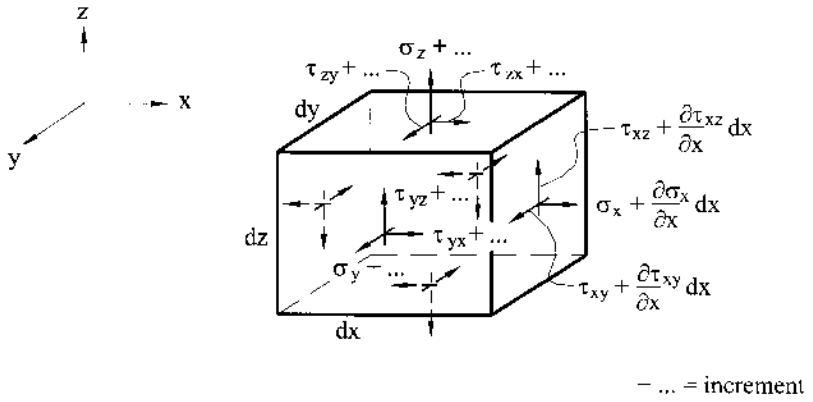

Fig. 1.5

Repeated subscripts will be omitted in the future, i.e., the normal stresses will have only one subscript indicating the stress direction. The following sign convention will be adapted for the stress components: the positive sign for the normal stress will correspond to a tensile stress, while the negative sign will correspond to a compressive stress. The sign agreement for the shear stresses follows from the relationship between the direction of an outer normal drawn to a particular face and the direction of the shear stress component on the same face. If both the outer normal and the shear stress are either in positive or negative directions relative to the coordinate axes, then the shear stress is positive. If the outer normal points in a positive direction while the stress is in a negative direction (or vice versa), the shear stress is negative. On this basis, all the stress components shown in Fig. 1.5 are positive. On any one face these three stress components comprise a vector, called a *surface traction*. The above-mentioned set of the stress components acting on the faces of the element forms the *stress tensor*, T_S, i.e.,

$$T_S = \begin{pmatrix} \sigma_x \tau_{xy} \tau_{xz} \\ \tau_{yx} \sigma_y \tau_{yz} \\ \tau_{zx} \tau_{zy} \sigma_z \end{pmatrix}, \tag{1.1}$$

which is symmetric with respect to the principal diagonal because of the *reciprocity law of shear stresses*, i.e.,

$$\tau_{xy} = \tau_{yx}; \ \tau_{xz} = \tau_{zx}; \ \tau_{yz} = \tau_{zy}. \tag{1.2}$$

Thus, only the six stress components out of nine in the stress tensor (1.1) are independent. The stress tensor, T_S, completely characterizes the three-dimensional state of stress at a point of interest.

For elastic stress analysis of plates, the two-dimensional state of stress is of special importance. In this case, $\sigma_z = \tau_{yz} = \tau_{xz} = 0$; thus, the two-dimensional stress tensor has a form

$$T_S = \begin{pmatrix} \sigma_x \tau_{xy} \\ \tau_{yx} \sigma_y \end{pmatrix}, \ \text{where } \tau_{xy} = \tau_{yx} \tag{1.3}$$

1.4.2 Strains and displacements

Assume that the elastic body shown in Fig. 1.6 is supported in such a way that rigid body displacements (translations and rotations) are prevented. Thus, this body deforms under the action of external forces and each of its points has small elastic displacements. For example, a point M had the coordinates x, y, and z in initial undeformed state. After deformation, this point moved into position $M'$and its coordinates became the following $x' = x + u$, $y' = y + v$, $z' = z' + w$, where u, v, and w are projections of the displacement vector of point M, vector $\mathbf{MM}'$, on the coordinate axes x, y and z. In the general case, u, v, and w are functions of x, y, and z.

Again, consider an infinitesimal element in the form of parallelepiped enclosing point of interest M. Assuming that a deformation of this parallelepiped is small, we can represent it in the form of the six simplest deformations shown in Fig. 1.7. The first three deformations shown in Fig. 1.7a, b, and c define the elongation (or contraction) of edges of the parallelepiped in the direction of the coordinate axes and can be defined as

$$\varepsilon_x = \frac{\delta(\mathrm{d}x)}{\mathrm{d}x}, \varepsilon_y = \frac{\delta(\mathrm{d}y)}{\mathrm{d}y}, \varepsilon_z = \frac{\delta(\mathrm{d}z)}{\mathrm{d}z}, \tag{1.4}$$

and they are called the *normal* or *linear strains*. In Eqs (1.4), the increments $\delta \mathrm{d}x$ can be expressed by the second term in the Taylor series, i.e., $\delta \mathrm{d}x = (\partial u/\partial x)\mathrm{d}x$, etc.; thus, we can write

$$\varepsilon_x = \frac{\partial u}{\partial x}, \varepsilon_y = \frac{\partial v}{\partial y}, \varepsilon_z = \frac{\partial w}{\partial z}. \tag{1.5a}$$

The three other deformations shown in Fig. 1.7d, e, and f are referred to as *shear strains* because they define a distortion of an initially right angle between the edges of the parallelepiped. They are denoted by γ_{xy}, γ_{xz}, and γ_{yz}. The subscripts indicate the coordinate planes in which the shear strains occur. Let us determine, for example, the shear strain in the xy coordinate plane. Consider the projection of the parallelepiped, shown in Fig. 1.7d, on this coordinate plane. Figure 1.8 shows this projec-

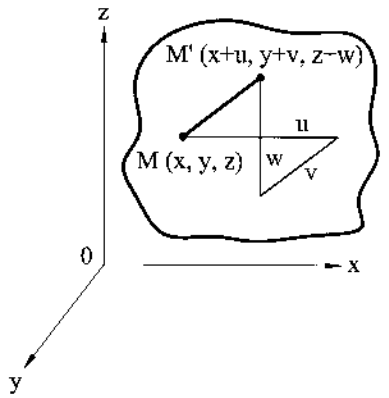

Fig. 1.6

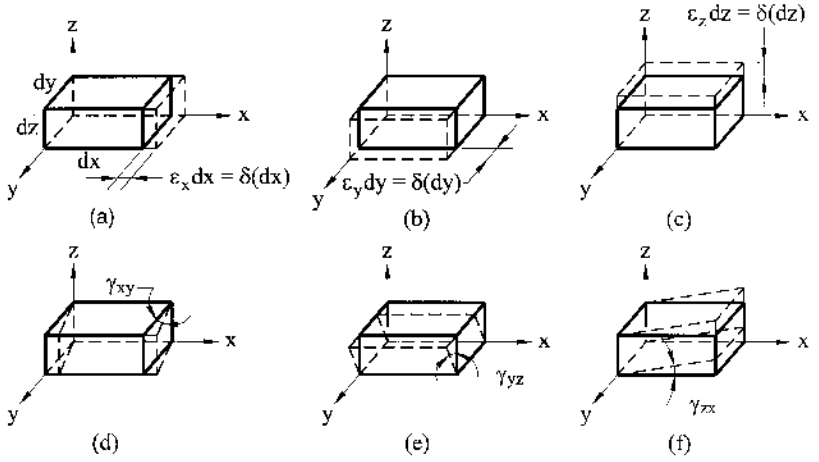

Fig. 1.7

tion in the form of the rectangle before deformation ($ABCD$) and after deformation ($A'B'C'D'$). The angle BAD in Fig. 1.8 deforms to the angle $B'A'D'$, the deformation being the angle $\gamma' + \gamma''$; thus, the shear strain is

$$\gamma_{xy} = \gamma' + \gamma'' \tag{a}$$

or it can be determined in terms of the in-plane displacements, u and v, as follows:

$$\gamma_{xy} = \frac{\frac{\partial v}{\partial x}\mathrm{d}x}{\mathrm{d}x + \frac{\partial u}{\partial x}\mathrm{d}x} + \frac{\frac{\partial u}{\partial y}\mathrm{d}y}{\mathrm{d}y + \frac{\partial v}{\partial y}\mathrm{d}y} = \frac{\frac{\partial v}{\partial x}}{1 + \frac{\partial u}{\partial x}} + \frac{\frac{\partial u}{\partial y}}{1 + \frac{\partial v}{\partial y}}.$$

Since we have confined ourselves to the case of very small deformations, we may omit the quantities $\partial u/\partial x$ and $\partial v/\partial y$ in the denominator of the last expression, as being negligibly small compared with unity. Finally, we obtain

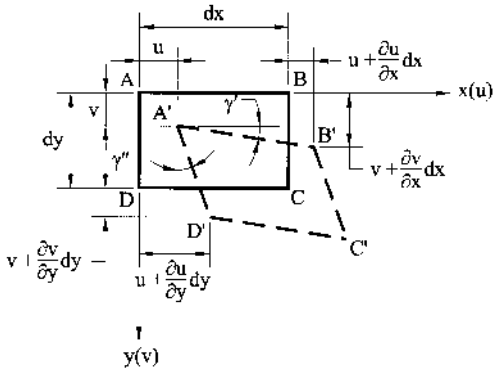

Fig. 1.8

$$\gamma_{xy} = \frac{\partial v}{\partial x} + \frac{\partial u}{\partial y}. \tag{b}$$

Similarly, we can obtain γ_{xz} and γ_{yz}. Thus, the shear strains are given by

$$\gamma_{xy} = \frac{\partial u}{\partial y} + \frac{\partial v}{\partial x},\ \gamma_{xz} = \frac{\partial u}{\partial z} + \frac{\partial w}{\partial x},\ \gamma_{yz} = \frac{\partial v}{\partial z} + \frac{\partial w}{\partial y}. \tag{1.5b}$$

Similar to the stress tensor (1.1) at a given point, we can define a strain tensor as

$$T_D = \begin{pmatrix} \varepsilon_x & \frac{1}{2}\gamma_{xy} & \frac{1}{2}\gamma_{xz} \\ \frac{1}{2}\gamma_{yx} & \varepsilon_y & \frac{1}{2}\gamma_{yz} \\ \frac{1}{2}\gamma_{zx} & \frac{1}{2}\gamma_{zy} & \varepsilon_z \end{pmatrix}. \tag{1.6}$$

It is evident that the strain tensor is also symmetric because of

$$\gamma_{xy} = \gamma_{yx},\ \gamma_{xz} = \gamma_{zx},\ \gamma_{yz} = \gamma_{zy} \tag{1.7}$$

1.4.3 Constitutive equations

The constitutive equations relate the stress components to strain components. For the linear elastic range, these equations represent the generalized Hooke's law. In the case of a three-dimensional isotropic body, the constitutive equations are given by [53].

$$\varepsilon_x = \frac{1}{E}\left[\sigma_x - \nu(\sigma_y + \sigma_z)\right],\ \varepsilon_y = \frac{1}{E}\left[\sigma_y - \nu(\sigma_x + \sigma_z)\right],\ \varepsilon_z = \frac{1}{2}\left[\sigma_z - \nu(\sigma_y + \sigma_x)\right], \tag{1.8a}$$

$$\gamma_{xy} = \frac{1}{G}\tau_{xy},\ \gamma_{xz} = \frac{1}{G}\tau_{xz},\ \gamma_{yz} = \frac{1}{G}\tau_{yz}, \tag{1.8b}$$

where E, ν, and G are the modulus of elasticity, Poisson's ratio, and the shear modulus, respectively. The following relationship exists between E and G:

$$G = \frac{E}{2(1+\nu)} \tag{1.9}$$

1.4.4 Equilibrium equations

The stress components introduced previously must satisfy the following differential equations of equilibrium:

$$\begin{aligned} &\frac{\partial \sigma_x}{\partial x} + \frac{\partial \tau_{xy}}{\partial y} + \frac{\partial \tau_{xz}}{\partial z} + F_x = 0, \\ &\frac{\partial \sigma_y}{\partial y} + \frac{\partial \tau_{yx}}{\partial x} + \frac{\partial \tau_{yz}}{\partial z} + F_y = 0, \\ &\frac{\partial \sigma_z}{\partial z} + \frac{\partial \tau_{zx}}{\partial x} + \frac{\partial \tau_{zy}}{\partial y} + F_z = 0, \end{aligned} \tag{1.10}$$

where F_x, F_y, and F_z are the body forces (e.g., gravitational, magnetic forces). In deriving these equations, the reciprocity of the shear stresses, Eqs (1.7), has been used.

1.4.5 Compatibility equations

Since the three equations (1.10) for six unknowns are not sufficient to obtain a solution, three-dimensional stress problems of elasticity are internally statically indeterminate. Additional equations are obtained to express the continuity of a body. These additional equations are referred to as *compatibility equations*. In Eqs (1.5) we have related the six strain components to the three displacement components. Eliminating the displacement components by successive differentiation, the following compatibility equations are obtained [53–55]:

$$\begin{aligned}
\frac{\partial^2 \varepsilon_x}{\partial y^2} + \frac{\partial^2 \varepsilon_y}{\partial x^2} &= \frac{\partial^2 \gamma_{xy}}{\partial x \partial y}, \\
\frac{\partial^2 \varepsilon_y}{\partial z^2} + \frac{\partial^2 \varepsilon_z}{\partial y^2} &= \frac{\partial^2 \gamma_{yz}}{\partial y \partial z}, \\
\frac{\partial^2 \varepsilon_z}{\partial x^2} + \frac{\partial^2 \varepsilon_x}{\partial z^2} &= \frac{\partial^2 \gamma_{xz}}{\partial x \partial z},
\end{aligned} \tag{1.11a}$$

$$\begin{aligned}
\frac{\partial}{\partial z}\left[\frac{\partial \gamma_{yz}}{\partial x} + \frac{\partial \gamma_{xz}}{\partial y} - \frac{\partial \gamma_{xy}}{\partial z}\right] &= 2\frac{\partial^2 \varepsilon_z}{\partial x \partial y}, \\
\frac{\partial}{\partial x}\left[\frac{\partial \gamma_{xz}}{\partial y} + \frac{\partial \gamma_{xy}}{\partial z} - \frac{\partial \gamma_{yz}}{\partial x}\right] &= 2\frac{\partial^2 \varepsilon_x}{\partial y \partial z}, \\
\frac{\partial}{\partial y}\left[\frac{\partial \gamma_{xy}}{\partial z} + \frac{\partial \gamma_{yz}}{\partial x} - \frac{\partial \gamma_{xz}}{\partial y}\right] &= 2\frac{\partial^2 \varepsilon_y}{\partial x \partial z}.
\end{aligned} \tag{1.11b}$$

For a two-dimensional state of stress ($\sigma_z = 0$, $\tau_{xz} = \tau_{yz} = 0$), the equilibrium conditions (1.10) become

$$\begin{aligned}
\frac{\partial \sigma_x}{\partial x} + \frac{\partial \tau_{xy}}{\partial y} + F_x &= 0, \\
\frac{\partial \sigma_y}{\partial y} + \frac{\partial \tau_{yx}}{\partial x} + F_y &= 0,
\end{aligned} \tag{1.12}$$

and the compatibility equation is

$$\frac{\partial^2 \varepsilon_x}{\partial y^2} + \frac{\partial^2 \varepsilon_y}{\partial x^2} = \frac{\partial^2 \gamma_{xy}}{\partial x \partial y} \quad \left(\gamma_{xz} = \gamma_{yz} = \varepsilon_z = 0\right). \tag{1.13}$$

We can rewrite Eq. (1.13) in terms of the stress components as follows

$$\left(\frac{\partial^2}{\partial x^2} + \frac{\partial^2}{\partial y^2}\right)\left(\sigma_x + \sigma_y\right) = 0. \tag{1.14}$$

This equation is called Levy's equation. By introducing Airy's stress function $\phi(x, y)$ which satisfies

$$\sigma_x = \frac{\partial^2 \phi}{\partial y^2}, \ \sigma_y = \frac{\partial^2 \phi}{\partial x^2}, \ \tau_{xy} = -\frac{\partial^2 \phi}{\partial x \partial y}, \tag{1.15}$$

Eq. (1.14) becomes

$$\nabla^2 \nabla^2 \phi = 0, \tag{1.16}$$

where

$$\nabla^2 \equiv \frac{\partial^2}{\partial x^2} + \frac{\partial^2}{\partial y^2} \tag{1.17}$$

is the two-dimensional Laplace operator.

SUMMARY

For an elastic solid there are 15 independent variables: six stress components, six strain components, and three displacements. In the case where compatibility is satisfied, there are 15 equations: three equilibrium equations, six constitutive relations, and six strain-displacement equations.

REFERENCES

1. Euler, L., De motu vibratorio tympanorum, *Novi Commentari Acad Petropolit*, vol. 10, pp. 243–260 (1766).
2. Chladni, E.F., *Die Akustik*, Leipzig, 1802.
3. Bernoulli, J., Jr., Essai theorique sur les vibrations de plaques elastiques rectangularies et libers, *Nova Acta Acad Petropolit,* vol. 5, pp. 197–219 (1789).
4. Germain, S., *Remarques sur la nature, les bornes et l'etendue de la question des surfaces elastiques et equation general de ces surfaces*, Paris, 1826.
5. Lagrange, J.L., *Ann Chim*, vol. 39, pp. 149–207 (1828).
6. Cauchy, A.L., Sur l'equilibre le mouvement d'une plaque solide, *Exercises Math*, vol. 3, p. 328 (1828).
7. Poisson, S.D., Memoire sur l'equilibre et le mouvement des corps elastique, *Mem Acad Sci*, vol. 8, p. 357 (1829).
8. Navier, C.L.M.H., *Bulletin des Sciences de la Societe Philomathique de Paris*, 1823.
9. Kirchhoff, G.R., Uber das gleichgewichi und die bewegung einer elastishem scheibe, *J Fuer die Reine und Angewandte Mathematik*, vol. 40, pp. 51–88 (1850).
10. Lord Kelvin and Tait, P.G., *Treatise on Natural Philosophy*, vol. 1, Clarendon Press, Oxford, 1883.
11. Clebsch, A. Theorie de l'Elasticite des Corps Solids, *Avec des Notes Entendues de Saint-Venant*, Dunod, Paris, pp. 687–706 (1883).
12. Levy, M., Memoire sur la theorie des plaques elastiques planes, *J Math Pure Appl*, vol 3, p. 219 (1899).
13. Krylov, A.N., On stresses experienced by a ship in a sea way, *Trans Inst Naval Architects*, vol. 40, London, pp. 197–209, 1898.
14. Bubnov, I.G., *Theory of Structures of Ships*, vol. 2, St . Petersburg, 1914.
15. Galerkin, B.G., *Thin Elastic Plates*, Gostrojisdat, Leningrad, 1933 (in Russian).
16. Timoshenko, S.P., On large deflections of circular plates, *Mem Inst Ways Commun*, 89, 1915.

17. Timoshenko, S.P., Sur la stabilite des systemes elastiques, *Ann des Points et Chaussees*, vol. 13, pp. 496–566; vol. 16, pp. 73–132 (1913).
18. Timoshenko, S.P. and Woinowsky-Krieger, S., *Theory of Plates and Shells*, 2nd edn, McGraw-Hill, New York, 1959.
19. Hencky, H., Der spanngszustand in rechteckigen platten (Diss.), *Z Andew Math und Mech*, vol. 1 (1921).
20. Huber, M.T., *Probleme der Static Techish Wichtiger Orthotroper Platten*, Warsawa, 1929.
21. von Karman, T., Fesigkeitsprobleme in Maschinenbau, *Encycl der Math Wiss*, vol. 4, pp. 348–351 (1910).
22. von Karman,T., Ef Sechler and Donnel, L.H. The strength of thin plates in compression, *Trans ASME*, vol. 54, pp. 53–57 (1932).
23. Nadai, A. *Die formanderungen und die spannungen von rechteckigen elastischen platten*, Forsch a.d. Gebiete d Ingeineurwesens, Berlin, Nos. 170 and 171 (1915).
24. Foppl, A., *Vorlesungen uber technische Mechanik*, vols 1 and 2, 14th and 15th edns, Verlag R., Oldenburg, Munich, 1944, 1951.
25. Gehring, F., *Vorlesungen uber Mathematieche Physik, Mechanik*, 2nd edn, Berlin,1877.
26. Boussinesq, J., Complements anne étude sur la theorie de l'equilibre et du mouvement des solides elastiques, *J de Math Pures et Appl* , vol. 3, ses. t.5 (1879).
27. Leknitskii, S.G., *Anisotropic Plates* (English translation of the original Russian work), Gordon and Breach, New York, 1968.
28. Reissner, E., The effect of transverse shear deformation on the bending of elastic plates, *J Appl Mech Trans ASME*, vol. 12, pp. A69–A77 (1945).
29. Volmir, A.S., *Flexible Plates and Shells*, Gos. Izd-vo Techn.-Teoret. Lit-ry, Moscow, 1956 (in Russian).
30. Panov, D.Yu., On large deflections of circular plates, *Prikl Matem Mech*, vol. 5, No. 2, pp. 45–56 (1941) (in Russian).
31. Bryan, G.N., On the stability of a plane plate under thrusts in its own plane, *Proc London Math Soc*, 22, 54–67 (1981)
32. Cox, H.L, *Buckling of Thin Plates in Compression*, Rep. and Memor., No. 1553,1554, (1933).
33. Hartmann, F., *Knickung, Kippung, Beulung*, Springer-Verlag, Berlin, 1933.
34. Dinnik, A.N., A stability of compressed circular plate, *Izv Kiev Polyt In-ta*, 1911 (in Russian).
35. Nadai, A., Uber das ausbeulen von kreisformigen platten, *Zeitschr VDJ*, No. 9,10 (1915).
36. Meissner, E., Uber das knicken kreisformigen scheiben, *Schweiz Bauzeitung*, 101, pp. 87–89 (1933).
37. Southwell, R.V. and Scan, S., On the stability under shearing forces of a flat elastic strip, *Proc Roy Soc*, A105, 582 (1924).
38. Timoshenko, S.P. and Gere, J.M., *Theory of Elastic Stability*, 2nd edn, McGraw-Hill, New York, 1961.
39. Karman, Th., Sechler, E.E. and Donnel, L.H., The strength of thin plates in compression, *Trans ASME*, 54, 53–57 (1952).
40. Levy, S., *Bending of Rectangular Plates with Large Deflections*, NACA, Rep. No.737, 1942.
41. Marguerre, K., Die mittragende briete des gedrückten plattenstreifens, *Luftfahrtforschung*, 14, No. 3, 1937.
42. Gerard, G. and Becker, H., *Handbook of Structural Stability*, Part1 – Buckling of Flat Plates, NACA TN 3781, 1957.
43. Volmir, A.S., *Stability of Elastic Systems*, Gos Izd-vo Fiz-Mat. Lit-ry, Moscow, 1963 (in Russian).
44. Cox, H.l., *The Buckling of Plates and Shells*. Macmillan, New York, 1963.

45. Voight, W, Bemerkungen zu dem problem der transversalem schwingungen rechteckiger platten, *Nachr. Ges (Göttingen*), No. 6, pp. 225–230 (1893).
46. Ritz, W., Theorie der transversalschwingungen, einer quadratischen platte mit frein rändern, *Ann Physic, Bd*., 28, pp. 737–786 (1909).
47. Timoshenko, S.P. and Young, D.H., *Vibration Problems in Engineering*, John Wiley and Sons., New York, 1963.
48. Den Hartog, J.P., *Mechanical Vibrations*, 4th edn, McGraw-Hill, New York, 1958.
49. Thompson, W.T., *Theory of Vibrations and Applications*, Prentice-Hill, Englewood Cliffs, New Jersey, 1973.
50. Leissa, A.W., *Vibration of Plates*, National Aeronautics and Space Administration, Washington, D.C., 1969.
51. Timoshenko, S.P., *History of Strength of Materials*, McGraw-Hill, New York, 1953.
52. Truesdell, C., *Essays in the History of Mechanic*., Springer-Verlag, Berlin, 1968.
53. Timoshenko, S.P. and Goodier, J.N., *Theory of Elasticity*, 3rd edn, McGraw-Hill, New York, 1970.
54. Prescott, J.J., *Applied Elasticity,* Dover, New York, 1946.
55. Sokolnikoff, I.S*., Mathematical Theory of Elasticity*, 2nd edn, McGraw-Hill, New York, 1956.

2

The Fundamentals of the Small-Deflection P late Bending Theory

2.1 INTRODUCTION

The foregoing assumptions introduced in Sec. 1.3 make it possible to derive the basic equations of the *classical* or *Kirchhoff's bending theory* for stiff plates. It is convenient to solve plate bending problems in terms of displacements. In order to derive the governing equation of the classical plate bending theory, we will invoke the three sets of equations of elasticity discussed in Sec. 1.4.

2.2 STRAIN–CURVATURE RELATIONS (KINEMATIC EQUATIONS)

We will use common notations for displacement, stress, and strain components adapted in elasticity (see Sec. 1.4). Let u, v, and w be components of the displacement vector of points in the middle surface of the plate occurring in the x, y, and z directions, respectively. The normal component of the displacement vector, w (called the *deflection*), and the lateral distributed load p are positive in the downward direction. As it follows from the assumption (4) of Sec. 1.3

$$\varepsilon_z = 0, \ \gamma_{yz} = 0, \ \gamma_{xz} = 0. \tag{2.1}$$

Integrating the expressions (1.5) for ε_z, γ_{yz}, and γ_{xz} and taking into account Eq. (2.1), we obtain

$$w^z = w(x, y), \ u^z = -z\frac{\partial w}{\partial x} + u(x, y), \ v^z = -z\frac{\partial w}{\partial y} + v(x, y), \tag{2.2}$$

where u^z, v^z, and w^z are displacements of points at a distance z from the middle surface. Based upon assumption (6) of Sec. 1.3, we conclude that $u = v = 0$. Thus, Eqs (2.2) have the following form in the context of Kirchhoff's theory:

$$w^z = w(x, y),\ \ u^z = -z\frac{\partial w}{\partial x},\ \ v^z = -z\frac{\partial w}{\partial y}. \tag{2.3}$$

As it follows from the above, the displacements u^z and v^z of an arbitrary horizontal layer vary linearly over a plate thickness while the deflection does not vary over the thickness.

Figure 2.1 shows a section of the plate by a plane parallel to Oxz, $y = \text{const.}$, before and after deformation. Consider a segment AB in the positive z direction. We focus on an arbitrary point B which initially lies at a distance z from the undeformed middle plane (from the point A). During the deformation, point A displaces a distance w parallel to the original z direction to point A_1. Since the transverse shear deformations are neglected, the deformed position of point B must lie on the normal to the deformed middle plane erected at point A_1(assumption (4)). Its final position is denoted by B_1. Due to the assumptions (4) and (5), the distance z between the above-mentioned points during deformation remains unchanged and is also equal to z.

We can also represent the displacement components u^z and v^z, Eqs (2.2), in the form

$$u^z = -z\vartheta_x,\ \ v^z = -z\vartheta_y, \tag{2.4}$$

where

$$\vartheta_x = \frac{\partial w}{\partial x},\ \ \vartheta_y = \frac{\partial w}{\partial y} \tag{2.5}$$

are the angles of rotation of the normal (normal I–I in Fig. 2.1) to the middle surface in the Oxz and Oyz plane, respectively. Owing to the assumption (4) of Sec. 1.3, ϑ_x and ϑ_y are also slopes of the tangents to the traces of the middle surface in the above-mentioned planes.

Substitution of Eqs (2.3) into the first two Eqs (1.5a) and into the first Eq. (1.5b), yields

$$\varepsilon_x^z = -z\frac{\partial^2 w}{\partial x^2},\ \ \varepsilon_y^z = -z\frac{\partial^2 w}{\partial y^2},\ \ \gamma_{xy}^z = -2z\frac{\partial^2 w}{\partial x \partial y}, \tag{2.6}$$

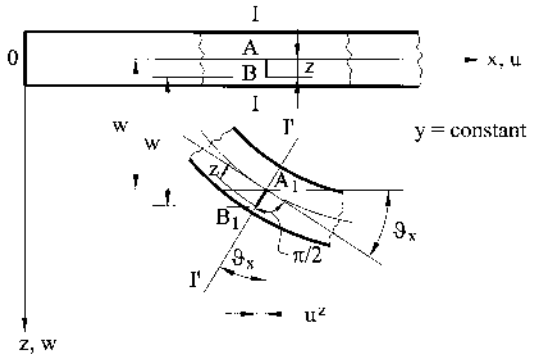

Fig. 2.1

where the superscript z refers to the in-plane strain components at a point of the plate located at a distance z from the middle surface. Since the middle surface deformations are neglected due to the assumption (6), from here on, this superscript will be omitted for all the strain and stress components at points across the plate thickness.

The second derivatives of the deflection on the right-hand side of Eqs. (2.6) have a certain geometrical meaning. Let a section MNP represent some plane curve in which the middle surface of the deflected plate is intersected by a plane $y = const$. (Fig. 2.2).

Due to the assumption 3 (Sec. 1.3), this curve is shallow and the square of the slope angle may be regarded as negligible compared with unity, i.e., $(\partial w/\partial x)^2 \ll 1$. Then, the second derivative of the deflection, $\partial^2 w/\partial x^2$ will define approximately the curvature of the section along the x axis, χ_x. Similarly, $\partial^2 w/\partial y^2$ defines the curvature of the middle surface χ_y along the y axis. The curvatures χ_x and χ_y characterize the phenomenon of bending of the middle surface in planes parallel to the Oxz and Oyz coordinate planes, respectively. They are referred to as *bending curvature* and are defined by

$$\chi_x = \frac{1}{\rho_x} = -\frac{\partial^2 w}{\partial x^2},\ \chi_y = \frac{1}{\rho_y} = -\frac{\partial^2 w}{\partial y^2} \tag{2.7a}$$

We consider a bending curvature positive if it is convex downward, i.e., in the positive direction of the z axis. The negative sign is taken in Eqs. (2.7a) since, for example, for the deflection convex downward curve MNP (Fig. 2.2), the second derivative, $\partial^2 w/\partial x^2$ is negative.

The curvature $\partial^2 w/\partial x^2$ can be also defined as the rate of change of the angle $\vartheta_x = \partial w/\partial x$ with respect to distance x along this curve. However, the above angle can vary in the y direction also. It is seen from comparison of the curves MNP and $M_1N_1P_1$ (Fig. 2.2), separated by a distance dy. If the slope for the curve MNP is $\partial w/\partial x$ then for the curve $M_1N_1P_1$ this angle becomes equal to $\left[\frac{\partial w}{\partial x} - \frac{\partial}{\partial y}\left(\frac{\partial w}{\partial x}\right)dy\right]$ or $\left(\frac{\partial w}{\partial x} - \frac{\partial^2 w}{\partial x \partial y}dy\right)$. The rate of change of the angle $\partial w/\partial x$ per unit length will be $(-\partial^2 w/\partial x \partial y)$. The negative sign is taken here because it is assumed

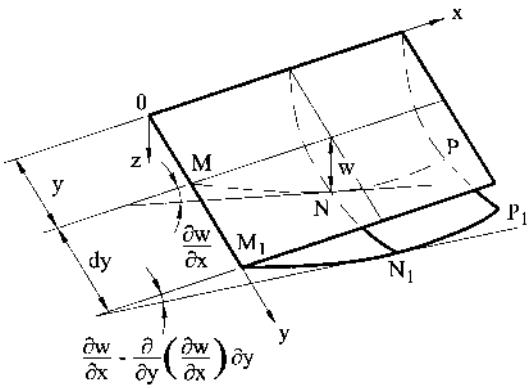

Fig. 2.2

that when y increases, the slope angle of the tangent to the curve decreases (by analogy with the sign convention for the bending curvatures χ_x and χ_y). Similarly, can be convinced that in the perpendicular section (for the variable x), the rate of change of the angle $\partial w/\partial y$ is characterized by the same mixed derivative $(-\partial^2 w/\partial x \partial y)$. By analogy with the torsion theory of rods, the derivative $\partial^2 w/\partial x \partial y$ defines the warping of the middle surface at a point with coordinates x and y is called the *twisting curvature with respect to the* x and y *axes and is denotes by* χ_{xy}. Thus,

$$\chi_{xy} = \chi_{yx} = \frac{1}{\rho_{xy}} = -\frac{\partial^2 w}{\partial x \partial y} \tag{2.7b}$$

Taking into account Eqs (2.7) we can rewrite Eqs (2.6) as follows

$$\varepsilon_x = z\chi_x; \;\; \varepsilon_y = z\chi_y; \;\; \gamma_{xy} = 2z\chi_{xy}. \tag{2.8}$$

2.3 STRESSES, STRESS RESULTANTS, AND STRESS COUPLES

In the case of a three-dimensional state of stress, stress and strain are related by the Eqs (1.8) of the generalized Hooke's law. As was mentioned earlier, Kirchhoff's assumptions of Sec. 1.3 brought us to Eqs (2.1). From a mathematical standpoint, this means that the three new equations (2.1) are added to the system of governing equations of the theory of elasticity. So, the latter becomes overdetermined and, therefore, it is necessary to also drop three equations. As a result, the three relations out of six of Hookes' law (see Eqs (1.8)) for strains (2.1) are discarded. Moreover, the normal stress component $\sigma_z = 0$. Solving Eqs (1.8) for stress components σ_x, σ_y, and τ_{xy}, yields

$$\sigma_x = \frac{E}{1-\nu^2}(\varepsilon_x + \nu\varepsilon_y); \;\; \sigma_y = \frac{E}{1-\nu^2}(\varepsilon_y + \nu\varepsilon_x); \;\; \tau_{xy} = G\gamma_{xy}. \tag{2.9}$$

The stress components are shown in Fig. 2.3a. The subscript notation and sign convention for the stresses were given in Sec. 1.4.

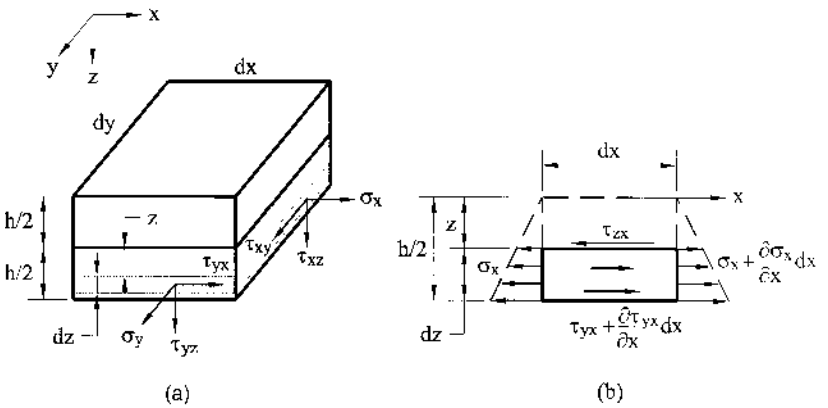

Fig. 2.3

Introducing the plate curvatures, Eqs (2.7) and using Eqs (2.8), the above equations appear as follows:

$$\sigma_x = \frac{Ez}{1-\nu^2}(\chi_x + \nu\chi_y) = -\frac{Ez}{1-\nu^2}\left(\frac{\partial^2 w}{\partial x^2} + \nu\frac{\partial^2 w}{\partial y^2}\right);$$
$$\sigma_y = \frac{Ez}{1-\nu^2}(\chi_y + \nu\chi_x) = -\frac{Ez}{1-\nu^2}\left(\frac{\partial^2 w}{\partial y^2} + \nu\frac{\partial^2 w}{\partial x^2}\right); \tag{2.10}$$
$$\tau_{xy} = \frac{Ez}{1+\nu}\chi_{xy} = -\frac{Ez}{1+\nu}\frac{\partial^2 w}{\partial x \partial y}.$$

It is seen from Eqs. (2.10) that Kirchhoff's assumptions have led to a completely defined law of variation of the stresses through the thickness of the plate. Therefore, as in the theory of beams, it is convenient to introduce, instead of the stress components at a point problem, the total statically equivalent forces and moments applied to the middle surface, which are known as the *stress resultants* and *stress couples*. The stress resultants and stress couples are referred to as the *shear forces*, Q_x and Q_y, as well as the *bending* and *twisting moments* M_x, M_y, and M_{xy}, respectively. Thus, Kirchhoff's assumptions have reduced the three-dimensional plate straining problem to the two-dimensional problem of straining the middle surface of the plate. Referring to Fig. 2.3, we can express the bending and twisting moments, as well as the shear forces, in terms of the stress components, i.e.,

$$\begin{Bmatrix} M_x \\ M_y \\ M_{xy} \end{Bmatrix} = \int_{-h/2}^{h/2} \begin{Bmatrix} \sigma_x \\ \sigma_y \\ \tau_{xy} \end{Bmatrix} z\,\mathrm{d}z \tag{2.11}$$

and

$$\begin{Bmatrix} Q_x \\ Q_y \end{Bmatrix} = \int_{-h/2}^{h/2} \begin{Bmatrix} \tau_{xz} \\ \tau_{yz} \end{Bmatrix} \mathrm{d}z. \tag{2.12}$$

Because of the reciprocity law of shear stresses ($\tau_{xy} = \tau_{yx}$), the twisting moments on perpendicular faces of an infinitesimal plate element are identical, i.e., $M_{yx} = M_{xy}$.

The sign convention for the shear forces and the twisting moments is the same as that for the shear stresses (see Sec. 1.4). A positive bending moment is one which results in positive (tensile) stresses in the bottom half of the plate. Accordingly, all the moments and the shear forces acting on the element in Fig. 2.4 are positive.

Note that the relations (2.11) and (2.12) determine the intensities of moments and shear forces, i.e., moments and forces per unit length of the plate midplane. Therefore, they have dimensional units as [*force* · *length*/*length*] or simply [*force*] for moments and [*force*/*length*] for shear forces, respectively.

It is important to mention that while the theory of thin plates omits the effect of the strain components $\gamma_{xz} = \tau_{xz}/G$ and $\gamma_{yz} = \tau_{yz}/G$ on bending, the vertical shear forces Q_x and Q_y are not negligible. In fact, they are necessary for equilibrium of the plate element.

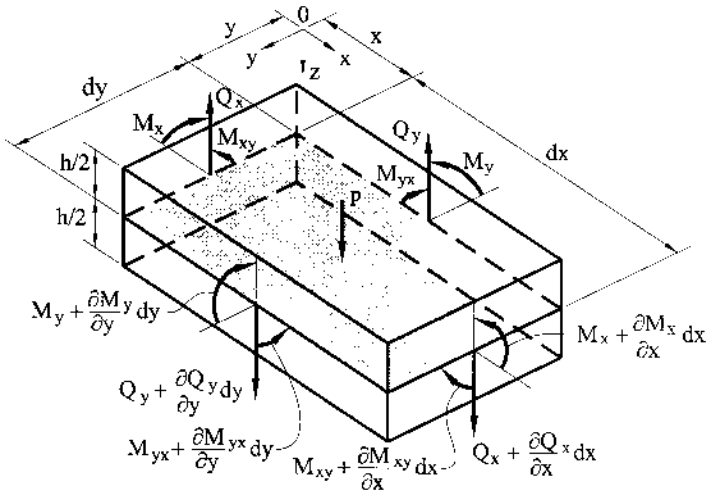

Fig. 2.4

Substituting Eqs (2.10) into Eqs (2.11) and integrating over the plate thickness, we derive the following formulas for the stress resultants and couples in terms of the curvatures and the deflection:

$$M_x = D(\chi_x + \nu\chi_y) = -D\left(\frac{\partial^2 w}{\partial x^2} + \nu\frac{\partial^2 w}{\partial y^2}\right),$$

$$M_y = D(\chi_y + \nu\chi_x) = -D\left(\frac{\partial^2 w}{\partial y^2} + \nu\frac{\partial^2 w}{\partial x^2}\right), \tag{2.13}$$

$$M_{xy} = M_{yx} = D(1-\nu)\chi_{xy} = -D(1-\nu)\frac{\partial^2 w}{\partial x \partial y},$$

where

$$D = \frac{Eh^3}{12(1-\nu^2)} \tag{2.14}$$

is the *flexural rigidity of the plate*. It plays the same role as the flexural rigidity EI in beam bending. Note that $D > EI$; hence, a plate is always stiffer than a beam of the same span and thickness. The quantities χ_x, χ_y and χ_{xy} are given by Eqs (2.7).

Solving Eqs (2.13) for the second derivatives of the deflection and substituting the above into Eqs (2.10), we get the following expressions for stresses

$$\sigma_x = \pm\frac{12M_x}{h^3}z, \sigma_y = \pm\frac{12M_y}{h^3}z, \ \tau_{xy} = \frac{12M_{xy}}{h^3}z. \tag{2.15}$$

Determination of the remaining three stress components τ_{xz}, τ_{yz}, and σ_z through the use of Hooke's law is not possible due to the fourth and fifth assumptions (Sec. 1.3), since these stresses are not related to strains. The differential equa-

tions of equilibrium for a plate element under a general state of stress (1.10) (assuming that the body forces are zero) serve well for this purpose, however. If the faces of the plate are free of any tangent external loads, then τ_{xz} and τ_{yz} are zero for $z = \pm h/2$. From the first two Eqs (1.10) and Eqs (2.9) and (2.10), the shear stresses τ_{xz} (Fig. 2.3(b)) and τ_{yz} are

$$\tau_{xz} = -\int_{-h/2}^{h/2} \left(\frac{\partial \sigma_x}{\partial x} + \frac{\partial \tau_{xy}}{\partial y}\right) dz = \frac{E\left(z^2 - h^2/4\right)}{2\left(1-\nu^2\right)} \frac{\partial}{\partial x} \nabla^2 w,$$
$$\tau_{yz} = -\int_{-h/2}^{h/2} \left(\frac{\partial \sigma_y}{\partial y} + \frac{\partial \tau_{yx}}{\partial x}\right) dz = \frac{E\left(z^2 - h^2/4\right)}{2\left(1-\nu^2\right)} \frac{\partial}{\partial y} \nabla^2 w, \tag{2.16}$$

where $\nabla^2( )$ is the *Laplace operator*, given by

$$\nabla^2 w = \frac{\partial^2 w}{\partial x^2} + \frac{\partial^2 w}{\partial y^2}. \tag{2.17}$$

It is observed from Eqs (2.15) and (2.16) that the stress components σ_x, σ_y, and τ_{xy} (in-plane stresses) vary linearly over the plate thickness, whereas the shear stresses τ_{xz} and τ_{yz} vary according to a parabolic law, as shown in Fig. 2.5.

The component σ_z is determined by using the third of Eqs (1.10), upon substitution of τ_{xz} and τ_{yz} from Eqs (2.16) and integration. As a result, we obtain

$$\sigma_z = -\frac{E}{2(1-\nu^2)} \left(\frac{h^3}{12} - \frac{h^2 z}{4} + \frac{z^3}{3}\right) \nabla^2 \nabla^2 w. \tag{2.18}$$

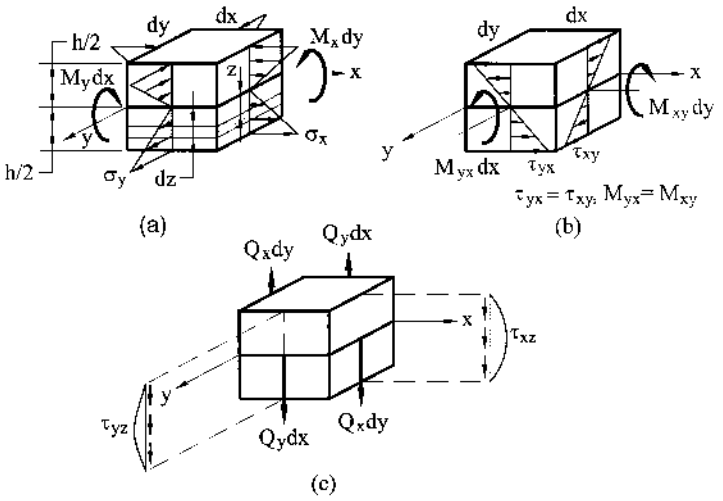

Fig. 2.5

2.4 GOVERNING EQUATION FOR DEFLECTION OF PLATES IN CARTESIAN COORDINATES

The components of stress (and, thus, the stress resultants and stress couples) generally vary from point to point in a loaded plate. These variations are governed by the static conditions of equilibrium.

Consider equilibrium of an element $\mathrm{d}x \times \mathrm{d}y$ of the plate subject to a vertical distributed load of intensity $p(x, y)$ applied to an upper surface of the plate, as shown in Fig. 2.4. Since the stress resultants and stress couples are assumed to be applied to the middle plane of this element, a distributed load $p(x, y)$ is transferred to the midplane. Note that as the element is very small, the force and moment components may be considered to be distributed uniformly over the midplane of the plate element: in Fig. 2.4 they are shown, for the sake of simplicity, by a single vector. As shown in Fig. 2.4, in passing from the section x to the section $x + \mathrm{d}x$ an intensity of stress resultants changes by a value of partial differential, for example, by $\partial M_x = \frac{\partial M_x}{\partial x}\mathrm{d}x$. The same is true for the sections y and $y + \mathrm{d}y$. For the system of forces and moments shown in Fig. 2.4 , the following three independent conditions of equilibrium may be set up:

(a) The force summation in the z axis gives

$$\frac{\partial Q_x}{\partial x}\mathrm{d}x\mathrm{d}y + \frac{\partial Q_y}{\partial y}\mathrm{d}x\mathrm{d}y + p\mathrm{d}x\mathrm{d}y = 0,$$

from which

$$\frac{\partial Q_x}{\partial x} + \frac{\partial Q_y}{\partial y} + p = 0. \tag{2.19}$$

(b) The moment summation about the x axis leads to

$$\frac{\partial M_{xy}}{\partial x}\mathrm{d}x\mathrm{d}y + \frac{\partial M_y}{\partial y}\mathrm{d}x\mathrm{d}y - Q_y\mathrm{d}x\mathrm{d}y = 0$$

or

$$\frac{\partial M_{xy}}{\partial x} + \frac{\partial M_y}{\partial y} - Q_y = 0. \tag{2.20}$$

Note that products of infinitesimal terms, such as the moment of the load p and the moment due to the change in Q_y have been omitted in Eq. (2.20) as terms with a higher order of smallness.

(c) The moment summation about the y axis results in

$$\frac{\partial M_{yx}}{\partial y} + \frac{\partial M_x}{\partial x} - Q_x = 0. \tag{2.21}$$

It follows from the expressions (2.20) and (2.21), that the shear forces Q_x and Q_y can be expressed in terms of the moments, as follows:

$$Q_x = \frac{\partial M_x}{\partial x} + \frac{\partial M_{xy}}{\partial y} \tag{2.22a}$$

$$Q_y = \frac{\partial M_{xy}}{\partial x} + \frac{\partial M_y}{\partial y} \tag{2.22b}$$

Here it has been taken into account that $M_{xy} = M_{yx}$. Substituting Eqs (2.22) into Eq. (2.19), one finds the following:

$$\frac{\partial^2 M_x}{\partial x^2} + 2\frac{\partial^2 M_{xy}}{\partial x \partial y} + \frac{\partial^2 M_y}{\partial y^2} = -p(x, y). \tag{2.23}$$

Finally, introduction of the expressions for M_x, M_y, and M_{xy} from Eqs (2.13) into Eq. (2.23) yields

$$\frac{\partial^4 w}{\partial x^4} + 2\frac{\partial^4 w}{\partial x^2 \partial y^2} + \frac{\partial^4 w}{\partial y^4} = \frac{p}{D}. \tag{2.24}$$

This is the *governing differential equation for the deflections* for thin plate bending analysis based on Kirchhoff's assumptions. This equation was obtained by Lagrange in 1811. Mathematically, the differential equation (2.24) can be classified as a linear partial differential equation of the fourth order having constant coefficients [1,2].

Equation (2.24) may be rewritten, as follows:

$$\nabla^2(\nabla^2 w) = \nabla^4 w = \frac{p}{D}, \tag{2.25}$$

where

$$\nabla^4( ) \equiv \frac{\partial^4}{\partial x^4} + 2\frac{\partial^4}{\partial x^2 \partial y^2} + \frac{\partial^4}{\partial y^4} \tag{2.26}$$

is commonly called the *biharmonic operator*.

Once a deflection function $w(x, y)$ has been determined from Eq. (2.24), the stress resultants and the stresses can be evaluated by using Eqs (2.13) and (2.15). In order to determine the deflection function, it is required to integrate Eq. (2.24) with the constants of integration dependent upon the appropriate boundary conditions. We will discuss this procedure later.

Expressions for the vertical forces Q_x and Q_y, may now be written in terms of the deflection w from Eqs (2.22) together with Eqs (2.13), as follows:

$$\begin{aligned} Q_x &= -D\frac{\partial}{\partial x}\left(\frac{\partial^2 w}{\partial x^2} + \frac{\partial^2 w}{\partial y^2}\right) = -D\frac{\partial}{\partial x}(\nabla^2 w), \\ Q_y &= -D\frac{\partial}{\partial y}\left(\frac{\partial^2 w}{\partial x^2} + \frac{\partial^2 w}{\partial y^2}\right) = -D\frac{\partial}{\partial y}(\nabla^2 w). \end{aligned} \tag{2.27}$$

Using Eqs (2.27) and (2.25), we can rewrite the expressions for the stress components τ_{xz}, τ_{yz}, and σ_z, Eqs (2.16) and (2.18), as follows

$$\tau_{xz} = \frac{3Q_x}{2h}\left[1 - \left(\frac{2z}{h}\right)^2\right], \quad \tau_{yz} = \frac{3Q_y}{2h}\left[1 - \left(\frac{2z}{h}\right)^2\right],$$

$$\sigma_z = -\frac{3p}{4}\left[\frac{2}{3} - \frac{2z}{h} + \frac{1}{3}\left(\frac{2z}{h}\right)^3\right]. \tag{2.28}$$

The maximum shear stress, as in the case of a beam of rectangular cross section, occurs at $z = 0$ (see Fig. 2.5), and is represented by the formula

$$\max .\tau_{xz} = \frac{3}{2}\frac{Q_x}{h}, \ \max .\tau_{yz} = \frac{3}{2}\frac{Q_y}{h}.$$

It is significant that the sum of the bending moments defined by Eqs (2.13) is invariant; i.e.,

$$M_x + M_y = -D(1+\nu)\left(\frac{\partial^2 w}{\partial x^2} + \frac{\partial^2 w}{\partial y^2}\right) = -D(1+\nu)\nabla^2 w$$

or

$$\frac{M_x + M_y}{1+\nu} = -D\nabla^2 w \tag{2.29}$$

Letting M denote the moment function or the so-called moment sum,

$$M = \frac{M_x + M_y}{1+\nu} = -D\nabla^2 w, \tag{2.30}$$

the expressions for the shear forces can be written as

$$Q_x = \frac{\partial M}{\partial x}, \ Q_y = \frac{\partial M}{\partial y} \tag{2.31}$$

and we can represent Eq. (2.24) in the form

$$\begin{aligned} &\frac{\partial^2 M}{\partial x^2} + \frac{\partial^2 M}{\partial y^2} = -p, \\ &\frac{\partial^2 w}{\partial x^2} + \frac{\partial^2 w}{\partial y^2} = -\frac{M}{D}. \end{aligned} \tag{2.32}$$

Thus, the plate bending equation $\nabla^4 w = p/D$ is reduced to two second-order partial differential equations which are sometimes preferred, depending upon the method of solution to be employed.

Summarizing the arguments set forth in this section, we come to the conclusion that the deformation of a plate under the action of the transverse load $p(x, y)$ applied to its upper plane is determined by the differential equation (2.24). This deformation results from:

(a) bending produced by bending moments M_x and M_y, as well as by the shear forces Q_x and Q_y;
(b) torsion produced by the twisting moments $M_{xy} = M_{yz}$.

Both of these phenomena are generally inseparable in a plate. Indeed, let us replace the plate by a flooring composed of separate rods, each of which will bend under the

action of the load acting on it irrespective of the neighboring rods. Let them now be tied together in a solid slab (plate). If we load only one rod, then, deflecting, it will carry along the adjacent rods, applying to their faces those shear forces which we have designated here by Q_x and Q_y. These forces will cause rotation of the cross section, i.e., twisting of the rod. This approximation of a plate with a grillage of rods (or beams) is known as the "grillage, or gridwork analogy" [3].

2.5 BOUNDARY CONDITIONS

As pointed out earlier, the boundary conditions are the known conditions on the surfaces of the plate which must be prescribed in advance in order to obtain the solution of Eq. (2.24) corresponding to a particular problem. Such conditions include the load $p(x, y)$ on the upper and lower faces of the plate; however, the load has been taken into account in the formulation of the general problem of bending of plates and it enters in the right-hand side of Eq. (2.24). It remains to clarify the conditions on the cylindrical surface, i.e., at the edges of the plate, depending on the fastening or supporting conditions. For a plate, the solution of Eq. (2.24) requires that two boundary conditions be satisfied at each edge. These may be a given deflection and slope, or force and moment, or some combination of these.

For the sake of simplicity, let us begin with the case of rectangular plate whose edges are parallel to the axes Ox and Oy. Figure 2.6 shows the rectangular plate one edge of which ($y = 0$) is built-in, the edge $x = a$ is simply supported, the edge $x = 0$ is supported by a beam, and the edge $y = b$ is free.

We consider below all the above-mentioned boundary conditions:

(1) *Clamped, or built-in, or fixed edge* $y = 0$

At the clamped edge $y = 0$ the deflection and slope are zero, i.e.,

$$w = 0|_{y=0} \quad \text{and} \quad \vartheta_y \equiv \frac{\partial w}{\partial y} = 0\Big|_{y=0}. \tag{2.33}$$

(2) *Simply supported edge* $x = a$

At these edges the deflection and bending moment M_x are both zero, i.e.,

$$w = 0|_{x=a}, \quad M_x = -D\left(\frac{\partial^2 w}{\partial x^2} + \nu\frac{\partial^2 w}{\partial y^2}\right) = 0\Big|_{x=a}. \tag{2.34}$$

The first of these equations implies that along the edge $x = a$ all the derivatives of w with respect to y are zero, i.e., if $x = a$ and $w = 0$, then $\frac{\partial w}{\partial y} = \frac{\partial^2 w}{\partial y^2} = 0$.

It follows that conditions expressed by Eqs (2.34) may appear in the following equivalent form:

$$w = 0|_{x=a}, \quad \frac{\partial^2 w}{\partial x^2} = 0\Big|_{x=a}. \tag{2.35}$$

(3) *Free edge* $y = b$

Suppose that the edge $y = b$ is perfectly free. Since no stresses act over this edge, then it is reasonable to equate all the stress resultants and stress couples occurring at points of this edge to zero, i.e.,

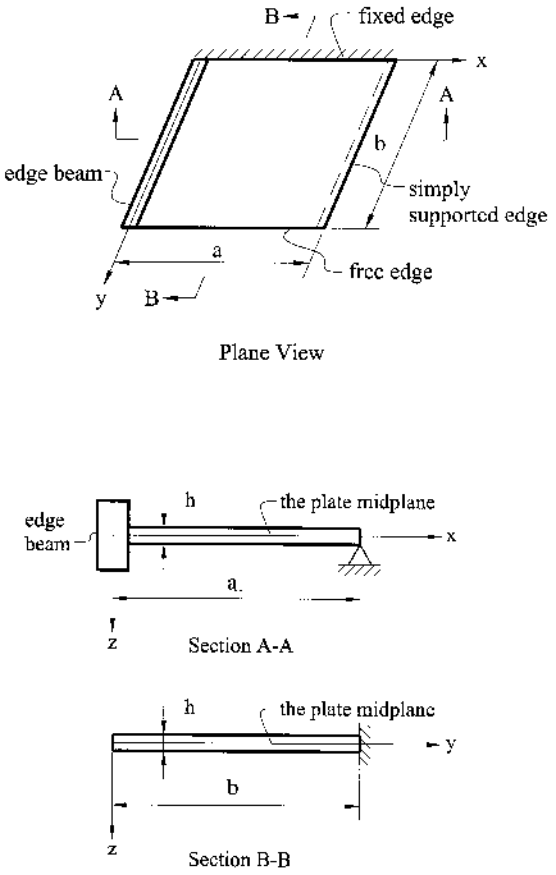

Fig. 2.6

$$M_y = 0\big|_{y=b},\ \ Q_y = 0\big|_{y=b},\ \ M_{yx} = 0\big|_{y=b} \tag{2.36}$$

and this gives three boundary conditions. These conditions were formulated by Poisson.

It has been mentioned earlier that three boundary conditions are too many to be accommodated in the governing differential equation (2.24). Kirchhoff suggested the following way to overcome this difficulty. He showed that conditions imposed on the twisting moment and shear force are not independent for the presented small-deflection plate bending theory and may be reduced to one condition only. It should be noted that Lord Kelvin (Thomson) gave a physical explanation of this reduction [4].

Figure 2.7a shows two adjacent elements, each of length $\mathrm{d}x$ belonging to the edge $y = b$. It is seen that, a twisting moment $M_{yx}\mathrm{d}x$ acts on the left-hand element, while the right-hand element is subjected to $\left[M_{yx} + \left(\partial M_{yx}/\partial x\right)\mathrm{d}x\right]\mathrm{d}x$. These moments are resultant couples produced by a system of horizontal shear stresses τ_{yx}. Replace them by couples of vertical forces M_{yx} and $M_{yx} + \frac{\partial M_{yx}}{\partial x}\mathrm{d}x$ with the

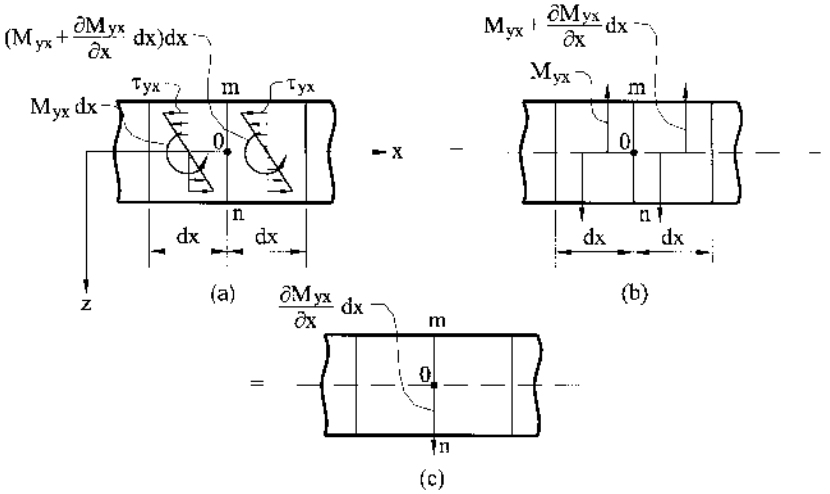

Fig. 2.7

moment arm dx having the same moment (Fig. 2.7b), i.e., as if rotating the above-mentioned couples of horizontal forces through 90°.

Such statically equivalent replacement of couples of horizontal forces by couples of vertical forces is well tolerable in the context of Kirchhoff's plate bending theory. Indeed, small elements to which they are applied can be considered as absolutely rigid bodies (owing to assumption (4)). It is known that the above-mentioned replacement is quite legal for such a body because it does not disturb the equilibrium conditions, and any moment may be considered as a free vector.

Forces M_{yx} and $M_{yx}+\frac{\partial M_{yx}}{\partial x}\mathrm{d}x$ act along the line mn (Fig. 2.7b) in opposite directions. Having done this for all elements of the edge $y=b$ we see that at the boundaries of two neighboring elements a single unbalanced force $(\partial M_{yx}/\partial x)\mathrm{d}x$ is applied at points of the middle plane (Fig. 2.7c).

Thus, we have established that the twisting moment M_{yx} is statically equivalent to a distributed shear force of an intensity $\partial M_{yx}/\partial x$ along the edge $y=b$, for a smooth boundary. Proceeding from this, Kirchhoff proposed that the three boundary conditions at the free edge be combined into two by equating to zero the bending moment M_y and the so-called *effective shear force* per unit length V_y. The latter is equal to the sum of the shear force Q_y plus an unbalanced force $\partial M_{yx}/\partial x$, which reflects the influence of the twisting moment M_{yx} (for the edge $y=b$). Now we arrive at the following two conditions at the free edge:

$$M_y = 0\big|_{y=b},\quad V_y = 0\big|_{y=b} \tag{2.37}$$

where

$$V_y = Q_y + \frac{\partial M_{xy}}{\partial x}. \tag{2.38}$$

The effective shear force V_y can be expressed in terms of the deflection w using Eqs (2.13) and (2.27). As a result, we obtain

$$V_y = -D\frac{\partial}{\partial y}\left[\frac{\partial^2 w}{\partial y^2} + (2-\nu)\frac{\partial^2 w}{\partial x^2}\right]. \tag{2.39a}$$

In a similar manner, we can obtain the effective shear force at the edge parallel to the x axis, i.e.,

$$V_x = -D\frac{\partial}{\partial x}\left[\frac{\partial^2 w}{\partial x^2} + (2-\nu)\frac{\partial^2 w}{\partial y^2}\right] \tag{2.39b}$$

Finally, the boundary conditions (2.37) may be rewritten in terms of the deflection as follows

$$\frac{\partial^2 w}{\partial y^2} + \nu\frac{\partial^2 w}{\partial x^2} = 0\Big|_{y=b} \quad \text{and} \quad -\frac{\partial}{\partial y}\left[\frac{\partial^2 w}{\partial y^2} + (2-\nu)\frac{\partial^2 w}{\partial x^2}\right] = 0\Big|_{y=b}. \tag{2.40}$$

Similarly, the boundary conditions for the free edge parallel to the x axis can be formulated. This form of the boundary conditions for a free edge is conventional.

It should be noted that transforming the twisting moments – as it was mentioned above – we obtain not only continuously distributed edge forces V_x and V_y but, in addition, also nonvanishing, finite concentrated forces at corner points (on each side of a corner) of a rectangular plate. These are numerically equal to the value of the corresponding twisting moment (Fig. 2.8). The direction and the total magnitude of the corner forces can be established by analyzing boundary conditions of a plate and the deflection surface produced by a given loading.

The concept of the corner forces is not limited to the intersection of two free boundaries, where they obviously must vanish. In general, any right angle corner where at least one of the intersecting boundaries can develop M_{xy} and M_{yx} will have a corner force. Consider, as an example, the case of symmetrically loaded, simply supported rectangular plate, as shown in Fig. 2.9.

At the corners, $x = a$ and $y = b$, the above-discussed action of the twisting moments (because $M_{xy} = M_{yx}$) results in

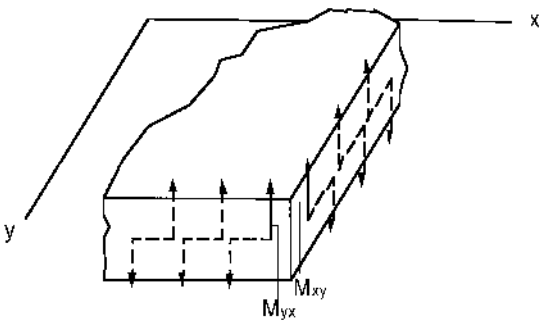

Fig. 2.8

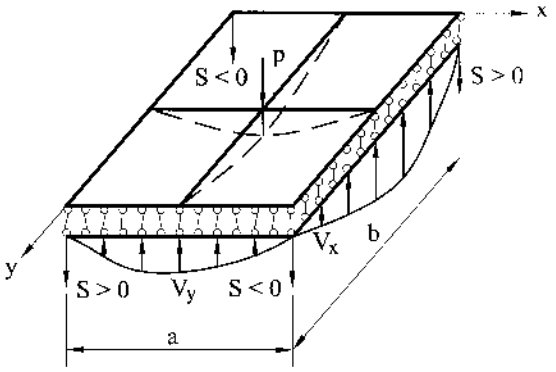

Fig. 2.9

$$S = 2M_{xy} = -2D(1-\nu)\left.\frac{\partial^2 w}{\partial x \partial y}\right|_{x=a,y=b}. \tag{2.41}$$

Thus, the distributed twisting moments are statically equivalent to the distributed edge forces $\partial M_{yx}/\partial x$ and $\partial M_{xy}/\partial y$ over the plate boundary, as well as to the concentrated corner forces, $S = 2M_{xy}$ for a given rectangular plate. Note that the directions of the concentrated corner forces, S, are shown in Fig. 2.9 for a symmetrical downward directed loading of the plate. At the origin of the coordinate system, taking into account the nature of torsion of an adjacent element, we obtain for the moment M_{xy} and, consequently, for the force S, the minus sign. If we rotate the twisting moment $M_{xy} < 0$ through 90°, then we obtain at this corner point $(x = 0,\ y = 0)$ a downward force $S = 2M_{xy}$. At other corner points the signs of M_{xy} will alternate, but the above-mentioned corner forces will be directed downward everywhere for a symmetrical loading of a plate.

The concentrated corner force for plates having various boundary conditions may be determined similarly. In general, any right angle corner where at least one of the intersecting boundaries can develop M_{xy} or M_{yx} will have a corner force. For instance, when two adjacent plate edges are *fixed* or *free,* we have $S = 0$, since along these edges no twisting moments exist. If one edge of a plate is fixed and another one (perpendicular to the fixed edge) is simply supported, then $S = M_{xy}$. The case of non-right angle intersections will be examined later.

It is quite valid to utilize the above replacement of the shear force Q_y and twisting moment M_{xy} by the effective shear force V_y in the context of the approximate Kirchhoff's theory of plate bending, as it was mentioned earlier. But with respect to a real plate, equating of the effective shear force to zero does not mean that both the shear force and twisting moment are necessarily equal to zero. Hence, according to Kirchhoff's theory, we obtain such a solution when along a free edge, e.g., $y = \text{const}$, some system of shear stresses τ_{yz} (corresponding to Q_y) and τ_{yx} (corresponding to M_{yx}) is applied (of course, such a system of stresses and corresponding to them the stress resultants and stress couples appear on this free edge). This system is mutually balanced on the edge $y = \text{const}$ and it causes an additional stress field. The latter, however, due

to Saint-Venant's principle, decays rapidly as we move away from this edge into the interior of the plate. The above-mentioned additional stress field cannot be determined by using the governing differential equation (2.24). Corrections can be obtained using the plate bending equations with regard to the shear strains γ_{xz} and γ_{yz} and will be discussed in Sec. 7.3. These corrections, as a rule, are negligible for solid isotropic plates.

(4) *Edge $x = 0$ supported by a beam*

The boundary conditions of the type (2.33), (2.35), and (2.37) are called *homogeneous* boundary conditions. *Nonhomogeneous* boundary conditions are commonly used in many important engineering structures – for example, when a plate is supported by an edge beam.

Assume that the cross section of the edge beam is symmetrical with respect to the middle surface of the plate and the edge beam has flexural and torsional rigidities. Since the edge beam and the plate are built monotonically (Fig. 2.10), they must have the same displacements and slopes.

$$w_{\mathrm{b}} = w\big|_{x=0} \quad \text{and} \quad \vartheta_{\mathrm{b}} = \vartheta\big|_{x=0} \quad \text{or} \quad \left(\frac{\partial \mathrm{w}}{\partial \mathrm{x}}\right)_{\mathrm{b}} = \left.\frac{\partial w}{\partial x}\right|_{x=0}, \tag{2.42}$$

where the subscript b refers to the edge beam, and quantities relating to the plate have no subscripts.

Consider an element dy of the edge beam as a free body, as shown in Fig. 2.10. Equilibrium conditions of this element result in the following equations:

$$\sum F_z = 0: -Q_{\mathrm{b}} - V_x \mathrm{d}y + Q_{\mathrm{b}} + \frac{\mathrm{d}Q_{\mathrm{b}}}{\mathrm{d}y}\mathrm{d}y = 0$$

$$\sum M_y = 0: +T + M_x \mathrm{d}y - \left(T + \frac{\mathrm{d}T}{\mathrm{d}y}\mathrm{d}y\right) = 0 \quad \text{or}$$

$$V_x = \frac{\mathrm{d}Q_{\mathrm{b}}}{\mathrm{d}y}(0, y), \quad M_x = \frac{\mathrm{d}T}{\mathrm{d}y}(0, y) \tag{a}$$

where T is the twisting moment in the beam.

As it follows from the beam theory [5]

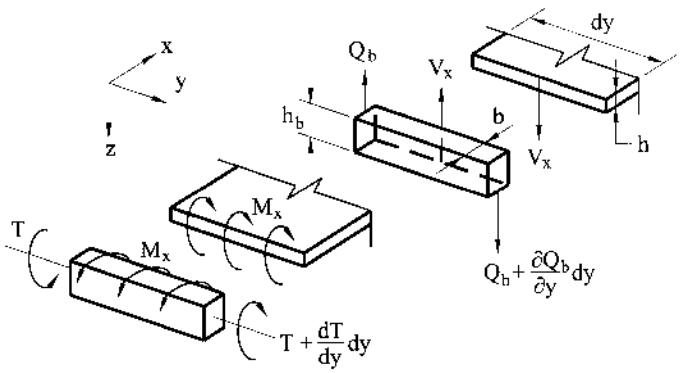

Fig. 2.10

$$\frac{dQ_b}{dy}(0,y) = -(EI)_b \frac{\partial^4 w_b}{\partial y^4}(0,y) \quad \text{and} \tag{b}$$

$$T(0,y) = -(GJ)_b \frac{d\vartheta_b}{dy}(0,y) = -(GJ)_b \frac{\partial^2 w_b}{\partial x \partial y}(0,y), \tag{c}$$

where $(EI)_b$ and $(GJ)_b$ are the flexural rigidity and the torsional stiffness of the beam cross section, respectively.

Substituting (b) and (c) into Eq. (a) and taking into account the compatibility conditions (2.42), gives the boundary conditions for the plate edge $x = 0$ supported by the beam:

$$V_x = -(EI)_b \left.\frac{\partial^4 w_b}{\partial y^4}\right|_{x=0}; \quad M_x = -(GJ)_b \left.\frac{\partial^3 w_b}{\partial x \partial y^2}\right|_{x=0} \tag{2.43a}$$

Using the expressions for M_x and V_x, Eqs. (2.13), (2.39b), and Eqs (2.42), we can rewrite the boundary conditions (2.43a) in terms of w, as follows:

$$D\left[\frac{\partial^3 w}{\partial x^3} + (2-\nu)\frac{\partial^3 w}{\partial x \partial y^2}\right] = (EI)_b \left.\frac{\partial^4 w}{\partial y^4}\right|_{x=0}; \quad D\left[\frac{\partial^2 w}{\partial x^2} + \nu \frac{\partial^2 w}{\partial y^2}\right] = (GJ)_b \left.\frac{\partial^3 w}{\partial x \partial y^2}\right|_{x=0}. \tag{2.43b}$$

Similar expressions can be written for edges $y = 0,\ b$.

Let us study the boundary conditions on skew edges. Consider a vertical section of the plate whose normal n makes an angle α with the x axis (Fig. 2.11a). Take the origin of the Cartesian coordinate system n (outward normal to the edge) and t (tangent to the edge) at some point of the edge. In a general case, the normal bending M_n and twisting M_{nt} moments, as well the transverse shear force Q_n will act at this section. Figure 2.11b shows the state of stress of a layer of the plate with the coordinate $z > 0$. The above moments at any point of the skew edge are

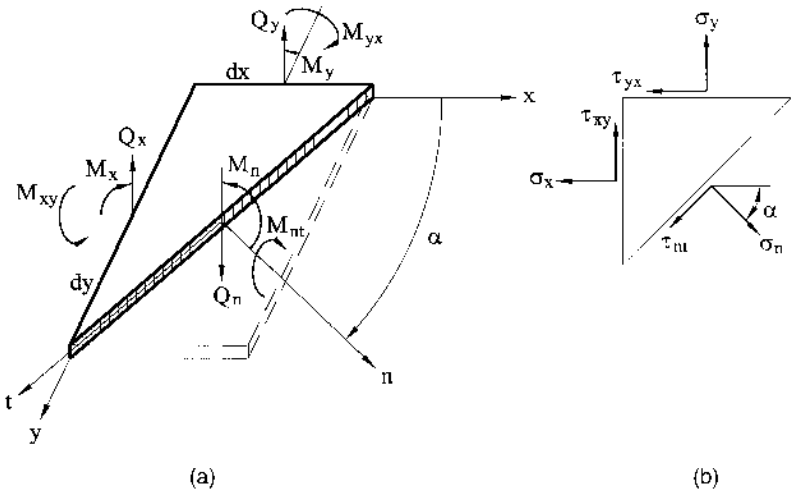

Fig. 2.11

$$M_n = \int_{-h/2}^{h/2} \sigma_n z \mathrm{d}z, \quad M_{nt} = \int_{-h/2}^{h/2} \tau_{nt} z \mathrm{d}z. \tag{2.44}$$

The relationship between the stress components shown in Fig. 2.11b is given by [6,7]

$$\sigma_n = \sigma_x \cos^2 \alpha + \sigma_y \sin^2 \alpha + 2\tau_{xy} \cos \alpha \sin \alpha;$$
$$\tau_{nt} = \tau_{xy} \cos 2\alpha - (\sigma_x - \sigma_y) \sin \alpha \cos \alpha.$$

Substituting the above into Eqs (2.44), integrating over the plate thickness and taking into account Eqs (2.11), one obtains the following relationships

$$\begin{aligned} M_n &= M_x \cos^2 \alpha + M_y \sin^2 \alpha + M_{xy} \sin 2\alpha; \\ M_{nt} &= M_{xy} \cos 2\alpha - (M_x - M_y) \sin \alpha \cos \alpha. \end{aligned} \tag{2.45}$$

The shear force Q_n acting at a section of the edge having a normal n can be evaluated from condition of equilibrium of the plate element shown in Fig. 2.11a, as follows:

$$\begin{aligned} Q_n \mathrm{d}s - Q_x \mathrm{d}y - Q_y \mathrm{d}x = 0, \text{ from which} \\ Q_n = Q_x \cos \alpha + Q_y \sin \alpha. \end{aligned} \tag{2.46}$$

The effective shear force at a point of the skew edge can be determined similarly to (2.38), i.e.,

$$V_n = Q_n + \frac{\partial M_{nt}}{\partial t}, \tag{2.47}$$

where $\partial/\partial t$ denotes a differentiation with respect to the tangent of the skew edge.

The boundary conditions discussed above for rectilinear edge can be generalized to some curvilinear edge. Let n and t be the outward normal making the angle α with the x axis and tangent to the curvilinear edge at a point of interest (Fig. 2.12). Then the prescribed boundary conditions (2.33), (2.35), and (2.37), taking into account (2.47), can be rewritten at an arbitrary point of the above curvilinear edge, as follows:

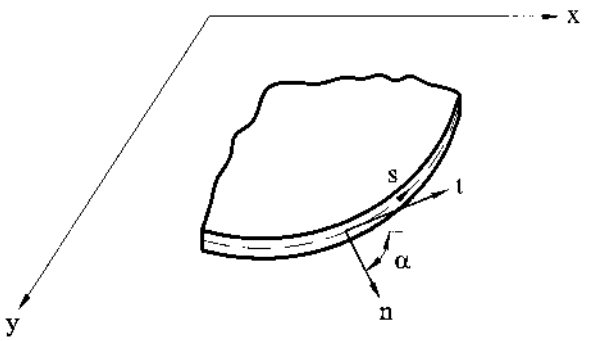

Fig. 2.12

(1) *Built-in curvilinear edge*

$$w = 0, \ \frac{\partial w}{\partial n} = 0. \tag{2.48a}$$

(2) *Simply supported edge*

$$w = 0, \ M_n = 0. \tag{2.48b}$$

(3) *Free curvilinear edge*

$$M_n = 0, V_n = Q_n + \frac{\partial M_{nt}}{\partial s} = 0. \tag{2.48c}$$

(4) *Curvilinear edge is elastically fixed*

$$w + \beta_1 V_n = 0, \frac{\partial w}{\partial n} + \beta_2 M_n = 0, \tag{2.48d}$$

where M_n and V_n are the normal bending moment and the normal effective shear force, respectively, defined by expressions (2.45) and (2.47). They can also be expressed in terms of the deflection w using Eqs (2.45)–(2.47) and Eqs (2.13) and (2.27). In Eqs (2.48) β_1 and β_2 are some coefficients that characterize a support compliance.

If adjacent edges of a plate have slopes of the normals α_1 and α_2 (Fig. 2.13), then the concentrated force S at a common corner point will be equal to

$$S = (M_{nt})_{\alpha_1} - (M_{nt})_{\alpha_2}. \tag{2.49}$$

When $\alpha_1 = 0$ *and* $\alpha_2 = \pi/2$ we will obtain the expression (2.41).

It is observed from the above that the boundary conditions are of the two basic kinds: *geometric* or *kinematic boundary conditions* describe edge constraint pertaining to deflection or slope; *static* or *natural boundary conditions* impose some restrictions on the internal forces and moments at the edges of the plate. Accordingly, in Eq. (2.48a) both conditions are kinematic; in Eq. (2.48c) they are both static; and in Eq. (2.48b) the boundary conditions are mixed.

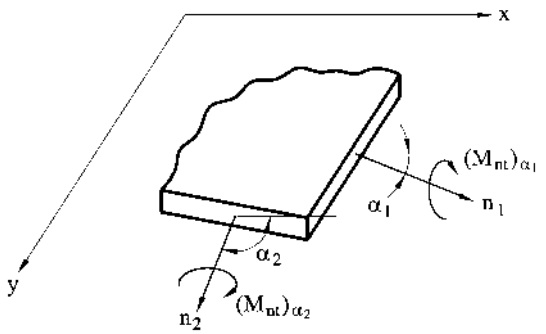

Fig. 2.13

2.6 VARIATIONAL FORMULATION OF PLATE BENDING PROBLEMS

It is known from the theory of elasticity that governing equations for stresses, strains, and displacements can be represented in the differential form. However, this is not a unique possible formulation of the problem for finding the stress–strain field of an elastic body. The problem of determining stresses, strains, and displacements can be reduced to some definite integral of one or another type of these functions called *functionals*. Then, the functions themselves (stresses, strains, and displacements) reflecting a real state of a body can be found from conditions of *extremum* for this functional. The mathematical techniques of such an approach is studied in the division of mathematics called the *calculus of variation*. Therefore, some postulates and statements that formulate properties of these functionals in the theory of elasticity are referred to as *variational principles*. The latter represent some basic theorems expressed in the form of integral equalities connecting stresses, strains, and displacements throughout the volume of a body and based on the properties of the work done by external and internal forces. A variety of powerful and efficient approximate methods for analysis of various linear and nonlinear problems of solid mechanics are based on the variational principles. Some of these methods will be described further in Chapter 6.

2.6.1 Strain energy of plates

A *functional* is a scalar quantity depending on some function or several functions, as from independent variables. The functional can be treated as a function of an infinite number of independent variables. The subject matter of the calculus of variation is searching of unknown functions $f_i(x, y, z)$ that give a maximum (minimum) or stationary value of a functional. For example,

$$\Pi = \int\int\int_V F\big[f_1(x,y,z), f_2(x,y,z), \ldots, f_n(x,y,z); f_1'(x,y,z), \ldots, f_n'(x,y,z); x, y, z\big]\mathrm{d}V.$$

The above-mentioned functions for which the functional is maximum (minimum) or stationary are referred to as *extremals* of the given functional [8–11].

Let us consider a functional expressing the total potential energy of a deformed elastic body and the loads acting on it. The total potential energy, Π, consists of the strain energy of deformation (the potential of internal forces), U, and the potential energy of external forces (the potential of external forces), Ω, i.e.,

$$\Pi = U + \Omega. \tag{2.50}$$

By convention, let us assume that the potential energy at the initial, undeformed state, Π_0, is zero. Hence, the total energy Π presents a variation of the energy of internal and external forces in the transition from initial to deformed states. The potential energy of a body is measured by the work done by external and internal forces when this body returns from its final to an initial position (where it was mentioned above, $\Pi_0 = 0$).

Our study is mainly limited to linearly elastic bodies that dissipate no energy and have only one equilibrium configuration. We also require that loads keep the

same orientation in space as they move. Such loads are called *conservative*. A mechanical system is called *conservative* if zero net work is done in carrying the system around any closed path: that is, in arbitrary changing a configuration and then restoring it. An extension of this study to nonlinear, or nonconservative, problems is possible.

First, let us set up an expression for the potential of the internal forces (strain energy of deformation). This potential is equal to the negative work of the internal forces, i.e., $U = -W_i$. Since the work done by the internal forces, W_i, is always negative (because displacements always occur in the opposite direction with respect to applied internal forces), the strain energy is positive.

The strain energy stored in an elastic body for a general state of stress is given by [6,7]

$$U = \frac{1}{2}\int\int\int_V \left(\sigma_x\varepsilon_x + \sigma_y\varepsilon_y + \sigma_z\varepsilon_z + \tau_{xy}\gamma_{xy} + \tau_{xz}\gamma_{xz} + \tau_{yz}\gamma_{yz}\right)\mathrm{d}V. \tag{2.51}$$

The integration extends over the entire body volume V. Based upon the assumptions of Kirchhoff's small-deflection plate bending theory, the stress components σ_z, τ_{xz}, and τ_{yz} may be omitted. Thus, introducing the generalized Hooke's law, the above expression reduces to the following form, involving only stresses and elastic constants,

$$U = \int\int\int_V \left[\frac{1}{2E}\left(\sigma_x^2 + \sigma_y^2 - 2\nu\sigma_x\sigma_y\right) + \frac{1+\nu}{E}\tau_{xy}^2\right]\mathrm{d}V. \tag{2.52}$$

Substituting for the stress components from Eq. (2.10) into Eq. (2.52) and integrating it over the thickness of the plate, we obtain

$$U = \frac{1}{2}\int\int_A D\left[\left(\frac{\partial^2 w}{\partial x^2}\right)^2 + \left(\frac{\partial^2 w}{\partial y^2}\right)^2 + 2\nu\frac{\partial^2 w}{\partial x^2}\frac{\partial^2 w}{\partial y^2} + 2(1-\nu)\left(\frac{\partial^2 w}{\partial x\partial y}\right)^2\right]\mathrm{d}A \tag{2.53}$$

or alternatively

$$U = \frac{1}{2}\int\int_A D\left\{\left(\frac{\partial^2 w}{\partial x^2} + \frac{\partial^2 w}{\partial y^2}\right)^2 - 2(1-\nu)\left[\frac{\partial^2 w}{\partial x^2}\frac{\partial^2 w}{\partial y^2} - \left(\frac{\partial^2 w}{\partial x\partial y}\right)^2\right]\right\}\mathrm{d}A \tag{2.54}$$

where A is the area of the plate middle surface.

We can also rewrite the expression (2.53) for the strain energy in terms of the bending and twisting moments, and the corresponding curvatures by the use of Eqs (2.13). As a result, for plates of a constant thickness the strain energy is

$$U = \frac{1}{2}\int\int_A \left(M_x\chi_x + M_y\chi_y + 2M_{xy}\chi_{xy}\right)\mathrm{d}A. \tag{2.55}$$

We observe from Eqs (2.53) and (2.54) that the strain energy is a nonlinear (quadratic) function of deformations. Hence, the principle of superposition is therefore not valid for the strain energy.

The expressions (2.53) and (2.54) are valid for plates of constant and variable thickness. It should be noted that the following integral

$$\iint_A \left[\frac{\partial^2 w}{\partial x^2} \frac{\partial^2 w}{\partial y^2} - \left(\frac{\partial^2 w}{\partial x \partial y} \right)^2 \right] \mathrm{d}A \tag{2.56}$$

entering in Eq (2.54) is equal to zero for fixed supports and for simply supported edges of plates, whose contour is traced by straight lines. This statement can be easily proven by transforming the integral (2.56) over the plate surface into the line integral over the plate boundary [3].

The potential of external forces, Ω, is defined as the work done by external forces through the corresponding displacements, assuming that these forces remain unchanged during the deformation. Further, when a positive displacement occurs, Ω decreases, so the potential of the external forces is always negative and may be evaluated as the product of these forces and the corresponding final displacement components. Determine the potential, Ω_p, of the distributed load $p(x, y)$ and concentrated P_i and M_j forces and moments applied to the middle surface of the plate as follows:

$$\Omega_\mathrm{p} = -\left[\iint_A p(x, y) w \mathrm{d}_A + \sum_i P_i w_i + \sum_j M_j \vartheta_j \right], \tag{2.57}$$

where w_i and ϑ_j are the deflection and the slope of the normal at the point of application of the ith force and jth moment in the plane of the action of this moment, respectively.

In the expression (2.57) the potential of edge loads, Ω_Γ, is not included. These loads have potentials only if compatible boundary displacements are permitted. In such cases, the potentials of the edge moments m_n, m_t and the transverse edge forces V_n can be expressed as

$$\Omega_\Gamma = -\oint_\Gamma \left(V_n w + m_n \frac{\partial w}{\partial n} + m_{nt} \frac{\partial w}{\partial t} \right) \mathrm{d}s, \tag{2.58}$$

where $\partial w/\partial n$ and $\partial w/\partial t$ are the derivatives of w with respect to the outward normal and the tangent directions, respectively, along the plate boundary to the boundary Γ.

The total potential of the external loads applied to the plate surface and to its boundary is

$$\Omega = \Omega_\mathrm{p} + \Omega_\Gamma, \tag{2.59}$$

where Ω_p and Ω_Γ are given by the expressions (2.57) and (2.58).

Using expressions (2.50), (2.54), (2.57) and (2.58), we can write the total potential energy of the plate in bending in the Cartesian coordinates as follows

$$\Pi = \frac{1}{2}\int\int_A D\left\{\left(\frac{\partial^2 w}{\partial x^2}+\frac{\partial^2 w}{\partial y^2}\right)^2 - 2(1-\nu)\left[\frac{\partial^2 w}{\partial x^2}\frac{\partial^2 w}{\partial y^2} - \left(\frac{\partial^2 w}{\partial x \partial y}\right)^2\right]\right\}\mathrm{d}A$$
$$- \left[\int\int_A p(x,y)w\mathrm{d}A + \sum_i P w_i + \sum_j M_j \vartheta_j + \right. \tag{2.60}$$
$$\left. \oint_\Gamma \left(\mathrm{V}_n w_n + m_n \frac{\partial w}{\partial n} + m_{nt}\frac{\partial w}{\partial t}\right)\mathrm{d}s\right],$$

or alternatively

$$\Pi = \frac{1}{2}\int\int_A \left(M_x \chi_x + M_y \chi_y + 2M_{xy}\chi_{xy}\right)\mathrm{d}A$$
$$- \left[\int\int_A p(x,y)w\mathrm{d}A + \sum_i P_i w_i + \sum_j M_j \vartheta_j + \right. \tag{2.61}$$
$$\left. \oint_\Gamma \left(\mathrm{V}_n w_n + m_n \frac{\partial w}{\partial n} + m_{nt}\frac{\partial w}{\partial t}\right)\mathrm{d}s\right].$$

As is seen from Eq. (2.58) that the value of the total potential energy of bending of plates is determined by an assignment of deflection w as a function of independent variables (x and y in the Cartesian coordinate system).

2.6.2 Variational principles

Let us consider some general concepts of the calculus of variation. *A variation* means an infinitesimal increment of a function for fixed values of its independent variables. The variation is designated by the symbol δ. The variational symbol δ may be treated as the differential operator d. The only difference between them lies in the fact that the symbol δ refers to some possible variations of a given function while the symbol d is associated with real variations of the same function. In what follows, only the following three operations are needed:

$$\frac{\mathrm{d}(\delta w)}{\mathrm{d}x} = \delta\left(\frac{\mathrm{d}w}{\mathrm{d}x}\right),\ \ \delta(w^2) = 2w(\delta w),\ \ \int(\delta w)\mathrm{d}x = \delta\int w\mathrm{d}x.$$

Consider an elastic body in equilibrium. This means that the body subjected to the maximum values of static (i.e., slowly piled-up) external forces has already reached its final state of deformation. Now we disturb this equilibrium condition by introducing small, arbitrary, but kinematically compatible, displacements. These displacements need not actually take place and need not be infinitesimal. Only one restriction is imposed on these displacements: they must be compatible with the support conditions (as discussed later, there are cases when satisfaction of geometric (or kinematic) boundary conditions is sufficient) and internal compatibility of the body. These displacements are called admissible *virtual*, because

they are imagined to take place (i.e., hypothetical), with the actual loads acting at their fixed values. The admissible virtual displacement produces an admissible configuration of the body. It follows from the above that virtual displacements cannot affect the equilibrium of the given system, when the full loads have been applied. Neither external loads nor internal forces and moments are altered by a virtual displacement [8–12, 14].

Now we can introduce the general variational principles of solid mechanics.

(a) The Principle of Conservation of Energy

This principle states that *the strain energy stored in an elastic body is equal to the work done by the applied external loads during the loading process, if we assume that there are no thermal or inertial effects*.

(b) The Principle of Virtual Work

The work done by actual forces through a virtual displacement of the actual configuration is called *virtual work*. It is assumed that during the virtual displacements all forces are held constant. The virtual work is designated by δW.

The principle of virtual work is formulated as follows:

> An elastic body is in equilibrium if and only if the total virtual work done by external and internal forces is zero for any admissible virtual displacements, i.e.,

$$\delta W = \delta W_{\mathrm{i}} + \delta W_{\mathrm{e}} = 0 \tag{2.62}$$

where δW_{i} and δW_{e} are the virtual works done by internal and external forces, respectively. As mentioned earlier, δW_{i} is negative. This principle was first proposed by J. Bernoulli in 1771. It can be interpreted as follows: if a body is in equilibrium then its resultant force and resultant couple are both zero; so, they produce no work.

(c) The Principle of Minimum Potential Energy

The principle of minimum potential energy may be looked upon as a specialization of the principle of virtual work (2.62). Indeed, the potential energy of the internal forces is equal to the negative work of the internal forces, i.e., $U = -W_{\mathrm{i}}$. On the other hand, $W_{\mathrm{e}} = -\Omega$. Therefore, we can write the equality (2.62), as follows:

$$\delta W = -\delta U - \delta\Omega = 0, \tag{2.63}$$

where $\delta U + \delta\Omega = \delta(U + \Omega) = \delta\Pi$ (because δ can be treated as a differential of a function) and $\delta\Pi$ is the variation in the total potential energy due to introducing compatible virtual displacements and is given by Eq. (2.60) or Eq. (2.61). Finally, the equality (2.63) can be written as

$$\delta\Pi = 0. \tag{2.64}$$

This equality expresses the principle of minimum potential energy proposed by Lagrange.

From calculus, an equality $\mathrm{d}f = 0$ means that the function f has an extremum (or a value corresponding to a point of inflection). It can be shown [9,10] that a variation of the total potential energy during any admissible virtual displacement (variation of the displacement) is positive for any stable configuration of equili-

brium. Hence, in this case, the total potential energy of a given system has a minimum. From the uniqueness theorem [6,7], the problem of the theory of elasticity, based on assumptions of small displacements and deformations defines only one equilibrium configuration, and this configuration of equilibrium is stable. Thus, if the small-deflection theory of an elastic body is being studied, then *the potential energy is a minimum in an equilibrium state*. So, the principle of minimum potential energy, proposed by Lagrange, can be formulated, as follows:

> Among all admissible configurations of an elastic body, the actual configuration (that satisfies static equilibrium conditions) makes the total potential energy, Π, stationary with respect to all small admissible virtual displacements. For stable equilibrium, Π is a minimum.

Notice that the above principle applies to a conservative system only.

It can be shown that the governing differential equation (2.24) and the boundary conditions (2.48) can be deduced from Lagrange's variational principle (2.64) [3,8–12]. However, the key importance of the variational principles discussed above is that they can be used to obtain approximate solutions of complicated problems of solid mechanics, in particular, plate-shell bending problems. These are obtained while avoiding mathematical difficulties associated with integration of differential equations in partial derivatives. The corresponding methods, called *variational methods* and based on the above-mentioned principles, are discussed further in Chapter 6. More complete information on the variational principles and their application in mechanics is available in the literature [8–12].

PROBLEMS

2.1 Verify the result given by Eq. (2.18).

2.2 Derive the governing differential equation for deflections of a plate subjected to a distributed moment load $m_x(x, y)$ and $m_y(x, y)$ applied to the middle surface.

2.3 Show that at the corner of a polygonal simply supported plate, $M_{xy} = 0$ unless the corner is 90°.

2.4 If a lateral deflection w is a known function of x and y, what are the maximum slope $\partial w/\partial n$ and the direction of axis n with respect to the x axis in terms of $\partial w/\partial x$ and $\partial w/\partial y$?

2.5 Show that the sum of bending curvatures in any two mutually perpendicular directions, n and t, at any point of the middle surface, is a constant, i.e.,

$$\chi_x + \chi_y = \chi_n + \chi_t = \text{const.}$$

2.6 Verify the expression given by Eq. (2.61).

2.7 Derive the expressions for the boundary quantities M_n, M_{nt}, and V_n in terms of the deflection w at a regular (smooth) point of the curvilinear contour of the plate using: (a) the local coordinates n and t where the coordinate n coincides with the direction of the outward normal and $\mathbf{t}$ – with the tangent direction to the boundary; (b) the intrinsic coordinates n and s, where s, is the arc length over the boundary.
Hint: use the following relations for part (b)

$$\frac{\partial \mathbf{n}}{\partial s} = \frac{1}{\rho}\mathbf{t}, \quad \frac{\partial \mathbf{t}}{\partial s} = -\frac{1}{\rho}\mathbf{n}$$

where $\mathbf{n}$ and $\mathbf{t}$ are the unit vectors of the intrinsic coordinate system directed along the outward normal and tangent to the boundary, respectively.

2.8 Derive Eq. (2.24) directly from the third equation of (1.10) by using the relations (2.16) and (2.17).

2.9 Assume that shear stresses in the plate are distributed according to the parabolic law for $-h/2 \leq z \leq h/2$. Show that when the expression $\tau_{xz} = \left(6Q_x/h^3\right)\left[(h/2)^2 - z^2\right]$ is substituted into the first relation (2.12) an identity is obtained.

2.10 Prove that the integral (2.56) is equal to zero for fixed supports and for simply supported edges.

REFERENCES

1. Webster, A.G., *Partial Differential Equations of Mathematical Physics*, Dover, New York, 1955.
2. Sommerfeld, A., *Partial Differential Equations in Physics*, Academic Press, New York, 1948.
3. Timoshenko, S.P. and Woinowsky-Krieger, S., *Theory of Plates and Shells,* 2nd edn, McGraw-Hill, New York, 1959.
4. Thomson, W. and Tait, P.G., *Treatise on Natural Philosophy*, Cambridge University Press, Cambridge, 1890.
5. Timoshenko, S.P., *Strength of Materials*, 3rd edn, Van Nostrand Company, New York, 1956.
6. Timoshenko, S.P. and Goodier, J.N., *Theory of Elasticity*, 3rd edn, McGraw-Hill, New York, 1970.
7. Prescott, J.J., *Applied Elasticity,* Dover, New York, 1946.
8. Forray, M.J., *Variational Calculus in Science and Engineering*, McGraw-Hill, New York, 1968.
9. Lanczos, C., *The Variational Principles of Mechanics*, The University of Toronto Press, Toronto, 1964.
10. Hoff, H.I., *The Analysis of Structures Based on the Minimal Principles and Principle of Virtual Displacements*, John Wiley and Sons, New York, 1956.
11. Reddy, J.N., *Energy and Variational Methods in Applied Mechanics*, John Wiley and Sons, New York, 1984.
12. Washizy, K., *Variational Methods in Elasticity and Plasticity*, 3rd edn, Pergamon Press, New York, 1982.

FURTHER READING

Gould, P.L., *Analysis of Shells and Plates*, Springer-Verlag, New York, Berlin, 1988.

Heins, C.P., *Applied Plate Theory for the Engineer*, Lexington Books, Lexington, Massachusetts, 1976.

McFarland, D.E., Smith, B.L. and Bernhart, W.D., *Analysis of Plates*, Spartan Books, New York, 1972.

Mansfield, E.H., *The Bending and Stretching of Plates,* Macmillan, New York, 1964.

Szilard, R., *Theory and Analysis of Plates*, Prentice-Hall, Inc., Englewood Cliffs, New York, 1974.

Ugural, A.C., *Stresses in Plates and Shells*, McGraw-Hill, New York, 1981.

Vinson, J.R., *The Behavior of Plates and Shells,* John Wiley and Sons, New York, 1974.

3

Rectangular Plates

3.1 INTRODUCTION

We begin the application of the developed plate bending theory with thin rectangular plates. These plates represent an excellent model for development and as a check of various methods for solving the governing differential equation (2.24).

In this chapter we consider some mathematically "exact" solutions in the form of double and single trigonometric series applied to rectangular plates with various types of supports and transverse loads, plates on an elastic foundation, continuous plates, etc.

3.2 THE ELEMENTARY CASES OF PLATE BENDING

Let us consider some elementary examples of plate bending of great importance for understanding how a plate resists the applied loads in bending. In addition, these elementary examples enable one to obtain closed-form solutions of the governing differential equation (2.24).

3.2.1 Cylindrical bending of a plate

Consider an infinitely long plate in the y axis direction. Assume that the plate is subjected to a transverse load which is a function of the variable x only, i.e., $p = p(x)$ (Fig. 3.1a). In this case all the strips of a unit width parallel to the x axis and isolated from the plate will bend identically. The plate as a whole is found to be bent over the cylindrical surface $w = w(x)$. Setting all the derivatives with respect to y equal zero in Eq. (2.24), we obtain the following equation for the deflection:

$$\frac{d^4 w}{dx^4} = \frac{p(x)}{D}. \tag{3.1}$$

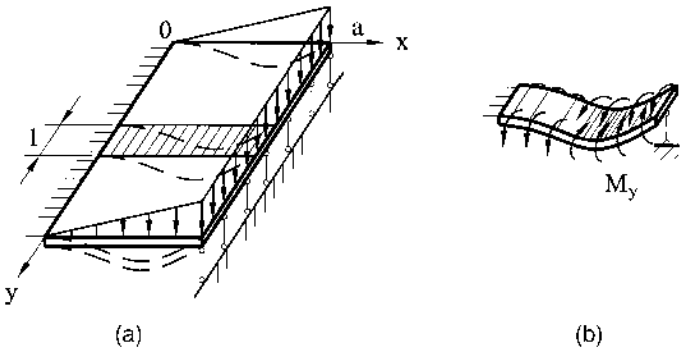

Fig. 3.1

We have applied here the ordinary derivative notation since w depends now only on the variable x. Equation (3.1) describes a *cylindrical bending of thin plates*. It is seen that this equation coincides with the corresponding equation of bending of a beam if we replace the flexural rigidity of the beam, EI, by the flexural rigidity of a plate, D. Since $D > EI$, the strip of the unit width within the plate (it is cross-hatched in Fig. 3.1a) is always stiffer than an isolated beam having the same span and thickness.

An integration of Eq. (3.1) should present no problems. Let, for example, $p = p_0 \frac{x}{a}$, then the general solution of Eq. (3.1) is of the following form:

$$w = w_{\mathrm{h}} + w_{\mathrm{p}} = C_1 + C_2 x + C_3 x^2 + C_4 x^3 + \frac{p_0 x^5}{120aD}, \tag{3.2}$$

where w_{h} is a solution of homogeneous equation (3.1) and w_p is a particular solution depending on the right-hand side of Eq. (3.1), i.e., on a given type of the applied loading.

The boundary conditions for the plate-strip can be written as follows (Fig. 3.1a)

$$w = 0|_{x=0}, \frac{\mathrm{d}w}{\mathrm{d}x} = 0\Big|_{x=0} \quad \text{and} \quad w = 0|_{x=a}, M_x = -D\frac{\mathrm{d}^2 w}{\mathrm{d}x^2} = 0\Big|_{x=a}. \tag{3.3}$$

The constants of integration C_i $(i = 1, 2, 3, 4)$ can be evaluated from the boundary conditions (3.3). Substituting for w from (3.2) into (3.3), we obtain the following:

$$C_1 = C_2 = 0, C_3 = \frac{7p_0 a^2}{240D}, \quad C_4 = \frac{9p_0 a}{240D}.$$

Substituting the above into Eq. (3.2), yields Eq. (3.4), as shown below:

$$w = \frac{p_0 a^4}{240D}\left(7\frac{x^2}{a^2} - 9\frac{x^3}{a^3} + 2\frac{x^5}{a^5}\right) \tag{3.4}$$

This is the equation for the deflection of the plate in cylindrical bending.

The bending moments M_x and M_y may be obtained from Eqs (2.13) making all the derivatives of w with respect to y equal zero, i.e.,

$$M_x = -D\frac{d^2w}{dx^2}, \quad M_y = -\nu D\frac{d^2w}{dx^2} = \nu M_x, \quad M_{xy} = 0. \tag{3.5}$$

Substituting Eq. (3.4) into Eq. (3.5), we obtain

$$M_x = -\frac{p_0 a^2}{120}\left(7 - 27\frac{x}{a} + 20\frac{x^3}{a^3}\right). \tag{3.6}$$

The moment $M_y = \nu M_x$ is proportional to M_x.

A cylindrical bending of a plate with a finite size in the y direction is possible only if the moment M_y will be applied to edges that are parallel to the x axis, as shown for the strip isolated from an infinite plate of Fig. 3.1b. In the absence of these moments, the surface of deflections will deviate from the cylindrical one over part of the length along the y axis.

3.2.2 Pure bending of plates

Consider a rectangular plate with a free boundary and assume that this plate is subjected to distributed bending moments over its edges $M_x = m_1 = \text{const}$ and $M_y = m_2 = \text{const}$ (Fig. 3.2). In this particular case, the governing differential equation (2.24) becomes

$$\frac{\partial^4 w}{\partial x^4} + 2\frac{\partial^4 w}{\partial x^2 \partial y^2} + \frac{\partial^4 w}{\partial y^4} = 0. \tag{3.7}$$

This equation will be satisfied if we make

$$w = 0.5\left(C_1 x^2 + C_2 y^2\right). \tag{3.8}$$

The constants of integration C_1 and C_2 may be evaluated from the following boundary conditions:

$$M_x = m_1 \quad \text{and} \quad M_y = m_2. \tag{3.9}$$

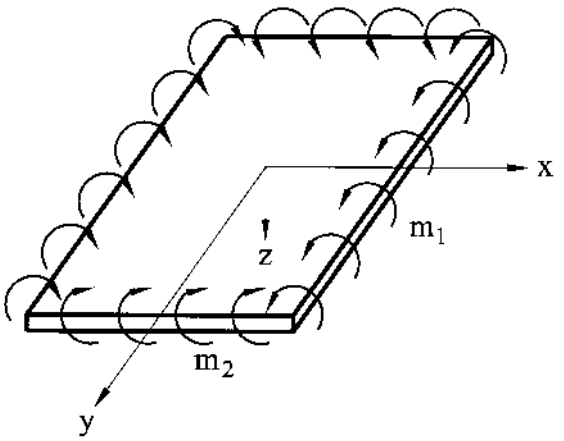

Fig. 3.2

Using Eqs (2.13), (3.8), and (3.9), we obtain

$$C_1 = \frac{\nu m_2 - m_1}{D(1-\nu^2)},\ C_2 = \frac{\nu m_1 - m_2}{D(1-\nu^2)}.$$

Substituting the above into Eq. (3.8) yields the deflection surface, as shown below:

$$w = \frac{1}{2D(1-\nu^2)}\left[(\nu m_2 - m_1)x^2 + (\nu m_1 - m_2)y^2\right] \tag{3.10}$$

Hence, in all sections of the plate parallel to the x and y axes, only the constant bending moments $M_x = m_1$ and $M_y = m_2$ will act. Other stress resultants and stress couples are zero, i.e.,

$$M_{xy} = Q_x = Q_y = 0.$$

This case of bending of plates may be referred to as a *pure bending*.

Let us consider some *particular cases of pure bending of plates*.

(a) Let $m_1 = m_2 = m$.

Then,

$$w = -\frac{m}{2D(1+\nu)}(x^2 + y^2). \tag{3.11}$$

This is an equation of the *elliptic paraboloid of revolution*. The curved plate in this case represents a part of a sphere because the radii of curvature are the same at all the planes and all the points of the plate.

(b) Let $m_1 = m, m_2 = 0$ (Fig. 3.3).

Then,

$$w = \frac{m}{2D(1-\nu^2)}\left(-x^2 + \nu y^2\right). \tag{3.12}$$

A surface described by this equation has a saddle shape and is called the *hyperbolic paraboloid of revolution* (Fig. 3.3). Horizontals of this surface are hyperbolas, asymptotes of which are given by the straight lines $\frac{x}{y} = \pm\sqrt{\nu}$. As is seen, due to the Poisson effect the plate bends not only in the plane of the applied bending moment $M_x = m_1 = m$ but it also has an opposite bending in the perpendicular plane.

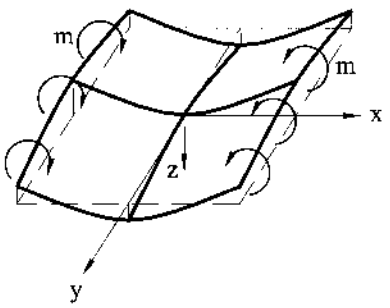

Fig. 3.3

(c) Let $m_1 = m, m_2 = -m$ (Fig. 3.4a).

Then

$$w = \frac{m}{2D(1-\nu)}(-x^2 + y^2). \tag{3.13}$$

This is an equation of an *hyperbolic paraboloid* with asymptotes inclined at 45° to the x and y axes.

Let us determine the moments M_n and M_{nt} from Eqs (2.45) in skew sections that are parallel to the asymptotes. Letting $\alpha = 45°$, we obtain

$$M_n = 0, \quad M_{nt} = -m.$$

Thus, a part of the plate isolated from the whole plate and equally inclined to the x and y axes will be loaded along its boundary by uniform twisting moments of intensity m. Hence, this part of the plate is subjected to *pure twisting* (Fig. 3.4b). Let us replace the twisting moments by the effective shear forces V_α, rotating these moments through 90° (see Sec. 2.4). Along the whole sides of the isolated part we obtain $V_\alpha = 0$, but at the corner points the concentrated forces $S = 2m$ are applied. Thus, for the model of Kirchhoff's plate, an application of self-balanced concentrated forces at corners of a rectangular plate produces a deformation of pure torsion because over the whole surface of the plate $M_{nt} = m = \text{const}$.

Remark

Since the plate described above in pure bending has no supports, its deflections have been determined with an accuracy of the displacements of an absolutely rigid body.

3.3 NAVIER'S METHOD (DOUBLE SERIES SOLUTION)

In 1820, Navier presented a paper to the French Academy of Sciences on the solution of bending of simply supported plates by double trigonometric series [1].

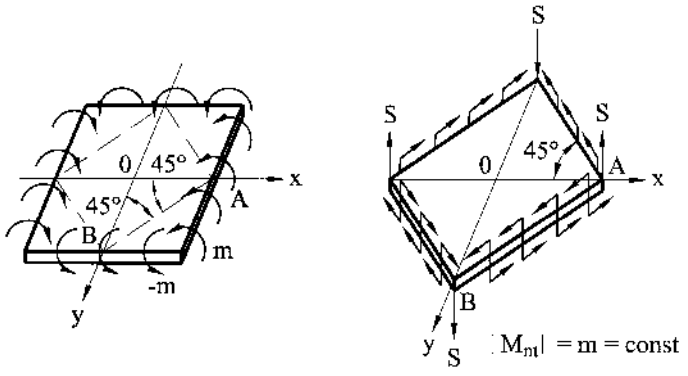

Fig. 3.4

Consider a rectangular plate of sides a and b, simply supported on all edges and subjected to a uniform load $p(x, y)$. The origin of the coordinates is placed at the upper left corner as shown in Fig. 3.5.

The boundary conditions for a simply supported plate are the following (see Eqs (2.35):

$$w = 0|_{x=0,a};\ \frac{\partial^2 w}{\partial x^2} = 0\Big|_{x=0,a} \quad \text{and} \quad w = 0|_{y=0,b};\ \frac{\partial^2 w}{\partial y^2} = 0\Big|_{y=0,b}. \tag{3.14}$$

In this case, the solution of the governing differential equation (2.24), i.e., the expressions of the deflection surface, $w(x, y)$, and the distributed surface load, $p(x, y)$, have to be sought in the form of an infinite Fourier series (see Appendix B), as follows:

$$w(x, y) = \sum_{m=1}^{\infty}\sum_{n-1}^{\infty} w_{mn} \sin\frac{m\pi x}{a}\sin\frac{n\pi y}{b}, \tag{3.15a}$$

$$p(x, y) = \sum_{m=1}^{\infty}\sum_{n=1}^{\infty} p_{mn} \sin\frac{m\pi x}{a}\sin\frac{n\pi y}{b}, \tag{3.15b}$$

where w_{mn} and p_{mn} represent coefficients to be determined. It can be easily verified that the expression for deflections (3.15a) automatically satisfies the prescribed boundary conditions (3.14).

Let us consider a general load configuration. To determine the Fourier coefficients p_{mn}, each side of Eq. (3.15b) is multiplied by $\sin\frac{l\pi x}{a}\sin\frac{k\pi y}{b}$ and integrated twice between the limits $0,a$ and $0,b$, as follows (see Appendix B):

$$\int_0^a\int_0^b p(x, y)\sin\frac{l\pi x}{a}\sin\frac{k\pi y}{b}\mathrm{d}x\mathrm{d}y = \sum_{m=1}^{\infty}\sum_{n=1}^{\infty} p_{mn}\int_0^a\int_0^b \sin\frac{m\pi x}{a}\sin\frac{n\pi y}{b}\sin\frac{l\pi x}{a}\sin\frac{k\pi y}{b}\mathrm{d}x\mathrm{d}y. \tag{a}$$

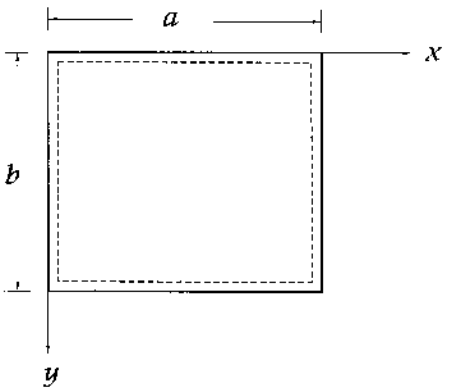

Fig. 3.5

It can be shown by direct integration that

$$\int_0^a \sin\frac{m\pi x}{a}\sin\frac{l\pi x}{a}\,\mathrm{d}x = \begin{cases} 0 \text{ ifm} \neq l \\ \\ a/2 \text{ if } m = l \end{cases}$$

$$\text{and } \int_0^b \sin\frac{n\pi y}{b}\sin\frac{k\pi y}{b}\,\mathrm{d}y = \begin{cases} 0 \text{ if } n \neq k \\ \\ b/2 \text{ if } n = k. \end{cases} \tag{3.16}$$

The coefficients of the double Fourier expansion are therefore the following:

$$p_{mn} = \frac{4}{ab}\int_0^a\int_0^b p(x,y)\sin\frac{m\pi x}{a}\sin\frac{n\pi y}{b}\,\mathrm{d}x\mathrm{d}y. \tag{3.17}$$

Since the representation of the deflection (3.15a) satisfies the boundary conditions (3.14), then the coefficients w_{mn} must satisfy Eq. (2.24). Substitution of Eqs (3.15) into Eq. (2.24) results in the following equation:

$$\sum_{m=1}^{\infty}\sum_{n=1}^{\infty}\left\{w_{mn}\left[\left(\frac{m\pi}{a}\right)^4 + 2\left(\frac{m\pi}{a}\right)^2\left(\frac{n\pi}{b}\right)^2 + \left(\frac{n\pi}{b}\right)^4\right] - \frac{p_{mn}}{D}\right\}\sin\frac{m\pi x}{a}\sin\frac{n\pi y}{b} = 0.$$

This equation must apply for all values of x and y. We conclude therefore that

$$w_{mn}\pi^4\left(\frac{m^2}{a^2}+\frac{n^2}{b^2}\right)^2 - \frac{p_{mn}}{D} = 0,$$

from which

$$w_{mn} = \frac{1}{\pi^4 D}\frac{p_{mn}}{\left[(m/a)^2 + (n/b)^2\right]^2}. \tag{3.18}$$

Substituting the above into Eq. (3.15a), one obtains the equation of the deflected surface, as follows:

$$w(x,y) = \frac{1}{\pi^4 D}\sum_{m=1}^{\infty}\sum_{n=1}^{\infty}\frac{p_{mn}}{\left[(m/a)^2 + (n/b)^2\right]^2}\sin\frac{m\pi x}{a}\sin\frac{n\pi y}{b}, \tag{3.19}$$

where p_{mn} is given by Eq. (3.17). It can be shown, by noting that $\left|\sin m\pi x/a\right| \leq 1$ and $|\sin n\pi y/b| \leq 1$ for every x and y and for every m and n, that the series (3.19) is convergent.

Substituting $w(x, y)$ into the Eqs (2.13) and (2.27), we can find the bending moments and the shear forces in the plate, and then using the expressions (2.15), determine the stress components. For the moments in the plate, for instance, we obtain the following:

$$M_x = \frac{1}{\pi^2}\sum_{m=1}^{\infty}\sum_{n=1}^{\infty} p_{mn}\frac{[(m/a)^2 + \nu(n/b)^2]}{[(m/a)^2 + (n/b)^2]^2}\sin\frac{m\pi x}{a}\sin\frac{n\pi y}{b},$$

$$M_y = \frac{1}{\pi^2}\sum_{m=1}^{\infty}\sum_{n=1}^{\infty} p_{mn}\frac{[(n/b)^2 + \nu(m/a)^2]}{[(m/a)^2 + (n/b)^2]^2}\sin\frac{m\pi x}{a}\sin\frac{n\pi y}{b}, \tag{3.20}$$

$$M_{xy} = -\frac{1_\nu}{\pi^2}\sum_{m=1}^{\infty}\sum_{n=1}^{\infty} p_{mn}\frac{mn}{ab[(m/a)^2 + (n/b)^2]^2}\cos\frac{m\pi x}{a}\cos\frac{n\pi y}{b}.$$

The infinite series solution for the deflection (3.19) generally converges quickly; thus, satisfactory accuracy can be obtained by considering only a few terms. Since the stress resultants and couples are obtained from the second and third derivatives of the deflection $w(x, y)$, the convergence of the infinite series expressions of the internal forces and moments is less rapid, especially in the vicinity of the plate edges. This slow convergence is also accompanied by some loss of accuracy in the process of calculation. The accuracy of solutions and the convergence of series expressions of stress resultants and couples can be improved by considering more terms in the expansions and by using a special technique for an improvement of the convergence of Fourier's series (see Appendix B and Ref. [2]).

Example 3.1

A rectangular plate of sides a and b is simply supported on all edges and subjected to a uniform pressure $p(x, y) = p_0$, as shown in Fig 3.5. Determine the maximum deflection, moments, and stresses.

Solution

The coefficients p_{mn} of the double Fourier expansion of the load are obtained from Eq. (3.17). Substituting $p(x, y) = p_0 = \text{const}$ and integrating, yields the following

$$p_{mn} = \frac{4p_0}{\pi^2 mn}(1 - \cos m\pi)(1 - \cos n\pi) \text{ or } p_{mn} = \frac{16p_0}{\pi^2 mn}(m, n = 1, 3, 5, \ldots). \tag{a}$$

It is observed that because $p_{mn} = 0$ for even values of m and n, these integers assume only for odd values.

Substituting for p_{mn} from (a) into Eqs (3.19) and (3.20), we can obtain the expressions for deflections and moments. We obtain the following:

$$w = \frac{16p_0}{D\pi^6}\sum_{m=1,3,\ldots}^{\infty}\sum_{n=1,3,\ldots}^{\infty}\frac{\sin\frac{m\pi x}{a}\sin\frac{n\pi y}{b}}{mn\left[(m/a)^2 + (n/b)^2\right]^2}, \tag{3.21a}$$

$$M_x = \frac{16p_0}{\pi^4}\sum_{m=1,3,\ldots}^{\infty}\sum_{n=1,3,\ldots}^{\infty}\frac{(m/a)^2 + \nu(n/b)^2}{mn\left[(m/a)^2 + (n/b)^2\right]^2}\sin\frac{m\pi x}{a}\sin\frac{n\pi y}{b}, \tag{3.21b}$$

$$M_y = \frac{16p_0}{\pi^4}\sum_{m=1,3,\ldots}^{\infty}\sum_{n=1,3,\ldots}^{\infty}\frac{\nu(m/a)^2 + (n/b)^2}{mn\left[(m/a)^2 + (n/b)^2\right]^2}\sin\frac{m\pi x}{a}\sin\frac{n\pi y}{b}, \tag{3.21c}$$

$$M_{xy} = -\frac{16(1-\nu)}{\pi^4 ab}\sum_{m}^{\infty}\sum_{n}^{\infty}\frac{1}{[(m/a)^2 + (n/b)^2]^2}\cos\frac{m\pi x}{a}\cos\frac{m\pi y}{b}. \tag{3.21d}$$

Based upon physical considerations and due to the symmetry of the plate and boundary conditions, the maximum deflection occurs at the center of the plate ($x = a/2,\ y = b/2$) and its value is shown next:

$$w_{\max} = \frac{16p_0}{\pi^6 D} \sum_{m=1,3,\ldots}^{\infty} \sum_{n=1,3,\ldots}^{\infty} \frac{(-1)^{\frac{m+n}{2}-1}}{mn\left[(m/a)^2 + (n/b)^2\right]^2}. \tag{b}$$

Here, $\sin m\pi/2$ and $\sin n\pi/2$ are replaced by $(-1)^{m-1/2}$ and $(-1)^{n-1/2}$, respectively. It can be observed that this series converges very rapidly, and the consideration of two terms gives an accuracy sufficient for all practical purposes. In particular, for the case of a square plate ($a = b$), we obtain

$$w_{\max} = \frac{16p_0a^4}{\pi^6 D}\left(\frac{1}{4} + \frac{1}{100} + \frac{1}{100} + \ldots\right) \approx \frac{4a^4p_0}{\pi^6 D} = 0.00416\frac{p_0a^4}{D},$$

or substituting for $D = \frac{Eh^3}{12(1-\nu^2)}$ and making $\nu = 0.3$, we obtain

$$w_{\max} \approx 0.0454\frac{p_0a^4}{Eh^3}.$$

The error of this result compared with an exact solution is about 2.5% [3].

It is observed that the series for the bending and twisting moments given by Eqs (3.21) do not converge as rapidly as that of the series for the deflections. The maximum bending moments, found at the center of the plate, are determined by applying Eqs (3.21b) and (3.21c). The first term of this series for a square plate for $\nu = 0.3$ yields

$$M_{x,\max} = M_{y,\max} = 0.0534p_0a^2. \tag{c}$$

The exact solution for the bending moments at the center of the square plate for $\nu = 0.3$ is the following [3]:

$$M_{x,\max} = M_{y,\max} = 0.0479p_0a^2. \tag{d}$$

The error of solution (c) is about 11.5 per;, and that is worse than that for the deflections.

The maximum normal stress at the center of the square plate produced by the moments of Eq. (d), by application of Eqs (2.15) is determined to be $\sigma_{x,\max} = \sigma_{y,\max} = 0.287\frac{p_0a^2}{h^2}$.

Let us study the essential characteristics of the transverse shear forces as applied to the simply supported rectangular plate of Example 3.1. To simplify our analysis, we use only a single harmonic approximation of a uniformly distributed loading and solution also. However, the general conclusions will be valid for any harmonic approximations of the solution. From Eq. (a), we compute the following for $m = n = 1$:

$$p_{11} = \frac{16p_0}{\pi^2} \quad \text{and} \quad p = \frac{16p_0}{\pi^2}\sin\frac{\pi x}{a}\sin\frac{\pi y}{b}.$$

Retaining also only one term in the series (a), we obtain the following expression for the deflection:

$$w = \frac{16p_0}{D\pi^6}\frac{\sin\dfrac{\pi x}{a}\sin\dfrac{\pi y}{b}}{\left(1/a^2+1/b^2\right)^2}. \tag{e}$$

The transverse shear forces, Q_x and Q_y, and effective shear forces, V_x and V_y, may be found by substituting for w from Eq. (e) into Eqs (2.27) and (2.39). We obtain

$$Q_x = \frac{16p_0}{\pi^3}\frac{\cos\dfrac{\pi x}{a}\sin\dfrac{\pi y}{b}}{a\left[(1/a)^2+(1/b)^2\right]}; \quad Q_y = \frac{16p_0}{\pi^3}\frac{\sin\dfrac{\pi x}{a}\cos\dfrac{\pi y}{b}}{b\left[(1/a)^2+(1/b)^2\right]}$$

$$V_x = \frac{16p_0}{\pi^3}\frac{\left[1/a^2+(2-\nu)1/b^2\right]}{a\left(1/a^2+1/b^2\right)^2}\cos\frac{\pi x}{a}\sin\frac{\pi y}{b}; \tag{f}$$

$$V_y = \frac{16p_0}{\pi^3}\frac{\left[(2-\nu)1/a^2+1/b^2\right]}{b\left(1/a^2+1/b^2\right)^2}\sin\frac{\pi x}{a}\cos\frac{\pi y}{b}$$

The resultant of the external distributed load carrying by the plate is

$$R_{\mathrm{p}} = \int_0^a\int_0^b p\,\mathrm{d}x\mathrm{d}y = \frac{16p_0}{\pi^2}\int_0^a\int_0^b \sin\frac{\pi x}{a}\sin\frac{\pi y}{b}\,\mathrm{d}x\mathrm{d}y \quad \text{or} \quad R_{\mathrm{p}} = \frac{64p_0}{\pi^4}ab. \tag{g}$$

which acts in the positive z direction (downward). Determine the resultant of the transverse effective shear forces, R_{V}, acting on the plate edges, as follows

$$R_{\mathrm{V}} = -\int_0^b\left[\left|V_x(0,y)\right|+\left|V_x(a,y)\right|\right]\mathrm{d}y - \int_0^a\left[\left|V_y(x,0)\right|+\left|V_y(x,b)\right|\right]\mathrm{d}x. \tag{h}$$

The negative sign on the right-hand side of Eq. (h) indicates that the resultant of the effective shear forces points in the negative z direction. Evaluating these integrals yields

$$R_{\mathrm{V}} = -\frac{64p_0}{\pi^4}\frac{ab}{\left(a^2+b^2\right)^2}\left[a^4+2(2-\nu)a^2b^2+b^4\right]. \tag{i}$$

Adding R_{p} and R_{V} given by Eqs (g) and (i), results in the following:

$$R_{\mathrm{p}} + R_{\mathrm{V}} = -128\frac{p_0(1-\nu)}{\pi^4}\frac{a^3b^3}{\left(a^2+b^2\right)^2} \tag{j}$$

as an apparently unbalanced force. However, we must include the corner forces given by Eqs (2.41) in the total equilibrium condition according to the classical plate theory. From Eq. (3.21d) for $m = n = 1$, we have the following

$$M_{xy} = -\frac{16(1-\nu)}{\pi^4 ab}\frac{\cos\dfrac{\pi x}{a}\cos\dfrac{\pi y}{b}}{\left(1/a^2+1/b^2\right)^2}. \tag{k}$$

As explained in Sec. 2.4, all the corner concentrated forces, S, for the simply supported rectangular plate that is subjected to a downward directed uniform load p_0, act downward also, i.e., in the positive z direction. Each such a force is given by Eq. (2.41), i.e.,

$$S = 2|M_{xy}| = 2\left[\frac{16(1-\nu)}{\pi^4 ab}\frac{a^3b^3}{\left(a^2+b^2\right)^2}\right].$$

Thus, a total force due to the corner forces acts in the positive z direction and is given by the following:

$$R_S = 4S = 128\frac{p_0(1-\nu)}{\pi^4}\frac{a^3b^3}{\left(a^2+b^2\right)^2}. \tag{l}$$

Now, adding Eqs (j) and (l), we get

$$R_p + R_V + R_S = 0.$$

The effective shear force distributions and concentrated corner forces are shown in Fig. 2.9. Thus, we have demonstrated the contribution of the corner forces to the overall equilibrium of the rectangular simply supported plate.

It is interesting to note that the boundary transverse shear forces, Q_x and Q_y, balance the external distributed load p_0. Indeed, let us compute the resultant R_Q of the shear forces on the boundary of the plate, as follows:

$$R_Q = -\int_0^b \left[|Q_x(0,y)| + |Q_x(a,y)|\right]dy - \int_0^a \left[|Q_y(x,0)| + |Q_y(x,b)|\right]dx.$$

Substituting for Q_x and Q_y from the first two equations (f) into the above, we obtain

$$R_Q = -\frac{64p_0}{\pi^4}ab, \tag{m}$$

where the negative sign indicates that R_Q points in the negative z direction, i.e., in the upward direction. Adding Eqs (g) and (m) results in

$$R_p + R_Q = 0.$$

However, following the logic of Kirchhoff's plate theory, the transverse shear force alone cannot be treated as the edge supporting reaction. Only the effective shear force may represent such a reaction. This result will also be discussed in detail later, in Sec. 7.3.

Example 3.2

A rectangular wall panel is taken to be simply supported on all edges and subjected to a patch load of intensity $p_0 = \text{const.}$ as shown in Fig. 3.6. Determine the deflected surface.

Solution

The constants of the Fourier expansion of the load are

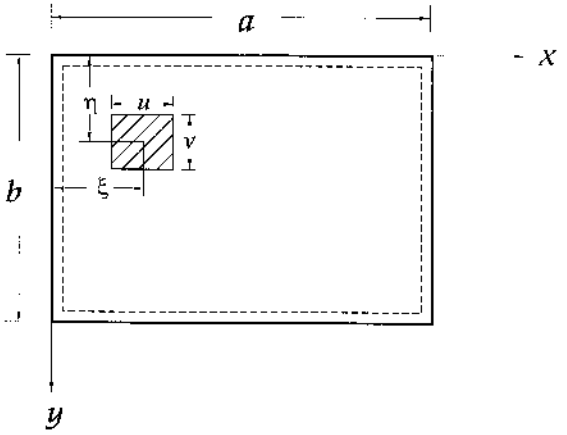

Fig. 3.6

$$p_{mn} = \frac{4p_0}{uv}\int_{\xi-u/2}^{\xi+u/2}\int_{\eta-v/2}^{\eta+v/2}\sin\frac{m\pi x}{a}\sin\frac{n\pi y}{b}\,\mathrm{d}x\mathrm{d}y$$
$$= \frac{16p_0}{\pi^2 mn}\sin\frac{m\pi\xi}{a}\sin\frac{n\pi\eta}{b}\sin\frac{m\pi u}{2a}\sin\frac{n\pi v}{2b}. \tag{3.22}$$

Inserting the above into Eqs (3.19), yields the double series expression of the following deflected surface

$$w(x,y) = \frac{16p_0}{\pi^6 D}\sum_{m=1}^{\infty}\sum_{n=1}^{\infty}\frac{\sin\frac{m\pi\xi}{a}\sin\frac{n\pi\eta}{b}\sin\frac{m\pi u}{2a}\sin\frac{n\pi v}{2b}\sin\frac{m\pi x}{a}\sin\frac{n\pi y}{b}}{mn\left[(m/a)^2+(n/b)^2\right]^2}. \tag{3.23}$$

The convergence of this solution is relatively fast if the dimensions u and v are not too small. The deflection can be obtained with sufficient accuracy by taking the first four terms of the series.

3.4 RECTANGULAR PLATES SUBJECTED TO A CONCENTRATED LATERAL FORCE *P*

Let us consider a rectangular plate simply supported on all edges of sides a and b and subjected to concentrated lateral force P applied at $x = \xi$ and $y = \eta$, as shown in Fig. 3.7.

Assume first that this force is uniformly distributed over the contact area of sides u and v (Fig. 3.6) i.e., its load intensity is defined as

$$p_0 = \frac{P}{uv}.$$

Substituting the above into Eq. (3.22), one obtains

$$p_{mn} = \frac{16P}{\pi^2 mnuv}\sin\frac{m\pi\xi}{a}\sin\frac{n\pi\eta}{b}\sin\frac{m\pi u}{2a}\sin\frac{n\pi v}{2b}. \tag{3.24}$$

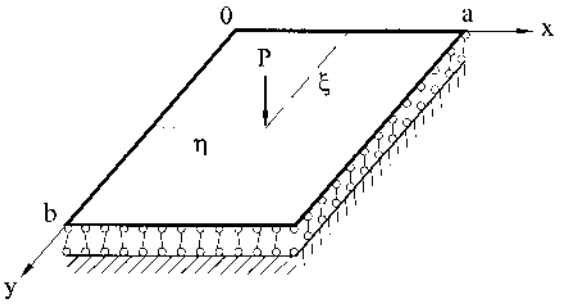

Fig. 3.7

Now we must let the contact area approach zero by permitting $u \to 0$ and $v \to 0$. In order to be able to use the limit approach first, Eq. (3.24) must be put in a more suitable form. For this purpose, the right-hand side is multiplied and divided by ab, giving the following:

$$p_{mn} = \lim_{u\to 0, v\to 0} \left[\frac{4P}{ab} \sin\frac{m\pi\xi}{a} \sin\frac{n\pi\eta}{b} \frac{\sin\dfrac{m\pi u}{2a} \sin\dfrac{n\pi v}{2b}}{(m\pi u/2a)(n\pi v/2b)} \right]. \tag{3.25}$$

Knowing that $\lim_{\alpha\to 0} \dfrac{\sin\alpha}{\alpha} = 1$, Eq. (3.25) becomes

$$p_{mn} = \frac{4P}{ab} \sin\frac{m\pi\xi}{a} \sin\frac{n\pi\eta}{b}, \tag{3.26}$$

and the deflection of the plate subjected to a concentrated force is obtained from Eq. (3.19), as follows:

$$w(x, y) = \frac{4P}{\pi^4 Dab} \sum_{m=1}^{\infty} \sum_{n=1}^{\infty} \frac{\sin\dfrac{m\pi\xi}{a} \sin\dfrac{n\pi\eta}{b}}{\left[(m/a)^2 + (n/b)^2\right]^2} \sin\frac{m\pi x}{a} \sin\frac{n\pi y}{b}. \tag{3.27}$$

The convergence of this series is fairly rapid. Let $\xi = a/2$ and $\eta = b/2$; then for even m and n, all the numbers p_{mn} are zero. For odd numbers, we derive the following from (3.27):

$$p_{mn} = \frac{4P}{ab} \sin\frac{m\pi}{2} \sin\frac{n\pi}{2}.$$

The deflected middle surface equation (3.27) in this case becomes

$$w(x, y) = \frac{4P}{\pi^4 Dab} \sum_{m=1,3,\ldots}^{\infty} \sum_{n=1,3,\ldots}^{\infty} \frac{\sin\dfrac{m\pi}{2} \sin\dfrac{n\pi}{2}}{\left[(m/a)^2 + (n/b)^2\right]} \sin\frac{m\pi x}{a} \sin\frac{n\pi y}{b}. \tag{3.28}$$

Furthermore, if the plate is square ($a = b$), the maximum deflection, which occurs at the center, is obtained from Eq. (3.28), as follows:

$$w_{\max} = \frac{4Pa^2}{\pi^4 D} \sum_{m=1,3,\ldots}^{\infty} \sum_{n=1,3,\ldots} \frac{1}{(m^2 + n^2)^2}.$$

Retaining the first nine terms of this series ($m = 1,\ n = 1, 3, 5;\ m = 3,\ n = 1, 3, 5;\ m = 5,\ n = 1, 3, 5$) we obtain

$$w_{\max} = \frac{4Pa^2}{\pi^4 D}\left[\frac{1}{4} + \frac{2}{100} + \frac{1}{324} + \frac{2}{625} + \frac{2}{1156} + \frac{1}{2500}\right] = 0.01142\frac{Pa^2}{D}.$$

The "exact" value is $w_{\max} = 0.01159\dfrac{Pa^2}{D}$ and the error is thus 1.5% [3].

This very simple Navier's solution, Eq. (3.28), converges sufficiently rapidly for calculating the deflections. However, it is unsuitable for calculating the bending moments and stresses because the series for the second derivatives $\partial^2 w/\partial x^2$ and $\partial^2 w/\partial y^2$ obtained by differentiating the series (3.28) converge extremely slowly. These series for bending moment, and consequently for stresses as well as for the shear forces, diverge directly at a point of application of a concentrated force, called a *singular point*. Thus, to calculate stress components in the vicinity of a concentrated force, it is necessary to use a more efficient technique, especially since the maximum stresses occur in the immediate vicinity of the singular point. Therefore, the problem of determining a correct stress distribution near such types of singular points is of practical interest.

We now consider one approach for determining the bending moment distribution near the above-mentioned singular point. Let us write the solution (3.27) in the form

$$w = \frac{4Pb^3}{\pi^4 a}\sum_{m=1}^{\infty} S_m \sin\frac{m\pi\xi}{a}\sin\frac{m\pi x}{a}, \tag{3.29a}$$

where

$$S_m = \frac{1}{2}\sum_{n=1}^{\infty}\frac{\cos\dfrac{n\pi}{b}(y-\eta) - \cos\dfrac{n\pi}{b}(y+\eta)}{\left(m^2b^2/a^2 + n^2\right)^2}. \tag{3.29b}$$

The series (3.29b) can be summed using the formula [4]:

$$\sum_{n=1}^{\infty}\frac{\cos nz}{(\alpha^2+n^2)^2} = -\frac{1}{2\alpha^4} + \frac{\pi}{4\alpha^3}\frac{\cosh\alpha(\pi-z)}{\sin\pi\alpha} - \frac{\pi(\pi-z)}{4\alpha^2} - \frac{\sinh\alpha(\pi-z)}{\sinh\pi\alpha} + \frac{\pi^2}{4\alpha^2}\frac{\cosh\alpha(\pi-z)\cosh\pi\alpha}{\sin h^2\pi\alpha}. \tag{a}$$

Using the above formula, we can represent the deflection surface (3.28) as

$$w(x,y) = \frac{Pa^2}{\pi^3 D}\sum_{m=1}^{\infty}\left(1 + \beta_m\coth\beta_m - \frac{\beta_m y_1}{b}\coth\frac{\beta_m y_1}{b} - \frac{\beta_m\eta}{b}\coth\frac{\beta_m\eta}{b}\right) \times \frac{\sinh\dfrac{\beta_m\eta}{b}\sin h\dfrac{\beta_m y_1}{b}\sin\dfrac{m\pi\xi}{a}\sin\dfrac{m\pi x}{a}}{m^3\sinh\beta_m}, \tag{3.30}$$

where $\beta_m = \frac{m\pi b}{a,}$ $y_1 = b - y$, and $y \geq \eta$. If $y < \eta$, then the values y_1 and η must be replaced by y and $\eta_1 = b - \eta$, respectively.

Let us use an infinitely long (in the y-direction) plate loaded by a concentrated force P applied at $x = \xi$ and $y = 0$, as shown in Fig. 3.8, to illustrate the above-

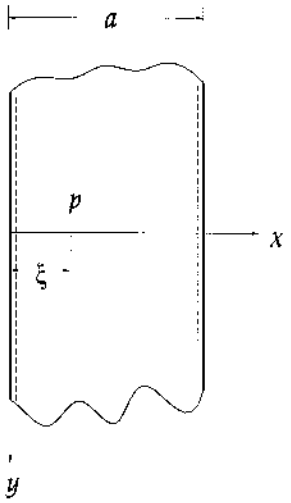

Fig. 3.8

mentioned approach. The deflection of such a plate-strip can be easily obtained from Eq. (3.30) by letting $b \to \infty$. Then, taking into account the following approximate equalities,

$$\begin{aligned}\tanh\alpha_m \approx 1, \cosh\alpha_m \approx \frac{1}{2}e^{\alpha_m}, \sinh\frac{\alpha_m}{b}(b-2y) \approx \cosh\frac{\alpha_m}{b}(b-2y)\\ \approx \frac{1}{2}e^{(\alpha_m/b)(b-2y)},\end{aligned} \tag{3.31}$$

we obtain the following expression for the deflection surface of the above-mentioned plate-strip:

$$w = \frac{Pa^2}{2\pi^3 D}\sum_{m=1}^{\infty}\frac{1}{m^3}\sin\frac{m\pi\xi}{a}\sin\frac{m\pi x}{a}\left(1+\frac{m\pi y}{a}\right)e^{-\frac{m\pi y}{a}}. \tag{3.32}$$

Differentiating the above expression twice in accordance with Eqs (2.13), we obtain the following expressions for the bending moments

$$M_x = \frac{P}{2\pi}\sum_{m=1}^{\infty}\frac{1}{m}\sin\frac{m\pi\xi}{a}\sin\frac{m\pi x}{a}\left[1+\nu+(1-\nu)\frac{m\pi y}{a}\right]e^{-\frac{m\pi y}{a}}, \tag{3.33a}$$

$$M_y = \frac{P}{2\pi}\sum_{m=1}^{\infty}\frac{1}{m}\sin\frac{m\pi\xi}{a}\sin\frac{m\pi x}{a}\left[1+\nu-(1-\nu)\frac{m\pi y}{a}\right]e^{-\frac{m\pi y}{a}}. \tag{3.33b}$$

Series in Eqs (3.33) can be summed up by using the formula [4]:

$$\sum_{m=1}^{\infty}\frac{1}{m}\sin\frac{m\pi x}{a}\sin\frac{m\pi\xi}{a}e^{-\frac{m\pi y}{a}} = \frac{1}{4\pi}\ln\frac{\cosh\frac{\pi y}{a}-\cosh\frac{\pi}{a}(x+\xi)}{\cosh\frac{\pi y}{a}-\cos\frac{\pi}{a}(x-\xi)}. \tag{3.34}$$

Let us present the equations for the bending and twisting moments for points that are in the immediate vicinity from the point of application of force P but necessarily lying on the x axis. In this case, the values $(x-\xi)$ and y are very small and the following approximate equalities hold:

$$\cos\frac{\pi(x-\xi)}{a} \approx 1 - \frac{\pi^2(x-\xi)^2}{2a^2}; \quad \cosh\frac{\pi y}{a} \approx 1 + \frac{\pi^2 y^2}{2a^2}. \tag{3.35}$$

Applying the expression (3.34) and the above approximate equalities to Eqs (3.33), we obtain the following equations for the bending moments:

$$\left.\begin{matrix} M_x \\ M_y \end{matrix}\right\} = \frac{P}{4\pi}\left\{(1+\nu)\ln\frac{2a\sin\dfrac{\pi\xi}{a}}{\pi r} \pm \frac{(1-\nu)y^2}{r^2}\right\}; \quad r^2 = (x-\xi)^2 + y^2. \tag{3.36}$$

As seen from Eqs (3.36), the bending moments and, consequently, shear forces are unbounded at $r = 0$, i.e., at a point where a concentrated force is applied. This is an evident reason of divergence of the Fourier series at the singular points. An occurrence of infinite stress resultants and stress couples can be physically explained. First, in reality there is no concentrated force. A load is always distributed over some finite area. It can be easily shown that a finite value of a concentrated force cannot balance the intensities of the shear forces and bending moments in the vicinity of a point of application of P. Indeed, let us cut from the square plate subjected to a center force P, a differential element of sides Δx and Δy surrounding this singular point (Fig. 3.9). Then, from a static equilibrium condition – namely, the force summation into the z direction is zero – we obtain

$$P - 2Q_x\Delta x - 2Q_y\Delta y = 0,$$

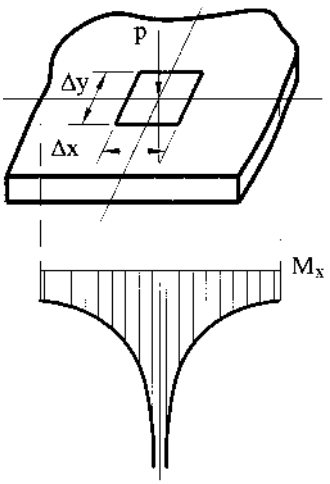

Fig. 3.9

or for square plates loaded by a centrally applied concentrated force, $Q_x = Q_y$ in the vicinity of the singular point, and for $\Delta x = \Delta y$, we have $Q_x = \frac{P}{4\Delta x}$. If $\Delta x \to 0$, the intensity of $Q_x \to \infty$.

Secondly, if a concentrated force P is replaced by a distributed load over a small area of radius c, surrounding a point of application of the above force, then it was shown that if $c < h$, the Kirchhoff hypotheses do not hold. A more accurate stress analysis in the vicinity of the above-mentioned loaded zone can be carried out with the use of three-dimensional (3D) elasticity theory (i.e., without Kirchhoff's assumptions). Such a rigorous treatment of stress distribution showed [3] that the classical plate bending theory based on Kirchhoff's assumptions determines stresses with sufficient high degree of accuracy if $c \geq 2h$. However, if $c < h$, then, near the loaded plate surface, the high local compressive vertical normal and transverse shear stresses occur. Both the above stresses were assumed to be negligible in the Kirchhoff plate theory.

Thus, the "defect" of the Kirchhoff theory can be removed if we replace a concentrated force by a distributed load over some small but finite area, say, over a circular region of radius c and $c \geq 2h$. It should also be noted that a replacement of a real load distributed over a small area by a concentrated force, or by a moment (the resultants of this load) represents a very suitable idealization.

The deflection surface of a plate due to the concentrated force can be used for calculating the deflections and stresses caused by an arbitrary load $p(x, y)$, as discussed later. Such singular solutions may also be convenient in analyzing the stress distribution near stress raisers of various nature. However, in the case of concentrated loads, the solutions in the form of series should be avoided for calculating stresses. Here, the closed-form solutions are desirable.

The expressions for bending moments in the long plate-strip loaded uniformly over a circular area of small radius c are given in [5]. Neglecting small terms of order c^2/a^2 for points near the center of a circular loading zone, these expressions have the following form

$$M_x = \frac{P}{4\pi}\left[-(1+\nu)\ln\frac{c}{a_0} + 1\right] - \frac{P(1-\nu)}{4\pi}; \quad M_y = \frac{P}{4\pi}\left[-(1+\nu)\ln\frac{c}{a_0} + 1\right], \tag{3.37}$$

where $a_0 = \frac{2a}{\pi}\sin\frac{\pi\xi}{a}$.

Now we can consider the expressions for bending moments in the vicinity of the point of application of a concentrated force P for rectangular plates of finite length. These solutions can be obtained by adding the boundary moments which satisfy new boundary conditions: namely,

$$w = 0|_{y=\pm b/2}, \quad M_x = 0\big|_{y=\pm b/2}.$$

Adding the solution obtained above for a long plate-strip with a new one, we obtain the following expressions of bending moments for points in the vicinity of an application of concentrated force P:

$$\begin{aligned} M_x &= -\frac{1+\nu}{4\pi}P\ln\frac{r}{a_0} + \gamma_1\frac{P}{4\pi} + \frac{1-\nu}{4\pi}P\frac{y^2}{r^2}, \\ M_y &= -\frac{1+\nu}{4\pi}P\ln\frac{r}{a_0} + \gamma_2\frac{P}{4\pi} + \frac{1-\nu}{4\pi}P\frac{y^2}{r^2}, \end{aligned} \tag{3.38}$$

Table 3.1

b/a	1.0	1.2	1.4	1.6	1.8	2.0	∞
γ_1	−0.565	−0.350	−0.211	−0.125	−0.073	−0.042	0
γ_2	0.135	0.115	0.085	0.057	0.037	0.023	0

where γ_1 and γ_2 are some coefficients depending on the plate dimensions. They are presented below in Table 3.1 [3].

Let us turn back to the expression (3.27) and write it in the following form

$$w = G(x, y; \xi, \eta) = \frac{4}{\pi^4 abD} \sum_{m=1}^{\infty} \sum_{n=1}^{\infty} \frac{\sin\frac{m\pi\xi}{a} \sin\frac{n\pi\eta}{b} \sin\frac{m\pi x}{a} \sin\frac{n\pi y}{b}}{\left[(m/a)^2 + (n/b)^2\right]^2}. \tag{3.39}$$

This is the equation of the deflected surface of the plate produced by a unit concentrated force $P = 1$ and it is denoted by $G(x, y; \xi, \eta)$. It is seen that $G(x, y; \xi, \eta)$ depends on two sets of coordinates: (a) the point of observation, (x, y) and (b) the point of application of the applied unit force, (ξ, η). This function is defined as *Green's function* and represents a deflection at the point of observation, (x, y), due to a unit force at the point of application, (ξ, η) or vice versa, because this function is symmetrical with respect to these coordinate sets, i.e., $G(x, y; \xi, \eta) = G(\xi, \eta; x, y)$. The latter immediately follows from the well-known reciprocity theorem. Sometimes, $G(x, y; \xi, \eta)$ is referred to as an *influence function*. Once Green's function is established for a plate, one can determine readily the deflection at any point of observation due to prescribed surface loading $p(\xi, \eta)$. Then, by superposition, we have the following:

$$w(x, y) = \iint_S p(\xi, \eta) G(x, y; \xi, \eta) d\xi d\eta.$$

The Green's function approach is widely used in mechanics [6,7].

3.5 LEVY'S SOLUTION (SINGLE SERIES SOLUTION)

In the preceding sections it was shown that the calculation of bending moments and shear forces using Navier's solution is not very satisfactory because of slow convergence of the series.

In 1900 Levy developed a method for solving rectangular plate bending problems with simply supported two opposite edges and with arbitrary conditions of supports on the two remaining opposite edges using single Fourier series [8]. This method is more practical because it is easier to perform numerical calculations for single series that for double series and it is also applicable to plates with various boundary conditions.

Levy suggested the solution of Eq. (2.24) be expressed in terms of complementary, $w_{h,}$ and particular, w_p, parts, each of which consists of a single Fourier series where unknown functions are determined from the prescribed boundary conditions. Thus, the solution is expressed as follows:

$$w = w_{\mathrm{h}} + w_{\mathrm{p}}. \tag{3.40}$$

Consider a plate with opposite edges, $x = 0$ and $x = a$, simply supported, and two remaining opposite edges, $y = 0$ and $y = b$, which may have arbitrary supports.

The boundary conditions on the simply supported edges are

$$w = 0|_{x=0,x=a} \text{ and } M_x = -D\left(\frac{\partial^2 w}{\partial x^2} + \nu\frac{\partial^2 w}{\partial y^2}\right) = 0\Bigg|_{x=0,x=a}. \tag{3.41a}$$

As mentioned earlier, the second boundary condition can be reduced to the following form:

$$\frac{\partial^2 w}{\partial x^2} = 0\Bigg|_{x=0,x=a} \tag{3.41b}$$

The complementary solution is taken to be

$$w_{\mathrm{h}} = \sum_{m=1}^{\infty} f_m(y)\sin\frac{m\pi x}{a}, \tag{3.42}$$

where $f_m(y)$ is a function of y only; w_{h} also satisfies the simply supported boundary conditions (3.41). Substituting (3.42) into the following homogeneous differential equation

$$\nabla^2\nabla^2 w = 0 \tag{3.43}$$

gives

$$\left[\left(\frac{m\pi}{a}\right)^4 f_m(y) - 2\left(\frac{m\pi}{a}\right)^2\frac{\mathrm{d}^2 f_m(y)}{\mathrm{d}y^2} + \frac{\mathrm{d}^4 f_m(y)}{\mathrm{d}y^4}\right]\sin\frac{m\pi x}{a} = 0,$$

which is satisfied when the bracketed term is equal to zero. Thus,

$$\frac{\mathrm{d}^4 f_m(y)}{\mathrm{d}y^4} - 2\left(\frac{m\pi}{a}\right)^2\frac{\mathrm{d}^2 f_m(y)}{\mathrm{d}y^2} + \left(\frac{m\pi}{a}\right)^4 f_m(y) = 0 \tag{3.44}$$

The solution of this ordinary differential equation can be expressed as

$$f_m(y) = \mathrm{e}^{\lambda y}. \tag{3.45}$$

Substituting the above into Eq. (3.44), gives the following characteristic equation:

$$\lambda^4 - 2\frac{m^2\pi^2}{a^2}\lambda^2 + \frac{m^4\pi^4}{a^4} = 0, \tag{3.46}$$

which has the two following two double roots

$$\lambda_{1,2} = \frac{m\pi}{a}, \quad \lambda_{3,4} = -\frac{m\pi}{a}. \tag{3.47}$$

According to the obtained values of the characteristic exponents, the solution of the homogeneous equation can be expressed in terms of either exponential functions

$$f_m(y) = A'_m\mathrm{e}^{m\pi y/a} + B'_m\mathrm{e}^{-m\pi y/a} + \frac{m\pi y}{a}\left(C'_m\mathrm{e}^{m\pi y/a} + D'_m\mathrm{e}^{-m\pi y/a}\right) \tag{3.48}$$

or hyperbolic functions

$$f_m(y) = A_m \sinh\frac{m\pi y}{a} + B_m \cosh\frac{m\pi y}{a} + \frac{m\pi y}{a}\left(C_m \sinh\frac{m\pi y}{a} + D_m \cosh\frac{m\pi y}{a}\right). \tag{3.49}$$

The second form, Eq. (3.49), is more convenient for calculations.

The complementary solution given by Eq. (3.42) becomes

$$\begin{aligned} w_{\mathrm{h}} = \sum_{m=1}^{\infty}\Big[& A_m \sinh\frac{m\pi y}{a} + B_m \cosh\frac{m\pi y}{a} \\ & + \frac{m\pi y}{a}\left(C_m \sinh\frac{m\pi y}{a} + D_m \cosh\frac{m\pi y}{a}\right)\Big] \sin\frac{m\pi x}{a}, \end{aligned} \tag{3.50}$$

where the constants A_m, B_m, C_m, and D_m are obtained from the boundary conditions on the edges $y = 0$ and $y = b$.

The particular solution, w_{p}, in Eq. (3.40), can also be expressed in a single Fourier series as

$$w_{\mathrm{p}}(x, y) = \sum_{m=1}^{\infty} g_m(y) \sin\frac{m\pi x}{a}. \tag{3.51}$$

The lateral distributed load $p(x, y)$ is taken to be the following (see Appendix B):

$$p(x, y) = \sum_{m=1}^{\infty} p_m(y) \sin\frac{m\pi x}{a}, \tag{3.52}$$

where

$$p_m(y) = \frac{2}{a}\int_0^a p(x, y) \sin\frac{m\pi x}{a}\mathrm{d}x. \tag{3.53}$$

Substituting Eqs (3.51) and (3.52) into Eq. (3.44), gives

$$\frac{\mathrm{d}^4 g_m(y)}{\mathrm{d}y^4} - 2\left(\frac{m\pi}{a}\right)^2 \frac{\mathrm{d}^2 g_m(y)}{\mathrm{d}y^2} + \left(\frac{m\pi}{a}\right)^4 g_m(y) = \frac{p_m(y)}{D}. \tag{3.54}$$

Solving this equation, we can determine $g_m(y)$ and, finally, find the particular solution, $w_{\mathrm{p}}(x, y)$.

The complementary components of the stress resultants and stress couples, $M_{x\mathrm{h}}$, $M_{y\mathrm{h}}$, $M_{xy\mathrm{h}}$, and $V_{x\mathrm{h}}$, $V_{y\mathrm{h}}$, can be expressed in terms of $f_m(y)$ by substituting Eq. (3.50) into Eqs (2.13) and (2.39), as follows:

$$M_{x\mathrm{h}} = D\sum_{m=1}^{\infty}\left(\frac{m^2\pi^2}{a^2}f_m - \nu\frac{\mathrm{d}^2 f_m}{\mathrm{d}y^2}\right)\sin\frac{m\pi x}{a},$$

$$M_{y\mathrm{h}} = D\sum_{m=1}^{\infty}\left(\nu\frac{m^2\pi^2}{a^2}f_m - \frac{\mathrm{d}^2 f_m}{\mathrm{d}y^2}\right)\sin\frac{m\pi x}{a},$$

$$M_{xy\mathrm{h}} = -D(1-\nu)\sum_{m=1}^{\infty}\frac{m\pi}{a}\frac{\mathrm{d}f_m}{\mathrm{d}y}\cos\frac{m\pi x}{a}, \tag{3.55}$$

$$V_{x\mathrm{h}} = D\sum_{m=1}^{\infty}\left[\left(\frac{m\pi}{a}\right)^3 f_m - \frac{m\pi}{a}(2-\nu)\frac{\mathrm{d}^2 f_m}{\mathrm{d}y^2}\right]\cos\frac{m\pi x}{a},$$

$$V_{y\mathrm{h}} = D\sum_{m=1}^{\infty}\left[-\frac{\mathrm{d}^3 f_m}{\mathrm{d}y^3} + (2-\nu)\left(\frac{m\pi}{a}\right)^2\frac{\mathrm{d}f_m}{\mathrm{d}y}\right]\sin\frac{m\pi x}{a}.$$

These homogeneous stress resultants and stress couple components must be complemented with particular ones.

Example 3.3

The rectangular simply supported plate on all edges and having dimensions a and b (Fig. 3.10) is subjected to a uniform load p_0. Determine the deflections and bending moments.

Solution

Since the boundary conditions are identical for all the edges of the plate and the load is constant, then we make the x axis coincident with the axis of symmetry of the plate. It will be shown later that this location of the x axis simplifies considerably the computational procedure.

For $p(x, y) = p_0$, Eq. (3.53) upon integration, becomes

$$p_m = \frac{2p_0}{a}\int_0^a \sin\frac{m\pi x}{a}\mathrm{d}x = \frac{4p_0}{m\pi} \quad (m = 1, 3, 5, \ldots). \tag{a}$$

Substituting the above into Eq. (3.54), one obtains

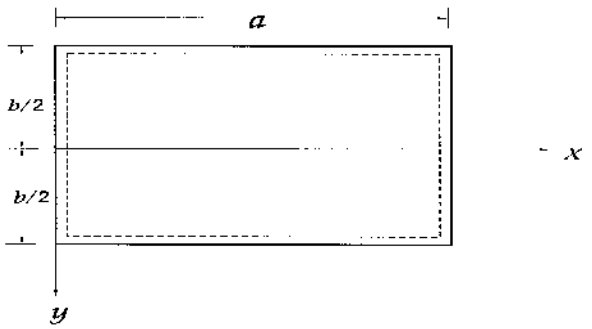

Fig. 3.10

$$\frac{\mathrm{d}^4 g_m}{\mathrm{d}y^4} - 2\left(\frac{m\pi}{a}\right)^2 \frac{\mathrm{d}^2 g_m}{\mathrm{d}y^2} + \left(\frac{m\pi}{a}\right)^4 g_m = \frac{4p_0}{m\pi D}. \tag{b}$$

Since the right-hand side of this equation is a constant, the particular solution of Eq. (b) will also be a constant. Setting, for example,

$$g_m = A, \tag{c}$$

and substituting the above into Eq. (b), gives

$$A = \left(\frac{a}{m\pi}\right)^4 \frac{4p_0}{m\pi D}. \tag{d}$$

So, using Eqs (c), (d), and (3.51), the particular solution is of the following form:

$$w_{\mathrm{p}}(x, y) = \frac{4p_0 a^4}{\pi^5 D} \sum_{m=1,3,5,\ldots}^{\infty} \frac{1}{m^5} \sin\frac{m\pi x}{a}. \tag{3.56a}$$

This series can be summed, and we obtain

$$w_{\mathrm{p}}(x, y) = \frac{4p_0 a^4}{\pi^5 D} \sum_{m=1,3,5,\ldots}^{\infty} \frac{1}{m^5} \sin\frac{m\pi x}{a} = \frac{p_0}{24D}\left(x^4 - 2ax^3 + a^3 x\right). \tag{3.56b}$$

The expression (3.56b) represents the equation for deflections of a uniformly loaded simply supported strip of unit width parallel to the x axis.

Due to the symmetry of the boundary conditions and applied loading, we can conclude that the plate deflection will be also symmetrical about the x axis, i.e., $w(x, y) = w(x, -y)$. This condition is satisfied by Eq. (3.50) if we let $A_m = B_m = 0$. Then, combining Eqs (3.50) and (3.56), we obtain

$$w = \sum_{m=1,3,5,\ldots}^{\infty} \left(B_m \cosh\frac{m\pi y}{a} + C_m \frac{m\pi y}{a} \sinh\frac{m\pi y}{a} + \frac{4p_0 a^4}{m^5 \pi^5 D}\right) \sin\frac{m\pi x}{a}, \tag{3.57a}$$

or alternatively, using expression (3.56b),

$$\begin{aligned} w = {} & \frac{p_0}{24D}\left(x^4 - 2ax^3 + a^3 x\right) \\ & + \sum_{m=1,3,5,\ldots}^{\infty} \left(B_m \cosh\frac{m\pi y}{a} + C_m \frac{m\pi y}{a} \sinh\frac{m\pi y}{a}\right) \sin\frac{m\pi x}{a}. \end{aligned} \tag{3.57b}$$

Equations (3.57) exactly satisfy Eq. (2.24) and the boundary conditions (3.41) at $x = 0$ and $x = a$. The remaining boundary conditions are, as follows:

$$w = 0\big|_{y=\pm\frac{b}{2}}, \frac{\partial^2 w}{\partial y^2} = 0\Bigg|_{y=\pm\frac{b}{2}}. \tag{3.58}$$

Application of the above to w leads to two equations for determining B_m and C_m. Solving these equations, one obtains

$$B_m = -\frac{2p_0 a^4(\alpha_m \sinh\alpha_m + 2\cosh\alpha_m)}{\pi^5 m^5 D \cosh^2\alpha_m}, \quad C_m = \frac{2p_0 a^4}{\pi^5 m^5 D \cosh\alpha_m}, \tag{e}$$

where $\alpha_m = m\pi b/2a$.

The deflection of the plate surface, Eq. (3.57a), may thus be expressed

$$w = \frac{4p_0a^4}{\pi^5 D}\sum_{m=1,3,..}^{\infty}\frac{1}{m^5}\left(1 - \frac{\alpha_m \tanh\alpha_m + 2}{2\cosh\alpha_m}\cosh\frac{2\alpha_m y}{b} + \frac{\alpha_m}{2\cosh\alpha_m}\frac{2y}{b}\right.$$
$$\left.\sinh\frac{2\alpha_m y}{b}\right)\sin\frac{m\pi x}{a}. \tag{3.59}$$

The maximum deflection is obtained at the plate center ($x = a/2, y = 0$), where

$$w_{\max} = \frac{4p_0a^4}{\pi^5 D}\sum_{m=1,3,...}^{\infty}\frac{(-1)^{\frac{m-1}{2}}}{m^5}\left(1 - \frac{\alpha_m \tanh\alpha_m + 2}{2\cosh\alpha_m}\right).$$

Since

$$\sum_{m=1,3,...}^{\infty}\frac{(-1)^{\frac{m-1}{2}}}{m^5} = \frac{5\pi^5}{2^9(3)}.$$

we can write the following expression for the maximum deflection of the plate:

$$w_{\max} = \frac{5p_0a^4}{384D} - \frac{4p_0a^4}{\pi^5 D}\sum_{m=1,3,...}^{\infty}\frac{(-1)^{\frac{m-1}{2}}(\alpha_m \tanh\alpha_m + 2)}{2\cosh\alpha_m\, m^5}. \tag{3.60}$$

The first term above represents the deflection $w_{\max}$ of the middle of a uniformly loaded, simply supported strip. The second term is a very rapidly converging series. For example, in the case of a square plate ($a = b$ and $\alpha_m = m\pi/2$), the maximum deflection is given as

$$w_{\max} = \frac{5p_0a^4}{384D} - \frac{4p_0a^4}{\pi^5 D}(0.68562 - 0.00025 + \ldots) = 0.00406\frac{p_0a^4}{D}.$$

It is seen that the second term of the series in parentheses is negligible and that by taking only the first term ($m = 1$), the formula for deflection is obtained correct to three significant figures.

Substituting the expression (3.57b) into the first and second equations (3.55), we obtain the following expressions for bending moments:

$$M_x = \frac{p_0x(a-x)}{2} + (1-\nu)p_0a^2\pi^2\sum_{m=1,3,...}^{\infty} m^2\left[B_m\cosh\frac{m\pi y}{a}\right.$$
$$\left.+C_m\left(\frac{m\pi y}{a}\sinh\frac{m\pi y}{a} - \frac{2\nu}{1-\nu}\cosh\frac{m\pi y}{a}\right)\right]\sin\frac{m\pi x}{a},$$
$$M_y = \nu\frac{p_0x(a-x)}{2} - (1-\nu)p_0a^2\pi^2\sum_{m=1,3,...}^{\infty} m^2\left[B_m\cosh\frac{m\pi y}{a}\right. \tag{3.61}$$
$$\left.+C_m\left(\frac{m\pi y}{a}\sinh\frac{m\pi y}{a} + \frac{2}{1-\nu}\cosh\frac{m\pi y}{a}\right)\right]\sin\frac{m\pi x}{a},$$

where B_m and C_m are given by Eqs (e).

Both series in Eqs (3.61) converge rapidly. At the center ($x = a/2, y = 0$) of the square plate the bending moments are given as

$$M_x = M_y = 0.0479 p_0 a^2.$$

If $b/a \gg 1$ (the plate-strip), then $M_x = p_0 a^2/8$, $M_y = \nu M_x$. The series for the effective shear forces V_x and V_y are also convergent.

Example 3.4

For the simply supported plate subjected to hydrostatic loading ($p(x) = p_0 \frac{x}{a}$), as shown in Fig. 3.11, determine the deflection and bending moment equations.

Solution

Determine the coefficients p_m from Eq. (3.53). We have

$$p_m = \frac{2}{a}\int_0^a p(x,y)\sin\frac{m\pi x}{a}\,dx = \frac{2p_0}{a}\int_0^a \frac{x}{a}\sin\frac{m\pi x}{a}\,dx$$
$$= \frac{2p_0}{m\pi}(-1)^{m+1}, \quad m = 1, 2, 3\ldots. \tag{a}$$

The given loading is a constant along the y axis. Hence, the function g_m will be also a constant. Substituting the expression (a) into the right-hand side of Eq. (3.54), we obtain

$$g_m = \frac{2p_0 a^4}{m^5\pi^5 D}(-1)^{m+1}. \tag{b}$$

Inserting (b) into Eq. (3.51), we obtain the particular solution of the following form:

$$w_p(x,y) = \frac{2p_0 a^4}{\pi^5 D}\sum_{m=1,2,\ldots}^{\infty}\frac{(-1)^{m+1}}{m^5}\sin\frac{m\pi x}{a}. \tag{c}$$

Using Eqs (3.50) and (c), and letting $A_m = D_m = 0$ (because of the symmetry of the loading and boundary conditions about the x axis), we obtain the equation of the plate deflection in the following form:

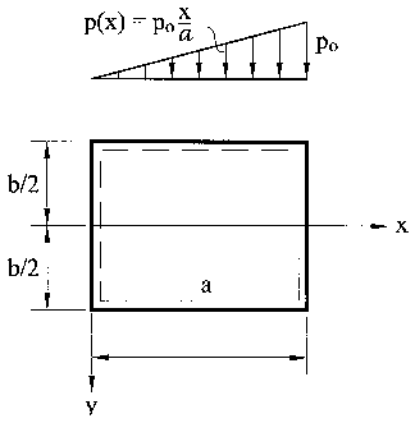

Fig. 3.11

$$w(x,y)=\sum_{m=1,2,\ldots}^{\infty}\left(B_m\cosh\frac{m\pi y}{a}+C_m\frac{m\pi y}{a}\sinh\frac{m\pi y}{a}+\frac{2p_0a^4}{\pi^5D}\frac{(-1)^{m+1}}{m^5}\right)\sin\frac{m\pi x}{a}, \tag{d}$$

where the constants of integration B_m and C_m are evaluated from the boundary conditions on edges $y=\pm b/2$: namely,

$$w=0|_{y=\pm b/2}\quad\text{and}\quad\left.\frac{\partial^2 w}{\partial y^2}=0\right|_{y=\pm b/2}. \tag{e}$$

Application of the above to w, Eq. (d), leads to two equations. Solving them for B_m and C_m yields

$$B_m=-\frac{(2+\alpha_m\tanh\alpha_m)(-1)^{m+1}}{\pi^5m^5\cosh\alpha_m},\quad C_m=\frac{(-1)^{m+1}}{\pi^5m^5\cosh\alpha_m}, \tag{f}$$

where $\alpha_m=m\pi b/2a$.

The deflection of the plate along the x axis is

$$(w)_{y=0}=\frac{p_0a^4}{D}\sum_{m=1}^{\infty}\left[\frac{2(-1)^{m+1}}{\pi^5m^5}+A_m\right]\sin\frac{m\pi x}{a}.$$

For a square plate we have $a=b$, from which one obtains the following:

$$(w)_{y=0}=\frac{p_0a^4}{D}\left(0.002055\sin\frac{\pi x}{a}-0.000177\sin\frac{2\pi x}{a}+0.000025\sin\frac{3\pi x}{a}-\ldots\right). \tag{g}$$

The center deflection is given as

$$(w)_{x=a/2,y=0}=0.00203\frac{p_0a^4}{D}. \tag{h}$$

As expected, this result is about one-half of the deflection of a uniformly laded plate (see Example 3.1). Equating the first derivative of the expression (g) to zero, we can find that the maximum deflection occurs at a point $x=0.557a$ and that $w_{\max}=0.00206(p_0a^4/D)$.

The bending moments can be found by substitution of Eq. (d) for deflection into Eq. (2.13). For example, the bending moment equation M_x along the x axis, i.e., for $y=0$, has the form

$$(M_x)_{y=0}=p_0a^2\sum_{m=1}^{\infty}\frac{2(-1)^{m+1}}{\pi^3m^3}\sin\frac{m\pi x}{a}$$

$$+p_0a^2\pi^2\sum_{m=1}^{\infty}m^2[(1-\nu)B_m-2\nu C_m]\sin\frac{m\pi x}{a},$$

where the constants B_m and C_m are given by the expressions (f). These series converge rapidly and several first terms give a sufficiently accurate result for M_x.

Example 3.5

Derive expressions for the deflected surface and the bending moments in a floor plate-strip subjected to a uniformly distributed load q_0 along line $y = 0$, as shown in Fig. 3.12a. Assume the edges $x = 0$ and $x = a$ are simply supported.

Solution

If a plate is strongly lengthened in one direction – for example, in the y direction – then such a plate in some problems can be considered as an infinite one in this direction. Levy's solution can be applied advantageously with some modifications to obtain the expressions for the deflections and bending moments.

The solution of the governing differential equation (2.24) is sought in the form of Eq. (3.48). At the same time, since for $y \to \infty$ deflections cannot approach infinity, then the terms containing $e^{m\pi y/a}$ should be equated to zero because these terms and their derivatives do not vanish at $y \to \infty$. Hence, w_h can be represented as follows:

$$w_h = \sum_{m=1}^{\infty} \left(B'_m + \frac{m\pi y}{a} D'_m \right) e^{-m\pi y/a} \sin \frac{m\pi x}{a}. \tag{a}$$

The above satisfies Eq. (2.24) and the boundary conditions on the edges $x = 0$ and $x = a$.

Let us consider the lower part of the plate where $y \geq 0$. The constants B'_m and D'_m can be evaluated from the conditions of symmetry of the plate and loading at $y = 0$. First, due to the symmetry of the deflected middle surface of the plate with respect to the x axis, the derivative $\partial w/\partial y$ is zero at $y = 0$; this condition is satisfied if $B'_m = D'_m$. Therefore, Eq. (a) becomes (for the lower part of the plate)

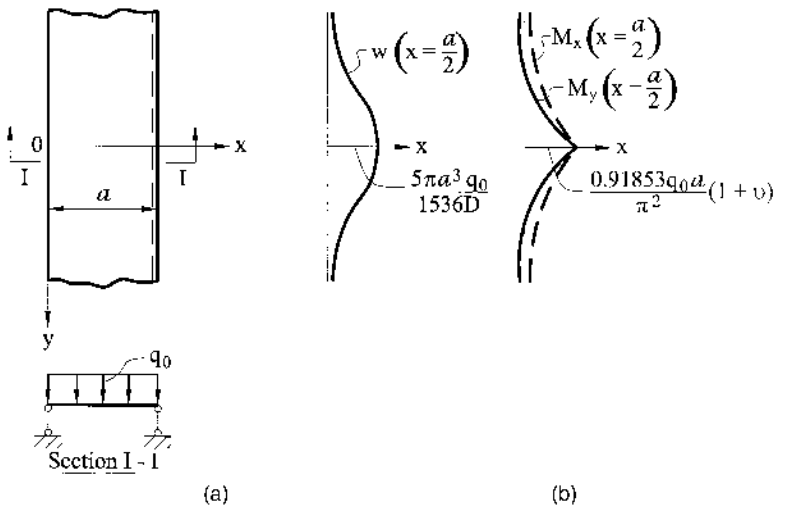

Fig. 3.12

$$w_{\mathrm{h}} = \sum_{m=1}^{\infty} B'_m \left(1 + \frac{m\pi y}{a}\right) \mathrm{e}^{-m\pi y/a} \sin \frac{m\pi x}{a}. \tag{b}$$

Secondly, the effective (Kirchhoff's) shear force at the section just below the x axis is numerically equal to one-half the line load $q(x)$. Taking into account the sign, this condition leads to the following:

$$V_y\big|_{y=+0} = -\frac{1}{2} q(x). \tag{c}$$

If the line load is uniformly distributed along the x axis, it can be expanded into a sine series in accordance with Eq. (3.52). The coefficients q_m of the single Fourier expansion are obtained from Eq. (3.53), as follows (for a uniformly distributed load q_0)

$$q_m = \frac{2}{a} \int_0^a q(x) \sin \frac{m\pi x}{a} \mathrm{d}x = \frac{4q_0}{m\pi} \text{ for } m = 1, 3, 5, \ldots. \tag{d}$$

Thus, the load is expressed as

$$q = \frac{4q_0}{\pi} \sum_{m=1,3,\ldots}^{\infty} \frac{1}{m} \sin \frac{m\pi x}{a}. \tag{e}$$

Now using the expression (c) and Eqs (3.55) and (e), we obtain

$$\left(V_y\right)_{y=0} = -D \frac{\partial}{\partial y} \nabla^2 w_{\mathrm{h}} = -\frac{2q_0}{\pi} \sum_{m=1,3,\ldots}^{\infty} \frac{1}{m} \sin \frac{m\pi x}{a}. \tag{f}$$

Substitution of Eq. (b) in the left-hand side of Eq. (f) gives

$$B'_m = \frac{q_0 a^3}{\pi^4 m^4 D} \ (m = 1, 3, 5, \ldots). \tag{g}$$

Since the plate at $y > 0$ and $y < 0$ carries no load, the particular solution of Eq. (2.24) is zero. Thus, the expression of the deflection surface of the plate becomes

$$w = w_{\mathrm{h}} = \frac{q_0 a^3}{\pi^4 D} \sum_{m=1,3,\ldots}^{\infty} \frac{1}{m^4} \left(1 + \frac{m\pi y}{a}\right) \mathrm{e}^{-m\pi y/a} \sin \frac{m\pi x}{a}. \tag{h}$$

When the above is inserted into Eqs (3.55), the expressions for bending moments will be obtained in the following form:

$$\begin{aligned} M_x &= \frac{q_0 a}{\pi^2} \sum_{m=1,3,\ldots}^{\infty} \frac{1}{m^2} \left[1 + \nu + (1 - \nu) \frac{m\pi y}{a}\right] \mathrm{e}^{-m\pi y/a} \sin \frac{m\pi x}{a}, \\ M_y &= \frac{q_0 a}{\pi^2} \sum_{m=1,3,\ldots}^{\infty} \frac{1}{m^2} \left[1 + \nu - (1 - \nu) \frac{m\pi y}{a}\right] \mathrm{e}^{-m\pi y/a} \sin \frac{m\pi x}{a}. \end{aligned} \tag{i}$$

The maximum values of the deflections and bending moments occur at the plate center, i.e., at $y = 0$ and $x = a/2$

$$w_{\max} = \frac{q_0 a^3}{\pi^4 D} \sum_{m=1,3,\ldots}^{\infty} \frac{(-1)^{\frac{m-1}{2}}}{m^4} = \frac{5 q_0 \pi a^3}{1536 D},$$

$$M_{x,\max} = M_{y,\max} = \frac{q_0 a(1+\nu)}{\pi^2} \sum_{m=1,3,..}^{\infty} \frac{(-1)^{\frac{m-1}{2}}}{m^2} = \frac{0.91853 q_0 a(1+\nu)}{\pi^2}.$$

For $y = a$ the factor $e^{\pi y/a} = e^{-\pi} \approx 0.045$ and it is possible to consider that the bending moments and deflections vanish practically at a distance $y \approx a$. The deflection and bending moment diagrams are shown in Fig. 3.12b.

Example 3.6

A simply supported rectangular plate shown in Fig. 3.13 is loaded by an edge moment $m_x = f(x)$ along edge $x = 0$. Determine the equation for deflections of the plate middle surface.

Solution

We expand the given moment function $f(x)$ into the following Fourier series:

$$m_x = f(x) = \sum_{n=1}^{\infty} F_n \sin \frac{n\pi y}{b}, \tag{a}$$

where F_n are the constants of the Fourier expansion. Since a lateral load $p(x, y)$ is zero, the solution must satisfy the homogeneous differential equation (3.43). The solution of this homogeneous equation may be taken in the form

$$\begin{aligned} w = \sum_{n=1}^{\infty} \frac{1}{\beta_n^2} (&C_{1n} \cosh \beta_n x + C_{2n} \beta_n x \sinh \beta_n x \\ &+ C_{3n} \sinh \beta_n x + C_{4n} \beta_n x \cosh \beta_n x) \sin \beta_n y, \end{aligned} \tag{b}$$

where $\beta_n = n\pi/b$. The constants of integration C_{in} $(i = 1, 2, 3, 4)$ can be evaluated from the prescribed boundary conditions on edges of the plate: namely,

$$w = 0|_{x=0,a}, \quad M_x = m_x\big|_{x=0}, \quad M_x = 0\big|_{x=a}, \tag{c}$$

$$w = 0|_{y=0,b}, \quad M_y = 0\big|_{y=0,b}; \tag{d}$$

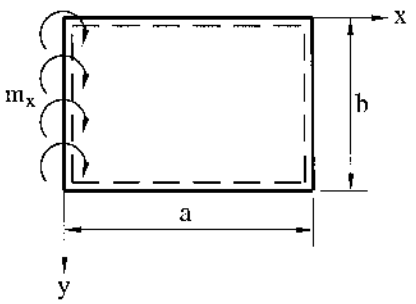

Fig. 3.13

w in the form of Eq. (b) satisfies Eq. (3.43) and the boundary conditions (d) exactly. Using the relations (2.12) and Eq. (a), the boundary conditions (c) can be rewritten, as follows

$$w = 0|_{x=0,a};\quad \left[-D\left(\frac{\partial^2 w}{\partial x^2} + \nu\frac{\partial^2 w}{\partial y^2}\right)\right]\Bigg|_{x=0} = F_n \sin\beta_n y \text{ and } \left(\frac{\partial^2 w}{\partial x^2} + \nu\frac{\partial^2 w}{\partial y^2}\right)\Bigg|_{x=a} = 0. \tag{e}$$

Substitution of Eqs (b) into (e) and solving the obtained equations for C_{in}, one obtains

$$C_{1n} = 0,\ C_{2n} = -\frac{F_n}{2D},\ C_{3n} = \frac{F_n}{2D}\left(1 - \coth^2\beta_n a\right)\beta_n a,\ C_{4n} = \frac{F_n}{2D}\coth\beta_n a. \tag{f}$$

Inserting the above into Eq. (f) yields the following:

$$w = \sum_{n=1}^{\infty} \frac{F_n}{2D\beta_n^2 \sinh\beta_n a}\left[\beta_n x\cosh\beta_n(a-x) - \beta_n a\frac{\sinh\beta_n x}{\sinh\beta_n a}\right]\sin\beta_n y. \tag{3.62}$$

As it follows from the above, in order to obtain a particular solution for plates subjected to various types of load distribution $p(x, y) = p_0 \cdot f(x)$ it is necessary to determine the coefficients p_m (see Eq. (3.53)). Table 3.2 furnishes the values of p_m for various types of load distributions.

3.6 CONTINUOUS PLATES

When a uniform plate extends over a support and has more than one span along its length or width, it is termed *continuous*. Such plates are of considerable practical interest.

Continuous plates are externally statically indeterminate members (note that a plate itself is also internally statically indeterminate). So, the well-known methods developed in structural mechanics can be used for the analysis of continuous plates. In this section, we consider the *force method* which is commonly used for the analysis of statically indeterminate systems. According to this method, the continuous plate is subdivided into individual, simple-span panels between intermediate supports by removing all redundant restraints. It can be established, for example, by introducing some fictitious hinges above the intermediate supports. In this way, the redundant moments acting along the intermediate supports are eliminated. Similar fictitious hinges can be used at the ends if those are fixed. The simple-span panel obtained in such a way is referred to as a *primary plate*. In order to restore the rejected restraints, the unknown redundant moments are applied to the primary plate. These moments can be determined from the solution of simultaneous algebraic equations expressing the compatibility of the slopes between the adjoining panels produced by both external loads and unknown redundant moments.

In our further discussion we assume that the supports are unyielding. For the sake of simplicity, we confine ourselves to a rectangular plate continuous in one direction only and having the same flexural rigidity. Obviously, the general procedure of the force method discussed below can be applied to plates continuous in both directions.

Table 3.2

No.	Load Geometry $p(x,y)=\sum_m p_m \sin\frac{m\pi x}{a}$	Expansion coefficient p_m [determined from Eq. (3.53)]
1	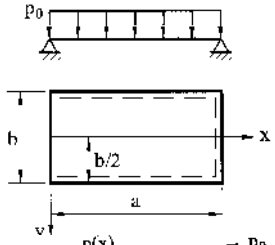	Uniform loading, $p_0 = \text{const}$ $p_m = \frac{4p_0}{m\pi}$ $(m = 1, 3, 5, \ldots)$
2	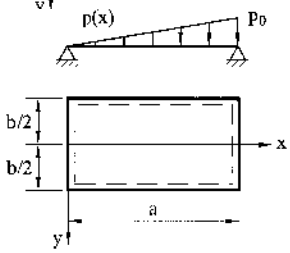	Hydrostatic loading, $p(x) = p_0 \frac{x}{a}$ $p_m = \frac{2p_0}{m\pi}(-1)^{m+1}$ $(m = 1, 2, \ldots)$
3	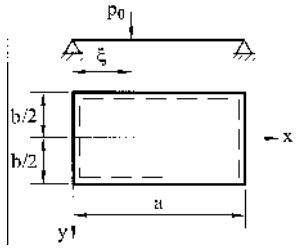	Line load p_0 at $x = \xi$ $p_m = \frac{2p_0}{a}\sin\frac{m\pi\xi}{a}$ $(m = 1, 2, 3, \ldots)$
4	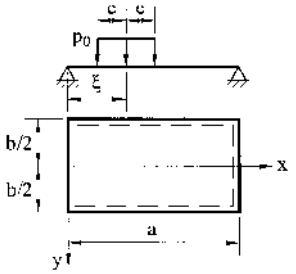	Uniform load from $(\xi - e)$ to $(\xi + e)$ $p_m = \frac{4p_0}{m\pi}\sin\frac{m\pi\xi}{a}\sin\frac{m\pi e}{a}$ $(m = 1, 2, \ldots)$
5	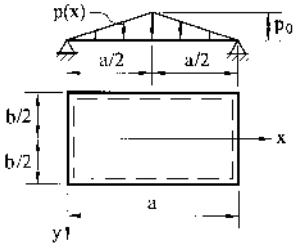	Triangular load $p(x) = 2p_0 \frac{x}{a}$ if $x \le a/2$ $p(x) = 2p_0 \frac{a-x}{a}$ if $x \ge a/2$ $p_m = \frac{8p_0}{m^2\pi^2}(-1)^{\frac{m-1}{2}}$ $(m = 1, 3, \ldots)$

Consider the three-span simply supported continuous plate. The plate is subjected to a uniform load of intensities p_1, p_2, and p_3 as shown in Fig. 3.14a. Figure 3.14b illustrates the primary plate obtained by introducing the fictitious hinges above the intermediate supports; $\mu_1(y)$ and $\mu_2(y)$ are the redundant, unknown distributed moments replacing the removed restraints at the intermediate supports. These unknown bending moments may be represented by the following Fourier series:

$$\mu_1(y) = \sum_{m=1,3,\ldots}^{\infty} \mu_{1m} \sin \lambda_m y, \quad \mu_2(y) = \sum_{m=1,3,\ldots}^{\infty} \mu_{2m} \sin \lambda_m y, \quad \lambda_m = \frac{m\pi}{b}. \tag{3.63}$$

Since the deflection is symmetric with respect to the line $y = b/2$, the numbers m in the expansions (3.63) must be odd only. It is seen from Fig. 3.14b that the

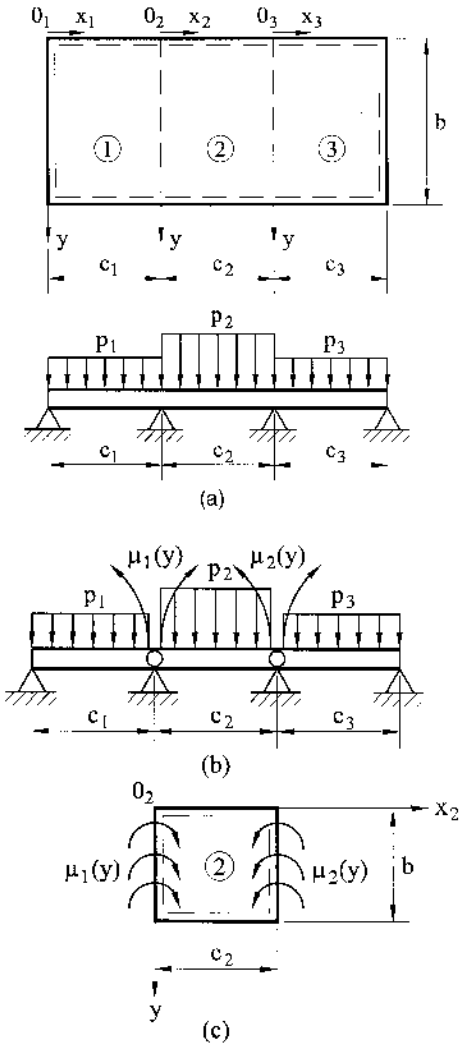

Fig. 3.14

primary plate consists of individual simple-span panels subjected to a given loading and the distributed edge moments $\mu_1(y)$ and $\mu_2(y)$, as shown in Fig. 3.14c.

The deflected surface of each simply supported individual panel may be obtained by application of Levy's method. The general solution for individual panels simply supported on all edges is given by Eqs (3.50) and (3.56a) if y is replaced by x_i, x by y, and a by b. We have the following:

$$w_i = \sum_{m=1,3,\ldots}^{\infty} \left(A_m^{(i)} \sinh \lambda_m x_i + B_m^{(i)} \cosh \lambda_m x_i + C_m^{(i)} \lambda_m x_i \sinh \lambda_m x_i + D_m^{(i)} \lambda_m x_i \cosh \lambda_m x_i + \frac{4 p_i b^4}{m^5 \pi^5 D} \right) \sin \lambda_m y, \quad i = 1, 2, 3. \tag{3.64}$$

The boundary conditions of each panel as well as the compatibility of deformations between any two panels across a common boundary (slopes continuity at the intermediate supports) are used to determine the constants in the solution (3.64) and the coefficients in the Fourier series (3.63). The boundary conditions for the plates 1, 2, and 3 are represented as follows:

$$w_1 = 0|_{x_1=0,c_1}, \ \frac{\partial^2 w_1}{\partial x_1^2} = 0 \Big|_{x_1=0}, \quad -D \frac{\partial^2 w_1}{\partial x_1^2} = \sum_{m=1,3,\ldots}^{\infty} \mu_{1m} \sin \lambda_m y \Big|_{x_1=c_1}, \tag{a}$$

$$w_2 = 0|_{x_2=0,c_2}, \ -D \frac{\partial^2 w_2}{\partial x_2^2} = \sum_{m=1,3,\ldots}^{\infty} \mu_{1m} \sin \lambda_m y \Big|_{x_2=0}, \quad -D \frac{\partial^2 w_2}{\partial x_2^2} = \sum_{m=1,3,\ldots}^{\infty} \mu_{2m} \sin \lambda_m y \Big|_{x_2=c_2} \tag{b}$$

$$w_3 = 0|_{x_3=0,c_3}, \ \frac{\partial^2 w_3}{\partial x_3^2} = 0 \Big|_{x_3=c_3}, \quad -D \frac{\partial^2 w_3}{\partial x_3^2} = \sum_{m=1,3,\ldots}^{\infty} \mu_{2m} \sin \lambda_m y \Big|_{x_3=0}. \tag{c}$$

The compatibility conditions are expressed as follows

$$\left(\frac{\partial w_1}{\partial x_1} \right)_{x_1=c_1} = \left(\frac{\partial w_2}{\partial x_2} \right)_{x_2=0}, \quad \left(\frac{\partial w_2}{\partial x_2} \right)_{x_2=c_2} = \left(\frac{\partial w_3}{\partial x_3} \right)_{x_3=0}. \tag{d}$$

Let us consider the middle panel 2 (Fig. 3.14c). Application of the edge conditions (b) to Eq. (3.64) for $i = 2$ leads to the following values of the constants

$$\begin{aligned} A_m^{(2)} &= \frac{1}{D \sinh \lambda_m c_2} \left[\frac{4 p_2 b^4}{m^5 \pi^5} (\cosh \lambda_m c_2 - 1)(1 + 0.5 \lambda_m \operatorname{csch} \lambda_m c_2) + \frac{c_2}{2 \lambda_m} (\mu_{1m} \operatorname{csch} \lambda_m c_2 - \mu_{2m} \coth \lambda_m c_2) \right], \\ B_m^{(2)} &= -\frac{4 p_2 b^4}{m^5 \pi^5 D}, \ C_m^{(2)} = \frac{2 p_2 b^4}{m^5 \pi^5 D} - \frac{\mu_{1m}}{2 D \lambda_m^2}, \\ D_m^{(2)} &= \frac{1}{2D \sinh \lambda_m c_2} \left[\frac{4 p_2 b^4}{m^5 \pi^5} (1 - \cosh \lambda_m c_2) - \frac{1}{\lambda_m^2} (\mu_{2m} - \mu_{1m} \cosh \lambda_m c_2) \right]. \end{aligned} \tag{e}$$

The coefficients $A_m^{(1)}$, $B_m^{(1)}$, $C_m^{(1)}$, and $D_m^{(1)}$ are also given by Eqs (e) if p_2 is replaced by p_1, c_2 by c_1, μ_{2m} by μ_{1m} and letting $\mu_{1m} = 0$. Similarly, the coefficients $A_m^{(3)}$, $B_m^{(3)}$, $C_m^{(3)}$, and $D_m^{(3)}$ can be obtained by replacing c_2 by c_3, p_2 by p_3, μ_{1m} by μ_{2m} and letting $\mu_{2m} = 0$. Introducing Eqs (3.64) for $i = 1$ and $i = 2$ into the compatibility conditions (d), we obtain the following two additional equations:

$$\begin{aligned} &A_m^{(1)} \cosh \lambda_m c_1 + B_m^{(1)} \sinh \lambda_m c_1 + C_m^{(1)}(\sinh \lambda_m c_1 + \lambda_m c_1 \cosh \lambda_m c_1) \\ &\quad + D_m^{(1)}(\cosh \lambda_m c_1 + \lambda_m c_1 \sinh \lambda_m c_1) = A_m^{(2)} + D_m^{(2)}, \\ &A_m^{(2)} \cosh \lambda_m c_2 + B_m^{(2)} \sinh \lambda_m c_2 + C_m^{(2)}(\sinh \lambda_m c_2 + \lambda_m c_2 \cosh \lambda_m c_2) \\ &\quad + D_m^{(2)}(\cosh \lambda_m c_2 + \lambda_m c_2 \sinh \lambda_m c_2) = A_m^{(3)} + D_m^{(3)}. \end{aligned} \tag{f}$$

Having coefficients $A_m^{(i)}$, $B_m^{(i)}$, $C_m^{(i)}$, and $D_m^{(i)}$ $(i = 1, 2, 3)$ available, from Eqs (f) we obtain the moment coefficients μ_{1m} and μ_{2m}. Equations (3.64) then give the deflection of the continuous plate from which the moments and stresses can also be computed.

The foregoing approach may be extended to include the case of a long rectangular plate with many supports (see Timoshenko and Woinowski-Krieger [3]). However, as the number of panels increases, it becomes more tedious to find a solution by the classical methods. A more practical approach for solving such plates is to use the numerical methods introduced in Chapter 6.

Example 3.7

Determine the deflections and bending moments in the three-span, simply supported continuous plate loaded as shown in Fig. 3.15.

Solution

Letting $p_1 = p_0$, $p_2 = p_3 = 0$, and $c_1 = c_2 = c_3 = b = 2a$, we can obtain coefficients of integration $A_m^{(i)}$, $B_m^{(i)}$, $C_m^{(i)}$, and $D_m^{(i)}$ $(i = 1, 2, 3)$ and moment coefficients μ_{1m} and μ_{2m} from Eqs (e) and (f), respectively. Equations (3.64) then give the deflection of the continuous plate from which the bending moments are computed using Eqs (3.55).

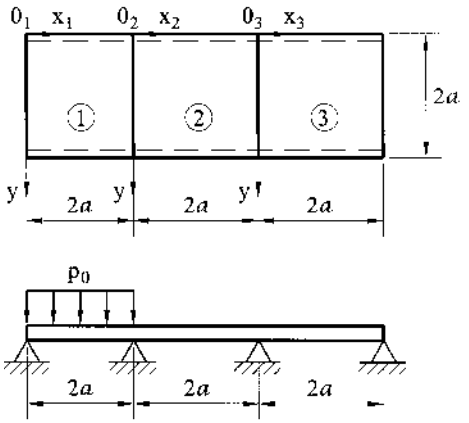

Fig. 3.15

The deflection w and bending moments M_x and M_y diagrams along the central section $y = a$ of the three-span plate are shown in Fig. 3.16 for $\nu = 0.3$.The maximum values of the deflection and bending moment are

$$w_{\max} = 0.64(1 - \nu^2)\frac{p_0 a^4}{Eh^3} \text{ and } M_{x\max} = 0.177pa^2.$$

3.7 PLATES ON AN ELASTIC FOUNDATION

Many problems of considerable practical importance can be related to the solution of plates resting on an elastic foundation. Reinforced concrete pavements of highways and airport runways, foundation slabs of buildings, etc., are well-known direct application. However, an indirect application of this type of plate bending problem is of equal importance. For example, the shallow shell bending problems may be reduced to the solution of the problem for a plate on an elastic foundation; i.e., an analogy exists between the governing differential equation of a shallow shell and that of a plate on elastic foundation.

The key difficulty of this type of problem is in the correct mathematical description of a real elastic foundation. There exist a lot of various hypotheses – models of elastic foundations. The simplest of them has been suggested by Winkler [11]. It is based on the assumption that the foundation's reaction $q(x, y)$ can be described by the following relationship:

$$q(x, y) = kw, \tag{3.65}$$

where k is a constant termed the *foundation modulus,* which has the dimensions of force per unit surface area of the plate per unit deflection, e.g. $(\text{lb/in}^2)(1/\text{in})$ in US units or $(\text{N/m}^2)(1/\text{m})$ in SI units. Values of k for various soils are given in numerous references such as [9,12]. In Eq. (3.65) $q(x, y)$ is the resisting pressure of the foundation and w is the deflection of the plate.

When the plate is supported by a continuous elastic foundation, the external load acting in the lateral direction consists of the surface load $p(x, y)$ and of the

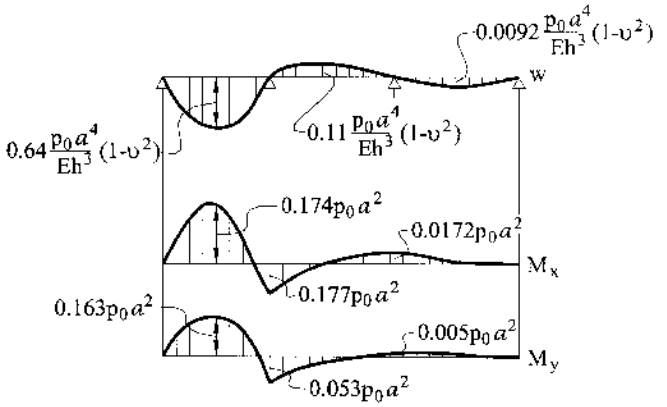

Fig. 3.16

reaction of the elastic foundation $q(x, y)$. Thus, the differential equation of the plate (2.24) becomes the following:

$$\frac{\partial^4 w}{\partial x^4} + 2\frac{\partial^4 w}{\partial x^2 \partial y^2} + \frac{\partial^4 w}{\partial y^4} = \frac{1}{D}[p(x, y) - q(x, y)]. \tag{3.66}$$

In this differential equation, the reactive force, $q(x, y)$, exerted by the elastic foundation is also unknown, because it depends on the deflection, $w(x, y)$, of the plate. Substituting Eq. (3.65) into (3.66), *the governing differential equation of the plate on an elastic foundation*, given by the Winkler model, can be written as

$$D\nabla^2\nabla^2 w + kw = p. \tag{3.67}$$

This equation can be solved for rectangular plates by the classical methods discussed earlier.

3.7.1 Application of Navier's solution

Let us consider a simply supported rectangular plate of sides $a \times b$ on an elastic foundation (Fig. 3.17). The deflection $w(x, y)$ and a given loading $p(x, y)$ can be expressed in the form of a double trigonometric series in the form of the expressions (3.15), as follows. Substituting the above expressions into the governing differential equation of the problem (3.67), we obtain the unknown amplitudes of the deflections, w_{mn}, for a specific set of m and n values, as follows:

$$w_{mn} = \frac{p_{mn}}{D\pi^4\left(m^2/a^2 + n^2/b^2\right)^2 + k}, \tag{3.68}$$

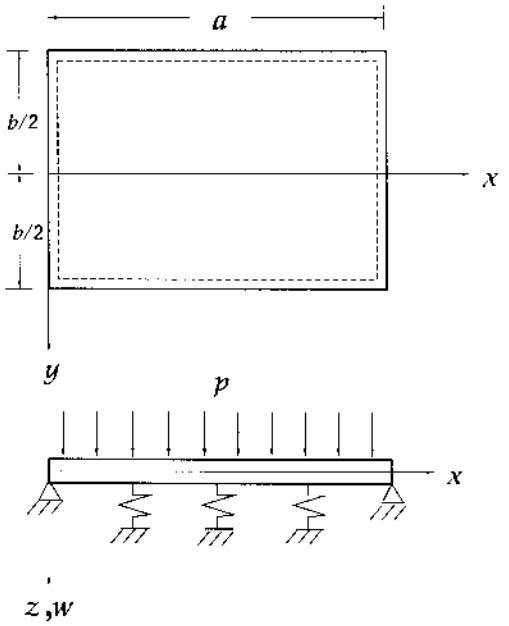

Fig. 3.17

which substituted into Eq. (3.15a) yields

$$w(x,y)=\sum_{n=1}^{\infty}\sum_{m=1}^{\infty}\frac{p_{mn}\sin\dfrac{m\pi x}{a}\sin\dfrac{n\pi y}{b}}{D\pi^4\left(m^2/a^2+n^2/b^2\right)^2+k}. \tag{3.69}$$

If a plate is subjected to a uniform load of intensity p_0, then Eq. (3.69) becomes

$$w=\frac{16p_0}{\pi^2}\sum_{n=1}^{\infty}\sum_{m=1}^{\infty}\frac{\sin\dfrac{m\pi x}{a}\sin\dfrac{n\pi y}{b}}{mn\left[\pi^4 D(m^2/a^2+n^2/b^2)^2+k\right]}. \tag{3.70}$$

If a plate is loaded by a concentrated force P applied at a point (ξ,η), then the deflected surface equation of the plate can be represented by the following form:

$$w=\frac{4P}{ab}\sum_{n=1}^{\infty}\sum_{m=1}^{\infty}\frac{\sin\dfrac{m\pi\xi}{a}\sin\dfrac{n\pi\eta}{b}}{\pi^4 D(m^2/a^2+n^2/b^2)^2+k}\sin\frac{m\pi x}{a}\sin\frac{n\pi y}{b}. \tag{3.71}$$

Having the deflection of the plate produced by a concentrated force, the deflection produced by any kind of lateral loading is obtained by the method of superposition.

3.7.2 Application of Levy's method

If any two opposite edges of the plate on an elastic foundation are simply supported, say, the edges $x=0$ and $x=a$, then Levy's solution presented earlier in Sec. 3.5 can be applied advantageously. The general solution of the governing differential equation of the plate on an elastic foundation, Eq. (3.67), may be represented again in the form of the sum of particular and complementary solutions, i.e.,

$$w=w_{\mathrm{p}}+w_{\mathrm{h}}. \tag{3.72}$$

Expressing the complementary solution by the Fourier series, yields

$$w_{\mathrm{h}}=\sum_{m=1}^{\infty}f_m(y)\sin\frac{m\pi x}{a}. \tag{3.73}$$

Substituting the above into the homogeneous part of Eq. (3.66) and solving it for $f_m(y)$, we obtain

$$\begin{aligned}f_m(y)=&A_m\sinh\alpha_m y\sin\beta_m y+B_m\sinh\alpha_m y\cos\beta_m y+C_m\cosh\alpha_m y\sin\beta_m y\\&+D_m\cosh\alpha_m y\cos\beta_m y,\end{aligned} \tag{3.74}$$

where

$$\alpha_m=\sqrt{\frac{1}{2}\left(\frac{m^2\pi^2}{a^2}+\sqrt{\frac{m^4\pi^4}{a^4}+\frac{k}{D}}\right)};\quad \beta_m=\sqrt{\frac{1}{2}\left(-\frac{m^2\pi^2}{a^2}+\sqrt{\frac{m^4\pi^4}{a^4}+\frac{k}{D}}\right)}. \tag{3.75}$$

Substituting (3.74) into (3.73), we can obtain the expression for complementary solution w_{h}. Similarly, if we express the particular solution as

$$w_p = \sum_{m=1}^{\infty} g_m(y) \sin \frac{m\pi x}{a}, \tag{3.76}$$

and the applied load as

$$p = \sum_{m=1}^{\infty} p_m(y) \sin \frac{m\pi x}{a}, \tag{3.77}$$

and then we substitute these equations into Eq. (3.66), we obtain

$$\frac{\mathrm{d}^4 g_m}{\mathrm{d}y^4} - 2\left(\frac{m\pi}{a}\right)^2 \frac{\mathrm{d}^2 g_m}{\mathrm{d}y^2} + \left(\frac{m^4\pi^4}{a^4} + \frac{k}{D}\right) g_m = \frac{p_m(y)}{D}. \tag{3.78}$$

Solving Eq. (3.78) for g_m, we can find the particular solution w_{p}. Therefore, Eq. (3.76) together with Eqs (3.73) and (3.74) describes the deflected surface of the plate.

Example 3.8

Find the equation for the deflection of a rectangular plate, resting on a Winkler foundation of modulus k and subjected to a uniform loading of intensity p_0. Assume that edges $x = 0$ and $x = a$ are simply supported while edges $y = \pm b/2$ are fixed.

Solution

For a uniform loading p, the right-hand side of Eq. (3.66) is constant. Thus, the particular solution is also a constant and may be taken in the following form:

$$g_m = B, \tag{a}$$

and the expression for p_m is given by (see Table 3.2)

$$p_m = \frac{4p_0}{m\pi}. \tag{b}$$

Substitution of (a) and (b) into Eq. (3.78) results in the following particular solution:

$$g_m = \frac{4p_0}{Dm\pi} \frac{1}{\left(\frac{m^4\pi^4}{a^4} + \frac{k}{D}\right)}. \tag{c}$$

Due to the symmetry of the deflection around the x axis, we can take $B_m = C_m = 0$ in Eq. (3.74) and the general solution for deflection becomes

$$w = \sum_{m=1}^{\infty} (A_m \sinh \alpha_m y \sin \beta_m y + D_m \cosh \alpha_m y \cos \beta_m y + g_m) \sin \frac{m\pi x}{a}, \tag{3.79}$$

where A_m and $B_m$are constants of integration. They have to be evaluated from the boundary conditions on the edges $y = \pm b/2$; namely,

$$w = 0|_{y=\pm b/2}, \frac{\partial w}{\partial y} = 0\Big|_{y=\pm b/2}: \tag{d}$$

Substituting the expressions (3.79) into these boundary conditions, gives

$$A_m = \frac{g_m}{\gamma_1\left(\cosh\alpha_m\frac{b}{2}\cos\beta_m\frac{b}{2}\right)}; \quad D_m = -A_m\tanh\alpha_m\frac{b}{2}\tanh\beta_m\frac{b}{2} - \frac{g_m}{\cosh\alpha_m\frac{b}{2}\cos\beta_m\frac{b}{2}} \tag{e}$$

where

$$\gamma_1 = \frac{\gamma_2+\gamma_3}{\gamma_4-\gamma_5} - \tanh\alpha_m\frac{b}{2}\tanh\beta_m\frac{b}{2};$$
$$\gamma_2 = \alpha_m\cosh\alpha_m\frac{b}{2}\sin\beta_m\frac{b}{2},\ \gamma_3 = \beta_m\sinh\alpha_m\frac{b}{2}\cos\beta_m\frac{b}{2}; \tag{f}$$
$$\gamma_4 = \alpha_m\sinh\alpha_m\frac{b}{2}\cos\beta_m\frac{b}{2},\ \gamma_5 = \beta_m\cosh\alpha_m\frac{b}{2}\sin\beta_m\frac{b}{2}.$$

Substituting the above into expression (3.79), we can obtain the deflection equation for the plate under consideration.

The Winkler model introduced above is the simplest model of an elastic foundation. It was based on the assumption that the subgrade of a foundation at some point of its surface is proportional to the pressure between the plate and the subgrade at the same point. This is correct in the case of a floating plate, but in the case of a coherent subgrade such a hypothesis approximates crudely the actual behavior of the subgrade. A better approximation can be obtained using the model of a semi-infinite elastic space, as shown in Fig. 3.18; the deflection of a semi-infinite space surface due to the distributed loads can be determined with the use of Boussinesq's solution [13]. So, the deflection at a point (x_i, y_i) of the semi-infinite space surface caused by an elementary distributed load $q\mathrm{d}x\mathrm{d}y$ applied at point (x, y) using the Boussinesq solution can be represented in the following form:

$$\mathrm{d}w_i = K[(x-x_i),(y-y_i)]q\mathrm{d}x\mathrm{d}y,$$

where $K[\ ]$ is an influence function (or Green's function). It represents a deflection at point (x_i, y_i) of a semi-infinite space caused by a unit force $P = 1$ applied at point (x, y). This function $K[\ldots]$ can be derived from Boussinesq's solution. Then, an

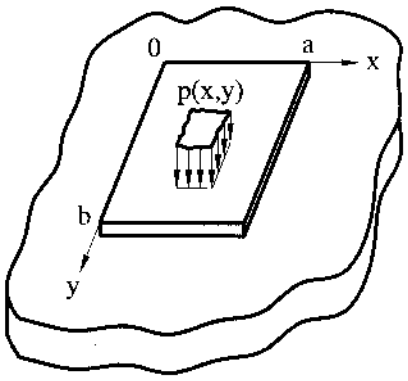

Fig. 3.18

arbitrary reaction load $q(x, y)$ occurring over a plate base causes the following deflection at point (x_i, y_i):

$$w(x_i, y_i) = \int_0^a \int_0^b K[(x - x_i), (y - y_i)]q(x, y)\mathrm{d}x\mathrm{d}y. \tag{3.80}$$

The above-mentioned function $K[\ldots]$ is given by the following [13]:

$$K[\ldots] = \frac{1 - \nu^2}{\pi E}\frac{1}{r}, \tag{3.81}$$

where r is the distance between the point of load application (x, y) and point of observation (x_i, y_i), $r^2 = (x - x_i)^2 + (y - y_i)^2$. With regard to expression (3.81) and replacing a unit force by $q\mathrm{d}x\mathrm{d}y$, Eq. (3.80) may be rewritten as

$$w(x_i, y_i) = \frac{1 - \nu^2}{\pi E}\int_0^a \int_0^b \frac{q(x, y)\mathrm{d}x\mathrm{d}y}{\sqrt{(x - x_i)^2 + (y - y_i)^2}}. \tag{3.82}$$

For this model, the relationship between the deflection of the foundation w and the foundation reaction q is much more complicated than for the Winkler model. Thus, the problem of bending of a plate resting on a semi-infinite space becomes more difficult. In the majority of cases, such plate bending problems can be solved numerically only.

3.8 PLATES WITH VARIABLE STIFFNESS

Let us consider bending of a rectangular plate having a variable thickness, $h = h(x, y)$. We assume that the above thickness varies gradually and there is no abrupt variation in thickness so that the expressions for the bending and twisting moments derived earlier for plates of constant thickness, Eqs (2.13), apply with sufficient accuracy to this case also. Substituting the above equations for the bending and twisting moments into the equation of static equilibrium (2.23) and taking into account that $D = D(x, y)$. One obtains the following:

$$\begin{aligned} D\nabla^2\nabla^2 w + 2\frac{\partial D}{\partial x}\frac{\partial}{\partial x}(\nabla^2 w) + 2\frac{\partial D}{\partial y}\frac{\partial}{\partial y}(\nabla^2 w) + \nabla^2 D(\nabla^2 w) \\ - (1 - \nu)\left(\frac{\partial^2 D}{\partial x^2}\frac{\partial^2 w}{\partial y^2} - 2\frac{\partial^2 D}{\partial x \partial y}\frac{\partial^2 w}{\partial x \partial y} + \frac{\partial^2 D}{\partial y^2}\frac{\partial^2 w}{\partial x^2}\right) = p. \end{aligned} \tag{3.83}$$

This is the governing fourth-order partial differential equation with variable coefficients in w describing the bending of thin plates with variable thickness. A closed-form solution of this equation is possible in very special cases only. Practically, plates of variable thickness can be treated by approximate and numerical methods introduced in Chapter 6. Among them, the variational (the Ritz method) and finite element methods are widely used in practice. Analysis of plates with variable thickness can be efficiently carried out by the small parameter method [3]. Let us illustrate an application of this method to rectangular plates of variable stiffness.

For simplicity, assume that the plate stiffness varies in one direction only, say, in the y direction. So, the plate thickness, h, varies according to the law

$$h = h_0[1 + \lambda\Phi(y)], \tag{3.84}$$

where λ is a constant and is in the range $0 < \lambda < 1$, $\Phi(y)$ is a given function describing a variation of the plate thickness over the y cordinate, and h_0 is some reference plate thickness.

Thus,

$$D = \frac{E[h(y)]^3}{12(1-\nu^2)} = D_0[1 + \lambda\Phi(y)]^3; \quad D_0 = \frac{Eh_0^3}{12(1-\nu^2)}. \tag{3.85}$$

The small parameter method introduces the value λ as a parameter of a solution of the given problem. Considering the deflection as a function of x, y, and λ, represent $w(x, y, \lambda)$ in the form

$$w = \sum_{m=0}^{\infty} w_m \lambda^m, \tag{3.86}$$

where $w_m = w_m(x, y)$. Substituting the expressions (3.85) and (3.86) into Eq. (3.83) and equating the coefficients for identical powers of λ to zero, we obtain the following sequence of differential equations:

$$\begin{aligned}
&\nabla^2\nabla^2 w_0 = \frac{p}{D_0},\\
&\nabla^2\nabla^2 w_1 = -3\left\{\Phi(y)\nabla^2\nabla^2 w_0 + 2\Phi'(y)\frac{\partial}{\partial y}\nabla^2 w_0 + \Phi''(y)\left[\nabla^2 w_0 - (1-\nu)\frac{\partial^2 w_0}{\partial x^2}\right]\right\},\\
&\nabla^2\nabla^2 w_2 = -3\left\{\Phi(y)\nabla^2\nabla^2 w_1 + 2\Phi'(y)\frac{\partial}{\partial y}\nabla^2 w_1 + \Phi''(y)\left[\nabla^2 w_1 - (1-\nu)\frac{\partial^2 w_1}{\partial x^2}\right]\right\}\\
&\qquad - 3\left\{[\Phi(y)]^2\nabla^2\nabla^2 w_0 + 4\Phi(y)\Phi'(y)\frac{\partial}{\partial y}\nabla^2 w_0 + 2\right.\\
&\qquad \left.\left[\left(\Phi'(y)\right)^2 + \Phi(y)\Phi''(y)\right]\left[\nabla^2 w_0 - (1-\nu)\frac{\partial^2 w_0}{\partial x^2}\right]\right\},\\
&\qquad \text{etc.}
\end{aligned} \tag{3.87}$$

where the prime notations indicate the derivatives of the function $\Phi(y)$ with respect to y. Assume for simplicity that the plate edges $x = 0$ and $x = a$ are simply supported. Then, following the Levy method, solutions of Eqs (3.87) are sought in the form of the following series:

$$
\begin{aligned}
w_0 &= \sum_{n=1}^{\infty} w_{0n} \sin \frac{n\pi x}{a};\\
w_1 &= \sum_{n=1}^{\infty} w_{1n} \sin \frac{n\pi x}{a};\\
w_2 &= \sum_{n=1}^{\infty} w_{2n} \sin \frac{n\pi x}{a}\\
&\text{etc} \ldots\ldots\ldots\ldots
\end{aligned}
\tag{3.88}
$$

where the coefficients w_{mn} $(m = 0, 1, 2, \ldots)$ are functions of the y only. Expand the given loading in the series also, as follows:

$$
p(x, y) = \sum_{n=1}^{\infty} p_n(y) \sin \frac{n\pi x}{a}. \tag{3.89}
$$

Substituting the first expression (3.88) and Eq. (3.89) into the first equation (3.87) and satisfying the boundary conditions prescribed on the plate edges $y = 0$ and $y = b$, we can determine w_{0n}. Then, substitution of the first and second expressions (3.88) into the second equation (3.87) gives w_{1n}. Similarly, each of the functions w_m can be found by substitution of $w_0, w_1, \ldots, w_{m-1}$ into the corresponding differential equation of the system (3.87) involving w_m into the left-hand side. Finally, the deflection surface of the plate is obtained by substituting for $w_0, w_1, w_2, \ldots, w_m$ from Eqs (3.88) into Eq. (3.86). The interested reader can find an application of this and other methods to plates of variable thickness in Ref. [14].

Example 3.9

A rectangular plate of variable thickness in the y direction is simply supported on edges $x = 0$ and $x = a$ and is fixed on edges $y = 0$ and $y = b$. The plate thickness varies according to the law $h = h_0(1 + \lambda y)$. The plate is subjected to a load $p = p_0 \sin \frac{n\pi x}{a} \sin \frac{m\pi y}{b}$. Find the deflections and bending moments in the plate.

Solution

This problem was solved numerically by using the above-presented general procedure of the small-parameter method. The boundary conditions are found to be as follows:

$$
w = \frac{\partial^2 w}{\partial x^2} = 0 \Big|_{x=0,a}; \; w = \frac{\partial w}{\partial y} = 0 \Big|_{y=0,b}.
$$

For the plate under consideration, $\Phi(y) \equiv y$. The values of the deflection and bending moment M_y at a plate section $x = a/2$ are given in Table 3.3**.** These results were obtained by using the three terms in the expansion (3.86) for a plate with the following geometric and mechanical parameters: $a = b = 1\,\text{m}$; $h_0 = 0.0625\,\text{m}$; $\lambda = 0.5$; and $\nu = 0.3$.

Table 3.3

y(m)	$\frac{w}{p_0/E}$	$M_y\left(\frac{1}{\rho_0}\right)$
0	0	−0.03510
0.2	15.851	0.00561
0.4	30.156	0.02321
0.6	26.04	0.02065
0.8	10.3432	−0.006025
1.0	0	−0.05646

3.9 RECTANGULAR PLATES UNDER COMBINED LATERAL AND DIRECT LOADS

To this point, it was assumed that a plate is bent by lateral load only and deflections are so small that the plate middle surface was assumed to be unstrained. Thus, the latter was considered as a neutral surface. Occasionally, however, direct forces (acting in the plane of the middle surface of the plate) are applied directly at the boundaries or they arise due to temperature changes (Chapter 7). The latter forces and the corresponding stresses are also referred to as the *membrane* or *in-plane forces* and the *membrane* or *in-plane stresses*, respectively.

Attention will now be directed to situations in which lateral and direct forces act on the plate simultaneously. We will distinguish two possible cases:

1. Stresses in the middle surface are small and, therefore, their influence on the plate bending is negligible. So, the total stress may be obtained by adding stresses caused by stretching and by bending of the plate middle surface.
2. Direct stresses are not small and their effect on the plate bending should be taken into account. These stresses may have a considerable effect on the bending of the plate and must be considered in deriving the corresponding differential equation of the deflection surface. The midsurface is strained subsequent to combined loading and assumption 6 of the Kirchhoff theory (see Sec. 1.3) is no longer valid. However, w is still regarded as small so that remaining assumptions of Sec. 1.3 hold, and yet large enough so that the products of the direct forces or their derivatives and the derivatives of w are of the same order of magnitude as the derivatives of the shear forces, Q_x and Q_y. Thus, as before, the internal forces and moments are given by Eqs (2.13) and (2.27).

We consider below the second case in detail. Let a plate element of sides dx and dy be subjected to direct forces N_x, N_y, and $N_{xy} = N_{yx}$ which are functions of x and y. The top and front views of such an element are shown in Fig. 3.19a and b, respectively. The lateral load of intensity $p(x, y)$ is applied to the element and the moments, due to this load, acting on the element are shown in Fig. 2.4. We will derive the differential equation of the plate straining due to the combined effect of direct and lateral loads.

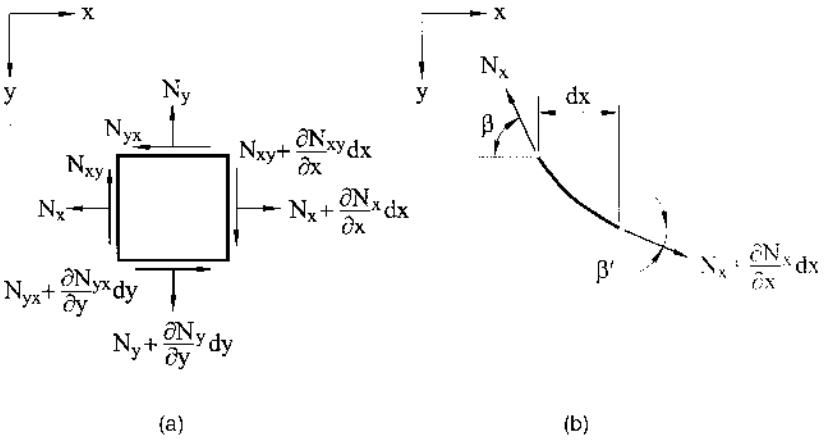

Fig. 3.19

Consider the equilibrium of the element shown in Fig. 3.19, which is subjected to the in-plane forces N_x, N_y, and N_{xy}, as well as to the lateral load $p(x, y)$. First, we apply the condition $\sum F_x = 0$. Referring to Fig. 3.19a, from the equilibrium of $N_x dy$ forces into the x-direction, we obtain the following:

$$\left(N_x + \frac{\partial N_x}{\partial x}dx\right)dy\cos\beta' - N_x dy\cos\beta, \tag{a}$$

where $\beta' = \beta + d\beta = \beta + \frac{\partial\beta}{\partial x}dx$. Noting that deflections are assumed to be very small and, hence, for β small $\cos\beta \approx 1$, and that likewise, $\cos\beta' \approx 1$, Eq. (a) reduces to $\frac{\partial N_x}{\partial x}dxdy$. The sum of the x components of $N_{xy}dx$ is treated in a similar way. Thus, the force summation in the x direction leads to

$$\frac{\partial N_x}{\partial x} + \frac{\partial N_{xy}}{\partial y} = 0. \tag{3.90a}$$

Furthermore, the condition $\sum F_y = 0$ results in the following:

$$\frac{\partial N_{xy}}{\partial x} + \frac{\partial N_y}{\partial y} = 0. \tag{3.90b}$$

Equations (3.90) are independent from the equilibrium equations of Sec. 2.3 and may be studied separately.

Considering the projection of all the forces (direct and lateral) on the z axis, the plate deflection must be taken into account. Due to the bending of the plate in the xz plane, the z component of the normal force N_x is equal to (Fig. 3.19b)

$$-N_x dy\sin\beta + \left(N_x + \frac{\partial N_x}{\partial x}dx\right)dy\sin\beta' \tag{b}$$

Inasmuch as β and β' are small, $\sin\beta \approx \beta \approx \partial w/\partial x$ and $\sin\beta' \approx \beta'$, where $\beta' = \beta + d\beta$. The latter can be represented as

$$\beta' \approx \beta + \frac{\partial\beta}{\partial x}dx = \frac{\partial w}{\partial x} + \frac{\partial^2 w}{\partial x^2}dx;$$

substituting the above into Eq. (b) gives

$$-N_x \mathrm{d}y \frac{\partial w}{\partial x} + \left(N_x + \frac{\partial N_x}{\partial x}\mathrm{d}x\right)\left(\frac{\partial w}{\partial x} + \frac{\partial^2 w}{\partial x^2}dx\right)\mathrm{d}y.$$

Neglecting higher-order terms in this equation yields

$$N_x \frac{\partial^2 w}{\partial x^2}\mathrm{d}x\mathrm{d}y + \frac{\partial N_x}{\partial x}\frac{\partial w}{\partial x}\mathrm{d}x\mathrm{d}y.$$

The z components of the in-plane shear forces N_{xy} on the x edges of the element are determined as follows. The slopes of the deflection surface in the y direction on the x edges are equal to $\partial w/\partial y$ and $\partial w/\partial y + (\partial^2 w/\partial x \partial y)\mathrm{d}x$, respectively. The z directed component of N_{xy}i s then

$$N_{xy}\frac{\partial^2 w}{\partial y \partial x}\mathrm{d}x\mathrm{d}y + \frac{\partial N_{xy}}{\partial x}\frac{\partial w}{\partial y}\mathrm{d}x\mathrm{d}y.$$

An expression identical to the above is found for the z projection of the in-plane shear forces N_{yx} acting on the y edges:

$$N_{yx}\frac{\partial^2 w}{\partial x \partial y}\mathrm{d}x\mathrm{d}y + \frac{\partial N_{yx}}{\partial y}\frac{\partial w}{\partial x}\mathrm{d}x\mathrm{d}y.$$

Finally, for the forces in Figs 3.19 and 2.4, from $\sum F_z = 0$, we have the following:

$$\frac{\partial Q_x}{\partial x} + \frac{\partial Q_y}{\partial y} + p + N_x\frac{\partial^2 w}{\partial x^2} + N_y\frac{\partial^2 w}{\partial y^2} + 2N_{xy}\frac{\partial^2 w}{\partial x \partial y}$$

$$+ \left(\frac{\partial N_x}{\partial x} + \frac{\partial N_{yx}}{\partial y}\right)\frac{\partial w}{\partial x} + \left(\frac{\partial N_{xy}}{\partial x} + \frac{\partial N_y}{\partial y}\right)\frac{\partial w}{\partial y} = 0.$$

As is seen from Eqs (3.90), the terms within the parentheses in the above expression vanish and we finally obtain the above equation in the following form:

$$\frac{\partial Q_x}{\partial x} + \frac{\partial Q_y}{\partial y} + p + N_x\frac{\partial^2 w}{\partial x^2} + N_y\frac{\partial^2 w}{\partial y^2} + 2N_{xy}\frac{\partial^2 w}{\partial x \partial y} = 0. \tag{3.91}$$

As the direct forces do not result in any moment along the edges of the element, Eqs (2.20) and (2.21), and, hence Eqs (2.27) are unchanged. Introduction of Eqs. (2.27) into Eq. (3.91), yields

$$\frac{\partial^4 w}{\partial x^4} + 2\frac{\partial^4 w}{\partial x^2 \partial y^2} + \frac{\partial^4 w}{\partial y^4} = \frac{1}{D}\left(p + N_x\frac{\partial^2 w}{\partial x^2} + N_y\frac{\partial^2 w}{\partial y^2} + 2N_{xy}\frac{\partial^2 w}{\partial x \partial y}\right). \tag{3.92}$$

Expressions (3.91) and (3.92) are *governing differential equations for a thin plate subjected to combined lateral and direct loads*. It is observed that Eq. (2.24) is now replaced by Eq. (3.92) to determine the deflection surface of the plate if the direct loads N_x, N_y, and N_{xy} are not small. Either Navier's or Levy's methods may be applied to obtain a solution.

Example 3.10

A rectangular plate with simply supported edges is subjected to the action of a combined uniform lateral load p and uniform tension N as shown in Fig. 3.20. Derive the equation of the deflection surface.

Solution

The lateral load p can be represented by the double trigonometric series (Eq. (a) of Example 3.1)

$$p = \frac{16p_0}{\pi^2} \sum_{m=1,3,5,\ldots}^{\infty} \sum_{n=1,3,5,\ldots}^{\infty} \frac{1}{mn} \sin\frac{m\pi x}{a} \sin\frac{n\pi y}{b}. \tag{a}$$

Inserting the above into Eq. (3.92), we obtain the following (letting $N_x = N$):

$$\frac{\partial^4 w}{\partial x^4} + 2\frac{\partial^4 w}{\partial x^2 \partial y^2} + \frac{\partial^4 w}{\partial y^4} - \frac{N}{D}\frac{\partial^2 w}{\partial x^2} = \frac{16p_0}{\pi^2} \sum_{m=1,3,5,\ldots}^{\infty} \sum_{n=1,3,5,\ldots}^{\infty} \frac{1}{mn} \sin\frac{m\pi x}{a} \sin\frac{n\pi y}{b}. \tag{b}$$

The boundary conditions of a simply supported plate will be satisfied if we take the deflection w in the form of series

$$w = \sum_m \sum_n w_{mn} \sin\frac{m\pi x}{a} \sin\frac{n\pi y}{b}. \tag{c}$$

Substituting this series into Eq. (b), we find the following values for coefficients w_{mn}:

$$w_{mn} = \frac{16p_0}{D\pi^6 mn\left[\left(m^2/a^2 + n^2/b^2\right)^2 + \dfrac{Nm^2}{\pi^2 Da^2}\right]}; \quad m, n = 1, 3, 5, \ldots. \tag{d}$$

Hence, the deflection surface of the plate is given by

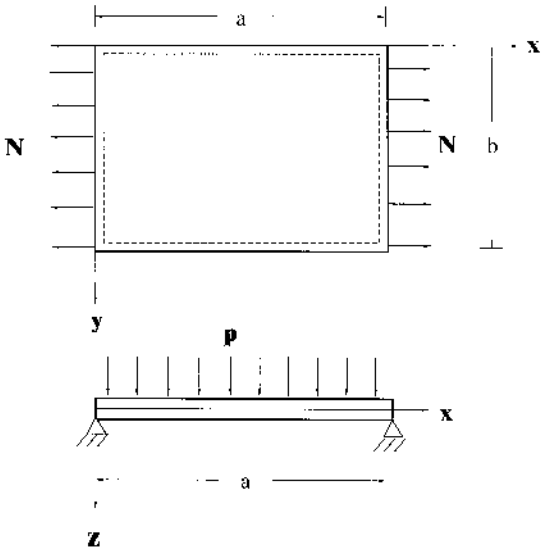

Fig. 3.20

$$w = \frac{16p_0}{\pi^6 D} \sum_{m=1,3,5,\ldots}^{\infty} \sum_{n=1,3,5,\ldots}^{\infty} \frac{\sin\dfrac{m\pi x}{a} \sin\dfrac{n\pi y}{b}}{mn\left[\left(m^2/a^2 + n^2/b^2\right)^2 + \dfrac{Nm^2}{\pi^2 Da^2}\right]}. \tag{e}$$

Comparing this result with the solution (3.21a), we conclude from the presence of the term $Nm^2/\pi^2 Da^2$ in the brackets of the denominator that the deflection of the plate is somewhat diminished by the action of the tensile forces N. This is as would be expected.

3.10 BENDING OF PLATES WITH SMALL INITIAL CURVATURE

Let us assume that a plate has an initial curvature of its middle surface, i.e., there is an initial deflection w_0 at any point of the above surface. It is assumed that w_0 is small compared with the plate thickness. If the plate is subject to lateral load and then an additional deflection w_1 occurs, the total deflection is thus

$$w = w_0 + w_1. \tag{3.93}$$

Here w_1 is the solution of Eq. (2.24) set up for the flat plate, i.e., without the above-mentioned initial deflection. It will be valid if the small initial deflection, w_0, is considered as a result of the action of some fictitious lateral load. Then, applying the superposition principle (recall that the above principle cannot be applied for large deflections), it is possible to determine the total deflection.

If besides the lateral load, the direct forces are also applied to an initially curved plate, then these forces produce bending also, which depends not only on w_1 but also on w_0. In order to determine the total deflection, w, we introduce $w = w_0 + w_1$ into the right hand side of Eq. (3.92). The left-hand side of this equation takes into account a change in curvature from the initial curved state due to the given lateral load. Therefore, w_1 has to be substituted for w on the left-hand side of Eq. (3.92). Thus, Eq. (3.92) for the initially curved plate is of the following form:

$$\frac{\partial^4 w_1}{\partial x^4} + 2\frac{\partial^4 w_1}{\partial x^2 \partial y^2} + \frac{\partial^4 w_1}{\partial y^4} = \frac{1}{D}\left[p + N_x \frac{\partial^2 (w_0 + w_1)}{\partial x^2} + N_y \frac{\partial^2 (w_0 + w_1)}{\partial y^2} + 2N_{xy} \frac{\partial^2 (w_0 + w_1)}{\partial x \partial y}\right]. \tag{3.94}$$

As mentioned previously, the influence of the initial curvature on the total deflection of the plate is equivalent to the influence of some fictitious lateral load of intensity p_f equal to

$$p_f = N_x \frac{\partial^2 w_0}{\partial x^2} + N_y \frac{\partial^2 w_0}{\partial y^2} + 2N_{xy} \frac{\partial^2 w_0}{\partial x \partial y}. \tag{3.95}$$

Hence, an initially curved plate will experience a bending under action of the direct forces, lying in the plate middle surface only.

Example 3.11

Consider a simply supported plate with sides a and b. Assume that the initial deflection is defined by the following equation:

$$w_0 = \alpha_{11} \sin\frac{\pi x}{a} \sin\frac{\pi y}{b}. \tag{a}$$

The plate edges $x = 0$ and $x = a$ are subjected to an in-plane uniform compressive force $N_x = -N$, as shown in Fig. 3.21. Find the deflected surface of the plate.

Solution

The differential equation (3.94) together with Eq. (a) will take the following form for the problem under consideration:

$$\frac{\partial^4 w_1}{\partial x^4} + 2\frac{\partial^4 w_1}{\partial x^2 \partial y^2} + \frac{\partial^4 w_1}{\partial y^4} = \frac{N}{D}\left(\frac{\alpha_{11}\pi^2}{a^2} \sin\frac{\pi x}{a} \sin\frac{\pi y}{b} - \frac{\partial^2 w_1}{\partial x^2}\right). \tag{b}$$

Let us represent a solution of the above equation in the form

$$w_1 = A \sin\frac{\pi x}{a} \sin\frac{\pi y}{b}, \tag{c}$$

where A is unknown parameter. This solution satisfies exactly the simply supported boundary conditions. Inserting Eq. (c) into Eq. (b) yields

$$A = \frac{\alpha_{11} N}{\frac{\pi^2 D}{a^2}\left(1 + \frac{a^2}{b^2}\right)^2 - N}. \tag{d}$$

Substituting for A from Eq. (d) into Eq. (c), one obtains the deflection w_1, caused by the compressive forces N. Adding this deflection to the initial deflection (a), gives the following total deflection of the plate:

$$w = w_0 + w_1 = \frac{\alpha_{11}}{1 - \beta} \sin\frac{\pi x}{a} \sin\frac{\pi y}{b}, \tag{e}$$

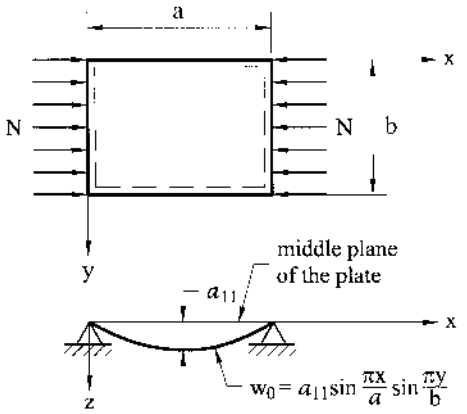

Fig. 3.21

where

$$\beta = \frac{N}{\frac{\pi^2 D}{a^2}\left(1+\frac{a^2}{b^2}\right)^2}. \tag{f}$$

The maximum deflection occurs at the plate center. Setting $x = a/2$ and $y = b/2$, we obtain

$$w_{\max} = \frac{\alpha_{11}}{1-\beta}. \tag{g}$$

In general case, a given initial deflection of the plate can be expanded into the following Fourier series:

$$w_0 = \sum_{m=1,3,\ldots}^{\infty} \sum_{n=1,3,\ldots}^{\infty} \alpha_{mn} \sin\frac{m\pi x}{a} \sin\frac{n\pi y}{b} \tag{h}$$

Substituting the above into Eq. (b) and solving yields

$$w_1 = \sum_{m=1,3,\ldots}^{\infty} \sum_{n=1,3,\ldots}^{\infty} b_{mn} \sin\frac{m\pi x}{a} \sin\frac{n\pi y}{b}, \tag{i}$$

where

$$b_{mn} = \frac{\alpha_{mn} N}{\frac{\pi^2 D}{a^2}\left(m+\frac{n^2 a^2}{m^2 b^2}\right)^2 - N}. \tag{k}$$

As follows from Eq. (k), the coefficients b_{mn} are increased with an increase of the force N.

To write the equation for a plate subjected to initial deflection and to in-plane uniform tensile forces, it is required to change the sign of N in Eq. (b) of the foregoing example only. By following the approach described above, the deflection of an initially curved plate subjected to a simultaneous action of in-plane forces N_x, N_y, and N_{xy}may also be readily obtained.

PROBLEMS

3.1 A rectangular plate with sides a and b ($0 \le x \le a$, $0 \le y \le b$) is bent according to the following equation $w = C \sin \pi x/a \sin \pi y/b$. Clarify the type of loading and static boundary conditions that correspond to the given deflection surface.

3.2 Given the deflection surface of the rectangular plate with sides a and b ($0 \le x \le a$, $0 \le y \le b$) in the form $w = Axy(x-a)(y-b)$, specify the type of loading and kinematic boundary conditions corresponding to the given deflection surface of the plate.

3.3 A square plate is subjected to uniformly distributed twisting moments $M_{xy} = M_{yx}$ applied to all its four edges. Determine the expression for the deflection surface.

3.4 Formulate the conditions under which a cylindrical bending can occur.

3.5 A rectangular plate of sides a and b is subjected to uniformly distributed bending moments m applied to all four edges of the plate (see Fig. 3.2, where $m_1 = m_2 = m$). Its curved middle surface should present a portion of a sphere because the radii of curvature are identical in all planes and at all points of the plate. However, as follows

from Eq. (3.11), the deflection surface of the above plate under the given moment loading m represents a paraboloid of revolution. Explain this discrepancy.

3.6 Consider a simply supported plate with sides a and b ($0 \le x \le a$, $0 \le y \le b$). If the applied load is represented by Eq. (3.15b) find the expressions for the coefficients p_{mn} for the following load distributions:

- **(a)** hydrostatic pressure given by the law $p(x, y) = p_0 x/a$;
- **(b)** uniform line load p_0 distributed over the line $x = \xi$;
- **(c)** uniform load p_0 distributed over a half of the rectangular plate middle surface, i.e., $0 \le \xi \le a/2$ and $0 \le \eta \le b$, where ξ and η are coordinates of a point of application of applied loading.

3.7 A steel door 2 m long, 1.2 m wide, and 20 mm thick is subjected is subjected to a uniform pressure p_0. The plate is simply supported at all edges. Using the Navier approach and retaining only the first four terms in the series expansion, determine: (a) the limiting value of p_0 that can be applied to the plate without causing yielding; (b) the maximum deflection w and bending moments M_x and M_y that would be produced when the pressure reaches its limiting value. Use $E = 210\,\text{GPa}$, $\nu = 0.3$, $\sigma_{YS} = 240\,\text{MPa}$

3.8 A rectangular wall panel is subjected to a uniform patch load of intensity p_0. The plate is regarded as simply supported (Fig. 3.6). Using the Navier approach and retaining the first four terms in the series solution, determine: (a) the maximum deflection w; (b) the maximum bending moment M_x. Take $a = b = 2\,\text{m}$, $h = 2 \times 10^{-2}\,\text{m}$, $\xi = \eta = a/2$, $u = v = 0.5\,\text{m}$, $v = 0.3$, $E = 200$ GPa. Express w and M_x in terms of p_0.

3.9 Consider a simply supported square plate with side a and subjected to a concentrated load P applied at its center (Fig. 3.7). Find the corner points and indicate their directions.

3.10 Verify Eq. (3.36).

3.11 A semi-infinite plate-strip ($0 \le y < \infty$) is simply supported on the edges $x = 0$ and $x = a$. The edge $y = 0$ is given by the following displacement and rotation:

$$w(x, 0) = A \sin \frac{\pi x}{a}; \quad \frac{\partial w}{\partial y}(x, 0) = B \sin \frac{\pi x}{a}.$$

Determine the bending moment M_y and the effective shear force V_y on the edge $y = 0$.

3.12 An infinite plate-strip ($-\infty < y < \infty$) is simply supported at $x = 0$ and $x = a$. A uniform line load q acts along the line $y = 0$. Determine the deflection w and bending moment M_y at the plate center, $x = a/2$, $y = 0$.

3.13 Consider a rectangular plate with two opposite sides ($x = 0$ and $x = a$) simply supported; the third edge ($y = 0$) is built-in, and the fourth edge ($y = b$) free. The plate is subjected to a uniform pressure of intensity p_0. Retaining only the first two terms of the Levy's solution, determine the deflection at the midpoint of the free edges and the bending moments at the midpoint of the clamped edge. Take $a = 2\,\text{m}$, $b = 3.5\,\text{m}$, $h = 0.15\,\text{m}$, $E = 210\,\text{GPa}$, $\nu = 0.3$.

3.14 A rectangular plate with two opposite sides $y = \pm b/2$ fixed and the sides $x = 0$ and $x = a$ simply supported is subjected to a hydrostatic loading, as shown in row 2 of Table 3.2. Derive the expressions for the deflections w and the reactional bending moments M_y along the clamped edges $y = \pm b/2$.

3.15 Consider a simply supported rectangular plate $0 \le x \le a$ and $0 \le y \le b$. The plate is loaded by the edge moments m_x along the edges $x = 0$ and $x = a$ and the edge moment m_y along the edges $y = 0$ and $y = b$. Applying the Levy approach, derive the expression for the deflection surface w.

3.16 Consider a three-span simply supported continuous plate shown in Fig. 3.15. The second span is subjected to a uniform load of intensity p_0. Draw the diagrams of the

deflections and bending moments along the central section $y = a$. Take $a = 1\,\text{m}$, $h = 10\,\text{mm}$, $E = 200\,\text{GPa}$, $\nu = 0.3$, $p_0 = 25\,\text{MPa}$.

3.17 A rectangular plate with two simply supported edges $x = 0$ and $x = a$ and two clamped edges $y = \pm b/2$ rests on an elastic foundation of the Winkler type. The plate is subjected to a uniform lateral surface load p_0. Determine the maximum deflection, $w_{\max}$, and the maximum bending moment, M_y, at the clamped edges. Take $a = 1.5\,\text{m}$, $b = 2.0\,\text{m}$, $h = 12\,\text{mm}$, $p_0 = 20\,\text{MPa}$, $k = 1.04\ \text{MPA/m}$, $E = 210\,\text{GPa}$, $\nu = 0.3$.

3.18 A rectangular plate has a small initial deviation of the middle surface $w_{\text{i}}(x, y)$. The plate is subjected to a lateral surface load p and in-plane forces N_x, N_y, and N_{xy}. Show that the governing differential equation of that initially curved plate under the above load and forces has the form

$$\frac{\partial^4 w_1}{\partial x^4} + 2\frac{\partial^4 w_1}{\partial x^2 \partial y^2} + \frac{\partial^4 w_1}{\partial y^4} = \frac{1}{D}\left[p + N_x.\frac{\partial^2 (w_{\text{i}} + w_1)}{\partial x^2} + 2N_{xy}\frac{\partial^2 (w_{\text{i}} + w_1)}{\partial x \partial y} + .N_y \frac{\partial^2 (w_{\text{i}} + w_1)}{\partial y^2}\right] \tag{P3.1}$$

3.19 A simply supported rectangular plate with sides a and b ($0 \le x \le a$, $0 \le y \le b$) has an initial deflection $w_{\text{i}} = C \sin\frac{\pi x}{a}\sin\frac{\pi y}{b}$ and uniform in-plane compression forces N_x applied to the edges $x = 0$ and $x = a$. With reference to Eq. (P3.1), show that the deflection surface of that plate is given by

$$w_1 = w_{\text{i}} + w_1 = \frac{C}{1-\alpha}\sin\frac{\pi x}{a}\sin\frac{\pi y}{b}, \text{ where } \alpha = \frac{N_x}{\pi^2 D/a^2\left(1 + a^2/b^2\right)_x}.$$

3.20 Verify Eqs (3.87).

3.21 A simply supported rectangular plate with sides a and b has an initial deflection $w_0(x, y)$, defined by Eq. (a) in Example 3.11. The plate is subject to uniform biaxial compressive forces N_x and N_y. Determine the maximum deflection for $a = b$ and $N_x = N_y = -N$.

3.22 A flat plate is subjected to lateral distributed load p and direct (in-plane) forces N_x, N_y, and N_{xy}. In addition, body forces F_x and F_y act in the middle plane of the plate. Show that the governing differential equation for deflections becomes

$$\nabla^2\nabla^2 w = \frac{1}{D}\left(p + N_x\frac{\partial^2 w}{\partial x^2} + N_y\frac{\partial^2 w}{\partial y^2} + 2N_{xy}\frac{\partial^2 w}{\partial x \partial y} - F_x\frac{\partial w}{\partial x} - F_y\frac{\partial w}{\partial y}\right). \tag{P3.2}$$

REFERENCES

1. Navier, C.L.M.N., *Bulletin des Science de la Societe Philomarhique de Paris*, 1823.
2. Kantorovich, L.V. and Krylov, V.I., *Approximate Methods of Higher Analysis*, John Wiley and Sons, New York, 1958.
3. Timoshenko, S.P. and Woinowski-Krieger, S., *Theory of Plates and Shells*, 2nd edn, McGraw-Hill, New York, 1959.
4. Gradshtein, I.S. and Ryzhik, I.M., *Table of Integrals, Series, and Products*, Academic Press, New York, 1980.
5. Lukasiewitz, S., *Local Loads in Plates and Shells*, Warszawa Noordhoff International Publishing, Leyden, 1979.
6. Ventsel, ES., *On One Approach of Construction of Green's Functions for Some Boundary Value Problems of the Theory of Plates and Shallow Shells*, Kharkov State University, Ukr. NIINTI, No. 2997-Ukr. 89, 1989 (in Russian).

7. Melnikov, Yu.A., *Green's Functions in Applied Mechanics*, Computational Mechanics Publications, Southampton, UK, and Boston, USA, 1995.
8. Levy, M., Memoire sur la theorie des plaques elastiques planes, *J Math Pures Appl*, vol. 3, p. 219 (1899).
9. Flugge, W. (ed.), *Handbook of Engineering Mechanics*, McGraw-Hill, New York, 1975.
10. Ponomarev, S.D. (ed.), *Stress Analyses in Mechanical Engineering*, Gos Nauchno-Tekh Izd-vo Mashinostr Lit-ry, Moscow, 1958 (in Russian).
11. Winkler, E., *Die Lehre von der Elastizität und Festigkeit*, Prague, 1867.
12. Hetenyi, M., *Beams on Elastic Foundation*, The University of Michigan Press, Ann Arbor, 1961.
13. Vlasov, V.Z. and Leont'ev, N.N., *Beams, Plates, and Shells on Elastic Foundation*, NASA TTF-357, Washington, D.C., 1966.
14. Ventsel, E.S., A solution of some linear boundary value problems of the theory of elasticity with a complex operator using simple boundary value problems, *Dokl Acad Sci, Ukraine*, Ser. E, No. 8, p. 43–47 (1980) (in Russian).

4

Circular Plates

4.1 INTRODUCTION

Circular plates are common in many structures such as nozzle covers, end closures in pressure vessels, pump diaphragms, turbine disks, and bulkheads in submarines and airplanes, etc. When circular plates are analyzed, it is convenient to express the governing differential equation (2.24) in polar coordinates. This can be readily accomplished by a coordinate transformation. An alternative approach based on the procedure presented in Chapter 3 for rectangular plates to derive the basic relationships for the lateral deflections of circular plates may be used also.

4.2 BASIC RELATIONS IN POLAR COORDINATES

As mentioned earlier, we use the polar coordinates r and φ in solving the bending problems for circular plates. If the coordinate transformation technique is used, the following geometrical relations between the Cartesian and polar coordinates are applicable (see Fig. 4.1a):

$$x = r\cos\varphi,\ \ y = r\sin\varphi \text{ and } r^2 = x^2 + y^2,\ \varphi = \tan^{-1}\frac{y}{x}. \tag{4.1}$$

Referring to the above

$$\begin{aligned} &\frac{\partial r}{\partial x} = \frac{x}{r} = \cos\varphi, \quad \frac{\partial r}{\partial y} = \frac{y}{r} = \sin\varphi, \\ &\frac{\partial \varphi}{\partial x} = -\frac{y}{r^2} = -\frac{\sin\varphi}{r}, \quad \frac{\partial \varphi}{\partial y} = \frac{x}{r^2} = \frac{\cos\varphi}{r}. \end{aligned} \tag{4.2}$$

Inasmuch as the deflection is a function of r and φ, the chain rule together with the relations (4.2) lead to the following

$$\frac{\partial w}{\partial x}=\frac{\partial w}{\partial r}\frac{\partial r}{\partial x}+\frac{\partial w}{\partial \varphi}\frac{\partial \varphi}{\partial x}=\frac{\partial w}{\partial r}\cos\varphi-\frac{1}{r}\frac{\partial w}{\partial \varphi}\sin\varphi. \tag{4.3}$$

To evaluate the expression $\partial^2 w/\partial x^2$, we can repeat the operation (4.3) twice. As a result, we obtain

$$\begin{aligned}\frac{\partial^2 w}{\partial x^2}&=\cos\varphi\frac{\partial}{\partial r}\left(\frac{\partial w}{\partial x}\right)-\frac{1}{r}\sin\varphi\frac{\partial}{\partial \varphi}\left(\frac{\partial w}{\partial x}\right)\\&=\frac{\partial^2 w}{\partial r^2}\cos^2\varphi-\frac{\partial^2 w}{\partial \varphi\partial r}\frac{\sin 2\varphi}{r}+\frac{\partial w}{\partial r}\frac{\sin^2\varphi}{r}+\frac{\partial w}{\partial \varphi}\frac{\sin 2\varphi}{r^2}+\frac{\partial^2 w}{\partial \varphi^2}\frac{\sin^2\varphi}{r^2}.\end{aligned} \tag{4.4a}$$

Similarly,

$$\frac{\partial^2 w}{\partial y^2}=\frac{\partial^2 w}{\partial r^2}\sin^2\varphi+\frac{\partial^2 w}{\partial r\partial \varphi}\frac{\sin 2\varphi}{r}+\frac{\partial w}{\partial r}\frac{\cos^2\varphi}{r}-\frac{\partial w}{\partial \varphi}\frac{\sin 2\varphi}{r^2}+\frac{\partial^2 w}{\partial \varphi^2}\frac{\cos^2\varphi}{r^2}, \tag{4.4b}$$

$$\frac{\partial^2 w}{\partial x\partial y}=\frac{\partial^2 w}{\partial r^2}\frac{\sin 2\varphi}{2}+\frac{\partial^2 w}{\partial r\partial \varphi}\frac{\cos 2\varphi}{r}-\frac{\partial w}{\partial \varphi}\frac{\cos 2\varphi}{r^2}-\frac{\partial w}{\partial r}\frac{\sin 2\varphi}{2r}-\frac{\partial^2 w}{\partial \varphi^2}\frac{\sin 2\varphi}{2r^2}. \tag{4.4c}$$

Adding term by term the relations (4.4a) and (4.4b), yields

$$\nabla_r^2 w\equiv\frac{\partial^2 w}{\partial x^2}+\frac{\partial^2 w}{\partial y^2}=\frac{\partial^2 w}{\partial r^2}+\frac{1}{r}\frac{\partial w}{\partial r}+\frac{1}{r^2}\frac{\partial^2 w}{\partial \varphi^2}. \tag{4.5}$$

After repeating twice the operation ∇_r^2, the governing differential equation for the plate deflection (2.26) in polar coordinates becomes

$$\nabla_r^4 w\equiv\left(\frac{\partial^2}{\partial r^2}+\frac{1}{r}\frac{\partial}{\partial r}+\frac{1}{r^2}\frac{\partial^2}{\partial \varphi^2}\right)\left(\frac{\partial^2 w}{\partial r^2}+\frac{1}{r}\frac{\partial w}{\partial r}+\frac{1}{r^2}\frac{\partial^2 w}{\partial \varphi^2}\right)=\frac{p}{D}, \tag{4.6a}$$

or in the expended form

$$\frac{\partial^4 w}{\partial r^4}+\frac{2}{r}\frac{\partial^3 w}{\partial r^3}-\frac{1}{r^2}\frac{\partial^2 w}{\partial r^2}+\frac{1}{r^3}\frac{\partial w}{\partial r}+\frac{2}{r^2}\frac{\partial^4 w}{\partial r^2\partial \varphi^2}-\frac{2}{r^3}\frac{\partial^3 w}{\partial \varphi^2\partial r}+\frac{4}{r^4}\frac{\partial^2 w}{\partial \varphi^2}+\frac{1}{r^4}\frac{\partial^4 w}{\partial \varphi^4}=\frac{p}{D}. \tag{4.6b}$$

Let us set up the relationships between moments and curvatures. Consider now the state of moment and shear force on an infinitesimal element of thickness h, described in polar coordinates, as shown in Fig. 4.1b. Note that, to simplify the derivations, the x axis is taken in the direction of the radius r, at $\varphi=0$ (Fig. 4.1b). Then, the radial M_r, tangential M_t, twisting M_{rt} moments, and the vertical shear forces Q_r, Q_t will have the same values as the moments M_x, M_y, and M_{xy}, and shears Q_x, Q_y at the same point in the plate. Thus, transforming the expressions for moments (2.13) and shear forces (2.27) into polar coordinates, we can write the following:

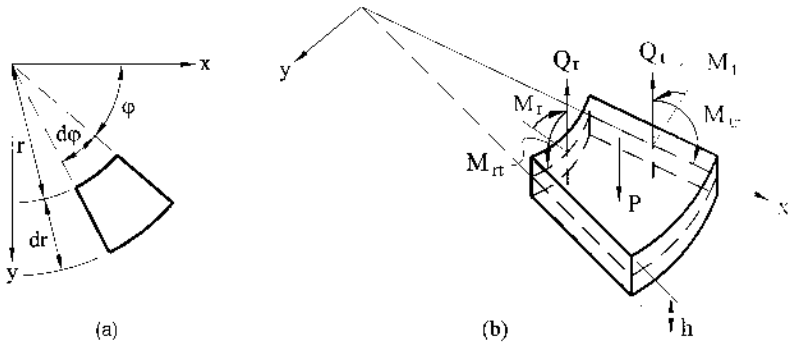

Fig. 4.1

$$M_r = -D\left[\frac{\partial^2 w}{\partial r^2} + \nu\left(\frac{1}{r}\frac{\partial w}{\partial r} + \frac{1}{r^2}\frac{\partial^2 w}{\partial \varphi^2}\right)\right]; \quad M_t = -D\left[\frac{1}{r}\frac{\partial w}{\partial r} + \frac{1}{r^2}\frac{\partial^2 w}{\partial \varphi^2} + \nu\frac{\partial^2 w}{\partial r^2}\right];$$

$$M_{rt} = M_{tr} = -D(1-\nu)\left(\frac{1}{r}\frac{\partial^2 w}{\partial r \partial \varphi} - \frac{1}{r^2}\frac{\partial w}{\partial \varphi}\right); \tag{4.7a}$$

$$Q_r = -D\frac{\partial}{\partial r}\left(\nabla_r^2 w\right); \; Q_t = -D\frac{1}{r}\frac{\partial}{\partial \varphi}\left(\nabla_r^2 w\right). \tag{4.7b}$$

Similarly, the formulas for the plane stress components, from Eqs (2.15), are written in the following form:

$$\sigma_r = \frac{12M_r}{h^3}z, \quad \sigma_t = \frac{12M_t}{h^3}z, \quad \tau_{rt} = \tau_{tr} = \frac{12M_{tr}}{h^3}z, \tag{4.8}$$

where M_r, M_t and M_{tr} are determined by Eqs (4.7). Clearly the maximum stresses take place on the surfaces $z = \pm h/2$ of the plate.

Similarly, transforming Eqs (2.38) and (2.39) into polar coordinates gives the effective transverse shear forces. They may be written for an edge with outward normal in the r and φ directions, as follows:

$$\begin{aligned} V_r &= Q_r + \frac{1}{r}\frac{\partial M_{rt}}{\partial \varphi} = -D\left[\frac{\partial}{\partial r}(\nabla_r^2 w) + \frac{1-\nu}{r}\frac{\partial}{\partial \varphi}\left(\frac{1}{r}\frac{\partial^2 w}{\partial r \partial \varphi} - \frac{1}{r^2}\frac{\partial w}{\partial \varphi}\right)\right], \\ V_t &= Q_t + \frac{\partial M_{rt}}{\partial r} = -D\left[\frac{1}{r}\frac{\partial}{\partial \varphi}(\nabla_r^2 w) + (1-\nu)\frac{\partial}{\partial r}\left(\frac{1}{r}\frac{\partial^2 w}{\partial r \partial \varphi} - \frac{1}{r^2}\frac{\partial w}{\partial \varphi}\right)\right]. \end{aligned} \tag{4.9}$$

The boundary conditions at the edges of a circular plate of radius a may readily be written by referring to Eqs. (2.48), namely:

(a) *Clamped edge* $r = a$

$$w = 0|_{r=a}, \frac{\partial w}{\partial r} = 0\Big|_{r=a}. \tag{4.10}$$

(b) *Simply supported edge* $r = a$

$$w = 0|_{r=a},\ M_r = 0\big|_{r=a}. \tag{4.11}$$

(c) *Free edge* $r = a$

$$M_r = 0\big|_{r=a},\ V_r = 0\big|_{r=a}. \tag{4.12}$$

If we use the transformations given by Eqs (4.1)–(4.4), the strain energy for a circular plate is

$$U = \frac{1}{2}\int\int_S D\left[\left(\frac{\partial^2 w}{\partial r^2} + \frac{1}{r}\frac{\partial w}{\partial r} + \frac{1}{r^2}\frac{\partial^2 w}{\partial \varphi^2}\right)^2 - 2(1-\nu)\frac{\partial^2 w}{\partial r^2}\left(\frac{1}{r}\frac{\partial w}{\partial r} + \frac{1}{r^2}\frac{\partial^2 w}{\partial \varphi^2}\right)\right.$$
$$\left. + 2(1-\nu)\left(\frac{1}{r}\frac{\partial^2 w}{\partial r \partial \varphi} - \frac{1}{r^2}\frac{\partial w}{\partial \varphi}\right)^2\right] r\mathrm{d}r\mathrm{d}\varphi. \tag{4.13}$$

4.3 AXISYMMETRIC BENDING OF CIRCULAR PLATES

When an applied loading and end restraints of the circular plate are independent of the angle φ, then the deflection of the plate and the stress resultants and stress couples will depend upon the radial position r only. Such a bending of the circular plate is referred to as *axially symmetrical* and the following simplifications can be made:

$$\frac{\partial^k(\ )}{\partial \varphi^k} = M_{rt} = Q_t = 0;\ k = 1, 2, 3, 4.$$

The previous equations for the bending of a circular plate can therefore be simplified to

$$M_r = -D\left(\frac{\mathrm{d}^2 w}{dr^2} + \frac{\nu}{r}\frac{\mathrm{d}w}{\mathrm{d}r}\right);\ M_t = -D\left(\frac{1}{r}\frac{\mathrm{d}w}{\mathrm{d}r} + \nu\frac{\mathrm{d}^2 w}{\mathrm{d}r^2}\right);$$
$$Q_r = -D\frac{\mathrm{d}}{\mathrm{d}r}\left(\frac{\mathrm{d}^2 w}{\mathrm{d}r^2} + \frac{1}{r}\frac{\mathrm{d}w}{\mathrm{d}r}\right) = -D\frac{\mathrm{d}}{\mathrm{d}r}\left[\frac{1}{r}\frac{\mathrm{d}}{\mathrm{d}r}\left(r\frac{\mathrm{d}w}{\mathrm{d}r}\right)\right]. \tag{4.14}$$

The differential equation of the deflected surface of the circular plate, Eq. (4.6a), reduces now to

$$\nabla_r^4 w \equiv \left(\frac{\mathrm{d}^2}{\mathrm{d}r^2} + \frac{1}{r}\frac{\mathrm{d}}{\mathrm{d}r}\right)\left(\frac{\mathrm{d}^2 w}{\mathrm{d}r^2} + \frac{1}{r}\frac{\mathrm{d}w}{\mathrm{d}r}\right) = \frac{p}{D}, \tag{4.15a}$$

and in the extended form

$$\frac{\mathrm{d}^4 w}{\mathrm{d}r^4} + \frac{2}{r}\frac{\mathrm{d}^3 w}{\mathrm{d}r^3} - \frac{1}{r^2}\frac{\mathrm{d}^2 w}{\mathrm{d}r^2} + \frac{1}{r^3}\frac{\mathrm{d}w}{\mathrm{d}r} = \frac{p}{D}. \tag{4.15b}$$

The formulas for stress components are given by Eq. (4.8), setting $\tau_{r\theta} = 0$, where M_r and M_θ can be determined from relations (4.14). Introducing the identity

$$\nabla_r^2 w \equiv \frac{\mathrm{d}^2 w}{\mathrm{d}r^2} + \frac{1}{r}\frac{\mathrm{d}w}{\mathrm{d}r} = \frac{1}{r}\frac{\mathrm{d}}{\mathrm{d}r}\left(r\frac{\mathrm{d}w}{\mathrm{d}r}\right), \tag{4.16}$$

Eq. (4.15a) appears in the form

$$\frac{1}{r}\frac{\mathrm{d}}{\mathrm{d}r}\left\{r\frac{\mathrm{d}}{\mathrm{d}r}\left[\frac{1}{r}\frac{\mathrm{d}}{\mathrm{d}r}\left(r\frac{\mathrm{d}w}{\mathrm{d}r}\right)\right]\right\}=\frac{p}{D}. \tag{4.17}$$

The rigorous solution of Eqs (4.15) or Eq. (4.17) is obtained as the sum of the complementary solution of the homogeneous differential equation, w_{h}, and the particular solution, w_{p}, i.e.,

$$w=w_{\mathrm{h}}+w_{\mathrm{p}}. \tag{4.18}$$

The complementary solution of Eqs (4.15) or Eq. (4.17) is given by

$$w_{\mathrm{h}}=C_1\ln r+C_2r^2\ln r+C_3r^2+C_4, \tag{4.19}$$

where $C_i(i=1,2,3,4)$ are constants that can be evaluated from the boundary conditions.

The particular solution, w_{p}, is obtained by successive integration of Eq. (4.17):

$$w_{\mathrm{p}}=\int\frac{1}{r}\int r\int\frac{1}{r}\int\frac{rp(r)}{D}\mathrm{d}r\mathrm{d}r\mathrm{d}r\mathrm{d}r. \tag{4.20}$$

If the plate is under a uniform loading $p=p_0=\text{const}$, the particular solution is

$$w_{\mathrm{p}}=\frac{p_0r^4}{64D}. \tag{4.21}$$

For purposes of calculation, the following quantities are given explicitly:

$$\begin{aligned}
w&=C_1\ln r+C_2r^2\ln r+C_3r^2+C_4+\frac{p_0r^4}{64D},\\
\frac{\mathrm{d}w}{\mathrm{d}r}&=C_1\frac{1}{r}+C_2(2r\ln r+r)+2C_3r+\frac{p_0r^3}{16D},\\
M_r&=-D\left[-C_1\frac{1-\nu}{r^2}+2C_2(1+\nu)\ln r+C_2(3+\nu)+2C_3(1+\nu)\right.\\
&\qquad\left.+\frac{p_0r^2}{16D}(3+\nu)\right],\\
M_t&=-D\left[C_1\frac{1-\nu}{r^2}+2C_2(1+\nu)\ln r+C_2(1+3\nu)+2C_3(1+\nu)\right.\\
&\qquad\left.+\frac{p_0r^2}{16D}(1+3\nu)\right],\\
Q_r&=-4D\left(C_2\frac{1}{r}+\frac{p_0r}{8D}\right).
\end{aligned} \tag{4.22}$$

Let us consider some solutions for axially symmetrical circular plates.

4.3.1 Solid plates

Consider a solid plate of radius a under an axisymmetric load $p(r)$. Take the origin of the coordinate system at a plate center. The solution of the governing differential

equation (4.17) is given by the expressions (4.18)–(4.20). For the solid plate, which contains no concentrated loads at $r = 0$, it is easy to see that the terms involving the logarithms in Eq. (4.19) yield an infinite displacement and bending moment, and the shear force for all values of C_1 and C_2, except zero; therefore, $C_1 = C_2 = 0$. Thus, for a solid circular plate subjected to an axisymmetric distributed load with arbitrary boundary conditions, the deflection surface is given by

$$w = C_3 r^2 + C_4 + w_{\mathrm{p}}. \tag{4.23}$$

The constants of integration C_3 and C_4 in this equation are determined from boundary conditions specified at boundary $r = a$. Let us consider some particular cases of plates and loadings that are commonly encountered in practice.

(a) Plate with simply supported edge under a uniform load p_0 (Fig. 4.2a).

The boundary conditions are

$$w = 0|_{r=a},\ M_r = 0\big|_{r=a}. \tag{a}$$

Substituting for w_{p} from Eq. (4.21) into Eq. (4.23), we obtain the equation for the deflected surface:

$$w = C_3 r^2 + C_4 + \frac{p_0 r^4}{64D}, \tag{4.24}$$

and the expression for M_r may be obtained from Eq. (4.22) by making $C_1 = C_2 = 0$:

$$M_r = -D\left[2C_3(1+\nu) + \frac{p_0 r^2}{16D}(3+\nu)\right]. \tag{4.25}$$

Introducing Eqs (4.24) and (4.25) into the boundary conditions (a), one obtains the system of two algebraic equations in C_3 and C_4. Solving the above system, yields

$$C_3 = -\frac{p_0 a^2}{32D}\frac{(3+\nu)}{(1+\nu)},\ C_4 = \frac{p_0 a^4 (5+\nu)}{64D(1+\nu)}. \tag{b}$$

Substituting the above into Eq. (4.24) gives the plate deflection in the form

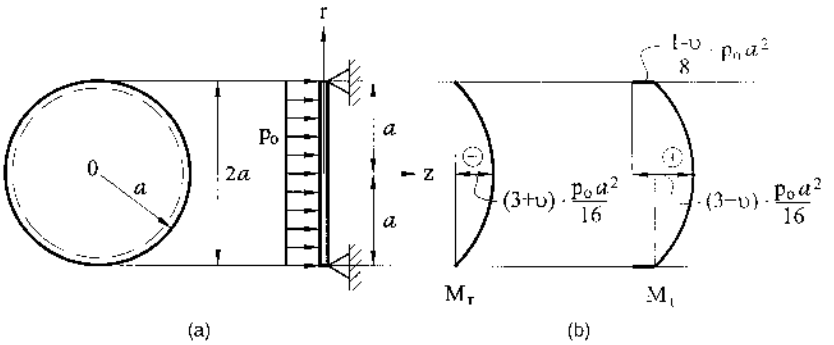

Fig. 4.2

$$w = \frac{p_0(a^2 - r^2)}{64D}\left(\frac{5+\nu}{1+\nu}a^2 - r^2\right). \tag{4.26}$$

The maximum deflection, which occurs at $r = 0$, is thus

$$w_{\max} = \frac{p_0 a^4}{64D}\left(\frac{5+\nu}{1+\nu}\right). \tag{c}$$

Given the deflection curve w, the moment equation can readily be obtained from Eqs (4.22) by substituting for C_3 and C_4 from (b) and making $C_1 = C_2 = 0$. Thus, we obtain

$$M_r = \frac{p_0}{16}(3+\nu)(a^2 - r^2),\ M_t = \frac{p_0}{16}\left[(3+\nu)a^2 - (1+3\nu)r^2\right]. \tag{4.27}$$

The bending moment diagrams are shown in Fig. 4.2b. The maximum moments also occur at the plate center, i.e., at $r = 0$. Thus, we have

$$\max M_r = \max M_t = \frac{p_0 a^2}{16}(3+\nu). \tag{4.28}$$

(b) Plate with clamped edge under a uniform load p_0 (Fig. 4.3a)

The boundary conditions are

$$w = 0|_{r=a},\quad \frac{dw}{dr} = 0\Big|_{r=a}. \tag{d}$$

Introducing the deflection surface in the form of Eq. (4.24) into the conditions (d), we obtain

$$C_3 = -\frac{p_0 a^2}{32D},\ C_4 = \frac{p_0 a^4}{64D}. \tag{e}$$

Similarly to the procedure for the previous case, the deflection is then

$$w = \frac{p_0}{64D}(a^2 - r^2)^2. \tag{4.29}$$

The maximum deflection occurs at the center of the plate:

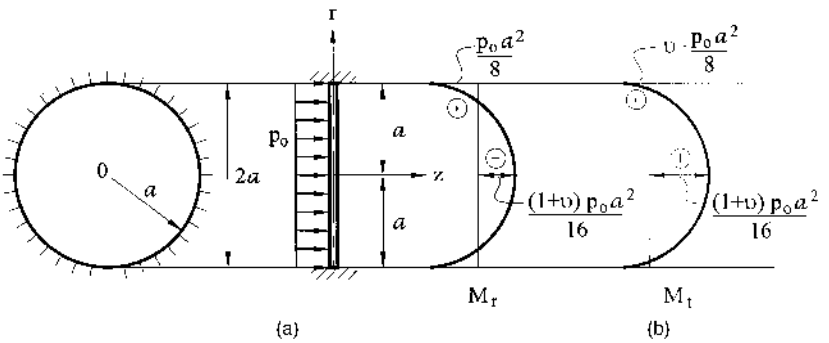

Fig. 4.3

$$w_{\max} = \frac{p_0 a^4}{64D}. \tag{f}$$

Expressions for the bending moments are calculated by means of Eqs (4.22). Substituting for C_3 and C_4 from Eqs (e) into Eqs (4.22) and letting $C_1 = C_2 = 0$, we obtain

$$M_r = \frac{p_0}{16}\left[(1+\nu)a^2 - (3+\nu)r^2\right]; \quad M_t = \frac{p_0}{16}\left[(1+\nu)a^2 - (1+3\nu)r^2\right]. \tag{4.30}$$

The bending moment distributions are shown in Fig. 4.3b. The maximum bending moment M_r occurs at the edge of the plate (at $r = a$), where

$$\max M_r = -\frac{p_0 a^2}{8}. \tag{4.31a}$$

The maximum bending moment M_t takes place at the plate center (at $r = 0$), where

$$\max M_t = \frac{p_0 a^2 (1+\nu)}{16}. \tag{4.31b}$$

If $\nu = 0.3$, comparing Eqs (c) and (f), we see that the maximum deflection for the simply supported plate is about four times as great as that for the plate with a clamped edge. For the same value of ν, the maximum bending moment for a simply supported plate is about 1.7 times as great as that for the plate with clamped edge.

(c) Circular plate under a concentrated force at its center

When a concentrated or a point load acts at the plate center, one can set $p_0 = 0$ and, thus, $w_p = 0$ in Eq. (4.18). Referring to Eq. (4.19), we can conclude that C_1 must be taken as zero in order that the deflection should be finite at $r = 0$. The term involving C_2 must now be retained because of the very high shear stresses present in the vicinity of the center (see Sec. 3.4). The deflection surface of the plate is then represented, as follows:

$$w = C_2 r^2 \ln r + C_3 r^2 + C_4. \tag{4.32}$$

The constants C_2, C_3, and C_4 are evaluated from the boundary conditions and from conditions at the point of application of the concentrated force. As an example, consider *the plate with clamped edge loaded by a concentrated force* P applied at plate center O, as shown in Fig. 4.4a. The boundary conditions (d), when introduced into Eq. (4.32) lead to

$$\begin{aligned} C_2 a^2 \ln a + C_3 a^2 + C_4 &= 0, \\ C_2 a(2\ln a + 1) + 2C_3 &= 0. \end{aligned} \tag{g}$$

The additional condition can be set up from the following consideration. Let us isolate a small cylinder of radius r in the vicinity of the application of P (Fig. 4.5).

From equilibrium of this cylinder, we obtain

$$\sum F_z = 0: \quad Q_r(2\pi r) + P = 0 \quad \text{or } Q_r = -\frac{P}{2\pi r}.$$

Substituting for Q_r from Eq. (4.22) into the above and letting $p_0 = 0$, we obtain

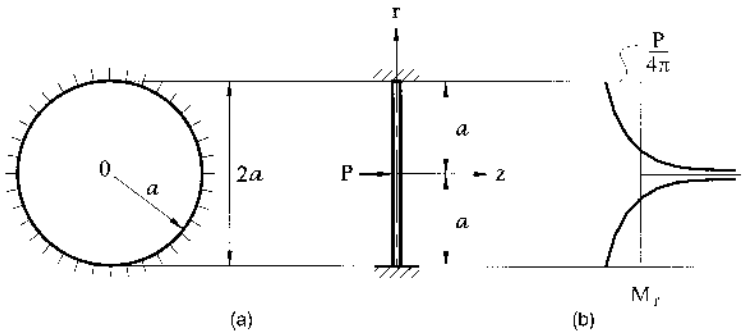

Fig. 4.4

$$4DC_2\frac{1}{r}=\frac{P}{2\pi r}. \tag{h}$$

Solving Eqs (g) and (h), the constants of integration are

$$C_2=\frac{P}{8\pi D},\quad C_3=-\frac{P}{16\pi D}(2\ln a+1),\quad C_4=\frac{Pa^2}{16\pi D}.$$

Upon substitution of the above into Eq. (4.32), we obtain an expression for the deflection:

$$w=\frac{P}{16\pi D}\left(2r^2\ln\frac{r}{a}+a^2-r^2\right). \tag{4.33}$$

The bending moments M_r and M_t may be obtained by inserting the constants of integration C_2, C_3, and C_4 ($C_1=0$) into Eqs (4.22) for $p_0=0$. We have the following:

$$M_r=\frac{P}{4\pi}\left[(1+\nu)\ln\frac{a}{r}-1\right];\quad M_t=\frac{P}{4\pi}\left[(1+\nu)\ln\frac{a}{r}-\nu\right]. \tag{4.34}$$

Applying the same procedure, we can obtain the deflection surface and bending moments for a plate with *simply supported edges and subjected to a concentrated force at its center*. For this plate, the deflection and bending moments are given by

$$\begin{aligned} w&=\frac{P}{16\pi D}\left[2r^2\ln\frac{r}{a}+\frac{3+\nu}{1+\nu}\left(a^2-r^2\right)\right];\\ M_r&=\frac{P}{4\pi}(1+\nu)\ln\frac{a}{r};\quad M_t=\frac{P}{4\pi}\left[(1+\nu)\ln\frac{a}{r}+1-\nu\right]. \end{aligned} \tag{4.35}$$

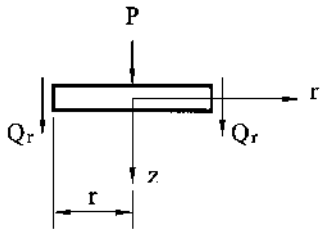

Fig. 4.5

As seen, the bending moments for both plates approach infinity at the point of application of concentrated force ($r \to 0$) (see Fig. 4.4b). The appearance here of a singularity in the bending moments has the same nature as that discussed earlier for rectangular plates loaded by a concentrated force. A detailed explanation of this phenomenon is provided in Sec. 3.4.

(d) Simply supported circular plate subjected to a symmetric lateral load which linearly increases from the center of the edge (Fig. 4.6)

Substituting $p = p_0 \frac{r}{a}$ into Eq. (4.20) for the particular solution gives

$$w_p = \int \frac{1}{r} \int r \int \frac{1}{r} \int \frac{1}{D} r \left(p_0 \frac{r}{a} \right) dr dr dr dr = \frac{p_0 r^5}{225 a D}. \tag{4.36}$$

Substituting the above into Eq. (4.23), yields the general solution of the form

$$w = C_3 r^2 + C_4 + \frac{p_0 r^5}{225 a D}. \tag{a}$$

Substituting (a) into the boundary conditions (4.11) leads to the following values of the constants of integration:

$$C_3 = -\frac{p_0 a^2}{90 D} \left(\frac{4+\nu}{1+\nu} \right), \quad C_4 = \frac{p_0 a^4}{45 D} \left[\frac{4+\nu}{2(1+\nu)} - \frac{1}{5} \right]. \tag{b}$$

Equation (a) with known coefficients C_3 and C_4 determines the deflected plate surface

$$w = \frac{p_0 a^2}{45 D} \left\{ \frac{r^2}{2} \left(\frac{4+\nu}{1+\nu} \right) + a^2 \left[\frac{4+\nu}{2(1+\nu)} - \frac{1}{5} \right] + \frac{r^5}{5 a^3} \right\}. \tag{c}$$

Example 4.1

A cylindrical tank and flat thin plate bottom are subjected to internal pressure p, as shown in Fig. 4.7a. Determine a required thickness of the bottom, h, and calculate its maximum deflection. Use $R = 0.25\,\text{m}$, $p = 2.5\,\text{MPa}$, $E = 200\,\text{GPa}$, and $\nu = 0.3$, respectively. The allowable stress σ_{all} is 150 MPa.

Solution

The cylindrical tank bottom represents a circular solid plate. It is necessary to establish a type of boundary conditions on the plate edge, which depends on a rigidity of the cylinder, and the presence of the gasket at the connection. If the

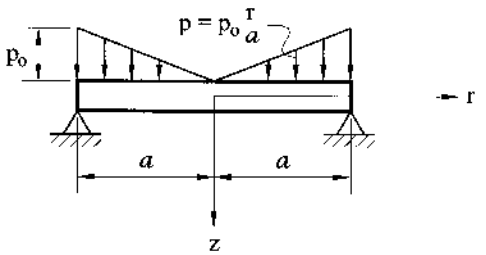

Fig. 4.6

cylinder itself is sufficiently rigid, the plate of radius is R (Fig. 4.7b) is thin and, in addition, the bottom is inserted without a soft gasket, then we can assume the circular plate edge to be clamped over the contour of the bolts arrangement and the plate. If the cylinder walls are compliant and the soft gaskets are at the connection, one can take the plate edge to be simply supported (Fig. 4.7c). In practice, a real type of plate support is an intermediate one between the above-mentioned extreme cases, i.e., they (the supports) represent an elastic restraint support. In order to gain a clear impression of real stresses and deformations occurring in the bottom, it makes sense to consider both extreme cases. The deflection surfaces and bending moments for these cases are given by Eqs (4.29), (4.30), and (4.26), (4.27). The bending moment, M_r and M_t, diagrams are shown in Figs 4.3 and 4.4 for both extreme cases. Referring to these diagrams, we can conclude that the maximum bending moment for a simply supported circular plate occurs at the center, while for the plate with clamped edge the maximum bending moment is at the plate edge. The value of the maximum bending moment for a simply supported plate is nearly 1.7 times larger than for a plate with a clamped edge (for $\nu = 0.3$). However, taking into account that the plate edge is rather clamped than simply supported, one can expect that the value of the maximum bending moment at the plate center does not exceed $p_0 R^2/8$, i.e., the value of the bending moment at the clamped edge. Therefore, the circular plate with a clamped edge can be taken as the design variant of the tank head. The maximum normal stress occurs at the clamped edge (i.e., for $r = R$ and $z = \pm h/2$). From Eq. (4.8), $\sigma_{\max}$ is given by

$$\sigma_{r,\max} = \frac{M_{r,\max}}{h^2/6} = \frac{6pR^2}{8h^2}, \quad \sigma_{t,\max} = \frac{M_{t,\max}}{h^2/6} = \nu\frac{6pR^2}{8h^2}.$$

The third principal stress $\sigma_3 = \sigma_z = 0$, according to the general assumptions adopted in the plate bending theory. Since the material of the plate is assumed to be a ductile, the maximum shear (Tresca) criterion of yielding (see Appendix A.6.2) can be applied: namely,

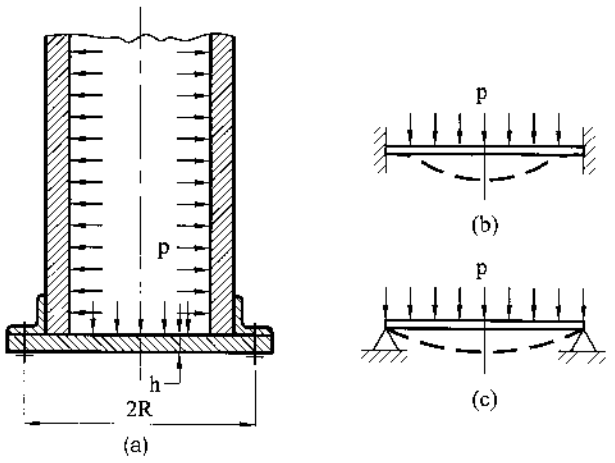

Fig. 4.7

$$\sigma_e = \sigma_1 - \sigma_3 = \frac{6pR^2}{8h^2} \le \sigma_{\text{all}}.$$

Solving this for the plate thickness, h, yields

$$h = \sqrt{\frac{6pR^2}{8\sigma_{\text{all}}}} = \sqrt{\frac{6(2.5 \times 10^6)(0.25)^2}{8(150 \times 10^6)}} \approx 28\,\text{mm};$$

$$D = \frac{Eh^3}{12(1-\nu^2)} = 40.2 \times 10^4 \text{N} \cdot \text{m}$$

Note that if the simply supported plate was chosen as a design variant, then the plate thickness was found to be $h \approx 36\,\text{mm}$.

The maximum deflection for the selected design variant of the tank head is given by Eq. (f) (case (b) in Sec. 4.3.1), as follows:

$$w_{\max} = \frac{pR^4}{64D}.$$

Substituting the given numerical data into the above equation gives

$$w_{\max} = 0.38\,\text{mm}.$$

Example 4.2

Find the expression for the deflection of the clamped solid plate shown in Fig. 4.8a due to line load p distributed along a circle with radius $r = b$.

Solution

To solve this problem, one first divides the plate problem into two parts (Fig. 4.8b): an inner solution for a solid plate 1 extending over the region $0 \le r \le b$, and an outer solution for an annular plate 2 over the region $b \le r \le a$. In each case, the governing equation are (for $p = 0$)

$$\nabla_r^4 w_1 = 0;\ \nabla_r^4 w_2 = 0.$$

For the inner plate 1 the solution w_1 is of the form (see Eq. (4.23))

$$w_1 = C_3^{(1)} r^2 + C_4^{(1)}, \tag{a}$$

and for plate 2 the corresponding solution is

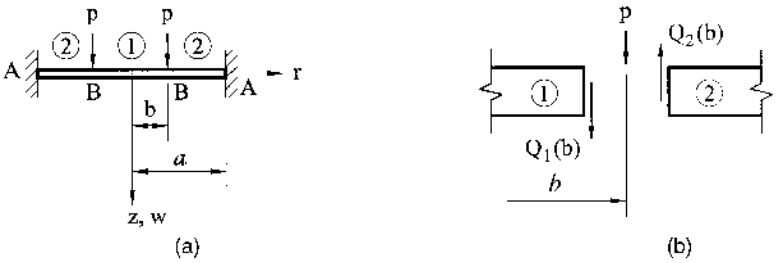

Fig. 4.8

$$w_2 = C_1^{(2)} \ln r + C_2^{(2)} r^2 \ln r + C_3^{(2)} r^2 + C_4^{(2)}. \tag{b}$$

The six constants in Eqs (a) and (b) are determined from the boundary conditions at $r = a$, i.e.,

$$w_2 = 0\big|_{r=a} \quad \frac{\mathrm{d}w_2}{\mathrm{d}r} = 0\bigg|_{r=a} \tag{c}$$

and from the continuity conditions at the junction of the two plate segments. The latter have the form

$$w_1\big|_{r=b} = w_2\big|_{r=b}; \quad \frac{\mathrm{d}w_1}{\mathrm{d}r}\bigg|_{r=b} = \frac{\mathrm{d}w_2}{\mathrm{d}r}\bigg|_{r=b}; \quad M_r^{(1)}\big|_{r=b} = M_r^{(2)}\big|_{r=b}; \quad p = Q_r^{(1)}\big|_{r=b} - Q_r^{(2)}\big|_{r=b}. \tag{d}$$

Since the inner plate is in pure bending (see Eq. (a)), then $Q_r^{(1)} = 0$ and the last condition (d) is of the form

$$p = -Q_r^{(2)}\big|_{r=b}. \tag{e}$$

The last condition (e) is illustrated in Fig. 4.8b. Introducing expressions (a) and (b) into conditions (c), (d), and (e) together with Eqs (4.14), we can find the six constants of integration. The final solution is, as follows:

– *for the inner plate* 1, $0 \le r \le b$

$$w = \frac{pb}{8a^2 D}\left[\left(a^2 - b^2\right)\left(a^2 + r^2\right) - 2a^2\left(b^2 + r^2\right)\ln\frac{a}{b}\right]; \tag{4.37a}$$

– *for the outer annular plate* 2, $b \le r \le a$

$$w = \frac{pb}{8a^2 D}\left[\left(a^2 + b^2\right)\left(a^2 - r^2\right) + 2a^2\left(b^2 + r^2\right)\ln\frac{r}{a}\right]. \tag{4.37b}$$

4.3.2 Annular circular plates

In this section, we discuss the bending of circular plates with concentric circular holes, the so-called *annular plates* (Fig. 4.9).

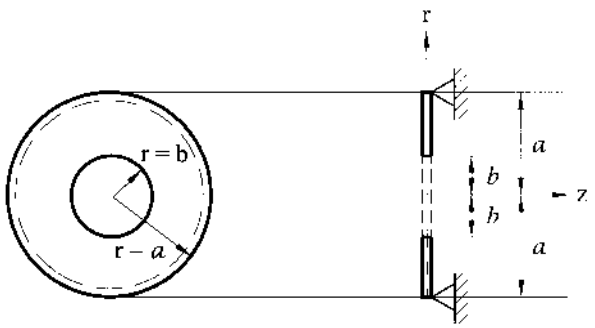

Fig. 4.9

The outer and inner radii of a plate are denoted by a and b, respectively. For annular plates the homogeneous solution is given by Eq. (4.19). The solution of an axially symmetric bending of circular plates with central holes may follow a procedure similar to the one discussed in the foregoing section, but one must consider the boundary conditions at the outer ($r = a$) as well as the inner ($r = b$) boundaries. Two typical cases of loading are illustrated below.

(a) Simply supported annular plate loaded by edge moments (Fig. 4.10)

For this case of loading, $w_p = 0$ and the general solution is given by

$$w = C_1 \ln r + C_2 r^2 \ln r + C_3 r^2 + C_4. \tag{4.38}$$

The boundary conditions are

$$M_r = m_1|_{r=b}; \quad Q_r = 0|_{r=b}; \quad M_r = m_2|_{r=a}; \quad w = 0|_{r=a}. \tag{a}$$

Introducing Eq. (4.38) into the boundary conditions (a), with the use of Eqs (4.14), yields the following expressions for the constants of integration:

$$\begin{aligned} C_1 &= \frac{(m_1 - m_2)a^2b^2}{D(1-\nu)(a^2-b^2)}, \quad C_2 = 0, C_3 = \frac{m_1b^2 - m_2a^2}{2D(1+\nu)(a^2-b^2)}, \\ C_4 &= -\frac{(m_1 - m_2)a^2b^2}{D(1-\nu)(a^2-b^2)}\ln a - \frac{(m_1b^2 - m_2a^2)}{2D(1+\nu)(a^2-b^2)}a^2. \end{aligned} \tag{b}$$

Substituting the above into Eq. (4.38) yields the expression for deflections:

$$w = \frac{(m_1 - m_2)a^2b^2}{D(1-\nu)(a^2-b^2)}\ln\frac{r}{a} + \frac{m_1b^2 - m_2a^2}{2D(1+\nu)(a^2-b^2)}(r^2 - a^2). \tag{4.39}$$

Substituting the above expression into Eqs (4.14) gives the expressions for bending moments:

$$M_r = -\frac{m_1b^2 - m_2a^2}{a^2-b^2} + \frac{a^2b^2(m_1 - m_2)}{r^2(a^2-b^2)}; \quad M_t = -\frac{m_1b^2 - m_2a^2}{a^2-b^2} - \frac{a^2b^2(m_1 - m_2)}{r^2(a^2-b^2)}. \tag{4.40}$$

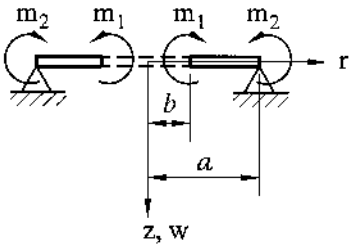

Fig. 4.10

(b) Simply supported plate under a line load uniformly distributed along the inner edge (Fig. 4.11)

Again, $w_p = 0$, and the general solution is given by Eqs (4.38). The boundary conditions are

$$w = 0|_{r=a}; \quad M_r = 0|_{r=a}; \quad M_r = 0|_{r=b}; \quad Q_r = -p|_{r=b}. \tag{4.41}$$

Substituting expressions (4.14) and (4.38) into boundary conditions (4.41), we find

$$C_1 = p\frac{b}{4D}\frac{2(1+\nu)\ln\frac{b}{a}}{(1-\nu)(a^2-b^2)}a^2b^2, \quad C_2 = p\frac{b}{4D},$$

$$C_3 = p\frac{b}{4D}\left(\frac{b^2\ln\frac{b}{a}}{a^2-b^2} - \ln a - \frac{3+\nu}{2(1+\nu)}\right),$$

$$C_4 = -p\frac{b}{4D}\left\{\frac{a^2b^2\ln\frac{b}{a}}{a^2-b^2}\left[\frac{2(1+\nu)}{1-\nu}+\right] - \frac{(3+\nu)a^2}{2(1+\nu)}\right\}.$$

Substitution of the above into Eq. (4.38) gives the following expression for the deflection:

$$w = p\frac{a^2b}{4D}\left\{\left(1-\frac{r^2}{a^2}\right)\left[\frac{3+\vartheta}{2(1+\vartheta)} - \frac{b^2}{a^2-b^2}\ln\frac{b}{a}\right] + \frac{r^2}{a^2}\ln\frac{r}{a} + \frac{2b^2}{a^2-b^2}\frac{1+\vartheta}{1-\vartheta}\ln\frac{b}{a}\ln\frac{r}{a}\right\}. \tag{4.42}$$

It is observed that if $b \to 0$, $b^2\ln(b/a)$ vanishes, and Eq. (4.42), letting $p = P/2\pi b$, reduces to the first equation (4.35) for a solid circular plate under a concentrated force applied at its center.

4.4 THE USE OF SUPERPOSITION FOR THE AXISYMMETRIC ANALYSIS OF CIRCULAR PLATES

The procedure discussed in Sec. 4.3 for determining the deflections and bending moments of symmetrically loaded circular plates is applicable to other cases of loading and boundary conditions. For complicated configurations of loads and boundary conditions, the method of superposition may be used to good advantage

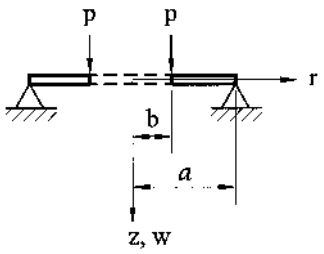

Fig. 4.11

to simplify the analysis. Superposition is a valid method of solution if the response of a structure is directly proportional to the load that produces it and deflections are small. Then, if a static loading is broken into simpler components, the final response is independent of whether component loads are applied simultaneously or added in arbitrary sequence. Let us illustrate an application of the method of superposition in the following examples.

Example 4.3

Find the center deflection, w_0, in the solid clamped plate loaded as shown in Fig. 4.12a.

Solution

Consider a solid plate with clamped edge loaded by a line load p around a circle of radius c, as shown in Fig. 4.12b. The center deflection, w_0, is given by expression (4.37a). Setting $b = c$ and $r = 0$, we obtain the center deflection, w_0, as follows:

$$w_0 = \frac{pc}{8D}\left(a^2 - c^2 + 2c^2 \ln\frac{c}{a}\right). \tag{a}$$

Having the deflection for a load uniformly distributed along a concentric circle, we can determine the deflection for the given loading using the method of superposition. In fact, consider an infinitesimal line load $p_0 dc$ around a circle of radius c on a plate, as shown in Fig. 4.12c. Then, the center deflection for the given loading is obtained from Eq. (a), replacing p by $p_0 dc$ and integrating from 0 to b. We have

$$\begin{aligned} w_c &= \frac{p_0}{8D}\int_0^b \left(a^2 c - c^3 + 2c^3 \ln c - 2c^3 \ln a\right) dc \\ &= \frac{p_0}{8D}\left[a^2\frac{c^2}{2} - \frac{c^4}{4} + 2\ln a \cdot \frac{c^4}{4} + 2\left(\frac{c^4}{4}\ln c - \frac{c^4}{16}\right)\right]\Bigg|_0^b. \end{aligned}$$

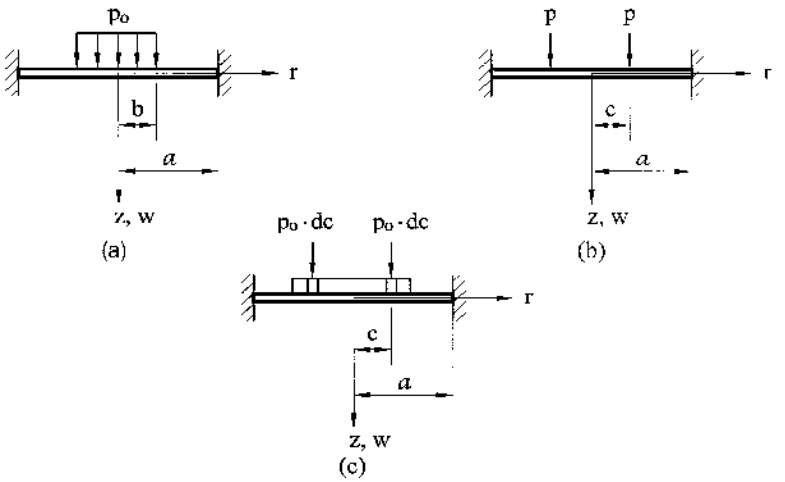

Fig. 4.12

Finally, we obtain

$$w_c = \frac{p_0 b^2}{16D}\left(a^2 - \frac{3}{4}b^2 + b^2 \ln\frac{b}{a}\right). \tag{4.43}$$

Example 4.4

The plate shown in Fig. 4.13a is stepped so that the central disk has twice the flexural rigidity of the outer annulus. Find the maximum deflection and bending moment M_r at $r = 0.5a$, caused by concentrated force P. Use $\nu = 0.3$.

Solution

The plate can be separated into two components (Fig. 4.13b): an inner part of the plate of radius $a/2$ and outer part in the form of an annular plate ($a/2 \le r \le a$). Continuity between the inner and outer plates is maintained by applying an unknown moment, M_r, as shown in Fig. 4.13b.

First, consider the solution for the inner plate. The slope at $r = a/2$ is

$$\frac{dw_i}{dr} = \frac{dw_i}{dr}(P) + \frac{dw_i}{dr}(M_r), \tag{a}$$

where $\frac{dw_i}{dr}(P)$ and $\frac{dw_i}{dr}(M_r)$ are the slopes of the inner plate at $r = a/2$ produced by an external concentrated force P and bending moment M_r, respectively. The above slopes can be obtained by differentiating the expressions for the deflections given by the first equation (4.35) and Eq. (4.39) and then setting $r = a/2$ in the equation for $\frac{dw_i}{dr}(P)$ and $r = a/2, m_1 = 0, b = 0$, and $m_2 = M_r$ in the equation for $\frac{dw_i}{dr}(M_r)$. Thus, we obtain the following:

$$\frac{dw_i}{dr}(P) = -0.0612\frac{P(0.5a)}{2D} = -0.0153\frac{Pa}{D};$$

$$\frac{dw_i}{dr}(M_r) = C_1\frac{0.5a}{2} + C_2\frac{1}{0.5a} = \frac{0.5a}{2}\left(-\frac{2(0.25a^2)M_r}{1.3(0.25a^2)2D}\right) = -0.1923\frac{M_r a}{D}. \tag{b}$$

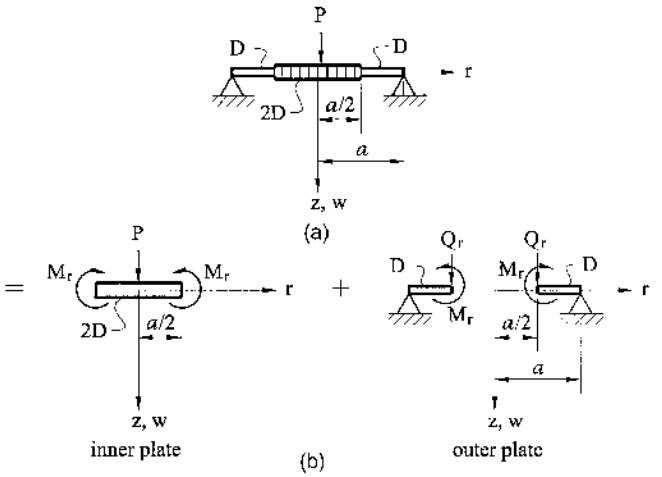

Fig. 4.13

Finally,

$$\frac{dw_i}{dr}(P) + \frac{dw_i}{dr}(M_r) = -0.0153\frac{Pa}{D} - 0.1923\frac{M_r a}{D}. \tag{c}$$

Then we can determine the slopes of the outer annular plate. This plate is loaded by the line shear forces Q_r and the line unknown bending moments M_r. The line shear force is

$$Q_r = \frac{P}{2\pi r} = \frac{P}{2\pi(0.5a)} = 0.318\frac{P}{a}. \tag{d}$$

The slope of the outer plate at $r = a/2$ is

$$\frac{dw_o}{dr} = \frac{dw_o}{dr}(Q_r) + \frac{dw_o}{dr}(M_r). \tag{e}$$

The slopes on the right-hand side of Eq. (e) can be obtained by differentiating the expressions for the deflections given by Eqs (4.39) and (4.42) and then setting $m_2 = 0$, $m_1 = M_r$, and $q = Q_r$.

We obtain the following:

$$\frac{dw_o}{dr}(M_r) = \frac{M_r b^2}{D(a^2 - b^2)}\left[\frac{a^2}{r(1-\nu)} + \frac{r}{1+\nu}\right], \tag{f}$$

$$\frac{dw_o}{dr}(Q_r) = Q_r\frac{a^2 b}{4D}\left\{\left(-\frac{2r}{a^2}\right)\left[\frac{3+\nu}{2(1+\nu)} - \frac{b^2}{a^2 - b^2}\ln\frac{b}{a}\right] + \frac{r}{a^2}\left(2\ln\frac{r}{a} + 1\right)\right. \tag{g}$$

$$\left. + \frac{2b^2}{a^2 - b^2}\frac{1+\nu}{1-\nu}\ln\frac{b}{a}\frac{1}{a}\right\}.$$

Making $b = a/2$ and $r = a/2$ in Eqs (f) and (g) and using Eq. (d), we obtain the following expressions for slopes at $r = a/2$:

$$\frac{dw_o}{dr}(M_r) = 1.0806\frac{M_r a}{D}; \quad \frac{dw_o}{dr}(Q_r) = -0.1353\frac{Pa}{D}. \tag{h}$$

Finally, the total slope at $r = a/2$ of the outer plate is given by

$$\frac{dw_o}{dr} = -0.1353\frac{Pa}{D} + 1.0806\frac{M_r a}{D}. \tag{i}$$

Equating slopes from Eqs (c) and (i), we find the following:

$$M_r = 0.094P. \tag{j}$$

The maximum deflection occurs under the point of application of the concentrated force. This center deflection is the sum of the following four contributions:

w at $r = 0$in the first equation (4.35);
w at $r = 0$ in Eq (4.39) with $m_1 = 0$ and $m_2 = M_r$, $b = 0$;
w at $r = b$ in Eq. (4.42) with $q = Q_r$; and
w at $r = b = 0.5a$ in Eq. (4.39) with $m_1 = M_r$ and $m_2 = 0$.

Thus, at the plate center, at $r = 0$, the maximum deflection is given as

$$w_{\max} = 0.0505\frac{P(0.25a^2)}{2D} + \frac{M_r a^2}{4D(1+\nu)} - \frac{M_r b^2}{D(a^2-b^2)} \left[\frac{2}{1+\nu}\frac{b^2-a^2}{4} + \frac{a^2}{1-\nu}\ln\frac{b}{a}\right] + 0.1934Q_r\frac{a^3}{D}.$$

Substituting here Q_r from Eq. (d) for M_r from Eq. (j), we compute the center deflection:

$$w_{\max} = 0.03224\frac{Pa^2}{D}$$

4.5 CIRCULAR PLATES ON ELASTIC FOUNDATION

We consider in this section circular plates loaded symmetrically with respect to their center and resting on a Winkler-type foundation, which was discussed earlier in chapter 3. The foundation reaction, $q(r)$, can be described by

$$q(r) = k \cdot w(r), \tag{4.44}$$

where $k (k = \text{const})$ is the modulus of the foundation.

Introducing the reaction of the foundation from Eq. (4.44) into Eq. (4.15b), we obtain the governing differential equation of bending of circular plates resting on a Winkler-type foundation:

$$\left(\frac{\mathrm{d}^2}{\mathrm{d}r^2} + \frac{1}{r}\frac{\mathrm{d}}{\mathrm{d}r}\right)\left(\frac{\mathrm{d}^2 w}{\mathrm{d}r^2} + \frac{1}{r}\frac{\mathrm{d}w}{\mathrm{d}r}\right) = \frac{1}{D}(p - kw), \tag{4.45}$$

where p is a given surface load. Denoting

$$l = \sqrt[4]{\frac{D}{k}}, \tag{4.46}$$

and introducing the dimensionless coordinate $\zeta = r/l$, one can write Eq. (4.45) in the form

$$\left(\frac{\mathrm{d}^2}{\mathrm{d}\zeta^2} + \frac{1}{\zeta}\frac{\mathrm{d}}{\mathrm{d}\zeta}\right)^2 w + w = \frac{pl^4}{D}. \tag{4.47}$$

Introducing the following notation

$$\nabla_\zeta^2 = \frac{\mathrm{d}^2}{\mathrm{d}\zeta^2} + \frac{1}{\zeta}\frac{\mathrm{d}}{\mathrm{d}\zeta}, \tag{4.48}$$

we can rewrite Eq. (4.47) as follows:

$$\nabla_\zeta^4 w + w = \frac{pl^4}{D}. \tag{4.49}$$

For $p = 0$, the homogeneous equation (4.49) is reduced to a system of the following two second-order differential equations:

$$\frac{d^2w}{d\zeta^2}+\frac{1}{\zeta}\frac{dw}{d\zeta}\pm iw=0, \tag{4.50}$$

where i is the imaginary unit, $i^2=-1$.

The solution of this system of differential equations is of the form [1]:

$$w=C_1J_0\left(\zeta\sqrt{i}\right)+C_2J_0\left(\zeta\sqrt{-i}\right)+C_3H_0^{(1)}\left(\zeta\sqrt{i}\right)+C_4H_0^{(1)}\left(\zeta\sqrt{-i}\right), \tag{4.51}$$

where $J_0\left(\zeta\sqrt{\pm i}\right)$ is the Bessel function of the first kind of zero order and $H_0^{(1)}\left(\zeta\sqrt{\pm i}\right)$ is the Hankel function of the first kind of zero order [2].

Since the functions $J_0\left(\zeta\sqrt{\pm i}\right)$ and $H_0^{(1)}(\zeta\sqrt{\pm i})$ are complex, whereas the solution w must be real, it is evident that the constants $C_i(i=1,2,3,4)$ must also be complex. In order to express the solution in terms of real functions, let us rewrite the expression (4.51) in the form

$$w=A_1u_0(\zeta)+A_2v_0(\zeta)+A_3f_0(\zeta)+A_4g_0(\zeta), \tag{4.52}$$

where the following expressions are the modified Bessel functions [1] tabulated in [3]:

$$\begin{aligned}
u_0(\zeta)&=\mathrm{Re}J_0\left(\zeta\sqrt{i}\right)=\frac{J_0\left(\zeta\sqrt{i}\right)+J_0\left(\zeta\sqrt{-i}\right)}{2},\\
v_0(\zeta)&=\mathrm{Im}J_0\left(\zeta\sqrt{i}\right)=\frac{J_0\left(\zeta\sqrt{i}\right)-J_0\left(\zeta\sqrt{-i}\right)}{2i},\\
f_0(\zeta)&=\mathrm{Re}H_0^{(1)}\left(\zeta\sqrt{i}\right)=\frac{H_0^{(1)}\left(\zeta\sqrt{i}\right)+H_0^{(1)}\left(\zeta\sqrt{-i}\right)}{2},\\
g_0(\zeta)&=\mathrm{Im}H_0^{(1)}\left(\zeta\sqrt{i}\right)=\frac{H_0^{(1)}\left(\zeta\sqrt{i}\right)-H_0^{(1)}\left(\zeta\sqrt{-i}\right)}{2i}.
\end{aligned} \tag{4.53}$$

Since the functions $u_0(\zeta)$, $v_0(\zeta)$, $f_0(\zeta)$, and $g_0(\zeta)$ are real, then the coefficients $A_i(i=1,2,3,4)$will also be real.

It can be shown that the functions u_0 and v_0, together with all of their derivatives, remain finite when $\zeta\to 0$ and tend toward infinity when $\zeta\to\infty$. The function f_0 for $\zeta\to 0$ has a singularity of the $\zeta^2\ln\zeta$ type, the function g_0 approaches infinity as $\ln\zeta$ when $\zeta\to 0$; both these functions approach zero when $\zeta\to\infty$ [1].

The following relationships exist between the functions u_0, v_0, f_0, and g_0:

$$\nabla_\zeta^2u_0=v_0;\ \nabla_\zeta^2v_0=-u_0;\quad \nabla_\zeta^2f_0=g_0;\quad \nabla_\zeta^2g_0=-f_0, \tag{4.54}$$

where the operator ∇_ζ^2 is given by Eq. (4.48). These relations and Eqs (4.14) enable us to write the expressions for bending moments and shear forces.

Example 4.6

Find the deflection surface equation for an infinite plate resting on an elastic foundation, subjected to a concentrated force P.

Solution

The deflection surface is given by Eq. (4.52). Thus, the problem is to evaluate the constants of integration A_i. The functions $u_0(\zeta)$ and $v_0(\zeta)$ tend toward infinity for $\zeta\to\infty$ whereas the deflections and bending moments for $\zeta\to\infty$ should vanish. As it follows from the physical sense of the problem, then $A_1=A_2=0$. For $\zeta=0$, the

deflection should be finite; since $g_0(\zeta)$ approaches infinity for $\zeta \to 0$, then $A_4 = 0$. Thus,

$$w = A_3 f_0(\zeta). \tag{4.55}$$

Notice that $f_0(\zeta)$ remains finite when $\zeta \to 0$. The constant A_3 is determined from the equilibrium condition at the point of application of P: the resultant of the radial shear force Q_r distributed over a lateral surface of an infinitesimal circular cylinder cut out from the plate at its center must be in the limit equal to a value of the applied force P, ie.,

$$\lim_{\zeta \to 0} Q_r = \frac{P}{2\pi r} = -\frac{P}{2\pi l \zeta}. \tag{4.56}$$

Substituting for w from Eq. (4.55) into the third Eq. (4.14) and taking into account the relations (4.54), we obtain the following expression for the shear force:

$$Q_r = -\frac{D}{l^3} A_3 g_0{}'(\zeta), \tag{4.57a}$$

where the prime notation indicates the first derivative of the function with respect to the variable ζ. From the theory of the Bessel functions [2], when $\zeta \to 0$ then $g_0'(\zeta) = -\frac{2}{\pi\zeta}$. Thus,

$$Q_r = -A_3 \frac{D}{l^3} \frac{2}{\pi\zeta}. \tag{4.57b}$$

Equating the right-hand sides of Eqs (4.56) and (4.57b), one obtains $A_3 = Pl^2/4D$ and the deflection surface is given by

$$w = \frac{Pl^2}{4D} f_0(\zeta). \tag{4.58}$$

Taking into account that the function $f_0(\zeta)$ tends toward 1/2 for $\zeta \to 0$ [2], we can determine the maximum deflection (under point of application of P), as follows:

$$w_{\max} = \frac{Pl^2}{8D}.$$

The bending moments may be determined from Eqs (4.14) by inserting Eqs (4.57). They are of the following form:

$$\begin{aligned} M_r &= \frac{P}{4\pi}\left[(1+\nu)\left(\ln\frac{2l}{r} - \gamma\right) - \frac{1}{2}(1-\nu)\right]; \\ M_\theta &= \frac{P}{4\pi}\left[(1+\nu)\left(\ln\frac{2l}{r} - \gamma\right) + \frac{1}{2}(1-\nu)\right], \end{aligned} \tag{4.59}$$

where $\gamma = 0.5772157\ldots$ is Euler's constant. These formulas are inapplicable for the point of application of the concentrated force.

The function (4.58) can be considered as a Green's function in polar coordinates for plates resting on a Winkler-type elastic foundation, i.e., it enables one to determine the deflection surface of an infinite plate subjected to any type of axisymmetric loading $p = p(r)$ by integrating the solution as a function of r.

Once the solution for an infinite plate on an elastic foundation is available, we can go to the solution for a circular plate of finite dimensions subjected to an

axisymmetric loading. For example, the deflection surface of solid circular plates on a Winkler-type foundation can be represented by Eq. (4.18), where w_p is a particular and w_h is a complementary solutions of Eq. (4.45), respectively. The particular solution can be determined using the superposition principle and Green's function (4.58). The homogeneous solution for the solid circular plate of finite dimensions is of the form

$$w_h = A_1 u_0(\zeta) + A_2 v_0(\zeta).$$

The constants of integration A_1 and A_2 can be evaluated from the prescribed boundary conditions on the plate edge.

4.6 ASYMMETRIC BENDING OF CIRCULAR PLATES

In the foregoing sections, our concern was with circular plates loaded axisymmetrically. We now turn to asymmetrical loading. For the analysis of deflections and stresses, we must obtain appropriate solutions of the governing differential equation (4.6). The general solution of this equation can also be presented in the form of (4.18). The complementary solution, w_h, can be expressed by the following series:

$$w_h = f_0(r) + \sum_{n=1}^{\infty} f_n(r)\cos n\varphi + \sum_{n=1}^{\infty} f_n^*(r)\sin n\varphi. \tag{4.60}$$

Substituting the above into Eq. (4.6), and noting the validity of the resulting expressions for all r and φ, leads to two ordinary differential equations with solutions

$$\begin{aligned} f_0(r) &= A_0 + B_0 r^2 + C_0 \ln\frac{r}{r^*} + D_0 r^2 \ln\frac{r}{r_0}, \\ f_1(r) &= A_1 r + B_1 r^{-1} + C_1 r^3 + D_1 r \ln\frac{r}{r_0} \quad \text{for } n = 1, \\ &\cdots\cdots\cdots\cdots\cdots\cdots\cdots\cdots\cdots\cdots\cdots\cdots \\ f_n(r) &= A_n r^n + B_n r^{-n} + C_n r^{n+2} + D_n r^{-n+2} (n \neq 1), \end{aligned} \tag{4.61}$$

Similar expressions can be written for $f_n^*(r)$ and $f_1^*(r)$. The first term in Eq. (4.61) represents an axisymmetric part of the deflection, discussed in Sec. 4.3. The terms containing $\cos n\varphi$ in Eq. (4.60) correspond to symmetrical components of the function w_h with respect to the plane $\varphi = 0$, while the terms containing $\sin n\varphi$ represent an inversely symmetrical part of w_h. The applied surface load $p = p(r, \varphi)$ can be expanded into a trigonometric series:

$$p(r,\varphi) = p_0(r) + \sum_{n=1}^{\infty} p_n(r)\cos n\varphi + \sum_{n=1}^{\infty} p_n^*(r)\sin n\varphi, \tag{4.62}$$

where

$$\begin{aligned} p_n(r) &= \frac{1}{\pi}\int_0^{2\pi} p(r,\varphi)\cos n\varphi \mathrm{d}\varphi, \quad p_n^*(r) = \frac{1}{\pi}\int_0^{2\pi} p(r,\varphi)\sin n\varphi \mathrm{d}\varphi, \\ p_0(r) &= \frac{1}{2\pi}\int_0^{2\pi} p(r,\varphi)\mathrm{d}\varphi. \end{aligned} \tag{4.63}$$

The constants of integration, $A_n, \ldots, D_n$, can be determined from boundary conditions of the plate. The boundary conditions on curvilinear edges of the circular plates are given by the expressions (4.10)–(4.12). The stress resultants and stress couples within the plate and on its edge are given by Eqs (4.7) and (4.9). Some details of an asymmetrical circular plate analysis are explained by considering the following illustrative problems.

Example 4.7

The edge of a solid circular plate of radius a is fixed over its boundary and the applied load is expressed as

$$p = p_0\left(1 + \frac{x}{a}\right) = p_0\left(1 + \frac{r}{a}\cos\varphi\right). \tag{a}$$

Find an expression for the deflections (Fig. 4.14).

Solution

Comparing Eq. (a) with Eq. (4.62), we can see that only two terms of the series are present in the example: an axisymmetric component p_0 and component $p_n(r)\cos n\varphi$ for $n = 1$ i.e., $p_1(r) = p_0\frac{r}{a}\cos\varphi$. The axisymmetric part of the solution, caused by load p_0,w_0, has been obtained in Sec. 4.3 and is expressed by formulas (4.29) and (4.30).

Find the asymmetrical part of the solution, w_1, that corresponds to the load component $p_1(r)$. The above part of the solution can also be represented in the form of Eq. (4.18). The homogeneous solution is given by the second equation (4.61), i.e.,

$$w_{\mathrm{h}}^{(1)} = f_1(r)\cos\varphi = \left(A_1 r + B_1 r^{-1} + C_1 r^3 + D_1 r\ln\frac{r}{a}\right)\cos\varphi, \tag{b}$$

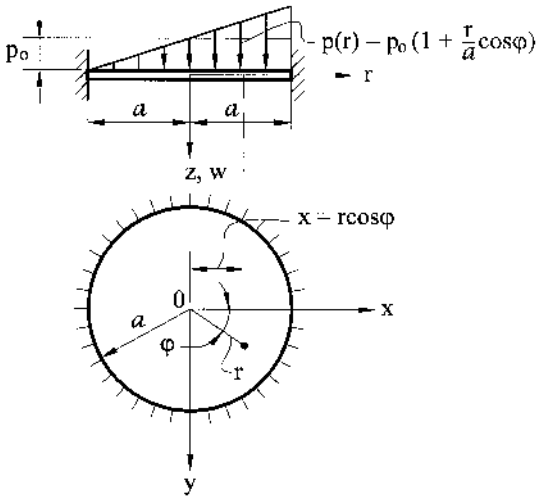

Fig. 4.14

where the superscript 1 indicates that this solution is obtained for $n = 1$. A particular solution must satisfy Eq. (4.6) with the right-hand side $\frac{p_0 r}{Da}\cos\varphi$. We will seek this particular solution in the following form:

$$w_{\mathrm{p}}^{(1)} = Ar^5 \cos\varphi. \tag{c}$$

Substituting the above into Eq. (4.6), we can find a constant A, i.e., $A = p_0/192Da$. Thus, the particular solution is

$$w_{\mathrm{p}}^{(1)} = \frac{p_0 r^5 \cos\varphi}{192Da}. \tag{d}$$

Hence, the general solution that corresponds to the asymmetrical part of loading is given by

$$w_1 = \left(A_1 r + B_1 r^{-1} + C_1 r^3 + D_1 r \ln r + \frac{p_0 r^5}{192Da}\right)\cos\varphi. \tag{e}$$

The boundary and continuity conditions are, as follows:

$$w \neq \infty\big|_{r=0};\ \frac{\partial w}{\partial r} \neq \infty\bigg|_{r=0};\ w = 0|_{r=a};\ \frac{\partial w}{\partial r} = 0\bigg|_{r=a}. \tag{f}$$

As it follows from the first two boundary conditions (f)

$$B_1 = 0 \quad \text{and} \quad D_1 = 0.$$

The third and fourth conditions (f) lead to the following two equations:

$$A_1 a + C_1 a^3 + \frac{p_0 a^4}{192D} = 0; \quad A_1 + 3C_1 a^2 + \frac{5p_0 a^3}{192D} = 0,$$

from which one derives A_1 and C_1, as follows:

$$A_1 = \frac{p_0 a^3}{192D},\ C_1 = -\frac{p_0 a}{96D}.$$

Hence, the deflection surface of the plate caused by the asymmetrical part of the given loading (a) is of the following form:

$$w_1(r,\varphi) = w_{\mathrm{h}}^{(1)} + w_{\mathrm{p}}^{(1)} = \frac{p_0 a^4}{192D}\left[\frac{r}{a} - 2\left(\frac{r}{a}\right)^3 + \left(\frac{r}{a}\right)^5\right]\cos\varphi. \tag{g}$$

Finally, the deflection surface of the plate due to the given loading (a) can be obtained by superposing the solutions given by formulas (4.29) and (g). We have

$$w(r,\varphi) = w_0 + w_1 = \frac{p_0 a^4}{64D}\left[1 - 2\left(\frac{r}{a}\right)^2 + \left(\frac{r}{a}\right)^4\right] + \frac{p_0 a^4}{192D}\left[\frac{r}{a} - 2\left(\frac{r}{a}\right)^3 + \left(\frac{r}{a}\right)^5\right]\cos\varphi. \tag{h}$$

The deflection at the center, w_C, can be obtained by setting $r = 0$. We obtain

$$w_C = \frac{p_0 a^4}{64D}. \tag{i}$$

The bending moments can be obtained by substitution for w from (g) into Eqs (4.7).

Stress analysis of circular plates having various boundary conditions and subjected to asymmetrical loading can be successfully carried out by numerical and approximate methods introduced in Chapter 6. Among other methods, the *reciprocity theorem* [4] may enable a simple approach for computation of the center displacements in circular plates with symmetrical boundary conditions under asymmetrical loading.

Consider a circular plate that carries two loads P_C and P_D applied at points C and D, respectively. Maxwell's reciprocal theorem is formulated, as follows [6]:

$$P_C \Delta_{CD} = P_D \Delta_{DC}, \tag{4.64}$$

where Δ_{CD} is the displacement component at point C in the direction of load P_C and due to load P_D; Δ_{DC} is the displacement component at point D in the direction of load P_D and due to load P_C. Equation (4.64) states that work done by the load P_C in moving through displacement produced by the load P_D is equal to work done by the load P_D in moving through displacement produced by the load P_C. The words "load" and "displacement" can be given by their general meanings, i.e., concentrated forces and deflections, couples and their rotations; at last, distributed load and the corresponding deflections are included.

Let point C be the center of a circular plate and point D be some point located at a distance r from that center. Denote $\Delta_{CD} = w_C$ and $\Delta_{DC} = w(r)$. Evidently $w(r)$ is a deflection at point D due to the unit force applied at the plate center. In the cases of fixed and simply supported plates, $w(r)$ is given by expressions obtained in Eqs (4.33) and (4.35), respectively. Then, let $P_C = 1$ and $P_D = p(r, \varphi)$. Substituting the above into Eq. (4.64), one obtains

$$w_C = \int_0^{2\pi} \int_0^a p(r, \varphi) w(r) r \mathrm{d}r \mathrm{d}\varphi \tag{4.65}$$

where a is the radius of a circular plate.

To illustrate the application of Eq. (4.65), reconsider Example 4.7. Upon substituting $p(r, \varphi) = p_0\left(1 + \frac{r}{a}\cos\varphi\right)$ and Eq. (4.33) into Eq. (4.65), setting $P = 1$ and integrating, we obtain

$$w_C = \frac{p_0}{16\pi D} \int_0^{2\pi} \int_0^a \left(1 + \frac{r}{a}\cos\varphi\right)\left(2r^2 \ln\frac{r}{a} + a^2 - r^2\right) r \mathrm{d}r \mathrm{d}\varphi = \frac{p_0 a^4}{64D}. \tag{4.66}$$

The above coincides exactly with the value given by Eq. (i) in Example 4.7.

4.7 CIRCULAR PLATES LOADED BY AN ECCENTRIC LATERAL CONCENTRATED FORCE

The solution for circular plates under an arbitrary concentrated load can be considered one of the fundamental problems in the theory of plates, because this solution can be used as the Green's function (see Sec. 3.4) for determining deflections of the plate caused by an arbitrary asymmetric loading.

Consider a bending problem for a clamped circular plate of radius R loaded by a concentrated force P applied at a distance b from the center of the plate. Represent the given concentrated force in the following form of series:

$$\frac{P}{\pi b}\left(\frac{1}{2}+\sum_{n=1}^{\infty}\cos n\varphi\right).$$

This series is quite analogous to the series applied earlier for the case of a rectangular plate loaded by a concentrated force. Then, the deflected surface of the plate, $w(r, \varphi)$, can be sought also in the form of the trigonometric series corresponding to the given loading. The next procedure for obtaining a solution of Eq. (4.6) will be quite similar to that discussed in Sec. 4.6. An approach for obtaining the solution of the problem leads to a rapidly convergent series for deflections. However the series in the solutions for the bending moments and shear forces do not convergent rapidly, and, directly at the point of application of the concentrated force these series are divergent (see Sec. 3.4). Therefore, a solution of this problem in the closed form is of a special interest. Such a solution was first obtained by Michell [5]. We present Michell's solution below.

At first, let us remind ourselves of one well-known definition of a circle given in analytical geometry. Let point M^0 be any point on the circumference, points O_1 and O_2 some fixed points on the xy coordinate plane and r_1^0 and r_2^0 some distances from point M^0 to points O_1 and O_2 as shown in Fig. 4.15a.

Then, any circle can be defined as a locus of points for which the ratio r_1^0/r_2^0 is a constant. In fact, as follows from Fig. 4.15a,

$$r_1^0=\sqrt{R^2+(\lambda R)^2-2R\cdot(\lambda R)\cos\varphi};\quad r_2^0=\sqrt{R^2+(R/\lambda)^2-2R\cdot(R/\lambda)\cos\varphi}, \tag{4.67}$$

where λ is some parameter. It can be shown that

$$\frac{r_1^0}{r_2^0}=\lambda=\text{const.} \tag{4.68}$$

Let the concentrated force P be applied at point O_1 at a distance λR from the center, as shown in Fig. 4.15b. Locate an arbitrary point M of the plate by coordinates r_1 and r_2, which are the distances from the above point to some fixed points O_1 and O_2.

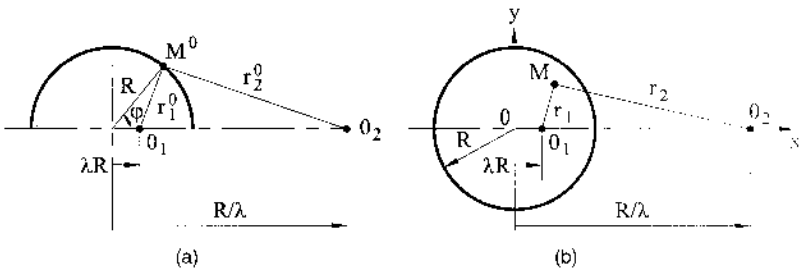

Fig. 4.15

The coordinates r_1 and r_2 are related to Cartesian coordinates by the following expressions:

$$r_1^2 = (x - \lambda R)^2 + y^2;\ r_2^2 = (x - R/\lambda)^2 + y^2. \tag{4.69}$$

Determine the expression for the Laplace operator of some function Ω in terms of the coordinates r_1 and r_2. For this purpose, first find the following

$$\begin{aligned}
\frac{\partial \Omega}{\partial x} &= \frac{\partial \Omega}{\partial r_1}\frac{\partial r_1}{\partial x} + \frac{\partial \Omega}{\partial r_2}\frac{\partial r_2}{\partial x} = \frac{\partial \Omega}{\partial r_1}\cdot\frac{x - \lambda R}{r_1} + \frac{\partial \Omega}{\partial r_2}\cdot\frac{x - R/\lambda}{r_2}, \\
\frac{\partial^2 \Omega}{\partial x^2} &= \frac{\partial^2 \Omega}{\partial r_1^2}\frac{(x - \lambda R)^2}{r_1^2} + \frac{\partial^2 \Omega}{\partial r_2^2}\frac{(x - R/\lambda)^2}{r_2^2} + \frac{\partial \Omega}{\partial r_1}\left[\frac{1}{r_1} - \frac{(x - \lambda R)^2}{r_1^3}\right] \\
&\quad + \frac{\partial \Omega}{\partial r_2}\left[\frac{1}{r_2} - \frac{(x - R/\lambda)^2}{r_2^3}\right].
\end{aligned} \tag{4.70}$$

Similarly,

$$\frac{\partial^2 \Omega}{\partial y^2} = \frac{\partial^2 \Omega}{\partial r_1^2}\frac{y^2}{r_1^2} + \frac{\partial^2 \Omega}{\partial r_2^2}\frac{y}{r_2^2} + \frac{\partial \Omega}{\partial r_1}\left(\frac{1}{r_1} - \frac{y^2}{r_1^3}\right) + \frac{\partial \Omega}{\partial r_2}\left(\frac{1}{r_2} - \frac{y^2}{r_2^3}\right). \tag{4.71}$$

Summing the above equations for the second derivatives, one obtains the expression for the Laplace operator. We have the following:

$$\nabla^2 \Omega \equiv \frac{\partial^2 \Omega}{\partial x^2} + \frac{\partial^2 \Omega}{\partial y^2} = \frac{\partial^2 \Omega}{\partial r_1^2} + \frac{\partial^2 \Omega}{\partial r_2^2} + \frac{1}{r_1}\frac{\partial \Omega}{\partial r_1} + \frac{1}{r_2}\frac{\partial \Omega}{\partial r_2}. \tag{4.72}$$

This expression can be rewritten in the form

$$\nabla^2 \Omega = \frac{1}{r_1}\frac{\partial}{\partial r_1}\left(r_1 \frac{\partial \Omega}{\partial r_1}\right) + \frac{1}{r_2}\frac{\partial}{\partial r_2}\left(r_2 \frac{\partial \Omega}{\partial r_2}\right). \tag{4.73}$$

Determination of the biharmonic operator $\nabla^2\nabla^2\Omega$ is reduced to the double implementation of the operator (4.73).

A solution of Eq. (4.6) for the circular plate loaded by a concentrated force P at point O_1 can be represented in the following form:

$$w = \frac{P}{8\pi D} r_1^2 \ln r_1 + C_1 r_1^2 \ln r_2 + C_2 r_1^2 + C_3 r_2^3, \tag{4.74}$$

where the first term on the right-hand side represents the deflection surface of the plate symmetrical about point O_1 and having a singularity at that point. The constants of integration C_1, C_2, and C_3 are evaluated from the boundary conditions. Since on the boundary, $r_1 = r_1^0$, $r_2 = r_2^0$, and also $r_1^0 = \lambda r_2^0$, then the boundary condition $w = 0$ will be satisfied if we put

$$C_1 = -\frac{P}{8\pi D},\ C_2 = -\frac{P}{8\pi D}\ln\lambda - \frac{C_3}{\lambda^2}. \tag{4.75}$$

In this case,

$$w = \frac{P}{8\pi D} r_1^2 \ln \frac{r_1}{\lambda r_2} + C_3 \left(r_2^2 - \frac{r_1^2}{\lambda^2} \right). \tag{4.76}$$

The constant C_3 is determined from the condition that on the boundary $\partial w/\partial n = 0$. Since $w = 0$, then to satisfy this boundary condition it is sufficient that $\partial w/\partial r_1 = 0$ on the boundary, i.e., for $r_1 = \lambda r_2$. As it follows from the above, $C_3 = \frac{P}{8\pi D} \frac{\lambda^2}{2}$. Finally, we obtain

$$w = \frac{P}{8\pi D} \left[r_1^2 \ln \frac{r_1}{\lambda r_2} + \frac{1}{2} (\lambda^2 r_2^2 - r_1^2) \right]. \tag{4.77}$$

At the point of application of the concentrated force, i.e., for $r_1 = 0$ and $r_2 = R\left(\frac{1}{\lambda} - \lambda\right)$ (see Fig. 4.15b), the deflection is

$$w = \frac{PR^2}{16\pi D} (1 - \lambda^2). \tag{4.78}$$

The closed-form equation for the deflections enables one to determine the bending moments in the closed form also. For this purpose, we first find the derivatives of w and the bending moments in the Cartesian coordinate system using Eqs (4.70). The bending moments at points of the diameter passing through the point of application of the force ($y = 0$) are found to be

$$\begin{aligned} M_x = M_r &= \frac{P}{8\pi D} \left[2(1+\nu) \ln \frac{r_1}{\lambda r_2} + 2 + \lambda^2 (1+\nu) + \frac{r_1^2}{r_2^2} (1-\nu) \right], \\ M_y = M_t &= \frac{P}{8\pi D} \left[2(1+\nu) \ln \frac{r_1}{\lambda r_2} + 2\nu + \lambda^2 (1+\nu) - \frac{r_1^2}{r_2^2} (1-\nu) \right]. \end{aligned} \tag{4.79}$$

where $r_1 = x - \lambda R$, $r_2 = R/\lambda - x$.

In the particular case of a clamped circular plate loaded by a concentrated force P applied at its center, $\lambda \to 0$ and Eqs (4.78) and (4.79) will coincide with those obtained in Sec. 4.3 for an axisymmetrically loaded circular plate (see Eqs (4.33) and (4.34)).

4.8 CIRCULAR PLATES OF VARIABLE THICKNESS

We limit ourselves to axisymmetric bending, since this is the type most widely encountered in engineering – for example, in many machine parts, such as turbine blades, bellows, springs, etc. Following Szillard [6], we derive the governing equation of these plates.

Due to the symmetry, Q_t and M_{rt} vanish and only internal forces and moments show in Fig. 4.16a act on the plate element, as follows

$$(Q_r + \mathrm{d}Q_r)(r + \mathrm{d}r)\mathrm{d}\varphi - Q_r r \mathrm{d}\varphi + p \mathrm{d}s \mathrm{d}r = 0, \tag{4.80}$$

$$\left(M_r + \frac{\mathrm{d}M_r}{\mathrm{d}r} \mathrm{d}r \right)(r + \mathrm{d}r)\mathrm{d}\varphi - M_r r \mathrm{d}\varphi - Q_r r \mathrm{d}\varphi \mathrm{d}r - M_t \mathrm{d}r \mathrm{d}\varphi = 0. \tag{4.81}$$

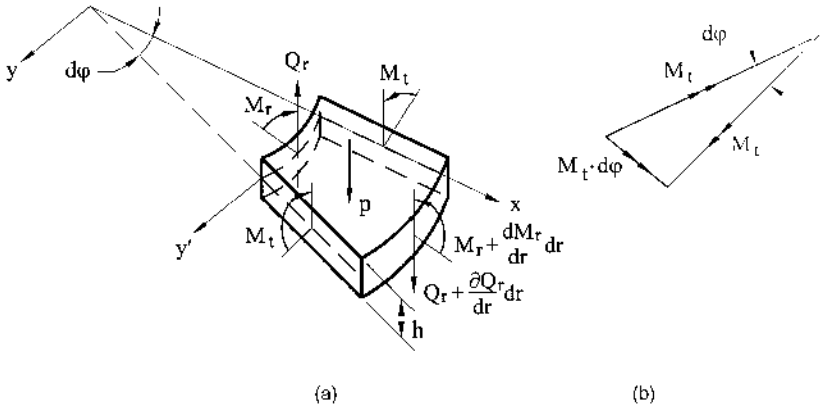

Fig. 4.16

The last term on the left-hand side of Eq. (4.81) is due to the resultant moment shown in Fig. 4.16b. Replacing $ds = r d\varphi$, canceling the common factor $dr d\varphi$ and neglecting small quantities of higher order, Eqs (4.80) and (4.81) become

$$-\frac{1}{r}\frac{d}{dr}(rQ_r) = p, \tag{4.82}$$

$$Q_r = \frac{dM_r}{dr} + \frac{1}{r}(M_r - M_t). \tag{4.83}$$

Substituting for M_r and $M_t$from Eqs (4.14) into Eq. (4.83) and making $D = D(r)$, we obtain

$$\frac{d^3w}{dr^3} + \frac{d^2w}{dr^2}\left(\frac{1}{D}\frac{dD}{dr} + \frac{1}{r}\right) + \frac{dw}{dr}\left(\frac{\nu}{rD}\frac{dD}{dr} - \frac{1}{r^2}\right) + \frac{Q_r}{D} = 0. \tag{4.84}$$

If we substitute for Q_r from the third equation (4.14) into Eq. (4.82), we obtain

$$\frac{1}{r}\frac{d}{dr}\left\{rD\frac{d}{dr}\left[\frac{1}{r}\frac{d}{dr}\left(r\frac{dw}{dr}\right)\right]\right\} = p(r). \tag{4.85}$$

Either of the two equations, (4.84) or (4.85), can be used as the governing differential equations of axisymmetrically loaded circular plates of variable thickness.

In order to lower the order of differential equation (4.84), let us introduce a new variable

$$\vartheta = -\frac{dw}{dr}, \tag{4.86}$$

where ϑ is the angle of rotation of the normal to the plate middle surface. The negative sign for ϑ is because, as seen from Fig. 4.17, this angle is counted off in the direction which is opposite to the rotation from the r axis to the z axis. The expressions for bending moments, Eqs (4.14), can be also written in terms of ϑ, as follows:

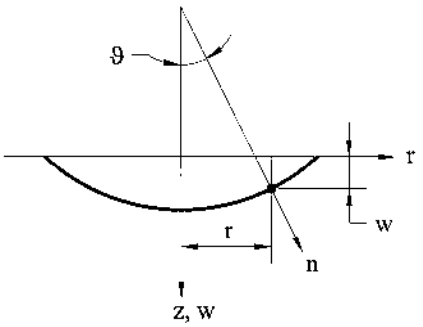

Fig. 4.17

$$M_r = D\left(\frac{\mathrm{d}\vartheta}{\mathrm{d}r} + \nu\frac{\vartheta}{r}\right);\ M_t = D\left(\frac{\vartheta}{r} + \nu\frac{\mathrm{d}\vartheta}{\mathrm{d}r}\right). \tag{4.87}$$

Finally, introducing ϑ in the form of Eq. (4.86) into Eq. (4.84) yields the following:

$$\frac{\mathrm{d}^2\vartheta}{\mathrm{d}r^2} + \left[\frac{1}{r} + \frac{1}{D}\frac{\mathrm{d}D}{\mathrm{d}r}\right]\frac{\mathrm{d}\vartheta}{\mathrm{d}r} + \left[\frac{\nu}{D}\frac{\mathrm{d}D}{\mathrm{d}r} - \frac{1}{r}\right]\frac{\vartheta}{r} = \frac{Q_r}{D}. \tag{4.88}$$

If $D = \text{const}$, Eq. (4.88) reduces to

$$\frac{\mathrm{d}^2\vartheta}{\mathrm{d}r^2} + \frac{1}{r}\frac{\mathrm{d}\vartheta}{\mathrm{d}r} - \frac{1}{r^2}\vartheta = \frac{Q_r}{D}. \tag{4.89}$$

Equation (4.88) can also be considered as the governing differential equation of bending of an axisymmetrically loaded circular plate having a variable stiffness. It is assumed that the right-hand side of this equation is a known function of r. Q_r can be obtained from the free-body equilibrium. In a general case, when h is an arbitrary function of r, Eq. (4.88) can be solved numerically only using the approximate methods introduced in Chapter 6. The small-parameter method, introduced in Chapter 3 for treating rectangular plates with a variable thickness, can also be applied to the solution of Eq. (4.88).

However, there is an important particular case when a closed-form solution of Eq. (4.88) is available. This is a case when the plate thickness varies according to the following law:

$$h = Cr^{\alpha}. \tag{4.90}$$

Depending on the exponent α, the shape of the plate may be different (Fig. 4.18). The problem of an axisymmetric bending of the circular plate having a form that corresponds to $\alpha < 0$ is encountered, in particular, in the analysis of turbine disks loaded by an axial load.

Let r_1 be the inner radius and h_1 the plate thickness on the inner edge of an annular circular plate. Taking into account Eq. (4.90), we can represent the plate thickness as

$$h = h_1\left(\frac{r}{r_1}\right)^{\alpha}. \tag{4.91}$$

The flexural rigidity of the arbitrary point of the plate for this case is

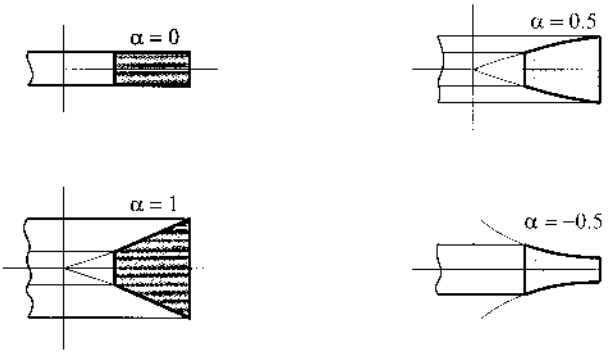

Fig. 4.18

$$D = \frac{Eh^3}{12(1-\nu^2)} = D_0\left(\frac{r}{r_i}\right)^{3\alpha}, \quad \text{and} \tag{4.92}$$

$D_0 = \dfrac{Eh_1^3}{12(1-\nu^2)}$ is the flexural rigidity on the inner edge. Substituting Eq. (4.92) into Eq. (4.88), yields

$$\frac{\mathrm{d}^2\nu}{\mathrm{d}r^2} + \frac{(1+3\alpha)}{r}\frac{\mathrm{d}\nu}{\mathrm{d}r} - \frac{(1-3\alpha\nu)}{r^2}\vartheta = \frac{Q_r}{D_0}\left(\frac{r_1}{r}\right)^{3\alpha}. \tag{4.93}$$

The general solution of this equation can be represented

$$\vartheta = \vartheta_{\mathrm{h}} + \vartheta_{\mathrm{p}}, \tag{4.94}$$

where the complementary solution ϑ_{h} is sought in the form

$$\vartheta_{\mathrm{h}} = Cr^x. \tag{4.95}$$

Substituting the above into the homogeneous equation (4.93), we obtain the following characteristic equation:

$$x^2 + 3\alpha x - (1 - 3\alpha\nu) = 0.$$

The roots of this equation are the following:

$$x_1 = -\frac{3\alpha}{2} + \sqrt{\frac{9\alpha^2}{4} + (1 - 3\nu\alpha)}; \quad x_2 = -\frac{3\alpha}{2} - \sqrt{\frac{9\alpha^2}{4} + (1 - 3\alpha\nu)}\ .$$

Hence, the complementary solution is given by

$$\vartheta_{\mathrm{h}} = C_1 r^{\left[-\frac{3\alpha}{2}+\sqrt{\frac{9\alpha^2}{4}+(1-3\alpha\nu)}\right]} + C_2 r^{\left[-\frac{3\alpha}{2}-\sqrt{\frac{9\alpha^2}{4}+(1-3\alpha\nu)}\right]}. \tag{4.96}$$

The particular solution, ϑ_{p}, depends on the type of loading. If the circular plate is subjected to a load $p_0 = \mathrm{const}$, then the shear force Q_r can be calculated from the equilibrium as follows:

$$Q_r = -p_0 \frac{r^2 - r_1^2}{2r}.$$

Substituting the above into the right-hand side of Eq. (4.93), we can seek a particular solution in the following form $\vartheta_p = Br^y$. After a simple transformation, we obtain

$$\vartheta_p = -\frac{p_0 r_1^{3\alpha}}{2D_0}\left[\frac{r^{3(1-\alpha)}}{8 - 9\alpha + 3\alpha\nu} + \frac{r^{(1-3\alpha)} r_1^2}{3\alpha(1-\nu)}\right]. \tag{4.97}$$

If a concentrated load P is distributed over the inner edge, we can find, by analogy, that

$$Q_r = -\frac{P}{2\pi r} \quad \text{and} \quad \vartheta_p = \frac{\mathrm{Pr}_1^{3\alpha} r^{(1-3\alpha)}}{6\pi D_0 \alpha(1-\nu)}. \tag{4.98}$$

The general solution of Eq. (4.93) for a plate subjected to uniform pressure p_0 and concentrated force P distributed over the inner edge of the plate can be represented in the form

$$\begin{aligned}\vartheta = {} & C_1 r^{\left[-\frac{3}{2}\alpha + \sqrt{\frac{9\alpha^2}{4} + (1 - 3\nu\alpha)}\right]} + C_2 r^{\left[-\frac{3}{2}\alpha - \sqrt{\frac{9\alpha^2}{4} + (1 - 3\alpha\nu))}\right]} \\ & - \frac{p_0 r_1^{3\alpha}}{2D_0}\left[\frac{r^{3(1-\alpha)}}{8 - 9\alpha + 3\alpha\nu} + \frac{r^{(1-3\alpha)} r_1^2}{3\alpha(1-\nu)}\right] + \frac{\mathrm{Pr}_1^{3\alpha} r^{(1-3\alpha)}}{6\pi D_0 \alpha(1-\nu)}.\end{aligned} \tag{4.99}$$

The bending moments can be determined from Eqs (4.87). The deflection w is determined by integrating the expression (4.86). We have

$$w = -\int \vartheta \mathrm{d}r + C_3. \tag{4.100}$$

The constants of integration, C_1, C_2, and C_3, are to be determined from boundary conditions. The above conditions are of the following form:

if the plate edge is fixed, then $\vartheta = 0$;
if the plated edge is simply supported, then $M_r = D\left(\frac{\mathrm{d}\vartheta}{\mathrm{d}r} + \nu\frac{\vartheta}{r}\right) = 0$;

The third boundary condition is formulated, as follows: the deflection on the restrained edge is zero. One can also take a definite integral instead of indefinite Eq. (4.100), i.e.,

$$w = -\int_{r_0}^{r} \vartheta \mathrm{d}\bar{r}, \tag{4.101}$$

where r_0 is the radius on the plate support and r is the radius at a point of interest.

Example 4.9

Find the expressions for stresses and deflections in the circular plate with linearly varying thickness. The plate is simply supported on its edges and loaded by line forces P, as shown in Fig. 4.19a. Given $r_2 = \beta r_1$, $\nu = 1/3$.

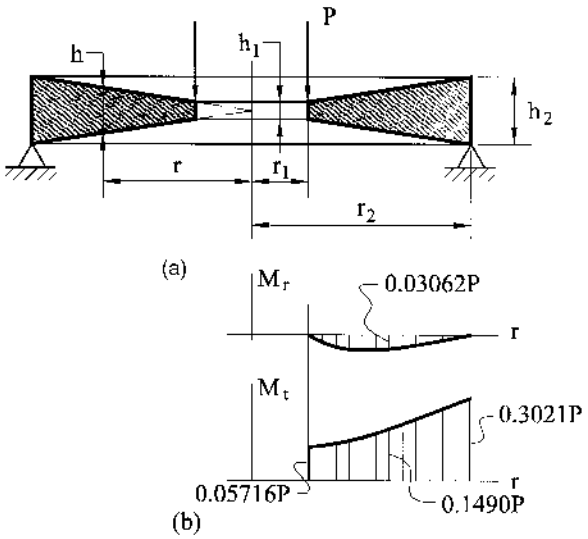

Fig. 4.19

Solution

The parameter α in this case is equal to unity. Thus, for $\alpha = 1$ and $\nu = 1/3$, Eq. (4.99) becomes

$$\vartheta = C_1 + C_2 r^{-3} + \frac{\mathrm{Pr}_1^3 r^{-2}}{4\pi D_0}. \tag{a}$$

Accordingly,

$$\frac{\vartheta}{r} = C_1 r^{-1} + C_2 r^{-4} + \frac{\mathrm{Pr}_1^3 r^{-3}}{4\pi D_0}; \quad \frac{\mathrm{d}\vartheta}{\mathrm{d}r} = -3C_2 r^{-4} - \frac{\mathrm{Pr}_1^3 r^{-3}}{2\pi D_0}. \tag{b}$$

The boundary conditions are

$$M_r = 0\big|_{r=r_1} \text{ or } \left(\frac{d\vartheta}{\mathrm{d}r} + \frac{1}{3}\frac{\vartheta}{r}\right) = 0\Big|_{r=r_1}; \; M_r = 0\big|_{r=r_2=3r_1} \text{ or } \left(\frac{\mathrm{d}\vartheta}{\mathrm{d}r} + \frac{1}{3}\frac{\vartheta}{r}\right) = 0\Big|_{r=r_2=\beta r_1}. \tag{c}$$

Substituting for ϑ and $\mathrm{d}\vartheta/\mathrm{d}r$ from Eqs (b) into the boundary conditions (c) leads to the following system of two algebraic equations:

$$-\frac{3C_2}{r_1^4} - \frac{P}{2\pi D_0} + \frac{C_1}{3r_1} + \frac{C_2}{3r_1^4} + \frac{P}{12\pi D_0} = 0,$$

$$-\frac{3C_2}{\beta^4 r_1^4} - \frac{P}{2\beta^3 \pi D_0} + \frac{C_1}{3\beta r_1} + \frac{C_2}{3\beta^4 r_1^4} + \frac{P}{12\beta^3 \pi D_0} = 0.$$

Solving these equations for C_1 and C_2 yields

$$C_1 = \frac{5}{4}\frac{P}{4\pi D_0} r_1 \left(1 + \frac{\beta^3 - \beta}{1 - \beta^3}\right), \quad C_2 = \frac{5}{32}\frac{P}{\pi D_0} r_1^4 \frac{\beta^3 - \beta}{1 - \beta^3}.$$

Substituting the above into the expression (a) gives the following

$$\vartheta = \frac{P}{4\pi D_0} r_1 \left[\frac{5(1-\beta)}{1-\beta^3} + \frac{5(\beta^3-\beta)}{8(1-\beta^3)} \frac{r_1^3}{r^3} + \frac{r_1^2}{r^2} \right]. \tag{d}$$

Knowing ϑ we can determine the bending moments M_r and M_t from Eqs (4.87). We have

$$\begin{aligned} M_r &= D_0 \frac{r^3}{r_1^3} \left(\frac{\mathrm{d}\vartheta}{\mathrm{d}r} + \nu \frac{\vartheta}{r} \right) = \frac{5P}{12\pi} \left[\frac{r_1(\beta^2-1)\beta}{r(\beta^3-1)} - 1 + \frac{\beta-1}{\beta^3-1} \frac{r^2}{r_1^2} \right], \\ M_t &= D_0 \frac{r^3}{r_1^3} \left(\frac{\vartheta}{r} + \nu \frac{\mathrm{d}\vartheta}{\mathrm{d}r} \right) = \frac{P}{4\pi} \left[\frac{5(\beta-1)}{\beta^3-1} \frac{r^2}{r_1^2} + \frac{1}{3} \right]. \end{aligned} \tag{e}$$

The moment diagrams for $\beta = 3$ are shown in Fig. 4.19b. The maximum stress at $r = r_1$ is

$$\sigma_{t,\max} = \frac{6M_t}{h_1^2} = 1.08 \frac{P}{\pi h_1^2},$$

and at $r = r_2$

$$\sigma_{t,\max} = \frac{6M_t}{(3h_1)^2} = 0.63 \frac{P}{\pi h_1^2}.$$

The maximum deflection for $\beta = 3$ is found from Eq. (4.101) by substituting for ϑ from Eq. (d) into the above and making $r_0 = r_2 = \beta r_1$:

$$w_{\max} = -\int_{3r_1}^{r_1} \vartheta \mathrm{d}r = 0.295 \frac{\mathrm{P}r_1^2}{\pi D_0}.$$

Numerical results, given in Fig. 4.19, were taken from Ref. [7].

PROBLEMS

4.1 A circular plate of radius a is bent according to the following equation (the origin of the coordinate system is at the plate center):

$$w = C(a^2 - r^2)$$

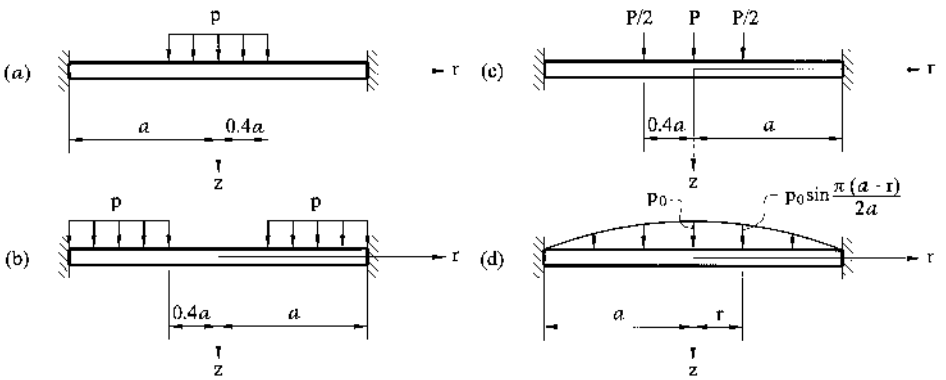

Fig. P4.1

How is the plate supported and what is the nature of the loading?

4.2 The equation of the deflected middle surface of the circular plate of radius a is given by the following equation:

$$w = C\left[(5+\nu)a^4 - 2(3+\nu)a^2r^2 + (1+\nu)r^4\right]$$

How is the plate supported and what is the nature of the loading?

4.3 It is known that at a concentrated load on a beam, the bending moment is finite at the point of application of the force. However, at a concentrated load on a plate, the bending moment is infinite at a point of application of the force according to Kirchhoff's plate bending theory. Explain physically, why there is this difference.

4.4 At each of the circular plates with the clamped edge and loaded, as shown in Fig. P.4.1, determine the deflection and bending moments equations. Find $w_{\max}$, $M_{r,\max}$, and $M_{t,\max}$.

4.5 At each of the circular plates with simply supported edge and loaded, as shown in Fig. P.4.2, determine the equations for deflections and bending moments. Find $w_{\max}$, $M_{r,\max}$, and $M_{t,\max}$.

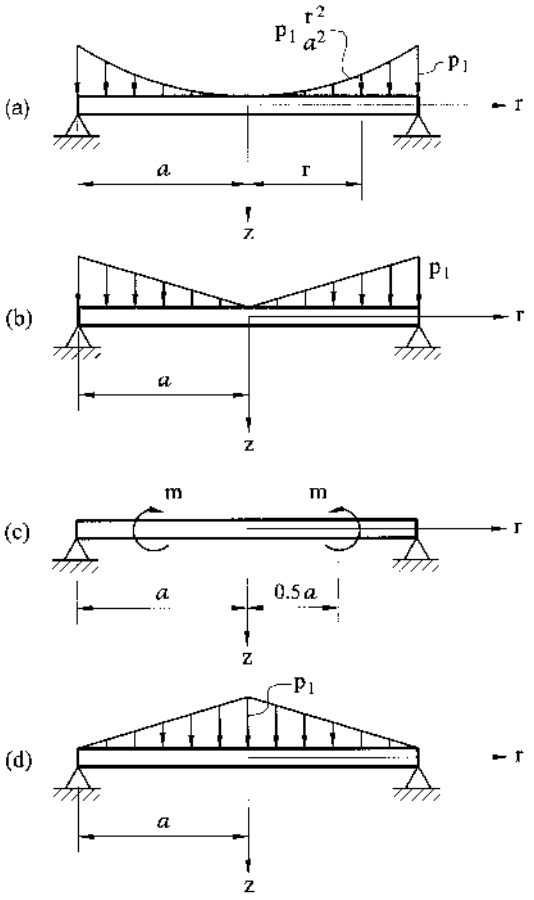

Fig. P4.2

4.6 Let a circular plate be subjected to an axially symmetric transverse load of intensity p. Show that $p = \frac{Q_r}{r} + \frac{dQ_r}{dr}$.

4.7 Show that the following relations are valid for the axisymmetrically loaded circular plate:

$$\frac{d}{dr}(\chi_r + \chi_t) = -\frac{Q_r}{D} \text{ and } \frac{d}{dr}(M_r + M_t) = -(1+\nu)Q_r.$$

4.8 At each of the annular circular plates and loaded, as shown in Fig. P.4.3, determine the equations for the deflections and bending moments. Find w_{max}, $M_{r,max}$, and $M_{t,max}$.

4.9 Calculate the stresses and deflections in a diaphragm intended for measuring the rate of liquid (see Fig. P.4.3b). The resistance created by the diaphragm in flowing the liquid

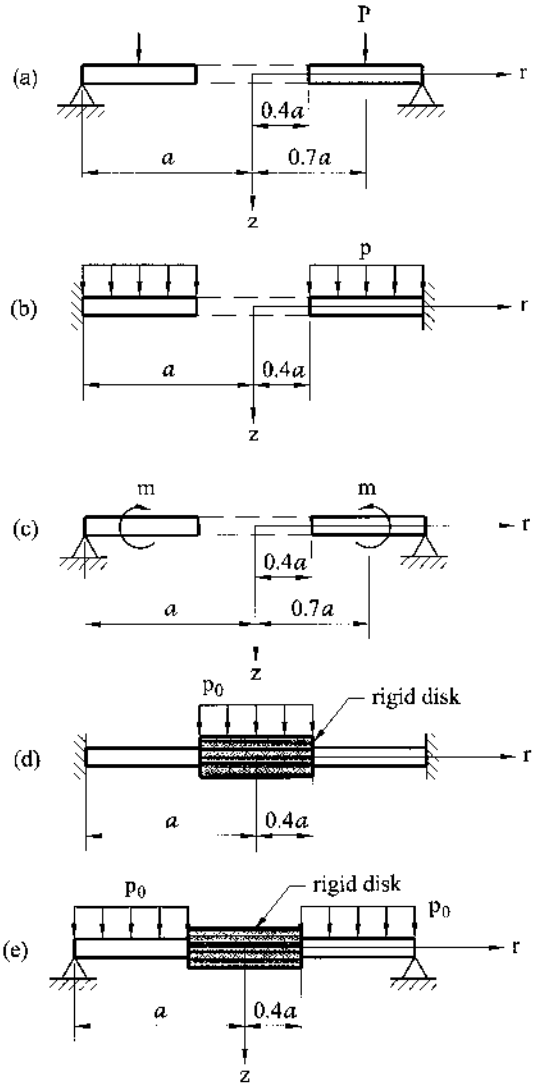

Fig. P4.3

causes a pressure drop of intensity p. Given: $a = 0.2\,\text{m}$, $p = 0.4\,\text{MPa}$, $\nu = 0.3$, $E = 220$ GPa, and $h = 0.02\,\text{m}$.

4.10 Calculate the stresses and deflections in the cap of a hatch. The cap is modeled by a circular plate simply supported on its outer edge and having a rigid cylinder welded to the plate's central part, as shown in Fig. P.4.3.e. Use: $a = 0.85\,\text{m}$, $p = 2\,\text{MPa}$, $E = 200\,\text{GPa}$, $\nu = 0.3$, and $h = 0.08\,\text{m}$.

4.11 Find the deflections and bending moments in the circular stepped plate shown in Fig. P.4.4. Assume $a = 2\,\text{m}$, $h = 0.2\,\text{m}$, $h_1 = 0.12\,\text{m}$, $p_0 = 1.5\,\text{MPa}$, $E = 200\,\text{GPa}$, and $\nu = 0.3$.

4.12 Redo Problem 4.11 for the case of the plate with fixed outer edge.

4.13 Find the expressions for deflections and bending moments in a circular plate subjected to load $p = \frac{p_0 r}{a}\cos\varphi$ (the origin is taken at the plate center) if the plate edge is fixed and a is the plate radius.

4.14 A circular simply supported plate is subjected to a transverse load $p = p_0\left(1 + \frac{r}{a}\cos\varphi\right)$ (the origin of the coordinate system is taken at the plate center) and a is the plate radius. Draw the deflection and bending moment diagrams along the diameter for $\varphi = \pi/4$. Use $a = 2.0\,\text{m}$, $h = 0.15\,\text{m}$, $p_0 = 5\,\text{MPa}$, $E = 200\,\text{GPa}$, and $\nu = 0.3$.

4.15 Derive expressions for the stress couples M_r, M_t, and M_{rt} in terms of the deflection, using the procedure presented in Sec. 2.3 for rectangular plates.

4.16 A concrete circular slab, simply supported on its edge, is subjected to the loading shown in Fig. P.4.5. Using the reciprocity theorem, determine the center deflection

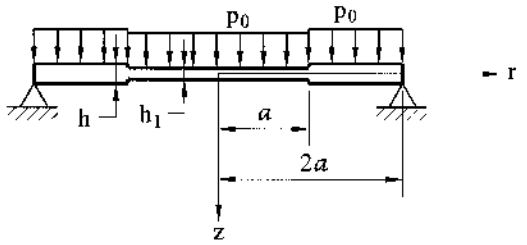

Fig. P4.4

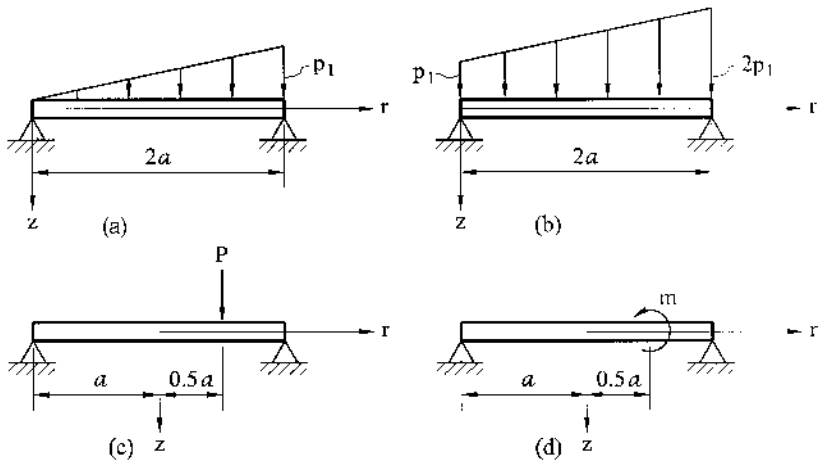

Fig. P4.5

of the plate due to a concentrated center force. A useful formula for a concentrated center force P and $v = 0$ is $w = \frac{1}{16\pi D}\left[2r^2 \ln\frac{r}{a} + 3(a^2 - r^2)\right]$.

4.17 For the circular plate, shown in Fig. P.4.5c, verify Eq. (4.64) using the Michell solution given by Eq. (4.77) and the solution (P.4.1) for the deflection due to a centrally applied concentrated force.

4.18 Derive the governing differential equation for a circular plate analogous to Eq. (2.44) for rectangular plates, using the procedure presented in Sec. 2.4.

REFERENCES

1. Korenev, B.G., *Besselevykh Funktsiiakh* Nekotorye Zadachi Teorii Uprugosti I Teploprovodnosti Reshaemye v, *Gos Izd Fiz-Mat Literatyru*, Moscow, 1960 (in Russian).
2. Watson, G.N., *Theory of Bessel Functions*, 2nd ed., Cambridge University Press, Cambridge, 1944.
3. Abramowitz, M. and Stegun, I.A., *Handbook of Mathematical Functions*, Bureau of Standards, Series No. 55, US Government Printing Office, Washington, DC, 1965.
4. Cook, R.D. and Young, W.C., *Advanced Mechanics of Materials*, Macmillan Publishing Company and Colliear Macmillan Publishers, New York and London, 1985.
5. Michell, J.H., *Proc. London Math. Soc.*, vol. 34, p. 223, 1902.
6. Szillard, R., *Theory and Analysis of Plates*, Prentice-Hall, Englewood Cliffs, New Jersey, 1974.
7. Boyarshinov, S.V., The Fundamentals of Structural Mechanics of Machines, Mashinostroenie, Moscow, 1973 (in Russian).

5

Bending of Plates of Various Shapes

5.1 INTRODUCTION

Structural members, common in engineering practice, consist of plates with shapes other than rectangular or circular. The analytical approaches to the solutions of such plate bending problems, discussed in Chapters 3 and 4, are usually too complicated to be considered for practical use. The more general forms are discussed in this chapter. We consider possible solutions, which can be obtained analytically with relative ease for some geometrical forms of plates different from rectangular and circular.

5.2 ELLIPTICAL PLATES

Elliptical plates with a clamped boundary, subjected to uniformly distributed loads, enable one to obtain an analytical solution. Let us consider the elliptical plate shown in Fig. 5.1. Take the origin of the coordinate system at the center of the plate. The equation of the contour of the plate (equation of the ellipse) is given by

$$\frac{x^2}{a^2}+\frac{y^2}{b^2}=1. \tag{a}$$

The boundary conditions for the clamped edge of the plate are

$$w=0,\frac{\partial w}{\partial n}=0. \tag{b}$$

It can be easily shown that these conditions are satisfied if the deflected surface is

$$w=w_0\left(\frac{x^2}{a^2}+\frac{y^2}{b^2}-1\right)^2, \tag{5.1}$$

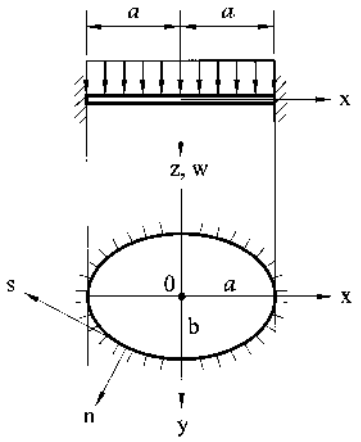

Fig. 5.1

where w_0 is the center deflection of the plate. Substituting for w into the governing differential equation (2.24), and letting $p = p_0$, gives

$$w_0\left(\frac{24}{a^4}+\frac{16}{a^2b^2}+\frac{24}{b^4}\right)=\frac{p_0}{D},$$

from which

$$w_0=\frac{p_0}{D\left(24/a^4+24/b^4+16/a^2b^2\right)}. \tag{5.2}$$

Substituting the above into Eq. (5.1), gives the following solution:

$$w_0=\frac{p_0}{8D}\frac{a^4b^4\left(x^2/a^2+y^2/b^2-1\right)^2}{\left(3a^4+3b^4+2a^2b^2\right)}. \tag{5.3}$$

Since the deflection surface w in the form of Eq. (5.1) satisfies Eq. (2.24) and the prescribed boundary conditions (b) exactly, then it is an exact solution of the given plate bending problem.

The maximum deflection is given by

$$w_{\max}=w(0,0)=\frac{p_0}{8D}\frac{a^4b^4}{(3a^4+3b^4+2a^2b^2)}.$$

Knowing the deflection surface Eq. (5.2), one can determine the bending moments in the plate using Eqs (2.13). The bending moments M_y at the end points of the semi-minor axis and at the plate center are

$$M_y\big|_{x=0,y=\pm b}=-\frac{8\nu w_0 D}{b^2},\quad M_y\Big|_{x=0,y=0}=4w_0D\left(\frac{1}{b^2}+\frac{\nu}{a^2}\right). \tag{5.4}$$

The bending moments M_x at the end point of the semi-major axis and at the plate center are given by

$$M_x\big|_{x=\pm a,y=0} = -\frac{8w_0D}{a^2}, \quad M_x\Big|_{x=0,y=0} = 4w_0D\left(\frac{1}{a^2}+\frac{\nu}{b^2}\right). \tag{5.5}$$

Comparing these values of the bending moments, we can conclude that the end point of the semi-minor axis of the ellipse is the most stressed point.

In the particular case, for $a = b = R$, the relation (5.3) gives a value of the maximum deflection for a circular plate with clamped boundary:

$$w_0 = \frac{p_0R^4}{64D}.$$

For an elliptical plate with a simply supported boundary, subjected to a uniformly distributed load, the deflected surface is a more intricate problem. Omitting the solution of this problem, we give only values of the maximum deflection

$$w_0 = \alpha\frac{p_0b^4}{D}$$

and the bending moments at the center of the plate

$$M_x = \beta p_0 b^3, \quad M_y = \beta_1 p_0 b^2.$$

The values of the coefficients α, β, and β_1 are given in the Table 5.1 [1] for $\nu = 0.3$.

5.3 SECTOR-SHAPED PLATES

The general solution for circular plates (Sec. 4.2) can be used with some modifications for a plate in the form of a sector plate. We consider a uniformly loaded sector plate subtending the angle α and bounded by the lines $r = r_0$ and $r = r_1$. The plate is assumed to be simply supported along the straight edges, as shown in Fig. 5.2.

By expanding the lateral load $p = p_0 = \text{const}$ into a trigonometric series containing the sine terms only, we obtain the following expression for the load:

$$p = \frac{4p_0}{\pi}\sum_{m=1,3,5,\ldots}^{\infty}\frac{1}{m}\sin\frac{m\pi\varphi}{\alpha}. \tag{5.6}$$

The general solution of the problem is sought in the form

$$w = w_{\mathrm{h}} + w_{\mathrm{p}},$$

where the particular solution for the deflections, w_{p}, which satisfies the conditions of simple supports along the edges $\varphi = 0, \alpha$, is given by [2]

Table 5.1

a/b	1.0	1.2	1.5	2.0	3.0	4.0	5.0	∞
α	0.70	0.96	1.26	1.58	1.88	2.02	2.10	2.28
β	0.206	0.219	0.222	0.210	0.188	0.184	0.17	0.15
β_1	0.206	0.261	0.321	0.379	0.433	0.465	0.48	0.5

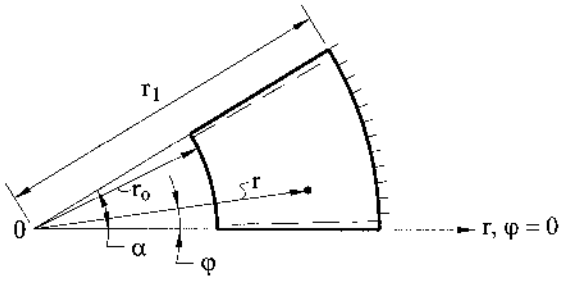

Fig. 5.2

$$w_{\mathrm{p}} = \frac{4p_0 r_0^4}{\pi}\rho^4 \sum_{m=1,3,5,\ldots}^{\infty} \frac{\sin\dfrac{m\pi\varphi}{\alpha}}{m\left(16 - m^2\pi^2/\alpha^2\right)\left(4 - m^2\pi^2/\alpha^2\right)}. \tag{5.7}$$

where $\rho = r/r_0$

The complementary solution, w_{h}, can be taken as

$$w_{\mathrm{h}} = F_0 + \sum_{m=1}^{\infty} F_m \sin\frac{m\pi\varphi}{\alpha}, \tag{5.8}$$

where

$$\begin{aligned} F_0 &= A_0 + B_0\rho^2 + C_0 \ln\rho + D_0\rho^2\ln\rho, \\ F_m &= A_m\rho^{m\pi/\alpha} + B_m\rho^{-m\pi/\alpha} + C_m\rho^{2+m\pi/\alpha} + D_m\rho^{2-m\pi/\alpha}. \end{aligned} \tag{5.9}$$

The coefficients A_0, B_0, C_0, D_0, and A_m, B_m, C_m, D_m are determined from the boundary conditions at $r = r_0$ and $r = r_1$. Some analytical solutions for sector plates with various values of the angle $\alpha(\alpha = \pi/2$ and $\alpha = \pi)$ are given in Timoshenko and Woinowski-Krieger [1].

If the uniformly loaded and simply supported plate sector takes the form of a semicircle ($\alpha = \pi$), as shown in Fig. 5.3, then its solution assumes the form

$$w = \sum_{m=1,3,5,\ldots}^{\infty} \left(A_m r^m + C_m r^{m+2}\right)\sin m\varphi + \frac{4p_0 r^4}{\pi D}\sum_{m=1,3,5,\ldots}^{\infty} \frac{\sin m\varphi}{m\left(16 - m^2\right)\left(4 - m^2\right)}. \tag{5.10}$$

This solution satisfies the boundary conditions on the straight edge of the semicircular plate. The constants A_m and C_m are determined from the boundary conditions along the curvilinear edge of the semicircle. Determining the above constants and inserting them into Eq. (5.10), one finds

$$\begin{aligned} w = \frac{p_o r_0^4}{D}\sum_{m=1,3,5,\ldots}^{\infty} \Bigg\{ & \frac{4\rho^4}{m\pi\left(16 - m^2\right)\left(4 - m^2\right)} \\ & + \frac{\rho^m(5 + m + \nu)}{m\pi\left(16 - m^2\right)(2 + m)[m + 0.5(1 + \nu)]} \\ & - \frac{\rho^{m+2}(3 + m + \nu)}{m\pi(4 + m)(4 - m^2)[m + 0.5(1 + \nu)]}\Bigg\}\sin m\varphi. \end{aligned} \tag{5.11}$$

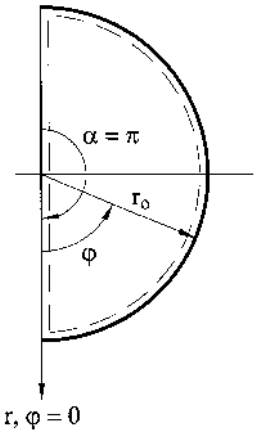

Fig. 5.3

5.4 TRIANGULAR PLATES

5.4.1 Isosceles right triangular plates

Consider a simply supported isosceles right triangular plate AOB, of length a under a concentrated force P acting at an arbitrary point $C(\xi, \eta)$, as shown in Fig. 5.4. To solve the given plate bending problem, the method of images, introduced by Nadai [2], may be used. According to this method, the given triangular plate is considered as one-half of a simply supported square plate, as indicated in Fig. 5.4 by dashed lines.

This square plate is subjected to the concentrated forces P (given force acting downward) and $-P$ (fictitious concentrated force acting upward) at points $C(\xi, \eta)$ and $C'(a-\xi, a-\eta)$, respectively. Point C' is the mirror or image point of C with respect to diagonal AB. The bending couple due to $+P$ and $-P$ results in a zero bending moment and deflection along diagonal AB of the square plate, i.e., the prescribed simply supported boundary conditions for the given triangular plate

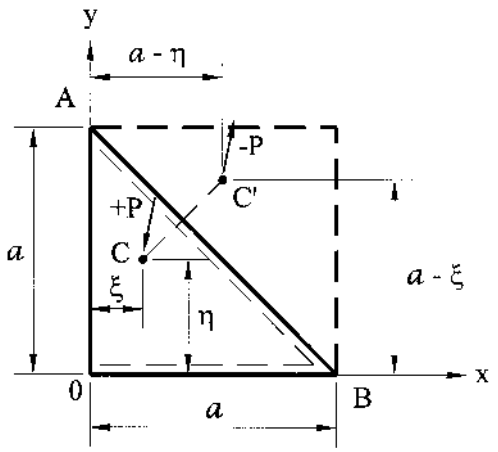

Fig. 5.4

will be satisfied. The deflection owing to the force P can be obtained from Eq. (3.27) by replacing b with a. Finally, we have

$$w_{+P} = \frac{4Pa^2}{\pi^4 D} \sum_{m=1}^{\infty} \sum_{n=1}^{\infty} \frac{\sin \dfrac{m\pi\xi}{a} \sin \dfrac{n\pi\eta}{b}}{\left(m^2 + n^2\right)^2} \sin \frac{m\pi x}{a} \sin \frac{n\pi y}{a}. \tag{5.12}$$

Upon substitution of $-P$ for P, $(a - \eta)$ for ξ, and $(a - \xi)$ for η in Eq. (5.12), we obtain the deflection due to the force $-P$ at C':

$$w_{-P} = -\frac{4Pa^2}{\pi^4 D} \sum_{m=1}^{\infty} \sum_{n=1}^{\infty} \frac{(-1)^{m+n} \sin \dfrac{m\pi\eta}{a} \sin \dfrac{m\pi\xi}{a}}{\left(m^2 + n^2\right)^2} \sin \frac{m\pi x}{a} \sin \frac{n\pi y}{a}. \tag{5.13}$$

The deflected surface of the triangular plate is obtained from

$$w = w_{+P} + w_{-P}, \tag{5.14}$$

where w_{+P} and w_{-P} are given by Eqs (5.12) and (5.13). Using the function w as Green's function, we can obtain the solution of an isosceles triangular, simply supported plate subjected to any type of loading $p(x, y)$. For example, the deflected surface of a triangular plate under a uniformly distributed load of intensity $p_0 = P/\mathrm{d}\xi\mathrm{d}\eta$ may be found from Eq. (5.14), after integration over the area of the plate, as follows:

$$\begin{aligned} w = \frac{16p_0a^4}{\pi^6 d} \Bigg[& \sum_{m=1,3\ldots}^{\infty} \sum_{n=2,4\ldots}^{\infty} \frac{n \sin \dfrac{m\pi x}{a} \sin \dfrac{n\pi y}{a}}{m\left(n^2 - m^2\right)\left(m^2 + n^2\right)^2} \\ & + \sum_{m=2,4\ldots}^{\infty} \sum_{n=1,3\ldots}^{\infty} \frac{m \sin \dfrac{m\pi x}{a} \sin \dfrac{n\pi y}{a}}{n\left(m^2 - n^2\right)\left(m^2 + n^2\right)^2} \Bigg]. \end{aligned} \tag{5.15}$$

This series converges very rapidly. With the expressions for the deflection of the plate determined, one can obtain the bending moments and stresses in the plate from Eqs (2.13) and (2.15), respectively.

5.4.2 Equilateral triangular plate

Consider a simply supported equilateral plate ABC shown in Fig. 5.5. The deflected surface of the equilateral triangular plate may be represented in the form

$$w = kF(x, y), \tag{5.16}$$

where k is a constant and $F(x, y)$ is some function that satisfies the prescribed simply supported boundary conditions for the plate. In particular, $F(x, y)$ can be represented as the product of the left-hand sides of equations of the three sides of the triangle. In this case,

$$\begin{aligned} F(x, y) &= \left(x + \frac{a}{3}\right)\left(\frac{x}{\sqrt{3}} + y - \frac{2a}{3\sqrt{3}}\right)\left(\frac{x}{\sqrt{3}} - y - \frac{2a}{3\sqrt{3}}\right) \\ &= \frac{x^3 - 3y^2x}{3} - \frac{a(x^2 + y^2)}{3} + \frac{4a^3}{81}. \end{aligned} \tag{5.17}$$

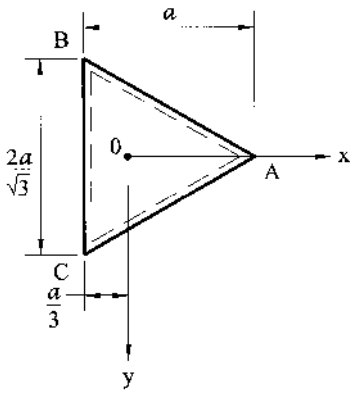

Fig. 5.5

It is evident that $F(x, y)$ is zero at the boundary. In the particular case of a uniformly loaded equilateral triangular plate, the deflection surface can be taken as [1]

$$w = \frac{p_0}{64aD}\left[x^3 - 3y^2x - a(x^2 + y^2) + \frac{4}{27}a^3\right]\left(\frac{4}{9}a^2 - x^2 - y^2\right), \tag{5.18}$$

where p_0 is the load intensity. It can be shown that this expression for w satisfies the governing differential equation (2.24) and the boundary conditions for a simply supported edge. Therefore, Eq. (5.18) is the solution. By employing Eqs (2.13), the bending moments may then be obtained. It can be shown that the center moments are

$$M_x = M_y = (1 + \nu)\frac{p_0 a^2}{54}. \tag{5.19}$$

The largest moments occur on the planes bisecting the angles of the triangle. For example, at points along the x axis (Fig. 5.5), for $\nu = 0.3$, we obtain the following expressions:

$$M_{x,\max} = 0.0248p_0a^2 \ (x = -0.062a, y = 0);$$

$$M_{y,\max} = 0.0259p_0a^2 \ (x = 0.129a, y = 0).$$

The maximum stress is given by $\sigma_{y,\max} = 0.155p_0a^2/h^2$.

5.5 SKEW PLATES

Skew plates are widely used in modern structures. Swept wings of airplanes and parallelogram slabs in buildings and bridges are examples of the application of skew plates in engineering. Following Szillard [3], let us derive the governing differential equation of bending of skew plates by introducing an oblique coordinate system, ξ, η, as shown in Fig. 5.6. The coordinates of the rectangular (x, y) and oblique (ξ, η) systems are related by

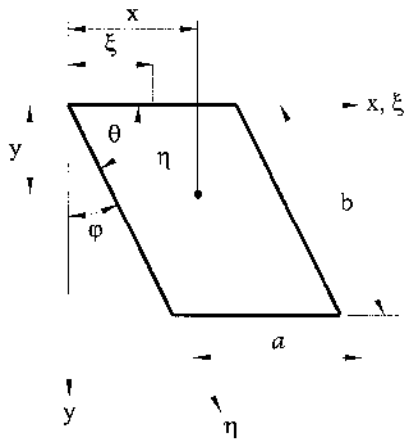

Fig. 5.6

$$\xi = x - y\tan\varphi \text{ and } \eta = \frac{1}{\cos\varphi}y. \tag{5.20}$$

Substitution of the expressions (5.20) into Eq. (2.17), transforms the Laplacian operator from the rectangular to oblique coordinate system, ∇_o^2, as follows:

$$\nabla_o^2 = \frac{1}{\cos^2\varphi}\left(\frac{\partial^2}{\partial\xi^2} - 2\sin\varphi\frac{\partial^2}{\partial\xi\partial\eta} + \frac{\partial^2}{\partial\eta^2}\right) \tag{5.21}$$

Therefore, the governing differential equation of plate bending, expressed in terms of the oblique coordinates, is of the form

$$\frac{D}{\cos^4\varphi}\left\{\frac{\partial^4 w}{\partial\xi^4} + 2\left(1 + 2\sin^2\varphi\right)\frac{\partial^4 w}{\partial\xi^2\partial\eta^2} - 4\sin\varphi\left(\frac{\partial^4 w}{\partial\xi^3\partial\eta} + \frac{\partial^4 w}{\partial\xi\partial\eta^3}\right) + \frac{\partial^4 w}{\partial\eta^4}\right\} = p(\xi, \eta). \tag{5.22}$$

or, more concisely,

$$D\nabla_o^2\nabla_o^2 w(\xi, \eta) = p(\xi, \eta). \tag{5.23}$$

The analytical solution of Eq. (5.22) or (5.23) is complicated by the absence of orthogonal relationships and by the presence of singularities occurring at the obtuse corners. It can be solved only for a few particular cases. Thus, the analysis of the skew plates mentioned above can be carried out, primarily, by numerical methods discussed in Chapter 6. Some numerical solution procedures and the corresponding examples are discussed in Szillard [3].

PROBLEMS

5.1 Derive the equation for the bending moments, M_x and M_y, for a clamped elliptical plate under a uniformly distributed surface load p_0.

5.2 Derive the equations for the shear forces, Q_x and Q_y, for a clamped elliptical plate under a uniformly distributed surface load p_0.

5.3 With reference to Problem 5.2, show that a clamped elliptical plate under a uniformly distributed load p_0 is in a state of equilibrium, i.e., show that $P + R = 0$, where P is the resultant of distributed load p_0 and R is the resultant of the reactive forces on the plate boundary, $R = \oint (V_x dy - V_y dx)$.

5.4 Determine the required thickness of a fixed elliptical plate with $a = 25$ in. and $b = 18$ in. The plate is loaded by a uniform pressure of 120 psi. Take $\nu = 0.3$ and the allowable stress of 16 ksi.

5.5 Verify Eq. (5.11).

5.7 A simply supported wing panel in the form of an isosceles right triangle is subjected to a uniform distributed load p_0 (Fig. 5.4). By retaining only the first term of the series solution at point $C(x = a/4, y = a/4)$, determine (a) the deflection and (b) the bending moments.

5.8 Consider a simply supported equilateral triangular plate under a uniformly distributed load p_0. With reference to Eqs (2.32), show that

$$\nabla^2 M = -p_0;\ M = \frac{p_0}{4a}\left(x + \frac{a}{3}\right)\left(x - \frac{2}{3}a + y\sqrt{3}\right)\left(x - \frac{2}{3}a - y\sqrt{3}\right).$$

.

5.9 Verify Eq. (5.22).

5.10 Consider a clamped plate in the form of a parallelogram (Fig. 5.6) subjected to a uniform surface load p_0. Taking a solution of Eq. (5.22) in the form

$$w(\xi, \eta) = \frac{A}{4}\left(1 - \cos\frac{2\pi\xi}{a}\right)\left(1 - \cos\frac{2\pi\eta}{b}\right)$$

determine at point $\xi = a/2$ and $\eta = b/2$: (a) the deflection, (b) the bending moments. Use $\varphi = 15^\circ$.

5.11 Determine the expressions for M_x, M_y, and M_{xy} for skew plates by using the geometrical relationship (5.20) between the Cartesian and oblique coordinates.

REFERENCES

1. Timoshenko, S.P. and Woinowsky-Krieger, S., *Theory of Plates and Shells*, 2nd edn, McGraw-Hill, New York, 1959.
2. Nadai, A., *Die Elastichen Platten*, Springer-Verlag, Berlin, 1925.
3. Szillard, R., *Theory and Analysis of Plates*, Prentice-Hall, Englewood Cliffs, New Jersey, 1974.

6

Plate Bending by Approximate and Numerical Methods

6.1 INTRODUCTION

An exact solution in analytical form (i.e., exact solution formula) of plate bending problems using classical methods, discussed in Chapters 3, 4, and 5, is limited to relatively simple plate geometry, load configuration, and boundary supports. If these conditions are more complicated, the classical analysis methods become increasingly tedious or even impossible. In such cases, approximate methods are the only approaches that can be employed for the solution of practically important plate bending problems. Nevertheless, the classical solutions remain very valuable because they enable one to gain insight into the variation of stresses and strains with basic shape and property changes, and they provide an understanding of the physical plate behavior under an applied loading. In addition, they can be used as a basis for incisively evaluating the results of approximate solutions through quantitative comparisons and order-of-magnitude bounds.

In this chapter we consider some approximate methods that are widely used for plate and shell bending analysis. By convention, these approximate methods may be divided into two groups.

6.1.1 Indirect methods

These methods enable us to obtain numerical values of unknown functions by, primarily, direct discretization of the governing differential equation of the corresponding boundary value problem. Also they can be defined as methods for solving problems on computers. Note that computers have changed, almost revolutionized, numerical methods. These changes of the field as a whole, as well as many individual methods, are continuing. Here, we introduce such well-known methods as the finite difference method, the method of boundary collocations, the boundary element method, and the Galerkin method.

6.1.2 Direct methods

These methods use the variational principles introduced in Sec. 2.6 for determining numerical fields of unknown functions (deflections, internal forces, and moments), avoiding the differential equations of the plate or shell theory. The Ritz method is considered first and then the most efficient and well-accepted method at the present time – the finite element method – is also be presented. It should be noted that the above-mentioned division is very conventional because some approximate methods combine some distinguishing features of both groups of methods. For instance, the variational difference method is based on variational principles but unknown functions of deflection are represented in a numerical form at nodal points of the mesh drawn on the area of a plate midplane. In this chapter, all the above-mentioned methods are discussed only with application to plate bending problems. Their application to shell problems is considered in Part II.

6.2 THE FINITE DIFFERENCE METHOD (FDM)

6.2.1 General concepts

This is a method of the solution of boundary value problems for differential equations. The essence of the FDM lies in the following:

1. The middle plane of the plate is covered by a rectangular, triangular, or other reference network (Fig. 6.1), depending on the geometry of the plate. This network is called a *finite difference mesh* and points of intersection of this mesh are referred to as *mesh* or *nodal points*.
2. The governing differential equation inside the plate domain is replaced by the corresponding finite difference equations at the mesh points using the special *finite difference operators*.
3. Boundary conditions are also formulated with the use of the above-mentioned finite difference operators at mesh points located on the plate boundary.

As a result of such replacement, we obtain a closed set of linear algebraic equations written for every nodal point within the plate. Solving this system of equations, one obtains a numerical field of the nodal displacements.

6.2.2 Approximation of derivatives by finite differences

The key point of the FDM is the finite difference approximation of derivatives. Consider a development of the above approximations for the derivatives of a one-dimensional, continuous function $f(x)$. It is known that the derivative of a function $f(x)$ at point x_i is defined, as follows (Fig. 6.2a):

$$\left(\frac{\mathrm{d}f}{\mathrm{d}x}\right)_i = \lim_{\Delta\to 0}\frac{f_{i+1}-f_i}{\Delta} \quad \text{or} \quad \left(\frac{\mathrm{d}f}{\mathrm{d}x}\right)_i = \lim_{\Delta\to 0}\frac{f_i-f_{i-1}}{\Delta},$$

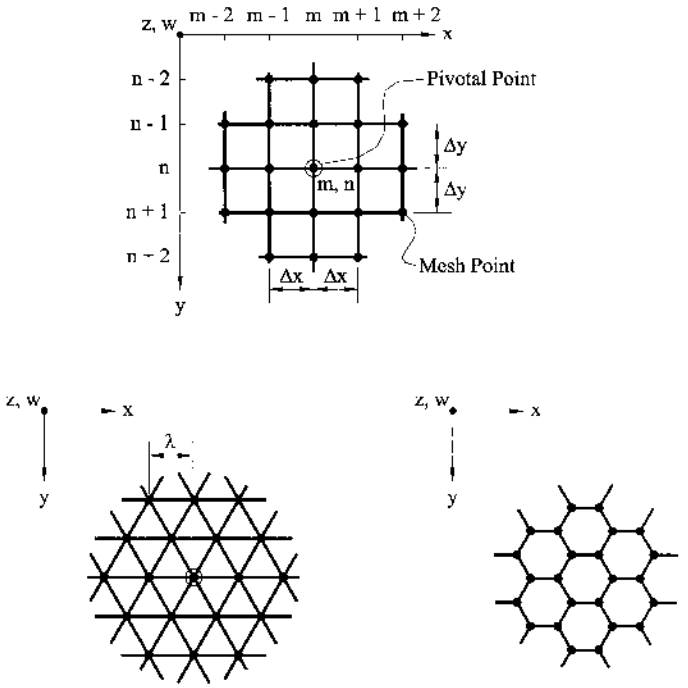

Fig. 6.1

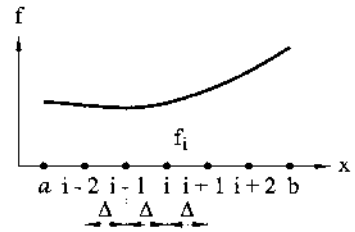

(a)

$$\left(\frac{d^2}{dx^2}\right)_i = (1)(-2)(1) \cdot \frac{1}{\Delta^2}$$

$$\left(\frac{d^3}{dx^3}\right)_i = (-1)(2)(0)(-2)(1) \cdot \frac{1}{2\Delta^3}$$

$$\left(\frac{d^4}{dx^4}\right)_i = (1)(-4)(6)(-4)(1) \cdot \frac{1}{\Delta^4}$$

(b)

Fig. 6.2

where $f_i = f(x_i)$, etc.; Δ is a finite increment of the variable x. Dropping the symbol of limit in the above equalities, we obtain

$$\left(\frac{\mathrm{d}f}{\mathrm{d}x}\right)_i \approx \frac{f_{i+1} - f_i}{\Delta}, \tag{6.1a}$$

$$\left(\frac{df}{dx}\right)_i \approx \frac{f_i - f_{i-1}}{\Delta}. \tag{6.1b}$$

Expressions (6.1a) and (6.1b) are called the first forward and backward approximations of the first derivative of $f(x)$ at point x_i, respectively. In practice, the expression for a central difference approximation of $(\mathrm{d}f/\mathrm{d}x)_i$ is often used, as follows:

$$\left(\frac{\mathrm{d}f}{\mathrm{d}x}\right)_i \approx \frac{f_{i+1} - f_{i-1}}{2\Delta}. \tag{6.2}$$

Expressions (6.1) and (6.2) are also referred to as the *finite difference operators of the first derivative*. It is clear that expressions (6.1) and (6.2) are more accurate as the value of Δ is smaller. From now on, for simplicity, we use the sign of equality in the above expressions instead of the sign of approximate equality.

Applying expressions (6.1) and (6.2) as operators we can derive the corresponding differential approximations of the second, third, and fourth derivatives of the function $f(x)$. We present below only the central difference approximations of the above derivatives, as follows:

$$\left(\frac{\mathrm{d}^2 f}{\mathrm{d}x^2}\right)_i = \frac{f_{i-1} - 2f_i + f_{i+1}}{\Delta^2}, \tag{6.3}$$

$$\left(\frac{\mathrm{d}^3 f}{\mathrm{d}x^3}\right)_i = \frac{f_{i+2} - 2f_{i+1} + 2f_{i-1} - f_{i-2}}{2\Delta^3}, \tag{6.4}$$

$$\left(\frac{\mathrm{d}^4 f}{\mathrm{d}x^4}\right)_i = \frac{f_{i+2} - 4f_{i+1} + 6f_i - 4f_{i-1} + f_{i-2}}{\Delta^4}. \tag{6.5}$$

The coefficient patterns for the central finite difference operators of a one-dimensional function $f(x)$ are given in Fig. 6.2b.

By using the quadratic interpolation, one can obtain the expressions of the above derivatives for a nonuniformly spaced finite difference mesh shown in Fig. 6.3.

For example,

$$\begin{aligned} \left(\frac{\mathrm{d}f}{\mathrm{d}x}\right)_i &= \frac{-\alpha^2 f_{i-1} - (1-\alpha^2) f_i + f_{i+1}}{\alpha(1+\alpha)\Delta}, \\ \left(\frac{\mathrm{d}^2 f}{\mathrm{d}x^2}\right)_i &= \frac{2[\alpha f_{i-1} - (1+\alpha) f_i + f_{i+1}]}{\alpha(1+\alpha)\Delta^2}. \end{aligned} \tag{6.6}$$

We now discuss the case of a continuous function $F(x, y)$ of two variables. For this purpose, assume that a plate middle plane is approximated by a mesh with the mesh widths of Δ_x and Δ_y in the x and y directions, respectively. Let us restrict our derivation and application to equally spaced square meshes by introducing $\Delta x = \Delta y = \Delta$. It is evident that $\partial^i F/\mathrm{d}x^i$ and $\partial^j F/\partial y^j$ $(i, j = 1, 2, 3, 4)$ are

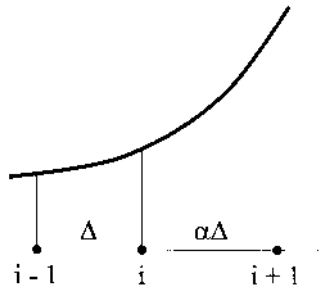

Fig. 6.3

approximated by the finite difference operators of the type (6.3)–(6.5). For example, for a central point k, we obtain

$$\left(\frac{\partial^2 F}{\partial x^2}\right)_k = \frac{F_a - 2F_k + F_c}{\Delta^2}; \quad \left(\frac{\partial^2 F}{\partial y^2}\right)_k = \frac{F_d - 2F_k + F_b}{\Delta^2}. \tag{6.7}$$

Adding the equalities (6.7), we obtain the finite difference approximation of the Laplace operator, as follows:

$$\left(\nabla^2 F\right)_k = \left(\frac{\partial^2 F}{\partial x^2} + \frac{\partial^2 F}{\partial y^2}\right) = \frac{F_a + F_b + F_c + F_d - 4F_k}{\Delta^2}. \tag{6.8}$$

The finite difference approximation of the biharmonic operator can be obtained by applying the Laplace operator (6.8) twice. We have the following:

$$\left(\nabla^2\nabla^2 F\right)_k = \frac{20F_k - 8(F_a + F_b + F_c + F_d) + 2\left(F_e + F_f + F_g + F_h\right) + (F_l + F_m + F_n + F_i)}{\Delta^4}. \tag{6.9}$$

The expression for the approximation of the second mixed derivative can be obtained following the pattern shown next:

$$\left(\frac{\partial^2 F}{\partial x \partial y}\right)_k = \frac{\partial}{\partial x}\left(\frac{\partial F}{\partial y}\right)_k = \frac{-(\partial F/\partial y)_a + (\partial F/\partial y)_c}{2\Delta} = \frac{F_h - F_e + F_f - F_g}{4\Delta^2}. \tag{6.10}$$

Applying this operator twice, one obtains the approximation of the fourth derivative of the function $F(x, y)$, $(\partial^4 F/\partial x^2 \partial y^2)_k$.

For reference purposes, some useful finite difference operators for a square mesh are represented in the form of coefficient patterns in Fig. 6.4. Notice that the center point in each case is the node about which each operator is written (the above point is outlined by a rectangle). In the case of a rectangular mesh with $\Delta x = \lambda_x$ and $\Delta y = \lambda_y$, one needs to replace Δ with λ_x, or Δ with λ_y. For example,

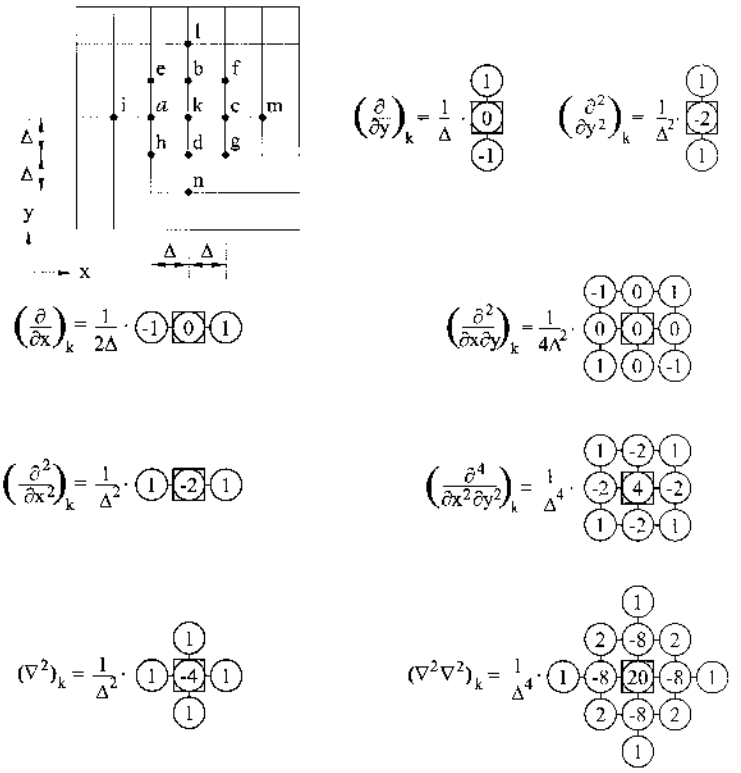

Fig. 6.4

$$\left(\frac{\partial F}{\partial x}\right)_k = \frac{F_a - F_c}{2\lambda_x}; \quad \left(\frac{\partial F}{\partial y}\right)_k = \frac{F_b - F_d}{2\lambda_y};$$
$$\left(\frac{\partial^2 F}{\partial x^2}\right)_k = \frac{F_a - 2F_k + F_c}{\lambda_x^2}; \left(\frac{\partial^2 F}{\partial y^2}\right)_k = \frac{F_b - 2F_k + F_d}{\lambda_y^2}; \text{ etc.} \tag{6.11}$$

Up to this point, the finite difference operators have been derived using only Cartesian coordinates. The latter are well adapted to the solution of plate bending problems involving domains bounded by straight lines. For curvilinear plate domains, polar coordinates, can be conveniently applied. The finite difference operators in polar, or other coordinates, can be developed through the transformation of the corresponding equations relating the x and y coordinates to the set of coordinates of interest and using the coefficient patterns for finite difference operators given in Fig. 6.4.

6.2.3 Application of the finite difference method to plate bending problems

We can set up, with the use of a biharmonic operator (6.9), a finite difference expression of the governing differential equation (2.25) for every kth nodal point of the finite difference mesh within the plate at which $w_k \neq 0$:

$$\left(\nabla^2\nabla^2 w\right)_k = \frac{p_k}{D}, \quad k = 1, 2, \ldots N, \tag{6.12}$$

where p_k is an average load over an area $\Delta \times \Delta$ enclosing the nodal point k. If a concentrated force P is applied at a kth point, then $p_k = P/\Delta^2$. The finite difference operators for some moments and the effective shear forces are given in Fig. 6.5. They were obtained by replacing the partial derivatives in Eqs (2.13) and (2.39b) by the corresponding finite difference expressions.

Let us consider some finite difference expressions for typical boundary conditions for the plate edge $x = \text{const}$.

(a) Simply supported edge (Fig. 6.6a)

According to the boundary conditions for a simply supported edge, we have

$$w_k = 0 \text{ and } \left(\frac{\partial^2 w}{\partial x^2}\right)_k = 0, \tag{6.13a}$$

and applying the finite difference operator of the second derivative (see Fig. 6.4) yields

$$\frac{w_a - 2w_k + w_b}{\Delta^2} = 0,$$

from which, taking into account that $w_k = 0$, we can obtain

$$w_b = -w_a. \tag{6.13b}$$

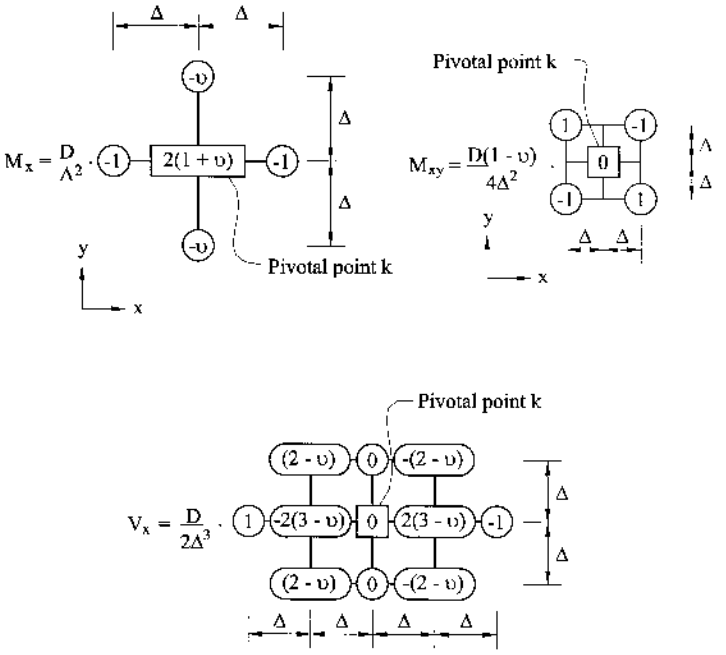

Fig. 6.5

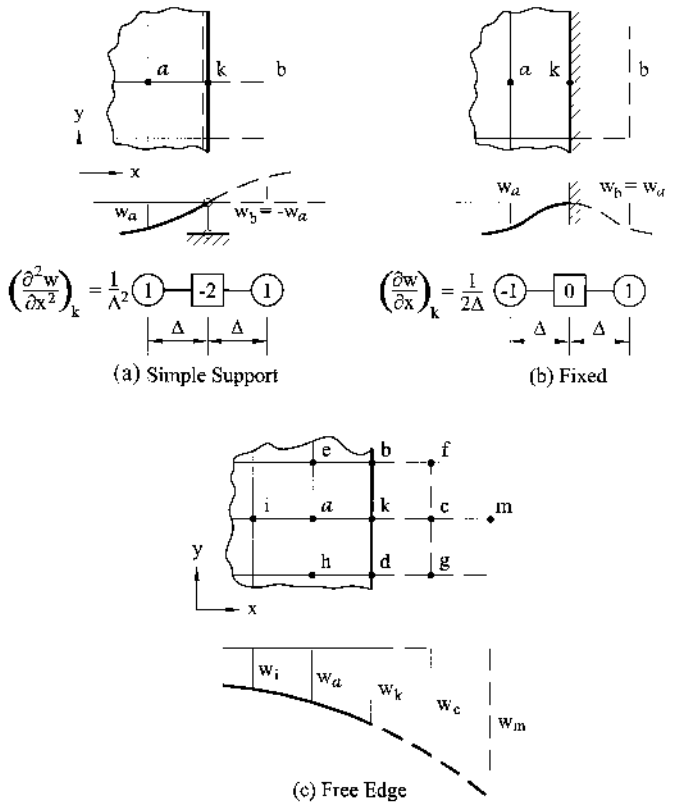

Fig. 6.6

(b) Clamped edge (Fig. 6.6b)

Boundary conditions for the clamped edge of a plate can be written for the kth point as follows:

$$w_k = 0 \text{ and } \left(\frac{\partial w}{\partial x}\right)_k = 0. \tag{6.14a}$$

Applying the operator of the first derivative of w, the latter boundary condition becomes (see Fig. 6.4)

$$\frac{w_b - w_a}{2\Delta} = 0,$$

from which

$$w_b = w_a. \tag{6.14b}$$

(c) Free edge (Fig. 6.6c)

As shown in Sec. 2.4, the boundary conditions for a free edge, for instance, $x = \text{const}$, have the form

$$M_x = 0 \text{ and } V_x = 0. \tag{6.15a}$$

Applying the finite difference operators of forces and moments, given in Fig. 6.5, to the above boundary conditions, the latter are represented for a kth point on the plate edge as follows:

$$\begin{gathered} 2(1+\nu)w_k - w_a - w_c - \nu(w_b + w_d) = 0, \\ 2(3-\nu)(w_c - w_a) + (2-\nu)\left(w_e + w_h - w_f - w_g\right) + w_i - w_m = 0. \end{gathered} \tag{6.15b}$$

There will be four fictitious nodes – f, c, g, and m – when the finite difference analog of the differential equation (6.12), Eq. (6.9) is applied to mesh point k on the free edge (Fig. 6.6c).

The expressions (6.13b), (6.14b), or (6.15b) are used either for eliminating the fictitious points mentioned above or for joining them to Eq. (6.9) as additional equations. As a result we obtain the closed system of linear algebraic equations with a square matrix. Solving this system of equations yields the numerical field of the plate deflections w_k $(k = 1, 2, \ldots, N)$.

Example 6.1

Find the approximate deflection values for a continuous rectangular plate, with loads and supports as shown in Fig. 6.7 [1].

Solution

The domain of the plate is divided into a number of small squares (28 squares, as shown in Fig. 6.7). We thus have $\Delta x = \Delta y = \Delta = 0.25a$. In labeling nodal points, the plate and loading symmetry about the x axis has been taken into account. At all the nodal points on the outer and inner $(x = a)$ boundaries the deflections are zero. At the fictitious nodes, located outside of the outer boundary, we have the following (with regard to the notation of the nodal points of Fig. 6.7):

$$\begin{gathered} w_{1''} = w_1, w_{6''} = w_6, w_{5''} = w_5, w_{10''} = w_{10}, \\ w_{1'} = -w_1, w_{2'} = -w_2, w_{3'} = -w_3. \end{gathered} \tag{a}$$

Nodal loads on the right field of the plate (just to the right of the line $x = a$) are $p_4 = p_5 = p_9 = p_{10} = 0$, and on the left field of the plate (just to the left of the line $x = a$) they are $p_1 = p_2 = p_3 = p_6 = p_7 = p_8 = p = \text{const}$.

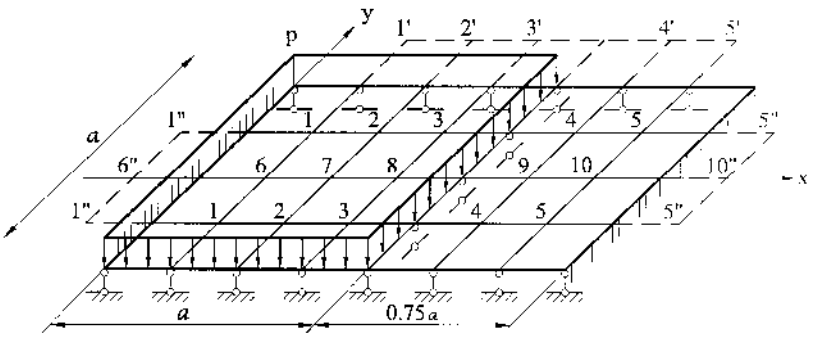

Fig. 6.7

Using the operator (6.9), we obtain a set of the algebraic equations (6.12) in the explicit form for the nodal points $1, 2, \ldots, 10$. Then, with the use of the relation for case (a), we can eliminate the deflections at the fictitious points $1''$, $5''$, $6''$, and $10''$ in the above system of equations. Solving the latter yields the following numerical values of the deflections at the nodal points of the mesh shown in Fig. 6.7:

$$w_1 = 0.00129\frac{pa^4}{D},\ w_2 = 0.002047\frac{pa^4}{D},\ w_3 = 0.001746\frac{pa^4}{D},$$

$$w_4 = -0.000246\frac{pa^4}{D},\ w_5 = -0.000133\frac{pa^4}{D},\ w_6 = 0.001746\frac{pa^4}{D}$$

$$w_7 = w_{\max} = 0.00278\frac{pa^4}{D},\ w_8 = 0.002019\frac{pa^4}{D},\ w_9 = -0.0003476\frac{pa^4}{D},$$

$$w_{10} = -0.0001875\frac{pa^4}{D}.$$

Having determined the numerical values of the deflections and applying the finite difference operators for moments (see Fig. 6.5), one can determine the bending and twisting moments, and then the corresponding stresses.

The FDM has become fairly popular in recent years. As mentioned earlier, according to this method the governing differential equation is replaced by a set of simultaneous algebraic equations: computers can be used to find the solution to these algebraic equations. The FDM has obvious advantages and disadvantages. Among its advantages, we can mention the following:

(a) it is straightforward in understanding and application;
(b) it is sufficiently universal, being applied to both linear and nonlinear problems; and
(c) it is well suited for computer application.

Disadvantages of this method are

(a) it requires (to a certain extent) mathematically trained operators;
(b) it requires more work to achieve complete automation of the procedure in program writing;
(c) the matrix of the approximating system of linear algebraic equations is asymmetric, causing some difficulties in numerical solution of this system; and
(d) an application of the FDM to domains of complicated geometry may run into serious difficulties.

This section contains only a brief description of the FDM and its application to plate bending problems. The interested reader is referred to other works [2,3].

6.3 THE BOUNDARY COLLOCATION METHOD (BCM)

The boundary collocation method (BCM) is among the simplest methods of solving partial differential equations, both from a conceptual, as well as a computational point of view. The solution is expressed as a sum of known solutions of the governing differential equation, and boundary conditions are satisfied at selected colloca-

tion points on the boundary. Thus, the obtained solution satisfies the governing differential equation exactly and the prescribed boundary conditions only approximately. An estimation of the error of approximation can be found by simply checking the boundary conditions at some intermediate points located between the collocation ones. The method is easily applied to irregular domains (simply or multiply connected) with arbitrary boundary conditions. This method can be considered as a particular case of the more general method, the so-called the weighted residual method [4], when the weighting functions are chosen in the form of the Dirac delta functions at discrete points of a boundary.

We describe the general procedure of the BCM applied to plate bending problems. The presentation of the method follows the spirit of Hutchinson's paper [5]. Consider a thin plate occupying a two-dimensional domain Ω with boundary Γ. When the plate is subjected to transverse loading p, its deflection w must satisfy the governing differential equation (2.24) within the domain and prescribed boundary conditions on its boundary, i.e.,

$$\mathbf{l}[w(x, y)] = \mathbf{f}(x, y)\big|_{\Gamma}, \tag{6.16}$$

where $\mathbf{l} = [l_1, l_2]^T$ is a known two-component, linear differential operator prescribed on the boundary Γ, whose explicit form is given by Eqs (2.48); $\mathbf{f} = [f_1, f_2]^T$ is also a known two-component vector-function specified on Γ. The superscript T indicates the symbol of transposition.

In the BCM an unknown deflection $w(x, y)$ is approximated by an expansion of the form

$$w(x, y) = \sum_{j=1}^{N} a_j \Phi_j(x, y) + w_p(x, y) \tag{6.17}$$

where $\Phi_j(x, y)$ are some prescribed trial (or basis) functions; a_j are unknown coefficients, and w_p is an appropriate particular solution of the nonhomogeneous equation (2.24). The trial functions $\Phi_j(x, y)$ are subject to the following conditions [6]:

(a) They must be linearly independent (i.e., any function from the expansion (6.17) can not be linearly expressed through the other functions of the same expansion);
(b) Every function from the expansion (6.17) satisfies the homogeneous differential equation (2.24) exactly.

Many possibilities exist for the choice of the basis functions Φ_j in the expansion (6.17). One possible choice is to represent them in polar coordinates for the plate bending problems, as follows [7]:

$$\begin{Bmatrix} r^k \\ r^{-k} \\ r^{k+2} \\ r^{-k+2} \end{Bmatrix} \quad \begin{Bmatrix} \sin k\varphi \\ \cos k\varphi \end{Bmatrix} \tag{6.18}$$

where $k = 1, 2, \ldots, \infty$ for sin terms and $k = 0, 1, 2, \ldots, \infty$ for cos terms. For $k = 0$ and $k = 1$ the basis functions are the following:

$$\Phi_0 = \left\{1, r^2 \ln r, r^2 \ln r\right\}^T, \quad \Phi_1 = \left\{r, r^3, r^{-1}, r \ln r\right\}^T \tag{6.19}$$

In the expressions (6.18) r and φ are polar coordinates of points of interest with the origin located somewhere within the plate. Each term in the left set of braces times each term in the right set of braces in (6.18) represents a solution form and satisfies the homogeneous differential equation (2.24). Other forms of the basic functions are discussed in [5, 8].

In dealing with solid plates with a centrally placed origin, all singular terms in the expressions (6.18) and (6.19) (*lnr*, *rlnr*, and r to any negative power) are omitted. As it follows from the above, $w(x, y)$ in the form of (6.17) satisfies Eq. (2.24) exactly. Thus, only the boundary conditions need to be satisfied. Substituting the expressions (6.17) into Eqs. (6.16) and assuming that the boundary conditions will be satisfied at some discrete points $(x_i, y_i; i = 1, 2, \ldots, M)$, called *collocation points,* along boundary Γ, leads to a system of $2M$ linear algebraic equations for N unknown constants a_j. This system can be written in the following form:

$$[A]\{a\} = \{b\}, \tag{6.20}$$

where $[A] = [A_{ij}, A_{i+M,j}]^T$ and $\{b\} = [b_i, b_{i+M}]^T$ are the partitioned matrices. The coefficients of these matrices are of the form

$$A_{ij} = l_1[\Phi_j(x_i, y)],\ A_{i+M,j} = l_2[\Phi_j(x_i, y_i)];$$
$$b_i = f_1(x_i, y_i) - l_1[w_p(x_i, y_i)],\ b_{i+M} = f_2(x_i, y_i) - l_2[w_p(x_i, y_i)]$$

$\{a\}$ is the column matrix of unknown coefficients a_j. In order to obtain a square matrix $[A]$, the number of terms in the expansion (6.17) would have to be twice the number of collocation points, that is, $N = 2M$. Such a variant of the BCM is called the *straightforward boundary collocation method.*

As an alternative to insuring that the matrix $[A]$ is square by a proper choice of terms and boundary conditions, one can go to the process known as the *overdetermined boundary collocation method.* In the latter approach, more collocation points are chosen than are necessary, i.e., $2M > N$, and the system (6.20) contains more equations than unknowns. This overdetermined system can be solved by the least squares method [2]. This numerical procedure is quite simple. Let $\{a^*\}$ be a trial solution of Eq. (6.20). $\{a^*\}$ does not exactly satisfy Eq. (6.20) but leads to some residual error $\{e\}$, so that

$$[A]\{a^*\} - \{b\} = \{e\} \tag{6.21}$$

It can be shown the condition for selecting the solution $\{a^*\}$ to minimize the error e_i is equivalent to the following matrix equation [5]

$$[A]^T \cdot [A] \cdot \{a^*\} = [A]^T \cdot \{b\} \tag{6.22}$$

The matrix $[A]^T \cdot [A]$ is square and positive definite. The system of linear algebraic equations (6.22) is called the *normal system*. The solution steps are the same as for a square matrix.

In conclusion, notice that the BCM has some advantages and disadvantages. Among the advantages one notes the following:

1. it is easy to understand and program the approach;
2. it is easily applied to arbitrary shapes and boundary conditions, and the solution appears in a closed form for the whole region.

However, the BCM has some disadvantages, among which are

(a) it is limited to linear problems;
(b) a complete set of solutions (the basic functions Φ_j) to the differential equations must be known; and
(c) the matrix [A] is full and sometimes ill-conditioned, and a known arbitrariness exists in the selection of the collocation points.

This section contains only a brief survey of the boundary collocation method. The interested reader is referred to other works [5,8,9].

Example 6.2

A 90° sectorial plate subjected to a uniform surface load of an intensity p_0 is simply supported along its straight edges. Determine the deflection, bending moments distribution along the x axis for (a) simply supported (Fig. 6.8a) and (b) clamped (Fig. 6.8b) conditions along its arc. Assume $\nu = 0.3$ (this example is taken from Ref. [9]).

Solution

The deflection $w(x, y)$ is approximated by the expression (6.17) and the trial functions are taken in polar coordinates according to Eqs (6.18), as follows:

$$w = \sum_{j=0}^{N} \left(a_j r^j + b_j r^{j+2}\right) \cos j\varphi + \frac{p_0 r^4}{64D}, \tag{a}$$

where the coefficients a_j and b_j are to be determined from the boundary conditions, and the upper limit of summation N is determined by the accuracy of solution desired from the BCM. The simply supported plate (Fig. 6.8a) is analyzed by using 14 boundary points and the plate simply supported along the straight edges and clamped along the arc (Fig. 6.8b) by using 12 boundary points. The results of the analysis are presented in Table 6.1, which shows these results, and in Fig. 6.9, where the moment distributions are shown.

In Table 6.1, the numerical results given by the BCM solutions are compared with exact solutions obtained in Ref. [7]. This comparison shows that the BCM solution agrees well with the exact solution both in the interior of the plate and at its boundary.

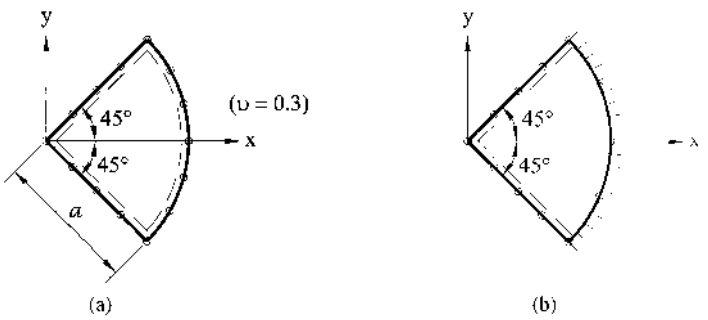

Fig. 6.8

Table 6.1

	Simple arc support						Clamped arc support			
	w		M_x		M_y		w		M_x	
x/a	Exact	BCM	Exact	BCM	Exact	BCM	Exact	BCM	Exact	BCM
0	0	0	—	−271	—	271	0	0	—	−199
0.25	92	93	36	38	319	322	63	64	68	70
0.50	225	226	353	354	352	353	132	132	272	273
0.75	203	203	381	381	286	287	82	81	113	116
1.00	0	0	0	0	88	88	0	1	−488	−486
Multi.	$10^{-5}p_0a^4/D$		$10^{-4}p_0a^2$		$10^{-4}p_0a^2$		$10^{-5}p_0a^4/D$		$10^{-4}p_0a^2$	

6.4 THE BOUNDARY ELEMENT METHOD

The boundary element method (BEM) is now used extensively for the analysis of two-dimensional (2D) and three-dimensional (3D) elastic, homogeneous, and isotropic bodies. It offers important advantages over domain-type methods, such as the finite element method and the finite difference method, since only the discretization of the boundary is needed. The BEM is well suited for treating complicated boundaries, for discontinuous internal actions, mixed boundary conditions, etc. In particular, the BEM has been applied successfully for the solutions of plate bending problems, demonstrating its advantages [10–14].

The BEM reduces a given boundary value problem for a plate, in the form of partial differential equations to the integral equations over the boundary of the plate. Then, the BEM proceeds to obtain an approximate solution by solving these integral equations. To make such a reduction possible, it is necessary, first, to express the solution as the sum of a particular integral corresponding to a given loading applied to the plate and of a complementary solution. That solution satisfies the homogeneous partial differential equation corresponding to the load-free plate, subject to certain boundary conditions.

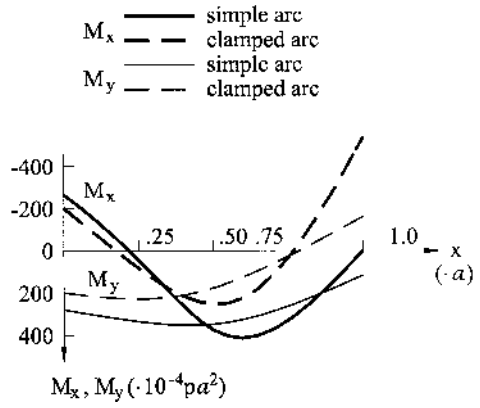

Fig. 6.9

Several different boundary element approaches have already been proposed for the construction of the complementary solution. They are frequently referred to as *direct* and *indirect BEM formulations* [12,13]. In the indirect BEM formulation, the complementary function is represented by an integral in terms of some arbitrary functions, called *source functions*, over the boundary of a domain of the plate. These source functions may be visualized, for example, as fictitious force and moment distributions acting on the boundary of the given plate embedded in an infinite elastic plate (the term "fictitious" is used here because these loads are not resulting in transverse loads assigned for the plate). Finding these source functions, one can determine the deflections, bending and twisting moments anywhere within the plate or on its boundary.

In the direct formulation, the partial differential equation of the plate bending problem for the complementary function is transformed by the use of the reciprocal work identity to an integral equation in terms of boundary values of the deflections and the stress resultants. Both BEM formulations have certain advantages and disadvantages that are discussed in detail in Refs [12,13]. It has been established now that these two formulations have the same origin and theoretical basis. We discuss below both approaches, as applied to plate bending problems.

6.4.1 Indirect BEM for plates

The presentation of the indirect BEM below follows the approach of Ventsel [14]. Assume that a given plate, originally occupying a 2D domain Ω with a smooth boundary Γ, is to be extended infinitely. Then, apply to an infinite plate the above-mentioned fictitious loads in the form of transverse loads $q(\xi, \eta)$ and moments $m_n(\xi, \eta)$ distributed continuously over Γ, where (ξ, η) is some point on Γ (called the *source point*). The moments m_n act in the direction of the outward normal n to Γ at the source point (Fig. 6.10).

In order to determine the deflection surface of the infinite plate caused by the above-mentioned fictitious loads, find the so-called singular solutions of the biharmonic equation (2.24). In our case, these singular solutions correspond to the deflection of point (x, y) of the infinite plate (called the *observation point*) caused by a unit normal concentrated force, and by a unit concentrated moment; both are applied at

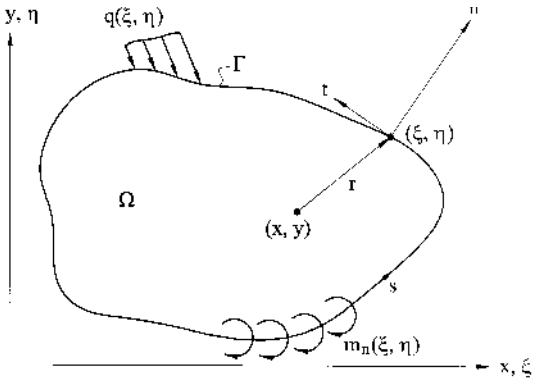

Fig. 6.10

a source point (ξ, η). The above singular solutions are denoted by $G_q(x, y; \xi, \eta)$ and $G_m(x, y; \xi, \eta)$, respectively.

Mathematically, the fundamental solution $G_q(x, y; \xi, \eta)$ of Eq. (2.25) is defined as

$$\nabla^2\nabla^2 G_q = \delta(x, y; \xi, \eta), \tag{6.23a}$$

where $\delta(x, y; \xi, \eta)$ is the Dirac delta function. The solution of the above equation has the form

$$G_q(x, y; \xi, \eta) = \frac{1}{8\pi D} r^2 \ln r, \tag{6.23b}$$

where $r^2 = (x - \xi)^2 + (y - \eta)^2$ is a distance between the source and observation points. Notice that the observation point may be found either inside the domain of the plate Ω, or on its boundary; the source point is always located on the boundary Γ.

Now we can assign the singular solution $G_m(x, y; \xi, \eta)$. Let us consider two normal and oppositely directed concentrated forces P and $-P$, applied at a source point (ξ, η) and at some neighboring point located on the normal n, at a distance Δn from the former. Then a unit concentrated moment at the above source point and acting in the direction of n can be obtained as follows:

$$m = \lim_{\substack{P\to\infty \\ \Delta n\to 0}} P \cdot \Delta n = 1 \tag{6.24a}$$

If one takes a sum of the solutions (6.23) of the above-mentioned concentrated forces and goes to the limit $\Delta n \to 0$, then, taking into account Eq. (6.24a), one finds the following expression for $G_m(x, y; \xi, \eta)$:

$$G_m(x, y; \xi, \eta) = -\frac{\partial G_q(x, y; \xi, \eta)}{\partial n}. \tag{6.24b}$$

The deflection surface of the infinite plate due to the fictitious and given loads can be represented in the following form:

$$w(x, y) = w_{\mathrm{p}}(x, y) + \int_{\Gamma} \left[q(x, y) G_q(x, y; \zeta, \eta) + m_n(\zeta, \eta) G_m(x, y; \zeta, \eta) \right] \mathrm{d}s; \qquad (x, y) \in \Omega, \tag{6.25}$$

where

$$w_{\mathrm{p}}(x, y) = \int\int_{\Omega} p(\xi, \zeta) G_q(x, y; \xi, \zeta) \mathrm{d}\xi \mathrm{d}z \tag{6.26}$$

is a particular solution of Eq. (2.24). Since a point (x, y) is inside the domain Ω whereas a point (ζ, η) is on the boundary Γ, the deflection function $w(x, y)$ as given by Eq. (6.25) will be a continuous function of x and y, with continuous derivatives of all orders, in the domain Ω. We can thus differentiate with respect to x and y, as

required to find the slopes, moments, and shear forces in the plate due to these fictitious loads applied along Γ.

Assume that the boundary conditions on Γ are nonhomogeneous, as follows:

$$\begin{aligned} w &= w^*|_\Gamma, \quad \vartheta_n, = \vartheta_n^*|_\Gamma \quad \text{(Problem 1)},\\ w &= w^*{}_\Gamma, \quad M_n = M_n^*|_\Gamma \quad \text{(Problem 2)},\\ M_n &= M_n^*|_\Gamma, \quad V_n = V_n^*|_\Gamma \quad \text{(Problem 3)}, \end{aligned} \tag{6.27}$$

where ϑ_n, M_n, and V_n are the slope, bending moment, and the effective shear force on the boundary with the outer normal n; ϑ_n^*, M_n^*, and V_n^* are given boundary functions specified on Γ. The boundary quantities ϑ_n, M_n, and V_n at a regular point on Γ are expressed in terms of the deflection w by the relations (2.45)–(2.48) and Eq. (2.13). We obtain the following:

$$\begin{aligned} \vartheta_n &= \frac{\partial w}{\partial n},\\ M_n &= -D\left(\frac{\partial^2 w}{\partial n^2} + \nu\frac{\partial^2 w}{\partial t^2}\right),\\ V_n &= -D\left[\frac{\partial^3 w}{\partial n^3} + (2-\nu)\frac{\partial^3 w}{\partial n \partial t^2}\right], \end{aligned} \tag{6.28}$$

where $\partial/\partial n$ and $\partial/\partial t$ denote differentiation along the outward normal and tangential directions, respectively.

The expression (6.25) satisfies the governing equation (2.24) exactly and does not satisfy the prescribed boundary conditions (6.27) for arbitrary chosen fictitious loads q and m_n. Inserting $w(x, y)$ in the form of Eq. (6.25) into the boundary conditions (6.27) and letting a point (x,y) from inside the domain approach the boundary, we obtain the integral representation of the deflection, slope, normal bending moment, and the effective shear force on Γ due to the given and fictitious loads. In so doing, it is necessary to take the limit as x, y approaches Γ, and to examine the limiting values of the above-mentioned integral representations. It can be shown that the deflections and slopes remain continuous, whereas the normal bending moments and effective shear forces undergo a finite jump for a passage through the boundary Γ. Equating the limiting values of $w(x, y)$, $\vartheta_n(x, y)$, $M_n(x, y)$, and $V_n(x, y)$ on Γ to the prescribed boundary functions according to Eqs (6.28), we finally obtain the boundary integral equations for the unknown fictitious loads $q(\zeta, \eta)$ and $m_n(\zeta, \eta)$. These equations can be represented in the general form for solving Problems 1, 2, and 3, as follows:

$$\int_\Gamma \left[q(\zeta,\eta)G_q(x,y;\zeta,\eta) + m_n(\zeta,\eta)G_m(x,y;\zeta,\eta)\right]\mathrm{d}s + w_\mathrm{p}(x,y) = w^*(x,y); \tag{6.29a}$$

$$\int_\Gamma \left[q(\zeta,\eta)\frac{\partial^2 G_q(x,y;\zeta,\eta)}{\partial n} + m_n(\zeta,\eta)\frac{\partial G_m(x,y;\zeta,\eta)}{\partial n}\right]\mathrm{d}s + \frac{\partial w_\mathrm{p}(x,y)}{\partial n} = \vartheta_n^*(x,y); \tag{6.29b}$$

$$\int_\Gamma \left[q(\zeta, n)\left(\frac{\partial^2 G_q(x, y; \zeta, \eta)}{\partial n^2} + \nu \frac{\partial^2 G_q(x, y; \zeta, \eta)}{\partial t^2} \right) \right] \mathrm{d}s + \frac{m_n(x, y)}{2}$$
$$+ \int_\Gamma \left[m_n(\zeta, \eta)\left(\frac{\partial^2 G_m(x, y; \zeta, \eta)}{\partial n^2} + \nu \frac{\partial^2 G_m(x, y; \zeta, \eta)}{\partial t^2} \right) \right] \mathrm{d}s$$
$$+ \left(\frac{\partial^2}{\partial n^2} + \nu \frac{\partial^2}{\partial t^2} \right) w_\mathrm{p}(x, y) = M_n^*(x, y); \tag{6.29c}$$

$$\frac{1}{2} q(x, y) + \int_\Gamma q(\zeta, \eta) \left[\frac{\partial^3 G_q(x, y; \zeta, \eta)}{\partial n^3} + (2 - \nu) \frac{\partial^3 G_q(x, y; \zeta, \eta)}{\partial n \partial t^2} \right] \mathrm{d}s$$
$$+ \int_\Gamma m_n(\zeta, \eta) \left[\frac{\partial^3 G_m(x, y; \zeta, \eta)}{\partial n^3} + (2 - \nu) \frac{\partial^3 G_m(x, y; \zeta, \eta)}{\partial n \partial t^2} \right] \mathrm{d}s$$
$$+ \left[\frac{\partial^3}{\partial n^3} + (2 - \nu) \frac{\partial^3}{\partial n \partial t^2} \right] w_\mathrm{p}(x, y) = V_n^*(x, y). \tag{6.29d}$$

It can be shown [14] that the kernels of the integrals in Eqs (6.29a)–(6.29c), as well as the first integral in Eq. (6.29d), are bounded when a point (x, y) from the domain Ω approaches (ζ, η) on Γ. Therefore, the integrals of these equations can be evaluated by using a standard numerical technique developed for the numerical implementation of regular integrals. The kernel of the second integral in Eq. (6.29d) behaves like r^{-2} when a point $(x, y) \to (\zeta, \eta)$ on the boundary. This integral does not exist neither as an improper nor singular integral and special care must be taken for representation and evaluation of such a type of integral. There are a number of efficient techniques for dealing with this strongly singular integral [14–16]. The first approach is to cancel out explicitly this higher-order singularity in advance, before limiting transition to the boundary (for example, by using integration by parts for the expression of the effective shear force when a point (x, y) is not on Γ). The second possibility is to assign a certain sense to this strongly singular integral. This is possible because it appears in the expression for the effective shear force which is finite on the boundary. Hadamard [17] defined this integral in the finite part integration sense and it is referred to as a hypersingular integral. Hypersingular integrals can be evaluated analytically, using either some regularization technique [14–17, etc.], or numerically, by special quadrature formulas that avoid any explicit performing of limiting processes [14,18,19].

Solving the boundary integral equations, we obtain the source functions $q(\zeta, \eta)$ and $m_n(\zeta, \eta)$ distributed over Γ. Once the fictitious loads q and m_n distributed over the boundary have been established from the numerical solution of the boundary integral equations, the values of the deflection and stress resultants anywhere within the plate and on its boundary can be calculated by using Eqs (6.25) and (2.13).

6.4.2 Direct BEM

Unlike the indirect BEM, the direct BEM is formulated in terms of the natural variables, interpretable as deflection, slope, bending moment, and effective shear force assigned along the plate boundary Γ.

The direct BEM can be obtained with the use of the Betti–Maxwell reciprocal theorem [12, 20]. This theorem states that for any two equilibrium states, say, A and B, of an elastic body, the work that would be done by the forces A if given the displacements B is equal to the work that would be done by the forces B if given the displacements A. This means that the following expression can be written for any elastic plate:

$$\int\int_{\Omega} p_{\mathrm{A}} w_{\mathrm{B}} \mathrm{d}\Omega + \int_{\Gamma} (V_{\mathrm{A}} w_{\mathrm{B}} - M_{\mathrm{A}} \vartheta_{\mathrm{B}}) \mathrm{d}s = \int\int_{\Omega} p_{\mathrm{B}} w_{\mathrm{A}} \mathrm{d}\Omega + \int_{\Gamma} (V_{\mathrm{B}} w_{\mathrm{A}} - M_{\mathrm{B}} \vartheta_{\mathrm{A}}) \mathrm{d}s. \tag{6.30}$$

Again, assume that the plate boundary is smooth. If the boundary has corner points, the expression (6.30) has to be complemented by the terms $\sum V_{\mathrm{A}} w_{\mathrm{B}}$ and $\sum V_{\mathrm{B}} w_{\mathrm{A}}$ on the left- and right-hand sides, respectively. Here, the summation is made over all corners.

Let us identify w_{A} with w and p_{A} with p (i.e., an actual deflection field and actual loading are chosen as the state A), while w_{B} is identified with the fundamental solution (6.23b) for a unit concentrated force replacing p_B and applied at a source point (ξ, η) of an infinite plate. Taking into account that

$$\int\int_{\Omega} w(x, y) \delta(x, y; \xi, \eta) \mathrm{d}\Omega = w(\xi, \eta), \tag{6.31}$$

one obtains from the expression (6.30), after the usual limiting process when the interior point (ξ, η) approach Γ [11–14], the following integral representation of the plate deflections:

$$cw(\xi, \eta) = \int_{\Gamma} \left[V_n \langle w \rangle G_q - M_n \langle w \rangle \frac{\partial G_q}{\partial n} - V_n \langle G_q \rangle w + M_n \langle G_q \rangle \vartheta_n \right] \mathrm{d}s(x, y) + \int\int_{\Omega} p(x, y) G_q \mathrm{d}\Omega(x, y) \tag{6.32}$$

In Eq. (6.32), n is the normal at point (x, y) on the boundary Γ and

$$c = \begin{cases} 1 & (\xi, \eta) \text{ inside } \Omega \\ \dfrac{1}{2} & (\xi, \eta) \text{ on } \Gamma \\ 0 & (\xi, \eta) \text{ outside } \Omega \end{cases} \tag{6.32}$$

Explicit expressions for the operators $M_n\langle \ldots \rangle$, and $V_n\langle \ldots \rangle$ at a point (x, y) are given by Eqs. (6.28); $G_q \equiv G_q(x, y; \xi, \eta)$ is a fundamental (singular) solution of Eq. (6.23a) given by Eq. (6.23b).

For solving well-posed plate bending boundary value problems, given by Eqs. (2.24) and (6.27), an additional equation is required. This can be an integral representation for the slopes. Let v is an arbitrary direction at point $(\xi, \eta) \in \Omega$. When the above point approaches the boundary, this direction will coincide with the corresponding direction of the outward normal at the source point $(\xi, \eta) \in \Gamma$. Thus,

differentiating Eq. (6.32) in a fixed direction v, we obtain, through a limiting process, the following integral representation of the slopes:

$$c\vartheta_v(\xi,\eta) = \int_\Gamma \left[V_n\langle w\rangle \frac{\partial G_q}{\partial v} - M_n\langle w\rangle \frac{\partial^2 G_q}{\partial n \partial v} - V_n\left\langle \frac{\partial G_q}{\partial v}\right\rangle w + M_n\left\langle \frac{\partial G_q}{\partial v}\right\rangle \vartheta_n \right] \mathrm{d}s(x,y) + \int\int_\Omega p(x,y)\frac{\partial G_q}{\partial v}\mathrm{d}\Omega(x,y) \tag{6.34}$$

where c for a smooth boundary at point (x, y) is given by (6.32), $\vartheta_v = \partial w/\partial v$.

The expressions (6.32) and (6.34) can be used to give the boundary integral equations of the direct BEM. Indeed, placing in the above equations the point (ξ, η) on the boundary Γ, replacing two out of four boundary quantities, w, ϑ_n, M_n, and V_n, by prescribed boundary functions according to Eqs. (6.27), and noting that the boundary functions on the left sides are the same boundary functions as on the right sides, we can formulate two coupled boundary integral equations for the two remaining boundary quantities.

Comparing the indirect and direct BEM formulations, it is easy to discover that the variables (x, y) and (ξ, η) change places in the resulting boundary integral equations (6.29) and (6.32), (6.34).

6.4.3 Numerical treatment of BEM

An analytical solution of the boundary integral equations of either direct or indirect BEM formulation is possible in the exceptional cases of a simple plate geometry, load, and boundary conditions. However, these equations can be solved numerically by employing the standard boundary element technique developed, for example, in Refs [11–13].

Let us describe briefly a possible numerical procedure for solving these boundary integral equations. The boundary of a given domain is divided into N smooth boundary elements (BEs), $\Delta\Gamma_k$ $(k = 1, 2, \ldots N)$. The geometry of $\Delta\Gamma_k$ is approximated by a straight line or a parabolic arc. Unknown source functions (either "fictitious" loads in the indirect BEM or natural variables in the direct BEM) are assumed to be uniformly or linearly varying along $\Delta\Gamma_k$ (of course, a higher order of approximation of these functions can be also assigned). The nodes of the unknown source functions and the given boundary functions are assigned either at the center of $\Delta\Gamma_k$ or at the interfaces between two adjacent boundary elements. The integrals are evaluated analytically or numerically using standard Gaussian quadrature [21]. In the case where the boundary integrals involve the previously mentioned strong singularities (when a point $(x, y) \in \Omega \to (\xi, \eta) \in \Gamma$), it is necessary to consider a neighborhood of such points separately and employ the special regularization formulas [14–19] for evaluating these singular integrals. Such an approximation of the boundary integral equations yields a system of algebraic equations with respect to nodal values of the unknown source functions. Once these unknowns have been established, the values of the deflections and stress resultants at any point either inside the plate domain or on its boundary can be evaluated from the discretized form of Eqs (6.25), (6.32), and (2.13).

Example 6.3

A square plate with a square central opening is subjected to a uniform surface load p. The external edges of the plate are simply supported and the internal edges are free, as shown in Fig. 6.11a. Determine the deflection at the points A, B, and C. Assume $\nu = 1/6$.

Solution

This problem has been analyzed by Tottenham [10]. He applied the direct and indirect BEM to the analysis of this plate. One-quarter of the plate was considered, with the nodes at the quarter points along each side, giving a total of 24 points – shown in Fig. 6.11b. Due to the symmetry, the boundary conditions were satisfied at 13 points – indicated also in Fig. 6.11b. The 26 algebraic equations for the 26 source functions specified at 13 points of the external and internal edges of the plate boundary have approximated the boundary integral equations of the indirect and direct BEM . The results obtained are compared with those using the finite element method (FEM) and variational finite difference method (VFDM) in Table 6.2. In both of the comparative cases (for BEM solutions) the mesh size was $a/16$ and the source functions are assumed to be constant over BEs along the boundary. In analyzing this problem, the corner points were ignored. As follows from Table 6.2, the numerical results obtained by BEM are very close to those obtained by FEM and VFDM (the discrepancy of the results does not exceed more than 2.5%).

Example 6.4

A quadrangular plate is subjected to a concentrated force P applied at the center of an inscribed circle, as shown in Fig. 6.12a. The radius of the inscribed circle $R = 2/3$ m. Poisson's ratio $\nu = 0.3$, the plate thickness $h = 2 \times 10^{-3}$ m, the modulus of elasticity $E = 2 \times 10^5$ Pa. Determine the deflection and bending moment distributions along section AB and along the boundary.

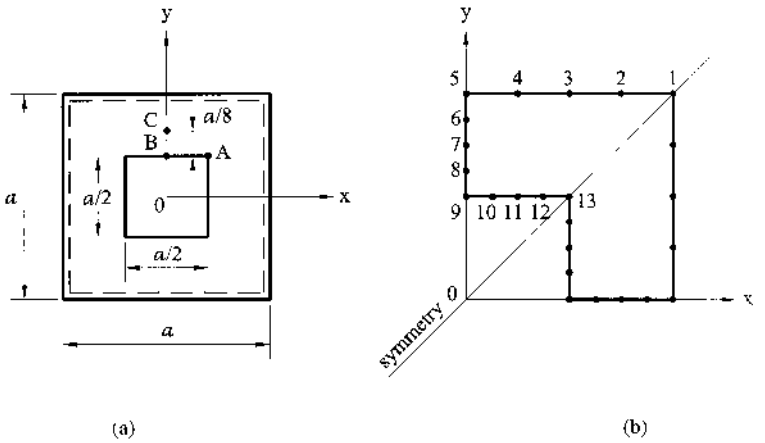

Fig. 6.11

Table 6.2

	Displacement ($\times pa^4/100D$)			
	Boundary element method			
Point	Indirect	Direct	Finite element method	Finite difference method
A	0.2188	0.2188	0.2185	0.2174
B	0.3107	0.3141	0.3156	0.3006
C	0.1558	0.1565	—	0.1541

Solution

This problem was analyzed by Ventsel [14]. He applied the indirect BEM to the analysis of the plate. The plate boundary was divided into 28 boundary elements (BEs), giving a total of 28 nodes. The boundary conditions were satisfied at these nodal points. Unknown edge forces, q, and the normal edge moments, m_n, were assumed to be constant over BEs. The two boundary integral equations (Eqs (6.29a) and (6.29b)) were approximated by 56 algebraic equations for the 56 nodal loads, $q^{(k)}$ and $m_n^{(k)}$ $(k = 1, 2, \ldots, 28)$. Some results of the numerical analysis are shown in Fig. 6.12a, b in the form of the deflection and bending moment distributions along section AB and the boundary. The deflection and bending moments ordinates are given in Fig. 6.12 to within the following constant multipliers: p/D for the w and P for the function M.

In conclusion, it should be noted that the BEM is very powerful and efficient as applied to various linear plate bending problems. The method has the following advantages:

1. It can be easily adapted to any complicated geometry of the domain involved and to arbitrary boundary conditions, like the finite element method. However, unlike the FEM, an application of the BEM to boundary value problems enables us to reduce the dimensionality of the problem. The latter results in a smaller, than the FEM, system of equations and considerable reductions in the data required to run a problem.
2. The BEM is easily programmed for arbitrary plate configurations, loads, and boundary conditions.
3. The numerical accuracy of the BEM is generally greater than that of the FEM and other numerical methods. The numerical discretization of the method leads to a stable system of linear algebraic equations. The error of an approximate solution introduced by the BEM can be estimated a posteriori when the problem under consideration has been solved [14].
4. The method has been adapted well for the solution of the so-called singular problems, such as plates with crack-like defects, plates having holes, corners, etc.

However, this method has some disadvantages:

1. It can be successfully applied primarily to linear problems.
2. The method requires that a fundamental solution of a governing differential equation or Green's function be represented in the explicit analy-

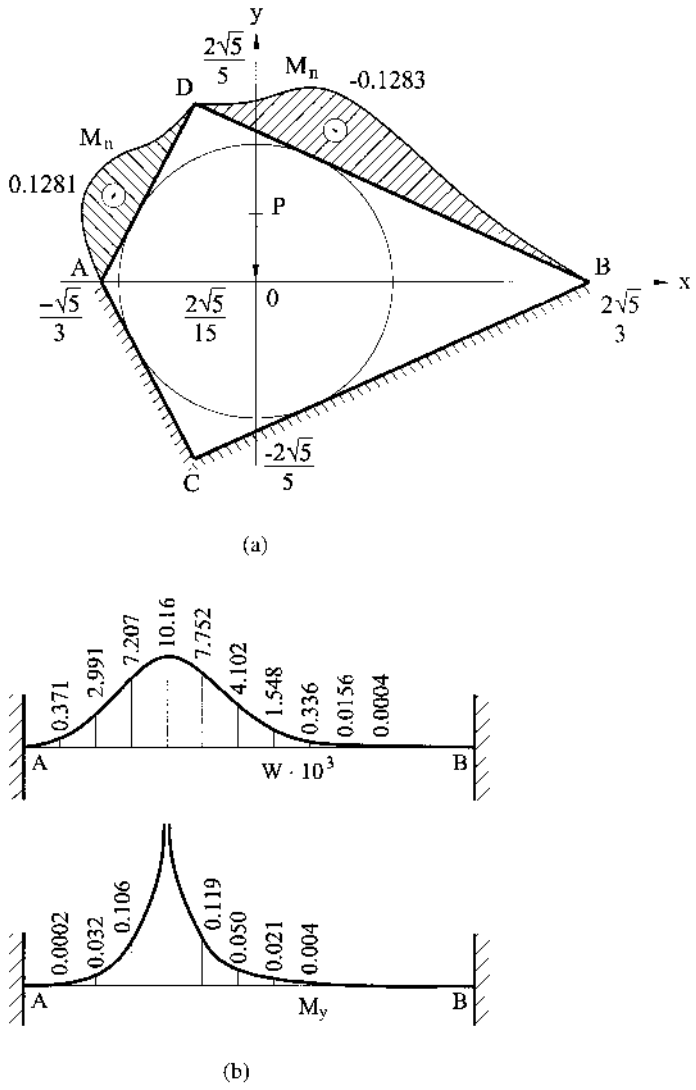

Fig. 6.12

tical form. Note, that for the plate bending problems discussed, the fundamental solution is of the very simple analytical form. If the above-mentioned fundamental solution is more awkward than for plate bending problems, the BEM formulation and numerical approximation becomes less efficient.

3. The matrix of the approximating system of linear algebraic equations is complete, unlike the FEM, which causes some difficulties in its numerical implementation.

This section contains only a brief description of the BEMs and their application to plate bending problems. The interested reader is referred to other publications [10–15].

6.5 THE GALERKIN METHOD

The method formulated by Galerkin [22] can be applied successfully to diverse types of problems of applied elasticity including the plate bending problems. Although the mathematical theory behind the Galerkin method is quite complicated, its physical interpretation is relatively simple. We consider now the general idea of the Galerkin method from the mathematical point of view.

Let a differential equation of a given 2D boundary value problem be of the form

$$L[w(x, y)] = p(x, y) \quad \text{in some 2D domain } \Omega, \tag{6.35}$$

where $w = w(x, y)$ is an unknown function of two variables (of course, the method can be applied to 3D problems also) and p is a given load term defined also in the domain Ω. The symbol L indicates either a linear or nonlinear differential operator. For instance, for plate bending problems, $L[\ldots] \equiv D\nabla^2\nabla^2(\ldots)$. The function w must satisfy the prescribed boundary conditions on the boundary Γ of that domain. An approximate solution of Eq. (6.35) is sought in the following form:

$$w_N(x, y) = \sum_{i=1}^{N} \alpha_i f_i(x, y), \tag{6.36}$$

where α_i are unknown coefficients to be determined and $f_i(x, y)$ are the linearly independent coordinate functions (they are also called trial functions) that satisfy all the prescribed boundary conditions but not necessarily satisfy Eq. (6.35).

From calculus, any two functions $f_1(x)$ and $f_2(x)$ are called mutually orthogonal in the interval (a, b) if they satisfy the condition

$$\int_a^b f_1(x) f_2(x) \mathrm{d}x = 0. \tag{a}$$

For example, a set of functions $1, \sin x, \cos x, \cos 2x, \sin 2x, \ldots, \cos kx, \sin kx, \ldots$ is orthogonal in the interval $(0, 2\pi)$ because any two functions from the this set satisfy the condition (a) in the above interval. If one of the functions – for example, $f_1(x)$ – is identically equal to zero, then the condition (a) is satisfied for any function $f_2(x)$.

Thus, if a function $w(x, y)$ is an exact solution of the given boundary value problem, then the function $[L(w) - p]$ will be orthogonal to any set of functions. Since the deflection function $w_N(x, y)$ in the form of (6.36) is an approximate solution only of Eq. (6.35), $[L(w_N) - p] \neq 0$, and it is no longer orthogonal to any set of functions. However, we can require that the magnitude of the function $[L(w_N) - p]$ be minimum. This requirement is equivalent to the condition that the above function should be orthogonal to some bounded set of functions: first of all, to the trial functions $f_i(x)$. It leads to the following Galerkin equation:

$$\iint_{\mathrm{A}} [L(w_N) - p] f_i(x, y) \mathrm{d}x \mathrm{d}y = 0, \tag{6.37}$$

Substituting for w_N from Eq. (6.36), one obtains

$$\int\int_{A}\left[L\left(\sum_{i=1}^{N}\alpha_i f_i(x,y)\right)-p\right]f_j(x,y)\mathrm{d}x\mathrm{d}y=0,\quad j=1,2,\ldots,N.$$

Introducing the residual error function $E(w_N)$, as follows,

$$E(w_N)=L\left(\sum_{i=1}^{N}\alpha_i f_i(x,y)\right)-p, \tag{6.38}$$

we can rewrite the above Galerkin equation in the form

$$\int\int_{A}E(\alpha_i,f_i(x,y);p)f_j(x,y)\mathrm{d}x\mathrm{d}y=0;\ i,j=1,2,\ldots,N. \tag{6.39}$$

The above requirement can be used as a condition for determining the coefficients α_i. Replacing the integral in Eq. (6.39) by the sum of integrals, we obtain the following system of linear algebraic equations:

$$\begin{aligned}&a_{11}\alpha_1+a_{12}\alpha_2+.....+a_{1N}\alpha_N=b_1\\&\ldots\ldots\ldots\ldots\ldots\ldots\ldots\ldots\\&a_{N1}\alpha_1+a_{N2}\alpha_2+.....+a_{NN}\alpha_N=b_N,\end{aligned} \tag{6.40a}$$

where

$$a_{ij}=\int\int_{A}L(f_i)\cdot f_j\mathrm{d}x\mathrm{d}y;\ b_i=\int\int_{A}p\cdot f_j\mathrm{d}x\mathrm{d}y\ \ i,j=1,2,\ldots,N. \tag{6.40b}$$

Solving Eqs (6.40a), we can determine the unknown coefficients α_i which, in conjunction with Eq. (6.36), gives the N-parameter Galerkin approximation of Eq. (6.35). Notice that if $N\to\infty$, the Galerkin solution approaches the exact solution if the system of functions $f_1,f_2,\ldots$ is complete and linearly independent [6].

Galerkin equations (6.37) had been derived above from the special mathematical condition of orthogonality of two functions, Eq. (a). However, the Galerkin method can be derived from the general variational principle of virtual work, introduced in Sec. 2.6.2.

As shown in Sec. 2.4, the governing equation of plate bending problems, Eq. (2.24), represents the condition of static equilibrium of an infinitesimal plate element. Then, the operator $[L(w_N)-p]$ can be interpreted as an intensity of some unbalanced total loading that occurs over the area of integration A (area of the plate) when the deflection function is sought in the form of Eq. (6.36). Retaining a finite number of N terms in the expansion (6.36) implies that an actual continual system is replaced by a system with N degrees of freedom (i.e., a discrete system). In turn, the constant coefficients α_i $(i=1,2,\ldots,N)$ can be treated as some generalized displacements, each of which corresponds to a deflected state of the plate defined by a function $f_i(x,y)$.

According to the principle of virtual work, any discrete system is in equilibrium if work done by all the elementary forces, i.e., $[L(w_N)-p]\mathrm{d}x\mathrm{d}y$, acting through some admissible for this system displacements, i.e., $\delta\alpha_i f_i(x,y)$, is equal to zero:

$$\delta W_i = \delta\alpha_j \int\int_A [L(w_N) - p] f_i(x, y) \mathrm{d}x\mathrm{d}y = 0. \tag{b}$$

This equality, after discarding the arbitrary variation $\delta\alpha_i$, yields Eqs (6.37).

Since the Galerkin equations (6.37) can be treated as an expression of the principle of virtual work, then, instead of factor $f_i(x, y)$, any of its derivatives can also be set depending on the sense of the operator $[L(w_N) - p]$. For example, in the governing differential equation of beam bending, $\mathrm{d}^2v/\mathrm{d}x^2 = -M/EI$, the operator $[EI(\mathrm{d}^2w/\mathrm{d}x^2) + M]$ represents the bending moments in dimension. Then, assigning the deflections in the form of the series $v_N = \sum_i^N \alpha_i f_i(x)$, it is necessary to take $f_i''(x)$, having the dimension of curvature, as a multiplier in the integrand of Eq. (6.39), but not f_i. In this case, the product $E(v_N) \cdot f_j'' \mathrm{d}x$ represents an elementary work and the Galerkin equations appear in the following form:

$$\int_0^L E(v_N) \cdot f_j'' \mathrm{d}x = 0, \quad i = 1, 2, \ldots, N.$$

The above variational interpretation of the method provides a way for justifying the so-called *generalized Galerkin method.* Let the trial functions $f_i(x, y)$, unlike the general requirements of the Galerkin method, satisfy kinematic boundary conditions only. This implies that, if for example, the bending moment M_n and effective shear force V_n at any point of the boundary Γ (n is outward normal at a point of the boundary) are equal to zero, then bending of a plate over surface $f_i(x, y)$ can cause an appearance of some moments $M_{ni} \neq 0$ and $V_{ni} \neq 0$. Then, the following equations, instead of Eqs (6.37), result from the variational principle $\delta W_i = 0$:

$$\int\int_A [L(w) - p] f_i(x, y) \mathrm{d}x\mathrm{d}y - \hat{W}_i = 0, \tag{6.41}$$

where $\hat{W}_i$ is work done by moments and forces on the boundary of the domain of integration A acting through displacements $f_i(x, y)$. For plate bending problems,

$$\hat{W}_i = \oint_\Gamma \Delta M_n \frac{\partial f_i}{\partial n} \mathrm{d}s + \oint_\Gamma \Delta V_n f_i \mathrm{d}s$$

where ΔM_n and ΔV_n are unbalanced portions of the moment and effective shear force on the boundary Γ in plate bending over the surface w. For example, on the edge $x = 0$ of the rectangular plate,

$$\Delta M_x = m_x - \left[-D\left(\frac{\partial^2 w}{\partial x^2} + \nu \frac{\partial^2 w}{\partial y^2} \right) \right],$$

$$\Delta V_x = q_x - \left[-D \frac{\partial}{\partial x} \left(\frac{\partial^2 w}{\partial x^2} + (2 - \nu) \frac{\partial^2 w}{\partial y^2} \right) \right],$$

where m_x and q_x are intensities of external load applied to the plate edge.

Hence, when the Galerkin method is applied to the solution of the boundary value problems of solid mechanics and an approximate solution of Eq. (6.35) is sought in the form of (6.36), the multiplier in the integrand of Eq. (6.37) should

be chosen in such a way that the operation of orthogonality would correspond to the application of the principle of virtual work to the given problem. Such an approach will result in a more rapid convergence of a solution.

Example 6.5

Find an analytical expression by Galerkin's method for the deflection of a uniformly loaded ($p = \text{const}$) rectangular plate with all edges clamped (Fig. 6.13).

Solution

The boundary conditions for the plate are given by

$$w = 0|_{\substack{x=\pm a \\ y=\pm b}}; \quad \frac{\partial w}{\partial x} = \frac{\partial w}{\partial y}\bigg|_{\substack{x=\pm a \\ y=\pm b}}. \tag{a}$$

Let us take the deflected plate surface in the following form

$$w = \alpha_1 f_1(x, y) + \alpha_2 f_2(x, y) + \alpha_3 f_3(x, y) + \ldots \tag{b}$$

where

$$f_1 = \left(x^2 - a^2\right)^2 \left(y^2 - b^2\right)^2; \quad f_2 = \left(x^2 - a^2\right)^2 \left(y^2 - b^2\right)^3; \text{ etc.}$$

The function (b) satisfies all the prescribed boundary conditions (a) exactly. To simplify the solution, let us consider only the first term in Eq. (b). Thus, Galerkin's equations (6.40) reduce to only one equation of the following type:

$$a_{11}\alpha_1 = b_1, \tag{c}$$

where

$$a_{11} = D \int_A \int \nabla^2 \nabla^2 f_1 \cdot f_1 \mathrm{d}x\mathrm{d}y; \quad b_1 = \int_A \int p \cdot f_1 \mathrm{d}x\mathrm{d}y. \tag{d}$$

We have the following

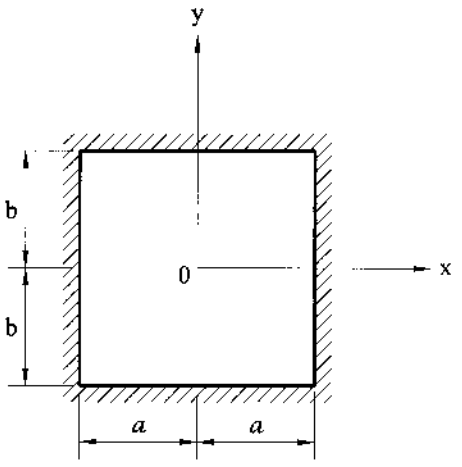

Fig. 6.13

$$f_1 = \left(x^2 - a^2\right)^2\left(y^2 - b^2\right)^2; \quad \frac{\partial^4 f_1}{\partial x^4} = 24\left(y^2 - b^2\right)^2; \quad \frac{\partial^4 f_1}{\partial y^4} = 24\left(x^2 - a^2\right)^2;$$

$$\frac{\partial^4 f_1}{\partial x^2 \partial y^2} = 16\left(3x^2 - a^2\right)\left(3y^2 - b^2\right);$$

$$a_{11} = D\iint_A \left(\frac{\partial^4 f_1}{\partial x^4} f_1 + 2\frac{\partial^4 f_1}{\partial x^4 \partial y^4} f_1 + \frac{\partial^4 f_1}{\partial y^4} f_1\right) \mathrm{d}x\mathrm{d}y$$

$$= 4D\int_0^a \int_0^b \Big[24\left(x^2 - a^2\right)^2\left(y^2 - b^2\right)^4 + 32\left(3x^2 - a^2\right)\left(3y^2 - b^2\right)\left(x^2 - a^2\right)^2$$

$$\left(y^2 - b^2\right)^2 + 24\left(x^2 - a^2\right)^4\left(y^2 - b^2\right)^2\Big]\mathrm{d}x\mathrm{d}y$$

$$= D\frac{4 \cdot 128 \cdot 64}{63 \cdot 25} a^5 b^5 \left(b^4 + \frac{4}{7}a^2 b^2 + a^4\right);$$

$$b_1 = \iint_A p \cdot f_1 \mathrm{d}x\mathrm{d}y = 4p\int_0^a \int_0^b \left(x^2 - a^2\right)^2\left(y^2 - b^2\right)^2 \mathrm{d}x\mathrm{d}y = 4p\frac{64}{225}a^5 b^5.$$

Inserting these values of a_{11} and b_1 into Eq. (c) yields the following:

$$\alpha_1 = \frac{b_1}{a_{11}} = \frac{7p}{128D\left(b^4 + \frac{4}{7}a^2 b^2 + a^4\right)}.$$

Thus,

$$w = \alpha_1 f_1 = \frac{7p}{128D\left(b^4 + \frac{4}{7}a^2 b^2 + a^4\right)}\left(x^2 - a^2\right)^2\left(y^2 - b^2\right)^2.$$

The maximum deflection occurs at the plate center or at $x = y = 0$, as shown below:

$$w_{\max} = \frac{7pa^4 b^4}{128D\left(b^4 + \frac{4}{7}a^2 b^2 + a^4\right)}.$$

For a square plate ($a = b$), we have

$$w = 0.0213\frac{p}{Da^4}\left(x^2 - a^2\right)^2\left(y^2 - a^2\right)^2 \text{ and } w_{\max} = 0.0213\frac{pa^4}{D}.$$

The exact solution obtained by a more rigorous approach is shown next [7]:

$$w_{\max} = 0.0202\frac{pa^4}{D}.$$

Although, only one term of the series expansion has been retained, the error of the approximate solution is about 5%. The bending moments can be determined from Eqs (2.13). Let us determine the bending moment M_x along the line $y = 0$ for a square plate ($a = b$). We have the following for this line $y = 0$:

$$w = \alpha_1 \left(x^2 - a^2\right)^2 a^4, \tag{e}$$

$$M_x = -D \left.\frac{\partial^2 w}{\partial x^2}\right|_{y=0} = -4D\alpha_1 \left(3x^2 - a^2\right) a^4. \tag{f}$$

The maximum bending moment occurs at midpoints of the sides $x = \pm a$, $y = 0$, and $M_{\max}$ is given by

$$M_{\max} = -8D\alpha_1 a^6 = -0.171pa^2.$$

The exact solution of $M_{\max}$ found by Galerkin is $-0.204pa^2$ [22]. The error is about 16%, which is higher than for the deflection. Taking more terms in the expression (b), we approach the above exact value of the bending moment.

It should be noted that the Galerkin method is more general that the Ritz method discussed in Sec. 6.6, because no quadratic functional or virtual work principle is necessary. If the governing equations are derivable from a variational principle, then the Galerkin method reduces to the Ritz method and leads to an identical set of linear algebraic equations produced by the Ritz method. Sometimes, the Galerkin method may be preferable if it is more convenient to work with the governing differential equations rather than with the energy functional. Moreover, there are problems for which no satisfactory variational principle has been formulated, but for which a set of governing differential equations is available. This suggests that the Galerkin method is even broader in application than the Ritz method.

6.6 THE RITZ METHOD

We are now coming to the presentation of the *direct methods*. We begin with a study of the Ritz method. The Ritz method belongs among the so-called *variational methods* that are commonly used as approximate methods for a solution of various boundary value problems of mechanics. These methods are based on variational principles of mechanics discussed in Sec. 2.6.

The energy method developed by Ritz [23] applies the principle of minimum potential energy (2.64). According to the Ritz method, the deflection surface of the plate is approximated by series of the form

$$w(x, y) = \sum_{i=1}^{\infty} C_i f_i(x, y), \tag{6.42}$$

where $f_i(x, y)$ are some coordinate functions that satisfy individually, at least, the kinematic boundary conditions (i.e., conditions imposed on the deflections and their first derivatives) and C_i are unknown constants to be determined from the minimum potential energy principle.

Introducing the expression for $w(x, y)$ in the form of (6.42) into Eq. (2.60) for the total potential energy of a plate, we obtain the following after integrating the total potential energy Π as a function of the unknown coefficients C_i:

$$\Pi = \Pi(C_1, C_2, \ldots). \tag{6.43}$$

Therefore, the extremum problem of the calculus of variations is transformed into the maximum–minimum problem of differential calculus, The latter problem, in turn, is solved by satisfying the following:

$$\frac{\partial \Pi}{\partial C_1} = 0, \quad \frac{\partial \Pi}{\partial C_2} = 0, \ldots, \quad \frac{\partial \Pi}{\partial C_i} = 0, \ldots . \tag{6.44}$$

Since U is a quadratic and Ω_p is a linear functional of w (see Eqs (2.54) and (2.57)), then Eqs (6.44) represent a system of linear nonhomogeneous algebraic equations for C_i. The solution of this system, being substituted into the expression (6.42), yields a final solution of the problem. It is evident that the accuracy of the Ritz method depends considerably on how well the assumed coordinate functions are capable of describing the actual deflection surface. These functions must satisfy the two conditions [6,24]:

1. For any i elements $f_1, f_2, \ldots, f_n$ should be linearly independent or, in other words, any element f_i cannot be expressed by a linear combination of others.
2. The sequence of elements (6.42) is a complete in the energy. This means that whatever element w and a number $\varepsilon > 0$ have been, one can find such a natural number N and such constants $C_1, C_2, \ldots, C_N$ that the following inequality could be satisfied:

$$\left\| w - \sum_{i=1}^{N} C_i f_i \right\| < \varepsilon.$$

where $\| \ \|$ is the norm in the energy space [6].

If the coordinate functions $f_i(x, y)$ satisfy the above-mentioned requirements (and the kinematic boundary conditions), then the infinite series (6.42) with the coefficients obtained from Eqs (6.44) represent an exact solution. In most cases, however, only several terms of the series (6.42) are retained. As a result, only an approximate solution of a problem is available, the accuracy of which depends to a greater degree on a selection of the coordinate functions $f_i(x, y)$ and on a number of terms N retained in the following expression:

$$w(x, y) = \sum_{i=1}^{N} C_i f_i(x, y). \tag{6.45}$$

Various methods for selecting suitable coordinate functions $f_i(x, y)$ for bending analysis of plates by the Ritz method are presented in Refs [24,25].

Example 6.6

Determine the deflection of a rectangular plate simply supported on two opposite edges $y = 0$ and $y = b$, clamped on edge $x = 0$, and free on the edge $x = a$, as shown in Fig. 6.14. The plate is subjected to a uniform load of intensity p_0.

Solution

The geometrical boundary conditions for the plate of Fig. 6.14 are

$$w = 0|_{y=0}; \quad w = 0|_{y=b}; \quad w = 0|_{x=0}; \quad \frac{\partial w}{\partial x} = 0\bigg|_{x=0}. \tag{a}$$

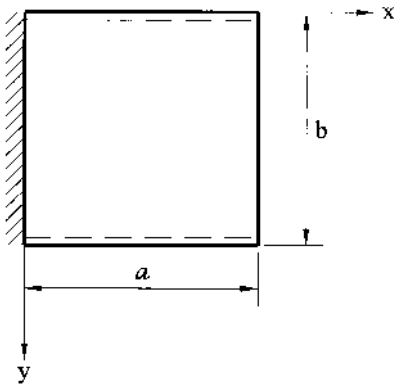

Fig. 6.14

The coordinate functions $f_i(x, y)$ must satisfy the boundary conditions (a) only and they must not satisfy the natural boundary conditions for the free edge $x = a$ and the second boundary condition ($M_y = 0$) for simply supported edges $y = 0$ and $y = b$. Let us take an approximate solution of the following form (the first approximation):

$$w(x, y) = C_1\left(\frac{x}{a}\right)^2 \sin\frac{\pi y}{b}, \tag{b}$$

where C_1 is an unknown coefficient. It can be easily shown that $w(x, y)$ in the form of Eq. (b) satisfies exactly the boundary conditions (a) and does not violate the conditions of $w \neq 0$ and $\partial w/\partial x \neq 0$ along the free edge, and $\partial w/\partial y \neq 0$ along the simply supported edges. Let us introduce new dimensionless coordinates ξ and η, as follows:

$$x = a\xi \quad \text{and} \quad y = b\eta. \tag{c}$$

Thus, we can rewrite the expression for the total potential energy (Eq. (2.60)) in new coordinates as

$$\Pi = \frac{Db}{2a^3}\int_0^1\int_0^1 \left\{\left[\left(\frac{\partial^2 w}{\partial \xi^2}\right) + \left(\frac{a}{b}\right)^2\left(\frac{\partial^2 w}{\partial \eta^2}\right)\right]^2 - 2(1-\nu)\left(\frac{a}{b}\right)^2\left[\frac{\partial^2 w}{\partial \xi^2}\frac{\partial^2 w}{\partial \eta^2} - \left(\frac{\partial^2 w}{\partial \xi \partial \eta}\right)^2\right]\right\} \mathrm{d}\xi \mathrm{d}\eta - ab\int_0^1\int_0^1 p \cdot w \mathrm{d}\xi \mathrm{d}\eta, \tag{d}$$

and the expression for the deflection surface is

$$w = C_1\xi^2 \sin \pi\eta. \tag{e}$$

Upon substituting the expression (e) for the deflection into Eq. (d), evaluating the integrals and taking the derivative $\partial\Pi/\partial C_1 = 0$, we can determine coefficient C_1. We have $C_1 = (a^4 p/D)(2/\Psi)$, where Ψ is given by

$$\Psi = 3\pi\left[2 + \frac{\pi^4}{10}\left(\frac{a}{b}\right)^4 + \frac{4}{3}\pi^2\left((1-\nu)\left(\frac{a}{b}\right)^2 - \frac{2}{3}\nu\pi^2\left(\frac{a}{b}\right)^2\right]. \tag{f}$$

The expression for the deflection is

$$w = \frac{a^4 p}{D} \cdot \frac{2(x/a)^2 \sin \pi y/b}{\Psi}.$$

If we evaluate the deflection for $a/b = 1$, $\nu = 0.3$, $x = a$, and $y = b/2$, we obtain

$$w = 0.1118 \frac{pa^4}{D},$$

which deviates from the exact solution by approximately 1%.

Example 6.7

Determine the deflection of a semicircular plate ($h = \text{const}$) subjected to a concentrated force P, as shown in Fig. 6.15. It is fixed along the straight edge and is free along the arc edge.

Solution

The geometrical boundary conditions for this problem have the form

$$w = 0|_{x=0}, \quad \frac{\partial w}{\partial x} = 0\Big|_{x=0}. \tag{a}$$

These conditions will be satisfied if we take $w(x, y)$ in the form

$$w = x^2\left(C_0 + C_{10}x + C_{01}y + C_{20}x^2 + C_{11}xy + C_{02}y^2 + \ldots\right). \tag{b}$$

After substitution of this expression into Eq. (2.60) and letting $p(x, y) = 0$, an integration should be performed over the area of the semicircle. With this purpose, it is convenient to go to the polar coordinates, r and φ, replacing x with $r\cos\varphi$, y with $r\sin\varphi$ and the area element $\mathrm{d}x\mathrm{d}y$ with $r\mathrm{d}r\mathrm{d}\varphi$. The limits of integration will be: over the variable φ – from 0 to π and over the variable r – from 0 to R. Notice that the potential of the external forces will involve only a non-integral term, namely

$$\Omega_s = -P \cdot w_0,$$

where w_0 is the deflection at a point of the force application that is calculated from Eq. (b). Fairly awkward calculations do not present any key difficulties and allow us to determine the deflection surface $w(x, y)$ and then the bending moments. The

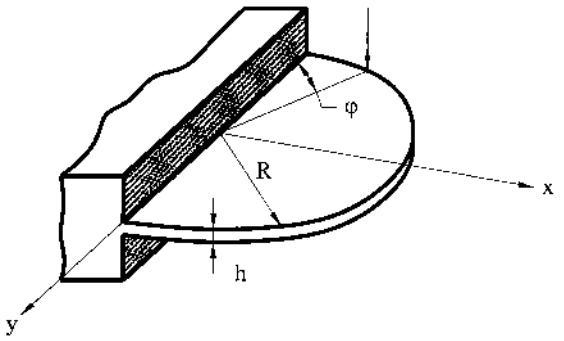

Fig. 6.15

accuracy of calculation of the bending moments depends mainly on the number of terms retained in the expansion (b).

If a plate has openings (Fig. 6.16), then the analysis can be performed similarly but the area of openings must be eliminated from the area of integration in calculating the total potential energy Π.

Let us discuss the advantages of the Ritz method.

(a) The basic advantage lies in the fact that the coordinate functions $f_i(x, y)$ must satisfy the kinematic (or geometrical) boundary conditions only. Therefore, the area of an application of the method to the plate bending problems is wider than of the classical analytical methods discussed in Chapter 3. Therefore, the Ritz method is very efficient for the analysis of plates having free edges, for plates with openings.

(b) The method can be also applied successfully to rectangular plates of variable thickness, because there is no difference between the expressions of Π for plates of constant and variable thicknesses.

(c) Another advantage of the method is that the matrix of the linear algebraic equations, following on from Eq. (6.44), is always symmetrical, resulting in stable and powerful logarithms for their numerical solution.

The basic disadvantages of the method are

(a) The Ritz method can be applicable only to simple configurations of plates (rectangular, circular, etc.), because of the complexity of selecting the coordinate functions for domains of complex geometry.

(b) The Ritz method approximation (6.44) results in the complete matrix of linear algebraic equations that produces some difficulties in its numerical implementation.

It should be noted that the Ritz method can serve as a basis for a such popular and powerful methods as the finite element method, which is discussed in the next section.

6.7 THE FINITE ELEMENT METHOD (FEM)

6.7.1 Introduction

The finite element method (FEM) is based on the concept that one can replace any continuum by an assemblage of simply shaped elements with well-defined force–

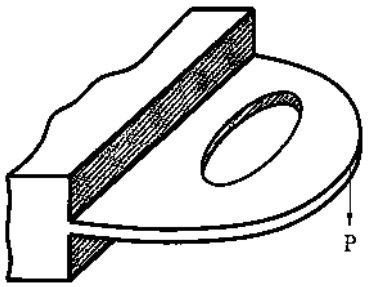

Fig. 6.16

displacement and material relationships. While one may not be able to derive a closed-form solution for the continuum, one can derive an approximate solution for the element assemblage that replaced it.

According to the FEM, a plate is discretized into a finite number of elements (usually, triangular or rectangular in shape), called *finite elements* and connected at their nodes and along interelement boundaries. Unknown functions (deflections, slopes, internal forces, and moments) are assigned in the form of undetermined parameters at those nodes. The equilibrium and compatibility conditions must be satisfied at each node and along the boundaries between finite elements. To determine the above-mentioned unknown functions at nodal points, one of the variational principles, introduced in Sec. 2.6, is applied. As a result, a system of algebraic equations is obtained. Its solution determines the state of stress and strain in a given plate.

There are a number of finite element methods. In this section we discuss only the commonly used finite element displacement approach wherein the governing set of algebraic equations is expressed in terms of unknown nodal displacements.

The FEM can be treated as some modification of the Ritz method. A difference between the classical Ritz approach and the FEM is in the technique of representation of displacements. In the Ritz method, the displacements are assigned in the entire domain occupied by the plate. A governing system of algebraic equations for this approach will have a completed, not banded structure. Since in the FEM the displacements are assigned element by element, the matrix of the system of algebraic equations is obtained as partially completed, and usually it has a banded structure. This is a profound advantage of the FEM compared with other numerical methods introduced in the preceding sections of this chapter.

The FEM has gained considerable attention and prominence after the publication of the classic paper by Turner *et al.* [26] that showed how one can use an assemblage of simple elements as a basis for computerized structural analysis. Courant [27], and later Argyris *et al.* [28] represent the initial attempts to provide the theoretical investigations of this method. Gallagher [29], Hughes [30], Zienkiewicz [31], and other investigators developed the general procedure of the FEM technique for plate and shell stress analysis.

For every finite plate (or shell) element there is a relationship between the generalized displacements at the nodal points and the corresponding forces and moments at the nodes. This relationship may be presented in the form of a matrix called a *stiffness matrix*. In this section, we discuss the stiffness matrices for rectangular and triangular plate elements. Then, we present the general procedure of the FEM for plate bending analysis. The derivations, given below, are based on the classical (Kirchhoff's) plate bending theory introduced in Chapter 2.

6.7.2 The rectangular plate element

Consider a flat rectangular plate which is subdivided into rectangular finite elements with dimensions c and d, as shown in Fig. 6.17. The properties belonging to such a finite element (abbreviated further as FE) is designated e. The geometrical position of a rectangular FE is determined by the four nodal (corner) points i, j, k, and l, and the straight line boundaries. At each node q ($q = i, j, k, l$) we consider the possible

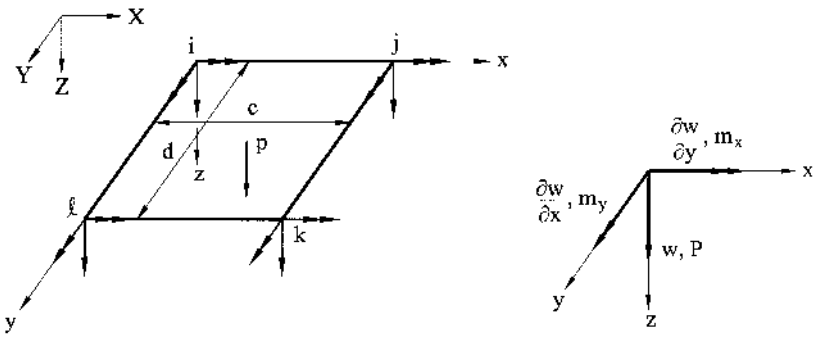

Fig. 6.17

nodal deflection w_q and rotations of the normal to the plate middle surface (slopes) about the x and y axes, i.e., $(\partial w/\partial y)_q$ and $(\partial w/\partial x)_q$, respectively.

The deflection w_q and two rotations $(\partial w/\partial y)_q$ and $(\partial w/\partial x)_q$ are referred to as a set of *nodal displacements*.

We assume that the FE is subjected to surface-distributed load $p(x, y)$ and external concentrated force P_q and moments m_{xq} and m_{yq}, applied at each nodal point q of the FE, as shown in Fig. 6.17. Do not confuse the external nodal moments m_{xq} and m_{yq} with the stress couples M_x and M_y introduced in Chapter 2. The nodal force and two moments are referred to as a set of *nodal forces*. The nodal displacements and nodal forces are assumed to be positive in the directions shown in Fig. 6.17. Two coordinate systems are introduced in Fig. 6.17: the coordinate set X, Y, Z is referred to as a global set for the entire structure while the set x, y, z is called the local set for the FE of interest.

We develop below a stiffness matrix for a given FE. Let us approximate the deflection field over the area of the rectangular FE shown in Fig. 6.17. The strain energy of the plate in bending involves the second derivatives of the deflections (see Eq. (2.60)). Hence, the degree of a polynomial that approximates this deflection field cannot be less than two. On the other hand, in order to characterize the shape of the FE by its nodal displacements with reference to Fig. 6.17, it is necessary to have 12 degrees of freedom (in the three degrees of freedom, w, $\partial w/\partial y$, $\partial w/\partial x$ at each of the four nodal points i, j, k, l of the above element). Consequently, we need to select a polynomial with 12 parameters. The polynomial selected is

$$w(x, y) = \alpha_1 + \alpha_2 x + \alpha_3 y + \alpha_4 x^2 + \alpha_5 y^2 + \alpha_6 xy + \alpha_7 x^2 y + \alpha_8 xy^2 + \alpha_9 x^3 + \alpha_{10} y^3 + \alpha_{11} x^3 y + \alpha_{12} xy^3. \tag{6.46}$$

Obviously, the above polynomial satisfies exactly the governing differential equation (2.24). However, this deflection function will not result in a fully compatible element. In the FEM formulation, it is required that the compatibility conditions (equality of the deflections and slopes) are satisfied at the nodal points. An accuracy of the FEM will be increased if the selected deflection function involves the compatibility of the deflections and slopes along a common boundary line of the adjacent FEs. It can be shown that the polynomial (6.46) provides the compatibility of deflections between

elements and some slopes (normal) are continuous while other slopes (tangential) may not be continuous. In order to correct this problem, one needs to define four degrees of freedom at each node and, correspondingly, employ a deflection function with 16 terms [29,30]. Of course, the above polynomial leads to improved results, but the analysis becomes more involved than described below. At the same time, numerical and theoretical investigations showed that the use of the polynomial (6.46) provides a convergence of the solution by the FEM. So, the polynomial (6.46) is frequently used in engineering practice.

Let us represent the above polynomial approximating the deflection field over the FE designated by e in the matrix form as follows:

$$w_e = [N]\{\alpha\}, \tag{6.47}$$

where

$$[N] = \left[1, x, y, x^2, y^2, xy, x^2y, xy^2, x^3, y^3, x^3y, xy^3\right] \text{ and } \{\alpha\} = [\alpha_1, \alpha_2, \ldots, \alpha_{12}]^T. \tag{6.48}$$

Here and further, the subscript e refers to a finite element designated by this letter. We introduce the braces $\{\ldots\}$ to indicate a matrix of one column, the brackets $[\ldots]$ to represent a matrix (both, a square and row matrices); and the superscript T to represent the transpose of a matrix.

Introduce the element displacement matrix $\{\delta\}_e$ as follows:

$$\{\delta\}_e = \left[\delta_i, \delta_j, \delta_k, \delta_l\right]^T, \tag{6.49}$$

where

$$\left\{\delta_i\right\} = \left[w_i, (\partial w/\partial y)_i, (\partial w/\partial x)_i\right]^T; \quad \left\{\delta_j\right\} = \left[w_j, (\partial w/\partial y)_j, (\partial w/\partial x)_j\right]^T; \text{ etc.}$$

If we express the coefficients $\alpha_m (m = 1, 2, 3, \ldots, 12)$ via the nodal displacements w_q, $(\partial w/\partial y)_q$, and $(\partial w/\partial x)_q$ $(q = i, j, k, l)$ in the local coordinate system x, y, z, then we can write the following relationship:

$$\{\delta\}_e = [C]\{\alpha\}, \tag{6.50}$$

where $[C]$ is 12×12 matrix whose elements depend on the x and y coordinates of the nodal points of the finite element shown in Fig. 6.17.

From the foregoing, the solution for the unknown constants is

$$\{\alpha\} = [C]^{-1}\{\delta\}_e. \tag{6.51}$$

The inverse matrix $[C]^{-1}$ is given below for the rectangular FE of Fig. 6.17 in the explicit form in Table 6.3.

Upon substitution of $\{\alpha\}$ from Eq. (6.51) into Eq. (6.47) one obtains

$$w_e = [L]\{\delta\}_e, \tag{6.52}$$

where

$$[L] = [N][C]^{-1} \tag{6.53}$$

Table 6.3

$$
[C]^{-1} = \begin{bmatrix}
1 & 0 & 0 & 0 & 0 & 0 & 0 & 0 & 0 & 0 & 0 & 0 \\
0 & 1 & 0 & 0 & 0 & 0 & 0 & 0 & 0 & 0 & 0 & 0 \\
0 & 0 & 1 & 0 & 0 & 0 & 0 & 0 & 0 & 0 & 0 & 0 \\
-\frac{3}{a^2} & -\frac{2}{a} & 0 & \frac{3}{a^2} & -\frac{1}{a} & 0 & 0 & 0 & 0 & 0 & 0 & 0 \\
-\frac{3}{b^2} & 0 & -\frac{2}{b} & 0 & 0 & 0 & 0 & 0 & 0 & \frac{3}{b^2} & 0 & -\frac{1}{b} \\
-\frac{1}{ab} & -\frac{1}{b} & -\frac{1}{a} & \frac{1}{ab} & 0 & \frac{1}{a} & -\frac{1}{ab} & 0 & 0 & \frac{1}{ab} & \frac{1}{b} & 0 \\
\frac{3}{a^2b} & \frac{2}{ab} & 0 & -\frac{3}{a^2b} & \frac{1}{ab} & 0 & \frac{3}{a^2b} & -\frac{1}{ab} & 0 & -\frac{3}{a^2b} & -\frac{2}{ab} & 0 \\
\frac{3}{ab^2} & 0 & \frac{2}{ab} & -\frac{3}{ab^2} & 0 & -\frac{2}{ab} & \frac{3}{ab^2} & 0 & -\frac{1}{ab} & -\frac{3}{ab^2} & 0 & \frac{1}{ab} \\
\frac{2}{a^3} & \frac{1}{a^2} & 0 & -\frac{2}{a^3} & \frac{1}{a^2} & 0 & 0 & 0 & 0 & 0 & 0 & 0 \\
\frac{2}{b^3} & 0 & \frac{1}{b^2} & 0 & 0 & 0 & 0 & 0 & 0 & -\frac{2}{b^3} & 0 & \frac{1}{b^2} \\
-\frac{2}{a^3b} & -\frac{1}{a^2b} & 0 & \frac{2}{a^3b} & -\frac{1}{a^2b} & 0 & -\frac{2}{a^3b} & \frac{1}{a^2b} & 0 & \frac{2}{a^3b} & \frac{1}{a^2b} & 0 \\
-\frac{2}{ab^3} & 0 & -\frac{1}{ab^2} & \frac{2}{ab^3} & 0 & \frac{1}{ab^2} & -\frac{2}{ab^3} & 0 & \frac{1}{ab^2} & \frac{2}{ab^3} & 0 & -\frac{1}{ab^2}
\end{bmatrix}
$$

is referred to as a shape function for the FE of interest.

Define the strain–displacement relationship as follows:

$$\{\varepsilon\}_e = z\{\chi\}_e, \tag{6.54}$$

where $\{\varepsilon\}_e = \left[\varepsilon_x, \varepsilon_y, \gamma_{xy}\right]^T$ is the *strain matrix* and $\{\chi\}_e = \left[\chi_x, \chi_y, 2\chi_{xy}\right]^T$ is the *curvature matrix*. Using Eqs (2.7), one can represent the latter matrix in terms of the deflections as follows:

$$\{\chi\}_e = \left[-\frac{\partial w}{\partial x^2}, -\frac{\partial^2 w}{\partial y^2}, -2\frac{\partial^2 w}{\partial x \partial y}\right]^T. \tag{6.55}$$

Substituting for w_e from Eq. (6.52) into Eq. (6.55), one can express the curvature matrix in terms of the polynomial (6.46) as follows:

$$\{\chi\}_e = [B]\{\delta\}_e, \tag{6.56}$$

where $[B] = \left[[B]_i, [B]_j, [B]_k, [B]_l\right]$ and

$$[B]_i = \left[-\frac{\partial^2 [L]_i}{\partial x^2}, -\frac{\partial^2 [L]_i}{\partial y^2}, -2\frac{\partial^2 [L]_i}{\partial x \partial y} \right]^T;$$

$$[B]_j = \left[-\frac{\partial^2 [L]_j}{\partial x^2}, -\frac{\partial^2 [L]_j}{\partial y^2}, -2\frac{\partial^2 [L]_j}{\partial x \partial y} \right]^T; \text{ etc.}$$

Now. let us introduce the stress resultants and stress couples relationships (see Eqs (2.13)) in the matrix form:

$$\{M\}_e = \begin{Bmatrix} M_x \\ M_y \\ M_{xy} \end{Bmatrix} = D \begin{bmatrix} 1 & \nu & 0 \\ \nu & 1 & 0 \\ 0 & 0 & (1-\nu)/2 \end{bmatrix} \begin{Bmatrix} \chi_x \\ \chi_y \\ 2\chi_{xy} \end{Bmatrix}, \tag{6.57a}$$

or symbolically as follows:

$$\{M\}_e = [D]\{\chi\}_e, \tag{6.57b}$$

where $[D]$ is the elasticity matrix. The stress–strain relationship, from Eqs (2.10), can be written in the matrix form as follows:

$$\{\sigma\}_e = z[D^*]\{\chi\}_e, \tag{6.58}$$

where the matrix $[D^*]$ is given by

$$[D^*] = \frac{12}{h^3}[D]. \tag{6.59}$$

To continue the development, it is necessary to define the set of discrete nodal forces corresponding to the prescribed nodal degrees, as shown in Fig. 6.17:

$$\{R\}_e = \left[R_i, R_j, R_k, R_l\right]^T, \tag{6.60a}$$

where

$$\left\{R_q\right\} = \left[P_q, m_{xq}, m_{yq}\right]^T; \quad q = i, j, k, l. \tag{6.60b}$$

We now employ the principle of minimum potential energy, introduced in Sec. 2.6.2, to derive the element stiffness matrix, $[k]_e$ and the element nodal force matrix $\{R\}_e$. Toward this end, we write the strain energy in the element as (see Eq. (2.61))

$$U_e = \frac{1}{2}\int\int_{A_e} [\chi]_e^T \{M\}_e \mathrm{d}A_e. \tag{6.61}$$

Substituting for $[\chi]_e^T$ from Eq. (6.56) and for $\{M\}_e$ from Eq. (6.57b) into the above, we obtain

$$U_e = \frac{1}{2}\int\int_{A_e} \{\delta\}_e^T [B]^T [D][B]\{\delta\}_e \mathrm{d}A_e = \{\delta\}_e^T \left\langle \frac{1}{2}\int\int_{A_e} [B]^T [D][B]\mathrm{d}A_e \right\rangle \{\delta\}_e$$

or

$$U = \frac{1}{2}\{\delta\}_e^T [k]_e \{\delta\}_e, \tag{6.62}$$

where A_e is the rectangular area $c \times d$ of the FE of interest (see Fig. 6.17) and

$$[k]_e = \int\int_{A_e} [B]^T [D][B] \mathrm{d}A_e \tag{6.63}$$

is the (symmetric) *element stiffness matrix*.

The potential of external forces, Ω_e, acting upon the element is

$$\Omega_e = -\{\delta\}_e^T \{R\}_e - \int\int_{A_e} pw \mathrm{d}A_e, \tag{6.64}$$

where the first term on the right-hand side is the potential of the discrete nodal forces and the second term is the potential of the distributed load $p(x, y)$. If we substitute for w from Eq. (6.52) into the above equation, we obtain

$$\Omega_e = -\{\delta\}_e^T \{R\}_e - \int\int_{A_e} p[L]\{\delta\}_e \mathrm{d}A_e.$$

Since the potential of external forces is a scalar quantity, we may take the transpose without changing its value

$$\Omega_e = -\{\delta\}_e^T \left\langle \{R\}_e + \int\int_{A_e} p[L]^T \mathrm{d}A_e \right\rangle. \tag{6.65}$$

It is convenient to write the above equation in the form

$$\Omega_e = -\{\delta\}_e^T \{Q\}_e, \tag{6.66}$$

where

$$\{Q\}_e = \{R\}_e + \iint_{A_e} p[L]^T \mathrm{d}A_e \tag{6.67}$$

is the *element nodal force matrix*.

If $\Pi_e = U_e + \Omega_e$ is the total potential energy associated with the element, we have

$$\Pi_e = \frac{1}{2}\{\delta\}_e^T [k]_e \{\delta\}_e - \{\delta\}_e^T \{Q\}_e. \tag{6.68}$$

If we apply the principle of minimum potential energy to Eq. (6.68), we obtain

$$\frac{\partial \Pi_e}{\partial \{\delta\}_e} = 0 \quad \text{or} \quad \frac{\partial \Pi_e}{\partial \{\delta_q\}} = 0; \quad q = i, j, k, l. \tag{6.69}$$

If we perform the operations prescribed by Eq. (6.69) and rearrange terms, we obtain the following expression that relates nodal displacements and corresponding nodal forces:

$$[k]_e\{\delta\}_e = \{Q\}_e. \tag{6.70}$$

This 12×12 system of linear algebraic equations characterizes the deformation of the rectangular plate element subjected to surface load and nodal forces.

When the elements are assembled, the total potential energy of the entire plate is characterized by the following (see Eq. (6.69):

$$\Pi = \sum_{e=1}^{E} \left\langle \frac{1}{2}\{\delta\}_e^T[k]_e\{\delta\}_e - \{\delta\}_e^T\{Q\}_e \right\rangle, \tag{6.71}$$

where E refers to the total number of finite elements comprising the given plate. This expression contains $12E$ unknowns, which is excessive. Since the value of $\{\delta\}_e$ for two adjacent elements that share a common nodal point must be the same, the displacement vector is reduced and can be represented as

$$\{\Delta\} = [\Delta_1, \Delta_2, \ldots, \Delta_M]^T, \tag{6.72}$$

where $M = 3N$ and N is the total number of nodal points in the mesh. Thus, the expression of Πin terms of the reduced displacement vector takes the form

$$\Pi = \frac{1}{2}\{\Delta\}^T[K]\{\Delta\} - \{\Delta\}^T\{Q\}, \tag{6.73}$$

where $[K]$ is the $M \times M$ *global stiffness matrix* of the entire plate and $\{Q\}$ is the *generalized global force matrix*.

If we apply the principle of minimum potential energy to Eq. (6.73):

$$\frac{\partial \Pi}{\partial\{\Delta_i\}} = 0; i = 1, 2, \ldots, M,$$

we obtain the following *governing equation of the FEM for the entire plate*:

$$[K]\{\Delta\} = \{Q\}. \tag{6.74}$$

The global stiffness matrix $[K]$ and the generalized global force matrix $\{Q\}$ can be assembled from 12×12 element stiffness, $[k]_e$, and the element force, $\{Q\}_e$, matrices. This assembly process is readily computerized once the individual element properties are known.

The matrix $[K]$ in Eq. (6.74) is singular, because in deriving the above equation possible rigid body motions of the entire plate have not been prevented. Applying appropriate kinematic boundary conditions (imposed on the components of the displacement vector $\{\delta\}_e$), we eliminate the rigid body motion. This results in deleting some rows and columns of the matrix $[K]$, corresponding to vanishing displacements, and the nonsingular stiffness matrix $[K^*]$ is obtained. As a result, Eq. (6.74) can be represented in the form

$$[K^*]\{\Delta^*\} = \{Q^*\}. \tag{6.75}$$

This set of algebraic equations is then solved for the unknown displacements. The order of this system will be equal to the total number of unknown displacements of the discretized plate. The matrix $[K^*]$ can always be written in banded, symmetric form.

Once all displacements have been determined, we can utilize Eqs (6.56) and (6.57) to determine the bending and twisting moments. The general procedure for solving plate (or shell) bending problems by FEM is summarized as follows:

1. For every FE, having a number e and certain nodes numbering and displacements, the nodal force $\{Q\}_e$ and the element stiffness $[k]_e$ matrices are determined in the local coordinate system. A transition of the above matrices from the local to global coordinate system is carried out.
2. The governing system of equations (6.74) is set up where the global matrices $[K]$ and $\{Q\}$ are simply generated in elements as follows: $[K] = \sum_e [k]_e$ and $\{Q\} = \sum_e \{Q\}_e$.
3. The prescribed kinematic boundary conditions are inserted in the global stiffness matrix, as indicated earlier, and the set of equations (6.75) is formed for the entire plate.
4. The set of Eqs (6.75) is solved.
5. Output data are calculated. The element deflections, internal forces, and moments, as well as the stress components, are computed at all nodal points.

It should be noted that the procedure described can be efficient only by using powerful digital computers. At present, new powerful computer programs, based on FEM, have been developed for solving various linear and nonlinear plate (and shell) bending problems.

6.7.3 The triangular plate element

The triangular element can easily accommodate irregular boundaries and can be graduated in size to permit small elements in regions of stress concentration. Consequently, this element is widely used in the finite element technique. Let a flat plate be subdivided into a set of triangular finite elements referred to the local coordinate system xyz, where one of the coordinate axes (for instance, the y axis, as shown in Fig. 6.18) is directed along a particular side of the FE.

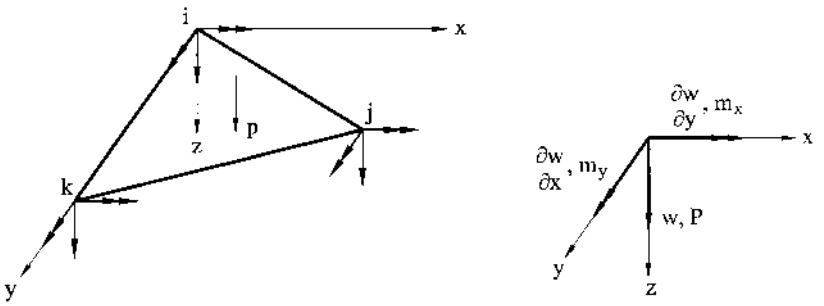

Fig. 6.18

The matrix of the nodal displacements for this FE includes the nodal deflections w_q and slopes $(\partial w/\partial y)_q, (\partial w/\partial x)_q$ where $q = i, j, k$. Thus, the triangular FE posseses nine degrees of freedom.

The problem of selecting a suitable polynomial to describe the displacement field over the triangular FE of interest is somewhat more difficult than for the rectangular element. The simplest expression for the deflection function $w(x, y)$ that satisfies all the general requirements, introduced in Sec. 6.7.2, is a cubic polynomial. However, a complete cubic polynomial contains 10 terms. Thus, one needs to fit this cubic polynomial to the nine-degree FE under consideration. Several different possibilities of the presentations of this polynomial were proposed to overcome this difficulty [29–31]. We consider only one of them. It was recommended to take the above cubic polynomial in the form

$$w(x, y) = \alpha_1 + \alpha_2 x + \alpha_3 y + \alpha_4 x^2 + \alpha_5 xy + \alpha_6 y^2 + \alpha_7 x^3 + \alpha_8 (x^2 y + y^2 x) + \alpha_9 y^3. \tag{6.76}$$

The triangular plate bending element, based on the polynomial (6.47), has several limitations. The continuity of slopes across element lines is not guaranteed. Further, its stiffness matrix may be singular for some orientations of sides of FE with respect to the local coordinate axes [30,31]. Thus, this type of element cannot always provide accurate results when used for the bending analysis of plates. However, because of its simplicity, this polynomial is used in engineering practice.

The nodal displacement matrix $\{\delta\}_e$ is of the form (see Fig. 6.18):

$$\{\delta\}_e = \left[\delta_i, \delta_j, \delta_k\right], \tag{6.77}$$

where

$$\left\{\delta_i\right\} = \left[w_i, (\partial w/\partial y)_i, (\partial w/\partial x)_i\right], \text{ etc.}$$

The matrix representing the deflection field is also given by Eq. (6. 47), but the matrices $[N]$ and $\{\alpha\}$ now have the following form:

$$[N] = \left[1, x, y, x^2, xy, y^2, x^3, x^2 y + y^2 x, y^3\right], \{\alpha\} = [\alpha_1, \alpha_2, \ldots, \alpha_9]^T. \tag{6.78}$$

Nodal displacements, upon introduction of Eq. (6.76) and the first derivatives of w with respect to x and y into Eq. (6.77), are next found. They are given by Eq. (6.50) in which the matrix $[C]$ is the 9×9 matrix that depends upon the nodal coordinates. Inversion of the above matrix provides the values of the unknown coefficients α_1, $\alpha_2, \ldots, \alpha_9$ and is given by Eq. (6.51). The displacement function is expressed by Eq. (6.52).

The nodal force matrix $\{R\}_e$ for the triangular FE represents a three-component vector of the form

$$\{R\}_e = \left[R_i, R_j, R_k\right]^T, \tag{6.79}$$

where $\{R\}_q (q = i, j, k)$ is given by Eq. (6.60b). The stiffness matrix, $[k]_e$, and the external nodal force matrix, $\left\{Q\right\}_e$, for the triangular plate element as well as the governing equation of the FEM for the entire plate can be obtained by employing the general procedure introduced in Sec. 6.7.2 for the rectangular plate element.

Let us discuss briefly some **advantages** of the FEM:

1. The solution by the FEM is obtained without the use of the governing differential equation.
2. The method has a clear and straightforward mechanical meaning and can be formulated in terms of a technique familiar to practicing engineers.
3. The method can be successfully applied to arbitrary boundary and loading conditions that can be handled in the same manner as simpler problems.
4. The complete automation of all procedures of the numerical process for solving boundary value problems by the FEM is permitted.
5. The FEM can be applied to the stress analysis of combined structures consisting of various structural elements such as plates, shells, beams, arches, etc.

Among the **disadvantages** of the FEM, the following can be mentioned:

1. The FEM requires the use of powerful computers of considerable speed and storage capacity.
2. It is difficult to ascertain the accuracy of numerical results when large structural systems are analyzed.
3. The method is poorly adapted to a solution of the so-called singular problems (e.g., plates and shells with cracks, corner points, discontinuity internal actions, etc.), and of problems for unbounded domains.
4. The method presents many difficulties associated with problems of C^1 continuity and nonconforming elements in plate (and shell) bending analysis.

Since the application of fundamental concepts of the FEM has recently extended to various linear and nonlinear boundary value problems, it is efficient to combine the BEM and FEM for the stress analysis of combined plate and shell structures [12,13].

Example 6.8

A square simply supported plate with side a is acted upon by (a) a uniform lateral surface load p_0 and (b) a concentrated force P applied at the plate center. Determine the deflections and the bending and twisting moments by the FEM. Use $\nu = 0.3$

Solution

Calculations are carried out with the use of the rectangular FEs under a varied number of the plate discretization. The deflection, w, the bending moments, M_x, M_y, at the plate center, and the twisting moment, M_{xy} at a corner point of the plate are assigned in the form:

– for a uniformly distributed load p_0, as follows:

$$w = \alpha \cdot 10^{-4} \frac{p_0 a^4}{D}; \quad M_x = M_y = \beta \cdot 10^{-2} p_0; \quad M_{xy} = \gamma \cdot 10^{-2} p_0 \text{ and}$$

– for a concentrated force P, as follows:

$$w = \alpha_1 \cdot 10^{-2} \frac{Pa^2}{D}; \quad M_x = M_y = \beta_1 \cdot 10^{-2} P; \quad M_{xy} = \gamma_1 \cdot 10^{-2} P.$$

Table 6.4

Discretization	Number of nodes	A uniform distributed load			Concentrated force		
		α	β	γ	α_1	β_1	γ_1
2×2	9	34.44	4.427	−3.492	1.378	23.18	−6.505
4×4	25	39.45	4.694	−3.317	1.233	24.72	−6.184
8×8	81	40.40	4.728	−3.296	1.183	25.18	−6.032
16×16	289	40.58	4.781	−3.251	1.167	25.34	−6.085
[7]	—	40.62	4.789	−3.247	1.160	—	—

The results of calculations are given in Table 6.4 (taken from Ref. [32]), where these numerical results for varied numbers of the FEs are compared with those obtained from Ref. [7]. As seen from Table 6.4, a discrepancy of the corresponding numerical data is small even for a sufficiently large mesh of the plate discretization. A reduction of mesh dimensions (an increase in the number of the FEs) provides a monotonic convergence of the obtained results to an exact solution.

This section provides only a brief survey of the FEM and its application to plate bending problems. The literature associated with this method and its application is voluminous. The interested reader is referred to Refs [28–31].

PROBLEMS

6.1 Derive the finite difference expressions for the effective shear forces V_x and V_y. Referring to Fig. 6.5 check the correctness of the result for V_x.

6.2 Determine the finite difference expression corresponding to Eq. (2.25) at a pivotal point k for nonuniform spaced rectangular mesh widths Δx and Δy in the x and y axes directions, respectively.

6.3 Verify Eqs (6.15b).

6.4 Consider a clamped plate shown in Fig. P.6.1. The plate is acted upon by a uniformly distributed load of intensity p_0. Find the deflection w at the nodal points 1 through 5

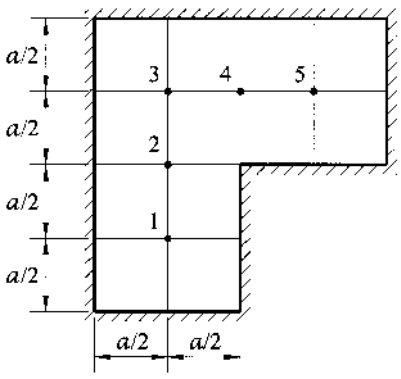

Fig. P6.1

and estimate the location of the point of maximum deflection and determine its magnitude. Use the method of finite differences.

6.5 With reference to Example 6.1 of Sec. 6.2, determine the bending moments M_x and M_y at nodal points of the mesh of the plate shown in Fig. 6.7 by utilizing the deflection field found at the nodal point in the above example.

6.6 Consider a square clamped plate with side a. The plate is subjected to a uniformly distributed load of intensity p_0. Analyze a convergence of numerical FDM solutions for the deflections w and the bending moments M_x and M_y at the plate center for varied plate mesh widths Δ. Take Δ equal to $a/2, a/4$, and $a/8$.

6.7 Derive Eq. (6.22) from the conditions of minimum of the error e_i, given by Eq. (6.21).

6.8 Consider a simply supported square plate ($0 \le x,\ y \le a$) subjected to a uniformly distributed load p_0. Using the approximate representation of the deflection in the form of (a) in Example 6.2, write out the straightforward BCM governing collocation equations (6.19) for the collocation points on the plate boundary. Take the three points for each side of the plate boundary.

6.9 With reference to Fig. 6.10 write the expression for the singular solution $G_m(x, y; \xi, \eta)$ in the explicit form.

6.10 Write the boundary integral equations of the direct BEM formulation for a simply supported rectangular plate ($0 \le x \le a;\ 0 \le y \le b$) subjected to a lateral surface load $p(x, y)$. Use the expressions (6.31) and (6.33).

6.11 Consider a square clamped plate with side a subjected to a uniformly distributed load p_0. Applying the indirect BEM approach, write the boundary integral equations in the explicit form. Use the expressions (6.25) and (6.27).

6.12 With reference to Example 6.5 of Sec. 6.5, find the maximum value of the bending moment M_x by retaining two and three terms in the expression (b) for the deflection surface. Compare the obtained value of $M_{\max}$ with the exact solution given in that example. Use the Galerkin method.

6.13 With reference to Fig. 6.13, solve the problem of Example 6.5 by taking the deflection surface of the plate in the following form

$$w = A \cos^2 \frac{\pi x}{2a} \cos^2 \frac{\pi y}{2b}$$

that satisfies all the boundary conditions of the plate. Applying the Galerkin method, find the maximum deflection and bending moments at the plate center and at a midpoint of the clamped edge.

6.14 Consider a rectangular plate under a uniformly distributed surface load p_0. The plate has edges $y = \pm b$ simply supported and the edges $x = \pm a$ clamped. Using the Galerkin method, determine the deflection and bending moments at the plate center and the bending moment M_x at the midpoint of the clamped edge $x = a$. Let $a = 1\,\text{m}$, $b = 1.5\,\text{m}$, $h = 12\,\text{mm}$, $p_0 = 25\,\text{MPa}$, $E = 200\,\text{GPa}$, and $\nu = 0.3$. Assume a solution of the following form:

$$w = \frac{1}{2} C \left(1 - \cos \frac{2\pi x}{a}\right) \cos \frac{\pi y}{2b}.$$

Check that the above solution satisfies all the prescribed boundary conditions of the plate.

6.15 A rectangular plate with sides a and b ($0 \le x \le a, 0 \le y \le b$) is subjected to a uniformly distributed load of intensity p_0. The plate edges $y = 0, b$ are simply supported, the edge $x = 0$ is clamped, while the edge $x = a$ is free. Determine the deflection w and stresses σ_x and σ_y at the plate center. Use the Ritz method and solution approximated by

$$w = C \left(\frac{x}{a}\right)^2 \sin \frac{\pi y}{b}.$$

Check that the above solution satisfies the kinematic boundary conditions on the plate boundary. Take $a = b = 1.5\,\text{m}$, $h = 15\,\text{mm}$, $E = 210\,\text{GPa}$, $p_0 = 30\,\text{MPa}$, and $\nu = 0.3$.

6.16 Determine the required thickness h of a rectangular plate platform of sides $2a$ and $2b$ ($-a \le x \le a$, $-b \le y \le b$). The plate is supported by columns at its corners and the plate edges are free. The plate is acted upon by a uniform lateral surface load p_0. Let $a = b = 2.0\,\text{m}$, $p_0 = 32\,\text{MPa}$, $E = 210\,\text{GPa}$, $\sigma_{YP} = 250\,\text{MPa}$, and $\nu = 0.3$; the factor of safety is 2. Assuming that the columns can be considered as point supports at the plate corners, take a solution in the form

$$w = C\left(\cos\frac{\pi x}{2a} + \cos\frac{\pi y}{2b}\right).$$

Use the Ritz method and Tresca criterion.

6.17 A uniformly loaded rectangular plate of sides a and b ($0 \le x \le a$, $0 \le y \le b$) has the following boundary conditions: the edge $x = 0$ is fixed, the edge $y = 0$ is simply supported, and the edges $y = b$ and $x = a$ are free. Determine the deflections at the midpoints of the free edges of the plate if a deflection surface of the plate is approximated by the following expression:

$$w = C\left(\frac{x}{a}\right)^2 \sin\frac{\pi y}{2b}.$$

Check that the above expression satisfies the kinematic boundary conditions prescribed on the plate edges. Use the Ritz method and take $\nu = 0.3$.

6.18 Derive the expression of the nodal force matrix $\{Q\}_e$ for the squarer finite element of side c, as shown in Fig. 6.17, subjected to a uniform distributed load p_0 only.

6.19 Redo Problem 6.18 for the triangular finite element representing a right isosceles triangle with legs a and b ($b = 2a$). The origin of the Cartesian coordinate system is taken at the centroid of the triangle.

6.20 A square plate of side a ($0 \le x \le a$, $0 \le y \le b$) with two opposite sides $x = 0$ and $x = a$ simply supported and the remaining edges clamped is subjected to a uniformly distributed load p_0. If the plate is discretized into four identical rectangular finite elements, compute the maximum deflection. Take $a = 4\,\text{m}$, $h = 30\,\text{mm}$, $p_0 = 50\,\text{MPa}$, $E = 210$ GPa, and $\nu = 0.3$. Analyze only one quarter-plate by the FEM.

REFERENCES

1. Alexandrov, A.V., and Potapov, V.D. *The Fundamentals of the Theory of Elasticity and Plasticity*, Izd-vo Vyshaia Shkola, Moscow, 1990 (in Russian).
2. Salvadori, M.G. and Baron, M.L., *Numerical Methods in Engineering*, Prentice-Hall, Englewood Cliffs, New Jersey, 1967.
3. Wang, P.Ch., *Numerical and Matrix Methods in Structural Mechanics*, John Wiley and Sons, New York, 1969.
4. Finlayson, B.A., *The Method of Weighted Residuals and Variational Principles*, Academic Press, New York, 1972.
5. Hutchinson, J.R., Analysis of plates and shells by boundary collocations. In: *Boundary Element Analysis of Plates and Shells* (ed. D.E. Beskos), Springer-Verlag, Berlin, pp. 341–368 (1991).
6. Mikhlin, S.G., *Variational Methods in Mathematical Physics*, Macmillan, New York, 1964.
7. Timoshenko, S.P, and Woinowsky-Krieger. S., *Theory of Plates and Shells*, McGraw-Hill, New York, 1959.
8. Kolodziej, J.A., Review of application of boundary collocation method in mechanics of continuum media, *Solid Mechanics Archives*, 12, pp. 187–231 (1987).

9. Johnson, D., Plate bending by a boundary point method, *Computers & Structures*, vol. 26, No. 4, pp. 673–680 (1987).
10. Tottenham, H., The boundary element method for plates and shells. In: *Developments in Boundary Element Methods – 1* (eds PK Banerjee and R Butterfield), Applied Science Publishers, London, pp. 173–207 (1979).
11. Hartmann, F., Static analysis of plates. In: *Boundary Element Analysis of Plates and Shells* (ed. D.E. Beskos), Springer-Verlag, Berlin, pp. 1–35 (1991).
12. Brebbia, C.A., Telles, J.C.F. and Wrobel, L.C., *Boundary Element Techniques. Theory and Application in Engineering*, Springer-Verlag, Berlin, 1984.
13. Banerjee, P.K. and Butterfield, R., *Boundary Element Methods in Engineering Science*, McGraw-Hill, New York, 1981.
14. Ventsel, E.S., An indirect boundary element method for plate bending analysis, *Int J Numer Meth Eng*, 9, pp. 1597–1611 (1997).
15. Krishnasamy, G., Schmerr, L.W., Rudolphi, T.J., and Rizzo, F.L., Hypersingular boundary integral equations: some applications in acoustic and elastic wave scattering, *J Appl Mech*, 57, pp. 404–414 (1990).
16. Rudolphi, T.J., Krishnasamy, G., Schmerr, L.W., and Rizzo, F.J., On the use of strongly singular integral equations for crack problems. In: *Boundary Elements X* (ed. C.A. Brebbia), Springer-Verlag, Berlin, pp. 249–263 (1988).
17. Hadamard, J.S., *Lectures on Cauch's Problem in Linear Partial Differential Equations*, Yale University Press, London, 1923.
18. Kutt, R., Quadrature formulas for finite-part integrals, *Report WISK, The National Research Institute for Mathematical Science*, 178, Pretoria, 1975.
19. Ioakimidis, N.I. and Pitta, M.S. Remarks on the Gaussian quadrature rule for finite-part integrals with a second-order singularity, *Comput Meth Appl Mech Eng*, 69, pp. 325–343 (1988).
20. Fung, Y.C., *Foundations of Solid Mechanics*, Prentice-Hall, Englewood Cliffs, 1965.
21. Stroud, A.H. and Secrest, D., *Gaussian Quadrature Formulas*, Prentice-Hall, Englewood Cliffs, New Jersey, 1966.
22. Galerkin, B.G., Series-solutions of some cases of equilibrium of elastic beams and plates, *Vestn Inshenernov*, vol. 1, pp. 897–903 (1915) (in Russian).
23. Ritz, W., Theorie der transversalschwingungen einer quadratischen plattemit freien randern, *Ann Phys*, vol. 28, pp. 737–786 (1909).
24. Washizu, K., *Variational Methods in Elasticity and Plasticity*, Pergamon Press, Oxford, 1968.
25. Szilard, R., *Theory and Analysis of Plates. Classical and Numerical Methods*, Prentice-Hall, Englewood Cliffs, New Jersey, 1974.
26. Turner, M.J., Clough, R.W., Martin, H.C., and Topp, L.J. Stiffness and deflection analysis of complex stuctures, *J Aeronaut Sci*, vol. 23, no.9, pp. 805–823 (1956).
27. Courant, R. Variational methods for the solution of problems of equilibrium and vibration, *Bulletin of the American Mathematical Society*, vol. 49, pp. 1–23 (1943).
28. Argyris, J.N., Kelsey, S., and Kamel, H., Matrix methods of structural analysis. In: *Matrix Methods of Structural analysis* (ed. Fraeijs de Veubeke), Pergamon Press, Oxford, 1964.
29. Gallagher, R.H., *Finite Element Analysis*, Prentice-Hill, Englewood Cliffs, New Jersey, 1975.
30. Hughes, T.J.R., *The Finite Element Method*, Prentice-Hill, Englewood Cliffs, New Jersey, 1987.
31. Zienkiewicz, O., *The Finite Element Method*, McGraw-Hill, London, 1977.
32. Grigorenko, Ia.M. and Mukoed, A.P. *Solutions of the Shell Theory Problems by Computers*. Gos. Izd-vo "Vysha Shkola", Kiev, 1974 (in Russian).

7

Advanced Topics

7.1 THERMAL STRESSES IN PLATES

7.1.1 Basic concepts

It was assumed in the foregoing discussions that the temperature of an elastic plate remains constant and has the same value at all points of the plate; hence, temperature effects were not taken into consideration. If the temperature of the plate is raised or lowered it expands or contracts, respectively. Within a certain temperature change, such expansion or contraction, for most structural materials, is directly proportional to the change in temperature. When a free plate made of homogeneous isotropic material is heated uniformly, there appear normal strains but no thermal stresses. The thermal stresses will occur in the following cases: first, if the plate experiences a nonuniform temperature field; secondly, if the displacements are prevented from occurring freely because of the restrictions placed on the boundary even with a uniform temperature; and thirdly, if the material displays anisotropy even with uniform heating – for example, if a heated plate consists of several layers of different materials (e.g., bimetallic plates).

A study of the deformations of an elastic solid in the presence of a temperature field is called *thermoelasticity*. Let us assume that the temperature of an infinitesimal plate element is increased from T_0 to T. The initial temperature, T_0, is defined as a reference state of uniform temperature distribution which does not produce stress or strain in the plate. The thermal field, $T = T(x, y, z)$, is assumed to be known from a solution of the heat conduction problem. The thermal strains are expressed for a two-dimensional body as follows [1,2]:

$$\varepsilon_{xT}^{z} = \alpha T, \varepsilon_{yT}^{z} = \alpha T, \gamma_{xyT}^{z} = 0, \tag{7.1}$$

where α is the coefficient of thermal expansion. Over a moderate temperature change, α remains reasonably constant and represents an experimentally determined material property. In Eqs (7.1), ε_{xT}^z, ε_{yT}^z, and γ_{xyT}^z are the normal and shear thermal strain components, respectively, at a distance z from the plate middle surface. From Eqs (7.1) it follows that the temperature field has no effect on the shear strain components.

Also, from Eqs (7.1), taking the temperature effects into account, we must modify the general plate bending equations. For the sake of simplicity, we assume that the material properties of the plate are not affected by temperature changes: i.e., the modulus of elasticity, E, and Poisson's ratio, ν, are assumed to be constant. In general, a temperature increase or decrease produces changes in a plate's curvature and in the dimensions of the plate's middle surface.

7.1.2 Thermoelastic plate equations

We begin by modifying Hooke's law relations for Kirchhoff's plate theory. These relations are obtained by adding to strains resulting from external forces, the strains due to the thermal effects. The latter are given by Eqs (7.1). We have the following:

$$\varepsilon_x^z = \frac{1}{E}\left(\sigma_x^z - \nu\sigma_y^z\right) + \alpha T, \quad \varepsilon_y^z = \frac{1}{E}\left(\sigma_y^z - \nu\sigma_x^z\right) + \alpha T, \gamma_{xy}^z = \frac{1}{G}\tau_{xy}^z. \tag{7.2}$$

Solving these equations for the stress components, yields

$$\begin{aligned} \sigma_x^z &= \frac{E}{1-\nu^2}\left[\varepsilon_x^z + \nu\varepsilon_y^z - (1+\nu)\alpha T\right]; \\ \sigma_y^z &= \frac{E}{1-\nu^2}\left[\varepsilon_y^z + \nu\varepsilon_x^z - (1+\nu)\alpha T\right]; \tau_{xy}^z = G\gamma_{xy.}^z \end{aligned} \tag{7.3}$$

The assumptions of Kirchhoff's plate bending theory, introduced in Sec. 1.3, can be applied to the thermoelastic analysis of plates, with the exception of assumption 6. As mentioned earlier, a change in the temperature of a plate may result in a change in the dimensions of the middle surface, i.e., points of the middle surface can displace not only in the z but also in the x and y directions. Let u and v, as before, be the displacement components along the x and y axes on the middle surface, respectively. Thus, the total strain components for thermoelastic plates can be obtained by superimposing the strains due to stretching or contracting of the middle surface (Eqs 1.5a) and the strains associated with bending of the middle surface (Eqs 2.6), derived in Sec. 2.2. As result, the following expressions for the strains in terms of displacement components in the middle surface can be written:

$$\varepsilon_x^z = \frac{\partial u}{\partial x} - z\frac{\partial^2 w}{\partial x^2}; \quad \varepsilon_y^z = \frac{\partial v}{\partial y} - z\frac{\partial^2 w}{\partial y^2}; \quad \gamma_{xy}^z = \left(\frac{\partial u}{\partial y} + \frac{\partial v}{\partial x}\right) - 2z\frac{\partial^2 w}{\partial x \partial y}. \tag{7.4}$$

In the foregoing, the first terms on the right-hand sides of the above equations represent the strain components in the middle surface due to its stretching, and terms with w represent the strain components due to bending.

Owing to the deformation of the plate middle surface, the stresses distributed over the thickness of the plate result in the in-plane forces, N_x, N_y, N_{xy} and moments, M_x, M_y, M_{xy}, per unit length, as shown in Figs 3.19 and 2.4. The in-plane force components are represented by

$$\begin{Bmatrix} N_x \\ N_y \\ N_{xy} \end{Bmatrix} = \int_{-h/2}^{h/2} \begin{Bmatrix} \sigma_x^z \\ \sigma_y^z \\ \tau_{xy}^z \end{Bmatrix} \mathrm{d}z, \tag{7.5}$$

and the moments are given by Eqs (2.11). Introducing Eqs (7.3) and (7.4) into Eqs (2.11) and (7.5), the stress resultants are obtained in the form

$$N_x = \frac{Eh}{1-\nu^2}\left(\frac{\partial u}{\partial x} + \nu\frac{\partial v}{\partial y}\right) - \frac{N_T}{1-\nu}; \quad N_y = \frac{Eh}{1-\nu^2}\left(\frac{\partial v}{\partial y} + \nu\frac{\partial u}{\partial x}\right) - \frac{N_T}{1-\nu};$$

$$N_{xy} = N_{yx} = \frac{E}{2(1+\nu)}\left(\frac{\partial u}{\partial y} + \frac{\partial v}{\partial x}\right); \tag{7.6}$$

$$M_x = -D\left(\frac{\partial^2 w}{\partial x^2} + \nu\frac{\partial^2 w}{\partial y^2}\right) - \frac{M_T}{1-\nu}; \quad M_y = -D\left(\frac{\partial^2 w}{\partial y^2} + \nu\frac{\partial^2 w}{\partial x^2}\right) - \frac{M_T}{1-\nu};$$

$$M_{xy} = M_{yx} = -D(1-\nu)\frac{\partial^2 w}{\partial x \partial y}. \tag{7.7}$$

Here the quantities

$$N_T = \alpha E \int_{-h/2}^{h/2} T(x, y, z)\mathrm{d}z \text{ and } M_T = \alpha E \int_{-h/2}^{h/2} T(x, y, z) z \mathrm{d}z \tag{7.8}$$

are termed the *thermal stress resultants*, i.e., the *thermal equivalent normal force and bending moment*, respectively.

The components of the stress tensor may now be derived in terms of the stress resultants by substitution of Eqs (7.4) into (7.3) and elimination of the displacement derivatives through the use of Eqs (7.7) and (7.8), as follows:

$$\sigma_x^z = \frac{1}{h}\left(N_x + \frac{N_T}{1-\nu}\right) + \frac{12z}{h^3}\left(M_x + \frac{M_T}{1-\nu}\right) - \frac{\alpha E T}{1-\nu};$$

$$\sigma_y^z = \frac{1}{h}\left(N_y + \frac{N_T}{1-\nu}\right) + \frac{12z}{h^3}\left(M_y + \frac{M_T}{1-\nu}\right) - \frac{\alpha E T}{1-\nu}; \tag{7.9}$$

$$\tau_{xy}^z = \frac{1}{h}N_{xy} + \frac{12z}{h^3}M_{xy}.$$

Substitution of Eqs (7.7) and the second equation of (7.8) into the plate equilibrium equation (2.25) gives the following:

$$\nabla^2\nabla^2 w = \frac{1}{D}\left(p - \frac{1}{1-\nu}\nabla^2 M_T\right). \tag{7.10}$$

This is the *governing differential equation for the bending of thin elastic Kirchhoff's plates due to the lateral pressure and thermal effects*. We observe from Eq. (7.10) that it is possible to superimpose the temperature-induced deflections with those induced only by the transverse load.

From the above, it follows that in addition to the thermal bending stresses resulting from the temperature variation across the thickness of the plate, membrane stresses are also produced, if the plate is heated uniformly throughout its thickness

and prescribed boundary conditions prevent free expansion or contraction of the middle surface of the plate. The equations governing the in-plane (membrane) resultants are given by Eqs (3.90). These equations are identically satisfied by introducing the stress function $\Phi(x, y)$, related to the force resultants, as follows:

$$N_x = \frac{\partial^2 \Phi}{\partial y^2}, \quad N_y = \frac{\partial^2 \Phi}{\partial x^2}, \quad N_{xy} = -\frac{\partial^2 \Phi}{\partial x \partial y}. \tag{7.11}$$

For a plate of a constant thickness and negligible weight, the equation of compatibility can be obtained by inserting Eqs (7.2) and (7.9) into Eq. (1.13) and making $M_x = M_y = M_{xy} = M_T = 0$. We obtain

$$\frac{\partial^2}{\partial y^2}\left(N_x - \nu N_y + N_T\right) + \frac{\partial^2}{\partial x^2}\left(N_y - \nu N_x + N_T\right) = 2(1+\nu)\frac{\partial^2 N_{xy}}{\partial x \partial y}. \tag{7.12}$$

Substitution of relations (7.11) into the above yields

$$\nabla^2 \nabla^2 \Phi = -\nabla^2 N_T \tag{7.13}$$

where N_T is given by Eq. (7.8). Equation (7.13) is the *governing differential equation for the two-dimensional thermoelastic problem of plane stress for thin plates*. Since we have assumed the validity of Kirchhoff's small-deflection theory, the governing equations of thermal bending, Equation (7.10), and thermal stretching or contracting, Eq. (7.13), are independent of each other. Equation (7.10) may be solved by the methods discussed in Chapters 3 and 6, while the methods discussed in the theory of elasticity for plane stress problems are available for solving Eq. (7.13) [1,2]. We discuss below some peculiarities associated with the solution of the thermoelastic plate bending problems. We modify the boundary conditions for thermoelastic plates. Let us consider the boundary conditions for rectangular plates again, as follows:

(a) *Simply supported edges* $x = 0$ and $x = a$

$$w = 0, \quad M_x = 0$$

From Eq. (7.7), the condition for the bending moment can be rewritten as

$$M_x = -D\left(\frac{\partial^2 w}{\partial x^2} + \nu \frac{\partial^2 w}{\partial y^2}\right) - \frac{M_T}{1-\nu} = 0\Bigg|_{x=0, x=a}. \tag{7.14}$$

Taking into account that for edges $x = 0, a$ the curvature $\partial^2 w/\partial y^2 = 0$, the above conditions can be simplified to the form

$$w = 0|_{x=0,a} \text{ and } D\frac{\partial^2 w}{\partial x^2} + \frac{M_T}{1-\nu} = 0\Bigg|_{x=0,a}. \tag{7.15}$$

(b) *Clamped edges* $x = 0$ and $x = a$

$$w = 0|_{x=0,a} \text{ and } \frac{\partial w}{\partial x} = 0|_{x=0,x=a}. \tag{7.16}$$

(c) *Free edges* $x = 0$ *and* $x = a$
The boundary conditions in this case are (see Chapter 2)

$$M_x = 0 \text{ and } V_x = 0. \tag{7.17}$$

The first condition (for the bending moment) is given by Eq. (7.14). The effective shear force is found to be (see Sec. 2.4) $V_x = Q_x + \partial M_{xy}/\partial y$. Using Eqs (2.22a) and (7.7), we can express V_x in the above equation in terms of the deflections w. Finally, the second equation (7.17) will take the following form:

$$\frac{\partial^3 w}{\partial x^3} + (2-\nu)\frac{\partial^3 w}{\partial x \partial y^2} + \frac{1}{D(1-\nu)}\frac{\partial M_T}{\partial x} = 0\Bigg|_{x=0,a}. \tag{7.18}$$

Similarly, the boundary conditions can be represented for edges $y = 0$ and $y = b$. We observe from Eqs (7.15)–(7.18) that the boundary conditions for simply supported and free edges of thermoelasic plates are nonhomogeneous.

Small-deflection thermal bending problems of plates can be readily solved by the so-called *isothermal analogy* [1,2]. Let us introduce a fictitious lateral load as follows:

$$p_T = -\frac{1}{1-\nu}\nabla^2 M_{\mathrm{T}}. \tag{7.19}$$

Then, the thermoelastic plate bending problems can be reduced to the corresponding isothermal problems for a plate subjected to two types of surface lateral loads: an actual surface lateral load of intensity $p(x, y)$ and a fictitious load of intensity $p_T(x, y)$. It should be noted that the isothermal analogy might also require a modification of the boundary conditions. This means that in the mathematical formulation of the static boundary conditions, the thermal equivalent moment M_T must be included in accordance with Eqs (7.15) and (7.18) for bending problems.

Example 7.1

Consider a simply supported rectangular plate (see Fig. 3.5) that is subjected to a nonuniform temperature distribution. Determine the deflection surface of the plate.

Solution

The boundary conditions on the edges $x = 0, a$ of the plate are given by Eqs (7.15). Similar expressions can be written for edges $y = 0, b$ by replacing the variable x with y in the second equation (7.15). In general, M_T is a function of x, y, and T. From Eqs (7.15) and (7.7), the following expression applies to the boundary

$$D\nabla^2 w = -M_T \frac{1}{1-\nu}\Bigg|_{\substack{x=0,a \\ y=0,b}}. \tag{a}$$

Equation (7.10), setting $p = 0$, can be represented in an equivalent form, as follows:

$$\begin{aligned} D\nabla^2 w + M_T \frac{1}{1-\nu} &= f(x, y); \\ \nabla^2 f &= 0. \end{aligned} \tag{b}$$

Equation (a) and the first equation (b) results in

$$f = 0, \tag{c}$$

which is an appropriate solution of the second Eq. (b).

Thus, the given thermoelastic problem can be reduced to the solution of the following equation:

$$D\nabla^2 w = -M_T \frac{1}{1-\nu}, \tag{7.20}$$

with the following boundary condition on all edges:

$$w = 0|_{\substack{x=0,a \\ y=0,b}}. \tag{d}$$

We apply Navier's method for solving the boundary value problem described by Eq. (7.20) and Eq. (d). The solution of Eq. (7.20) is sought in the following form of a double Fourier series:

$$w(x, y) = \sum_{m=1}^{\infty} \sum_{n=1}^{\infty} w_{mn} \sin \frac{m\pi x}{a} \sin \frac{n\pi y}{b}. \tag{e}$$

Each term of this series satisfies the boundary conditions (d). The right-hand side of Eq. (7.20) is expressed in a similar form, i.e.,

$$M_T(x, y) = \sum_{m=1}^{\infty} \sum_{n=1}^{\infty} \mu_{mn}^{(T)} \sin \frac{m\pi x}{a} \sin \frac{n\pi y}{b}, \tag{f}$$

where the Fourier coefficients $\mu_{mn}^{(T)}$ are the following:

$$\mu_{mn}^{(T)} = \frac{4}{ab} \int_0^a \int_0^b M_T(x, y) \sin \frac{m\pi x}{a} \sin \frac{n\pi y}{b} \mathrm{d}x\mathrm{d}y. \tag{g}$$

Substituting these two series into Eq. (7.20), and equating coefficients of like terms, we obtain

$$w_{mn} = \frac{\mu_{mn}^{(T)}}{(1-\nu)\pi^2 D} \left[\frac{1}{(m/a)^2 + (n/b)^2} \right]. \tag{h}$$

If, for example, the temperature varies through thickness only, i.e., $T = T(z)$, then

$$\mu_{mn}^{(T)} = \frac{4M_T}{\pi^2 mn} [1 - (-1)^m][1 - (-1)^n], \tag{i}$$

and the deflection surface becomes

$$w(x, y) = \frac{16M_T}{(1-\nu)\pi^2 D} \sum_{m=1,3,\ldots}^{\infty} \sum_{n=1,3,\ldots}^{\infty} \frac{\sin \frac{m\pi x}{a} \sin \frac{n\pi y}{b}}{mn\left[(m/a)^2 + (n/b)^2\right]}. \tag{7.21}$$

The bending moments and stresses in the plate may be calculated from Eqs (7.7) and (7.9).

The thermoelastic problem above has been considered in Cartesian coordinates for rectangular plates. However, all previously introduced thermoelastic analysis can be applied to circular plates in polar coordinates. This section covers only some general ideas and fundamental concepts of the thermoelastic stress analysis of plates in the context of Kirchhoff's bending theory. The interested reader is referred to Refs [1,2].

7.2 ORTHOTROPIC AND STIFFENED PLATES

7.2.1 General

Up to this point, all our previous discussions of plates have assumed the plate material to be isotropic according to assumption 1 in Sec. 1.3. We recall that the assumption of isotropy implies that material properties at a point are the same in all directions. This means, that if an isotropic material is subjected to an axial stress in a principal direction, the major deformation occurs in the direction of the applied load. Lateral deformations of smaller magnitude occur in the other principal directions. Also, shear stress causes only shear deformation. So, normal strains and stresses are not coupled to shear strains and stresses. The deformations are dependent on the two independent elastic constants – for instance, E and ν. Many construction materials such as steel, aluminum, etc., fall into this category.

However, certain materials display direction-dependent properties; consequently, these materials are referred to as *anisotropic*. In anisotropic materials stressed in one of the principal directions, the lateral deformations in the other principal directions could be smaller or larger than the deformation in the direction of the applied stress depending on the material properties. For a general anisotropic material, the matrix of material constants, because of symmetry, contains 21 independent material constants. This means that all the strains are coupled to all the stresses. Some materials such as wood, plywood, delta wood, and fiber-reinforced plastics, etc., fall into this category. These materials possess *natural anisotropy*. Besides plates made of anisotropic materials, a number of manufactured plates made of isotropic materials also may fall into the category of anisotropic plates: examples include corrugated and stiffened plates, etc. Such a type of anisotropy is referred to as *structural anisotropy* and that of an anisotropic plate can approximately replace their structural behavior. Such an approximation is possible if, for example, stiffeners are arranged sufficiently close to each other so that the given stiffened plate can be replaced by an orthotropic homogeneous plate with "distributed" stiffened rigidities along the plate. Experimental data indicate a good agreement with this idealization provided that the flexural rigidities are uniformly distributed in the x and y directions.

If an anisotropic material has three mutually perpendicular planes of symmetry with respect to its elastic properties, it is called *orthotropic* (i.e., orthogonally anisotropic). Practical applications of orthotropic plates in civil, marine, and aerospace engineering are numerous and include decks of contemporary steel bridges, composite-beam gridworks, plates and reinforced with closely spaced flexible ribs, and reinforced concrete plates.

The fundamental equations for the small-deflection theory of bending of thin orthotropic plates are presented in this section.

7.2.2 Basic relationships

Let us consider bending of plates of constant thickness and made of orthotropic material. Assume that the principal directions of orthotropy coincide with the x and y coordinate axes which, in turn, lie in the middle plane of the plate. The stress–strain relations (2.9) used for isotropic plates are not valid for orthotropic plates. Thus, we

must obtain a new set of stress–strain relations that reflects the orthotropic properties of a material of the plate. Such a set of relations is shown below [3]:

$$\varepsilon_x = \frac{\sigma_x}{E_x} - \nu_y \frac{\sigma_y}{E_y}; \quad \varepsilon_y = \frac{\sigma_y}{E_y} - \nu_x \frac{\sigma_x}{E_x}; \quad \gamma_{xy} = \frac{\tau_{xy}}{G}, \tag{7.22}$$

where E_x, E_y, ν_x, ν_y, and G are assumed to be elastic constants of an orthotropic material, i.e., E_x, E_y, and ν_x, ν_y are the moduli of elasticity and Poisson's ratios in the x and y directions, respectively. They are independent of one another. G is the shear modulus, which is the same for both isotropic and orthotropic materials. It can be expressed in terms of E_x and E_y as follows:

$$G \approx \frac{\sqrt{E_x E_y}}{2\left(1 + \sqrt{\nu_x \nu_y}\right)}. \tag{7.23}$$

The following relationship exists between independent elastic constants introduced above:

$$\frac{\nu_x}{E_x} = \frac{\nu_y}{E_y}. \tag{7.24}$$

This equality directly results from Betti's reciprocal theorem. Solving Eqs (7.22) for the stress components and taking into account (7.24), we obtain

$$\begin{aligned} &\sigma_x = \frac{E_x}{1 - \nu_x \nu_y}\left(\varepsilon_x + \nu_y \varepsilon_y\right); \quad \sigma_y = \frac{E_y}{1 - \nu_x \nu_y}\left(\varepsilon_y + \nu_x \varepsilon_x\right); \\ &\tau_{xy} = G\gamma_{xy}. \end{aligned} \tag{7.25}$$

The derivation of the governing differential equation of bending of an orthotropic plate is based on the general hypotheses introduced in Sec. 1.3. The strain-deflection relations (2.6) hold for orthotropic plates also. So, substituting the relations (2.6) into Eqs (7.25) gives the following:

$$\begin{aligned} &\sigma_x = -\frac{E_x}{1 - \nu_x \nu_y}\left(\frac{\partial^2 w}{\partial x^2} + \nu_y \frac{\partial^2 w}{\partial y^2}\right) z; \quad \sigma_y = -\frac{E_y}{1 - \nu_x \nu_y}\left(\frac{\partial^2 w}{\partial y^2} + \nu_x \frac{\partial^2 w}{\partial x^2}\right) z; \\ &\tau_{xy} = -2Gz \frac{\partial^2 w}{\partial x \partial y}. \end{aligned} \tag{7.26}$$

Substituting the above into Eqs (2.11) and integrating over the plate thickness, yields the following bending and twisting moments deflection relations for orthotropic plates:

$$\begin{aligned} &M_x = -\left[D_x \frac{\partial^2 w}{\partial x^2} + D_{xy} \frac{\partial^2 w}{\partial y^2}\right]; \quad M_y = -\left[D_y \frac{\partial^2 w}{\partial y^2} + D_{yx} \frac{\partial^2 w}{\partial x^2}\right]; \\ &M_{xy} = -2D_s \frac{\partial^2 w}{\partial x \partial y}, \end{aligned} \tag{7.27}$$

where D_x, D_y, D_{xy}, D_{yx}, and D_s are the flexural and torsional rigidities of an orthotropic plate, respectively, and are given as

$$D_x = \frac{E_x}{1-\nu_x\nu_y}\frac{h^3}{12}; \quad D_y = \frac{E_y}{1-\nu_x\nu_y}\frac{h^3}{12}; \quad D_{xy} = \frac{E_x\nu_y}{1-\nu_x\nu_y}\frac{h^3}{12};$$
$$D_{yx} = \frac{E_y\nu_x}{1-\nu_x\nu_y}\frac{h^3}{12}; \quad D_s = \frac{Gh^3}{12}. \tag{7.28}$$

In view of the expressions (7.24), one can conclude that $D_{xy} = D_{yx}$. The shear force expressions (2.22) become

$$Q_x = -\frac{\partial}{\partial x}\left(D_x\frac{\partial^2 w}{\partial x^2} + H\frac{\partial^2 w}{\partial y^2}\right); \quad Q_y = -\frac{\partial}{\partial y}\left(H\frac{\partial^2 w}{\partial x^2} + D_y\frac{\partial^2 w}{\partial y^2}\right), \tag{7.29}$$

where

$$H = D_{xy} + 2D_s. \tag{7.30}$$

The governing differential equation (2.24) for orthotropic plates becomes

$$D_x\frac{\partial^4 w}{\partial x^4} + 2H\frac{\partial^4 w}{\partial x^2\partial y^2} + D_y\frac{\partial^4 w}{\partial y^4} = p(x,y). \tag{7.31}$$

We give below the expression for the potential energy of bending for orthotropic plates, which follows from Eqs (2.52) and (7.26):

$$U = \frac{1}{2}\int\int_A \left[D_x\left(\frac{\partial^2 w}{\partial x^2}\right)^2 + 2D_{xy}\frac{\partial^2 w}{\partial x^2}\frac{\partial^2 w}{\partial y^2} + D_y\left(\frac{\partial^2 w}{\partial y^2}\right)^2 + 4D_s\left(\frac{\partial^2 w}{\partial x\partial y}\right)^2\right]\mathrm{d}A. \tag{7.32}$$

Equations (7.31) and (7.32) are valid for both naturally and structurally orthotropic plates provided structural elements causing orthotropy are arranged sufficiently close together, so as to ignore a jump change of elastic properties in a plate.

7.2.3 Determination of rigidities for structurally orthotropic plates

The solution of Eq. (7.31) requires specific values of the flexural and torsional rigidities of naturally and structurally orthotropic plates and plate structures. As mentioned earlier, the orthotropic moduli and Poisson's ratios E_x, E_y, ν_x, ν_y, and G can be obtained experimentally for naturally orthotropic materials – for example, from tension or shear tests, as in the case of isotropic materials. The plate rigidities may be then calculated from Eqs (7.28) and (7.30).

The flexural and torsional rigidities of structurally ortotropic plates are determined using the following approximate procedure. A structurally orthotropic plate is reduced to a naturally orthotropic plate with elastic properties equal to the average properties of components of the original plates [4]. Such a plate is termed an *equivalent* or *transformed orthotropic plate*. Subsequently, the rigidities (7.28) and (7.30) of such an equivalent orthotropic plate are approximated, depending on the type of structural orthotropy. The suitable formulas for the plate rigidities for some com-

monly encountered cases of structurally orthotropic plates, shown in Fig. 7.1 [5], are listed below [4–6,7]:

(a) *Plate reinforced by equidistant stiffeners in one direction* (the x-direction) (Fig. 7.1a)

$$D_x = \frac{Eh^3}{12(1-\nu^2)} + \frac{E'b(H_1^3 - h^3)}{12t}, \quad D_y = H = \frac{Eh^3}{12(1-\nu^2)}. \tag{a}$$

(b) *Plate reinforced by a set of equidistant ribs* in one direction (Fig. 7.1b)

$$D_x = \frac{EI}{t}, D_y = \frac{Eh^3}{12\left(1 - \frac{b}{t} + \frac{bh^3}{tH_1^3}\right)}, \quad D_{xy} = 0, D_s \approx \frac{Ch^3}{12} + \frac{C}{2t}, \tag{b}$$

where I is the moment of inertia of a T-shaped section corresponding to one spacing of the rib location about its center axis (shown as shaded in Fig. 7.1c); C is the torsional rigidity of one rib about its centroidal axis. In Eqs (a), (b), and (c), E and

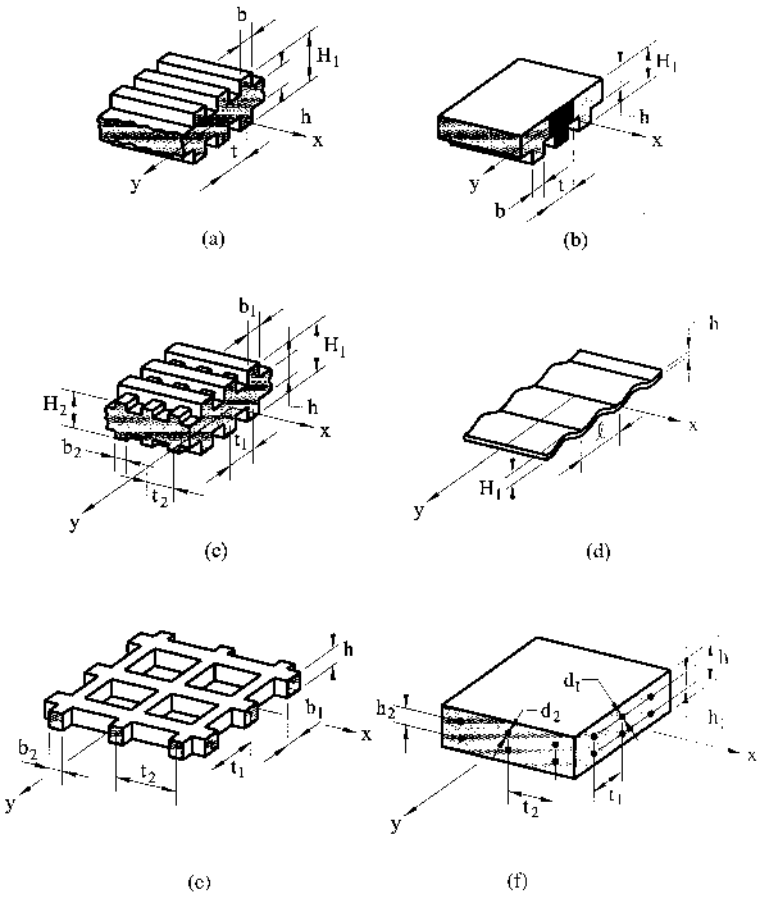

Fig. 7.1

E' are the elastic moduli of the plating and stiffeners or ribs, respectively; ν is Poisson's ratio of plating.

(c) *Plate reinforced by equidistant* stiffeners in two directions (Fig.7.1c)

$$D_x = \frac{Eh^3}{12(1-\nu^2)} + \frac{E'b_1(H_1^3 - h^3)}{12t_1},$$
$$D_y = \frac{Eh^3}{12(1-\nu^2)} + \frac{E'b_2(H_2^3 - h^3)}{12t_2}, H \approx \frac{Eh^3}{12(1-\nu^2)}, \tag{c}$$

(d) *Corrugated plate with a sinusoidal corrugation* $z = H_1 \sin\frac{\pi y}{l}$ (Fig. 7.1d)

$$D_x = EI, \quad D_y = \frac{l}{s}\frac{Eh^3}{12(1-\nu^2)}, \quad D_{xy} = 0, H = \frac{s}{l}\frac{Eh^3}{12(1+\nu)} \tag{d}$$

where

$$I = 0.5H^2h\left[1 - \frac{0.81}{2.5(H/2l)^2}\right]$$

is the moment of inertia of one wave of the corrugation, and $s = l(1 + \pi^2 H_1^2/4l^2)$ is an unfolded length of the one wave.

(e) *Open gridworks* (Fig. 7.1e)

$$D_x = \frac{b_1h^3}{12t_1}, \quad D_y = \frac{b_2h^3}{12t_2}, \quad D_{xy} \cong 0, \quad H = 2D_s = \frac{1}{2}\left(\frac{C_1}{t_1} + \frac{C_2}{t_2}\right), \tag{e}$$

where C_1 and C_2 are the torsional rigidities of the ribs that are parallel to the x and y axes.

(f) *Two-way reinforced concrete slab* (Fig. 7.1f)

$$D_x = \frac{E_c}{(1-\nu_c^2)}\left[\frac{h^3}{12} - I_{xs} + \frac{E_s}{E_c}I_{xs}\right], \quad D_y = \frac{E_c}{(1-\nu_c^2)}\left[\frac{h^3}{12} - I_{ys} + \frac{E_s}{E_c}I_{ys}\right],$$
$$D_s = \frac{1-\nu_c}{2}\sqrt{D_xD_y}, H = \sqrt{D_xD_y}, D_{xy} = \nu_c\sqrt{D_xD_y}, \tag{f}$$

where E_c, ν_c are the modulus of elasticity and Poisson's ratio for concrete, respectively; E_s is the modulus of elasticity for steel; and I_{xs}, I_{ys} are the moments of inertia of steel bars about the x and y axes, respectively.

Notice when $E_x = E_y = E$ and $\nu_x = \nu_y = \nu$, Eqs (7.23), (7.28), and (7.30) become

$$G = \frac{E}{2(1+\nu)}; \quad D_x = D_y = D = \frac{Eh^3}{12(1-\nu^2)}; \quad D_{xy} = \nu D = \nu\frac{Eh^3}{12(1-\nu^2)};$$
$$D_s = \frac{Eh^3}{24(1+\nu)}; \quad H = D_{xy} + 2D_s = D = \frac{Eh^3}{12(1-\nu^2)}.$$

and Eq. (7.31) reduces to that of an isotropic plate, Eq. (2.24), for this particular case.

7.2.4 Rectangular naturally and structurally orthotropic plates

The general procedure for the determination of the deflection, bending moments, and stress components in orthotropic plates is identical with that employed for isotropic plates. The analytical and numerical methods described earlier in Chapters 3 and 6 can be used for determining the deflections, stress resultants, and stress couples.

Example 7.2

A rectangular orthotropic plate with principal directions parallel to the sides is simply supported on all four edges (see Fig. 3.5) and bends under a normal load distributed according to some arbitrary law, i.e., $p = p(x, y)$. Determine the deflection surface for the plate.

Solution

The simply supported boundary conditions are given by Eqs (3.14). We now apply Navier's method discussed in Chapter 3 to treat this plate. Introduction of Eqs (3.15) into (7.31) yields the following:

$$\sum_{m=1}^{\infty}\sum_{n=1}^{\infty}\left\{w_{mn}\left(\frac{m^4\pi^4}{a^4}D_x + 2\frac{m^2n^2\pi^4}{a^2b^2}H + \frac{n^4\pi^4}{b^4}D_y\right) - p_{mn}\right\}\sin\frac{m\pi x}{a}\sin\frac{n\pi y}{b} = 0. \tag{a}$$

Since the above must be valid for all x and y, the terms in the braces must be zero. We obtain

$$w_{mn} = \frac{p_{mn}}{D_x\left(m^4\pi^4/a^4\right) + 2H\left(m^2n^2\pi^4/a^2b^2\right) + D_y\left(n^4\pi^4/b^4\right)}. \tag{b}$$

Substituting Eqs (b) and (3.17) into Eq. (3.15a), we obtain the expression for the following deflections:

$$w = \frac{4}{ab}\sum_{m=1}^{\infty}\sum_{n=1}^{\infty}\int_0^a\int_0^b \frac{p(x, y)\sin\frac{m\pi x}{a}\sin\frac{n\pi y}{b}\,\mathrm{d}x\mathrm{d}y}{D_x\left(m^4\pi^4/a^4\right) + 2H\left(m^2n^2\pi^4/a^2b^2\right) + D_y\left(n^4\pi^4/b^4\right)}. \tag{c}$$

In the particular case of a rectangular plate under a uniformly distributed load of intensity p_0, referring to Sec. 3.3, Eq. (c) is reduced to the following:

$$w = \frac{16p_0}{\pi^6}\sum_{m=1,3,\ldots}^{\infty}\sum_{n=1,3,\ldots}^{\infty}\frac{\sin\frac{m\pi x}{a}\sin\frac{n\pi y}{b}}{mn\left[D_x\left(m^4/a^4\right) + 2H\left(m^2n^2/a^2b^2\right) + D_y\left(n^4/b^4\right)\right]}. \tag{7.33}$$

For isotropic materials, letting $D_x = D_y = D_{xy} = D$, the above equation will coincide with Eq. (3.21a).

Example 7.3

An infinitely long (in the y direction) plate is reinforced by equidistant stiffeners in the direction of the x axis located symmetrically about the middle surface. This plate is modeled by an equivalent orthotropic plate with elastic properties given by Eqs (a) of Sec. 7.2.3. Assuming that the plate is simply supported on edges $x = 0, a$ and subjected to a uniform surface load p_0 (Fig. 7.2), determine the plate deflection surface.

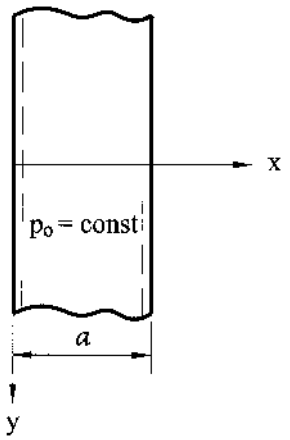

Fig. 7.2

Solution

We apply Levy's method discussed in Sec. 3.5 to treat this splate-strip. The deflection can be expressed by Eq. (3.40), where the complementary solution w_h is given by Eq. (3.42). Substituting the above into the homogeneous differential equation (7.31) gives

$$D_x\left(\frac{m\pi}{a}\right)^4 f_m - 2H\left(\frac{m\pi}{a}\right)^2 \frac{\mathrm{d}^2 f_m}{\mathrm{d}y^2} + D_y \frac{\mathrm{d}^4 f_m}{\mathrm{d}y^4} = 0. \tag{a}$$

The solution of this ordinary differential equation is of the following form:

$$f_m = C\mathrm{e}^{sy}.$$

Then

$$D_x\left(\frac{m\pi}{a}\right)^4 - 2Hs^2\left(\frac{m\pi}{a}\right)^2 + D_y s^4 = 0. \tag{b}$$

The roots of this equation are

$$\begin{aligned} s_{1,2} &= \pm\frac{m\pi}{a}\sqrt{\frac{1}{D_y}\left(H + \sqrt{H^2 - D_x D_y}\right)}; \\ s_{3,4} &= \pm\frac{m\pi}{a}\sqrt{\frac{1}{D_y}\left(H - \sqrt{H^2 - D_x D_y}\right)}. \end{aligned} \tag{c}$$

The particular solution can be determined by using the procedure discussed in Sec. 3.5. Taking the distributed load $p(x, y)$ in the form of a single Fourier series (3.52), where p_m is given by Eq. (3.53), and for a uniformly distributed load – by Eq. (a) of Example 3.3:

$$p_m = \frac{4p_0}{m\pi}; \quad m = 1, 3, 5, \ldots . \tag{d}$$

The particular solution is given by Eq. (3.51). Substituting for w_p and p from Eqs (3.51) and (d) into Eq. (7.31), yields the following:

$$D_x\left(\frac{m\pi}{a}\right)^2 g_m - 2H\left(\frac{m\pi}{a}\right)^2 \frac{d^2 g_m}{dy^2} + D_y \frac{d^4 g_m}{dy^4} = p_m.$$

The particular solution of this equation is presented next:

$$g_m = \frac{p_m}{D_x}\left(\frac{a}{m\pi}\right)^4 \quad \text{and}$$

$$w_p = \sum_{m=1,3,\ldots}^{\infty} \frac{p_m}{D_x}\left(\frac{a}{m\pi}\right)^4 \sin\frac{m\pi x}{a} = \frac{4p_0}{\pi D_x}\left(\frac{a}{\pi}\right)^4 \sum_{m=1,3,\ldots}^{\infty} \frac{1}{m^5}\sin\frac{m\pi x}{a} \tag{e}$$

The general solution w becomes

$$w = \sum_{m=1,3,\ldots}^{\infty}\left[C_{1m}e^{s_{1}y} + C_{2m}e^{s_{2}y} + C_{3m}e^{s_{3}y} + C_{4m}e^{s_{4}y} + \frac{4p_0}{\pi D_x}\left(\frac{a}{\pi}\right)^4 \frac{1}{m^5}\right]\sin\frac{m\pi x}{a} \tag{7.34}$$

As y gets larger, the quantities $e^{s_1 y}$ and $e^{s_3 y}$ tend to approach infinity. Thus, we must set $C_{1m} = C_{3m} = 0$ and Eq. (7.34) reduces to the following:

$$w = \sum_{m=1,3,\ldots}^{\infty}\left[C_{2m}e^{s_{2}y} + C_{4m}e^{s_{4}y} + \frac{4p_0}{\pi D_x}\left(\frac{a}{\pi}\right)^4 \frac{1}{m^5}\right]\sin\frac{m\pi x}{a} \tag{7.35}$$

7.2.5 Circular structurally orthotropic plates

Circular plates with frequently arranged annular ribs (Fig. 7.3a) or with rectangular corrugation (Fig. 7.3b) can be considered as examples of structurally orthotropic plates. These plates have a different stiffness in the radial and circumferential directions. In this case, as mentioned in Sec. 7.2.1, an inhomogeneouty of elastic properties of the plate in different directions is explained not by material properties, which are assumed to be isotropic and homogeneous, but the plate structure only. Strictly

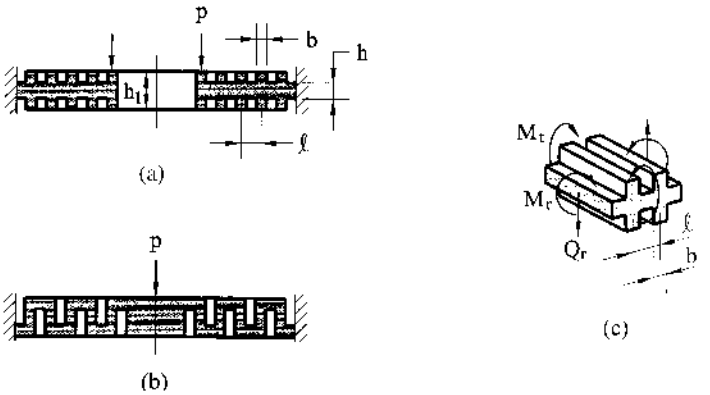

Fig. 7.3

speaking, the flexural rigidity of such plates varies along a radius by some periodical law: it has one value between ribs while another value along them. However, if the ribs are arranged sufficiently close to one other, then it can be assumed that the rigidity in the radial and circumferential directions has some average values, constant or smoothly varying along the radius, and the plates themselves are structurally orthotropic.

We derive the governing differential equation and general relationships for structurally orthotropic circular plates in the context of Kirchhoff's theory. As an example, consider an axisymmetric bending of a circular plate with annular ribs (Fig. 7.3a). We assume that the state of stress in the annular rib is uniaxial, i.e., $\sigma_z = \sigma_r = 0$. In deriving this governing equation, we follow the approach discussed in Sec. 4.8. Let $\vartheta = -\mathrm{d}w/\mathrm{d}r$ be the angle of rotation of the normal to the middle surface (Fig. 4.17). For axisymmetric deformation of the circular plate and uniaxial deformation of the rib, the following expressions for the strain and stress components can be set up:

For the plate

$$\begin{aligned} &\varepsilon_r = \frac{\mathrm{d}\vartheta}{\mathrm{d}r} z; \quad \varepsilon_t = \frac{\vartheta}{r} z; \\ &\sigma_r = \frac{Ez}{1-\nu^2}\left(\frac{\mathrm{d}\vartheta}{\mathrm{d}r} + \nu\frac{\vartheta}{r}\right); \quad \sigma_t = \frac{Ez}{1-\nu^2}\left(\frac{\vartheta}{r} + \frac{\mathrm{d}\vartheta}{\mathrm{d}r}\right). \end{aligned} \tag{7.36a}$$

For the rib

$$\varepsilon_t = \frac{\vartheta}{r} z; \quad \sigma_t = Ez\frac{\vartheta}{r}, \tag{7.36b}$$

where the subscripts r and t denote the radial and circumferential strain and stress components, respectively; z is a distance counted from the middle surface.

Integrating the stresses over the plate thickness and over the cross-sectional area of the rib, we can obtain the bending moments (per unit length) (see Fig. 7.3c) as follows:

$$\begin{aligned} M_r &= \int_{-h/2}^{h/2} \sigma_r z \mathrm{d}z = D_r\left(\frac{\mathrm{d}\vartheta}{\mathrm{d}r} + \nu\frac{\vartheta}{r}\right); \\ M_t &= \int_{-h/2}^{h/2} \sigma_t z \mathrm{d}z + \frac{1}{l}\int_A \sigma_t z \mathrm{d}A = D\left(\frac{\vartheta}{r} + \nu\frac{\mathrm{d}\vartheta}{\mathrm{d}r}\right) + \frac{EI_x}{l}\frac{\vartheta}{r}; \end{aligned} \tag{7.37}$$

or

$$M_t = D_t\frac{\vartheta}{r} + \nu D_r\frac{\mathrm{d}\vartheta}{\mathrm{d}r}, \tag{7.38}$$

where l is the spacing of the ribs; $D = Eh^3/12(1-\nu^2)$ is the flexural rigidity of an unstiffened plate; $D_r = D$; $D_t = D(1 + EI_x/Dl)$ are transformed rigidities in the radial and circumferential directions, respectively; and $I_x = b\left(h_1^3 - h^3\right)/12$ is the moment of inertia of the area of the rib.

Substituting the expressions for the bending moments, Eqs (7.37) and (7.38), into the equation of equilibrium of a differential element of a circular axisymmetric

plate, Eq. (4.83), we obtain, after some simple transformations, the following governing differential equation:

$$\frac{\mathrm{d}^2\vartheta}{\mathrm{d}r^2}+\frac{1}{r}\frac{\mathrm{d}\vartheta}{\mathrm{d}r}-\frac{1}{r^2}\frac{D_t}{D_r}\vartheta=\frac{Q_r}{D_r}. \tag{7.39}$$

Note that for isotropic plates, letting $D_r = D_t = D$, Eq. (7.39) coincides with Eq. (4.89).

A solution of the corresponding homogeneous equation is sought in the following form:

$$\vartheta_{\mathrm{h}} = Cr^{\eta}.$$

Substituting the above into Eq. (7.39) for zero right-hand side results in the following characteristic equation:

$$\eta^2=\frac{D_t}{D_r}, \tag{7.40}$$

the roots of which are

$$\eta_1=\sqrt{\frac{D_t}{D_r}}=\eta; \quad \eta_2=-\sqrt{\frac{D_t}{D_r}}=-\eta. \tag{7.41}$$

Then, the complementary solution, ϑ_{h}, is of the following form:

$$\vartheta_{\mathrm{h}} = C_1r^{\eta}+C_2r^{-\eta}. \tag{7.42}$$

The particular solution of Eq. (7.39) depends on the type of loading. If, for example, a plate is subjected to a uniformly distributed load of intensity p_0, then

$$Q_r=\frac{p_0r}{2},$$

and Eq. (7.39) takes the form

$$\frac{\mathrm{d}^2\vartheta}{\mathrm{d}r^2}+\frac{1}{r}\frac{\mathrm{d}\vartheta}{\mathrm{d}r}-\eta^2\frac{1}{r^2}\vartheta=p_0\frac{r}{2D_r}. \tag{7.43}$$

The particular solution of this equation is sought in the following form of power function:

$$\vartheta_{\mathrm{p}} = Cr^{\alpha}.$$

Substitution of the above into Eq. (7.43) leads to

$$Cr^{(\alpha-2)}(\alpha^2+\eta^2)=p_0\frac{r}{2D_r}.$$

This equality must be satisfied for any value of r; thus, the following is determined: $r^{(\alpha-2)} = r; \quad \alpha-2=1 \quad \text{and} \quad \alpha=3; \quad \text{and} \quad C=\dfrac{p_0}{2D_r(9-\eta^2)}.$

Therefore, the particular solution of Eq. (7.39) for the case of a uniform loading is

$$\vartheta_{\mathrm{p}}=\frac{p_0r^3}{2D_r(9-\eta^2)}, \tag{7.44}$$

and the general solution is of the form

$$\vartheta = C_1 r^{\eta} + C_2 r^{-\eta} + \frac{pr^3}{2D_r\left(9 - \frac{D_t}{D_r}\right)}. \tag{7.45}$$

For the corrugated plate shown in Fig. 7.3b, the governing differential equation is of the same form as Eq. (7.39) but the flexural rigidities will be different – namely

$$D_r = \frac{Eh^3}{12(1-\nu^2)}\frac{l}{s}; \quad D_t = \frac{EI_x}{l(1-\nu^2)}, \tag{7.46}$$

where l is the spacing of the corrugation; s is an unfolded length of the middle line of one corrugation; h is a thickness which is assumed to be constant; and I_x is the moment of inertia of the cross section of one corrugation about the axis coinciding with the middle plane. The expressions for the bending moments and stresses in the corrugated plate have the form

$$\begin{aligned} &M_r = D_r\frac{\mathrm{d}\vartheta}{\mathrm{d}r}; \quad M_t = D_t\frac{\vartheta}{r}; \\ &\sigma_{r,\max} = \frac{6M_r}{h^2} + \nu\frac{M_t l}{I_x}z_{\max}; \quad \sigma_{t,\max} = \frac{M_t l}{I_x}z_{\max} + \nu\frac{6M_r}{h^2}, \end{aligned} \tag{7.47}$$

where $z_{\max}$ is the largest distance from the plate middle plane.

Analysis of circular plates with radial ribs can also be performed using the above-mentioned scheme of structural orthotropy (for a sufficiently larger number of stiffeners). However, this case is more complicated because the distances between such ribs vary along the plate radius and, therefore, the flexural rigidity is also variable. In addition, for a one-sided arrangement of ribs, stretching of the plate middle plane becomes significant and must be taken into account. Many references are available for orthotropic plate design. An interested reader is referred to other works [4–6,7].

7.3 THE EFFECT OF TRANSVERSE SHEAR DEFORMATION ON THE BENDING OF ELASTIC PLATES

7.3.1 Introduction

Kirchhoff's hypotheses, discussed in Sec. 1.3, permitted the creation of the classical (Kirchhoff's) bending theory of thin plates which for more than a century has been the basis for the calculation and design of structures in various areas of engineering and has yielded important theoretical and numerical results. However, just as for any other approximation theory, Kirchhoff's theory has some obvious drawbacks and deficiencies, two of which are:

1. A well-known disagreement exists between the order of Eq. (2.24) and the number of the boundary conditioners on the plate free edge. As a result, the boundary conditions of the classical theory take into account only two characteristics on the free edge of the plate rather than three characteristics corresponding to the reality (see Sec. 2.5). Of the two conditions of (2.37), only the first condition (imposed on the bending moment) has a clear physical interpretation. The reduction of the twisting moment

to a transverse shear force is not justified in the general case [8,9]. As a result of the replacement of the transverse shear force $Q_x(Q_y)$ and twisting moment M_{xy} by their combination, effective shear force $V_x(V_y)$, the self-balanced tangential stresses remain at the free edge of a plate and the concentrated forces arise at the corner points of a rectangular or polygonal plate when this reduction is used. The role of the latter forces is still not clear [8,9].

2. Certain formal contradictions take place between the Kirchhoff plate theory and the three-dimensional equations of elasticity. The most important of the above contradictions is associated with Hooke's law (Eq. (1.8b)) for the transverse shear stresses τ_{xz} and τ_{yz}. In fact, the deformations γ_{xz} and γ_{yz} are absent according to the hypotheses of the classical theory. However, the stresses τ_{xz} and τ_{yz} cannot be equal to zero, as it would be expected from Eqs. (1.8b), because the shear forces Q_x and Q_y, which are resultants of the above-mentioned stresses, are necessary for an equilibrium of the plate differential element.

Notice that as a result of an inaccuracy of Kirchhoff's theory, we cannot guarantee that the stress distribution predicted by this theory will agree well with the actual stresses in the immediate vicinity of the plate edge. The latter statement acquires a practical importance of a refinement of the classical plate theory for plate fields neighboring to a boundary or to openings whose diameter (or another typical dimension) is not too large compared with the plate thickness.

Numerous researchers have attempted to refine Kirchhoff's theory and such attempts continue to this day. E. Reissner made the most important advance in this direction [10,11]. Reissner's theory takes into account the influence of the transverse shear deformation on the deflection of the plate and leads to a sixth-order system of governing differential equations, and accordingly, to three boundary conditions on the plate edge. Here it is unnecessary to introduce the effective transverse shear force. Reissner's theory is free from the drawbacks of Kirchhoff's theory discussed above.

The correct interpretation of Reissner's theory is complicated substantially by the fact that this theory involves the variational procedure to derive the governing equations, which was essentially based on the use of Kirchhoff's theory to approximate the stress distribution over the thickness of the plate. Therefore, another approach is presented below for obtaining the governing differential equations of the refined plate bending theory, which takes into account the transverse shear deformations. According to this approach, the above equations are derived from the equations of the theory of elasticity and certain physical hypotheses. This approach was developed by Vasil'ev [12] and we follow the outline given in this reference.

7.3.2 The governing equations of the refined plate bending theory

Let us introduce again three familiar hypotheses:

1. the straight line normal to the middle plane of the plate does not change its length and remains rectilinear when the plate is subjected to bending;
2. the transverse normal stress σ_z is small compared with the stresses σ_x and σ_y; and

3. the middle plane remains unstrained subsequent to bending.

The only difference between these hypotheses and Kirchhoff's hypotheses discussed in Sec. 1.3 is that the former hypotheses do not require the straight line of the plate to be orthogonal to the bent midsurface of the plate, In this case, the straight line normal to the midsurface, called also the normal element, acquires three independent degrees of freedom corresponding to the deflection $w(x, y)$ and the angles of rotation ϑ_x and ϑ_y which are not related to the deflection w as it has taken place in Kirchhoff's theory (see Eqs (2.5)).

It has been shown in Sec. 2.2 that the displacement components over the plate thickness, according to the above-mentioned hypotheses, obey the following law (see Eqs (2.3)–(2.5)):

$$u = -z\vartheta_x(x, y), \quad v = -z\vartheta_y(x, y), \quad w = w(x, y). \tag{7.48}$$

By repeating the derivation of relations (2.13) discussed in Sec. 2.3, we obtain

$$\begin{aligned} M_x &= -D\left(\frac{\partial \vartheta_x}{\partial x} + \nu\frac{\partial \vartheta_y}{\partial y}\right); \quad M_y = -D\left(\frac{\partial \vartheta_y}{\partial y} + \nu\frac{\partial \vartheta_x}{\partial x}\right); \\ M_{xy} &= -\frac{1}{2}D(1-\nu)\left(\frac{\partial \vartheta_x}{\partial y} + \frac{\partial \vartheta_y}{\partial x}\right). \end{aligned} \tag{7.49}$$

Note that if the angles of rotation are related to the deflections by relations of the type of (2.5), the bending and twisting moment equations (7.49) will coincide with the relations (2.13) derived for the classical (Kirchhoff's) theory.

The stresses σ_x, σ_y, and τ_{xy} are related to the stress resultants M_x, M_y, and M_{xy} by relations (2.11) and the transverse shear forces, Q_x and Q_y are resultants of the transverse shear stresses, τ_{xz} and τ_{yz} (see Eqs (2.12)). As mentioned previously, the transverse shear forces cannot be obtained directly by integrating Eqs (2.12) in Kirchhoff's theory because of the hypotheses (2.1) adapted in this theory. However, the refined theory makes it possible to obtain Q_x and Q_y in terms of the deflection w and the angles of rotation ϑ_x and ϑ_y by integrating Eqs (2.12). Substituting for τ_{xz} and τ_{yz} from Eq. (1.8b) into Eqs (2.12) and using the second and third relations (1.5b) and (7.48), we obtain the following

$$Q_x = G\int_{-h/2}^{h/2}\left(\frac{\partial u}{\partial z} + \frac{\partial w}{\partial x}\right)\mathrm{d}z = Gh\left(-\vartheta_x + \frac{\partial w}{\partial x}\right). \tag{7.50}$$

Thus, within the framework of the theory, one can obtain the transverse shear forces as the stress resultants of the shear stress τ_{xz} and τ_{yz}. We have the following:

$$Q_x = C\eta_x; \quad Q_y = C\eta_y, \tag{7.51}$$

where

$$C = Gh; \quad \eta_x = -\vartheta_x + \frac{\partial w}{\partial x}; \quad \eta_y = -\vartheta_y + \frac{\partial w}{\partial y} \tag{7.52}$$

and C describes the shear stiffness of the plate in the planes xz and yz.

Considering the equilibrium of the plate element, as shown in Fig. 2.4, we obtain Eqs (2.19) and (2.22). Substituting for the stress resultants from the relations (7.49), (7.51) into Eqs (2.19) and (2.22), we arrive at the system of equations for

ϑ_x, ϑ_y, and w. It is possible to simplify this system. To this end, we use Eq. (2.23). By substituting the moments according Eqs. (7.49) into the above equation, we obtain

$$D\nabla^2\left(\frac{\partial\vartheta_x}{\partial x}+\frac{\partial\vartheta_y}{\partial y}\right)-p=0. \tag{7.53}$$

Let us introduce the so-called *potential function* $\phi(x, y)$ of the displacement field in a plane $z = \text{const}$ which satisfies the following relations:

$$\vartheta_x=\frac{\partial\phi}{\partial x};\quad \vartheta_y=\frac{\partial\phi}{\partial y}. \tag{7.54}$$

Using this function, we can reduce Eq. (7.53) to the form

$$D\nabla^2\nabla^2\phi=p. \tag{7.55}$$

Using Eqs (2.22), and substituting there the expressions (7.49) and (7.51) for moments and forces together with relations (7.54), we obtain

$$\frac{\partial F_\phi}{\partial x}=0;\quad \frac{\partial F_\phi}{\partial y}=0;\quad F_\phi=\frac{D}{C}\nabla^2\phi-\phi+w. \tag{7.56}$$

From the first two Eqs (7.56), it follows that $F_\phi = \text{const}$. The value of this constant is unessential for the potential function and, hence, can be assumed to be equal to zero without loss of generality. Then, $F_\phi = 0$ and we obtain the following from Eq. (7.56):

$$w=\phi-\frac{D}{C}\nabla^2\phi, \tag{7.57}$$

where the function ϕ is given by Eq. (7.54). This potential is sometimes referred to as the penetrating potential, because it describes solutions that penetrate into the plate domain. However, this potential cannot describe completely the bending behavior of the plate. It does not take into account the rotation of the plate element in its own plane, which can be described by the so-called *stream function* ψ. This function may be introduced as follows:

$$\vartheta_x=-\frac{\partial\psi}{\partial y};\quad \vartheta_y=\frac{\partial\psi}{\partial x};\ w=0. \tag{7.58}$$

It can be easily verified that the relations (7.58) represent the solution of the homogeneous equation (7.53) (i.e., for $p = 0$).

Substituting the expressions (7.49) for the moments and expressions (7.51) and (7.52) for the shear forces into Eqs. (2.22) and using Eqs (7.58), we obtain

$$\frac{\partial F_\psi}{\partial x}=0,\quad \frac{\partial F_\psi}{\partial y}=0,\quad F_\psi=\Delta\psi-k^2\psi, \tag{7.59}$$

where

$$k^2=\frac{2C}{D(1-\nu)}. \tag{7.60}$$

By repeating the reasoning that led to Eq. (7.57), we arrive at the Helmholtz equation:

$$\nabla^2\psi-k^2\psi=0. \tag{7.61}$$

Since the plate bending problem is assumed to be linear, we can use the method of superposition and represent the angles of rotation of the normal element of the plate as follows:

$$\vartheta_x = \frac{\partial \phi}{\partial x} - \frac{\partial \psi}{\partial y}; \quad \vartheta_y = \frac{\partial \phi}{\partial y} + \frac{\partial \psi}{\partial x}, \tag{7.62}$$

where the functions ϕ and ψ are defined by Eqs (7.54) and (7.58), respectively. Equations (7.55) and (7.61) represent *the sixth-order system of governing differential equations of the plate bending theory by taking into account the transverse shear deformations*. This theory is sometimes referred to as the *shear or refined plate theory*.

The deflection w is given by Eq. (7.57). Taking into account the relations (7.49) and (7.62), we can express the bending and twisting moments, as well as shear forces, in terms of the following functions ϕ and ψ:

$$M_x = -D\left[\frac{\partial^2 \phi}{\partial x^2} + \nu \frac{\partial^2 \phi}{\partial y^2} - (1-\nu)\frac{\partial^2 \psi}{\partial x \partial y}\right];$$

$$M_y = -D\left[\frac{\partial^2 \phi}{\partial y^2} + \nu \frac{\partial^2 \phi}{\partial x^2} + (1-\nu)\frac{\partial^2 \psi}{\partial x \partial y}\right];$$

$$M_{xy} = -D(1-\nu)\left[\frac{\partial^2 \phi}{\partial x \partial y} + \frac{1}{2}\left(\frac{\partial^2 \psi}{\partial x^2} - \frac{\partial^2 \psi}{\partial y^2}\right)\right]; \tag{7.63}$$

$$Q_x = -D\frac{\partial}{\partial x}\Delta\phi + C\frac{\partial \psi}{\partial y}; \quad Q_y = -D\frac{\partial}{\partial y}\Delta\phi + C\frac{\partial \psi}{\partial x}. \tag{7.64}$$

As $C \to \infty$ (i.e., the transverse shear deformation is ignored) it follows from Eqs (7.57) and (7.61) that $\psi = 0$ and $w = \phi$ and the resulting system of Eqs (7.55) and (7.61) degenerates into the governing differential equation (2.24) of the Kirchhoff theory.

From the above it follows that the effect of the transverse shear strains is twofold. Consider the second term on the right-hand side of Eq. (7.57). It determines the effect of the shear strain on the deflection. The asymptotic analysis, conducted in Ref. [12], showed that the coefficient $\nabla^2\phi$ in Eq. (7.57) contains the factor of h^2/a^2, where a is the characteristic length of the plate. Since h^2/a^2 is a very small value for thin plates, we can set $w = \phi$ with a high degree of accuracy. The second effect of the shear strains is associated with the existence of the Helmholtz equation (Eq. (7.61)). The key difference between Kirchhoff's theory and the refined theory presented is directly related to that equation. It was established [12,13] that the Helmholtz equation determines the state of stress of the plate near the plate edge or other perturbation line along which the continuity of the plate geometry is violated, or in the vicinity of the applied load, etc. It is known that solutions of this equation vary rapidly only when remote from the edge. Therefore, the potential ψ is a function of the boundary layer type, i.e., it describes solutions that decay with increasing distance from the boundary. It was established that ψ decays at a distance equal approximately to two thicknesses from the boundary. At interior points of the plate domain that are farther than

$2h$ from the boundary, therefore, the solution is described practically exactly by the penetrating potential ϕ. This, of course, does not mean that the boundary layer potential ψ can be ignored, because it may influence significantly the penetrating potential via the boundary conditions.

Let us determine the stress components corresponding to the displacements (7.48). Repeating the derivation of the stress–moments relations (2.15), it can be shown that the stresses σ_x, σ_y, and τ_{xy} are defined by the same relations (2.15) as in the case for Kirchhoff's plate bending theory.

Now we can proceed to determining the shear stresses τ_{xz} and τ_{yz}. If we substitute for the transverse shear strains γ_{xz} and γ_{yz} from Eq. (1.5b), together with the relations (7.48), into the constitutive equations (1.8b) for the transverse shear stresses, we obtain

$$\tau_{xz} = G\left(-\vartheta_x + \frac{\partial w}{\partial x}\right), \quad \tau_{yz} = G\left(-\vartheta_y + \frac{\partial w}{\partial y}\right). \tag{7.65}$$

These stresses do not satisfy the following static boundary conditions

$$\tau_{xz} = 0\big|_{z=\pm\frac{h}{2}}, \quad \tau_{yz} = 0\big|_{z=\pm\frac{h}{2}} \tag{7.66}$$

because the theory under consideration is based on the displacement approximation in the form of Eq. (7.48). Note that these relations also do not coincide with the relations (2.16), which follow from the equilibrium equations. Kirchhoff's theory is free from this contradiction because it does not involve the constitutive relations (1.8b).

Boundary conditions

As mentioned earlier, Eqs (7.55) and (7.61) form a sixth-order system of differential equations; hence, the corresponding boundary value problem requires three boundary conditions. To be specific, we consider the typical boundary conditions for the edge $x = \text{const}$.

(a) *The edge* $x = \text{const}$ *is perfectly fixed*
For this edge the boundary conditions are

$$u = 0, \quad v = 0, \quad w = 0. \tag{7.67}$$

Using Eqs (7.48) and (7.62), we can rewrite these boundary conditions in terms of the functions ϕ and ψ, as follows

$$\frac{\partial \phi}{\partial x} = \frac{\partial \psi}{\partial y}; \quad \frac{\partial \phi}{\partial y} = -\frac{\partial \psi}{\partial x}; \quad \phi - \frac{D}{C}\Delta\phi = 0. \tag{7.68}$$

(b) *The edge* $x = \text{const}$. *is free*
This type of boundary conditions implies that the stresses σ_x, τ_{xy}, and τ_{xz} must vanish. For the bending problems of thin plates described by the refined theory presented above, these requirements can be reduced to the following conditions:

$$M_x = 0; \quad M_{xy} = 0; \quad Q_x = 0. \tag{7.69}$$

Applying the relations ((7.63) and (7.64), we can rewrite these boundary conditions in terms of the functions ϕ and ψ, as follows:

$$\frac{\partial^2\phi}{\partial x^2}+\nu\frac{\partial^2\phi}{\partial y^2}-(1-\nu)\frac{\partial^2\psi}{\partial x\partial y}=0;$$
$$\frac{\partial^2\phi}{\partial x\partial y}+\frac{1}{2}\left(\frac{\partial^2\psi}{\partial x^2}-\frac{\partial^2\psi}{\partial y^2}\right)=0; \tag{7.70}$$
$$\frac{D}{C}\frac{\partial}{\partial x}\Delta\phi-\frac{\partial\psi}{\partial y}=0.$$

Let us transform the second boundary condition (7.70). Eliminating $\partial^2\psi/\partial x^2$ with the use of (7.61), differentiating with respect to y (along the plate edge), and eliminating ϕ with the use of the third condition (7.70), we obtain

$$\frac{\partial}{\partial x}\left[\frac{\partial^2\phi}{\partial x}+(2-\nu)\frac{\partial^2\phi}{\partial y^2}-\frac{D}{C}(1-\nu)\frac{\partial^2}{\partial y^2}\Delta\phi\right]=0. \tag{7.71}$$

If $\psi=0$ and $C\to\infty$, then the third condition (7.71) disappears and the first boundary condition (7.70) and Eq. (7.70) become equivalent to the conditions $M_x=0$ and $V_x=0$ in Kirchhoff's theory. Note that the condition $V_x=0$ is obtained without reduction of the twisting moment to a force performed in Kirchhoff's theory (see Sec. 2.4).

(c) *The edge* $x=$ const *is simply supported*

The shear plate bending theory allows two types of boundary conditions for a simply supported edge in contrast to Kirchhoff's theory:

– *The first case* corresponds to a plate whose contour is supported by the diaphragms that are absolutely rigid in their own planes. We then have

$$w=0,\quad M_x=0,\quad \vartheta_y=0. \tag{7.72}$$

Using the relations (7.63), we can represent these conditions in terms of functions ϕ and ψ after some transformations, as follows [12]:

$$\phi=0,\frac{\partial^2\phi}{\partial x^2}=0,\quad \frac{\partial\psi}{\partial x}=0. \tag{7.73}$$

– *The second possible case* of a simply supported edge corresponds to a plate free-resting on a supporting contour. The corresponding boundary conditions for this edge are

$$w=0,\quad M_x=0,\quad M_{xy}=0. \tag{7.74}$$

Again, using Eqs (7.63), we can rewrite these conditions in terms of the following functions ϕ and ψ :

$$\phi-\frac{D}{C}\Delta\phi=0,$$
$$\frac{\partial^2\phi}{\partial x^2}+\nu\frac{\partial^2\phi}{\partial y^2}-(1-\nu)\frac{\partial^2\psi}{\partial x\partial y}=0, \tag{7.75}$$
$$\frac{\partial^2\phi}{\partial x\partial y}+\frac{1}{2}\left(\frac{\partial^2\psi}{\partial x^2}-\frac{\partial^2\psi}{\partial y^2}\right)=0.$$

Note that the governing differential equations (7.57) and (7.63) can be obtained from the following conditions of the minimum for the Lagrange functional:

$$U = \int\int\left[\frac{1}{2}\left(M_x\frac{\partial\vartheta_x}{\partial x} + M_y\frac{\partial\vartheta_y}{\partial y} + M_{xy}\left(\frac{\partial\vartheta_x}{\partial y} + \frac{\partial\vartheta_y}{\partial x}\right)\right.\right.$$
$$\left.\left. + Q_x\eta_x + Q_y\eta_y\right) - pw\right]\mathrm{d}x\mathrm{d}y. \tag{7.76}$$

7.3.3 Application of the refined theory

In order to illustrate an application of this theory, let us consider the classical commonly encountered problem: a simply supported rectangular plate with sides a and b ($0 \le x \le a$; $0 \le y \le b$) subjected to a uniformly distributed load of intensity p (see Fig. 3.5). This problem has been analyzed comprehensively by Kirchhoff's theory in Sec. 3.3. The deflected surface of the plate was given by Eq. (3.21a). We have ascertained that the edge supporting reactions (V_x and V_y) did not balance the given uniform load exerted on the plate (see Example 3.1). Note that the contour transverse shear forces, Q_x and Q_y, balance the external load, but according to Kirchhoff's theory they cannot be treated as the edge supporting reactions. Thus, as already discussed in the above example, there will be the concentrated reactions, S, at each corner to satisfy the equilibrium conditions for the plate as a solid.

Let us now consider the solution of this problem using the shear plate bending theory discussed above. To satisfy the boundary conditions (7.73), we seek the solution in the form of the series

$$\phi = \sum_m\sum_n \phi_{mn}\sin\lambda_m x\sin\lambda_n y; \qquad \psi = \sum_m\sum_n \psi_{mn}\cos\lambda_m x\cos\lambda_n y, \tag{7.77}$$

where

$$\lambda_m = \frac{m\pi}{a}, \quad \lambda_n = \frac{n\pi}{b}. \tag{7.78}$$

By substituting the second series into Eq. (7.61), we obtain $\psi_{mn} = 0$, i.e., $\psi = 0$. Inserting the first series into Eqs (7.55) and expanding the surface load $p(x, y)$ into a similar series, we find ϕ_{mn} and then, using relation (7.57), we obtain the following expression for the plate deflections:

$$w = \frac{1}{D}\sum_m\sum_n \frac{p_{mn}\left[1 + \frac{D}{C}\left(\lambda_m^2 + \lambda_n^2\right)\right]}{\left(\lambda_m^2 + \lambda_n^2\right)^2}\sin\lambda_m x\sin\lambda_n y. \tag{7.79}$$

For a thin plate, the numerical difference between the solutions (3.21a) and (7.79) is small, but these solutions are sufficiently different. Unlike Kirchhoff's theory, in the shear theory the supporting reactions coincide with the contour transverse shear forces, Q_x and Q_y, given by Eqs (7.64); these forces balance the applied uniform load p exerted on the plate and exclude the existence of any corner forces. As mentioned earlier, the existence of these corner forces is also not confirmed by the solution of the three-dimensional theory of elasticity for this problem. Thus, Kirchhoff's plate bending theory leads to the edge supporting reactions that differ significantly from the reactions resulting from the refined plate theory discussed above.

Concluding remarks

The refined plate theory presented above is referred to as a first-order shear theory because it deals with the resultant stresses (the forces and moments). There are a number of first-order shear theories of plate bending developed by E. Reissner [10,11], Timoshenko [4], Vasil'ev [12], Green [14], Mindlin [15], etc. All these theories were constructed in a reasonably correct manner and are reducible to a sixth-order system of equations which may be different from Eqs (7.55) and (7.61). However, it is significant that these theories, independently of particular hypotheses on which they are based, can be reduced to a biharmonic equation similar to Eq. (7.55) and to the Helmholtz equation of the type of Eq. (7.61). In essence, all these theories differ from the classical (Kirchhoff's) theory.

A refined higher-order theory of plates was developed by Reddy [16]. The distinction between the first- and second-order theories is associated with the accuracy of the shear stress-free conditions (7.66) on the plate surfaces $\pm h/2$. Reddy's theory satisfies the stress-free boundary conditions and accounts for shear rotations and parabolic variations of the transverse shear stresses.

Concluding our general observations on the influence of shear deformations on the state of stress in plate bending problems, we can note the following. The nondimensional analysis shows that the stresses σ_x, σ_y, and τ_{xy} are of order pa^2/h^2, whereas τ_{xz} and τ_{yz} are of the order pa/h, and σ_z is of order p, where a is the characteristic length of the plate. Therefore, for thin plates with the ratio $a/h > 10$, the transverse normal σ_z and shear stresses τ_{xz} and τ_{yz} are negligible when compared with the remaining stresses σ_x, σ_y, and τ_{xy}. Then, as mentioned earlier, the influence of the transverse shear strains on the deflections is also very small and can be neglected. Its application gives no practical improvement of results obtained by Kirchhoff's theory for thin plates. Thus, for thin isotropic plates, the refined (shear) plate bending theory is of a fundamental rather than applied nature. This theory makes it possible to eliminate the contradictions and drawbacks of the classical (Kirchhoff's) theory discussed above. In particular, one of the significant corrections to the classical plate bending theory is associated with the effective shear forces that appear in this theory as a formal quantity for matching the number of the natural boundary conditions on a free edge with the order of the governing differential equation (2.24).

However, the transverse shear strain correction is of considerable importance for analyzing the state of stress in plate fields adjacent to the boundary or to various geometrical and load discontinuities (cracks, holes whose diameter is so small as to be of the order of magnitude of the plate thickness, concentrated load, etc.). Also it has been observed that the effect of the shear strains is more pronounced in orthotropic plates than in isotropic plates.

7.4 LARGE-DEFLECTION THEORY OF THIN PLATES

7.4.1 General

The Kirchhoff's linear plate bending theory discussed in earlier chapters, is valid only for small deflections ($w \leq 0.2h$). In this case, the theory gives sufficiently accurate results and lateral loads are carried by a bending action of the plate only. The linear theory ignores straining of the middle surface of the plate and the correspond-

ing in-plane stresses are neglected. However, if the magnitude of the lateral deflections increases beyond a certain level ($w \geq 0.3h$), these deflections are accompanied by stretching of the middle surface. Coincidentally, the load-carrying mechanism of a plate is changed: the membrane forces produced by such stretching help appreciably in resisting the lateral loads (such a plate is referred to as a flexible plate – see Sec. 1.1). As the ratio w/h increases, the role of the membrane forces becomes more pronounced. When the magnitude of the maximum deflection reaches the order of the plate thickness ($w \approx h$), the membrane action becomes comparable to that of bending. Beyond this ($w > h$), the membrane action predominates (as mentioned in Sec. 1.1., such a plate is called a membrane). When constructing the large-deflection plate bending theory, we use two assumptions: the hypothesis of the straight normals (assumption 4 of Sec. 1.3) and the hypothesis of an absence of reciprocal pressure of horizontal layers (assumption 5 of Sec. 1.3). However, the assumption about absence of membrane deformations of the middle plane (assumption 6 of Sec. 1.3) is dropped.

The large-deflection theory assumes that the deflections w are sufficiently large (they can be comparable with the plate thickness or larger), but they should remain small relative to the other dimensions of the plate (except for its thickness). Thus, the bent (deformed) midsurface of the plate may be considered as a shallow surface due to the smallness of the w/a ratio, where a is some typical dimension of the plate middle plane. Moreover, the displacement components u and v that were neglected in the linear theory are taken into account. But these components will be assumed to be small compared with deflections, i.e., $|u| \ll |w|$, $|v| \ll |w|$. This assumption is quite understandable: the deflection w occurs in the direction of the least rigidity, while the displacements u and v occur in the direction of the largest rigidity of the plate. It is also assumed that the derivatives of the displacements u and v with respect to the x and y coordinates are small compared with the values of $\partial w/\partial x$ and $\partial w/\partial y$. It should be also noted that the deflections of the plate are not assumed to be small, compared with its thickness, but at the same time still sufficiently small to justify an application of the simplified formulas (2.7) for the plate curvatures. Finally, the large-deflection theory deals with finite deflections. However, the relative deformations (strains) are assumed to be small quantities (for instance, in steel structures they are of the order of 1/1000).

Flexible plates and membranes are widely used in engineering. For example, a part of a plane skin of an aircraft wing, reinforced by the longitudinal stiffeners (stringers) and transverse ribs, should be classified as a flexible plate. Flexible plates also occupy a highly permanent place in shipbuilding. The skin of a ship bottom is subjected to compression and it also participates in the overall bending of the ship hull; in addition, the ship's bottom undergoes a significant water pressure. As a rule, the deflections of the skin are comparable with its thickness. The theory of flexible plates can also be applied to the stress analysis of a ship's deck because for certain positions of a ship with respect to the crests of waves, the deck is found to be strongly compressed. Therefore, the stress analysis of such decks requires an application of the large-deflection theory.

In designing thin-walled beams with high and thin webs in civil engineering structures, the web should be analyzed as a flexible plate: buckling can occur due to shear, with formation of inclined bulgings.

Circular flexible plates and membranes are frequently met in instrument-making. For example, corrugated membrane plates with initial imperfections are used as

elastic-sensitive elements of manometric devices. They can undergo significant deflections.

7.4.2 The rectangular flexible plates

In deriving the governing differential equations for large deflections in rectangular plates, the Cartesian coordinate system will be used. We consider all the three sets of equations: equilibrium of a plate element; compatibility conditions; and constitutive relations.

We begin our analysis with the *equilibrium equations*. Note that in the large-deflection force analysis of thin plates, in-plane forces N_x, N_y, and N_{xy} depend now not only on external forces applied at the middle plane but also on the stretching of the middle surface caused by its bending. A fundamental feature of the large-deflection plate bending problems is that the equations of static equilibrium must be set up for the *deformed (bent) configuration of plates*. However, in the case of a shallow bent surface of the plate, this point is of fundamental importance only for analyzing the force summation in the z direction. Thus, the assumptions adapted in the large-deflection theory, and discussed in Sec. 7.4.1, make it possible to employ the equilibrium equations (3.90) and (3.91) in the force analysis of a plate under transverse loading, resulting in relatively large elastic deflections.

We are coming now to the analysis of *deformations of the middle surface* of the plate caused by its bending. Let us attach the Cartesian fixed coordinate axes x and y to the middle plane of the plate. Consider three points $A(x, y, 0)$, $B(x + \mathrm{d}x, y, 0)$, and $C(x, y + \mathrm{d}y, 0)$ on the undeformed midplane of the plate (Fig. 7.4).

After deformation, the coordinates of these points will be

$$A_1(x + u, y + v, w),\ B_1\left(x + \mathrm{d}x + u + \frac{\partial u}{\partial x}\mathrm{d}x,\ y + v + \frac{\partial v}{\partial x}\mathrm{d}x,\ w + \frac{\partial w}{\partial x}\mathrm{d}x\right),$$

$$C_1\left(x + u + \frac{\partial u}{\partial y}\mathrm{d}y,\ y + v + \frac{\partial v}{\partial y}\mathrm{d}y,\ w + \frac{\partial w}{\partial y}\mathrm{d}y\right),$$

where u, v, and w are the displacement components of any point of the plate middle surface along the x, y, and z axes, respectively. Determine the distance between points A_1 and B_1:

$$A_1B_1 = \sqrt{\left(\mathrm{d}x + \frac{\partial u}{\partial x}\mathrm{d}x\right)^2 + \left(\frac{\partial v}{\partial x}\mathrm{d}x\right)^2 + \left(\frac{\partial w}{\partial x}\mathrm{d}x\right)^2}. \tag{a}$$

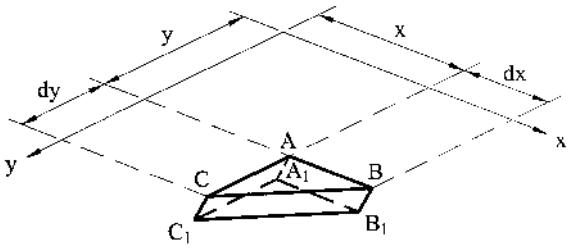

Fig. 7.4

The relative stretching of the line segment $AB = \mathrm{d}x$ on the plate middle surface in the direction of the x axis is

$$\varepsilon_x = \frac{A_1B_1 - AB}{AB} = \frac{\sqrt{\left(\mathrm{d}x + \frac{\partial u}{\partial x}\mathrm{d}x\right)^2 + \left(\frac{\partial v}{\partial x}\mathrm{d}x\right)^2 + \left(\frac{\partial w}{\partial x}\mathrm{d}x\right)^2} - \mathrm{d}x}{\mathrm{d}x}$$
$$= \sqrt{1 + 2\frac{\partial u}{\partial x} + \left(\frac{\partial u}{\partial x}\right)^2 + \left(\frac{\partial v}{\partial x}\right)^2 + \left(\frac{\partial w}{\partial x}\right)^2} - 1. \tag{b}$$

Due to the smallness of displacements u and v, one can neglect $(\partial u/\partial x)^2$ and $(\partial v/\partial x)^2$ under the radical sign (if w is comparable with the plate thickness, we can assume that $\partial u/\partial x$ and $\partial v/\partial y$ has the same order of smallness as the values $(\partial w/\partial x)^2$ and $(\partial w/\partial y)^2$, respectively). Thus, we can rewrite ε_x as follows:

$$\varepsilon_x = \sqrt{1 + 2\frac{\partial u}{\partial x} + \left(\frac{\partial w}{\partial x}\right)^2} - 1, \tag{c}$$

and after approximately taking the root, we obtain

$$\varepsilon_x = \frac{\partial u}{\partial x} + \frac{1}{2}\left(\frac{\partial w}{\partial x}\right)^2. \tag{7.80a}$$

Similarly,

$$\varepsilon_y = \frac{\partial v}{\partial y} + \frac{1}{2}\left(\frac{\partial w}{\partial y}\right)^2. \tag{7.80b}$$

Now we can proceed to determining a shear strain at point A (Fig. 7.4). Let us introduce the following designations:

S_1 is the distance A_1B_1; S_2 is the distance A_1C_1; S is the distance B_1C_1.

From the triangle $A_1B_1C_1$ we obtain

$$S^2 = S_1^2 + S_2^2 - 2S_1S_2\cos\beta, \tag{d}$$

where β represents the angle between line segments A_1B_1 and A_1C_1. Solving the above equation for $\cos\beta$, yields

$$\cos\beta = -\frac{S^2 - S_1^2 - S_2^2}{2S_1S_2}. \tag{e}$$

The distance S_1 may be found from Eq. (a), as follows:

$$S_1^2 = \left[\left(1 + \frac{\partial u}{\partial x}\right)^2 + \left(\frac{\partial v}{\partial x}\right)^2 + \left(\frac{\partial w}{\partial x}\right)^2\right]\mathrm{d}x^2 = (1 + \varepsilon_x)^2\mathrm{d}x^2.$$

Similarly, we can determine the following

$$S_2^2 = \left[\left(\frac{\partial u}{\partial x}\right)^2 + \left(1 + \frac{\partial v}{\partial x}\right)^2 + \left(\frac{\partial w}{\partial y}\right)^2\right]\mathrm{d}y^2 = (1 + \varepsilon_y)^2\mathrm{d}y^2;$$

$$S^2 = \left[\left(1 + \frac{\partial u}{\partial x}\right)\mathrm{d}x - \frac{\partial u}{\partial y}\mathrm{d}y\right]^2 + \left[\frac{\partial v}{\partial x}\mathrm{d}x - \left(1 + \frac{\partial v}{\partial y}\right)\mathrm{d}y\right]^2 + \left[\frac{\partial w}{\partial x}\mathrm{d}x - \frac{\partial w}{\partial y}\mathrm{d}y\right]^2.$$

Substitution of the above into Eq. (e) yields the following:

$$\cos\beta = \frac{\dfrac{\partial u}{\partial y}\left(1 - \dfrac{\partial u}{\partial x}\right) + \dfrac{\partial v}{\partial x}\left(1 + \dfrac{\partial v}{\partial y}\right) + \dfrac{\partial w}{\partial x}\dfrac{\partial w}{\partial y}}{(1+\varepsilon_x)(1+\varepsilon_y)}.$$

Since the strain components are assumed to be small, we can drop ε_x and ε_y compared with unity and the products

$$\frac{\partial u}{\partial y}\frac{\partial u}{\partial x}, \frac{\partial v}{\partial x}\frac{\partial v}{\partial y}$$

may also be dropped compared with

$$\frac{\partial w}{\partial x}\frac{\partial w}{\partial y}.$$

Finally, we obtain

$$\cos\beta = \frac{\partial u}{\partial y} + \frac{\partial v}{\partial x} + \frac{\partial w}{\partial x}\frac{\partial w}{\partial y}.$$

The shear strain γ_{xy} is defined as follows:

$$\gamma_{xy} = \frac{\pi}{2} - \beta \approx \sin\left(\frac{\pi}{2} - \beta\right) = \cos\beta.$$

Thus, the shear strain in the plate middle surface is

$$\gamma_{xy} = \frac{\partial u}{\partial y} + \frac{\partial v}{\partial x} + \frac{\partial w}{\partial x}\frac{\partial w}{\partial y}. \tag{7.81}$$

Finally, the strain components in the plate middle surface are

$$\varepsilon_x = \frac{\partial u}{\partial x} + \frac{1}{2}\left(\frac{\partial w}{\partial x}\right)^2; \quad \varepsilon_y = \frac{\partial v}{\partial y} + \frac{1}{2}\left(\frac{\partial w}{\partial y}\right)^2; \quad \gamma_{xy} = \frac{\partial u}{\partial y} + \frac{\partial v}{\partial x} + \frac{\partial w}{\partial x}\frac{\partial w}{\partial y}. \tag{7.82}$$

Eliminating the tangential components of displacements u and v from Eqs (7.82), one can obtain the following *equation of the compatibility of deformations* in the middle surface of the plate:

$$\frac{\partial^2 \varepsilon_x}{\partial y^2} + \frac{\partial^2 \varepsilon_y}{\partial x^2} - \frac{\partial^2 \gamma_{xy}}{\partial x \partial y} = \left(\frac{\partial^2 w}{\partial x \partial y}\right)^2 - \frac{\partial^2 w}{\partial x^2}\frac{\partial^2 w}{\partial y^2}. \tag{7.83}$$

Consider now the constitutive equations. It should be noted that due to the adapted assumptions in Sec. 7.4.1, the constitutive relations for the large-deflection plate analysis are of the same form as for the classical plate theory. In particular, the strain–membrane force relations, according to Hooke's law, are of the form

$$\varepsilon_x = \frac{1}{Eh}(N_x - \nu N_y), \quad \varepsilon_y = \frac{1}{Eh}(N_y - \nu N_x), \quad \gamma_{xy} = \frac{N_{xy}}{Gh}. \tag{7.84}$$

Upon substitution of Eqs (7.84) into Eqs (7.83), we derive the following:

$$\frac{1}{Eh}\left[\frac{\partial^2}{\partial y^2}(N_x - \nu N_y) + \frac{\partial^2}{\partial x^2}(N_y - \nu N_x) - 2(1+\nu)\frac{\partial^2 N_{xy}}{\partial x \partial y}\right] = \left(\frac{\partial^2 w}{\partial x \partial y}\right)^2 - \frac{\partial^2 w}{\partial x^2}\frac{\partial^2 w}{\partial y^2} \tag{7.85}$$

Thus, the system of the four equations (Eqs (3.90), (3.91), and (7.85)) is found to be closed, i.e., it involves the four unknown functions, N_x, N_y, N_{xy}, and w. However, this system of four equations can be reduced to the corresponding system of two equations by introducing a stress function ϕ for in-plane stress components, as follows:

$$N_x = \frac{\partial^2 \Phi}{\partial y^2}, \quad N_y = \frac{\partial^2 \Phi}{\partial x^2}, \quad N_{xy} = -\frac{\partial^2 \Phi}{\partial x \partial y}, \tag{7.86}$$

where $\Phi = \phi h$. In doing so, as it can be easily verified, Eqs (3.90) are identically satisfied. Substituting for Φ from Eqs (7.86) into Eqs (7.85) and (3.91), we obtain

$$\begin{aligned} &\frac{\partial^4 \Phi}{\partial x^4} + 2\frac{\partial^4 \Phi}{\partial x^2 \partial y^2} + \frac{\partial^4 \Phi}{\partial y^4} = Eh\left[\left(\frac{\partial^2 w}{\partial x \partial y}\right)^2 - \frac{\partial^2 w}{\partial x^2}\frac{\partial^2 w}{\partial y^2}\right]; \\ &\frac{\partial^4 w}{\partial x^4} + 2\frac{\partial^4 w}{\partial x^2 \partial y^2} + \frac{\partial^4 w}{\partial y^4} = \frac{1}{D}\left(p + \frac{\partial^2 \Phi}{\partial y^2}\frac{\partial^2 w}{\partial x^2} + \frac{\partial^2 \Phi}{\partial x^2}\frac{\partial^2 w}{\partial y^2} - 2\frac{\partial^2 \Phi}{\partial x \partial y}\frac{\partial^2 w}{\partial x \partial y}\right). \end{aligned} \tag{7.87}$$

These are the *governing differential equations for large deflections of thin plates*. Equations (7.87) are coupled, nonlinear, partial differential equations, each of fourth order. The first equation can be interpreted as an *equilibrium equation*, while the second one is a *compatibility equation* in terms of the stress function. They were first introduced in 1910 by von Karman [17].

Once the stress function Φ and the deflection w have been determined, the in-plane forces N_x, N_y, and N_{xy}, as well the bending M_x, M_y and twisting M_{xy} moments can be obtained through the use of Eqs (7.86) and (2.13). The functions Φ and w must satisfy not only Eqs (7.87) but also the prescribed boundary conditions. If we consider a rectangular plate, then two conditions must be imposed on the functions Φ and w separately on each side of the plate. In the large-deflection theory of plate bending, the support conditions (simple support, built-in support, etc.) require some correction [17]. In particular, for built-in or hinged supports, the boundary conditions mentioned above will be similar to those of shallow shells discussed later in Sec. 17.4.

Unfortunately, where realistic problems are concerned, solving these coupled, nonlinear, partial differential equations represents a stubborn mathematical task. The usual numerical procedure is to reduce the nonlinear differential equations (7.87) to a system of nonlinear algebraic equations using the variational methods, finite difference methods, or finite element methods. Inasmuch as the analytical solution of these nonlinear algebraic equations is possible only in the exceptional cases, an iterative numerical procedures can be used (see Sec. 18.7). Only as a result of recent progress in the development of various numerical approaches has the large-deflection analysis of plates been treated satisfactory [17–20].

The governing differential equations (7.87) have been derived assuming that the material of the plate was isotropic. For plates made of orthotropic material (in the case when the axes of elastic symmetry coincide with the coordinate axes x and y), equations analogous to Eqs (7.87) have the following form [3]:

$$\frac{1}{h}\left(A_y\frac{\partial^4\Phi}{\partial x^4}+2A_{xy}\frac{\partial^4\Phi}{\partial x^2\partial y^2}+A_x\frac{\partial^4\Phi}{\partial y^4}\right)=\left(\frac{\partial^2 w}{\partial x\partial y}\right)^2-\frac{\partial^2 w}{\partial x^2}\frac{\partial^2 w}{\partial y^2},$$

$$D_x\frac{\partial^4 w}{\partial x^4}+2H\frac{\partial^4 w}{\partial x^2\partial y^2}+D_y\frac{\partial^4 w}{\partial y^4}=p+\left(\frac{\partial^2\Phi}{\partial y^2}\frac{\partial^2 w}{\partial x^2}-2\frac{\partial^2\Phi}{\partial x\partial y}\frac{\partial^2 w}{\partial x\partial y}+\frac{\partial^2\Phi}{\partial x^2}\frac{\partial^2 w}{\partial y^2}\right), \tag{7.88}$$

where D_x, D_y, and H are given by Eqs (7.28) and (7.30). $A_x = 1/Ex$, $A_y = 1/Ey$, $A_{xy} = 1/2G - \partial y/Ey = 1/2G - \partial x/Ex$.

Example 7.4

Consider a rectangular plate subjected to a uniformly distributed load of intensity p (Fig. 7.5a). The plate is supported along all the edges by diaphragms that are absolutely rigid in their own plane and flexible out of their plane. This corresponds to the following boundary conditions:

$$w=0,\frac{\partial^2 w}{\partial x^2}=0,\quad N_x=0,v=0\Big|_{x=0,a}. \tag{a}$$

Similarly, the boundary conditions can be formulated on edges $y = 0$ and $y = b$. Carry out a qualitative bending analysis of the plate.

Solution

The solution of Eqs (7.87) will be sought in the following form:

$$w=\sum_{m,n}f_{mn}\sin\frac{m\pi x}{a}\sin\frac{n\pi y}{b};\quad \Phi=\sum_{i,j}\zeta_{ij}\sin\frac{i\pi x}{a}\sin\frac{j\pi y}{b}, \tag{7.89}$$

where f_{mn} and ζ_{ij} are unknown constants. It can be easily verified that the functions w and Φ in the form of (7.89) satisfy the prescribed boundary conditions (a).

We use the Galerkin method (see Sec. 6.5) to determine constants f_{mn} and ζ_{ij}. Substitute the expansions (7.89) into Eqs (7.87) and multiply the first equation by $\sin(i\pi x/a)\sin(j\pi y/b)$ and the second one by $\sin(m\pi x/a)\sin(n\pi y/b)$. Integrating each of the expressions obtained over the plate area and equating the results to

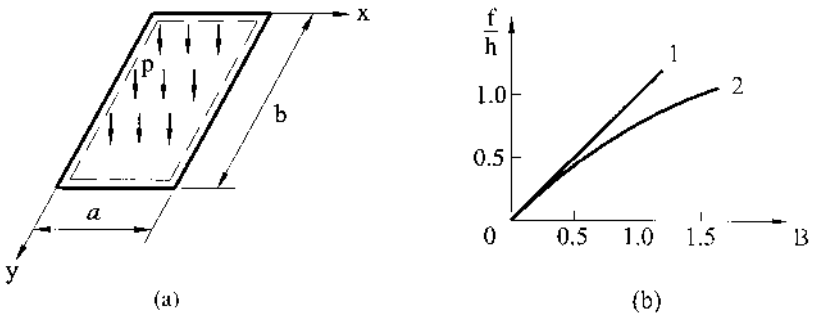

Fig. 7.5

zero, we obtain the system of nonlinear algebraic equations for the constants f_{mn} and ζ_{ij}.

The numerical procedure is illustrated for the case when only one term is retained in the expansion (7.89), i.e.,

$$w = f \sin\frac{\pi x}{a}\sin\frac{\pi y}{b}; \quad \Phi = \zeta \sin\frac{\pi x}{a}\sin\frac{\pi y}{b}.$$

Upon substitution of the above into Eqs (7.87), one obtains

$$\begin{aligned} E_1^{(1)} &= \zeta\frac{1}{Eh}\left(\frac{\pi^2}{a^2}+\frac{\pi^2}{b^2}\right)^2 \sin\frac{\pi x}{a}\sin\frac{\pi y}{b} \\ &\quad - f\frac{\pi^4}{a^2b^2}\left(\cos^2\frac{\pi x}{a}\cos^2\frac{\pi y}{b} - \sin^2\frac{\pi x}{a}\sin^2\frac{\pi y}{b}\right); \\ E_2^{(1)} &= fD\left(\frac{\pi^2}{a^2}+\frac{\pi^2}{b^2}\right)^2 \sin\frac{\pi x}{a}\sin\frac{\pi y}{b} \\ &\quad - 2f\zeta\left(\frac{\pi^4}{a^2b^2}\right)\left(\sin^2\frac{\pi x}{a}\sin^2\frac{\pi y}{b} - \cos^2\frac{\pi x}{a}\cos^2\frac{\pi y}{b}\right) - p, \end{aligned}$$

where $E_1^{(1)}$ and $E_2^{(1)}$ are the first term approximation of the residual error functions of the first and second equations (7.87), respectively. Applying the Galerkin method (see Sec. 6.5), multiply $E_1^{(1)}$ and $E_2^{(1)}$ by $\sin(\pi x/a)\sin(\pi y/b)$ and integrate over the plate area. We have

$$\begin{aligned} &\zeta\left(\frac{\pi^2}{a^2}+\frac{\pi^2}{b^2}\right)^2 + f^2\frac{16\pi^2 Eh}{3a^2b^2} = 0; \\ &fD\left(\frac{\pi^2}{a^2}+\frac{\pi^2}{b^2}\right)^2 - f\zeta\frac{32\pi^2}{3a^2b^2} = \frac{16}{\pi^2}p. \end{aligned} \tag{7.90}$$

This system of two equations can be reduced to one equation for the deflection amplitude f_{11}. For example, if $a/b = 1$, we have

$$\frac{f}{h} + \frac{128(1-\nu^2)}{3\pi^4}\frac{f^3}{h^3} = B, \tag{7.91}$$

where

$$B = \frac{4pa^4}{\pi^6 Dh}.$$

Equation (7.91) enables one to carry out a qualitative large-deflection bending analysis of the square plate. In order to obtain a more accurate result, it is necessary to retain in the expressions (7.89) a larger number of terms. Figure 7.5b illustrates the relationship of f/h versus B corresponding to the bending of square stiff (curve 1) and flexible (curve 2) plates for $\nu = 0.3$. A difference of 10% is already reached for the stiff plate for $f/h \approx 0.5$ in this case. The above example is taken from Ref. [21].

7.4.3 Axisymmetric bending of circular flexible plates and membranes

We use the polar coordinate system for the axisymmetric bending analysis of the flexible circular plates and membranes (see Fig. 4.1). Let u be a radial displacement of points in the middle surface, and ε_r and ε_t are the strain components in the radial and tangential (i.e., perpendicular to the radial) directions, respectively. In the analysis of flexible circular plates and membranes subjected to axisymmetric load p we follow the outline of Ref. [19].

Using the line of reasoning as in Sec. 7.4.2, we can conclude that ε_r is expressed by the relation similar to Eq. (7.80a) by replacing the partial derivatives in x with the ordinary derivatives in r. We have

$$\varepsilon_r = \frac{\mathrm{d}u}{\mathrm{d}r} + \frac{1}{2}\left(\frac{\mathrm{d}w}{\mathrm{d}r}\right)^2. \tag{7.92a}$$

Since for axisymmetric deformation of circular plates, $v = 0$ and $\partial^k(\ldots)/\partial\varphi^k = 0$ $(k = 1, 2, \ldots)$, the in-plane circumferential (or tangential) strain, ε_t, can occur as a result of the radial displacements only. So, if points on an infinitesimal arc length $\mathrm{d}s = r\mathrm{d}\varphi$ displace along the plate radius r by an amount u, then, after deformation, the arc length becomes $(r + u)\mathrm{d}\varphi$ and the corresponding circumferential strain component is

$$\varepsilon_t = \frac{(r+u)\mathrm{d}\varphi - r\mathrm{d}\varphi}{r\mathrm{d}\varphi} \quad \text{or} \qquad \varepsilon_t = \frac{u}{r}. \tag{7.92b}$$

The shear deformation is zero in axisymmetric bending. Substituting $u = \varepsilon_t r$ into Eq. (7.92a) results in the following compatibility of deformations equation:

$$\frac{\mathrm{d}}{\mathrm{d}r}(r\varepsilon_t) - \varepsilon_r = -\frac{1}{2}\left(\frac{\mathrm{d}w}{\mathrm{d}r}\right)^2. \tag{7.93}$$

The middle surface curvatures in the radial, χ_r, and tangential, χ_t, directions, can be obtained from Eqs (2.7) using the relations (4.4) and the conditions of axial symmetry discussed above. Thus, we have

$$\chi_r = -\frac{\mathrm{d}^2 w}{\mathrm{d}r^2}, \quad \chi_t = -\frac{1}{r}\frac{\mathrm{d}w}{\mathrm{d}r}. \tag{7.94a}$$

The twist of the middle surface, $\chi_{rt} = 0$.

Let ϑ be the angle of rotation of the normal to the plate middle surface (see Fig. 4.17), introduced by Eq. (4.86). Then, Eqs (7.94a) can be rewritten in terms of the above angle ϑ, as follows:

$$\chi_r = \frac{\mathrm{d}\vartheta}{\mathrm{d}r}, \; \chi_t = \frac{\vartheta}{r}. \tag{7.94b}$$

Consider now the state of moments and shear forces on an infinitesimal element of the plate, described in polar coordinates and shown in Fig. 7.6a. The x and y axes are taken in the radial and tangential directions, respectively, in the middle surface, as shown in Fig. 7.6a.

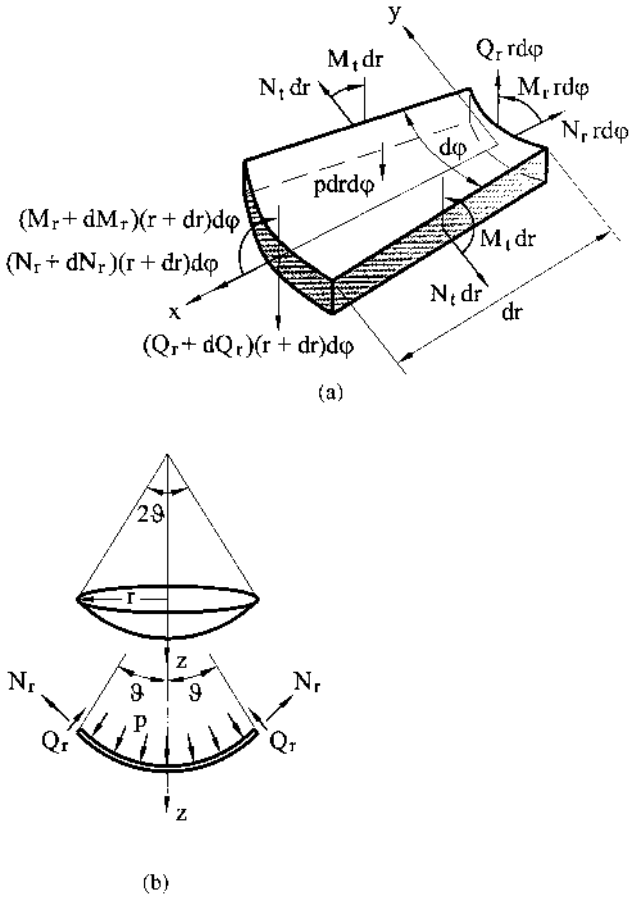

Fig. 7.6

The condition that the sum of the x-directed forces equals zero leads to

$$(N_r + \mathrm{d}N_r)(r + \mathrm{d}r)\mathrm{d}\varphi - N_r r\mathrm{d}\varphi - 2N_t \mathrm{d}r\frac{\mathrm{d}\varphi}{2} = 0.$$

Neglecting the high-order terms in the above equation yields

$$r\mathrm{d}N_r + N_r\mathrm{d}r - N_t\mathrm{d}r \quad \text{or}$$
$$\frac{\mathrm{d}}{\mathrm{d}r}(rN_r) - N_t = 0. \tag{7.95a}$$

The equilibrium of moments about the x axis is governed by the following equation:

$$(M_r + \mathrm{d}M_r)(r + \mathrm{d}r)\mathrm{d}\varphi - M_r r\mathrm{d}\varphi + Qr\mathrm{d}\varphi\mathrm{d}r - 2M_t\mathrm{d}r\frac{\mathrm{d}\varphi}{2} + pr\mathrm{d}\varphi\mathrm{d}r\frac{\mathrm{d}r}{2} = 0\,.$$

Omitting the higher-order terms yields

$$\frac{\mathrm{d}M_r}{\mathrm{d}r} + \frac{M_r}{r} - \frac{M_t}{r} = -Q. \tag{7.95b}$$

To describe equilibrium of the circular plate in the z direction, it is necessary, as we have seen in Sec. 3.9, to consider the plate in the deflected state. For the forces in Fig. 7.6b, acting on the interior part of the circular plate of radius r, from $\sum F_z = 0$, we have

$$Q(2\pi r) + N_r(2\pi r)\vartheta =, R, \tag{7.96}$$

where

$$R = \int_0^r p(2\pi r)\mathrm{d}r \tag{7.97}$$

is the resultant of the external distributed load.

Introduce the load function Ψ, as follows:

$$\Psi = \frac{1}{r}\frac{R}{2\pi} = \frac{1}{r}\int_0^r pr\mathrm{d}r. \tag{7.98}$$

Then, the shear force, Q, can be found from Eq. (7.96), as follows:

$$Q = \Psi - N_r\vartheta, \tag{7.99}$$

and the load intensity is given by

$$p = \frac{1}{r}\frac{\mathrm{d}}{\mathrm{d}r}(r\Psi). \tag{7.100}$$

The in-plane force–strain relations can be obtained by transforming Eqs (7.84) from Cartesian to polar coordinates. Solving the above equations for the in-plane forces, we obtain

$$N_r = \frac{Eh}{1-\nu^2}(\varepsilon_r + \nu\varepsilon_t),\ N_t = \frac{Eh}{1-\nu^2}(\varepsilon_t + \nu\varepsilon_r). \tag{7.101}$$

The bending moment–curvature relations are given by Eqs (4.14).

The equation of equilibrium (7.95a) will be satisfied if one introduces the stress function Φ by the following relations:

$$N_r = \frac{1}{r}\frac{\mathrm{d}\Phi}{\mathrm{d}r}, \quad N_t = \frac{\mathrm{d}^2\Phi}{\mathrm{d}r^2}. \tag{7.102}$$

Comparing Eqs (7.95b) and (7.99), one finds

$$\frac{\mathrm{d}M_r}{\mathrm{d}r} + \frac{M_r}{r} - \frac{M_t}{r} = -\Psi + N_r\vartheta. \tag{7.103}$$

Substituting for M_r from the first equation of Eq. (4.14) into Eq. (7.103) and using Eqs (7.102) and (4.86), we obtain, after some mathematics,

$$D\frac{\mathrm{d}}{\mathrm{d}r}\left[\frac{1}{r}\frac{\mathrm{d}}{\mathrm{d}r}\left(r\frac{\mathrm{d}w}{\mathrm{d}r}\right)\right] = \Psi + \frac{1}{r}\frac{\mathrm{d}\Phi}{\mathrm{d}r}\frac{\mathrm{d}w}{\mathrm{d}r} \tag{7.104}$$

or in the following form

$$D\frac{\mathrm{d}}{\mathrm{d}r}\left(\nabla^2 w\right) = \Psi + \frac{1}{r}\frac{\mathrm{d}\Phi}{\mathrm{d}r}\frac{\mathrm{d}w}{\mathrm{d}r}, \tag{7.105}$$

where

$$\nabla^2 w = \frac{1}{r}\frac{\mathrm{d}}{\mathrm{d}r}\left(r\frac{\mathrm{d}w}{\mathrm{d}r}\right) \tag{7.106}$$

is the Laplace operator in the polar coordinates for axisymmetric deformation.

Let us express the strain components in terms of the stress function Φ. We obtain

$$\varepsilon_r = \frac{1}{Eh}\left(\frac{1}{r}\frac{\mathrm{d}\Phi}{\mathrm{d}r} - \nu\frac{\mathrm{d}^2\Phi}{\mathrm{d}r^2}\right), \quad \varepsilon_t = \frac{1}{Eh}\left(\frac{\mathrm{d}^2\Phi}{\mathrm{d}r^2} - \frac{\nu}{r}\frac{\mathrm{d}\Phi}{\mathrm{d}r}\right). \tag{7.107}$$

Introducing the above relations into the compatibility equation (7.93), one obtains

$$\frac{\mathrm{d}^3\Phi}{\mathrm{d}r^3} + \frac{1}{r}\frac{\mathrm{d}^2\Phi}{\mathrm{d}r^2} - \frac{1}{r^2}\frac{\mathrm{d}\Phi}{\mathrm{d}r} = -\frac{Eh}{2}\left(\frac{\mathrm{d}w}{\mathrm{d}r}\right)^2. \tag{7.108}$$

Applying again the Laplace operator (7.106), we can rewrite the above equation, as follows:

$$\frac{\mathrm{d}}{\mathrm{d}r}\left(\nabla^2\Phi\right) = -\frac{Eh}{2r}\left(\frac{\mathrm{d}w}{\mathrm{d}r}\right)^2. \tag{7.109}$$

Thus, the governing differential equations for an axisymmetrically loaded, flexible circular plate have the following form

$$D\frac{d}{\mathrm{d}r}\left(\nabla^2 w\right) = \Psi + \frac{1}{r}\frac{\mathrm{d}\Phi}{\mathrm{d}r}\frac{\mathrm{d}w}{dr}, \tag{7.110a}$$

$$\frac{\mathrm{d}}{\mathrm{d}r}\left(\nabla^2\Phi\right) = -\frac{Eh}{2r}\left(\frac{\mathrm{d}w}{\mathrm{d}r}\right)^2. \tag{7.110b}$$

For the small-deflection stiff, axisymmetrically loaded circular plates, Eq. (7.110b) is omitted and Eq. (7.110a) appears in the form

$$D\frac{\mathrm{d}}{\mathrm{d}r}\left(\nabla^2 w\right) = \Psi. \tag{7.111}$$

Differentiating both parts of this equation with respect to r, one obtains Eq. (4.17), as expected. On the contrary, for an *absolutely flexible plate* (i.e., membrane), the term containing D should be neglected and we obtain the following system of differential equations:

$$\frac{1}{r}\frac{\mathrm{d}\Phi}{\mathrm{d}r}\frac{\mathrm{d}w}{\mathrm{d}r} = -\Psi, \tag{7.112a}$$

$$\frac{\mathrm{d}}{\mathrm{d}r}\left(\nabla^2\Phi\right) = -\frac{Eh}{2r}\left(\frac{\mathrm{d}w}{\mathrm{d}r}\right)^2. \tag{7.112b}$$

Let us consider now the *boundary conditions* for flexible circular plates, described by Eqs (7.110). If a circular plate is simply supported along edge $r = a$, then the boundary conditions are

$$w = 0|_{r=a}, \left(\frac{\mathrm{d}^2 w}{\mathrm{d}r^2} + \frac{\nu}{r}\frac{\mathrm{d}w}{\mathrm{d}r}\right) = 0|_{r=a}. \tag{7.113a}$$

If a circular plate is fixed along edge $r = a$, then the boundary conditions are of the form

$$w = 0|_{r=a}, \frac{dw}{dr} = 0|_{r=a}. \tag{7.113b}$$

For solid plates having no concentric circular hole, the above boundary conditions must be complemented by the condition of no slope at the plate center, i.e.,

$$\vartheta = -\frac{dw}{dr} = 0|_{r=a}. \tag{7.114}$$

Let us describe the boundary conditions for the stress function Φ.

In the case when the edge points of the plate cannot displace in the radial direction, the following condition must be satisfied:

$$u = 0|_{r=a}. \tag{7.115}$$

Using the relations (7.92b) and (7.107), one obtains

$$\frac{u}{r} = Eh\left(\frac{d^2\Phi}{dr^2} - \frac{\nu}{r}\frac{d\Phi}{dr}\right),$$

and the boundary conditions (7.115) can be written in the form

$$\left(\frac{d^2\Phi}{dr^2} - \frac{\nu}{r}\frac{d\Phi}{dr}\right) = 0\Big|_{r=a}. \tag{7.116}$$

If the edge points of the plate are free to displace in the radial direction, then the corresponding boundary condition is of the form

$$N_r = \frac{1}{r}\frac{d\Phi}{dr} = 0\Big|_{r=a}. \tag{7.117}$$

The conditions (7.116) and (7.117) must be supplemented by the condition of boundedness of the derivative of the stress function, $d\Phi/dr$, for the entire plate: in particular, at $r = 0$. The value of N_r, and hence, σ_r, should be also bounded. Then, as seen from the expression (7.102), the following condition must be satisfied:

$$\frac{d\Phi}{dr} = 0\Big|_{r=0}. \tag{7.118}$$

Example 7.5

Consider a flexible circular plate of radius a with clamped edge under a uniform load p_0, as shown in Fig. 4.3a. Find the bending moments and normal stresses.

Solution

Let us approximate the deflected surface of the flexible circular plate with clamped edge by the expression

$$w = f\left(1 - \frac{r^2}{a^2}\right)^2, \tag{a}$$

where f is the maximum deflection at the plate center, i.e., at $r = 0$. Note that this equation corresponds to the solution of the same problem for stiff circular plates according to the small-deflection plate bending theory (see Sec. 4.3).

Substituting for w from Eq. (a) into Eq. (7.110b), gives

$$\frac{\mathrm{d}}{\mathrm{d}r}\left(\nabla^2\Phi\right) = -\frac{8Ehf^2}{a^2 r}\left(\frac{r}{a} - \frac{r^3}{a^3}\right)^2.$$

Integrating this equation, one obtains

$$\nabla^2\Phi = -\frac{8Ehf^2}{a^2}\left(\frac{r^2}{2a^2} - \frac{r^4}{2a^4} + \frac{r^6}{6a^6}\right) + C_1.$$

Multiplying this equation by r and integrating repeatedly, we obtain

$$\frac{\mathrm{d}\Phi}{\mathrm{d}r} = -\frac{2Ehf^2}{a}\left(\frac{r^3}{2a^3} - \frac{r^5}{3a^5} + \frac{r^7}{12a^7}\right) + C_1\frac{r}{2} + C_2\frac{1}{r}. \tag{b}$$

The constant $C_2 = 0$ due to the condition (7.118). The constant C_1 is evaluated from boundary conditions on the plate edge. We consider below two types of possible boundary conditions for function Φ.

(a) *Points of the plate edge are free to displace in the plane of the middle surface*
Using the condition (7.117), one finds

$$C_1 = \frac{Ehf^2}{r^2}. \tag{c}$$

Then, we obtain

$$\frac{\mathrm{d}\Phi}{\mathrm{d}r} = \frac{Ehf^2}{6a}\left(3\frac{r}{a} - 6\frac{r^3}{a^3} + 4\frac{r^5}{a^5} - \frac{r^7}{a^7}\right). \tag{d}$$

Since $p = p_0 = \text{const}$, the function Ψ in (7.98) is shown next:

$$\Psi = \frac{p_0 r}{2}.$$

On the other hand,

$$\nabla^2 w = -\frac{8f}{a^2}\left(1 - 2\frac{r^2}{a^2}\right).$$

Hence,

$$\frac{\mathrm{d}}{\mathrm{d}r}\left(\nabla^2 w\right) = \frac{32fr}{a^4}. \tag{e}$$

Let us apply the Galerkin method in the form of the principle of virtual work (see Sec. 6.5) to solving Eq. (7.110a). In this case, the differential operator of the problem is of the form

$$D\frac{\mathrm{d}}{\mathrm{d}r}(\nabla^2 w) - \Psi - \frac{1}{r}\frac{\mathrm{d}\Phi}{\mathrm{d}r}\frac{\mathrm{d}w}{\mathrm{d}r}.$$

It has a sense of bending moments in dimension. Seeking the deflected surface of the plate in the form of the series

$$w = \sum_{i=1}^{N} A_i \eta_i(r), \tag{f}$$

we can represent the Galerkin equation (6.39), according to the principle of virtual work for solving Eq. (7.110a), as follows

$$\int_0^a E(w_N) \frac{\mathrm{d}\eta_j}{\mathrm{d}r} r \mathrm{d}r = 0, \quad j = 1, 2, \ldots, N. \tag{g}$$

Retaining only one term in the expansion (f) and setting according to (a),

$$\eta_1 = \left(1 - \frac{r^2}{a^2}\right)^2.$$

Hence, the function $E(w_1)$ is equal to

$$E_1(w) = D\frac{32fr}{a^4} - \frac{p_0 r}{2} + \frac{2}{3}\frac{Eh}{r} f^3 \left(\frac{5-3\nu}{1-\nu}\frac{r}{a} - 6\frac{r^3}{a^3} + 4\frac{r^5}{a^5} - \frac{r^7}{a^7}\right)\left(\frac{r}{a} - \frac{r^3}{a^3}\right).$$

Introducing the dimensionless variable

$$\rho = \frac{r}{a},$$

and substituting for E and η_1 from the above equations into Eq. (g), one obtains

$$\int_0^1 \left[32Df\rho - \frac{1}{2}p_0 \rho a^4 + \frac{2}{3}\frac{Eh}{\rho} f^3 \left(\frac{5-3\nu}{1-\nu}\rho - 6\rho^3 + 4\rho^5 - \rho^7\right)\left(\rho - \rho^3\right)\right]\rho \mathrm{d}\rho = 0.$$

Evaluating this integral, we obtain the following equation:

$$\frac{6}{7}\zeta^3 + \frac{16}{3(1-\nu^2)}\zeta = p^*, \tag{h}$$

where

$$\zeta = \frac{f}{h}, \quad p* = \frac{p_0}{E}\left(\frac{a}{h}\right)^4. \tag{i}$$

For $\nu = 0.3$, the above equation appears in the form

$$0.857\zeta^3 + 5.862\zeta = p^*.$$

Solving this equation, gives ζ. Having determined ζ, we can determine the deflections, bending moments, and normal stresses. The bending moments can be determined from Eqs (4.14) by substituting for w from Eq. (a). We have

$$M_r = 4D\frac{f}{a^2}\left[(1+\nu) - (3+\nu)\rho^2\right], \tag{j}$$

$$M_t = 4D\left[(1+\nu) - (1+3\nu)\rho^2\right]. \tag{k}$$

The in-plane normal stresses, σ_{r0} and σ_{t0}, are given by

$$\sigma_{r0} = \frac{N_r}{h} = \frac{1}{hr}\frac{\mathrm{d}\Phi}{\mathrm{d}r}, \quad \sigma_{t0} = \frac{N_t}{h} = \frac{1}{h}\frac{\mathrm{d}^2\Phi}{\mathrm{d}r^2},$$

or substituting for $\mathrm{d}\Phi/\mathrm{d}r$ from Eq. (b), and (c), and determining $\mathrm{d}^2\Phi/\mathrm{d}r^2$, we obtain

$$\begin{aligned}\sigma_{r0} &= \frac{Ef^2}{6a^2}\left(3 - 6\rho^2 + 4\rho^4 - \rho^6\right),\\ \sigma_{t0} &= \frac{Ef^2}{6a^2}\left(3 - 18\rho^2 + 20\rho^4 - 7\rho^6\right).\end{aligned} \tag{l}$$

It is seen from the above equations that, near the plate edge, the tangential stresses σ_{t0} are compressive.

The bending normal stresses, σ_{rb} and σ_{tb}, are shown next:

$$\sigma_{rb} = \frac{6M_r}{h^2}, \quad \sigma_{tb} = \frac{6M_t}{h^2}.$$

At the plate center, the bending normal stresses are (for $\nu = 0.3$)

$$\sigma^*_{rb} = \sigma^*_{tb} = 2.86\zeta, \tag{m}$$

and near the plate edge the above stresses are

$$\sigma^*_{rb} = 4.4\zeta, \sigma^*_{tb} = 1.32\zeta, \tag{n}$$

where

$$\sigma^*_{rb} = \frac{\sigma_{rb}}{E}\left(\frac{a}{h}\right)^2, \quad \sigma^*_{tb} = \frac{\sigma_{tb}}{E}\left(\frac{a}{h}\right)^2. \tag{o}$$

(b) *The edge points are not displaced in the radial direction*
From Eq. (7.116), it follows that the constant C_1 in Eq. (b) is equal to

$$C_1 = \frac{Ehf^2}{3a^2}\frac{5 - 3\nu}{1 - \nu},$$

from which

$$\frac{\mathrm{d}\Phi}{\mathrm{d}r} = \frac{Ehf^2}{6a}\left(\frac{5 - 3\nu}{1 - \nu}\rho - 6\rho^3 + 4\rho^5 - \rho^7\right).$$

In this case of the boundary conditions, the Galerkin equation (6.39) is of the form

$$\int_0^1 \left[32Df\rho - \frac{1}{2}p_0\rho a^4 + \frac{2}{3}\frac{Ehf^3}{\rho}\left(\frac{5 - 3\nu}{1 - \nu}\rho - 6\rho^3 + 4\rho^5 - \rho^7\right)(\rho - \rho^3)\right]$$

$$(\rho - \rho^3)\rho\mathrm{d}\rho = 0.$$

Evaluating this integral, yields the following equation:

$$\frac{2}{21}\frac{23 - 9\nu}{1 - \nu}\zeta^3 + \frac{16}{3(1 - \nu^2)}\zeta = p^*, \tag{p}$$

or for $\nu = 0.3$,

$$2.762\zeta^3 + 5.862\zeta = p^*. \tag{q}$$

The in-plane normal stresses are

$$\sigma_{r0} = \frac{Ef^2}{6a^2}\left(\frac{5-3\nu}{1-\nu} - 6\rho^2 + 4\rho^4 - \rho^6\right),$$
$$\sigma_{t0} = \frac{Ef^2}{6a^2}\left(\frac{5-3\nu}{1-\nu} - 18\rho^2 + 20\rho^4 - 7\rho^6\right). \tag{r}$$

At the plate center these stresses are

$$\sigma^*_{r0} = \sigma^*_{t0} = \frac{5-3\nu}{6(1-\nu)}\zeta^2,$$

and near the plate edge the in-plane normal stresses are given by

$$\sigma^*_{r0} = \frac{1}{3(1-\nu)}\zeta^2, \quad \sigma^*_{t0} = \frac{\nu}{3(1-\nu)}\zeta^2.$$

The bending normal stresses are determined by the previous equations (m) and (n).

7.5 MULTILAYERED PLATES

Plates composed of two or more thin bonded layers of isotropic or anisotropic materials are called *multilayered plates*. Such plates offer certain advantages over homogeneous plates. When suitably designed, they combine a moderate weight with a sufficient strength. Such multilayered plates are used extensively for flight structures, in plywood laminates, and "sandwich" structural assemblies; each layer may possess a different thickness orientation of the principal axes, and anisotropic properties. In formulating the governing differential equations within the frame of the classical plate bending theory, we assume that the individual layers are isotropic and that sliding between them is prevented. So, the strain–displacement relations for the kth layer (Fig. 7.7) can be written as follows:

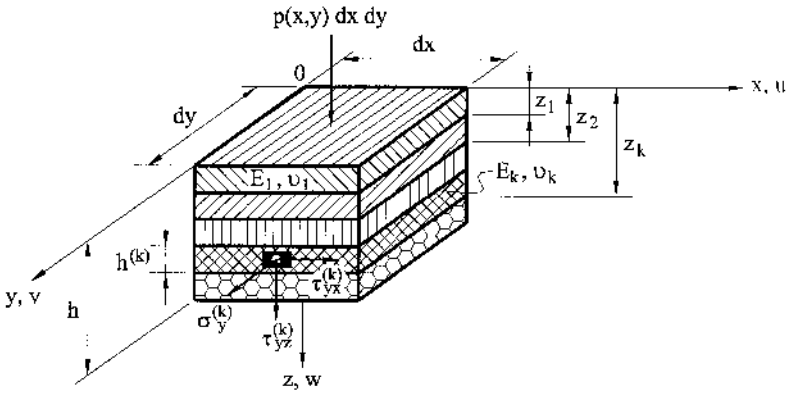

Fig. 7.7

$$\varepsilon_x^{(k)} = -z_k \frac{\partial^2 w}{\partial x^2}, \quad \varepsilon_y^{(k)} = -z_k \frac{\partial^2 w}{\partial y^2}, \gamma_{xy}^{(k)} = -2z_k \frac{\partial^2 w}{\partial x \partial y} \tag{7.119}$$

From Hooke's law, Eqs (2.9), we obtain

$$\begin{aligned} \sigma_x^{(k)} &= \frac{E_k}{1-\nu_k^2}\left(\varepsilon_x^{(k)} + \nu_k \varepsilon_y^{(k)}\right); \quad \sigma_y^{(k)} = \frac{E_k}{1-\nu_k^{(k)}}\left(\varepsilon_y^{(k)} + \nu_k \varepsilon_x^{(k)}\right); \\ \tau_{xy}^{(k)} &= \frac{E_k}{2(1+\nu_k)} \gamma_{xy}^{(k)}. \end{aligned} \tag{7.120}$$

Substituting the strains defined by Eqs (7.119) into the above, integrating over each layer and summing the results, we obtain the following bending and twisting moments:

$$\begin{Bmatrix} M_x \\ M_y \\ M_{xy} \end{Bmatrix} = \sum_k \int_{z_{k-1}}^{z_k} \begin{Bmatrix} \sigma_x \\ \sigma_y \\ \tau_{xy} \end{Bmatrix}^{(k)} z \mathrm{d}z. \tag{7.121}$$

The stress components defined in the kth layer can be calculated from

$$\begin{aligned} \sigma_x^{(k)} &= -z_k \frac{E_k}{1-\nu_k^2}\left(\frac{\partial^2 w}{\partial x^2} + \nu_k \frac{\partial^2 w}{\partial y^2}\right); \quad \sigma_y^{(k)} = -z_k \frac{E_k}{1-\nu_k^2}\left(\frac{\partial^2 w}{\partial y^2} + \nu_k \frac{\partial^2 w}{\partial x^2}\right); \\ \tau_{xy}^{(k)} &= -z_k \frac{E_k}{1+\nu_k} \frac{\partial^2 w}{\partial x \partial y}. \end{aligned} \tag{7.122}$$

The governing differential equation for multilayered plates can be derived similarly, as described in Sec. 2.4. This equation will be similar to that for homogeneous plates, but replacing the rigidity D by the so-called *transformed rigidity*, D_t, of the multilayered plates, as follows [22,23]:

$$D_\mathrm{t} \nabla^2 \nabla^2 w(x, y) = p(x, y), \tag{7.123}$$

where D_t is given by Pister and Dong in the form [22]

$$D_\mathrm{t} = \frac{AC - B^2}{A}, \tag{7.124}$$

and the constants A, B, and C are given by

$$\begin{aligned} A &= \sum_k \frac{E_k}{1-\nu_k^2}(z_k - z_{k-1}); \; B = \sum_k \frac{E_k}{1-\nu_k^2}\left(\frac{z_k^2 - z_{k-1}^2}{2}\right); \\ C &= \sum_k \frac{E_k}{1-\nu_k^2}\left(\frac{z_k^3 - z_{k-1}^3}{3}\right). \end{aligned} \tag{7.125}$$

The deflected surface of the multilayered plates can be determined by the same analytical and numerical methods as those discussed for homogeneous plates in Chapters 3, 4, and 6.

If multilayered plates are composed from $2n+1$ symmetrical isotropic layers, about the midplane then the transformed flexural rigidity D_t and Poisson's ratio ν_t can be determined from [21]

$$D_t = \frac{2}{3}\left[\sum_{k=1}^{n}\frac{E_k}{1-\nu_k^2}\left(h_k^3 - h_{k+1}^3\right) + \frac{E_{n+1}h_{n+1}^3}{1-\nu_{n+1}^2}\right];$$
$$\nu_t = \frac{2}{3D_t}\left[\sum_{k=1}^{n}\frac{E_k\nu_k}{1-\nu_k^2}\left(h_k^3 - h_{k+1}^3\right) + \frac{E_{n+1}\nu_{n+1}h_{n+1}^3}{1-\nu_{n+1}^2}\right]. \tag{7.126}$$

Lekhnitskii [3] and Ambartsumyan [23] gave similar expressions for multilayered orthotropic plates.

7.6 SANDWICH PLATES

Sandwich plates are frequently used in aerospace structures, shipbuilding, building structures, etc. There are many varieties of sandwich construction, but the basic notion is to separate two thin flat sheets (skins or faces) of strong material (metal or fiber composite) by a core material that is lightweight and comparatively weak. The latter is a hardened foam or has a honeycomb or corrugated construction.

Figure 7.8 shows a rectangular sandwich plate of dimensions $a \times b$. The middle plane of the plate lies in the xy plane. The faces are each of thickness t and the core is of thickness c. The small-deflection theory of the sandwich plates was first developed by Libove and Batdorf [24]. The difference between the sandwich and classical plate bending theories is the low transverse shear stiffness of the core, which can no longer be neglected and must be included in all sandwich calculations.

Following Libove and Batdorf [24], we present below the small-deflection plate bending theory. It is based on the following assumptions:

(a) The faces are made from different orthotropic materials and they are assumed to be thin in comparison with the thickness of the core, i.e., $t \ll c$. Thus, the flexural rigidity of the faces can be neglected.
(b) The faces carry all the bending and twisting moments. The core makes no contribution to the bending stiffness of the sandwich plate.
(c) The core may also be orthotropic. The material of the core is assumed to be absolutely rigid in the direction perpendicular to the middle surface of

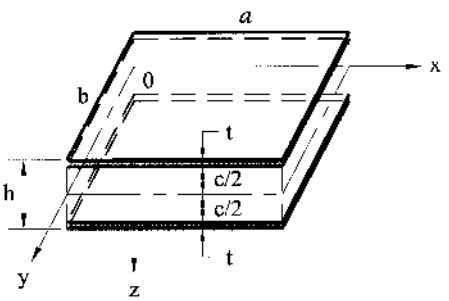

Fig. 7.8

the plate and quite compliant in the tangential direction. Therefore, only the transverse shear stresses τ_{xz} and τ_{yz} arise in the core material. They are nearly uniform throughout the thickness of the core.

(d) The x and y axes are the principal axes of orthotropy.

(e) A general small-deflection theory for flat orthotropic plates, in which deflections due to shear are taken into account, is applied to the sandwich plate. It is assumed that the sandwich behaves essentially as a plate, provided certain physical constants serve to describe the sandwich plate flexural behavior and they may be regarded as the fundamental properties of the plate.

These constants are:

– *flexural and twisting stiffnesses*, D_x, D_y, and D_{xy}:

$$D_x = -\frac{M_x}{\partial^2 w/\partial x^2}, \quad D_y = -\frac{M_y}{\partial^2 w/\partial y^2}; \quad D_{xy} - \frac{M_{xy}}{\partial^2 w/\partial x \partial y}.$$

– *the two transverse stiffnesses*, D_{Qx} and D_{Qy}:

$$D_{Qx} = \frac{Q_x}{\gamma_{xz}}, \quad D_{Qy} = \frac{Q_y}{\gamma_{yz}}. \tag{7.127}$$

– *the two Poisson's ratios*, ν_x and ν_y:

$$\nu_x = \frac{\partial^2 w/\partial y^2}{\partial^2 w/\partial x^2}, \quad \nu_y = -\frac{\partial^2 w/\partial x^2}{\partial^2 w/\partial y^2}.$$

The four constants, D_x, D_y, ν_x, and ν_y are not independent of each other. If three of them are known, the fourth can be determined from the following relation:

$$\nu_x D_y = \nu_y D_x,$$

which can be derived from Betti's reciprocal theorem [4]. For simpler types of sandwich construction the physical constants can be evaluated theoretically from the geometry and physical properties of the material used. For more complicated types of construction, these constants can be evaluated experimentally only. In the general case of the orthotropic faces and core, the expressions for the rigidities introduced above are presented for some practically important cases in Refs [26,27].

Let w be the deflection of the middle surface of the sandwich plate; the stress resultants and stress couples are also associated with the plate middle surface. We apply the same sign convention for the bending moments, and shear and in-plane forces as for homogeneous plates in Chapter 2. The deflection of the sandwich plates is produced by bending in the faces and by shear in the core. Thus, the curvatures in the xz and yz directions are made up of the components that are due to the bending moments, M_x and M_y, and that are due to the variation of the shear forces, Q_x and Q_y. The differential equations for the bending curvatures $\partial^2 w/\partial x^2$ can be represented in the form

$$\frac{\partial^2 w}{\partial x^2} = -\frac{M_x}{D_x} + \nu_y \frac{M_y}{D_y} + \frac{1}{D_{Q_x}} \frac{\partial Q_x}{\partial x}; \quad \frac{\partial^2 w}{\partial y^2} = \nu_x \frac{M_x}{D_x} - \frac{M_y}{D_y} + \frac{1}{D_{Q_y}} \frac{\partial Q_y}{\partial y}. \tag{7.128a}$$

The twist, $\partial^2 w/\partial x \partial y$, is also made up of the components due to the twisting moment, M_{xy}, and that due to the variation of the shear forces, Q_x and Q_y. The differential equation of the twist curvature is given by

$$\frac{\partial^2 w}{\partial x \partial y} = -\frac{M_{xy}}{D_{xy}} + \frac{1}{2}\frac{1}{D_{Q_x}}\frac{\partial Q_x}{\partial y} + \frac{1}{2}\frac{1}{D_{Q_y}}\frac{\partial Q_y}{\partial x}. \tag{7.128b}$$

It is convenient to invert Eqs (7.128) as follows:

$$\begin{aligned}
M_x &= -D_x^*\left[\frac{\partial}{\partial x}\left(\frac{\partial w}{\partial x} - \frac{Q_x}{D_{Q_x}}\right) + \nu_y \frac{\partial}{\partial y}\left(\frac{\partial w}{\partial y} - \frac{Q_y}{D_{Q_y}}\right)\right];\\
M_y &= -D_y^*\left[\frac{\partial}{\partial y}\left(\frac{\partial w}{\partial y} - \frac{Q_y}{D_{Q_y}}\right) + \nu_x \frac{\partial}{\partial x}\left(\frac{\partial w}{\partial x} - \frac{Q_x}{D_{Q_x}}\right)\right];\\
M_{xy} &= -\frac{D_{xy}}{2}\left[\frac{\partial}{\partial x}\left(\frac{\partial w}{\partial y} - \frac{Q_y}{D_{Q_y}}\right) + \frac{\partial}{\partial y}\left(\frac{\partial w}{\partial x} - \frac{Q_x}{D_{Q_X}}\right)\right],
\end{aligned} \tag{7.129}$$

where

$$D_x^* = \frac{D_x}{1-\nu_x\nu_y}; \quad D_y^* = \frac{D_y}{1-\nu_x\nu_y}. \tag{7.130}$$

Substituting the relations (7.129) into the equilibrium equations, Eqs (2.19)–(2.22), one finds

$$\begin{aligned}
(D_{xy} + \nu_y D_x^*)\frac{\partial^3 w}{\partial x \partial y^2} + D_x^*\frac{\partial^3 w}{\partial x^3} &= \frac{D_x^*}{D_{Qx}}\frac{\partial^2 Q_x}{\partial x^2} + \frac{1}{2}\frac{D_{xy}}{D_{Qx}}\frac{\partial^2 Q_x}{\partial y^2}\\
&\quad + \left(\frac{1}{2}\frac{D_{xy}}{D_{Q_y}} + \frac{\nu_y D_x^*}{D_{Q_y}}\right)\frac{\partial^2 Q_y}{\partial x \partial y} - Q_x,
\end{aligned} \tag{7.131a}$$

$$\begin{aligned}
\left(D_{xy} + \nu_x D_y^*\right)\frac{\partial^3 w}{\partial x^2 \partial y} + D_y^*\frac{\partial^3 w}{\partial y^3} &= \frac{D_y^*}{D_{Q_y}}\frac{\partial^2 Q_y}{\partial y^2} + \frac{1}{2}\frac{D_{xy}}{D_{Q_y}}\frac{\partial^2 Q_y}{\partial x^2}\\
&\quad + \left(\frac{1}{2}\frac{D_{xy}}{D_{Q_x}} + \frac{\nu_x D_y^*}{D_{Q_x}}\right)\frac{\partial^2 Q_x}{\partial x \partial y} - Q_y,
\end{aligned} \tag{7.131b}$$

$$\frac{\partial Q_x}{\partial x} + \frac{\partial Q_y}{\partial y} = -p. \tag{7.131c}$$

This is the *system of the governing differential equations in* w, Q_x, and Q_y *for the small-deflection theory of sandwich plate bending problems* based on the assumptions introduced earlier.

Assuming general values for the middle surface deflection w and the shear forces Q_x and Q_y, which satisfy Eqs (7.131) and the relevant boundary conditions, it is possible to solve a number of bending problems of sandwich plates. The boundary conditions on the edges of the sandwich plate should be consistent with Eqs (7.131). We present below a simplified variant of the boundary conditions: namely,

(a) *Simply supported edge* ($y = \text{const}$) in which all points in the boundary are prevented from moving parallel to the edge.

$$w = 0, \quad M_y = 0, \quad \frac{Q_x}{D_{Qx}} = 0. \tag{7.132a}$$

(b) *Free edge* ($y = \text{const}$)

$$M_y = 0, \quad M_{xy} = 0, \quad Q_y = 0. \tag{7.132b}$$

(c) *Clamped edge* ($y = \text{const}$) in which the points in the boundary are prevented from moving parallel to the edge.

$$w = 0, \quad \frac{Q_x}{D_{Qx}} = 0, \quad \frac{\partial w}{\partial y} - \frac{Q_y}{D_{Qy}} = 0. \tag{7.132c}$$

Similarly, the boundary conditions may be formulated on edges $x = \text{const}$.

Let us consider a special case of the *sandwich plate having isotropic faces of equal thicknesses and an isotropic non-direct stress-carrying core*. For this special case, assuming that $t \ll c$, we have

$$\begin{gathered} D_x^* = D_y^* = D_s = \frac{E_{\mathrm{f}} t d^2}{2(1-\nu_{\mathrm{f}}^2)}; \quad \nu_x = \nu_y = \nu_{\mathrm{f}}; \\ D_{Q_x} = D_{Q_y} = D_Q = G_{\mathrm{c}} \frac{d^2}{c}; \quad D_{xy} = D_s(1-\nu_{\mathrm{f}}), \end{gathered} \tag{7.133}$$

where E_{f} and ν_{f} are the modulus of elasticity and Poisson's ratio, respectively, of isotropic sandwich plate faces; G_{c} is the modulus of rigidity of the isotropic core; $d = c + t$ is the distance between the centerlines of the faces; D_s and D_Q are the flexural and transverse shear stiffnesses of the isotropic sandwich plate.

For this special case, the system of the three governing differential equations (7.131) can be reduced to a single equation. In fact, the equations of equilibrium (Eqs (2.19)–(2.22)) are reduced to Eq. (2.23). Substituting for M_x, M_y, and M_{xy} from Eqs (7.129) into Eq. (2.23) and taking into account the relations (7.133), one obtains

$$D_s \nabla^2 \nabla^2 w - \frac{D_s}{D_Q}\left(\frac{\partial^3 Q_x}{\partial x^3} + \frac{\partial^3 Q_y}{\partial y^3} + \frac{\partial^3 Q_x}{\partial x \partial y^2} + \frac{\partial^3 Q_y}{\partial x^2 \partial y}\right) = p. \tag{7.134}$$

It can be easily verified that the following equality takes place:

$$\frac{\partial^3 Q_x}{\partial x^3} + \frac{\partial^3 Q_y}{\partial y^3} + \frac{\partial^3 Q_x}{\partial x \partial y^2} + \frac{\partial^3 Q_y}{\partial x^2 \partial y} = \nabla^2\left(\frac{\partial Q_x}{\partial x} + \frac{\partial Q_y}{\partial y}\right) = -\nabla^2 p.$$

Thus, Eq. (7.134) finally can be rewritten in the following form:

$$D_s \nabla^2 \nabla^2 w = \left(1 - \frac{D_s}{D_Q}\nabla^2\right) p. \tag{7.135}$$

This is the *governing differential equation of the isotropic sandwich plate*. In the limiting case when $G_{\mathrm{c}} \to \infty$, Eq. (7.135) is reduced to the governing differential equation of isotropic homogeneous plate bending, Eq. (2.24) with the flexural stiffness D_s, i.e., with the stiffness of the composed section consisting of the two layers of thickness t each and separated by a distance c. In another limiting case when $G_{\mathrm{c}} \to 0$, Eq. (7.135) is reduced to the corresponding equation for the separated faces.

Here only basic concepts have been given of the theory of sandwich plates. The interested reader is referred to Refs [24–28].

PROBLEMS

7.1 Calculate the maximum deflection and maximum moments in Example 7.1 of Sec. 7.1. Take $m = n = 1$, $T = T_0 z/h$, $b = 2a$, $\nu = 0.3$.

7.2 Redo Problem 7.1 for the temperature field given by $T = T_0(2z/h)$.

7.3 With reference to Eqs. (7.8), derive the additional potential energy for the thermal bending and thermal stretching into the total potential energy of the plate (Eq. (2.60)).

7.4 Consider a built-in edge, rectangular plate ($-a/2 \le x \le a/2$, $-b/2 \le y \le b/2$) under a transverse temperature field $T = T_0(z^2/h)$. Find the expression for the deflection surface of the plate. Use the Ritz method and results of the Problem 7.3. Assume that w is given by

$$w = \frac{1}{4} w_0 \left(1 + \cos\frac{2\pi x}{a}\right)\left(1 + \cos\frac{2\pi y}{b}\right).$$

7.5 A simply supported plate with sides $a = 35$ in. and $b = 45$ in. and having a thickness of 3 in. is heated from both top and bottom such that, at a certain time, three thermocouples read $T(+h/2) = 350^\circ$F, $T(0) = 100^\circ$F, and $T(-h/2) = 350^\circ$F. If the stress-free temperature is 80°F, calculate the maximum deflection of the plate. Retain only one term ($m = n = 1$) in the series solution. Assume that the plate is made of aluminum with the following mechanical parameters: $E_{al} = 10 \times 10^6$ psi, $\alpha_{al} = 10 \times 10^{-6}$in./in.$^\circ$F , and $\nu = 0.3$.

7.6 Verify Eq. (7.32).

7.7 A rectangular, simply supported plate with sides a and b ($b = 1.5a$) is reinforced by single equidistant stiffeners (Fig. 7.1a). Compute the maximum deflection, w_{max}. The plate and stiffeners are made of steel with $E = 200$ GPa, $\nu = 0.3$. Take $a = 1280$ mm, $t = 180$ mm, $h = 40$ mm, and $H_1 = 80$ mm.

7.8 Determine the rigidities of a steel bridge deck that may be approximated as a steel plate reinforced by a set of equidistant ribs in one direction (Fig. 7.1b). Take $h = 12$ mm, $H_1 = 36$ mm, $t = 120$ mm, $E = 210$ GPa, $\nu = 0.3$, and the torsional rigidity of one rib is $C = JG = 0.246b^3(H_1 - h)G$.

7.9 A rectangular, simply supported building floor slab with sides a and b is made of reinforced concrete. It is subjected to a uniformly distributed load of intensity p_0. Determine the expressions for (a) the deflection surface and (b) the bending moments. Take $b = 2a$, $m = n = 1$, $t_1 = a/10$, $t_2 = a/8$, $h = a/15$, $d_2 = d_1 = h/10$, $E_c = 21.4$ GPa, $\nu_c = 0.15$, $E_s = 200$ GPa, $\nu_s = 0.28$.

7.10 Find the maximum stresses in a simply supported rectangular plate with sides a and b. The plate is subjected to a uniformly applied load of intensity p_0. It is constructed of a alumina/epoxy laminate with $E_x = 33,000$ ksi, $E_y = 3000$ ksi, $G = 1000$ ksi, $\nu_x = 0.28$, and $\nu_y = 0.3$. Let $a = 35$ in., $b = 20$ in., and $h = 0.20$ in. Compare the result with that of an equivalent isotropic plate of $E = 17400$ ksi and $\nu = 0.35$.

7.11 An infinitely long plate of Example 7.3 of Sec. 7.2 is reinforced by a set of equidistant ribs in the x direction (Fig. 7.1b). The plate is subjected to a uniformly distributed load of intensity p_0. Determine the deflections and bending moments in the plate if $a = 12$ ft., $t = 12$ in., $h = 0.2$ in., $H_1 = 2.5$ in., and $b = 1.5$ in. Assume that the plate and ribs are made of the same material with $E = 30{,}000$ ksi and $\nu = 0.3$. Retain only one term in the series solution.

7.12 Verify Eq. (7.39).

7.13 Determine the particular solution of Eq. (7.39) for an orthotropic circular plate subjected to a concentrated force P applied at its center.

7.14 A circular, simply supported plate of radius R is reinforced by equidistant annular ribs (Fig. 7.3a). The plate is subjected to a uniform load p_0. Determine the maximum allowable value of p_0 if $w_{max} = 0.2$ in. Take $R = 10$ ft, $h = 1$ in., $t = 10$ in., $b = 4$ in.,

and $h_1 = 6$ in. Assume that the plate and ribs are made of the same material with $E = 29{,}000$ ksi and $\nu = 0.29$.

7.15 Verify Eqs (7.55) and (7.56).

7.16 Verify the boundary conditions for the free edge given by Eqs (7.70).

7.17 Solve the problem of Example 3.1 within the framework of the refined (shear) plate bending theory. Determine the deflection surface w and the bending moments M_x and M_y. Check the overall equilibrium of the plate.

7.18 Verify Eq. (7.87).

7.19 Transform Eqs (7.86) to plane polar coordinates r and φ. Show that in this case

$$N_r = \frac{1}{r}\frac{\partial \Phi}{\partial r} + \frac{1}{r^2}\frac{\partial^2 \Phi}{\partial \varphi^2}, \quad N_t = \frac{\partial^2 \Phi}{\partial r^2}, \quad N_{rt} = -\frac{\partial}{\partial r}\left(\frac{1}{r}\frac{\partial \Phi}{\partial \varphi}\right), \quad \text{and} \tag{P7.1}$$

$$\nabla^2\nabla^2 \Phi = -\frac{1}{2} EhL(w, w),$$

$$\nabla^2\nabla^2 w = \frac{1}{D}[p + L(w, \Phi)], \tag{P7.2}$$

where

$$L(w, \Phi) = \frac{\partial^2 w}{\partial r^2}\left(\frac{1}{r}\frac{\partial \Phi}{\partial r} + \frac{1}{r^2}\frac{\partial^2 \Phi}{\partial \varphi^2}\right) + \left(\frac{1}{r}\frac{\partial w}{\partial r} + \frac{1}{r^2}\frac{\partial^2 w}{\partial \varphi^2}\right)\frac{\partial^2 \Phi}{\partial r^2} - 2\frac{\partial}{\partial r}\left(\frac{1}{r}\frac{\partial \Phi}{\partial \varphi}\right)\frac{\partial}{\partial r}\left(\frac{1}{r}\frac{\partial w}{\partial \varphi}\right) \tag{P.7.3}$$

and $L(w, w)$ is obtained by replacing Φ with w in the above equation.

7.20 Consider a rectangular isotropic, sandwich plate shown in Fig. 7.8. Following Plantema [28], introduce w_b and w_s as follows

$$w = w_b + w_s, \quad \gamma_{xz} = \frac{\partial w_s}{\partial x}, \quad \gamma_{yz} = \frac{\partial w_s}{\partial y}, \tag{P.7.4}$$

where w_b and w_s are the deflections of the above plate due to bending and shear, respectively. Show that Eqs (7.127), (7.129), and (7.135) will be transformed in terms of the partial deflections to the following relations and equations

$$M_x = -D_s\left(\frac{\partial^2 w_b}{\partial x^2} + \nu\frac{\partial^2 w_b}{\partial y^2}\right), \quad M_y = -D_s\left(\frac{\partial^2 w_b}{\partial y^2} + \nu\frac{\partial^2 w_b}{\partial x^2}\right),$$

$$M_{xy} = -D_s(1 - \nu)\frac{\partial^2 w_b}{\partial x \partial y},$$

$$Q_x = D_Q\frac{\partial w_s}{\partial x}, \quad Q_y = D_Q\frac{\partial w_s}{\partial y}, \tag{P7.5}$$

$$\nabla^2\nabla^2 w_b = \frac{1}{D_s}p(x, y). \tag{P7.6}$$

Verify also that the relationship between the partial deflections is of the form

$$w_s = -\frac{D_s}{D_Q}\nabla^2 w_b + C, \tag{P7.7}$$

where C is an arbitrary integration constant which is to be determined from boundary conditions prescribed for w_s on the plate edges (see [27] for more detail). For a verification of Eq. (P7.7), use Eqs (2.22) together with Eqs (P7.2).

REFERENCES

1. Boley, B.A. and Weiner, J.H., *Theory of Thermal Stresses*, John Wiley and Sons, New York, 1960.
2. Johns, D.J., *Thermal Stress Analysis*, Pergamon Press, Elmsford, New York, 1965.
3. Lekhnitskii, S.G., *Anisotropic Plates*, Gordon and Breach, New York, 1968.
4. Timoshenko, S.P and Woinowski-Krieger S., *Theory of Plates and Shells*, 2nd. edn, McGraw-Hill, New York, 1959.
5. Boyarshinov SV., *The Fundamentals of Structural Mechanics of Machines*, Mashinostroenie, Moscow, 1973 (in Russian).
6. Troitsky, M.S., *Orthotropic Bridges – Theory and Design*, The James Lincoln Arc Welding Foundation, Cleveland, 1987.
7. Huffington, H.J., Theoretical determination of rigidity properties of orthotropic stiffened plates, *J Appl Mech*, vol. 23, No. 1, pp. 15–20 (1956).
8. Donnel, L.H., *Beams, Plates, and Shells*, McGraw-Hill, New York, 1976.
9. Alfutov, N.A., On paradoxes of the theory of thin elastic plates, *Mechanics of Solids*, No. 3, pp. 65–72 (1992).
10. Reissner, E., On the theory of bending of elastic plates, *J Math Phys*, vol. 23, 184–191 (1944).
11. Reissner, E., The effect of transverse shear deformation on the bending of elastic plates, *J Appl Mech*, vol. 12, pp A69–A77 (1945).
12. Vasil'ev, V.V., Classical theory of plates: historical perspective and state-of-the-art, *Mechanics of Solids*, vol. 33, No. 3, pp. 35–45 (1998).
13. Zihlin, P.A., On Poisson's and Kirchhoff's theories of plates from the point of view of the modern theory of plates, *Mechanics of Solids*, No. 3, pp. 65–72 (1992).
14. Green, A., On Reissner's theory of bending of elastic plates, *Quart Appl Math*, vol. 7, No. 2, pp. 223–228 (1949).
15. Mindlin, R.D., Influence of rotary inertia and shear on flexural motions of isotropic elastic plates, *J Appl Mech*, vol. 18, No.1, pp. 31–38 (1951).
16. Reddy, J.N., *Energy and Variational Methods in Applied Mechanics*, John Wiley and Sons, New York, 1984.
17. Von Karman, Th., *Encyklop. die der Mathematischen*, Wissenschaften, vol .IV, 1910.
18. Levy, S., Large deflection theory for rectangular plates, *Proc. Symp. on Non-Linear Problems, Symp Appl Math*., I, pp. 197–210 (1947).
19. Volmir, A.S., *Flexible Plates and Shells*, AFFDL-TR-66-216, Air Force Flight Dynamics Laboratory, Wright-Patterson Air Force Base, Ohio, 1967.
20. Zienkiewitcz, D.C., *The Finite Element Method*, McGraw-Hill, New York, 1977.
21. Alexandrov, A.P. and Potapov, V.D., *The Fundamentals of the Theory of Elasticity and Plasticity*, Izd-vo "Vyshaia Shkola," Moscow, 1990 (in Russian).
22. Pister, K.S. and Dong, S.B., Elastic bending of layered plates, *Proc ASCE J Eng Mech Div*, October, 84, pp. 1–10 (1950).
23. Ambartsumyan, S.A., *Theory of Anisotropic Plates* (translation from the Russian), Technomic, Stamford, CT, 1970.
24. Libove, C. and Butdorf, S.B., *A General Small-Deflection Theory for Flat Sandwich Plates*, NACA TN 1526, 1948.
25. Robinson, J.R., The buckling and bending of orthotropic sandwich plates with all edges simply supported, *Aeronautical Quart*, vol. 6, No. 2, pp. 125–148 (1955).
26. Libove, C. and Hubka, R.E., *Elastic Constants for Corrugated Core Sandwich Plates*, NACA TN 2289, 1951.
27. Allen, H.G., *Analysis and Design of Structural Sandwich Panels*, Pergamon Press, London, 1969.
28. Plantema, F.J., *Sandwich Construction*, John Wiley and Sons, New York, 1966.

8

Buckling of Plates

8.1 INTRODUCTION

Thin plates of various shapes used in naval and aeronautical structures are often subjected to normal compressive and shearing loads acting in the middle plane of the plate (in-plane loads). Under certain conditions such loads can result in a plate buckling. Buckling or elastic instability of plates is of great practical importance. The buckling load depends on the plate thickness: the thinner the plate, the lower is the buckling load. In many cases, a failure of thin plate elements may be attributed to an elastic instability and not to the lack of their strength. Therefore, plate buckling analysis presents an integral part of the general analysis of a structure.

In this chapter, we consider a systematic but simplified analysis of plate buckling and obtain some useful relations between the critical loads and plate parameters.

8.2 GENERAL POSTULATIONS OF THE THEORY OF STABILITY OF PLATES

This section contains some fundamentals of classical stability analysis of thin elastic plates. It should be noted that the stability analysis of plates is qualitatively similar to the Euler stability analysis of columns [1].

Consider an ideal thin, elastic plate which is assumed initially to be perfectly flat and subjected to external in-plane compressive and shear loads acting strictly in the middle plane of the plate. The resulting deformations of this plate are characterized by the absence of deflections ($u \neq 0$, $v \neq 0$, and $w = 0$) and, consequently, of the bending and twisting moments, as well as the transverse shear forces. Such a plane stress condition of the plate is referred to as an *initial* or *flat configuration of equilibrium,* assuming the equilibrium conditions between applied external loads and the corresponding in-plane stress resultants.

Depending mainly on values of the applied in-plane loads, an initial, flat configuration of a plate equilibrium may be stable or unstable. The initial configuration of elastic equilibrium is *stable*, if when the plate is displaced from this equilibrium state by an infinitesimal disturbance, say a small lateral force, the deflected plate will tend to come back to its initial, flat configuration when the disturbance is removed. The initial configuration of equilibrium is said to be *unstable* if, when the plate is displaced from this equilibrium position by a small lateral load, it will tend to displace still further when the load is removed. The unstable plate will find other (new) equilibrium state(s), which may be in the vicinity of the initial state or may be far away from the initial equilibrium configuration. If the plate remains at the displaced position even after the small lateral load is removed, it is said to be in *neutral equilibrium*; thus, the plate in neutral equilibrium is neither stable nor unstable.

The transition of the plate from the stable state of equilibrium to the unstable one is referred to as *buckling* or *structural instability*. The smallest value of the load producing buckling is called the *critical* or *buckling load*.

The importance of buckling is the initiation of a deflection pattern, which if the loads are further increased above their critical values, rapidly leads to very large lateral deflections. Consequently, it leads to large bending stresses, and eventually to complete failure of the plate.

It is important to note that a plate leading from the stable to unstable configuration of equilibrium always passes through the neutral state of equilibrium, which thus can be considered as a bordering state between the stable and unstable configurations. In the mathematical formulation of elastic stability problems, neutral equilibrium is associated with the existence of bifurcation of the deformations. According to this formulation, the *critical load can be identified with the load corresponding to the bifurcation of the equilibrium states, or in other words, the critical load is the smallest load at which both the flat equilibrium configuration of the plate and slightly deflected configuration are possible*.

The goal of the buckling analysis of plates is to determine the critical buckling loads and the corresponding buckled configuration of equilibrium. We consider below the linear buckling analysis of plates based on the following assumptions:

(a) Prior to loading, a plate is ideally flat and all the applied external loads act strictly in the middle plane of the plate.
(b) States of stress is described by equations of the linear plane elasticity. Any changes in the plate dimensions are neglected prior to buckling.
(c) All the loads applied to the plate are dead loads; that is, they are not changed either in magnitude or in direction when the plate deforms.
(d) The plate bending is described by Kirchhoff's plate bending theory discussed in Chapter 2.

The linear buckling analysis of plates based on these assumptions makes it possible to determine accurately the critical loads, which are of practical importance in the stability analysis of thin plates. However, this analysis gives no way of describing the behavior of plates after buckling, which is also of considerable interest. The postbuckling analysis of plates is usually difficult because it is basically a nonlinear problem. Some postbuckling plate problems will be discussed in Sec. 8.5. Classical

buckling problems of plates can be formulated using (1) the equilibrium method, (2) the energy method, and (3) the dynamic method.

The equilibrium method

Consider an initial state of equilibrium of a plate subjected to the external edge loads acting in the middle plane of the plate. Let the corresponding in-plane stress resultants in this initial state be N_x, N_y, and N_{xy}. They may be found from the solution of the plane stress problem for the given plate geometry and in-plane external loading. However, for a complex plate geometry and complex in-plane load configurations, such a problem may involve sufficient difficulties. We confine the bucking analysis in this chapter by considering such load configurations and plate geometry, when determining the above-mentioned in-plane resultants presents no difficulties, and they can be directly expressed via the given external forces. Note that such problems are of a practical importance. Next, assume that for certain values of the external forces, the plate has buckled slightly. We formulate the differential equation of equilibrium for this neighboring state assuming that the latter represents a slightly bent configuration of equilibrium. For the plate, the in-plane external edge loads that result in an elastic instability as in the case of a beam column, are independent of the lateral loads. Thus, the governing differential equation of the linear buckling analysis of plates is obtained from Eq. (3.92) by making p equal zero. We have the following:

$$\frac{\partial^4 w}{\partial x^4} + 2\frac{\partial^4 w}{\partial x^2 \partial y^2} + \frac{\partial^4 w}{\partial y^4} = \frac{1}{D}\left(N_x \frac{\partial^2 w}{\partial x^2} + 2N_{xy}\frac{\partial^2 w}{\partial x \partial y} + N_y \frac{\partial^2 w}{\partial y^2}\right), \tag{8.1}$$

where N_x, N_y, and N_{xy} are the internal forces acting in the middle surface of the plate due to the applied in-plane loading. The right-hand side of Eq. (8.1) can be interpreted as some fictitious, transverse surface load, p_f, created by the normal projections of the in-plane internal forces acting in the slightly curved configuration of the plate.

Equation (8.1) is a homogeneous, partial differential equation. The mathematical problem is to solve this equation with appropriate homogeneous boundary conditions. In general, such a problem has only a trivial solution corresponding to the initial, flat configuration of equilibrium (i.e., $w = 0$). However, the coefficients of the governing equation depend on the magnitudes of the stress resultants, which are, in turn, connected with the applied in-plane external forces, and we can find values of these loads for which a nontrivial solution is possible. The smallest value of these loads will correspond to a critical load.

A more general formulation of the equilibrium method transforms the stability problem into an eigenvalue problem. For this purpose, we multiply a reference value of the stress resultants ($\bar{N}_x$, $\bar{N}_y$, and $\bar{N}_{xy}$) by a load parameter λ, i.e.,

$$N_x = -\lambda \bar{N}_x, \quad N_y = -\lambda \bar{N}_y, N_{xy} = -\lambda \bar{N}_{xy}. \tag{8.2}$$

Substituting Eqs (8.2) into Eq. (8.1), we obtain an alternative form of the governing differential equation of plate buckling problems:

$$\nabla^4 w + \frac{\lambda}{D}\left(\bar{N}_x \frac{\partial^2 w}{\partial x^2} + \bar{N}_y \frac{\partial^2 w}{\partial y^2} + 2\bar{N}_{xy}\frac{\partial^2 w}{\partial x \partial y}\right) = 0. \tag{8.3}$$

The solution of Eq. (8.3), $w(x, y)$, obtained by some analytical or numerical methods, introduced in Chapters 3 and 6, involves arbitrary constant coefficients C_i $(i = 1, 2, \ldots, n)$ to be determined from the prescribed boundary conditions. Consequently, Eq. (8.3) is reduced to a system of homogeneous, linear algebraic equations in C_i. For an existence of a nontrivial solution of the system, its determinant must be equal to zero. This results in the so-called characteristic equation in λ. Solving this characteristic equation, we obtain some specific values $\lambda_1, \lambda_2, \ldots, \lambda_n$ (the *characteristic numbers* or *eigenvalues*) and the corresponding nonzero solutions, called *characteristic functions* or *eigenfunctions*. The smallest of the characteristic numbers or eigenvalues not equal to zero will be the *critical value*, λ_{cr}, and the corresponding eigenfunctions will be the *buckling modes*. Then, the critical load is calculated by multiplying λ_{cr} and the corresponding reference value of the load.

The energy method

The energy method is based on the general theorems and principles of the equilibrium of mechanical systems discussed in Sec. 2.6. As mentioned in Sec. 2.6, the potential energy of a system has an extremum at equilibrium. Based on this statement, we can reformulate the concepts of stability and instability presented earlier. The equilibrium will be *stable* if the potential energy in that state has a minimum value in comparison with values corresponding to any possible states close to the state of equilibrium, *unstable* if the potential energy is a maximum, and *neutral* if the potential energy in the equilibrium state is neither a maximum nor a minimum.

Let us apply this potential energy criterion to the buckling analysis of plates. Two states of the plate are considered: an initial state of equilibrium under the given in-plane edge loads, in which the middle surface remains flat; a neighboring state, in which the middle surface is slightly curved due to small virtual displacements applied to the plate. Let Π_0 and Π be the potential energies in the flat and neighboring states of equilibrium, respectively. The equilibrium will be stable if for all possible small deflections $\Pi_0 < \Pi$, unstable if $\Pi_0 > \Pi$, and neutral if $\Pi_0 = \Pi$.

The increment in the total potential energy of the plate loaded by the edge in-plane external loads, after the transition of this plate from an initial configuration of equilibrium to the above-mentioned neighboring configuration of equilibrium is given by the following relationship:

$$\Delta\Pi = \Pi - \Pi_0 = \Delta U_0 + U_b + \Delta\Omega_\Gamma, \tag{8.4}$$

where ΔU_0 is the increment of the strain energy of the plate middle surface in buckling; U_b is the strain energy of bending and twisting of the plate; and $\Delta\Omega_\Gamma$ is the increment in the potential of the in-plane external edge forces applied to the plate. Bifurcation of an initial configuration of equilibrium (corresponding to the neutral equilibrium) occurs when

$$\Delta\Pi = 0. \tag{8.5a}$$

This is *the general energy criterion for the buckling analysis of plates* (*and shells also*). The critical loads may be determined from this criterion at an additional condition of the minimum of the load parameter λ.

It can be shown [1,2] that the governing differential equation (8.1) can be obtained from the condition (8.5a). The latter can also be employed for constructing an approximate solution of the plate buckling problems, in particular for determin-

ing the critical loads, by the Ritz method (see Sec. 6.6). In this case, the deflection surface of the plate, $w(x, y)$, in the neighboring state of equilibrium is sought in the form of Eq. (6.42). If all external forces acting on the plate vary in the proportion to a load parameter λ, then substituting Eq. (6.42) into the condition (8.5a) yields

$$\Delta\Pi = \Delta\Pi(\lambda, C_1, C_2, \ldots, C_n) = 0, \tag{8.5b}$$

where C_i $(i = 1, 2, \ldots, C_n)$ are undetermined coefficients. Numerical implementation of the conditions (8.5) requires the usual minimization process (Eq. (6.44)). The latter also leads to a system of linear algebraic, homogeneous equations. So, applying the procedure discussed earlier for determining a nontrivial solution in the equilibrium method, we can find all the characteristic numbers λ_i, and their smallest value corresponding to the critical eigenvalue, λ_{cr}.

Dynamic or kinematic method

This method is the most general and universal and is associated with the mathematical problem of the stability of motion. The method is based on examining transverse oscillations of a thin plate subjected to in-plane edge loads. The smallest value of the load that results in unbounded growth of the amplitude of these oscillations in time is considered as a critical value of the applied loads.

The equilibrium and energy methods are now discussed in more detail.

8.3 THE EQUILIBRIUM METHOD

8.3.1 Buckling of rectangular plates

According to the equilibrium method, the critical values of applied in-plane forces may be found from the solution of the governing differential equation (8.1) or its equivalent analog (8.3). As mentioned in Sec. 8.2, this equation is a homogeneous, linear partial differential equation with, generally speaking, variable coefficients. It is impossible to find its analytical solution in the general case. However, for some particular but practically important cases this equation makes it possible to obtain an exact solution. The following examples illustrate the equilibrium method for obtaining the exact solutions associated with determining the critical forces in rectangular plates.

Example 8.1

Determine the critical buckling load for a simply supported plate subjected to a uniformly distributed compressive edge load q_x acting in the x direction, as shown in Fig. 8.1.

Solution

For this particular case $N_x = -q_x$ and $N_y = N_{xy} = 0$. The differential equation (8.1) becomes

$$D\nabla^2\nabla^2 w + N_x \frac{\partial^2 w}{\partial x^2} = 0. \tag{8.6}$$

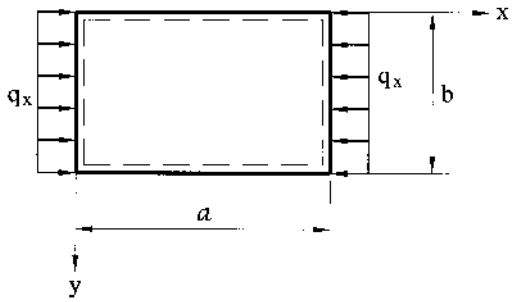

Fig. 8.1

We seek the solution of this equation in the form of Eq. (3.15a) that satisfies the simply supported boundary conditions. Inserting this solution into Eq. (8.1) leads to the following equation:

$$\sum_{m=1}^{\infty}\sum_{n=1}^{\infty}\left[D\pi^4\left(\frac{m^2}{a^2}+\frac{n^2}{b^2}\right)^2-q_x\pi^2\frac{m^2}{a^2}\right]w_{mn}\sin\frac{m\pi x}{a}\sin\frac{n\pi y}{b}=0.$$

One possible solution is $w_{mn}=0$; however, this represents the trivial solution, $w(x, y)=0$, and corresponds to an equilibrium in the unbuckled, flat state of the plate and is of no interest. Another possible solution is obtained by setting the quantity in square brackets to zero, or

$$\pi^4 D\left(\frac{m^2}{a^2}+\frac{n^2}{b^2}\right)^2-q_x\pi^2\frac{m^2}{a^2}=0,$$

from which

$$q_x=\frac{\pi^2 D}{b^2}\left(\frac{mb}{a}+\frac{n^2 a}{mb}\right)^2. \tag{a}$$

The constants w_{mn} remain undetermined. Expression (a) gives all values of q_x corresponding to $m=1, 2, 3, \ldots$; $n=1, 2, 3, \ldots$ as possible forms of the defected surface (Eq. (3.15a)). From all of these values one must select the smallest, which will be the critical value. Evidently the smallest value of q_x is obtained for $n=1$. For $n=1$ the formula for q_x takes the form

$$N_x=\frac{\pi^2 D}{b^2}\left(\frac{mb}{a}+\frac{a}{mb}\right)^2 \tag{8.7a}$$

or, in an equivalent form,

$$q_x=K\frac{\pi^2 D}{b^2}, \tag{8.7b}$$

where

$$K=\left(\frac{mb}{a}+\frac{a}{mb}\right)^2 \tag{8.8}$$

is the *buckling load parameter*. For a given value of m, the parameter K depends only on the ratio a/b, called the *aspect ratio* of the plate. As follows from Eqs (8.7) and (8.8), the smallest value of q_x, and consequently, the value of the critical force $q_{x,\mathrm{cr}}$, depends on the number of half-sine waves in the longitudinal direction, m. For a given aspect ratio the critical load is obtained by selecting m so that it makes Eq. (8.7b) a minimum. Since only K depends on m, we have the following:

$$\frac{\mathrm{d}K}{\mathrm{d}m} = 2\left(\frac{mb}{a} + \frac{a}{mb}\right)\left(\frac{b}{a} - \frac{a}{m^2 b}\right) = 0.$$

Since the first factor in parentheses of the above is nonzero, we obtain

$$m = \frac{a}{b}. \tag{8.9}$$

This provides the following minimum values of the critical load:

$$\min q_x = q_{x,\mathrm{cr}} = \frac{4\pi^2 D}{b^2}. \tag{8.10}$$

The corresponding value of the buckling load parameter is $K = 4$. The corresponding critical stress is found to be

$$\sigma_{x,\mathrm{cr}} = \frac{N_{x,\mathrm{cr}}}{h} = \frac{q_{x,\mathrm{cr}}}{h} = \frac{4\pi^2 D}{b^2 h} = \frac{\pi^2 E}{3(1-\upsilon^2)}\left(\frac{h}{b}\right)^2. \tag{8.11}$$

Thus, the critical values of q_x and σ_x correspond to such plate dimensions when its width, b, fits in its length, a, by whole numbers. In this case a bent plate is subdivided into square cells of side dimensions b. In the general case, $q_{x,\mathrm{cr}}$ may be determined from Eqs (8.7) and (8.8).

The variation of the buckling load parameter K as a function of the aspect ratio a/b for $m = 1, 2, 3, 4$ is shown in Fig. 8.2. Referring to this figure, the magnitude of $q_{x,\mathrm{cr}}$ and the number of half-waves m (in the direction of the applied compressive forces) for any value of the aspect ratio can readily be found. For example, if $a/b = 1.5$, we can find that $K = 4.34$ and $m = 2$. The corresponding critical load for this particular case is

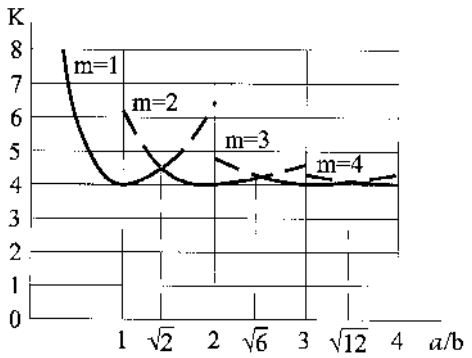

Fig. 8.2

$$q_{x,\mathrm{cr}} = 4.34\frac{\pi^2 D}{b^2}.$$

The plate will buckle under this load into two half-waves in the direction of the applied compressive loads and one-half in the perpendicular direction.

An analysis of the curves in Fig. 8.2 shows that for short and broad plates (for $a/b < 1$) a minimum value of the critical force is obtained for $m = 1$. For $a/b \ll 1$, that is for very short and broad plates, the ratio a/b can be neglected compared with the ratio b/a in Eq. (8.8). As a result, $\min.K \cong b^2/a^2$ and the value of the critical force for this particular case is

$$q_{x,\mathrm{cr}} = \frac{\pi^2 D}{a^2}.$$

Thus, in this case, the critical force does not depend on the plate width and depends only upon its length. The above expression represents the Euler critical load for a strip of unit width and of length a whose smallest value of flexural rigidity, EI, is replaced with the flexural rigidity of the plate, D.

Example 8.2

Determine the buckling critical load for a plate subjected to a uniformly distributed compressive edge load acting in the x direction. Assume that the edges $x = 0$ and $x = a$ are simply supported, the edge $y = 0$ is fixed, and the edge $y = b$ is free, as shown in Fig. 8.3.

Solution

It is convenient for this problem to employ Levy's method (see Sec. 3.5) for the solution. The boundary conditions at the edges $x = 0$ and $x = a$ will be automatically satisfied by setting

$$w(x, y) = \sum_{m=1}^{\infty} f_m(y) \sin\frac{m\pi x}{a}. \tag{a}$$

For this case, we also can set $N_x = -q_x$ and $N_y = N_{xy} = 0$. Substituting the above into Eq. (8.1) and imposing the condition that at least one of the terms multiplying $\sin(m\pi x/a)$ must vanish, we determine for $f_m(y)$ the following ordinary differential equation:

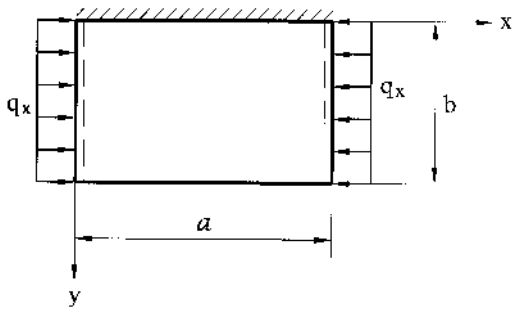

Fig. 8.3

$$\frac{d^4 f_m}{dy^4} - 2\left(\frac{m\pi}{a}\right)^2 \frac{d^2 f}{dy^2} + \left[\left(\frac{m\pi}{a}\right)^4 - \frac{q_x}{D}\left(\frac{m\pi}{a}\right)^2\right] f_m = 0. \tag{8.12}$$

The solution of Eq. (8.12) is shown below:

$$f_m(y) = C_1 e^{-\alpha y} + C_2 e^{\alpha y} + C_3 \cos \beta y + C_4 \sin \beta y, \tag{8.13}$$

where

$$\alpha, \beta = \left[\pm\left(\frac{m\pi}{a}\right)^2 + \sqrt{\frac{q_x}{D}\left(\frac{m\pi}{a}\right)^2}\right]^{1/2}. \tag{8.14}$$

The constants C_i $(i = 1, 2, 3, 4)$ are evaluated from the boundary conditions prescribed on the edges $y = 0$ and $y = b$, i.e.,

$$w = 0|_{y=0}, \quad \left.\frac{\partial w}{\partial y} = 0\right|_{y=0} \tag{8.15a}$$

$$\left. M_y = -D\left(\frac{\partial^2 w}{\partial y^2} + \nu \frac{\partial^2 w}{\partial x^2}\right) = 0\right|_{y=b}, \left. V_y = -D\left[\frac{\partial^3 w}{\partial y^3} + (2 - \nu)\frac{\partial^3 w}{\partial x \partial y^2}\right] = 0\right|_{y=b}. \tag{8.15b}$$

Introducing (a) with (8.13) into the boundary conditions (8.15a), we obtain two algebraic equations for the unknown constants. Solving the above equations, one finds

$$C_1 = -\frac{C_3}{2} + \frac{\beta C_4}{2\alpha}, \quad C_2 = -\frac{C_3}{2} - \frac{\beta C_4}{2\alpha}. \tag{b}$$

Substituting the above into Eq. (8.13), gives

$$f_m(y) = C_3(\cos \beta y - \cosh \alpha y) + C_4\left(\sin \beta y - \frac{\beta}{\alpha}\sinh \alpha y\right). \tag{8.16}$$

Introducing $w(x, y)$ with $f_m(y)$ in the form of Eq. (8.16) into the boundary conditions (8.15b) results in two simultaneous homogeneous algebraic equations. In order to obtain a nontrivial solution, we equate the determinant of these equations to zero, and obtain

$$2gh\left(g^2 + \zeta^2\right)\cos \beta b \cosh \alpha b = \frac{1}{\alpha\beta}\left(\alpha^2 \zeta^2 - \beta^2 g^2\right)\sin \beta b \sinh \alpha b, \tag{8.17}$$

where

$$g = \alpha^2 - \nu\left(\frac{m\pi}{a}\right)^2, \quad \zeta = \beta^2 + \nu\left(\frac{m\pi}{a}\right)^2.$$

For $m = 1$, the minimum eigenvalue of Eq. (8.17), i.e., the critical value of the applied force is

$$q_{x,\mathrm{cr}} = K\frac{\pi^2 D}{b^2}, \tag{8.18}$$

where for $\nu = 0.25$, $K = 1.328$.

It can be observed that a type of the plate boundary support has an effect on values of critical forces and buckling modes. For example, fixed supports increase a plates stability compared with hinged supports; the presence of a free edge leads to a

sharp decrease in critical forces, etc. If the boundary conditions of a plate differ from simply supported ones, determining the critical forces even for simple cases of loadings represents a sufficiently complicated mathematical problem and can be obtained by numerical methods only [2–8].

For rectangular plates subjected to uniform compressive forces acting in the direction of one coordinate axis only (either the x or the y axis) with various boundary conditions, the critical stress, σ_{cr}, can be determined from the expression

$$\sigma_{cr} = K\frac{\pi^2 D}{b^2 h}, \tag{8.19}$$

where the coefficients K are given in Fig. 8.4 versus the aspect ratios a/b [4].

Example 8.3

Determine the critical forces for the rectangular plate with simply supported edges and uniformly compressed in two directions, as shown in Fig. 8.5.

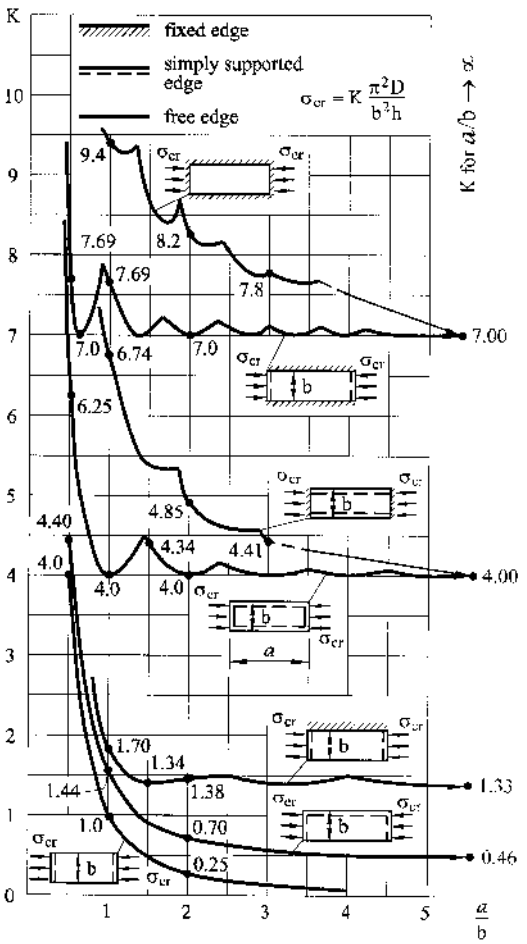

Fig. 8.4

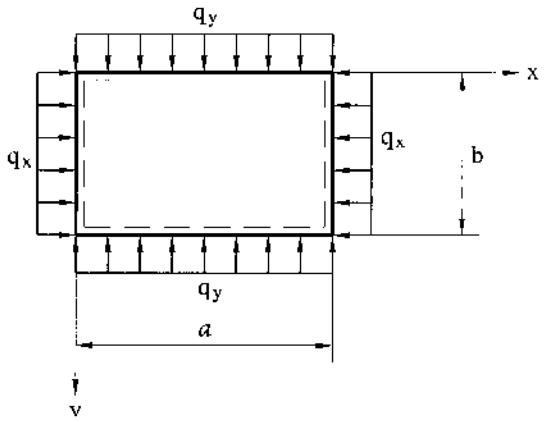

Fig. 8.5

Solution

For this problem, first analyzed by Bryan [9] in 1861, the stress resultants may be easily found: they are $N_x = -q_x$, $N_y = -q_y$, $N_{xy} = 0$. Equation (8.1) for this type of loading becomes

$$\frac{\partial^4 w}{\partial x^4} + 2\frac{\partial^4 w}{\partial x^2 \partial y^2} + \frac{\partial^4 w}{\partial y^4} + \frac{1}{D}\left(N_x \frac{\partial^2 w}{\partial x^2} + N_y \frac{\partial^2 w}{\partial y^2}\right) = 0. \tag{8.20}$$

Let us take w in the form of the expression (3.15a). The deflection surface equation in this form satisfies the simply supported boundary conditions. Substituting the above into Eq. (8.20) gives

$$w_{mn}\left\{\left(\frac{m^2}{a^2} + \frac{n^2}{b^2}\right)^2 - \frac{1}{\pi^2 D}\left[q_x \frac{m^2}{a^2} + q_y \frac{n^2}{b^2}\right]\right\} = 0. \tag{8.21}$$

The trivial solution of this equation is $w_{mn} = 0$. As mentioned earlier, this solution corresponds to unbuckled, i.e., flat, configuration of equilibrium of the plate and is of no interest for buckling analysis. A nontrivial solution can be obtained by equating the term in braces in Eq. (8.21) to zero, i.e.,

$$q_x\left(\frac{m}{a}\right)^2 + q_y\left(\frac{n}{b}\right)^2 = D\pi^2\left[\left(\frac{m}{a}\right)^2 + \left(\frac{n}{b}\right)^2\right]^2. \tag{8.22}$$

Let us consider *several particular cases:*

1. Assume, first, that $q_x = q_y = q = \text{const}$ (a uniform all-round compression). In this case, it follows from Eq. (8.22) that

$$q = \frac{\pi^2 D}{b^2}\left[n^2 + \left(\frac{mb}{a}\right)^2\right].$$

It can be easily shown that the minimum value of q, q_{cr}, corresponds to $m = n = 1$. Thus,

$$q_{cr} = \frac{\pi^2 D}{b^2}\left[1 + \left(\frac{b}{a}\right)^2\right]. \tag{8.23}$$

In particular, for the square plate ($a = b$), the above expression appears, as follows:

$$q_{cr} = 2\frac{\pi^2 D}{b^2}.$$

Hence, if the square plate is compressed in two directions by the two equal system of forces, q, the critical value of these forces is two times less than that for the square plate compressed by the same force acting in one direction only (see Example 8.1).

2. Assume now that the compressive forces q_x and q_y applied to the plate of Fig. 8.5 will increase in the proportion to one parameter. For example, $q_x = \lambda$ and $q_y = \alpha\lambda$, where $\alpha > 0$ is some fixed known parameter. Then, from Eq. (8.22), we obtain

$$\lambda = \frac{\pi^2 D}{b^2}\frac{\left[\left(\frac{mb}{a}\right)^2 + n^2\right]}{\left(\frac{mb}{a}\right)^2 + \alpha n^2}. \tag{8.24}$$

For $a > b$, the minimum value of λ may be reached for $n = 1$ only. Thus,

$$\lambda_{cr} = K\frac{\pi^2 D}{b^2}, \tag{8.25}$$

where

$$K = \frac{\left[(mb/a)^2 + 1\right]}{(mb/a)^2 + \alpha}. \tag{8.26}$$

For each ratio of a/b and each value of α it should be selected a number of the half-sine waves m from the condition of minimum of K as discussed in Example 8.1.

8.3.2 Buckling of circular plates

Circular plates in some measuring instruments are used as sensitive elements reacting to a change in the lateral pressure. In some cases – in temperature changes, in the process of their assembly – these elements are subjected to the action of radial compressive forces from a supporting structure. As a result, buckling of the circular plates can take place.

Let us consider a circular solid plate subjected to uniformly distributed in-plane compressive radial forces q_r, as shown in Fig. 8.6. We confine our buckling analysis to considering only axisymmetric configurations of equilibrium for the plate.

We can use the polar coordinates r and φ to transfer the governing differential equation of plate buckling (Eq. (8.1)), derived for a rectangular plate, to a circular plate. For the particular case of axisymmetric loading and equilibrium configurations, we have

$$N_x = N_y = N_r = -q_r, \quad N_{xy} = 0. \tag{8.27}$$

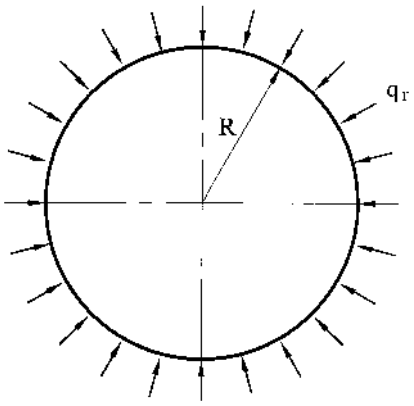

Fig. 8.6

Denoting

$$\mu^2 = \frac{q_r}{D}, \tag{8.28}$$

and using the relations between the polar and Cartesian coordinates, Eqs (4.1)–(4.4), we obtain the following differential equation of the axisymmetrically loaded circular plate subjected to in-plane compressive forces q_r:

$$\frac{\mathrm{d}^4 w}{\mathrm{d}r^4} + \frac{2}{r}\frac{\mathrm{d}^3 w}{\mathrm{d}r^3} - \frac{1}{r^2}\frac{\mathrm{d}^2 w}{\mathrm{d}r^2} + \frac{1}{r^3}\frac{\mathrm{d}w}{\mathrm{d}r} + \mu^2\left[\frac{\mathrm{d}^2 w}{\mathrm{d}r^2} + \frac{1}{r}\frac{\mathrm{d}w}{\mathrm{d}r}\right] = 0. \tag{8.29}$$

Let us introduce the following new variable:

$$\rho = \mu r, \tag{8.30}$$

which represents a dimensionless polar radius. Using the new variable ρ, we can rewrite Eq. (8.29), as follows:

$$\frac{\mathrm{d}^4 w}{\mathrm{d}\rho^4} + \frac{2}{\rho}\frac{\mathrm{d}^3 w}{\mathrm{d}\rho^3} + \left(1 - \frac{1}{\rho^2}\right)\frac{\mathrm{d}^2 w}{\mathrm{d}\rho^2} + \frac{1}{\rho}\left(1 + \frac{1}{\rho^2}\right)\frac{\mathrm{d}w}{\mathrm{d}\rho} = 0. \tag{8.31}$$

This is a fourth-order linear, homogeneous differential equation. The general solution of this equation is given by [1] as

$$w(\rho) = C_1 + C_2 \ln \rho + C_3 J_0(\rho) + C_4 Y_0(\rho), \tag{8.32}$$

where $J_0(\rho)$ and $Y_0(\rho)$ are the Bessel functions of the first and second kind of zero orders, respectively. They are tabulated in Ref. [10]. In Eq. (8.32), C_i $(i = 1, \ldots, 4)$ are constants of integration. Since $w(\rho)$ must be finite for all values of ρ, including $\rho = 0$, then the two terms $\ln \rho$ and $Y_0(\rho)$, having singularities at $\rho = 0$, must be dropped for the solid plate because they approach an infinity when $\rho \to \infty$. Thus, for the solid circular plate, Eq. (8.32) must be taken in the form

$$w(\rho) = C_1 + C_3 J_0(\rho). \tag{8.33}$$

Determine the critical values of the radial compressive forces, q_r, applied to the middle plane of solid circular plates for two types of boundary supports.

(1) Circular plate with fixed edge

Let the radius of the plate be R. We denote the corresponding value of μR by β, i.e., $\beta = \mu R$. The boundary conditions are

$$w(\beta) = 0\big|_{\rho=\beta}, \quad \vartheta(\beta) = 0\big|_{\rho=\beta}, \tag{a}$$

where the slope of the plate midsurface, $\vartheta(\rho)$, is given by

$$\vartheta(\rho) = \mu \frac{\mathrm{d}w}{\mathrm{d}\rho} = \mu C_3 \frac{\mathrm{d}}{\mathrm{d}\rho} J_0(\rho). \tag{b}$$

From the Bessel function theory [10], that it follows

$$J_1(\rho) = -\frac{\mathrm{d}}{\mathrm{d}\rho} J_0(\rho). \tag{c}$$

Thus, we can write the following representations for the slope

$$\vartheta(\rho) = -\mu C_3 J_1(\rho), \tag{8.34}$$

and

$$\vartheta(\beta) = -\mu C_3 J_1(\beta) \quad \text{on the boundary}, \tag{8.35}$$

where $J_1(\ )$ is the Bessel function of the first kind of the first order.

Substituting the expressions (8.34) and (8.35) into the boundary conditions (a) yields the following system of two linear homogeneous equations:

$$C_1 + C_3 J_0(\beta) = 0,$$
$$-\mu C_3 J_1(\beta) = 0.$$

For a nontrivial solution of these equations:

$$J_1(\beta) = 0.$$

From the tables of roots of the Bessel functions [10] it follows that the smallest root of the function $J_1(\beta)$ is $\beta_{\min} = 3.8317$.

Noting that $\beta^2 = (\mu R)^2 = q_r / DR^2$, we obtain the critical value of the compressive forces as

$$q_{r,\mathrm{cr}} = (3.8317)^2 \frac{D}{R^2} = 14.68 \frac{D}{R^2}. \tag{8.36}$$

(2) Circular plate with simply supported edge

The boundary conditions for this type of support are

$$w(\beta) = 0|_{\rho=\beta}, M_r(\beta) = 0|_{\rho=\beta}. \tag{d}$$

The radial bending moment, M_r, for an axisymmetrically loaded circular plate is given by Eq. (4.14). When passing from variable r to the variable ρ, the expression for M_r becomes

$$M_r = -D\mu^2 \left(\frac{\mathrm{d}^2 w}{\mathrm{d}\rho^2} + \frac{\nu}{\rho} \frac{\mathrm{d}w}{\mathrm{d}\rho} \right). \tag{8.37}$$

Using Eq. (8.33) for the deflections and Eq. (8.37) for the radial bending moments, we can represent the second boundary condition (d) in the form

$$-D\mu^2\left[\frac{\mathrm{d}^2}{\mathrm{d}\rho^2}J_0(\rho)+\frac{\nu}{\rho}\frac{d}{d\rho}J_0(\rho)\right]=0\Bigg|_{\rho=\beta}. \tag{8.38}$$

Using the relationships between the Bessel functions of the first kind [10], we have

$$\frac{\mathrm{d}^2}{\mathrm{d}\rho^2}J_0(\rho)=-J_0(\rho)+\frac{1}{\rho}J_1(\rho). \tag{e}$$

Substituting the expression for the deflections (8.33) into the boundary conditions (d) and taking into account Eqs (8.38) and (e), we arrive at the following system of linear homogeneous equations:

$$\begin{aligned} C_1+C_3J_0(\beta)&=0\\ -D\mu^2C_3[\beta J_0(\beta)-(1-\nu)J_1(\beta)]&=0 \end{aligned} \tag{f}$$

A nontrivial solution of this system of equations leads to the following:

$$\beta J_0(\beta)-(1-\nu)J_1(\beta)=0. \tag{g}$$

Letting $\nu=0.3$ and using the tables of the Bessel function [10], we can determine the smallest nonzero root of Eq. (g). We have

$$\beta_{\min}=2.0485,$$

and the critical value of an intensity of the radial compressive forces is

$$q_{r,\mathrm{cr}}=4.196\frac{D}{R^2}. \tag{8.39}$$

Comparing the values of the critical compressive forces for the clamped and simply supported circular solid plates, we can conclude that the replacement of the supported edges with clamped ones increases the critical force by a factor of 3.5.

8.4 THE ENERGY METHOD

Practical application of the equilibrium method runs into serious mathematical obstacles when determining the buckling loads of the plates with complex geometry and mixed boundary conditions. Under these circumstances a possibility for obtaining a rigorous solution of the differential equation (8.1) becomes very doubtful and, practically, impossible. Therefore, the use of the energy method can be very advantageous.

We will apply the energy criterion (8.5) to the buckling analysis of plates. The increment in the total potential energy of the plate upon buckling is given by Eq. (8.4). Let us derive the expression for the increment in the strain energy of the middle surface of the plate. In deriving this expression, we assume that the in-plane stress resultants are entirely due to external edge loading in the plane of the plate, in which case they are unchanged during bending (created by buckling). The increment of the strain energy of the plate middle surface due to buckling can be obtained from the general expression of the potential energy of an elastic body given by Eq. (2.51). Based on the assumptions 4 and 5 of the classical plate theory, the above expression

is simplified and has the following form for the above-mentioned increment of the middle surface:

$$\Delta U = \frac{1}{2}\int\int\int_{V}\left(\sigma_x\varepsilon_x + \sigma_y\varepsilon_y + \tau_{xy}\gamma_{xy}\right)\mathrm{d}V. \tag{a}$$

This increment of the strain energy can also be expressed in terms of the in-plane stress resultants. The latter are related to the stress components as follows:

$$\sigma_x = \frac{N_x}{h}, \quad \sigma_y = \frac{N_y}{h}, \quad \text{and} \quad \tau_{xy} = \frac{N_{xy}}{h}. \tag{b}$$

Substituting the above into Eq. (a) and integrating over the plate thickness, h, results in the following expression for the increment in the strain energy of the plate middle surface:

$$\Delta U_0 = \int\int_{A}\left(N_x\varepsilon_x + N_y\varepsilon_y + N_{xy}\gamma_{xy}\right)\mathrm{d}x\mathrm{d}y. \tag{8.40}$$

Note that there is no 1/2 coefficient in Eq. (8.40), since the in-plane stress resultants are already acting when additional middle surface strains (due to the buckling) occur. For the sake of simplicity, we derive the expression for ΔU_0 for a rectangular plate of dimensions $a \times b$. Inserting Eqs (7.82) into Eq. (8.40) results in the following expression for the increment of the strain energy of the plate middle surface:

$$\begin{aligned}\Delta U_0 = &\int_0^b\int_0^a\left[N_x\frac{\partial u}{\partial x} + N_y\frac{\partial v}{\partial y} + N_{xy}\left(\frac{\partial u}{\partial y} + \frac{\partial v}{\partial x}\right)\right]\mathrm{d}x\mathrm{d}y \\ &+\frac{1}{2}\int_0^b\int_0^b\left[N_x\left(\frac{\partial w}{\partial x}\right)^2 + N_y\left(\frac{\partial w}{\partial y}\right)^2 + 2N_{xy}\frac{\partial w}{\partial x}\frac{\partial w}{\partial y}\right]\mathrm{d}x\mathrm{d}y.\end{aligned} \tag{8.41}$$

We transform the first integral of the right-hand side of Eq. (8.41). Integrating this expression term-by-term, we obtain

$$\begin{aligned}\int_0^b\int_0^a\left[N_x\frac{\partial u}{\partial x} + N_y\frac{\partial v}{\partial y} + N_{xY}\left(\frac{\partial u}{\partial y} + \frac{\partial v}{\partial x}\right)\right]\mathrm{d}x\mathrm{d}y &= \int_0^b\left[\left|N_x u\right|_0^a + \left|N_{xy}v\right|_0^a\right]\mathrm{d}y \\ &+\int_0^b\left[\left|N_y v\right|_0^b + \left|N_{xy}u\right|_0^b\right]\mathrm{d}x - \int_0^b\int_0^a u\left[\frac{\partial N_x}{\partial x} + \frac{\partial N_{xy}}{\partial y}\right]\mathrm{d}x\mathrm{d}y \\ &-\int_0^b\int_0^a v\left[\frac{\partial N_{xy}}{\partial x} + \frac{\partial N_y}{\partial y}\right]\mathrm{d}x\mathrm{d}y.\end{aligned} \tag{8.42}$$

Using Eqs (3.90a) and (3.90b), we can conclude that the two last integrals on the right-hand side in the above expression vanish. The first two integrals on the right-hand side of Eq. (8.42) represent the work, W_e, done by the in-plane external forces applied to the middle surface of the plate. Thus, the expression (8.42) can be represented in the form

$$\Delta U_0 = W_e + \frac{1}{2}\int_0^b \int_0^a \left[N_x \left(\frac{\partial w}{\partial x}\right)^2 + N_y \left(\frac{\partial w}{\partial y}\right)^2 + 2N_{xy} \frac{\partial w}{\partial x}\frac{\partial w}{\partial y} \right] dx dy. \tag{8.43}$$

It can be shown that the expression for ΔU_0 in the form of Eq. (8.43) is valid (replacing the limits of integration) for a plate of any geometry, not necessarily, rectangular.

The increment in the potential of the external, in-plane forces applied to the plate is equal to the negative value of the work done by these forces, i.e.,

$$\Delta \Omega_\Gamma = -W_e. \tag{8.44}$$

The strain energy of the bending and twisting of a plate, U_b, is given by Eq. (2.53). Therefore, the increment in the total potential energy of the plate upon buckling, $\Delta\Pi$, can be obtained by substituting Eqs (2.53) and (8.43) with taking into account Eq. (8.44) on the right-hand side of Eq. (8.4).

$$\begin{aligned} \Delta\Pi = \frac{1}{2}\int\int_A D \left\{ \left(\frac{\partial^2 w}{\partial x^2} + \frac{\partial^2 w}{\partial y^2}\right)^2 + 2(1-\nu)\left[\left(\frac{\partial^2 w}{\partial x \partial y}\right)^2 - \frac{\partial^2 w}{\partial x^2}\frac{\partial^2 w}{\partial y^2} \right] \right\} dx dy \\ + \frac{1}{2}\int\int_A \left[N_x \left(\frac{\partial w}{\partial x}\right)^2 + N_y \left(\frac{\partial w}{\partial y}\right)^2 + 2N_{xy}\frac{\partial w}{\partial x}\frac{\partial w}{\partial y} \right] dx dy \end{aligned} \tag{8.45}$$

As mentioned in Sec. 8.2, the energy criterion (8.5) may be employed be obtain the exact and approximate solutions of the plate buckling problems. In the latter case, this criterion may be combined with, for instance, the Ritz method together with the eigenvalue technique introduced in Sec. 8.2.

Note that in practice $\Delta\Pi = 0$ only if the form chosen for the deflection is exact. Any approximation form, when Eq. (8.45) is applied, will give a value of the critical force higher than the true value. Let us demonstrate the advantages of the energy criterion in illustrative examples.

Example 8.4

Using the Ritz method, determine the critical buckling load for the plate with three simply supported edges $x = 0, a$ and $y = 0$ and one free edge $y = b$, as shown in Fig. 8.7. The plate is loaded by linearly distributed compressive in-plane forces $q_x = q\left(1 + \eta\frac{y}{b}\right)$ along the simply supported edges $x = 0, a$, where $\eta > 0$ is some fixed parameter.

Solution

The deflection surface of the plate can be approximated, as follows:

$$w = \sin\frac{n\pi x}{a}\sum_{i=1}^{N} C_i y^i. \tag{a}$$

This approximate solution satisfies exactly the prescribed geometric boundary conditions, i.e.,

$$w = 0|_{x=0,a}, \quad w = 0|_{y=0}. \tag{b}$$

Retaining only one term ($i = 1$) in the series (a), we can find the following:

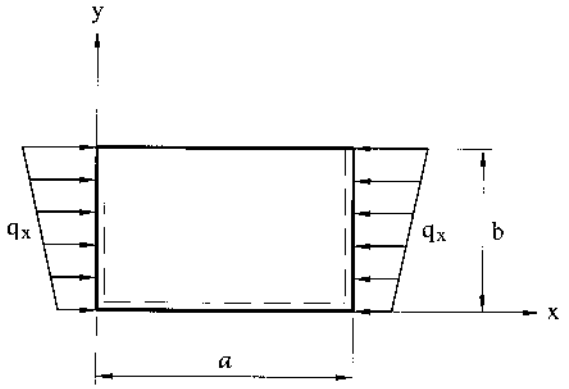

Fig. 8.7

$$\frac{\partial w}{\partial x} = C_1 y\left(\frac{n\pi}{a}\cos\frac{n\pi x}{a}\right), \frac{\partial^2 w}{\partial x^2} = -C_1 y\left(\frac{n\pi}{a}\right)^2 \sin\frac{n\pi x}{a},$$
$$\frac{\partial^2 w}{\partial x \partial y} = C_1\left(\frac{n\pi}{a}\cos\frac{n\pi x}{a}\right), \frac{\partial^2 w}{\partial y^2} = 0.$$

For this type of loading, the solution of the plane stress problem is $N_x = -q_x$, $N_y = N_{xy} = 0$. Substituting the above into Eq. (8.45), and performing the operations of integration, we obtain

$$\Delta\Pi = C_1^2 \frac{ab}{4}\left\{D\left[\frac{b^2}{3}\left(\frac{n\pi}{a}\right)^4 + 2(1-\nu)\left(\frac{n\pi}{a}\right)^2\right] - q\left(\frac{n\pi}{a}\right)^2 b^2\left(\frac{1}{3}+\frac{\eta}{4}\right)\right\}.$$

The eigenvalues of the load q_x can be found from equation $\partial\Pi/\partial C_1 = 0$. We have

$$q_n = \frac{n^2\pi^2 D}{b^2}\left[\frac{b^2/a^2 + 6(1-\nu)/n^2\pi^2}{1+3\eta/4}\right].$$

For $n = 1$, the smallest eigenvalue is approximately equal to the critical value, i.e.,

$$q_{\text{cr}} = \frac{b^2/a^2 + 6(1-\nu)/\pi^2}{1-3\eta/4}\cdot\frac{\pi^2 D}{b^2}. \tag{8.46}$$

Example 8.5

Determine the critical value of uniformly distributed in-plane shear forces q_{xy} for the simply supported rectangular plate shown in Fig. 8.8.

Solution

We assume that the deflection surface is adequately approximated as follows:

$$w = C_1 \sin\frac{\pi x}{a}\sin\frac{\pi y}{b} + C_2 \sin\frac{2\pi x}{a}\sin\frac{2\pi y}{b}, \tag{a}$$

where C_1 and C_2 are two unknown coefficients. It is obvious that w in the form of (a) satisfies exactly the prescribed geometrical boundary conditions ($w = 0$ on the boundary).

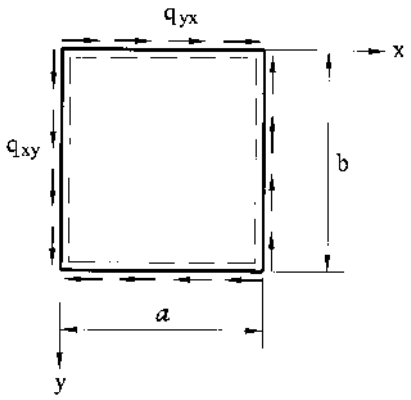

Fig. 8.8

Substituting for w from (a) into the potential energy expression $\Delta\Pi$ given by Eq. (8.45) and setting $N_{xy} = -q_{xy}$, $N_x = N_y = 0$, we obtain

$$\Delta\Pi = -\frac{\pi^4}{8} Dab\left(\frac{1}{a^2} + \frac{1}{b^2}\right)^2 \left(C_1^2 + 16C_2^2\right) - \frac{32}{9} q_{xy} C_1 C_2. \tag{b}$$

Applying the conditions for a stationary value of $\Delta\Pi$ – namely, $\partial(\Delta\Pi)/\delta C_1$ and $\partial(\Delta\Pi)/\partial C_2 = 0$ – results in the following two homogeneous linear equations:

$$\frac{\pi^4}{4} Dab\left(\frac{1}{a^2} + \frac{1}{b^2}\right)^2 C_1 - \frac{32}{9} q_{xy} C_2 = 0,$$

$$-\frac{32}{9} SC_1 + 4\pi^4 Dab\left(\frac{1}{a^2} + \frac{1}{b^2}\right)^2 C_2 = 0.$$

A nontrivial solution can be obtained by equating the determinant of these equations to zero. Consequently, we have

$$\pi^8 D^2 a^2 b^2 \left(a^{-2} + b^{-2}\right)^4 - \left(\frac{32 q_{xy}}{9}\right)^2 = 0,$$

which gives the following approximation for the critical shear forces:

$$q_{xy,\mathrm{cr}} = \pm\frac{9}{32}\pi^4 Dab\left(\frac{1}{a^2} + \frac{1}{b^2}\right)^2. \tag{8.47}$$

This result, which is larger by 15% than an exact solution for a square plate ($a = b$) [1], can be improved by retaining more terms in the expression (a) [1–3].

8.5 BUCKLING ANALYSIS OF ORTHOTROPIC AND STIFFENED PLATES

8.5.1 Orthotropic plates

Consider a rectangular orthotropic plate whose elastic properties are characterized by four independent constants: the moduli of elasticity E_x and E_y in the two

mutually perpendicular principal directions x and y; the shear modulus G; and Poisson's ratio ν_x. The second Poisson's ratio ν_y is related to ν_x by the expression (7.24). The constitutive equations, stress resultants–curvature equations, and the governing differential equation for the orthotropic plate in the framework of small-deflection plate bending theory have been derived in Sec. 7.2. Repeating the derivation of Eq. (3.92), we can represent the governing differential equation of the orthotropic plate buckling, as follows:

$$D_x\frac{\partial^4 w}{\partial x^4}+2H\frac{\partial^4 w}{\partial x^2\partial y^2}+D_y\frac{\partial^4 w}{\partial y^4}+N_x\frac{\partial^2 w}{\partial x^2}+N_y\frac{\partial^2 w}{\partial y^2}+2N_{xy}\frac{\partial^2 w}{\partial x\partial y}=0. \tag{8.48}$$

Let us analyze the stability of a rectangular, simply supported orthotropic plate subjected to in-plane compressive forces q_x, as shown in Fig. 8.1. The boundary conditions for simply supported edges of the orthotropic plate are

$$w=0|_{\substack{x=0,a\\y=0,b}},\ \frac{\partial^2 w}{\partial x^2}+\nu_y\frac{\partial^2 w}{\partial y^2}=0\Bigg|_{x=0,a},\ \frac{\partial^2 w}{\partial y^2}+\nu_x\frac{\partial^2 w}{\partial x^2}=0\Bigg|_{y=0,b}. \tag{a}$$

We take the deflection surface of the plate in the form

$$w=w_{11}\sin\frac{m\pi x}{a}\sin\frac{n\pi y}{b}. \tag{b}$$

The deflection surface in the form of (b) satisfies exactly the boundary conditions (a). Substituting (b) into Eq. (8.48) and letting $N_x=-q_x$, $N_y=N_{xy}=0$, we obtain from the solution of this equation the following expression for the compressive forces q_x:

$$q_x=\frac{\pi^2\sqrt{D_xD_y}}{b^2}\left[\sqrt{\frac{D_x}{D_y}}\left(\frac{mb}{a}\right)^2+\frac{2H}{\sqrt{D_xD_y}}n^2+\sqrt{\frac{D_y}{D_x}}\left(\frac{a}{mb}\right)^2\right]. \tag{8.49}$$

It is evident that a minimum value of q_x is reached for $n=1$. The critical value of the compressive force can be obtained by varying a number of half-waves m. For a plate that is lengthened along the x axis ($a\gg b$), we have the following:

$$q_{x,\mathrm{cr}}=\frac{2\pi^2\sqrt{D_xD_y}}{b^2}\left(1+\frac{H}{\sqrt{D_xD_y}}\right). \tag{8.50}$$

For a plate with a finite ratio of sides, it should be taken [4], that

$$m=1 \text{ for } 0<\frac{a}{b}<\sqrt[4]{4\frac{D_x}{D_y}},$$

$$m=2 \text{ for } \sqrt[4]{4\frac{D_x}{D_y}}<\frac{a}{b}<\sqrt[4]{36\frac{D_x}{D_y}},$$

$$m=3 \text{ for } \sqrt[4]{36\frac{D_x}{D_y}}<\frac{a}{b}<\sqrt[4]{144\frac{D_x}{D_y}}, \text{ and so on.}$$

Making $D_x = D_y = H = D$, we obtain the expression (8.10) for $q_{x,\mathrm{cr}}$ in a rectangular, simply supported isotropic plate.

8.5.2 Stiffened plates

In the stability analysis of stiffened plates, two modes of buckling are usually considered. One possible mode is the local buckling of the plate between the stiffeners, provided that the plate is reinforced with strong stiffeners. In the second case, an overall buckling of the plate–stiffener combination occurs. The latter is called primary buckling in the pertinent literature.

A more economical design can be obtained if we permit simultaneous local and primary buckling at about the same stress level. Consequently, in the elastic stability analysis of stiffened plates, the structural interaction of plate and stiffeners should be taken into account.

Two approaches to the stability analysis of stiffened plates are possible. If a plate is reinforced with many equally spaced parallel stiffeners of the same size (or with a grid-stiffening arrangement), such an assembly can effectively be approximated by the orthotropic (structurally orthotropic) plate theory. This approach makes it possible to consider Eq. (8.48) for the buckling analysis of structurally orthotropic plates, and the rigidities on the left-hand side of this equation are determined according to the procedure introduced in Sec. 7.2.3. Evidently, this approach is applicable only in the case when the stiffeners are located close to one another: the value $1/n$ (n is the number of stiffeners or ribs taken over all the width of the plate) should be small compared with unity.

Another approach involves the buckling analysis of a plate which is reinforced with few stiffeners. For such a type of stiffened plates, the convenient orthotropic plate idealization cannot be used to obtain reliable values for the critical loads. Since the stiffeners are rigidly fastened to the plate, we should treat the plate and stiffeners as a structural unit; consequently, at mutual points, the stiffener deflects and twists in the same way as the plate. Since the numerical procedure of the first approach is quite similar to the one discussed in Sec. 8.5.1 and involves no new ideas and principles, the second approach will be introduced below only. The critical load may be determined by the equilibrium or energy methods. The following examples illustrate the application of both methods for the buckling analysis of the stiffened plate.

Example 8.6

This problem was analyzed by Timoshe [1]. Determine the critical load for a simply supported rectangular plate which is reinforced by a single longitudinal rib located along its centerline, as shown in Fig. 8.9. The plate is subjected to the in-plane compressive forces q_x uniformly distributed along the edges $x = 0, a$.

Solution

In our buckling analysis, we take into account only the bending stiffness of the rib in the plane perpendicular to the middle plane of the plate. We apply the differential equation (8.6) to one of the halves of the plate. Its integral is represented in the form

$$w(x, y) = F(y) \sin \frac{m\pi x}{a}. \tag{8.51}$$

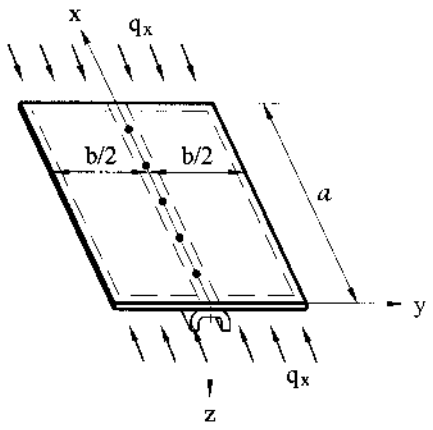

Fig. 8.9

Substituting the above into Eq. (8.6) and letting $N_x = -q_x$, $N_y = 0$, $N_{xy} = 0$, gives

$$\frac{\mathrm{d}^4F(y)}{\mathrm{d}y^4} - 2\left(\frac{m\pi}{a}\right)^2\frac{\mathrm{d}^2F(y)}{\mathrm{d}y^2} + \left(\frac{m\pi}{a}\right)^2\left[\left(\frac{m\pi}{a}\right)^2 - \frac{q_x}{D}\right]F(y) = 0. \tag{8.52}$$

Its solution is of the form

$$F(y) = C_1\cosh\alpha y + C_2\sinh\alpha y + C_3\cos\beta y + C_4\sin\beta y, \tag{8.53}$$

where

$$\alpha = \sqrt{\mu\left(\mu + \sqrt{\frac{q_x}{D}}\right)}, \quad \beta = \sqrt{\mu\left(\sqrt{\frac{q_x}{D}} - \mu\right)} \text{ and } \mu = \frac{m\pi}{a}. \tag{8.54}$$

The boundary conditions on the edge $y = b/2$ are

$$w = 0, \frac{\partial^2 w}{\partial y^2} = 0\Big|_{y=b/2}. \tag{8.55}$$

Assume that the plate is buckled together with the rib; then the bent surface of the plate must be symmetric about the line $y = 0$. This results in the following condition:

$$\frac{\partial w}{\partial y} = 0\Big|_{y=0}. \tag{8.56}$$

The difference in the reaction forces from the two strips of the plate given by the expression

$$R_y = -D\left[\frac{\partial^3 w}{\partial y^3} + (2-\nu)\frac{\partial^3 w}{\partial y \partial x^2}\right] \tag{8.57}$$

will be transmitted to the rib. Assume that the plate and rib are made of one and the same material. Due to the assumption adopted above for deformations of the rib, it can be easily shown that only the first term in the brackets of Eq. (8.57) should be taken into account. If we assume that the rib together with the plate is subjected to

the compressive forces q_x, then the equation for the elastic curve of the rib may be represented in the form

$$\left(EI_i\frac{\partial^4 w}{\partial x^4}+q_x\frac{\partial^2 w}{\partial x^2}+2D\frac{\partial^3 w}{\partial y^3}\right)_{y=0}=0,$$

or replacing $q_x = N_x = \sigma_x A_i$ for the rib, we obtain

$$\left(EI_i\frac{\partial^4 w}{\partial x^4}+\sigma_x A_i\frac{\partial^2 w}{\partial x^2}+2D\frac{\partial^3 w}{\partial y^3}\right)_{y=0}=0, \tag{8.58}$$

where I_i and A_i are the second moment of inertia and area of the rib cross section, respectively.

Let us introduce the following parameters:

$$\xi=\frac{a}{b},\quad \gamma=\frac{EI_i}{Db},\quad \delta=\frac{A_i}{bh}. \tag{8.59}$$

Introducing Eq. (8.53) into the conditions (8.55), (8.56), and (8.58), we obtain a system of linear algebraic homogeneous equations for $C_1,\ldots,C_4$. Equating the determinant of this system to zero, yields the following equation:

$$\left(\frac{1}{b\alpha}\tanh\frac{b\alpha}{2}-\frac{1}{b\beta}\tan\frac{b\beta}{2}\right)\left(\frac{\gamma m^2}{\alpha^2}-K\delta\right)\frac{m^2\pi^2}{\alpha^2}-4\frac{m}{\alpha}\sqrt{K}=0, \tag{8.60}$$

where

$$K=\frac{\sigma_{x,\mathrm{cr}}}{\sigma_{x,\mathrm{E}}} \tag{8.61}$$

and

$$\sigma_{x,\mathrm{cr}}=\frac{q_{x,\mathrm{cr}}}{h},\quad \sigma_{x,\mathrm{E}}=4\frac{\pi^2 D}{b^2 h} \tag{8.62}$$

where $\sigma_{x,E}$ is the critical stress for a rectangular, simply supported, unstiffened plate with the dimensions of Fig. 8.9 (see Eq. (8.11)). Equation (8.60) may be solved by the method of trial and errors. For $m = 1$ and $\xi > 2$, its solution, using the parameters introduced in Eqs (8.59), gives the following expression for $\sigma_{x,\mathrm{cr}}$:

$$\sigma_{x,\mathrm{cr}}=\frac{\pi^2 D}{b^2 h}\frac{\left(1+\xi^2\right)^2+2\gamma}{\xi^2(1+2\delta)}. \tag{8.63}$$

Now we analyze the stability problems for stiffened plates by the energy method.

Example 8.7

Determine the critical value of the in-plane compressive forces q_x acting on the plate reinforced by two equally spaced stiffeners, as shown in Fig. 8.10. The plate is simply supported on all edges. Let A_i and B_i ($B_i = EI_i$) be the area of the cross section and the bending stiffness of a stiffener, and c_i be spacing of the stiffeners.

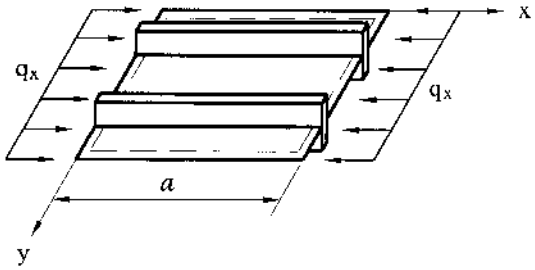

Fig. 8.10

Solution

The expression for the increment in the total potential energy in buckling for the plate reinforced by the discrete stiffeners, $\Delta\Pi_s$, may be represented as follows:

$$\Delta\Pi_s = \Delta\Pi + U_i - W_i, \tag{8.64}$$

where $\Delta\Pi$ is the increment in the potential energy of the unstiffened plate given by Eq. (8.45), U_i is the strain energy of the stiffener in bending, and W_i is the work done by the compressive forces $q_{xi} = q_x A_i/h$ acting on the stiffener, as shown below:

$$U_i = \frac{B_i}{2}\int_0^a \left(\frac{\partial^2 w}{\partial x^2}\right)_{y=c_i} \mathrm{d}x \tag{8.65}$$

and

$$W_i = \frac{q_{xi}}{2}\int_0^a \left(\frac{\partial w}{\partial x}\right)^2_{y=c_i} \mathrm{d}x. \tag{8.66}$$

Let the deflection surface of the plate be approximated by Eq. (3.15a). Substituting for w from the above equation into Eqs (8.45), (8.65), and (8.66), and finally, into Eq. (8.64) for $\Delta\Pi_s$, we obtain the following:

$$\begin{aligned}\Delta\Pi_s = {} & \frac{\pi^4 D}{2}\frac{ab}{4}\sum_m\sum_n {w_{mn}}^2\left(\frac{m^2}{a^2}+\frac{n^2}{b^2}\right)^2 - \frac{q_x}{2}\frac{ab}{4}\sum_m\sum_n \frac{m^2\pi^2}{a^2}w_{mn}^2 \\ & + \frac{\pi^4 B_i}{4a^3}\sum_m m^4\left(w_{m1}\sin\frac{\pi c_i}{b} + w_{m2}\sin\frac{2\pi c_i}{b} + \ldots\right)^2 \\ & - \frac{q_{xi}A_i}{h}\frac{\pi^2}{4a}\sum_m m^2\left(w_{m1}\sin\frac{\pi c_i}{b} + w_{m2}\sin\frac{2\pi c_i}{b} + \ldots\right)^2,\end{aligned} \tag{8.67}$$

where D is the flexural rigidity of the unstiffened plate. The critical value of the applied compressive forces, $q_{x,\mathrm{cr}}$, may be found from the energy criterion (8.5). Differentiating $\Delta\Pi_s$ in the form of (8.67) with respect to w_{mn}, we can determine $q_{x,\mathrm{cr}}$ from the nontrivial solution of the system of linear algebraic homogeneous equations, equating the determinant of this system to zero. Dropping the intermediate algebra, we present the final results. The critical force is given by

$$q_{x,\mathrm{cr}} = \frac{\pi^4 D}{b^2} \frac{\left(1+\xi^2\right)+3\gamma}{\xi^2(1-3\delta)}, \tag{8.68}$$

where ξ, δ, and γ are given by formulas (8.59). The solution (8.68) is done in the first approximation, i.e., for $m = n = 1$. If a rectangular, simply supported plate is reinforced by i equally spaced stiffeners then the critical value of the compressive forces is the following:

$$q_{x,\mathrm{cr}} = \frac{\pi^2 D}{b^2} \frac{\left(1+\xi^2\right)^2 + 2\sum_i \gamma_i \sin^2(\pi c_i/b)}{\xi^2\left[1+2\sum_i \delta_i \sin^2(\pi c_i/b)\right]}. \tag{8.69}$$

8.6 POSTBUCKLING BEHAVIOR OF PLATES

8.6.1 Large deflections of plates in compression

Using the linearized buckling analysis introduced in Sec. 8.2, we have considered only the initial elastic buckling of flat plates and the critical forces and stresses have been found for some typical loadings and boundary conditions. The critical force is the force at which bifurcation of equilibrium states occurs and is of fundamental significance to the designer. So, the critical loads found in the previous sections represent merely the loads at which buckling begins. It should be noted that the postbuckling behavior of plates is markedly different from that of thin rods. While a small increase in the critical load for rods will produce a complete collapse, the load-carrying capacity of the plate is not exhausted and elastic plate can carry stresses higher than σ_{cr}. It can be explained, first of all, by the effect of large deflections in the postbuckling stage and, then, by the fact that the longitudinal edges of the plate are usually constrained to remain straight. Thus, the postbuckling mechanism of elastic plates is characterized not only by bending but also by the direct (or in-plane) stresses. It is important that the latter become comparable in magnitude with the former stresses.

The use of an additional strength due to the postbuckling effects is of great practical importance in the design of ship and aerospace structures. By considering the postbuckling behavior of plates, considerable weight savings can be achieved. In these structures, the edges of the plates are usually supported by stringers in such a way that they remain straight during buckling. After buckling, the central part of the plate bulges out, and an increasingly larger portion of the load is carried by the material close to the supported edges (stringers) of the plate.

The nonlinear, large-deflection plate bending theory, discussed in Sec. 7.4, can be used for the analysis of the postbuckling behavior of plates. Because of a nonlinearity of the governing differential equations of this analysis, the resulting mathematical difficulties are considerable and exact solutions can very seldom be obtained. The most generally used techniques for the treatment of postbuckling of plates are based on numerical methods [11,12].

For some simple cases an analytical solution can be obtained under some assumptions regarding the plate behavior, boundary conditions, etc. Consider a rectangular, simply supported plate, as shown in Fig. 8.1. The plate is subjected to

the in-plane compressive forces q_x. An approximate expression for the buckled middle surface of the plate is taken in the following form ($m = n = 1$):

$$w = w_{11} \sin\frac{\pi x}{a} \sin\frac{\pi y}{b}. \tag{8.70}$$

The governing differential equations for the investigation of the postbuckling behavior of thin plates of a constant thickness are von Karman's large-deflection equations (7.87), derived in Sec. 7.4. Assuming that the lateral load p is zero, we can rewrite these equations in terms of the stress function ϕ ($\phi = \Phi/h$), as follows:

$$\frac{1}{E}\nabla^4\phi = \left(\frac{\partial^2 w}{\partial x \partial y}\right)^2 - \frac{\partial^2 w}{\partial x^2}\frac{\partial^2 w}{\partial y^2}, \tag{8.71a}$$

$$\frac{D}{h}\nabla^4 w = \frac{\partial^2 \phi}{\partial y^2}\frac{\partial^2 w}{\partial x^2} + \frac{\partial^2 \phi}{\partial x^2}\frac{\partial^2 w}{\partial y^2} - 2\frac{\partial^2 \phi}{\partial x \partial y}\frac{\partial^2 w}{\partial x \partial y}. \tag{8.71b}$$

Substituting for w from Eq. (8.70) into Eq. (8.71a), we obtain

$$\frac{1}{E}\nabla^4\phi = \frac{1}{2}w_{11}^2 \frac{\pi^4}{a^2 b^2}\left(\cos\frac{2\pi x}{a} + \cos\frac{2\pi y}{b}\right). \tag{8.72}$$

Assume that the edge supports do not prevent the in-plane motions of the plate in the y direction or, in other words, the in-plane shear stresses are zero. A particular integral of Eq. (8.72) is taken, as follows:

$$\phi_{\mathrm{p}} = A\cos\frac{2\pi x}{a} + B\cos\frac{2\pi y}{b}.$$

Determine the unknown coefficients A and B by calculating $\nabla^4\phi_{\mathrm{p}}$ and comparing the left- and right-hand sides of Eq. (8.72). We obtain the following:

$$\phi_{\mathrm{p}} = E\frac{w_{11}^2}{32}\left[\left(\frac{a}{b}\right)^2 \cos\frac{2\pi x}{a} + \left(\frac{b}{a}\right)^2 \cos\frac{2\pi y}{b}\right]. \tag{8.73}$$

Assuming that the edge supports do not prevent the in-plane motions of the plate in the y direction, we take the solution of the homogeneous Eq. (8.72) in the form

$$\phi_{\mathrm{h}} = -\frac{q_x y^2}{2h}. \tag{8.74}$$

Finally, the general solution of Eq. (8.72) is

$$\phi = \phi_{\mathrm{p}} + \phi_{\mathrm{h}} = E\frac{w_{11}^2}{32}\left[\left(\frac{a}{b}\right)^2 \cos\frac{2\pi x}{a} + \left(\frac{b}{a}\right)^2 \cos\frac{2\pi y}{b}\right] - \frac{q_x y^2}{2h}. \tag{8.75}$$

In-plane stresses in the plate middle surface are

$$\sigma_x = \frac{\partial^2 \phi}{\partial y^2} = -E\frac{\pi^2}{8}\left(\frac{w_{11}}{a}\right)^2 \cos\frac{2\pi y}{b} - \frac{q_x}{h}; \quad \sigma_y = \frac{\partial^2 \phi}{\partial x^2} = -E\frac{\pi^2}{8}\left(\frac{w_{11}}{b}\right)^2 \cos\frac{2\pi x}{a};$$

$$\tau_{xy} = -\frac{\partial^2 \phi}{\partial x \partial y} = 0. \tag{8.76}$$

As seen, the in-plane shear stresses are zero. Let us apply the Galerkin method to solve Eq. (8.71b). Using the general procedure of the method discussed in Sec. 6.5, we obtain

$$\int_0^a \int_0^b E \sin\frac{\pi x}{a} \sin\frac{\pi y}{b} \mathrm{d}x\mathrm{d}y = 0, \tag{8.77}$$

where

$$E \equiv \frac{D}{h}\nabla^4 w - \frac{\partial^2\phi}{\partial y^2}\frac{\partial^2 w}{\partial x^2} - \frac{\partial^2\phi}{\partial x^2}\frac{\partial^2 w}{\partial y^2} + 2\frac{\partial^2\phi}{\partial x \partial y}\frac{\partial^2 w}{\partial x \partial y}. \tag{8.78}$$

Substituting for w and ϕ from Eqs (8.70) and (8.75) into (8.77) and performing the corresponding operations of differentiation and integration, yields the following:

$$D\frac{\pi^4 ab}{4} w_{11}\left(\frac{1}{a^2}+\frac{1}{b^2}\right)^2 - q_x w_{11}\frac{\pi^2}{a^2}\frac{ab}{4} + E\frac{\pi^4 w_{11}^3}{64} h\left(\frac{1}{a^4}+\frac{1}{b^4}\right)ab = 0. \tag{8.79}$$

Assuming that $w_{11} \neq 0$, we obtain

$$q_x = N_x = \sigma_x h = D\frac{\pi^2}{b^2}\left(\frac{b}{a}+\frac{a}{b}\right)^2 + E\frac{\pi^2 h}{16b^2} w_{11}^2\left(\frac{b^2}{a^2}+\frac{a^2}{b^2}\right). \tag{8.80}$$

Since the first term on the right-hand side of the above equation represents the critical force of the linear buckling analysis, $q_{x,\mathrm{cr}}$, introduced in Sec. 8.3, it is evident that the plate can sustain a compression load greater than the linear buckling. It should be noted that the load-carrying capacity is more pronounced when the unloaded edges are constrained to remain straight ($N_y \neq 0$).

The first detailed analysis of the postbuckling behavior of plates loaded by compressive loads was conducted by von Karman *et al*. [13], who suggested a simplified approach to obtain an estimate for the ultimate load carried by the buckled plate. Based on experimental observations, this simplified method assumes that the ultimate buckling load of the plate is carried exclusively by two strips of equal width (the so-called effective width), located along the unloaded edges, and the stringers, jointly with the effective width portion of the plate, act as columns. A detailed numerical analysis of the postbuckling behavior of thin plates with various boundary conditions using the simplified method based on the effective width concept in compression for routine design purposes was developed by Marguerre [14], Cox [2], Schade [15], etc. The interested reader is referred to these references and to Refs [1,3].

8.6.2 Load-carrying capacity of plates in compression

We have seen that a plate after buckling may carry in some cases a compressive force that is many times higher than the critical load at which buckling begins. So, in cases when issues of weight economy are of fundamental importance, as for example in the aircraft industry, it is expedient to determine not only the critical load but also the ultimate load which the plate can carry without failure, which corresponds to the plate load-carrying capacity in compression.

We consider below a rectangular plate that is pin-connected along its edges with rigid stiffeners. The plate is subjected to compressive forces in one direction, as shown in Fig. 8.11a.

Prior to buckling of the plate, the compressive stresses are uniformly distributed over its width, b, but after buckling the distribution of stresses along the loaded edges becomes progressively nonlinear: they increase more intensively in the vicinity of the plate edges and the stresses differ little from their critical values in the central part of the plate. A typical compressive stress distribution along the plate cross section is shown in Fig. 8.11b. The actual distribution of the compressive stresses depends on the boundary conditions and on the length-to-width ratio, a/b, provided that this ratio is less than 3.

When failure of the plate is impending, almost the total compressive load is carried by two strips, located along the unloaded edges.

Following the simplified approach proposed by von Karman *et al.* [13], we determine the ultimate load carried by the compressed plate. This approach is based on the following assumptions:

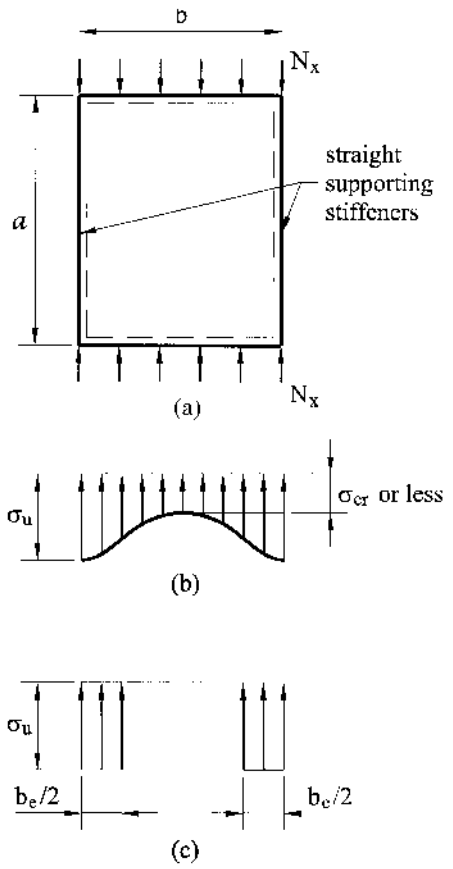

Fig. 8.11

(a) The initial (unloaded) plate is perfectly flat.
(b) The ultimate buckling load is carried exclusively by two strips of equal width, b_e, located along the unloaded edges.
(c) The maximum stress in the edge fiber of the plate, located in the middle surface, σ_u, is uniformly distributed over the two plate strips, b_e, as shown in Fig. 8.11c.
(d) The supporting stiffeners remain straight during the buckling and, jointly with the effective width portion of the plate, b_e, they act as columns.

Since the normal compressive stress is not uniform along the plate cross section, let us introduce the mean compressive stress, σ_m. From the above assumptions, it follows that the effective width, b_e, is

$$b_e = \frac{1}{\sigma_u}\int_0^b \sigma_m \mathrm{d}y. \tag{8.81}$$

Now we can determine the effective width of the bunched plate by using the reference value of the critical stress, σ_{cr}, in the following form:

$$\sigma_{cr} = \frac{N_{1cr}}{h} = K\frac{D}{h}\left(\frac{\pi}{b}\right)^2. \tag{8.82}$$

Due to the assumption (b), an expression similar to Eq. (8.82) can be written for the equivalent plate of width b_e:

$$\sigma_u = K\frac{D}{h}\left(\frac{\pi}{b_e}\right)^2. \tag{8.83}$$

Comparing Eqs (8.82) and (8.83) yields the following:

$$b_e = b\sqrt{\frac{\sigma_{cr}}{\sigma_u}}. \tag{8.84}$$

A more accurate postbuckling analysis estimates b_e as follows [16]:

$$b_e = b\cdot\sqrt[3]{\frac{\sigma_{cr}}{\sigma_u}}. \tag{8.85a}$$

Koiter [17] received the expressions for the effective width of flat plate in the form

$$b_e = b\left[1.2\left(\frac{\sigma_{cr}}{\sigma_u}\right)^{0.4} - 0.65\left(\frac{\sigma_{cr}}{\sigma_u}\right)^{0.8} + 0.45\left(\frac{\sigma_{cr}}{\sigma_u}\right)^{1.2}\right]. \tag{8.85b}$$

The ultimate load carried by the compressed plate is

$$P_u = \sigma_u b_e h. \tag{8.86}$$

To obtain estimates for the maximum edge stresses, σ_u, two cases are considered:

1. If the supporting stiffeners are relatively strong, the yield criterion can be conveniently used, in connection with the effective width concept, to determine σ_u the plate is able to carry. In this case, σ_u is simply equal to the yield stress σ_y, provided that the stiffeners and the adjacent plate

strips reach the yield stresses simultaneously without buckling. The ultimate load carried by the plate in this case is

$$P_{\mathrm{u}} = \sigma_{\mathrm{y}} b_{\mathrm{e}} h. \tag{8.87}$$

2. If the supporting stiffeners are relatively weak, they may fail by buckling before yield stress is developed. In this case, a trial and error procedure should be used to obtain an estimate for the maximum edge stresses, σ_{u}. First, we assign an effective width b_{e} in the first approximation as $b_{\mathrm{e}} = (0.3 - 0.6)b$, and determine $\sigma_u^{(1)}$, considering that the longitudinal supporting stiffener and the effective width portion of the plate act as a column. Using the $\sigma_u^{(1)}$ value obtained, a new estimate for $b_{\mathrm{e}}^{(2)}$ can be calculated, etc. The procedure is repeated until the interrelationship between these two variables is satisfied.

8.7 BUCKLING OF SANDWICH PLATES

The stability analysis of sandwich plate structure has to be taken with regard to various types of its buckling modes as a whole and its separate elements. Let a sandwich plate be loaded by the external in-plane edge loads (compressive and/or shear) symmetrically with respect to its middle plane. Two possible modes of buckling should be distinguished: a general, resulting from bending of the middle surface of the sandwich plate; a local, manifested as bending (wrinkling) of the upper and lower sheets and occurring without bending of the plate as a whole. In this book we consider only the buckling analysis of the general stability of sandwich plates. The local stability problems for sandwich plates were studied in Ref. [18].

The governing differential equations of the small-deflection bending theory of orthotropic and isotropic sandwich plates were derived in Sec. 7.6. The above equations will be valid for the buckling analysis if, according to the general procedure introduced in Sec. 8.2 for plate stability problems, instead of the transverse surface load p, a fictitious load p_{f} (see Sec. 8.2) is inserted in Eqs (7.131) for orthotropic sandwich plates or in Eq. (7.135) for isotropic ones:

$$p_{\mathrm{f}} = N_x \frac{\partial^2 w}{\partial x^2} + N_y \frac{\partial^2 w}{\partial y^2} + 2N_{xy} \frac{\partial^2 w}{\partial x \partial y}, \tag{8.88}$$

where N_x, N_y, and N_{xy} are the internal forces acting in the middle plane of the plate corresponding to the applied in-plane loading. Thus, the stability problem of the sandwich orthotropic plate is described by a system of governing equations consisting of Eqs (7.131a) and (7.131b), and (7.131c), where the latter equation is of the form

$$\frac{\partial Q_x}{\partial x} + \frac{\partial Q_y}{\partial y} = -p_{\mathrm{f}}, \tag{8.89}$$

p_{f} is given by Eq. (8.88). In a special case, substituting for p_{f} from Eq. (8.88) into Eq. (7.135), we obtain the following governing differential stability equation for isotropic sandwich shells:

$$D_s \nabla^2 \nabla^2 w = \left(1 - \frac{D_s}{D_Q} \nabla^2\right) \left(N_x \frac{\partial^2 w}{\partial x^2} + N_y \frac{\partial^2 w}{\partial y^2} + 2N_{xy} \frac{\partial^2 w}{\partial x \partial y}\right) \tag{8.90}$$

Example 8.8

A rectangular simply supported isotropic sandwich plate of Fig. 7.8 is subjected to an in-plane edge compressive load of intensity q_x, as shown in Fig. 8.1. Determine the critical value of this load if $a = 20\,\text{in.}$, $b = 10\,\text{in.}$, $t = 0.02\,\text{in.}$, $c = 0.2\,\text{in.}$, $E_f = 10 \times 10^6\,\text{psi}$, $G_c = 12{,}000\,\text{psi}$, $\nu = 0.3$.

Solution

The simply supported boundary conditions in terms of the deflections are given by Eqs (3.14). For the problem under consideration, $N_x = -q_x$ and $p_f = -q_x \partial^2 w/\partial x^2$. Therefore, Eq. (8.90) simplifies to the following form:

$$D_s \nabla^2 \nabla^2 w + q_x \left(1 - \frac{D_s}{D_Q} \nabla^2\right) \frac{\partial^2 w}{\partial x^2} = 0. \tag{a}$$

Equation (a) is a constant-coefficient equation. A solution of the form

$$w = C_1 \sin \frac{m\pi x}{a} \sin \frac{n\pi y}{b}; \quad m, n = 1, 2, 3, \ldots, \tag{b}$$

where C_1 is a constant, is seen to satisfy the boundary conditions (3.14). Introduction of that expression for w into Eq. (a) and rearrangement gives

$$q_x = \frac{\pi^2 D_s}{b^2} \frac{\left[(mb/a) + (n^2 a/mb)\right]^2}{1 + \psi\left[(mb/a)^2 + n^2\right]}, \tag{c}$$

where m and n are positive integers and

$$\psi = \frac{\pi^2 D_s}{b^2 D_Q}. \tag{d}$$

Equation (c) may now be written in the following alternative form:

$$q_x = K_s \frac{\pi^2 D_s}{b^2}, \tag{e}$$

where the nondimensional buckling coefficient K_s for sandwich plates is defined as

$$K_s = \frac{[mb/a + n^2 a/mb)]^2}{1 + \psi\left[n^2 + (mb/a)^2\right]}. \tag{f}$$

For given values of the plate aspect ratio a/b and the shear stiffness parameter ψ, the value of the wave–length parameters m and n may be chosen by trial to give the smallest value of q_x, i.e., $q_{x,\text{cr}}$.

It is seen that for $G_c \to \infty$, $\psi = 0$ and the buckling parameter $K_s \to K$ given by Eq. (8.8) (for $n = 1$). Thus, for this particular case when the transverse shear deformation is neglected, Eq. (c) reduces to the corresponding expression (8.7b) derived for buckling of homogeneous plates.

Using the numerical data of the problem, let us compute the rigidities. We have

$$D_s = \frac{E_s t(c+t)^2}{2(1-\nu^2)} = 5318 \text{ lb-in}, \quad D_Q = G_c \frac{(c+t)^2}{c} = 2904 \text{ lb/in},$$

$$\psi = \frac{\pi^2 D_s}{b^2 D_Q} = 1.831.$$

Introduction of these data into Eq. (f) reveals that the smallest value of the coefficient K_s corresponds to $n = 1$ and $m = 3$. For this value Eq. (g) gives $q_{x,\text{cr}} = 973.2$ lb/in.

If the core were omitted and the two face sheets bonded together to form a thin homogeneous plate 0.04 in. thick, the corresponding critical load would be only 23.4 lb.

PROBLEMS

8.1 Figure 8.2 shows the variation of the buckling load parameter K as a function of aspect ratio a/b for $m = 1, 2, 3, 4$. Based on this figure, determine the condition at which a transition from m to $m+1$ half-sine waves across the span of the plate, compressed in the x direction by a uniform edge loads.

8.2 Calculate the critical value of the uniform compressive edge loads q_x applied over two simply supported edges of length b if two opposite edges of the length a are fixed. Use $a = 2\,\text{m}$, $b = 1\,\text{m}$, $h = 0.1\,\text{m}$, $E = 210\,\text{GPa}$, and $\nu = 0.3$.

8.3 Calculate the critical value of the uniformly applied compressive edge loads for a rectangular plate of sides a and b with two simply supported opposite edges and two other opposite edges free. Assume that the load is applied over the free edges. Take $a = 10\,\text{m}$, $b = 5\,\text{m}$, $h = 0.15\,\text{m}$, $E = 220\,\text{GPa}$, and $\nu = 0.3$.

8.4 Let a rectangular, simply supported plate of sides a and b be loaded by uniformly distributed compressive q_x and tensile q_y forces. The q_x forces are applied parallel to the side a and q_y forces act in the direction parallel to the side b. Find the nontrivial solution of Eq. (8.20) for this type of loading and calculate the critical value of the parameter λ if $q_y = \lambda q_x$ and $a = b$. Compare this result with the case when the above plate is compressed in two directions (see Fig. 8.5).

8.5 Consider a circular plate uniformly compressed by in-plane radial forces q_r. Compare the critical values of q_r for two types of plate supports: (a) simply supported edge and (b) fixed edge. Use the radius of the plate $a = 40\,\text{in.}$, $h = 2.5\,\text{in.}$, $E = 25{,}000\,\text{ksi}$, and $\nu = 0.3$.

8.6 Consider a rectangular plate of sides $2a$ and $2b$. The origin of the Cartesian coordinate system is taken at the plate center. The plate rests at its center upon columns and is compressed by uniformly distributed forces q_x applied parallel to the side $2a$. Assuming that the column support can be approximated by a point support, determine the critical value of q_x. Use the Ritz method and the approximate expression for the deflection in the form

$$w = C\left[\cos\frac{\pi x}{2a} + \cos\frac{\pi y}{2b}\right].$$

8.7 Let a rectangular plate of sides a and b $(a > b)$ with fixed edges be subjected to compressive linearly varying loads $q_x = q_0(1 - \eta y/b)(\eta < 1)$. The load is applied to short plate edges. The origin of the Cartesian coordinate system is attached at the left upper corner of the plate. Determine the critical value of the applied compressive load by the Ritz method. Assume that $a = 3\,\text{m}$, $b = 1.5\,\text{m}$, $h = 0.15\,\text{m}$, $\eta = 0.5$, $E = 200\,\text{GPa}$, and $\nu = 0.28$, and the approximate expression for deflections is

$$w = C\left(x^2 - a^2\right)^2\left(y^2 - b^2\right)^2.$$

8.8 Derive Eq. (8.48).

8.9 Consider an unstiffened, simply supported rectangular plate of sides a and b and a plate of the same geometry and boundary conditions but reinforced by a single longitudinal rib located along its centerline, as shown in Fig. 8.9. Compare the critical values of the compressive forces q_x uniformly distributed along the edges $x = 0, a$ for the above two plates. Assume that $a = b = 2\,\text{m}$, $h = 0.15\,\text{m}$, $E = 220\,\text{GPa}$, and $\nu = 0.3$, and the rib has a cross section in the form of a channel section C75 × 6. In the buckling analysis, take into account the buckling stiffness of the rib in the plane that is perpendicular to the plate middle plane.

8.10 A simply supported square plate is reinforced by three equally spaced stiffeners of rectangular cross section of depth h_1 and of width t. The plate is subjected to in-plane uniform compressive forces q_x that act parallel to the stiffeners. Determine the critical value of the applied forces. Assume that the stiffeners and plate are made of the same material and stiffeners are symmetrical about the plate middle plane. Use $a = 5\,\text{m}$, $h = 0.2\,\text{m}$, $h_1 = 0.4\,\text{m}$, $t = 0.1\,\text{m}$, $E = 210\,\text{GPa}$, and $\nu = 0.3$.

8.11 A long, simply supported rectangular plate ($a/b = 3$), subjected to uniform compressive forces q_x acting parallel to the long side a was reinforced by stiffeners symmetrically placed about the plate middle surface. Three variants of locations of the stiffeners had been discussed:

(a) First, the equally spaced transverse stiffeners (i.e., located in the perpendicular direction with respect to q_x) were suggested to locate at a distance equal to b;

(b) Secondly, the equally spaced transverse stiffeners were suggested to locate at a distance $b/2$;

(c) Thirdly, only one longitudinal stiffener located along the plate centerline (i.e., in the direction of the applied load) was suggested to apply.

Assuming buckling of the reinforced plate as a whole, determine the critical values of the applied forces q_x for all the above cases. If the geometrical and mechanical properties of the plate and stiffeners are known, draw conclusions about the efficient arrangement of stiffeners for the problem under consideration from the point of view of the buckling analysis.

8.12 Estimate the ultimate edge load of a rectangular plate, stiffened along both longitudinal edges and uniformly compressed in the x direction. Assume that the plate is simply supported along its edges and that the stiffeners and adjacent plate strips simultaneously approach the compressive yield strength. Let $a = 900\,\text{mm}$, $b = 450\,\text{mm}$, $h = 1\,\text{mm}$, $E = 73\,\text{GPa}$, $\nu = 0.3$, and $\sigma_y = 415\,\text{MPa}$.

REFERENCES

1. Timoshenko, S.P. and Gere, J.M., *Theory of Elastic Stability*, McGraw-Hill, New York, 1961.
2. Cox, H.L., *The Buckling of Plates and Shells*, The Macmillan Company, New York, 1963.
3. Bulson, P.S., *The Stability of Plates*, American Elsevier Publishing Company, New York, 1969.
4. Volmir, A.S., *Stability of Elastic Systems*, Gos. Izd-vo Fiz.-Mat. Lit-ry, Moscow, 1963 (in Russian).
5. Carson, W.G. and Newton, R.E., Plate buckling analysis using a fully compatible finite elements, *AIAAJ*, vol. 7, No. 3, pp. 527–529, (1969).
6. Kapur, K.K. and Hartz, B.J., Stability of plates using the finite element method, J *Engng Mech Div, Proc ASCE*, vol. 92, pp. 177–195, 1966.

7. Costa, J.A. and Brebbia, C.A. Elastic buckling of plates using the boundary element methods. In *Boundary Elements, VII* (eds C.A. Brebbia and G. Maier), Springer-Verlag, Berlin, 4-29–4-43 (1985).
8. Manolis, G.D., Beskos, D.E. and Pineros, M.F. Beam and plate stability by boundary elements, *Comput Struct*, vol. 22, pp. 917–923, (1986).
9. Bryan, G.N., On the stability of a plane plate under thrusts in its own plane with application to the buckling of the sides of a ship, *Proc Lond Math Soc*, vol. 22, pp. 54–67, (1891).
10. Watson, G.N., *Theory of Bessel Functions*, 2nd edn, Cambridge University Press, Cambridge, 1944.
11. Murray, D.W. and Wilson, E.L., Finite-element large-deflection analysis of plates, *Proc. ASCE, J Engng Mech, Div EMI*, p. 143 (1969).
12. Yang, T. J., Elastic postbuckling prediction of plates using discrete elements, *AIAAJ*, vol. 9, No. 9, pp. 1665–1666 (1971).
13. von Karman, T., Sechler, E.E., and Donnel, L.H., The strength of thin plates in compression, *Trans ASME*, vo. 54, pp. 53–57 (1932).
14. Marguerre, K., Die mittragende breite der gedrückten platte, *Luftfahrtforschung*, vol. 14, no. 3, pp. 121–128 (1937).
15. Schade, H.A., Larguer effective de toles reinforcees travaillant sous l'action de forces de flexion, *Bulletin Technique du Bureau Veritas*, pp. 215–227 (1953).
16. Marguerre, K., The apparent width of the plate in compression, *Tech Memo* No. 833, NACA, Washington, D.C, 1937.
17. Koiter, W.T., The effective width of flat plates for various longitudinal edge conditions at loads far beyond the buckling load, Rep. No. 5287, *National Luchtvaart Laboratorium* (The Netherlands).
18. Yusuff, S., Theory of wrinkling in sandwich construction, *J Roy Aeron Soc*, vol. 59, No. 529 (1955).

9

The Vibration of Plates

9.1 INTRODUCTION

In the preceding chapters, we have assumed that all external forces are applied slowly: so slowly that the loads and the resulting stresses and deformations are independent of time. In engineering practice, however, many components of machines and structures are subjected to dynamic effects, produced by time-dependent external forces or displacements. Dynamic loads may be created by moving vehicles, wind gusts, seismic disturbances, unbalanced machine vibrations, flight loads, sound, etc. Dynamic effects of time-dependent loads on structures are studied in structural dynamics. Structural dynamics deals with time-dependent motions of structures, primarily, with vibration of structures, and analyses of the internal forces associated with them. Thus, its objective is to determine the effect of vibrations on the performance of the structure or machine.

The dynamics of plates, which are continuous elastic systems, can be modeled mathematically by partial differential equations based on Newton's laws or by integral equations based on the considerations of virtual work. In practical applications only the lateral vibration is of interest, and the effects of extensional vibrations in the middle plane may be neglected. Therefore, the inertia forces, associated with the lateral translation of the plate, are considered. In this chapter only the simplified theory of plate vibrations is introduced; some physical phenomena, associated with, for instance, damping effects, are not considered.

Damping effects are caused either by internal friction or by the surrounding media. Although structural damping is theoretically present in all plate vibrations, it has usually little or no effect on (a) the natural frequencies and (b) the steady-state amplitudes; consequently, it can be safely ignored in the initial treatment of the problem. We follow the same pattern, as used in earlier chapters, of looking first

for exact solutions by solving the differential equations, then looking for approximate solutions.

The derivation of the governing differential equation of motion of plates is, in most cases, a simple extension of the static case by adding effective forces to the plate that result from accelerations of the mass of the plate. These are the *inertia forces*. For the most part, we take advantage of D'Alambert's principle to add the inertia forces as reversed effective forces. Other time-dependent forces may also be considered. The most common of these are *damping forces*.

We consider various kinds of motion of plates. There is a *free vibration,* which occurs in the absence of applied loads but may be initiated by applying initial conditions to the plate. The free vibration deals with natural characteristics of the plates, and these natural vibrations occur at discrete frequencies, depending only on the geometry and material of the plates. Then, there is a *forced vibration*, which results from an application of time-dependent loads. Forced vibrations come in two kinds: a harmonic response, when a periodic force is applied to the plate; and a transient response, when the applied force is not a periodic force.

In deriving the governing differential equation of motion, we use the general assumptions of Kirchhoff's plate bending theory introduced in Sec. 1.3. To adapt the elastic static equations derived for thin plates in Chapter 2, to model undamped structural dynamics, we need to consider only the dependent variables (the deflections, strains, and stresses) as functions of time. Let the applied loads be some functions of time, and explicitly include inertia forces in the surface lateral loads according to D'Alambert's principle. In this case, the forcing function appearing on the right-hand side of the governing differential equation (2.24) for the bending of thin plates becomes

$$p(x, y, t) - \rho h \frac{\partial^2 w}{\partial t^2}(x, y, t), \tag{9.1}$$

where both p and w are functions of time, as well as space; ρ is the mass density of the material, and h is the plate thickness. In the forced vibrations $p(x, y, t)$ causes the dynamic response.

Thus, the differential equation of forced, undamped motion of plates has the form

$$D\nabla^2\nabla^2 w(x, y, t) = p(x, y, t) - \rho h \frac{\partial^2 w}{\partial t^2}(x, y, t). \tag{9.2}$$

9.2 FREE FLEXURAL VIBRATIONS OF RECTANGULAR PLATES

Consider a rectangular plate with arbitrary supports. Let us assume that certain transverse surface loads distributed on the surface cause the particles, located in the middle surface, to attain the deflections and velocities directed perpendicularly to the initial (undeformed) middle surface. At a certain time, which is assumed to be the initial, the plate is suddenly released from all external loads. The unloaded plate, which has initial deflection and velocity, begins to vibrate. The particles located in the middle surface move in the direction perpendicular to the plate and, as a result, the plate becomes curved. Such vibrations are called *free* or *natural transverse vibrations*. The plate will execute *free* or *natural lateral vibrations*.

As stated previously, natural vibrations are functions of the material properties and the plate geometry only, and are inherent properties of the elastic plate, independent of any load. Thus, for natural or free vibrations, $p(x, y, t)$ is set equal to zero, and Eq. (9.2) becomes

$$D\nabla^2\nabla^2 w(x, y, t) + \rho h \frac{\partial^2 w}{\partial t^2}(x, y, t) = 0. \tag{9.3}$$

Deflection w must satisfy the boundary conditions at the plate edge (these conditions practically do not differ from those in the case of static equilibrium) and the following initial conditions:

$$\text{when } t = 0: \quad w = w_0(x, y), \quad \frac{\partial w}{\partial t} = v_0(x, y), \tag{9.4}$$

where w_0 and v_0 are the initial deflection and initial velocity for point (x, y).

Equation (9.3) is the governing, fourth-order homogeneous partial differential equation of the undamped, free, linear vibrations of plates. A complete solution of the problem of a freely vibrating plate is reduced to determining the deflections at any point for any moment of time. However, the most important part of the problem of free flexural vibrations of plates is to determine the *natural frequencies* and the *mode shapes of the vibration* (deflection surfaces in two dimensions) associated with each natural frequency. For such a problem (like in buckling), Eq. (9.3) is an eigenvalue problem. The natural frequencies are the *eigenvalues* and associated shape functions are the *eigenfunctions*. Values of these parameters are necessary for establishing the dynamic stresses caused by a variable load. A solution of Eq. (9.3) can be obtained by applying the classical analytical and approximate methods discussed in Chapters 3, 4, and 6 for static plate bending problems.

Let us describe a general *analytical method* (the Fourier method) for determining the natural frequencies of a freely vibrating plate. To solve Eq. (9.3) and obtain $w(x, y, t)$ in general, one can assume the following solution:

$$w(x, y, t) = (A \cos \omega t + B \sin \omega t) W(x, y), \tag{9.5}$$

which is a separable solution of the *shape function* $W(x, y)$ describing the modes of the vibration and some harmonic function of a time; ω is the natural frequency of the plate vibration which is related to vibration period T by the relationship $\omega = 2\pi/T$.

Introducing Eq. (9.5) into Eq. (9.3), we have

$$D\nabla^2\nabla^2 W(x, y) - \omega^2 \rho h W = 0. \tag{9.6}$$

Let us represent a solution of this equation in the form of a Fourier series. Requiring the function W to satisfy the boundary conditions and to be the solution of Eq. (9.6), we obtain a system of homogeneous equations for the unknown constants. This system has solutions that differ from zero only in the case when its determinant $\Delta(\omega)$ is equal to zero; therefore we obtain the *frequency* or *characteristic equation,* which is

$$\Delta(\omega) = 0. \tag{9.7}$$

This equation will have an infinite number of solutions which constitute the frequency spectrum for a given plate. In general, the frequencies will depend on two parameters: m and n ($m = 1, 2, \ldots$; $n = 1, 2, \ldots$). The lowest frequency is called the

frequency of the fundamental mode or the *fundamental natural frequency* and all other frequencies are called the *frequencies* of *higher harmonics*, or *overtones*. For each frequency ω_{mn}, there is a corresponding shape function $W_{mn}(x, y)$ that, on the basis of the homogeneous equations, is determined by a constant multiplier (which can be assumed as being equal to unity). For example, in the case of a rectangular, simply supported plate, the shape function may be taken as

$$W(x, y) = \sum_{m=1}^{\infty} \sum_{n=1}^{\infty} C_{mn} \sin \frac{m\pi x}{a} \sin \frac{n\pi y}{b}, \tag{9.8}$$

where a and b are the plate dimensions and C_{mn} is the vibration amplitude for each value of m and n. Substitution of Eq. (9.8) into Eq. (9.6) results in the homogeneous algebraic equation

$$\frac{m^4\pi^4}{a^4} + 2\frac{m^2\pi^2}{a^2}\frac{n^2\pi^2}{b^2} + \frac{n^4\pi^4}{b^4} - \frac{\omega^2\rho h}{D} = 0. \tag{9.9}$$

Solving this equation for ω gives the natural frequencies

$$\omega_{mn} = \pi^2 \left(\frac{m^2}{a^2} + \frac{n^2}{b^2} \right) \sqrt{\frac{D}{\rho h}}. \tag{9.10}$$

The *fundamental natural frequency* can be obtained by letting $m = 1$, $n = 1$. Note that, again (as in the buckling analysis), the amplitude C_{mn} cannot be determined from the linear eigenvalue problem.

For a square plate of dimension a, Eq. (9.10) becomes

$$\omega_{mn} = \frac{\pi^2}{a^2} \sqrt{\frac{D}{\rho h}} (m^2 + n^2), \tag{9.11}$$

and the fundamental natural frequency is

$$\omega_{11} = \frac{2\pi^2}{a^2} \sqrt{\frac{D}{\rho h}}. \tag{9.12}$$

The fundamental mode of the flexural vibration is a single sine wave in the x and y directions. Figure 9.1a shows a plate view executing the vibrations of the fundamental tone with the natural frequency ω_{11}. The maximum deflection is at the plate center. The deflected surfaces that correspond to the natural frequencies ω_{21} and ω_{12} are depicted in Fig. 9.1b and c; in each case there are the two maximum deflections and one of the axes of symmetry is a nodal line.

9.3 APPROXIMATE METHODS IN VIBRATION ANALYSIS

9.3.1 Variational methods

An exact solution of the governing differential equation (9.3) in closed form is possible only for a limited number of cases regarding a plate's geometry and its boundary conditions. As mentioned previously, the natural fundamental frequencies are of the greatest importance in practice. Therefore, one has to determine these frequencies by the approximate methods discussed in Chapter 6.

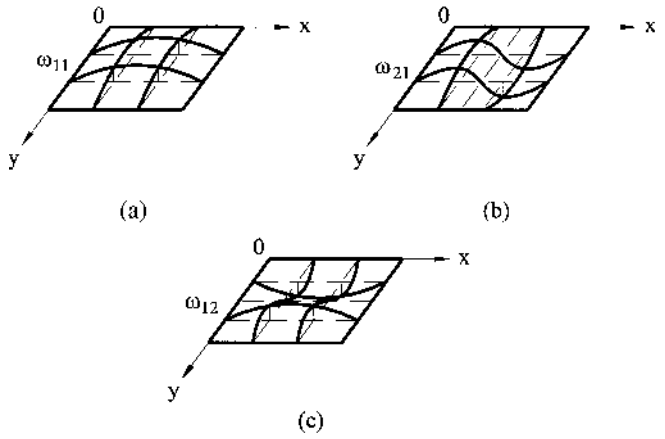

Fig. 9.1

Here, we consider some variational methods for determining natural frequencies of freely vibrating plates. First we apply *Rayleigh's principle* for finding the lowest natural frequency of a vibrating plate, which is of great interest in applied vibration analysis. This principle is based on the following statement: if the vibrating system is conservative (no energy is added or lost), then the maximum kinetic energy, $K_{\max}$, must be equal to the maximum potential (strain) energy, $U_{\max}$. Applying this principle, we consider an elastic plate undergoing free vibrations with the fundamental mode as a system with one degree of freedom. Taking into account that only free flexural vibrations are of interest, we can present the above principle as follows:

$$U_{\max} = K_{\max}. \tag{9.13}$$

This principle is essentially a restatement of the principle of conservation of energy (see Sec. 2.6). The strain energy of the plate is described in detail in Sec. 2.6. The kinetic energy of the plate is

$$K = \frac{1}{2}\int\int_A \rho h\left[\frac{\partial w(x, y, t)}{\partial t}\right]^2 \mathrm{d}x\mathrm{d}y. \tag{9.14}$$

Assuming that the plate is undergoing harmonic vibrations, we can approximate the vibrating middle surface of the plate by the equation

$$w(x, y, t) = W(x, y)\sin\omega t, \tag{9.15}$$

where $W(x, y)$ is a given continuous function that approximately represents the shape of the plate's deflected middle surface and satisfies at least the kinematic boundary conditions and ω represents the unknown natural frequency of the plate pertinent to the assumed shape function. Substituting the expression (9.15) into Eq. (9.14) for the kinetic energy, we obtain

$$K = \frac{\omega^2}{2}\cos^2\omega t\int\int_A \rho h W^2(x, y)\mathrm{d}x\mathrm{d}y. \tag{9.16}$$

It is evident, that the kinetic energy is a maximum when $\cos\omega t = 1$. Thus, we have

$$K_{\max} = \frac{\omega^2}{2} \int\int_A \rho h W^2(x, y) \mathrm{d}x\mathrm{d}y \tag{9.17}$$

The strain energy is a maximum when the deflection is a maximum. For the deflected middle surface, which is approximated by Eq. (9.15), $U_{\max}$ occurs when $\sin \omega t = 1$. It can be easily shown that under this condition the maximum strain energy of the vibrating plate is identical to Eq. (2.54), derived in Sec. 2.6 for the static case.

Substituting the expressions (2.54) and (9.17) for the maximum values of the strain and kinetic energies, respectively, into Rayleigh's principle (9.13), we obtain

$$\omega^2 = \frac{2U_{\max}}{\int\int_A \rho h W^2(x, y) \mathrm{d}x\mathrm{d}y}, \tag{9.18}$$

where

$$U_{\max} = \frac{1}{2} \int\int_A D \left\{ \left(\nabla^2 W\right)^2 + 2(1 - \upsilon) \left[\left(\frac{\partial^2 W}{\partial x \partial y} \right)^2 - \frac{\partial^2 W}{\partial x^2} \frac{\partial^2 W}{\partial y^2} \right] \right\} \mathrm{d}x\mathrm{d}y. \tag{9.19}$$

The accuracy of determining the natural frequencies by Eq. (9.18) depends to a considerable extent on the successful selection of the expression for W. Frequently, the function W is chosen as an expression that is proportional to a static deflection of a plate of interest with the same boundary conditions as for the plate of interest under a uniformly distributed lateral surface load p. This is equivalent to the assumption that the plate surface that corresponds to the fundamental mode is identical to that deflected by a uniform distributed load. The approximate lowest or fundamental frequency calculated from Rayleigh's principle is always higher than the "exact" values, since we have arbitrarily stiffened the plate by assuming a modal shape, thus increasing its frequency.

Equation (9.18) determines a frequency ω only in the first approximation. A more accurate frequency value can be obtained by using the *Ritz method* discussed in Sec. 6.6 for static plate problems. Being applied to the plate vibration problems, this method represents a generalization of Rayleigh's principle by including more than one parameter in the expression of the shape function. In this way, not only a more accurate value for the lowest natural frequency can be obtained but also additional information concerning the higher frequencies and pertinent mode shapes is gained.

Assuming the shape function $W(x, y)$ in the form of a series, we can write

$$W(x, y) = \sum_{i=1}^{n} C_i W_i(x, y). \tag{9.20}$$

The unknown coefficients C_i are obtained from the minimum total energy principle (see Secs 2.6 and 6.6). Thus, based on Eq. (6.44), we may write

$$\frac{\partial(U_{\max} - K_{\max})}{\partial C_i} = 0 \quad (i = 1, 2, 3, \ldots, n). \tag{9.21}$$

Inserting Eq. (9.20) into Eqs (9.17), (9.19) and performing the Ritz procedure, described by Eq. (9.21), we obtain, after integration of the definite integrals, the set of homogeneous linear algebraic equations in C_i. In order that at least one coefficient be different from zero, we equate the determinant of this system to zero and obtain

the frequency (or the characteristic) equation (9.7), whose solutions, as mentioned previously, constitute the frequency spectrum for a given plate.

Example 9.1

Determine an approximate value of the natural frequencies for the clamped rectangular plate with dimensions $2a$ and $2b$, as shown in Fig. 9.2.

Solution

Assume that $W(x, y)$ is given by the following expression (the first approximation):

$$W(x, y) = C\left(x^2 - a^2\right)^2\left(y^2 - b^2\right)^2. \tag{a}$$

This function satisfies the boundary conditions on the plate edges, i.e.,

$$W = \frac{\partial W}{\partial x} = 0\Big|_{x=\pm a}, \; W = \frac{\partial W}{\partial y} = 0\Big|_{y=\pm b}.$$

Substituting the expression (a) into Eq. (9.18) and evaluating the integrals, we obtain the fundamental natural frequencies in the form

$$\omega_{11} = 4\sqrt{2\left[\frac{1}{a^4} + \frac{1}{b^4} + \frac{2^8}{3^2 7^2}\frac{1}{a^2 b^2}\right]}\sqrt{\frac{D}{\rho h}}.$$

For a square plate ($a = b$), the frequency becomes

$$\omega_{11} = \frac{9.08}{a^2}\sqrt{\frac{D}{\rho h}}.$$

This result agrees (within 1.04%) with the value obtained from more accurate computation [1,2].

Approximate values of natural frequencies in rectangular plates with various combinations of boundary conditions, obtained by the Ritz method, are given in Ref. [2,3].

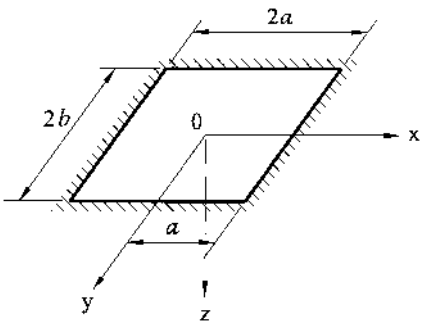

Fig. 9.2

9.3.2 The Galerkin method

The Galerkin method, introduced in Sec. 6.5, also may be used for determining the natural frequencies in vibrating plates. Assume again that a shape function for the plate is approximated by a series (9.20), which satisfies, term by term, all boundary conditions. Then, following the general procedure of the Galerkin method (see Sec. 6.5), the unknown coefficients C_i can be determined from the orthogonality conditions (6.37). For the vibration plate problems described by Eq. (9.6), the orthogonality conditions together with the expansion (9.20) result in the following equation:

$$\int\int_A \left(D \sum_{i=1}^{n} C_i \nabla^2 \nabla^2 W_i - \rho h \omega^2 \sum_{i=1}^{n} C_i W_i \right) W_k \mathrm{d}x\mathrm{d}y = 0; \quad k = 1, 2, \ldots, n. \tag{9.22}$$

The numerical implementation of the above condition leads to the Galerkin system of linear algebraic homogeneous equations of the form

$$\begin{aligned} &a_{11}C_1 + a_{12}C_2 + \ldots\ldots\ldots\ldots\ldots = 0 \\ &\ldots\ldots\ldots\ldots\ldots\ldots\ldots\ldots\ldots\ldots\ldots \\ &a_{n1}C_1 + a_{n2}C_2 + \ldots\ldots\ldots\ldots\ldots = 0, \end{aligned} \tag{9.23}$$

where

$$a_{ik} = a_{ki} = \int\int_A \left[D \nabla^2 \nabla^2 W_i - \rho h \omega^2 W_i \right] W_k \mathrm{d}x\mathrm{d}y. \tag{9.24}$$

This system of homogeneous equations has a nontrivial solution if its determinant made up of the coefficients a_{ik} is equal to zero. The latter results in the nth order characteristic equation (9.7) for determining the natural frequencies.

Let us represent the shape function $W(x, y)$ for a rectangular plate with dimensions a and b in the form

$$W(x, y) = \sum_i \sum_k C_{ik} W_{ik}(x, y), \tag{9.25}$$

where C_{ik} are unknown coefficients representing the amplitudes of the free vibration modes and $W_{ik}(x, y)$ is the product of the pertinent eigenfunctions of lateral beam vibrations,

$$W_{ik}(x, y) = F_i(x) F_k(y), \tag{9.26}$$

which satisfy the prescribed boundary conditions on the edges $x = 0$, $x = a$, and $y = 0$, $y = b$. In Eq. (9.26), $F_i(x)$ and $F_k(y)$ represent the ith and kth modes of freely vibrating beams with spans a and b, respectively.

Example 9.2

Determine the natural frequencies of the rectangular, simply supported plate of sides a and b with a uniformly distributed mass m and with four concentrated masses M, as shown in Fig. 9.3.

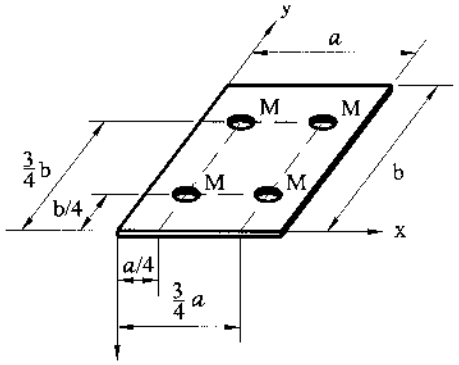

Fig. 9.3

Solution

We apply the Galerkin method for the solution of this problem. We modify slightly Eq. (9.24) for the coefficients a_{ik} of Galerkin's system of equations, to the present problem, as follows:

$$a_{ik} = a_{ki} = \int\int_A \left[D\nabla^2\nabla^2 W_i - m\omega^2 W_i\right] W_k \mathrm{d}x\mathrm{d}y - \sum M\omega^2 W_i W_k, \tag{9.27}$$

where m and M are uniformly distributed and concentrated masses, respectively. The deflected surface of the vibrating plate is approximated by the series

$$W(x, y) = \sum_{i=1}^{\infty}\sum_{k=1}^{\infty} C_{ik} \sin\frac{i\pi x}{a}\sin\frac{k\pi y}{b}, \tag{a}$$

which satisfies the simply supported boundary conditions.

The first approximation

Retaining only the first term in the expansion (a), we obtain

$$a_{11} = \int\int_A \left[D\left(\frac{\partial^4 W_1}{\partial x^4} + 2\frac{\partial^4 W_1}{\partial x^2\partial y^2} + \frac{\partial^4 W_1}{\partial y^4}\right) - m\omega^2 W_1\right] W_1 \mathrm{d}x\mathrm{d}y - 4M\omega^2 W_1. \tag{9.28}$$

Introducing in the above $W_1 = \sin(\pi x/a)\sin(\pi y/b)$ and substituting for a_{11} from (9.28) into the Galerkin equation (9.24), we obtain, after some operations, this equation in the following form:

$$\left[D\pi^4\left(\frac{1}{a^2} + \frac{1}{b^2}\right)^2 - m\omega^2\right]\int_0^a\int_0^b \sin^2\frac{\pi x}{a}\sin^2\frac{\pi y}{b}\mathrm{d}x\mathrm{d}y - 4M\omega^2\frac{1}{4} = 0. \tag{f}$$

Integrating Eq. (f) yields the following expression for the natural frequency:

$$\omega = \pi^2\left(\frac{1}{a^2} + \frac{1}{b^2}\right)\sqrt{\frac{D}{m + \dfrac{4M}{ab}}}. \tag{9.29}$$

Using more additional terms in Eq. (a), the "exact" value of the natural frequency may be obtained. The application of the fourth approximation to this problem for the square plate ($a = b$) has shown that the refinement over the first approximation does not exceed 1.2%. Thus, the accuracy of the first approximation may be considered as quite satisfactory.

9.4 FREE FLEXURAL VIBRATIONS OF CIRCULAR PLATES

Let us consider a freely vibrating, solid, circular plate of radius a, having a constant thickness h. Using the polar coordinates, r and φ, with the origin at the center of the plate, we can rewrite the governing differential equation of the free vibration of plates, Eq. (9.3), as follows:

$$D\nabla_r^2\nabla_r^2 w + \rho h\frac{\partial^2 w}{\partial t^2} = 0, \tag{9.30}$$

where ∇_r^2 is the Laplace operator given by Eq. (4.5). Assume that the deflection of the middle surface of the plate can be approximated as

$$w(r, \varphi, t) = W(r, \varphi)F(t). \tag{9.31}$$

Introducing the above into Eq. (9.30), yields

$$DF(t)\nabla_r^2\nabla_r^2 W + \rho h W\frac{\mathrm{d}^2 F}{\mathrm{d}t^2} = 0 \quad \text{or} \quad \frac{D\nabla_r^2\nabla_r^2 W}{\rho h W} = -\frac{\dfrac{\mathrm{d}^2 F}{\mathrm{d}t^2}}{F}. \tag{9.32}$$

Since the left-hand side of this equation is a function of variables r and φ whereas the right-hand side depends only on time variable t, we can conclude that the ratios in the left- and right-hand sides of Eq. (9.32) must be constant. Denote the aforementioned constant ratio on the right-hand side of Eq. (9.32) by ω^2, i.e.,

$$\frac{\mathrm{d}^2 F}{\mathrm{d}t^2} = -\omega^2 F, \tag{9.33}$$

where ω is the natural frequency of vibrations. Solving this for F, yields

$$F = A\sin(\omega t + \varphi_0), \tag{9.34}$$

where φ_0 is an arbitrary constant. The shape function $W(r, \varphi)$ satisfies the differential equation

$$\frac{D\nabla_r^2\nabla_r^2 W}{\rho h W} = \omega^2 \quad \text{or} \quad \nabla_r^2\nabla_r^2 W - \lambda^4 W = 0, \tag{9.35}$$

where

$$\lambda^4 = \frac{\omega^2\rho h}{D}. \tag{9.36}$$

Let us go from the variable r to the dimensionless variable $\zeta = \lambda r$. Then, Eq. (9.35) becomes

$$\left(\frac{\partial^2}{\partial\zeta^2} + \frac{1}{\zeta}\frac{\partial}{\partial\zeta} + \frac{1}{\zeta^2}\frac{\partial^2}{\partial\varphi^2}\right)^2 W - W = 0. \tag{9.37}$$

Its solution is of the following form [4,5]:

$$W(r, \varphi) = [C_1 J_n(\zeta) + C_2 I_n(\zeta) + C_3 Y_n(\zeta) + C_4 K_n(\zeta)] \sin(n\varphi + \alpha), \tag{9.38}$$

where $n = 0, 1, \ldots, \infty$; $C_1, \ldots, C_4$ are constants of integration; and $J_n()$, $I_n()$, $Y_n()$, and $K_n()$ are Bessel functions of the first and second kind of the real and imaginary arguments, respectively [4,5], and α is a constant. Since the origin of the polar coordinate system is taken to coincide with the center of the circular plate having no internal holes or supports at the center, the terms $Y_n(\zeta)$ and $K_n(\zeta)$ must be discarded ito avoid infinite deflections and stresses at $r = 0$. When these simplifications are employed, Eq. (9.38) becomes, for a typical mode,

$$W = [C_1 J_n(\zeta) + C_2 I_n(\zeta)] \sin(n\varphi + \alpha). \tag{9.39}$$

Assume that the plate is clamped along its contour. The boundary conditions are

$$W = \frac{\partial W}{\partial r} = 0 \Big|_{r=a} \tag{9.40}$$

When Eq. (9.39) is substituted into the above boundary conditions, the existence of a nontrivial solution yields the following characteristic determinant:

$$\begin{vmatrix} J_n(\zeta) & I_n(\zeta) \\ J_n'(\zeta) & I_n'(\zeta) \end{vmatrix} = 0, \tag{9.41}$$

where the primes are used to indicate a differentiation with respect to the argument, in this case to ζ. Using the following recursion relationships [4,5]:

$$\begin{aligned} \zeta J_n'(\zeta) &= n J_n(\zeta) - \zeta J_{n+1}(\zeta) \\ \zeta I_n'(\zeta) &= n I_n(\zeta) + \zeta I_{n+1}(\zeta), \end{aligned} \tag{9.42}$$

and expanding Eq. (9.41) gives

$$J_n(\zeta) I_{n+1}(\zeta) + I_n(\zeta) J_{n+1}(\zeta) = 0. \tag{9.43a}$$

The eigenvalues ζ determining the frequencies ω are the roots of Eq. (9.43a). The Bessel functions are widely tabulated for small values of n [4].

For circular plates simply supported all around ($w = 0$ and $M_r = 0$), the frequency equation is of the form

$$\frac{J_{n+1}(\zeta)}{J_n(\zeta)} + \frac{I_{n+1}(\zeta)}{I_n(\zeta)} = \frac{2\zeta}{1 - \nu}. \tag{9.43b}$$

If a plate edge is completely free ($M_r = 0$ and $V_r = 0$), then the frequency equation can be represented as follows (for $\zeta \gg n$) [3]:

$$\frac{J_n(\zeta)}{J_n'(\zeta)} \cong \frac{\left[\zeta^2 + 2(1 - \nu)n^2\right]\left[I_n(\zeta)/I_n'(\zeta)\right] - 2\zeta(1 - \zeta)}{\zeta^2 - 2(1 - \nu)n^2} \tag{9.43c}$$

For more information concerning the above problems, see Ref. [3].

The natural frequencies and pertinent mode shapes for solid circular plates can be also calculated by using the Ritz or Galerkin methods, as indicated in Sec. 9.3. Let us illustrate this procedure.

Example 9.3

Determine the fundamental natural frequency of axisymmetric vibrations of a solid circular plate with radius R. The plate is clamped along its boundary.

Solution

We take the shape function in the first approximation as follows:

$$W = C\left(R^2 - r^2\right).^2 \tag{a}$$

Evidently, the above expression satisfies the given boundary conditions ($w = 0$ and $\partial w/\partial r = 0$) exactly. We apply the Ritz method. It can be shown that for circular plates with a fastened edge the expression for the potential energy (4.13) becomes simplified:

$$U_{\max} = \int\int_A \frac{D}{2}\left(\frac{\partial^2 W}{\partial r^2} + \frac{1}{r}\frac{\partial W}{\partial r} + \frac{1}{r^2}\frac{\partial^2 W}{\partial \varphi^2}\right)^2 r\mathrm{d}r\mathrm{d}\varphi. \tag{9.44a}$$

The corresponding expression for the kinetic energy in polar coordinates has the form

$$K_{\max} = \frac{\omega^2}{2}\int\int_A \rho h W^2(r,\varphi) r\mathrm{d}r\mathrm{d}\varphi. \tag{9.44b}$$

Substituting for W from Eq. (a) into expressions (9.44) and evaluating the corresponding integrals, one obtains

$$U_{\max} = C^2 D\frac{\pi}{2}R^6\frac{32}{3} \quad \text{and} \quad K_{\max} = \frac{\omega^2}{2}C^2\pi R^{10}\frac{1}{10}\rho h. \tag{b}$$

Then, the fundamental natural frequency (the first approximation) may be found from Eq. (9.18), as follows:

$$\omega_{11} = \frac{10.33}{R^2}\sqrt{\frac{D}{\rho h}}.$$

Notice that the second approximation of this frequency differs from the above value by 1.175% only.

9.5 FORCED FLEXURAL VIBRATIONS OF PLATES

The equation of motion of plates under a variable, time-dependent, transverse load $p(x, y, t)$ is given by Eq. (9.2). A solution of the above nonhomogeneous, partial differential equation must satisfy the prescribed boundary and initial conditions. An exact solution can be obtained by using the following procedure. First, let us solve the problem of free vibrations of a plate, and determine the natural frequencies ω_{mn} and the corresponding mode shapes W_{mn}. Then, let us introduce a load $p(x, y, t)$ in the form of series extended in eigenfunctions (the mode shapes), i.e.,

$$p = \sum_{m=1}^{\infty}\sum_{n=1}^{\infty} f_{mn}(t) W_{mn}(x, y). \tag{9.45}$$

We seek a solution of Eq. (9.2) in the form

$$w = \sum_{m=1}^{\infty} \sum_{n=1}^{\infty} F_{mn}(t) W_{mn}(x, y). \tag{9.46}$$

The following equation takes place for the function F_{mn}:

$$\ddot{F}_{mn} + \omega_{mn}^2 F_{mn} = \frac{1}{\rho h} f_{mn}(t), \tag{9.47}$$

from which

$$F_{mn} = A_{mn} \cos \omega_{mn} t + B_{mn} \sin \omega_{mn} t + F_{mn}^{(\mathrm{p})}(t) \tag{9.48}$$

and

$$w = \sum_{m=1}^{\infty} \sum_{n=1}^{\infty} \left[A_{mn} \cos \omega_{mn} t + B_{mn} \sin \omega_{mn} t + F_{mn}^{(\mathrm{p})}(t) \right] W_{mn}(x, y) \tag{9.49}$$

where $F_{mn}^{(\mathrm{p})}$ is a particular solution of Eq. (9.2); its form depends on f_{mn}, i.e., how a given load p varies with time. The constants A_{mn} and B_{mn} are determined from initial conditions: namely, at $t = 0$

$$w = w_0(x, y) \quad \text{and} \quad \frac{\partial w}{\partial t} = v_0(x, y). \tag{9.50}$$

Example 9.4

Determine the vibration modes for a simply supported rectangular plate with dimensions a and b. The plate is subjected to a surface transverse load varying as $p = p_0(x, y) \cos \Omega t$, where Ω is the frequency of forced vibrations, which is equal to the frequency of a disturbing loading.

Solution

Let us expand an applied load into the series

$$p(x, y, t) = \cos \Omega p_o(x, y) = \cos \Omega t \sum_{m}^{\infty} \sum_{n}^{\infty} A_{mn} \sin \alpha_m x \sin \beta_n y, \tag{9.51}$$

where

$$A_{mn} = \frac{4}{ab} \int_0^a \int_0^b p_0(x, y) \sin \alpha_m x \sin \beta_n y \mathrm{d}x \mathrm{d}y, \quad \alpha_m = \frac{m\pi}{a}, \quad \beta_n = \frac{n\pi}{b}. \tag{9.52}$$

The deflected surface of the vibrating plate can be approximated by the series (9.46) where

$$W_{mm}(x, y) = \sin \alpha_m x \sin \beta_n y \tag{9.53}$$

The particular solution, $F_{mn}^{(p)}(t)$, may be found from Eq. (9.47) by letting $f_{mn}(t) = \cos \Omega t$.

We obtain

$$F_{mn}^{(t)} = \frac{1}{\rho h} \frac{\cos \Omega t}{\omega_{mn}^2 - \Omega^2} \tag{9.54}$$

Substituting the above into Eq. (9.49) and evaluating the constants A_{mn} and B_{mn} from the assumption that the plate is at rest at the initial moment (i.e., at $t = 0 \quad w = 0$ and $\partial\omega/\partial t = 0$), we obtain the following expression for the deflected surface of the vibrating plate:

$$w = \frac{1}{\rho h}\sum_{m=1}^{\infty}\sum_{n=1}^{\infty}\frac{A_{mn}}{\omega_{mn}^2 - \Omega^2}(\cos\Omega t - \cos\omega_{mn}t)\sin\alpha_m x \sin\beta_n y \tag{9.55}$$

In the case when the load frequency Ω will coincide with any natural frequencies of the plate, the plate will vibrate in the *resonance state*. In fact, if for any m and n, $\Omega = \omega_{mn}$, then the corresponding term of the series (9.55) becomes indetermined of the type 0/0. Evaluating this indeterminate form yields

$$w_{mn} = \frac{1}{\rho h}\frac{A_{mn}}{2\omega_{mn}} t \sin\omega_{mn}t \sin\alpha_m x \sin\beta_n y. \tag{9.56}$$

This expression represents a vibration with an amplitude that indefinitely increases with time.

If $p_0 = const$, then $\quad A_{mn} = 16p_0/mn\pi^2 \quad$ for $\quad m = 1, 3, 5\ldots; \quad n = 1, 3, 5, \ldots$ Eq. (9.55) will be of the form:

$$w = \frac{16p_0}{\rho h \pi^2}\sum_{m=1,3,\ldots}^{\infty}\sum_{n=1,3,\ldots}^{\infty}\frac{\cos\Omega t - \cos\omega_{mn}t}{mn(\omega_{mn}^2 - \Omega^2)}\sin\alpha_m x \sin\beta_n y \tag{9.57}$$

Here, we did not take into account the resistance of surrounding media and internal friction. These factors can have a pronounced effect on the vibration process. As a result, the vibrations will have a gradually diminishing amplitude.

This chapter can serve only as introduction to the dynamic behavior of plates; for further analysis, the interested reader is referred to other works [1,3,6,7].

PROBLEMS

9.1 Consider free harmonic vibrations of a rectangular plate with simply supported edges $x = 0$ and $x = a$. Determine the natural frequencies and associated mode shapes if (a) the edges $y = 0$ and $y = b$ are free, (b) the edges $y = 0$ and $y = b$ are clamped, (c) the edge $y = 0$ is simply supported and the edge $y = b$ is free, and (d) the edge $y = 0$ is simply supported and the edge $y = b$ is clamped. Use $w(x, y, t) = F(y)\sin(m\pi x/a)\cos\omega t$.

9.2 Determine an approximate value of the lowest natural frequency of a rectangular plate. The edges $x = 0$ and $x = a$ are built-in and the edges $y = 0$ and $y = b$ are simply supported. Use the Galerkin method. Take the shape function, $W(x, y)$, in the form of Eq. (9.25), where

$$F_i(x) = \sin\lambda_i x - \sinh\lambda_i x - a(\cos\lambda_i x - \cosh\lambda_i x);$$

$$F_k(y) = \sin\mu_k y; \text{ and } \lambda_i = i\pi/a, \mu_k = k\pi/b; \ i = (2n+1)/2; \ (n = 1, 2, \ldots)$$

9.3 Redo Problem 9.1 by employing the Ritz method. Take $W(x, y)$ in the form

$$W(x, y) = \sum_{m=1}^{\infty}\sum_{n=1}^{\infty}A_{mn}\left(1 - \cos\frac{2m\pi x}{a}\right)\sin\frac{n\pi y}{b}.$$

9.4 Determine an approximate value of the fundamental natural frequency for a rectangular plate. The edges $y = 0$ and $y = b$ are simply supported while the edge $x = 0$ is clamped at the edge.

9.5 Consider free, axisymmetric harmonic vibrations of a circular solid plate with radius R. Calculate the three lowest natural frequencies if (a) the plate edge $r = R$ is simply supported and (b) the plate edge $r = R$ is clamped.

9.6 Determine the lowest natural frequency of the rectangular, simply supported plate of sides a and b with a uniformly distributed mass m and with a concentrated mass M applied at the plate center ($x = a/2$ and $y = b/2$).

9.7 Determine the amplitude of the forced vibrations of a rectangular simply supported plate of sides a and b. The plate is subjected to the following time-dependent, transverse surface load:

$$p = p_0 \sin\frac{\pi x}{a}\sin^2\frac{\pi y}{a}\sin\theta t.$$

.

9.8 For approximate description of elastic vibrations of a rectangular plate ($0 \le x \le a$, $0 \le y \le b$) with thickness h, this plate is replaced by a single degree of freedom system. The mass of the plate is concentrated at the plate center. Determine the corresponding reduction coefficient (mass factor), ensuring such an equivalent replacement if the plate is simply supported and its deflection surface is approximated by the following expression that satisfies all the boundary conditions:

$$W = A\cos\frac{\pi x}{2a}\cos\frac{\pi y}{2b}$$

(the origin of the coordinate system is taken at the plate center).

9.9 Redo Problem 9.8 for the plate clamped along edges $x = \pm a$ and $y = \pm b$. Take W in the form:

$$W = \frac{A}{a^4 b^4}\left(x^2 - a^2\right)^2\left(y^2 - b^2\right)^2.$$

REFERENCES

1. Nowacki, W., *Dynamics of Elastic Systems*, John Wiley and Sons, New York, 1963.
2. Warburton, G., The vibration of rectangular plates, *Proc J Mech Engrs*, vol. 168, No. 12, pp. 371–384 (1954).
3. Leissa, A.W., *Vibrations of Plates,* National Aeronautics and Space Administration, Washington, D.C., 1969.
4. Watson, G.N., *Theory of Bessel Functions*, 2nd. edn, Cambridge University Press, Cambridge, 1944.
5. McLachlan, N., *Bessel Functions for Engineers,* Oxford Eng Sci Ser, Oxford University Press, London, 1948.
6. Thomson, W.T., *Vibration Theory and Applications*, Prentice-Hall, Englewood Cliffs, New Jersey, 1973.
7. Dill, E.N. and Pister, K.S., Vibration of rectangular plates and plate systems, *Proc 3rd US Natl Congr Appl Mech*, pp. 123–132 (1958).

Part II

Thin Shells

10

Introduction to the General Shell Theory

10.1 SHELLS IN ENGINEERING STRUCTURES

Thin shells as structural elements occupy a leadership position in engineering and, in particular, in civil, mechanical, architectural, aeronautical, and marine engineering (Fig. 10.1). Examples of shell structures in civil and architectural engineering are large-span roofs, liquid-retaining structures and water tanks, containment shells of nuclear power plants, and concrete arch domes. In mechanical engineering, shell forms are used in piping systems, turbine disks, and pressure vessels technology. Aircrafts, missiles, rockets, ships, and submarines are examples of the use of shells in aeronautical and marine engineering. Another application of shell engineering is in the field of biomechanics: shells are found in various biological forms, such as the eye and the skull, and plant and animal shapes. This is only a small list of shell forms in engineering and nature.

The wide application of shell structures in engineering is conditioned by their following advantages:

1. *Efficiency of load-carrying behavior*.
2. *High degree of reserved strength and structural integrity*.
3. *High strength : weight ratio*. This criterion is commonly used to estimate a structural component efficiency: the larger this ratio, the more optimal is a structure. According to this criterion, shell structures are much superior to other structural systems having the same span and overall dimensions.
4. *Very high stiffness*.
5. *Containment of space*.

In addition to these mechanical advantages, shell structures enjoy the unique position of having extremely high aesthetic value in various architectural designs.

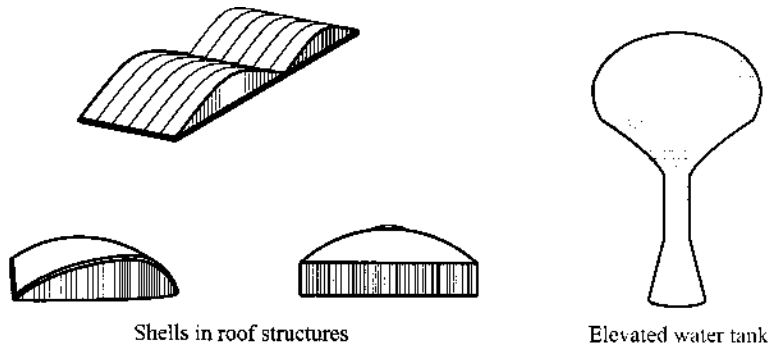

Shells in roof structures

Elevated water tank

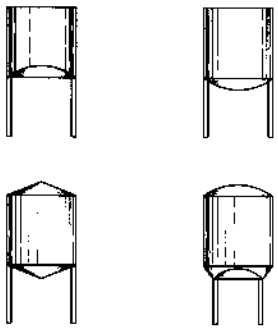

Liquid retaining cylindrical shells

(a)

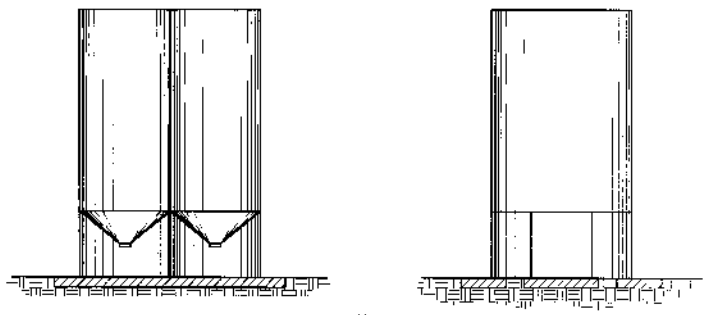

Silos

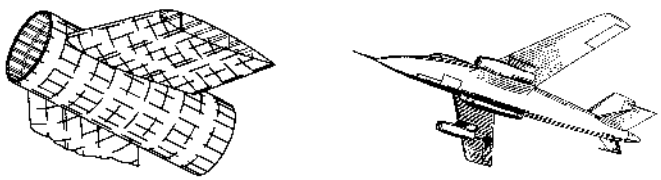

Aircraft structures

(b)

Fig. 10.1

Contemporary engineers using scientifically justified methods of design tend to develop a structure that combines maximum strength, functional perfection, and economy during its lifetime. In addition, it is important that the best engineering solution ensues, other things being equal, at the expense of the selection of structural form and by not increasing the strength properties of the structure, e.g., by increasing its cross section. Note that the latter approach is easier. Shell structures support applied external forces efficiently by virtue of their geometrical form, i.e., spatial curvatures; as a result, shells are much stronger and stiffer than other structural forms.

10.2 GENERAL DEFINITIONS AND FUNDAMENTALS OF SHELLS

We now formulate some definitions and principles in shell theory. The term *shell* is applied to bodies bounded by two curved surfaces, where the distance between the surfaces is small in comparison with other body dimensions (Fig. 10.2).

The locus of points that lie at equal distances from these two curved surfaces defines the *middle surface* of the shell. The length of the segment, which is perpendicular to the curved surfaces, is called the *thickness* of the shell and is denoted by h. The geometry of a shell is entirely defined by specifying the form of the middle surface and thickness of the shell at each point. In this book we consider mainly shells of a constant thickness.

Shells have all the characteristics of plates, along with an additional one – curvature. The curvature could be chosen as the primary classifier of a shell because a shell's behavior under an applied loading is primarily governed by curvature (see Sec. 10.4). Depending on the curvature of the surface, shells are divided into cylindrical (noncircular and circular), conical, spherical, ellipsoidal, paraboloidal, toroidal, and hyperbolic paraboloidal shells. Owing to the curvature of the surface, shells are more complicated than flat plates because their bending cannot, in general, be separated from their stretching. On the other hand, a plate may be considered as a special limiting case of a shell that has no curvature; consequently, shells are sometimes referred to as curved plates. This is the basis for the adoption of methods from the theory of plates, discussed in Part I, into the theory of shells.

There are two different classes of shells: thick shells and thin shells. A shell is called *thin* if the maximum value of the ratio h/R (where R is the radius of curvature of the middle surface) can be neglected in comparison with unity. For an engineering accuracy, a shell may be regarded as thin if [1] the following condition is satisfied:

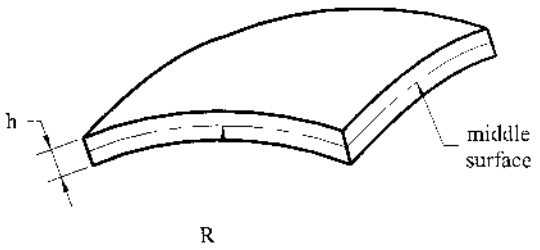

Fig. 10.2

$$\max\left(\frac{h}{R}\right) \leq \frac{1}{20}. \tag{10.1}$$

Hence, shells for which this inequality is violated are referred to as *thick shells*. For a large number of practical applications, the thickness of shells lies in the range

$$\frac{1}{1000} \leq \frac{h}{R} \leq \frac{1}{20},$$

i.e., in the range of thin shells, and therefore the theory of thin shells presented in this book is of great practical importance.

Note also that the inequality (10.1) defines very roughly the boundary between thin and thick shells. In reality, it depends also upon other geometrical parameters of shells, the character of their boundary conditions, smoothness of a variation of external loads over the shell surface, etc.

10.3 BRIEF OUTLINE OF THE LINEAR SHELL THEORIES

The most common shell theories are those based on linear elasticity concepts. Linear shell theories predict adequately stresses and deformations for shells exhibiting small elastic deformations; i.e., deformations for which it is assumed that the equilibrium equation conditions for deformed shell surfaces are the same as if they were not deformed, and Hooke's law applies.

For the purpose of analysis, a shell may be considered as a three-dimensional body, and the methods of the theory of linear elasticity may then be applied. However, a calculation based on these methods will generally be very difficult and complicated. In the theory of shells, an alternative simplified method is therefore employed. According to this method and adapting some hypotheses (see Sec. 12.1), the 3D problem of shell equilibrium and straining may be reduced to the analysis of its middle surface only, i.e. the given shell, as discussed earlier as a thin plate, may be regarded as some 2D body. In the development of thin shell theories, simplification is accomplished by reducing the shell problems to the study of deformations of the middle surface.

Shell theories of varying degrees of accuracy were derived, depending on the degree to which the elasticity equations were simplified. The approximations necessary for the development of an adequate theory of shells have been the subject of considerable discussions among investigators in the field. We present below a brief outline of elastic shell theories in an historical context.

Love was the first investigator to present a successful approximation shell theory based on classical linear elasticity [2]. To simplify the strain–displacement relationships and, consequently, the constitutive relations, Love applied, to the shell theory, the Kirchhoff hypotheses developed originally for the plate bending theory, together with the small deflection and thinness of the shell assumptions. This set of assumptions is commonly called the *Kirchhoff–Love assumptions*. The Love theory of thin elastic shells is also referred to as *the first-order approximation shell theory*. In spite of its popularity and common character, Love's theory was not free from some deficiencies, including its inconsistent treatment of small terms, where some were retained and others were rejected, although they were of the same order. This meant that, for certain shells, Love's differential operator matrix on the displacements, in

the equations of equilibrium, became unsymmetric. Obviously, this violated Betti's theorem of reciprocity. Love's theory also contained some other inconsistencies. The need for a mathematically rigorous two-dimensional set of the shell equations employing the Kirchhoff–Love assumptions led to different versions of the first-order approximation theories.

E. Reissner [3] developed the linear theory of thin shells (also the first-order approximation theory) where some inadequacies of Love's theory were eliminated. He derived equations of equilibrium, strain–displacement relations, and stress resultants expressions for thin shells directly from the three-dimensional theory of elasticity, by applying the Love–Kirchhoff hypotheses and neglecting small terms of order z/R_i (where R_i $(i = 1, 2)$ are the radii of the curvature of the middle surface) compared with unity in the corresponding expressions.

Sanders [4] also developed the first-order-approximation shell theory from the principle of virtual work and by applying the Kirchhoff–Love assumptions. Sanders' theory of thin shells has removed successfully the inconsistencies of the Love theory. A version that retains terms of magnitude compatible with those retained by E. Reissner and resolves the inconsistency in the expression for twist was developed by Koiter [5].

Timoshenko's theory of thin shells [6] was very close to the Love theory. General relations and equations were obtained by applying the Kirchhoff–Love hypotheses and neglecting terms z/R_i in comparison with unity. Naghdi [7,8] analyzed the accuracy of the Love–Kirchhoff theory of thin elastic shells.

A second class of thin elastic shells, which is commonly referred to as *higher-order approximation,* has also been developed. To this grouping it is possible to assign all linear shell theories in which one or another of the Kirchhoff–Love hypotheses are suspended. First, we consider some representative theories in which the thinness assumption is delayed in derivation while the rest of the postulates are retained. In this case, the order of a particular approximate theory will be established by the order of the terms in the thickness coordinate that is retained in the strain and constitutive equations.

Lur'ye [9], Flügge [10], and Byrne [11] independently developed *the second-order approximation theory of shells*. The general relations and equations of this theory are the direct result of the application of the Kirchhoff hypotheses together with the small-deflection assumption to the corresponding equations of the three-dimensional theory of elasticity. The second-order approximation theory attempts a more careful discard of terms z/R_i. It retains these terms in comparison with unity in the strain–displacement relations and stress resultant equations. Applications of this theory have generally been restricted to circular cylindrical shells. In addition, the general relations and equations of this second-order approximation shell theory are found to be cumbersome for application.

Novozhilov [1] developed another version of the second-order approximation theory. Just as Lur'ye–Flügge–Byrne theory, he obtained the strain–displacement relations from the three-dimensional theory of elasticity by applying Kirchhoff's assumptions. Then, he made use of the strain energy expression to derive the formulas for the stress resultants and couples (again by applying the Kirchhoff hypotheses) and for determining the terms to be disregarded. Novozhilov developed the criterion for simplifying the governing equations and relations of the general theory of thin shells based on Kirchhoff's hypotheses. He proved that the errors introduced

by Kirchhoff's assumptions into the small-deflection shell theory were of the order h/R_i in comparison with unity [12].

Valuable contributions to the general theory of thin shells were given by Gol'denveizer [13]. He was the first to formulate the conditions for compatibility of strain components in the general theory of shells.

The second-order approximation equations were derived by Vlasov [14] directly from the general three-dimensional linear elasticity equations for a thick shell. The assumption that the transverse normal and shear strain components may be neglected for thin shells was made, and the remaining strains were represented by the first three terms of their series expansion. The assumption of zero transverse normal strain as well as zero transverse shear strains permits a rapid transition from the three-dimensional theory to the two-dimensional equations of the thin shell theory.

Another class of second-order approximation theories appeared in which the assumptions on the vanishing of the transverse normal strain and on the preservation of the normals was abandoned. Such theories, which incorporated the transverse shear and normal stress effects, were proposed by E. Reissner [15,16], Naghdi [17], and others. A comprehensive analysis of the first- and higher-order approximation theories and of the corresponding governing equations for elastic shells was made by Kraus [18], Leissa [19], etc.

The small-defection shell theories discussed above were formulated from the classical linear theory of elasticity. It is known that the equations of these theories, which are based on Hooke's law and the omission of nonlinear terms in both the equations for strain components and equilibrium equations, have a unique solution in every case. In other words, a linear shell theory determines a unique position of equilibrium for every shell with prescribed load and constraints. In reality, however, a solution of physical shell problems is not always unique. A shell under identical conditions of loading and constraints may have several possible positions of equilibrium. A theory that takes into account finite or large deformations is referred to as a *geometrically nonlinear theory of thin shells*. Additionally, a shell may be *physically nonlinear* with respect to the stress–strain relations.

E. Reissner [20] derived a nonlinear theory of symmetrically loaded shells of revolution. In this theory, the small-deflection assumption was abandoned while the remaining assumptions of the general higher-order approximation theories were retained. Derivations of a more general geometrically nonlinear theory of thin shells have been carried out by Naghdi and Nordgren [21], Sanders [22], and Koiter [23]. Vlasov [14] derived a set of equations for nonlinear shallow shells. From these equations, as a particular case, von Karman equations describing finite deformations for plates, discussed in Sec. 7.4, followed. A subsequent development of the general nonlinear theory of thin shells has been made by Mushtari and Galimov [24], Simmonds and Danielson [25], etc.

A number of specialized shell theories were developed to include features of special types of shells, in parallel with the evolution of the general theories of thin shells discussed above. The factors influencing the assumptions and domains of applications of these specialized shell theories have been a shell geometry, the deformation ranges, the loading and stress conditions, the particular shell behavior desired, etc. Most of these theories are based on Love's first-order approximation.

The membrane theory of thin shells may be presented as the first example of such a type of the specialized shell theory. The general form of the governing equations of the membrane theory of thin shells was established by Beltrami [26] and Lecornu [27] in the last century. The membrane theory of shells was intensively evolving. H. Reissner [28] developed the membrane theory of thin shells of revolution under unsymmetric loads. Sokolovskii [29] reduced the equations of the membrane theory to canonical form and revealed a number of their characteristic properties. Pucher [30] discovered the usefulness of Airy's stress function for the solution of membrane problems in shells of an arbitrary form.

Another example of the specialized shell theory is the theory of shallow shells. Donnel [31], Vlasov [14], and Mushtari [32] independently developed a simplified engineering theory of thin shells of a general form. Due to their simplicity, the governing equations of this theory were found to be extremely convenient for solving many engineering shell problems. Apart from the Kirchhoff–Love hypotheses, some additional assumptions that simplify the strain–displacement relations, equilibrium, and compatibility equations were used in deriving these equations. It turned out that the Donnel–Vlasov–Mushtari theory could be applied with sufficient accuracy to shallow shells. Shallow shells have geometries that are close to that of a thin plate. Such shells have a wide application in engineering, for example in roof structures, which have a relatively small rise compared with their span. Notice that the above-mentioned theory may also be applied to non-shallow shells whose state of stress is characterized by rapidly varying stress components along the coordinates of the middle surface. Shallow shells are commonly referred to as curved plates. Marguerre established the governing equations for plates having an initial curvature [33].

Shells of revolution, a very important class of thin shells, have many technical applications in engineering. The theory of thin shells of revolution may serve as one more example of the specialized shell theories. H. Reissner presented a classical formulation of the bending problems for a shell of revolution [28] and studied a spherical shell under axisymmetric bending. He reduced the differential equations of the spherical shell to a convenient form and then applied the asymptotic method for their integration. Meissner [34] was able to generalize Reissner's results to symmetrical deformation of shells of revolution of an arbitrary shape and having a variable thickness. Hoff [35] analyzed circular conical shells under an arbitrary loading. Flügge gave general solutions for spherical and conical shells subjected to asymmetrical loading [36]. His approach was based on the classical displacement method.

Wissler analyzed toroidal shells [37]. By convention, cylindrical shells are frequently considered apart from the shells of revolution, although they technically fall into this class of shells. The analysis of cylindrical shells for general surface loading occupies a prominent place in the literature because of their wide practical significance and the relative simplicity of the theory. We should mention that Flügge derived the governing differential equations for circular cylindrical shells in terms of displacements [36]. Parkus derived the equations for a cylinder of an arbitrary cross section [38]. It should be noted that radical simplifications underlying the relations and equations of the general theory of cylindrical shells were introduced by Donnel [31], Dishinger [39], Hoff [40], and Vlasov [14]. Novozhilov [1] derived the governing differential of the general theory of cylindrical shells of an arbitrary shape

using complex variables and pointed out some possible simplifications of these equations.

The concept of the *edge effect*, introduced first by Love [2], applied to shells of revolution, is of greatest importance in an engineering analysis of thin shells. Love showed that a first approximation to a general solution might be obtained in the form of the sum of the solutions of the membrane equations and the equations for the edge effect. Integrals of the latter equations are expressed in terms of rapidly varying functions. Gol'denveizer [13] defined the conditions for which the rapidly decaying solutions of the equations of the general shell theory may be obtained, and analyzed a number of possible special cases. Geckeler [41] applied this concept to symmetrically loaded spherical shells. His approximate method was based on the reduction of the system of the two-coupled differential equations to two independent differential equations, assuming that for very thin shells the derivatives of the given functions will be greater than the functions themselves.

Shell buckling problems have been a subject of investigations by many scientists and engineers. For a circular cylindrical shell subjected to a uniform compressive axial load, the differential equations have been formulated and solutions have been found by Lorentz [42] and Timoshenko [43]. Mises [44] and Mushtari and Sachenkov [45] treated a linear buckling problem for cylindrical shells subjected to combined loading (external pressure and axially applied compressive forces). The combined effect of axial and internal pressure was studied by Flügge [36] for cylindrical shells. It should be noted that, unlike the plate bending problems, a theoretically determined buckling load, calculated by the small-deflection theory, is rarely attained or even approached in experiment. It was shown that initial imperfections were the most influential contributor to the discrepancy between theoretical and experimental results in determining the buckling loads. Donnel and Wan [46] derived the general equations and analyzed the effect of imperfections on the buckling of thin cylindrical shells under uniform, axial compressive forces.

The buckling problem for a spherical shell under an external pressure was presented by Zoelly [47] in linear and by von Karman and Tsien [48] in nonlinear formulations, respectively. Koiter [49] analyzed the postbuckling behavior of a cylindrical shell under axial compression. Buckling of shallow shells under normal surface load was studied by Budansky [50] (linear problem) and Kaplan and Fung [51] (nonlinear problem).

Equations of motion for the vibration analysis of shells may be derived as a simple extension of the static case by adding the inertia forces to body forces and body moment terms that result from accelerations of the mass of the shell according to the D'Alambert principle. The equations of free vibrations of thin elastic shells were first derived by Love [2]. Then, the equations of motion for shells of various shape according to the first- and higher-order approximations were presented by Kraus [18], Flügge [52], Epstein [53], etc. Analysis of various equations of motion of thin elastic shells, as well as a comprehensive presentation of available results for free vibration frequencies and mode shapes which can be used for design was made by Leissa [19].

This historical survey is aimed at only providing a brief background on the formation of the shell theory. The interested reader who wants to be more acquainted with the shell's history in more details is referred to other works [1,18,19,36].

10.4 LOADING-CARRYING MECHANISM OF SHELLS

The general theories of beams, arches, plates, and shells are usually based upon the unified set of assumptions. However, the load–resistance mechanisms of these members do not resemble one another. The load–resistance mechanism of flat plates was discussed in Secs 1.1 and 1.3. We can say that shells fall into a class of plates as arches relate to straight beams under the action of transverse loading. It is known that the efficiency of the arch form lies primarily in resisting the transverse load with a thrust N, thus minimizing the shear force V and bending moment M. It is possible to specify the arch shape and the manner of its loading in such a way that the arch does not experience bending at all. In this case, the arch is in the so-called momentless state of stress. For example, for a parabolic arch, bending will not be induced by a vertical load uniformly distributed over its chord. Thus, the ability of arches to support certain transverse loads without bending is the reason for their structural advantage over straight beams.

A shell mainly balances an applied transverse load, much like an arch, by means of tensile and compressive stresses, referred to as the *membrane or direct stresses*. These stresses are uniformly distributed over the shell thickness. Such a state of stress is called the *momentless or membrane state of stress*. Although the shear force and bending and twisting moments are still present in the general case of loading, the efficiency of the shell form rests with the presence of the membrane stresses, as the primary means of resistance with the bending stress resultants and couples are minimized. Thus, shells, like arches over beams, possess an analogous advantage over plates; however, with the following essential difference – *while an arch of a given form will support only one completely determined load without bending, a shell of a given shape has, provided its edges are suitably supported, as a rule, the same property for a wide range of loads which satisfy only very general requirements.*

The membrane stress condition is an ideal state at which a designer should aim. It should be noted that structural materials are generally far more efficient in an extensional rather in a flexural mode because:

1. Strength properties of all materials can be used completely in tension (or compression), since all fibers over the cross section are equally strained and load-carrying capacity may simultaneously reach the limit for the whole section of the component.
2. The membrane stresses are always less than the corresponding bending stresses for thin shells under the same loading conditions.

Thus, the momentless or membrane stress conditions determine the basic advantages of shells compared with beams, plates, etc.

The highest efficiency of a shell, as a *structural member, is associated with its curvature and thinness*. Owing to the shell curvature, the projections of the direct forces on the normal to the middle surface develop an analog of an ''elastic foundation'' under the shell. So, it can be said that a shell resists an applied transverse loading as a flat plate resting on an elastic foundation. This phenomenon can explain an essential increase in strength and stiffness of a shell compared with a plate. Thus, as a result of the curvature of the surface, a shell acquires a spatial stiffness that gives to it a larger load-carrying capacity and develops the direct stresses. Owing to its

thinness, a shell may balance an applied transverse loading at the expense of the membrane stresses mainly, with bending actions minimized.

Note that the pure bending conditions have no advantages and should be avoided because shells, in view of their small thickness, possess a low strength for this deformation. However, sometimes bending conditions cannot be avoided. It turns out that strong severe bending conditions are localized only in a small domain near some discontinuities in loading and geometrical conditions, as well as near supports, etc. As we move away from such a disturbance zone, the bending stresses will diminish rapidly and a considerable part of the shell will be in the momentless stress condition. Therewith, the thinner the shell the faster this decrease of bending stresses.

As mentioned above, shell thinness demonstrates the high efficiency of shells. It is associated with the shell's low weight and simultaneously its high strength. However, a shell's thinness is, at the same time, a weak point because all the advantages mentioned earlier hold for a tensile state of stress. In this case, a shell material is stretched and its strength properties are used completely. On the other hand, a thinness of shells manifests itself in compression. External forces, as before, are effectively transformed in the constant membrane stresses over the shell thickness. However, the trouble is that the level of the critical stresses at buckling be sufficiently low. This level is just determined by the shell thickness. The thinner the shell, the lower is the level of the critical stresses. The latter can be many factors smaller than the proportional limit of the shell material. In this case, the efficiency of thin shells can be reduced considerably. To avoid the possibility of buckling, a shell structure should be designed in such a way that a dominant part of the structure is in tension.

REFERENCES

1. Novozhilov, V.V., *Theory of Thin Elastic Shells*, 2nd edn, P. Noordhoff, Groningen, 1964.
2. Love, A.E.H., *A Treatise on the Mathematical Theory of Elasticity*, 1st edn, Cambridge University Press, 1892; 4th. edn, Dover, New York, 1944.
3. Reissner, E., A new derivation of the equations of the deformation of elastic shells, *Am J Math*, vol. 63, No.1, pp. 177–184 (1941).
4. Sanders, J.L., *An Improved First Approximation Theory for Thin Shells*, NASA TR-R24, 1959.
5. Koiter, W.T., A consistent first approximation in the general theory of thin elastic shells, *Proc. Symp. on Theory of Thin Elastic Shells* (Delft, August 1959), North-Holland, Amsterdam, pp. 12–33 (1960).
6. Timoshenko, S. and Woinowsky-Krieger, S., *Theory of Plates and Shells,* McGraw-Hill, New York, 1959.
7. Naghdi, P.M., A survey on resent progress in the theory of thin elastic shells, *Appl Mech Revs*, vol, 9, pp. 365–368 (1956).
8. Naghdi, P.M., Foundations of elastic shell theory. In: *Progress in Solid Mechanics* (eds I.N. Sneedon and R. Hill), North-Holland, Amsterdam, IV, Chapter 1, 1963.
9. Lur'ye, A.I., General theory of elastic shells, *Prikl Mat Mekh*, vol. 4, No. 4, pp. 7–34 (1940) (in Russian).
10. Flügge, W., *Stresses in Shells*, 2nd edn, Springer-Verlag, Berlin, 1962.
11. Byrne, R., Theory of small deformations of a thin elastic shell, *Seminar Reports in Math*, University of California, Publ in Math, N.S., vol. 2, No. 1, pp. 103–152 (1944).

12. Novozhilov, V.V. and Finkelshtein, R.O., On the error in Kirchhoff's hypothesis in the theory of shells, *Prikl Mat Mekh*, vol. 7, No. 5, pp. 35–46 (1943) (in Russian).
13. Gol'denveizer, A.L., *Theory of Thin Shells*, Pergamon Press, New York, 1961.
14. Vlasov, V.Z., *General Theory of Shells and its Applications in Engineering*, NASA TT F-99, 1964.
15. Reissner, E., Stress strain relations in the theory of thin elastic shells, *J Math Phys*, vol. 31, pp. 109–119 (1952).
16. Reissner, E., On the theory of thin elastic shells, *H. Reissner Anniv Vol*, J.W. Edwards, Ann Arbor, pp. 231–247 (1949).
17. Naghdi, P.M., On the theory of thin elastic shells, *Q Appl Math*, vol. 14, pp. 369–380 (1957).
18. Kraus, H., *Thin Elastic Shells*, John Wiley and Sons, New York, 1967.
19. Leissa, A.W., *Vibrations of Shells*, NASA SP-288, Washington, DC, 1973.
20. Reissner, E., On axisymmetrical deformation of thin shells of revolution, *Proc Symp Appl Math*, vol. 3, pp. 27–52 (1950).
21. Naghdi, P.M. and Nordgren, R.P., On the nonlinear theory of shells under the Kirchhoff hypothesis, *Q Appl Math*, vol. 21, pp. 49–60 (1963).
22. Sanders, J.L., Nonlinear theories for thin shells, *Q Appl Math*, vol. 21, pp. 21–36 (1963).
23. Koiter, W.T., The stability of elastic equilibrium (Chapter 5: Shell theory for finite deflections), *Diss, Tech Rept, AFFDL-TR-70-25*, Air Force System Command, Wright-Patterson AFB, 1970.
24. Mushtari, Kh.M. and Galimov, K.Z., *Nonlinear Theory of Thin Shells*, The Israel Program for Scientific Translations, Jerusalem, 1961.
25. Simmonds, J.G. and Danielson, D.A., Nonlinear shell theory with finite rotation and stress-function vectors, *J Appl Mech*, vol. 39, pp. 1085–1090 (1972).
26. Beltrami, E., Sull'equilibrio delle supperficial flessibili ed inestendibili, *Mem R, Acad Sci di Bologna*, 1881.
27. Lecornu, L., Sur l'equilibre des surfaces flexible et inextendibles, *J de L'Ecole Polytechnique,* c. XLVIII.
28. Reissner, H., *Spaunnungen in Kugelschalen*, Müller-Breslau-Festschrift, Leipzig, 1912.
29. Sokolovskii, V.V., Momentless shells of revolution, *Prikl Mat Mekh*, vol. 1, No. 3, pp. 81–88 (1938) (in Russian).
30. Pucher, A., Über den spannungszustand in gekrümmten flächen, *Beton u Eisen*, vol. 33, pp. 298–304 (1934).
31. Donnel, L.H., *Beams, Plates, and Shells*, McGraw-Hill, New York, 1976.
32. Mushtari, Kh.M., Certain generalizations of the theory of thin shells, *Izv Fiz Mat O-va pri Kazan Un-te*, vol. 11, No. 8 (1938) (in Russian).
33. Marguerre, K., Zur theorie der gekrümmten platten grosser formänderung, *Proc 5th Int Congr Appl Mech*, Cambridge, Mass., pp. 93–101 (1939).
34. Meissner, E., Das elastizitätsproblem für dünne schalen von ringflächen, *Kugel-und Kegelvj-Schr Naturf Ges*, Zürich, vol. 60, pp. 23–47 (1915).
35. Hoff, N.J., Thin circular conical shells under arbitrary loads, *J Appl Mech*, vol. 22, pp. 557–562 (1955).
36. Flügge, W., Die Stabilität der Kreiszylinderschale, *Ing-Arch*, vol. 3, pp. 463–506 (1932).
37. Wissler, H., Festigkeitsberechnung von Ringflächenschalen, Diss, Zürich, 1916.
38. Parkus, H., Die Grundleichungen der allegemeinen zylinderschale, *Österr Ing-Arch,* vol. 6, pp. 30–35 (1951).
39. Dishinger, F., Die strenge berechnung der kreiszylinderschale in ihrer anwendung auf die Zeics-Dywidag-Schalen, *Beton u. Eisen*, vol. 34, pp. 257–264, 283–294 (1935).
40. Hoff, N.J., Boundary value problems of thin-walled circular cylinders, *J Appl Mech*, vol. 21, pp. 343–350 (1954).
41. Geckeler, J., Die festigkeit achsensymmetrischer schalen, *Ing Arch*, Bd. 1, 1930.

42. Lorentz, R., Die nichtachsensymmetrische knickung dünnwandiger hohlzylinder, *Phys Z*, vol. 12, pp. 241–260 (1911).
43. Timoshenko, S.P. and Gere, J., *Theory of Elastic Stability*, McGraw-Hill, New York, 1961.
44. Mises, R., Der kritische aubendruck für alldeits belastete cylindrischer rohre, *Festschr Zum 70 Geburtstag von prof A Stodola*, Zürich, pp. 418–432 (1929).
45. Mushtari, Kh.M. and Sachenkov, A.V., A stability of cylindrical and conical shells of circular cross sections under axial compression and external normal pressure, *Prikl Mat Mekh*, vol. 18, No. 6, pp. 667–674 (1954).
46. Donnel, L.H. and Wan, C.C., Effect of imperfection on the buckling of thin cylinders and columns under axial compression, *J Appl Mech*, vol. 17, No. 1, pp. 73–83 (1950).
47. Zoelly, R., *Über ein Knickungsproblem an der Kugelschal*e, Diss, Zürich, 1915.
48. Von Karman, T. and Tsien, H.S., The buckling of thin cylindrical shells under elastic compression, *J Aeronaut Sci*, vol. 8, pp. 303–312 (1941).
49. Koiter, W.T., *Buckling and Postbuckling Behavior of a Cylindrical Panel under Axial Compression*, Nat Luchtvaart Laboratory, Report No. 476, Amsterdam, 1956.
50. Budansky, B., Buckling of clamped shallow spherical shells, *Proc IUTAM Symposium on the Theory of Thin Elastic Shells*, Amsterdam, pp. 64–94 (1960).
51. Kaplan, A. and Fung, Y.C., *A Nonlinear Theory of Bending and Buckling of Thin Elastic Shallow Spherical Shells*, NASA TN 3212, 1954.
52. Flügge, W., *Static und Dynamik der Schalen*, Julius Springer, Berlin, 1934.
53. Epstein, P.S., On the theory of elastic vibrations in plates and shells, *J Math Phys*, vol. 21, pp. 198–209 (1942).

11

Geometry of the Middle Surface

11.1 COORDINATE SYSTEM OF THE SURFACE

A surface Ω can be defined as a locus of points whose position vector, $\mathbf{r}$, directed from the origin 0 of the global coordinate system, $OXYZ$, is a function of two independent parameters α and β (see Fig. 11.1).

The parametric representation of the surface can be given, as follows:

in vector form as $\mathbf{r} = \mathbf{r}(\alpha, \beta)$; (11.1)

or

in scalar form as $X = X(\alpha, \beta), \quad Y = Y(\alpha, \beta), \quad Z = Z(\alpha, \beta),$ (11.2)

where $X(\alpha, \beta)$, $Y(\alpha, \beta)$, and $Z(\alpha, \beta)$ are some definite, continuous, and single-valued functions of two variable coordinates α and β. If we eliminate the parameters α and β from Eqs (11.2), then the equation of the surface becomes

$$F(X, Y, Z) = 0. \tag{11.3}$$

The parametric equation (11.1) may also be written in the form

$$\mathbf{r} = X(\alpha, \beta)\mathbf{i} + Y(\alpha, \beta)\mathbf{j} + Z(\alpha, \beta)\mathbf{k}, \tag{11.4}$$

in which $\mathbf{i}, \mathbf{j}$, and $\mathbf{k}$ are unit vectors along the X, Y, and Z axes, respectively.

We assume that there is a one-to-one correspondence between the pairs of numbers (α, β) belonging to Ω and points of the surface. Therefore these parameters, α and β, can be called *curvilinear coordinates of a given surface*. If one of the coordinates, e.g., α, is incremented $\alpha = \alpha_1$, $\alpha = \alpha_2, \ldots, \alpha = \alpha_n$, we define a series of parametric curves on the surface, along which only a parameter β varies. These curves are termed the *α-coordinate lines*. Similarly, if a parameter β takes on the values $\beta = \beta_1$, $\beta = \beta_2, \ldots, \beta = \beta_n$, we obtain the *$\beta$-coordinate lines*.

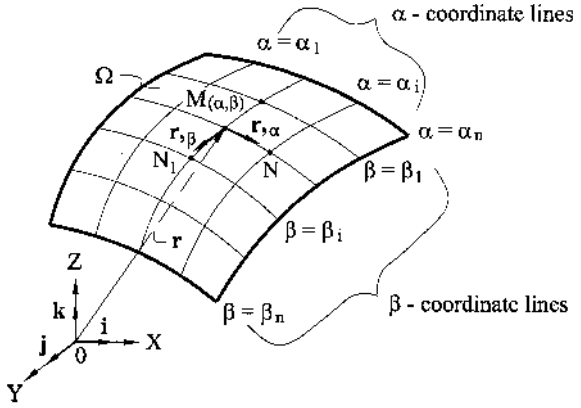

Fig. 11.1

If the α- and β-coordinate lines are mutually perpendicular at all points on a surface Ω (i.e., the angles between the tangents to these lines are equal to 90°), the *curvilinear coordinates* are said to be *orthogonal*. Orthogonal curvilinear coordinates are used extensively in this book.

The derivatives of the position vector $\mathbf{r}$ with respect to the curvilinear coordinates α and β are given by the following:

$$\frac{\partial \mathbf{r}}{\partial \alpha} = \mathbf{r}_{,\alpha} \quad \text{and} \quad \frac{\partial \mathbf{r}}{\partial \beta} = \mathbf{r}_{,\beta}\,, \tag{11.5}$$

where we have introduced the comma notation to denote partial derivatives with respect to α and β; $\mathbf{r}_{,\alpha}$ and $\mathbf{r}_{,\beta}$ are the tangent vectors at any point of the surface to the α- and β-coordinate lines, respectively (Fig. 11.1). Indeed, since α and β are scalar quantities, the directions of vectors $\mathbf{r}_{,\alpha}$ and $\mathbf{r}_{,\beta}$ coincide with directions of the vector $d\mathbf{r}$. This vector $d\mathbf{r}$ points to the chords joining points M and N for $\mathbf{r}_{,\alpha}$, and M and N_1 for $\mathbf{r}_{,\beta}$. In the limit, as $\Delta\alpha \to 0$ and $\Delta\beta \to 0$, these chords approach the tangents at a point M along the coordinate lines α and β, respectively. Since the latter are assumed to be orthogonal, then

$$\mathbf{r}_{,\alpha} \cdot \mathbf{r}_{,\beta} = 0. \tag{11.6}$$

11.2 PRINCIPAL DIRECTIONS AND LINES OF CURVATURE

Consider a small region of a smooth surface Ω near a typical point M. By "smooth" we mean that the surface is continuous, and contains no discontinuities of slope, i.e., creases or vertices. If we draw various curves along the surface Ω through point M, then the tangents to these curves are placed on one plane called the *tangent plane* to the surface at M (plane P in Fig. 11.2). A line that is perpendicular to the tangent plane and passes through point M is called the *normal* to the surface Ω at point M, and it is denoted by $\mathbf{n}$. Since the surface is smooth (as defined above), the tangent plane and, hence, the normal are uniquely determined.

A *normal section* of the surface Ω at point M can be defined as the section by some plane containing a normal to the surface at that point. Such a section repre-

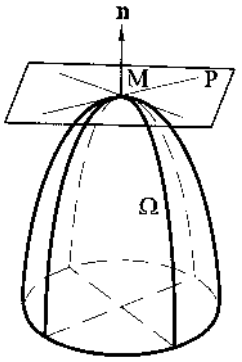

Fig. 11.2

sents a plane curve. Obviously, an infinite number of different normal sections may be drawn through point M of surface Ω (sections aa, bb, cc, etc., in Fig. 11.3)

Consider one of such normal sections as a plane curve, as shown in Fig. 11.4. The position of a point M on the curve is determined by a single arc length coordinate s, measured from a suitable datum point. Let M and M_1 be two neighboring points defining a short arc of length $\mathrm{d}s$. At M and M_1 the normals OM and OM_1 are drawn to the curve (there is only one normal at each point, since the curve is smooth) and they are inclined with respect to a suitable datum direction at angles ϕ and $\phi+\mathrm{d}\phi$, respectively. Assume that the two normals intersect at a point O (the *center of curvature of the arc*). The center of curvature is defined strictly in terms of a limiting process in which $\mathrm{d}s \to 0$. The length OM (i.e., the distance from the center of curvature to point M) is called the *radius of curvature,* ρ, of the given curve at point M.

It follows by simple trigonometry from the above description that

$$\rho = \frac{\mathrm{d}s}{\mathrm{d}\phi}. \tag{11.7a}$$

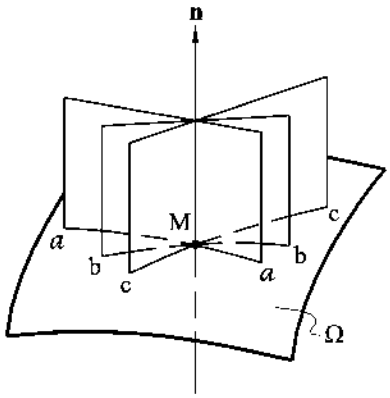

Fig. 11.3

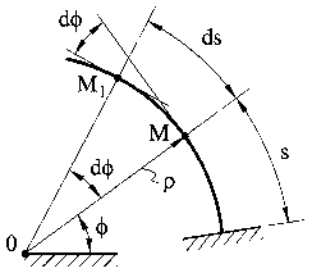

Fig. 11.4

In practice it is more convenient to use the *curvature* κ as a variable; this is defined as

$$\kappa = 1/\rho. \tag{11.7b}$$

It follows from the above that there are an infinite number of possible radii of curvature and curvatures at a point M of the surface because an infinite number of normal sections may be drawn through that point. However, there are two orthogonal normal sections at any point of a surface oriented such that one radius of curvature is the maximum of all possible, whereas the second radius of curvature is the minimum of all possible. These normal sections are called *principal normal sections* or *principal directions*. The curvatures of these sections and the corresponding radii are referred to as *principal curvatures* (denoted by κ_1 and κ_2) and *principal radii* (denoted by $R_1 = 1/\kappa_1$ and $R_2 = 1/\kappa_2$) at a point.

We also introduce *lines of the principal curvature* or simply *lines of curvature*. A *line of curvature* is a curve on the surface with the property that, at any point of the curve, it has a common tangent with the principal directions. From the above, it follows that the curvature takes on an extreme value at that point of the lines of curvature. Hence, at any point of a smooth surface there is at least one set of principal directions and two orthogonal lines of curvature.

The principal directions and lines of curvature may coincide or may not coincide, depending upon the surface geometry. Figure 11.5a shows the surface of revolution. It is described by rotating a plane curve (called a *meridian*) about the axis of rotation (the Z axis in Fig. 11.5).

The meridional plane L contains the axis of rotation. Each point of the meridian, when it rotates about the Z axis, describes a rotating *parallel circle* whose plane T is perpendicular to the Z axis. Normals to the surface of revolution, $\mathbf{n}$ and $\mathbf{n}_1$, drawn at neighboring points of the meridian, M and M_1, lie in plane L and they intersect in the same plane at point O_1. Thus, *meridians* at any point of the surface are one of the *lines of curvature* and, at the same time, one of the *principal normal sections*. The *radius of curvature of the meridian* equals MO_1 and it is the *first principal radius of curvature of the surface of revolution*, R_1. Normals to the surface, $\mathbf{n}$ and $\mathbf{n_2}$, drawn at neighboring points of the parallel circle, M and M_2, do not lie in plane T. They are located on some conical surface K and intersect at its vertex O_2 (Fig. 11.5b). The latter always lies on the Z axis, independently of the shape of a meridian curve. The *second principal normal section* of the surface of revolution is a curve, Γ, which lies in the plane that is tangent to the conical surface K at point M. It follows from the above that the second principal section

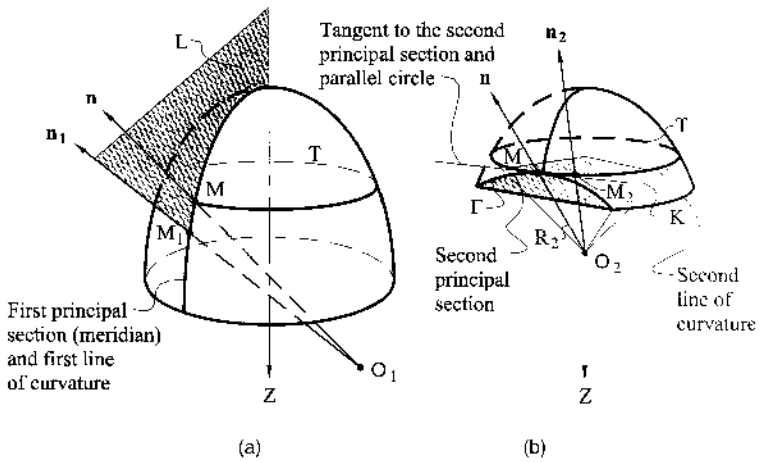

Fig. 11.5

and parallel circle have a common tangent at point M. Thus, the *parallel circles* of the surface of revolution represent the *second lines of curvature* but they are not the second principal normal sections or principal directions. The *generator* MO_2 of the conical surface K is the *second principal radius of curvature of the surface of revolution*, R_2. This radius is numerically equal to the distance along a normal to the meridian curve from a point of interest of this curve to the axis of rotation (the Z axis).

In Sec. 11.1 we made no special assumptions about the curvilinear coordinates of a shell middle surface. However, from now on we assume that the *coordinate lines* α and β *are the lines of curvature*. This system of the coordinate lines has particularly simple properties, so that the equations of the theory of shells acquire a relatively simple form in this system. To be able to use the corresponding formulas of the general theory of shells, knowledge of the lines of curvature is required, and the determination of these curves for a given surface is, in general, a fairly complicated problem. However, for many of types of shells used in practice, the geometry of the middle surface is of a simple nature (e.g., surfaces of revolution, cylindrical surfaces, etc.), so that the lines of curvature are already known.

11.3 THE FIRST AND SECOND QUADRATIC FORMS OF SURFACES

Let us study a surface Ω of an arbitrary geometry near typical point M, as shown in Fig. 11.6. Consider two points $M(\alpha, \beta)$ and $M_1(\alpha + d\alpha, \beta + d\beta)$ arbitrarily near to each other and both lying on the surface. Let their position vectors be $\mathbf{r}$ and $\mathbf{r} + d\mathbf{r}$, respectively.

Determine the length of the arc ds joining the points M and M_1 on the surface. In the limit, ds approaches $|d\mathbf{r}|$, where $|d\mathbf{r}|$ is the modulus of the increment in the vector $\mathbf{r}$ going from point M to point M_1, as defined by

$$d\mathbf{r} = \mathbf{r}_{,\alpha}\, d\alpha + \mathbf{r}_{,\beta}\, d\beta. \tag{11.8}$$

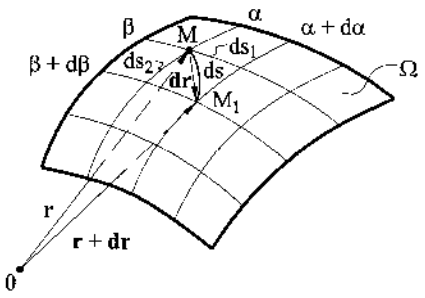

Fig. 11.6

The square of this differential of the arc length is

$$ds^2 = |d\mathbf{r}|^2 = d\mathbf{r} \cdot d\mathbf{r} = \mathbf{r}_{,\alpha} \cdot \mathbf{r}_{,\alpha} (d\alpha)^2 + 2\mathbf{r}_{,\alpha} \cdot \mathbf{r}_{,\beta} d\alpha d\beta + \mathbf{r}_{,\beta} \cdot \mathbf{r}_{,\beta} (d\beta)^2. \tag{11.9}$$

Denoting

$$a_{11} = (\mathbf{r}_{,\alpha} \cdot \mathbf{r}_{,\alpha}); \quad a_{12} = (\mathbf{r}_{,\alpha} \cdot \mathbf{r}_{,\beta}); \quad a_{22} = (\mathbf{r}_{,\beta} \cdot \mathbf{r}_{,\beta}), \tag{11.10}$$

we can rewrite Eq. (11.9), as follows:

$$ds^2 = a_{11}(d\alpha)^2 + 2a_{12} d\alpha d\beta + a_{22}(d\beta)^2. \tag{11.11}$$

The expression on the right-hand side of this equation is called *the first quadratic form of the surface* defined by the vector $\mathbf{r}(\alpha, \beta)$ and a_{ik} $(i, k = 1, 2)$ are the *coefficients of that form.*

If the coordinate lines α and β form an orthogonal net, then $\mathbf{r}_{,\alpha} \cdot \mathbf{r}_{,\beta} = 0$ and, hence, $a_{12} = 0$. Denoting

$$A = (a_{11})^{1/2}; \quad B = (b_{11})^{1/2}, \tag{11.12}$$

we can rewrite the first quadratic form (Eq. (11.11)) for this particular case as

$$ds^2 = A^2(d\alpha)^2 + B^2(d\beta)^2. \tag{11.13}$$

The quantities A and B are termed the *Lamé parameters*. To interpret the meaning of A and B geometrically, we rewrite Eq. (11.13), as follows:

$$ds^2 = ds_1^2 + ds_2^2, \tag{11.14a}$$

where ds_1 and ds_2 are the lengths of linear arc elements corresponding to the increments in the curvilinear coordinates α and β, respectively (Fig.11.6), and

$$ds_1 = A d\alpha \quad \text{and} \quad ds_2 = B d\beta. \tag{11.14b}$$

We can see that the Lamé parameters are quantities which relate a change in arc length on the surface to the corresponding change in curvilinear coordinate or, in other words, they may be treated as some distortion coefficients transforming the change in curvilinear coordinates (dimensional or dimensionless) into the change in arc length of linear segments, ds_1 and ds_2.

The coefficients of the first quadratic form can also be computed in terms of the Cartesian coordinates by substituting Eq. (11.4) into the relations (11.10). We obtain

$$a_{11} = (X_{,\alpha})^2 + (Y_{,\alpha})^2 + (Z_{,\alpha})^2;\ a_{12} = X_{,\alpha} X_{,\beta} + Y_{,\alpha} Y_{,\beta} + Z_{,\alpha} Z_{,\beta};$$
$$a_{22} = \left(X_{,\beta}\right)^2 + \left(Y_{,\beta}\right)^2 + \left(Z_{,\beta}\right)^2. \tag{11.15}$$

The first quadratic form generally pertains to the measurement of distances along an arc between two points on a surface, to areas on the surface, and to angles between any two curves passing through a point (i.e., the angle between the tangents to these curves), etc. Thus, the first quadratic form defines the *intrinsic geometry* of the surface. However, it does not involve the specific shape of the surface. For instance, this form cannot be a measure of curvature of curves lying on a surface or if we change a curvature of the surface (say, by its bending) without its stretching or contracting, the first quadratic form remains unchanged. So, the representation of the surface by the Lamé parameters only is not sufficient and the first quadratic form must be complemented with the second quadratic form to describe uniquely the intrinsic and extrinsic geometries of a surface.

The *second quadratic form* describes a shape of the surface, given by Eq. (11.1). This problem is associated with finding a curvature of the surface at a point. The notion of curvature of the surface is an extension of the notion of curvature of a plane curve, discussed in Sec. 11.2.

Consider a normal section which traces a plane curve with a unit inward normal $\mathbf{e_3}$ directed toward the center of curvature of the curve. The curvature of that normal section, called *the normal curvature* and denoted by κ_{n}, is of the following form (a detailed derivation of this expression is given in Appendix C.2):

$$\kappa_{\mathrm{n}} = \frac{II}{I} = \frac{b_{11}(\mathrm{d}\alpha)^2 + 2b_{12}\mathrm{d}\alpha\mathrm{d}\beta + b_{22}(\mathrm{d}\beta)^2}{a_{11}(\mathrm{d}\alpha)^2 + 2a_{12}\mathrm{d}\alpha\mathrm{d}\beta + a_{22}(\mathrm{d}\beta)^2}, \tag{11.16}$$

where

$$b_{11} = \mathbf{e}_3 \cdot \frac{\partial^2 \mathbf{r}}{\partial \alpha^2}; \quad b_{12} = \mathbf{e}_3 \cdot \frac{\partial^2 \mathbf{r}}{\partial \alpha \partial \beta}; \quad b_{22} = \mathbf{e}_3 \cdot \frac{\partial^2 \mathbf{r}}{\partial \beta^2}, \tag{11.17}$$

and the coefficients a_{ik} $(i, k = 1, 2)$ are given by Eqs (11.10). It can be seen that expression I in the denominator of Eq. (11.16) represents the first quadratic form of the surface for any coordinate curves that are not orthogonal (see Eq. (11.11)).

Expression II is called *the second quadratic form of surfaces*:

$$II = b_{11}(\mathrm{d}\alpha)^2 + 2b_{12}\mathrm{d}\alpha\mathrm{d}\beta + b_{22}(\mathrm{d}\beta)^2, \tag{11.18}$$

and the quantities b_{11}, b_{12}, and b_{22} are referred to as *the coefficients of the second quadratic form of surfaces*. The coefficients b_{11} and b_{22} characterize the normal curvature of lines $\beta = \text{const.}$ and $\alpha = \text{const}$, respectively, whereas the coefficient b_{12} describes the twisting of the surface. Thus, the second quadratic form defines completely a curved shape of a surface in the neighborhood of a point of interest.

The coefficients of the second quadratic form b_{ik} $(i, k = 1, 2)$ were given in terms of the curvilinear coordinates α and β. They can also be expressed in terms of the Cartesian coordinates X, Y, and Z (see Eqs (C.11) in the Appendix C.2).

As mentioned previously, the simultaneous use of the first and second quadratic forms define completely and uniquely a surface with the accuracy of its location in the space. This means that two surfaces having the same first and second quadratic

forms coincide in their configuration and can be different only by their location in the space.

11.4 PRINCIPAL CURVATURES

As mentioned in Sec. 11.2, through every point M of a smooth surface the normal curvature, κ_n, in general varies with the direction through the point. However, there are two orthogonal directions on which κ_n is extremal ($\kappa_{max} = \kappa_1$ and $\kappa_{min} = \kappa_2$) and these are what have been named in Sec. 11.2 the principal directions. It is seen from Eq. (11.16) that the normal curvature at point M of a surface depends on a direction of the section, $\lambda = d\beta/d\alpha$. Determine the values of λ that correspond to the extremal values of κ_n. For this purpose, transform Eq. (11.16), by inserting the parameter λ, to the form

$$\kappa_n(\lambda) = \frac{b_{11} + 2b_{12}\lambda + b_{22}\lambda^2}{a_{11} + 2a_{12}\lambda + a_{22}\lambda^2}. \tag{11.19}$$

The desired values of λ are evaluated from the condition $d\kappa_n/d\lambda = 0$. The latter results in the following equation:

$$(b_{12}a_{22} - b_{22}a_{12})\lambda^2 + (b_{11}a_{22} - b_{22}a_{11})\lambda + (b_{11}a_{12} - b_{12}a_{11}) = 0.$$

This equation defines the two roots, λ_1 and λ_2, corresponding to the two principal directions, i.e.,

$$\lambda_{1,2} = \frac{-(b_{11}a_{22} - b_{22}a_{11}) \pm \sqrt{(b_{11}a_{22} - a_{11}b_{22})^2 - 4(b_{12}a_{22} - b_{22}a_{12})(b_{11}a_{12} - b_{12}a_{11})}}{2(b_{12}a_{22} - b_{22}a_{12})}. \tag{11.20}$$

One of the roots, λ_1, being substituted into Eq. (11.19), corresponds to the maximum value of the normal curvature, κ_1, while the second one, λ_2, corresponds to the minimum value, κ_2.

We have postulated in Sec. 11.2 that the curvilinear coordinate lines α and β are to be the principal directions. It can be shown (see Appendix C.2) that the principal directions are mutually orthogonal. From the orthogonality condition (C.13) or (C.14) (see Appendix C.2), and from Eqs (11.10), we obtain that

$$a_{12} = b_{12} = 0 \tag{11.21}$$

if the curvilinear coordinate lines α and β are chosen to coincide with the principal directions. The values of the principal curvature can be immediately determined from Eq. (11.16) by setting $a_{12} = b_{12} = 0$ and then letting $d\alpha = 0$ and $d\beta = 0$, in turn, to give

$$\kappa_1 = \frac{1}{R_1} = \frac{b_{11}}{a_{11}}; \quad \kappa_2 = \frac{1}{R_2} = \frac{b_{22}}{a_{22}}. \tag{11.22}$$

The expression of the second quadratic form, Eq. (11.18), when the principal directions (or the lines of curvature) are used as the curvilinear coordinate curves, simplifies to the form

$$II = b_{11}(d\alpha)^2 + b_{22}(d\beta)^2. \tag{11.23}$$

11.5 UNIT VECTORS

As mentioned previously, all vector quantities in the theory of shells, which are functions of points on the middle surface, will be given in terms of their projections on the directions of the tangents to some reference axes (the coordinate lines α and β, and normal to the surface at a point of interest). Since these reference axes change their directions when passing from one point of the surface to another one, it is necessary to investigate the differentiation of these vector quantities with respect to α and β.

A triad of the unit orthogonal vectors composed at a point on the middle surface of tangent vectors $\mathbf{e}_1$ and $\mathbf{e}_2$ to the coordinate lines α and β, and an inward normal vector $\mathbf{e}_3$ directed toward the center of curvature of the shell, represent a local vectorial basis to which the displacements, stress resultants, and stress couples are assigned. This basis defines a right-hand system, as shown in Fig. 11.7. Taking into account the expressions (11.5), (11.10), and (11.12), we can introduce the unit vectors as follows:

$$\mathbf{e}_1 = \frac{\mathbf{r}_{,\alpha}}{|\mathbf{r}_{,\alpha}|} = \frac{\mathbf{r}_{,\alpha}}{A}, \quad \mathbf{e}_2 = \frac{\mathbf{r}_{,\beta}}{|\mathbf{r}_{,\beta}|} = \frac{\mathbf{r}_{,\beta}}{B}, \quad \mathbf{e}_3 = \mathbf{e}_1 \times \mathbf{e}_2 = \frac{1}{AB}(\mathbf{r}_{,\alpha} \times \mathbf{r}_{,\beta}) \tag{11.24}$$

Any vector $\mathbf{T}$ may be represented in terms of the introduced orthogonal unit vectors, as follows:

$$\mathbf{T} = T_1\mathbf{e}_1 + T_2\mathbf{e}_2 + T_3\mathbf{e}_3,$$

where T_1, T_2, and T_3 are components of the vector in the coordinate basis (Eq. (11.24)). A partial derivative of the above vector $\mathbf{T}$ with respect to any coordinate may be represented as

$$\frac{\partial \mathbf{T}}{\partial \alpha} = \frac{\partial T_1}{\partial \alpha}\mathbf{e}_1 + \frac{\partial T_2}{\partial \alpha}\mathbf{e}_2 + \frac{\partial T_3}{\partial \alpha}\mathbf{e}_3 + T_1\frac{\partial \mathbf{e}_1}{\partial \alpha} + T_2\frac{\partial \mathbf{e}_2}{\partial \alpha} + T_3\frac{\partial \mathbf{e}_3}{\partial \alpha}. \tag{11.25}$$

The laws of differentiating the vectors, represented by Eq. (11.25), are reduced to the following form (a detailed derivation of these expressions is given in Appendix C.3):

$$\begin{aligned}
&\frac{\partial \mathbf{e}_1}{\partial \alpha} = -\frac{1}{B}\frac{\partial A}{\partial \beta}\mathbf{e}_2 + \frac{A}{R_1}\mathbf{e}_3, \quad \frac{\partial \mathbf{e}_1}{\partial \beta} = \frac{1}{A}\frac{\partial B}{\partial \alpha}\mathbf{e}_2, \\
&\frac{\partial \mathbf{e}_2}{\partial \alpha} = \frac{1}{B}\frac{\partial A}{\partial \beta}\mathbf{e}_1, \quad \frac{\partial \mathbf{e}_2}{\partial \beta} = -\frac{1}{A}\frac{\partial B}{\partial \alpha}\mathbf{e}_1 + \frac{B}{R_2}\mathbf{e}_3, \\
&\frac{\partial \mathbf{e}_3}{\partial \alpha} = -\frac{A}{R_1}\mathbf{e}_1, \quad \frac{\partial \mathbf{e}_3}{\partial \beta} = -\frac{B}{R_2}\mathbf{e}_2.
\end{aligned} \tag{11.26}$$

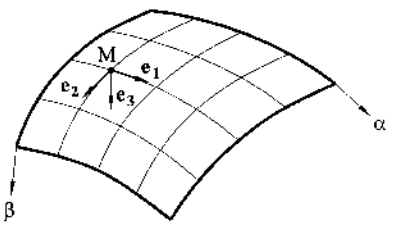

Fig. 11.7

11.6 EQUATIONS OF CODAZZI AND GAUSS. GAUSSIAN CURVATURE.

We present some important relations between the Lamé parameters A and B and the principal curvatures $k_1 = 1/R_1$ and $k_2 = 1/R_2$. These relations will be given below without proof (a detailed derivation is given in Appendix C.4), as follows:

$$\frac{\partial}{\partial\beta}\left(\frac{A}{R_1}\right) = \frac{1}{R_2}\frac{\partial A}{\partial\beta}; \quad \frac{\partial}{\partial\alpha}\left(\frac{B}{R_2}\right) = \frac{1}{R_1}\frac{\partial B}{\partial\alpha} \tag{11.27a}$$

and

$$\frac{\partial}{\partial\alpha}\left(\frac{1}{A}\frac{\partial B}{\partial\alpha}\right) + \frac{\partial}{\partial\beta}\left(\frac{1}{B}\frac{\partial A}{\partial\beta}\right) = -\frac{AB}{R_1R_2}. \tag{11.27b}$$

Equations (11.27a) are referred to as the *conditions of Codazzi*, whereas Eq. (11.27b) is known as the *condition of Gauss*.

Thus, the four functions A, B, R_1, and R_2 of the two parameters α and β are the Lamé parameters and principal radii of curvature of any surface only in the case when they are related to one another by the conditions of Codazzi and Gauss (11.27). From the above, it follows that the latter equations constitute necessary conditions for the existence of a surface.

Let us determine the product and semi-sum of the principal curvatures based on Eq. (11.19), as follows:

$$\Gamma = k_1k_2 = \frac{b_{11}b_{22} - b_{12}^2}{a_{11}a_{22} - a_{12}^2}, \tag{11.28}$$

$$K = \frac{k_1 + k_2}{2} = -\frac{2a_{12}b_{12} - a_{11}b_{22} - a_{22}b_{11}}{2\left(a_{11}a_{22} - a_{12}^2\right)}. \tag{11.29}$$

The first of these quantities is called the *Gaussian curvature* and the second is the *mean curvature* of a surface. The concept of Gaussian curvature is fundamental in the theory of surfaces. If the coordinate curves are lines of curvature, then the expression for Γ, Eq. (11.28), is reduced to the following equation (because $a_{12} = b_{12} = 0$) :

$$\Gamma = k_1k_2 = \frac{b_{11}b_{22}}{A^2B^2}, \tag{11.30}$$

where b_{11} and b_{22} are given by Eqs (11.17).

From the algebraic sign of the Gaussian curvature, the form of a surface in the neighborhood of a given point can be inferred. If $\Gamma > 0$, then, as follows from Eq. (11.28), the principal curvatures have the same sign. This means that both centers of principal curvature (O_1 and O_2 in Fig.11.8a) lie on the same side of the surface. The centers of curvature of all other normal sections will also lie on the segment $O_1\ O_2$. Point M of a surface whose centers of a curvature are located in such a way, called the *elliptic* point. On the contrary, for the centers of curvature O_1 and O_2 lie on opposite sides of the surface, as shown in Fig. 11.8b. The corresponding point of the surface is called *hyperbolic*. At last, if $\Gamma = 0$, then one of the two principal curvatures is zero, and the corresponding center of curvature (Fig.11.8c) is on an infinity. Point M of the surface in this case is called a *parabolic*.

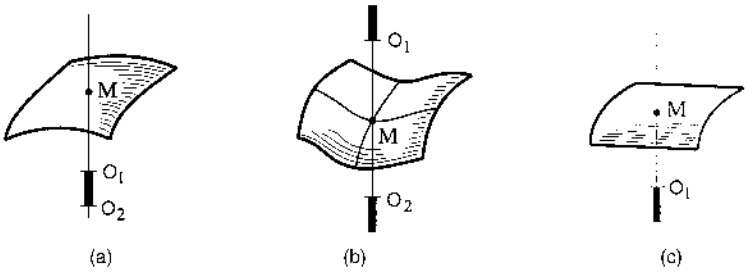

Fig. 11.8

For example, a sphere and an ellipsoid are examples of surfaces with positive Gaussian curvature. The so-called pseudo-sphere has a negative Γ that is a constant for all points. Cylindrical and conical surfaces have zero Gaussian curvatures.

The above sections contain only a brief survey of the geometry of surfaces. The interested reader is referred to Appendix C of the book and to Refs [1–3].

11.7 CLASSIFICATION OF SHELL SURFACES

We define here some of the surfaces that are commonly used for shell structures in engineering practice. There are several possible classifications of these surfaces. One such classification, associated with the Gaussian curvature, was discussed in Sec. 11.6. Following Ref. [4], we now discuss other categories of shell surfaces associated with their shape and geometric developability.

11.7.1 Classification based on geometric form

(a) Surfaces of revolution (Fig. 11.9)

As mentioned previously, surfaces of revolution are generated by rotating a plane curve, called the meridian, about an axis that is not necessarily intersecting the meridian. Circular cylinders, cones, spherical or elliptical domes, hyperboloids of revolution, and toroids (see Fig. 11.9) are some examples of surfaces of revolution. It can be seen that for the circular cylinder and cone (Fig. 11.9a and b), the meridian is a straight line, and hence, $k_1 = 0$, which gives $\Gamma = 0$. These are shells of zero Gaussian curvature. For ellipsoids and paraboloids of revolution and spheres (Fig. 11.9c, d, and e), both the principal curvatures are in the same direction and, thus, these surfaces have a positive Gaussian curvature ($\Gamma > 0$). They are synclastic surfaces. For the hyperboloid of revolution (Fig. 11.9f), the curvatures of the meridian and the second line of curvature are in opposite directions (i.e., the principal radii R_1 and R_2 lie on opposite sides of the surface for all points on the surface). For the toroid (Fig. 11.9g), the Gaussian curvature changes from positive to negative as we move along the surface.

(b) Surfaces of translation (Fig. 11.10)

A surface of translation is defined as the surface generated by keeping a plane curve parallel to its initial plane as we move it along another plane curve. The two planes containing the two curves are at right angles to each other. An elliptic paraboloid is

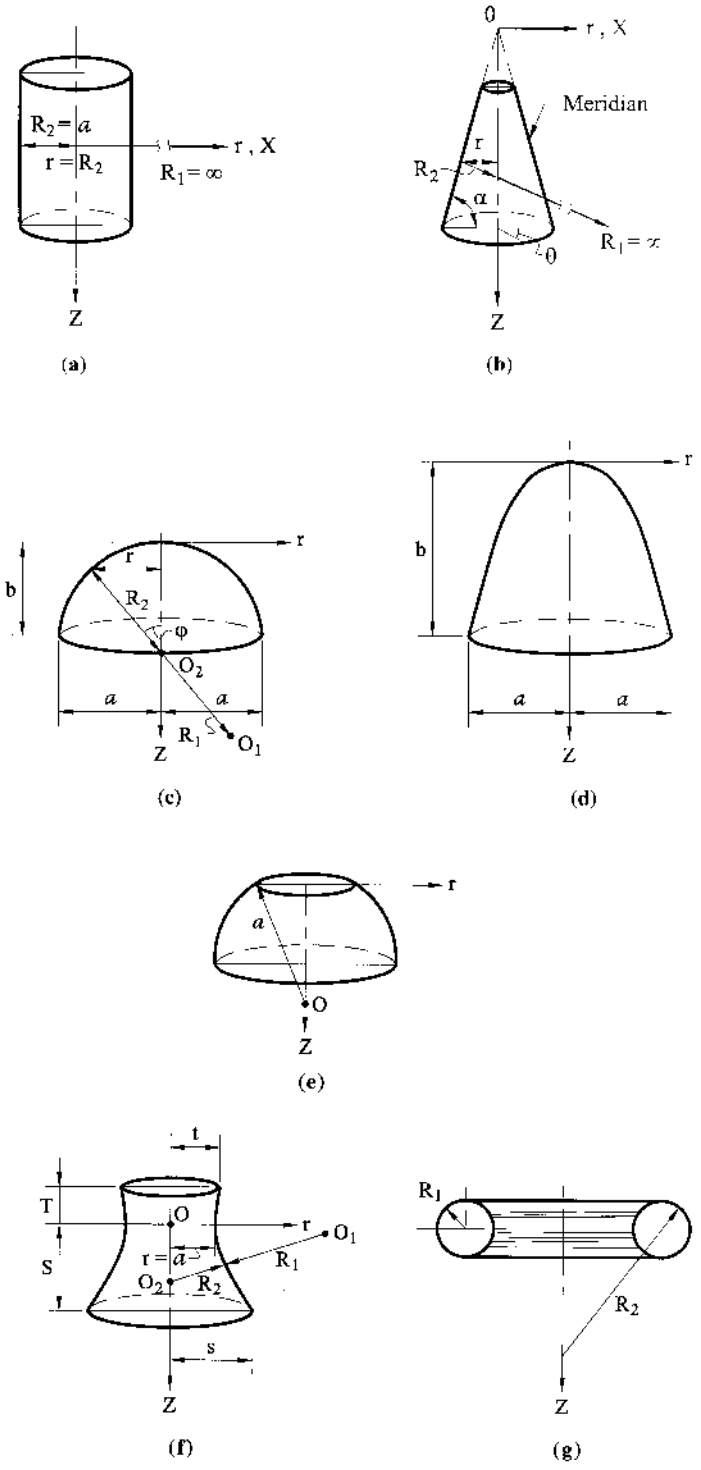

Fig. 11.9

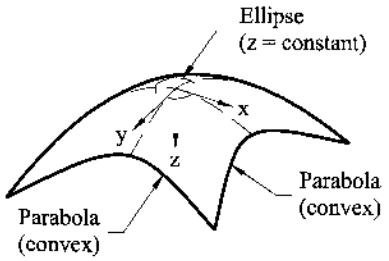

Fig. 11.10

shown in Fig. 11.10 as an example of such a type of surfaces. It is obtained by translation of a parabola on another parabola; both parabolas have their curvatures in the same direction. Therefore, this shell has a positive Gaussian curvature. For this surface sections $x = \text{const}$ and $y = \text{const}$ are parabolas, whereas a section $z = \text{const}$ represents an ellipse: hence its name, "elliptic paraboloid."

(c) Ruled surfaces (Fig. 11.11)

Ruled surfaces are obtained by the translation of straight lines over two end curves (Fig. 11.11). The straight lines are not necessarily at right angles to the planes containing the end curves. The frustum of a cone can thus be considered as a ruled surface, since it can be generated by translation of a straight line (the generator) over two curves at its ends. It is also, of course, a shell of revolution. The hyperboloid of revolution of one sheet, shown in Fig. 11.11a, represents another example of ruled surfaces. It can be generated also by the translation of a straight line over two circles at its ends. Figure 11.11b shows a surface generated by a translation of a straight line on a circular curve at one end and on a straight line at the other end. Such surfaces are referred to as conoids. Both surfaces shown in Fig. 11.11 have negative Gaussian curvatures.

11.7.2 Classification based on shell curvature

(a) Singly curved shells

These shells have a zero Gaussian curvature. Some shells of revolution (circular cylinders, cones), shells of translation, or ruled surfaces (circular or noncircular cylinders and cones) are examples of singly curved shells.

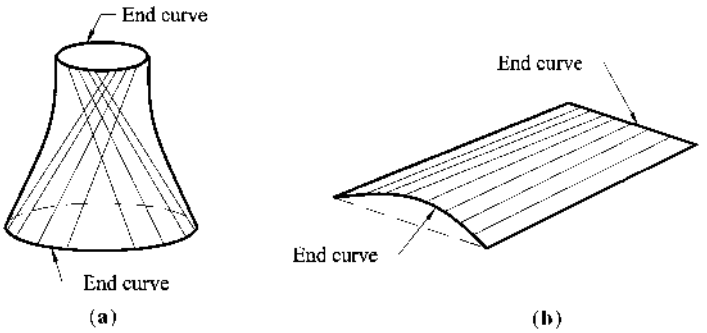

Fig. 11.11

(b) Doubly curved shells of positive Gaussian curvature

Some shells of revolution (circular domes, ellipsoids and paraboloids of revolution) and shells of translation and ruled surfaces (elliptic paraboloids, paraboloids of revolution) can be assigned to this category of surfaces.

(c) Doubly curved shells of negative Gaussian curvature

This category of surfaces consists of some shells of revolution (hyperboloids of revolution of one sheet) and shells of translation or ruled surfaces (paraboloids, conoids, hyperboloids of revolution of one sheet).

It is seen from this classification that the same type of shell may appear in more than one category.

11.7.3 Classification based on geometrical developability

(a) Developable surfaces

Developable surfaces are defined as surfaces that can be "developed" into a plane form without cutting and/or stretching their middle surface. All singly curved surfaces are examples of developable surfaces.

(b) Non-developable surfaces

A non-developable surface is a surface that has to be cut and/or stretched in order to be developed into a planar form. Surfaces with double curvature are usually non-developable.

The classification of shell surfaces into developable and non-developable has a certain mechanical meaning. From a physical point of view, shells with non-developable surfaces require more external energy to be deformed than do developable shells, i.e., to collapse into a plane form. Hence, one may conclude that non-developable shells are, in general, stronger and more stable than the corresponding developable shells having the same overall dimensions. On the other hand, developable shells have some advantages associated with their technological effectiveness.

11.8 SPECIALIZATION OF SHELL GEOMETRY

It is shown in the next chapter that the governing equations and relations of the general theory of thin shells are formulated in terms of the Lamé parameters A and B as well as of the principal curvatures $\kappa_1 = 1/R_1$ and $\kappa_2 = 1/R_2$. In the general case of shells having an arbitrary geometry of the middle surface, the coefficients of the first and second quadratic forms and the principal curvatures are some functions of the curvilinear coordinates. We determine the Lamé parameters for some shell geometries that are commonly encountered in engineering practice.

11.8.1 Shells of revolution

The shells of revolution were discussed in Secs 11.2 and 11.7. As for the curvilinear coordinate lines α and β, the meridians and parallels may be chosen: they are the lines of principal curvatures and form an orthogonal mesh on the shell middle surface. Figure 11.12a shows a surface of revolution where R_1 is the principal radius of the meridian, R_2 is the principal radius of the parallel circle (as shown in Sec.11.2, R_2

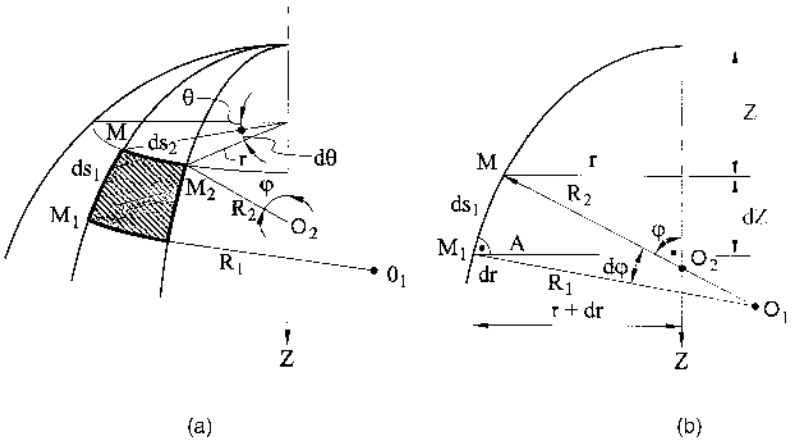

Fig. 11.12

is the distance along a normal to the meridional curve drawn from a point of interest to the axis of revolution of the surface), and r is the radius of the parallel circle.

There are several possibilities for a choice of the curvilinear coordinates α and β.

(a) First, consider the *cylindrical coordinate system*, taking

$$\alpha = Z, \quad \beta = \theta, \tag{11.31}$$

where Z indicates the vertical position of a point M and θ denotes an angular position of the point along the parallel circle from some arbitrary origin. The latter angle may be referred to as the *circumferential angle*.

Consider a differential element isolated by two neighboring meridional sections and two parallel circles (the cross-hatched element in Fig. 11.12a). Let the arc lengths of sidesMM_1 and MM_2 be $\mathrm{d}s_1$ and $\mathrm{d}s_2$, respectively. From the triangle AMM_1 of Fig. 11.12b, we have

$$\cos\left(\frac{\pi}{2} - \varphi\right) = \frac{\mathrm{d}Z}{\mathrm{d}s_1}, \tag{11.32}$$

from which

$$\mathrm{d}s_1 = \frac{\mathrm{d}Z}{\sin\varphi} = \mathrm{d}Z\sqrt{1 + \cot^2\varphi}, \tag{11.33}$$

where φ is the angle formed by the extended normal to the surface at point M and the axis of rotation. This angle is referred to as the *meridional angle*.

For shells of revolution the radius of a parallel circle, r, is a function of Z, i.e., $r = r(Z)$. By inspection of Fig. 11.12b, we have the following:

$$\mathrm{d}s_1 = \sqrt{\mathrm{d}Z^2 + AM_1^2} = \sqrt{\mathrm{d}Z^2 + (\mathrm{d}r)^2} = \mathrm{d}Z\sqrt{1 + r_{,z}^2}. \tag{11.34}$$

On the other hand, as follows from Fig. 11.12a, we have

$$MM_2 = \mathrm{d}s_2 = r\mathrm{d}\theta. \tag{11.35}$$

Using the general expressions (11.14b), and taking into account that for the cylindrical coordinates given by the expression (11.31), $d\alpha = dZ$ and $d\beta = d\theta$, we can finally determine the Lamé parameters in the following form:

$$A = \sqrt{1 + \left(\frac{dr}{dZ}\right)^2}, \quad B = r. \tag{11.36}$$

(b) Next, consider the *spherical coordinate system*, taking

$$\alpha = \varphi, \quad \beta = \theta. \tag{11.37}$$

It can be easily shown that the spherical coordinates (Eqs (11.37)) also define uniquely a point M on the surface of revolution. By inspection of Fig. 11.12, the following obvious relations hold:

$$ds_1 = R_1 d\varphi = R_1 d\alpha \quad \text{and} \quad ds_2 = r d\theta = r d\beta. \tag{11.38}$$

Comparing the above with the expressions (11.14), we obtain the Lamé parameters in the form

$$A = R_1, \quad B = r, \tag{11.39}$$

or noting that $r = R_2 \sin\varphi$ (see Fig. 11.12b), we can rewrite the expressions (11.39) as follows:

$$A = R_1, \quad B = R_2 \sin\varphi. \tag{11.40}$$

The first two of the relations of the Codazzi–Gauss equations (Eqs (11.27a)) are identically satisfied in this case, whereas the third equation (Eq. (11.27b)) gives the following:

$$\frac{d(R_2 \sin\varphi)}{d\varphi} = R_1 \cos\varphi. \tag{11.41}$$

Determine *the principal curvatures and principal radii of curvatures for shells of revolution*. Let a shell of revolution be assigned in the global coordinate system by the following equations:

$$X = r(Z)\cos\theta, \quad Y = r(Z)\sin\theta, \quad Z = Z, \tag{11.42}$$

where r is the radius of the parallel circle at a section $Z = \text{const}$ and θ is the angle of rotation of the meridional plane. Substituting Eqs (11.42) into Eqs (11.15) and (C.12), we obtain, after some mathematics, the following:

$$\begin{aligned} &a_{11} = 1 + r_{,Z}^2, \quad a_{12} = 0, \quad a_{22} = r^2, \quad \omega = r\sqrt{1 + r_{,Z}^2}, \\ &b_{11} = -\frac{r_{,ZZ}}{\sqrt{1 + r_{,Z}^2}}, \quad b_{12} = 0, \quad b_{22} = \frac{r}{\sqrt{1 + r_{,Z}^2}} \end{aligned}. \tag{11.43}$$

Substituting the above into Eqs (11.22), yields the following expressions for the principal curvatures:

$$\kappa_1 = \frac{1}{R_1} = -\frac{r_{,ZZ}}{\left(1 + r_{,Z}^2\right)^{3/2}}, \quad \kappa_2 = \frac{1}{r\left(1 + r_{,Z}^2\right)^{1/2}}. \tag{11.44}$$

It can be seen from Eqs (11.44) that κ_2 is always positive, whereas κ_1 may be either positive or negative depending upon the sign of the value of $r_{,ZZ}$. If a convexity of the meridian curve is directed to the Z axis, as in Fig. 11.9f, then, $r_{,ZZ} > 0$, and κ_1 for such a shell is negative.

Hence, if the equation of the meridional curve, i.e., $r = r(Z)$, is known, one can determine the principal curvatures and principal radii of shells of revolution using Eqs (11.44).

We consider below some specific forms of shells of revolution that are commonly used in applications and present the principal curvatures and principal radii for them.

(a) Ellipsoid of revolution (Fig. 11.9c)

The equation of the meridian of an ellipsoid has the form

$$b^2r^2 + a^2Z^2 = a^2b^2, \tag{a}$$

where a and b are lengths of the major and minor semi-axes, respectively. So, Eq. (a) can be written as

$$\frac{r^2}{a^2} + \frac{Z^2}{b^2} = 1,$$

which gives us r as a function of Z, as follows:

$$r = \frac{a}{b}\sqrt{b^2 - Z^2}. \tag{b}$$

Upon determining $r_{,Z}$ and $r_{,ZZ}$, and substituting into Eqs (11.44), we can readily obtain the expressions for the principal radii of curvature, as follows:

$$R_1 = \frac{1}{\kappa_1} = a^2b^2\left(\frac{r^2}{a^4} + \frac{Z^2}{b^4}\right)^{3/2}, \quad R_2 = \frac{1}{\kappa_2} = \frac{1}{b^2}\left(b^4r^2 + Z^2a^4\right)^{1/2}. \tag{11.45}$$

We would prefer to have R_1 and R_2 as functions of φ (see Fig. 11.12a), and hence, we must eliminate Z and r from the above. To do this, we consider a triangle formed by the sides $\mathrm{d}s_1$ (along the meridian), $\mathrm{d}r$, and dZ (see Fig. 11.12b). We can write the following:

$$\tan\varphi = \frac{\mathrm{d}Z}{\mathrm{d}r}.$$

Using this equation and Eq. (b), we can express r and Z as functions of φ and the lengths of ellipse axes, a and b. We have the following:

$$r = \frac{a^2\sin\varphi}{\left(a^2\sin^2\varphi + b^2\cos^2\varphi\right)^{1/2}} \text{ and } Z = \pm\frac{b^2\cos\varphi}{\left(a^2\sin^2\varphi + b^2\cos^2\varphi\right)^{1/2}}. \tag{c}$$

Substituting for r and Z from Eqs (c) into the expressions for R_1 and R_2, Eqs (11.45), gives

$$R_1 = \frac{a^2b^2}{\left(a^2\sin^2\varphi + b^2\cos^2\varphi\right)^{3/2}}, \quad R_2 = \frac{a^2}{\left(a^2\sin^2\varphi + b^2\cos^2\varphi\right)^{1/2}}. \tag{11.46}$$

(b) Paraboloid of revolution (Fig. 11.9d)

The equation of the meridional curve is given by

$$r^2 - 2pZ = 0 \quad \text{or} \quad r^2 = \frac{a^2}{b} Z, \tag{d}$$

where p is a parameter of the parabola. Using the technique considered above for the ellipsoid of revolution, we present below the final expressions for the principal radii of curvature for the paraboloid, dropping the intermediate mathematics,

$$R_1 = \frac{a^2}{2b} \frac{1}{(\cos^2 \varphi)^{3/2}}, \quad R_2 = \frac{a^2}{2b} \frac{1}{\cos \varphi}, \tag{11.47}$$

where b is the height of the paraboloid and a is one-half the length of the paraboloid base.

(c) Sphere (Fig. 11.9e)

Consider a spherical shell of radius a. It can be easily shown that the principal radius of the meridian is equal to the radius of the generating circle a. Indeed, the equation of the meridian is

$$Z^2 + r^2 = a^2.$$

With $r_{,Z} = -Z/r$ and $r_{,ZZ} = -(1/r)\left(1 + Z^2/r^2\right)$, we find from Eq. (11.45) that the principal radii of the sphere are

$$R_1 = \frac{\left[1 + (Z/r)^2\right]^{3/2}}{(1/r)\left(1 + Z^2/r^2\right)} = \sqrt{Z^2 + r^2} = a \text{ and } R_2 = r\left(1 + \frac{z^2}{r^2}\right)^{1/2} = \sqrt{r^2 + Z^2} = a.$$

Thus, for a spherical shell, both the principal radii of curvature are equal to the radius of the generating circle a.

(d) Hyperboloid of revolution (Fig. 11.9f)

The equation of the generating curve (hyperbola) is

$$\frac{r^2}{a^2} - \frac{Z^2}{b^2} = 1, \tag{e}$$

where a is one-half the length of the reference section of the hyperboloid and b is some characteristic dimension of the hyperboloid. The latter may be evaluated by substituting the base coordinates (s, S) and the top coordinates (t, T) into the equation of the hyperbola, i.e.,

$$b = \frac{aT}{\sqrt{t^2 - a^2}} = \frac{aS}{\sqrt{s^2 - a^2}}.$$

For the radii of curvature we have to use the same formulas as for the ellipsoid (i.e., Eqs (11.46)), replacing b^2 by $-b^2$. Thus, we obtain

$$R_1 = -\frac{a^2 b^2}{\left(a^2 \sin^2 \varphi - b^2 \cos^2 \varphi\right)^{3/2}}, \quad R_2 = \frac{a^2}{\left(a^2 \sin^2 \varphi - b^2 \cos^2 \varphi\right)^{1/2}}. \tag{11.48}$$

The principal radii of curvature for convex shells of revolution formed by rotating curves of the second order about their axes of symmetry can also be computed from the following equations [5]:

$$R_1 = \frac{R_0}{\left(1 + \gamma \sin^2 \varphi\right)^{3/2}}, \quad R_2 = \frac{R_0}{\left(1 + \gamma \sin^2 \varphi\right)^{1/2}}, \tag{11.49}$$

where the parameter R_0 equals the value of the radii of curvature at $\varphi = 0$, i.e., at the vertex of the corresponding shell, and the parameter γ takes on the following values:

$\gamma = 0$ for a spherical shell;

$\gamma = -1$ for paraboloids;

$\gamma > -1$ for ellipsoids; and

$\gamma < -1$ for hyperboloids.

11.8.2 Cylindrical shells

A cylinder is generated by moving a straight line along a curve while maintaining it parallel to its original position. It follows from this definition that through every point of the cylinder one may pass a straight line that lies entirely on this surface. These lines are called the *generators*. All planes that are normal to the generators intersect the cylinder in identical curves, which are called *profiles*. The cylinder is named after the shape of the profile, i.e., a circular, elliptical, or parabolic cylinder. Of these shells, only the circular cylinder is a shell of revolution, whereas the others represent shells of translation (see Sec. 11.7.1(b)) since they can be generated by the translation of a straight line.

Let us consider a cylindrical shell of a general shape, as shown in Fig. 11.13.

We use the cylindrical coordinate system to describe the position of a reference point on a cylindrical shell middle surface. Thus, the curvilinear coordinates of the reference point may be taken as

$$\alpha = x, \quad \beta = \theta, \tag{11.50}$$

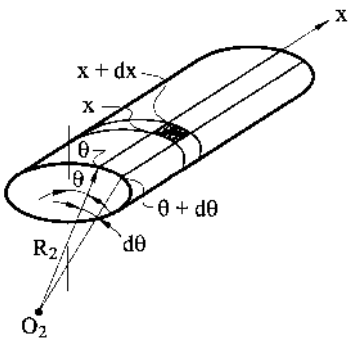

Fig. 11.13

where x is the distance measured from some reference profile to the point of interest and θ is the angle between the normal to the shell at a point and a reference normal at a chosen origin.

Consider an element of the shell, bounded by sections $x, x + \mathrm{d}x$ and $\theta, \theta + d\theta$ (Fig. 11.13). The first quadratic form of the surface will be here, as follows:

$$\mathrm{d}s^2 = \mathrm{d}x^2 + R_2^2 \mathrm{d}\theta^2, \tag{11.51}$$

where R_2 is the second principal radius of curvature, while the first principal radius is infinite, i.e., $R_1 = \infty$. Comparing the above with the relation (11.12), one can obtain the Lamé parameters for the cylindrical shell of a general shape, as follows:

$$A = 1, \quad B = R_2. \tag{11.52}$$

For a circular cylindrical shell, $R_2 = \text{const} = R$, where R is the radius of the circular cylinder. So, the Lamé parameters for the circular cylindrical shell are

$$A = 1, \quad B = R = \text{const}. \tag{11.53}$$

11.8.3 Conical shells

In a conical shell, the meridional angle φ is a constant and can no longer serve as a coordinate of the meridian. The location of a point on the middle surface will be defined by the radius vector $\mathbf{r}$ taken from the top of the cone (point O in Fig. 11.14) along its generator, and angle θ formed by a meridional plane passing through that point with some reference meridional plane. Let the length of the vector $\mathbf{r}$ be s and the slope of the generator to the cone base be α. The projections of $\mathbf{r}$ on the global coordinate axes, X, Y, and Z (see Fig. 11.14) are

$$X = s\cos\alpha\cos\theta, \quad Y = s\cos\alpha\sin\theta, \quad Z = s\sin\alpha. \tag{11.54}$$

The vector $\mathbf{r}$ can be resolved along the unit vectors $\mathbf{i}, \mathbf{j}$, and $\mathbf{k}$, as follows:

$$\mathbf{r} = s(\mathbf{i}\cos\alpha\cos\theta + \mathbf{j}\cos\alpha\sin\theta + \mathbf{k}\sin\alpha). \tag{11.55}$$

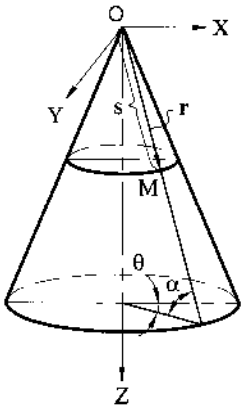

Fig. 11.14

The values s and θ will be considered as the curvilinear coordinates on the middle surface, as follows:

$$\alpha = s \quad \text{and} \quad \beta = \theta. \tag{11.56}$$

The coefficients of the first quadratic form are determined from Eqs (11.12) and (11.10), i.e.,

$$A^2 = \left(\frac{\partial \mathbf{r}}{\partial \alpha}\right)^2 \quad \text{and} \quad B^2 = \left(\frac{\partial \mathbf{r}}{\partial \beta}\right)^2.$$

Substituting for $\mathbf{r}$ from Eq. (11.55), then differentiating with respect to α and β and taking into account relations (11.56), we obtain the Lamé parameters for a conical shell in the form

$$A = 1 \quad \text{and} \quad B = s\cos\alpha. \tag{11.57}$$

11.8.4 Shallow shells

A shallow shell is defined as a shell having a relatively small raise as compared to its spans (Fig. 11.15).

A shell is said to be a shallow if at any point of its middle surface the following inequalities hold:

$$\left(\frac{\partial z}{\partial x}\right)^2 \ll 1, \quad \left(\frac{\partial z}{\partial y}\right)^2 \ll 1 \tag{11.58}$$

where $z = z(x, y)$ represents the equation of the shell middle surface. Referring to Fig. 11.15b, one sees the effect of this simplification. Consider a differential element of the middle surface bounded by the intersections with two planes parallel to the Oyz coordinate plane and separated by a distance dx, and two planes parallel to the Oxz coordinate plane separated by a distance dy. From Fig. 11.15b, it follows that

$$\mathrm{d}s_1 \cong \mathrm{d}x\left[1 + (z, x)^2\right]^{1/2} \tag{11.59a}$$

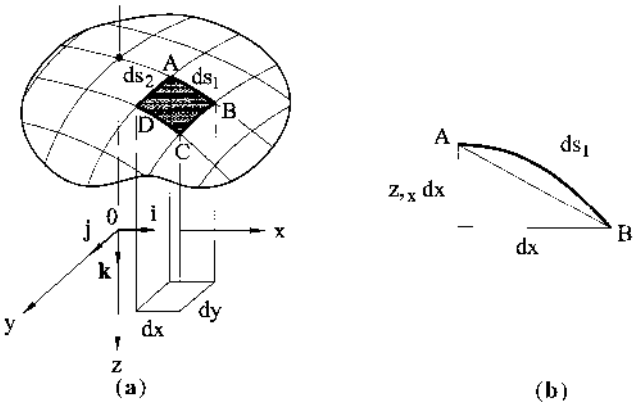

Fig. 11.15

Similarly, we can write

$$ds_2 \cong dy\left[1 + (z, y)^2\right]^{1/2}. \tag{11.59b}$$

These expressions, due to the geometric simplification (Eq. (11.58)), may be written simply as

$$ds_2 \approx dy \quad \text{and} \quad ds_1 \approx dx. \tag{11.60}$$

Practically, the above imply that the curvilinear coordinates α and β may be selected as the Cartesian coordinates x and y with the following Lamé parameters:

$$A = B = 1. \tag{11.61}$$

PROBLEMS

11.1 Verify Eqs (11.28) and (11.29).

11.2 Draw sketches of the following meridians and calculate the principal curvatures κ_1 and κ_2 in each case: (a) $Z = Ar^2$, and (b) $(r/a)^2 - (z/b)^2 = 1$.

11.3 Explain the difference between the first and second quadratic forms from the geometric point of view.

11.4 Roof shell structures often have a shape of surfaces of translation (see Sec. 11.7.1(b)). The equation of such a surface can be assigned as $Z = \varphi(X) + \psi(Y)$. Assuming that a location of a point on this surface is given by the Cartesian coordinates $\alpha = x$ and $\beta = y$, determine the coefficients of the first quadratic form for the nonshallow shell of translation.

11.5 Verify Eqs. (11.45) and (11.47).

11.6 Verify that the Gauss–Codazzi relations are satisfied for a shell of revolution with the parameter A given by equation $A = [1 + (r_{,Z})^2]^{1/2}$.

11.7 Verify Eqs (11.48).

11.8 Calculate the Lamé parameters for a conical shell in terms of the coordinates Z and θ (see Fig. 11.15), i.e., for $\alpha = Z$ and $\beta = \theta$.

11.9 Prove that surfaces possessing the same Lamé parameters will have the same Gaussian curvature.

REFERENCES

1. Louis, A., *Differential Geometry*, Harper and Row, New York, 1967.
2. Stoker, J.J., *Differential Geometry*, Wiley-Interscience, New York, 1969.
3. Kreyszig, E., *Differential Geometry*, University of Toronto, Toronto, 1959.
4. Kelkar, V.S. and Sewell, R.T., *Analysis & Design of Shell Structures*, Prentice-Hall, Englewood Cliffs, New Jersey, 1987.
5. Novozhilov, V.V., *Thin Shell Theory*, P. Noordholf, Groningen, The Netherlands, 1964.

12

The General Linear Theory of Shells

12.1 BASIC ASSUMPTIONS

The linear theory of thin elastic shells with arbitrary shape of the middle surface is derived on the basis of Kirchhoff's assumptions that were used in the development of the plate bending theory introduced in Part I. These assumptions are formulated for the linear theory of thin shells of an arbitrary shape, as follows:

1. *Normals to the undeformed middle surface remain straight and normal to the deformed middle surface and undergo no extension*. This assumption implies that all the strain components (normal and shear) in the direction of the normal to the middle surface vanish.
2. *The transverse normal stress is small compared with other normal stress components and may be neglected.*

Novozhilov showed [1] that the error introduced by the Kirchhoff hypotheses in the theory of thin shells is of the order h/R in comparison with unity, in which h and R are the shell thickness and radius of curvature of the middle surface, respectively. It is assumed that the thickness of the shell is small compared with other dimensions, for example, the smallest radius of the middle surface of the shell (see the inequality (10.1)).

We also assume that the *displacements of an arbitrary point of a shell are small in comparison to its thickness*. As a consequence of this assumption, the products of the displacements and their partial derivatives will be neglected as second-order quantities of smallness. Furthermore, we can refer all calculations to the original configuration of the shell and ensure the differential equations will be linear.

From here on we assume that the material of the shells is homogeneous, isotropic and that it obeys Hooke's law.

As was mentioned in Sec. 10.3, the above Kirchhoff's hypotheses together with small displacement and thinness of shell assumptions are called the Kirchhoff–Love assumptions. According to the Kirchhoff assumptions, deformations throughout the whole volume of the shell material are completely defined by deformations and changes in curvature of the middle surface. Thus, the adoption of these hypotheses reduces the three-dimensional (3D) shell problem to the two-dimensional (2D) problem of equilibrium and straining of the middle surface of a shell. So, the shell will be regarded as a 2D body, i.e., a collection of material points situated on the middle surface.

The general linear theory of thin shells includes the three sets of equations: kinematic (strain–displacement relations), constitutive, and equilibrium. These equations must be complemented with prescribed boundary conditions on the shell edges.

12.2 KINEMATICS OF SHELLS

12.2.1 Variation of the displacements across the shell thickness

Let the middle surface of the undeformed shell be associated with the curvilinear coordinates α and β, and the coordinate lines α and β coincide with the lines of curvature, as shown in Fig. 12.1. Apart from the global (fixed) Cartesian coordinate system adopted in Chapter 11, let us introduce the local (movable) Cartesian coordinate system $Oxyz$. The x and y axes coincide with the directions of tangents to the curvilinear coordinate lines α and β at a point O of the middle surface, and the z axis points along the normal to this surface at the same point. Notice that the previously introduced triad of unit vectors, $\mathbf{e}_1$, $\mathbf{e}_2$, and $\mathbf{e}_3$ (see Sec. 11.5) form the basis of this local coordinate system. The positive directions of the x, y, and z axes coincide with the positive directions of the unit vectors, respectively. In particular, the positive direction of the z axis is to the center of curvature of the shell (for elliptic and parabolic points of the middle surface), as shown in Fig. 12.1. Such a direction of the z axis is consistent with the previously adopted positive direction of that axis in the plate bending theory (see Sec. 2.2).

Consider a material point M on the middle surface, as shown in Fig. 12.2. As a result of a deformation, this point moves from M on the undeformed middle surface to a point M_1 on the deformed middle surface. We identify this displacement of point M by the vector $\mathbf{D}$. This vector will be a function of the coordinates α and β, i.e.,

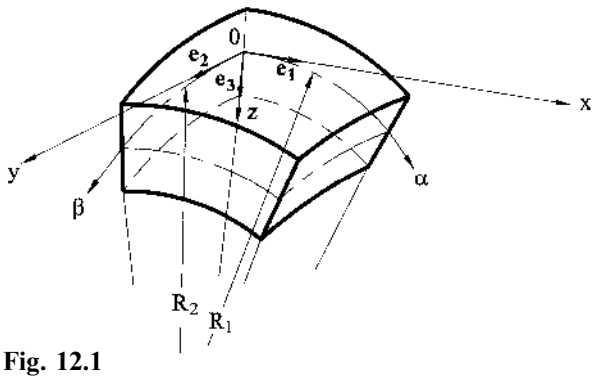

Fig. 12.1

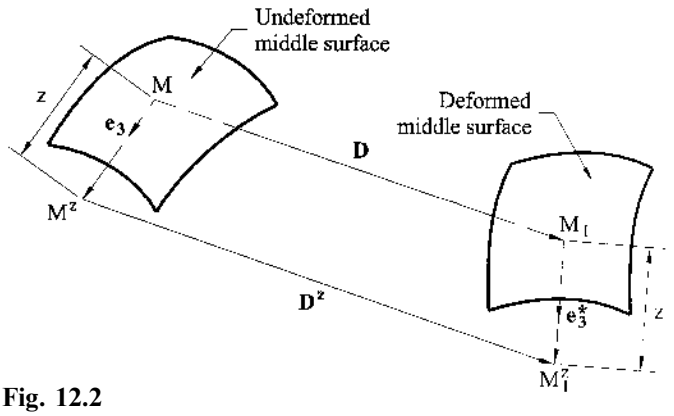

Fig. 12.2

points of the middle surface and, hence, it will completely define the deformed position of the middle surface.

Denote the projections of the *displacement vector* **D** *on the directions of the* x, y, *and* z *axes of the local coordinate system by* u, v, *and* w, respectively. Here u and v are tangential displacements and w is the normal displacement or deflection. The positive directions of the displacement components u, v, and w coincide with the positive directions of the local coordinate axes x, y, and z at a point of the middle surface. Let point M^z be within the shell, at a distance z from point M on the middle surface, and its displacement vector be $\mathbf{D}^z$. The components of this vector along the coordinate axes x, y, and z u^z, v^z, and w^z, can be expressed in terms the displacement components of the point M, as follows (the detailed derivation of these equations is given in Appendix D.):

$$u^z = u - z\vartheta_1, \quad v^z = v - z\vartheta_2, \quad w^z = w, \tag{12.1}$$

where ϑ_1 and ϑ_2 are the angles of rotation of the normal to the middle surface about tangents to the coordinate lines β and α, respectively. They are given by the following (for derivation of these equations see Appendix D):

$$\vartheta_1 = \frac{u}{R_1} + \frac{1}{A}\frac{\partial w}{\partial \alpha}, \quad \vartheta_2 = \frac{v}{R_2} + \frac{1}{B}\frac{\partial w}{\partial \beta}. \tag{12.2}$$

12.2.2 Strain–displacement relations

First, let us introduce the strain components at a point of the middle surface. We denote by ε_1 and ε_2 the linear strain components in the α and β directions, respectively, and by γ_{12} the shear strain component in the middle surface. These strain components can be expressed in terms of the displacement components, u, v, and w, introduced earlier, as follows (the detailed derivation of these expressions is given in Appendix D):

$$\varepsilon_1 = \frac{1}{A}\frac{\partial u}{\partial \alpha} + \frac{1}{AB}\frac{\partial A}{\partial \beta}v - \frac{w}{R_1}, \tag{12.3}$$

$$\varepsilon_2 = \frac{1}{B}\frac{\partial v}{\partial \beta} + \frac{1}{AB}\frac{\partial B}{\partial \alpha}u - \frac{w}{R_2}, \tag{12.4}$$

$$\gamma_{12} = \frac{B}{A}\frac{\partial}{\partial \alpha}\left(\frac{v}{B}\right) + \frac{A}{B}\frac{\partial}{\partial \beta}\left(\frac{u}{A}\right). \tag{12.5}$$

Let us examine a variation of the strain components across the shell thickness. For this purpose, we pass within the shell an equidistant surface located at a distance z from the middle surface, where $-h/2 \le z \le h/2$. Locate a point on this surface by the same coordinates α and β that were used for the middle surface. According to Kirchhoff's assumptions, points lying on one normal to the middle surface remain on the same normal after deformation. Therefore, the above coordinates remain valid for the equidistant surface too. It can be proven (see Appendix D) that if the α- and β-coordinate lines coincide with the lines of curvature on the middle surface, then they are orthogonal, and may also serve as lines of curvature for the equidistant surface.

Figure 12.3 shows a section of the shell by a plane normal to the middle surface. Consider two pairs of neighboring points, M and N, lying along line $\alpha = \text{const.}$ on the middle surface, and their counterparts M^z and N^z on the equidistant surface, located at a distance z from the middle surface. In virtue of Kirchhoff's assumptions, adopted in the general shell theory, all these points will be located on the same normals after deformation and the distance between them in the normal direction (in the z direction) remains unchanged.

If the radius of curvature of arc MN on the middle surface is R_1, then the corresponding radius of curvature of arc M^zN^z on the equidistant surface (by inspection of Fig. 12.3) is

$$R_1^z = R_1 - z. \tag{12.6}$$

It follows from the above that R_1^z is the first principal radius of curvature of the equidistant surface. Moreover, if the length of arc MN is $\mathrm{d}s_1 = A\mathrm{d}\alpha$, then the length of the corresponding arc M^zN^z of the equidistant surface and its Lamé parameter are determined as follows:

$$\mathrm{d}s_1^z = A^z\mathrm{d}\alpha = A\left(1 - \frac{z}{R_1}\right)\mathrm{d}\alpha, \tag{12.7}$$

$$A^z = A\left(1 - \frac{z}{R_1}\right). \tag{12.8}$$

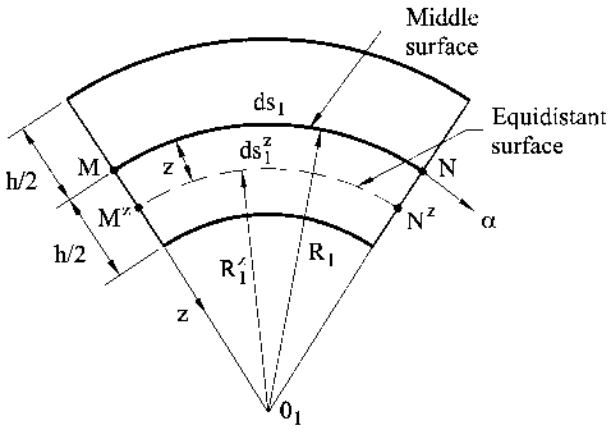

Fig. 12.3

Similarly, the formulas for determining the second principal radius of curvature, R_2^z, and the second Lamé parameter of the equidistant surface, B^z, can be obtained as follows:

$$B^z = B\left(1 - \frac{z}{R_2}\right), \quad R_2^z = R_2 - z. \tag{12.9}$$

When points of the middle surface undergo displacements u, v, and w, then, according to the adapted assumptions, the corresponding points of the equidistant surface undergo displacements u^z, v^z, and w^z given by Eqs (12.1). Therefore, we can obtain the relationships for determining the strain components in the equidistant surface, ε_1^z, ε_2^z, and γ_{12}^z by replacing in Eqs (12.3)–(12.5) the quantities R_1, R_2, A, B, and u, v, w with R_1^z, R_2^z, A^z, B^z, and u^z, v^z, w^z according to Eqs (12.1), (12.6), (12.8), and (12.9). After some algebra, we obtain

$$\varepsilon_1^z = \frac{1}{1 - \frac{z}{R_1}}(\varepsilon_1 + z\chi_1), \quad \varepsilon_2^z = \frac{1}{1 - \frac{z}{R_2}}(\varepsilon_2 + z\chi_2), \tag{12.10}$$

$$\gamma_{12}^z = \frac{1}{1 - \frac{z}{R_1}}(\omega_1 + z\tau_1) + \frac{1}{1 - \frac{z}{R_2}}(\omega_2 + z\tau_2), \tag{12.11}$$

where

$$\chi_1 = -\left(\frac{1}{A}\frac{\partial \vartheta_1}{\partial \alpha} + \frac{1}{AB}\frac{\partial A}{\partial B}\vartheta_2\right) = -\left[\frac{1}{A}\frac{\partial}{\partial \alpha}\left(\frac{u}{R_1} + \frac{1}{A}\frac{\partial w}{\partial \alpha}\right) + \frac{1}{AB}\frac{\partial A}{\partial \beta}\left(\frac{v}{R_2} + \frac{1}{B}\frac{\partial w}{\partial \beta}\right)\right], \tag{12.12}$$

$$\chi_2 = -\left(\frac{1}{B}\frac{\partial \vartheta_2}{\partial \beta} + \frac{1}{AB}\frac{\partial B}{\partial \alpha}\vartheta_1\right) = -\left[\frac{1}{B}\frac{\partial}{\partial \beta}\left(\frac{v}{R_2} + \frac{1}{B}\frac{\partial w}{\partial \beta}\right) + \frac{1}{AB}\frac{\partial B}{\partial \alpha}\left(\frac{u}{R_1} + \frac{1}{A}\frac{\partial w}{\partial \alpha}\right)\right], \tag{12.13}$$

$$\omega_1 = \frac{1}{A}\frac{\partial v}{\partial \alpha} - \frac{1}{AB}\frac{\partial A}{\partial \beta}u, \quad \omega_2 = \frac{1}{B}\frac{\partial u}{\partial \beta} - \frac{1}{AB}\frac{\partial B}{\partial \alpha}v, \tag{12.14}$$

$$\tau_1 = -\left(\frac{1}{A}\frac{\partial \vartheta_2}{\partial \alpha} - \frac{1}{AB}\frac{\partial A}{\partial \beta}\vartheta_1\right), \quad \tau_2 = -\left(\frac{1}{B}\frac{\partial \vartheta_1}{\partial \beta} - \frac{1}{AB}\frac{\partial B}{\partial \alpha}\vartheta_2\right). \tag{12.15}$$

In Eqs (12.15), the angles of rotation, ϑ_1 and ϑ_2, are given by Eqs (12.2); ω_1 and ω_2 can be identified with the angles of rotation of the unit vectors $\mathbf{e}_1$ and $\mathbf{e}_2$, respectively, about the normal direction to the middle surface given by the unit vector $\mathbf{e}_3$ (see Appendix D.1). The terms χ_1 and χ_2 correspond to the familiar bending curvatures introduced in the plate bending theory (see Sec. 2.2). However, for shells they are more properly called *the changes in curvatures of the middle surface in the directions of the α- and β-coordinate lines*, since shells, by definition, are initially curved.

Equation (12.11) contains four different functions ($\omega_1, \omega_2, \tau_1,$ and τ_2). However, one can bring it to a form consisting of only two different functions of the curvilinear coordinates of the middle surface. With this purpose, first of all, note that the following identity holds:

$$\tau_1 - \frac{\omega_2}{R_1} = \tau_2 - \frac{\omega_1}{R_2}. \tag{12.16}$$

The validity of this identity can be easily verified if we substitute for τ_1, τ_2, ω_1, and ω_2 from Eqs (12.15) and (12.14) in terms of u, v, and w, and perform a differentiation with regard to the Codazzi relations (11.27a). Then, comparing Eqs (12.5) and (12.14), it is easily verified that

$$\gamma_{12} = \omega_1 + \omega_2. \tag{12.17}$$

Let us introduce the following geometric quantity:

$$\chi_{12} = \tau_1 - \frac{\omega_2}{R_1} = \tau_2 - \frac{\omega_1}{R_2}. \tag{12.18}$$

The term χ_{12} represents *the twist of a differential element of the middle surface due to the shell bending*. It can be defined as the limit of the ratio of the relative angle of rotation of two opposite sides of the above element, caused by shell straining, and a distance between these sides, as the element shrinks to zero. The twist has the dimensions of reciprocal of length and is thereby analogous to curvature.

Substituting for τ_1 and ω_2 or for τ_2 and ω_1 from Eqs (12.14) and (12.15) into the above, yields

$$\begin{aligned}\chi_{12} = &-\frac{1}{R_1}\left(\frac{u}{AB}\frac{\partial A}{\partial \beta} - \frac{1}{B}\frac{\partial u}{\partial \beta}\right) + \frac{1}{R_2}\left(\frac{v}{AB}\frac{\partial B}{\partial \alpha} - \frac{1}{A}\frac{\partial v}{\partial \alpha}\right)\\ &-\frac{1}{AB}\left(\frac{\partial^2 w}{\partial \alpha \partial \beta} - \frac{1}{B}\frac{\partial B}{\partial \alpha}\frac{\partial w}{\partial \beta} - \frac{1}{A}\frac{\partial A}{\partial \beta}\frac{\partial w}{\partial \alpha}\right).\end{aligned} \tag{12.19}$$

Finally, reducing terms of Eq. (12.11) to the common denominator and using Eqs (12.17) and (12.18), we can rewrite the above equation in the form

$$\gamma_{12}^z = \frac{1}{\left(1 - \frac{z}{R_1}\right)\left(1 - \frac{z}{R_2}\right)}\left[\gamma_{12} + 2z\chi_{12} - \frac{z^2}{R_1 R_2}(\tau_1 R_1 + \tau_2 R_2)\right]. \tag{12.20}$$

It follows from Eq. (12.18) and (12.17) that

$$\tau_1 R_1 + \tau_2 R_2 = \chi_{12}(R_1 + R_2) + \gamma_{12}.$$

Substituting the above into Eq. (12.20), after some algebra, we obtain

$$\gamma_{12}^z = \frac{1}{\left(1 - \frac{z}{R_1}\right)\left(1 - \frac{z}{R_2}\right)}\left\{\gamma_{12}\left(1 - \frac{z^2}{R_1 R_2}\right) + 2z\chi_{12}\left[1 - \frac{z}{2}\left(\frac{1}{R_1} + \frac{1}{R_2}\right)\right]\right\}. \tag{12.21}$$

Equations (12.10) and (12.21) determine the strain components variation across the shell thickness according to the second-order approximation of the general, linear shell theory. However, for thin shells used in engineering practice, the ratio $h/R_{\min}$ (where $R_{\min}$ is the smallest radius of curvature of the middle surface) is less than 1/50. Therefore, the ratio $z/R_{\min}$ does not exceed 1%. It should be kept in mind that as mentioned previously, the Kirchhoff assumptions stipulate the error of the linear theory of the order of $h/R_{\min}$. So, retaining in the expressions (12.10) and (12.21) the terms of the order h/R_i ($i = 1, 2$) in comparison with unity is not justified. Hence, the above expressions for the strain components at an arbitrary point of the

shell may be simplified to the form (neglecting here the value of z/R_i in comparison with unity)

$$\varepsilon_1^z = \varepsilon_1 + z\chi_1, \tag{12.22a}$$

$$\varepsilon_2^z = \varepsilon_2 + z\chi_2, \tag{12.22b}$$

$$\gamma_{12}^z = \gamma_{12} + 2z\chi_{12}. \tag{12.22c}$$

In so doing, it cannot be stated that the linear in z Eqs (12.22) are less accurate than Eqs (12.10) and (12.21).

The relations (12.22) are of primary importance in the theory of shells. They express the normal and shear strain components at any point across the shell thicknesses as a linear combination of the following two terms:

(a) the in-plane strain components on the middle surface that are expressed in terms of the middle surface displacements by Eqs (12.3)–(12.5);
(b) the changes in curvature and twist that are also given in terms of the middle surface displacements by Eqs (12.12), (12.13), and (12.19).

Therefore, as mentioned previously, the relations (12.22) enable one to reduce the 3D problem of the shell straining to the 2D problem of the deformation of the shell middle surface. The relationships between the in-plane strains, changes in curvature, and twist on the one hand, and the displacements of the middle surface on the other, are called the generalized *strain–displacement* or *kinematic equations*. They establish the conditions of *compatibility* of the strains and displacements, suitably specialized for the shell theory under consideration. Let us summarize these equations, as follows:

$$\varepsilon_1 = \frac{1}{A}\frac{\partial u}{\partial \alpha} + \frac{1}{AB}\frac{\partial A}{\partial \beta}v - \frac{w}{R_1},$$

$$\varepsilon_2 = \frac{1}{B}\frac{\partial v}{\partial \beta} + \frac{1}{AB}\frac{\partial B}{\partial \alpha}u - \frac{w}{R_2},$$

$$\gamma_{12} = \frac{B}{A}\frac{\partial}{\partial \alpha}\left(\frac{v}{B}\right) + \frac{A}{B}\frac{\partial}{\partial \beta}\left(\frac{u}{A}\right), \tag{12.23}$$

$$\chi_1 = -\left[\frac{1}{A}\frac{\partial}{\partial \alpha}\left(\frac{u}{R_1} + \frac{1}{A}\frac{\partial w}{\partial \alpha}\right) + \frac{1}{AB}\frac{\partial A}{\partial \beta}\left(\frac{v}{R_2} + \frac{1}{B}\frac{\partial w}{\partial \beta}\right)\right],$$

$$\chi_2 = -\left[\frac{1}{B}\frac{\partial}{\partial \beta}\left(\frac{v}{R_2} + \frac{1}{B}\frac{\partial w}{\partial \beta}\right) + \frac{1}{AB}\frac{\partial B}{\partial \alpha}\left(\frac{u}{R_1} + \frac{1}{A}\frac{\partial w}{\partial \alpha}\right)\right],$$

$$\chi_{12} = -\left[\frac{1}{AB}\left(-\frac{1}{A}\frac{\partial A}{\partial \beta}\frac{\partial w}{\partial \alpha} - \frac{1}{B}\frac{\partial B}{\partial \alpha}\frac{\partial w}{\partial \beta} + \frac{\partial^2 w}{\partial \alpha \partial \beta}\right) + \frac{1}{R_1}\frac{A}{B}\frac{\partial}{\partial \beta}\left(\frac{u}{A}\right) + \frac{1}{R_2}\frac{B}{A}\frac{\partial}{\partial \alpha}\left(\frac{v}{B}\right)\right], \tag{12.24}$$

$$\varepsilon_3 = \gamma_{13} = \gamma_{23} = 0. \tag{12.25}$$

It follows from the above equations that a deformation of the shell middle surface is completely defined by the six strain parameters, $\varepsilon_1, \varepsilon_2, \gamma_{12}, \chi_1, \chi_2$, and χ_{12} that are

called the *strain components*. The first three strain components characterize the changes in linear and angular dimensions of a differential element of the middle surface, while the last three strain components are associated with the change in space shape of the above element, i.e., with its bending and twisting. It is pertinent to draw the analogy between shells and curved beams. It is known from the strength of materials [2] that any change in linear dimensions of a curved bar is accompanied by a change in its curvature and vice versa.

Taking in Eqs (12.22)–(12.24) $A = B = 1$, $R_1 = R_2 = \infty$, and $\alpha = x$, $\beta = y$, we obtain the strain–displacement relationships for the bending theory of flat plates:

$$\varepsilon_1 = -z\frac{\partial^2 w}{\partial x^2}; \quad \varepsilon_2 = -z\frac{\partial^2 w}{\partial y^2}; \quad \gamma_{12} = -2z\frac{\partial^2 w}{\partial x \partial y}. \tag{12.26}$$

These are identified with the x- and y-coordinate axes, respectively.

It can be seen from Eqs (12.22)–(12.24) that the six quantities determining deformations of the middle surface of the shell and changes in its curvature (ε_1, ε_2, γ_{12}, $\chi_1 \cdot \chi_2$, and χ_{12}) are expressed in terms of the three displacement components (u, v, and w). Therefore, there are some identical relationships between the six parameters. The meaning of these relationships, called the *compatibility equations*, lies in the fact that elements of the middle surface obtaining the linear deformations, ε_1, ε_2, and γ_{12}, as well as changes in curvature and twist, χ_1, χ_2, and χ_{12}, must form a unique and continuous surface. The simplest way to obtain these equations is to demand that the coefficients that characterize the first and second quadratic forms of the deformed surface would satisfy the Codazzi and Gauss equations (11.27). The compatibility equations were derived by Gol'denveizer [3], accordingly; they are presented below without derivation:

$$\begin{aligned}
&\frac{\partial}{\partial\alpha}(\chi_2 B) - \frac{1}{A}\frac{\partial}{\partial\beta}\left(\chi_{12}A^2\right) - \frac{\partial B}{\partial\alpha}\chi_1 + \frac{1}{R_2}\frac{\partial A}{\partial\beta}\gamma_{12} \\
&\qquad + \frac{1}{R_1}\left[-\frac{\partial}{\partial\alpha}(\varepsilon_2 B) + \frac{\partial B}{\partial\alpha}\varepsilon_1 + \frac{\partial}{\partial\beta}(\gamma_{12}A)\right] = 0, \\
&\frac{\partial}{\partial\beta}(\chi_1 A) - \frac{1}{B}\frac{\partial}{\partial\alpha}\left(\chi_{12}B^2\right) - \frac{\partial A}{\partial\beta}\chi_2 + \frac{1}{R_1}\frac{\partial B}{\partial\alpha}\gamma_{12} \\
&\qquad + \frac{1}{R_2}\left[-\frac{\partial}{\partial\beta}(\varepsilon_1 A) + \frac{\partial A}{\partial\beta}\varepsilon_2 + \frac{\partial}{\partial\alpha}(\gamma_{12}B)\right] = 0, \\
&\frac{1}{AB}\frac{\partial}{\partial\alpha}\left\{\frac{1}{A}\left[-\frac{\partial}{\partial\alpha}(\varepsilon_2 B) + \frac{\partial B}{\partial\alpha}\varepsilon_1 + \frac{1}{2A}\frac{\partial}{\partial\beta}\left(\gamma_{12}A^2\right)\right]\right\} \\
&\qquad + \frac{1}{AB}\frac{\partial}{\partial\beta}\left\{\frac{1}{B}\left[-\frac{\partial}{\partial\beta}(\varepsilon_1 A) + \frac{\partial A}{\partial\beta}\varepsilon_2 + \frac{1}{2B}\frac{\partial}{\partial\alpha}\left(\gamma_{12}B^2\right)\right]\right\} - \left(\frac{\chi_1}{R_2} + \frac{\chi_2}{R_1}\right) = 0.
\end{aligned} \tag{12.27}$$

As in problems of the theory of elasticity, the compatibility equations (12.27) are used in the theory of shells for solving problems formulated in terms of the stress resultants and stress couples. When we solve problems in displacements, these equations are identically satisfied. This can be proven by substituting the expressions for deformations and parameters of a change in curvature from Eqs (12.23) and (12.24)

into Eqs (12.27) and performing the transformations of these equations with the use of the Codazzi and Gauss relationships.

12.3 STATICS OF SHELLS

In the previous section we dealt with geometrical description of the shell (deformations and displacements). In the present section we consider the equilibrium conditions of the shell.

12.3.1 Hooke's law for thin shells

The constitutive equations for a 3D homogeneous isotropic body are given by Eqs (1.8). Applying the same system of notations as that adapted above for the strain components in Sec. 12.2.2, we can rewrite the above equations, as follows:

$$\varepsilon_1^z = \frac{1}{E}[\sigma_1^z - \nu(\sigma_2^z + \sigma_3^z)], \quad \varepsilon_2^z = \frac{1}{E}[\sigma_2^z - \nu(\sigma_1^z + \sigma_3^z)], \quad \varepsilon_3^z = \frac{1}{E}[\sigma_3^z - \nu(\sigma_2^z + \sigma_1^z)], \tag{12.28}$$

$$\gamma_{12}^z = \frac{\tau_{12}^z}{G}, \quad \gamma_{13}^z = \frac{\tau_{13}^z}{G}, \quad \gamma_{23}^z = \frac{\tau_{23}^z}{G}, \tag{12.29}$$

where σ_1^z, σ_2^z, and σ_3^z are the normal stresses acting on planes whose normals are parallel to the directions α, β, and z axes, respectively; $\varepsilon_1^z, \varepsilon_2^z$, and ε_3^z are the linear strains along the same directions; τ_{12}^z, τ_{13}^z, and τ_{23}^z are shear stresses; and $\gamma_{12}^z, \gamma_{13}^z$, and γ_{23}^z are the corresponding shear strains.

Returning to Kirchhoff's postulates, note that the assumption of the preservation of the normal implies that all of the strain components in the direction of the normal to the middle surface (hypothesis 1) vanish. This means that

$$\varepsilon_3^z = \gamma_{13}^z = \gamma_{23}^z = 0, \tag{12.30}$$

and, in view of Eqs (12.29), the shear stress components τ_{13}^z and τ_{23}^z also vanish. The next Kirchhoff's assumption for thin shells states that the transverse normal stress is negligible compared with the in-plane normal stresses (hypothesis 2), so we can set

$$\sigma_3^z = 0. \tag{12.31}$$

This assumption proves itself because the normal stress σ_3^z on the external and internal shell surfaces is equal to the intensity of the applied transverse external load. It can be shown that the in-plane normal stresses, σ_1^z and σ_2^z, are, at least, R/h times greater than σ_3^z [1]. Due to the shell thinness, we can conclude that σ_3^z will also be small at interior points of the shell.

Solving Eqs (12.28) and (12.29) for the stress components and taking into account the relation (12.31), we can obtain the following expressions for determining the stress components in terms of the strain components:

$$\sigma_1^z = \frac{E}{1-\nu^2}(\varepsilon_1^z + \nu\varepsilon_2^z); \quad \sigma_2^z = \frac{E}{1-\nu^2}(\varepsilon_2^z + \nu\varepsilon_1^z); \quad \tau_{12}^z = G\gamma_{12}^z = \frac{E}{2(1+\nu)}\gamma_{12}^z. \tag{12.32}$$

Substituting for the strain components from Eqs (12.22) into the above, we express the stress components at any point across the thickness of the shell in terms of the middle surface strain components, changes in curvature, and twist, as follows:

$$\sigma_1^z = \frac{E}{1-\nu^2}[\varepsilon_1 + \nu\varepsilon_2 + z(\chi_1 + \nu\chi_2)], \quad \sigma_2^z = \frac{E}{1-\nu^2}[\varepsilon_2 + \nu\varepsilon_1 + z(\chi_2 + \nu\chi_1)],$$

$$\tau_{12}^z = \frac{E}{1+\nu}\left(\frac{1}{2}\gamma_{12} + z\chi_{12}\right). \tag{12.33}$$

Figure 12.4 shows a space differential element isolated from a shell by means of four sections normal to its middle surface and tangential to the lines α and $\alpha + d\alpha$, β and $\beta + d\beta$. The height of this element is finite and equals the shell thickness h. In this figure, the stresses acting on the volume element are indicated. The sign convention and subscript notation of the stress components are that of the theory of elasticity (see Sec. 1.4) and adapted in the treatment of thin shells, where the subscripts 1, 2, and 3 correspond to the axes α, β, and z, respectively. So, all stresses are shown positive in Fig. 12.4. For any orthogonal coordinates, the condition of equilibrium of moments on a differential element requires that

$$\tau_{12}^z = \tau_{21}^z, \quad \tau_{13}^z = \tau_{31}^z, \quad \text{and} \quad \tau_{23}^z = \tau_{32}^z. \qquad .$$

12.3.2 The stress resultants and stress couples in shells

It follows from Eq. (12.33) that the stress components are linearly distributed across the thickness of the elastic shell; therefore, it is convenient to integrate the stress distribution through the shell thickness, and then to replace the usual consideration of stresses by a consideration of statically equivalent *stress resultants and stress couples* applied to the middle surface, just as was done in the plate bending theory (see Sec. 2.3). These stress resultants and stress couples are also referred to as the *internal forces and moments*, respectively. By performing such integrations, the variations with respect to z are completely eliminated to give a 2D theory of thin shells. The elements of area of the cross sections (shaded in Fig.12.4) are

$$ds_1^z = A^z d\alpha dz = A\left(1 - \frac{z}{R_1}\right)d\alpha dz; \quad ds_2^z = B^z d\beta dz = B\left(1 - \frac{z}{R_2}\right)d\beta dz. \tag{12.34}$$

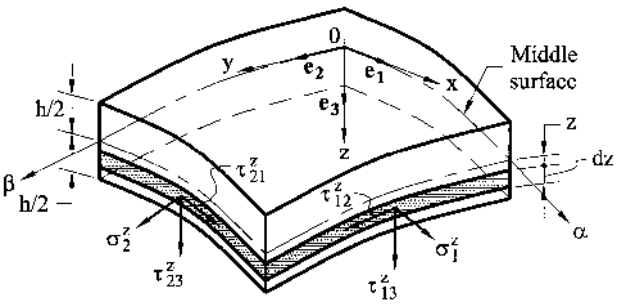

Fig. 12.4

Let us define the in-plane normal force N_1 as the resultant of the normal stresses σ_1 acting on plane face yz per unit length of the element. Thus, we have the following:

$$N_1 B \mathrm{d}\beta = \int_{-h/2}^{h/2} \sigma_1^z \mathrm{d}s_2^z = \int_{-h/2}^{h/2} \sigma_1^z B\left(1 - \frac{\mathrm{z}}{R_2}\right)\mathrm{d}\beta \mathrm{d}z,$$

from which

$$N_1 = \frac{1}{B\mathrm{d}\beta}\int_{-h/2}^{h/2} \sigma_1^z B\mathrm{d}\beta\left(1 - \frac{z}{R_2}\right)\mathrm{d}z \quad \text{or} \quad N_1 = \int_{-h/2}^{h/2} \sigma_1^z\left(1 - \frac{z}{R_2}\right)\mathrm{d}z. \tag{12.35a}$$

Similarly, we can define the in-plane shear force N_{12} and the transverse shear force Q_1, which are the resultants of the shear stress components τ_{12} and τ_{13}, respectively, and act on the same yz plane face:

$$N_{12} = \int_{-h/2}^{h/2} \tau_{12}^z\left(1 - \frac{z}{R_2}\right)\mathrm{d}z \tag{12.35b}$$

$$Q_1 = \int_{-h/2}^{h/2} \tau_{13}^z\left(1 - \frac{z}{R_2}\right)\mathrm{d}z. \tag{12.35c}$$

Expression for the remaining stress resultants per unit length are derived in a similar manner. They are given by the following:

$$N_2 = \int_{-h/2}^{h/2} \sigma_2^z\left(1 - \frac{z}{R_1}\right)\mathrm{d}z, \tag{13.35d}$$

$$N_{21} = \int_{-h/2}^{h/2} \tau_{21}^z\left(1 - \frac{z}{R_1}\right)\mathrm{d}z, \tag{12.35e}$$

$$Q_2 = \int_{-h/2}^{h/2} \tau_{23}^z\left(1 - \frac{z}{R_1}\right)\mathrm{d}z. \tag{12.35f}$$

Taking, next, the moments of the stress components σ_1^z and τ_{12}^z about the y and x axes, we will arrive to the following two new quantities:

$$M_1 = \int_{-h/2}^{h/2} \sigma_1^z z\left(1 - \frac{z}{R_2}\right)\mathrm{d}z \tag{12.36a}$$

and

$$M_{12} = \int_{-h/2}^{h/2} \tau_{12}^z z\left(1 - \frac{z}{R_2}\right)\mathrm{d}z, \tag{12.36b}$$

which are referred to, as mentioned previously, as the stress couples or the *bending* and *twisting moments*, respectively, acting on plane face yz. These moments are given to per unit length of the element of Fig. 12.4. Similarly, we can define the stress couples or the bending and twisting moments assigned on plane face xz, as follows:

$$M_2 = \int_{-h/2}^{h/2} \sigma_2^z z\left(1 - \frac{z}{R_1}\right)\mathrm{d}z, \tag{12.36c}$$

$$M_{21} = \int_{-h/2}^{h/2} \tau_{21}^z z\left(1 - \frac{z}{R_1}\right)\mathrm{d}z. \tag{12.36d}$$

The positive senses of the stress resultants and stress couples are shown in Fig. 12.5; the sign convention adopted in this figure is the same as for thin plates (see Sec. 2.3).

Notice in the above definitions of the stress resultants and stress couples that the symmetry of the stress tensor ($\tau_{12} = \tau_{21}$) does not necessarily imply that N_{12} and N_{21} are either equal or that M_{12} and M_{21} are equal for a thin shell of an arbitrary shape, except for a spherical shell.

In the general linear theory of thin shells presented above, six internal forces, N_1, N_{12}, N_{21}, N_2, Q_1, and Q_2, and four moments, M_1, M_2, M_{12} and M_{21}, characterize completely the state of stress of the shell, because the knowledge of these quantities enables one to determine the stress components at any point of the shell, as follows:

$$\begin{aligned}
\sigma_1^z &= \left(\frac{N_1}{h} + \frac{12M_1}{h^3}z\right)\frac{1}{1-\frac{z}{R_2}} \approx \frac{N_1}{h} + \frac{12M_1}{h^3}z; \\
\sigma_2^z &= \left(\frac{N_2}{h} + \frac{12M_2}{h^3}z\right)\frac{1}{1-\frac{z}{R_1}} \approx \frac{N_2}{h} + \frac{12M_2}{h^3}z, \\
\tau_{12}^z &= \frac{1}{2h}(N_{12} + N_{21}) + \frac{6}{h^3}(M_{12} + M_{21})z.
\end{aligned} \tag{12.37}$$

The determination of the transverse shear stresses τ_{13} and τ_{23} from their resultants Q_1 and Q_2 is not as precise, even within the framework of the present theory, as is the determination of σ_1, σ_2, and τ_{12}. In this case, it is reasoned, as in the theory of beams and thin plates, that the transverse shear stresses are parabolically distributed across the thickness of the shell. Assuming that the shear stresses are lacking on the outer and inner surfaces of the shell, we obtain the following expression for the transverse shear stresses:

$$\tau_{i3}^z = \frac{6}{5}\frac{Q_i}{h}\left[1 - \left(\frac{2z}{h}\right)^2\right], \quad i = 1, 2, \tag{12.38}$$

where, for the sake of convenience, a "form factor" of 6/5 is introduced. It represents the ratio of peak shear stress to average shear stress across the thickness of the shell.

As mentioned previously, general theory of thin shells presented was based on the Kirchhoff–Love assumptions. Now is the time to discuss these assumptions applied to the preceding derivations of the stress resultants and stress couples.

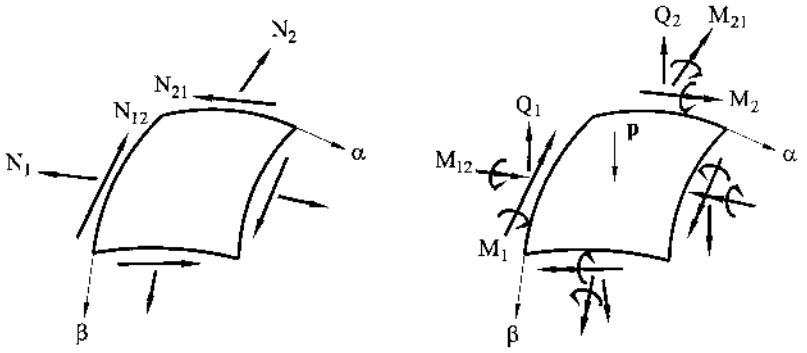

Fig. 12.5

1. We have found that, as a result of the first Kirchhoff assumption, $\gamma_{13} = \gamma_{23} = 0$ and therefore $\tau_{13} = \tau_{23} = 0$ from Hooke's law (Eqs 12.29). Nevertheless, we have defined the nonvanishing shear stress resultants Q_1 and Q_2 as integrals of τ_{13} and τ_{23} over the shell thickness. A similar situation has been observed in the plate bending theory (see Sec. 2.3), as well as in the elementary theory of beams. Here, as in the plate bending theory, the Q_1 and Q_2 resultants must be retained for purposes of equilibrium. However, they cannot be determined directly by integrating the shear stresses τ_{13} and τ_{23} over the shell thickness as was done for other stress resultants. As in the plate bending theory, the transverse shear forces Q_1 and Q_2 may be found from equilibrium conditions set up for a differential element; this is shown later.

2. We have also found that, as a result of the first and second Kirchhoff's assumptions, $\varepsilon_3 = \sigma_3 = 0$. If only σ_3 were assumed to vanish, then the following expression for the normal strain ε_3 could be obtained from Eqs (12.28) by setting $\sigma_3 = 0$. We have

$$\varepsilon_3 = -\frac{\nu}{1-\nu}(\varepsilon_1 + \varepsilon_2). \tag{12.39}$$

From this expression it would appear that the simultaneous vanishing of both the transverse normal stress and normal strain is inconsistent. These inconsistencies and deficiencies specify an approximate character of the general linear thin shell theory. However, as mentioned previously, the error introduced by Kirchhoff's assumptions into the shell theory is of the order of h/R_i in comparison with unity.

12.3.3 Equilibrium of the shell element

Consider a differential element isolated from a shell and bounded by two pairs of the normal sections passing through the α- and β-coordinate lines (Fig. 12.4) and specify its equilibrium under all external and internal forces. The external forces will comprise some surface loads applied to the upper and lower surfaces of the element. As mentioned previously, the stress components, continuously distributed across the shell thickness, are replaced by statically equivalent internal forces and moments and applied to the middle surface (Fig. 12.5). An analogous operation can be executed for the external loads by replacing them by statically equivalent forces distributed over the middle surface. Let us resolve the surface load $\mathbf{p}$ into components in the directions of $\mathbf{e_1}$, $\mathbf{e_2}$, and $\mathbf{e_3}$ are denoted by p_1, p_2, and p_3. Thus,

$$\mathbf{p} = p_1\mathbf{e}_1 + p_2\mathbf{e}_2 + p_3\mathbf{e_3}. \tag{12.40}$$

Hence, instead of considering the equilibrium of the 3D element of the shell shown in Fig. 12.4, one can study the equilibrium of the 2D element of the middle surface shown in Fig. 12.5.

Let us consider the equilibrium conditions of this element of the middle surface loaded by the external and internal forces and moments. The force and moment equilibrium for the shell element (the resultant force and resultant moment of all the external and internal forces applied to the middle surface are zero) results in the following scalar equations:

$$\frac{\partial}{\partial\alpha}(N_1B)+\frac{\partial}{\partial\beta}(N_{21}A)+N_{12}\frac{\partial A}{\partial\beta}-N_2\frac{\partial B}{\partial\alpha}-Q_1\frac{AB}{R_1}+p_1AB=0,$$

$$\frac{\partial}{\partial\beta}(N_2A)+\frac{\partial}{\partial\alpha}(N_{12}B)+N_{21}\frac{\partial B}{\partial\alpha}-N_1\frac{\partial A}{\partial\beta}-Q_2\frac{AB}{R_2}+p_2AB=0,$$

$$\frac{\partial}{\partial\alpha}(Q_1B)+\frac{\partial}{\partial\beta}(Q_2A)+N_1\frac{AB}{R_1}+N_2\frac{AB}{R_2}+p_3AB=0, \tag{12.41}$$

$$\frac{\partial}{\partial\alpha}(BM_{12})+\frac{\partial}{\partial\beta}(AM_2)-M_1\frac{\partial A}{\partial\beta}+M_{21}\frac{\partial B}{\partial\alpha}-Q_2AB=0,$$

$$\frac{\partial}{\partial\beta}(AM_{21})+\frac{\partial}{\partial\alpha}(BM_1)-M_2\frac{\partial B}{\partial\alpha}+M_{12}\frac{\partial A}{\partial\beta}-Q_1AB=0,$$

$$N_{12}-N_{21}-\frac{M_{12}}{R_1}+\frac{M_{21}}{R_2}=0. \tag{12.42}$$

The detailed derivations of Eqs (12.41) and (12.42) are given in Appendix E. The above equations represent *a set of the differential equations of static equilibrium of a shell element of the general theory of thin elastic shells*.

It can be easily shown that the third Eq. (12.42) is identically satisfied. To prove that, one needs to substitute for N_{12}, N_{21}, and M_{12}, M_{21} from Eqs (12.35) and (12.36) into the third Eq. (12.42). We obtain the following:

$$\int_{-h/2}^{h/2}\tau_{12}^z\left(1-\frac{z}{R_2}\right)\mathrm{d}z-\int_{-h/2}^{h/2}\tau_{21}^z\left(1-\frac{z}{R_1}\right)\mathrm{d}z-\int_{-h/2}^{h/2}\tau_{12}^z\frac{z}{R_1}\left(1-\frac{z}{R_2}\right)\mathrm{d}z$$

$$=\int_{-h/2}^{h/2}\tau_{21}^z\frac{z}{R_2}\left(1-\frac{z}{R_1}\right)\mathrm{d}z=\int_{-h/2}^{h/2}\left(1-\frac{z}{R_2}\right)\left(1-\frac{z}{R_1}\right)(\tau_{12}^z-\tau_{21}^z)\mathrm{d}z\equiv 0$$

because $\tau_{12}^z=\tau_{21}^z$.

Hence, the system of three equations (Eqs (12.42)) can be reduced to two equations and the third equation may be disregarded, although we may mention it from time to time.

Novozhilov [1] suggested that we reduce the number of unknowns in the above equations by setting

$$M_{12}=M_{21}=H,\quad S=N_{12}+\frac{H}{R_2}=N_{21}+\frac{H}{R_1}. \tag{12.43}$$

It can be shown that the substitution of these expressions for N_{12}, N_{21}, M_{12}, and M_{21} from Eqs (12.43) into the third Eq. (12.42) results in the identity, $0\equiv 0$. Thus, taking into account relations (12.43), the equilibrium equations (12.41) and (12.42) are finally reduced to the system of five partial differential equations for eight unknown stress resultants and couples: i.e., N_1, N_2, S, M_1, M_2, H, Q_1, and Q_2.

Determining the transverse shear forces Q_1 and Q_2 from the first and second Eqs (12.42) and substituting them into Eqs (12.41) with the replacement $N_{12}=S-H/R_2$ and $N_{21}=S-H/R_1$, we arrive at three equations of equilibrium in the following form:

$$\frac{\partial}{\partial\alpha}(N_1B)+\frac{1}{A}\frac{\partial}{\partial\beta}\left(SA^2\right)-\frac{2}{R_2}\frac{\partial A}{\partial\beta}H-\frac{1}{R_1}\left[\frac{\partial}{\partial\alpha}(M_1B)-M_2\frac{\partial B}{\partial\alpha}+2\frac{\partial}{\partial\beta}(HA)\right]$$
$$-N_2\frac{\partial B}{\partial\alpha}+ABp_1=0,$$
$$\frac{\partial}{\partial\beta}(N_2A)+\frac{1}{B}\frac{\partial}{\partial\alpha}\left(SB^2\right)-\frac{2}{R_1}\frac{\partial B}{\partial\alpha}H-\frac{1}{R_2}\left[\frac{\partial}{\partial\beta}(M_2A)-M_1\frac{\partial A}{\partial\beta}+2\frac{\partial}{\partial\alpha}(HB)\right]$$
$$-N_1\frac{\partial A}{\partial\beta}+ABp_2=0,$$
$$N_1\frac{AB}{R_1}+N_2\frac{AB}{R_2}+\frac{\partial}{\partial\alpha}\left\{\frac{1}{A}\left[\frac{1}{A}\frac{\partial}{\partial\beta}\left(HA^2\right)+\frac{\partial}{\partial\alpha}(M_1B)-M_2\frac{\partial B}{\partial\alpha}\right]\right\}$$
$$+\frac{\partial}{\partial\beta}\left\{\frac{1}{B}\left[\frac{1}{B}\frac{\partial}{\partial\alpha}\left(HB^2\right)+\frac{\partial}{\partial\beta}(AM_2)-M_1\frac{\partial A}{\partial\beta}\right]\right\}+ABp_3=0. \tag{12.44}$$

12.3.4 Constitutive equations (stress resultants–strain and stress couple–curvature relations)

In shell problems, the constitutive equations are required to relate the stress resultants and stress couples, instead of merely stresses, to the corresponding strains and curvatures.

Since we have already neglected the terms of order z/R_i $(i=1,2)$ in determining deformations (hence, also stresses), then the factor $(1-z/R_i)$ can be dropped. Thus, substituting for σ_1^z, σ_2^z, and τ_{12}^z from Eqs (12.33) into Eqs (12.35) and (12.36), as well as taking into account expressions (12.43) and integrating over the thickness of the shell, we obtain the following stress resultant–strain and stress couple–curvature relations:

$$N_1=\frac{Eh}{1-\nu^2}(\varepsilon_1+\nu\varepsilon_2),\quad N_2=\frac{Eh}{1-\nu^2}(\varepsilon_2+\nu\varepsilon_1),$$
$$N_{12}=S-\frac{H}{R_2},\quad N_{21}=S-\frac{H}{R_1},\quad S=\frac{Eh}{2(1+\nu)}\gamma_{12}, \tag{12.45}$$
$$M_1=D(\chi_1+\nu\chi_2),\quad M_2=D(\chi_2+\nu\chi_1),$$
$$M_{12}=M_{21}=H,\quad H=D(1-\nu)\chi_{12}, \tag{12.46}$$

where

$$D=\frac{Eh^3}{12(1-\nu^2)} \tag{12.47}$$

is the *flexural rigidity (or stiffness) of the shell*. Equations (12.45) and (12.46) are referred to as the *constitutive equations or stress resultants–strain and stress couple–curvature relations of the general linear theory of thin shells*. As for the transverse shear forces, Q_1 and Q_2 – as mentioned previously, they can be determined from the equations of static equilibrium only, Eqs (12.42).

In the first-order approximation shell theory, the constitutive relations for N_{12} and N_{21} are usually simplified to the form

$$N_{12} = N_{21} = S = \frac{Eh}{2(1+\nu)}\gamma_{12}. \tag{12.48}$$

In this form, the constitutive equations (12.45), (12.46), and (12.48) remind us of the corresponding stress resultants–strains and stress couple–curvatures relations discussed previously in the plate bending theory (Sec. 2.3). The difference between the two constitutive equations is that the strain–displacement relations in the general shell theory have a more complex form than in the plate theory. However, as mentioned in Ref. [1], although the error introduced by the simplified relation (12.48) does not exceed the corresponding errors of the general assumptions adopted in the shell theory, the application of the above equation brings some contradictions. But these contradictions do not practically influence the accuracy of the calculations of the stress and displacement components.

12.4 STRAIN ENERGY OF SHELLS

The strain energy of the shell can be determined by means of Kirchhoff's assumptions discussed previously, i.e., the transverse normal, σ_3, and shear, τ_{13} and τ_{23}, stress components are neglected. Therefore, the strain energy density (strain energy per unit volume) $\hat{u}$ is given by [1]:

$$\hat{u} = \frac{1}{2E}\left[(\sigma_1^z)^2 + (\sigma_2^z)^2 - 2\nu\sigma_1^z\sigma_2^z\right] + \frac{1}{2G}(\tau_{12}^z)^2$$

or

$$\hat{u} = \frac{E}{2\left(1-\nu^2\right)}\left[(\varepsilon_1^z)^2+(\varepsilon_2^z)^2+2\nu\varepsilon_1^z\varepsilon_2^z\right] + \frac{G}{2}(\gamma_{12}^z)^2. \tag{12.49a}$$

Since $G = E/2(1+\nu)$, the last equation may be rewritten as

$$\hat{u} = \frac{E}{2\left(1-\nu^2\right)}\left[(\varepsilon_1^z + \varepsilon_2^z)^2+2(1-\nu)\left(\frac{1}{4}(\gamma_{12}^z)^2 - \varepsilon_1^z\varepsilon_2^z\right)\right]. \tag{12.49b}$$

Substituting for ε_1^z, ε_2^z, and γ_{12}^z from Eqs (12.22) into the above:

$$\begin{aligned}\hat{u} = \frac{E}{2\left(1-\nu^2\right)}\Bigg\{&[\varepsilon_1 + \varepsilon_2 + z(\chi_1+\chi_2)]^2 \\ &+ 2(1-\nu)\left[\frac{1}{4}(\gamma_{12}+2\chi_{12}z)^2 - (\varepsilon_1+\chi_1 z)(\varepsilon_2+\chi_2 z)\right]\Bigg\}.\end{aligned} \tag{12.50}$$

To calculate the total strain energy of the shell, it is necessary to multiply the strain density $\hat{u}$ by an elementary volume of the layer of the shell, as follows:

$$\mathrm{d}V = A^z B^z \mathrm{d}\alpha\mathrm{d}\beta\mathrm{d}z = \left(1-\frac{z}{R_1}\right)\left(1-\frac{z}{R_2}\right)AB\mathrm{d}\alpha\mathrm{d}\beta\mathrm{d}z,$$

and to integrate over the shell thickness ($-h/2 \le z \le h/2$) and over the area of its middle surface.

Accepting the same accuracy that has been used to derive the values of the strain components, neglecting the small terms of the order z/R_i in the expressions for the volume of shell, element and integrating over the shell thickness, we obtain the following expression for the strain energy of the shell:

$$U = \int_\alpha \int_\beta \frac{Eh}{2(1-\nu^2)}\left[(\varepsilon_1+\varepsilon_2)^2+2(1-\nu)\left(\frac{\gamma_{12}^2}{4}-\varepsilon_1\varepsilon_2\right)\right]AB\mathrm{d}\alpha\mathrm{d}\beta + \int_\alpha \int_\beta \frac{D}{2}\left[(\chi_1+\chi_2)^2+2(1-\nu)\left(\chi_{12}^2-\chi_1\chi_2\right)\right]AB\mathrm{d}\alpha\mathrm{d}\beta. \tag{12.51}$$

The first integral in the expression (12.51) represents the membrane strain energy of the shell, whereas the second term expresses its bending strain energy. Using Eqs (12.45) and (12.46), one can express the strain energy of the shell in terms of the internal forces and moments, as follows:

$$U = \int_\alpha \int_\beta \left[\frac{1}{2Eh}(N_1+N_2)^2+2(1+\nu)\left(S^2-N_1N_2\right)\right]AB\mathrm{d}\alpha\mathrm{d}\beta + \int_\alpha \int_\beta \frac{12}{2Eh^3}\left[(M_1+M_2)^2+2(1+\nu)\left(H^2-M_1M_2\right)\right]AB\mathrm{d}\alpha\mathrm{d}\beta. \tag{12.52}$$

At last, the strain energy can be calculated using the following equation:

$$U = \frac{1}{2}\int_\alpha \int_\beta [N_1\varepsilon_1 + N_2\varepsilon_2 + S\gamma_{12} + M_1\chi_1 + M_2\chi_2 + 2H\chi_{12}]AB\mathrm{d}\alpha\mathrm{d}\beta. \tag{12.53}$$

The expressions (12.51)–(12.53) are valid for shells with both constant and variable thicknesses.

12.5 BOUNDARY CONDITIONS

In the previous sections we have derived a set of differential equations (kinematic, equilibrium, and constitutive), which must be satisfied everywhere on the middle surface. However, the solutions of the above equations, naturally, do not yet determine completely the state of stress and strain in a shell, as long as they are not subject to boundary conditions. We now clarify how many boundary conditions must be imposed on the shell edges and set up their formulation for the general linear theory of thin shells. We consider three cases.

1. *A shell has no boundaries*, i.e., it is completely closed. The coordinate lines α and β on the middle surface of the closed shell will be, in turn, also closed. It is evident that in this case the concept of the boundary conditions loses its meaning. However, it does not follow from this that any solution satisfying the previously mentioned governing differential equations of the general linear shell theory is in this case a solution of the shell problem under consideration. A true solution must be a periodic function of the coordinates α and β for a passage through the shell along these closed coordinate lines, and hence, in moving along any closed curve belonging to the middle surface. Thus, in the *case of complete or closed shells, the boundary conditions are replaced by the conditions of periodicity*.

2. *A shell is closed with respect to one coordinate and open with respect to another*, as is, for example, the case for cylindrical shells. It is evident that in the

direction of the closed coordinate the conditions of periodicity must be formulated as the boundary conditions. Along the other, the open coordinate, it is necessary to set up the boundary conditions, which are to be satisfied in solving the governing differential equations of the general shell theory.

3. A *shell is open with regard to both coordinate lines α and β.* In this case, it is required to set up certain boundary conditions in the directions of both principal directions. Proceeding now to this general case, we confine ourselves to the simplest case where the boundaries coincide with the lines of principal curvature of the middle surface (the α- and β- coordinate lines), since this case is encountered most frequently in practice.

Let, for example, the line $\beta = \beta^*$ be a boundary of the shell. The stresses acting on the boundary can be reduced to the three internal forces N_2, N_{21}, and Q_2 and two moments M_2 and M_{21}. The deformations on the same boundary are characterized by the three displacement components u, v, and w and two slopes ϑ_1 and ϑ_2. Thus, at first glance, five boundary conditions must be prescribed on the edge line $\beta = \beta^*$. However, this is not true: due to the Kirchhoff kinematic hypothesis (the first Kirchhoff assumption), not all the above-mentioned quantities are independent. The slope of the normal to the shell boundary, ϑ_2, is connected with the displacements w and v on this boundary by the condition of the preservation of the normal. Therefore, the number of independent displacements (and hence, the corresponding generalized forces) equals four, and only the four boundary conditions can be assigned on each edge of the shell. By the way, as follows from the above, such a number of independent boundary conditions corresponds to the eighth order of the governing differential equations of the general linear theory of thin shells.

Thus, the five forces and moments assigned for the *static boundary conditions* on the shell boundary (i.e., the boundary conditions expressed in terms of the internal forces and moments) can be reduced to four quantities in accordance with Kirchhoff's postulates. This can be carried out in a similar manner to that done in the plate theory (Sec. 2.5): namely, the three boundary quantities, N_2, N_{21}, and M_{21}, may be replaced with the two boundary quantities with an acceptable accuracy.

Figure 12.6 shows two adjacent differential segments of the boundary $\beta = \beta^*$ of the middle surface, each of length $\mathrm{d}s_1$, near some point m_1. The boundary curve mm_1m_2 may be approximated by a polygon formed by two small segments of equal length. The length of each such segment with a high order of accuracy may be set equal to the length of the arc spanning, i.e., $mm_1 = m_1m_2 \approx \mathrm{d}s_1$. Let points n_1 and n_2 be halfway between the points m and m_1, m_1 and m_2, respectively. It is evident that $n_1n_2 \approx \mathrm{d}s_1$. Let $M_{21}ds_1$ and

$$\left(M_{21} + \frac{\partial M_{21}}{\partial s_1}\mathrm{d}s_1\right)\mathrm{d}s_1$$

be the resultants of the twisting moments distributed over segments mm_1 and m_1m_2, respectively. These act at the midpoints n_1 and n_2. Further, we replace each of the above resultant couples by a pair of equal and opposite forces with the moment arms $\mathrm{d}s_1$ and applied at end points of the corresponding segments. So, at end points m and m_1 the forces $(M_{21}ds_1)/ds_1 = M_{21}$, acting normal to the chord mm_1, are applied. Similarly, the forces $M_{21} + (\partial M_{21}/\partial s_1)ds_1$, acting normal to the chord m_1m_2, will be applied at end points m_1 and m_2. Thus at each point of the corners of the polygon,

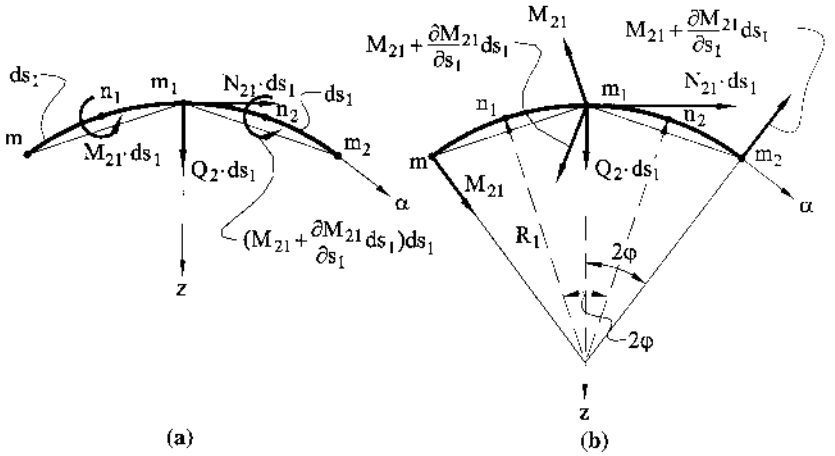

Fig. 12.6

two concentrated forces from twisting moments distributed over the adjacent segments are applied, as shown in Fig. 12.6b for corner point m_1.

Projecting both these forces, acting at a point m_1, on the direction of the normal to the middle surface (the direction of the transverse shear force Q_2) and on the direction of the tangent to the middle surface (the direction of the in-plane shear force N_{21}), we obtain:

(a) in the first case

$$+M_{21}\frac{\partial M_{21}}{\partial s_1}\mathrm{d}s_1 - M_{21} = \frac{\partial M_{21}}{\partial s_1}\mathrm{d}s_1; \tag{a}$$

(b) in the second case

$$-\left(2M_{21} + \frac{\partial M_{21}}{\partial s_1}\mathrm{d}s_1\right)\varphi, \tag{b}$$

where 2φ is the angle between the normals to the middle surface at points n_1 and n_2, i.e., $2\varphi = \mathrm{d}s_1/R_1$. Substituting this value for φ into the expression (b) and retaining only the first-order quantities, one finds $-(M_{21}/R_1)\mathrm{d}s_1$. Thus, along the shell edge $\beta = \beta^*$, the twisting moment can be replaced by the distributed normal (transverse) shear forces $\partial M_{21}/\partial s_1$ and distributed tangential (in-plane) shear forces $-M_{21}/R_1$.

As mentioned previously (see Sec. 2.5), the replacement of the twisting moment by statically equivalent forces results in a certain redistribution of the stresses over the thickness of the shell along its boundaries. By the St.Venant principle, the effect of this approximation cannot be significant; it can only be noticeable within the immediate neighborhood of the boundaries (at distances of the order of the shell thickness).

It follows from the above that the boundary conditions on the edge $\beta = \beta^*$ can be formulated in terms of the following four quantities:

$$N_2, \quad T_2 = N_{21} - \frac{M_{21}}{R_1}, \quad V_2 = Q_2 + \frac{1}{A}\frac{\partial M_{21}}{\partial \alpha}, \quad M_2, \tag{12.54}$$

where T_2 and V_2 are referred to as the *in-plane and transverse effective shear forces*, respectively. These boundary quantities define completely the state of stress on the above-mentioned shell edge; therefore, the number of boundary conditions on the edge must be equal to four, and not five.

Note that the static boundary conditions (12.54) can also be expressed in terms of functions S and H by using the relations (12.43). In this case, the boundary quantities on the edge $\beta = \beta^*$ are of the form

$$N_2, \quad T_2 = S - \frac{2H}{R_1}, \quad V_2 = Q_2 + \frac{1}{A}\frac{\partial H}{\partial \alpha}, \quad M_2. \tag{12.55}$$

Using the above results, it is not difficult to deduce, similarly, the boundary quantities assigned for the edge $\alpha = \alpha^*$.

We have considered the so-called static boundary conditions expressed in terms of the four generalized force and moment quantities prescribed on the shell edges. Of course, the boundary conditions of the shell can be expressed in terms of the prescribed displacements or slopes on its edges (the so-called kinematic boundary conditions). Sometimes, the mixed boundary conditions expressed in terms of the displacements and forces prescribed on the shell boundaries are also encountered in practice.

Let us list some typical boundary conditions that are frequently encountered in engineering applications. These conditions are formulated below for a boundary of the shell, which is a part of the β curve, i.e., for the boundary $\beta = \beta^*$:

(1) *Free edge*

$$N_2 = 0, \quad T_2 = N_{21} - \frac{M_{21}}{R_1} = 0, \quad V_2 = Q_2 + \frac{1}{A}\frac{\partial M_{21}}{\partial \alpha} = 0, \quad M_2 = 0 \tag{12.56}$$

(2) *Clamped edge*

$$u = 0, \quad v = 0, \quad w = 0, \quad \vartheta_2 = 0, \tag{12.57}$$

where ϑ_2 is given by Eq. (12.2).

(3) *Hinged edge with the support free to move in the normal direction*

$$M_2 = 0, \quad V_2 = Q_2 + \frac{1}{A}\frac{\partial M_{21}}{\partial \alpha} = 0, \quad u = 0, \quad v = 0. \tag{12.58}$$

(4) *Hinged edge with fixed support*

$$M_2 = 0, \quad u = 0, \quad v = 0, \quad w = 0. \tag{12.59}$$

Similarly, the boundary conditions for the shell edge $\alpha = \alpha^*$ can be assigned.

12.6 DISCUSSION OF THE GOVERNING EQUATIONS OF THE GENERAL LINEAR SHELL THEORY

At this point, the governing equations of the general linear theory of thin shells are now complete. They can be classified in the following manner:

(1) The strain–displacement relations

Six strain–displacement equations are summarized for the general linear shell theory by Eqs (12.23) and (12.24). They involve six components of strain, ε_1, ε_2, γ_{12}, χ_1, χ_2, and χ_{12}, which are given explicitly in terms of the three displacement components u, v, and w. Note that the six strain components must satisfy the equations of compatibility (Eqs (12.27)). The latter equations are used only for solving the shell problems in forces–strain components. If the problem under consideration is solved in terms of the displacement components, then these conditions are satisfied automatically.

(2) The constitutive equations

The eight equations are summarized in the general case by Eqs (12.45) and (12.46). They express the eight stress resultants and stress couples, N_1, N_2, N_{12}, N_{21}, M_1, M_2, M_{21}, and M_{12}, as explicit functions of the six strain components, ε_1, ε_2, γ_{12}, χ_1, χ_2, and χ_{12}. The number of these constitutive equations can be reduced for a practical stress analysis of shells to six by accepting the assumption (12.43).

(3) Equations of equilibrium

Five equations of equilibrium must be satisfied. They are given by Eqs (12.41) and (12.42). These five equations involve the 10 stress resultants and couple resultants, N_1, N_2, N_{12}, N_{21}, M_1, M_2, M_{12}, $M_{21,}$ Q_1, and Q_2. The number of the these forces and moments can be reduced to eight by using Eqs (12.43).

(4) Boundary conditions

Boundary conditions relate the stress resultants and stress couples or displacement components specified on the shell boundaries to prescribed boundary quantities (in a particular case, the latter may be equal to zero). These boundary conditions are summarized by Eqs (12.56)–(12.59).

Thus, in general, there are 19 equations relating 19 unknowns, u, v, w; ε_1, ε_2, γ_{12}; χ_1, χ_{12}; N_1, N_2, N_{12}, N_{21}, M_1 , M_2, M_{12}, M_{21}, Q_1, and Q_2. For a simplified general linear theory of shells, one can take $N_{12} = N_{21}$ and $M_{12} = M_{21}$, thereby reducing the number of equations and unknowns to 17.

As for the theory of elasticity, shell problems may be solved either in terms of displacements or in terms of the internal forces and moments. According to the first technique, the internal forces and moments are replaced in the equilibrium equations (12.41) and (12.42) by the displacement components u, v, and w, using the constitutive and strain–displacement relations (12.45), (12.46) and (12.23), (12.24), respectively. As a result, the eight-order system of the three governing partial differential equations for displacements is obtained. The second technique consists of simultaneous treatment of equations of equilibrium (12.41) and (12.42) or (12.44) and compatibility relations (12.27). In so doing, the eight-order system of six governing differential equations for N_1, N_2, S, M_1, M_2, and H will be obtained.

12.7 TYPES OF STATE OF STRESS FOR THIN SHELLS

All equations mentioned in Sec. 12.6 are linear for both techniques, which, of course, greatly simplifies their study and solution. However, shell problems associated with calculations of the stress and strain components remain very difficult. As a rule, the governing, eight-order partial differential equations of the general shell theory have variable coefficients. Mathematical difficulties associated with integration of such a type of differential equations are evident. Even for the simplest circular cylindrical shells for which the governing equations have constant coefficients, cumbersome computations remain involved and,by far, not all problems of practical interest for such shells have been solved. Consequently, attempts of scientists and engineers engaged in the practical stress analysis of shell structures were directed towards the search for possibilities of simplifying the above governing differential equations of the general shell theory and shell problems themselves. Several approximate methods and the corresponding shell models based upon some additional assumptions and upon simplified governing equations are considered in Chapter 17.

Previously, in presenting the general linear shell theory, it was assumed that the flexural stresses are values of the same order as the stresses caused by in-plane (membrane) stresses. If one of the above-mentioned types of stresses is negligible in comparison with another one, then it is possible to introduce considerable simplifications in the general linear shell theory. Consider some possible types of state of stress for thin shells.

1. If the flexural stresses are negligible compared with the membrane stresses then such a type of state of stress is called a *membrane or momentless state of stress*. The governing equations of the membrane theory can be obtained directly from the equations of the general shell theory by neglecting the effect of the bending and twisting moments, as well as the transverse shear forces, on the state of stress and strain of thin shells. In some cases, the membrane theory describes the state of stress and strain with reasonable accuracy, since the bending and twisting moments are of negligible magnitudes: for example, hollow spherical shells subjected to inside and outside uniform pressure are in the pure membrane state of stress.

2. If, to the contrary, the membrane stresses are negligible in comparison with the flexural stresses, then such a type of state of stress is referred to as a pure *flexural or moment state of stress*. Note that the definitions of the ''membrane'' and ''pure flexural'' states of stress are not quite correct because the membrane state of stress admits an existence of small flexural stresses and, in turn, small membrane stresses may occur in a pure flexural state of stress. It was mentioned previously that shells, due to their small thickness, possess a relatively small flexural stiffness and, therefore, they are poorly adapted to resisting in bending. Even relatively small bending moments may cause considerable flexural stresses and displacements in shells. Therefore, a pure flexural type of the state of stress is dangerous and technically disadvantageous for thin shells. It should be avoided by introducing some intermediate reinforcements, by selecting the corresponding shape of the shell, by choosing the type of supports, etc. Conversely, the membrane state of stress, at which the shell is uniformly stressed across its thickness, is technically the most advantageous. So, engineers designing a shell should aim at such a state of stress.

3. If the flexural and membrane stresses are of the same order, then such a state of stress is called a *mixed state of stress, or edge effect*. The term ''edge effect'' is

associated with the fact that the above-mentioned mixed state of stress often occurs near edges of the shell. Note that all attempts to generate the membrane state of stress throughout the shell surface were not successful, except for a few particular cases. At the main portion of a shell the state of stress, which is close to the membrane, can be generated. However, near the shell edges or some reinforcing stiffeners, the mixed state of stress takes place. This edge effect is, as a rule, localized in a comparatively small area. The latter circumstance is commonly used for the decomposition of a given state of stress into the membrane and edge effect. As shown in Sec. 17.5, such decomposition results in considerable simplifications in solving the shell problems.

PROBLEMS

12.1 Verify Eqs (12.10)–(12.15).

12.2 Verify Eq. (12.16).

12.3 Explain and show the physical meaning of the twist of a differential element of the middle surface, χ_{12}.

12.4 Equations (12.22) are not unique linear relations in the general linear theory of thin shells. Using the expansions of the type

$$\frac{1}{1 - z/R_i} = 1 + \frac{z}{R_i} + \left(\frac{z}{R_i}\right)^2 + \dots \quad (i = 1, 2)$$

and Eqs (12.10) and (12.11), derive the corresponding strain relations in the equidistant surface. Compare the accuracy of the above equations with the relations (12.22).

12.5 Would the accuracy of Eqs (12.24) be changed if the terms of the order ε_i/R_i $(i = 1, 2)$ were added to the right-hand sides?

12.6 Give the physical explanation of the assumption $\sigma_z = 0$ adopted in the general linear theory of thin shells. Compare the orders of the direct stresses σ_1 and σ_2 with the above stress σ_3.

12.7 Generalize the equilibrium equations (12.41) to include surface loading that consists of distributed moments $m_1(x, y)$ and $m_2(x, y)$.

12.8 Verify Eqs (12.44).

12.9 What are the formal contradictions, brought by the approximate relations (12.48), in the general linear shell theory?

12.10 Verify Eqs. (12.52) and (12.53).

12.11 Derive the boundary conditions of the type (12.56)–(12.59) for the shell boundary $\alpha = \alpha^*$.

REFERENCES

1. Novozhilov, V.V., *Thin Shell Theory* (translated from 2nd Russian ed. by P.G. Lowe), Groningen, Noordholf, The Netherlands, 1964.
2. Cook, R.D. and Young, W.C., *Advanced Mechanics of Materials*, Prentice-Hall, New Jersey, 1964.
3. Gol'denveizer, A.L., *Theory Of Elastic Shells* (translated from Russian by G. Herrmann), Pergamon Press, New York, 1961.

13

The Membrane Theory of Shells

13.1 PRELIMINARY REMARKS

It was shown in Chapter 12 that a thin elastic shell supports an arbitrary external loading by means of stress resultants (internal forces) and stress couples (bending and twisting moments). Under appropriate loading and boundary conditions, however, the resulting bending and twisting moments are either zero, or so small that they may be neglected. Such a state of stress is referred to as the *membrane state of stress* because of the analogy to membranes that cannot support bending and twisting moments. The corresponding theory of thin shells that deals with this state of stress is called the *membrane theory of shells*. It follows from the above that the membrane theory neglects all moments, i.e.,

$$M_1 = M_2 = H = 0. \tag{13.1}$$

In turn, it follows from the corresponding moment relations

$$M_1 = D(\chi_1 + \nu\chi_2), \quad M_2 = D(\chi_2 + \nu\chi_1), \quad H = D(1-\nu)\chi_{12}, \tag{13.2}$$

that neglecting the moments will be justified either when the shell has a very small flexural stiffness, D, or when the changes in curvature and in twist of the middle surface, χ_1, χ_2, and χ_{12}, are very small. In the first case, we deal with an absolutely flexible shell, the *membrane*; in the second case, with the momentless or the membrane state of stress of a shell that has a finite flexural stiffness. Although, both these problems are described by one and the same theory, a distinction must be made between them because they resist the applied loading differently. An absolutely flexible shell (for instance, made from cloth) is not able to sustain compressive forces since any small compression forces will cause the loss of stability of its shape. Therefore, these shells may resist the applied loads only in tension.

Shells with finite flexural stiffness, in contrast to absolutely flexible shells, may resist in both the membrane states of compressive as well as tensile forces. They lose

stability only when the compressive forces exceed a certain critical value. For absolutely flexible shells, since they do not possess a resistance to bending, only the membrane state of stress is possible, while for shells with finite stiffness such a state of stress is only one of the possible stress conditions. In this chapter we consider only shells with a finite flexural stiffness.

13.2 THE FUNDAMENTAL EQUATIONS OF THE MEMBRANE THEORY OF THIN SHELLS

The governing equations of the membrane theory can be obtained directly from the equations of the general theory of thin shells derived in Chapter 12. For this purpose, it is assumed that, in view of the smallness of the changes of curvature and twist, the moment terms in the equations of equilibrium for a shell element are unimportant, although in principle the shell may resist the external loads in bending. Note that neglecting the moments leads to neglecting the normal shear forces. Thus, for the membrane theory of thin shells, we can assume that

$$M_1 = M_2 = H = Q_1 = Q_2 = 0. \tag{13.3}$$

Introducing Eq. (13.3) into Eqs (12.44) and taking into account Eq. (12.43), one arrives at the following system of differential equations:

$$\begin{aligned}
&\frac{\partial}{\partial\alpha}(N_1 B) + \frac{1}{A}\frac{\partial}{\partial\beta}\left(A^2 S\right) - N_2\frac{\partial B}{\partial\alpha} + ABp_1 = 0,\\
&\frac{\partial}{\partial\beta}(N_2 A) + \frac{1}{B}\frac{\partial}{\partial\alpha}\left(B^2 S\right) - N_1\frac{\partial A}{\partial\beta} + ABp_2 = 0,\\
&N_1\frac{1}{R_1} + N_2\frac{1}{R_2} + p_3 = 0,
\end{aligned} \tag{13.4}$$

where $N_{12} = N_{21} = S$ (since $H = 0$).

In this system, the number of unknowns is equal to the number of equations, so the problem of the membrane theory of shells is statically determinate (that is true for the equilibrium of an infinitely small shell element but is not always true for the equilibrium of the entire shell). This means that if the external load components, p_1, p_2, and p_3, are known, then the membrane forces and stresses for such a shell are uniquely determined from Eqs (13.4).

Having determined the membrane forces, the shell displacements may be found. Solving the constitutive equations (12.45) for strains, and substituting them into Eqs (12.23), yields the following system of the three partial differential equations for the displacements:

$$\begin{aligned}
\varepsilon_1 &= \frac{1}{A}\frac{\partial u}{\partial\alpha} + \frac{v}{AB}\frac{\partial A}{\partial\beta} - \frac{w}{R_1} = \frac{1}{Eh}(N_1 - \nu N_2),\\
\varepsilon_2 &= \frac{1}{B}\frac{\partial v}{\partial\beta} + \frac{u}{AB}\frac{\partial B}{\partial\alpha} - \frac{w}{R_2} = \frac{1}{Eh}(N_2 - \nu N_1),\\
\gamma_{12} &= \frac{B}{A}\frac{\partial}{\partial\alpha}\left(\frac{v}{B}\right) + \frac{A}{B}\frac{\partial}{\partial\beta}\left(\frac{u}{A}\right) = \frac{2(1+\nu)}{Eh}S.
\end{aligned} \tag{13.5}$$

The system of the differential equations (13.4) in the membrane theory for determining the membrane internal forces (and stresses) is of the second order. Accordingly, the system (13.5) for the displacements is also of the second order. However, the stress resultants (N_1, N_2, and S) on the right-hand sides of Eqs (13.5) are themselves solutions of the second-order equations. Hence, the displacements in the membrane theory must satisfy a fourth-order system of differential equations. The latter can be obtained by substituting into Eqs (13.4) for the stress resultants from the corresponding expressions in terms of the strains.

The mathematical formulation of the theory of membrane shells is completed by adding appropriate boundary conditions. In the membrane theory, it follows from the above that only two boundary conditions may be specified on each edge of the shell. If the boundary conditions are given in terms of the stress resultants, then only the membrane (or in-plane) forces (N_1, N_2, and S) are specified on edges of the shell. If the boundary conditions are formulated in terms of displacements, then only displacement components that are tangent to the middle surface, i.e., u and v, must be prescribed on the shell boundary. In the membrane theory it is impossible to specify the edge displacements w and slopes ϑ, since their assignment may result in the appearance of the corresponding boundary transverse shear forces and bending moments. This is in a conflict with the general postulates of the membrane theory of thin shells introduced above.

Since the differential equations of the membrane theory for the stress resultants (13.4) and for the displacements (13.5) have different orders (the second and fourth, respectively), the boundary conditions cannot be prescribed in terms of forces only for membrane shells: half of the boundary conditions should be assigned in terms of displacements.

13.3 APPLICABILITY OF THE MEMBRANE THEORY

As mentioned previously (see Sec. 10.1), the advantages of a shell as a structural member can be only completely realized when its wall resists the applied loads in tension (or compression) under membrane state of stress conditions. We now express some considerations which provide a good insight into the range of applicability of the membrane theory.

Membrane strains are associated with deformations of line elements that lie in the middle surface of the shell. If a shell is bent without straining of the middle surface, it is said to be bent *inextensionally*. For example, if we roll a sheet of paper into a cone or a cylinder, we bend it inextensionally. It is known that shells offer high resistance to membrane strains. In fact, we can bend a piece of thin sheet metal easily with our fingers, but we cannot stretch it noticeably.

However, there are many cases in which inextensional bending is impossible. There is Lagrange's theorem (see, for instance [1]), which asserts that a convex closed surface cannot be deformed inextensionally. For example, a Ping-Pong ball cannot be bent inextensionally. Cones, cylinders, and convex domes cannot be bent inextensionally if their edges are reinforced by rigid rings. Since shells offer high resistance to membrane stresses, those that cannot be bent inextensionally are usually very stiff. Generally, the membrane theory is permissible only for shells that cannot be bent inextensionally, or for shells that experience only very small bending moments.

Now we present, without proof, the general conditions under which the membrane theory is valid. It can be shown that these conditions are necessary and sufficient for an existence of the momentless state of stress in thin shells and that they correspond to the minimum of strain energy stored by a shell during its straining. These conditions are [2]:

(a) The boundaries of a shell are free from transverse shear forces and moments. Loads applied to the shell boundaries must lie in planes that are tangent to the middle surface of the shell.
(b) The normal displacements and rotations at the shell edges are unconstrained: that is, these edges can displace freely in the direction of the normal to the middle surface.
(c) A shell must have a smoothly varying and continuous surface.
(d) The components of the surface and edge loads must be also smooth and continuous functions of the coordinates.

If these conditions are violated, fully or partially, flexural stresses occur. If designers do not succeed in eliminating these stresses completely, they must aim at localizing them and limiting their magnitude. Thus, the solutions given by the membrane theory must, in many cases, be supplemented by a solution of the equations of the bending theory in those parts of the shell where bending proves to be important. Such a combination of the bending and membrane theories is one of the important ideas on the basis of which the majority of problems of the shell theory are being solved at present. It should be also noted that even if the membrane stresses are sometimes combined with flexural stresses, the membrane theory does not lose its significance because already at a small distance from a bending zone, the state of stress may be usually considered as momentless.

13.4 THE MEMBRANE THEORY OF SHELLS OF REVOLUTION

Consider a particular case of a shell described by a surface of revolution (Fig. 11.12). The midsurface of such a shell of revolution, as mentioned in Sec. 11.8, is generated by rotating a meridian curve about an axis lying in the plane of this curve (the Z axis).

The geometry of shells of revolution is addressed in Sec. 11.8. There it is mentioned that meridians and parallel circles can be chosen as the curvilinear coordinate lines for such a shell because they are lines of curvature, and form an orthogonal mesh on its midsurface. Let us locate a point on the middle surface by the spherical coordinates θ and φ (see Sec. 11.8), where θ is the circumferential angle characterizing a position of a point along the parallel circle, whereas the angle φ is the meridional angle, defining a position of that point along the meridian. The latter represents the angle between the normal to the middle surface and the shell axis (Fig. 11.12a). As before, R_1, R_2 are the principal radii of curvature of the meridian and parallel circle, respectively, and r is the radius of the parallel circle. The Lamé parameters for shells of revolution in the above-mentioned spherical coordinate system are given by Eqs (11.39). Notice that, due to the symmetry of shells of revolution about the Z axis, these parameters are functions of φ only and do not depend upon θ. Referring to Fig. 11.12a and b, we can obtain by inspection the following relations:

$$r = R_2 \sin\varphi;$$
$$AM_1 = \mathrm{d}r = \frac{\mathrm{d}r}{\mathrm{d}\varphi}\mathrm{d}\varphi \approx MM_1 \cos\varphi = R_1 \mathrm{d}\varphi \cos\varphi \tag{13.6a}$$

or

$$\frac{\mathrm{d}r}{\mathrm{d}\varphi} = \frac{\mathrm{d}}{\mathrm{d}\varphi}(R_2 \sin\varphi) = R_1 \cos\varphi. \tag{13.6b}$$

Finally from Eqs (13.6a) and (13.6b) we obtain

$$\frac{1}{r}\frac{\mathrm{d}r}{\mathrm{d}\varphi} = \frac{R_1}{R_2}\cot\varphi. \tag{13.6c}$$

Substituting for A and B from Eqs (11.39) into the system of differential equations (13.4) and taking into account the relations (13.6), yields

$$\begin{aligned} R_1\frac{\partial S}{\partial\theta} + \frac{\partial}{\partial\varphi}(rN_1) - N_2 R_1 \cos\varphi + rR_1 p_1 = 0, \\ R_1\frac{\partial N_2}{\partial\theta} + \frac{1}{r}\frac{\partial}{\partial\varphi}\left(r^2 S\right) + rR_1 p_2 = 0, \\ \kappa_1 N_1 + \kappa_2 N_2 + p_3 = 0, \end{aligned} \tag{13.7}$$

where

$$\kappa_1 = \frac{1}{R_1} \quad \text{and} \quad \kappa_2 = \frac{1}{R_2}.$$

The last equation in the above system is known as the *Laplace equation*. Note that the membrane forces N_1, N_2, and S are, in a general case of loading, some functions of θ and φ.

Equations (13.7) can be reduced to one single, second-order differential equation for some function U. For this purpose, rewrite the above equations using the relations (13.6), as follows

$$\frac{1}{R_1}\frac{\partial N_1}{\partial\varphi} + \frac{N_1 - N_2}{R_2}\cot\varphi + \frac{1}{R_2\sin\varphi}\frac{\partial S}{\partial\theta} + p_1 = 0, \tag{13.8a}$$

$$\frac{1}{R_2\sin\varphi}\frac{\partial N_2}{\partial\theta} + \frac{1}{R_1}\frac{\partial S}{\partial\varphi} + \frac{2\cot\varphi}{R_2}S + p_2 = 0, \tag{13.8b}$$

$$\frac{N_1}{R_1} + \frac{N_2}{R_2} + p_3 = 0. \tag{13.8c}$$

Solving Eq. (13.8c) for N_2 and substituting this into Eqs (13.8a) and (13.8b), one finds the following:

$$\begin{aligned} \frac{1}{R_1}\frac{\partial N_1}{\partial\varphi} + N_1\left(\frac{1}{R_1} + \frac{1}{R_2}\right)\cot\varphi + \frac{1}{R_2\sin\varphi}\frac{\partial S}{\partial\theta} = -p_1 - p_3\cot\varphi \\ -\frac{1}{R_1\sin\varphi}\frac{\partial N_1}{\partial\theta} + \frac{1}{R_1}\frac{\partial S}{\partial\varphi} + 2\frac{\cot\varphi}{R_2}S = \frac{1}{\sin\varphi}\frac{\partial p_3}{\partial\theta} - p_2. \end{aligned} \tag{13.9}$$

We introduce new variables, U and V instead of N_1 and S, as follows:

$$N_1 = \frac{U}{R_2 \sin^2 \varphi}, \quad S = \frac{V}{R_2^2 \sin^2 \varphi}. \tag{13.10}$$

Substituting the above into Eqs (13.9), we obtain, after some simple transformations, the following system of equations:

$$\begin{aligned} \frac{R_2^2 \sin \varphi}{R_1} \frac{\partial U}{\partial \varphi} + \frac{\partial V}{\partial \theta} &= -(p_3 \cos \varphi + p_1 \sin \varphi) R_2^3 \sin^2 \varphi, \\ -\frac{R_2}{\sin \varphi} \frac{\partial U}{\partial \theta} + \frac{\partial V}{\partial \varphi} &= \left(\frac{\partial p_3}{\partial \theta} - p_2 \sin \varphi \right) R_1 R_2^2 \sin \varphi. \end{aligned} \tag{13.11}$$

Differentiating then the first equation (13.11) with respect to φ and the second one with respect to θ, and subtracting the second equation from the first, we obtain the following second-order differential equation for U:

$$\frac{1}{R_1 R_2 \sin \varphi} \frac{\partial}{\partial \varphi} \left(\frac{R_2^2 \sin \varphi}{R_1} \frac{\partial U}{\partial \varphi} \right) + \frac{1}{R_1 \sin^2 \varphi} \frac{\partial^2 U}{\partial \theta^2} = F(\theta, \varphi), \tag{13.12}$$

where

$$F(\theta, \varphi) = -\frac{1}{R_1 R_2 \sin \varphi} \frac{\partial}{\partial \varphi} \left[R_2^3 \sin^2 \varphi (p_3 \cos \varphi + p_1 \sin \varphi) \right] + R_2 \left(\frac{\partial p_2}{\partial \theta} \sin \varphi - \frac{\partial^2 p_3}{\partial \theta^2} \right). \tag{13.13}$$

Equation (13.12) may be written in the operator form

$$\mathbf{L}U = F(\theta, \varphi), \tag{13.14}$$

where the differential operator $\mathbf{L}$ is of the form

$$\mathbf{L}(\ldots) \equiv \frac{1}{R_1 R_2 \sin \varphi} \frac{\partial}{\partial \varphi} \left(\frac{R_2^2 \sin \varphi}{R_1} \frac{\partial (\ldots)}{\partial \varphi} \right) + \frac{1}{R_1 \sin^2 \varphi} \frac{\partial^2}{\partial \theta^2} (\ldots). \tag{13.15}$$

The kinematic equations for displacements of shells of revolution in spherical coordinates are

$$\begin{aligned} \frac{1}{R_1} \frac{\partial u}{\partial \varphi} - \frac{w}{R_1} &= \frac{1}{Eh}(N_1 - \nu N_2) = \varepsilon_1, \\ \frac{1}{r} \frac{\partial v}{\partial \theta} + \frac{u}{r} \cos \varphi - \frac{w}{R_2} &= \frac{1}{Eh}(N_2 - \nu N_1) = \varepsilon_2, \\ \frac{r}{R_1} \frac{\partial}{\partial \varphi} \left(\frac{v}{r} \right) + \frac{1}{r} \frac{\partial u}{\partial \theta} &= \frac{S}{Gh} = \gamma_{12}. \end{aligned} \tag{13.16}$$

Now transform the above kinematic equations. Introducing the functions

$$\xi = \frac{u}{\sin \varphi}, \quad \eta = \frac{v}{R_2 \sin \varphi}, \tag{13.17}$$

and making subsequent transformations associated with an elimination of deflection w and then ξ, the system of equations (Eqs (13.16)) may be reduced to one second-order differential equation for the unknown function η. In the operator form, this equation has the form

$$\mathbf{L}\eta = f(\theta, \varphi), \tag{13.18}$$

where

$$f(\theta,\varphi) = \frac{1}{R_1 R_2 \sin\varphi}\left\{\frac{1}{Gh}\frac{\partial(R_2 S)}{\partial\varphi} - \frac{1}{EhR_1}\left(R_1^2 + R_2^2 + 2\nu R_1 R_2\right)\frac{\partial N_1}{\partial\theta} - \frac{R_2}{Eh}(R_2 + \nu R_1)\frac{\partial p_3}{\partial\theta}\right\}, \tag{13.19}$$

and the operator $\mathbf{L}$ is given by Eq. (13.15). Thus, the governing differential equations for determining the membrane forces, Eq. (13.14), and displacements, Eq. (13.18), have an identical form. These equations can be solved by using the well-known method of separation of variables.

Let us represent the load components p_1, p_2, and p_3 in the form of the Fourier series

$$\begin{aligned} p_1 &= \sum_{n=0}^{\infty} p_{1n}\cos n\theta + \sum_{n=1}^{\infty} p_{1n}^{*}\sin n\theta; \quad p_2 = \sum_{n=1}^{\infty} p_{2n}\sin n\theta + \sum_{n=0}^{\infty} p_{2n}^{*}\cos n\theta, \\ p_3 &= \sum_{n=0}^{\infty} p_{3n}\cos n\theta + \sum_{n=1}^{\infty} p_{3n}^{*}\sin n\theta \end{aligned}, \tag{13.20}$$

where $p_{1n}, \ldots, p_{3n}^{*}$ are functions of φ only. The first of the two sums in each line represents that part of the load that is symmetric in θ and the second sum represents the antisymmetric part. The coefficients p_{in} and p_{in}^{*} $(i = 1, 2, 3)$ are evaluated from well-known formulas (see, for example, Appendix B). For the shell analysis, it is sufficient to consider only one harmonic of the load, say, $p_i^{(n)}$, i.e.,

$$p_1^{(n)} = p_{1n}\cos n\theta, \quad p_2^{(n)} = p_{2n}\sin n\theta, \quad p_3^{(n)} = p_{3n}\cos n\theta \tag{13.21}$$

and then a solution may be obtained by summing the membrane forces, displacements, etc., due to individual load components. Inserting Eq. (13.21) into Eq. (13.12) and introducing the expression

$$U = U_n \cos n\theta, \tag{13.22}$$

we obtain, in the general case, the following ordinary differential equations with variable coefficients:

$$\frac{1}{R_1 R_2 \sin\varphi}\frac{\mathrm{d}}{\mathrm{d}\varphi}\left(\frac{R_2^2 \sin\varphi}{R_1}\frac{\mathrm{d}U_n}{\mathrm{d}\varphi}\right) - \frac{n^2}{R_1 \sin^2\varphi}U_n = F_n(\varphi), \tag{13.23}$$

where

$$F_n(\varphi) = -\frac{1}{R_1 R_2 \sin\varphi}\frac{\mathrm{d}}{\mathrm{d}\varphi}\left[(p_{3n}\cos\varphi + p_{1n}\sin\varphi)R_2^3 \sin^2\varphi\right] + R_2 n(p_{2n}\sin\varphi + n p_{3n}). \tag{13.24}$$

In turn, the expression for V can be introduced in the form

$$V = V_n \sin n\theta. \tag{13.25}$$

Once the expression U_n has been determined by solving Eq. (13.23), we can introduce Eqs (13.21), (13.22), and (13.25) into the first equation (Eq. (13.11)). Solving this equation, we obtain V_n as follows:

$$V_n = -\frac{R_2^2 \sin\varphi}{nR_1}\frac{\mathrm{d}U_n}{\mathrm{d}\varphi} - (p_{3n}\cos\varphi + p_{1n}\sin\varphi)R_2^3 \sin^2\varphi. \tag{13.26}$$

Finally, using the expressions (13.10) and Eq. (13.8c), the membrane forces for the considered harmonic of load can be determined in the following form

$$N_1^{(n)} = N_{1n}\cos n\theta, \quad N_2^{(n)} = N_{2n}\cos n\theta, \quad S^{(n)} = S_n \sin n\theta. \tag{13.27}$$

Then, we can come to determining the displacements. For this purpose, we represent the previously introduced function η in the form

$$\eta^{(n)} = \eta_n \sin n\theta. \tag{13.28}$$

Substituting the expressions (13.28), (13.21), and (13.27) into Eq. (13.18), we obtain an ordinary differential equation for η_n. The latter will be identical to Eq. (13.23), if we replace in it U_n with η_n and $F_n(\varphi)$ with $f_n(\varphi)$, as follows:

$$f_n(\varphi) = \frac{1}{R_1 R_2 \sin\varphi}\left[\frac{1}{Gh}\frac{\mathrm{d}R_2 S_n}{\mathrm{d}\varphi} + n\frac{N_{1n}}{EhR_1}\left(R_1^2 + R_2^2 + 2\vartheta R_1 R_2\right) + \frac{R_2}{Eh}(R_2 + \nu R_1)np_{3n}\right]. \tag{13.29}$$

A solution of the differential equation for η_n involves four constants of integration: two constants from Eq. (13.23) for the forces and the remaining two constants from the equation for displacements. These constants are evaluated from the boundary conditions discussed in Sec. 13.2.

Using the solution obtained for η_n, as well as Eqs (13.17) and (13.16), and introducing the displacements in the form

$$u^{(n)} = u_n \cos n\theta, \quad v^{(n)} = v_n \sin n\theta, \quad w^{(n)} = w_n \cos n\theta, \tag{13.30}$$

we can determine the expressions for u_n, v_n, and w_n, and then the displacements themselves.

13.5 SYMMETRICALLY LOADED SHELLS OF REVOLUTION

Let us assume that the shell of revolution is subjected to loading that is symmetrical about the shell axis, i.e., the Z axis. A self-weight of a shell and a uniformly distributed snow load are examples of such a type of loading. In this case, the governing differential equations of the membrane theory of shells of revolution will be simplified considerably. All the derivatives with respect to θ will vanish because a given load, and hence all the membrane forces and displacements, does not change in the circumferential direction. The externally applied loads per unit area of the middle surface are represented at any point by the components p_1 and p_3 acting in the directions of the y and z axes of the local coordinate system at the above point

(see Sec. 12.2), respectively, where the y axis points in the tangent direction along the meridian and the z axis is a normal to the middle surface at that point (Fig. 13.1). The load component p_2 (acting along the x axis) is assumed to be absent. The presence of this component implies that the shell is twisted about its axis. If $p_2 = 0$ and edge forces in the circumferential direction are also zero, then, as follows from the second Eq. (13.7), in the case of axisymmmetrical loading,

$$S = N_{12} = N_{21} = 0. \tag{13.31}$$

The nonzero membrane forces are shown in Fig. 13.1.

The first and third equations of the system (13.7) after some algebra transformations, eliminating N_2, and taking into account Eqs (13.6), may be reduced to the following equation:

$$\frac{\mathrm{d}}{\mathrm{d}\varphi}(N_1 r \sin\varphi) + rR_1(p_1 \sin\varphi + p_3 \cos\varphi) = 0. \tag{13.32}$$

Integrating this equation from φ_0 to φ, one finds

$$\begin{aligned} [N_1 r \sin\varphi]_{\varphi_0}^{\varphi} &= -\int_{\varphi_0}^{\varphi} rR_1(p_1 \sin\bar{\varphi} + p_3 \cos\bar{\varphi})\mathrm{d}\bar{\varphi} \quad \text{or} \\ N_1 r \sin\varphi &= -\int_{\varphi_0}^{\varphi} rR_1(p_1 \sin\bar{\varphi} + p_3 \cos\bar{\varphi})\mathrm{d}\bar{\varphi} + N_1^{(0)} b \sin\varphi_0, \end{aligned} \tag{13.33a}$$

where φ_0 is the angle corresponding to the shell edge (for instance, at the top) where the boundary conditions are specified; $N_1^{(0)}$ and $r_0 = b$ are the meridional force, and the radius of the parallel circle, respectively, at the shell edge $\varphi = \varphi_0$ (Fig. 13.2); and $\bar{\varphi}$ is a dummy variable.

Solving Eq. (13.33a) for N_1 and taking into account Eq. (13.6a), yields

$$N_1 = -\frac{1}{R_2 \sin^2\varphi}\int_{\varphi_0}^{\varphi} R_1 R_2(p_1 \sin\bar{\varphi} + p_3 \cos\bar{\varphi}) \sin\bar{\varphi}\mathrm{d}\bar{\varphi} + \frac{N_1^{(0)} R_2^{(0)} \sin^2\varphi_0}{R_2 \sin^2\varphi} \tag{13.33b}$$

where $b = R_2^{(0)} \sin\varphi_0$. $R_2^{(0)}$is the principal radius of curvature at the shell edge $\varphi = \varphi_0$.

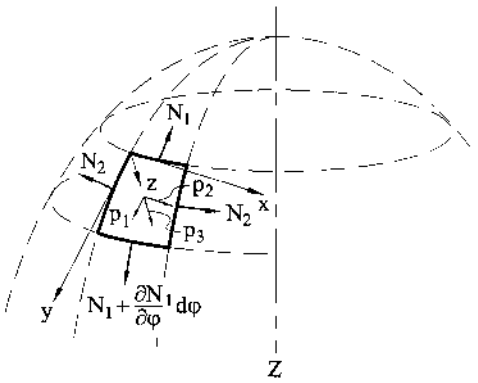

Fig. 13.1

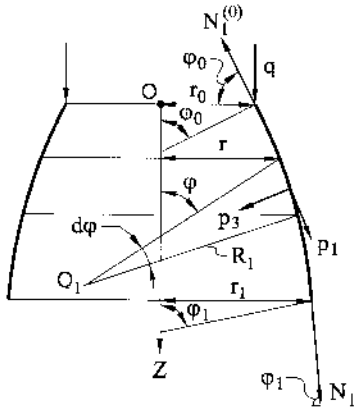

Fig. 13.2

Let a shell, in addition to the surface load components p_1 and p_3, be subjected to some line load q per unit length of the top parallel circle, $\varphi = \varphi_0$. This may be, for example, the weight of a skylight of a dome. From Fig. 13.2, $N_1^{(0)} = -q/\sin\varphi_0$; substituting into Eq. (13.33a) gives

$$N_1 r \sin\varphi = -\left[\int_{\varphi_e}^{\varphi} rR_1(p_1 \sin\bar{\varphi} + p_3 \cos\bar{\varphi})\mathrm{d}\bar{\varphi} + qb\right]. \tag{13.34}$$

This equation may be easily interpreted if we multiply both sides of Eq. (13.34) by 2π. We have

$$N_1(2\pi r)\sin\varphi = -2\pi\int_{\varphi_0}^{\varphi} rR_1(p_1 \sin\bar{\varphi} + p_3 \cos\bar{\varphi})\mathrm{d}\bar{\varphi} - 2\pi bq. \tag{13.35}$$

Referring to Fig. 13.2, one can conclude that the left-hand side of this equation is the vertical component of the resultant of meridional forces N_1over a parallel circle determined by angle φ. As seen from Fig.13.2, $2\pi r R_1 \mathrm{d}\varphi$ is the area of an elementary ring corresponding to an infinitesimal angle $\mathrm{d}\varphi$; and $p_1 \sin\varphi$ and $p_3 \cos\varphi$ are the vertical components of the surface load. Hence, the integrand function of Eq. (13.35) represents a vertical component of the surface load corresponding to the elementary ring. Integrating over φ, we obtain the vertical component of the resultant of all surface loads acting on the shell above the parallel circle φ where $N_1$is to be determined. So, we can rewrite Eq. (13.35), as follows:

$$N_1(2\pi r)\sin\varphi = -F,$$

from which

$$N_1 = -\frac{F}{2\pi r \sin\varphi}, \tag{13.36}$$

where

$$F = 2\pi\left[\int_{\varphi_0}^{\varphi} rR_1(p_1 \sin\bar{\varphi} + p_3 \cos\bar{\varphi})\mathrm{d}\bar{\varphi} + qb\right] \tag{13.37}$$

is the vertical component of all external loading applied above the parallel circle φ of the shell where N_1 is desired. Thus, Eq. (13.35) represents the static equilibrium condition: i.e., the force summation in the direction of the shell axis (the Z axis) is zero. Note that in the case of a shell closed at its apex, $\varphi_0 = 0$ and N_1 becomes

$$N_1 = -\frac{1}{r \sin \varphi} \int_0^{\varphi} r R_1 (p_1 \sin \bar{\varphi} + p_3 \cos \bar{\varphi}) \mathrm{d}\bar{\varphi}. \tag{13.38}$$

Having determined N_1 from Eq. (13.34) or Eq. (13.36), or Eq. (13.38), we can calculate N_2 from the third Eq. (13.7), as follows:

$$N_2 = -R_2 \left(p_3 + \frac{N_1}{R_1} \right). \tag{13.39}$$

Now we can discuss the *displacements in symmetrically loaded shells of revolution*. For this particular case, $v = 0$ and $\gamma_{12} = 0$ and the system of Eqs (13.16) may be simplified to the following:

$$\begin{aligned} \frac{1}{R_1} \frac{\mathrm{d}u}{\mathrm{d}\varphi} - \frac{w}{R_1} &= \frac{1}{Eh} (N_1 - \nu N_2) = \varepsilon_1, \\ \frac{u}{R_2} \cot \varphi - \frac{w}{R_2} &= \frac{1}{Eh} (N_2 - \nu N_1) = \varepsilon_2, \end{aligned} \tag{13.40}$$

where u and w are displacements along the tangent and normal to the meridian curve (or along the y and z axes, as shown in Fig. 13.1), respectively. Knowing N_1 and N_2 for a given shell problem, we can evaluate the strain components, ε_1 and ε_2, and then, u and w from Eqs. (13.40). For this purpose, eliminating w from Eqs (13.40), one finds that

$$\frac{1}{R_2} \left(\frac{\mathrm{d}u}{\mathrm{d}\varphi} - u \cot \varphi \right) = \left(\frac{R_1}{R_2} \right) \varepsilon_1 - \varepsilon_2. \tag{13.41}$$

Multiplying both sides of the above equation by $R_2 \csc \varphi$, we have, after some mathematics,

$$\frac{\mathrm{d}}{\mathrm{d}\varphi} (u \csc \varphi) = f_1(\varphi), \tag{13.42a}$$

where

$$f_1(\varphi) = \frac{R_2}{\sin \varphi} \left(\frac{R_1}{R_2} \varepsilon_1 - \varepsilon_2 \right). \tag{13.42b}$$

The function $f_1(\varphi)$ can be found when N_1 and N_2 have been determined. Integrating Eq. (13.42a), we obtain the following expression for u:

$$u = \sin \varphi \int f_1(\varphi) \mathrm{d}\varphi + C_1 \sin \varphi, \tag{13.43}$$

where C_1 is a constant of integration. Substituting for u from Eq. (13.43) into the second Eq. (13.40), one finds the following expression for w:

$$w = \cos \varphi \int f_1(\varphi) \mathrm{d}\varphi + C_1 \cos \varphi - \varepsilon_2 R_2. \tag{13.44}$$

The constant of integration is evaluated from the boundary condition at either the top or the bottom of the shell, i.e., for $\varphi = \varphi_0$ or $\varphi = \varphi_1$.

Note that the normal displacements w for various points of a shell, including its edges, are related to tangential displacements u. Thus, for a membrane shell, the boundary conditions must not be simultaneously imposed on u and w. If a displacement component is given along one of parallels, then the constant C_1 can be evaluated from Eqs (13.43) or (13.44). Thus, we have the freedom of prescribing u or w at only one of the shell boundaries, and we must permit only other displacements yielded by our analysis; otherwise, incompatibility problems will arise.

In analysis of shell structures consisting of thin shells of revolution and other structural members (ring beams, flat or curved plates, supports, etc.), the horizontal displacements and rotation of the tangent to the meridian at the shell boundaries are of considerable interest. These quantities are required for satisfying the compatibility conditions at the junction of a thin shell and the structural members.

First, determine the horizontal expansion or contraction of the membrane shell at its edge, ξ. We have the following conditions for the rings:

$$\xi = r\varepsilon_2 = \frac{r}{Eh}(N_2 - \nu N_1), \tag{13.45a}$$

or

$$\xi = \frac{R_2 \sin\varphi}{Eh}(N_2 - \nu N_1). \tag{13.45b}$$

For a spherical shell, letting $R_1 = R_2 = R$, Eq. (13.45b) becomes

$$\xi = \frac{R \sin\varphi}{Eh}(N_2 - \nu N_1). \tag{13.45c}$$

For example, determine the horizontal expansion of the sphere edge $\varphi = \varphi_1$ under the internal pressure p. Taking into account that due to the symmetry of the shell and loading, $N_1 = N_2 = N$, and making $p_3 = -p$ (for internal pressure), one can bring the third Eq. (13.7) to the form $2N/R = p$, from which one derives $N = pR/2$. Substituting the above into Eq. (13.45c) gives

$$\xi = p\frac{R^2 \sin\varphi_1}{2Eh}(1 - \nu). \tag{13.46a}$$

For a hemisphere, $\varphi_1 = \pi/2$ and ξ becomes

$$\xi = p\frac{R^2}{2Eh}(1 - \nu). \tag{13.46b}$$

Now, we can proceed to determine the rotation of the tangent to the meridian. It can be easily shown that it is equal to the rotation of the normal to the middle surface during deformation about the axis which is tangent to the parallel circle. The latter expression was introduced in Sec. 12.2.1 as ϑ_1, given by the first Eq. (12.2). Setting $A = R_1$ and $\alpha = \varphi$, we obtain

$$\vartheta_1 = \frac{1}{R_1}\left(u + \frac{\partial w}{\partial \varphi}\right). \tag{13.47a}$$

By differentiating Eq. (13.44), we have

$$\frac{dw}{d\varphi} = \cos\varphi \cdot f_1(\varphi) - \sin\varphi \int f_1(\varphi) d\varphi - C_1 \sin\varphi - \varepsilon_2 \frac{dR_2}{d\varphi} - R_2 \frac{d\varepsilon_2}{d\varphi}. \tag{13.47b}$$

The displacement u is given by Eq. (13.43). Adding the right-hand sides of Eqs (13.47b) and (13.43), we obtain ϑ_1, as follows:

$$\vartheta_1 = \frac{1}{R_1}\left(\cos\varphi \cdot f_1(\varphi) - \varepsilon_2 \frac{dR_2}{d\varphi} - R_2 \frac{d\varepsilon_2}{d\varphi}\right),$$

or substituting for $f_1(\varphi)$ from Eq. (13.42b) results in the following:

$$\vartheta_1 = \cot\varphi\left(\varepsilon_1 - \frac{R_2}{R_1}\varepsilon_2\right) - \frac{\varepsilon_2}{R_1}\frac{dR_2}{d\varphi} - \frac{R_2}{R_1}\frac{d\varepsilon_2}{d\varphi}. \tag{13.48a}$$

Let us present this expression in the explicit form for a special case of spherical shells only. Substituting $R_1 = R_2 = R$ into the above equation, we obtain

$$\vartheta_1 = \cot\varphi(\varepsilon_1 - \varepsilon_2) - \frac{d\varepsilon_2}{d\varphi}. \tag{13.48b}$$

Inserting the strains in terms of N_1 and N_2 into this equation, we obtain the following expression of ϑ_1 for a sphere:

$$Eh\vartheta_1 = \cot\varphi(1+\nu)(N_1 - N_2) - \frac{dN_2}{d\varphi} + \nu\frac{dN_1}{d\varphi}. \tag{13.48c}$$

13.6 MEMBRANE ANALYSIS OF CYLINDRICAL AND CONICAL SHELLS

Cylindrical and conical shells have straight generators and, therefore, the radius of the curvature in the meridional direction is infinite. It will be shown that the vanishing one out of the two principal curvatures leads to a great simplification in the analysis of such a type of shells. For this reason, we treat these shells as a separate category of membrane shells.

13.6.1 General cylindrical shells

We consider cylindrical shells with an arbitrary shape of the cross section (or profile): e.g., circular, elliptical, parabolic, and cylinders of open or closed types. The peculiarities of the geometry of these shells were analyzed in Sec. 11.8. Since the generators of cylindrical shells are straight, such shells have zero Gaussian curvatures and, hence, have developable surfaces (see Sec. 11.7).

Using the cylindrical coordinates x and θ to describe the position of a reference point on the cylindrical shell middle surface (Fig. 11.13), the Lamé parameters are given by the relations (11.52), i.e.,

$$A = 1, \quad B = R_2, \tag{13.49}$$

where $R_2 = R_2(\theta)$ is the second principal radius of curvature, while the first radius of curvature $R_1 = \infty$. Notice that for a circular cylindrical shell $R_2 = \text{const} = R$, where

R is the radius of the circular cross section of the shell. With the cylindrical coordinates defined above and the Lamé parameters given by Eqs (13.49), the equilibrium Eqs (13.4) are significantly simplified and become (making $\alpha = x$ and $\beta = \theta$ in the above equations):

$$\begin{aligned} \frac{\partial N_1}{\partial x} + \frac{1}{R_2}\frac{\partial S}{\partial \theta} + p_1 &= 0, \\ \frac{\partial S}{\partial x} + \frac{1}{R_2}\frac{\partial N_2}{\partial \theta} + p_2 &= 0, \\ N_2 + R_2 p_3 &= 0, \end{aligned} \tag{13.50}$$

where p_1, p_2, and p_3 are the load components in the directions of the shell generator, tangent to its profile, and the normal to the middle surface, respectively.

The strain–displacement relations for cylindrical shells can be obtained from Eqs (13.5) by substituting for the Lamé parameters from Eqs (13.49) and making $R_1 = \infty$ and $\alpha = x$ and $\beta = \theta$. As a result, we obtain these relations in the following form:

$$\begin{aligned} \varepsilon_1 &= \frac{\partial u}{\partial x} = \frac{1}{Eh}(N_1 - \nu N_2), \\ \varepsilon_2 &= \frac{1}{R_2}\frac{\partial v}{\partial \theta} - \frac{w}{R_2} = \frac{1}{Eh}(N_2 - \nu N_1), \\ \gamma_{12} &= \frac{1}{R_2}\frac{\partial u}{\partial \theta} + \frac{\partial v}{\partial x} = \frac{1}{Gh}S. \end{aligned} \tag{13.51}$$

A general solution of Eqs (13.50) may be obtained in the following manner. From the third Eq. (13.50), we obtain the circumferential force N_2, i.e.,

$$N_2 = -R_2 p_3. \tag{13.52a}$$

The other two Eqs (13.50) may be solved by simple integration in the x direction, i.e.,

$$S = -\int \left(p_2 + \frac{1}{R_2}\frac{\partial N_2}{\partial \theta} \right) \mathrm{d}x + f_1(\theta), \tag{13.52b}$$

$$N_1 = -\int \left(p_1 + \frac{1}{R_2}\frac{\partial S}{\partial \theta} \right) \mathrm{d}x + f_2(\theta), \tag{13.52c}$$

where $f_1(\theta)$ and $f_2(\theta)$ are unknown functions of θ, to be determined from two boundary conditions. Each must be of the kind that on a profile $x = \text{const}$ (one end of the shell or a plane of symmetry) one of the forces S or N_1 will be given as an arbitrary function of θ.

Similarly, the general solution of Eqs (13.51) may be found once the membrane forces have been determined. For $h = \text{const}$, this solution is given by

$$Ehu = \int (N_1 - \nu N_2)\mathrm{d}x + f_3(\theta), \tag{13.53a}$$

$$Ehv = 2(1+\nu)\int S\mathrm{d}x - \frac{Eh}{R_2}\int \frac{\partial u}{\partial \theta}\mathrm{d}x + f_4(\theta), \tag{13.53b}$$

$$Ehw = Eh\frac{\partial v}{\partial \theta} - R_2(N_2 - \nu N_1), \tag{13.53c}$$

where $f_3(\theta)$ and $f_4(\theta)$ are two additional arbitrary functions which may be used to fulfill two boundary conditions on the edges $x = \text{const}$ of the shell. Equations (13.52) and (13.53) represent a complete general solution of the cylindrical membrane shell problem.

It should be noted that since the arbitrary functions $f_i(\theta)$ $(i = 1, 2, 3, 4)$ depend upon θ, boundary conditions can only be assigned for edges $x = \text{const}$. As a rule, we cannot satisfy boundary conditions on the longitudinal edges ($\theta = \text{const}$) of an open cylindrical shell, when, for example, a segment of a cylindrical membrane shell is under consideration. These must, therefore, be abandoned, which represents a severe limitation of the theory of the membrane shells as applied to open cylindrical shells. This limitation can only be remedied by including the bending resistance of the shell. However, such difficulties do not arise if a shell is closed with respect to the coordinate θ,

For most practical problems, we will have $p_1 = 0$ and p_2 and p_3 will be independent of x. Thus, from Eqs (13.52), one finds that

$$N_2 = -p_3 R_2, \tag{13.54a}$$

$$S = -\left(p_2 + \frac{1}{R_2}\frac{\partial N_2}{\partial \theta}\right)x + f_1(\theta) \quad \text{or} \quad S = -xF(\theta) + f_1(\theta), \tag{13.54b}$$

where

$$F(\theta) = p_2 + \frac{1}{R_2}\frac{\partial N_2}{\partial \theta} = p_2 - \frac{1}{R_2}\frac{\mathrm{d}}{\mathrm{d}\theta}(p_3 R_2). \tag{13.54c}$$

Hence, taking the partial derivative of S with respect to θ and integrating, we obtain

$$\frac{\partial S}{\partial \theta} = -x\frac{\mathrm{d}F}{\mathrm{d}\theta} + \frac{\mathrm{d}f_1(\theta)}{\mathrm{d}\theta}.$$

Substituting this expression and $p_1 = 0$ into Eq. (13.52c), we find that

$$N_1 = \left(\frac{x^2}{2R_2}\right)\frac{\mathrm{d}F}{\mathrm{d}\theta} - \frac{x}{R_2}\frac{\mathrm{d}f_1}{\mathrm{d}\theta} + f_2(\theta). \tag{13.54d}$$

Substituting next for the membrane forces from Eqs (13.54) into Eqs (13.53) and evaluating the integrals, we can represent the displacement components in terms of the introduced function $F(\theta)$, as follows

$$
\begin{aligned}
Ehu &= \frac{x^3}{6R_2}\frac{\mathrm{d}F}{d\theta} - \nu(x)N_2 - \frac{x^2}{2R_2}\frac{\mathrm{d}f_1}{\mathrm{d}\theta} + x\cdot f_2 + f_3,\\
Ehv &= -\frac{x^4}{24R_2}\frac{\mathrm{d}}{\mathrm{d}\theta}\left(\frac{1}{R_2}\frac{\mathrm{d}F}{\mathrm{d}\theta}\right) - (1+\nu)x^2F + \frac{\nu\cdot x^2}{2R_2}\frac{\mathrm{d}N_2}{\mathrm{d}\theta}\\
&\quad + \frac{x^3}{6R_2}\frac{\mathrm{d}}{\mathrm{d}\theta}\left(\frac{1}{R_2}\frac{\mathrm{d}f_1}{\mathrm{d}\theta}\right) - \frac{x^2}{2R_2}\frac{\mathrm{d}f_2}{\mathrm{d}\theta} + x\left[2(1+\nu)f_1 - \frac{1}{R_2}\frac{\mathrm{d}f_3}{\mathrm{d}\theta}\right] + f_4,\\
Ehw &= \frac{x^4}{24}\frac{\mathrm{d}}{\mathrm{d}\theta}\left[\frac{1}{R_2}\frac{\mathrm{d}}{\mathrm{d}\theta}\left(\frac{1}{R_2}\frac{\mathrm{d}F}{\mathrm{d}\theta}\right)\right] + \frac{x^2}{2}\left[(2+\nu)\frac{\mathrm{d}F}{\mathrm{d}\theta} - \nu\frac{\mathrm{d}}{\mathrm{d}\theta}\left(\frac{1}{R_2}\frac{\mathrm{d}N_2}{\mathrm{d}\theta}\right)\right]\\
&\quad + R_2N_2 - \frac{x^3}{6}\frac{\mathrm{d}}{\mathrm{d}\theta}\left[\frac{1}{R_2}\frac{\mathrm{d}}{\mathrm{d}\theta}\left(\frac{1}{R_2}\frac{\mathrm{d}f_1}{\mathrm{d}\theta}\right)\right] + \frac{x^2}{2}\frac{\mathrm{d}}{\mathrm{d}\theta}\left(\frac{1}{R_2}\frac{\mathrm{d}f_2}{\mathrm{d}\theta}\right)\\
&\quad - x\left[(2+\nu)\frac{\mathrm{d}f_1}{\mathrm{d}\theta} - \frac{\mathrm{d}}{\mathrm{d}\theta}\left(\frac{1}{R_2}\frac{\mathrm{d}f_3}{\mathrm{d}\theta}\right)\right] - \nu(R_2)f_2 - \frac{\mathrm{d}f_4}{\mathrm{d}\theta}.
\end{aligned}
\tag{13.55}
$$

For a circular cylindrical shell $R_2 = R = \text{const}$ and Eqs (13.54) and (13.55) may be simplified.

Consider the boundary conditions for a closed cylindrical shell. For statically determinate shells, the two conditions should be assigned for determining arbitrary functions $f_1(\theta)$ and $f_2(\theta)$. These conditions should be imposed on the membrane forces N_1 and S on the shell edges. In so doing, since the expression for S contains only one function $f_1(\theta)$, the shear force can be prescribed on one edge of the shell only. The functions $f_3(\theta)$ and $f_4(\theta)$ are evaluated from the two kinematic boundary conditions assigned for the displacement components u and v on the shell edges – e.g., $x = 0$ and $x = L$, where L is the length of the cylindrical shell.

For statically indeterminate cylindrical shells the number of kinematic boundary conditions increases at the expense of static boundary conditions. For example, if both ends of the shell, $x = 0$ and $x = L$, are built-in, all the boundary functions mentioned previously are evaluated from the following conditions:

$$u|_{x=0} = u|_{x=L} = v|_{x=0} = v|_{x=L}, = 0.$$

Comparing the flexural deformations at surface layers in the shell, $\varepsilon_1^{(\mathrm{f})} = \chi_1 h/2$ and $\varepsilon_2^{(\mathrm{f})} = \chi_2 h/2$, with the membrane deformations, ε_1 and ε_2, one can establish that the former deformations are small compared with the latter only in the case when arbitrary functions $f_i(\theta)$ $(i = 1, 2, 3, 4)$ satisfy the limitations

$$\frac{h}{R}\left(\frac{\mathrm{d}^2 f_i}{\mathrm{d}\theta^2}\right) \ll f_i.$$

These inequalities express the general requirement of slowly varying deformations in the direction of θ. The above requirements impose additional limitations on admissible character of distribution of boundary loads $N_1^{(0)}$ and $S^{(0)}$.

It follows from Eqs (13.55) that the continuous expressions for the displacement components in the membrane theory can only be obtained in the case when

arbitrary functions $f_1(\theta)$ and $f_2(\theta)$, which arise in integrating the equilibrium equations, are continuous together with their derivatives up to the second and third derivatives. This also imposes certain limitations on admissible types of loading and boundary conditions in order that membrane theory can be applied.

One important comment should be mentioned. It follows from Eqs (13.54) and (13.55) that the membrane forces and displacements increase without limit with an increase of the shell length. This is a natural result of the membrane analysis of a cylindrical shell in which th flexural rigidity of the circumferential cross sections of the shell is neglected and all loading is directly transmitted to the shell ends. Therefore, the area of application of the membrane theory of cylindrical shells is restricted by fairly short shells ($l/R \ll \sqrt{R/h}$) [2]. So, there is a variety of requirements that govern the applicability of the membrane theory of cylindrical shells. These requirements are concerned with the type of shell supports, type of loading, and length of the shell.

An impression may be formed that the membrane theory of cylindrical shells is practically of no use because of the limitations mentioned above. However, this is not true. In some cases, the membrane theory of cylindrical shells allows one to obtain simple and, at the same time, sufficiently accurate solutions. In particular, it is applicable to the analysis of cylindrical shells reinforced by stiffeners. In this case, the external loading applied to the closely spaced at equal distances stiffeners is distributed by the stiffener elements in such a way that the condition of slowly varying deformation in the circumferential direction is satisfied.

13.6.2 Conical shells

Figure 13.3a shows a conical shell in the form of a frustum of a cone. The meridian of the shell has zero curvature, while the radius of the second principal curve is R_2. The radius of the parallel circle is denoted by r. In this typical case, the angle φ is a constant and can no longer serve as a coordinate on the meridian. Instead, we introduce the coordinate s, the distance of a point of the middle surface, usually measured from the vertex, along the generator, i.e., $\alpha = s$. Another coordinate is the

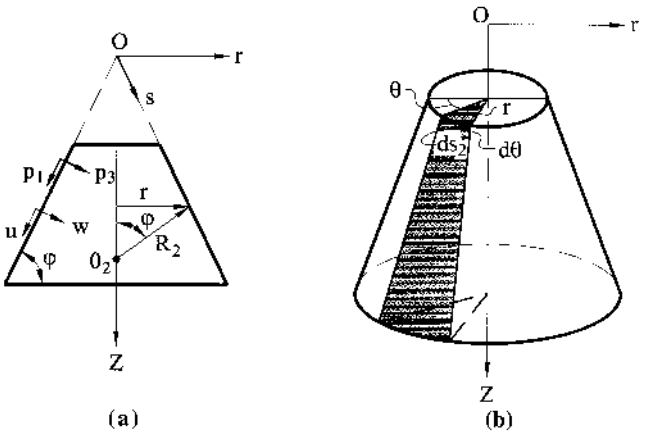

Fig. 13.3

circumferential angle θ in the horizontal plane measured on the parallel circle, i.e., $\beta = \theta$.

For such a shell, a length of the element along the meridian is ds_1 and along the parallel circle is $ds_2 = rd\theta$. It follows from Fig. 13.3a and b that

$$R_2 = s\cot\varphi, \quad r = s\cos\varphi. \tag{13.56}$$

Thus, the Lamé parameters for the given coordinate system are

$$A = 1 \quad \text{and} \quad B = r = s\cos\varphi. \tag{13.57}$$

Substituting the above into Eqs (13.4) and (13.5), we obtain the equilibrium and kinematic equations, respectively. The equilibrium equations for the conical shell are given by

$$\begin{aligned} &\frac{\partial}{\partial s}(N_1 s) + \frac{1}{\cos\varphi}\frac{\partial S}{\partial\theta} - N_2 + sp_1 = 0, \\ &\frac{1}{\cos\varphi}\frac{\partial N_2}{\partial\theta} + \frac{1}{s}\frac{\partial}{\partial s}\left(Ss^2\right) + sp_2 = 0, \\ &\frac{1}{s}\tan\varphi N_2 + p_3 = 0. \end{aligned} \tag{13.58}$$

The kinematic equations for displacement components have the form

$$\begin{aligned} &\frac{\partial u}{\partial s} = \varepsilon_1 \\ &\frac{1}{\cos\varphi}\frac{\partial v}{\partial\theta} + u - w\tan\varphi = \varepsilon_2 s \\ &s\frac{\partial}{\partial s}\left(\frac{v}{s}\right) + \frac{1}{s\cos\varphi}\frac{\partial u}{\partial\theta} = \gamma_{12} \end{aligned} \tag{13.59}$$

We come now to determining the membrane forces and displacements for conical shells. From the last Eq. (13.58), we have

$$N_2 = -p_3 s\cdot\cot\varphi. \tag{13.60}$$

Substituting the above into the second Eq. (13.58), one finds that

$$\frac{\partial}{\partial s}\left(Ss^2\right) = -s^2\left(p_2 - \frac{1}{\sin\varphi}\frac{\partial p_3}{\partial\theta}\right).$$

Integrating this expression over s, we obtain

$$S = \frac{1}{s^2}\left[f_1(\theta) - \int_s s^2\left(p_2 - \frac{1}{\sin\varphi}\frac{\partial p_3}{\partial\theta}\right)ds\right]. \tag{13.61}$$

Substituting for N_2 and S from Eqs (13.60) and (13.61) into the first Eq. (13.58), and integrating over s, gives the following expression:

$$N_1 = \frac{1}{s^2 \cos\varphi} f_1'(\theta) + \frac{1}{s} f_2(\theta) - \frac{1}{s \sin\varphi} \int_s s(p_3 \cos\varphi + p_1 \sin\varphi) \mathrm{d}s + \frac{1}{s \cos\varphi} \int_s \frac{1}{s^2} \left[\int_s \left(\frac{\partial p_2}{\partial \theta} - \frac{1}{\sin\varphi} \frac{\partial^2 p_3}{\partial \theta^2} \right) s^2 \mathrm{d}s \right] \mathrm{d}s. \tag{13.62}$$

Let us determine the displacements. From the first Eq. (13.59), we have

$$u = \int_s \varepsilon_1 \mathrm{d}s + f_3(\theta). \tag{13.63}$$

Substituting for u from Eq. (13.63) into the third Eq. (13.59) and integrating over s, one finds that

$$v = \frac{1}{\cos\varphi} f_3'(\theta) + s f_4(\theta) + s \int_s \frac{\gamma_{12}}{s} \mathrm{d}s - \frac{s}{\cos\varphi} \frac{\partial}{\partial \theta} \int_s \left[\int_s \varepsilon_1 \mathrm{d}s \right] \frac{\mathrm{d}s}{s^2}. \tag{13.64}$$

The displacement w is determined from the second Eq. (13.59), i.e.,

$$w = u \cot\varphi + \frac{1}{\sin\varphi} \frac{\partial v}{\partial \theta} - \varepsilon_2 s \cot\varphi. \tag{13.65}$$

As for the case of the cylindrical shell, four arbitrary functions depend only upon the angular coordinate θ; therefore, the boundary conditions on edges $\theta = \text{const}$ of open shells cannot be satisfied.

A continuity and slowly varying of loads with respect to the angular coordinate are necessary conditions of applicability of the membrane theory to a conical shell.

Let us pay attention to one peculiarity of conical shells: a closed at a vertex conical shell is not capable of carrying a self-balanced load applied to its free edge according to the membrane theory. The reason for that is an unlimited increase of forces, and hence, deformations in the vicinity of the vertex, i.e., for $s = 0$ (see formulas (13.60)–(13.62)). In so doing, the displacements determined from Eqs (13.64) and (13.65) become also unlimited: a moment state of stresses will occur near the vertex of a closed conical shell.

For an axisymmetrically (with respect to the shell axis) loaded conical shell, the system of equations (13.58) may be simplified. Putting the derivatives of all functions with respect to θ equal zero and $S = 0$ together with $p_2 = 0$, we obtain the above-mentioned system in the following form:

$$\begin{aligned} \frac{\mathrm{d}}{\mathrm{d}s}(N_1 s) - N_2 &= -p_1 s, \\ N_2 &= -p_3 s \cot\varphi. \end{aligned} \tag{13.66}$$

Adding these equations member by member, we obtain the following first-order differential equation for N_1:

$$\frac{\mathrm{d}}{\mathrm{d}s}(N_1 s) = -s(p_1 + p_3 \cot\varphi). \tag{13.67}$$

Integrating the above, yields

$$N_1 = -\left[\frac{1}{s}\int (p_1 + p_3 \cot\varphi) s\,ds + \frac{C}{s}\right], \tag{13.68}$$

where C is a constant of integration.

13.7 THE MEMBRANE THEORY OF SHELLS OF AN ARBITRARY SHAPE IN CARTESIAN COORDINATES

The boundary contour of shells of an arbitrary shape does not usually coincide with the lines of curvature. As an example, one can mention shells of double curvature which are commonly used for roofs of buildings. A membrane analysis of such shells is more conveniently performed using Cartesian coordinates whose x and y axes lie in a horizontal plane with the z axis pointing in the vertical direction to the plane above. The middle surface of the shell can be assigned by the following equation in the Cartesian coordinate system:

$$z = f(x, y). \tag{13.69}$$

In this coordinate system, we consider an element $ABCD$ of the shell obtained by making sections at the locations $x, x + dx$, and $y, y + dy$ (Fig. 13.4).

These sections are not necessarily the lines of curvature in a general case (the exceptions are cylindrical surfaces for which the x axis is directed along generators). They are not mutually perpendicular. Hence, angle ω between sides AB and AD is not necessarily a right angle and element $ABCD$ is a skew quadrilateral with sides ds_1 and ds_2 in space. Its projection in the xy plane is a rectangle $\bar{A}\bar{B}\bar{C}\bar{D}$ with sides dx and dy. Let φ and ϕ be the angles which sides AD and AB make with the xy plane. Correspondingly, the lengths AD and AB of the shell element are $(dx/\cos\varphi)$ and $(dy/\cos\phi)$, respectively. The midsurface area of the element $ABCD$ becomes $(dx/\cos\varphi)(dy/\cos\phi)\sin\omega$.

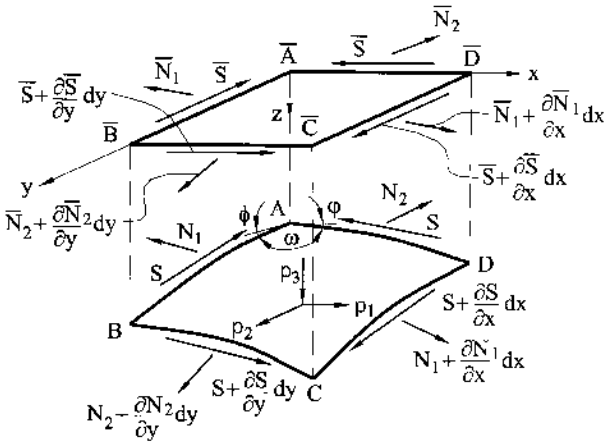

Fig. 13.4

The curves $x = \text{const}$ and $y = \text{const}$ on the shell midsurface can be used as coordinate curves, and we denote by N_1, N_2, and S the membrane stress resultants at any point on the shell. It should be noted that the directions of these forces make up non-right angles with the corresponding sides of the element. These membrane forces are shown in Fig. 13.4. Two out of all unknown forces (N_1 and S) are parallel to the plane Oxz, and, therefore, have no components in the direction of the y axis. Two others (N_2 and S on sides AD and BC) have no components in the x direction. These considerations simplify setting up the equation of equilibrium.

Figure 13.4 also shows the surface load components, where p_1 and p_2 are parallel to the x and y axes, respectively, and p_3 acts in the z direction. These load components are defined per unit are of the shell midsurface.

We set up the equation of equilibrium in the direction of the x axis. Consider a side AB. The membrane force per unit length acting on this side is $N_1(\mathrm{d}y/\cos\phi)$ and its component in the x direction is $N_1(\mathrm{d}y/\cos\phi)\cos\varphi$. The in-plane shear force S of the same direction has a component in the x direction of the form $S(\mathrm{d}x/\cos\varphi)\cos\varphi$. By analogy, the components of the membrane forces acting on the opposite side CD can be represented, as follows:

$$\left(N_1 + \frac{\partial N_1}{\partial x}\mathrm{d}x\right)\frac{\mathrm{d}y}{\cos\left(\phi + \frac{\partial\phi}{\partial x}\mathrm{d}x\right)}\cos\left(\varphi + \frac{\partial\varphi}{\partial x}\mathrm{d}x\right),$$

$$\left(S + \frac{\partial S}{\partial y}\mathrm{d}y\right)\cos\left(\varphi + \frac{\partial\varphi}{\partial y}\mathrm{d}y\right)\frac{\mathrm{d}x}{\cos\left(\varphi + \frac{\partial\varphi}{\partial y}\mathrm{d}y\right)}.$$

Summing these forces with the corresponding signs, taking into account that the resultant force due to the loading p_1 is obtained by multiplying p_1 by the area of the element $ABCD$, and canceling out the common factor $\mathrm{d}x\mathrm{d}y$, we obtain the following after some simplifications and assuming that the angles φ and ϕ are small:

$$\frac{\partial}{\partial x}\left(N_1\frac{\cos\varphi}{\cos\phi}\right) + \frac{\partial S}{\partial y} + p_1\frac{\sin\omega}{\cos\phi\cos\varphi} = 0. \tag{13.70a}$$

Similarly, we can obtain the following equilibrium equation for the components of the membrane forces in the y direction:

$$\frac{\partial}{\partial y}\left(N_2\frac{\cos\phi}{\cos\varphi}\right) + \frac{\partial S}{\partial x} + p_2\frac{\sin\omega}{\cos\phi\cos\varphi} = 0. \tag{13.70b}$$

Let us set up an equation of equilibrium for all the membrane forces in the z direction. The component of the force N_1 in the z direction is $N_1(\mathrm{d}y/\cos\phi)\sin\varphi$ and the component of the in-plane shear force S in the same direction referred to the same side of the element $ABCD$ is $S(\mathrm{d}y/\cos\phi)\sin\varphi$. The corresponding expressions can be obtained for the two other components of the membrane forces. So, the equation of equilibrium for the membrane forces in the z direction is derived after some simplifications, as follows:

$$\frac{\partial}{\partial x}\left(N_1\frac{\sin\varphi}{\cos\phi}\right) + \frac{\partial}{\partial y}\left(N_2\frac{\sin\phi}{\cos\varphi}\right) + \frac{\partial}{\partial y}(S\tan\varphi) + \frac{\partial}{\partial x}(S\tan\phi) + p_3\frac{\sin\omega}{\cos\phi\cos\varphi} = 0. \tag{13.70c}$$

The values of the trigonometric functions entering into Eqs (13.70) can be expressed in terms of the partial derivatives of the equation of a surface given by Eq. (13.69), i.e.,

$$\tan\varphi = \frac{\mathrm{d}z}{\mathrm{d}x}, \quad \tan\phi = \frac{\mathrm{d}z}{\mathrm{d}y}; \tag{13.71a}$$

hence,

$$\cos\varphi = \frac{1}{\sqrt{1+\left(\frac{\partial z}{\partial x}\right)^2}}, \quad \sin\varphi = \frac{\partial z/\partial x}{\sqrt{1+\left(\frac{\partial z}{\partial x}\right)^2}}, \quad \text{etc.} \tag{13.71b}$$

It can be easily noted that the expressions

$$\left(N_1\frac{\mathrm{d}y}{\cos\phi}\right)\cos\varphi, \left(N_2\frac{\mathrm{d}x}{\cos\varphi}\right)\cos\phi; \quad \left(S\frac{\mathrm{d}y}{\cos\phi}\right)\cos\phi, \left(S\frac{\mathrm{d}x}{\cos\varphi}\right)\cos\varphi$$

represent projections of the membrane forces acting on sides of the shell skew quadrilateral element $ABCD$ on the coordinate plane xy or the membrane forces acting on sides of the rectangle $\bar{A}\bar{B}\bar{C}\bar{D}$, as shown in Fig. 13.4. Let us denote these projections by $\bar{N}_1\mathrm{d}y$, $\bar{N}_2\mathrm{d}x$, and $\bar{S}\mathrm{d}x$, i.e.,

$$\bar{N}_1 = N_1\frac{\cos\varphi}{\cos\phi}, \quad \bar{N}_2 = N_2\frac{\cos\phi}{\cos\varphi}, \quad \bar{S} = S. \tag{13.72}$$

Using these notations, we can rewrite equations of equilibrium, Eqs (13.70), as follows

$$\frac{\partial\bar{N}_1}{\partial x} + \frac{\partial\bar{S}}{\partial y} + \bar{p}_1 = 0, \tag{13.73a}$$

$$\frac{\partial\bar{S}}{\partial x} + \frac{\partial\bar{N}_2}{\partial y} + \bar{p}_2 = 0, \tag{13.73b}$$

$$\frac{\partial}{\partial x}\left(\bar{N}_1\tan\varphi\right) + \frac{\partial}{\partial y}\left(\bar{N}_2\tan\phi\right) + \frac{\partial}{\partial y}\left(\bar{S}\tan\varphi\right) + \frac{\partial}{\partial x}\left(\bar{S}\tan\phi\right) + \bar{p}_3 = 0. \tag{13.73c}$$

where

$$\bar{p}_1 = p_1\frac{\sin\omega}{\cos\phi\cos\varphi}, \quad \bar{p}_2 = p_2\frac{\sin\omega}{\cos\phi\cos\varphi}, \quad \bar{p}_3 = p_3\frac{\sin\omega}{\cos\phi\cos\varphi} \tag{13.74}$$

are the surface load components per unit area of the projection of the shell element on the xy plane in the x, y, and z directions, respectively.

Equation (13.73c) can be rewritten by substituting for the tangents from Eqs (13.71a), as follows:

$$\bar{N}_1\frac{\partial^2 z}{\partial x^2} + 2\bar{S}\frac{\partial^2 z}{\partial x\partial y} + \bar{N}_2\frac{\partial^2 z}{\partial y^2} = -\bar{p}_3 - \left(\frac{\partial\bar{N}_1}{\partial x} + \frac{\partial\bar{S}}{\partial y}\right)\frac{\partial z}{\partial x} - \left(\frac{\partial\bar{S}}{\partial x} + \frac{\partial\bar{N}_2}{\partial y}\right)\frac{\partial z}{\partial y}. \tag{13.75}$$

Taking into account Eqs (13.73a) and (13.73b), this equation may be represented in the form

$$\bar{N}_1 \frac{\partial^2 z}{\partial x^2} + 2\bar{S} \frac{\partial^2 z}{\partial x \partial y} + \bar{N}_2 \frac{\partial^2 z}{\partial y^2} = -\bar{p}_3 + \bar{p}_1 \frac{\partial z}{\partial x} + \bar{p}_2 \frac{\partial z}{\partial y}. \tag{13.76}$$

For a given shell surface $z = f(x, y)$ and given loading, Eqs (13.73a), (13.73b), and (13.76) govern the membrane forces in the shell under consideration. This system of equations can be reduced to one differential equation. In fact, Eqs (13.73a) and (13.73b) coincide with the corresponding equations of the plane elasticity [3]. We now introduce the Pucher stress function Φ [4], which is defined by the following

$$\bar{N}_1 = \frac{\partial^2 \Phi}{\partial y^2} - \int \bar{p}_1 \mathrm{d}x, \quad \bar{N}_2 = \frac{\partial^2 \Phi}{\partial x^2} - \int \bar{p}_2 \mathrm{d}y, \quad \bar{S} = -\frac{\partial^2 \Phi}{\partial x \partial y}. \tag{13.77}$$

It is easily verified by substitution that if Φ is a continuous function with continuous partial derivatives, Eqs (13.73a) and (13.73b) are identically satisfied. Introducing the relations (13.77) into Eq. (13.76), yields the following:

$$\frac{\partial^2 \Phi}{\partial x^2}\frac{\partial^2 z}{\partial y^2} - 2\frac{\partial^2 \Phi}{\partial x \partial y}\frac{\partial^2 z}{\partial x \partial y} + \frac{\partial^2 \Phi}{\partial y^2}\frac{\partial^2 z}{\partial x^2} = -\bar{p}_3 + \bar{p}_1 \frac{\partial z}{\partial x} + \bar{p}_2 \frac{\partial z}{\partial y} + \frac{\partial^2 z}{\partial x^2}\int \bar{p}_1 \mathrm{d}x + \frac{\partial^2 z}{\partial y^2}\int \bar{p}_2 \mathrm{d}y. \tag{13.78}$$

Equation (13.78) represents the *governing differential equation for a membrane shell of an arbitrary shape in Cartesian coordinates*.

Solving this equation and satisfying the boundary conditions, we obtain the function Φ and, then, the membrane forces from Eqs (13.77) and (13.72), i.e.,

$$N_1 = \bar{N}_1 \sqrt{\frac{1 + (\partial z/\partial x)^2}{1 + (\partial z/\partial y)^2}}, \quad N_2 = \bar{N}_2 \sqrt{\frac{1 + (\partial z/\partial y)^2}{1 + (\partial z/\partial x)^2}}, \quad S = \bar{S}. \tag{13.79}$$

For most practical problems, loadings $\bar{p}_1$ and $\bar{p}_2$ are zero. Substituting $\bar{p}_1 = \bar{p}_2 = 0$ into Eq. (13.76), we obtain the following expression:

$$\bar{N}_1 \frac{\partial^2 z}{\partial x^2} + 2\bar{S} \frac{\partial^2 z}{\partial x \partial y} + \bar{N}_2 \frac{\partial^2 z}{\partial y^2} = -\bar{p}_3. \tag{13.80}$$

PROBLEMS

13.1 Derive Eq. (13.18).

13.2 Derive Eqs (13.33) and (13.39) in cylindrical coordinates z and r (see Eqs (11.31)).

13.3 Using the nondimensional analysis procedure, it can be shown that the membrane forces, strain components, and displacements obtained by the membrane theory are of the order

$$\{N_1, N_2, S\} \sim \tilde{L}p, \sim \{\varepsilon_1, \varepsilon_2, \gamma_{12}\} \frac{\tilde{L}p}{Eh}, \quad \{u, v, w\} \sim \frac{L^2 p}{Eh}; \tag{a}$$

on other hand, the changes in curvature and in twist and the moments in the framework of the membrane theory have the order

$$\{\chi_1, \chi_2, \chi_{12}\} \sim \frac{p}{Eh}, \quad \{M_1, M_2, H\} \sim h^2 p, \tag{b}$$

where L is some typical linear dimension of a shell (for example, radius of curvature of the shell midsurface), p is a loading parameter, h is the shell thickness, and the symbol $\sim$ means that the quantities on the left- and right-hand sides have the same order. Estimate the order of the membrane and bending stresses in the framework of applicability of the membrane theory.

13.4 Consider a circular plate and hemispherical shell having the same radii R and thicknesses h. Assume that the plate and shell carry the same uniform normal pressure p (the resultant of this pressure, $F = \pi R^2 p$, is the same for both plate and shell). However, the plate carries p by bending and the shell carries p by membrane action. Compare the maximum normal stresses in the plate and shell.

13.5 Using the expressions (a) and (b) of Problem 13.3, verify that the membrane theory satisfies the equilibrium equations of the general linear theory of thin shells (Eqs (12.44)) with the error of the order of h^2/C^2 compared with unity.

13.6 Formulate a complete set of boundary conditions for a shell of revolution according to the membrane shell theory.

13.7 Compare the flexural and membrane stresses in a circular, closed cylindrical shell under a uniform internal pressure of intensity p_0. Take $R/h = 30$, $\nu = 0$.

13.8 Formulate the restrictions imposed by the membrane theory on the stress analysis of closed and open cylindrical shells.

13.9 Verify Eq. (13.65).

13.10 Derive Eq. (13.70c).

13.11 Based on Eq. (13.80), derive the governing equations of:

- **(a)** a cable structure lying in the xz plane and subjected to a "live load" p and self-weight q;
- **(b)** a thin membrane.

13.12 Specify Eq. (13.76) for shells with surfaces defined by the following equations:

- **(a)** dome: $z^2 + x^2 + y^2 = a^2$;
- **(b)** cone: $z^2 = (x^2 + y^2)\tan^2\alpha$;
- **(c)** elliptic paraboloid: $z = x^2/2h_1 + y^2/2h_2$;
- **(d)** hyperbolic paraboloid: $z = x^2/2h_1 - y^2/2h_2$; and
- **(e)** hypar with the coordinate axes along straight-line generators: $z = Cxy$.

Assume that all shells are subjected to a normal uniform pressure p_0.

13.13 Derive the governing differential equations of the membrane theory in displacements.

REFERENCES

1. Calladine, C.R., *Theory of Shell Structures*, Cambridge University Press, Cambridge, 1983.
2. Novozhilov, V.V., *The Shell Theory* [translated from 2nd Russian edn. by P.G. Lowe], Noordhoff, Groningen, The Netherlands, 1964.
3. Timoshenko, S.P. and Goodier, J.N., *Theory of Elasticity*, 2nd edn, McGraw-Hill, New York, 1951.
4. Pucher, A., Über den spannungszustand in gekrümmten flächen, *Beton u Eisen*, vol. 33 (1934).

14

Application of the Membrane Theory to the Analysis of Shell Structures

We consider below an application of the membrane theory of thin shells, developed in Chapter 13, to the analysis of various shell structures. The membrane theory can be applied with various levels of accuracy to the stress analysis of two kinds of shell structures: facilities for storage of water, gas, oil, etc. (elevated water towers, silos, pressure vessels, tanks, closures, etc.) and long-span roofs of buildings or domes.

14.1 MEMBRANE ANALYSIS OF ROOF SHELL STRUCTURES

14.1.1 Axisymmetrically loaded dome roofs

(a) Spherical domes: self-weight

First, we consider a dome closed at its apex and subjected to a dead load of p per unit area of the middle surface (e.g., own weight, weight of cladding, etc.), as shown in Fig. 14.1a.

Resolving the dead load p into components along the normal, p_3, and meridional, p_1, directions, with respect to the middle surface of the dome, we obtain the following relationships:

$$p_3 = p\cos\varphi, p_1 = p\sin\varphi. \tag{14.1}$$

Substituting the above into Eq. (13.38), taking into account Eq. (13.6a) and noting that for a sphere $R_1 = R_2 = R$, we obtain the following expression for the meridional force:

$$N_1 = -\frac{1}{R\sin^2\varphi}\int_0^{\varphi} R^2\sin\bar{\varphi}(p\sin^2\bar{\varphi} + p\cos^2\bar{\varphi})\mathrm{d}\bar{\varphi},$$

or

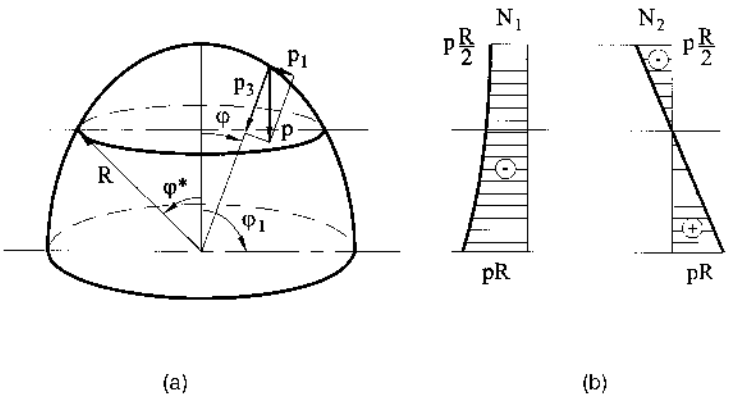

Fig. 14.1

$$N_1 = -pR\frac{1-\cos\varphi}{1-\cos^2\varphi} = -\frac{pR}{1+\cos\varphi}. \tag{14.2}$$

Then, substituting Eq. (14.2) into Eq. (13.39) gives the expression for the circumferential force, as follows:

$$N_2 = -pR\cos\varphi + \frac{pR}{1+\cos\varphi} = -pR\left(\cos\varphi - \frac{1}{1+\cos\varphi}\right). \tag{14.3}$$

At the crown of the dome where $\varphi = 0$, we have the following:

$$N_1 = N_2 = -\frac{pR}{2}.$$

The meridional force, N_1, is compressive along the meridian of the dome, increasing from the apex to the bottom of the dome. The circumferential compressive force N_2, near the crown, decreases gradually with the increase of φ and changes sign. Diagrams of the distribution of the membrane forces N_1 and N_2 are shown in Fig. 14.1b.

Denote by φ^* the coordinate of the parallel circle on which $N_2 = 0$. This parallel circle is called the *line of transition*. Below this line, the circumferential force,N_2, is tensile only under the loading shown in Fig. 14.1a. The coordinate φ^* of the line of transition may be found from Eq. (14.3), equating the term in the parenthesis to zero and putting $\varphi = \varphi^*$. We have

$$\cos\varphi^* - \frac{1}{1+\cos\varphi^*} = 0,$$

from which $\varphi^* = 51^\circ 49'$.

Spherical domes whose opening angle is less then $2\varphi^*$ are free from tensile stresses. At the base of a semi-sphere ($\varphi = \varphi_1 = 90^\circ$), $N_2 = pR$, $N_1 = -pR$.

The presence of the line of transition enables one to avoid considerable bending near the base of a dome. Let us consider this statement in detail. Resolve the membrane force $N_1^{(1)}$, acting at the base of the dome ($\varphi = \varphi_1$), into two components: the vertical V and horizontal H, as shown in Fig. 14.2a. The vertical component V

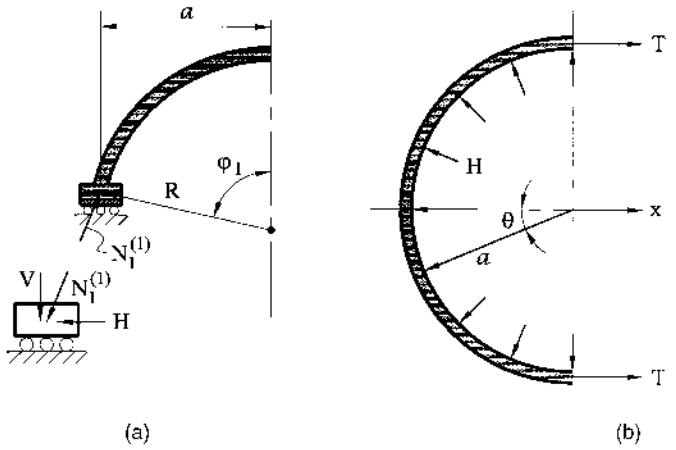

Fig. 14.2

will be transmitted to the wall on which the dome rests, while the assimilation of the horizontal component H requires a special structural element called a thrust (or supporting) ring. A half-plan of the ring is shown in Fig. 14.2b. The shell is assumed to extend to the centroid of the ring to eliminate the introduction of eccentricity.

The vertical and horizontal components of the membrane force N_1 are found to be

$$V = N_1^{(1)} \sin \varphi_1, \quad H = -N_1^{(1)} \cos \varphi_1. \tag{14.4}$$

The horizontal component, H, being applied to the thrust ring produces its tension in the circumferential direction. Let T be the circumferential tension in the ring. We can evaluate T by summing forces in the x direction on Fig. 14.2b and assuming that the radius of the ring is approximately equal to a, i.e., to the radius of the parallel circle at the shell base ($\varphi = \varphi_1$), as follows:

$$2T = \int_{-\pi/2}^{\pi/2} -N_1^{(1)} \cos \varphi_1 \cos \theta (a \mathrm{d}\theta) \quad \text{or} \quad T = -N_1^{(1)} a \cos \varphi_1. \tag{14.5}$$

For the spherical shell we have $a = R \sin \varphi_1$. So that

$$T = -N_1^{(1)} R \cos \varphi_1 \sin \varphi_1. \tag{14.6}$$

For the self-weight case, we find by substituting Eq. (14.2) into Eq. (14.6) that

$$T = pR^2 \frac{\cos \varphi_1 \sin \varphi_1}{1 + \cos \varphi_1}. \tag{14.7}$$

Comparing Eq. (14.7) and the graph for N_2 in Fig. 14.1b, we can conclude that there could be a strain incompatibility at the junction between the shell edge and the thrust ring. For $\varphi_1 < 51^\circ 49'$, the circumferential force N_2 is compressive while the ring force T is tensile for all $\varphi_1 < 90^\circ$. Thus, the dome, which has been shown to be in a state of compression through the membrane stress analysis, must accommodate somewhat the circumferential expansion of the base ring accompanying the tensile

force T. Clearly, this cannot be accomplished with membrane action alone, and bending must be considered to satisfy deformational continuity. It should be noted that the bending effects introduced are usually confined to a relatively small portion of the shell adjacent to the base, and membrane action will still predominate throughout most of the shell.

However, if $\varphi > 51°49'$ the circumferential force N_2 will be tensile and, hence, will coincide with the sign of the circumferential tension in the ring. So, the possibility arises of selecting the cross-sectional area of the thrust ring in such a way that the elongation of the shell edge would be equal to stretching the ring. The circumferential strains of the shell edge, $\varepsilon_2^{(s)}$, and the thrust ring, $\varepsilon_2^{(r)}$, are found to be

$$\varepsilon_2^{(s)} = \frac{1}{E_s h}\left(N_2^{(1)} - \nu_s N_1^{(1)}\right); \quad \varepsilon_2^{(r)} = \frac{\sigma_2^{(r)}}{E_r} = \frac{T}{E_r A_r} = -\frac{N_1^{(1)} a}{E_r A_r}\cos\varphi_1. \tag{14.8}$$

In Eqs (14.8), $N_1^{(1)}$ and $N_2^{(1)}$ are the meridional and circumferential forces at the shell base, respectively, i.e., at $\varphi = \varphi_1$; E_s and ν_s are the modulus of elasticity and Poisson's ratio, respectively, of the shell material; E_r and A_r are the modulus of elasticity and cross-sectional area of the thrust ring, respectively. The required cross-sectional area of the thrust ring can be determined from the following compatibility condition:

$$\varepsilon_2^{(s)} = \varepsilon_2^{(r)}. \tag{14.9}$$

Substituting Eqs (14.8) into Eq. (14.9) yields the required area of the cross section of the thrust ring, as follows:

$$A_r = \left|\frac{\cos\varphi_1}{\dfrac{N_2^{(1)}}{N_1^{(1)}} - \nu_s}\right| \frac{E_s}{E_r} ah, \tag{14.10}$$

where $N_1^{(1)}$ and $N_2^{(1)}$are given by Eqs (14.2) and (14.3) by substituting φ_1 for φ.

Having determined the internal forces, we can calculate the meridional, σ_1, and circumferential, σ_2, membrane stress components, as follows:

$$\sigma_1 = \frac{N_1}{h} = -\frac{p}{h}\frac{R}{1+\cos\varphi}, \quad \sigma_2 = \frac{N_2}{h} = -\frac{p}{h}R\left(\cos\varphi - \frac{1}{1+\cos\varphi}\right). \tag{14.11}$$

Let us now determine the displacements of the spherical dome supporting its own weight (Fig. 14.1a). Substituting for the membrane forces N_1 and N_2 from Eqs (14.2) and (14.3) into the right-hand sides of Eqs (13.5) gives the strains ε_1 and ε_2. Introducing the latter into Eqs (13.42b) results in the following expressions for $f_1(\varphi)$:

$$f(\varphi) = \frac{R^2 p(1+\nu)}{Eh}\left(\cos\varphi - \frac{2}{1+\cos\varphi}\right). \tag{14.12}$$

Inserting the above expression into Eq. (13.43), and evaluating the integrals, yields the following expression for u:

$$u = \frac{pR^2(1+\nu)}{Eh}\left[\sin\varphi\ln(1+\cos\varphi) - \frac{\sin\varphi}{1+\cos\varphi}\right] + C_1\sin\varphi, \tag{14.13}$$

where C_1 is a constant of integration that can be evaluated from boundary conditions on the dome base, i.e., Fig.14.2a, $u = 0|_{\varphi=\varphi_1}$. It follows from the above that

$$C_1 = \frac{pR^2(1+\nu)}{Eh}\left[\frac{1}{1+\cos\varphi_1} - \ln(1+\cos\varphi_1)\right].$$

Upon substitution of this value into Eq. (14.13), the deflection u is obtained in the form

$$u = \frac{pR^2(1+\nu)}{Eh}\sin\varphi\left[\ln\frac{1+\cos\varphi}{1+\cos\varphi_1} + \frac{\cos\varphi - \cos\varphi_1}{(1+\cos\varphi)(1+\cos\varphi_1)}\right]. \tag{14.14}$$

Then Eq. (13.44) yields w.

Up to this point, we have assumed that domes were closed at their apex. Now let us analyze the membrane forces distribution in a spherical dome under self-weight, which has a skylight at its top (Fig. 14.3).

In this case, the dome has the form of a truncated sphere with a reinforcing ring used to support the upper structure (skylight). We assume that p is the weight of the shell surface per unit area and there is a line load q per unit length at the top of the dome, due to the weight of the skylight, hood, etc. To find N_1, we substitute $R_1 = R_2 = R$, and $p_3 = p\cos\varphi$, $p_1 = p\sin\varphi$, and $r = R\sin\varphi$ into Eq. (13.34). We have the following:

$$\begin{aligned} N_1 &= -\frac{1}{R\sin^2\varphi}\left[\int_{\varphi_0}^{\varphi} R^2\sin^2\bar{\varphi}\left(p\sin^2\bar{\varphi} + p\cos^2\bar{\varphi}\right)\sin\bar{\varphi}\,\mathrm{d}\bar{\varphi} + qb\right] \\ &= pR\frac{\cos\varphi - \cos\varphi_0}{\sin^2\varphi} - q\frac{b}{R\sin^2\varphi}, \end{aligned}$$

where b is the radius of the parallel circle at the dome top. Since $b = R\sin\varphi_0$, we obtain

$$N_1 = \frac{1}{\sin^2\varphi}[pR(\cos\varphi - \cos\varphi_0) - q\sin\varphi_0]. \tag{14.15}$$

Substituting the above into Eq. (13.39), we obtain

$$N_2 = \frac{1}{\sin^2\varphi}\left[-pR\left(\cos\varphi\sin^2\varphi - \cos\varphi_0 + \cos\varphi\right) + q\sin\varphi_0\right]. \tag{14.16}$$

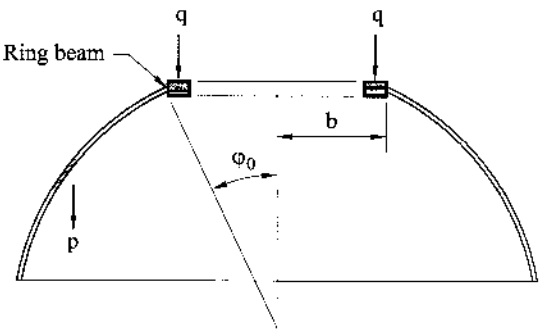

Fig. 14.3

(b) Spherical domes: live or snow loads

Live or snow loads are applied in such a way that they are uniformly distributed over the plan area of the shell surface as opposed to self-weight loading, which is uniformly distributed over the surface area. If q is the loading defined on the plan area, then referring to Fig. 14.4a, we can obtain an equivalent load p defined on the surface area from the following relationship ($ds = R d\varphi$):

$$pR d\varphi = (qR d\varphi)\cos\varphi \quad \text{or} \quad p = q\cos\varphi. \tag{14.17}$$

Thus, from Eqs (14.1), we obtain

$$p_3 = q\cos^2\varphi, \quad p_1 = q\sin\varphi\cos\varphi. \tag{14.18}$$

Substituting these values into Eq. (13.38) and again setting $R_1 = R_2 = R$ and $r = R\sin\varphi$, we have

$$N_1 = -\frac{1}{R\sin^2\varphi}\int_0^{\varphi} qR^2\left(\sin^2\bar{\varphi}\cos\bar{\varphi} + \cos^3\bar{\varphi}\right)\sin\bar{\varphi}\, d\bar{\varphi}.$$

Evaluating this integral yields the following expression for the meridional force:

$$N_1 = -\frac{qR}{2}. \tag{14.19}$$

Substituting this into Eq. (13.39) we obtain the circumferential force:

$$N_2 = -\frac{qR}{2}\cos 2\varphi. \tag{14.20}$$

The meridional and circumferential forces distributions are shown in Fig. 14.4b. Referring to these diagrams, we can see that N_1 is compressive throughout the dome, from $\varphi = 0^\circ$ to $\varphi = 90^\circ$, while N_2 is a tensile force beyond $\varphi = 45^\circ$.

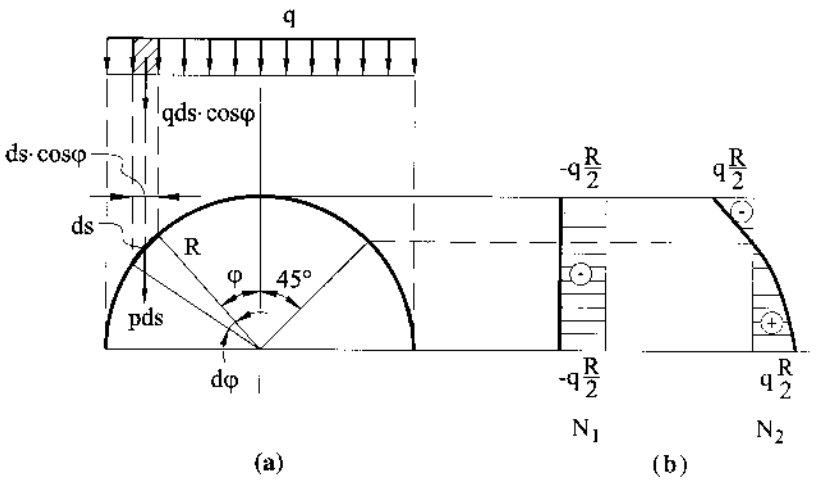

Fig. 14.4

14.1.2 Conic roofs: axisymmetric loading

Consider a planetarium dome that may be approximated as an edge-supported truncated cone. We derive expressions for the circumferential and meridional forces for two conditions of loading: (a) self-weight of the shell per unit area of its middle surface (Fig. 14.5a) and (b) snow load uniformly distributed over the shell plan (Fig. 14.5b). Both types of loading are axisymmetric.

For the analysis of this dome under its self-weight, we use the equations derived in Sec. 13.6.2 for conical shells. For the axisymmetric loading, these equations are simplified – namely, $S = 0$ – and the remaining membrane forces are functions of the s coordinate only. The circumferential force N_2 is given by Eq. (13.60). We have the following:

$$N_2 = -p_3 s \cot \varphi, \tag{14.21}$$

where the coordinate s defines the distance of a point of the middle surface measured from the vertex along the generator of the shell, as shown in Fig. 14.5a.

Substituting for N_2 from Eq. (14.21) into the first Eq. (13.58) and setting $S = 0$, we obtain the following expression for the meridional force N_1:

$$N_1 = -\frac{1}{s}\left[\int (p_1 + p_3 \cot \varphi) s \mathrm{d}s + C\right], \tag{14.22}$$

where C is a constant of integration. Substituting for p_1 and p_3 from Eq. (14.1) into Eq. (14.22), yields the following:

$$N_1 = -\frac{p}{s}\int_{s_0}^{s} (\sin \varphi + \cos \varphi \cot \varphi) \bar{s} \mathrm{d}\bar{s} + \frac{C}{s}. \tag{14.23}$$

As no force acts at the top edge of the shell, $C = 0$ and we obtain

$$N_1 = -\frac{p}{s}\int_{s_0}^{s} \frac{\bar{s}}{\sin \varphi} \mathrm{d}\bar{s}.$$

and, finally,

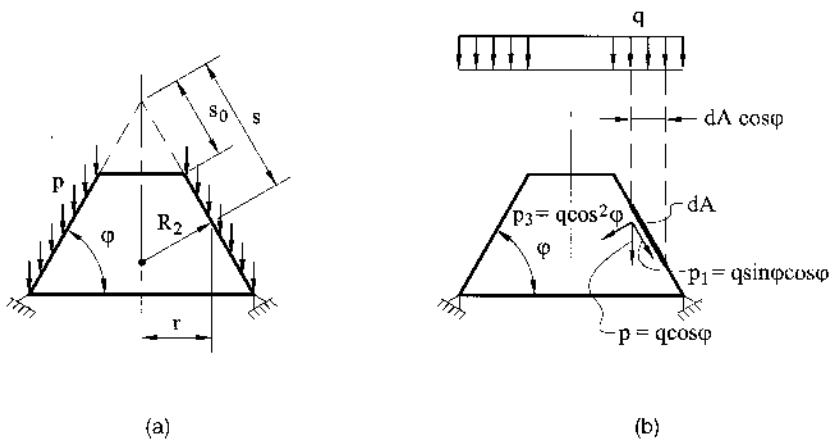

Fig. 14.5

$$N_1 = -\frac{p}{2s}\frac{s^2 - s_0^2}{\sin\varphi}. \tag{14.24}$$

The circumferential force N_2 may be determined from Eq. (14.21) by substituting $p_3 = p\cos\varphi$. We have

$$N_2 = -ps\frac{\cos^2\varphi}{\sin\varphi}. \tag{14.25}$$

To analyze the force components due to the snow load q, defined on the plan area, we use the relations (14.18) to determine the equivalent load components defined on the surface area. Substituting the above relations into Eq. (14.22) yields

$$N_1 = -\frac{1}{s}\int (q\sin\varphi\cos\varphi + q\cos^2\varphi\cot\varphi)s\mathrm{d}s + \frac{C}{s}. \tag{14.26}$$

Evaluating this integral gives the following expression for the meridional force:

$$N_1 = -\frac{qs}{2}\cot\varphi + \frac{C}{s}.$$

The condition that $N_1 = 0$ at $s = s_0$ leads to the following expression for C:

$$C = 0.5qs_0\cot\varphi.$$

Hence,

$$N_1 = -\frac{q}{2s}\left(s^2 - s_0^2\right)\cot\varphi. \tag{14.27}$$

The circumferential force N_2 may be found from Eq. (13.60) by substituting for p_3 from the first relation (14.18), as follows:

$$N_2 = -qs\frac{\cos^3\varphi}{\sin\varphi}. \tag{14.28}$$

The membrane stresses are obtained by dividing the membrane forces given by Eqs (14.27) and (14.28) by the shell thickness h.

14.1.3 Cylindrical shell roofs

Circular cylindrical shells, or "barrel" shells, are frequently used for roof structures. Such a roof structure represents an open cylindrical shell having two curvilinear and two straight edges, as shown in Fig. 14.6a. Cylindrical shell roofs may be supported along curvilinear edges by rigid arches, frames, or solid wall supports that are stiff against deformations in their own planes but that are nearly perfectly flexible for deformations perpendicular to their planes; such supports are called diaphragms. Along the rectilinear edges, these cylindrical shells are supported by the edge beams. The shell roof may be either dome-type convex or suspended membrane-type concave: the former is made of reinforced concrete and is used for relatively small spans, while membrane shell roofs are made of metal (e.g., steel, aluminum alloys) and can cover large span structures.

Consider a circular cylindrical barrel shell of length L under its self-weight (Fig. 14.6a). If p is the dead load per unit area of the shell surface, we can resolve it into components along the normal and circumferential directions.

We have

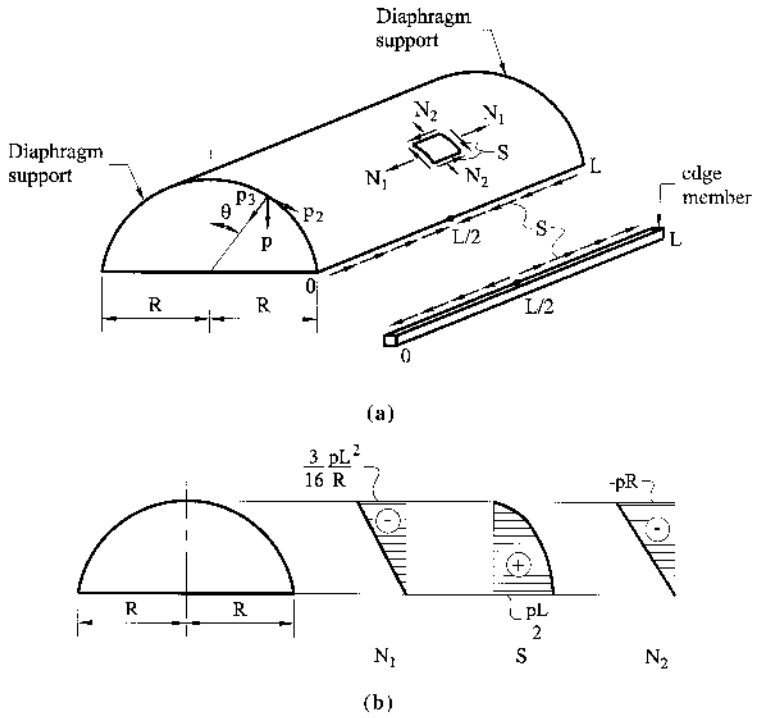

Fig. 14.6

$$p_3 = p\cos\theta, \quad p_2 = p\sin\theta. \tag{14.29}$$

Substituting this loading and $R_2 = R$ into Eqs (13.54), we obtain

$$\begin{aligned} N_2 &= -pR\cos\theta; \quad S = -xF(\theta) + f_1(\theta), \\ N_1 &= \frac{x^2}{2R}\frac{\mathrm{d}F}{\mathrm{d}\theta} - \frac{x}{R}\frac{\mathrm{d}f_1}{\mathrm{d}\theta} + f_2(\theta), \end{aligned} \tag{14.30}$$

where

$$F(\theta) = p_2 - \frac{1}{R}\frac{\mathrm{d}}{\mathrm{d}\theta}(p_3 R). \tag{14.31}$$

The unknown functions $f_1(\theta)$ and $f_2(\theta)$ may be evaluated from the prescribed boundary conditions on the shell edges $x = 0$ and $x = L$. The above conditions for the barrel shells supported by the diaphragms at the edges $x = 0$, L can be formulated, as follows:

$$N_1 = 0\big|_{\substack{x=o \\ x=L}}. \tag{14.32a}$$

Substituting these into the third Eq. (14.30), we have at $x = 0$ and $x = L$:

$$N_1(0) = f_2(\theta) = 0; \quad N_1(L) = \frac{L^2}{2R}\frac{\mathrm{d}F}{\mathrm{d}\theta} - \frac{L}{R}\frac{\mathrm{d}f_1}{\mathrm{d}\theta} = 0.$$

Thus,

$$f_1(\theta) = \frac{L}{2}F(\theta) + C. \tag{14.33}$$

For a given constant loading along x, we expect that the membrane forces N_1 and N_2 will be symmetrical, while S will be inversely symmetrical about the shell midspan, i.e., at $x = L/2$. Thus,

$$S = 0|_{x=L/2} \tag{14.32b}$$

Substituting for p_3 and p_2 from Eq. (14.29) into Eq. (14.31), we obtain

$$F(\theta) = p\sin\theta + \frac{p}{R}R\sin\theta = 2p\sin\theta, \tag{14.34}$$

and inserting the above together with Eq. (14.33) into the second Eq. of (14.30), we can write the expression for S in the following explicit form:

$$S = -2px\sin\theta + \frac{L}{2}2p\sin\theta + C = 2p\sin\theta\left(\frac{L}{2} - x\right) + C. \tag{14.35}$$

Applying the condition (14.32b), we obtain

$$C = 0.$$

Finally, all the membrane forces for the given loading may be represented in the form

$$N_1 = -\frac{px}{R}(L - x)\cos\theta; \quad N_2 = -pR\cos\theta; \quad S = 2p\left(\frac{L}{2} - x\right)\sin\theta. \tag{14.36}$$

The variation of N_1, N_2, and S over the depth of the cross section x = L/4of the semicircular barrel shell under self-weight is shown in Fig. 14.6b.

It follows from Eqs (14.36) that $N_2 = 0$ at $\theta = \pm\pi/2$. However, the shear force S does not vanish on the straight edges of the shell, as it is required there for the free edges. Figure 14.6a shows the variation of the membrane shear forces S from $x = 0$ to $x = L$ at the edge $\theta = \pi/2$. From this diagram, it is seen that these edge forces are self-equilibrating. To resist these forces, the edge members are employed. The latter are loaded by forces equal and opposite to the edge forces on the shell, i.e., S. Since the edge shell is compressed by the shear forces S, the edge member is stressed in tension only (Fig. 14.6a). Thus, the edge members are subjected to tensile axial loads $2p(L/2 - x)$ (for $\theta = \pi/2$) and they have free ends at the diaphragm supports. This tensile loading is balanced by the internal axial forces $T(x)$, which are zero at $x = 0$, L and may be found from the free-body diagram of the part of this edge member. We obtain from equilibrium the following expressions:

$$T(x) = \int_0^x 2p\left(\frac{L}{2} - x\right)\mathrm{d}x = 2p\left(\frac{L}{2}x - x^2\right).$$

This force has a maximum at $x = L/2$, which is given by

$$T_{\max} = \frac{pL^2}{4}.$$

The total compressive force on the cross section of the shell at $x = L/2$ may be obtained by substituting $x = L/2$ into the first Eq. (14.36) and integrating over the cross section. We have, at $x = L/2$,

$$R = 2\int_0^{\pi/2} N_1 R\mathrm{d}\theta = -\frac{pL^2}{2}\int_0^{\pi/2} \cos\theta \mathrm{d}\theta = -\frac{pL^2}{2}.$$

It is seen that this unbalanced compressive force on the shell cross section is balanced by the tensile forces $T_{\max}$ in the two edge beams, which must be provided. Similarly, equilibrium will be satisfied on any other section along the shell span. Thus, a semicircular barrel shell can support dead load under membrane conditions if the tension edge members are provided at their bottom edges. However, the membrane conditions are not satisfied because of the incompatibility of deformations at the shell edges. Indeed, as follows from the first Eq. (14.36), $N_1 = 0$ at $\theta = \pm\pi/2$. On the other hand, the edge member has tensile forces $T(x)$, which will cause it to extend in the axial direction. Moreover, due to its own weight, the edge member will tend to deflect vertically. These deflections will be different from the vertical deformations of the shell and edge members. The membrane theory alone cannot eliminate these incompatibilities of deformations and must be complemented by the bending theory (see Chapter 15).

When a cylindrical shell cross section has edges with an angle θ different from 90° (e.g., less than 90°), there arise further complications associated with an application of the membrane theory. In fact, in this case, N_2 (see the second Eq. of (14.36)) will now be nonzero at the longitudinal edges. Thus, the edge member has to resist both N_2 and S forces from the shell edges. This gives rise to further incompatibilities of deformation and requires an application of the bending theory of shells.

The procedure for the membrane analysis of cylindrical shells under self-weight described above is a particular case of a more general approach based on a Fourier series expansion. The governing differential equations for the membrane forces in cylindrical shells are given by Eqs (13.50). These equations have constant coefficients in x and, hence, they can be solved by representing solutions in the form of cosine and sine functions in x.

For barrel shells having simply supported edges $x = 0$ and $x = L$, which are commonly constructed as roof structures, the solutions of Eqs (13.50) can be represented as follows:

$$N_1 = \sum_{n=1}^{\infty} N_{1n} \sin\frac{n\pi x}{L}, \quad S = \sum_{n=0}^{\infty} S_n \cos\frac{n\pi x}{L}, \quad N_2 = \sum_{n=1}^{\infty} N_{2n} \sin\frac{n\pi x}{L}. \qquad (14.37)$$

It can be shown that the above solutions satisfy the simply supported boundary conditions. The load components are also expanded into Fourier series in x. This can be done by assuming odd extensions of the loads in the interval $(0, L)$ (refer to Appendix B). Introducing Eqs (14.37) and the load expansions into Eqs (13.50), solutions for membrane stress resultants can be obtained (after solving the resulting ordinary differential equations).

14.1.4 Shell roofs in the form of an elliptic or hyperbolic paraboloid covering rectangular areas

Such a type of roof is commonly used for covering public and sports buildings. Elliptic and hyperbolic paraboloids, considered in this section, fall into the category of shells of translation introduced in Sec. 11.7.

At first, assume that an *elliptic paraboloid* covers a rectangular area with the dimensions $2a \times 2b$ and that it is subjected to a uniform vertical surface load of intensity $p_3 = p$ (Fig. 14.7a). The equation of the shell middle surface in this case can be represented as

$$z = f\left(\frac{x^2}{2a^2} + \frac{x^2}{2a^2}\frac{y^2}{2b^2}\right)y^2. \tag{14.38}$$

Taking into account, we obtain

$$\frac{\partial^2 z}{\partial x^2} = \frac{f}{a^2}, \frac{\partial^2 z}{\partial y^2} = \frac{f}{b^2}, \quad \text{and} \quad \frac{\partial^2 z}{\partial x \partial y} = 0.$$

Assume, for simplicity, that $\bar{p}_3 \approx p_3 = p$, i.e., the vertical surface load per unit area of the middle surface is approximately equal to the vertical load of the horizontal projection of the middle surface. Then, substituting the above into Eq. (13.78), yields the following:

$$\frac{1}{b^2}\frac{\partial^2 \Phi}{\partial x^2} + \frac{1}{a^2}\frac{\partial^2 \Phi}{\partial y^2} = -\frac{p}{f}. \tag{14.39}$$

Assume then that the shell edges are attached to supporting arches, so that the membrane forces N_1 and N_2 are zero and the vertical load is transmitted to the supports by means of the membrane shear forces. Express these boundary conditions in terms of the function Φ. Taking into account the relations (13.77) and (13.72), we can write the boundary conditions on the shell edges as follows:

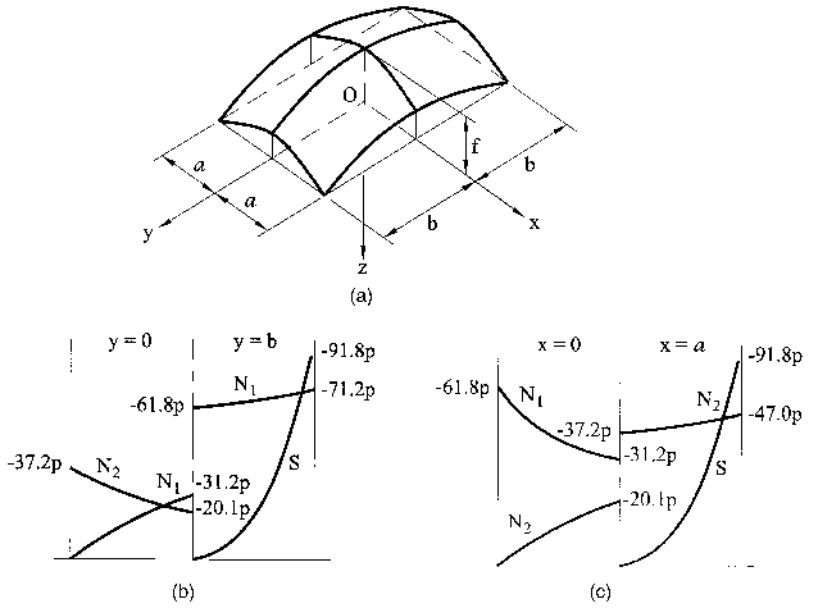

Fig. 14.7

$$N_1 = 0 \quad \text{and} \quad \frac{\partial^2 \Phi}{\partial y^2} = 0 \Bigg|_{x=\pm a}, \tag{14.40a}$$

$$N_2 = 0 \quad \text{and} \quad \frac{\partial^2 \Phi}{\partial x^2} = 0 \Bigg|_{y=\pm b}. \tag{14.40b}$$

The solution of Eq. (14.39) is sought in the form

$$\Phi = \sum_n C_n \cos \alpha_n x \cosh \beta_n y - \frac{p}{2f} b^2 x^2, \tag{14.41}$$

where

$$\alpha_n = \frac{n\pi}{2a}, \quad \beta_n = \frac{n\pi}{2b}; \quad n = 1, 3, 5, \ldots.$$

It can be easily shown that Φ in the form of Eq. (14.41) satisfies exactly the homogeneous equation (14.39) and the boundary conditions (14.40a). The constants of integration C_n are evaluated from the boundary conditions (14.40b). We have

$$\left.\frac{\partial^2 \Phi}{\partial x^2}\right|_{y=\pm b} = -\frac{\pi^2}{4a^2} \sum_n n^2 C_n \cos \alpha_n x \cosh \beta_n y - \frac{pb^2}{f} = 0.$$

Next, expand the value $\left(-pb^2/f\right)$ into the Fourier series

$$-\frac{pb^2}{f} = \sum_n A_n \cos \alpha_n x, \tag{14.42a}$$

where

$$A_n = \frac{2}{a} \int_0^a \left(-\frac{pb^2}{f}\right) \cos \frac{n\pi x}{2a} \, \mathrm{d}x = -\frac{4pb^2}{\pi f} \frac{1}{n} \sin \frac{n\pi}{2}. \tag{14.42b}$$

Then,

$$\left.\frac{\partial^2 \Phi}{\partial x^2}\right|_{y=\pm b} = \sum_n \left(-\frac{\pi^2}{4a^2} n^2 \cosh \beta_n b C_n - \frac{4pb^2}{\pi f} \frac{1}{n} \sin \frac{n\pi}{2}\right) \cos \alpha_n x. \tag{14.43}$$

This expression is equal to zero if

$$C_n = -\frac{16pa^2b^2 \sin \frac{n\pi}{2}}{n^3 \pi^3 f \cosh(n\pi/2)}. \tag{14.44}$$

Introducing C_n from Eq. (14.44) into Eq. (14.41), we obtain the expression for Φ, that satisfies the differential equation (14.39) and the prescribed boundary conditions (14.40).

Knowing the function Φ, we can determine $\bar{N}_1$, $\bar{N}_2$, and $\bar{S}$ using the relations (13.55) as follows:

$$\bar{N}_1 = -\frac{4pa^2}{\pi f}\sum_n \frac{\sin(n\pi/2)}{n\cosh(n\pi/2)}\cos\alpha_n x\cosh\beta_n y,$$

$$\bar{N}_2 = \frac{4pb^2}{\pi f}\sum_n \frac{\sin(n\pi/2)}{n\cosh(n\pi/2)}\cos\alpha_n x\cosh\beta_n y - \frac{pb^2}{f}, \tag{14.45}$$

$$\bar{S} = -\frac{4pab}{\pi f}\sum_n \frac{\sin(n\pi/2)}{n\cosh(n\pi/2)}\sin\alpha_n x\sinh\beta_n y.$$

Having determined the components of the horizontal projections of the membrane forces, we can calculate the membrane forces themselves using the relations (13.72).

Figures 14.7b and c show the membrane force diagrams for a shell with the following dimensions: $a = 25\,\text{m}$, $b = 20\,\text{m}$, and $f_x = f_y = 5\,\text{m}$ (from Ref. [1]). It follows from these diagrams that the membrane shear forces increase very rapidly approaching infinity at the corner points. This testifies that the membrane theory alone cannot be applied near the corner points. However, the given formulas and relations describe quite accurately the stress state throughout the shell, except for comparatively small areas near the corner points. In addition, they indicate that these areas should be reinforced due to the presence of the bending and twisting moments.

A roof in the form of a *hyperbolic paraboloid,* covering the rectangular area, can be analyzed similarly. The equation of such surface is given by

$$z = f\left(\frac{x^2}{2a^2} - \frac{y^2}{2b^2}\right) \tag{14.46}$$

The governing differential equation for the function Φ will differ from Eq. (14.39) by the sign for the first term only, i.e.,

$$-\frac{1}{b^2}\frac{\partial^2\Phi}{\partial x^2} + \frac{1}{a^2}\frac{\partial^2\Phi}{\partial y^2} = -\frac{p}{f}. \tag{14.47}$$

Its solution can be represented in the form

$$\Phi = \sum_n C_n \sin\alpha_{n-1}x\cos\beta_{n-1}y - \frac{pb^2}{2f}x^2, \tag{14.48}$$

where

$$\alpha_{n-1} = \frac{\pi(n-1)}{2a}, \quad \beta_{n-1} = \frac{\pi(n-1)}{2b}; \quad n = 1, 3, 5, \ldots.$$

Here

$$C_n = -\frac{16pa^2b^2(1 - \cos\frac{n-1}{2}\pi)}{(n-1)^3\pi^3 f\cos\frac{n-1}{2}\pi}.$$

Having determined Φ, we can calculate $\bar{N}_1$, $\bar{N}_2$, and $\bar{N}_{12}$ as follows:

$$\bar{N}_1 = -\sum_n C_n \beta_{n-1}^2 \sin \alpha_{n-1} x \cos \beta_{n-1} y,$$

$$\bar{N}_2 = -\sum_n C_n \alpha_{n-1}^2 \sin \alpha_{n-1} x \cos \beta_{n-1} y - \frac{pb^2}{f}. \tag{14.49}$$

$$\bar{N}_{12} = \sum_n C_n \alpha_{n-1} \beta_{n-1} \cos \alpha_{n-1} x \sin \beta_{n-1} y$$

Roofs with hyperbolic paraboloid surfaces are commonly made as suspended shells, because in this shape the roof's state of stress is in good agreement with the momentless scheme of the analysis.

14.1.5 Asymmetrically loaded domes: wind loading

In the general case of asymmetrically loaded domes, the governing equations of the membrane theory of shells of revolution must be solved without the simplifications provided by the axisymmetric membrane theory. As an example of the application of the general membrane theory, we consider shells subjected to wind loads.

The value and distribution of the wind loading can be established by testing models of structures in wind tunnels. There are special standard relationships that allow us to determine the value and distribution of wind loading for commonly used types of structures.

It is usual to represent dynamic loading, such as wind and earthquake effects, by statically equivalent for the purposes of design. The wind load on shell structures is composed of pressure on the wind side and suction on the leeward side. Here the load component acting perpendicular to the middle surface p_3 is taken into account. The components p_1 and p_2 are due to the friction forces and are of negligible magnitude. Assuming, for the sake of simplicity, that the wind acts in the direction of the meridian plane $\theta = 0^\circ$, the components of the wind pressure are of the form [2]

$$p_1 = p_2 = 0, \;\; p_3 = p \sin \varphi \cos \theta, \tag{14.50}$$

where p represents the static wind pressure intensity. Figure 14.8 shows the distribution of the wind load given by Eq. (14.50) on a spherical dome.

The differential equation (13.23) for the wind loading, given by Eq. (14.50), has the following form (making $n = 1$):

$$\frac{1}{R_1 R_2 \sin \varphi} \frac{\mathrm{d}}{\mathrm{d}\varphi} \left(\frac{R_2^2 \sin \varphi}{R_1} \frac{\mathrm{d}U_1}{\mathrm{d}\varphi} \right) - \frac{U_1}{R_1 \sin^2 \varphi} = F_1(\varphi), \tag{14.51}$$

where

$$F_1(\varphi) = -p \left[\frac{1}{R_1 R_2 \sin \varphi} \frac{\mathrm{d}}{\mathrm{d}\varphi} \left(R_2^3 \sin^3 \varphi \cos \varphi \right) - R_2 \sin \varphi \right]. \tag{14.52}$$

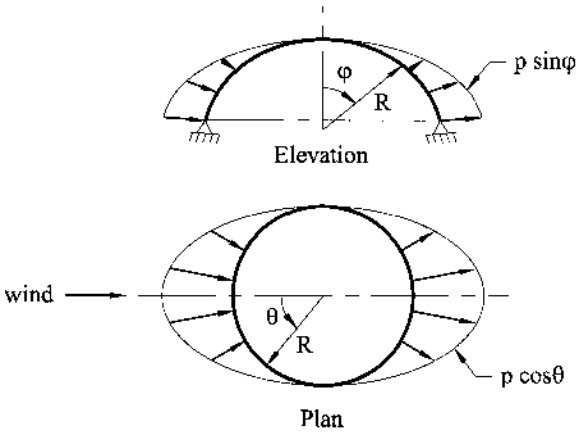

Fig. 14.8

Let us introduce some additional function

$$U_1^* = U_1 R_2 \sin\varphi. \tag{14.53}$$

The replacement of U_1 with U_1^* changes Eq. (14.51) to the form

$$\frac{\mathrm{d}}{\mathrm{d}\varphi}\left(\frac{1}{R_1 \sin\varphi}\frac{\mathrm{d}U_1^*}{\mathrm{d}\varphi}\right) = R_1 F_1(\varphi). \tag{14.54}$$

The function U_1^* can be evaluated as a result of two successive integrations and using the integration by parts formula. Dropping intermediate mathematics, one obtains the following final result:

$$U_1^* = -p\left[C_1 \int_{\varphi_0}^{\varphi} R_1 \sin\bar{\varphi}\mathrm{d}\bar{\varphi} + \int_{\varphi_0}^{\varphi} \Phi(\bar{\varphi}) R_1 \sin\bar{\varphi}\mathrm{d}\bar{\varphi} + C_2\right], \tag{14.55}$$

where φ_0 can be chosen arbitrarily. Further, it will be identified with the angle determining the upper edge of a shell (for truncated shells). The function $\Phi(\varphi)$ is given by

$$\Phi(\varphi) = R_2^2 \sin^2\varphi\cos\varphi - \int_{\varphi_0}^{\varphi} R_1 R_2 \sin^3\bar{\varphi}\,\varphi\mathrm{d}\bar{\varphi}. \tag{14.56}$$

In Eq. (14.55), C_1 and C_2 are the constants of integration. Using Eq. (14.53), we determine U_1 as follows:

$$U_1 = \frac{U_1^*}{R_2 \sin\varphi} = -\frac{p}{R_2 \sin\varphi}\left[C_1 \int_{\varphi_0}^{\varphi} R_1 \sin\bar{\varphi}\mathrm{d}\bar{\varphi} + \int_{\varphi_0}^{\varphi} \Phi(\bar{\varphi}) R_1 \sin\bar{\varphi}\mathrm{d}\bar{\varphi} + C_2\right], \tag{14.57}$$

Using the relations (13.10), (13.8c), and (13.22), we find the membrane forces N_1 and N_2, as follows (for simplicity, the superscripts 1, corresponding to the first term in the expansion (13.27), are dropped below):

$$N_1 = -\frac{p}{R_2^2 \sin^3 \varphi}\left[C_1 \int_{\varphi_0}^{\varphi} R_1 \sin\bar{\varphi} \mathrm{d}\bar{\varphi} + \int_{\varphi_0}^{\varphi} \Phi(\bar{\varphi}) R_1 \sin\bar{\varphi}\mathrm{d}\bar{\varphi} + C_2\right]\cos\theta, \tag{14.58}$$

$$N_2 = -p\left\{R_2 \sin\varphi - \frac{1}{R_1 R_2 \sin^3\varphi}\left[C_1 \int_{\varphi_0}^{\varphi} R_1 \sin\bar{\varphi}\mathrm{d}\bar{\varphi} + \int_{\varphi_0}^{\varphi} \Phi(\bar{\varphi}) R_1 \sin\bar{\varphi}\mathrm{d}\bar{\varphi} + C_2\right]\right\}\cos\theta. \tag{14.59}$$

Knowing U_1, we can determine V_1 from the first Eq. (13.11). We have the following

$$\frac{\partial V}{\partial\theta} = -p_3 R_2^3 \sin^2\varphi\cos\varphi - \frac{R_2^2 \sin\varphi}{R_1}\frac{\partial U}{\partial\varphi} = -p\left\{R_2^3 \sin^3\varphi\cos\varphi - \left[C_1\left(R_2\sin\varphi - \cot\varphi\int_{\varphi_0}^{\varphi} R_1\sin\bar{\varphi}\mathrm{d}\bar{\varphi}\right) + \Phi(\varphi)R_2\sin\varphi - \cot\varphi\int_{\varphi_0}^{\varphi}\Phi(\bar{\varphi})R_1\sin\bar{\varphi}\mathrm{d}\bar{\varphi} - C_2\cot\varphi\right]\right\}\cos\theta.$$

Taking into account the second relation (13.10), we obtain the following (again dropping the superscript 1 for the membrane shear force):

$$S = \frac{V}{R_2^2\sin^2\varphi} = -p\left[R_2\sin\varphi - C_1\left(\frac{1}{R_2\sin\varphi} - \frac{\cos\varphi}{R_2^2\sin^3\varphi}\int_{\varphi_0}^{\varphi} R_1\sin\bar{\varphi}\mathrm{d}\bar{\varphi}\right) - \frac{\Phi(\varphi)}{R_2\sin\varphi} + \frac{\cos\varphi}{R_2^2\sin^3\varphi}\int_{\varphi_0}^{\varphi}\Phi(\bar{\varphi})R_1\sin\bar{\varphi}\mathrm{d}\bar{\varphi} + \frac{C_2\cos\varphi}{R_2^2\sin^3\varphi}\right]\sin\theta. \tag{14.60}$$

The constants of integration, C_1 and C_2, are to be evaluated by assigning the membrane forces N_1 and N_2 on the upper edge of the shell, i.e., at $\varphi = \varphi_0$. Denoting these forces by $N_1^{(0)}$ and $S^{(0)}$, and letting $\varphi = \varphi_0$ in Eqs (14.58) and (14.60), we obtain the following expressions:

$$C_1 = -\frac{1}{p}\left[N_1^{(0)}\left(R_2^{(0)}\right)^2 \sin\varphi_0\cos\varphi_0 - S^{(0)}R_2^{(0)}\sin\varphi_0\right],$$
$$C_2 = -\frac{\left[\left(R_2^{(0)}\right)^2\sin^3\varphi_0\right]}{p}N_1^{(0)}. \tag{14.61}$$

For domes closed at the vertex, we have $\varphi_0 = 0$ and $C_1 = C_2 = 0$.

As an example, let us determine the expressions for the membrane forces for a spherical dome of radius R (see Fig. 14.8). For this particular case, $R_1 = R_2 = R$, $\varphi_0 = 0$ and

$$\Phi(\varphi) = R^2\left(\sin^2\varphi\cos\varphi - \int_0^{\varphi}\sin^3\bar{\varphi}\,\mathrm{d}\bar{\varphi}\right) = R^2[\sin^2\varphi\cos\varphi - (1-\cos\varphi) + \frac{1}{3}(1-\cos^3\varphi)]$$

$$N_1 = -\frac{pR}{\sin^3\varphi}\int_0^{\varphi}\left[\sin^3\bar{\varphi}\cos\bar{\varphi} - (1-\cos\bar{\varphi})\sin\bar{\varphi} + \frac{1}{3}(1-\cos^3\bar{\varphi})\sin\bar{\varphi}\right]\mathrm{d}\bar{\varphi}\cos\theta$$

$$= -\frac{pR}{3\sin^3\varphi}\left[\sin^2\varphi(1+\sin^2\varphi) - 2(1-\cos\varphi)\right]\cos\theta,$$

$$S = -\frac{pR}{3\sin^3\varphi}\left[2-\cos\varphi(2+\sin^2\varphi)\right]\sin\theta,$$

$$N_2 = -\frac{pR}{3\sin^3\varphi}\left[\sin^2\varphi(2\sin^2\varphi - 1) + 2(1-\cos\varphi)\right]\cos\theta. \tag{14.62}$$

It is seen from Eqs (14.62) that the maximum values of the membrane forces occur as follows:

- for the meridional forces, N_1, at $\varphi \approx \pi/4$ and $\theta = 0,\pi$;
- for the circumferential forces, N_2 at $\varphi = \pi/2$ and $\theta = 0,\pi$; and
- for the shear forces, S, at $\varphi = \pi/2$ and $\theta = \pi/2, 3\pi/2$.

At the top of the dome ($\varphi = 0$), all the membrane forces are zero. Figure 14.9 depicts the variations of N_1 and N_2 along the meridian $\theta = 0$ and the variation of S along the meridian $\theta = 90^\circ$.

14.2 MEMBRANE ANALYSIS OF LIQUID STORAGE FACILITIES

14.2.1 Introduction

Liquid storage facilities in the form of tanks, elevated water towers, cooling towers, etc., are widely used. They are made of steel or concrete and represent multishell structures, i.e., a combination of spherical, cylindrical, and conical shells, and

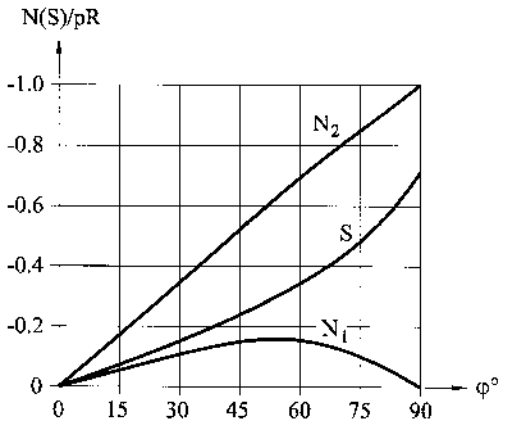

Fig. 14.9

circular plate, and circular rings located axisymmetrically. They are loaded axisymmetrically, to withstand water or gas pressure, dead or live loads, etc., or asymmetrically, for example, to withstand wind pressure. First, we consider the axisymmetric-type loading.

The walls of closed tanks designed for carrying liquids and gases are subjected to normal pressure forces p_3 (see Fig. 14.10). These forces consist of an excess pressure of gases p^* and the hydrostatic liquid pressure. The law of varying of the hydrostatic pressure over the tank depth can be expressed as

$$p_3 = -[p^* + \gamma_l(x - x^*)], \tag{14.63}$$

where γ_l is the specific weight of the liquid; x and x^* are the coordinates of parallels corresponding to the cross section of interest and the upper level of liquid, respectively. These coordinates are measured from a vertex of the tank or from its upper edge (Fig. 14.10).

Let us go from the x coordinate to the angular coordinate φ. Using the relationships

$$\frac{\mathrm{d}x}{\mathrm{d}r} = \tan\varphi, \quad \frac{\mathrm{d}r}{\mathrm{d}\varphi} = R_1 \cos\varphi, \tag{14.64}$$

we find

$$\mathrm{d}x = \tan\varphi \mathrm{d}r, \quad x = \int_{\varphi_0}^{\varphi} \tan\bar{\varphi}\mathrm{d}r = \int_{\varphi_0}^{\varphi} R_1 \sin\bar{\varphi}\mathrm{d}\bar{\varphi} \tag{14.65}$$

and

$$x - x^* = \int_{\varphi_0}^{\varphi} R_1 \sin\bar{\varphi}\mathrm{d}\bar{\varphi} - \int_{\varphi_0}^{\varphi^*} R_1 \sin\bar{\varphi}\mathrm{d}\bar{\varphi} = \int_{\varphi^*}^{\varphi} R_1 \sin\bar{\varphi}\mathrm{d}\bar{\varphi}. \tag{14.66}$$

Substituting the above into Eq. (14.63), we obtain

$$p_3 = -\left[p^* + \gamma_l \int_{\varphi^*}^{\varphi} R_1 \sin\bar{\varphi}\mathrm{d}\bar{\varphi}\right], \tag{14.67}$$

where φ_0 and φ^* are the meridional angles corresponding to the coordinates $x = 0$ and $x = x^*$, respectively.

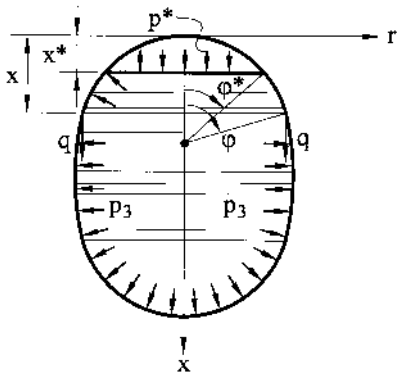

Fig. 14.10

The meridional forces for tanks can be determined from Eq. (13.33b) and Eq. (13.39). The former equation can be rewritten for tanks, taking into account Eq. (14.67) and noting that $p_1 = 0$, as follows:

$$N_1 = \frac{1}{R_2 \sin^2 \varphi}\left[p^* \int_{\varphi_0}^{\varphi} R_1 R_2 \cos\bar{\varphi} \sin\bar{\varphi} \mathrm{d}\bar{\varphi}\right.$$

$$\left. + \gamma_l \int_{\varphi_0}^{\varphi} R_1 R_2 \cos\bar{\varphi} \sin\bar{\varphi} \mathrm{d}\bar{\varphi} \int_{\varphi^*}^{\varphi} R_1 \sin\bar{\varphi} \mathrm{d}\bar{\varphi}\right] + \frac{N_1^{(0)} R_2^{(0)} \sin^2 \varphi_0}{R_2 \sin^2 \varphi} \tag{14.68}$$

If we take into account relation (13.6b), then the first integral in the square brackets can be represented as follows:

$$\int_{\varphi_0}^{\varphi} R_2 \sin\bar{\varphi} \cdot \mathrm{d}(R_2 \sin\bar{\varphi}) = \frac{1}{2}\left(R_2^2 \sin^2 \varphi - (R_2^{(0)})^2 \sin^2 \varphi_0\right).$$

Then, Eq. (14.68) appears as

$$N_1 = \frac{p^* R_2}{2} + \frac{\gamma_l}{R_2 \sin^2 \varphi} \int_{\varphi^*}^{\varphi} R_1 R_2 \cos\bar{\varphi} \sin\bar{\varphi} \mathrm{d}\bar{\varphi} \int_{\varphi^*}^{\varphi} R_1 \sin\bar{\varphi} \mathrm{d}\bar{\varphi}$$
$$+ \left(N_1^{(0)} - \frac{p^* R_2^{(0)}}{2}\right) \frac{R_2^{(0)} \sin^2 \varphi_0}{R_2 \sin^2 \varphi}. \tag{14.69}$$

In the second term of Eq. (14.69), the lower limit of the first integral is φ^*, because for $\varphi < \varphi^*$ the hydrostatic pressure of the liquid is zero.

Below we consider the membrane analysis of liquid storage facilities made of various forms of shells of revolution under axisymmetric and asymmetric loads.

14.2.2 Spherical storage tank with supports in its diametrical plane: axisymmetric loading

For a closed spherical shell $R_1 = R_2 = R_1^{(0)} = R_2^{(0)} = R$ and $\varphi_0 = 0$. Then, it follows from Eq. (14.69) that

$$N_1 = \frac{p^* R}{2} + \frac{\gamma_l R^2}{6 \sin^2 \varphi}\left[\cos^3 \varphi^* - \cos^2 \varphi (3 \cos\varphi^* - 2 \cos\varphi)\right]. \tag{14.70}$$

Since the meridional forces N_1 have an obvious abrupt change at the support ($\varphi = \pi/2$), Eq. (14.70) is valid for $\varphi < \pi/2$.

The circumferential force can be found from Eq. (13.39) as follows:

$$N_2 = -(p_3 R + N_1), \tag{14.71}$$

where

$$p_3 = p^* + \gamma_l R \int_{\varphi^*}^{\varphi} \sin\bar{\varphi} \mathrm{d}\bar{\varphi} = p^* + \gamma_l R(\cos\varphi^* - \cos\varphi).$$

Let us determine the meridional forces in the lower portion of the sphere tank, i.e., for $\varphi > \pi/2$. Taking the lower vertex of the sphere as a reference point for the reading of the meridional angles φ, we replace the lower limit in the first integral of Eq. (14.69) with π, i.e., $\varphi_0 = \pi$. We obtain the following:

$$N_1 = \frac{p^* R}{2} + \frac{\gamma_l R^2}{\sin^2 \varphi} \int_{\pi}^{\varphi} \cos \bar{\varphi} \sin \bar{\varphi} \mathrm{d}\bar{\varphi} \int_{\varphi^*}^{\varphi} \sin \bar{\varphi} \mathrm{d}\bar{\varphi} = \frac{p^* R}{2} + \frac{\gamma_l R^2}{6} \left(3 \cos \varphi^* + 2 \frac{1 + \cos^3 \varphi}{\sin^2 \varphi} \right) \tag{14.72}$$

It follows from Eq. (14.70) that, at the support, for $\varphi = \pi/2$, we derive

$$N_1^{'} = \frac{p^* R}{2} + \frac{\gamma_l R^2}{6} \cos^3 \varphi^*.$$

On the other hand, from Eq. (14.72), for $\varphi = \pi/2$, the meridional force is

$$N_1^{''} = \frac{p^* R}{2} + \frac{\gamma_l R^2}{6} (3 \cos \varphi^* + 2).$$

Thus, the value of the abrupt change in the meridional force at the support level in the diametrical plane is

$$\Delta N_1 = N_1^{''} - N_1^{'} = \frac{\gamma_l R^2}{6} (3 \cos \varphi^* + 2 - \cos^3 \varphi^*). \tag{14.73}$$

In particular, if the spherical tank is completely filled by a liquid only, i.e., $p^* = 0$ and $\varphi^* = 0$, then

$$\Delta N_1 = \frac{2}{3} \gamma_l R^2. \tag{14.74a}$$

Recalling that the volume of the sphere is $V = \frac{4}{3} \pi R^3$, we can rewrite Eq. (14.74a), as follows:

$$\Delta N_1 = \frac{V \gamma_l}{2 \pi R}. \tag{14.74b}$$

The above represents the meridional force, which balances the liquid weight filling the spherical tank. Thus, the meridional forces N_1 at the sphere portion $0 \leq \varphi < \pi/2$ are to be determined from Eq. (14.70) and at the portion $\pi/2 \leq \varphi \leq \pi$ from Eq. (14.72). The circumferential force N_2 is determined from Eq. (14.71) for both portions of the sphere, taking into account that N_1 for the upper and lower portions are given by Eqs (14.70) and (14.72), respectively. It is seen from the above equations that the maximum values of the meridional forces take place when the spherical storage tank is completely filled by a liquid.

Determine the limit of the second term in parentheses of Eq. (14.72) when $\varphi \to \pi$. Using the L'Hospital's rule, we obtain

$$N_1\big|_{\varphi=\pi} = \frac{p^* R}{2} + \frac{\gamma_l R^2}{2} (1 + \cos \varphi^*). \tag{14.75}$$

With the use of Eq. (14.71), it will be easily established that

$$N_1|_{\varphi=\pi} = N_2|_{\varphi=\pi}.$$

The meridional and circumferential force, N_1 and N_2, diagrams for the spherical storage tank filled completely by a liquid of a specific weight γ_l are shown in Fig. 14.11.

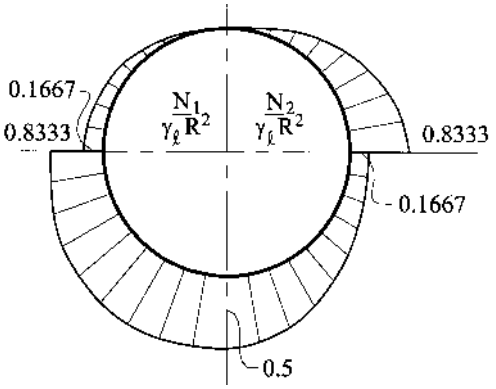

Fig. 14.11

Determination of the meridional and circumferential forces in the spherical tank caused by a *self-weight and snow loading* should present no problems. We denote the load intensity due to the self-weight and snow cover by q_1 and q_2, respectively. The latter will be assumed to be uniform at the portion from the tank vertex to the parallel that corresponds to some value $\varphi = \varphi_2$.

It follows from Eq. (14.1) and Eq. (14.10) that

$$p_1 = q\sin\varphi \quad \text{and} \quad p_3 = q\cos\varphi.$$

Substituting the above into Eq. (13.33b) and taking into account that for a closed spherical tank $R_1 = R_2 = R$ and $\varphi_0 = 0$ and $N_1^{(0)} = 0$, we obtain

$$N_{1q} = -\frac{qR}{\sin^2\varphi}\int_0^{\varphi}\sin\bar{\varphi}\mathrm{d}\bar{\varphi} = -\frac{qR}{\sin^2\varphi}(1-\cos\varphi). \tag{14.76}$$

Here, by q it is meant that $q = q_1 + q_2$ for $0 \le \varphi \le \varphi_2$ and q_1 for $\varphi_2 \le \varphi \le \pi/2$.

The meridional force at the lower portion of the tank is derived from Eq. (14.76). Assuming again that the reference point for angles φ is taken at the lower sphere vertex, we obtain

$$N_{1q} = -\frac{qR}{\sin^2\varphi}\int_{\pi}^{\varphi}\sin\bar{\varphi}\mathrm{d}\bar{\varphi} = \frac{qR}{\sin^2\varphi}(1+\cos\varphi). \tag{14.77}$$

Referring to Eqs (14.76) and (14.77) we can conclude that the meridional forces due to the self-weight are compressive over the sphere portion $0 \le \varphi \le \pi/2$, i.e., they are opposite in sign to the forces due to the internal excessive pressure. Over the sphere portion $\pi/2 \le \varphi \le \pi$, the meridional forces load the shell. It can be shown that the values of N_1 change abruptly for $\varphi = \pi/2$ and the amount of this change is equal to the weight of the sphere and snow load per unit the perimeter of the diametrical section of the sphere.

14.2.3 Cylindrical tank with bottom in the form of ellipsoid of revolution: axisymmetric loading

Assume that a cylindrical tank is filled by a liquid with a specific weight γ_l to the level x^* from the top of its cylindrical part, as shown in Fig. 14.12a. In addition, it is

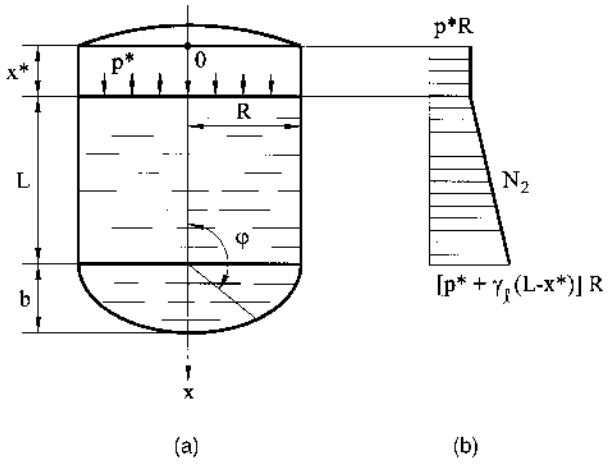

Fig. 14.12

subjected to the gas vapor pressure p^*. Hence, the total normal pressure is determined, as before, by Eq. (14.63). The origin of the coordinate x is taken at the top of the cylinder.

At first, we consider the cylindrical portion of the tank. For the cylinder, $R_1 = \infty$, $R_2 = R$ and from the third Eq. (13.7) and Eq. (14.63), it follows that

$$N_2 = R[p^* + \gamma_l(x - x^*)] \quad \text{for} \quad x \geq x^*. \tag{14.78}$$

The distribution of N_2 for the cylindrical portion of the tank is shown in Fig. 4.12b. As seen from this diagram, N_2 is constant and it equals p^*R over the cylindrical portion where the hydrostatic pressure of the liquid is absent. Then, this force varies according to the linear law of the rise of the hydrostatic pressure and reaches its maximum value at the lower edge of the cylinder. The value of the meridional force N_1 depends on the location of the tank supports. In any case, this force can be directly found from equilibrium of the portion of the cylinder intersected by a plane, perpendicular to the axis of the tank. So, if the tank is suspended at the upper edge of its cylinder, the meridional force is expressed

$$N_1 = \frac{p^* R}{2} + \frac{G_\Sigma}{2\pi R} \tag{14.79}$$

where, $G_\Sigma = G_q + G_l$; $G_q = \int_x^L q_t \mathrm{d}x$ is the self-weight of a portion of the tank located below the section of the interest; q_t is the self-weight of the tank per unit length; and G_l is the self-weight of a liquid filling the cylinder. If the tank is supported at the junction with the lower bottom, then

$$N_1 = \frac{p^* R}{2} - \frac{1}{2\pi R}\int_0^x q_t \mathrm{d}\bar{x}. \tag{14.80}$$

If q_t= const, then the meridional force is

$$N_1 = \frac{p^* R}{2} - \frac{q_t x}{2\pi R}. \tag{14.81}$$

It should be noted that if a tank is filled by a gas only, then the circumferential force N_2 is always greater than the meridional force N_1(twice as large if the self-weight of the tank is ignored in the formulas (14.79) and (14.80)). Therefore, a wall thickness should be selected, as a rule, corresponding to the maximum value of the circumferential forces.

We proceed now to determining the membrane forces for the bottom. The total pressure on the surface of the bottom is

$$p_3 = p^* + \gamma_l(L + \int_{\pi/2}^{\varphi} R_1 \sin\bar{\varphi} \mathrm{d}\bar{\varphi}), \tag{14.82}$$

where L is the height of the cylindrical part of the liquid column. The principal radii of curvature for the ellipsoid of revolution are given by Eqs (11.49). We rewrite these formulas as follows:

$$R_1 = \frac{R(1+\gamma)^{1/2}}{(1+\gamma\sin^2\varphi)^{3/2}}, \quad R_2 = \frac{R(1+\gamma)^{1/2}}{(1+\gamma\sin^2\varphi)^{1/2}}, \tag{14.83}$$

where $\gamma = \dfrac{R^2}{b^2} - 1$, b is the length of the semiaxis of the ellipse (the bottom depth), and R is the radius of the cylindrical portion of the tank. Substituting the expression for R_1 from Eq. (14.83) into Eq. (14.82) and integrating, we obtain after some algebra

$$p_3 = p^* + \gamma_l\left[L - b\frac{\cos\varphi}{(1+\gamma\sin^2\varphi)^{1/2}}\right]. \tag{14.84}$$

Introducing the above into Eq. (14.69) and integrating, we obtain the following expression for the meridional force:

$$\begin{aligned} N_1 = {} & \frac{p^* R_2}{2} + \frac{\gamma_l}{R_2\sin^2\varphi}\int_{\pi/2}^{\varphi} R_1 R_2 \cos\bar{\varphi}\sin\bar{\varphi}\left[L - b\frac{\cos\bar{\varphi}}{(1+\gamma\sin^2\bar{\varphi})^{1/2}}\right]\mathrm{d}\bar{\varphi} \\ & + \left(N_1^{(0)} - \frac{p^* R_2^{(0)}}{2}\right)\frac{R_2^{(0)}\sin^2\varphi_0}{R_2\sin^2\varphi}. \end{aligned} \tag{14.85}$$

Near the bottom edge,

$$N_1^{(0)} = \frac{R(p^* + \gamma_l L)}{2} + \frac{\gamma_l V}{2\pi R} = \frac{R(p^* + \gamma_l L)}{2} + \frac{\gamma_l}{3}Rb, \quad R_2^{(0)} = R, \quad \varphi_0 = \pi/2,$$

where $V = \dfrac{2}{3}\pi R^2 b$ is the volume of the liquid filling the bottom. Substituting R_1, R_2, $N_1^{(0)}$, $R_2^{(0)}$, into Eq. (14.85) and integrating, one obtains

$$N_1 = \frac{R_2(p^* + \gamma_l L)}{2} + \frac{\gamma_l R^2 b}{3R_2\sin^2\varphi}\left[1 + \frac{\cos^3\varphi}{(1+\gamma\sin^2\varphi)^{3/2}}\right]. \tag{14.86}$$

With the use of Eq. (13.39) the circumferential force, N_2, can be found, as follows:

$$N_2 = -R_2\left[p^* + \gamma_l\left(L - b\frac{\cos\varphi}{(1+\gamma\sin^2\varphi)^{1/2}}\right)\right] - N_1\frac{R_2}{R_1}. \tag{14.87}$$

The maximum values of the meridional and circumferential forces occur at the pole of the bottom (for $\varphi = \pi$). Using the L'Hospital rule, we can determine $N_{1\max}$ and $N_{2\max}$ from Eqs. (14.86) and (14.87), as follows:

$$N_{1\max} = N_{2\max}\big|_{\varphi=\pi/2} = \frac{R^2}{b}[p^* + \gamma_l(L+b)].$$

The meridional force, N_1, for the bottom is tensile. The circumferential force, N_2, for shallow bottoms changes its sign as it approaches the junction with the cylindrical portion of the tank, i.e., from a tensile force it becomes compressive. The meridional and circumferential force diagrams for a shallow bottom are shown in Fig. 14.13.

It should be kept in mind that at the transition from the cylindrical part of the tank to its bottom, the meridional curvature changes abruptly. The compatibility of deformations is achieved here owing to the occurrence of additional circumferential forces and bending moments. In this zone, called also "the edge effect zone," the membrane shell theory can give significant errors. However, the moment state of stress will diminish quickly, as we go away from the junction. Therefore, the thickness of the wall for both the cylindrical portion of the tank and its bottom can be selected from the membrane shell theory. However, at the edge effect zone, the corresponding reinforcement of the tank is needed (e.g., this reinforcement can be provided by setting up a ring beam or sheets of larger thickness, etc.).

14.2.4 The axisymmetrically loaded Intze tank

Elevated tanks of different forms of shells of revolution serve for water storage in a city or town. These water tanks are made of steel or concrete. An economical form of these tanks that is commonly constructed is the *Intze tank,* which is shown schematically in Fig. 14.14a.

The Intze tank consists of a roof shell, cylindrical wall, conical shell, ring beam, bottom shell, and supporting structure. The tank is filled with a liquid up to the top of the cylindrical wall. We consider below the membrane analysis of the Intze tank made of concrete and shown in Fig. 14.14a. The Intze tank can be separated into the elementary shell components as mentioned above, shown in Fig. 14.14b. Each shell component will be treated as a membrane shell according to the general procedure introduced in Chapter 13.

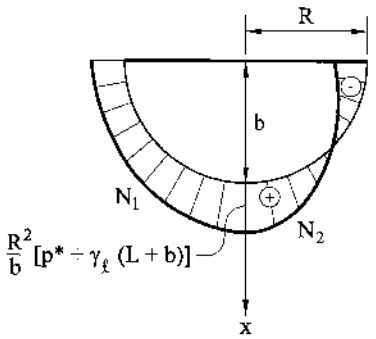

Fig. 14.13

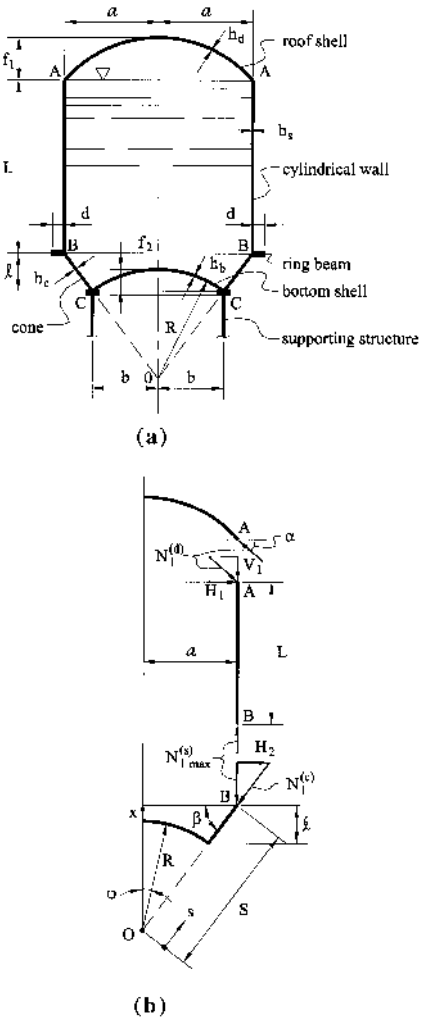

Fig. 14.14

Roof shell

The roof shell is subjected to a dead load (e.g., the weight of the roof) and live or snow loading. The membrane analysis of this shell is quite similar to that given in Sec. 14.1 for a spherical dome. At the base of the shell, the compressive membrane forces (if $\varphi_1 < 51^\circ 49'$), $N_1^{(d)}$ and $N_2^{(d)}$ will act.

Cylindrical wall

The cylindrical wall at its top, from the shell roof, is loaded by the vertical membrane force $V_1 = N_1^{(d)} \sin\alpha$ and the horizontal force $H_1 = N_1^{(d)} \cos\alpha$. Since we restricted our analysis to the membrane theory only, the above horizontal force will be resisted

jointly by the edge zones of the roof and the wall near the junction. A more accurate stress analysis of such a junction, including the moment shell theory, is given in the next chapter.

The water load acting on the cylindrical part of the tank causes the circumferential membrane forces only, $N_2^{(s)}$. It is equal to

$$N_2^{(s)} = \gamma_l a x, \tag{14.88a}$$

where γ_l is the water density. The maximum compressive meridional force $N_1^{(s)}$ occurs at the base of the cylinder and is

$$N_{1\max}^{(s)} = V_1 + \gamma_c h_s L, \tag{14.88b}$$

where γ_c and h_s are the concrete density and the wall thickness of the cylinder, respectively. The maximum circumferential force acts at the base of the cylinder. It is equal to

$$N_{2\max}^{(s)} = \gamma_l a L. \tag{14.88c}$$

Ring beam

At the top of the cone, the meridional compressive force $N_{1\max}^{(s)}$ is given by Eq. (14.88b). Neglecting the self-weight of the ring, this force is directly applied to the top of the cone, as shown in Fig. 14.14b. The above force can be resolved into a component along the cone, $N_1^{(c)} = N_{1\max}^{(s)}/\sin\beta$, and the horizontal component, $H_2 = N_{1\max}^{(s)}\cot\beta$. The latter component is resisted by the ring beam. The hoop tension in the ring beam is given by

$$T^{(r)} = H_2(a + d/2).$$

Conical shell

The conical shell is subjected to dead and water loads. The dead load consists of the self-weight of the conical frustum, W_c, and the total vertical load carried on top of the cone, which comes from the roof shell and the cylindrical wall, W_s. The above load components are

$$W_c = U_c h_c \gamma_c$$

where $U_c = \pi(a + r)\left[x^2 + (a - r)^2\right]^{1/2}$ $(0 \le \times \le l)$ is the volume of the frustum, h_c is the cone thickness, and r is the radius of the cone parallel circle of interest;

$$W_s = N_{1\max}^{(s)} 2\pi(a).$$

Then, the meridional force due to dead load and carried by the cone, $N_{1D}^{(c)}$, is given by

$$N_{1D}^{(c)} = -\frac{W_c + W_s}{2\pi r(\sin\beta)}. \tag{14.89a}$$

The circumferential force in the cone shell, $N_{2D}^{(c)}$ due to the dead load, can be obtained from the third Eq. (13.7) by letting $R_1 = \infty$ and $p_3 = \gamma_c h_c \cos\beta$.

The water load components are (using the coordinates s and β where s is measured along line OB starting from point O, as shown in Fig. 14.14b)

$$p_1 = 0, \quad p_3 = -\gamma_l[L + (S - s)\sin\beta]. \tag{14.90}$$

Substituting the above into Eq. (13.68), integrating, and using the boundary conditions for the case of water loading

$$N_{1W}^{(c)} = 0|_{s=S},$$

we obtain

$$N_{1W}^{(c)} = -\frac{\gamma_l \cot\beta}{6s}\left[2s^3 \sin\beta - 3s^2(L + S\sin\beta) + S^2(3L + S\sin\beta)\right]. \qquad (14.89b)$$

The circumferential membrane force due to the water loading can be again obtained from Eq. (13.39) by letting $R_1 = \infty$ and substituting for p_3 from Eq. (14.90).

Bottom shell

The membrane forces, $N_{1D}^{(b)}$ and $N_{2D}^{(b)}$, due to dead load (the self-weight of the bottom shell) are readily obtained from Eqs (14.2) and (14.3).

Referring to Fig. 14.14b, we can find water load components, as follows:

$$p_1 = 0, \quad p_3 = \gamma_l[H_W + R(1 - \cos\varphi)],$$

where $H_W = L + f_2$ is the height of water above the top of the bottom shell. Substituting the above into Eq. (13.38), setting $R_1 = R$ and $r = R\sin\varphi$, and evaluating the integral, one obtains

$$N_{1W}^{(b)} = \frac{\gamma_l R}{6\sin^2\varphi}\left[-3H_W \sin^2\varphi + R(3\cos^2\varphi - 2\cos^3\varphi - 1)\right]. \qquad (14.91)$$

The circumferential force due to water load, $N_{2W}^{(b)}$, can be obtained then from Eq. (13.39).

Finally the resultant membrane forces N_1 and N_2 from the cone and bottom shell are transmitted to the tank supports. The latter may have a variety of structures. For example, the tank may be supported on a circular ring beam (resisting the horizontal components of the cone meridional membrane force) that spans over a row of columns (resisting the vertical components of the membrane resultants). The membrane analysis of a supporting circular ring beam is quite similar to the analysis of the ring beam between conical and cylindrical shells given above.

14.2.5 Asymmetrically loaded liquid storage facilities: wind loading

In the operating conditions, liquid storage facilities (tanks, reservoirs, containers, etc.) and high-rise structures (chimneys, etc.) are subjected to unsymmetric, primarily, wind loading. In such facilities, which are not filled by liquid, as well as in high-rise structures, the wind loads can cause significant stresses and strains. If the material of these structures behaves elastically, then stresses and strains can be represented as a sum of two components. The first component corresponds to the beam state of stress of a shell with undistorted contour of its cross section. It is figured out using the well-known formulas of strength of materials [3]. The second term accounts for an additional state of stress due to the distortion of the shell cross-section contour. The ratio of these two terms depends on the geometric and rigidity parameters of a shell structure.

Wind loading is characterized by a little variation, which makes it possible to break down the general state of stress associated with a deformation of the contour

of the shell cross section into pure membrane and moment (of the edge effect type) stress states. The former usually governs over the considerable part of the shell. Moreover, it determines particular solutions of the governing differential equations for the moment state of stress also. Therefore, a study of the character and value of the membrane stresses and strains due to static wind loading is of considerable interest in engineering practice. As mentioned previously, the value and law of distribution of the wind loading over the shell surface can be established by testing some models of circular cylindrical shells in wind tunnels. The experimental results obtained showed that the wind loading can be taken as a normal pressure to the shell at all points and it can be approximated by the following truncated Fourier series:

$$p_1 = p_2 = 0, \quad p_3 = p^* \sum_n p_n \cos n\theta, \tag{14.92}$$

where p^* is the maximum value of the face pressure. Wind tunnel experimental investigations showed that it is possible to be restricted by the three terms in the expansion (14.92), taking $p_0 = -0.7$, $p_1 = 0.5$, and $p_2 = 1.2$.

The distribution of the normal pressure p_3, based on the trinomial approximation mentioned above is shown in Fig. 14.15a. For not-too-high shells, one can assume the pressure to be constant along their generators. For high-level cylindrical shell structures, a variation of the wind pressure over the shell depth may be taken into account by replacing the given variable wind load with some equivalent constant load over the shell depth.

Let us consider a circular cylindrical reservoir of radius R and depth H. Assume that it is fixed at the base and is free from the shear and meridional force at the top. Then, taking the origin of the coordinate system at the shell top, we can write the above boundary conditions as follows:

$$S(\theta) = N_1(\theta) = 0\big|_{x=0}. \tag{14.93}$$

Directly from Eq. (13.52a) we obtain the expression for the membrane circumferential forces by letting $R_2 = R$:

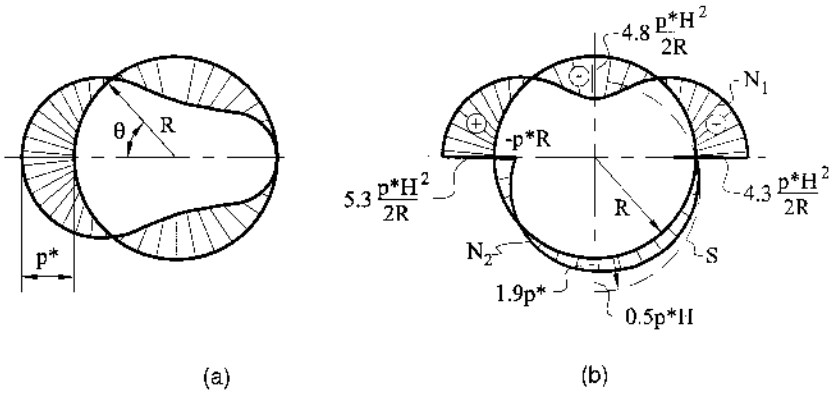

Fig. 14.15

$$N_2 = -p_3 R = -p^* R \sum_n p_n \cos n\theta. \tag{14.94a}$$

Then, taking into account that $R_2 = R, p_2 = 0$, and $f_1(\theta) = 0$ (due to the boundary conditions described above), we obtain from Eq. (13.52b) the following:

$$S = -\int_0^x \frac{\mathrm{d}(-p_3 R)}{R\mathrm{d}\theta}\,\mathrm{d}\bar{x} = -p^* \cdot x \sum_n p_n n \sin n\theta \tag{14.94b}$$

From Eq. (13.52c) it follows that (letting $f_2(\theta) = 0$ and $p_1 = 0$)

$$N_1 = -\int_0^x \frac{1}{R}\frac{\partial S}{\partial \theta}\mathrm{d}\bar{x} = \frac{p^* x^2}{2R}\sum_n p_n n^2 \cos n\theta. \tag{14.94c}$$

In Eqs (14.94b) and (14.94c), the unknown functions $f_1(\theta)$ and $f_2(\theta)$ are equal to zero due to the prescribed boundary conditions (14.93). The diagrams of the membrane forces N_1, N_2, and S are shown in Fig. 14.15b at a section $x = H$. The circumferential force N_2 is a constant over the shell depth in the membrane theory. However, it should be noted that when we approach the supporting cross section, the bending affects the state of stress significantly. Consequently, the membrane forces N_1, N_2, and S are redistributed over the length and cross sections of the shell.

14.3 AXISYMMETRIC PRESSURE VESSELS

Pressure vessels are commonly used to resist internal pressure (pressurized liquids or gases). They are usually made of metals or composite materials. In such constructions, the stresses due to the self-weight of the vessel are negligible compared with the stresses due to the internal pressure.

Let us consider a pressure vessel in the form of a shell of revolution with an arbitrary shape of the meridian, which intersects the axis of revolution at a right angle (Fig. 14.16).

In this section, we determine the membrane forces due to the axisymmetric internal pressure, p. Thus, the applied load components are

$$p_1 = 0, p_2 = 0, \quad \text{and} \quad p_3 = -p.$$

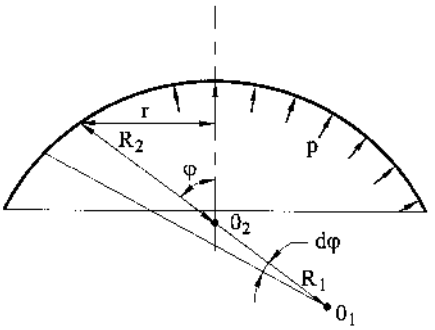

Fig. 14.16

Substituting the above into Eq. (13.38) and noting that $r = R_2 \sin\varphi$ and $dr = ds\cos\varphi = R_1 d\varphi \cos\varphi$, we obtain the following expression for the meridional force:

$$N_1 = \frac{1}{R_2 \sin^2\varphi}\int_{r_0=0}^{r_0} p\bar{r}d\bar{r} = \frac{pr^2}{2R_2\sin^2\varphi},$$

or upon substituting $r = R_2 \sin\varphi$, we can simplify this expression, as follows:

$$N_1 = \frac{pR_2}{2}, \tag{14.95a}$$

which is valid for any shape of meridian. Now, using Eq. (13.39), we can determine N_2 as follows:

$$N_2 = pR_2\left(1 - \frac{R_2}{2R_1}\right). \tag{14.95b}$$

Let us now consider a *cylindrical pressure vessel* with *hemispherical heads* under an internal pressure p, as shown in Fig. 14.17.

For the spherical head with $R_1 = R_2 = R$, we obtain from the above

$$N_1 = N_2 = \frac{pR}{2}.$$

For the cylinder, we have $N_2 = pR$ and $N_1 = pR/2$. Determine the radial displacements of the two neighboring points A and B at the junction of the cylinder and sphere (see Fig. 14.17a). We have

$$\xi_c = R\varepsilon_2^{(C)} = \frac{R}{Et_C}(N_2^{(C)} - \nu N_1^{(C)}) = \frac{pR^2}{2Et_C}(2-\nu). \tag{14.96a}$$

$$\xi_s = R\varepsilon_2^{(S)} = \frac{R}{Et_S}(N_2^{(S)} - \nu N_1^{(S)}) = \frac{pR^2}{2Et_S}(1-\nu) \tag{14.96b}$$

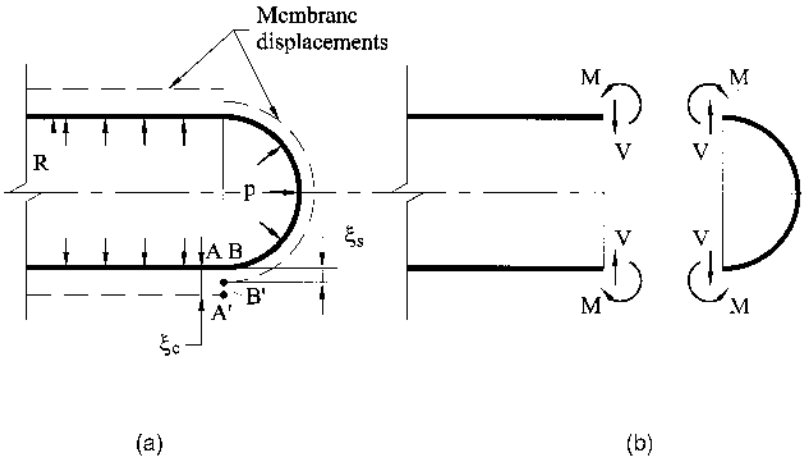

Fig. 14.17

where ξ_c and ξ_s are the radial displacements of the cylinder and sphere, respectively, at the above-mentioned neighboring points.

It follows from Eqs (14.96), that the radial displacement of the cylinder is greater than that of the sphere. Hence, in order to provide the compatibility of the radial displacements at the junction of the two shells, the shear forces, V, and bending moments, M, are to be applied at this junction, as shown in Fig. 14.17b. The situation becomes more complicated if we have a shallow spherical shell instead of a hemispherical shell as a head. In this case, the radial membrane force N_1 in the sphere, at the junction with the cylinder, has to be restricted by the cylinder as an edge load. Consequently, the displacement of the two shells is much greater and a ring beam needs to be provided at the junction to resist the radial membrane force N_1. The actual state of stress at the above junction will be discussed in detail in the next chapter.

A *toroidal shell* is also used for pressure vessels. A toroid is generated by the rotation of a closed curve about an axis passing outside. Figure 14.18a shows a shell in the shape of a toroid or doughut of circular section subjected to internal pressure p. The membrane force N_1 may be found from conditions of equilibrium of a shell segment shown in Fig. 14.18b, i.e.,

$$N_1(2\pi r)\sin\varphi = p\pi(r^2 - b^2),$$

from which

$$N_1 = \frac{p}{2}\cdot\frac{r^2 - b^2}{r\sin\varphi}.$$

Taking into account that $r = b + a\sin\varphi$, we represent N_1 in the form

$$N_1 = \frac{pa}{2}\frac{2b + a\sin\varphi}{b + a\sin\varphi}. \tag{14.97a}$$

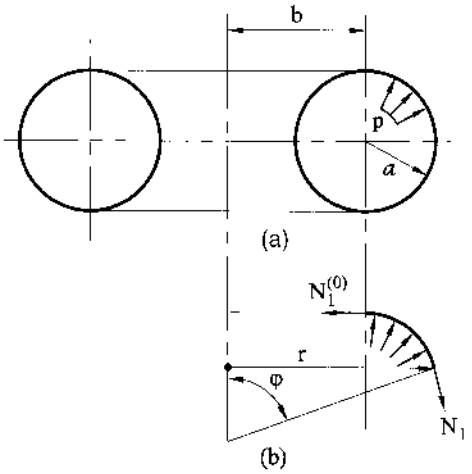

Fig. 14.18

The circumferential membrane force N_2 may be found from Eq. (13.39); substituting there $R_1 = a$, $R_2 = a + \dfrac{b}{\sin\varphi}$ and $p_3 = -p$, we have

$$N_2 = -\left(p_3 R_2 + N_1 \frac{R_2}{R_1}\right) = pR_2 - N_1 \frac{R_2}{R_1} = \frac{1}{2} pa. \tag{14.97b}$$

The radial displacement w can be determined in the usual fashion, i.e.,

$$w = r\varepsilon_2 = \frac{r}{Eh}(N_2 - \vartheta N_1).$$

However, if we try to calculate the longitudinal component of the displacement, which is parallel to the axis of the shell, u, one can show that the integral in the expression (13.43) diverges, since its integrand approaches infinity as φ goes to zero. It follows from the above that in the domain of the shell near a point $\varphi = 0$, the membrane theory does not describe the state of stress and strain of the toroidal shell, even loaded by a uniform pressure.

PROBLEMS

14.1 A hemispherical roof dome in Fig. 14.1 is subjected to its own weight. Assume that the dome is constructed of masonry having a radius of curvature $R = 40\,\text{m}$. Determine the required thickness of the dome according to the maximum principal stress theory if the compressive ultimate stress $\sigma_u = 22\,\text{MPa}$ and the factor of safety is 1.9.

14.2 A spherical roof dome in Fig. 14.2 is subjected to its own weight. Determine the required cross-sectional area of the thrust ring. Take $R = 35\,\text{m}$, $\varphi_1 = 55^\circ$, and $h_s = 10\,\text{cm}$ (thickness of the dome). Assume that the dome and the thrust ring are constructed of concrete with $\nu = 0.15$.

14.3 A planetarium dome may be approximated as an edge-supported truncated cone, as shown in Fig. 14.5b. It is subjected to a snow load with a maximum accumulation over the dome $q = 2.5\,\text{kPa}$. Assume that the dome is constructed of 12 cm thick concrete having the radii of the parallel circles equal to 40 m at the base and 25 m at the top, respectively. Determine the membrane stresses in the dome.

14.4 A cooling tower may be approximated by a one-sheet hyperboloid of revolution (see Fig. 11.9f). The equation of its meridian is $r = \dfrac{a}{b}\sqrt{b^2 + z^2}$, where a and b are the parameters of the hyperbola. Determine the membrane forces, N_1 and N_2, distribution over the depth of the cooling tower under its own weight. Assume that the tower is made of concrete and $T = 22.0\,\text{m}$, $S = 116.0\,\text{m}$, $a = 51.5\,\text{m}$, $b = 73.42\,\text{m}$, and $h = 0.2\,\text{m}$.
Hint: use cylindrical coordinates for the solution.

14.5 The four different dome configurations of the same height, $H = 0.5a$, are shown in Fig. P.14.1. The first dome is spherical with $R_0 = R = 1.25a$; the second dome is parabolic with $R_0 = a$; the third dome has the form of a semiellipsoid with $R_0 = 2a$ and $\gamma = 3$; and the fourth dome represents a segment of ellipsoid (the tangents of the dome meridian at its edges are not vertical) with $R_0 = 1.625a$ and $\gamma = 1.5$. All the four domes cover the same areas (of radius a) and they are made of concrete. (a) Find the meridional and circumferential forces distribution over the height of the above domes under their self-weight p in terms of a and p. (b) Determine the cross-sectional area of the thrust ring for all domes if the ring is assumed to be also made of the reinforced concrete. Take the thickness of the shell $h = a/50$ and $\nu_c = 0.15$. (c) Analyze

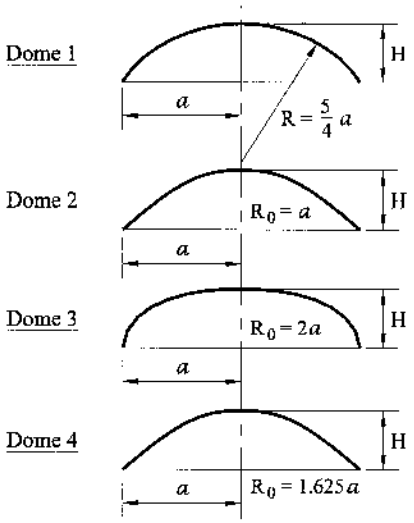

Fig. P14.1

and compare the states of stress of the four domes and on this basis select a more appropriate configuration of the dome. Justify your decision.

14.6 A circular cylindrical barrel shell of semicircular cross section is simply supported at $x = 0$ and $x = L$ (Fig. 14.6a). The shell is subjected to its self-weight p. The edge beams are employed along the rectilinear edges of the barrel shell to resist the membrane shear forces S. (a) Determine the membrane forces N_1, N_2, and S. (b) Select the required cross-sectional area of the edge beam if the shell and the above beam are made of an aluminum with $\sigma_y = 414\,\text{MPa}$, $\nu = 0.3$, and factor of safety is 2.0. Take $a = 10\,\text{m}$, $L = 30\,\text{m}$, and $h = a/100$. (c) Discuss the applicability of the membrane theory for the above barrel shell.

14.7 A horizontal circular pipe of radius a, length L, and thickness h, supporting its own weight, is made of concrete. (a) Determine the membrane forces distribution over the pipe length and over its cross section. (b) Determine the deflections u, v, and w for section $x = L/2$. (c) Analyze the applicability of the membrane theory for the above shell. Take $p_1 = 0$, $p_2 = p\sin\theta$, $p_3 = p\cos\theta$, and $\nu = 0$. The boundary conditions are of the form: $N_1 = 0, v = 0|_{x=0, x=L}$.

14.8 A simply supported at ($x = 0$ and $x = L$) semicircular cylindrical shell (Fig. 14.6) is subjected to a snow load q which is uniformly distributed over its plane area. Given the radius of the shell is a, thickness is h, modulus of elasticity and Poisson's ratio are E and ν, respectively, determine the membrane stresses in the shell.

14.9 Show that the governing equation of the membrane theory for an elliptic paraboloid under the action of a symmetric normal surface loading p, Eq. (14.39), can be reduced to the following governing equation of torsion of the prismatic rod:

$$\frac{\partial^2 \Psi}{\partial \xi^2} + \frac{\partial^2 \Psi}{\partial \eta^2} = -2, \tag{P14.1}$$

where Ψ is the stress function, $\xi = x/a$, and $\eta = y/b$.

14.10 Using the results of Problem 14.9, determine the membrane forces in the shell roof approximated by an elliptic paraboloid of revolution on an equilateral triangular plan

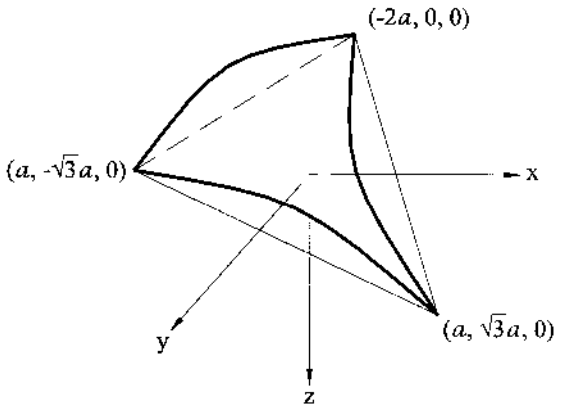

Fig. P14.2

(Fig P.14.2) due to a dead load p. Assume reasonable values for any additional properties and parameters required.

Hint: it is known from the theory of elasticity that the stress function Ψ for the torsion of the rod having a cross section in the form of an equilateral triangle is expressed in the following form:

$$\Psi = -\left[\frac{1}{6a}(x^3 - 3xy^2) - \frac{2}{3}a^2 + \frac{1}{2}(x^2 + y^2)\right]. \tag{P.14.2}$$

14.11 An auditorium dome of span 350 ft is approximated by a spherical shell of radius 280 ft. The dome is simply supported at its ends. Determine the maximum membrane forces in the dome under the action of a wind pressure. The components of the wind pressure are given by Eqs (14.50) and $p = 15$ psf. Assume reasonable values for any additional properties required.

14.12 A circular cylindrical chimney shell of height L and radius R is subjected to a wind pressure p_3. The chimney shell is fixed at its base and free at the top. Assuming that the wind pressure is constant over the height of the chimney and in the circumferential direction is approximated by the polynomial $p_3 = p(-0.7 + 0.5\cos\theta + 1.2\cos 2\theta)$, determine the membrane forces in the shell.

14.13 A steel cylindrical pressure vessel with conical end caps is subjected to an internal pressure of $p = 1.5$ MPa, as shown in Fig. P.14.3. Using the membrane theory alone, determine the required thickness of the cylinder if the yield stress of the steel is 250 MPa. Where may additional strengthening be required?

14.14 The tank shown in Fig. P.14.4 has a cylindrical top and a conical bottom. The tank is supported by a structure (not shown) that applies only vertical forces around the parallel AB. The tank is filled to depth $H = 2.5R$ with water of weight density γ_l. Determine the expressions for the membrane forces just above and just below the parallel AB.

14.15 Redo Problem 14.14 replacing the conical bottom with a hemispherical bottom of radius R. Consider two cases: (a) the bottom convexity is directed down and (b) the bottom convexity is directed up.

14.16 The spherical tank is filled with water at a distance H from the top, as shown in Fig. P.14.5a. The tank is supported by the outlet pipe. Determine the expressions for the membrane forces if the radius of the tank is R and water density is γ_l

Hint: the volume of a spherical segment is $U = \dfrac{\pi l}{6}(3r_A^2 + 3r_B^2 + l^2), \quad 0 < l < 2R.$

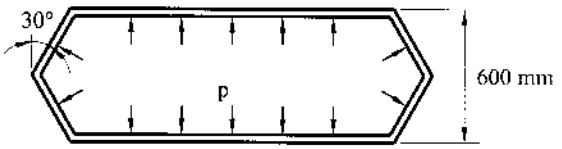

Fig. P14.3

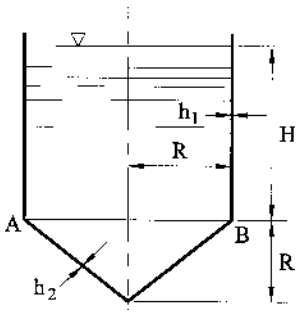

Fig. P14.4

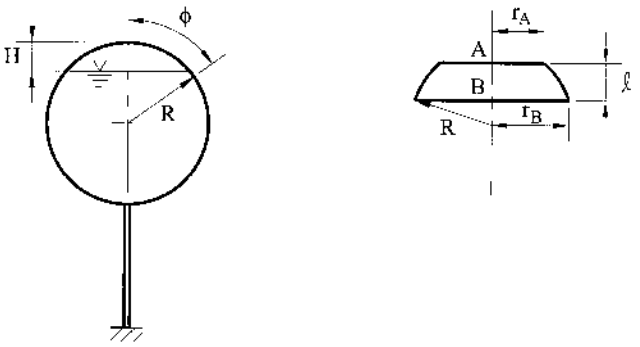

Fig. P14.5

14.17 A horizontal circular pipe of radius R, length l, and thickness h is subjected to internal gas pressure p. Determine the membrane stresses in the pipe if its ends are assumed to be built-in.

14.18 The Intze tank, shown in Fig. 14.14a, is filled with water up to the top of the cylindrical wall. The tank is made of concrete. The total load on the roof shell is taken as $p = 3.5$ kPa over its surface area. Determine (a) the membrane stresses in the roof shell, cylindrical wall, conical shell, and bottom shell; (b) the tension forces in the ring beam at the junction of the wall and cone, and in the supporting ring beam. Let $a = 7.6\,\text{m}$, $L = 7.2\,\text{m}$, $b = 4.8\,\text{m}$, $f_1 = 2.0\,\text{m}$, $f_2 = 1.3\,\text{m}$, $h_r = 95\,\text{mm}$, $h_s = 250\,\text{mm}$, and $h_b = 280\,\text{mm}$

14.19 A circular toroidal shell is subjected to internal pressure $p = 2.5\,\text{MPa}$, as shown in Fig. 14.18. The dimensions of the toroid are $a = 0.09\,\text{m}$, $b = 0.60\,\text{m}$, and $h = 1.8\,\text{mm}$. Determine the membrane stresses in the shell.

14.20 A spherical concrete dome having a span of $2a$ and height H ($H = 0.5a$) supports its own weight p. The ends of the dome have roller supports (they can freely displace in the horizontal direction). Determine (a) the horizontal displacements at the dome base and (b) the vertical displacement at its apex.

14.21 Redo Problem 14.20, except now assume that the dome is subjected to snow loading q.

REFERENCES

1. Novozhilov, V.V., *The Shell Theory* [translated from 2nd Russian edn by P.G. Lowe], Noordhoff, Groningen, The Netherlands, 1964.
2. Timoshenko, S.P. and Woinowsky-Krieger, S., *Theory of Plates and Shells*, 2nd edn, McGraw-Hill, New York, 1959.
3. Gere, J.M. and Timoshenko, S.P., *Mechanics of Materials*, 4th edn, PWS Publishing Company, Boston, 1997.

15

Moment Theory of Circular Cylindrical Shells

15.1 INTRODUCTION

The membrane theory of thin shells, discussed in previous chapters, is sufficient to analyze with a high degree of accuracy many commonly encountered loading conditions. However, at locations where the deflections are restricted, or there is a change in geometry, such as the cylindrical-to-spherical shell junction (see Sec. 14.7), the membrane theory is inadequate to maintain deflection and rotation compatibility between the shells. At these locations, discontinuity forces and moments are developed that result in bending and shear stresses in the shell. It should be noted that these bending and shear stresses are localized over a small area of the shell, and they dissipate rapidly along the shell. Many structures, such as shell roof structures, storage tanks, pressure vessels, missiles, etc., are designed according to the membrane theory and the total stress at discontinuities is determined from the membrane and moment theories. Thus, a complete analysis of various thin shell forms would require an appropriate moment theory, which is to be combined with the previously discussed membrane theory.

It should be noted that, due to the small thickness of the shell, even small bending moments cause large stresses in the shell. Therefore, it is very important to determine the bending stress–strain field correctly to insure a design reliability. The complete moment theory of thin shells is mathematically intricate. The governing differential equations of the moment theory of shells enable analytical or exact solutions only for some particular cases. Therefore, approximate shell theories were developed (see Chapter 17). The numerical methods, usually the finite element method (FEM), discussed in Chapters 6 and 18, were also applied for the moment analysis of thin shells.

We begin the moment analysis of thin shells with cylindrical shells. A cylindrical shell presents one of the most generally acceptable and optimal structural form

of shells employed in engineering. A cylindrical shell, as mentioned previously, is successful in combining simplicity, compactness, and almost an ideal technological effectiveness. The latter enables one to develop items by usual rolling-up a given sheet skelps. Therefore, pattern cutting of a material and the subsequent process of manufacturing of a given structural form requires a minimum of technological effort. On the other hand, unlike the other shell forms – say, noncircular shells of revolution – the governing differential equations of the moment theory of a circular cylindrical shell of constant thickness represent a system of equations with constant coefficients, which gives us the possibility to analyzing their solutions in the general form.

15.2 CIRCULAR CYLINDRICAL SHELLS UNDER GENERAL LOADS

Here we will use the same coordinates x and θ as we did for the membrane theory of cylindrical shells (Fig. 11.13), where x is the distance of a point of interest from a datum plane normal to the generators (this plane usually coincide with one edge of the shell) and θ measures the angular distance of the point from a datum generator. In this case, the Lamé parameters are given by Eqs (11.53) and the principal radii of curvature are

$$R_1 = \infty, \quad R_2 = R. \tag{15.1}$$

The equilibrium equations of the general classical shell theory, Eqs.(12.41) and (12.42), and the relations (12.43), appear in the following form:

$$\begin{aligned}
R\frac{\partial N_1}{\partial x} + \frac{\partial S}{\partial \theta} + p_1 R &= 0,\\
\frac{\partial N_2}{\partial \theta} + R\frac{\partial S}{\partial x} - Q_2 - \frac{\partial H}{\partial x} + p_2 R &= 0,\\
\frac{\partial Q_2}{\partial \theta} + R\frac{\partial Q_1}{\partial x} + N_2 + p_3 R &= 0,\\
\frac{\partial M_2}{\partial \theta} + R\frac{\partial H}{\partial x} - RQ_2 &= 0,\\
R\frac{\partial M_1}{\partial x} + \frac{\partial H}{\partial \theta} - RQ_1 &= 0.
\end{aligned} \tag{15.2, 15.3}$$

This system of five differential equations of equilibrium can be reduced to the following system of three equations, by eliminating the shear forces, Q_1 and Q_2, from Eqs (15.3):

$$\begin{aligned}
R\frac{\partial N_1}{\partial x} + \frac{\partial S}{\partial \theta} + p_1 R &= 0,\\
\frac{\partial N_2}{\partial \theta} + R\frac{\partial S}{\partial x} - \frac{1}{R}\frac{\partial M_2}{\partial \theta} - 2\frac{\partial H}{\partial x} + p_2 R &= 0,\\
\frac{1}{R}\frac{\partial^2 M_2}{\partial \theta^2} + 2\frac{\partial^2 H}{\partial x \partial \theta} + R\frac{\partial^2 M_1}{\partial x^2} + N_2 + p_3 R &= 0.
\end{aligned} \tag{15.4}$$

The kinematic relations for thin cylindrical shells may be obtained from the corresponding equations of the general shell theory, Eqs (12.23) and (12.24), by using Eqs (15.1) and (15.2). We have the following:

$$\varepsilon_1 = \frac{\partial u}{\partial x}, \quad \varepsilon_2 = \frac{1}{R}\frac{\partial v}{\partial \theta} - \frac{w}{R}, \quad \gamma_{12} = \frac{1}{R}\frac{\partial u}{\partial \theta} + \frac{\partial v}{\partial x}, \tag{15.5a}$$

$$\chi_1 = -\frac{\partial^2 w}{\partial x^2}, \quad \chi_2 = -\frac{1}{R^2}\left(\frac{\partial v}{\partial \theta} + \frac{\partial^2 w}{\partial \theta^2}\right), \quad \chi_{12} = -\frac{1}{R}\left(\frac{\partial v}{\partial x} + \frac{\partial^2 w}{\partial x \partial \theta}\right). \tag{15.5b}$$

Substituting the above into Eqs (12.45) and (12.46), we obtain the following stress resultant – and stress couples – displacements relations for circular cylindrical shells

$$N_1 = \frac{Eh}{1-\nu^2}\left[\frac{\partial u}{\partial x} + \frac{\nu}{R}\left(\frac{\partial v}{\partial \theta} - w\right)\right]; \quad N_2 = \frac{Eh}{1-\nu^2}\left[\frac{1}{R}\left(\frac{\partial v}{\partial \theta} - w\right) + \nu\frac{\partial u}{\partial x}\right];$$

$$S = \frac{Eh}{2(1+\nu)}\left(\frac{\partial v}{\partial x} + \frac{1}{R}\frac{\partial u}{\partial \theta}\right); \tag{15.6a–c}$$

$$M_1 = -D\left[\frac{\partial^2 w}{\partial x^2} + \frac{\nu}{R^2}\left(\frac{\partial v}{\partial \theta} + \frac{\partial^2 w}{\partial \theta^2}\right)\right]; \quad M_2 = -D\left[\frac{1}{R^2}\left(\frac{\partial v}{\partial \theta} + \frac{\partial^2 w}{\partial \theta^2}\right) + \nu\frac{\partial^2 w}{\partial x^2}\right];$$

$$H = -D(1-\nu)\left(\frac{\partial v}{\partial x} + \frac{\partial^2 w}{\partial x \partial \theta}\right)\frac{1}{R} \tag{15.6d–f}$$

Then, upon substituting Eqs (15.6) into Eqs (15.4) and introducing the dimensionless coordinate $\xi = x/R$ in place of x, one derives a set of three expressions in the three displacements u, v, and w. It is convenient to write this system of equations in the matrix form

$$\mathbf{Lu} = \mathbf{g}, \tag{15.7}$$

where

$$\mathbf{u} = \begin{Bmatrix} u \\ v \\ w \end{Bmatrix}, \quad \mathbf{L} = \begin{bmatrix} l_{11} & l_{12} & l_{13} \\ l_{21} & l_{22} & l_{23} \\ l_{31} & l_{32} & l_{33} \end{bmatrix}, \quad \mathbf{g} = \frac{1-\nu^2}{Eh}R^2\begin{Bmatrix} -p_1 \\ -p_2 \\ p_3 \end{Bmatrix}, \tag{15.8}$$

and elements of the differential matrix $\mathbf{L}$ are

$$l_{11} = \frac{\partial^2}{\partial \xi^2} + \frac{1-\nu}{2}\frac{\partial^2}{\partial \theta^2}, \quad l_{12} = l_{21} = \frac{1+\nu}{2}\frac{\partial^2}{\partial \xi \partial \theta}, \quad l_{13} = l_{31} = -\nu\frac{\partial}{\partial \xi},$$

$$l_{22} = \frac{1-\nu}{2}\frac{\partial^2}{\partial \xi^2} + \frac{\partial^2}{\partial \theta^2} + a^2\left[2(1-\nu)\frac{\partial^2}{\partial \xi^2} + \frac{\partial^2}{\partial \theta^2}\right],$$

$$l_{23} = l_{32} = -\frac{\partial}{\partial \theta} + a^2\left[(2-\nu)\frac{\partial^3}{\partial \xi^2 \partial \theta} + \frac{\partial^3}{\partial \theta^3}\right], \quad l_{33} = 1 + a^2\left(\frac{\partial^2}{\partial \xi^2} + \frac{\partial^2}{\partial \theta^2}\right)^2, \tag{15.9}$$

where

$$a^2 = h^2/12R^2 \tag{15.10}$$

For thin shells the values of a^2 are very small (10^{-4}–10^{-6}). These are the *governing differential equations for the displacements in circular cylindrical shells under general loading*.

Following Gol'denveizer [1] the problem of solving Eqs (15.7) is reduced to the integration of a single differential equation for some potential function. For this purpose, it is convenient to use the operator method introduced in [1]. Noting that the coefficients of Eqs. (15.7) are constants; we will consider those relations, according to the above method, as algebraic equations in u, v, and w. These have coefficients in which the symbols of differentiation, $\partial^k/\partial\xi^k$ and $\partial^k/\partial\theta^k$ ($k = 1, 2, 3, 4$) occur together with other quantities (the symbol of multiple differentiation is to be considered as the product of appropriate degrees of $\partial/\partial\xi$ and $\partial/\partial\theta$). Let us set these as follows:

$$\begin{aligned} &u = \Xi_{11}\Psi_1 + \Xi_{12}\Psi_2 + \Xi_{13}\Psi_3; \quad v = \Xi_{21}\Psi + \Xi_{22}\Psi_2 + \Xi_{23}\Psi_3; \\ &w = \Xi_{31}\Psi_1 + \Xi_{32}\Psi_2 + \Xi_{33}\Psi_{31}, \end{aligned} \tag{15.11}$$

where

$$\Xi = \begin{bmatrix} l_{11} & l_{12} & l_{13} \\ l_{21} & l_{22} & l_{23} \\ l_{31} & l_{32} & l_{33} \end{bmatrix} \tag{15.12}$$

is the determinant made up of the operators given by Eq. (15.7) and Ξ_{ik} ($i, k = 1, 2, 3$) are the minors of the above determinant, i.e., the determinants obtained by excluding the ith and the kth column from Ξ_{ik}.

Substituting the expressions (15.11) into Eqs (15.7) and using the well-known theorems of the theory of linear algebraic equations, one finds the following relations:

$$\Xi\Psi_1 + g_1 = 0; \quad \Xi\Psi_2 + g_2 = 0; \quad \Xi\Psi_3 + g_3 = 0. \tag{15.13}$$

Equations (15.13) are nonhomogeneous. Their solutions can be represented in the form

$$\Psi_1 = \Psi_{10} + \Psi_{11}; \quad \Psi_2 = \Psi_{20} + \Psi_{21}; \quad \Psi_3 = \Psi_{30} + \Psi_{31}, \tag{15.14}$$

where the second subscript 0 refers to the solutions of the homogeneous equations (complementary solutions) and the second subscript 1 stands for particular solutions. The former solutions of Eqs (15.13) are found from the following equations:

$$\Xi\Psi_{10} = 0; \quad \Xi\Psi_{20} = 0; \quad \Xi\Psi_{30} = 0. \tag{15.15}$$

Thus, the functions u_0, v_0, and w_0 are defined as

$$\begin{aligned} &u_0 = \Xi_{11}\Psi_{10} + \Xi_{12}\Psi_{20} + \Xi_{13}\Psi_{30}; \quad v_0 = \Xi_{21}\Psi_{10} + \Xi_{22}\Psi_{20} + \Xi_{23}\Psi_{30}; \\ &w_0 = \Xi_{31}\Psi_{10} + \Xi_{32}\Psi_{20} + \Xi_{33}\Psi_{30} \end{aligned} \tag{15.16}$$

They correspond to solutions of the homogeneous equations (15.7) for any Ψ_{10}, Ψ_{20}, and Ψ_{30} that satisfy Eqs (15.15). In particular, we can let

$$\Psi_{10} = 0; \quad \Psi_{20} = 0; \quad \Psi_{30} = \frac{2}{1-\nu}F. \tag{15.17}$$

Then, each solution of the equation

$$\Xi F = 0 \tag{15.18}$$

corresponds to an integral of the homogeneous equations (15.7), given by the expressions

$$u_0 = \frac{2}{1-\nu}\Xi_{13}F; \quad v_0 = \frac{2}{1-\nu}\Xi_{23}F; \quad w_0 = \frac{2}{1-\nu}\Xi_{33}F, \tag{15.19}$$

or using the explicit form of the symbols Ξ_{13}, Ξ_{23}, and Ξ_{33} from Eqs (15.9) and (15.12), we obtain

$$\begin{aligned}
u_0 &= \left\{-\frac{\partial^3}{\partial\xi\partial\theta^2}\cdot + \nu\frac{\partial^3}{\partial\xi^3} + a^2\left[\frac{(1+\nu)(2-\nu)}{1-\nu}\cdot\frac{\partial^5}{\partial\xi^3\partial\theta^2} + \frac{1+\nu}{1-\nu}\frac{\partial^5}{\partial\xi\partial\theta^4} + 4\nu\frac{\partial^3}{\partial\xi^3}\right.\right.\\
&\quad \left.\left. + \frac{2\nu}{1-\nu}\frac{\partial^3}{\partial\xi\partial\theta^2}\right]\right\}F;\\
v_0 &= \left\{(2+\nu)\frac{\partial^3}{\partial\xi^2\partial\theta} + \frac{\partial^3}{\partial\theta^3} - a^2\left[\frac{2(2-\nu)}{1-\nu}\frac{\partial^5}{\partial\xi^4\partial\theta} + \frac{4-3\nu+\nu^2}{1-\nu}\frac{\partial^5}{\partial\xi^2\partial\theta^3} + \frac{\partial^5}{\partial\theta^5}\right]\right\}F;\\
w_0 &= \left\{\frac{\partial^4}{\partial\xi^4} + 2\frac{\partial^4}{\partial\xi^2\partial\theta^2} + \frac{\partial^4}{\partial\theta^4} + a^2\left[4\frac{\partial^4}{\partial\xi^4} + \frac{2(2-2\nu+\nu^2)}{1-\nu}\frac{\partial^4}{\partial\xi^2\partial\theta^2} + \frac{\partial^4}{\partial\theta^4}\right]\right\}F.
\end{aligned} \tag{15.20}$$

Substituting for the operators l_{ik} from the relations (15.9) into (15.12) and (15.18), we obtain the latter equation in the explicit form, as follows:

$$\begin{aligned}
&(1+4a^2)\frac{\partial^8 F}{\partial\xi^8} + 4(1+a^2)\frac{\partial^8 F}{\partial\xi^6\partial\theta^2} + \left[6+a^2(1-\nu^2)\right]\frac{\partial^8 F}{\partial\xi^4\partial\theta^4} + 4\frac{\partial^8 F}{\partial\xi^2\partial\theta^6} + \frac{\partial^8 F}{\partial\theta^8}\\
&\quad + (8-2\nu^2)\frac{\partial^6 F}{\partial\xi^4\partial\theta^2} + 8\frac{\partial^6 F}{\partial\xi^2\partial\theta^4} + 2\frac{\partial^6 F}{\partial\theta^6} + (1-\nu^2)\left(\frac{1}{a^2}+4\right)\frac{\partial^4 F}{\partial\xi^4}\\
&\quad + 4\frac{\partial^4 F}{\partial\xi^2\partial\theta^2} + \frac{\partial^4 F}{\partial\theta^4} = 0.
\end{aligned} \tag{15.21}$$

Thus, the problem is reduced to funding solutions of one single eighth-order differential equation (15.21) and the function F can be considered as a potential function for the integration of the homogeneous equations (15.7). Solving Eq. (15.21), we can determine the function F and then, using the relations (15.20), find the complementary solutions, u_0, v_0, and w_0. The particular solutions for nonhomogeneous equations (15.7), u_1, v_1, and w_1, can be reduced to determining the particular integrals for the nonhomogeneous equations (15.13). In many cases, the particular solutions can be obtained from the membrane theory introduced in Chapter 13.

Thus, the analysis of arbitrarily loaded cylindrical shells is reduced to the integration of differential equations (15.7) with operators (15.9) or equivalent equations (15.13). In the general case of loading and boundary conditions, solutions of the above equations can be obtained only by numerical methods, such as the FEM and the finite difference method (FDM), etc. However, in some particular cases, it is possible to obtain closed-form solutions. Such solutions, even if approximate, are of great theoretical importance because they provide the possibility of carrying out a comprehensive analysis of a shell's state of stress and strain under general loads. As a result, one can introduce various simplifications into the governing equations. In particular, it was shown in Refs [1–3] that a complete state of stress of cylindrical shells under general loads can be represented as a sum of the following elementary stress states, based on fulfillment of some assumptions about the variation of the stress and strain components or the potential function:

- *the beam state* that provides a static equilibrium of a shell as a rigid body;
- *the membrane state*, corresponding to a particular solution of the governing equations of a shell carrying surface loads;
- *the so-called basic state*, corresponding to the stress and strain components varying slightly along the shell generator;
- *the edge effect state*, corresponding to rapidly varying the stress and strain components along the shell generator.

We now discuss briefly the stress analysis of cylindrical shells based on the closed-form solutions of the governing equations and possible simplifications that can be introduced from this analysis.

15.2.1 Analysis of closed cylindrical shells

For closed cylindrical shells, it is convenient to seek a solution of Eq. (15.21) in the form of the trigonometric series in the variable θ, as follows:

$$F = \sum_{n=2}^{\infty} (F_n \cos n\theta + F_n^* \sin n\theta), \tag{15.22}$$

in which $n = 0$ and $n = 1$, the terms corresponding to axisymmetric and beam states of stress, are eliminated. The axisymmetric state of stress of cylindrical shells is studied in detail in Sec. 15.3, while the state of stress of a beam type is presented in Mechanics of Materials (see, for example, [4]). The first term in the parenthesis of Eq. (15.22) refers to symmetric states and the second term refers to skew-symmetric states of stress about the reference meridional plane $\theta = 0$. Substituting Eq. (15.22) into the differential equation (15.21), yields

$$\sum_{n=2}^{\infty} [d_n(F_n) \cos n\theta + d_n(F_n^*) \sin n\theta] = 0, \tag{15.23}$$

where $d_n$is a differential operator to be defined below. By requiring that each term on the left-hand side of this equality be zero, we obtain for F_n and F_n^* one and the same

ordinary linear differential equation with constant coefficients. We present this equation for the function F_n:

$$d_n(F_n) \equiv (1+4a^2)\frac{d^8F_n}{d\xi^8} - 4(1+a^2)n^2\frac{d^6F_n}{d\xi^6} + \left[6n^4 + a^2(1-\nu^2)n^4. - (8-2\nu^2)n^2 + (1-\nu^2)\left(\frac{1}{a^2}+4\right)\right]\frac{d^4F_n}{d\xi^4} - 4n^2(n^2-1)^2\frac{d^2F_n}{d\xi^2} + n^4(n^2-1)^2F_n = 0. \tag{15.24}$$

Its solution can be represented in the form

$$F_n = Ae^{\lambda\xi} \quad (A = \text{const}).$$

Inserting the above into Eq. (15.24) and neglecting small quantities of the order of a^2 in comparison with those of order unity in its coefficients, yields the following characteristic equation for determining roots λ:

$$\lambda^8 - 4n^2\lambda^6 + 6n^4\lambda^4 - (8-2\nu^2)n^2\lambda^4 + (1-\nu^2)a^{-2}\lambda^4 - 4n^2(n^2-1)^2\lambda^2 + n^4(n^2-1)^2 = 0. \tag{15.25}$$

The detailed investigation of the roots of this equation and the corresponding analysis of the state of stress and strain of closed cylindrical shells has been carried out by Gol'denveizer [1]. In particular, it was shown in the above reference that if $n \ll a^{-1/2} = \sqrt{12}R/h$, the roots of the characteristic equation are broken down into small ($|\lambda| \approx a^{1/2}n^2$) and large ($|\lambda| \approx a^{-1/2}$) roots. The above inequality holds for closed cylindrical shells having a large and an intermediate relative reduced lengths, L/R. The small roots correspond to the basic state of stress for the shell, described by the simplified equations of the semi-membrane theory of shells (Sec. 17.2). By the way, if the relative length is not too large, so that $L/R < \dfrac{0.8}{n^2}\sqrt{\dfrac{R}{h}}$, the membrane theory can also be applied to describe a slowly varying state of stress. The large roots correspond to the edge effect state of stress described by simplified equations introduced in Sec. 17.5. Both the approximate theories mentioned above are introduced and analyzed in Chapter 17.

If $n \geq a^{-1/2}$, the above division of the roots into the small and large is impossible. The above inequality holds for closed cylindrical shells having a small and very small reduced length L/R. These shells are in a complete state of stress, which cannot be uncoupled into the previously introduced elementary stress states. However, for an analysis of these shells under general loading, the Donnell–Mushtari–Vlasov approximate theory, introduced in Sec. 17.3, can be applied. According to that theory, the characteristic equation (15.25) may be simplified significantly. It has eight mutually complex conjugate roots of the form

$$\lambda_{1-4} = \pm p_1 \pm iq_1; \quad \lambda_{5-8} = \pm p_2 \pm iq_2,$$

where p_1, q_1, p_2, and q_2 are real positive numbers. To eliminate the complex quantities, the arbitrary constants are replaced according to the following expressions:

$$A_1 = \frac{1}{2i}(C_1 + iC_2); \quad A_2 = -\frac{1}{2i}(C_1 - iC_2); \quad A_3 = \frac{1}{2i}(-C_3 + iC_4);$$
$$A_4 = \frac{1}{2i}(C_3 + iC_4);$$
$$A_5 = \frac{1}{2i}(C_5 + iC_6); \quad A_6 = -\frac{1}{2i}(C_5 - iC_6); \quad A_7 = \frac{1}{2i}(-C_7 + iC_8); \tag{15.26}$$
$$A_8 = \frac{1}{2i}(C_7 + iC_8).$$

Then, a solution of the homogeneous equation (15.24) can be represented, as follows

$$F_n = e^{p_1\xi}(C_1 \sin q_1\xi + C_2 \cos q_1\xi) + e^{-p_1\xi}(C_3 \sin q_1\xi + C_4 \cos q_1\xi) + e^{p_2\xi}(C_5 \sin q_2\xi + C_6 \cos q_2\xi) + e^{-p_2\xi}(C_7 \sin q_2\xi + C_8 \cos q_2\xi). \tag{15.27}$$

Equation (15.27) involves eight constants of integration. They are evaluated from the boundary conditions on the curvilinear shell edges for the expression of the potential function, including the complementary (Eq. (15.27) and particular solutions. As mentioned previously, the latter can be obtained from the membrane shell theory. The boundary conditions (four on each curvilinear shell edge) are formulated in terms of the three displacements u, v, w, slope ϑ_2, internal forces N_1, T_1, V_1, and moment M_1. Having determined these constants, we can then calculate the potential function, the displacements and, finally, using Eqs (15.6), the stress resultants and stress couples for a closed cylindrical shell under general loads. The problem of an analysis of the shell is completed if an axisymmetric and beam states of stress, corresponding to the harmonics $n = 0$ and $n = 1$ (previously eliminated from the consideration) are added.

15.2.2 Analysis of open cylindrical shells

Open circular cylindrical shells are commonly used in civil engineering for roof structures. The curvilinear edges of these shells rest upon some supporting elements in the form of solid diaphragms, tied arches, elevated gridwork, arched truss, etc. These supports are rigid for deformations in their own planes but are flexible for deformations outside their planes (Fig. 15.1).

Such cylindrical shells are sometimes referred to as barrel shells (see also Sec. 14.1.3). If the length of such a barrel shell (along its meridian) is L, the above boundary conditions are of the form

$$w = 0; \quad v = 0; \quad N_1 = 0; \quad \text{and} \quad M_1 = 0\big|_{\xi=0,\xi=L/R}, \tag{15.28a}$$

or in terms of the displacement components,

$$w = 0; \quad v = 0; \quad \frac{\partial u}{\partial \xi} = 0; \quad \text{and} \quad \frac{\partial^2 w}{\partial \xi^2} = 0\Bigg|_{\xi=0,\xi=L/R}. \tag{15.28b}$$

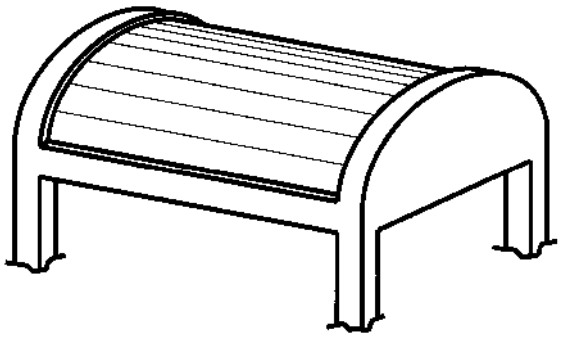

Fig. 15.1

The boundary conditions on the rectilinear shell edges, $\theta = \text{const}$, can be arbitrary. These edges are usually supported by edge beams. In the case of a multiwave shell structure, neighboring shells are joined by their longitudinal edges.

For open cylindrical shells, the boundary conditions (15.28) on the curvilinear edges will be satisfied if the potential function, F, is represented in the form of the trigonometric series

$$F = \sum_{m=1}^{\infty} F_m(\theta) \sin \beta_m \xi, \tag{15.29}$$

where,

$$\beta_m = \frac{m\pi R}{L}. \tag{15.30}$$

The problem of determining the complementary solution of the partial differential equation then leads to the integration of a sequence of ordinary differential equations of the form (see Eq. (15.21):

$$\begin{aligned} &\frac{\mathrm{d}^8 F_m}{\mathrm{d}\theta^8} - (4\beta_m^2 - 2)\frac{\mathrm{d}^6 F_m}{\mathrm{d}\theta^6} + \left[6\beta_m^4 + a^2(1-\nu^2)\beta_m^4 - 8\beta_m^2 + 1\right]\frac{\mathrm{d}^4 F_m}{\mathrm{d}\theta^4} \\ &\quad - \left[4(1+a^2)\beta_m^6 - (8-2\nu^2)\beta_m^4 + 4\beta_m^2\right]\frac{\mathrm{d}^2 F_m}{\mathrm{d}\theta^2} \\ &\quad + \left[(1+4a^2)\beta_m^8 + (1-\nu^2)\left(\frac{1}{a^2}+4\right)\beta_m^4\right]F_m = 0. \end{aligned} \tag{15.31}$$

We seek a solution of the above equation in the form

$$F_m = A\mathrm{e}^{\lambda\theta}..$$

Inserting the above into Eq. (15.31) and again neglecting the quantities of the order of a^2 in comparison with those of order unity in the coefficients of the equation, yields the following characteristic equation:

$$\begin{aligned} &\lambda^8 - (4\beta_m^2 - 2)\lambda^6 + (6\beta_m^4 - 8\beta_m^2 + 1)\lambda^4 - \left[4\beta_m^6 - (8-2\nu^2)\beta_m^4 + 4\beta_m^2\right]\lambda^2 \\ &\quad + \left(\beta_m^8 + \frac{1-\nu^2}{a^2}\beta_m^4\right) = 0. \end{aligned} \tag{15.32}$$

The eight roots of this characteristic equation can be expressed as

$$\lambda_{1-4} = \pm\mu_1 \pm i\mu_2; \quad \lambda_{5-8} = \pm\varsigma_1 \pm i\varsigma_2, \tag{15.33}$$

where μ_1, μ_2, ς_1, and ς_2 are real and positive numbers. As mentioned in Sec. 15.2.1, for a closed cylindrical shell, the eight roots of the characteristic equation can be divided into the small and large roots. For an open shell, that cannot be achieved. Thus, a solution of the homogeneous equation (15.31), after replacing the complex quantities with real constants C_i by using Eqs (15.26), is of the form

$$\begin{aligned} F_m = {} & e^{\mu_1\theta}(C_1 \sin\mu_2\theta + C_2 \cos\mu_2\theta) + e^{-\mu_1\theta}(C_3 \sin\mu_2\theta + C_4 \cos\mu_2\theta) \\ & + e^{\varsigma_1\theta}(C_5 \sin\varsigma_2\theta + C_6 \cos\varsigma_2\theta) + e^{-\varsigma_1\theta}(C_7 \sin\varsigma_2\theta + C_8 \cos\varsigma_2\theta) \end{aligned}. \tag{15.34}$$

The eight constants of integration are evaluated from the boundary conditions on the shell edges $\xi = 0$ and $\xi = L/R$ for the summarized expression of F_m, including a particular and complementary solution (Eq. (15.34)).

As for closed cylindrical shells, open cylindrical shells may also be classified, depending on the parameter β_m. Following Gol'denveizer [1], the classification has the following form:

1. shells of very large relative reduced length, for which $\beta_m \ll a^{1/2}$;
2. shells of large relative reduced length, for which $\beta_m \approx a^{1/2}$;
3. shells of an intermediate relative reduced length, for which $a^{1/2} \ll \beta_m \ll a^{-1/2}$;
4. shells of small relative reduced length, for which $\beta_m \approx a^{-1/2}$;
5. shells of very small relative reduced length, for which $\beta_m \gg a^{-1/2}$.

Let us analyze the states of stress for the above classes of open cylindrical shells under general loads and discuss the corresponding approximate methods for determining the stress and strain components for those shells.

The shells of the Class 1 can be treated as thin-walled bars, because deformations of these shells are only slightly constrained in the circumferential direction. The shells of the Class 2 are in the basic state of stress, because the stress and strain components (or the potential function) are characterized by a small variation along the shell generator. Such shells can be analyzed using the approximate semi-membrane theory of thin shells (Sec. 17.2). The shells of the Class 3 are in the simplified basic state of stress, which is characterized by a small variation of the potential function along the generator and by a rapid variation in the circumferential direction. So, further simplifications of the semi-membrane theory are possible for such shells (see, for example Ref. [2]). The complete state of stress for Class 4 of open cylindrical shells cannot be broken down into the elementary states of stress. However, such shells can be treated by the Donnell–Mushtari–Vlasov approximate theory (see Sec. 17.3). Finally, the shells of the Class 5 can be considered as cylindrical plates [2]. The equilibrium equations for such plates may be broken down as follows: two of them represent the plane stress problem and the third equation is the biharmonic equation of the plate bending problem.

15.3 AXISYMMETRICALLY LOADED CIRCULAR CYLINDRICAL SHELLS

Pipes, tanks, boilers, and various other vessels subjected to internal pressure can be classified as axisymmetrically loaded cylindrical shells.

A closed circular cylindrical shell of radius R will be deformed axisymmetrically if its external load and boundary conditions on ends are symmetrical about the axis of the shell, i.e., $p_1 = p_1(x), p_2 = 0$, and $p_3 = p_3(x)$ and the boundary conditions do not depend upon the angular coordinate θ. Under these conditions, the displacements, strains, internal forces, and moments will be functions of the coordinate x only, and the tangential displacement $v = 0$, because the displacement v, being independent of θ, will cause a skew-symmetric deformation of the shell about its axis.

Subject to the foregoing simplifications, the terms $S, H, Q_2, \gamma_{12}, \chi_2$ and χ_{12} drop out. Correspondingly, only three out of the five equilibrium equations (15.2) and (15.3) remain to be satisfied. These remaining equations of static equilibrium are of the following form:

$$\frac{dN_1}{dx} + p_1 = 0, \tag{15.35a}$$

$$\frac{dQ_1}{dx} + N_2\frac{1}{R} + p_3 = 0, \tag{15.35b}$$

$$\frac{dM_1}{dx} - Q_1 = 0. \tag{15.35c}$$

From Eq. (15.35a), the meridional force N_1 is

$$N_1 = -\int p_1 dx + C, \tag{15.36}$$

where C is a constant of integration. It may be expressed via the meridional force $N_1^{(0)}$ in a reference cross section of the shell, $x = 0$, $N_1^{(0)}$. We have

$$N_1 = -\int p_1 dx + N_1^{(0)}. \tag{15.37}$$

The kinematic relations (Eqs (15.5)), from symmetry, are of the form

$$\varepsilon_1 = \frac{du}{dx}, \quad \varepsilon_2 = -\frac{w}{R}, \quad \chi_1 = -\frac{d^2w}{dx^2}. \tag{15.38}$$

The corresponding stress resultant and stress couples-displacement relations (Eqs (15.6)) take the form

$$N_1 = \frac{Eh}{1-\nu^2}\left(\frac{du}{dx} - \nu\frac{w}{R}\right); \quad N_2 = \frac{Eh}{1-\nu^2}\left(\nu\frac{du}{dx} - \frac{w}{R}\right); \tag{15.39}$$

$$M_1 = -D\frac{d^2w}{dx^2}, \quad M_2 = -D\nu\frac{d^2w}{dx^2} = \nu M_1. \tag{15.40}$$

Eliminating Q_1 from Eqs (15.35b) and (15.35c), yields

$$\frac{d^2M_1}{dx^2} + N_2\frac{1}{R} + p_3 = 0. \tag{15.41}$$

Then, using the first and second of Eqs (15.39), we can express N_2 in terms of N_1 and w:

$$N_2 = -\frac{Eh}{R}w + \nu N_1. \tag{15.42}$$

Substituting Eq. (15.42) and Eq. (15.39) into Eq. (15.41), and assuming that $h = \text{const}$, we obtain the following equation:

$$D\frac{d^4w}{dx^4} + \frac{Eh}{R^2}w = p_3 + \frac{\nu}{R}N_1. \tag{15.43}$$

A more convenient form of this equation is shown below:

$$\frac{d^4w}{dx^4} + 4\beta^4 w = \frac{1}{D}\left(p_3 + \frac{\nu}{R}N_1\right), \tag{15.44}$$

where,

$$\beta^4 = \frac{Eh}{4R^2D} = \frac{3(1-\nu^2)}{R^2h^2} \tag{15.45}$$

β is a geometric parameter of the dimension [length]$^{-1}$. Equation (15.44) or Eq. (15.43) represent the *governing differential equation of an axsymmetrically loaded circular cylindrical shell.*

It can be easily shown that Eq. (15.44) coincides with the governing differential equation of bending of a strip-beam cut off from the shell by two neighboring longitudinal sections θ and $\theta + d\theta$ and resting on an elastic Winkler foundation [5] (shaded in Fig. 15.2). The elastic foundation for the strip-beam is the support part of the shell (not shaded in Fig. 15.2), resisting its deflections at the expense of the circumferential membrane forces N_2. These forces produce a projection in the normal direction that equals $N_2 d\theta$, which can be interpreted as the reactive forces of the foundation.

The shear force Q_1 is given by

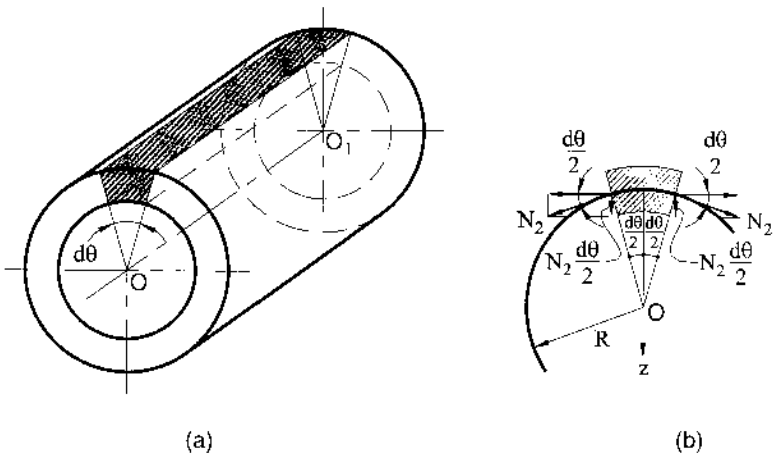

Fig. 15.2

$$Q_1 = \frac{\mathrm{d}M_1}{\mathrm{d}x} = -D\frac{\mathrm{d}^3 w}{\mathrm{d}x^3}. \tag{15.46}$$

The general solution of Eq. (15.44) can be represented in the form

$$w = w_\mathrm{h} + w_\mathrm{p} \tag{15.47}$$

where w_h is a complementary solution of the homogeneous equation (15.44) and w_p is a particular solution of the above equation with the right-hand side. w_h is sought in the form

$$w_\mathrm{h} = C\mathrm{e}^{kx}.$$

Substituting the above into Eq. (15.44), yields the following characteristic equation:

$$k^4 + 4\beta^4 = 0.$$

The roots of this equation are

$$k_{1,2} = (1 \pm i)\beta, \quad k_{3,4} = -(1 \pm i)\beta.$$

Therefore, the complementary solution of Eq. (15.44) is of the form

$$w_\mathrm{h} = \mathrm{e}^{\beta x}(C_1\mathrm{e}^{i\beta x} + C_2\mathrm{e}^{-i\beta x}) + \mathrm{e}^{-\beta x}(C_3\mathrm{e}^{i\beta x} + C_4\mathrm{e}^{-i\beta x}), \tag{15.48}$$

where C_i $(i = 1, 2, 3, 4)$ are constants of integration (complex). Applying Euler's formula

$$\mathrm{e}^{i\varphi} = \cos\varphi + i\sin\varphi, \quad \mathrm{e}^{-i\varphi} = \cos\varphi - i\sin\varphi,$$

we can replace the exponential functions (15.48) with trigonometric functions. We have the following:

$$w_\mathrm{h} = \mathrm{e}^{-\beta x}(A_1\sin\beta x + A_2\cos\beta x) + \mathrm{e}^{\beta x}(A_3\sin\beta x + A_4\cos\beta x), \tag{15.49}$$

where A_i $(i = 1, 2, 3, 4)$ are new, real arbitrary constants of integration.

The particular solution of Eq. (15.44), w_p, depends upon the law of distribution of the surface loads p_1 and p_3. If the latter vary along the longitudinal coordinate x as a power law with an exponent not more than three, then the particular solution has the form

$$w_\mathrm{p} = \frac{p_3 R^2}{Eh} + \nu\frac{N_1 R}{Eh}. \tag{15.50}$$

If the surface loads mentioned above vary according to another law, but fairly smoothly, then the expression (15.50) may also be used as an approximate particular solution of the equation. The following strong inequality is a necessary condition for the validity of the last statement:

$$\left|\frac{\mathrm{d}^4 w_\mathrm{p}}{\mathrm{d}x^4}\right| \ll |\beta^4 w_\mathrm{p}|.$$

It is possible to write the exact expression for the particular solution of Eq. (15.44) for arbitrary surface loads p_1 and p_3, by using the well-known method of variation of parameters [6], i.e.,

$$w_p = 4\beta \int_0^x K[\beta(x-\xi)]\Phi(\xi)\mathrm{d}\xi, \tag{15.51}$$

where

$$K(\beta x) = \frac{1}{4}(\cosh \beta x \sin \beta x - \sinh \beta x \cos \beta x) \quad \text{and} \quad \Phi(x) = \frac{p_3 R^2}{Eh} + \nu \frac{N_1 R}{Eh}.$$

The particular, w_p, and the complementary solutions of Eq. (15.44) can be interpreted as follows. The particular solution is the solution obtained by assuming the membrane action for the shell. This solution may not satisfy the prescribed boundary conditions of the shell. The complementary solution expresses the correction to the particular one, i.e., membrane solution, so that the prescribed boundary conditions can be satisfied for the sum of w_p and w_h.

The constants of integration, A_i, are evaluated from the boundary conditions assigned on the edges of a shell. Two boundary conditions are usually prescribed on any edge. Let us consider some typical boundary conditions for the closed cylindrical shell shown in Fig. 15.3.

(a) *The shell edge is built-in.*
In this case the boundary conditions are (Fig. 15.3a)

$$w = 0, \quad \frac{\mathrm{d}w}{\mathrm{d}x} = 0. \tag{15.52a}$$

(b) *The shell edge is simply supported.*
In this case the boundary conditions are (Fig. 15.3b)

$$w = 0, \quad \frac{\mathrm{d}^2 w}{\mathrm{d}x^2} = 0 \quad (\text{since } M_1 = 0), \tag{15.52b}$$

(c) *The shell edge is free.*
The boundary conditions are, for this case (Fig. 15.3c),

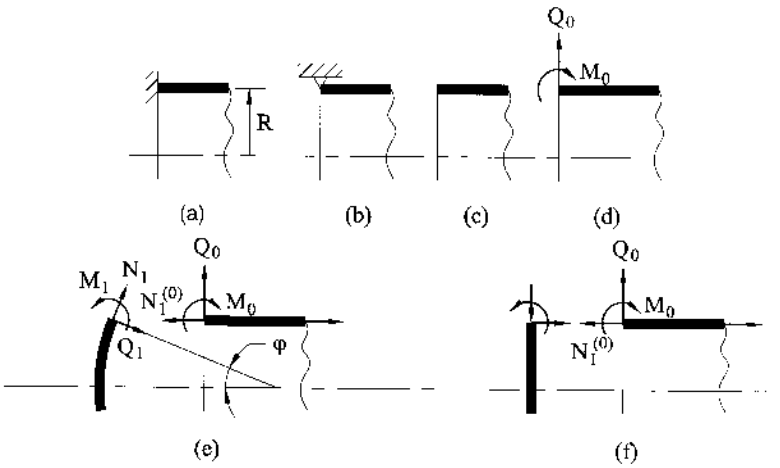

Fig. 15.3

$$\frac{d^2w}{dx^2} = 0 \quad (\text{since } M_1 = 0), \frac{d^3w}{dx^3} = 0 \quad (\text{since } Q_1 = 0). \tag{15.52c}$$

(d) *The shell edge is loaded by a given force Q_0 and moment M_0* (Fig. 15.3d)
The boundary conditions for this case are of the following form:

$$-D\frac{d^2w}{dx^2} = M_0, -D\frac{d^3w}{dx^3} = Q_0. \tag{15.52d}$$

In the case of joining a cylindrical shell with a shell of another geometry (Fig. 15.3e), it is necessary to satisfy the following four boundary conditions (two conditions are required for each edge of the joining shells): equality of the deflections w or circumferential strains ε_2; equality of slopes dw/dx; equality of moments M_1; and equality of thrusts, i.e.,

$$(-N_1 \cos\varphi + Q_1 \sin\varphi)_h = (Q_0)_c, \tag{15.52e}$$

where the subscripts h and c refer to the head shell and cylindrical shell, respectively.

If a cylindrical shell is joined with the flat bottom (Fig. 15.3f), then the boundary conditions are somewhat simplified because the first condition of joining, due to the assumption of nonstretching the middle surface of the plate, has a form $w_0 = 0$, the fourth condition, (15.52e), is not needed.

15.3.1 Analysis of long cylindrical shells

To evaluate the constants of integration it is necessary to solve a system of four linear algebraic equations for four unknowns A_i $(i = 1, 2, 3, 4)$. However, for some practically important cases this procedure may be simplified. Consider a long thin cylindrical shell. Take the origin of the x axis at one of the shell edges. It is seen from Eq. (15.49) that the first two terms, which are multiplied by $e^{-\beta x}$ will diminish quickly as we go away from the edge $x = 0$. Hence, for a long cylinder, these first two terms have a negligible effect at the edge $x = L$ (where L is the length of the shell). The second two terms involving $e^{\beta x}$, in contrast, increase quickly. Taking into account that the deflections w for large values of x should be finite and small quantities, one can conclude that the constants A_3 and A_4 should be very small for the above-mentioned long shell. Thus, in the field located near the origin of the coordinates, the second two terms may be neglected, i.e., it is possible to set $A_3 = A_4 = 0$. Then, the solution becomes the following:

$$w = e^{-\beta x}(A_1 \sin\beta x + A_2 \cos\beta x) + w_p, \tag{15.53}$$

where A_1 and A_2 are constants of integration, to be determined from the boundary conditions at $x = 0$. The function w in the form of Eq. (15.53) is applicable for the shell field near its edge $x = 0$. For the field located near the opposite edge of the shell, $x = L$, the second two terms in Eq. (15.49) cannot be dropped because the factor $e^{\beta x}$ takes very large values. However, one can take a new origin of the coordinate system, locating it at the second edge of the shell and pointing the x axis out to the opposite side. Then, we can again employ the expression (15.53) and, evaluating

new constants of integration A_1 and A_2, obtain the function w for the field located near the second edge of the shell.

Let us define more precisely the conditions under which a shell can be regarded as long. Assume that the permissible error of the shell stress analysis is, say, 5%. It can be easily shown that this requirement will be achieved if the following inequalities hold in this case (for $\nu = 0.3$):

$$\beta L \geq 3 \quad \text{or} \tag{15.54}$$

$$L \geq \frac{3}{\beta} = \frac{3}{\sqrt[4]{3(1-\nu^2)}}\sqrt{Rh} \approx 2.3\sqrt{Rh}, \quad \text{i.e.,} \quad L \geq 2.3\sqrt{Rh}. \tag{15.55}$$

Shells satisfying the above inequality will be referred to as *long,* or *semi-infinite shells,* and the error of approximate solutions, by using Eq. (15.53), will not be more than 5%.

Consider a long shell loaded by a uniform internal pressure $p_3 = -p = \text{const}$, an axial force $N_1^{(0)}$, and p_1, as well as the edge loads M_0 and Q_0, as shown in Fig. 15.4.

The boundary conditions for the shell edge $x = 0$ are of the form

$$-D\frac{\mathrm{d}^2 w}{\mathrm{d}x^2} = M_0\Big|_{x=0}; \quad -D\frac{\mathrm{d}^3 w}{\mathrm{d}x^3} = Q_0\Big|_{x=0}. \tag{15.56}$$

The general solution for the semi-infinite shell is taken in the form of Eq. (15.53). Substituting this solution into the conditions (15.56) yields the following values of the constants of integration:

$$A_1 = \frac{M_0}{2\beta^2 D}, \quad A_2 = -\frac{1}{2\beta^3 D}(Q_0 + \beta M_0).$$

Substituting the above constants into Eq. (15.53) yields the following equation for the deflections:

$$w = \frac{M_0}{2D\beta^2}\mathrm{e}^{-\beta x}(\sin\beta x - \cos\beta x) - \frac{Q_0}{2D\beta^3}\mathrm{e}^{-\beta x}\cos\beta x + w_{\mathrm{p}}. \tag{15.57a}$$

Inserting the above into Eqs (15.39), (15.40), and (15.46), and letting $p_3 = -p$, we obtain

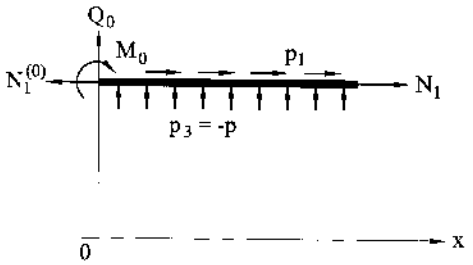

Fig. 15.4

$$\vartheta = \frac{dw}{dx} = \frac{M_0}{D\beta} e^{-\beta x} \cos \beta x + \frac{Q_0}{2D\beta^2} e^{-\beta x} (\cos \beta x + \sin \beta x) + \frac{dw_p}{dx}, \tag{15.57b}$$

$$M_1 = -D \frac{d^2 w}{dx^2} = M_0 e^{-\beta x} (\cos \beta x + \sin \beta x) + \frac{Q_0}{\beta} e^{-\beta x} \sin \beta x - D \frac{d^2 w_p}{dx^2}, \tag{15.57c}$$

$$M_1 = -D \frac{d^2 w}{dx^2} = M_0 e^{-\beta x} (\cos \beta x + \sin \beta x) + \frac{Q_0}{\beta} e^{-\beta x} \sin \beta x - D \frac{d^2 w_p}{dx^2}, \tag{15.57d}$$

$$Q_1 = -D \frac{d^3 w}{dx^3} = -2M_0 \beta e^{-\beta x} \sin \beta x + Q_0 e^{-\beta x} (\cos \beta x - \sin \beta x) - D \frac{d^3 w_p}{dx^3}, \tag{15.57e}$$

$$N_2 = -\frac{Ehw}{R} + \nu N_1 = 2R \cdot e^{-\beta x} \beta^2 \left[M_0 (\cos \beta x - \sin \beta x) + \frac{Q_0}{\beta} \cos \beta x \right] + p_0 R. \tag{15.57f}$$

The normal stress components are given by

$$\sigma_1 = \frac{N_1}{h} + \frac{12M_1}{h^3} z, \quad \sigma_2 = \frac{N_2}{h} + \frac{12M_2}{h^3} z. \tag{15.58}$$

Example 15.1

A long cylindrical shell is subjected to end moment m, as shown in Fig. 15.5a. Derive and plot the values of w and M_1 along the βx axis.

Solution

From Eqs (15.57), setting $M_0 = -m$, we have the following:

$$w = -\frac{m}{2D\beta^2} e^{-\beta x} (\sin \beta x - \cos \beta x); \quad M_1 = -m e^{-\beta x} (\cos \beta x + \sin \beta x).$$

On the loaded edge of the shell, $x = 0$, we obtain the following:

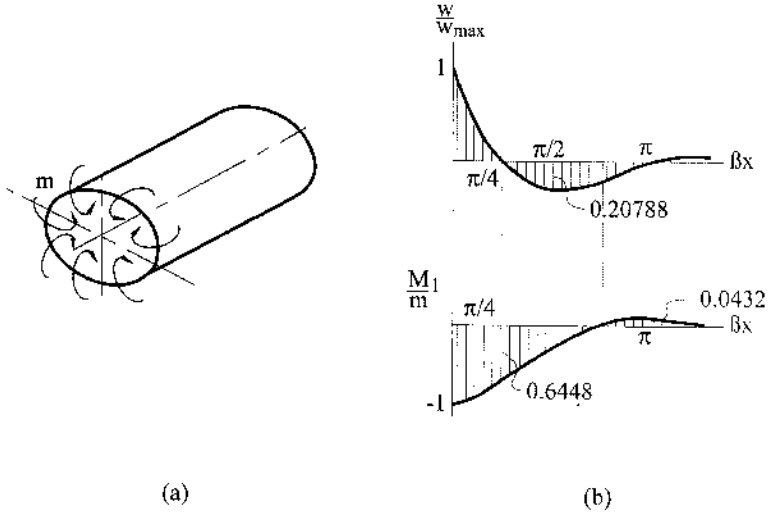

Fig. 15.5

$$w|_{x=0} = w_{\max} = \frac{m}{2D\beta^2}; \quad M_1\big|_{x=0} = M_{1\max} = -m.$$

Figure 15.5b shows the plots of the deflections and moments in a dimensionless form over the shell length. It is seen that all these values practically diminish at a distance $x = 2.3\sqrt{Rh}$ from the loaded edge of the shell. Such a sharp decrease of the moment state components, as we move away from the loaded shell edge, is called the *edge effect*. It will be discussed in more detail later, in Sec. 17.5.

Example 15.2

Determine the stresses and deformations in a long thin-walled cylinder with a rigid end, as shown in Fig. 15.6a. The cylinder is subjected to an internal pressure of intensity p. Assume that $R = 1.2\,\text{m}$, $h = 0.01\,\text{m}$, $p_3 = -p = \text{const}$, and $\nu = 0.3$.

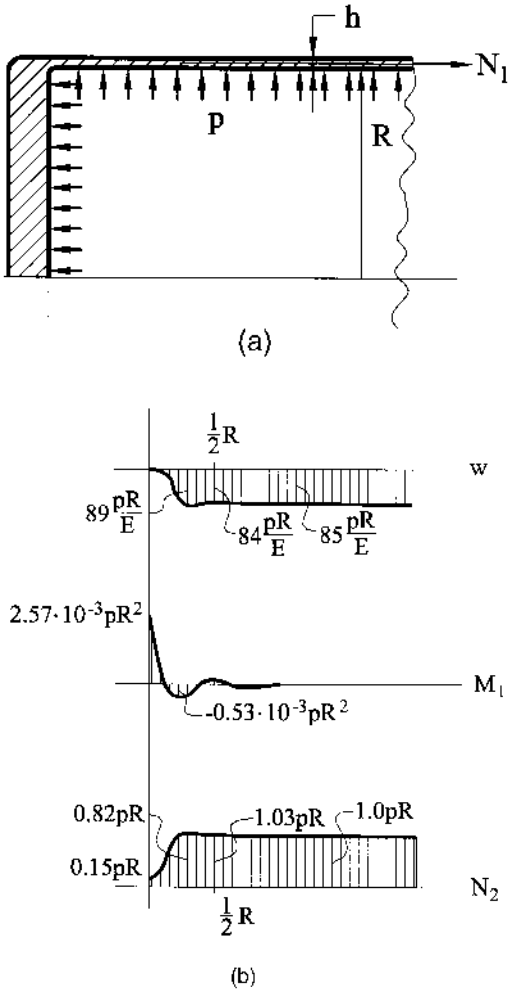

Fig. 15.6

Solution

Since the end is absolutely rigid, the shell edge may be assumed to be built-in with the end, and the boundary conditions are given by Eqs (15.52a). Making $p_1 = 0$, we can find the meridional force at the edge $x = 0$ from the equilibrium of part of the shell cut off along the circle $x = \text{const}$. We have the following:

$$N_1^{(0)}(2\pi R) = p(\pi R^2), \text{ from which } N_1^{(0)} = \frac{pR}{2}.$$

Thus $N_1 = N_1^{(0)} = pR/2 = \text{const}$ and the particular solution (Eq. (15.50)) is of the form

$$w_{\text{p}} = -\frac{pR^2}{Eh}(1 - \nu/2).$$

The geometric parameter is

$$\beta = \sqrt[4]{\frac{3(1-\nu^2)}{R^2h^2}} = 11.73(1/\text{m}).$$

Substituting for w and $\vartheta = \text{d}w/\text{d}x$ from Eqs (15.57a) and (15.57b) into the boundary conditions (15.52a), we obtain the two following equations:

$$-\frac{M_0}{2D\beta^2} - \frac{Q_0}{2D\beta^3} - p\frac{R^2}{Eh}\left(1 - \frac{\nu}{2}\right) = 0; \quad \frac{M_0}{\beta D} + \frac{Q_0}{2\beta^2 D} = 0.$$

Solving these equations for M_0 and Q_0 gives

$$M_0 = \frac{p}{2\beta^2}\left(1 - \frac{\nu}{2}\right), \quad Q_0 = -\frac{p}{\beta}\left(1 - \frac{\nu}{2}\right).$$

Then, using Eqs (15.57), we can determine the following deflections, internal forces, and moments:

$$w = \frac{pR^2}{Eh}\left(1 - \frac{\nu}{2}\right)\left[\text{e}^{-\beta x}(\sin\beta x + \cos\beta x) - 1\right],$$

$$N_2 = pR\left[1 - \left(1 - \frac{\nu}{2}\right)\text{e}^{-\beta x}(\cos\beta x + \sin\beta x)\right],$$

$$M_1 = \frac{p}{2\beta^2}\left(1 - \frac{\nu}{2}\right)\text{e}^{-\beta x}(\cos\beta x - \sin\beta x), \; M_2 = \nu M_1.$$

Figure 15.6b shows the diagrams of w, M_1, and N_2 along the shell length. The maximum bending moments occur at the junction of the shell and the head (at $x = 0$) and they are, as follows:

$$M_{1\,\max} = \frac{p}{2\beta^2}\left(1 - \frac{\nu}{2}\right) = 3.08 \times 10^{-3} p \text{ (Nm/m)},$$

$$M_{2\,\max} = \nu M_{1\,\max} = 0.924 \times 10^{-3} p \text{ (Nm/m)}.$$

The tensile membrane forces at $x = 0$ are

$$N_1 = \frac{pR}{2} = 0.6p, \quad N_2 = pR(1 - (1 - \nu/2)) = 0.18p \text{ (N/m)}.$$

The maximum normal stresses at outside points of the shell section located at the junction of the shell and head ($x = 0$) are the following:

$$\sigma_1 = \frac{6M_1}{h^2} + \frac{N_1}{h} = 184.8p + 60p = 244.8p \ (\mathrm{N/m^2}),$$

$$\sigma_2 = \frac{6M_2}{h^2} + \frac{N_2}{h} = 55.4p + 18p = 73.4p \ (\mathrm{N/m^2}).$$

At sections of the cylinder remote from the end, the bending moments vanish and the tensile membrane forces take the following values:

$$N_1 = \frac{pR}{2} = 0.6p, \quad N_2 = pR = 1.2p \ (\mathrm{N/m}).$$

The zone of the bending stresses is very small and at a distance of $R/16$ from the head, the bending stresses vanish.

Example 15.3

Determine the normal stresses in the cylinder of Example 15.2, (Fig. 15.6a), assuming that the flat end has a thickness comparable with the thickness of cylinder wall. Given: h (thickness of the cylinder wall) $= 0.01\,\mathrm{m}$, h_1 (thickness of the head) $= 0.04\,\mathrm{m}$, $R = 1.2\,\mathrm{m}$, $\nu = 0.3$, $E = 200\,\mathrm{GPa}$, and $p = \mathrm{const}$.

Solution

Separate mentally the cylinder and end into two independent components by taking a section at the point of intersection of the middle surfaces of the cylinder and end. This point may be regarded as a junction. Since the deformations of the independent components (cylinder and end) do not match each other at the junction, we have to apply unknown forces and couples, Q_0, M_0, and $N_1^{(0)}$, as shown in Fig. 15.7. These unknown forces and couples are to be determined from the compatibility conditions at the junction of the cylinder and end. We make the following reasonable assumption that stretching of the flat end may be neglected, i.e., the end is infinitely rigid for any in-plane deformations. Then, the compatibility conditions can be formulated as follows:

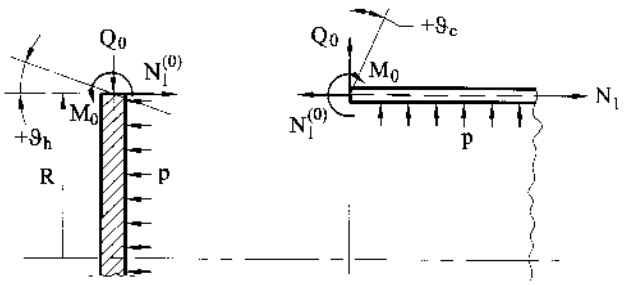

Fig. 15.7

$$w_c = 0\big|_{x=0}\ (a) \quad \text{and} \quad \vartheta_c\big|_{x=0} = \vartheta_h\big|_{r=R}\ (b), \tag{15.59}$$

i.e., the deflection of the cylinder at the junction is zero and the relative rotation of the wall of cylinder, ϑ_c, and flat end, ϑ_h, at the junction is also zero. The positive directions of the rotations are shown in Fig. 15.7. We have two equations and three unknowns. However, the meridional membrane force can be directly determined from the equilibrium conditions of the head, i.e.,

$$p(\pi R^2) = N_1(2\pi R), \quad \text{from which } N_1 = \frac{pR}{2}. \tag{a}$$

Deflections and slopes of the edge of the cylinder may be determined from Eqs (15.57) and (15.50) with regard to Eq. (a), as follows:

$$w_c\big|_{x=0} = -\left[\frac{M_0}{2D\beta^2} + \frac{Q_0}{2D\beta^3} + \frac{pR^2}{Eh}\left(1 - \frac{\nu}{2}\right)\right], \quad \vartheta_c\big|_{x=0} = \frac{M_0}{D\beta} + \frac{Q_0}{2D\beta^2}. \tag{b}$$

The angle of rotation of a normal of the end edge, ϑ_h, due to p and M_0 can be obtained by differentiating Eqs (4.26) and (4.38) with respect to r. Letting $p_0 = -p$ and $a = R$ in Eq. (4.26) and $b = 0$, $m_2 = 0$, and $m_1 = M_0$ in Eq. (4.39), yields, after differentiation the following expression for ϑ_h,

$$\vartheta_h\big|_{r=R} = \vartheta_h(p)\big|_{r=R} + \vartheta_h(M_0)\big|_{r=R} = \frac{pR^3}{8D_1(1+\nu)} - \frac{M_0 R}{D_1(1+\nu)}. \tag{c}$$

In writing this equation, it has been taken into account that the angles of rotation of normals to the end middle surface produced by p and M_0 have different signs (see Fig. 15.7) at the junction.

Substituting for w_c, ϑ_c, and ϑ_h from Eqs (b) and (c) into Eq. (15.59) yields the following equations for the unknowns M_0 and Q_0:

$$\frac{M_0}{2D\beta^2} + \frac{Q_0}{2D\beta^3} + \frac{pR^2}{Eh}\left(1 - \frac{\nu}{2}\right) = 0; \quad \frac{M_0}{D\beta} + \frac{Q_0}{2D\beta^2} = -\frac{M_0 R}{D_1(1+\nu)} + \frac{pR^3}{8D_1(1+\nu)} \tag{d}$$

where

$$\beta = 11.734\ (1/\text{m})\ \text{(see Example 15.2)},$$

$$D = \frac{Eh^3}{12(1-\nu^2)} = 18.315 \times 10^3(\text{Nm}), \ \text{and}$$

$$D_1 = \frac{Eh_1^3}{12(1-\nu^2)} = 1172 \times 10^3(\text{Nm}).$$

Using the above numerical data, and solving Eqs (d) for M_0 and Q_0, yields the following:

$$M_0 = 0.04783p\ (\text{Nm/m}), \quad Q_0 = -0.5972 \times 10^{-2}p\ (\text{N/m}).$$

Note that for an absolutely rigid end, the bending moment at the junction was

$$M_1 = 0.00308p \text{ (Nm/m)}.$$

Thus, because of the compliance of the flat end, the bending moment at the cylinder edge increases more than 10 times. This can be explained by the fact that the end is deflected as if it turns the edge of the cylinder inside out. The bending moment diagrams are shown in Fig. 15.8.

The maximum stresses at the center of the head are

$$\sigma_r = \sigma_t = \frac{6M_1}{h_1^2} = \frac{0.252p(6)}{4^2(10^{-4})} = 945p \text{ (N/m}^2\text{)}.$$

The maximum stresses in the cylinder occur in the neighborhood of the edge. They are

$$\sigma_1 = \frac{pR}{2h} + \frac{6M_1}{h^2} = 2930p \text{ N/m}^2); \quad \sigma_2 = \nu\left(\frac{pR}{2h} + \frac{6M_1}{h^2}\right) = 879p \text{ (N/m}^2\text{)}.$$

The tensile stresses in the cylinder away from the edge are

$$\sigma_1 = \frac{pR}{2h} = 60p, \quad \sigma_2 = \frac{pR}{h} = 120p \text{ (N/m}^2\text{)}.$$

Example 15.4

A long thin-walled cylindrical shell is subjected to a circumferential line load P (force/length), as shown in Fig. 15.9. Determine the expressions for the deflections, internal forces, and bending moments.

Solution

Consider a free-body diagram of the small ring cut from the shell and enclosing the line load P, as shown in Fig. 15.10. For the right half of the cylinder, the following boundary conditions may be formulated from the symmetry of the loading:

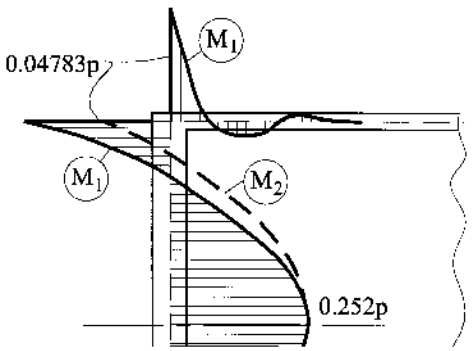

Fig. 15.8

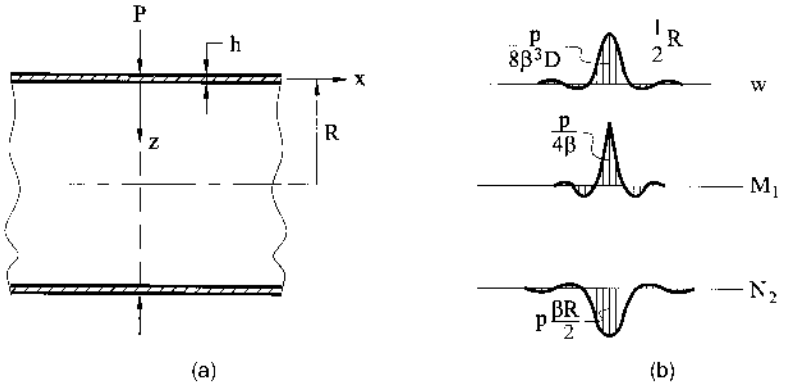

Fig. 15.9

$$\left.\frac{dw}{dx}=0\right|_{x=0}, \tag{15.60a}$$

$$Q_0=-\left.\frac{P}{2}\right|_{x=0} \quad \text{(see Fig. 15.10).} \tag{15.60b}$$

Substituting for dw/dx from Eq. (15.57b) into Eq. (15.60a) yields

$$\frac{M_0}{\beta D}+\frac{Q_0}{2\beta^2 D}=0,$$

or taking into account Eq. (15.60b), we obtain from the above $M_0=\dfrac{P}{4\beta}$.

Inserting the above into Eqs (15.57), we obtain the following expressions for the deflections, internal forces, and bending moments:

$$w=\frac{P}{8\beta^3 D}e^{-\beta x}(\sin\beta x+\cos\beta x), \tag{15.61a}$$

$$M_1=\frac{P}{4\beta}e^{-\beta x}(\cos\beta x-\sin\beta x),\ M_2=\nu M_1, \tag{15.61b}$$

$$N_2=-\frac{EhP}{8\beta^3 RD}e^{-\beta x}(\sin\beta x+\cos\beta x),\ N_1=0. \tag{15.61c}$$

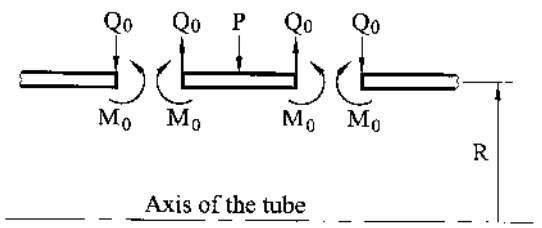

Fig. 15.10

The deflection, bending moment, and circumferential force diagrams are shown in Fig. 15.9b.

Expressions (15.61) may be used as Green's functions for determining the deflections, internal forces, and bending moments in long cylindrical shells subjected to radial loading uniformly distributed around the circumference of a shell, but arbitrarily distributed along the x axis (along the shell meridian), as shown in Fig. 15.11. For the use of w in the form of Eq. (15.61a) as Green's function, we rewrite it as follows:

$$w(x) = \frac{P}{8\beta^3 D} \cdot F(\beta x), \tag{15.62a}$$

where

$$F(\beta x) = e^{-\beta x}(\sin \beta x + \cos \beta x). \tag{15.62b}$$

First, we assume that a point of observation A (point where the deflection is to be determined) is located outside the loaded region $p(\xi)$, as shown in Fig. 15.11a. Take the origin of the Cartesian coordinate system at a point A. The elementary deflection at point A caused by an elementary radial line load $p(\xi)d\xi$ applied at a distance ξ from the origin is given by Eq. (15.62a), replacing P with $pd\xi$, and x with ξ:

$$dw_A = p(\xi)dx\frac{F(\beta\xi)}{8\beta^3 D}.$$

The deflection at point A produced by the entire load is derived as follows:

$$w_A = \frac{1}{8\beta^3 D}\int_a^{a+L} p(\xi)F(\beta\xi)d\xi, \tag{15.63}$$

which can be calculated once $p(\xi)$ is specified. Consider a particular case, $p = \text{const}$. Inserting Eq. (15.62b) into the above and letting $p = \text{const}$, we obtain the following after integration:

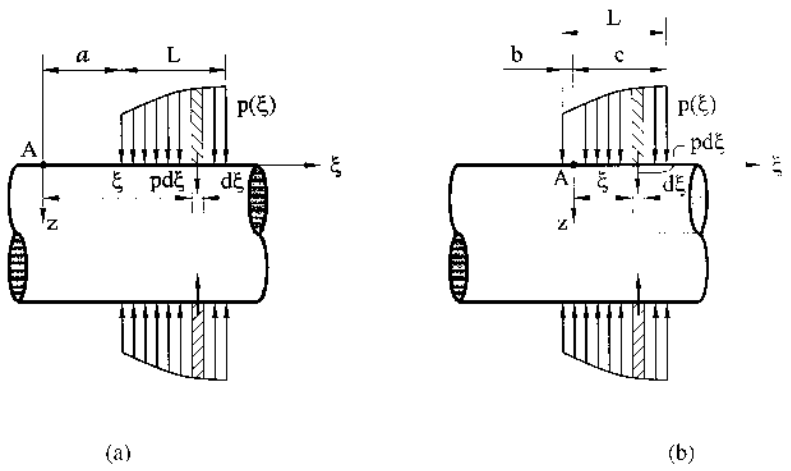

(a) (b)

Fig. 15.11

$$w_A = \frac{pR^2}{2Eh} e^{-\beta a}\left[\cos \beta a - e^{-\beta L} \cos \beta(a + L)\right]. \tag{15.64}$$

Secondly, locate the point of observation, A, within the loaded region, as shown in Fig. 15.11b. Let us take the origin of the Cartesian coordinates again at point A. An elementary deflection at that point owing to load $p\mathrm{d}\xi$ is given by Eq. (15.62). Thus, the resulting deflection at point A produced by the entire load can be again obtained by integration of Eq. (15.62). We have

$$w_A = \frac{1}{8\beta^3 D}\left[\int_0^b p(\xi)F(\beta\xi)\mathrm{d}\xi + \int_0^c p(\xi)F(\beta\xi)\mathrm{d}\xi\right]. \tag{15.65}$$

If $p = \text{const}$, then inserting Eq. (15.62b) into the above and putting $p = \text{const}$, we obtain the following after integration:

$$w_A = \frac{pR^2}{2Eh}\left[2 - e^{-\beta b}\cos \beta b - e^{-\beta c}\cos \beta c\right]. \tag{15.66}$$

Note that if the distance a is large and L is finite, then, as follows from Eq. (15.64), $w_A \approx 0$. This agrees well with the physical meaning. If b and c are large in Eq. (15.66), then the deflection will be approximately equal to pR^2/Eh, which represents the deflection of a long cylindrical shell subjected to an axisymmetrical uniform load of intensity $p = \text{const}$.

Example 15.5

A stiffening ring is placed around a long cylinder at a distance remote from the ends, as shown in Fig. 15.12a. The cylinder is subjected to an internal pressure of intensity p. The radius of the shell middle surface is R and the wall thickness is h. The ring dimensions are h_i (thickness of the ring) and b_i (the width of the ring). Determine the stresses at the ring attachment. Assume that the ring does not resist rotation, the dimensions of the ring cross section are small compared with the shell radius, and the shell and ring are made of one and the same material.

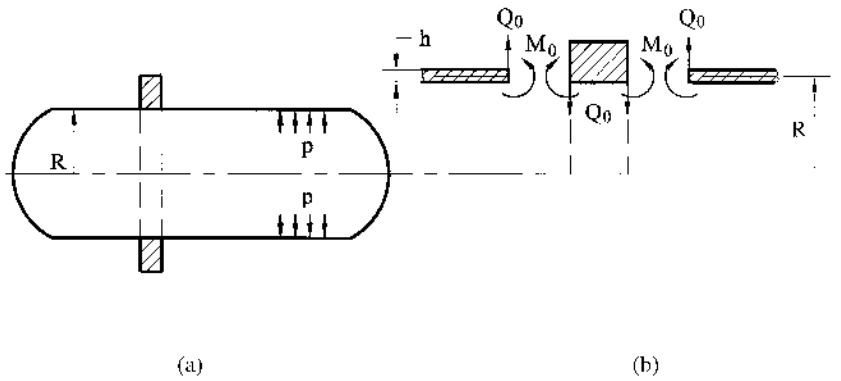

Fig. 15.12

Solution

Figure 15.12b shows the free-body diagram of the ring and adjacent parts of the cylinder walls. The contact forces and moments between the cylinder and ring are the shear force Q_0 and the bending moment M_0. Compatibility of the deflections for the shell, w_s, and for the ring, w_r, require that

$$w_s = w_r. \tag{a}$$

From symmetry, the angle of rotation of the shell, ϑ_s, due to the pressure and contact forces, Q_0, and moments, M_0, must be zero. So, the second compatibility equation is the following:

$$\vartheta_s = 0. \tag{b}$$

The deflection of the ring due to $2Q_0$ is

$$w_r = \frac{(2Q_0R)R}{A_iE}, \tag{c}$$

where $A_i = b_i \cdot h_i$ is the cross-sectional area of the ring. The deflection of the shell due to the pressure and contact forces and moments is determined by Eq. (15.57a), as follows:

$$w_s = -\left[\frac{M_0}{2D\beta^2} + \frac{Q_0}{2D\beta^3} + \frac{pR^2}{Eh}\left(1 - \frac{\nu}{2}\right)\right]. \tag{d}$$

The signs for w_r and w_s due to the internal pressure and contact forces and moments are in an agreement with the general sign convention adopted in this book for the deflections w in thin shells. The angle of rotation of the shell due to the pressure and contact forces and moments at the ring attachment is determined by Eq. (15.57b) as follows:

$$\vartheta_s = \frac{\mathrm{d}w_s}{\mathrm{d}x} = \frac{M_0}{\beta D} + \frac{Q_0}{2\beta^2 D} \tag{e}$$

(it can be easily shown by inspection that M_0 and Q_0 produce rotation of the same signs).

Substituting for w_s and ϑ_s from Eqs (d) and (e) into Eqs (a) and (b), results in the following equations:

$$\begin{aligned} &\frac{2Q_0R^2}{A_iE} = -\left[\frac{M_0}{2D\beta^2} + \frac{Q_0}{2D\beta^3} + \frac{pR^2}{Eh}\left(1 - \frac{\nu}{2}\right)\right], \\ &\frac{M_0}{\beta D} + \frac{Q_0}{2\beta^2 D} \end{aligned} \tag{f}$$

Solving this system of equations for M_0 and Q_0 gives the following:

$$M_0 = \frac{p}{2h\beta}\frac{1 - \nu/2}{(2/A_i + \beta/h)}, \quad Q_0 = -\frac{p}{h}\frac{1 - \nu/2}{(2/A_i + \beta/h)}. \tag{15.67}$$

Stress in the ring is

$$\sigma_r = \frac{2Q_0 R}{A_i} = -\frac{2pR(1-\nu/2)}{h(2+A_i\beta/h)}. \tag{15.68}$$

The maximum longitudinal stress in the shell occurs at the ring attachment and is given by

$$\sigma_1^{(s)} = \frac{pR}{2h} + \frac{6M_1}{h^2} = \frac{pR}{2h} + \frac{3p(1-\nu/2)}{h^3\beta(2/A_i+\beta/h)}. \tag{15.69}$$

The deflection of the shell at the ring junction is

$$w_s = -\frac{2pR^2(1-\nu/2)}{E(2h+A_i\beta)}. \tag{15.70}$$

The circumferential membrane force is given by Eq. (15.57e). Substituting for M_0 and Q_0 from Eqs (15.67) into the above, and letting $x = 0$, gives the following:

$$N_2 = pR\left[-\frac{\beta(1-\nu/2)}{h(2/A_i+\beta/h)} + 1\right]. \tag{15.71}$$

The circumferential bending moment is

$$M_2 = \nu M_1 = \frac{\nu p}{2h\beta}\frac{1-\nu/2}{(2/A_i+\beta/h)}.$$

Finally, the circumferential stress in the shell is given by

$$\sigma_2^{(s)} = \frac{N_2}{h} + \frac{6M_2}{h^2} = \frac{p}{h}\left[R + \frac{(1-\nu/2)}{h(2/A_i+\beta/h)}\left(\frac{3\nu}{\beta h} - \beta R\right)\right]. \tag{15.72}$$

15.3.2 Analysis of short cylindrical shells

It was shown in the above analysis of long cylindrical shells that the deflection and stress components due to the applied edge shear forces and bending moments dissipate rapidly as x increases and it becomes larger than $2.3\sqrt{Rh}$. This rapid reduction in deflections and stresses, as x increases, simplifies the solution (15.49) by letting $A_3 = A_4 = 0$. When the length of the cylinder, L, is less than about $2.3\sqrt{Rh}$, A_3 and A_4 cannot be ignored and all four constants in Eq. (15.49) must be evaluated. Thus, when the length of the shell is comparatively small, a mutual effect of the shell edges is so considerable that the constants of integration in Eq. (15.49) cannot be determined separately. Shells whose length does not satisfy the inequality (15.55) are referred to as *short shells*. A solution for short shells involves all the four constants of integration.

To simplify the procedure of evaluating the constants A_i $(i = 1, 2, 3, 4)$, we introduce the so-called Krylov's functions [7], as follows:

$$V_1(\beta x) = \cosh \beta x \cos \beta x;\ V_2(\beta x) = \frac{1}{2}[\cosh \beta x \sin \beta x + \sinh \beta x \cos \beta x],$$

$$V_3(\beta x) = \frac{1}{2}\sinh \beta x \sin \beta x;\ V_4(\beta x) = \frac{1}{4}[\cosh \beta x \sin \beta x - \sinh \beta x \cos \beta x]. \tag{15.73}$$

A transition from the exponential functions to Krylov's functions is implemented with the use of Euler's expression, as follows:

$$e^{i\varphi} = \cos \varphi + i \sin \varphi,\ e^{\varphi} = \cosh \varphi + \sinh \varphi.$$

As a result, the general solution (15.47) may be transformed to the following form:

$$w = C_1 V_1(\beta x) + C_2 V_2(\beta x) + C_3 V_3(\beta x) + C_4 V_4(\beta x) + w_{\mathrm{p}}, \tag{15.74}$$

where $C_1, \ldots, C_4$ are new constants of integration.

Krylov's functions possess the following properties. First, they are related to one another by the following simple differential relationships:

$$\frac{\mathrm{d}}{\mathrm{d}x} V_1(\beta x) = -4\beta V_4(\beta x), \frac{\mathrm{d}}{\mathrm{d}x} V_2(\beta x) = \beta V_1(\beta x),$$
$$\frac{\mathrm{d}}{\mathrm{d}x} V_3(\beta x) = \beta V_2(\beta x), \frac{\mathrm{d}}{\mathrm{d}x} V_4(\beta x) = \beta V_3(\beta x). \tag{15.75}$$

Secondly, when $x = 0$, all these functions vanish except for the function V_1, which is equal to unity, i.e.,

$$V_1(0) = 1, \quad V_2(0) = 0, \quad V_3(0) = 0, \quad V_4(0) = 0. \tag{15.76}$$

These properties of Krylov's functions enable one to express the constants of integration C_i $(i = 1, 2, 3, 4)$ in terms of the so-called initial parameters w_0, ϑ_0, M_{10}, and Q_{10}, i.e., the deflection, slope, bending moment, and shear force prescribed at the shell edge $x = 0$. Taking into account Eqs (15.57) and (15.74)–(15.76), one can write the following:

$$w_0 = C_1 + w_{\mathrm{p}0'}, \tag{15.77a}$$

$$\vartheta_0 = \beta C_2 + w'_{\mathrm{p}0}, \tag{15.77b}$$

$$M_{10} = -D(\beta^2 C_3 + w''_{\mathrm{p}0}), \tag{15.77c}$$

$$Q_{10} = -D(\beta^3 C_4 + w_{\mathrm{p}0}). \tag{15.77d}$$

where $w_{\mathrm{p}0}$, $w'_{\mathrm{p}0}$, $w''_{\mathrm{p}0}$, and w'''_{p0} are the particular solution and its derivatives with respect to x at the shell edge $x = 0$. Evaluating $C_1, \ldots, C_4$ from Eqs (15.77) in terms of the initial parameters and inserting them into Eq. (15.74), we obtain the following expressions for the deflections in terms of the initial parameters:

$$w = (w_0 - w_{\mathrm{p}0})V_1(\beta x) + \frac{1}{\beta}\left(\vartheta_0 - w'_{\mathrm{p}0}\right)V_2(\beta x) - \frac{1}{\beta^2}\left(\frac{M_{10}}{D} + w''_{\mathrm{p}0}\right)V_3(\beta x)$$
$$- \frac{1}{\beta^3}\left(\frac{Q_{10}}{D} + w'''_{\mathrm{p}0}\right)V_4(\beta x) + w_{\mathrm{p}}. \tag{15.78}$$

Differentiating the above and using relations (15.75) leads to the following expressions for ϑ, M_1, and Q_1

$$\vartheta = -4\beta(w_0 - w_{p0})V_4(\beta x) + (\vartheta_0 - w'_{p0})V_1(\beta x) - \frac{1}{\beta}\left(\frac{M_{10}}{D} + w''_{p0}\right)V_2(\beta x)$$

$$-\frac{1}{\beta^2}\left(\frac{Q_{10}}{D} + w'''_{p0}\right)V_3(\beta x) + w'_p, \tag{15.79}$$

$$M_1 = 4D\beta^2(w_0 - w_{p0})V_3(\beta x) + 4D\beta(\vartheta_0 - w'_{p0})V_4(\beta x) + (M_{10} + Dw''_{p0})V_1(\beta x)$$

$$+\frac{1}{\beta}(Q_{10} + Dw'''_{p0})V_2(\beta x) - Dw''_p, \tag{15.80}$$

$$Q_1 = 4D\beta^3(w_0 - w_{p0})V_2(\beta x) + 4D\beta^2(\vartheta_0 - w'_{p0})V_3(\beta x) - 4\beta(M_{10} + Dw''_{p0})V_4(\beta x)$$

$$+(Q_{10} + Dw'''_{p0})V_1(\beta x) - Dw'''_p. \tag{15.81}$$

The particular solution is determined by Eq. (15.50). If $p_3 = \text{const}$ and $N_1 = \text{const}$, then $w'_p = w_p{}'' = w'''_p = 0$.

Since two out of the four initial parameters are usually known from the boundary conditions on the shell edge $x = 0$, then the problem of evaluating the constants of integration is reduced to a solution of a system of algebraic equations for two unknowns. The latter is set up from the boundary conditions at the shell edge $x = L$ (where L is the shell length).

Example 15.6

Determine the equation of the deflected surface of a short cylindrical shell of radius R loaded by uniformly distributed moments m along the edge $x = L$, as shown in Fig. 15.13.

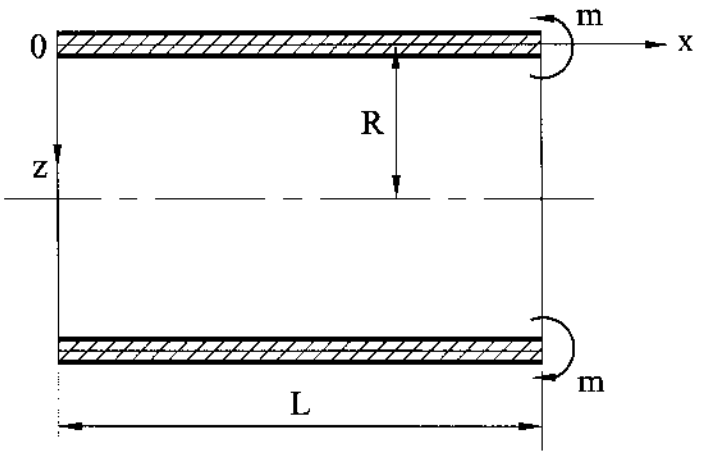

Fig. 15.13

Solution

Since for the edge $x = 0$, $M_1 = 0$, $Q_1 = 0$, and no transverse load is applied to the shell, then the deflection surface of the shell is of the form

$$w = w_0 V_1(\beta x) + \frac{1}{\beta}\vartheta_0 V_2(\beta x). \tag{a}$$

The initial parameters, w_0 and ϑ_0, may be evaluated from the boundary conditions on the edge $x = L$. The boundary conditions are

$$M_1 = m\big|_{x=L}, \quad Q_1 = 0\big|_{x=L}. \tag{b}$$

Inserting the expressions for the bending moment and shear force, Eqs (15.80) and (15.81), into the above, yields the following equations:

$$\begin{aligned} 4D\beta^2 w_0 V_3(\beta L) + 4D\beta\vartheta_0 V_4(\beta L) &= m, \\ 4D\beta^3 w_0 V_2(\beta L) + 4D\beta^2\vartheta_0 V_3(\beta L) &= 0. \end{aligned} \tag{c}$$

Solving these equations for w_0 and ϑ_0 gives

$$w_0 = -\frac{mV_3(\lambda)}{4D\beta^2[V_4(\lambda)V_2(\lambda) - V_3^2(\lambda)]}, \quad \vartheta_0 = \frac{mV_2(\lambda)}{4D\beta[V_4(\lambda)V_2(\lambda) - V_3^2(\lambda)]},$$

where $\lambda = \beta L$. Substituting the above into Eq. (15.78) gives the deflection surface of the short cylindrical shell loaded by a uniformly distributed moment m applied along the edge $x = L$:

$$w(x) = \frac{m}{4D\beta^2[V_4(\lambda)V_2(\lambda) - V_3^2(\lambda)}[-V_3(\lambda)V_1(\beta x) + V_2(\lambda)V_2(\beta x)]. \tag{15.82}$$

In a general case of loading, a cylindrical shell may be subjected to circumferential axisymmetric line loads P and moments m, respectively, as well as to uniform pressure p distributed over some shell length, as shown in Fig. 15.14. This shell can be divided into several segments (I, II, III, etc.) between sections where the loading conditions change. For each such segment, the function w will be different. To avoid the determination of a large number of constants of integration, it is convenient to set up a *general-purpose equation* of the middle surface of the shell which is continuous function of x throughout a shell in spite of the discontinuity of the loading diagram.

In setting up the general-purpose equation of the deflection surface of the shell, it should be taken into account that the function w and its first derivative should be continuous everywhere. The second derivative changes abruptly at sections where the radial moments m are applied, the third derivative may have a jump at sections where the radial forces P are applied, etc.

Dropping intermediate mathematics, we present below the general-purpose equation of the deflections for a cylindrical shell subjected to discontinuous loads, as shown in Fig.15.14:

$$w(x) = (w_0 - w_{p0})V_1(\beta x) + \frac{1}{\beta}(\vartheta_0 - w'_{p0})V_2(\beta x) - \frac{1}{\beta^2}\left(\frac{M_{10}}{D} + w''_{p0}\right)V_3(\beta x)$$
$$- \frac{1}{\beta^2}\left(\frac{Q_{10}}{D} + w'''_{p0}\right)V_4(\beta x) + w_{p1}\Big|_{I} - \frac{P}{D\beta^3}V_4[\beta(x - l_P)]\Big|_{II}$$
$$- \frac{m}{D\beta^2}V_3[\beta(x - l_m)]\Big|_{III} + \left(-p + \frac{\nu N_1}{R}\right)\frac{R^2}{Eh}\{1 - V_1[\beta(x - l_N)]\}\Big|_{IV}, \tag{15.83}$$

where w_{p1} is a particular solution for the first segment; l_P, l_m, and l_N are the coordinates of an application of the applied line forces P, moments m, and meridional forces N_1, respectively. In a general case, a number of terms in Eq. (15.83) depend on a number of discontinuous loads applied to the shell. The signs of the terms adopted in this equation correspond to directions of loads indicated in Fig. 15.14 and to the sign convention for deflections used in this book. The initial parameters w_0, ϑ_0, M_{10}, and Q_{10} are determined, as usual, from the boundary conditions. Two of them are known for $x = 0$, the remaining two parameters are evaluated from the boundary conditions at the shell edge $x = L$.

Example 15.7

A short cylinder is loaded by two moments m uniformly distributed along circular sections $x = 2.5$ in. and $x = 7.5$ in., respectively, as shown in Fig. 15.15. Assuming that $R = 20$ in., $h = 1$ in., $\nu = 0.3$, and $L = 10$ in., determine the equation of the deflected midsurface of the cylinder.

Solution

For the given data,

$$\beta = \sqrt[4]{\frac{3(1-\nu^2)}{h^2R^2}} = \sqrt[4]{\frac{3(1-0.3^2)}{(1)^2(20)^2}} = 0.28741/\text{in.}$$

Taking the origin of the coordinate system at the left edge of the shell, we can write the general-purpose equation (Eq. (15.83)) for the problem under consideration:

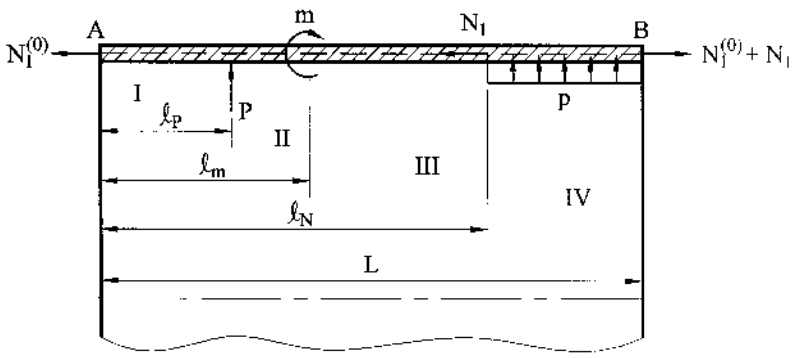

Fig. 15.14

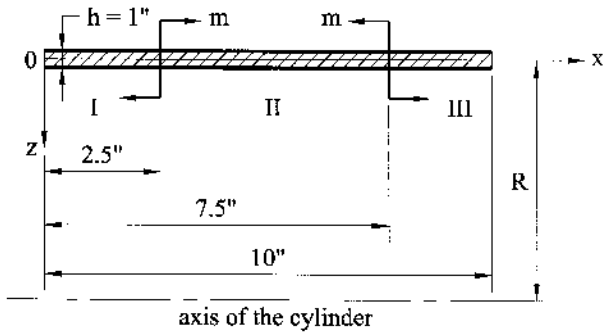

Fig. 15.15

$$w = w_0 V_1(\beta x) + \frac{1}{\beta}\vartheta_0 V_2(\beta x) - \frac{M_{10}}{\beta^2 D} - \frac{Q_{10}}{\beta^3 D}\Big|_{\mathrm{I}} - \frac{m}{\beta^2 D} V_3[\beta(x-2.5)]\Big|_{\mathrm{II}} + \frac{m}{\beta^2 D} V_3[\beta(x-7.5)]\Big|_{\mathrm{III}}. \tag{a}$$

Taking into account that $M_{10} = Q_{10} = 0$, this equation simplifies to the form

$$w = w_0 V_1(\beta x) + \frac{\vartheta_0}{\beta} V_2(\beta x)\Big|_{\mathrm{I}} - \frac{m}{\beta^2 D} V_3[\beta(x-2.5)]\Big|_{\mathrm{II}} + \frac{m}{\beta^2 D} V_3[\beta(x-7.5)]\Big|_{\mathrm{III}} \tag{b}$$

Applying Eqs (15.39), (15.46), and (15.73), one obtains the corresponding equations for the bending moments and shear forces:

$$\begin{aligned} M_1 &= -D\left\{-4\beta^2 w_0 V_3(\beta x) - 4\beta\vartheta_0 V_4(\beta x)\Big|_{\mathrm{I}} - \frac{m}{D} V_1[\beta(x-2.5]\Big|_{\mathrm{II}} + \frac{m}{D} V_1[\beta(x-7.5)]\Big|_{\mathrm{III}}\right\}, \\ Q_1 &= -D\left\{-4\beta^3 w_0 V_2(\beta x) - 4\beta^2\vartheta_0 V_3(\beta x)\Big|_{\mathrm{I}} + m\frac{4\beta}{D} V_4[\beta(x-2.5)]\Big|_{\mathrm{II}} - m\frac{4\beta}{D} V_4[\beta(x-7.5)]\Big|_{\mathrm{III}}\right\}. \end{aligned} \tag{c}$$

Boundary conditions on the right edge of the shell are of the form

$$M_1 = 0\big|_{x=10\,\mathrm{in.}}, \quad Q_1 = 0\big|_{x=10\,\mathrm{in.}} \tag{d}$$

Substituting Eqs (c) into the above boundary conditions, we obtain the system of two equations for w_0 and ϑ_0. Solving this system of equations, yields the following values of the initial parameters:

$$w_0 = -3.67\frac{m}{D}, \quad \vartheta_0 = 1.56\frac{m}{D}.$$

Inserting the above values of the initial parameters into Eq. (b) yields the equation of the deflected middle surface of the shell in the form

$$w = \frac{m}{D}\{-3.67V_1(0.2874x) + 5.428V_2(0.2874x)\big|_{\mathrm{I}} + 12.107V_3[0.2874(x-2.5)]\big|_{\mathrm{II}} + 12.107V_3[0.2874(x-7.5)]\big|_{\mathrm{III}}\}.$$

15.4 CIRCULAR CYLINDRICAL SHELL OF VARIABLE THICKNESS UNDER AXISYMMETRIC LOADING

Consider a state of stress and strain of circular cylindrical shells whose thickness varies only along the shell generator, i.e., $h = h(x)$, and remains symmetrical with respect to the middle surface. This shell is subjected to axisymmetrically applied edge and distributed loads. It follows from the preceding sections that in this case a deformation of the shell does not depend on the circumferential angle θ.

The governing differential equation for bending of an axisymmetrically loaded circular cylindrical shell, Eq. (15.43), can be generalized to the case of the above-mentioned shell with variable thickness, as follows:

$$\frac{\mathrm{d}^2}{\mathrm{d}x^2}\left[D(x)\frac{\mathrm{d}^2 w}{\mathrm{d}x^2}\right] + \frac{Eh}{R^2}w = p_3 + \frac{\nu}{R}N_1, \tag{15.84}$$

where

$$D(x) = \frac{Eh^3(x)}{12(1-\nu^2)}. \tag{15.85}$$

is the flexural stiffness of the shell with variable thickness $h = h(x)$. Equation (15.84) is a fourth-order ordinary differential equation with variable coefficients. It may be solved analytically for some particular laws of $D = D(x)$ only. For instance, Timoshenko provided an analytical solution of this equation when $h = \alpha x$ ($\alpha > 0$) using the Bessel functions [8]. In a general case, when $D(x)$ is an arbitrary function of x, a solution of Eq. (15.84) can be obtained only numerically. For this purpose, one has to transform Eq. (15.84) in the following way. Using Eqs (15.39), (15.41), and (15.46), one can reduce the fourth-order differential equation to the system of four first-order differential equations, as follows:

$$\begin{aligned} &\frac{\mathrm{d}w}{\mathrm{d}x} = \vartheta_1; \quad \frac{\mathrm{d}\vartheta_1}{\mathrm{d}x} = \frac{\mathrm{d}^2 w}{\mathrm{d}x^2} = -\frac{M_1}{D}; \quad \frac{\mathrm{d}M_1}{\mathrm{d}x} = Q_1; \\ &\frac{\mathrm{d}Q_1}{\mathrm{d}x} = -\left(p_3 + \frac{N_2}{R}\right) = -p_3 - \nu\frac{N_1}{R} + \frac{Eh}{R^2}w. \end{aligned} \tag{15.86}$$

Let us introduce a dimensionless variable ξ and dimensionless parameters of the state of stress and strain at any section of the cylinder X_i ($i = 1, 2, 3, 4$), as follows:

$$\begin{aligned} &\xi = \frac{x}{R}, \quad X_1 = \frac{w}{R}, \quad X_2 = \vartheta_1 = \frac{\mathrm{d}w}{\mathrm{d}x}, \\ &X_3 = \frac{R}{D_0}M_1 = -R\frac{D}{D_0}\frac{\mathrm{d}^2 w}{\mathrm{d}x^2}, \quad X_4 = \frac{R^2}{D_0}Q_1 = -R^2\frac{D}{D_0}\frac{\mathrm{d}^3 w}{\mathrm{d}x^3} \end{aligned} \tag{15.87}$$

where $D_0 = \text{const}$ is the flexural stiffness of the shell at some reference section, say, at $\xi = 0$; $D = D(x)$ is the flexural stiffness at a section of interest.

Applying the above-introduced dimensionless variables and parameters (Eqs (15.87)), one can represent Eqs (15.86) in the form

$$\frac{1}{d\xi} = X_2, \quad \frac{\mathrm{d}X_2}{\mathrm{d}\xi} = -\frac{D_1}{D}X_3, \quad \frac{\mathrm{d}X_3}{\mathrm{d}\xi} = X_4,$$
$$\frac{\mathrm{d}X_4}{\mathrm{d}\xi} = \frac{EhR^2}{D_0}X_1 - \frac{R^3}{D_0}\left(p_3 + \nu\frac{N_1}{R}\right). \tag{15.88}$$

This system of first-order ordinary differential equations is equivalent to the fourth-order single differential equation (15.84). In turn, the former system may be written in the following matrix form:

$$\frac{d\mathbf{X}}{d\xi} = \mathbf{A}(\xi)\mathbf{X} + \mathbf{f}, \tag{15.89}$$

where

$$\mathbf{X} = \begin{bmatrix} X_1 \\ X_2 \\ X_3 \\ X_4 \end{bmatrix} \tag{15.90}$$

is the column vector that characterizes the parameters of the state of stress and strain at a section of interest and

$$\mathbf{A} = \begin{bmatrix} 0 & 1 & 0 & 0 \\ 0 & 0 & -D_0/D & 0 \\ 0 & 0 & 0 & 1 \\ \frac{EhR^2}{D_0} & 0 & 0 & 0 \end{bmatrix}, \quad \mathbf{f} = \begin{bmatrix} 0 \\ 0 \\ 0 \\ -\frac{R^3}{D_0}\left(p_3 + \nu\frac{N_1}{R}\right) \end{bmatrix} \tag{15.91}$$

are the square matrix (4×4) and the column vector of the right-hand sides, respectively. The system of differential equations (15.89) may be efficiently solved numerically using, for example, the sweep method [9] or Godunov's method of discrete orthogonalization [10].

Example 15.8

Consider a circular cylindrical shell of variable thickness under the action of pressure p. Two cases of variation of the shell thickness are analyzed: (a) $h_1 = h_0\left(-\frac{1}{c^2}x^2 + \frac{4}{3}\right)$ and (b) $h_2 = h_0 = \text{const}$, as shown in Fig. 15.16a and b, respec-

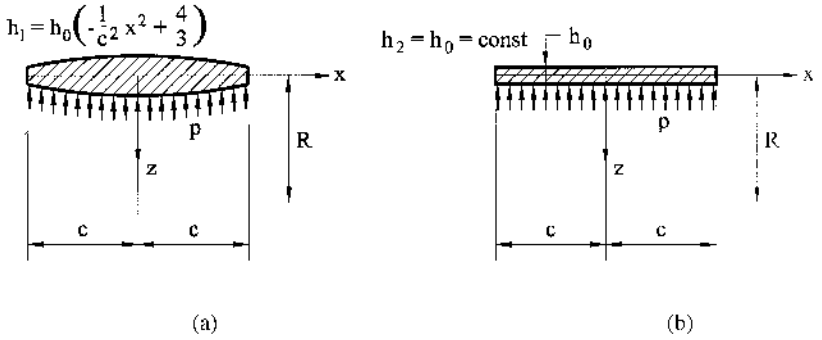

Fig. 15.16

tively. As this takes place, the area of an axial cross section for all the three shells is identical in the interval $-c \le x \le c$, i.e., the above shells are of the same weight. The parallel edges of the shells are simply supported. Assuming that $h_0 = 0.5$, $c = 20$, $R = 15$, and $\nu = 0.3$, determine the deflections, internal forces, and moments in the shell.

Solution

Since the shells and loading are symmetrical about $x = 0$, all the above problems are solved for the interval $0 \le x \le c$. Boundary conditions of the simply supported type for the shell edge $x = c$ and the symmetry conditions for the section $x = 0$ are prescribed. The numerical values of the components of the state of stress and strain are given in Table 15.1 for $h = h_1$. Analogous results are given in Table 15.2 for $h = h_2$. The system of ordinary differential equations (15.89) was solved by Godunov's method of discrete orthogonalization. From these tables it is seen how the thickness redistribution of the shell influences the state of stress and strain under the condition of the conservation of the shell weight. It makes it possible to select the most efficient parameters of shell structures.

Table 15.1

x	$(M_1/p) \times 10$	$(N_1/p) \times 10^{-1}$	Q_1/p	$(w/\frac{p}{E}) \times 10^{-3}$
0	−0.31633	0.40996	0	0.30976
2	−0.32035	0.40996	-0.39650×10^{-3}	0.31210
4	−0.33230	0.40996	-0.82848×10^{-3}	0.31931
6	−0.35740	0.40996	-1.18812×10^{-2}	0.33193
8	−0.42139	0.40996	-0.50151×10^{-2}	0.35117
10	−0.58015	0.40996	-0.11284×10^{-1}	0.37985
12	−0.86017	0.40996	-0.14980×10^{-1}	0.42531
14	−0.99610	0.40996	-0.97754×10^{-2}	0.50433
16	0.1056×10^{-1}	0.40996	0.10333	0.63605
18	0.29781	0.40996	0.14807	0.71609
20	0	0.40996	−0.73044	0

Table 15.2

x	M_1/p	N_1/p	Q_1/p	$(w/\frac{p}{E}) \times 10^{-3}$
0	0.13028×10^{-4}	0.42808×10	0	0.41154
2	0.31492×10^{-3}	0.42808×10	0.29494×10^{-3}	0.41153
4	0.10442×10^{-2}	0.42808×10	0.33756×10^{-3}	0.41140
6	0.82148×10^{-3}	0.42808×10	-0.91417×10^{-3}	0.41095
8	-0.44991×10^{-2}	0.42808×10	-0.48864×10^{-2}	0.41030
10	-0.18990×10^{-1}	0.42808×10	-0.97479×10^{-2}	0.41154
12	-0.27954×10^{-1}	0.42808×10	0.55193×10^{-2}	0.41935
14	0.39696×10^{-1}	0.42808×10	0.73855×10^{-1}	0.43480
16	0.30266	0.42808×10	0.18704	0.43047
18	0.65488	0.42808×10	0.82290×10^{-1}	0.31639
20	0	0.42808×10	−0.97407	0

This example has been taken from Ref. [10]

PROBLEMS

15.1 Indicate cases when the membrane theory alone cannot describe adequately the state of stress of cylindrical shells under applied transverse loading.

15.2 Verify Eqs (15.21) and (15.24).

15.3 What are the conditions at which a complete state of stress in open and closed cylindrical shells can be broken down into elementary states of stress? Characterize these elementary stress states.

15.4 A long steel pipe is subjected to the edge line load Q_0 that is applied uniformly around the circumference $x = 0$. The radius and thickness of the pipe are $R = 0.5\,\text{m}$ and $h = 5\,\text{mm}$, respectively. (a) Derive and plot the values of w and M vs. βx. (b) Determine the distance x at which the deflections and moments are 5% of their absolute maximum values. Take $E = 200\,\text{GPa}$, and $\nu = 0.3$.

15.5 A very long cylinder of radius R and of thickness h is subjected to uniform loading p_0 over L of its length (Fig. 15.11) (a) Determine the ratio of maximum bending stress to maximum magnitude of membrane stress. (b) Calculate the deflections and bending moments at a point A for two cases of location of that point, as shown in Figs 15.11a and b. Take $R = 1.5\,\text{m}$, $h = 6\,\text{mm}$, $p_0 = 5\,\text{kPa}$, $E = 200\,\text{GPa}$, and $\nu = 0.3$.

15.6 Verify Eqs (15.57).

15.7 The infinite circular cylinder of radius R is subjected to a uniformly distributed around a circumference moment m, as shown in Fig. P.15.1. Assuming that the moment is applied near the center of the cylinder, find the expressions for w, ϑ, M_1, and Q_1 as functions of m and x.

15.8 A stiffening ring is placed around a long steel cylindrical shell at a distance remote from the ends, as shown in Fig. 15.12a. The cylinder is loaded by an internal pressure p_0. Determine stress at the ring attachment if: (a) the ring is assumed to be infinitely rigid and (b) the ring is assumed to be 100 mm wide and 10 mm thick. Take the radius of the cylinder as 1.25 m and its thickness as 6 mm, $p_0 = 10\,\text{kPa}$, $E = 200\,\text{GPa}$, and $\nu = 0.3$.

15.9 Determine stresses in a cylindrical component reinforced by a ring and subjected to internal pressure $p = 4$ MPa (Fig. P.15.2). All dimensions in Fig. P.15.2 are given in mm. Take $E = 200\,\text{GPa}$, and $\nu = 0.3$.

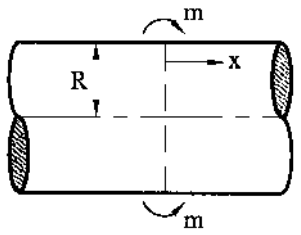

Fig. P15.1

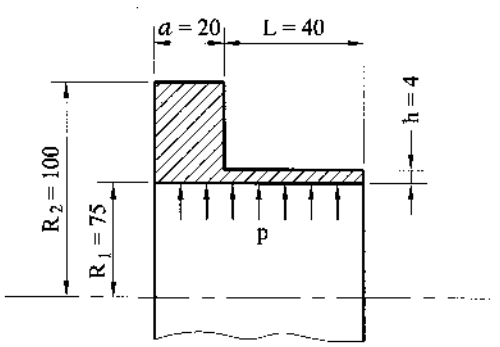

Fig. P15.2

15.10 A long cylindrical shell is reinforced by two equal stiffening rings at a distance 5 cm from one another. Both stiffening rings are placed far from the shell ends. The shell is loaded by an internal pressure p_0. Determine the deflections and stresses at the ring attachments if each ring has a rectangular cross section 2.5 cm wide and 0.5 cm thick. The parameters of the shell are $R = 1.5\,\text{m}$. $h = 5\,\text{mm}$. Take $p_0 = 500\,\text{kPa}$, $E = 200\,\text{GPa}$, and $\nu = 0.3$.

15.11 A long cylindrical pipe of diameter $D = 1.0$ m and of wall thickness $h = 6$ mm is subjected to load P, uniformly distributed along a circular cross section (Fig. 15.9). Determine the value of P required according to the Tresca criterion. Use $\sigma_{ys} = 220$ MPa, $E = 200\,\text{GPa}$, and $\nu = 0.3$.

15.12 Consider a semi-infinite cylindrical shell of radius R and thickness h loaded by an internal pressure $p_0 = \text{const}$. Compare the maximum values of bending stresses, σ_1, for two types of boundary conditions, prescribed on the shell edge $x = 0$: built-in and simply supported edges. Indicate in the solution the locations of these maximum stresses.

15.13 A stepped water tower, shown in Fig. P.15.3, is filled to capacity with a liquid of specific weight γ. Determine the values of the discontinuity moments and shear forces along the joint and at the base of the tower. Assume that the water tower is built-in at its base. The self-weight of the tower can be neglected. Take $H = 4.0\,\text{m}$, $R = 1\,\text{m}$, $H_1 = 1.0\,\text{m}$, $h_1 = 25\,\text{mm}$, $h_2 = 15\,\text{mm}$, $E = 30\,\text{GPa}$, $\gamma = 9800\,\text{N/m}^3$, and $\nu = 0.15$.

15.14 Solve a problem of Example 15.7 (see Fig. 15.15) replacing the two moments applied to the short shell by two equal line forces P distributed along circular sections of a shell $x = 2.5\,\text{in.}$ and $x = 7.5\,\text{in.}$

15.15 Verify the general-purpose equation of the middle surface deflections, Eq. (15.83).

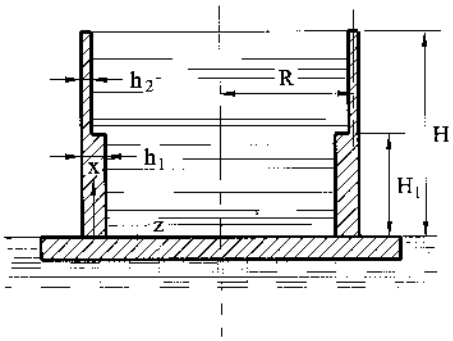

Fig. P15.3

REFERENCES

1. Gol'denveizer, A.L., *Theory of Thin Shells*, Pergamon Press, New York, 1961.
2. Novozhilov, V.V., *The Theory of Thin Elastic Shells*, P. Noordhoff LTS, Groningen, The Netherlands, 1964.
3. Vlasov, V.X., *General Theory of Shells and its Application in Engineering* (translated from Russian), NASA TT F-99, National Aeronautic and Space Administration, Washington, DC, 1964.
4. Cook, D. and Young, W.C., *Advanced Mechanics of Materials*, 2nd edn., Prentice Hall, New Jersey, 1999.
5. Winkler, E., *Die Lehre von der Elastizität und Festigkeit*, Prague, 1867.
6. Kreyszig, E., *Advanced Engineering Mathematics*, 7th edn, John Wiley and Sons, New York, 1993.
7. Krylov, A.N., *On Stresses Experienced by a Ship in a Sea Way*, Trans Inst Naval Architects, London, p. 44, 1902.
8. Timoshenko, S.P. and Woinowsky-Krieger, S., *Theory of Plates and Shells*, 2nd edn, McGraw-Hill, New York, 1959.
9. Collatz, L., *The Numerical Treatment of Differential Equations*, 3rd edn, Springer-Verlag, Berlin, 1966.
10. Godunov, S.K., *Ordinary Differential Equations with Constant Coefficients* (translated from Russian), Providence, R.I. American Mathematical Society, 1997.
11. Grigorenko, Ia.M. and Mukoed, A.P., *The Solution of Problems of the Shell Theory on Computers*, Vushcha Shkola, Kiev, 1979.

16

The Moment Theory of Shells of Revolution

16.1 INTRODUCTION

As mentioned, shells of revolution belong to a highly general class of shells frequently used in engineering. One representative of this class, cylindrical shells, was considered in Chapter 15, and we will not dwell on these shells. The shell types analyzed in this chapter are subclasses of shells of revolution having non-zero Gaussian curvature. As mentioned in Sec. 11.7, such shells have non-developable surfaces. Hence, they are stronger, stiffer, and more stable than shells with zero Gaussian curvature. These shells are frequently used to cover the roofs of sport halls and large liquid storage tanks. The containment shield structures of nuclear power plants also have dome-like roofs. Various pressure vessels are either completely composed of a single rotational shell or have shells of revolution at their end caps. Conical shells with zero Gaussian curvature are also representative of this class of shells: they are used to cover liquid storage tanks and the nose cones of missiles and rockets.

In the membrane analysis of shells of revolution considered in Chapters 13 and 14, we saw that the membrane theory alone cannot accommodate all the loads, support conditions, and geometries in actual shells. Thus, in a general case, shells of revolution experience both stretching and bending to resist an applied loading, which distinguishes significantly the bending of shells from the elementary behavior of plates (see also Sec. 10.4).

However, the character of bending deformation may be different. If a shell of revolution is subjected to a concentrated force (Fig. 16.1a), bending exerts a crucial effect on its strength, because, in this case, the bending deformation increases with a growth of the forces until the load-carrying capacity of the shell structure is exhausted. In places of junction of a shell with its supports (Fig. 16.1b) or other structural members (shell of another geometry, ring beam, etc.), or in places of jump change in

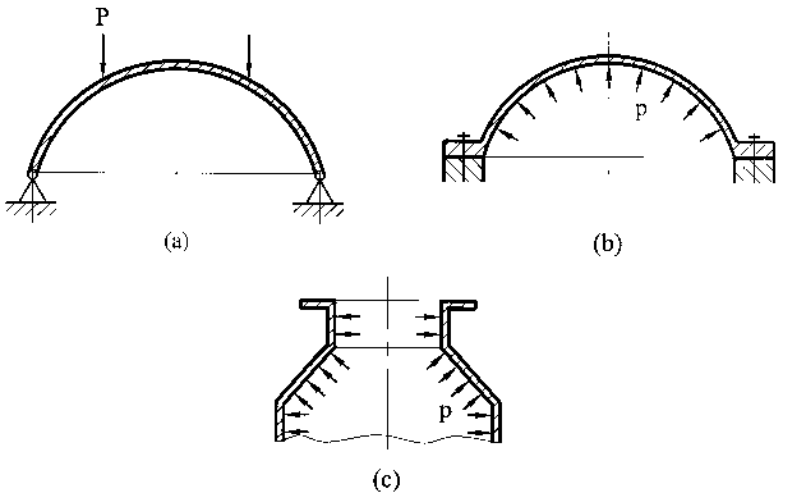

Fig. 16.1

the radii of curvature (Fig. 16.1c), the bending has another character; here, bending propagates only if it is needed to eliminate the discrepancies between the membrane displacements or to satisfy the conditions of statics. If a shell material is ductile, the bending deformations of the latter type are usually decreased and do not practically influence the load-carrying capacity of shell structures. If the material of the shell is brittle, the bending deformations remain proportional to the applied loads until failure and can result in a significant decrease in the strength of the shell structure

In this chapter we consider the bending theory of shells of revolution. It should be noted that the solutions of the governing differential equations involve many difficulties for a general shell of revolution, and therefore, we solve these equations for some particular shell geometries and load configurations that are frequently used in engineering practice.

16.2 GOVERNING EQUATIONS

We present below the governing differential equations of the moment theory of shells of revolution of an arbitrary shape. As curvilinear coordinates α and β of a point on the shell middle surface, it is convenient to take the spherical coordinates, introduced in Sec. 11.8, and used in the membrane theory of shells of revolution in Chapters 13 and 14. Thus, we take $\alpha = \varphi$ and $\beta = \theta$. As before, the angle φ defines the location of a point along the meridian, whereas θ characterizes the location of a point along the parallel circle (see Fig. 11.12). Let R_1 and R_2 be the principal radii of curvature of the meridian and parallel circle, respectively. Obviously, R_1 and R_2 will be functions of φ only, i.e., $R_1 = R_1(\varphi)$ and $R_2 = R_2(\varphi)$. The Lamé parameters in this case are determined by the following formulas (see Sec. 11.8):

$$A = R_1(\varphi), \quad B = R_2(\varphi)\sin\varphi, \quad r = R_2\sin\varphi. \tag{16.1}$$

The Codazzi and Gauss conditions are given by Eqs (11.41).

Let us consider the kinematic relations of the moment theory of shells of revolution. Displacement components of the middle surface along the given coordi-

nate axes are u (in the meridional direction), v (in the circumferential direction), and w (in the normal direction to the middle surface). The strain–displacement relations (12.23) and (12.24) of the general shell theory – taking into account Eqs (16.1) and (11.41) – take the following form for shells of revolution:

$$\begin{aligned}
\varepsilon_1 &= \frac{1}{R_1}\left(\frac{\partial u}{\partial \varphi} - w\right),\\
\varepsilon_2 &= \frac{1}{R_2 \sin\varphi}\left(\frac{\partial v}{\partial \theta} + u\cos\varphi - w\sin\varphi\right),\\
\gamma_{12} &= \frac{1}{R_1}\frac{\partial v}{\partial \varphi} - \frac{\cos\varphi}{R_2 \sin\varphi}v + \frac{1}{R_2 \sin\varphi}\frac{\partial u}{\partial \theta},
\end{aligned} \tag{16.2}$$

$$\begin{aligned}
\chi_1 &= -\frac{1}{R_1}\frac{\partial}{\partial \varphi}\left[\frac{1}{R_1}\left(u + \frac{\partial w}{\partial \varphi}\right)\right],\\
\chi_2 &= -\frac{1}{(R_2 \sin\varphi)^2}\left(\frac{\partial v}{\partial \theta}\sin\varphi + \frac{\partial^2 w}{\partial \theta^2}\right) - \frac{\cos\varphi}{R_1 R_2 \sin\varphi}\left(u + \frac{\partial w}{\partial \varphi}\right),\\
\chi_{12} &= \frac{1}{R_2 \sin\varphi}\left[\frac{\cos\varphi}{R_2 \sin\varphi}\frac{\partial w}{\partial \theta} - \frac{1}{R_1}\frac{\partial^2 w}{\partial \theta \partial \varphi} - \frac{1}{R_1}\frac{\partial u}{\partial \theta} - \frac{\sin\varphi}{R_1}\frac{\partial v}{\partial \varphi} + \frac{\cos\varphi}{R_2}v\right],
\end{aligned} \tag{16.3}$$

where ε_1 and ε_2 are in-plane meridional and circumferential strain components in the middle surface, γ_{12} characterizes a shear of the middle surface; χ_1 and χ_2 represent the changes in curvature of the coordinate lines in the middle surface due to its bending, and χ_{12} characterizes a twist of the middle surface. The rotations of the shell edges that coincide with the coordinate lines θ and φ, respectively, can be obtained from Eqs (12.2) using the relations (16.1) and (11.41). We obtain

$$\vartheta_1 = \frac{u}{R_1} + \frac{1}{R_1}\frac{\partial w}{\partial \varphi}, \quad \vartheta_2 = \frac{1}{R_2 \sin\varphi}\left(\frac{\partial w}{\partial \theta} + v\sin\varphi\right). \tag{16.4}$$

Equations of static equilibrium (12.41) and (12.42) with regard to relations (12.43), (11.41), and (16.2) take the form

$$\begin{aligned}
&\frac{\partial}{\partial \varphi}(N_1 R_2 \sin\varphi) + R_1\frac{\partial}{\partial \theta}\left(S - \frac{H}{R_1}\right) - N_2 R_1 \cos\varphi - Q_1 R_2 \sin\varphi\\
&\qquad + p_1 R_1 R_2 \sin\varphi = 0,\\
&R_1\frac{\partial N_2}{\partial \theta} + \frac{\partial}{\partial \varphi}\left[R_2 \sin\varphi\left(S - \frac{H}{R_2}\right)\right] + \left(S - \frac{H}{R_1}\right) R_1 \cos\varphi\\
&\qquad - Q_2 R_1 \sin\varphi + p_2 R_1 R_2 \sin\varphi = 0,\\
&\frac{\partial}{\partial \varphi}(Q_1 R_2 \sin\varphi) + \frac{\partial}{\partial \theta}(Q_2 R_1) + N_1 R_2 \sin\varphi + N_2 R_1 \sin\varphi + p_3 R_1 R_2 \sin\varphi = 0,\\
&\frac{\partial}{\partial \varphi}(H R_2 \sin\varphi) + R_1\frac{\partial M_2}{\partial \theta} + H R_1 \cos\varphi - Q_2 R_1 R_2 \sin\varphi = 0,\\
&R_1\frac{\partial H}{\partial \theta} + \frac{\partial}{\partial \varphi}(M_1 R_2 \sin\varphi) - M_2 R_1 \cos\varphi - Q_1 R_1 R_2 \sin\varphi = 0.
\end{aligned} \tag{16.5}$$

Taking into account the relations for the effective shear forces (in-plane and out-of-plane) introduced in Sec. 12.5, the following static quantities can be assigned on a boundary coinciding with the edge parallel circle $\varphi = \varphi_e$:

$$N_1,\ T_1 = S - \frac{2H}{R_2}, \quad M_1, \quad \text{and} \quad V_1$$

where

$$V_1 = Q_1 + \frac{1}{R_2 \sin\varphi}\frac{\partial H}{\partial \theta} = \frac{1}{R_2 \sin\varphi}\left[2\frac{\partial H}{\partial \theta} + \frac{\partial (M_1 R_2 \sin\varphi)}{R_1 \partial \varphi} - M_2 \cos\varphi\right]. \tag{16.6}$$

The constitutive relations are found to be in the form of Eqs (12.45) and (12.46).

The governing equations and relations introduced above allow one to determine the stress and displacement components that occur in a shell of revolution supported along its edges and subjected to given external loads. The unknown functions characterizing the state of stress and strain (deformations and stress resultants and couples) depend upon variables θ and φ in Eqs (16.3), (16.5), and (12.45), (12.46). These unknowns are periodic functions of variable θ for shells of revolution. Thus, one can apply the separation of variables method for solving the governing differential equations of shells of revolution. This method implies that all loads, displacements, and stress resultants and couples may be represented in the form

$$\begin{aligned} f_i(\theta, \varphi) &= \sum_{k=0}^{\infty} f_{ik}^{(s)} \cos k\theta + \sum_{k=1}^{\infty} f_{ik}^{(a)} \sin k\theta, \\ \zeta_i(\theta, \varphi) &= \sum_{k=1}^{\infty} \zeta_{ik}^{(s)} \sin k\theta - \sum_{k=0}^{\infty} \zeta_{ik}^{(a)} \cos k\theta, \end{aligned} \tag{16.7}$$

where by functions f_i are meant the functions $p_1, p_3, u, w, \varepsilon_1, \varepsilon_2, \vartheta_1, \kappa_1, \kappa_2, N_1, N_2, M_1, M_2$, and Q_1, and by functions ζ_i are meant the functions $p_2, v, \gamma_{12}, \vartheta_2, S, H$, and Q_2. It can be seen that the functions having the superscripts s and a correspond to symmetric and skew-symmetric of the above-mentioned functions about a zero meridian, respectively. It is easily verified that the symmetric and skew-symmetric components of the displacements, stress resultants, etc., determined by the same system of equations. Therefore, we present the corresponding relations and equations for functions having the superscript s only, without using this index. So, substituting the expressions (16.7) into the kinematic relations (16.2) and (16.3), equilibrium equations (16.5), and eliminating the shear forces, Q_1 and Q_2, we obtain some systems of ordinary differential equations for unknown functions of deformations, and stress resultants and couples. Note that the constitutive equations (12.45) and (12.46) remain unchanged. It is required only to provide all the quantities involving in these equations with the index k. Let us present these equations:

Kinematic equations (strain–displacement relations)

$$
\begin{aligned}
\varepsilon_{1k} &= \frac{1}{R_1}\left(\frac{\mathrm{d}u_k}{\mathrm{d}\varphi} - w_k\right),\\
\varepsilon_{2k} &= \frac{1}{R_2 \sin\varphi}(kv_k + u_k \cos\varphi - w_k \sin\varphi),\\
\gamma_{12k} &= \frac{1}{R_1}\frac{\mathrm{d}v_k}{\mathrm{d}\varphi} - \frac{\cos\varphi}{R_2 \sin\varphi} v_k - \frac{ku_k}{R_2 \sin\varphi},\\
\chi_{1k} &= -\frac{1}{R_1}\frac{\mathrm{d}}{\mathrm{d}\varphi}\left[\frac{u_k}{R_1} + \frac{1}{R_1}\frac{\mathrm{d}w_k}{\mathrm{d}\varphi}\right],\\
\chi_{2k} &= -\frac{1}{(R_2 \sin\varphi)^2}\left(kv_k \sin\varphi - k^2 w_k\right) - \frac{\cos\varphi}{R_1 R_2 \sin\varphi}\left(u_k + \frac{\mathrm{d}w_k}{\mathrm{d}\varphi}\right),\\
\chi_{12k} &= \frac{1}{R_2 \sin\varphi}\left[-\frac{\cos\varphi}{R_2 \sin\varphi} k w_k + \frac{k}{R_1}\frac{\mathrm{d}w_k}{\mathrm{d}\varphi} + \frac{k}{R_1}u_k - \frac{\sin\varphi}{R_1}\frac{\mathrm{d}v_k}{\mathrm{d}\varphi} + \frac{\cos\varphi}{R_2} v_k\right],\\
\vartheta_{1k} &= \frac{1}{R_1}\left(u_k + \frac{\mathrm{d}w_k}{\mathrm{d}\varphi}\right),\ \vartheta_{2k} = \frac{1}{R_2 \sin\varphi}(-kw_k + v_k \sin\varphi)
\end{aligned}
\tag{16.8}
$$

Equations of static equilibrium

$$
\begin{aligned}
&\frac{\mathrm{d}}{d\varphi}(N_{1k} R_2 \sin\varphi) + R_1 k S_k - \frac{1}{R_1}\frac{\mathrm{d}}{\mathrm{d}\varphi}(M_{1k} R_2 \sin\varphi) + M_{2k} \cos\varphi\\
&\quad - 2kH_k - N_{2k} R_1 \cos\varphi + p_{1k} R_1 R_2 \sin\varphi = 0\\
&\quad - R_1 k N_{2k} + \frac{1}{R_2 \sin\varphi}\frac{\mathrm{d}}{\mathrm{d}\varphi}\left[S_k (R_2 \sin\varphi)^2\right]\\
&\quad - \frac{1}{R_2}\left[R_1(-k)M_{2k} + 2R_2 \sin\varphi \frac{\mathrm{d}H_k}{\mathrm{d}\varphi} + 2\cos\varphi H_k (R_1 + R_2)\right]\\
&\quad + p_{2k} R_1 R_2 \sin\varphi = 0.\\
&\frac{N_{1k}}{R_1} + \frac{N_{2k}}{R_2} + \frac{1}{R_1 R_2 \sin\varphi}\left\{\frac{\mathrm{d}}{\mathrm{d}\varphi}\left[H_k k + \frac{1}{R_1}\frac{\mathrm{d}}{\mathrm{d}\varphi}(M_{1k} R_2 \sin\varphi) - M_{2k} \cos\varphi\right]\right.\\
&\quad \left. + \frac{1}{R_2 \sin\varphi}\left[\frac{k}{R_2 \sin\varphi}\frac{\mathrm{d}}{\mathrm{d}\varphi}\left((R_2 \sin\varphi)^2 H_k\right) - k^2 R_1 M_{2k}\right]\right\} + p_{3k} = 0.
\end{aligned}
\tag{16.9}
$$

Equations (16.8) and (16.9), together with the constitutive equations (12.45) and (12.46) and proper boundary conditions, form the closed eight-order system of the ordinary differential equations for each kth harmonic of the expansion (16.7). This system of the governing equations describes the state of stress and strain for the general moment theory of shells of revolution having a meridian of an arbitrary shape. This system of ordinary equations may be solved by applying the standard numerical methods intended for a solution of ordinary differential equations and introduced, for example, in Refs. [1,2]. The finite element method can also be applied to the analysis of the state of stress and strain for shells of revolution of a general shape [3,4].

It should be noted that numerical difficulties associated with a solution of the differential equations (16.8) and (16.9) may be partially eliminated for some specific shapes of shells of revolution and loading.

16.3 SHELLS OF REVOLUTION UNDER AXISYMMETRICAL LOADS

When a shell of revolution is subjected to rotationally symmetrical loads ($p_2 = 0$), its deformations and stress resultants and couples do not depend upon the variable θ. The conditions of symmetry dictate that

$$S = Q_2 = H = 0 \quad \text{and} \quad v = \gamma_{12} = \kappa_{12} = 0. \tag{16.10}$$

For this particular case of loading, the strain–displacement relations (16.2) and (16.3) and equilibrium equations (16.5) and constitutive equations (12.45) and (12.46) take the following form:

Strain–displacement relations

$$\begin{aligned}
&\varepsilon_1 = \frac{1}{R_1}\left(\frac{\mathrm{d}u}{\mathrm{d}\varphi} - w\right), \quad \varepsilon_2 = \frac{1}{R_2}(u\cot\varphi - w),\\
&\chi_1 = -\frac{1}{R_1}\frac{\mathrm{d}}{\mathrm{d}\varphi}\left[\frac{1}{R_1}\left(u + \frac{\mathrm{d}w}{\mathrm{d}\varphi}\right)\right], \quad \chi_2 = -\cot\varphi\frac{1}{R_1R_2}\left(u + \frac{\mathrm{d}w}{\mathrm{d}\varphi}\right),\\
&\vartheta_1 = \frac{u}{R_1} + \frac{1}{R_1}\frac{\mathrm{d}w}{\mathrm{d}\varphi},
\end{aligned} \tag{16.11}$$

where ϑ_1 is the angle of rotation of the tangent to the shell meridian.

Equilibrium equations

$$\begin{aligned}
&\frac{\mathrm{d}}{\mathrm{d}\varphi}(N_1R_2\sin\varphi) - N_2R_1\cos\varphi - Q_1R_2\sin\varphi + p_1R_1R_2\sin\varphi = 0,\\
&\frac{\mathrm{d}}{\mathrm{d}\varphi}(Q_1R_2\sin\varphi) + N_1R_2\sin\varphi + N_2R_1\sin\varphi + p_3R_1R_2\sin\varphi = 0,\\
&\frac{\mathrm{d}}{\mathrm{d}\varphi}(M_1R_2\sin\varphi) - M_2R_1\cos\varphi - Q_1R_1R_2\sin\varphi = 0.
\end{aligned} \tag{16.12}$$

Constitutive equations

$$\begin{aligned}
&N_1 = \frac{Eh}{1-\nu^2}(\varepsilon_1 + \nu\varepsilon_2), \quad N_2 = \frac{Eh}{1-\nu^2}(\varepsilon_2 + \nu\varepsilon_1),\\
&M_1 = D(\chi_1 + \nu\chi_2), \quad M_2 = D(\chi_2 + \nu\chi_1).
\end{aligned} \tag{16.13}$$

It is convenient to express the fourth and fifth Eqs (16.11) in terms of ϑ_1. So, inserting the fifth Eq. (16.11) into the above equations, one obtains the following

$$\chi_1 = -\frac{1}{R_1}\frac{\mathrm{d}\vartheta_1}{\mathrm{d}\varphi}, \quad \chi_2 = -\cot\varphi\frac{1}{R_2}\vartheta_1. \tag{16.14}$$

Substituting for the strain components from the first two Eqs (16.11) and Eqs (16.14) into Eqs (16.13), gives the following stress resultants and couples–displacement relations

$$N_1 = B\left[\frac{1}{R_1}\left(\frac{\mathrm{d}u}{\mathrm{d}\varphi} - w\right) + \frac{\nu}{R_2}(u\cot\varphi - w)\right], \tag{16.15a}$$

$$N_2 = B\left[\frac{1}{R_2}(u\cot\varphi - w) + \frac{\nu}{R_1}\left(\frac{\mathrm{d}u}{d\varphi} - w\right)\right], \tag{16.15b}$$

$$M_1 = -D\left[\frac{1}{R_1}\frac{\mathrm{d}\vartheta_1}{\mathrm{d}\varphi} + \frac{\nu}{R_2}\vartheta_1\cot\varphi\right], \tag{16.15c}$$

$$M_2 = -D\left[\frac{1}{R_2}\vartheta_1\cot\varphi + \frac{\nu}{R_1}\frac{\mathrm{d}\vartheta_1}{\mathrm{d}\varphi}\right], \tag{16.15d}$$

where

$$B = \frac{Eh}{1-\nu^2}, D = \frac{Eh^3}{12(1-\nu^2)}. \tag{16.16}$$

Equations (16.11), (16.12), and (16.13) or (16.15) form a closed system of 12 ordinary differential equations for 12 unknowns (strains, stress resultants and couples). Solving this system of equations, one obtains the internal forces, moments, and displacements. The stress components are calculated by the following formulas:

$$\sigma_{1\max} = \frac{N_1}{h} + \frac{6M_1}{h^2}, \quad \sigma_{2\max} = \frac{N_2}{h} + \frac{6M_2}{h^2}. \tag{16.17}$$

Let us bring the above system of equations to two symmetric governing equations for two unknowns. Following Meissner [5], we introduce the new variables

$$\vartheta_1 \quad \text{and} \quad U = R_2 Q_1(\varphi). \tag{16.18}$$

We now express the internal forces and moments in terms of the new variables. Canceling the circumferential force N_2 from the first and second Eqs (16.12), we obtain the following equation:

$$\frac{1}{R_1}\frac{\mathrm{d}}{\mathrm{d}\varphi}[(N_1\sin\varphi + Q_1\cos\varphi)r] + (p_1\sin\varphi + p_3\cos\varphi)r = 0. \tag{16.19}$$

Integrating this equation over φ, we obtain

$$(N_1\sin\varphi + Q_1\cos\varphi)r = -F(\varphi), \tag{16.20}$$

where

$$F(\varphi) = \int_{\varphi_e}^{\varphi} R_1 r(p_1\sin\bar{\varphi} + p_3\cos\bar{\varphi})\mathrm{d}\bar{\varphi} + C; \tag{16.21}$$

here $\bar{\varphi}$ is a dummy variable; φ_e is the angular coordinate of one of the shell edges – say, the top edge; $F(\varphi)$ represents the resultant of all external surface loads applied to an isolated part of the shell per unit φ; and C takes into account an axial component of the external loads applied to the top edge of the shell.

Comparing Eqs (16.21) and (13.37), we can conclude that a particular solution of Eq. (16.19), corresponding to the integral $F(\varphi)$, represents a membrane solution of the general bending theory of axisymmetrically loaded shells of revolution.

Taking into account Eq. (16.18), we can express the meridional force N_1 in terms of U from Eq. (16.20), as follows:

$$N_1 = -\frac{\cot\varphi}{R_2}U - \frac{F(\varphi)}{R_2\sin^2\varphi}. \tag{16.22}$$

Substituting for N_1 from (16.22) into the second Eq. (16.12) and using Eq. (16.18), we obtain the expression for the meridional circumferential force in the form

$$N_2 = -\frac{\mathrm{d}U}{\mathrm{d}\varphi}\frac{1}{R_1} + \frac{F(\varphi)}{R_1\sin^2\varphi} - p_3R_2. \tag{16.23}$$

According to Eqs (16.11) and Eqs (16.15a) and (16.15b), we have

$$\begin{aligned} \frac{\mathrm{d}u}{\mathrm{d}\varphi} - w &= \frac{R_1}{Eh}(N_1 - \nu N_2), \\ u\cot\varphi - w &= \frac{R_2}{Eh}(N_2 - \nu N_1) \end{aligned} \tag{16.24}$$

Eliminating w from the above equations yields

$$\frac{\mathrm{d}u}{\mathrm{d}\varphi} - u\cot\varphi = \frac{1}{Eh}[(R_1 + \nu R_2)N_1 - (R_2 + \nu R_1)N_2]. \tag{16.25}$$

Differentiating the last Eq. (16.24), we obtain

$$\frac{\mathrm{d}u}{\mathrm{d}\varphi}\cot\varphi - \frac{u}{\sin^2\varphi} - \frac{dw}{d\varphi} = \frac{d}{d\varphi}\left[\frac{R_2}{Eh}(N_2 - \nu N_1)\right]. \tag{16.26}$$

Eliminating the derivative $\mathrm{d}u/\mathrm{d}\varphi$ from Eqs (16.25) and (16.26), one obtains

$$u + \frac{\mathrm{d}w}{\mathrm{d}\varphi} = R_1\vartheta_1 = \frac{\cot\varphi}{Eh}[(R_1 + \nu R_2)N_1 - (R_2 + \nu R_1)N_2] - \frac{\mathrm{d}}{\mathrm{d}\varphi}\left[\frac{R_2}{Eh}(N_2 - \nu N_1)\right]. \tag{16.27}$$

Inserting Eqs (16.22) and (16.23) into the above equation, taking into account the third equation (16.11) and substituting for M_1, M_2, and Q_1 from (16.15c) and (16.15d), together with the notations (16.18) into the third Eq. (16.12), yields the following equations for ϑ_1 and U (for shells of constant thickness):

$$\begin{aligned} &\frac{R_2}{R_1}\frac{\mathrm{d}^2U}{\mathrm{d}\varphi^2} + \left[\frac{\mathrm{d}}{\mathrm{d}\varphi}\left(\frac{R_2}{R_1}\right) + \frac{R_2}{R_1}\cot\varphi\right]\frac{\mathrm{d}U}{\mathrm{d}\varphi} - \left(\frac{R_1}{R_2}\cot^2\varphi - \nu\right)U = EhR_1\vartheta_1 + \Phi(\varphi), \\ &\frac{R_2}{R_1}\frac{d^2\vartheta_1}{d\varphi^2} + \left[\frac{\mathrm{d}}{\mathrm{d}\varphi}\left(\frac{R_2}{R_1}\right) + \frac{R_2}{R_1}\cot\varphi\right]\frac{\mathrm{d}\vartheta_1}{\mathrm{d}\varphi} - \left(\nu + \frac{R_1}{R_2}\cot^2\varphi\right)\vartheta_1 = -\frac{R_1}{D}U, \end{aligned} \tag{16.28}$$

where

$$\begin{aligned} \Phi(\varphi) = \cot\varphi&\left[\frac{R_1 + \nu R_2}{R_2\sin^2\varphi}F(\varphi) + (R_2 + \nu R_1)\left(\frac{F(\varphi)}{R_1\sin^2\varphi} - p_3R_2\right)\right] \\ &+ \frac{\mathrm{d}}{\mathrm{d}\varphi}\left[\frac{F(\varphi)}{\sin^2\varphi}\left(\frac{R_2}{R_1} + \nu\right) - p_3R_2^2\right]. \end{aligned} \tag{16.29}$$

Equations (16.28) may be rewritten in the following operator form:

$$L(U) + \nu U = EhR_1\vartheta_1 + \Phi(\varphi),$$
$$L(\vartheta_1) - \nu\vartheta_1 = -\frac{R_1}{D}U. \tag{16.30}$$

where

$$L(..) = \frac{R_2}{R_1}\frac{\mathrm{d}^2(..)}{\mathrm{d}\varphi^2} + \left[\frac{\mathrm{d}}{\mathrm{d}\varphi}\left(\frac{R_2}{R_1}\right) + \frac{R_2}{R_1}\cot\varphi\right]\frac{\mathrm{d}(..)}{\mathrm{d}\varphi} - \cot^2\varphi(..)\left(\frac{R_1}{R_2}\right) \tag{16.31}$$

Equations (16.30) are the governing differential equations of the axisymmetric bending of shells of revolution of constant thickness. A particular solution of the system of ordinary differential equations (16.30) can be found from the membrane theory of axisymmetrically loaded shells of revolution (see Sec. 13.5).

Setting

$$U = \frac{1}{R_1}(L(\psi) - \nu\psi), \quad \vartheta_1 = -\frac{1}{D}\psi, \tag{16.32}$$

where ψ is some function of forces and displacements. We identically satisfy the second Eq. (16.30). Inserting Eqs (16.32) into the first Eq. (16.30), we obtain

$$L\left[\frac{1}{R_1}L(\psi)\right] - \nu L\left(\frac{\psi}{R_1}\right) + \frac{\nu}{R_1}L(\psi) + \left(\frac{EhR_1}{D} - \frac{\nu^2}{R_1}\right)\psi = \Phi(\varphi). \tag{16.33}$$

If the radius of the shell curvature $R_1 = \text{const}$ (sphere, cone, toroid), then Eq. (16.33) takes the following form:

$$LL(\psi) + \mu^2\psi = R_1\Phi(\varphi), \tag{16.34}$$

where

$$\mu^2 = \frac{EhR_1^2}{D} - \nu^2 \approx b^2 \tag{16.35}$$

and $b^2 = 12(1-\nu^2)R_1^2/h^2$ is the basic characteristic of a shell. Equation (16.34) can be represented in the form

$$[L + i\mu][L(\psi) - i\mu\psi] = R_1\Phi(\varphi), \tag{16.36}$$

and its general solution can be obtained in a complex form.

It is convenient to express the boundary conditions of the shell of revolution via the horizontal, ξ, and vertical, η, displacements of a point of the middle surface, as shown in Fig. 16.2. The formulas that relate the displacement components u and v to the displacements ξ and η can be directly obtained from Fig, 16.2, i.e.,

$$\xi = w\sin\varphi - u\cos\varphi, \eta = w\cos\varphi + u\sin\varphi. \tag{16.37}$$

Let us consider some typical boundary conditions for the shells of revolution shown in Fig. 16.3.

(a) *The edge of a shell is built-in* (Fig. 16.3a)
The boundary conditions are of the form

$$\vartheta_1 = \xi = 0|_{\varphi=\varphi_e}. \tag{16.38a}$$

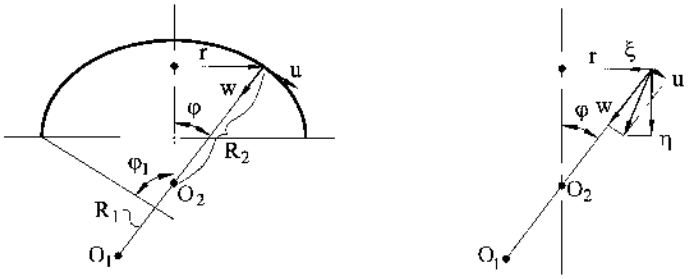

Fig. 16.2

The relative stretching in the circumferential direction is

$$\varepsilon_2 = \frac{\xi}{r} = \frac{\xi}{R_2 \sin\varphi}, \quad \text{from which } \xi = \varepsilon_2 R_2 \sin\varphi. \tag{a}$$

Using the above relation (a) and Eqs (16.13), the second boundary condition (Eq. (16.38a)) can be rewritten as follows:

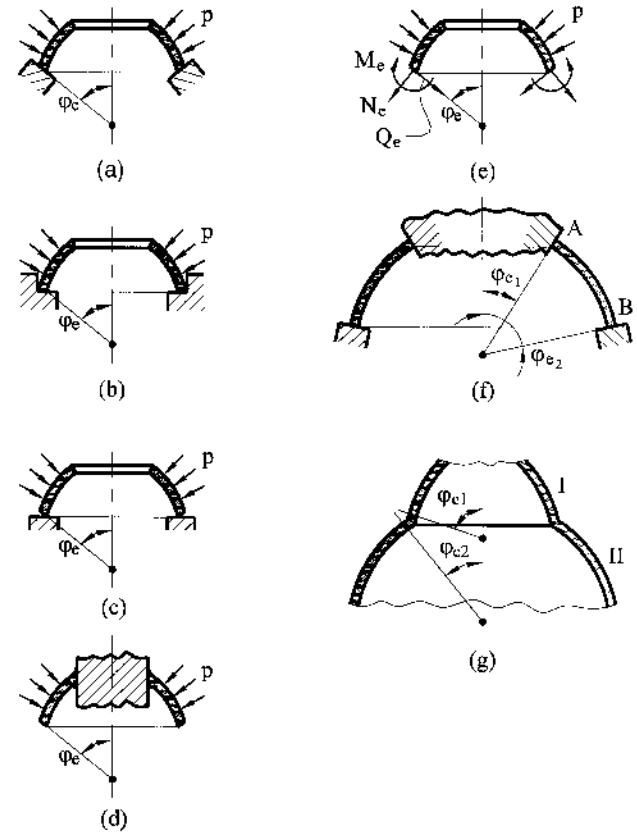

Fig. 16.3

$$\varepsilon_2 = 0|_{\varphi=\varphi_e} \quad \text{or} \quad N_2 - \nu N_1 = 0|_{\varphi=\varphi_e} \tag{16.38b}$$

(b) *The edge of a shell is pinned* (Fig. 16.3b)
In this case

$$\begin{aligned} &\xi = 0|_{\varphi=\varphi_e} \quad \text{or} \quad \varepsilon_2 = 0, \quad N_2 - \nu N_1 = 0|_{\varphi=\varphi_e} \quad \text{and} \\ &M_1 = 0|_{\varphi=\varphi_e} \quad \text{or} \quad \frac{1}{R_1}\frac{\mathrm{d}\vartheta_1}{\mathrm{d}\varphi} + \nu\frac{\cot\varphi}{R_2}\vartheta_1 = 0|_{\varphi=\varphi_e}. \end{aligned} \tag{16.38c}$$

(c) *The edge of a shell is simply supported* (Fig. 16.3c)
In this case the boundary conditions are of the form

$$\begin{aligned} &M_1 = 0\Big|_{\varphi=\varphi_e} \quad \text{or} \quad \frac{1}{R_1}\frac{\mathrm{d}\vartheta}{\mathrm{d}\varphi} + \nu\frac{\cot\varphi}{R_2}\vartheta_1 = \Big|_{\varphi=\varphi_e} \quad \text{and} \\ &N_1\cos\varphi_e + Q_1\sin\varphi_e = 0\Big|_{\varphi=\varphi_e}. \end{aligned} \tag{16.38d}$$

(d) *The edge of a shell is free* (Fig. 16.3d)
Here the boundary conditions are

$$\begin{aligned} &M_1 = 0|_{\varphi=\varphi_e} \quad \text{or} \quad \frac{1}{R_1}\frac{\mathrm{d}\vartheta_1}{\mathrm{d}\varphi} + \nu\frac{\cot\varphi}{R_2}\vartheta_1 = 0|_{\varphi=\varphi_e} \\ &Q_1 = 0|_{\varphi=\varphi_e} \quad \text{or} \quad U = 0|_{\varphi=\varphi_e}. \end{aligned} \tag{16.38e}$$

(e) *The edge of a shell is loaded by edge forces* N_e, Q_e, *and* M_e (Fig. 16.3e)
In this case the boundary conditions are

$$\begin{aligned} &M_1 = M_e\big|_{\varphi=\varphi_e} \quad \text{or} \quad \frac{1}{R_1}\frac{\mathrm{d}\vartheta_1}{\mathrm{d}\varphi} + \nu\frac{\cot\varphi}{R_2}\vartheta_1 = M_e\big|_{\varphi=\varphi_e} \\ &Q_1 = Q_e\big|_{\varphi=\varphi_e} \quad \text{or} \quad U = Q_e R_2\big|_{\varphi=\varphi_e}. \end{aligned} \tag{16.38f}$$

(f) *A shell is built-in from both sides* (Fig. 16.3f)
Since such a shell is statically indeterminate, we must impose the following five conditions:

$$\begin{aligned} &\vartheta_1 = 0|_{\varphi=\varphi_{e_1}}, \quad \varepsilon_2 = 0|_{\varphi=\varphi_{e_1}}; \quad \vartheta_1 = 0|_{\varphi=\varphi_{e_2}}, \quad \varepsilon_2 = 0|_{\varphi=\varphi_{e_2}}, \\ &\eta_{A/B} = 0 \quad \text{or} \quad \int_{\varphi=\varphi_{e_1}}^{\varphi=\varphi_{e_2}} (\varepsilon_1\sin\varphi + \vartheta_1\cos\varphi)R_1\mathrm{d}\varphi = 0. \end{aligned} \tag{16.38g}$$

(g) *Two joined shells* (Fig. 16.3g)
It is necessary for this case to satisfy the four boundary conditions, namely,

$$\begin{aligned} &\xi_e^{(1)} = \xi_e^{(2)} \quad \text{or} \quad \varepsilon_{2e}^{(1)} = \varepsilon_{2e}^{(2)}, \\ &\vartheta_{1e}^{(1)} = \vartheta_{1e}^{(2)}, \quad M_{1e}^{(1)} = M_{1e}^{(2)}, \\ &N_{1e}^{(1)}\cos\varphi_{e_1} + Q_{1e}^{(1)}\sin\varphi_{e_1} = N_{1e}^{(2)}\cos\varphi_{e_2} - Q_1^{(2)}\sin\varphi_{e_2}. \end{aligned} \tag{16.38h}$$

The last condition expresses the equality of the radial forces (thrusts).
(h) If a shell is closed at its vertex, for $\varphi = 0$, then the following conditions must be satisfied:

$$\vartheta_1 = 0|_{\varphi=0} \quad \text{and} \quad Q_1 = 0|_{\varphi=0}. \tag{16.39}$$

16.4 APPROXIMATE METHOD FOR SOLUTION OF THE GOVERNING EQUATIONS (16.30)

The solution of the governing differential equations (16.30) is quite complicated. In the present section, we introduce one approximate method for the bending analysis of shells of revolution under axisymmetric edge loads.

Figure 16.4 shows two shells of revolution subjected to distributed over the edge loads N_{1e}, M_e and Q_e. The first shell (Fig. 16.4a) is a shallow one. In axisymmetric bending of such a shell, the radial displacements and the corresponding circumferential tensile deformations are small near the loaded edge. Therefore, deformations caused by the bending moments diminish slowly and their influence may extend over, practically, the entire shell.

In the second case, shown in Fig. 16.4b, the slope of the normal, ϑ_1, is large. Here, considerable circumferential tension occurs near the loaded edge as the shell bends axisymmetrically. As a consequence, the bending deformations diminish rapidly and they practically vanish at a small distance from the edge.

The effect of the circumferential tension in an axisymmetric bending of a shell with large angle of rise is similar to that of an elastic foundation. A similar effect of rapid decrease of the bending deformations near the loaded edge was observed in the axisymmetrically loaded cylindrical shells in Sec. 15.5. Based on this analogy, a very efficient approximate method may be developed for shells of revolution with large angle of a rise and subjected to edge loading. This method uses the following assumptions:

(a) *All functions characterizing the stress and strain components in a shell near its edge, as well as their first derivatives, are small compared with their higher derivatives.* This assumption is based on that fact that all the considered functions will contain multipliers of the type $e^{-\alpha\varphi}$, where φ is the angle measured from the shell edge of interest and α is some parameter. In differentiating these functions, the parameter αappears every time in the form of the multiplier. Since these functions are rapidly decaying, the value of the parameter α is large. Therefore, values of the first derivative are sufficiently greater than the values of the functions themselves, and values of the second derivatives are greater than the first derivatives, etc., i.e.,

$$\frac{d^n U_n}{d\varphi^n} \gg \frac{d^{(n-1)} U_n}{d\varphi^{n-1}} \quad \text{and} \quad \frac{d^n \vartheta_1}{d\varphi^n} \gg \frac{d^{(n-1)} \vartheta_1}{d\varphi^{n-1}}.$$

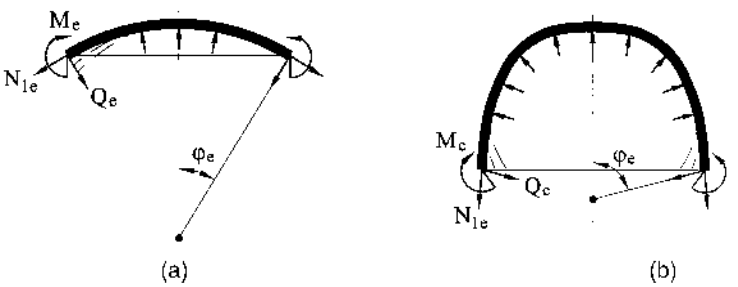

Fig. 16.4

On this basis, terms containing the functions themselves and their first derivatives on the left-hand side of Eqs (16.30) are dropped. The function $\Phi(\varphi)$ on the right-hand side of Eqs (16.30) is zero for loads applied to the edge of the shell. As a result, the governing differential equations (16.30) take the form

$$\frac{R_2}{R_1}\frac{\mathrm{d}^2 U}{\mathrm{d}\varphi^2} = EhR_1\vartheta_1, \tag{16.40a}$$

$$\frac{R_2}{R_1}\frac{\mathrm{d}^2 \vartheta_1}{\mathrm{d}\varphi^2} = -\frac{R_1}{D}U. \tag{16.40b}$$

(b) *The radii of curvature, R_1 and R_2, are assumed to be constant near the shell edge.* This is true for spherical shells only. For shells of other shapes this assumption is carried out the more precisely the closer the shape of a shell approaches a spherical one.

The approximate method for the bending analysis of axisymmetrically loaded spherical shells of revolution based on the above-mentioned assumptions was first introduced by H. Reissner [6] and Geckeler [7]; it was then generalized to shells of revolution of an arbitrary shape of a meridian by Meissner [5,8]. Equations (16.40) can be reduced to a single differential equation with one unknown. Differentiating Eq. (16.40a) twice with regard to the second assumption, and inserting $\mathrm{d}^2\vartheta_1/\mathrm{d}\varphi^2$ into Eq. (16.40b), we obtain the following fourth-order governing differential equation:

$$\frac{\mathrm{d}^4 U}{\mathrm{d}\varphi^4} + 4\alpha^4 U = 0, \tag{16.41}$$

where

$$\alpha = R_1\sqrt[4]{\frac{3(1-\nu^2)}{R_2^2 h^2}}. \tag{16.42}$$

Note that it is impossible to neglect the function U compared with its fourth derivative in Eq. (16.41) because the multiplier $4\alpha^4$ is sufficiently large.

Equation (16.41) is referred to as the *edge effect differential equation* because its solution is expressed in terms of rapidly damped functions. The edge effect governing equation and the corresponding numerical procedure for the general theory of thin shells is discussed in more detail in Sec. 17.5. Equation (16.41) is analogous to that of an axisymmetric deformation of a circular cylindrical shell (see Eq. (15.44)). Hence, we can apply the edge effect technique developed in Sec. 15.3 to axisymmetric bending analysis of shells of revolution. The general solution of Eq. (16.41) for U can be written in the form

$$U = \mathrm{e}^{-\alpha\varphi}(B_1\sin\alpha\varphi + B_2\cos\alpha\varphi) + \mathrm{e}^{\alpha\varphi}(B_3\sin\alpha\varphi + B_4\cos\alpha\varphi). \tag{16.43}$$

It is convenient to introduce a new independent variable ω, representing also the angular coordinate and counting off from the shell edge, as shown in Fig. 16.5.

If the lower shell edge is of interest (Fig. 16.5a), then

$$\omega = \varphi_e - \varphi. \tag{16.44a}$$

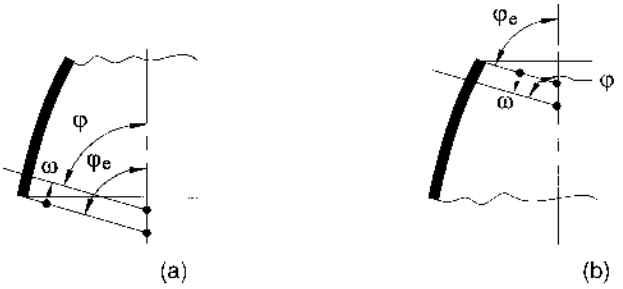

Fig. 16.5

If the upper shell edge is of interest (Fig. 16.5b), then the angle ω is counted off oppositely and

$$\omega = \varphi - \varphi_e. \tag{16.44b}$$

Since, in both the above-mentioned cases,

$$\frac{\mathrm{d}^4 U}{\mathrm{d}\varphi^4} = \frac{\mathrm{d}^4 U}{d\omega^4},$$

in the transition to a new variable, the differential equation remains unchanged, i.e.,

$$\frac{\mathrm{d}^4 U}{\mathrm{d}\omega^4} + 4\alpha^4 U = 0. \tag{16.45}$$

The solution of this equation can be written in the form

$$U = \mathrm{e}^{-\alpha\omega}(C_1 \sin\alpha\omega + C_2 \cos\alpha\omega) + \mathrm{e}^{\alpha\omega}(C_3 \sin\alpha\omega + C_4 \cos\alpha\omega), \tag{16.46}$$

where $C_1, \ldots, C_4$ are constants to be determined from the boundary conditions. Since the function U has to die down as the angle ω increases, the second term in Eq. (16.46), involving the multiplier $\mathrm{e}^{\alpha\omega}$, must vanish as we move away from the loaded edge of the shell. Therefore, the constants C_3 and C_4 should be equal to zero and the above solution takes the form

$$U = \mathrm{e}^{-\alpha\omega}(C_1 \sin\alpha\omega + C_2 \cos\alpha\omega). \tag{16.47}$$

This solution describes the moment state of stress and strain near a loaded edge (either bottom or top). However, in differentiating Eq. (16.47), it should be taken into account that on the top edge of the shell angle ω is counted off in the side of an increase of angle φ; therefore, $\mathrm{d}U/\mathrm{d}\varphi = \mathrm{d}U/d\omega$. On the bottom edge, reference directions of angles φ and ω are opposite, therefore, $\mathrm{d}U/\mathrm{d}\varphi = -\mathrm{d}U/\mathrm{d}\omega$. Let us determine the derivatives of the function U with respect to φ, as follows:

$$\frac{\mathrm{d}U}{\mathrm{d}\varphi} = \pm\alpha\mathrm{e}^{-\alpha\omega}[C_1(\cos\alpha\omega - \sin\alpha\omega) - C_2(\cos\alpha\omega + \sin\alpha\omega)],$$

$$\frac{\mathrm{d}^2 U}{\mathrm{d}\varphi^2} = 2\alpha^2\mathrm{e}^{-\alpha\omega}[-C_1 \cos\alpha\omega + C_2 \sin\alpha\omega],$$

$$\frac{\mathrm{d}^3 U}{\mathrm{d}\varphi^3} = \pm 2\alpha^3\mathrm{e}^{-\alpha\omega}[C_1(\cos\alpha\omega + \sin\alpha\omega) + C_2(\cos\alpha\omega - \sin\alpha\omega)].$$

Signs indicated at the top of the right-hand sides of these expressions stand for the upper edge of the shell; signs indicated at the bottom stand for the lower edge. Since, for this case, only the edge loads are of interest, we can put $p_1 = 0$, $p_3 = 0$, and $F(\varphi) = 0$, $\Phi(\varphi) = 0$ (see Eq. (16.28) and (16.29)). The stress resultants and couples and the displacement components are related to function U, as follows:

$$N_1 = -\frac{\cot\varphi}{R_2}U, \quad N_2 = -\frac{1}{R_1}\frac{\mathrm{d}U}{\mathrm{d}\varphi}, \quad Q_1 = \frac{U}{R_2},$$

$$\vartheta_1 = \frac{R_2}{EhR_1^2}\frac{\mathrm{d}^2U}{\mathrm{d}\varphi^2}, \quad M_1 = -\frac{D}{R_1}\frac{\mathrm{d}\vartheta_1}{\mathrm{d}\varphi} = -\frac{DR_2}{R_1^3Eh}\frac{\mathrm{d}^3U}{\mathrm{d}\varphi^3}, \tag{16.48}$$

$$M_2 \cong \nu M_1, \quad \varepsilon_2 = \frac{1}{Eh}(N_2 - \nu N_1), \quad \xi = \varepsilon_2 r.$$

Based on the smallness of ϑ_1 compared with its first derivative, the terms containing ϑ_1 in the expressions for bending moments (see Eqs (16.15c and d)) have been dropped in the above equations.

Let us consider a shell of revolution subjected to the edge loads in the form of the shear force Q_e and bending moment M_e applied either to the top or to the bottom edges of the shell. The boundary conditions for these types of loading are

$$M_1 = M_e\big|_{\omega=0}, Q_1 = Q_e\big|_{\omega=0}. \tag{16.49}$$

Substituting for U from Eq. (16.47) into Eqs (16.48) for M_1 and Q_1 and then the latter equations into the above boundary conditions, results in the following algebraic equations:

$$M_e = \mp\frac{R_1}{2R_2\alpha}(C_1 + C_2), \quad Q_e = \frac{1}{R_2}C_2,$$

from which

$$C_1 = \mp\frac{2M_eR_2\alpha}{R_1} - Q_eR_2, \quad C_2 = Q_eR_2.$$

Substituting the above into Eqs (16.47) and (16.48), gives the following expressions for the internal forces, moments, and deformations:

$$N_1 = \cot\varphi\left[\pm M_e\frac{2\alpha}{R_1}\mathrm{e}^{-\alpha\omega}\sin\alpha\omega - Q_e\mathrm{e}^{-\alpha\omega}(\cos\alpha\omega - \sin\alpha\omega)\right],$$

$$N_2 = \frac{2\alpha R_2}{R_1}\left[M_e\frac{\alpha}{R_1}\mathrm{e}^{-\alpha\omega}(\cos\alpha\omega - \sin\alpha\omega) \pm Q_e\mathrm{e}^{-\alpha\omega}\cos\alpha\omega\right],$$

$$M_1 = M_e\mathrm{e}^{-\alpha\omega}(\cos\alpha\omega + \sin\alpha\omega) \pm \frac{Q_eR_1}{\alpha}\mathrm{e}^{-\alpha\omega}\sin\alpha\omega, M_2 = \nu M_1, \tag{16.50}$$

$$\vartheta_1 = \pm M_e\frac{R_1}{\alpha D}\mathrm{e}^{-\alpha\omega}\cos\alpha\omega + Q_e\frac{R_1^2}{2\alpha^2 D}\mathrm{e}^{-\alpha\omega}(\cos\alpha\omega + \sin\alpha\omega).$$

On the shell edge, for $\omega = 0$, one obtains the following:

$$\vartheta_{1e} = \pm\frac{M_e}{\alpha D}R_1 + \frac{Q_e R_1^2}{2\alpha^2 D},$$

$$N_{1e} = -Q_e \cot\varphi_e,\ N_{2e} = M_e\frac{2R_2\alpha^2}{R_1^2} \pm Q_e\frac{2R_2\alpha}{R_1},$$

$$\varepsilon_{2e} = \frac{1}{Eh}\left[M_e\frac{2R_2\alpha^2}{R_1^2} \pm Q_e\frac{2R_2\alpha}{R_1} + \nu Q_e\cot\varphi_e\right], \quad \xi_e = \varepsilon_{2e}r_e = \varepsilon_{2e}R_{2e}\sin\varphi_e. \tag{16.51}$$

The upper signs in all the above equations refer to the top edge of the shell, whereas the lower signs refer to the bottom edge. If a shell of revolution is loaded by the horizontal force (thrust) H_e per unit length applied to the shell edge $\varphi = \varphi_e$, then the internal forces and deformations can also be determined from Eqs (16.50) and (16.51) by substituting for Q_e from the following equation:

$$Q_e = \pm H_e \sin\varphi_e. \tag{16.52}$$

If an arbitrary surface load is applied to the shell of revolution, then the solutions (16.48) must be complemented by a particular solution of the nonhomogeneous equations. This particular solution in most cases is determined from the membrane theory of shells introduced in Chapter 13 .

The accuracy of the introduced approximate Geckeler's analysis was analyzed in Refs [5–9]. It has been established that for thin shells with fairly big angle of rise, these formulas give satisfactory accurate results. The error of approximate formulas of the edge effect theory has an order of $\sqrt{h\cot^2\varphi/R}$. Practically, this method can be used if the angle of the shell edge $\varphi_e > 35^\circ$.

In the next section we apply the approximate solution procedure discussed above to the analysis of some specific geometric forms of shells of revolution used in practical application. We assume that for the geometry of the shells under consideration all requirements about accuracy of applicability of the approximate method introduced above are satisfied.

16.5 AXISYMMETRIC SPHERICAL SHELLS, ANALYSIS OF THE STATE OF STRESS AT THE SPHERICAL-TO-CYLINDRICAL JUNCTION

For spherical shells, $R_1 = R_2 = R$, and the governing equations of axisymmetric bending of shells of revolution, Eqs (16.40) are simplified. The solution procedure based on the approximate method introduced in Sec. 16.4, as applied to the bending analysis of axisymmetrically loaded spherical shells, is illustrated below by the following examples.

Example 16.1

Calculate stresses in the hemispherical shell stiffened on its edge by a flange and loaded by an internal pressure p which is balanced by a force P, as shown in Fig. 16.6a. Given $R = 50\,\text{cm}$, $h = 0.3\,\text{cm}$, $r_1 = 49.85\,\text{cm}$, $r_2 = 53\,\text{cm}$, $r_3 = 51.6\,\text{cm}$, $b = 3.15\,\text{cm}$, $h_1 = 0.8\,\text{cm}$, $\nu = 0.3$, and $E = 20\,\text{GPa}$.

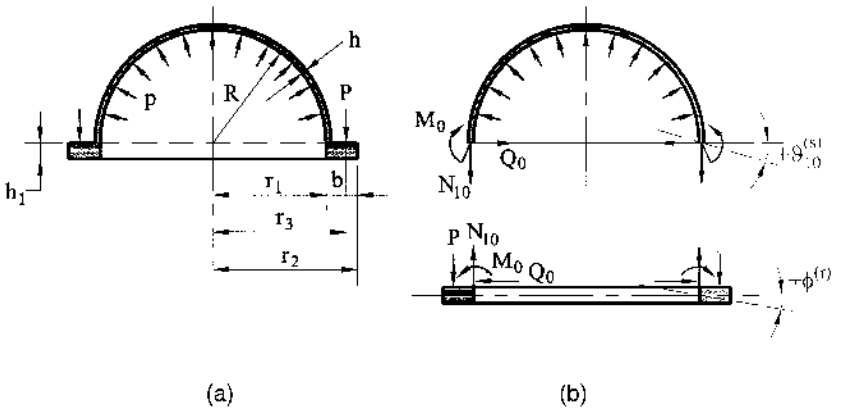

Fig. 16.6

Solution

Detach the spherical shell from the flange and apply to them the interface forces and moments M_0, Q_0, and N_{10}, as shown in Fig. 16.6b. The meridional force can be determined from the equilibrium condition, i.e.,

$$N_{10} = \frac{p(\pi r_1^2)}{2\pi R} = 24.8p(\text{N/cm}).$$

The bending moment M_0 and shear force Q_0 must be found from the compatibility of deformations conditions at the junction of the shell and flange.

Deformations of the flange may be calculated from the corresponding formulas of the theory of axisymmetrical deformations of rings [11,12]. Geometrical properties of the ring cross section are

$$I_1 = \int_A \frac{\mathrm{d}A}{r} = h_1 \ln\frac{r_2}{r_1} = 0.049\,\text{cm}, \quad I_3 = \int_A \frac{z^2}{r}\mathrm{d}A = \frac{h_1^3}{12}\ln\frac{r_2}{r_1} = 2.614 \times 10^{-3}\text{cm}^2.$$

Determine the internal bending moment $M^{(\mathrm{r})}$ and the membrane normal force $N^{(\mathrm{r})}$ at a cross section of the ring. We have

$$N^{(\mathrm{r})} = ph_1r_1 + Q_0R = 39.9p + 50Q_0,$$

$$M^{(\mathrm{r})} = pr_3^2 - N_{10}R^2 + M_0R + Q_0R\frac{h_1}{2} = 1.99 \times 10^3 p + 50M_0 + 20Q_0.$$

The angle of rotation of the ring section is

$$\phi^{(\mathrm{r})} = \frac{M^{(\mathrm{r})}}{EI_3} = \frac{1}{E}\left[0.7605 \times 10^6 p + 19.13 \times 10^3 M_0 + 7.65 \times 10^3 Q_0\right](\text{rad}). \qquad \text{(a)}$$

The radial displacement of the ring, $\xi^{(\mathrm{r})}$, at a point of the junction with the shell is

$$\xi^{(\mathrm{r})} = \frac{N^{(\mathrm{r})}}{EI_1} + \frac{\phi^{(\mathrm{r})}h_1}{2} = \frac{1}{E}\left[0.305 \times 10^6 p + 7.65 \times 10^3 M_0 + 4.08 \times 10^3 Q_0\right](\text{cm}).$$

(b)

The state of stress of the shell can be represented as a sum of the membrane state caused by the internal pressure p and membrane force N_{10}, and the moment state caused by the edge loads M_0 and Q_0.

For the membrane state of stress of the shell corresponding to a particular solution of the governing equations, we have

$$\vartheta_{1\mathrm{p}}^{(\mathrm{s})} = 0, \quad U_{\mathrm{p}} = 0, \quad N_{1\mathrm{p}} = N_{2\mathrm{p}} = \frac{pr_1^2}{2R} = N_{10} = 24.8p,$$

where the subscript p refers to the quantities associated with the membrane state. It can also be assumed that $r_1 \approx R$; then

$$N_{1\mathrm{p}} = N_{2\mathrm{p}} = \frac{pR}{2} = 25p.$$

The radial (horizontal) displacement of the shell edge, $\xi_{\mathrm{p}}^{(\mathrm{s})}$, corresponding to the membrane state of stress, is given by

$$\xi_{\mathrm{p}}^{(\mathrm{s})} = \frac{R}{Eh}\left(N_{2\mathrm{p}} - \nu N_{1\mathrm{p}}\right) = \frac{50 \times 24.8p(1 - 0.3)}{0.3(E)} = 2.9 \times 10^3 \frac{p}{E}(\mathrm{cm}). \tag{c}$$

Now, we can calculate the linear and angular displacements on the shell edge caused by the edge loads, M_0 and Q_0. These displacement components are determined with the use of the approximate solution procedure introduced in Sec. 16.4. In this case, a particular solution is zero. The general solution of the governing equations of the edge effect is given by Eqs (16.49). First, let us compute the parameter α (see Eq. (16.42)) and the flexural stiffness. We have

$$\alpha = R\sqrt[4]{\frac{3(1 - \nu^2)}{R^2h^2}} = 16.6(\mathrm{cm}), \quad D = \frac{Eh^3}{12(1 - \nu^2)} = 2.475 \times 10^{-3}E(\mathrm{N} \cdot \mathrm{cm}).$$

Substituting $R_1 = R_2 = R$ into Eq. (16.51), determine $\vartheta_{10}^{(\mathrm{s})}$, $\varepsilon_{20}^{(\mathrm{s})}$, and $\xi_0^{(\mathrm{s})}$ at the junction of the shell and ring which are caused by the above-mentioned edge loads. Taking the bottom signs in the above equations and letting $\varphi = 90^\circ$, one obtains

$$\vartheta_{10}^{(\mathrm{s})} = -\frac{M_0R}{\alpha D} + \frac{Q_0R^2}{2\alpha^2 D} = -\frac{1220M_0}{E} + \frac{1840Q_0}{E}, \tag{d}$$

$$\xi_0^{(\mathrm{s})}\Big|_{\varphi=90^\circ} = R\varepsilon^{(\mathrm{s})} = \frac{R}{Eh}\left[\frac{M_0 2\alpha^2}{R} - Q_0 2\alpha\right] = \frac{1835M_0}{E} - \frac{5330Q_0}{E}. \tag{e}$$

Let us set up the compatibility equations at the junction of the shell and ring:

$$\begin{aligned} \xi_{\mathrm{p}}^{(\mathrm{s})} + \xi_0^{(\mathrm{s})} &= \xi^{(\mathrm{r})}, \\ \vartheta_{10}^{(\mathrm{s})} &= \phi^{(\mathrm{r})} \end{aligned} \tag{f}$$

Substituting for all the components on the left- and right-hand sides of Eqs (f) from Eqs (a), (b), (c), (d), and (e), we obtain the following system of algebraic equations:

$$\begin{aligned} 2.90 \times 10^3 \frac{p}{E} - 5530\frac{Q_0}{E} + 1835\frac{M_0}{E} &= 305 \times 10^3 \frac{p}{E} + 4080\frac{Q_0}{E} + 7650\frac{M_0}{E}, \\ 1840\frac{Q_0}{E} - 1220\frac{M_0}{E} &= 760.5 \times 10^3 \frac{p}{E} + 7650\frac{Q_0}{E} + 19130\frac{M_0}{E} \end{aligned}$$

Solving these equations, yields

$$M_0 = -33.8p(\mathrm{N}\cdot\mathrm{cm/cm}), \quad Q_0 = -10.7p(\mathrm{N/cm}).$$

The maximum stresses occur at an outside point of the shell at $\varphi = 90^\circ$. They are

$$\sigma_{1\,\max} = \frac{N_1}{h} - \frac{6M_1}{h^2}; \quad \sigma_{2\,\max} = \frac{N_2}{h} - \frac{6M_2}{h^2}, \tag{g}$$

where

$$N_1 = N_{10} = 24.8p(\mathrm{N/cm}), \quad M_1 = M_0 = -33.8p(\mathrm{N}\cdot\mathrm{cm/cm});$$

$$N_2 = N_{20} + N_{2p}(\mathrm{N/cm}), \quad M_2 = \nu M_1 = -10.1p(\mathrm{N}\cdot\mathrm{cm/cm}),$$

and N_{20} is given by Eq. (16.49), i.e.,

$$N_{20} = M_0\frac{2\alpha^2}{R} - Q_0(2\alpha) = -17.32p\ (\mathrm{N/cm}).$$

Finally, N_2 can be determined as follows:

$$N_2 = N_{2\mathrm{p}} + N_{20} = 24.8p - 17.32p = 7.48p\ (\mathrm{N/cm}).$$

Substituting all the above data into Eqs (g) yields the following values of the maximum stresses:

$$\sigma_{1\,\max} = \frac{24.8p}{0.3} + \frac{6(33.8p)}{(0.3)^2} = 2336p(\mathrm{N/cm^2});$$

$$\sigma_{2\max} = \frac{7.48p}{0.3} + \frac{6(10.1p)}{(0.3)^2} = 698.2(\mathrm{N/cm^2}).$$

These values of the normal stresses coincide with the numerical data obtained in Ref. [12], where the same problem had been solved using the exact governing equations (16.30). The above-mentioned coincidence for this case can be explained by the fact that the meridional angle at the shell edge, φ_e, is equal to 90° and the radii of curvature had constant values throughout the shell.

Example 16.2

Consider a cylindrical vessel, made of steel, with a hemispherical head, as shown in Fig. 16.7a, under an internal pressure p. Determine the internal forces, moments, and stresses at the junction of the cylindrical and spherical shells. Given the radii of the cylinder and sphere are assumed to be the same and equal $R = 1.5$ m, the thickness of the cylinder and shell is $h = 0.01$ m, $E = 200$ GPa, and $\nu = 0.3$.

Solution

First, consider the *membrane state* of stress of the cylinder and head separately (Fig. 16.7b). *In the spherical shell* (*at the junction*):

$$N_{1\mathrm{p}}^{(\mathrm{s})} = N_{2\mathrm{p}}^{(\mathrm{s})} = \frac{pR}{2}, \quad \xi_{\mathrm{p}}^{(\mathrm{s})} = -\frac{pR^2}{2Eh}(1-\nu).$$

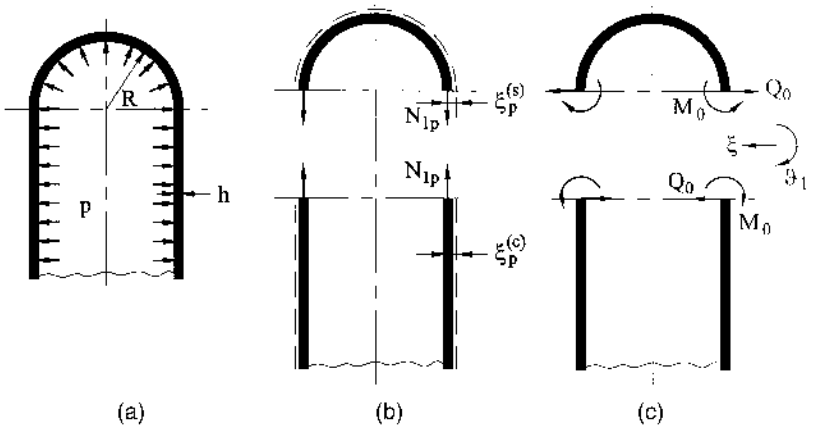

Fig. 16.7

In the cylindrical shell (at the junction):

$$N_{1p}^{(c)} = \frac{pR}{2}, \quad N_{2p}^{(c)} = pR, \quad \xi_p^{(c)} = -\frac{R}{Eh}\left(N_{2p}^{(c)} - \nu N_{1p}^{(c)}\right) = -\frac{pR^2}{Eh}(2-\nu).$$

In the above equations $\xi_p^{(s)}$ and $\xi_p^{(c)}$ refer to the membrane radial (horizontal) displacements at the juncture of the hemisphere and cylinder, respectively. Since at the junction of two shells $N_{1p}^{(s)} = N_{1p}^{(c)}$, then the membrane state of stress satisfies the static conditions of joint operation of the two shells. However, conditions of deformations' compatibility are not satisfied because the radial displacements of the cylindrical shell at the juncture are greater than the corresponding radial displacements of the spherical shell. Therefore, at the junction of the two shells, the interface force Q_0 and moment M_0 occur (Fig. 16.7c). These interface force and moment cause the *moment stress of the edge effect type* in the vicinity of the joint (see also Sec. 17.5). The values of the interface force and moment may be found from the conditions of compatibility of deformations at the junction of the spherical and cylindrical shells. Equating the total (i.e., caused by both the membrane state and edge effect) radial displacements and the angles of rotation at the juncture of the shells (the positive directions for displacements and angles of rotation are shown on the right part of Fig. 16.6c), we obtain the following:

$$\begin{aligned} &-\xi_p^{(s)} - Q_0\xi_Q^{(s)} - M_0\xi_M^{(s)} = -\xi_p^{(c)} + Q_0\xi_Q^{(c)} - M_0\xi_M^{(c)} \\ &-M_0\vartheta_{1M}^{(s)} - Q_0\vartheta_{1Q}^{(s)} = M_0\vartheta_{1M}^{(c)} - Q_0\vartheta_{1Q}^{(c)}, \end{aligned} \tag{a}$$

where ξ_Q, ξ_M and $\vartheta_{1Q}, \vartheta_{1M}$ refer to the radial displacements and slopes at the juncture caused by the unit interface shear force, $Q_0 = 1$, and unit bending moment, $M_0 = 1$; superscripts s and c stand for the hemisphere and cylinder, respectively. The deformation components at the junction for both cylindrical and spherical shells may be determined from Eqs (16.51) by setting $\varphi_e = \pi/2$ and making $R_1 = \infty$, $R_2 = R$ and $\alpha = \beta R$ for the cylindrical shell and letting $R_1 = R_2 = R$ and $\varphi = \pi/2$ for the spherical shell. Consequently, we obtain

$$\xi_Q^{(s)} = \xi_Q^{(c)} = \frac{1}{2D\beta^3},\ \xi_M^{(s)} = \xi_M^{(c)} = \frac{1}{2D\beta^2},\ \vartheta_{1M}^{(s)} = \vartheta_{1M}^{(c)} = \frac{1}{D\beta},\ \vartheta_{1Q}^{(s)} = \vartheta_{1Q}^{(s)} = \frac{1}{2D\beta^2},$$

where

$$\beta = \frac{\alpha}{R} = \frac{\sqrt[4]{3(1-\nu^2)}}{\sqrt{Rh}} = 10.4931\ (1/\text{m}).$$

Then, it follows from the compatibility equations (a) that

$$M_0 = 0, Q_0 = \frac{\xi_p^{(c)} - \xi_p^{(s)}}{\xi_Q^{(s)} + \xi_Q^{(c)}} = \frac{pR^2(D\beta^3)}{2Eh} = \frac{p\sqrt{Rh}}{8\sqrt[4]{3(1-\nu^2)}} = 0.01191p\ (\text{N}\cdot\ \text{m/m}).$$

Using Eqs (16.48) and (15.57), we can obtain the displacements and stress resultants and couples caused by the edge loads and the given internal pressure in both the cylindrical and spherical shells.

Figure 16.8a and b shows the bending moment M_1 and circumferential force N_{2m} diagrams, where N_{2M} is due to the edge loads only.

The maximum values of M_1 and N_{2M} at the junction of the two shells are found to be

$$M_{1\,\max} = \frac{pR^2}{2Eh} D\beta^2 \mathrm{e}^{-\pi/4} \frac{\sqrt{2}}{2} = 3.6 \times 10^{-4} p\ (\text{N}\cdot\text{m/m});$$

$$|N_{2M}| = Q_0 2\alpha = 0.375p\ (\text{N/m}).$$

Note that N_{2M} has different signs for the cylindrical and spherical shells at the juncture (see Fig. 16.8b).

The normal stresses due to the bending edge effect are

$$\sigma_{1M} = \frac{6M_{1\,\max}}{h^2} = 0.146\frac{pR}{h} = 21.9p,\ \sigma_{2M} = 0.1\sigma_{1M} = 2.19p.$$

The circumferential force N_{2M} eliminates a discontinuity in the forces of the membrane state. It can be easily shown that the total membrane force $N_2 = N_{2p} + N_{2M}$ is identical for both shells at the junction and equal $N_2 = 1.125p$. Thus, the total circumferential force N_2 varies continuously in the compound shell, as shown in Fig. 16.8c.

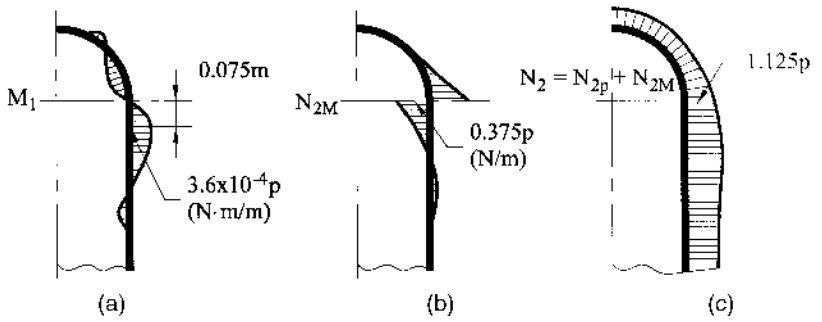

Fig. 16.8

It is seen that the stresses due to the edge effect have a magnitude of the same order (pR/h) as the membrane stresses in the shells under consideration. This is typical for shells at which the edge effect occurs, because the compatibility of deformations is not satisfied by the membrane state only.

Example 16.3

A compound steel shell consists of a cylinder (radius R and wall thickness h) and of a head in the form of a spherical segment (radius $R_s = 2R$ and thickness h), as shown in Fig. 16.9a. This compound shell is subjected to an internal pressure p. Determine the internal forces and moments in the compound shell if $R = 1.5\,\text{m}$, $h = 0.02\,\text{m}$, $\nu = 0.3$, $E = 200\,\text{GPa}$, and $\varphi_1 = 30^\circ$.

Solution

First, consider the membrane state of the head and cylinder separately, as shown in Fig. 16.9b. From the membrane shell theory, it follows that

$$N_{1p}^{(s)} = N_{2p}^{(s)} = \frac{pR_s}{2} = pR; \quad N_{1p}^{(c)} = \frac{pR}{2}, N_{2p}^{(c)} = pR \tag{a}$$

where, again, the subscript p refers to the membrane solution and superscripts s and c stand for the sphere and cylinder, respectively. It is seen from Fig. 16.9b that, apart from the latter example, the membrane state alone does not satisfy the conditions of static equilibrium in the head and cylinder. Therefore, the *edge effect* occurs at the junction of the compound shell to satisfy both the statics and compatibility of deformations conditions.

Consider the edge effect procedure being applied to the given compound shell. The membrane force $N_{1p}^{(s)}$ at the edge of the head has a horizontal component, which is equal to

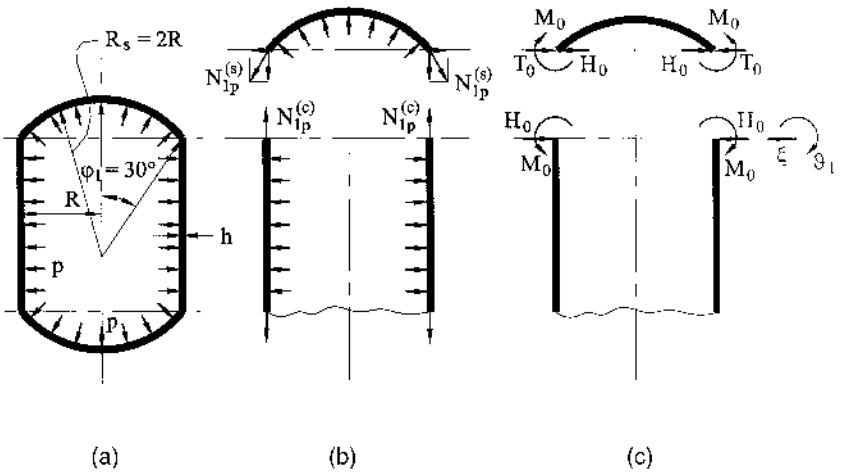

Fig. 16.9

$$T_0 = N_{1p}^{(s)} \cos\varphi_1 = pR\frac{\sqrt{3}}{2}. \tag{b}$$

To ensure that the shell loading by the membrane scheme (Fig. 16.9b), together with the edge effect, would be equivalent to the given loading applied to the compound shell, it is necessary to include the thrust that is equal and oppositely directed to T_0 among the edge effect forces, as shown in Fig. 16.8c. Thus, in applying the edge effect solution procedure, we should assume that the cylindrical shell is loaded by the edge moment M_0 and shear force H_0, whereas the spherical shell is loaded by the edge moment M_0 and thrust $(H_0 - T_0)$, as shown in Fig. 16.9c. The unknown quantities M_0 and H_0 are evaluated from the compatibility of deformations' conditions, i.e., the radial (horizontal) displacements and angles of rotation of normals should be identical at the juncture of both shells. Equating the edge radial displacements of the sphere and cylinder at the juncture, we obtain

$$\xi^{(s)} = \xi^{(c)} \tag{c}$$

where,

$$\begin{aligned}
\xi^{(s)} &= -\frac{R}{Eh}(N_{2p}^{(s)} - \nu N_{1p}^{(s)}) + (T_0 - H_0)\xi_H^{(s)} - M_0\xi_M^{(s)} \\
\xi^{(c)} &= -\frac{R}{Eh}\left(N_{2p}^{(c)} - \nu N_{1p}^{(c)}\right) + H_0\xi_H^{(c)} - M_0\xi_M^{(c)}.
\end{aligned} \tag{d}$$

In Eqs (c) and (d), the first terms on the right-hand sides correspond to the membrane solution.

The conditions of compatibility for the slopes (the positive direction of the slopes is shown in Fig. 16.9c to the right) has the form

$$(T_0 - H_0)\vartheta_{1H}^{(s)} - M_0\vartheta_{1M}^{(s)} = -H_0\vartheta_{1H}^{(c)} + M_0\vartheta_{1M}^{(c)}. \tag{e}$$

In Eqs. (d) and (e), the subscripts H and M indicate the cause of the corresponding displacements. The coefficients $\xi_H^{(s)}$, $\xi_M^{(s)}$, $\vartheta_{1H}^{(s)}$, $\vartheta_M^{(s)}$ and $\xi_H^{(c)}$, $\xi_M^{(c)}$, $\vartheta_{1H}^{(c)}$, $\vartheta_{1M}^{(c)}$ can be calculated from Eqs (16.51) by setting $R_1 = R_2 = R_s = 2R$, $\varphi_e = \varphi_1$, and replacing Q_0 with $H_0 \sin\varphi_1$ or $T_0 \sin\varphi_1$) according to Eq. (16.50) for the spherical shell, and by setting $R_1 = \infty$, $R_2 = R$, and $\varphi_e = \varphi_1$ for the cylindrical shell. As a result, we obtain

$$\begin{aligned}
&\xi_H^{(s)} = \frac{\sin^2\varphi_1}{2D\beta_s^3}, \quad \xi_M^{(s)} = \frac{\sin\varphi_1}{2D\beta_s^2}; \quad \vartheta_{1M}^{(s)} = \frac{1}{D\beta_s}; \quad \vartheta_{1H}^{(s)} = \xi_M^{(s)}, \\
&\xi_H^{(c)} = \frac{1}{2D\beta_c^3}, \quad \xi_M^{(c)} = \frac{1}{2D\beta_c^2}, \quad \vartheta_M^{(c)} = \frac{1}{D\beta_c}, \quad \vartheta_{1H}^{(c)} = \xi_M^{(c)}, \\
&\beta_s = \frac{\sqrt[4]{3(1-\nu^2)}}{\sqrt{2Rh}}, \quad \beta_c = \frac{\sqrt[4]{3(1-\nu^2)}}{\sqrt{Rh}}.
\end{aligned} \tag{f}$$

Substituting the numerical data into the relations (a), (b), (d), and (f), one obtains the following:

$$D = \frac{Eh^3}{12(1-\nu^2)} = 146.52 \times 10^3 (\text{Nm}); \quad \beta_c = 7.4213(1/\text{m}); \quad \beta_s = 5.2477(1/\text{m});$$

$$N_{1p}^{(s)} = N_{2p}^{(s)} = 1.5p \ (\text{N/m}); \quad N_{1p}^{(c)} = 0.75p \ (\text{N/m}); \quad N_{2p}^{(c)} = 1.5p; \quad T_0 = 1.3p \ (\text{N/m});$$

$$\xi_H^{(s)} = 0.005903 \times 10^{-6} (\text{m}^2/\text{N}); \quad \xi_M^{(s)} = 0.06196 \times 10^{-6} (\text{m/N});$$

$$\vartheta_M^{(s)} = 1.301 \times 10^{-6} (1/\text{N});$$

$$\xi_H^{(c)} = 0.008362 \times 10^{-6} (\text{m}^2/\text{N}); \quad \xi_M^{(c)} = 0.06196 \times 10^{-6} (\text{m/N});$$

$$\vartheta_M^{(c)} = 0.9196 \times 10^{-6} (1/\text{N}).$$

Substituting the above into the compatibility equations (c) and (e) and taking into account the relations (d), we can calculate H_0 and M_0. We have

$$H_0 = 0.5401p \ (\text{N/m}); \quad M_0 = 0.03627p \quad (\text{N} \cdot \text{m/m}).$$

Using Eqs (16.48) for a spherical shell and Eqs (15.57) for the cylindrical shell, we can determine the membrane forces N_2, N_1 and bending moments M_1, M_2 in the spherical and cylindrical parts of the given compound shell. The equations for the membrane forces and bending moments are of the following form:

– for the cylindrical shell

$$\begin{aligned} N_2^{(c)} &= 1.5p\left[1 - 4.0075e^{-\beta_c x}(\cos\beta_c x + \sin\beta_c x)\right]; \quad N_1^{(c)} = 0.75p; \\ M_1^{(c)} &= 0.03627pe^{-\beta_c x}(\cos\beta_c x - \sin\beta_c x), \end{aligned} \tag{g}$$

where the coordinate x is counted off from the juncture of the spherical and cylindrical shells.

–for the spherical shell

$$\begin{aligned} N_2^{(s)} &= 1.5p[1 - 4.0075e^{-\alpha\omega}(\cos\alpha\omega + \sin\alpha\omega)]; \\ N_1^{(s)} &= 1.5p[1 - 0.44e^{-\alpha\omega}\cos\alpha\omega]; \\ M_1^{(s)} &= 0.03627pe^{-\alpha\omega}(\cos\alpha\omega - \sin\alpha\omega), \end{aligned} \tag{h}$$

where $\alpha = R_s\beta_s$ and $\omega = \varphi_1 - \varphi = 30^\circ - \varphi$.

The diagrams of the membrane force N_2 and bending moment M_1 are shown in Fig. 16.10.

The maximum normal stresses occur in the cylindrical shell at points in its inner surface at the junction with the sphere segment. The total meridional stress is tensile at the above points and is equals to

$$\sigma_1 = \frac{N_1}{h} + \frac{6M_1}{h^2} = 37.5p + 544p = 581.5p. \tag{i}$$

The circumferential stress at the same points is compressive and is given by

$$\sigma_2 = \frac{N_2}{h} + \nu\frac{6M_1}{h^2} = -61.8p. \tag{j}$$

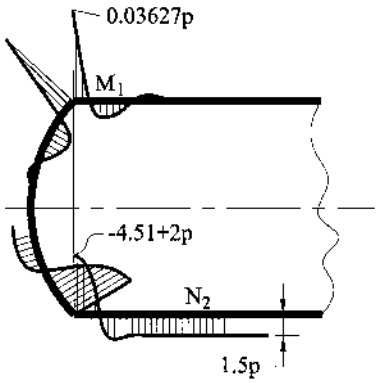

Fig. 16.10

It can be shown that in the given compound shell the edge effect normal stress is larger by an order of magnitude $\sqrt{(R/h)}$ than the corresponding membrane stress. Therefore, the compound shell, like that analyzed in this example, is inefficient.

However, it is possible to essentially decrease the stresses at the junction of compound shell structures. Figure 16.11a shows two shells, cylindrical and spherical, joined by a ring. The latter is supposed to support the thrust T_0 (Fig. (16.11a)). In the analysis of such shell structures, one can assume that the bending stiffness of the ring in the direction perpendicular to its plane is negligible. Thus, the ring resists only the radial load in its own plane. The free-body diagrams of the shells and ring are shown in Fig. 16.11b.

Let us determine the stress components at the junction of the two shells, shown in Fig. 16.11. The geometrical and mechanical parameters of the shells are taken from Example 16.3.

The values of the unknown interface forces, H_1 and H_2, as well the moment M_0, are evaluated from the conditions of deformations, compatibility of the shell parts and ring. Let the shell and ring be made of the same material. Assume that the

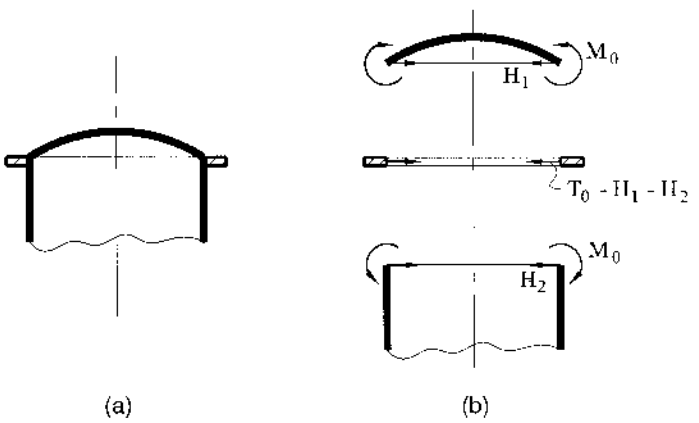

Fig. 16.11

cross-sectional area of the ring, A_r, has an order of magnitude Rh and the terms of the order of magnitude $\sqrt{h/R}$ can be neglected compared with unity. In this case, the radial compliance of the ring, R^2/A_rE, will be significantly lower than the radial compliance of the shells, i.e.,

$$\xi_H^{(c)} = \frac{1}{2D\beta_c^3} = 2\sqrt[4]{3(1-\nu^2)}\frac{R}{Eh}\sqrt{\frac{R}{h}}.$$

Therefore, one can assume that the thrust T_0 is completely carried by the ring and the ring's horizontal displacement, T_0R^2/EA_r, determines the corresponding displacements of the shell parts (cylindrical and spherical shells). Thus, the above-mentioned compatibility equations can be represented in the following form:

$$\begin{aligned}
-\frac{R}{Eh}(N_{2p}^{(s)} - \nu N_{1p}^{(s)}) + H_1\xi_H^{(s)} - M_0\xi_M^{(s)} &= \frac{T_0R^2}{EA_r},\\
-\frac{R}{Eh}(N_{2p}^{(c)} - \nu N_{1p}^{(c)}) + H_2\xi_H^{(c)} - M_0\xi_M^{(c)} &= \frac{T_0R^2}{EA_r},\\
M_0\vartheta_M^{(c)} - H_2\vartheta_H^{(c)} &= -M_0\vartheta_M^{(s)} + H_1\vartheta_H^{(s)}.
\end{aligned} \tag{k}$$

Let us select the cross-sectional area of the ring, A_r, from the condition

$$\sigma_r = \sigma_{2p} \tag{l}$$

where

$$\sigma_r = \frac{T_0R}{A_r} = \frac{pR^2\sqrt{3}}{2A_r},$$

is the compressive stress in the ring and

$$\sigma_{2p} = \frac{pR}{h}$$

is the maximum tensile stress in the shell by the membrane theory. Thus, we have

$$A_r = \frac{\sqrt{3}}{2}Rh = 0.02598(\text{m}^2). \tag{m}$$

Substituting for the coefficients $\xi_H, \xi_M, \vartheta_H$, and ϑ_M from Eqs (f) and taking into account Eq. (k), we can solve Eqs (p) for H_1, H_2, and M_0. We obtain

$$M_0 = 0.01605p; \quad H_1 = 0.2434p; \quad H_2 = 0.3308p.$$

Having determined the edge effect forces and moments, we can calculate the internal forces and bending moments in the spherical and cylindrical parts of the given compound shell by using Eqs (16.48) and (15.57), respectively. It can be seen that for this compound shell reinforced by the ring, the maximum edge effect bending stresses will have the same order of magnitude as the membrane stresses. In particular, the maximum edge effect bending stress in the zone of the junction of the two shells is given by

$$\sigma_1 = \frac{6M_1}{h^2} = 240.75p.$$

Comparing this bending stress due to the edge effect with the corresponding stress from the previous example, we can conclude that the setup of the ring allows one to decrease the edge effect maximum stress by more than two times, although the above stress remains quite considerable.

16.6 AXISYMMETRICALLY LOADED CONICAL SHELLS

For a conical shell, a distance s measured from the vertex of the cone along the straight meridian may be conveniently taken as a meridional coordinate of a point on the middle surface (see Sec. 13.6.2). Replacing the variable φ with a new variable s, we use the following obvious relationships

$$ds = R_1 d\varphi, \frac{d(\ldots)}{d\varphi} = R_1 \frac{d(\ldots)}{ds} \tag{16.53a}$$

For conical shells R_1 is a constant at infinity and does not vary with s, so that $dR_1/ds = 0$; hence,

$$\frac{d^2(\ldots)}{d\varphi^2} = R_1^2 \frac{d^2(\ldots)}{ds^2} \quad \text{and} \quad R_2 = s\cot\varphi, \frac{dR_2}{ds} = \cot\varphi. \tag{16.53b}$$

where φ is the constant value for all points on the straight meridian (Fig. 13.3).

In this section, we are concerned with the bending theory of a conical shell subjected to axisymmetrically applied edge loads. Therefore, we seek only solutions of the homogeneous bending theory equations (the edge effect solutions), because the membrane solution may be used as a particular integral of the general theory equations for conical shells. Using the relationships (16.53), we can rewrite the governing equation (16.28) in terms of the variable s, setting $R_1 = \infty$ for conical shells and $\Phi(\varphi) = 0$, as follows:

$$\begin{aligned} &\frac{d^2\vartheta_1}{ds^2} + \frac{1}{s}\frac{d\vartheta_1}{ds} - \frac{1}{s^2}\vartheta_1 = -\frac{1}{DR_2}U, \\ &\frac{d^2U}{ds^2} + \frac{1}{s}\frac{dU}{ds} - \frac{1}{s^2}U = \frac{Eh}{R_2}\vartheta_1, \end{aligned} \tag{16.54a}$$

or in the following operator form

$$\begin{aligned} &L_1(\vartheta_1) + \frac{1}{D}U = 0 \\ &L_1(U) - Eh\vartheta_1 = 0 \end{aligned} \tag{16.54b}$$

where the operator $L_1(..)$ is given by

$$L_1(\ldots) \equiv \cot\varphi\left[s\frac{d^2(\ldots)}{ds^2} + \frac{d(\ldots)}{ds} - \frac{1}{s}(\ldots)\right].$$

The solution of the governing differential equations (16.54b) can be expressed in terms of the Bessel functions or their modifications [13]. However, this rigorous approach is not suited to practical engineering calculations, as it is too lengthy even when tables of the Bessel functions are available. The problem of straining the conical shells may be solved by using the numerical methods introduced in Chapter 6 or by the finite element method technique [3,4].

A simpler solution for the conical shell problems, analogous to the Geckeler approximation, (see Sec. 16.4) is now introduced. Dropping terms with ϑ_1 and $d\vartheta_1/ds$ and the terms U and dU/ds from the left-hand sides of Eqs (16.54a), yields the following approximate equations:

$$\begin{aligned} \frac{d^2\vartheta_1}{ds^2} &\approx -\frac{U}{DR_2}, \\ \frac{d^2U}{ds^2} &\approx \frac{Eh}{R_2}\vartheta_1. \end{aligned} \tag{16.55}$$

Differentiating the second equation twice with respect to s and substituting it into the first equation, gives the following governing differential equation of the edge effect for conical shells:

$$\begin{aligned} &\frac{d^4U}{ds^4} + \frac{Eh}{R_2^2 D}U = 0 \quad \text{or} \\ &\frac{d^4U}{ds^4} + 4\beta^4 U = 0, \end{aligned} \tag{16.56}$$

where

$$\beta = \sqrt[4]{\frac{3(1-\nu^2)}{R_2^2 h^2}}. \tag{16.57}$$

Remember that in deriving the governing differential equation of the edge effect the following assumptions have been adopted: the lower derivatives of functions and functions themselves are small compared with the higher derivatives and the radius R_2 varies slightly near the shell edge. It has been shown that these assumptions are fairly fulfilled if $\sqrt{h/(r\sin\varphi)} \ll 1$ (r is the radius of the parallel circle) [14] or for conical shells with a considerable slope of the meridian ($\varphi > 35^\circ - 40^\circ$).

Let x be the coordinate measured from the edge of interest. Then we have

– for the top edge $x = s - s_0$,
– for the bottom edge $x = s_0 - s$,

where s_0 is some coordinate that corresponds to the given edge of the shell. In transition to the variable x, Eq. (16.56) remains unchanged, i.e.,

$$\frac{d^4U}{dx^4} + 4\beta^4 U = 0. \tag{16.58}$$

Using the edge effect procedure, developed in Sec. 16.4, we can obtain the solution of Eq. (16.58) and the following expressions for the deformations, internal forces, and moments in a conical shell subjected to the edge loads M_e and Q_e in terms of the variable x, as follows:

$$
\begin{aligned}
U &= \mp M_e 2\beta R_2 e^{-\beta x} \sin \beta x + Q_e R_2 e^{-\beta x}(\cos \beta x - \sin \beta x),\\
N_1 &= \cot \varphi\left[\pm M_e 2\beta e^{-\beta x} \sin \beta x - Q_e e^{-\beta x}(\cos \beta x - \sin \beta x)\right],\\
N_2 &= 2\beta R_2\left[M_e \beta e^{-\beta x}(\cos \beta x - \sin \beta x) \pm Q_e e^{-\beta x} \cos \beta x\right],\\
M_1 &= M_e e^{-\beta x}(\cos \beta x + \sin \beta x) \pm Q_e \frac{1}{\beta} e^{-\beta x} \sin \beta x,\ M_2 = \nu M_1,\\
\vartheta_1 &= \pm M_e \frac{1}{\beta D} e^{-\beta x} \cos \beta x + Q_e \frac{1}{2\beta^2 D} e^{-\beta x}(\cos \beta x + \sin \beta x),\\
\xi &= \varepsilon_2 r = R_2 \sin \varphi \frac{1}{Eh}(N_2 - \nu N_1).
\end{aligned}
\tag{16.59}
$$

The positive directions of the edge force Q_e and moment M_e are shown in Fig. 16.12. The upper sign in Eqs (16.59) refers to the top edge (at $\varphi = \varphi_{e1}$) and the lower sign refers to the bottom edge (at $\varphi = \varphi_{e2}$) of the shell.

Example 16.4

Determine the internal forces in a conical shell subjected to the edge loads m and H, as shown in Fig. 16.13. Given $h = 0.5\,\text{in}$, $\varphi = 60^\circ$, $s_1 = 10\,\text{in.}$, $s_2 = 30\,\text{in.}$, $R_2 = s_2 \cot \varphi = 17.3\,\text{in.}$, and $\nu = 0.3$.

Solution

The parameter β for the bottom edge is obtained from Eq. (16.57):

$$
\beta = \sqrt[4]{\frac{3(1-\nu^2)}{R_2^2 h^2}} = 0.4371 \quad (1/\text{in.}).
$$

The edge loads on the bottom edge are

$$
M_e = m, \quad Q_e = H \sin 60^\circ = 0.866H.
$$

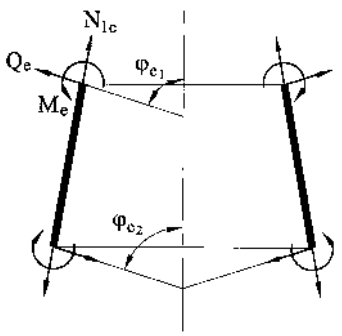

Fig. 16.12

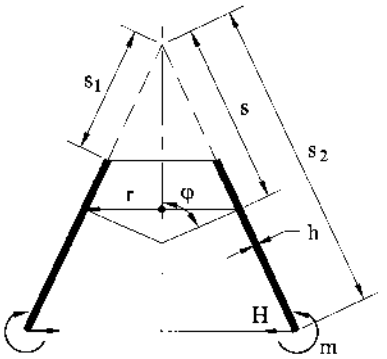

Fig. 16.13

Using Eqs (16.59) and setting $x = 0$, we can calculate the angle of rotation of the normal to the meridian, ϑ_1, and the internal forces at the bottom edge. We have

$$\vartheta_1 = -\frac{m}{\beta D} + \frac{Q_e}{2\beta^2 D} = -2.29\frac{m}{D} + 2.28\frac{H}{D},$$

$$N_1 = -Q_e \cot\varphi = -0.5H,$$

$$N_2 = 2\beta R_2(m\beta - Q_e) = 6.58m - 13.1H.$$

Comparing these numerical data with those obtained by using the exact edge effect procedure based on the use of the Bessel functions [12], we can conclude that the error of this approximate analysis does not exceed 1% for the given case.

16.7 AXISYMMETRIC DEFORMATION OF TOROIDAL SHELLS

Structural components having a form of toroidal shells are commonly used in mechanical engineering. Housings of pumps, hydraulic clutches, tanks, bellows, etc., are examples of such shape of a shell. The shape of a toroidal shell is characterized by the radii R and a and by the following parameters (Fig.16.14):

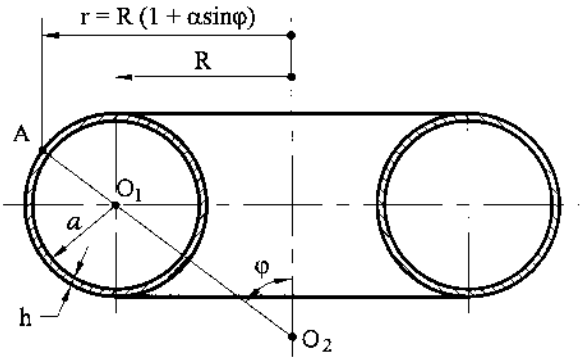

Fig. 16.14

$$\alpha = \frac{a}{R}, \quad \beta = \frac{a}{h}. \tag{16.60}$$

For a toroidal shell, the principal radii of curvature are (Fig. 16.13)

$$O_1A = R_1 = a = \text{const}, \quad O_2A = R_2 = R\frac{1+\alpha\sin\varphi}{\sin\varphi}, \tag{16.61}$$

where φ is the angular coordinate varying in the range $-180^\circ < \varphi < 180^\circ$. Toroidal shells, except for shallow part near $\varphi = 0$, can be successfully analyzed by the methods of the theory of edge effect (see Sec. 16.4).

For shells including the shallow part near $\varphi = 0$, the problem becomes more complicated. Considerable difficulties are associated with determining a particular solution of the nonhomogeneous governing differential equations, because the membrane solution near $\varphi = 0$ becomes invalid. Thus, toroidal shells must be analyzed by using the governing equations of the general moment theory of axisymmetric shells of revolution. Substituting for the principal radii of curvature from the relations (16.61) into Eqs (16.30), we obtain the following governing differential equations of the axisymmetric deformation of toroidal shells:

$$\begin{aligned} L_2(U) + \nu L_2(U) &= Eha\vartheta_1(\varphi) + \Phi^*(\varphi), \\ L_2(\vartheta_1) - \nu\vartheta_1 &= -\frac{a}{D}U, \end{aligned} \tag{16.62}$$

where

$$\begin{aligned} L_2(\ldots) &= \frac{1+\alpha\sin\varphi}{\sin\varphi}\frac{\mathrm{d}^2(\ldots)}{\mathrm{d}\varphi^2} + \cot\varphi\frac{\mathrm{d}(\ldots)}{\mathrm{d}\varphi} - \frac{\alpha\cot\varphi\cos\varphi}{1+\alpha\sin\varphi}(\ldots), \\ \Phi^*(\varphi) &= a^2\frac{\mathrm{d}}{\mathrm{d}\varphi}\left[p_3\frac{(1+\alpha\sin\varphi)^2}{\alpha^2\sin^2\varphi}\right] + p_1a^2\frac{(1+\alpha\sin\varphi)}{\alpha\sin\varphi}\left(\frac{1+\alpha\sin\varphi}{\alpha\sin\varphi} + \nu\right) \\ &\quad + F(\varphi)\frac{\cos\varphi(2+3\alpha\sin\varphi)}{\alpha\sin^4\varphi(1+\alpha\sin\varphi)}. \end{aligned} \tag{16.63}$$

The solution of Eqs (16.62) can be obtained by numerical methods introduced in Chapter 6 – in particular, by the finite element method.

PROBLEMS

16.1 Derive Eqs (16.5).

16.2 Derive Eqs (16.9).

16.3 Show that the vertical displacement of a point in the middle surface of shell of revolution, η (see Fig. 16.1) are governed by the following equation

$$\eta = \int_{\varphi_0}^{\varphi} (\varepsilon_1\sin\bar{\varphi} + \vartheta_1\cos\bar{\varphi})R_1\mathrm{d}\bar{\varphi}.$$

16.4 Verify Eqs (16.50).

16.5 Consider a spherical dome supporting its own weight and described in Sec. 14.1.1. Assume that the supports are as shown in Fig. 14.2a. (a) Determine the bending stresses and (b) compare the bending and membrane stresses. Assume reasonable values for any additional properties and parameters required.

16.6 A dome in the form of a spherical segment is clamped around its base and is loaded by an external pressure $p = 1.5$ MPa. Determine the force and moment applied to the base of the shell by support. Take φ_1 (the meridional angle at the shell base) $= 55^\circ$, $E = 200$ GPa, $\nu = 0.3$, $h = 20$ mm, and $R = 1500$ mm.

16.7 A cylindrical tank is capped by a hemispherical shell, as shown in Fig. 16.6. The tank is loaded by an internal pressure $p = 1.4$ MPa. Determine the discontinuity stresses at the junction. Take the allowable membrane stress $\sigma_{all} = 120$ Mpa, $E = 200$ GPa $\nu = 0.3$, $R = 1000$ mm, $h_c = h_s = 12$ mm, where h_c and h_s are the thicknesses of the cylindrical tank and hemispherical shell, respectively.

16.8 A hemispherical cap of radius R and thickness h is loaded by uniformly applied to the free edge of the cap moments M_0. Determine the length L, measured along the meridian from the loaded edge of the cap, where the internal moment M_1 diminishes to 1% of moment M_0. How does this length compare with that in Example 15.1 for a cylindrical shell?

16.9 Redo Problem 16.8 replacing the moments M_0 with uniformly applied horizontal forces Q_0 to the free edge of the cap.

16.10 What is the maximum stress at the junction of the flat circular plate and (a) hemispherical shell (Fig. P.16.1a) and (b) conical shell with $\alpha = 37^\circ$ (Fig. P.16.1b)? Both shells are subject to an internal pressure of $p = 1.5$ MPa. Let $E = 200$ GPa, and $\nu = 0.27$.

16.11 A conical frustum has a free edge at its top and it is built-in at the base. The shell is subject to internal pressure p. Determine the internal forces and bending moments in the shell. Let the radii of the parallel circles at the shell top and its base be 5.5 m and 8.5 m, respectively, $h = 60$ mm, $E = 200$ GPa, and $\nu = 0.3$. Employ the approximate method of Sec. 16.4 to determine the bending stress resultants and couples.

16.12 Calculate the displacements of the edge of the hemispherical shell shown in Fig. 16.5a. For your calculations use the numerical data in Example 16.1.

16.13 Compare the values of the normal stresses in the spherical shell segment for four variants of boundary conditions at its base: (a) the shell is loaded by a normal meridional force N_e applied to its free edge; (b) the shell is built-in; (c) the shell has roller supports at its free edge; and (d) the shell is simply supported. The shell is subjected to an external normal pressure p. Let $R = 30h$ and $\varphi_1 = 35^\circ$(meridional angle at the shell base) for all the above-mentioned shells. Employ the approximate method of Sec. 16.4 for the solution.

16.14 Consider the Intze-type water tank of Problem 14.18 (Fig. 14.14a). (a) Find the bending stress resultants and couples in the wall and the roof and plot their diagrams. (b) Assume that there is no ring beam at B. Find the final value of N_2 in the cone at B using the moment theory. Neglect the effects of discontinuities at C on the stresses

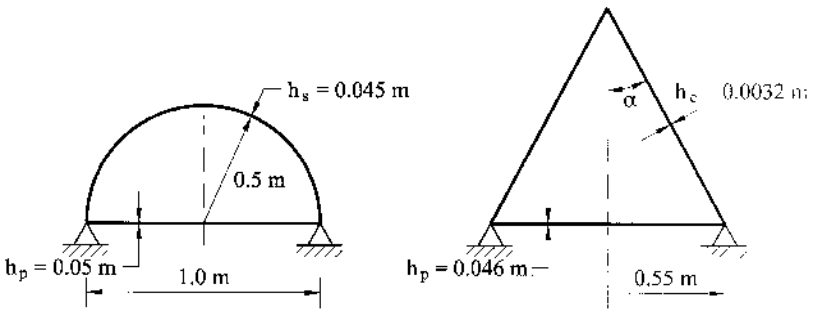

Fig. P16.1

at B. In your calculations assume that the modulus of elasticity of the wall and the roof are the same and Poisson's ratios are zero. Use the numerical data in Problem 14.18 for the solution.

16.15 Find the bending field in the intersection of the cylindrical wall and its conical end caps in the cylindrical pressure vessel shown in Fig. P.14.4. Take $H = 2R = 2\,\text{m}$, $h_1 = 10$ mm, $h_2 = 12\,\text{mm}$, $E = 200$ GPa, $\nu = 0.3$.

16.16 Consider the water tank shown in Fig. P.14.3. Perform a complete analysis of this tank. Let $R = 500\,\text{mm}$, $H = 2R$, and $h_1 = h_2 = 5\,\text{mm}$. Assume reasonable values for any additional properties required.

16.17 Consider a conical shell with a central angle α, the base radius a, and thickness h. The lower edge of this cone is fixed against rotation and translation. The shell is subjected to its own weight with intensity p. Perform a complete analysis of this shell.

16.18 Verify Eqs 16.62.

REFERENCES

1. Collatz, L., The *Numerical Treatment of Differential Equations*, 3rd edn, Springer-Verlag, Berlin, 1966.
2. Godunov, S.K., *Ordinary Differential Equations with Constant Coefficients* (translated from Russian), Providence, R.I. American Mathematical Society, 1997.
3. Zienkiewicz, O.C., *The Finite Element Method*, McGraw-Hill, New York, 1977.
4. Ashwell, D.G. and Gallagher, R.H. (eds) *Finite Elements for Thin Shells and Curved Members*, Wiley, London, 1976.
5. Meissner, E., Das elastizitatsproblem für dünne schalen von ringflächen, kugel-, and kegelform, *Physik Zeit*., vol. 14, pp. 343–349 (1913).
6. Reissner, H., *Spannungen in Kugelschalen* , Müller, Breslau-Festscher, 1912.
7. Geckeler, J., *Über die Festigkeit Achsensymmetrischer Schalen*, Forschg.-Arb. Ingwes, p. 276, Berlin, 1926.
8. Meissner, E., Über elastizität und festigkeit dünner schalen, *Viertelschr d Natur, Ges*, Bd. 60, Zürich, 1915.
9. Novozhilov, V.V., *The Theory of Thin Elastic Shells,* P. Noordhoff Ltd, Groningen, the Netherlands, 1964.
10. Timoshenko, S.P. and Goodier, J.N., *Theory of Elasticity*, 3rd edn, McGraw-Hill, New York, 1970.
11. Feodosyev, V., *Strength of Materials*, Izdatelstvo Mir, Moscow, 1968.
12. Boyarshinov, S.V., *The Fundamentals of Structural Mechanics of Machines*, Izdatelstvo Mashinostroenie, Moscow, 1973 (in Russian).
13. Watson, G.N., *Theory of Bessel Functions*, 2nd edn, Cambridge University Press, Cambridge, 1944.
14. Biderman, V.L., *Mechanics of Thin-Walled Structures*, Izdatelstvo Mashinostroenie, Moscow, 1977 (in Russian).

17

Approximate Theories of Shell Analysis and Their Applications

17.1 INTRODUCTION

The complexity of the governing equations of the general linear theory of thin shells motivated the development of a wide range of approximate theories associated with simplifications of these equations.

There are two principal avenues in developing these approximate theories. The first avenue is based on introducing some additional hypotheses (except for the general Kirchhoff–Love assumptions) that follow from the mechanical analysis of shell straining under applied loading, numerical results of solving various particular shell problems, and from experimental investigations [1–4, etc.]. The second avenue is based on the asymptotic analysis of the governing differential equations of the general linear theory of thin shells having a small parameter a (see Sec. 15.2) [5]. Both avenues arrive at the same results. However, the second avenue provides a way for an error estimation of the corresponding approximate equations. Note that the possibility of introducing one or other simplification is determined by the character of loading (its variation), boundary conditions, and the shell stiffness and its other geometric parameters.

In this chapter we consider only the first avenue of simplifications and the corresponding approximate theories.

17.2 THE SEMI-MEMBRANE THEORY OF CYLINDRICAL SHELLS

In the analysis of long closed and open cylindrical shells, the so-called semi-membrane theory has enabled a wide range of applications. It enables one to analyze the above-mentioned shells with the use of simple (and well-known for engineers) mathematical technique in situations when the membrane theory is not applicable.

17.2.1 The governing differential equations of the semi-membrane theory

It was mentioned previously that the membrane theory is inapplicable for the stress analysis of long cylindrical shells. Another deficiency of the membrane theory is the impossibility of satisfying the prescribed boundary conditions on the longitudinal edges of an open cylindrical shell. Vlasov [1] proposed an approximate approach, the so-called *semi-membrane theory of cylindrical shells*, which is free of those drawbacks. Moreover, this theory is significantly simpler than the general theory of cylindrical shells. As a result, Vlasov's theory has been widely adapted in engineering practice for the analysis of cylindrical shell structures.

The semi-membrane theory is based on the following assumptions (along with the general Kirchhoff–Love hypotheses):

1. *The bending, M_1, and twisting, H, moments at sections normal to the shell generator are insignificant and may be neglected.* This means that the normal stresses are assumed to be uniformly distributed across the shell thickness at a section, perpendicular to the longitudinal axis of the shell.
2. *The circumferential strain ε_2 and shear strain γ_{12} in the middle surface are neglected.*
3. *Poisson's ratio is zero, i.e., $\nu = 0$.*

Introducing these assumptions implies that a real shell is replaced by the model depicted in Fig. 17.1a. According to this model, a shell consists of innumerable sets of transverse elementary curvilinear strips connected by hinged bonds. Each such strip works in bending in the plane of the shell cross section. Forces are transmitted from strip to strip by means of rods. The latter can transmit only in-plane normal and shear forces, N_1 and S, respectively. Non-zero stress resultants and couples are shown in Fig. 17.1b.

The assumptions introduced above are justified by some physical considerations. Gol'denveizer [5] and Novozhilov [2] showed that these assumptions are mathematically equivalent to the inequality

$$\left|\frac{\partial^2 f}{\partial x^2}\right| \ll \left|\frac{\partial^2 f}{\partial \theta^2}\right|, \tag{17.1}$$

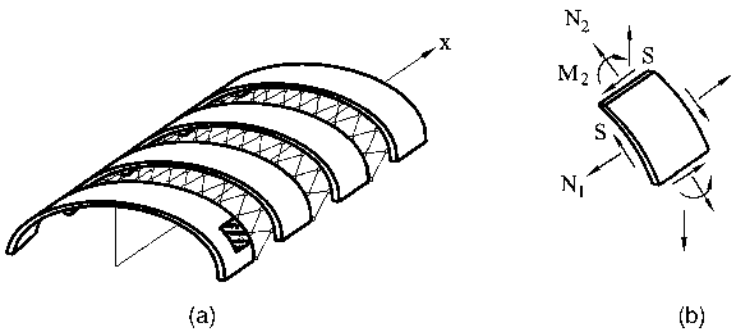

Fig. 17.1

which states that the second derivative of any function (displacement, strain, stress resultant or couple) in the longitudinal direction is negligible compared with its second derivative in the circumferential direction. As mentioned in Sec. 15.2, such a state of stress and strain is referred to as the basic one.

The equations of equilibrium (Eqs (15.4)) with regard to the introduced assumptions ($M_1 = Q_1 = H = 0$) are of the following form (for circular cylindrical shells):

$$\begin{aligned} R\frac{\partial N_1}{\partial x} + \frac{\partial S}{\partial \theta} + p_1 R &= 0, \\ \frac{\partial N_2}{\partial \theta} + R\frac{\partial S}{\partial x} - \frac{1}{R}\frac{\partial M_2}{\partial \theta} + p_2 R &= 0, \\ \frac{1}{R}\frac{\partial^2 M_2}{\partial \theta^2} + N_2 + p_3 R &= 0. \end{aligned} \tag{17.2}$$

Eliminating from the above equations the membrane forces S and N_2 results in the following equation that relates N_1 to M_2:

$$\frac{\partial^2 N_1}{\partial x^2} + \frac{1}{R^3}\Omega(M_2) = -\frac{\partial p_1}{\partial x} + \frac{1}{R}\frac{\partial p_2}{\partial \theta} - \frac{1}{R}\frac{\partial^2 p_3}{\partial \theta^2}, \tag{17.3}$$

where the operator Ω, called *Vlasov's operator*, is given as follows:

$$\Omega(\ldots) \equiv \frac{\partial^4(\ldots)}{\partial \theta^4} + \frac{\partial^2(\ldots)}{\partial \theta^2}. \tag{17.4}$$

We come now to the derivation of equations for strains and displacements. Taking into account the assumptions of the semi-membrane theory ($\varepsilon_2 = \gamma_{12} = 0$, $\chi_1 = 0$), the kinematic relations (15.5) take the form

$$\varepsilon_1 = \frac{\partial u}{\partial x}, \quad \varepsilon_2 = \frac{1}{R}\frac{\partial v}{\partial \theta} - \frac{w}{R} = 0, \quad \gamma_{12} = \frac{\partial v}{\partial x} + \frac{1}{R}\frac{\partial u}{\partial \theta} = 0, \tag{17.5a}$$

$$\chi_1 = 0, \quad \chi_2 = -\frac{1}{R^2}\left(\frac{\partial v}{\partial \theta} + \frac{\partial^2 w}{\partial \theta^2}\right) \quad \text{and} \quad \chi_{12} = -\frac{1}{R}\left[\frac{\partial v}{\partial x} + \frac{\partial^2 \omega}{\partial x \partial \theta}\right] = 0 \tag{17.5b}$$

The angles of rotations of the normal to the middle surface in the circumferential and meridional directions, ϑ_1 and ϑ_2 respectively, can be obtained from Eqs (12.2) by setting $\alpha = x$, $\beta = \theta$, $A = 1$ and $B = R$. We have

$$\vartheta_1 = \frac{\partial w}{\partial x}, \quad \vartheta_2 = \frac{v}{R} + \frac{1}{R}\frac{\partial w}{\partial \theta}. \tag{17.5c}$$

Using the relations (17.5a) and (17.5b), express the displacements u, w, and curvature χ_2 in terms of the circumferential displacement v. We obtain

$$w = \frac{\partial v}{\partial \theta}; \quad u = -\int_\theta \frac{\partial v}{\partial x} R\,\mathrm{d}\theta; \quad \chi_2 = -\frac{1}{R^2}\left(\frac{\partial v}{\partial \theta} + \frac{\partial^3 v}{\partial \theta^3}\right). \tag{17.6}$$

The constitutive equations (15.6), with regard to the adopted assumptions, can be represented in the form

$$N_1 = Eh\frac{\partial u}{\partial x}; \quad M_2 = D\chi_2 = \frac{Eh^3}{12}\chi_2. \tag{17.7}$$

Let us write the expressions for N_1 and M_2 in terms of the circumferential displacement v. From Eqs. (17.6) it follows that

$$N_1 = -Eh \int_\theta \frac{\partial^2 v}{\partial x^2} R \mathrm{d}\theta, \tag{17.8a}$$

$$M_2 = -\frac{Eh^3}{12R^2}\left(\frac{\partial v}{\partial \theta} + \frac{\partial^3 v}{\partial \theta^3}\right). \tag{17.8b}$$

The remaining stress resultants and couples are not equal to zero, as this seemingly follows from the adopted assumptions, and they can be also expressed in terms of v using the equations of equilibrium (Eqs (17.2) and (15.3)). We have

$$Q_2 = \frac{1}{R}\frac{\partial M_2}{\partial \theta} = -\frac{Eh^3}{12R^3}\left(\frac{\partial^2 v}{\partial \theta^2} + \frac{\partial^4 v}{\partial \theta^4}\right) = -\frac{Eh^3}{12R^2}\Omega(v), \tag{17.9}$$

$$S = -\int_\theta \frac{\partial N_1}{\partial x} R \mathrm{d}\theta - \int_\theta p_1 R \mathrm{d}\theta = Eh \int_\theta \left[\int_\theta \frac{\partial^2 v}{\partial x^2} R^2 \mathrm{d}\theta\right] \mathrm{d}\theta - \int_\theta p_1 R \mathrm{d}\theta, \tag{17.10}$$

$$N_2 = -\frac{1}{R}\frac{\partial^2 M_2}{\partial \theta^2} - p_3 R = \frac{Eh^3}{12R^3}\frac{\partial}{\partial \theta}\left(\frac{\partial^2 v}{\partial \theta^2} + \frac{\partial^4 v}{\partial \theta^4}\right) - p_3 R = \frac{Eh^3}{12R^3}\frac{\partial}{\partial \theta}\Omega(v) - p_3 R. \tag{17.11}$$

Indeterminate functions in θ resulting in integrating over x were dropped because the above functions must be periodical.

Now all the stress resultants and couples, as well as the displacements, have been expressed in terms of the circumferential displacement v. To determine this function, we can apply Eq. (17.3). Substituting for N_1 and M_2 from Eqs (17.8) into Eq. (17.3) and, then, differentiating it with respect to θ, we obtain the following *governing equation of the semi-membrane theory*:

$$Eh\frac{\partial^4 v}{\partial x^4} + \frac{Eh^3}{12R^6}\Omega\Omega(v) = P(x, \theta), \tag{17.12}$$

where

$$P(x, \theta) = \frac{1}{R}\frac{\partial^2 p_1}{\partial x \partial \theta} - \frac{1}{R^2}\frac{\partial^2 p_2}{\partial \theta^2} + \frac{1}{R^2}\frac{\partial^3 p_3}{\partial \theta^3} \tag{17.13}$$

is a function of a given surface loading. Equation (17.12) can be integrated in series; the given loads are expanded into a Fourier series and the function v is sought in the form of a Fourier series also. The constants of integration are evaluated from the boundary conditions on the shell edges.

Having determined the function v, it is possible to calculate all the stress resultants and couples from Eqs (17.8)–(17.11). The displacement components are given by Eqs (17.6). The stress components can be determined by using the relations

$$\sigma_1 = \frac{N_1}{h}, \quad \sigma_2 = \frac{N_2}{h} \pm \frac{6M_2}{h^2}, \quad \tau_{12} = \frac{S}{h}.$$

We can also present the governing differential equation of the semi-membrane theory in terms of the displacement function F, introduced as follows:

$$u = -\frac{\partial F}{\partial x}, \quad v = \frac{1}{R}\frac{\partial F}{\partial \theta}, \quad w = \frac{\partial^2 F}{R\partial\theta^2}. \tag{17.14}$$

Substituting the above into Eqs (17.5a), it is easily shown that the second assumption of the semi-membrane theory ($\varepsilon_2 = \gamma_{12} = 0$) will be automatically satisfied. Then, inserting Eq. (17.14) into Eqs (15.6a) and (15.6e) and using the above-introduced assumptions, leads to the following:

$$N_1 = -Eh\frac{\partial^2 F}{\partial x^2}, \quad M_2 = -\frac{Eh^3}{12R^3}\left(\frac{\partial^2 F}{\partial\theta^2} + \frac{\partial^4 F}{\partial\theta^4}\right). \tag{17.15}$$

Finally, substituting the above into Eq. (17.3), one obtains the following alternative governing equation of the semi-membrane theory of cylindrical shells:

$$B\frac{\partial^4 F}{\partial x^4} + \frac{D}{R^6}\left(\frac{\partial^8 F}{\partial\theta^8} + 2\frac{\partial^6 F}{\partial\theta^6} + \frac{\partial^4 F}{\partial\theta^4}\right) = \frac{\partial p_1}{\partial x} - \frac{1}{R}\frac{\partial p_2}{\partial\theta} + \frac{1}{R}\frac{\partial^2 p_3}{\partial\theta^2}, \tag{17.16}$$

where $B = Eh$ is the shell stiffness in tension; $D = Eh^3/12$ is the flexural shell stiffness ($\nu = 0$ due to the third assumption of the semi-membrane theory).

17.2.2 Analysis of cylindrical shells by the semi-membrane theory

Assume that a surface load is symmetrical about the plane $\theta = 0$. In this case, the load components p_1, p_2, and p_3 may be expended into a Fourier series, as follows:

$$p_1 = p_{10} + \sum_{k=1}^{\infty} p_{1k}\cos k\theta, \quad p_2 = p_{20} + \sum_{k=1}^{\infty} p_{2k}\sin k\theta, \quad p_3 = p_{30} + \sum_{k=1}^{\infty} p_{3k}\cos k\theta. \tag{17.17}$$

Substituting Eq. (17.17) into the expression (17.13), yields the load function $P(x, \theta)$, as follows:

$$P(x,\theta) = \sum_{k=1}^{\infty}\left[-\frac{k}{R}\frac{\mathrm{d}p_{1k}}{\mathrm{d}x} + \frac{k^2}{R^2}p_{2k} + \frac{k^3}{R^2}p_{3k}\right]\sin k\theta \text{ or}$$
$$P(x,\theta) = \sum_{k=1}^{\infty} P_k \sin k\theta, \tag{17.18a}$$

where

$$P_k = -\frac{k}{R}\frac{\mathrm{d}p_{1k}}{\mathrm{d}x} + \frac{k^2}{R^2}p_{2k} + \frac{k^3}{R^2}p_{3k.} \tag{17.18b}$$

The circumferential displacement v is sought in the form of the series

$$v = \sum_{k=1}^{\infty} V_k \sin k\theta, \tag{17.19}$$

where $V_k = V_k(x)$. Substituting for v and P from Eqs (17.18) and (17.19) into Eq. (17.12), yields

$$Eh\sum_{k=1}^{\infty}\left[\frac{\mathrm{d}^4V_k}{\mathrm{d}x^4}+\frac{h^2}{12R^6}V_k k^4(k^2-1)^2\right]\sin k\theta=\sum_{k=1}^{\infty}P_k\sin k\theta. \tag{17.20a}$$

The above results in the following system of ordinary differential equations of the following type:

$$\begin{aligned}
\frac{\mathrm{d}^4V_1}{\mathrm{d}x^4}&=\frac{1}{Eh}P_1,\\
\frac{\mathrm{d}^4V_2}{\mathrm{d}x^4}+\frac{h^2}{12R^6}2^4(2^2-1)^2V_2&=\frac{1}{Eh}P_2,\\
&\cdots\cdots\cdots\cdots\cdots\cdots\cdots\cdots\\
\frac{\mathrm{d}^4V_k}{\mathrm{d}x^4}+\frac{h^2}{12R^6}k^4(k^2-1)^2V_k&=\frac{1}{Eh}P_k,\\
&\cdots\cdots\cdots\cdots\cdots\cdots\cdots\cdots
\end{aligned} \tag{17.20b}$$

The first equation of the above system characterizes a bending deformation of the shell with no distortion of the circumference shape. It can be easily shown that stresses and displacements corresponding to the first equation completely coincide with those obtained by the elementary beam bending theory. The second and subsequent equations of the system (17.20b) represent deformation of the shell associated with a distortion of the shape of its cross section.

Let us consider the kth equation of the system (17.20b). We represent this equation in the form

$$\frac{\mathrm{d}^4V_k}{\mathrm{d}x^4}+4\beta_k^4V_k=\frac{1}{Eh}P_k(x), \tag{17.21}$$

where

$$4\beta_k^4=\frac{h^2k^4(k^2-1)^2}{12R^6}\quad\text{and}\quad\beta_{\mathrm{k}}=\sqrt[4]{\frac{h^2k^4(k^2-1)^2}{48R^6}}. \tag{17.22}$$

Equation (17.21) is analogous to that treated previously for the axisymmetric deformation of a circular cylindrical shell (see Eq. (15.44)). Its integral is of the form

$$V_k=V_{kh}+V_{k\mathrm{p}}, \tag{17.23}$$

where V_{k0} is a solution of the homogeneous equation (17.21) and $V_{k\mathrm{p}}$ represents its particular solution. As discussed in Sec. 15.3, V_{kh} may be represented in the form

$$\begin{aligned}
V_{kh}=&A_{1k}\cosh\beta_kx\sin\beta_kx+A_{2k}\cosh\beta_kx\cos\beta_kx+A_{3k}\sinh\beta_kx\cos\beta_kx\\
&+A_{4k}\sinh\beta_kx\sin\beta_kx.
\end{aligned} \tag{17.24a}$$

The particular solution of the nonhomogeneous equation (17.21) depends upon the type of surface loading. In the case when $\frac{\partial^4}{\partial x^4}P_k(x)=0$, the particular solution is of the form

$$V_{k\mathrm{p}}=\frac{P_k(x)}{4Eh\beta_k^4}. \tag{17.24b}$$

The constants of integration are evaluated from boundary conditions prescribed on the edges of a shell for the total solution (Eq. (17.23)).

For a very long shell that satisfies the following condition

$$\beta_k L \geq 3 \quad \text{or} \quad L \geq 2.5R\sqrt{\frac{R}{h}} \quad (k \geq 2) \tag{17.25}$$

it is advantageous to represent the total solution in the following form, analogous to the expression (15.53):

$$V_k = C_{1k}\mathrm{e}^{-\beta_k x}\sin\beta_k x + C_{2k}\mathrm{e}^{-\beta_k x}\cos\beta_k x + V_{k\mathrm{p}}. \tag{17.26}$$

The constants C_{1k} and C_{2k} are evaluated from boundary conditions prescribed at the shell edge $x = 0$.

Example 17.1

A simply supported thin-walled cylindrical tube with flat ends is filled by water up to the level H, as shown in Fig. 17.2. Determine the deformations and stresses due to the water pressure. Given $L = 40\,\mathrm{m}$, $2R = 3.2\,\mathrm{m}$, and $H = 0.516\,\mathrm{m}$.

Solution

The water pressure on the cylindrical wall of the tube and on its ends is given by the following:

$$\text{for } -\theta_0 \leq \theta \leq \theta_0 \quad p_3 = -\gamma_l R(\cos\theta - \cos\theta_0), \tag{a}$$

$$\text{for } \theta_0 \leq \theta \leq (2\pi - \theta_0) \quad p_3 = 0, \tag{b}$$

where γ_l is the specific weight of water. The negative sign in Eq. (a) is taken because p_3 is assumed to be positive in the inward direction.

The pressure on the bottoms and on the cylindrical surface may be considered independent from one another. Since the ends have a significant stiffness against deformations in their own planes that excludes the possibility of distortion of the shape of the circumference near the tube edge, the pressure on the bottom will cause an eccentric tension of the tube.

Determine the deformation of the tube caused by the water pressure on the cylindrical surface of the tube. Let us expend the pressure into the following series in θ:

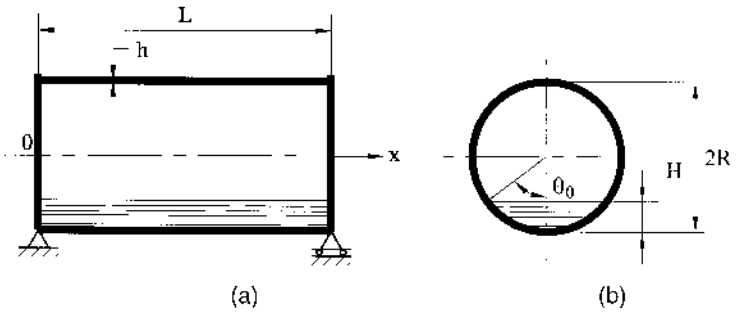

Fig. 17.2

$$p_3 = p_{30} + \sum_{k=1}^{\infty} p_{3k} \cos k\theta. \tag{c}$$

Integrating the right- and left-hand sides of the expression (c) together with (a) from 0 to 2π, one finds p_{30} as follows:

$$-\gamma_l R \int_{-\theta_0}^{\theta_0} (\cos\theta - \cos\theta_0) \mathrm{d}\theta = 2\pi(p_{30}),$$

from which

$$p_{30} = -\frac{\gamma_l R}{\pi}(\sin\theta_0 - \theta_0 \cos\theta_0). \tag{d}$$

To determine the coefficient p_{3k}, we multiply the left- and right-hand sides of the expression (c) by $\cos k\theta$ and integrate from 0 to 2π. We obtain

$$-\gamma_l R \int_{-\theta_0}^{\theta_0} (\cos\theta - \cos\theta_0) \cos k\theta \mathrm{d}\theta = \int_0^{2\pi} p_{3k} \cos^2 k\theta \mathrm{d}\theta,$$

from which

$$p_{3k} = -\frac{2\gamma_l R}{\pi} f_k. \tag{e}$$

where

$$\begin{aligned} f_k &= \frac{\sin[(k+1)\theta_0]}{2(k+1)} + \frac{\sin[(k-1)\theta_0]}{2(k-1)} - \frac{\sin k\theta_0 \cos k\theta_0}{k} \quad \text{for } k \neq 1 \quad \text{and} \\ f_k &= \frac{\theta_0}{2} - \frac{1}{4}\sin\theta_0 \quad \text{for} \quad k = 1. \end{aligned} \tag{f}$$

The component of pressure p_{30}, causing an axisymmetric deformation of the tube, has no significant meaning and it will not be considered in what follows. Determine the function of the surface load, P. According to Eq. (17.18), for $p_1 = p_2 = 0$ and $p_3 = p_{3k}$,

$$P_{\mathrm{k}} = \frac{k^3}{R^2} p_{3k} = -\frac{2\gamma_l k^3}{\pi R} f_k,$$

and one has the following:

$$P = -\sum_{k=1}^{\infty} \frac{2\gamma_l f_k k^3}{\pi R} \sin k\theta. \tag{g}$$

Hence, the kth equation (Eq. (17.20b)) takes the form

$$\frac{d^4 V_k}{dx^4} + 4\beta_k^4 V_k = -\frac{2\gamma_l k^3 f_k}{\pi E h R}, \tag{h}$$

where β_k is given by Eq. (17.22). The solution of this fourth-order differential equation can be obtained in the form of the sum of a complementary solution of the homogeneous equation, and of a particular solution. However, there is a good reason to choose another way for solving Eq. (h). The boundary conditions for this problem are symmetrical, i.e.,

$$v = 0|_{x=0,L} \quad \text{and} \quad N_1 = 0\big|_{x=0,L}. \tag{i}$$

(It is assumed that the shell ends offer no resistance to the displacements that are perpendicular to the end planes. The water pressure is of no concern here; it may be taken into account separately.) Using Eqs (17.8a) and (17.19), we can rewrite the boundary conditions (k) in terms of the function V_k as follows:

$$V = 0_k\big|_{x=0,L} \quad \text{and} \quad \left(\frac{\mathrm{d}^2 V_k}{\mathrm{d}x^2}\right) = 0\Bigg|_{x=0,L}. \tag{j}$$

Due to the symmetry of the boundary conditions, the general solution of the differential equation (h) can be conveniently represented in the form of the following trigonometric series:

$$V_k = \sum_{m=1,3,5,\ldots}^{\infty} A_{km} \sin\frac{m\pi x}{L}. \tag{k}$$

It can be easily shown that V_k in the form of the series (k) satisfies all the boundary conditions (i). Inserting the series (m) into the differential equation (h) results in the equality

$$\sum_{m=1,3,5,\ldots}^{\infty} A_{km}\left(\frac{m\pi}{L}\right)^4 \sin\frac{m\pi x}{L} + 4\beta_k^4 \sum_{m=1,3,5,\ldots}^{\infty} A_{km} \sin\frac{m\pi x}{L} = -\frac{2k^3\gamma_l f_k}{\pi EhR}. \tag{l}$$

To determine the coefficients A_{km}, we multiply both sides of the above equation by $\sin m\pi x/L$ and integrate from 0 to L. As a result, we obtain

$$A_{km} = -\frac{8k^3\gamma_l f_k L^4}{m\pi^2 REh(m^4\pi^4 + 4\beta_k^4 L^4)}. \tag{m}$$

Inserting the above into Eqs (k) and (17.19), yields the following trigonometric series for v:

$$v = -\sum_{k=1,2,\ldots}^{\infty} \sum_{m=1,3,5,\ldots}^{\infty} \frac{8k^3\gamma_l f_k L^4}{m\pi^2 REh(m^4\pi^4 + 4\beta_k^4 L^4)} \sin\frac{m\pi x}{L} \sin k\theta. \tag{n}$$

These series converge very rapidly. Knowing v, we can calculate the remaining displacement components u and w (see Eqs (17.6)) and the stress resultants and couples (see Eqs (17.7)–(17.11)). For $k = 1$, the parameter $\beta_k = 0$ and the corresponding solution will coincide with the elementary solution of the bending theory of a beam.

Let us present the solution of the same problem assuming that the tube is supported by a rigid collar at its midspan, as shown in Fig. 17.3. It is assumed that the collar prevents completely a distortion of the circular cross section of the tube.

In this case, the shell has two segments. Taking the origin of the coordinate system at a middle point of the shell length, one can write the following boundary conditions for function V_k $(k \geq 2)$:

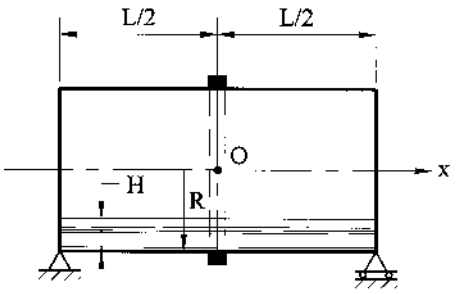

Fig. 17.3

$$u = 0, \quad v = 0, \quad V_k = 0, \quad \left.\frac{dV_k}{dx} = 0\right|_{x=0} \quad \text{and}$$
$$v = 0, \quad N_1 = 0, \quad V_k = 0, \quad \left.\frac{d^2V_k}{dx^2} = 0\right|_{x=L/2}. \tag{o}$$

Since these boundary conditions are asymmetric, the solution should be sought in the form of Eq. (17.23), (17.24) i.e., as the sum of V_{kc} and V_{kp}. Evaluating the constants of integration A_{ik} $(i = 1, 2, 3, 4)$ in the above solution from the boundary conditions (o), we can determine the circumferential displacement v from Eq. (17.19) and then can calculate all the displacement and stress components. Figure 17.4 depicts the diagrams of the meridional normal stresses $\sigma_1$over the middle cross section of the tube:

(a) according to the elementary beam bending theory (Fig. 17.4a);
(b) based on Vlasov's theory, in the absence of the reinforcing collar (Fig. 17.4b); and
(c) based on Vlasov's theory but with the rigid collar at the tube midspan (Fig. 17.4c).

Figure 17.5 shows the diagrams of the meridional normal stresses σ_1 in the lower stretched fiber along the tube length for the above-mentioned three cases.

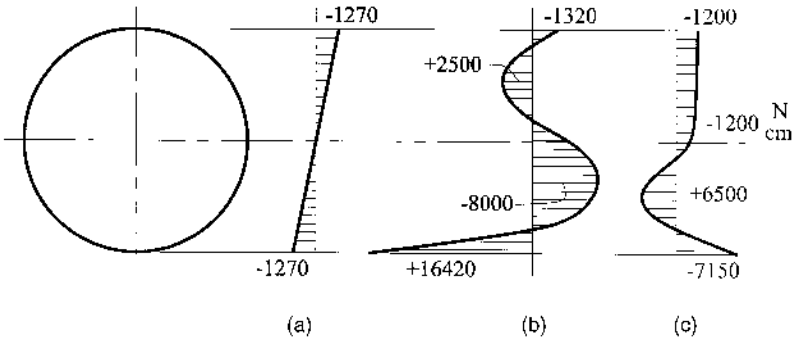

Fig. 17.4

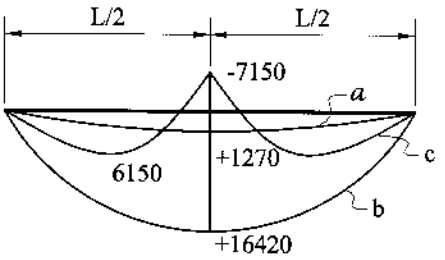

Fig. 17.5

The last two solutions (for Cases b and c) were obtained by retaining four terms in the expansion (m).

Comparing the bending stress diagrams depicted in Figs 17.4 and 17.5, one concludes that:

(a) Stresses in the shell for the given loading differ significantly from those calculated by the elementary beam bending theory.
(b) The bending stresses are noticeably reduced if a rigid collar, preventing a distortion of the tube cross section, is present. The character of the stress distribution is also changed.

This example was taken from Ref. [6].

If a large number of rigid collars were placed over the shell length in such a way that all its cross sections remained circular and undistorted, the deformations and stresses would not be different from those calculated by the beam bending theory. Based on the above, one can conclude that the most efficient way of decreasing stresses in shell structures is to attach rigid collars to the shells. If a shell is loaded by a concentrated force, normal to the shell middle surface, then it is sufficient to set up only one rigid collar at a place of the force application. In this case, the shell will deform as a beam, i.e., without distortion of its cross section.

In conclusion, let us discuss some issues regarding accuracy and area of application of the semi-membrane theory. It was indicated earlier (see Chapter 13) that the accuracy of solutions given by the membrane theory depends on the smoothness of a shell geometry, the smoothness of an applied loading, and on the formulation of boundary conditions. However, for a cylindrical shell, in addition to these requirements, one more requirement is added – namely, a shell length (see Sec. 13.6). It was shown in that section that the accuracy of the membrane solution decreases with an increase in the shell length, even if the other requirements of the existence of the membrane state of stress are satisfied. From a physical point of view, this means that for a long cylindrical shell the boundary conditions have little effect on the stresses and deformations in its middle part and these boundary conditions cannot prevent the appearance of significant bending stresses in this part of the shell (if an external loading is capable of causing the bending stresses).

Thus, the semi-membrane theory holds an intermediate place between the membrane theory and the general theory of thin shells (see Chapter 12). It can be applied to relatively long open and closed cylindrical shells with an arbitrary shape of the cross section if the variation of the displacement and stress components in the direction of the shell generator is smoother than their variation in the circumferential

direction. It follows from the above that a simple criterion for an estimate of the accuracy of solutions of the semi-membrane theory can be established. This criterion lies in the comparison of $\partial^2 f/\partial x^2$ and $\partial^2 f/\partial\theta^2$ (where f is any displacement, strain, internal force, or stress component), according to the inequality (17.1).

It should be noted, however, that for very long shells, subjected to smoothly varying loads along their generator, distortions of the shell cross section can be neglected. Such shells may be treated as thin-walled bars. On other hand, for small values of L/R, the membrane theory is more accurate than the semi-membrane theory because the former theory takes into account the in-plane cross-section deformations ε_2 and γ_{12}. However, for very small values of L/R ($L/R < 3\sqrt{h/R}$) [7], both the theories are inapplicable because, in this case, the deformations vary rapidly in the shell longitudinal direction. Finally, the semi-membrane theory can be recommended for medium-length cylindrical shells ($L/2R = 2 \div 8$)

17.3 THE DONNELL–MUSHTARI–VLASOV THEORY OF THIN SHELLS

This section will continue the discussion about simplified theories of thin shells. We introduce below the Donnell [3], Mushtari [4], and Vlasov [1] theory (abbreviated as the DMV theory). Conceptually, the DMV theory represents a simplified variant of the general linear theory of thin shells. Usually, this theory is based on the following physical assumptions (along with the Kirchhoff–Love hypotheses):

(a) *the effect of the transverse shear forces* Q_1 and Q_2 *in the in-plane equilibrium equations is negligible* (the static assumption);
(b) *the influence of the deflections,* w*, will predominate over the influences of the in-plane displacements* u and v *in the bending response of the shell* (the geometric assumption).

It should be noted that the static and geometric assumptions agree well with each other as predicted by the static–geometric analogy established for thin shells by Gol'denveizer [5]. Further, it was shown by Novozhilov [2] that the above physical assumptions are well justified in the following two cases:

1. *A shell is shallow* (see Sec. 11.8.4).
2. *The state of stress is of such a type that displacements, and hence, stresses, are rapidly varying functions at least in the direction of one of the coordinates* α *and* β. As a result, the derivatives of these functions are significantly greater than the functions themselves – the second derivatives are greater than the first derivatives, etc.

The second case is more general than the first case because it is applied not only to open but also to closed shells, i.e., to essentially non-shallow shells.

A variation of any function $f(s)$ can be characterized by the order of the value

$$\frac{1}{|f(s)|}\left|\frac{\mathrm{d}f(s)}{\mathrm{d}s}\right| \sim \frac{1}{b}, \tag{17.27}$$

where b is a typical linear dimension of the shell and the symbol $\sim$ indicates the identity of the values order. It is assumed that the state of stress and strain of a shell is rapidly varying, say in the α direction, if for any functions $f(\alpha, \beta)$ (displacements, stress resultants, and and couples) the following strong inequality holds [2,5]:

$$\frac{|R|_{\min}}{|f|}\left|\frac{\partial f}{A\partial\alpha}\right| \gg 1. \tag{17.28}$$

Based on the physical assumptions of the DMV theory, the kinematic relations (12.24) and the first two (the in-plane) equilibrium Eqs (12.41) are simplified to the following form:

The kinematic relations

$$\begin{aligned}
\chi_1 &= -\left[\frac{1}{A}\frac{\partial}{\partial\alpha}\left(\frac{1}{A}\frac{\partial w}{\partial\alpha}\right)+\frac{1}{AB^2}\frac{\partial A}{\partial B}\frac{\partial w}{\partial\beta}\right],\\
\chi_2 &= -\left[\frac{1}{B}\frac{\partial}{\partial\beta}\left(\frac{1}{B}\frac{\partial w}{\partial\beta}\right)+\frac{1}{A^2B}\frac{\partial B}{\partial\alpha}\frac{\partial w}{\partial\alpha}\right],\\
\chi_{12} &= -\frac{1}{AB}\left[\frac{\partial^2 w}{\partial\alpha\partial\beta}-\frac{1}{B}\frac{\partial B}{\partial\alpha}\frac{\partial w}{\partial\beta}-\frac{1}{A}\frac{\partial A}{\partial\beta}\frac{\partial w}{\partial\alpha}\right].
\end{aligned} \tag{17.29}$$

(the terms containing the in-plane displacements u and v for the changes in the curvature and twist of the middle surface were dropped in the above equations);

The in-plane equilibrium equations

$$\begin{aligned}
&\frac{\partial}{\partial\alpha}(BN_1)+\frac{\partial}{\partial\beta}(AS)+\frac{\partial A}{\partial\beta}S-\frac{\partial B}{\partial\alpha}N_2+ABp_1=0,\\
&\frac{\partial}{\partial\beta}(AN_2)+\frac{\partial}{\partial\alpha}(BS)+\frac{\partial B}{\partial\alpha}S-\frac{\partial A}{\partial\beta}N_1+ABp_2=0
\end{aligned} \tag{17.30}$$

(the transverse shear forces Q_1 and Q_2 were neglected here, and $N_{12}=N_{21}=S$). The third Eq. (12.41) and Eqs (12.42) remain unchanged. Taking into account the approximate nature of the DMV theory, we also can set $M_{12}=M_{21}=H$. The constitutive equations (12.45) and (12.46) will also remain unchanged.

Vlasov [1] introduced a scalar function of stresses $\Phi(\alpha,\beta)$ as follows:

$$\begin{aligned}
N_1 &= \frac{1}{B}\frac{\partial}{\partial\beta}\left(\frac{1}{B}\frac{\partial\Phi}{\partial\beta}\right)+\frac{1}{A^2B}\frac{\partial B}{\partial\alpha}\frac{\partial\Phi}{\partial\alpha},\\
N_2 &= \frac{1}{A}\frac{\partial}{\partial\alpha}\left(\frac{1}{A}\frac{\partial\Phi}{\partial\alpha}\right)+\frac{1}{AB^2}\frac{\partial A}{\partial\beta}\frac{\partial\Phi}{\partial\beta},\\
S &= -\frac{1}{AB}\left(\frac{\partial^2\Phi}{\partial\alpha\partial\beta}-\frac{1}{B}\frac{\partial B}{\partial\alpha}\frac{\partial\Phi}{\partial\beta}-\frac{1}{A}\frac{\partial A}{\partial\beta}\frac{\partial\Phi}{\partial\alpha}\right).
\end{aligned} \tag{17.31}$$

Substituting for N_1, N_2, and S from Eqs (17.31) into Eqs (17.30), taking into account the Codazzi–Gauss relations (11.27), and setting $p_1=p_2=0$, it can be established that the latter equations will not be satisfied identically. The left-hand sides of these equations do not turn out to equal zero; they are equal to

$$-\frac{\partial\Phi}{A\partial\alpha}\frac{AB}{R_1R_2} \quad \text{and} \quad -\frac{\partial\Phi}{B\partial\beta}\frac{AB}{R_1R_2},$$

respectively. Thus, an exact realization of the homogeneous equations of equilibrium (17.30) is reached only for shells of zero Gaussian curvature. However, these equations are satisfied approximately also in the case when the state of stress is rapidly varying in the direction of the coordinate lines α and β. It can be shown that in this

case, the non-zero terms may be disregarded because of their smallness, even if the Gaussian curvature differs from zero. Therefore, it can be concluded that for a sufficiently rapid variability of the state of stress, the expressions (17.31) satisfy approximately Eqs (17.30) (for $p_1 = p_2 = 0$) for an arbitrary shell geometry with an accuracy comparable to neglecting the first derivatives of Φ compared with its second and third derivatives.

Substituting for Q_1 and Q_2 from Eqs (12.42) into the third Eq. (12.41), and using the relations (12.46) and (17.29), we obtain the following equation:

$$-D\nabla^2\nabla^2 w + \frac{N_1}{R_1} + \frac{N_2}{R_2} + p_3 = 0. \tag{17.32}$$

Finally, substituting for N_1 and N_2 from the first two Eqs (17.31) into the above equation, after some manipulations and taking into account the Codazzi–Gauss relations (11.27), yields the following equation:

$$D\nabla^2\nabla^2 w - \nabla_k^2\Phi = p_3, \tag{17.33a}$$

where

$$\nabla^2(\ldots) \equiv \frac{1}{AB}\left[\frac{\partial}{\partial\alpha}\left(\frac{B}{A}\frac{\partial(\ldots)}{\partial\alpha}\right) + \frac{\partial}{\partial\beta}\left(\frac{A}{B}\frac{\partial(\ldots)}{\partial\beta}\right)\right] \tag{17.34a}$$

is the *Laplace elliptic operator* and,

$$\nabla_k^2(\ldots) = \frac{1}{AB}\left[\frac{\partial}{\partial\alpha}\left(\frac{B}{A}\kappa_2\frac{\partial(\ldots)}{\partial\alpha}\right) + \frac{\partial}{\partial\beta}\left(\frac{A}{B}\kappa_1\frac{\partial(\ldots)}{\partial\beta}\right)\right] \tag{17.34b}$$

is the *Vlasov's operator* [1]; $\kappa_1 = 1/R_1, \kappa_2 = 1/R_2$ are the principal curvatures in the directions of the coordinate lines α and β, respectively.

Equation (17.33a) involves two unknown functions, w and Φ. The second differential equation, connecting the same two functions, can be obtained from the compatibility equations (12.27). The parameters χ_1, χ_2, and χ_{12} are expressed in terms of w and the in-plane components of deformation. The latter components are connected with in-plane forces, and hence, by Hooke's law, with the function Φ. However, the in-plane deformations appear in the first two Eqs (12.27) only as secondary terms of the form ε/R, but the terms of the same order compared with χ (changes in curvature and twist) have been already disregarded. Thus, according to the DMV theory, the compatibility equations (12.27) can be also simplified to the form

$$\begin{aligned}
&\frac{\partial}{\partial\alpha}(B\chi_2) - \frac{\partial B}{\partial\alpha}\chi_1 - \frac{1}{A}\frac{\partial}{\partial\beta}(A^2\chi_{12}) = 0,\\
&\frac{\partial}{\partial\beta}(A\chi_1) - \frac{\partial A}{\partial\beta}\chi_2 - \frac{1}{B}\frac{\partial}{\partial\alpha}(B^2\chi_{12}) = 0,\\
&\frac{1}{AB}\frac{\partial}{\partial\alpha}\left\{\frac{1}{A}\left[-\frac{\partial}{\partial\alpha}(\varepsilon_2 B) + \frac{\partial B}{\partial\alpha}\varepsilon_1 + \frac{1}{2A}\frac{\partial}{\partial\beta}(\gamma_{12}A^2)\right]\right\}\\
&\qquad + \frac{1}{AB}\frac{\partial}{\partial\beta}\left\{\frac{1}{B}\left[-\frac{\partial}{\partial\beta}(\varepsilon_1 A) + \frac{\partial A}{\partial\beta}\varepsilon_2 + \frac{1}{2B}\frac{\partial}{\partial\alpha}(\gamma_{12}B^2)\right]\right\} - \left(\frac{\chi_2}{R_1} + \frac{\chi_1}{R_2}\right) = 0.
\end{aligned} \tag{17.35}$$

It can be shown that the first two equations of the above system are automatically satisfied if we substitute for χ_1, χ_2, and χ_{12} from the kinematic relations (17.29). The third equation of the system (17.35), after substituting for $\varepsilon_1, \varepsilon_2$, and γ_{12} from Eqs (12.45) together with Eqs (17.31), and for χ_1, χ_2, and χ_{12} from Eqs (17.29), and after some transformations with the use of the Codazzi–Gauss relations, takes the form

$$\nabla^2\nabla^2\Phi + Eh\nabla_k^2 w = 0. \tag{17.33b}$$

Thus, the *system of the governing differential equations of the approximate DMV theory* of thin shells have the following form:

$$\begin{aligned} -\nabla_k^2\Phi + D\nabla^2\nabla^2 w &= p_3, \\ \nabla^2\nabla^2\Phi + Eh\nabla_k^2 w &= 0. \end{aligned} \tag{17.36}$$

The first equation of the above system is the equilibrium equation, whereas the second one represents the compatibility equation. For a flat plate, $\kappa_1 = 0$ and $\kappa_2 = 0$, and therefore, $\nabla_k^2(\ldots) = 0$. Hence, for flat plates, the first and second Eqs (17.36) are uncoupled. The second equation, $\nabla^2\nabla^2\Phi = 0$, determines the Airy stress function of the plane stress problem, and the second one, $D\nabla^2\nabla^2 w = p_3$, describes the plate bending problem, as discussed in Part I of the book. The operator ∇_k^2, depending upon the shell curvatures, characterizes in Eqs (17.36) the coupled effect between the bending and membrane stress resultants.

In conclusion, let us briefly discuss a practical application of the DMV theory of thin shells. As mentioned previously, it can be applied to closed or open shells of any geometry if the state of stress is rapidly varying, at least, in one direction. It should be noted that solutions of the membrane shell problem and problem of pure bending are given by slowly varying functions. Therefore, the DMV theory can give a serious error in the stress analysis of such shell problems only if a shell area under consideration is not small compared with the radius $|R|_{\min}$. The DMV theory can be applied successfully to the analysis of thin shells whose state of stress is described by rapidly varying functions as, for instance, in the edge effect state of stress, discussed in detail in Sec. 17.5 for thin shells of any geometry. The DMV theory can also be correctly applied to the stress analysis of the shallow shells introduced in the next section. Lur'e [8] showed that the analysis of not too long $\left(\frac{L}{R} \le 0.75\sqrt{\frac{R}{h}}\right)$ cylindrical shells, based on the DMV theory, gives sufficiently accurate results even for slowly varying loads.

17.4 THEORY OF SHALLOW SHELLS

Shallow shells are frequently used for roof structures of industrial and public buildings. They are also used in mechanical and aerospace engineering applications. The theory of shallow shells can be also used to analyze shells that become locally shallow when the original shell is divided into finite segments or elements (see, for instance, Chapter 19).

Shallow shells were introduced in Sec. 11.8.4. Let us define a shallow shell in a more rigorous manner. Take the Cartesian coordinates x and y of the projections of points of the shell's middle surface on the coordinate plane Oxy as curvilinear

coordinates α and β of that surface, i.e., define the middle surface of the shell by the following equation:

$$z = z(x, y). \tag{17.37}$$

This can be done because of the single-valued correspondence of points of the middle surface and their rectangular projections on the plane Oxy.

A *shell may be called shallow if at any point of its middle surface the inequalities (11.58) hold.*

If we confine our analysis to the accuracy of the theory of thin shells (see inequality (10.1)), i.e., consider a shell as shallow for

$$\left(\frac{\partial z}{\partial x}\right)^2 < 0.05, \left(\frac{\partial z}{\partial y}\right)^2 < 0.05, \tag{17.38}$$

then the angle of 0.224 rad or $\sim 13^\circ$ may be taken as the limiting angle between the tangent plane to the shell's middle surface and the coordinate plane Oxy. Notice that Vlasov [1] defined a shallow shell as a shell whose rise does not exceed 1/5 of the smallest dimension of the shell in its plane (projection on the coordinate plane Oxy). However, it can be shown [2] that this practical limitation of the applicability of the shallow shell theory corresponds to the error noticeably exceeding the above-mentioned error of 5%.

Consider an element of the middle surface $ABCD$ (Fig. 11.15a). Let its projection on the coordinate plane Oxy be the rectangle with sides $\mathrm{d}x$ and $\mathrm{d}y$, as shown in Fig. 11.15a. The sides of the element $ABCD$ are the following:

$$\mathrm{d}s_1 = \sqrt{1 + \left(\frac{\partial z}{\partial x}\right)^2}\,\mathrm{d}x; \quad \mathrm{d}s_2 = \sqrt{1 + \left(\frac{\partial z}{\partial y}\right)^2}\,\mathrm{d}y.$$

However, by virtue of the assumption (17.38), one can use the following approximations:

$$\mathrm{d}s_1 \approx \mathrm{d}x; \quad \mathrm{d}s_2 \approx \mathrm{d}y, \tag{17.39}$$

i.e., one can identify the increments of arcs of the coordinate lines on the shell's middle surface with the increments of the corresponding rectangular coordinates. The cosine of angle between the lines x and y is equal to

$$\cos(\mathrm{d}s_1\hat{}, \mathrm{d}s_2) = \frac{\frac{\partial z}{\partial x}\frac{\partial z}{\partial y}}{\sqrt{1 + \left(\frac{\partial z}{\partial x}\right)^2}\sqrt{1 + \left(\frac{\partial z}{\partial y}\right)^2}}.$$

It follows from the above that for shallow shells, again because of the inequalities (17.38), one can assume that

$$\cos(\mathrm{d}s_1\hat{}, \mathrm{d}s_2) \approx 0, \tag{17.40}$$

i.e., it is possible to consider the curvilinear system x, y as approximately orthogonal. The curvatures of the coordinate lines x and y, κ_1 and κ_2, and "twist," κ_{12}, of the undeformed middle surface at any point of the middle surface of the shallow shell can be identified with the second derivatives of Eq. (17.37), i.e.,

$$\kappa_1 = \frac{1}{R_1} \approx \frac{\partial^2 z}{\partial x^2}, \quad \kappa_2 = \frac{1}{R_2} \approx \frac{\partial^2 z}{\partial y^2}, \quad \kappa_{12} \approx \frac{\partial^2 z}{\partial x \partial y}. \tag{17.41}$$

Taking Eqs (17.39) and (17.40) as exact equalities, we obtain that the following Lamé parameters for a shallow shell of any geometry:

$$A = 1, \quad B = 1, \tag{17.42}$$

i.e., the *intrinsic geometry of a shallow shell is identical to the geometry of a plane of its projection*. This actually represents the *first basic assumption of the theory of shallow shells*. It follows from the above that the shallow shell has the Gaussian curvature $\Gamma = \frac{1}{R_1 R_2} \approx 0$ because the latter is an exact zero only for flat plates. In particular cases the Gaussian curvature of shallow shells is also exactly equal to zero (for instance, if a shallow shell is a cylindrical or conical shell).

As mentioned in Sec. 17.3, the DMV theory can be applied to the analysis of shallow shells. Hence, the next, *second basic assumption of the theory of shallow shells is the basic assumption of the more general DMV theory of neglecting the tangential (membrane) displacements* u and v *in the kinematic expressions for the changes in curvature and twist,* Eqs (12.24) and *the transverse shear forces* Q_1 and Q_2 *in the two first equations of equilibrium (*12.41) (see Sec. 17.3).

The DMV theory, as the general theory of thin shells, was constructed in terms of the lines of curvature as curvilinear coordinate lines. Therefore, from now on, assume that the coordinate lines x and y coincide with the lines of curvature of the shell's middle surface. The error of this assumption is not beyond the limits of the accuracy of the shallow shell theory.

The shallowness of shells makes it possible to make further simplifications to the DMV theory. Making $\alpha = x, \beta = y$, and $A = B = 1$, we obtain the following relations for the strain components (Eqs (12.23)) and changes in curvature (Eqs (12.24)):

$$\begin{aligned} &\varepsilon_1 = \frac{\partial u}{\partial x} - \frac{w}{R_1}, \quad \varepsilon_2 = \frac{\partial v}{\partial y} - \frac{w}{R_2}, \quad \gamma_{12} = \frac{\partial v}{\partial x} + \frac{\partial u}{\partial y}, \\ &\chi_1 = -\frac{\partial^2 w}{\partial x^2}, \quad \chi_2 = -\frac{\partial^2 w}{\partial y^2}, \quad \chi_{12} = -\frac{\partial^2 w}{\partial x \partial y}. \end{aligned} \tag{17.43}$$

The Laplace operator (17.34a) is easily simplified to the form

$$\nabla^2(\ldots) \equiv \frac{\partial^2(\ldots)}{\partial x^2} + \frac{\partial^2(\ldots)}{\partial y^2}. \tag{17.44a}$$

The Codazzi conditions (11.27a) for shallow shells, and taking into account Eqs (17.42), are

$$\frac{\partial}{\partial \beta}\left(\frac{1}{R_1}\right) = 0 \quad \text{and} \quad \frac{\partial}{\partial \alpha}\left(\frac{1}{R_2}\right) = 0.$$

Also, the Vlasov operator ∇_k^2, introduced in Sec. 17.3 (see Eq.(17.34b)), taking into account the above relations, can be simplified to the following form:

$$\nabla_k^2(\ldots) \equiv \frac{1}{R_2}\frac{\partial^2(\ldots)}{\partial x^2} + \frac{1}{R_1}\frac{\partial^2(\ldots)}{\partial y^2} = \kappa_1 \frac{\partial^2(\ldots)}{\partial x^2} + \kappa_2 \frac{\partial^2(\ldots)}{\partial y^2}. \tag{17.44b}$$

Although the operators ∇^2 and ∇_k^2 were notably simplified, the system of governing equations for the theory of shallow shells will be of the same form as the system of equations (17.36) derived in Sec. 17.3 for the general DMV approximate theory of thin shells.

Solving the system of differential equations (17.36), gives Φ and w. Having determined the above functions, we can then determine the internal forces and moments using Eqs (17.31), (17.29) and (12.46). Let us present below all these equations for shallow shells, as follows:

$$N_1 = \frac{\partial^2 \Phi}{\partial y^2}, \quad N_2 = \frac{\partial^2 \Phi}{\partial x^2}, \quad S = -\frac{\partial^2 \Phi}{\partial x \partial y}, \tag{17.45a}$$

$$M_1 = -D\left(\frac{\partial^2 w}{\partial x^2} + \nu \frac{\partial^2 w}{\partial y^2}\right), \quad M_2 = -D\left(\frac{\partial^2 w}{\partial y^2} + \nu \frac{\partial^2 w}{\partial x^2}\right),$$

$$H = -(1-\nu)\frac{\partial^2 w}{\partial x \partial y}, \tag{17.45b}$$

$$Q_1 = -D\frac{\partial}{\partial x}(\nabla^2 w), \quad Q_2 = -D\frac{\partial}{\partial y}(\nabla^2 w).$$

The solution of Eqs (17.36) must satisfy the boundary conditions prescribed on the shell edges. We present below some typical boundary conditions for a shallow shell of an arbitrary geometry whose boundaries form a rectangular plane. For the sake of simplicity, assume that the shell edges coincide with the x- and y-coordinate lines and these lines are the lines of curvature. As mentioned previously, Eqs (17.36) have the eighth order, so the four boundary conditions must be prescribed on each edge of the shell (by two conditions on each of the functions Φ and w). Let us consider the boundary conditions for the shell edge $x =$ const. Note that the boundary conditions, depending on the shell deflections, have the same form as that for flat plates (see Eqs (2.48)). Therefore, we introduce below some typical boundary conditions imposed on the function Φ (or on the in-plane displacements in the directions of the x and y axes, u and v). We have (for example, for the shell edge $x =$ const.)

(a) Points of the shell edge can freely displace in the direction of the x axis. This means that

$$N_1 = 0 \quad \text{or} \quad \frac{\partial^2 \Phi}{\partial y^2} = 0. \tag{17.46a}$$

(b) Points of the shell edge can freely displace in the direction of the y axis. Then, we have

$$\tau_{12} = 0 \quad \text{or} \quad \frac{\partial^2 \Phi}{\partial x \partial y} = 0. \tag{17.46b}$$

(c) No displacements of the shell edge are allowed in the x direction, i.e.,

$$u = 0. \tag{17.47a}$$

(d) No displacements of the shell edge are allowed in the y direction, i.e.,

$$v = 0. \tag{17.47b}$$

In solving real design problems, various combinations of these boundary conditions can be met. For example, for a clamped shell edge that is parallel to the y axis, the boundary conditions are given by

$$u = v = w = \frac{\partial w}{\partial x} = 0. \tag{17.48}$$

If a shell edge rests on a diaphragm that is absolutely rigid in its own plane and flexible out of the plane, the boundary conditions have the form

$$\frac{\partial^2 \Phi}{\partial y^2} = 0, \quad v = w = \frac{\partial^2 w}{\partial x^2} = 0. \tag{17.49a}$$

If a shell edge can displace freely along this diaphragm, then we have

$$\frac{\partial^2 \Phi}{\partial y^2} = \frac{\partial^2 \Phi}{\partial x \partial y} = 0, \quad w = \frac{\partial^2 w}{\partial x^2} = 0. \tag{17.49b}$$

Similarly, the boundary conditions can be presented for the shell edge $y = \text{const}$.

For the analysis of shallow shells it is necessary to solve the system of equations (17.36), satisfying the above boundary conditions for the functions w and Φ. For a solution of these equations, some analytical and numerical methods, introduced in Chapter 6, may be applied. One of the most adapted analytical methods for solving this system of linear differential equations for a shallow shell with constant curvatures whose edges form a rectangular plane is the Fourier method of double series, which is similar to the Navier method discussed in Sec. 3.3 for bending of rectangular plates. Variational methods are frequently used for analyses of shallow shells. In order to apply the variational methods introduced in Chapter 6, let us set up the expression for the strain energy of shallow shells. Substituting for N_1, N_2, and S from Eqs (17.45a) and for M_1, M_2, and H from Eqs (17.45b) into Eq. (12.52) and setting $A = B = 1$, we obtain the following expression for the strain energy of shallow shells:

$$U = \frac{1}{2Eh} \int\int_A \left\{ \left(\frac{\partial^2 \Phi}{\partial x^2} + \frac{\partial^2 \Phi}{\partial y^2} \right)^2 - 2(1+\nu) \left[\frac{\partial^2 \Phi}{\partial x^2} \frac{\partial^2 \Phi}{\partial y^2} - \left(\frac{\partial^2 \Phi}{\partial x \partial y} \right)^2 \right] \right\} dA$$
$$+ \int\int_A \frac{D}{2} \left\{ \left(\frac{\partial^2 w}{\partial x^2} + \frac{\partial^2 w}{\partial y^2} \right)^2 - 2(1-\nu) \left[\frac{\partial^2 w}{\partial x^2} \frac{\partial^2 w}{\partial y 2} - \left(\frac{\partial^2 w}{\partial x \partial y} \right)^2 \right] \right\} dA, \tag{17.50}$$

where A is the area of the middle surface of the shallow shell.

Writing the corresponding expressions for work done by external loads, W_e, and the total potential energy, Π, we can apply the Ritz method (see Sec. 6.6) for solving various problems of shallow shell analysis.

Example 17.2

A shallow, rectangular in a plane, shell of sides a and b, is subjected to a normal uniform surface load $p_0 = \text{const}$ directed downward. The middle surface of the shell has the form of an elliptic paraboloid:

$$z = f\left[\frac{f_1}{f}\left(2\frac{x}{a}-1\right)^2+\frac{f_2}{f}\left(2\frac{y}{b}-1\right)^2-1\right], \tag{a}$$

where $f = f_1 + f_2$ is the rise of the shell (Fig. 17.6). The shell rests on the diaphragms along its edges. These diaphragms are absolutely rigid in their planes and flexible out of the planes. Determine the deflections, internal forces, and moments.

Solution

Determine the principal curvatures of the shell. It follows from Eqs (17.41) that we have

$$\kappa_1 = 8\frac{f_1}{a^2}, \kappa_2 = 8\frac{f_2}{b^2}, \quad \kappa_{12} = 0. \tag{a}$$

Substituting the above into the expressions (17.44), we can write the system of equations (17.36), as follows (making $p_3 = p_0$):

$$\begin{aligned} &D\nabla^2\nabla^2 w - 8\frac{f_1}{a^2}\frac{\partial^2\Phi}{\partial y^2} - 8\frac{f_2}{b^2}\frac{\partial^2\Phi}{\partial x^2} = p_0, \\ &\frac{1}{Eh}\nabla^2\nabla^2\Phi + 8\frac{f_1}{a^2}\frac{\partial^2 w}{\partial y^2} + 8\frac{f_2}{b^2}\frac{\partial^2 w}{\partial x^2} = 0. \end{aligned} \tag{b}$$

The boundary conditions on the shell edges have a form of Eqs (17.49a). Taking into account the expressions (17.45), these boundary conditions can be represented, as follows:

$$w = 0\big|_{x=0,a}; \quad \frac{\partial^2 w}{\partial x^2} = 0\Big|_{x=0,a}; \quad \frac{\partial^2\Phi}{\partial y^2} = 0\Big|_{x=0,a}; \quad v = 0\big|_{x=0.a}; \tag{c}$$

$$w = 0\big|_{y=0,b}; \quad \frac{\partial^2 w}{\partial y^2} = 0\Big|_{y=0,b}; \quad \frac{\partial^2\Phi}{\partial x^2} = 0\Big|_{y=0,b}; \quad u = 0\big|_{y=0,b}. \tag{d}$$

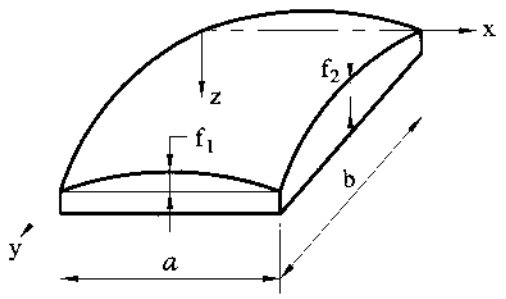

Fig. 17.6

A solution of Eqs (b) is sought in the following form of the Fourier series in two variables:

$$w = \sum_{m=1}^{\infty}\sum_{n=1}^{\infty} w_{mn} \sin\frac{m\pi x}{a}\sin\frac{n\pi y}{b}, \tag{e}$$

$$\Phi = \sum_{m=1}^{\infty}\sum_{n=1}^{\infty} \varphi_{mn} \sin\frac{m\pi x}{a}\sin\frac{n\pi y}{b}. \tag{f}$$

It can be shown that the expressions (e) and (f) satisfy exactly the three first conditions in (c) and (d). Let us check the fulfillment of the fourth conditions. Find the strain, as follows:

$$\varepsilon_2 = \frac{1}{Eh}(N_2 - \nu N_1) = \frac{1}{Eh}\left(\frac{\partial^2\Phi}{\partial x^2} - \nu\frac{\partial^2\Phi}{\partial y^2}\right).$$

Substituting for Φ from Eq. (f) into the above, results in the following:

$$\varepsilon_2 = -\frac{1}{Eh}\sum_{m=1}^{\infty}\sum_{n=1}^{\infty}\varphi_{mn}\left(\frac{m^2\pi^2}{a^2} - \nu\frac{n^2\pi^2}{b^2}\right)\sin\frac{m\pi x}{a}\sin\frac{n\pi y}{b}.$$

It is evident, that $\varepsilon_2 = 0$ for $x = 0$ and $x = a$. Taking into account the second relation (17.43), we can conclude that v is a constant along the shell edges $x = 0$ and $x = a$. So, we can put it equal to zero. Similarly, it is possible to show that the displacement $u = 0$ along edges $y = 0$ and $y = b$.

Next, represent the given load p_0 in the form of the Fourier series too, as follows:

$$p(x, y) = \sum_{m=1}^{\infty}\sum_{n=1}^{\infty} p_{mn}\sin\frac{m\pi x}{a}\sin\frac{n\pi y}{b},$$

where

$$p_{mn} = \frac{4}{ab}\int_0^a\int_0^b p(x, y)\sin\frac{m\pi x}{a}\sin\frac{n\pi y}{b}\mathrm{d}x\mathrm{d}y.$$

Since

$$p(x, y) = p_0 = \text{const}, \text{ then } p_{mn} = \frac{16p_0}{\pi^2 mn}; \quad m, n = 1, 3, 5, \ldots. \tag{g}$$

Inserting the expressions (e), (f), and (g) into Eqs (b), we obtain the following system of linear algebraic equations:

$$\frac{1}{Eh}\left(\frac{m^2\pi^2}{a^2} + \frac{n^2\pi^2}{b^2}\right)^2\varphi_{mn} - \frac{8\pi^2}{a^2b^2}(n^2f_1 + m^2f_2)w_{mn} = 0,$$

$$\frac{8\pi^2}{a^2b^2}(n^2f_1 + m^2f_2)\varphi_{mn} + D\left(\frac{m^2\pi^2}{a^2} + \frac{n^2\pi^2}{b^2}\right)^2 w_{mn} = p_{mn}. \tag{h}$$

Solving this system for unknown functions φ_{mn} and w_{mn}, gives

$$w_{mn} = \left[\frac{\pi^4 n^4 h^4}{12(1-\nu^2)b^4} A_{mn} + \frac{64 f^2 h^2}{A_{mn} a^4}\left(\frac{f_1}{f} + \frac{m^2}{n^2}\frac{f_2}{f}\right)^2\right]^{-1} \frac{p_{mn} h}{E},$$
$$\varphi_{mn} = \frac{8Eb^2 fh}{\pi^2 A_{mn} a^2 n^2}\left(\frac{f_1}{f} + \frac{m^2 f_2}{n^2 f}\right) w_{mn}, \tag{i}$$

where

$$A_{mn} = \left(\frac{m^2 b^2}{n^2 a^2} + 1\right)^2; \quad m, n = 1, 3, 5, \ldots. \tag{j}$$

Having determined the functions w and Φ, the internal forces and moments may be found from Eqs (17.45). We have the following:

$$M_1 = D \sum_{m=1,3,\ldots}^{\infty} \sum_{n=1,3,\ldots}^{\infty} w_{mn}\left(\frac{m^2\pi^2}{a^2} + \nu\frac{n^2\pi^2}{b^2}\right) \sin\frac{m\pi x}{a} \sin\frac{n\pi y}{b},$$
$$M_2 = D \sum_{m=1,3,\ldots}^{\infty} \sum_{n=1,3,\ldots}^{\infty} w_{mn}\left(\frac{n^2\pi^2}{b^2} + \nu\frac{m^2\pi^2}{a^2}\right) \sin\frac{m\pi x}{a} \sin\frac{n\pi y}{b},$$
$$H = -D(1-\nu) \sum_{m=1,3,\ldots}^{\infty} \sum_{n=1,3,\ldots}^{\infty} w_{mn} \frac{mn\pi^2}{ab} \cos\frac{m\pi x}{a} \cos\frac{n\pi y}{b},$$
$$N_1 = -\sum_{m=1,3,\ldots}^{\infty} \sum_{n=1,3,\ldots}^{\infty} \varphi_{mn} \frac{n^2\pi^2}{b^2} \sin\frac{m\pi x}{a} \sin\frac{n\pi y}{b}, \tag{k}$$
$$N_2 = -\sum_{m=1,3,\ldots}^{\infty} \sum_{n=1,3,\ldots}^{\infty} \varphi_{mn} \frac{m^2\pi^2}{a^2} \sin\frac{m\pi x}{a} \sin\frac{n\pi y}{b},$$
$$S = -\sum_{m=1,3,\ldots}^{\infty} \sum_{n=1,3,\ldots}^{\infty} \varphi_{mn} \frac{mn\pi^2}{ab} \cos\frac{m\pi x}{a} \cos\frac{n\pi y}{b}.$$

Setting in the relations (i) $f_1 = f_2 = 0$, we obtain the expressions for w_{mn}, which are valid for a rectangular simply supported plate, i.e.,

$$w_{mn} = \frac{p_{mn}}{D}\left(\frac{m^2\pi^2}{a^2} + \frac{n^2\pi^2}{b^2}\right)^2. \tag{l}$$

Some numerical values of the deflections, internal forces and moments were calculated with the use of Eqs (k) for the given shallow shell. The values of dimensionless coefficients $\bar{w}$, $\bar{M}$, $\bar{N}$ are given in Table 17.1 at the central point of the square shallow shell ($a = b$) for various dimensionless parameters $\lambda = f/h$ (λ characterizes the shallowness of a shell). The values of the deflections, internal forces, and moments are determined from the following relations:

$$w = \bar{w}\frac{p_0 a^4}{D10^4}; \quad N_1 = N_2 = -\bar{N}\frac{p_0 a^2}{h10^2}; \quad M_1 = M_2 = \bar{M}\frac{p_0 a^2}{10^2}. \tag{m}$$

Table 17.1

Parameter λ	Values of the dimensionless coefficients at the central point of the shell				
	Shallow shell			Plate (λ = 0)	
	$\bar{w}$	$\bar{N}$	$\bar{M}$	$\bar{w}$	$\bar{M}$
0.5	36.2101	4.2401	3.7985	39.4215	4.250
1.0	27.2112	6.3618	2.7911	39.4215	4.250
1.5	19.200	6.7200	1.9396	39.4215	4.250
2.0	13.4115	6.2501	1.1988	39.4215	4.250
3.0	7.0851	4.9501	0.5066	39.4215	4.250
4.0	4.1200	3.8102	0.2106	39.4215	4.250
5.0	2.6100	3.0115	0.07086	39.4215	4.250
6.0	1.7511	2.4510	0.01398	39.4215	4.250
10.0	0.5601	1.3102	−0.02180	39.4215	4.250
20.0	0.1364	0.6201	−0.00021	39.4215	4.250

The given numerical data for the shallow shell are compared in the table with the values of the deflections and bending moments in a rectangular simply supported plate having the same linear dimensions (a and b) as the shallow shell and subjected to the same load p_0. It follows from Table 17.1 that with an increase in the parameter λ, the load-carrying mechanism of the shallow shell changes: its stiffness increases and bending moments are diminished, i.e., for large values of λ the shallow shell supports a given normal surface load p_3 practically due to the membrane action only. Of course, this qualitative conclusion is valid not only for the considered shell but also for all of the classes of shallow shells. Comparison of the ordinates of bending moments (and deflections) in shallow shells and flat plates shows that the above-mentioned values are significantly greater (by one order) in flat plates than in shallow shells for certain values of the parameter $\lambda = f/h$ ($f = f_1 + f_2$).

To analyze the load-carrying mechanism of shallow shells subjected to a normal surface load, Fig. 17.7 illustrates some numerical results of the analysis of the shallow shell with the following geometrical and mechanical characteristics: $a = b = 10\,\text{m}$, $h = 0.1\,\text{m}$, $f_1 = f_2 = 0.5\,\text{m}$, $E = 40\,\text{GPa}$, $\nu = 0.17$, and $p_3 = p_0 = \text{const}$. For this shell $D = \frac{Eh^3}{12(1-\nu^2)} = 3.4326 \times 10^6\ \text{N} \cdot \text{m}$.

Figure 17.7 shows the diagrams of the deflection, w, membrane force, N_1, and bending moment, M_1, along the central section ($x = a/2$) of the shell. It should be noted that the location of the maximum deflection in the shallow shell shifts from the center (as it was in a flat plate) towards the supports. The bending moment distributions in the shell, both qualitatively and quantitatively, differ from those in flat plates. The numerical results in Fig. 17.7 and in Table 17.1 were obtained by retaining the six terms in the series (e), and eight and 10 terms in the series (k) for the deflections, membrane forces, and bending moments, respectively. In conclusion, let us make some comments.

1. When a shallow shell rise, f, increases, the shell geometry will differ noticeably from plane geometry, i.e., the first basic assumption of the shallow shell theory

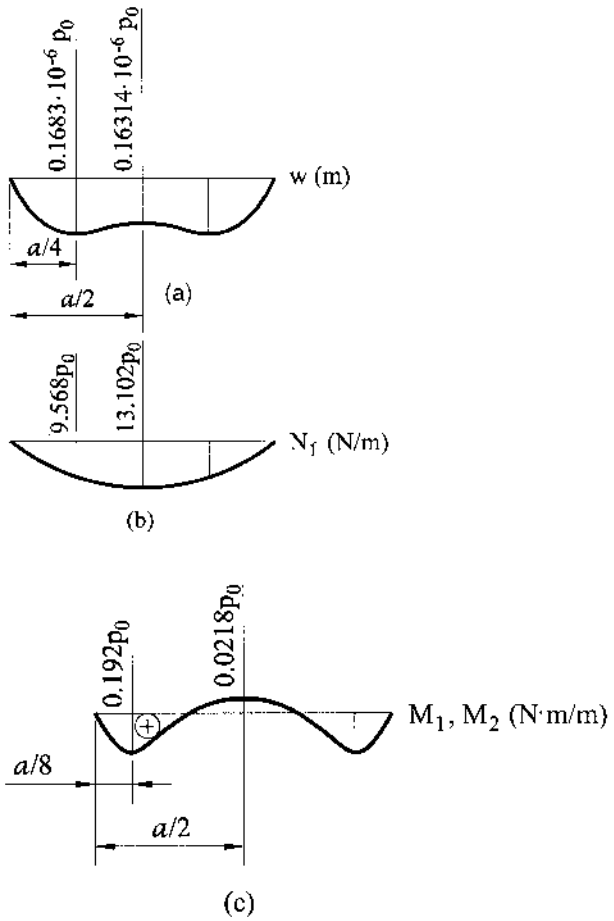

Fig. 17.7

will become more and more rough. The second basic assumption (the basic assumption of the DMV theory) remains still to be justified up to some value of $f = f^*$. The latter is determined by peculiarities of the shell geometry and loading. Therefore, for $f > f^*$ there is a good reason to analyze such shells by applying the more general DMV theory.

2. As mentioned previously, a shallow shell is an open shell that differs little from a plane. However, in some exceptional cases, non-shallow shells and closed shells can also be analyzed by the shallow shell theory. Such a case may be when a non–shallow shell is divided into parts some of which can be approximated by shallow shells. The most important such cases are (a) a non-shallow shell reinforced by equally spaced stiffeners for which any shell part between the stiffeners can be treated as a shallow shell and (b) buckling of shells of any geometry when this buckling is accompanied by a large number of bulgings whose dimensions are small compared with the minimum radius of the shell curvature (see Chapter 19).

17.5 THE THEORY OF EDGE EFFECT

In this section we introduce one more approximate theory of thin shells. As mentioned in Sec. 17.3, a thin shell can be found in the basic state of stress that is characterized by slowly varying deformations and stresses. The membrane (see Chapters 13 and 14) and pure bending stress states fall into the category of the basic state of stress. The pure bending state rarely occurs. It is possible for nonrigid shells only whose constraints allow such a type of bending. In some cases, the state of stress in thin shells can be separated into the following two components: the basic (mainly, membrane) for the entire shell and the mixed, mostly, a moment state, called *edge effect*, localizing near shell boundaries or near other sites at which the membrane theory does not apply. The latter state of stress can be superimposed on the basic state that essentially simplifies the obtaining of the general state of stress in a shell. It was indicated in Chapters 13–16 that the membrane solution alone for some shell geometries, loadings, and supports cannot satisfy the prescribed boundary conditions at the shell edges, the known conditions of continuity, equilibrium and/or kinematic constraints at the edge effect zones. Gol'denveizer termed the sources of edge effects "*lines of distortion*." To facilitate their identification, Gol'denveizer listed these as [5]:

(a) the physical edges of a shell;
(b) lines along which discontinuities of the components of external loads or of certain their derivatives occur;
(c) lines along which the middle surface of a shell has a break or the curvature of the middle surface changes abruptly; and
(d) lines along which the rigidity of a shell or its thickness undergoes sudden changes.

The edge effect can be defined as such a state of stress and strain at which stresses and displacements vary slightly along the lines of distortion, but decay rapidly in the normal direction to those lines.

The edge effect concept was demonstrated in Chapters 15 and 16 for axisymmetrically loaded circular cylindrical shells and shells of revolution, respectively. This section is concerned with constructing the general theory of the edge effect for shells of any geometry subjected to asymmetric loading.

In deriving the governing differential equations of the theory of edge effect, we make the following assumptions:

1. The lines of distortion coincide with one of the lines of curvature (for definiteness sake, with the β-coordinate line).

   Let us introduce the so-called *asymptotic line* as a line along which the normal curvature of the surface, $1/R_i$, is zero. For example, a generator of a cylindrical surface can be considered as an asymptotic line. In the theory of edge effect, it is assumed that the lines of distortion at any point of the middle surface do not touch the asymptotic line. In this case, the edge effect always takes place and it is called *simple edge effect*. If the distortion line touches an asymptotic line, then such an edge effect is referred to as a *complex* one. In this section we analyze only the simple edge effect.
2. The normal component of displacement, w, in zones of the edge effect is significantly greater than the in-plane components, u and v.

3. Functions f that characterize the state of stress and strain (displacements, internal forces, and moments) vary significantly more rapidly in the direction of the α-coordinate line than in the direction of the β-coordinate line, i.e.,

$$\left|\frac{\partial f}{A\partial\alpha}\right| \gg \left|\frac{\partial f}{B\partial\beta}\right|. \tag{17.51}$$

(4) The Lamé parameters, A and B, as well as the radii of curvature, have a small variation in the direction of the α-coordinate line, i.e.,

$$\begin{aligned} &\frac{\partial A}{\partial\alpha} \ll A; \quad \frac{\partial B}{\partial\alpha} \ll B, \\ &\frac{\partial R_1}{\partial\alpha} \ll R_1; \quad \frac{\partial R_2}{\partial\alpha} \ll R_2. \end{aligned} \tag{17.52}$$

A rapid decay of the edge effect state of stress, as we move away along the normal to the line of distortion is a very important characteristic of a shell. It is caused by the shell thinness and by the curvilinearity of its surface. Let us explain this phenomenon in more detail in the following simple example.

Figure 17.8 shows a flat cantilever plate and an open circular cylindrical shell loaded by uniformly distributed bending moments, $m = \text{const}$, applied to the free edges of the plate and shell.

It is evident, that the cantilever plate will resist the external moment load by means of bending only (producing the bending and twisting moments, and shear forces); no membrane forces occur in its middle surface (Fig. 17.8a). The cantilever shell will support the applied distributed moments m not only by means of the bending but also by straining the middle surface. The latter is accompanied by an appearance of the circumferential membrane forces N_2 in the longitudinal sections of the shell $\varphi = \text{const}$, i.e., in the sections perpendicular to the edge $x = a$ (Fig. 17.8b). The larger the shell curvature $1/R$, the stiffer is the shell in its middle surface and the greater is the role of the membrane forces N_2 in resisting the applied bending load. The availability of the circumferential forces N_2 will cause the internal bending moment to decrease rapidly as we move away from the loaded edge in the normal direction to the edge. This phenomenon is quite understandable if we recall the

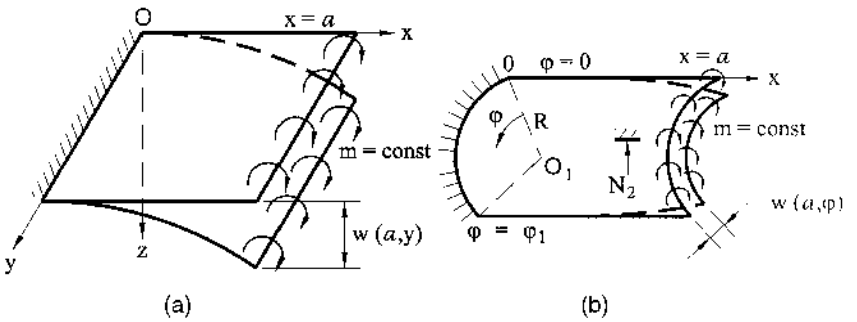

Fig. 17.8

analogy between a shell and a flat plate resting on an elastic Winkler-type foundation. The normal projections of the circumferential forces N_2 are interpreted as the reactions of the Winkler-type foundation (see Fig. 15.2 and the corresponding explanations in Sec. 15.3). Thus, the cylindrical shell shown in Fig. 17.8b acts as a flat cantilever plate resting on some elastic foundation. It is well known that stresses and displacements in such a flat cantilever plate, loaded by the distributed moments m applied along its free edge, decay rapidly as we move away from this loaded edge due to the distributed character of the elastic foundation.

For a more complete insight into the physical nature of the edge effect phenomenon, it is instructive to turn our attention to the general principles of mechanics: in particular, to the principle of minimum potential energy (see Sec. 2.6.2). It is easy to verify that the potential energy caused by bending moments is considerably larger than the potential energy due to the membrane forces. Hence, if we move away from a loaded zone that causes bending (for example, from a fixed shell edge) then, based on the principle of minimum potential energy, the process of the moment and shear force damping should begin. This a reason for the occurrence of rapidly decaying state of stress-edge effects.

Another situation occurs near the straight edges and other lines of disturbance of the state of stress and strain of a shell (the asymptotic lines). Assume, for example, that the edge $\varphi = 0$ is fixed and the other edges are free to displace. If the external moment m is applied to the edge $\varphi = \varphi_1$ then the circumferential forces N_2 are not needed for equilibrium. Therefore, the bending moments decrease slightly as we move away from the line of disturbance (in this case $\varphi = \varphi_1$) and a given state of stress cannot be separated into the membrane type and edge effect. Thus, near straight edges of open cylindrical shells, the simple edge effect concept cannot be applicable. The possibilities of simplifying the governing differential equations are more restricted here than in the case of the simple edge effect.

Now we derive the governing differential equation of the simple edge effect assuming the β-coordinate line is the distortion line. Due to the adopted assumptions (see assumptions 3 and 4), the Laplace operator, $\nabla^2 f$, and the operator $\nabla_k^2 f$ can be simplified to the form

$$\nabla^2 f \approx \frac{\partial}{A\partial\alpha}\left(\frac{\partial f}{A\partial\alpha}\right); \quad \nabla_k^2 f \approx \frac{1}{R_2}\frac{\partial}{A\partial\alpha}\left(\frac{\partial f}{A\partial\alpha}\right). \tag{17.53}$$

Since all functions describing the state of stress and strain in the zone of the simple edge effect represent some rapidly varying functions, we can use the differential equations of the DMV theory introduced in Sec. 17.3. These equations will be homogeneous for the edge effect problems. Taking into account the relations (17.53), the differential equations (17.36) for the edge effect analysis can be written in the following form:

$$\begin{aligned} &D\frac{\partial}{A\partial\alpha}\frac{\partial}{A\partial\alpha}\frac{\partial}{A\partial\alpha}\frac{\partial w}{A\partial\alpha} - \frac{1}{R_2}\frac{\partial}{A\partial\alpha}\frac{\partial\Phi}{A\partial\alpha} = 0, \\ &\frac{1}{Eh}\frac{\partial}{A\partial\alpha}\frac{\partial}{A\partial\alpha}\frac{\partial}{A\partial\alpha}\frac{\partial\Phi}{A\partial\alpha} + \frac{1}{R_2}\frac{\partial}{A\partial\alpha}\frac{\partial w}{A\partial\alpha} = 0. \end{aligned} \tag{17.54}$$

As mentioned previously, only the rapidly varying functions are of interest in the theory of the edge effect. Therefore, in integrating Eqs (17.54), arbitrary functions that depend linearly upon α should be dropped (these functions characterize the

displacements and stresses that vary slowly and they are taken into account by the membrane and pure moment solutions). Integrating twice the second equation of the system (17.54) and discarding the arbitrary functions, one finds the following:

$$\frac{\partial}{A\partial\alpha}\frac{\partial\Phi}{A\partial\alpha} = -\frac{Eh}{R_2}w. \tag{17.55}$$

Substituting the above into the first Eq. (17.54) and putting $A\mathrm{d}\alpha = \mathrm{d}s_1$, we bring this equation to the form

$$\frac{\partial^4 w}{\partial s_1^4} + \frac{12(1-\nu^2)}{R_2^2 h^2}w = 0. \tag{17.56}$$

This is the governing homogeneous differential equation of the simple edge effect. It differs from the corresponding equation of the axisymmetric edge effect in a circular cylindrical shell (see Eq. (15.43)) by the fact that the partial derivatives of w enter in this equation, because w is a function of two variables (this function varies slowly along the curvilinear coordinate β too).

A solution of Eq. (17.56), which decays, as we move away from the edge $\alpha = 0$, is of the following form:

$$w = e^{-\lambda s_1}[f_1(s_2)\cos\lambda s_1 + f_2(s_2)\cos\lambda s_1], \tag{17.57}$$

where f_1 and f_2 are some slowly varying functions, $B\mathrm{d}\beta = \mathrm{d}s_2$, and

$$\lambda = \sqrt[4]{3(1-\nu^2)}\frac{1}{\sqrt{R_2 h}}. \tag{17.58}$$

The internal forces and moments, which occur in the edge effect state, can be determined next. Using Eqs (17.29) and neglecting, due to the assumptions of the edge effect theory, the variation of the shell geometry in the zone of the simple edge effect, and also assuming that

$$\frac{\partial w}{\partial s_2} \ll \frac{\partial w}{\partial s_1},$$

one finds that

$$\chi_1 \approx -\frac{\partial^2 w}{\partial s_1^2}; \quad \chi_2 \approx 0; \quad \chi_{12} \approx 0.$$

Then, inserting the above into Eqs (12.46), we obtain

$$M_1 = -D\frac{\partial^2 w}{\partial s_1^2}; \quad M_2 = \nu M_1; \quad H = 0. \tag{17.59}$$

The stress function Φ can be determined by integrating twice the first Eq. (17.54). We have

$$\Phi = R_2 D\frac{\partial^2 w}{\partial s_1^2}. \tag{17.60}$$

The membrane forces N_1, N_2, and S are related to the function Φ by Eqs (17.31), which due to the adopted assumptions of the edge effect theory, result in the expressions

$$N_1 \approx 0; \quad N_2 \approx \frac{\partial^2\Phi}{\partial s_1^2} = R_2 D\frac{\partial^4 w}{\partial s_1^4} = -\frac{Eh}{R_2}w; \quad S \approx 0. \tag{17.61}$$

The transverse shear forces may be found from the corresponding equilibrium equations of the DMV theory, i.e.,

$$Q_1 = -D\frac{\partial}{A\partial\alpha}(\nabla^2 w); \quad Q_2 = -D\frac{\partial}{B\partial\beta}(\nabla^2 w).$$

Using the relations (17.53), the above relations appear, as follows:

$$Q_1 = -D\frac{\partial^3 w}{\partial s_1^3}; \quad Q_2 \approx 0. \tag{17.62}$$

The above relations and equations of the general edge effect theory were introduced for the case when the distortion line coincides with the β-coordinate line. Similarly, the corresponding equations can be presented for the α-coordinate line as a distortion line and, generally, for the case when the shell edge does not coincide with the line of curvature [5].

In conclusion, one notes the following:

1. The edge effect theory introduced above cannot be applied to the case when the shell boundary or another distortion line coincides with the asymptotic line.
2. If a considered state of stress and strain varies rapidly not only in the direction of the normal to the shell boundary but also along the boundary itself, the stress analysis of such a shell can be carried out by the DMV theory introduced in Sec. 17.3.
3. The governing differential equation of the edge effect, Eq. (17.56), is only approximate. The exact solution of the shell problems by the edge effect theory requires an integration of the system of the partial differential equations of the general theory of thin shells and therefore has no advantages from separation of a given state of stress into the membrane state and edge effect. Thus, the latter is taken into account only approximately.
4. The solution (17.57) makes it possible to satisfy the two boundary conditions on the corresponding shell edge. It is evident that these boundary conditions must be formulated for the sum of the membrane solution and the solution given by Eq. (17.56).

PROBLEMS

17.1 Verify Eqs (17.12) and (17.16).

17.2 Specify the area of application of the semi-membrane theory to the analysis of open and closed cylindrical shells.

17.3 A simply supported, at $x = 0$ and $x = L$, cylindrical tube is filled by water up to the level H (Fig. 17.2). The tube is reinforced by two equally spaced, rigid along the tube length, collars in such a way that they prevent a distortion of the tube cross sections. Applying the semi-membrane theory, determine the axial normal stress, σ_1, distribution over the shell cross section where the collar is attached to the tube. Let $L = 30\,\text{m}$, $R = 5.5\,\text{m}$, $h = 5.0\,\text{cm}$, $H = 1.2\,\text{m}$, $E = 210\,\text{GPa}$, and $\nu = 0.3$.

17.4 A simply supported, at $x = 0$ and $x = L$, closed circular cylindrical shell is subjected to a uniform vertical line load q, as shown in Fig. P.17.1. Determine the axial normal stress, σ_1, distribution in the lower stretched fiber along the shell length. Compare this

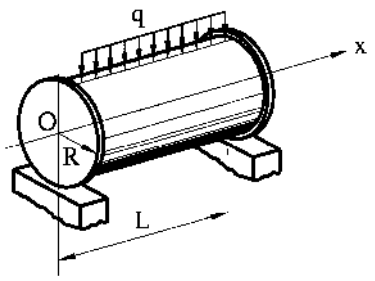

Fig. P.17.1

stress with that obtained by the elementary beam bending theory. Take $L = 15.0\,\text{m}$, $R = 2.0\,\text{m}$, $h = 1.5\,\text{cm}$, $E = 200\,\text{GPa}$, and $\nu = 0.3$.

17.5 Derive Eqs (17.36).

17.6 Substitute for N_1, N_2, and S from Eqs (17.31) into Eqs (17.30). Setting $p_1 = p_2 = 0$ and taking into account the Codazzi–Gauss relations (11.27), specify the accuracy of satisfying Eqs (17.30) in the framework of the assumptions of the DMV theory.

17.7 Show that the system of the governing equations (17.36) can be reduced to a single, eight-order differential equation, as follows:

$$a\nabla_k^2\nabla_k^2\Psi + \nabla^2\nabla^2\nabla^2\nabla^2\Psi = \frac{p_3}{D} \tag{P17.1}$$

where Ψ is some solving function introduced, as follows:

$$w = \nabla^2\nabla^2\Psi, \quad \Phi = -Eh\nabla_k^2\Psi \tag{P.17.2}$$

and

$$a = 12(1-\nu^2)/h^2. \tag{P.17.3}$$

17.8 Show that for a spherical shallow shell ($R_1 = R_2 = R$), the system of equations (17.36) can be broken down into the following equations:

$$\text{(a)} \quad D\nabla^2\nabla^2 w^* + \frac{Eh}{R^2}w = p_3 \tag{P.17.3a}$$

$$\text{(b)} \quad \nabla^2 w_0 = 0 \tag{P.17.3b}$$

$$\text{(c)} \quad \nabla^2\Phi = \frac{Eh}{R}w^* \tag{P.17.3c}$$

where

$$\nabla^2\Phi + \frac{Eh}{R}w = \frac{Eh}{R}w_0 \quad \text{and} \quad w = w_0 + w^* \tag{P.17.3d}$$

Hint: use the spherical coordinates φ and θ.

17.9 Give a physical interpretation of Eqs (P.17.3) of the previous problem.

17.10 Verify Eq. (17.50).

17.11 Consider a shallow shell in polar coordinates $\alpha = r$ and β, where r is the polar radius and β is the polar angle of a point of the middle surface on the horizontal plane. For this case, the Lamé parameters are $A = 1$ and $B = r$. Show that the shallow shell in this coordinate system is governed by the same equations (17.36) and the differential operators (17.34) are given by

$$\nabla^2(\ldots) \equiv \frac{1}{r}\left[\frac{\partial}{\partial r}\left(r\frac{\partial(\ldots)}{\partial r}\right)+\frac{1}{r}\frac{\partial^2(\ldots)}{\partial\beta^2}\right],$$
$$\nabla_k^2(\ldots) \equiv \frac{1}{r}\left[\frac{\partial}{\partial r}\left(rk_2\frac{\partial(\ldots)}{\partial r}\right)+\frac{\partial}{\partial\beta}\left(\frac{k_1}{r}\frac{\partial(\ldots)}{\partial\beta}\right)\right]. \tag{P.17.4}$$

17.12 Show that the membrane forces N_1, N_2, and S in the shallow shell theory are expressed in terms of the displacements, as follows:

$$N_1 = B\left[\frac{\partial u}{\partial x}+\nu\frac{\partial v}{\partial y}-(\kappa_1+\upsilon\kappa_2)w\right], \quad N_2 = B\left[\frac{\partial v}{\partial y}+\nu\frac{\partial u}{\partial x}-(\kappa_1+\nu\kappa_2)w\right],$$
$$S = \frac{B(1-\nu)}{2}\left(\frac{\partial v}{\partial x}+\frac{\partial u}{\partial y}\right) \tag{P.17.5}$$

where

$$B = \frac{Eh}{1-\nu^2}.$$

17.13 Using the equations of equilibrium (12.44), Eqs (17.45b), (P.17.5), and the relations (17.42), show that the governing equations of the shallow shell of double curvature in Cartesian coordinates are of the following form:

$$\frac{\partial^2 u}{\partial x^2}+\frac{1-\nu}{2}\frac{\partial^2 u}{\partial y^2}+\frac{1+\nu}{2}\frac{\partial^2 v}{\partial x\partial y}-(\kappa_1+\nu\kappa_2)\frac{\partial w}{\partial x} = -\frac{p_1}{B},$$
$$\frac{1-\nu}{2}\frac{\partial^2 u}{\partial x\partial y}+\left(\frac{\partial^2}{\partial y^2}+\frac{1-\nu}{2}\frac{\partial^2}{\partial x^2}\right)v-(\kappa_2+\nu\kappa_1)w = -\frac{p_2}{B}, \tag{P.17.6}$$
$$\frac{\partial u}{\partial x}(\kappa_1+\nu\kappa_2)+\frac{\partial v}{\partial y}(\kappa_2+\nu\kappa_1)-(\kappa_1^2+\kappa_2^2+2\nu\kappa_1\kappa_2)w-\frac{h^2}{12}\nabla^2\nabla^2 w = -\frac{p_3}{B}.$$

17.14 The governing equations (17.36) for the shallow shell theory were derived assuming that $p_1 = p_2 = 0$, and $p_3 \neq 0$. Show that if all the load components are nonzero, the relations (17.45a) should be replaced with

$$N_1 = \frac{\partial^2\Phi}{\partial y^2}-\int p_1 \mathrm{d}x, \quad N_2 = \frac{\partial^2\Phi}{\partial x^2}-\int p_2 \mathrm{d}y, \quad S = -\frac{\partial^2\Phi}{\partial x\partial y}, \tag{P.17.7}$$

and Eqs. (17.36) for this case appear as follows:

$$-\nabla_k^2\Phi + D\nabla^2\nabla^2 w = p_3-\kappa_1\int p_1\mathrm{d}x-\kappa_2\int p_2\mathrm{d}y,$$
$$\nabla^2\nabla^2\Phi + Eh\nabla_k^2 w = \int\frac{\partial^2 p_1}{\partial y^2}\mathrm{d}x+\int\frac{\partial^2 p_2}{\partial x^2}\mathrm{d}y-\nu\left(\frac{\partial p_1}{\partial x}+\frac{\partial p_2}{\partial y}\right). \tag{P.17.8}$$

17.15 Consider a square in a plan shallow shell of double curvature. Let the equation of its middle surface be given by (the origin of the Cartesian coordinate system is taken at the center of the projection of the shell on the horizontal plane)

$$z = f\left(1-\frac{x^2+y^2}{2a^2}\right),$$

where $f = f_1 + f_2$ is the total rise. The shell edges, $x = \pm a$ and $y = \pm a$, have the same supports as described in Example 17.1. The shell is subjected to a uniformly distributed load p. Determine the deflection w, the membrane forces N_1, N_2, and S, the bending moments M_1 and M_2, and the twisting moment H. Take four terms ($m = 1$, $n = 1$; m

$= 1$, $n = 3$; $m = 3$, $n = 1$; $m = 3$, $n = 3$) in the expansions (e) and (f) in Example 17.1. Let $a = 2.0\,\text{m}$, $h = 20\,\text{mm}$, $f_1 = f_2 = 250\,\text{mm}$, $p = 2\,\text{kPa}$, $G = 30\,\text{GPa}$, and $\upsilon = 0$.

17.16 A shallow shell of double curvature, shown in Fig. 17.6, is supported by diaphragms at its edges (the boundary conditions are given by Eqs (c) and (d) in Example 17.1). The shell is subjected to a uniformly distributed load of intensity p. Determine the deflections, in-plane forces, and bending moments in the shell. Take four terms in the expansions (e) and (f) (see problem 17.15). Take $a = 10\,\text{m}$, $b = 12\,\text{m}$, $\kappa_1 = 0.04/l, \text{m}$, $\kappa_2 = 0.02781/\text{m}$, $h = 30\,\text{mm}$, $E = 22\,\text{GPa}$, and $\upsilon = 0$.

17.17 Show that if deflection w is a rapidly varying function, at least in one of the coordinate directions, then the following estimate takes place:

$$\frac{|\nabla^2 w|}{\left|\frac{w}{R_1 R_2}\right|} \sim C^2$$

where $C \gg 1$.

17.18 Based on the results of Problem 17.7, derive Eqs (17.62).

17.19 Specify the area of application of the edge effect theory for open and closed cylindrical shells loaded asymmetrically.

REFERENCES

1. Vlasov, V.Z., *General Theory of Shells and its Applications in Engineering*, NASA Technical Translation TTF-99, Washington DC, 1964.
2. Novozhilov, V.V., *Thin Shell Theory* (translated from 2nd Russian edn. by P.G. Lowe), Noordhoff, Groningen, The Netherlands, 1964.
3. Donnell, L.H., *Stability of Thin Walled Tubes under Torsion*, NACA, Report No. 479, Washington, DC, 1933.
4. Mushtari, Kh.M., Certain generalizations of the theory of thin shells, *Izv Fiz Mat ob-va pri Kaz Un-te*, vol. 11, No. 8 (1938) (in Russian).
5. Gol'denveizer, A.L, *Theory of Elastic Shells* (translated from Russian by G. Herrmann), Pergamon Press, New York, 1961.
6. Boyarshinov, S.V., *The Fundamentals of Structural Mechanics of Machines*, Mashinostroenie, Moscow, 1973 (in Russian).
7. Biderman, V. L., *Mechanics of Thin-Walled Structures*, Izdatel'stvo "Mashinostroenie", Moscow, 1977 (in Russian).
8. Lur'e, A.L., General theory of elastic shells, *Prikl Mat Mekh*, vol. 4, No. 1, pp. 7–34 (1940) (in Russian).

18

Advanced Topics

18.1 THERMAL STRESSES IN THIN SHELLS

18.1.1 General

This section is concerned with the influence of high temperature on the state of stress and strain in thin shells. This issue has been studied in Sec. 7.1, as applied to thin plates. It should be noted that the thermal stresses and deformations in thin shells are a major factor in the design of structures such as boilers, heat exchangers, pressure vessels, nuclear piping, and supersonic aircraft skin. The basic concepts of the thermoelastic stress analysis of thin shells are quite similar to those introduced in Sec. 7.1 for thin plates. Similarly, the thermoelastic problems require modifying the constitutive equations of the general shell theory.

Let a shell be subjected to a nonuniform temperature field $T(\alpha, \beta, z)$ measured from some specified reference value. The temperature distribution T can be obtained from a solution of the equation of heat conduction [1], represented in terms of the shell coordinates. Taking into account the relations (7.1), we can modify the constitutive equations (12.28) by taking into account the temperature effects, as follows:

$$\varepsilon_1^z = \frac{1}{E}(\sigma_1^z - \nu\sigma_2^z) + \alpha T; \quad \varepsilon_2^z = \frac{1}{E}(\sigma_2^z - \nu\sigma_1^z) + \alpha T; \quad \gamma_{12}^z = \frac{1}{G}\tau_{12}^z, \tag{18.1}$$

where α is the coefficient of thermal expansion (see Sec. 7.1). It is assumed that E, ν, and d are constant for a given temperature field. Solving Eqs (18.1) for the stress components yields

$$\sigma_1^z = \frac{E}{1-\nu^2}[\varepsilon_1^z + \nu\varepsilon_2^z - (1+\nu)\alpha T]; \quad \sigma_2^z = \frac{E}{1-\nu^2}[\varepsilon_2^z + \nu\varepsilon_1^z - (1+\nu)\alpha T];$$

$$\tau_{12}^z = G\gamma_{12}^z.$$

Substituting Eqs (18.2) into Eqs (12.35) and (12.36) with the use of the relations (12.22), and integrating over z from $-h/2$ to $h/2$, one obtains

$$N_1 = B(\varepsilon_1 + \nu\varepsilon_2) - \frac{N_T}{1-\nu}; \quad N_2 = B(\varepsilon_2 + \nu\varepsilon_1) - \frac{N_T}{1-\nu};$$

$$N_{12} = N_{21} = S = B\frac{1-\nu}{2}\gamma_{12}; \tag{18.3}$$

$$M_1 = D(\kappa_1 + \nu\kappa_2) - \frac{M_T}{1-\nu}; \quad M_2 = D(\kappa_2 + \nu\kappa_1) - \frac{M_T}{1-\nu};$$

$$M_{12} = M_{21} = H = D(1-\nu)\kappa_{12}, \tag{18.4}$$

where

$$B = Eh/(1-\nu^2) \tag{18.5}$$

is the shell stiffness in tension and N_T and M_T are the thermal stress resultants, as given by Eqs (7.8). The equations of static equilibrium, Eqs (12.41) and (12.42), and kinematic equations, Eqs (12.23) and (12.24), of the general shell theory remain unchanged. Thus, a set of thermoelastic governing differential equations within the framework of the Kirchhoff–Love postulates consists of Eqs (12.23), (12.24), (12.41), (12.42), and (18.3)–(18.5). As mentioned in Chapter 12, these equations in some cases must be complemented with the equations of compatibility. The solutions of the above equations must satisfy the prescribed boundary conditions on shell edges.

As for thin plates, the thermal stresses in a shell can occur in the following cases: in a nonuniform heating; if thermal deformations are restricted by imposed constraints; in heating of multilayered shells composed of heterogeneous materials, etc. However, not any nonuniform heating causes the thermal stresses. For instance, if the temperature varies linearly over the length of a cylindrical shell and is constant over its circumference and thickness, then the shell's middle surface becomes a conical surface, but no stresses occur.

The isothermal analogy, introduced in Sec. 7.1 for the thermoelastic plate bending problems, can be applied also for solving the thermoelastic governing shell equations together with appropriate boundary conditions. According to this analogy, the thermoelastic terms entering on the right-hand side of the governing equations may be treated as some fictitious and known surface loading. In the next sections, the thermoelastic shell equations will be applied for stress analysis of some particular shell forms and loadings.

18.1.2 Circular cylindrical shells under axisymmetric nonuniform heating

Assume that the heating of a circular cylindrical shell is axisymmetric and varies linearly across its thickness according to the following law:

$$T = T_0 + \Delta T\frac{z}{h}, \tag{18.6}$$

where $T_0 = (T_1 + T_2)/2$ is an average temperature of the shell wall; $\Delta T = T_1 - T_2$ is a temperature change; and T_1 and T_2 are the temperatures of the lower and upper surfaces of the shell, respectively.

Derivation of the governing differential equation of the thermoelastic axisymmetric shell analysis is analogous to the derivation described in Sec. 15.3 for the static analysis. A distinction lies in the fact that constitutive equations of this problem must be complemented with thermal terms, as indicated in Sec. 18.1.1. Taking into account Eqs (12.22) and (15.38), we can rewrite the constitutive equations (18.2) in terms of the displacement components, as follows:

$$\sigma_1^z = \frac{E}{1-\nu^2}\left[\frac{\mathrm{d}u}{\mathrm{d}x} - z\frac{\mathrm{d}^2 w}{\mathrm{d}x^2} - \nu\frac{w}{R} - (1+\nu)\alpha T\right],$$
$$\sigma_2^z = \frac{E}{1-\nu^2}\left[-\frac{w}{R} + \nu\left(\frac{\mathrm{d}u}{\mathrm{d}x} - z\frac{\mathrm{d}^2 w}{\mathrm{d}x^2}\right) - (1+\nu)\alpha T\right]. \tag{18.7}$$

Then, using Eqs (12.35) and (12.36), and Eqs (15.38), we can rewrite the constitutive equations (Eqs (18.3)–(18.5)) in terms of the displacement components:

$$N_1 = B\left[\frac{\mathrm{d}u}{\mathrm{d}x} - \nu\frac{w}{R} - (1+\nu)\alpha T_0\right]; \tag{18.8a}$$

$$N_2 = B\left[\nu\frac{\mathrm{d}u}{\mathrm{d}x} - \frac{w}{R} - (1+\nu)\alpha T_0\right] = \nu N_1 - w\frac{Eh}{R} - Eh\alpha T_0; \tag{18.8b}$$

$$M_1 = -D\left[\frac{\mathrm{d}^2 w}{\mathrm{d}x^2} + (1+\nu)\alpha\frac{\Delta T}{h}\right]; \quad M_2 = -D\left[\nu\frac{\mathrm{d}^2 w}{\mathrm{d}x^2} + (1+\nu)\alpha\frac{\Delta T}{h}\right]. \tag{18.9}$$

Accordingly, the expressions of the shear force, Eq. (15.46), and the governing differential equation (15.44) are

$$Q_1 = \frac{\mathrm{d}M_1}{\mathrm{d}x} = -D\left[\frac{\mathrm{d}^3 w}{\mathrm{d}x^3} + (1+\nu)\frac{\alpha}{h}\frac{\mathrm{d}(\Delta T)}{\mathrm{d}x}\right], \tag{18.10}$$

$$\frac{\mathrm{d}^4 w}{\mathrm{d}x^4} + 4\beta^4 w = \frac{p_3}{D} + \frac{\nu N_1}{DR} - \frac{(1+\nu)\alpha}{h}\frac{\mathrm{d}^2(\Delta T)}{\mathrm{d}x^2} - \frac{Eh}{DR}\alpha T_0, \tag{18.11}$$

where β is given by Eq. (15.45). A solution of Eq. (18.11) is given by the expression (15.53) for long shells and by (15.74) for short shells. The particular solution, w_p, depends upon an assigned thermal field and given loading. If the thermal field and loading are such that

$$\frac{\mathrm{d}^4 T_0}{\mathrm{d}x^4} = 0, \quad \frac{\mathrm{d}^2(\Delta T)}{\mathrm{d}x^2} = 0,$$
$$\frac{\mathrm{d}^4 p_3}{\mathrm{d}x^4} = 0, \quad \frac{\mathrm{d}^4 N_1}{\mathrm{d}x^4} = 0,$$

then the particular solution is of the following type:

$$w_\mathrm{p} = \frac{R^2}{Eh}\left(p_3 + \nu\frac{N_1}{R}\right) - \alpha R T_0. \tag{18.12}$$

The technique of integrating Eq. (18.11) is not different from that discussed in Sec. 15.3.

As mentioned previously, the thermal terms on the right-hand side of Eq. (18.11) can be interpreted as some fictitious surface load, q_T. So, we can rewrite Eq. (18.11), as follows:

$$\frac{d^4w}{dx^4} + 4\beta^4 w = \frac{1}{D}\left(p_3 - q_T + \frac{\nu N_1}{R}\right), \tag{18.13}$$

where

$$q_T = \frac{D(1+\nu)\alpha}{h}\frac{d^2(\Delta T)}{dx^2} + \frac{Eh}{R}\alpha T_0. \tag{18.14}$$

Using the principle of superposition, the given thermoelastic problem for a circular cylindrical shell can be broken down into two independent problems. The first problem involves only thermal effects produced by q_T. In this case, only the particular solution is of interest (all constants of integration are assumed to be zero). The second problem deals with external forces, p_3 and N_1. Its solution was presented in Sec. 15.3. The constants of integration are evaluated in such a way that the sum of the solutions of these two problems satisfies the prescribed boundary conditions.

Example 18.1

An infinitely long circular cylindrical shell is heated according to Eq. (18.6). The temperature is a constant along the shell length. Determine the thermal stresses.

Solution

A given thermal field can be represented as a superposition of a uniform heating $T_0 = (T_1 + T_2)/2$, which produces no stresses, and of the thermal change $\Delta T = T_1 - T_2$ (Fig. 18.1).

Let us consider the state of stress corresponding to the thermal jump mentioned above. Since the temperature does not vary along the shell length, then all values are constant over the length, and, hence, a general solution of the thermal homogeneous equation is nonexistent. The particular solution (Eq. (18.12)) for $p_3 = 0$, $N_1 = 0$, and $T_0 = 0$ is also zero. Thus, the deflections of points of the middle surface w and the circumferential force N_2, according to Eq. (18.8b), are also equal

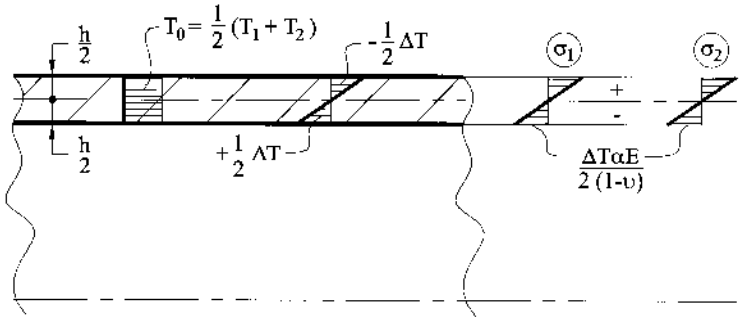

Fig. 18.1

to zero. However, the bending moments in this case are not equal to zero; it follows from Eqs. (18.9) that they are

$$M_1 = M_2 = -(1+\nu)\frac{\alpha D}{h}\Delta T. \tag{18.15}$$

A special feature of this thermal problem is that, in spite of the presence of the bending moments, the curvature of the middle surface does not change. It can be explained as follows: change in curvature caused by a nonuniform heating is compensated by a curvature change produced by the bending moments given by Eq. (18.15). The values of the bending stresses at the upper and lower points of the shell surfaces are found to be the following:

$$\sigma_{1\max} = \mp\frac{6M_1}{h^2} = \pm\frac{\alpha E}{2(1-\nu)}\Delta T; \quad \sigma_{2\max} = \mp\frac{6M_2}{h^2} = \pm\frac{\alpha E}{2(1-\nu)}\Delta T.$$

The bending stress diagrams across the shell thickness are shown in Fig. 18.1. They also illustrate the above statement about the lack of a change in curvature for the given thermal field.

Example 18.2

A cylindrical stepped shell is shown in Fig. 18.2a. The shell is heated over its lower surface up to the temperature $T_1 = 120^\circ\text{C}$ and over the upper surface to the temperature $T_2 = 50^\circ\text{C}$. The temperatures are constant over the shell length. Given $R = 0.5\,\text{m}$, $h_1 = 2 \times 10^{-2}\,\text{m}$, $h_2 = 1 \times 10^{-2}\,\text{m}$, the shell material is a structural steel with $\nu = 0.3$, $E = 200\,\text{GPa}$, and $\alpha = 12 \times 10^{-6}/^\circ C$. Determine the thermal stresses. Assume that the shell is sufficiently long.

Solution

The given thermal field can again be broken down into a uniform heating $T_0 = (T_1 + T_2)/2 = 85^\circ\text{C}$ and temperature jump $\Delta T = T_1 - T_2 = 70^\circ\text{C}$. Since the uniform heating produces no thermal stresses, it will not be taken into further account. Assume that the given shell is cut into two parts: the first of constant thickness h_1 and the second of constant thickness h_2. If they were really separated then they would be subjected to the thermal jump ΔT and, consequently, were additionally loaded by

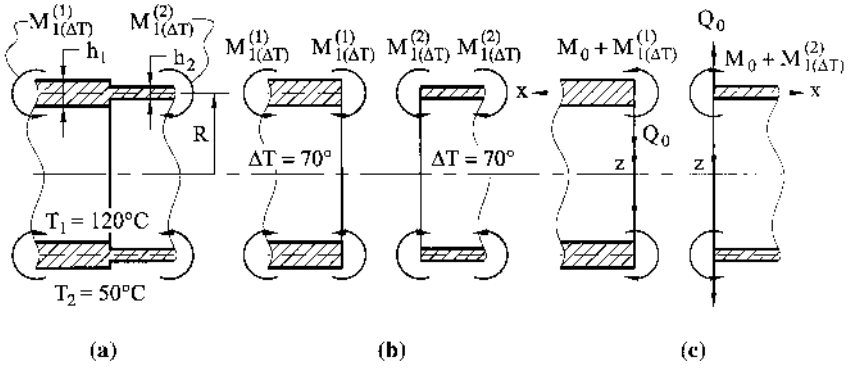

Fig. 18.2

the bending moments at shell edges, as shown in Fig. 18.2b. These moments can be calculated from Eqs. (18.15):

– for the first part of the shell ($h = h_1$),

$$M^{(1)}_{1(\Delta T)} = -\alpha \Delta T(1+\nu)\frac{D_1}{h_1} = -\frac{\alpha \Delta T E h_1^2}{12(1-\nu)} = -8000 \text{ N} \cdot \text{m/m};$$

– for the second part of the shell ($h = h_2$),

$$M^{(2)}_{1(\Delta T)} = -\alpha \Delta T(1+\nu)\frac{D_2}{h_2} = -\frac{\alpha \Delta T E h_2^2}{12(1-\nu)} = -2000 \text{ N} \cdot \text{m/m}.$$

At a state shown in Fig. 18.2c, the shell is loaded by the interface moments, M_0 and shear forces, Q_0 at the junction of the two shell parts only, where M_0 and Q_0 are the interface bending moment and shear force that actually act at the junction of the stepped shell and $M^{(1)}_{1(\Delta T)}$ and $M^{(2)}_{1(\Delta T)}$ have been added to compensate the moments applied to the shell in the state shown in Fig. 18.2b. To determine the interface moment M_0 and shear force Q_0, it is sufficient to consider only the state shown in Fig. 18.2c and set up the conditions of compatibility for deformations at the junction of the two shell parts. The latter are of the following form:

$$w^{(1)} = w^{(2)}; \quad \vartheta_1^{(1)} = -\vartheta_1^{(2)}; \tag{a}$$

i.e., the deflections and slopes of the normals for the two shell parts at the junction should be the same. The negative sign in Eq. (a) is taken because the direction of the x axis for the first and second parts of the shell is opposite. The deflections, $w^{(1)}$ and $w^{(2)}$, and slopes, $\vartheta_1^{(1)}$ and $\vartheta_1^{(2)}$, may be determined from Eqs (15.57). For the first (left) shell part, setting $x = 0$ and $w_p = 0$, we obtain

$$w^{(1)} = -\frac{M_0 + M^{(1)}_{1(\Delta T)}}{2D_1\beta_1^2} + \frac{Q_0}{2D_1\beta_1^3}; \quad \vartheta_1^{(1)} = \frac{M_0 + M^{(1)}_{1(\Delta T)}}{D_1\beta_1} - \frac{Q_0}{2D_1\beta_1^2}. \tag{b}$$

Similarly, for the second shell part, again setting $x = 0$ and $w_p = 0$, we have the following:

$$w^{(2)} = -\frac{M_0 + M^{(2)}_{1(\Delta T)}}{2D_2\beta_2^2} - \frac{Q_0}{2D_2\beta_2^3}; \quad \vartheta_1^{(2)} = \frac{M_0 + M^{(2)}_{1(\Delta T)}}{D_2\beta_2} + \frac{Q_0}{2D_2\beta_2^2}. \tag{c}$$

Computing the geometric properties of the stepped shell, we have

$$D_1 = \frac{Eh_1^3}{12(1-\nu^2)} = 146.8 \text{ kN} \cdot \text{m}; \quad D_2 = \frac{Eh_2^3}{12(1-\nu^2)} = 18.33 \text{ kN} \cdot \text{m}$$

$$\text{or} \quad D_2 = \frac{D_1}{8};$$

$$\beta_1 = \sqrt[4]{\frac{3(1-\nu^2}{R^2h_1^2}} = 12.85 \ \frac{1}{\text{m}}; \quad \beta_2 = \sqrt[4]{\frac{3(1-\nu^2)}{R^2h_2^2}} = 18.13 \ \frac{1}{\text{m}} = \beta_1\sqrt{2};$$

$$M^{(1)}_{1(\Delta T)} = 8000 \text{N} \cdot \text{m/m}; \quad M^{(2)}_{1(\Delta T)} = 2000 \text{N} \cdot \text{m/m} = \frac{1}{4}M^{(1)}_{1(\Delta T)}.$$

Substituting Eqs (b) and (c) into the compatibility equations (a), we obtain the following system of two equations:

$$3M_0 + 0.298Q_0 = 0 \quad \text{and} \quad 10^{-3}(3.539M_0 + 0.0623Q_0) = -10.258.$$

Solving these equations for M_0 and Q_0, yields

$$M_0 = -3523 \text{ N} \cdot \text{m/m}; \quad Q_0 = 35480 \text{ N/m}.$$

Having determined M_0 and Q_0, we can calculate the deflections, internal forces, and bending moments from Eqs (15.57). Summing them with the corresponding values of the state shown in Fig. 18.2b, we obtain the final expressions of the thermoelastic deflections and stress resultants and couples for the given problem (Fig. 18.2a). The most stressed point is located at the outside surface of the thinner part of the shell, near the stepped transition. The internal forces, bending moments, and normal stresses in this place are

$$M_1 = -3523 \text{ N} \cdot \text{m/m}; \quad M_2 = -2460 \text{ N} \cdot \text{m/m}; \quad N_1 = 0;$$

$$N_2 = 142656 \text{ N/m}; \quad w = 0.413 \times 10^{-3} \text{ m} = 0.413 \text{ mm};$$

$$\sigma_1 = \frac{6M_1}{h_2^2} = 211.4 \text{ MPa}; \quad \sigma_2 = \frac{N_2}{h_2} + \frac{6M_2}{h_2^2} = 161.9 \text{ MPa}.$$

As we move away from the stepped transition, the bending moments, $M_{1(\Delta T)}$ and $M_{2(\Delta T)}$, occur in the shell wall. These moments induce the normal stresses, which are found to be

$$\sigma_1 = \sigma_2 = 120 \text{ MPa}.$$

18.1.3 Thermoelastic stress analysis of shallow shells

The general assumptions and governing equations of the shallow shell theory were developed in Sec. 17.4. As mentioned in Sec. 18.1, the equilibrium and kinematic equations of the shell theory remain unchanged, whereas the constitutive relations should be changed in the thermoelastic stress analysis.

Solving the first two equations (18.3) for the strain components ε_1 and ε_2 yields the following:

$$\varepsilon_1 = \frac{1}{Eh}(N_1 - \nu N_2 + N_T); \quad \varepsilon_2 = \frac{1}{Eh}(N_2 - \nu N_1 + N_T). \tag{18.16}$$

Now repeating the procedure of deriving the governing differential equations of the shallow shell described in Secs 17.3 and 17.4, with the use of the constitutive equations (18.3), (18.4), and (18.16), yields the following equations:

$$\begin{aligned} D\nabla^2\nabla^2 w - \nabla_k^2 \Phi &= p_3 - \frac{1}{1-\nu}\nabla^2 M_T, \\ \frac{1}{Eh}\nabla^2\nabla^2 \Phi + \nabla_k^2 w &= -\frac{1}{Eh}\nabla^2 N_T, \end{aligned} \tag{18.17}$$

where the stress function Φ and operator ∇_k^2 were introduced in Sec. 17.4, and the quantities N_T and M_T are given by Eqs (7.8). This system of equations represents the *thermoelastic governing differential equations of the shallow shell*. Hence, if the values of N_T and M_T remain constant or vary linearly along the coordinate lines x and y, then the governing differential equations of the thermoelastic shallow shell stress analysis remain of the same type as for a non-thermally affected shell. However, a thermal

effect can influence the stress state of the shallow shell through the boundary conditions. Such a case is typical for stiffened shells. If a shell wall is heated faster than its stiffening ribs, then the thermal deformation of the shell itself will be restrained and significant compressive stresses may occur in the shell, causing buckling.

18.2 THE GEOMETRICALLY NONLINEAR SHELL THEORY

18.2.1 Introduction

The general shell theories presented previously were based on linear elasticity concepts. Linear shell theories predict adequately stresses and displacements for shells exhibiting small elastic deformations. The governing differential equations of these theories were based on Hooke's law, and the omission of rotations in the expressions for strains and equilibrium. As a result, the above governing equations were linearized. A theory of shells in which the small-displacement assumption is abandoned and the remaining assumptions are retained is called the *geometrically nonlinear theory*. This theory is based on the analysis of large, or finite displacements. Therefore, the geometrically nonlinear theory is also referred to as a large- or finite-displacement theory. In developing the governing equations of the geometrically nonlinear theory of thin shells, rotations are taken into account in both the strain–displacement and equilibrium equations. Additionally a shell may be a physically nonlinear with respect to constitutive relations. This type of nonlinearity forms the basis of *inelastic shell theory* and is not discussed in this book.

The large-displacement shell theory is often required when dealing with shallow shells, highly elastic membranes, and with buckling problems. The reason for that lies in the following. Shallow shells are less stiff than rising shells: the same transverse load produces larger displacements in shallow shells than in rising shells having the same planar dimensions. Hence, the displacements of the shallow shell can be beyond the limits of the applicability of the small-displacement theory (the commonly used criterion of an applicability of the linear shell theory is formulated as follows: the above theory is applicable if $|\mathbf{D}|/h \leq (0.2 \div 0.5)$ where $\mathbf{D} = [u, v, w]^T$ is the displacement vector. However, such a classification may be considered as arbitrary only since here too the decisive influence is that of the preassigned error limits in the solution of the boundary conditions of the theory of shells. Another approach to the criteria of applicability of the linear shell theory was given in Ref. [5]). The small-displacement theory determines a unique configuration of equilibrium for every shell with a prescribed load and assigned constraints. However, in reality, a solution of a physical shell problem is not always unique. A shell under identical conditions of loading and constraints may have several possible equilibrium configurations. Analyses of possible equilibrium configurations under prescribed loads provides a basis for studies of shell buckling problems that will be discussed in the next chapter. Membranes or flexible thin shells may be defined as shells whose bending stiffness is negligible compared with their in-plane stiffness. Such shells may resist applied loads in tension only. Displacements of the membranes, as a rule, exceed their thickness. Therefore, the geometrically nonlinear theory must be applied to characterize adequately the state of stress and strain of membranes.

We present in this section the geometrically nonlinear theory of shallow shells for which the displacements by modulus are equal or exceed the shell thickness but are

considerably less than the other linear dimensions of the shell (from now on, the term "geometrically" will be dropped because only this type of nonlinearity is discussed herein). The large-displacement theory of thin plates and shells originates from von Karman's work [2]. E. Reissner developed the geometrically nonlinear theory of thin shells [3]. Considerable contributions in the nonlinear shell theory were made by Saunders [4], Mushtari [5], etc. We will present here Vlasov's approach for deriving the governing differential equations of the nonlinear shallow shell theory [6].

A geometric nonlinearity manifests to the theory in two ways. At first, because of moderately large displacements, the strain components are related to these displacements by means of nonlinear equations. Secondly, a shell element undergoes so much changes in its shape after deformation, i.e., it moves and rotates in space through such finite distances and angles, that it is impossible to set up its equilibrium equations based on an undeformed shell configuration as has been done in the linear shell theory.

18.2.2 Nonlinear theory of shallow shells

As in the classical shell theory, assume that the coordinate lines coincide with the lines of principal curvatures. We start the nonlinear shallow shell analysis with the strain–displacement relations. In the classical, linear shell theory, it was assumed that strains were small and that the rotations were of the same order of magnitude as the strains. As mentioned earlier, the above rotations should be taken into account in developing the kinematic relations of the nonlinear theory of shallow shells. However, it will be assumed that the nonlinear strains of the middle surface remain still small compared with unity and they are of the order of the rotations squared.

It follows from the above that the nonlinear theory deals with the more complicated strain–displacement equations. However, for shallow shells, these equations can be simplified. Indeed, since the geometry of a shallow shell is close to a flat plate, the stiffness of the shell in the tangent plane is significantly greater than the flexural stiffness (see Sec. 7.4.1). Therefore, say, the angle of rotation ω_1 of the element ds_1 in the tangential plane (about the unit vector $\mathbf{e}_3$) is much smaller than the angle of rotation ϑ_1 of the same element in the normal plane (about the unit vector $\mathbf{e}_2$). However, although the angles ϑ_1 and ϑ_2 are larger in modulus than the angles ω_1 and ω_2, the former angles themselves remain still small because of the following limitation for the deflections adopted in the nonlinear theory of shallow shells: $|w| \leq 5h$. Therefore, the squares of the angles ϑ_1 and ϑ_2 can be neglected in comparison with unity.

Thus, the basic assumption of the linear shell theory about the smallness of the squares of all the angles of rotation compared with unity and about the equivalence of orders of their values is now reduced and it is postulated that

$$\omega_1^2 \ll \vartheta_1^2 \ll 1; \omega_2^2 \ll \vartheta_2^2 \ll 1. \tag{18.18}$$

As a result of the above assumption, the strain–displacement relations of the linear theory of shallow shells, Eqs (17.43), are complemented by the same nonlinear terms as in the theory of flexible plates (see Eqs (7.82)):

$$\begin{aligned} \varepsilon_1 &= \frac{\partial u}{\partial x} - \frac{w}{R_1} + \frac{1}{2}\left(\frac{\partial w}{\partial x}\right)^2; \quad \varepsilon_2 = \frac{\partial v}{\partial y} - \frac{w}{R_2} + \frac{1}{2}\left(\frac{\partial w}{\partial y}\right)^2; \\ \gamma_{12} &= \frac{\partial u}{\partial y} + \frac{\partial v}{\partial x} + \frac{\partial w}{\partial x}\frac{\partial w}{\partial y}. \end{aligned} \tag{18.19}$$

Notice that the shear strain expression for shallow shells is absolutely identical to that obtained in the large-deflection theory of thin plates (see the third Eq. (7.82)). Hence, the shell curvature does not affect the shear deformation of the middle surface, if the coordinate lines x and y are the lines of the principal curvatures in the framework of the theory of shallow shells.

The expressions for changes in curvature and for twist of the middle surface also coincide with those obtained in the small-deflection theory of shallow shells, i.e.,

$$\chi_1 = -\frac{\partial^2 w}{\partial x^2}; \quad \chi_2 = -\frac{\partial^2 w}{\partial y^2}; \quad \chi_{12} = -\frac{\partial^2 w}{\partial x \partial y}. \tag{18.20}$$

The tangential strain components, ε_1^z, ε_2^z, and γ_{12}^z, at points in an equidistant surface of the shell from the z coordinate, are determined, as previously, by Eqs (12.22).

The expressions for the stress resultants and stress couples, as well as the constitutive equations of the nonlinear shallow shell theory remain identical to those introduced in Sec. 12.3 for the linear shell theory. Introducing the relations (18.19) into the constitutive equations (12.45) and letting $N_{12} = N_{21} = S$, we obtain the following relations between the membrane forces and displacements at points of the middle surface:

$$\begin{aligned}
N_1 &= \frac{Eh}{1-\nu^2}\left[\frac{\partial u}{\partial x} + \nu\frac{\partial v}{\partial y} + \frac{1}{2}\left(\frac{\partial w}{\partial x}\right)^2 + \frac{\nu}{2}\left(\frac{\partial w}{\partial y}\right)^2 - \frac{w}{R_1} - \nu\frac{w}{R_2}\right], \\
N_2 &= \frac{Eh}{1-\nu^2}\left[\frac{\partial v}{\partial y} + \nu\frac{\partial u}{\partial x} + \frac{1}{2}\left(\frac{\partial w}{\partial y}\right)^2 + \frac{\nu}{2}\left(\frac{\partial w}{\partial x}\right)^2 - \frac{w}{R_2} - \nu\frac{w}{R_1}\right], \\
S &= \frac{Eh}{2(1+\nu)}\left(\frac{\partial u}{\partial y} + \frac{\partial v}{\partial x} + \frac{\partial w}{\partial x}\frac{\partial w}{\partial y}\right).
\end{aligned} \tag{18.21}$$

Let us eliminate the tangential displacements u and v from Eqs (18.21), and express the forces N_1, N_2, and S in terms of the deflections w. For this purpose, first, transform the two first relations (18.21), as follows:

$$N_1 - \nu N_2 = Eh\left[\frac{\partial u}{\partial x} + \frac{1}{2}\left(\frac{\partial w}{\partial x}\right)^2 - \frac{w}{R_1}\right]; \quad N_2 - \nu N_1 = Eh\left[\frac{\partial v}{\partial y} + \frac{1}{2}\left(\frac{\partial w}{\partial y}\right)^2 - \frac{w}{R_2}\right]. \tag{18.22}$$

Using the above relations, set up the following equation:

$$\begin{aligned}
&\frac{\partial^2}{\partial y^2}(N_1 - \nu N_2) + \frac{\partial^2}{\partial x^2}(N_2 - \nu N_1) - 2(1+\nu)\frac{\partial^2 S}{\partial x \partial y} \\
&\quad = Eh\left\{\frac{\partial^2}{\partial y^2}\left[\frac{1}{2}\left(\frac{\partial w}{\partial x}\right)^2\right] + \frac{\partial^2}{\partial x^2}\left[\frac{1}{2}\left(\frac{\partial w}{\partial y}\right)^2\right] - \frac{\partial^2}{\partial x \partial y}\left(\frac{\partial w}{\partial x}\frac{\partial w}{\partial y}\right)\right. \\
&\qquad \left. - \frac{1}{R_1}\frac{\partial^2 w}{\partial y^2} - \frac{1}{R_2}\frac{\partial^2 w}{\partial x^2}\right\}.
\end{aligned}$$

According to the general rules of differentiating, the following equalities hold:

$$\frac{\partial^2}{\partial y^2}\left[\frac{1}{2}\left(\frac{\partial w}{\partial x}\right)^2\right]=\left(\frac{\partial^2 w}{\partial x\partial y}\right)^2+\frac{\partial w}{\partial x}\frac{\partial^3 w}{\partial x\partial y^2};\ \frac{\partial^2}{\partial x^2}\left[\frac{1}{2}\left(\frac{\partial w}{\partial y}\right)^2\right]=\left(\frac{\partial^2 w}{\partial x\partial y}\right)^2+\frac{\partial w}{\partial y}\frac{\partial^3 w}{\partial x^2\partial y};$$

$$\frac{\partial^2}{\partial x\partial y}\left(\frac{\partial w}{\partial x}\frac{\partial w}{\partial y}\right)=\frac{\partial^3 w}{\partial x^2\partial y}\frac{\partial w}{\partial y}+\left(\frac{\partial^2 w}{\partial x\partial y}\right)^2+\frac{\partial^2 w}{\partial x^2}\frac{\partial^2 w}{\partial y^2}+\frac{\partial w}{\partial x}\frac{\partial^3 w}{\partial x\partial y^2}.$$

Inserting these equalities in the above equation yields the following:

$$\begin{aligned}&\frac{\partial^2}{\partial y^2}(N_1-\nu N_2)+\frac{\partial^2}{\partial x^2}(N_2-\nu N_1)-2(1+\nu)\frac{\partial^2 S}{\partial x\partial y}\\ &\quad=\quad Eh\left[\left(\frac{\partial^2 w}{\partial x\partial y}\right)^2-\frac{\partial^2 w}{\partial x^2}\frac{\partial^2 w}{\partial y^2}-\frac{1}{R_1}\frac{\partial^2 w}{\partial y^2}-\frac{1}{R_2}\frac{\partial^2 w}{\partial x^2}\right].\end{aligned}\tag{18.23}$$

Equation (18.23) represents the *equation of compatibility of deformations* of the nonlinear shallow shell theory in terms of the membrane forces and deflections.

Let us introduce the stress function Φ according to the relations (17.45a). Substituting for Φ from the above relations into Eqs (18.23), results in

$$\nabla^2\nabla^2\Phi=Eh\left[\left(\frac{\partial^2 w}{\partial x\partial y}\right)^2-\frac{\partial^2 w}{\partial x^2}\frac{\partial^2 w}{\partial y^2}-\nabla_k^2 w\right],\tag{18.24}$$

where the operators ∇^2 and ∇_k^2 are given by Eqs (17.44).

Now we are coming to constructing the equations of equilibrium for a shallow shell element subjected to a transverse surface load p_3. The positive directions of the internal forces and moments acting on the element are shown in Fig. 12.5. The derivation of the equations of equilibrium in the nonlinear theory of shallow shells has some peculiarities. The force summations in the x and y directions, as well as the moment summations about the above axes, are set up as for the linear shell theory. This involves neglecting the changes in transition of the shell element from its initial (undeformed) to the deflected state, and the initial curvatures of the above element are also neglected. However, the force summation into the z direction is set up by taking into account both the initial curvatures of the element and its consequent distortion acquired as a result of shell straining under action of applied loads. It can be shown that the above equation of equilibrium will have the form of the third Eq. (12.41), derived for the linear shell theory, but complemented by the same terms as for the corresponding equilibrium equation of the nonlinear theory of flat plates (see Eq. (3.91). The system of simplifications adopted in the nonlinear shallow shell theory results in the following equations of equilibrium:

$$\begin{aligned}&\frac{\partial N_1}{\partial x}+\frac{\partial S}{\partial y}=0;\\ &\frac{\partial N_2}{\partial y}+\frac{\partial S}{\partial x}=0;\end{aligned}\tag{18.25}$$

$$\frac{\partial Q_1}{\partial x}+\frac{\partial Q_2}{\partial y}=-p_3-\frac{N_1}{R_1}-\frac{N_2}{R_2}-N_1\frac{\partial^2 w}{\partial x^2}-N_2\frac{\partial^2 w}{\partial y^2}-2S\frac{\partial^2 w}{\partial x\partial y}; \tag{18.26}$$

$$Q_1=\frac{\partial M_1}{\partial x}+\frac{\partial H}{\partial y}; \tag{18.27a}$$

$$Q_2=\frac{\partial M_2}{\partial y}+\frac{\partial H}{\partial x}. \tag{18.27b}$$

Using the relations (18.27), it is possible to eliminate the shear forces Q_1 and Q_2 from Eq. (18.26). As a result, the equations of static equilibrium of the element of a shallow shell in the nonlinear theory are reduced to the following equations:

$$\begin{aligned}
&\frac{\partial N_1}{\partial x}+\frac{\partial S}{\partial y}=0,\\
&\frac{\partial N_2}{\partial y}+\frac{\partial S}{\partial x}=0,\\
&\frac{\partial^2 M_1}{\partial x^2}+2\frac{\partial^2 H}{\partial x\partial y}+\frac{\partial^2 M_2}{\partial y^2}+N_1\left(\frac{1}{R_1}+\frac{\partial^2 w}{\partial x^2}\right)+N_2\left(\frac{1}{R_2}+\frac{\partial^2 w}{\partial y^2}\right)+2S\frac{\partial^2 w}{\partial x\partial y}+p_3=0.
\end{aligned} \tag{18.28}$$

Substituting for the bending and twisting moments from Eqs (17.45b) into the third Eq. (18.28) and introducing again the stress function Φ from Eq. (17.45a), we obtain that the first two equations of (18.28) will be identically satisfied and the third equation becomes

$$D\nabla^2\nabla^2 w-\left[\nabla_k^2\Phi+\left(\frac{\partial^2\Phi}{\partial y^2}\frac{\partial^2 w}{\partial x^2}+\frac{\partial^2\Phi}{\partial x^2}\frac{\partial^2 w}{\partial y^2}-2\frac{\partial^2\Phi}{\partial x\partial y}\frac{\partial^2 w}{\partial x\partial y}\right)\right]=p_3. \tag{18.29}$$

Eqsuations (18.24) and (18.29) are the governing differential equations of the nonlinear theory of shallow shells. By introducing the operator

$$L(U,V)\equiv\frac{\partial^2 U}{\partial x^2}\frac{\partial^2 V}{\partial y^2}-2\frac{\partial^2 U}{\partial x\partial y}\frac{\partial^2 V}{\partial x\partial y}+\frac{\partial^2 U}{\partial y^2}\frac{\partial^2 V}{\partial x^2}, \tag{18.30}$$

we can rewrite the governing equations (18.24) and (18.29), as follows:

$$\begin{aligned}
&\nabla^2\nabla^2\Phi=-Eh\left[\frac{1}{2}L(w,w)+\nabla_k^2 w\right],\\
&D\nabla^2\nabla^2 w-\left[\nabla_k^2\Phi+L(\Phi,w)\right]=p_3.
\end{aligned} \tag{18.31}$$

Letting in Eqs (18.31) $\kappa_1=1/R_1=0$ and $\kappa_2=1/R_2=0$, we obtain Eqs (7.87) for the large-deflection theory of plates. Boundary conditions on edges of the large-deflection shallow shell are formulated in a similar manner to those of the small-deflection shallow shell or of the large-deflection plate (see Secs 17.4 and 7.4, respectively).

In conclusion, let us formulate some qualitative considerations about the mechanical behavior of a geometrically nonlinear shell under applied loading. For simplicity, consider a flexible spherical shallow shell. Such a shell is governed by Eqs (18.31), if we let $R_1 = R_2 = R$. We obtain the following system of equations:

$$\begin{aligned} \frac{1}{Eh}\nabla^2\nabla^2\Phi + \left[\frac{1}{2}L(w,w) + \frac{1}{R}\nabla^2 w\right] &= 0, \\ D\nabla^2\nabla^2 w - \left[\frac{1}{R}\nabla^2\Phi + L(\Phi,w)\right] &= p_3. \end{aligned} \tag{a}$$

Assume that the stress function Φ is assigned in the first approximation, as follows:

$$\Phi = A(p_3)\cdot w, \tag{b}$$

where $A(p_3)$ is a function of loading only. Substituting for Φ from Eq. (b) into Eq. (a), one obtains

$$\begin{aligned} \frac{A}{Eh}\nabla^2\nabla^2 w + \frac{1}{R}\nabla^2 w + \frac{1}{2}L(w,w) &= 0, \\ D\nabla^2\nabla^2 w - \frac{A}{R}\nabla^2 w - AL(w,w) &= p_3. \end{aligned}$$

Eliminating the nonlinear term $L(w,w)$ from the above equations, we obtain the following equation:

$$D^*\nabla^2\nabla^2 w + \frac{1}{R}\nabla^2 w = p_3^*, \tag{c}$$

where

$$D^*(p_3) = \frac{2A}{Eh} + \frac{D}{A}, \quad p_3^* = \frac{p_3}{A}. \tag{d}$$

The quantity $D^*(p_3)$ is made up of the extensional stiffness Eh and the flexural stiffness D. Therefore, it can be called the composite stiffness of the shell. Obviously, the latter depends on the loading p_3.

For a flexible plate, $R = \infty$, and Eq. (c) becomes

$$D^*\nabla^2\nabla^2 w = p_3^*. \tag{e}$$

Equations (c) and (e) are linear equations. Thus, a geometrically nonlinear shell or plate can be considered as a linear system whose flexural and extensional stiffnesses are replaced with some variable composite stiffness, D, given by the first Eq (d) and depending on the applied loading. The above consideration can be used for an approximate shell or plate analysis.

Example 18.3

Analyze the state of stress and strain in a cylindrical shallow shell of radius R having a rectangular configuration in a plan (see Fig. 18.3a). Assume that the shell is lengthened in the y direction ($b \gg a$) and is subjected to a uniform transverse surface load of intensity p. The straight edges of the shell are hinged and the displacement along the x axis is eliminated.

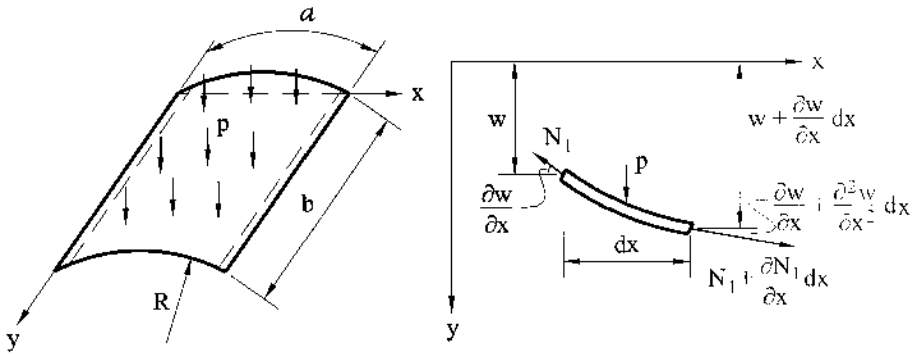

Fig. 18.3

Solution

Let us confine our study to the analysis of the middle part of the shell that is sufficiently remote from the short curvilinear edges. A curved surface of this part of the shell can be considered as a cylindrical surface. Just as has been done for the cylindrical bending of flat plates (see Sec. 3.2.1), the bending of the given part of the shell will be identical to the bending of a unit curvilinear, simply supported at $x = 0$ and $x = a$, shallow strip, isolated from the shell. For such a strip, $w = w(x)$. Since the deformations in the y direction of such a strip are restrained because of an interaction of neighboring strips, then it can be assumed that the relative deformation in the y direction is zero, i.e., $\varepsilon_2 = 0$. It can also be shown that the membrane force $N_1 =$ const over the shell width. The latter can be checked by considering the equilibrium of a shell element detached from the transverse shell strip, which is subjected to the membrane forces and given loading p, as shown in Fig. 18.3b. For a shallow shell and assumptions adopted in the nonlinear theory, the tangent to the curved axis of the shell strip can be neglected, i.e., it is possible to assume that N_1 is a constant over the shell width.

Thus, the equation of equilibrium (18.29) of the nonlinear shallow shell theory acquires, in this particular case, the following form (taking into account that $N_1 = \partial^2\Phi/\partial y^2$):

$$D\frac{\mathrm{d}^4 w}{\mathrm{d}x^4} - N_1\frac{\mathrm{d}^2 w}{\mathrm{d}x^2} - \frac{N_1}{R} = p. \tag{18.32}$$

The solution of this equation is sought in the form of the following series:

$$w(x) = \sum_{m=1}^{\infty} f_m \sin\frac{m\pi x}{a}. \tag{18.33}$$

It is evident that $w(x)$ in the form of Eq. (18.33) satisfies the prescribed boundary conditions for the deflections.

We solve the above problem in the first approximation, retaining the first term in the expansion (18.33) only. We apply the Galerkin method (see Sec. 6.5) for the solution of Eq. (18.32). Let us introduce

$$E \equiv D\frac{\mathrm{d}^4 w}{\mathrm{d}x^4} - N_1\left(\frac{\mathrm{d}^2 w}{\mathrm{d}x^2} + \frac{1}{R}\right) - p = 0. \tag{18.34}$$

Write the Galerkin equation (6.38) in the form

$$\int_0^a E \sin\frac{\pi x}{a}\mathrm{d}x = 0. \tag{18.35}$$

Substituting for w from Eq. (18.33) into the above and retaining only one term in the expansion, one finds the following after integration:

$$Df_1\frac{\pi^5}{4a^4} + N_1\left(f_1\frac{\pi^3}{a^3} - \frac{1}{R}\right) - p = 0. \tag{18.36}$$

Determine the expression for the constant membrane force N_1. From the first Eq. (18.19), one obtains

$$\frac{\partial u}{\partial x} = \varepsilon_1 + \frac{w}{R} - \frac{1}{2}\left(\frac{\partial w}{\partial x}\right)^2. \tag{18.37}$$

Integrating the above over the width of the shell, yields the following:

$$u(a) - u(0) = \int_0^a \left[\varepsilon_1 + \frac{w}{R} - \frac{1}{2}\left(\frac{\partial w}{\partial x}\right)^2\right]\mathrm{d}x. \tag{18.38}$$

The given boundary conditions prescribed along the straight edges of the shell are of the form

$$w = 0|_{x=0,a}; \quad \frac{\partial^2 w}{\partial x^2} = 0\Big|_{x=0,a}; \quad u = 0|_{x=0,a}.$$

Taking into account that $\varepsilon_2 = 0$, we can obtain from the constitutive equations (12.45):

$$\varepsilon_1 = \frac{1-\nu^2}{Eh}N_1.$$

Substituting for ε_1 from the above relation into Eq. (18.38) and taking into account the boundary conditions, we can express the membrane force N_1, as follows:

$$N_1 = -\frac{Eh}{(1-\nu^2)a}\int_0^a \left[\frac{w}{R} - \frac{1}{2}\left(\frac{\partial w}{\partial x}\right)^2\right]\mathrm{d}x.$$

Substituting for w from Eq. (18.33) into the above and integrating, we obtain (for $m = 1$)

$$N_1 = \frac{Eh}{1-\nu^2}\left(\frac{f_1^2\pi^2}{4a^2} - \frac{2f_1}{\pi R}\right). \tag{18.39}$$

Substituting the above expression into Eq. (18.36), we obtain the following cubic equation for the amplitude of deflections:

$$\frac{\pi^5 f_1^3}{16 h^3} - \frac{3\pi^2}{4}\frac{f_1^2}{Rh^3} + \left(\frac{\pi^5}{48} + \frac{2a^4}{4R^2h^2}\right)\frac{f_1}{h} = (1-\nu^2)\frac{pa^4}{Eh^4}. \tag{18.40}$$

The relationship between the dimensionless parameters $p^* = (1-\nu^2)pa^4/Eh^4$ and f_1/h is illustrated in Fig. 18.4 (taken from Ref. [7]). The curves of this figure are given for various values of $k^* = a^2/Rh$. Figure 18.4 shows the four different plots; the straight line 1 indicates the relationship p^* of f_1/h due to the linear theory of shallow shells, whereas the three other curves describe the relationship in the large-deflection theory for various values of the parameter k^*.

It is seen that for a relatively small parameter k^*, the relationship p^* of f_1/h is single-valued (curve 2 refers to a flexible flat plate with $k^* = 0$; and curve 3 stands for $k^* = 4.475$). However, for larger values of this parameter (curve 4 stands for $k^* = 40$) the above relationship is not uniquely defined, i.e., the three real roots of Eq. (18.40) correspond to one and the same value of p^*. This is a consequence of some peculiarities of straining the large-deflection shallow shell in the process of increasing the applied loading. As long as the parameter p^* increases from zero to the value of 1025 (the ordinate of point A on the curve), the deflection amplitude grows continuously up to the value $\sim 2.2h$, as is indicated by the branch OA of the curve. However, as soon as the load parameter p^* becomes larger than a certain value (about 1025), the given cylindrical shallow shell undergoes the so-called snap through, i.e., the deflection changes its value by jumping from approximately $2.2h$ (the abscissa of point A on the curve) to approximately $11.1h$ (the abscissa of point D on the curve). Upon unloading after this snap through, the shell does not return to its initial configuration of equilibrium. The permanent deflection measured by the abscissa of point E remains in the shell. To return the panel to its initial configuration it is necessary to apply to it a load of another sign whose dimensional parameter $p^* = -959.7$ (the ordinate of point B on the curve 4). At this load, an inverse snap through of the panel occurs. This snap through corresponds to the transition from point B to point F on curve 4.

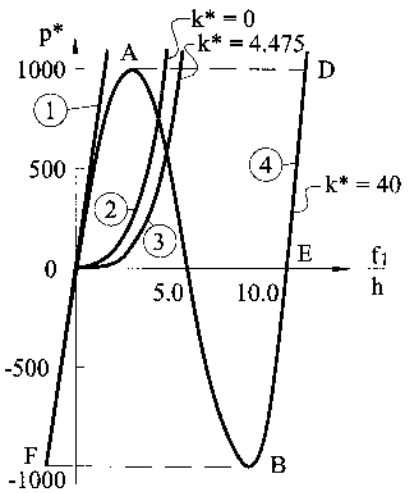

Fig. 18.4

It is clear that the linear relationship between p^* and f_1/h presented by the straight line 1 leads to incorrect quantitative and qualitative results of the stress and strain analysis of the given shell.

18.3 ORTHOTROPIC AND STIFFENED SHELLS

18.3.1 Introduction

In the previous chapters of Part II, only homogeneous and isotropic shells were considered. This permitted the study of the effects of different types of a shell geometry, edge constraints, loading, etc., upon stress and strain components using various shell theories. In this section, the complicated effects associated with material anisotropy and geometric nonhomogeneity, e.g., shell reinforcement, are considered. Obviously, each such effect causes complications in the governing differential equations of the general shell theory. We present below the general equations and relations for orthotropic and stiffened (structurally orthotropic) shells in the framework of the linear (classical) shell theory. It should be noted that the governing differential equations of the theory of orthotropic and stiffened shells may be derived in much the same way as was done for the theory of isotropic and homogeneous shells in Chapter 12. In fact, as mentioned in Sec. 12.5, the general linear theory of thin isotropic shells consists of the three sets of equations: the strain–displacement relations, Eqs (12.22)–(12.24); equations of equilibrium (or motion for dynamic problems), Eqs (12.41) and (12.42); and the constitutive equations (12.32) or (12.45) and (12.46). These three sets of equations are to be completed by appropriate boundary conditions. The first two sets of equations, without changes, are carried over into the theory of the orthotropic shells, whereas the constitutive equations (12.32) or (12.45) and (12.46), used for isotropic shells, are not valid for the above orthotropic shells and must be modified. First, we consider the stress–strain relations for orthotropic shells and then generalize them for stiffened shells.

18.3.2 Orthotropic shells

A material is orthotropic if its mechanical characteristics are specified along two mutually orthogonal directions (for a two-dimensional space). Such a material has different values for E, G, and ν for each direction (see Sec. 7.2). For instance, shells made of delta wood, plywood, fiberglass, metallic composites, and other composite materials fall into the category of orthotropic shells. We assume that the orthotropic material of the shell is so arranged that at each point of the shell its mutually orthogonal directions of elastic symmetry coincide with the principal lines of curvature on the shell's middle surface. For such orthotropic material of a shell, the stress components are related to strain components at any point located at a distance z from the middle surface, as follows:

$$\sigma_1^z = \frac{E_1}{1-\nu_1\nu_2}(\varepsilon_1^z + \nu_2\varepsilon_2^z); \quad \varepsilon_2^z = \frac{E_2}{1-\nu_1\nu_2}(\varepsilon_2^z + \nu_1\varepsilon_1^z); \quad \tau_{12}^z = G\gamma_{12}^z, \tag{18.41}$$

where E_1 and E_2 are the moduli of elasticity in the directions of the α- and β-coordinate axes, respectively; ν_1 and ν_2 are the Poisson's ratios corresponding to the above axes; and G is the shear modulus. It should be noted that the moduli of

elasticity and Poisson's ratios are not independent and are related by the following expression (see Eq. (7.24)):

$$\nu_1 E_2 = \nu_2 E_1.$$

Substituting for the strain components from Eqs (12.22) into Eqs (18.41), one obtains

$$\begin{aligned}
\sigma_1^z &= \frac{E_1}{1-\nu_1\nu_2}[\varepsilon_1 + \nu_2\varepsilon_2 + z(\chi_1 + \nu_2\chi_2)];\\
\sigma_2^z &= \frac{E_2}{1-\nu_1\nu_2}[\varepsilon_2 + \nu_1\varepsilon_1 + z(\chi_2 + \nu_1\chi_1)];\\
\tau_{12}^z &= G(\gamma_{12} + 2z\chi_{12}).
\end{aligned} \tag{18.42}$$

These are the *general constitutive relations of the linear theory of orthotropic shells based on the Kirchhoff–Love postulates*. They relate the stress components at a point of the shell located at a distance z from the middle surface to the in-plane strain components and changes in curvature and twist of the middle surface.

Substituting Eqs (18.41) into the stress and couple resultants' expressions (12.35) and (12.36), integrating over the shell thickness, and neglecting the terms of order z/R_i compared with unity, yields the following:

$$N_1 = B_1(\varepsilon_1 + \nu_2\varepsilon_2); \quad N_2 = B_2(\varepsilon_2 + \nu_1\varepsilon_1); \quad N_{12} = N_{21} = S = B_G\gamma_{12}; \tag{18.43}$$

$$M_1 = D_1(\chi_1 + \nu_2\chi_2); \quad M_2 = D_2(\chi_2 + \nu_1\chi_1); \quad M_{12} = M_{21} = H = D_G\chi_{12}, \tag{18.44}$$

where B_1, B_2, and B_G are the extensional and shear stiffnesses, respectively, defined as

$$B_1 = \frac{E_1 h}{1-\nu_1\nu_2}; \quad B_2 = \frac{E_2 h}{1-\nu_1\nu_2}; \quad B_G = Gh, \tag{18.45a}$$

and D_1, D_2, and D_G are the flexural and torsional stiffnesses, respectively, defined as

$$D_1 = \frac{E_1 h^3}{12(1-\nu_1\nu_2)}; \quad D_2 = \frac{E_2 h^3}{12(1-\nu_1\nu_2)}; \quad D_G = \frac{Gh^3}{6}. \tag{18.45b}$$

Equations (18.43) and (18.44) represent the stress resultant–in-plane strain and stress couple–curvature relations for the orthotropic linear shell theory based on the Kirchhoff–Love postulates.

18.3.3 Stiffened shells

Stiffened shells are commonly used in the aerospace and civil engineering fields. For example, a stiffened circular cylindrical shell is a widely used structural configuration for an aircraft fuselage or a launch vehicle fuel tank. Being suitably designed, the stiffened shells are more efficient and economical configurations than the corresponding unstiffened shells. They correspond, to a great extent, to specifications for low-weight structural configurations that are very important for aerospace structures.

Basically, two approaches are possible for the analysis of stiffened shells. If the distance between the stiffeners is too large, then the shell structure must be presented as a combination of shell and stiffener elements, each having its own governing equations and coupled to one another by equations of continuity. However, if the stiffening elements are relatively closely spaced, then a shell structure can be considered as orthotropic, the *structurally orthotropic shell* (see Sec. 7.2). In the latter case, the rigidities of the stiffeners can be "smeared" along the shell middle surface to yield an equivalent homogeneous orthotropic shell. Only the second approach is considered in this book.

Consider a thin shell, reinforced by closely spaced stiffeners, in two mutually perpendicular directions, attached to the inside of the shell skin, as illustrated in Fig. 18.5. Assume that the depth of the stiffeners is small compared with the principal radii of curvature of the shell middle surface and that the stiffeners, unlike the shell skin, undergo a uniaxial state of stress. For the sake of simplicity, assume that the stiffeners and skin are made of the same isotropic material. As mentioned previously, such a gird-stiffened shell is replaced by a structurally orthotropic unstiffened (homogeneous) shell. Let us set up the constitutive equations for the above shell by modifying the expressions (12.45) and (12.46). For the shell wall construction that is not symmetrical relative to the shell middle surface (see Fig. 18.5b), there is coupling between extensional forces and curvature change and between bending moments and extensional strain. Taking into account the above considerations and neglecting the terms of order z/R_i with respect to unity in Eqs (12.35) and substituting for the stress components from Eqs. (12.33), one can write the above expressions for the stress resultants for the structurally orthotropic shells. The membrane force N_1 is given by

$$N_1 d_\beta = d_\beta \int_{-h/2}^{h/2} \sigma_1^z dz + \int_{A_\alpha} \sigma_1^z dA_\alpha = d_\beta \frac{Eh}{1-\nu^2}(\varepsilon_1 + \nu\varepsilon_2) + \varepsilon_1 EA_\alpha + \chi_1 EF_\alpha. \tag{18.46}$$

Dividing both sides of the above equation by d_α, one obtains the following expression for N_1:

$$N_1 = \varepsilon_1 B_{11} + \varepsilon_2 B_{12} + \chi_1 K_{11}. \tag{18.47a}$$

In a similar manner, the expressions for the membrane force N_2 and S are given by

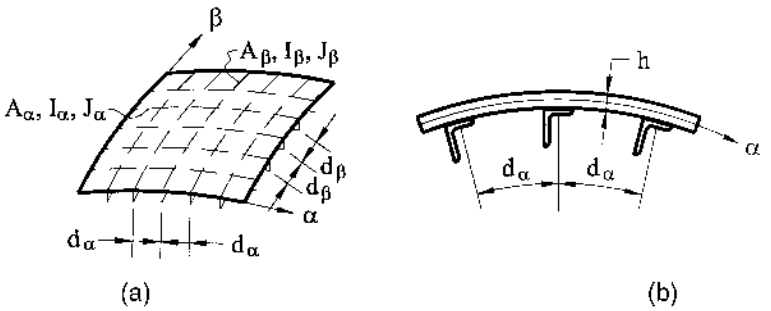

Fig. 18.5

$$N_2 = \varepsilon_2 B_{22} + \varepsilon_1 B_{21} + \chi_2 K_{22}. \tag{18.47b}$$

$$S = B_{33}\gamma_{12}. \tag{18.47c}$$

In Eqs (18.47)

$$\begin{aligned} &B_{11} = B + \frac{EA_\alpha}{d_\beta}; \quad B_{12} = B_{21} = B\nu; \quad K_{11} = \frac{EF_\alpha}{d_\beta}; \\ &B_{22} = B + \frac{EA_\beta}{d_\alpha}; \quad K_{22} = \frac{EF_\beta}{d_\alpha}; \quad B_{33} = \frac{1-\nu}{2}B; \quad B = \frac{Eh}{1-\nu^2}; \end{aligned} \tag{18.48}$$

A_α and A_β are the cross-sectional areas of the stiffeners in the α- and β-directions, respectively; $F_\alpha = \int_{A_\alpha} z\mathrm{d}A_\alpha$ and $F_\beta = \int_{A_\beta} z\mathrm{d}A_\beta$ are the first moments of area of the stiffeners about the tangents to the middle surface.

Note that $K_{11} > 0, K_{22} > 0$ for internally spaced stiffeners and $K_{11} < 0$, $K_{22} < 0$ for externally spaced stiffeners; $K_{11} = K_{22} = 0$ if the stiffeners are located symmetrically with respect to the shell middle surface.

Analogously, we can introduce the expressions for the bending moments in the structurally orthotropic shells. We have the following:

$$M_1 d_\beta = d_\beta \int_{-h/2}^{h/2} \sigma_1^z z\mathrm{d}z + \int_{A_\alpha} \sigma_1^z z\mathrm{d}A_\alpha,$$

or

$$M_1 = \varepsilon_1 K_{11} + \chi_1 D_{11} + \chi_2 D_{12}. \tag{18.49a}$$

Similarly, the bending moment M_2 is given by

$$M_2 = D_{22}\chi_2 + D_{21}\chi_1 + K_{22}\varepsilon_2 \tag{18.49b}$$

and

$$H = \chi_{12} D_{33}, \tag{18.49c}$$

where

$$\begin{aligned} &D_{11} = D + \frac{EI_\alpha}{d_\beta}; \quad D_{12} = D_{21} = \nu D; D_{22} = D + \frac{EI_\beta}{d_\alpha}; \\ &D_{33} = D(1-\nu) + \frac{1}{2}\left(\frac{GJ_\alpha}{d_\beta} + \frac{GJ_\beta}{d_\alpha}\right); \quad D = \frac{Eh^3}{12(1-\nu^2)}, \end{aligned} \tag{18.50}$$

where $I_\alpha = \int_{A_\alpha} z^2\mathrm{d}A_\alpha$ and $I_\beta = \int_{A_\beta} z^2\mathrm{d}A_\beta$ are the moments of inertia of the stiffeners about the tangents to the middle surface; J_α and J_β are the torsional constants for the α- and β-directed stiffeners. For thin-walled open cross sections, the torsional constant is given approximately by the following relation [8]:

$$J = \frac{1}{3}\sum l_i h_i^3,$$

where $\sum l_i$ is the developed length of the middle line of the cross section of the stiffener and h_i is its wall thickness. Note that the twisting rigidity of stiffened shells reinforced by thin-walled members with open cross sections differs little from the correponding rigidity of unstiffened shells. Therefore, in the analysis of the above stiffened shells, one can take

$$D_{33} \approx D(1-\nu). \tag{18.51}$$

By way of illustration of the above theory of orthotropic and stiffened shells, let us now derive the governing differential equation for some shell problems.

1. Axisymmetrically loaded stiffened circular cylindrical shell subjected to internal pressure p

Assume that the shell is stiffened by closely spaced circular circumferential rings. According to the above theory, first replace the given naturally orthotropic and stiffened circular shell by a structurally orthotropic shell having the extensional and flexural rigidities given by Eqs (18.48) and (18.50). Inserting the expressions (15.38) into Eqs (18.47a and b) and (18.49a) yields the following stress resultants–displacement relations:

$$\begin{aligned} &N_1 = B_{11}\frac{\mathrm{d}u}{\mathrm{d}x} - B_{12}\frac{w}{R} - K_{11}\frac{d^2w}{dx^2}, \quad N_2 = -B_{22}\frac{w}{R} + B_{21}\frac{\mathrm{d}u}{\mathrm{d}x}; \\ &M_1 = -D_{11}\frac{\mathrm{d}^2w}{\mathrm{d}x^2} + K_{11}\frac{\mathrm{d}u}{\mathrm{d}x}. \end{aligned} \tag{18.52}$$

Using the first Eq. (18.52), express $\mathrm{d}u/\mathrm{d}x$ in terms of N_1 and w, and then substitute the result into the second and third Eq. (18.52). We obtain the following:

$$\begin{aligned} N_2 &= \frac{1}{B_{11}}\left[B_{21}N_1 + \frac{w}{R}\left(B_{21}^2 - B_{22}B_{11}\right) + B_{21}K_{11}\frac{\mathrm{d}^2w}{\mathrm{d}x^2}\right], \\ M_1 &= \frac{1}{B_{11}}\left[K_{11}N_1 + \frac{w}{R}K_{11}B_{12} + \left(K_{11}^2 - B_{11}D_{11}\right)\frac{\mathrm{d}^2w}{\mathrm{d}x^2}\right]. \end{aligned} \tag{18.53}$$

Inserting the above equations into the equilibrium equation (15.41) results in the following governing differential equation for an axisymmetrically loaded, structurally orthotropic circular cylindrical shell (stiffened by circumferential rings):

$$\frac{\mathrm{d}^4w}{\mathrm{d}x^4} - 2\lambda^2\frac{\mathrm{d}^2w}{\mathrm{d}x^2} + 4\beta_s^4 w = f(p_3, N_1), \tag{18.54}$$

where

$$\begin{aligned} &\lambda^2 = \frac{K_{11}B_{12}}{2RD_s}; \quad \beta_s^4 = \frac{B_s}{4D_sR^2}; \quad D_s = B_{11}D_{11} - K_{11}^2; \quad B_s = B_{11}B_{22} - B_{12}^2; \\ &f(p_3, N_1) = \frac{1}{D_s}\left(B_{11}p_3 + K_{11}\frac{\mathrm{d}^2N_1}{\mathrm{d}x^2} + \frac{B_{21}}{R}N_1\right). \end{aligned} \tag{18.55}$$

The membrane meridional force N_1 may be found from Eq. (15.36), i.e.,

$$N_1 = -\int p_1 \mathrm{d}x + N_1^{(0)}, \tag{18.56}$$

where $N_1^{(0)}$ is the meridional force in a reference section of the shell, $x = 0$.

For an unstiffened, isotropic, circular cylindrical shell, axisymmetrically loaded by a pressure p_3, one obtains the following:

$$K_{11} = 0, \quad B_{11} = B_{22} = B, \quad B_{21} = \nu B; \quad B_s = B^2(1-\nu^2),$$

$$D_{11} = D = \frac{Eh^3}{12(1-\nu^2)}, \lambda = 0, \beta_s^4 = \beta^4$$

$$D_s = BD, \quad f(p_3, N_1) = \frac{1}{BD}\left(p_3 + \frac{\nu B}{R} N_1\right),$$

and Eqs (18.55) will be reduced to Eq. (15.43) derived in Sec. 15.3 for an isotropic circular cylindrical shell loaded axisymmetrically by a pressure p_3 (if $p_1 = 0$ then $N_1 = \text{const}$, and $\mathrm{d}^2 N_1/\mathrm{d}x^2 = 0$).

2. Shallow structurally orthotropic shells with unsymmetrical over-the-shell thickness composition

Assume that all the assumptions adopted for the theory of shallow shells and introduced in Sec. 17.4 hold. Thus, the equations of equilibrium of a differential shell element of the middle surface and compatibility equations presented in Sec. 17.4 remain unchanged. Only the constitutive equations will be changed, which results in new governing differential equations.

The equations of static equilibrium of the linear shallow shell theory can be obtained either from the equilibrium equations of the general linear shell theory, Eqs (12.41) and (12.42), using the assumptions adopted in the shallow shell theory (see Sec. 17.4), or from Eqs (18.28) by making all the nonlinear terms equal to zero. In any case, the equations of equilibrium of the linear shallow shell theory, using the Cartesian coordinates as the lines of curvature of the shallow shell middle surface, are of the following form (assuming that $p_1 = p_2 = 0$):

$$\frac{\partial N_1}{\partial x} + \frac{\partial S}{\partial y} = 0,$$

$$\frac{\partial S}{\partial x} + \frac{\partial N_2}{\partial y} = 0, \tag{18.57}$$

$$\frac{\partial^2 M_1}{\partial x^2} + 2\frac{\partial^2 H}{\partial x \partial y} + \frac{\partial^2 M_2}{\partial y^2} + \frac{N_1}{R_1} + \frac{N_2}{R_2} = -p_3 \tag{18.58}$$

The compatibility equations for the linear shallow shell theory are given by Eqs (17.35). In particular, the third equation of this system can be represented in the following form for the shallow shell (making $\alpha = x$, $\beta = y$, and $A = B = 1$):

$$\frac{\partial^2 \varepsilon_1}{\partial y^2} + \frac{\partial^2 \varepsilon_2}{\partial x^2} - \frac{\partial^2 \gamma_{12}}{\partial x \partial y} = -\frac{\partial^2 w}{\partial y^2}\frac{1}{R_1} - \frac{\partial^2 w}{\partial x^2}\frac{1}{R_2}. \tag{18.59}$$

The constitutive equations for shallow shells, reinforced in both directions by stiffeners, may be presented in the form of Eqs (18.47) and (18.49). The strain–displacement relations and the curvature changes–displacement expressions for the shallow composite shells are given by Eqs (17.43).

Solving Eq. (18.47) for the strain components yields the following:

$$\varepsilon_1 = \frac{1}{B_s}(N_1 B_{22} - N_2 B_{12} - \chi_1 K_{11} B_{22} + \chi_2 K_{22} B_{12});$$
$$\varepsilon_2 = \frac{1}{B_s}(N_2 B_{11} - N_1 B_{12} + \chi_1 K_{11} B_{12} - \chi_2 K_{22} B_{11}); \tag{18.60}$$
$$\gamma_{12} = \frac{S}{B_{33}}.$$

Substituting the above expressions into Eqs (18.49), one obtains

$$M_1 = \frac{K_{11}B_{22}}{B_s}N_1 - \frac{K_{11}B_{12}}{B_s}N_2 + \left(D_{11} - \frac{K_{11}^2 B_{22}}{B_s}\right)\chi_1 + \left(D_{12}\frac{K_{11}K_{22}B_{12}}{B_c}\right)\chi_2,$$
$$M_2 = \frac{K_{22}B_{11}}{B_s}N_2 - \frac{K_{22}B_{21}}{B_s}N_1 + \left(D_{21} + \frac{K_{11}K_{22}B_{21}}{B_s}\right)\chi_1 + \left(D_{22} - \frac{K_{22}^2 B_{11}}{B_s}\right)\chi_2,$$
$$H = D_{33}\chi_{12}. \tag{18.61}$$

Inserting the above expressions into Eq. (18.58) yields

$$\frac{K_{11}B_{22}}{B_s}\frac{\partial^2 N_1}{\partial x^2} - \frac{K_{11}B_{12}}{B_s}\frac{\partial^2 N_2}{\partial x^2} + \left(D_{11} - \frac{K_{11}^2 B_{22}}{B_s}\right)\frac{\partial^2 \chi_1}{\partial x^2}$$
$$+ \left(D_{12} + \frac{K_{11}K_{22}B_{12}}{B_s}\right)\frac{\partial^2 \chi_2}{\partial x^2} + 2D_{33}\frac{\partial^2 \chi_{12}}{\partial x \partial y} + \frac{K_{22}B_{11}}{B_s}\frac{\partial^2 N_2}{\partial y^2} - \frac{K_{22}B_{12}}{B_s}\frac{\partial^2 N_1}{\partial y^2}$$
$$+ \left(D_{21} + \frac{K_{11}K_{22}B_{21}}{B_s}\right)\frac{\partial^2 \chi_1}{\partial y^2} + \left(D_{22} - \frac{K_{22}^2 B_{11}}{B_s}\right)\frac{\partial^2 \chi_2}{\partial y^2} = -p_3 - \left(\frac{N_1}{R_1} + \frac{N_2}{R_2}\right). \tag{18.62}$$

Introduce again the stress function Φ by Eqs (17.45a). Substituting for the changes in curvature and twist from Eqs (17.43) and for the membrane forces from Eqs (17.45a) into Eq. (18.62), we obtain the following:

$$L_K \Phi + \nabla_{1s}^4 w = p_3, \tag{18.63}$$

where

$$L_K(\ldots) \equiv \frac{\partial^4}{\partial x^4}(\ldots)\frac{K_{11}B_{12}}{B_s} + \frac{\partial^4}{\partial y^4}(\ldots)\frac{K_{22}B_{12}}{B_s} - \frac{\partial^4}{\partial x^2 \partial y^2}(\ldots)\frac{(K_{11}B_{22} + K_{22}B_{11})}{B_s} - \nabla_k^2(\ldots),$$
$$\nabla_{1s}^4 \equiv \frac{\partial^4}{\partial x^4}(\ldots)\left(D_{11} - \frac{K_{11}^2 B_{22}}{B_s}\right) + 2\frac{\partial^4}{\partial x^2 \partial y^2}(\ldots)\left(D_{21} + D_{33} + \frac{K_{11}B_{12}K_{22}}{B_s}\right)$$
$$+ \frac{\partial^4}{\partial y^4}(\ldots)\left(D_{22} - \frac{K_{22}^2 B_{11}}{B_s}\right); \quad \nabla_k^2(\ldots) \equiv \frac{1}{R_1}\frac{\partial^2}{\partial y^2}(\ldots) + \frac{1}{R_2}\frac{\partial^2}{\partial x^2}(\ldots). \tag{18.64}$$

Then, let us use the compatibility equations (17.35). As mentioned in Sec. 17.3, the first two equations of the above system (17.35) will be automatically satisfied if one

substitutes for χ_1, χ_2, and χ_3 from the kinematic relations (17.29). Substituting for the in-plane strain components from Eqs (18.60) into the third compatibility equation (18.59) yields

$$\frac{1}{B_s}\left[B_{22}\frac{\partial^2 N_1}{\partial y^2} - B_{12}\frac{\partial^2 N_2}{\partial y^2} - K_{11}B_{22}\frac{\partial^2 \kappa_1}{\partial y^2} + K_{22}B_{12}\frac{\partial^2 \kappa_2}{\partial y^2} + B_{11}\frac{\partial^2 N_2}{\partial x^2} - B_{12}\frac{\partial^2 N_1}{\partial x^2}\right.$$
$$\left. + K_{11}B_{12}\frac{\partial^2 \chi_1}{\partial x^2} - K_{22}B_{11}\frac{\partial^2 \chi_2}{\partial x^2}\right] - \frac{1}{B_{33}}\frac{\partial^2 S}{\partial x \partial y} = \nabla_k^2 w \tag{18.65}$$

or, using the strain–displacement relations (17.43) and Eqs (17.45), we obtain

$$\nabla_{2s}^4 \Phi - L_K w = 0, \tag{18.66}$$

where

$$\nabla_{2s}^4(\ldots) \equiv \frac{B_{11}}{B_s}\frac{\partial^4}{\partial x^4}(\ldots) + 2\left(\frac{1}{2B_{33}} - \frac{B_{12}}{B_s}\right)\frac{\partial^4}{\partial x^2 \partial y^2} + \frac{B_{22}}{B_s}\frac{\partial^4}{\partial y^4}(\ldots). \tag{18.67}$$

Equations (18.63) and (18.66) form the *system of governing differential equations for the shallow structurally orthotropic shells.*

It can be shown that for shallow unstiffened and isotropic shells, the operators (18.64) and (18.67) become

$$L_K(\ldots) = -\nabla_k^2(\ldots); \quad \nabla_{1s}^4(\ldots) = D\nabla^4(\ldots); \quad \nabla_{2s}^4(\ldots) = \frac{1}{Eh}\nabla^4(\ldots), \tag{18.68}$$

where $\nabla^4(\ldots)$ is the biharmonic operator given by Eq. (2.26). Equations (18.63) and (18.66) will be reduced to the system of equations (17.36) introduced in Secs 17.3 and 17.4.

18.4 MULTILAYERED SHELLS

Consider a thin multilayered shell of revolution of a constant thickness, composed of n isotropic and orthotropic layers of variable thickness, whose mechanical parameters vary along the meridian only (see Fig. 18.6). Many of structures made of composite materials can be presented as multilayered orthotropic shells of revolution.

It is supposed that the above layers deform without slipping and separation. The stress components on planes, that are tangent to the contact surface, have no discontinuities and the material of the shell layers obeys Hooke's law.

The coordinate surface does not necessarily coincide with the contact surface of two adjacent layers. If a shell is composed of layers of identical thickness, then the coordinate surface is chosen to be parallel to the contact surfaces. It is also assumed that the deformations are small, the Kirchhoff–Love hypotheses are valid for the entire shell packet, and the mechanical parameters of each layer are not too different from one another, i.e., the shell is not significantly nonhomogeneous across its thickness. The axes of orthotropy in all layers of the shell packet are assumed to be parallel to the coordinate lines. Let the coordinate surface of the multilayered shell, chosen from some considerations, be referred to the curvilinear orthogonal coordinate system $\alpha = s$ and $\beta = \theta$, where s is the length of the meridian arc, measured

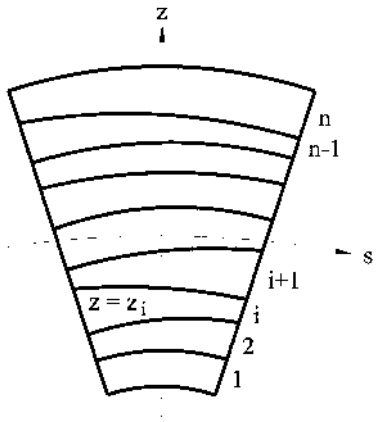

Fig. 18.6

from some reference shell cross section and θ is the circumferential angle measured from some reference meridian. For this coordinate system, the Lamé parameters are

$$A = 1 \quad \text{and} \quad B = r, \tag{18.69}$$

where r is the radius of the parallel circle.

There exists an obvious relationship between the spherical coordinates adopted in Sec. 11.8 and the coordinates mentioned above, i.e.,

$$\cos\theta \mathrm{d}s = \mathrm{d}r. \tag{18.70}$$

The entire shell is referred to the coordinate system z, θ, s. Then, the equations $z_i = z_i(s, \theta)$ $(i = 1, 2, \ldots, n-1)$ assign the contact surfaces for the i and $i+1$ layers, and bounding (lower and upper) surfaces are given by the equations $z_0 = z_0(s, \theta)$ and $z_n = z_n(s, \theta)$ (Fig. 18.6). Due to the above-mentioned assumptions adopted in the multi-layered shell theory, it is possible to replace the usual consideration of stresses over the entire shell packet by a consideration of statically equivalent stress resultants and stress couples, just as has been done for isotropic shells in Sec. 12.3.2. So, by analogy with Eqs (12.35) and (12.36), we obtain the following expressions for the internal forces and moments:

$$\begin{aligned}
N_1 &= \sum_{i=1}^{n} \int_{z_{i-1}}^{z_i} \sigma_1^i \left(1 - \frac{z}{R_2}\right) \mathrm{d}z; \quad N_2 = \sum_{i=1}^{n} \int_{z_{i-1}}^{z_i} \sigma_2^i \left(1 - \frac{z}{R_1}\right) \mathrm{d}z; \\
N_{12} &= \sum_{i=1}^{n} \int_{z_{i-1}}^{z_i} \tau_{12}^i \left(1 - \frac{z}{R_1}\right) \mathrm{d}z; \quad N_{21} = \sum_{i=1}^{n} \int_{z_{i-1}}^{z_i} \tau_{21}^i \left(1 - \frac{z}{R_2}\right) \mathrm{d}z; \\
Q_1 &= \sum_{i=1}^{i=n} \int_{z_{i-1}}^{z_i} \tau_{1z}^i \left(1 - \frac{z}{R_2}\right) \mathrm{d}z; \quad Q_2 = \sum_{i=1}^{n} \int_{z_{i-1}}^{z_i} \tau_{2z}^i \left(1 - \frac{z}{R_1}\right) \mathrm{d}z; \\
M_1 &= \sum_{i=1}^{n} \int_{z_{i-1}}^{z_i} \sigma_1^i \left(1 - \frac{z}{R_2}\right) z \mathrm{d}z; \quad M_2 = \sum_{i=1}^{n} \int_{z_{i-1}}^{z_i} \sigma_2^i \left(1 - \frac{z}{R_1}\right) z \mathrm{d}z; \\
M_{12} &= \sum_{i=1}^{n} \int_{z_{i-1}}^{z_i} \tau_{12}^i \left(1 - \frac{z}{R_1}\right) z \mathrm{d}z; \quad M_{21} = \sum_{i=1}^{n} \int_{z_{i-1}}^{z_i} \tau_{21}^i \left(1 - \frac{z}{R_2}\right) z \mathrm{d}z.
\end{aligned} \tag{18.71}$$

It should be noted that these stress resultants and stress couples are referred to the coordinate surface, unlike a single-layered isotropic shell, when they were referred to the middle surface. It is assumed that the stress resultants, N_{12} and N_{21}, and stress couples, M_{12} and M_{21}, can be reduced by using Novozhilov's suggestion (Eq. (12.43)).

Equations of static equilibrium and kinematic relations for the multilayered shells of revolution are coincident with those obtained in Sec. 16.2 for isotropic shells of revolution, taking into account that the internal forces and moments are given by the relations (18.71). Following a procedure similar to the one described in Sec. 12.3.4, we can obtain the constitutive equations for the multilayered orthotropic shells of revolution under axisymmetrical loading. We have

$$\begin{aligned} N_1 &= C_{11}\varepsilon_1 + C_{12}\varepsilon_2 + K_{11}\chi_1 + K_{12}\chi_2, \\ N_2 &= C_{12}\varepsilon_1 + C_{22}\varepsilon_2 + K_{12}\chi_1 + K_{22}\chi_2, \\ S &= C_{66}\gamma_{12} + 2K_{66}\chi_{12}, \end{aligned} \tag{18.72}$$

$$\begin{aligned} M_1 &= K_{11}\varepsilon_1 + K_{12}\varepsilon_2 + D_{11}\chi_1 + D_{12}\chi_2, \\ M_2 &= K_{12}\varepsilon_1 + K_{22}\varepsilon_2 + D_{12}\chi_1 + D_{22}\chi_2, \\ H &= K_{66}\gamma_{12} + 2D_{66}\chi_{12}, \end{aligned} \tag{18.73}$$

where S and H are given by Eqs (12.43) and the constants C_{mp}, K_{mp}, and D_{mp} depend upon the mechanical characteristics of layers and are of the following form:

$$C_{mp} = \sum_{i=1}^{n} \int_{z_{i-1}}^{z_i} B_{mp}^i \mathrm{d}z; \quad K_{mp} = \sum_{i=1}^{n} \int_{z_{i-1}}^{z_i} B_{mp}^i z \mathrm{d}z; \quad D_{mp} = \sum_{i=1}^{n} \int_{z_{i-1}}^{z_i} B_{mp}^i z^2 \mathrm{d}z. \tag{18.74}$$

The expressions of B_{mp}^i for the ith ayer have the following form:

– *for orthotropic shells*

$$B_{11} = \frac{E_1}{1-\nu_1\nu_2}; \quad B_{12} = \frac{\nu_1 E_2}{1-\nu_1\nu_2} = \frac{\nu_2 E_1}{1-\nu_1\nu_2}; \quad B_{22} = \frac{E_2}{1-\nu_1\nu_2}; \quad B_{66} = G; \tag{18.75}$$

– *for homogeneous isotropic shells*

$$\begin{aligned} &C_{11} = C_{22} = \frac{Eh}{1-\nu^2}; \quad C_{12} = \nu C_{11}; \quad C_{66} = \frac{Eh}{2(1+\nu)}; \\ &D_{11} = D_{22} = \frac{Eh^3}{12(1-\nu^2)}; \quad D_{12} = \nu D_{11}; \quad D_{66} = \frac{Eh^3}{24(1+\nu)}; \\ &K_{11} = K_{22} = K_{12} = K_{66} = 0. \end{aligned} \tag{18.76}$$

In Eqs (18.75), E_1 and E_2 are the moduli of elasticity in the direction of the meridian and parallel, respectively; ν_1 and ν_2 are Poisson's ratios in those directions, respectively; and G is the shear modulus in a plane that is parallel to the coordinate surface. In Eqs (18.76), E and ν are the modulus of elasticity and Poisson's ratio for the isotropic shell material.

The equations of equilibrium, kinematic relations, and constitutive equations (18.73) can be reduced to the eight-order system of 12 governing differential equations involving 12 unknown functions of the displacements, internal forces, and moments for the multilayered orthotropic shells of revolution. The higher order of this system and large number of equations and unknown functions present major problems for its solving. So, only numerical and approximate methods discussed in Chapter 6 can be employed for the analysis of the state of stress and strain of multilayered orthotropic shells.

18.5 SANDWICH SHELLS

Sandwich shells are commonly used in aircraft construction, shipbuilding, industrial building, etc., because they are quite efficient constructions: high strength is successfully combined with low weight. In this section we present a small-deflection elastic theory of orthotropic sandwich shallow shells that takes into account deformations due to the transverse shear. This theory represents a natural extension of the small-deflection theory of orthotropic sandwich plates introduced in Sec. 7.6.

The sandwich shell construction is quite similar to the sandwich plate introduced in Sec. 7.6 (see Fig. 7.8). The load-carrying flexural mechanism of a sandwich shell is also analogous to that of a sandwich plate. Assume that all the sandwich construction notations introduced in the plate sandwich theory in Sec. 7.6 are also adopted in the shell sandwich.

The basic theory of orthotropic sandwich cylindrical shells was developed by Stein and Mayers [9]. We present this theory as applied to shallow sandwich shells. It is assumed that a sandwich shell – just as discussed previously for a sandwich plate – behaves elastically as a homogeneous orthotropic shell with some mechanical properties, which characterize its mechanical behavior and peculiarities of its load-carrying mechanism under applied loads. The seven physical constants that characterize the flexural mechanism of flat plates have been presented in Sec. 7.6 (the subscripts x and y adopted in the sandwich plate theory are replaced by the subscripts 1 and 2 for the sandwich shell). These constants were the flexural stiffnesses D_1 and D_2, the flexural Poisson's ratios ν_1 and ν_2, the twisting stiffness D_{12}, and the shear stiffnesses D_{Q_1} and D_{Q_2}. Four of constants are related to each other by the following equality (see Sec. 7.6):

$$\nu_1 D_2 = \nu_2 D_1.$$

As mentioned previously, the behavior of a shell under applied loading differs essentially from the behavior of a flat plate. The applied loading is resisted predominantly by the in-plane stressing of the shell (see Chapter 10). Thus, the seven physical constants characterizing the flexural mechanism must be complemented by some physical constants that represent the membrane actions of a sandwich shell. The five additional constants appearing in the sandwich shell theory were introduced in Ref. [9] and are the extensional stiffnesses, Λ_1 and Λ_2, the extensional Poisson's ratios, ν_1' and ν_2', and the in-plane shear stiffness Λ_{12}. They can be introduced as follows:

$$\Lambda_1 = \frac{N_1}{\varepsilon_1}; \quad \Lambda_2 = \frac{N_2}{\varepsilon_2}; \quad \nu_1' = -\frac{\varepsilon_2}{\varepsilon_1}; \quad \nu_2' = -\frac{\varepsilon_1}{\varepsilon_2}; \quad \Lambda_{12} = \frac{N_{12}}{\gamma_{12}} = \frac{N_{21}}{\gamma_{21}} = \frac{S}{\gamma_{12}}. \tag{18.77}$$

These physical constants can be determined either theoretically in some simple cases or experimentally [9,10].

The equilibrium and strain–displacement relations for the small-deflection orthotropic shallow shell theory will coincide with the corresponding equations derived in Sec. 17.3 and 17.4 for the homogeneous isotropic shallow shells. The equilibrium equations of the small-deflection theory of shallow shells can be obtained from Eqs (12.41) and (12.42), letting $\alpha = x$, $\beta = y$, and $A = B = 1$. The above equations have the following form (for $p_1 = p_2 = 0$):

$$\begin{aligned}
&\frac{\partial N_1}{\partial x} + \frac{\partial S}{\partial y} = 0; \quad \frac{\partial N_2}{\partial y} + \frac{\partial S}{\partial x} = 0; \\
&\frac{\partial Q_1}{\partial x} + \frac{\partial Q_2}{\partial y} + \frac{N_1}{R_1} + \frac{N_2}{R_2} + p_3 = 0; \\
&Q_1 - \frac{\partial M_1}{\partial x} - \frac{\partial H}{\partial y} = 0; \quad Q_2 - \frac{\partial M_2}{\partial y} - \frac{\partial H}{\partial x} = 0
\end{aligned} \tag{18.78a-e}$$

where all the stress resultants and stress couples are referred to the middle surface of the sandwich shell. The sign convention for the internal forces and moments coincides with that adopted for the general shell theory of a homogeneous shell. It is also assumed that, due to the assumptions adopted in the general shallow shell theory, $N_{12} = N_{21} = S$ and $M_{12} = M_{21} = H$.

Now, we can turn our attention to the constitutive relations. The bending and twisting moments, changes in curvature, and twist relations remain analogous to those derived in the sandwich plate theory (see Eqs (7.129)). The relations between the elastic membrane strains and the membrane forces, taking into account Eqs (18.77), can be represented in the form

$$\varepsilon_1 = \frac{N_1}{\Lambda_1} - \nu_2' \frac{N_2}{\Lambda_2}; \quad \varepsilon_2 = \frac{N_2}{\Lambda_2} - \nu_1' \frac{N_1}{\Lambda_1}; \quad \gamma_{12} = \frac{S}{\Lambda_{12}}. \tag{18.79}$$

Solving these equations for the membrane forces yields the following:

$$N_1 = \frac{\Lambda_1}{1 - \nu_1'\nu_2'}(\varepsilon_1 + \nu_2'\varepsilon_2); \quad N_2 = \frac{\Lambda_2}{1 - \nu_1'\nu_2'}(\varepsilon_2 + \nu_1'); \quad S = \Lambda_{12}\gamma_{12}. \tag{18.80}$$

Substituting the expressions for the middle surface strains from Eqs (17.43) into the above equations, one obtains

$$\begin{aligned}
N_1 &= \frac{\Lambda_1}{1 - \nu_1'\nu_2'}\left[\frac{\partial u}{\partial x} - \frac{w}{R_1} + \nu_2'\left(\frac{\partial v}{\partial Y} - \frac{w}{R_2}\right)\right], \\
N_2 &= \frac{\Lambda_2}{1 - \nu_1'\nu_2'}\left[\frac{\partial v}{\partial y} - \frac{w}{R_2} + \nu_1'\left(\frac{\partial u}{\partial x} - \frac{w}{R_1}\right)\right], \\
S &= \Lambda_{12}\left(\frac{\partial v}{\partial x} + \frac{\partial u}{\partial y}\right).
\end{aligned} \tag{18.81}$$

Equations (18.78), (7.129), and (18.81) represent the 11 basic equations that are necessary for determining the internal forces, moments, and displacements acting in the sandwich shallow shell. The number of the governing equations can be reduced to five by substituting Eqs (7.129) and (18.81) into Eqs (18.78). As a result, the five differential equations with five unknowns – the shear forces Q_1 and Q_2 and

displacements u, v, and w – are obtained. Because of the awkwardness of these five differential equations for the orthotropic sandwich shallow shell, they are not given here. The interested reader is referred to Refs [9–11], where these equations are presented.

For a special case of an isotropic sandwich shallow shell with non-direct-stress-carrying core, the physical constants are simplified to the following form:

$$\begin{aligned} &D_{Q_1} = D_{Q_2} = D_Q = \frac{d^2}{c} G_c; \quad \nu_1 = \nu_2 = \nu_1' = \nu_2' = \nu, \\ &D_1^* = D_2^* = D_s = \frac{E_f t d^2}{2(1-\nu_f^2)}; \quad D_{12} = D_s(1-\nu), \\ &\Lambda_1 = \Lambda_2 = 2E_f t; \quad \Lambda_{12} = \frac{E_f t}{1+\nu}; \quad d = c + t, \end{aligned} \tag{18.82}$$

where all the above notations are explained in Sec.7.6. For this special case, the system of the five governing differential equations for an orthotropic sandwich shallow shell can be reduced to a single eight-order differential equation in w. Dropping the intermediate and lengthy mathematical manipulations associated with deriving this equation, we present below only the final result:

$$D_s \nabla^4 \nabla^4 w + \left(1 - \frac{D_s}{D_Q}\nabla^2\right)\left[2E_f t\left(\frac{1}{R_2}\frac{\partial^2}{\partial x^2} + \frac{1}{R_1}\frac{\partial^2}{\partial y^2}\right)^2 w - \nabla^4 p_3\right] = 0, \tag{18.83}$$

where

$$\nabla^4(\ldots) \equiv \frac{\partial^4(\ldots)}{\partial x^4} + 2\frac{\partial^4(\ldots)}{\partial x^2 \partial y^2} + \frac{\partial^4(\ldots)}{\partial y^4}$$

is a biharmonic operator.

It can be easily shown that if $R_1 \to \infty$ and $R_2 \to \infty$, this equation is equivalent to Eq. (7.135) derived in Sec. 7.5.1 for isotropic sandwich flat plates. Note that in the limiting case when the shear modulus approaches infinity, Eq. (18.83) is reduced to the governing differential equation of the homogeneous isotropic shallow shell theory with the flexural stiffness D_f, i.e., with the stiffness of a composite section composed from two facings separated by a distance which is equal to the depth of the core.

18.6 THE FINITE ELEMENT REPRESENTATIONS OF SHELLS

18.6.1 Introduction

We have seen in previous chapters of Part II that the shell problems associated with determining displacements, internal forces, and moments are described by high-order partial differential equations with variable coefficients. Only in very special cases of shell geometry, boundary conditions, and loadings is it possible to obtain reasonably accurate closed-form solutions and to develop relatively general analytical expressions for deformations and stresses (see Chapters 14–17). Such closed-form expressions, obtained in terms of arbitrary parameters defining a shell geometry, boundary conditions, and loading, are of considerable interest for a designer. In

fact, the analytical solutions permit any desired parametric studies to be conducted, rapid calculation of actual stresses and deformations in shell structures, and they provide a basis for error estimates of numerical solutions obtained by approximate methods.

However, available analytical solutions of shell structural problems are, nevertheless, limited in scope and, in general, do not apply to arbitrary shapes, loading, irregular stiffening, cutouts, support conditions, and many other aspects of practical design. Therefore, not surprisingly, the development of numerical formulations over the past 50 years, notably the finite element method (FEM), has enabled one to analyze thin shell structures. As mentioned in Sec. 6.7, the FEM is a general numerical procedure that can be used to tackle any problem of structural stress analysis, including shell problems, to any desired degree of accuracy. However, initially, one needs to understand the response of the basic individual elements making up a shell structure, and then to assemble such elements by enforcing compatibility of deformations between elements at their common nodes, and equilibrium of forces and moments at all nodes, as well as constraint conditions at the boundary nodes of the structure. Then, the overall response of the complete shell structure can be predicted.

The general procedure of an application of the FEM to thin shell structures is quite similar to that discussed in Sec. 6.7 for plate bending problems. We discuss in this section some issues regarding the peculiarities of the FEM representation and formulation for thin shell structural analysis.

There are three distinct approaches to the finite element representation of thin shell structures [12]:

(a) in "faceted" form with flat elements;
(b) via curved elements formulated on the basis of thin shell theory; and
(c) by means of the three-dimensional (solid) elements.

This section is concerned with the flat and curved shell elements only. Various applications of the solid finite elements to the stress analysis are given in Refs [12,13,14, etc.]. We consider below several applications of the FEM to some shell geometries.

18.6.2 The finite element solutions of axisymmetrically loaded shells of revolution

The axisymmetric bending of shells of revolution was studied in Sec. 16.3. It was shown in the above section that the state of stress and strain of such shells is governed by the ordinary differential equations: i.e., the displacements, internal forces, moments, and stresses are functions of one variable (meridional coordinate) only. Let us take the length of the meridian arc, s, measured from some reference point of the shell, as the meridional coordinate of a point in the middle surface.

If we apply the FEM to the bending analysis of axisymmetrically loaded shells of revolution, then the finite element should be one dimensional. Such an element may be represented in the form of a frustum: i.e., as a ring, generated by the straight line segment between two parallel circles or "nodes", say, i and j, as shown in Fig. 18.7. The thickness may vary from element to element. To increase the accuracy of a solution, finite elements with curved generators are employed in some cases.

The displacement vector of a point in the midsurface is specified by two components u and w in the meridional and normal directions, respectively (see Sec. 16.3).

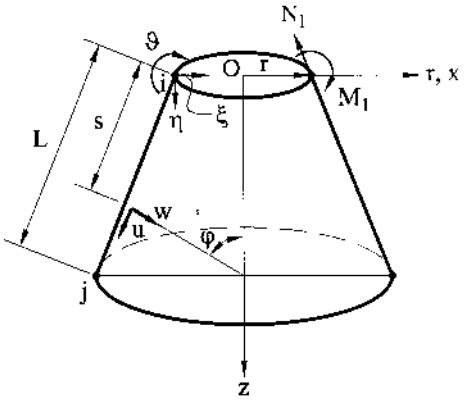

Fig. 18.7

Using the relationships $r = R_2 \sin\varphi$ and $\mathrm{d}s = R_1 \mathrm{d}\varphi$, we can rewrite the strain–displacement equations (16.11) in terms of variable s, as follows:

$$\begin{aligned} \varepsilon_1 &= \frac{\mathrm{d}u}{\mathrm{d}s} - \frac{w}{R_1}, \quad \varepsilon_2 = \frac{1}{r}(u\cos\varphi - w\sin\varphi), \\ \chi_1 &= -\frac{\mathrm{d}\vartheta_1}{\mathrm{d}s}, \quad \chi_2 = -\frac{\cos\varphi}{r}\vartheta_1, \\ \vartheta_1 &= \frac{u}{R_1} + \frac{\mathrm{d}w}{\mathrm{d}s} \end{aligned} \tag{18.84}$$

(for simplicity from hereon the subscript 1 in the notation for the angle of rotation ϑ is omitted).

The Codazzi–Gauss condition for shells of revolution is

$$\frac{\mathrm{d}r}{\mathrm{d}s} = \cos\varphi. \tag{18.85}$$

Introduce the displacement $\{f\}$ and strain $\{\varepsilon\}$ vectors, respectively, as follows:

$$\{f\}^T = [u, w], \tag{18.86a}$$

$$\{\varepsilon\}^T = [\varepsilon_1, \varepsilon_2, \chi_1, \chi_2]. \tag{18.86b}$$

Using the above notations, we can rewrite the kinematic relationships (18.84) for the finite element shown in Fig. 18.7 in the following matrix form:

$$\{\varepsilon\} = [R]\{f\}, \tag{18.87}$$

where

$$[R] = \begin{bmatrix} \dfrac{\mathrm{d}}{\mathrm{d}s} & -\dfrac{1}{R_1} \\ \dfrac{\cos\varphi}{r} & -\dfrac{\sin\varphi}{r} \\ -\dfrac{\mathrm{d}}{\mathrm{d}s}\left(\dfrac{1}{r_1}\right) & -\dfrac{\mathrm{d}^2}{\mathrm{d}s^2} \\ -\dfrac{\cos\varphi}{rR_1} & -\dfrac{\cos\varphi}{r}\dfrac{\mathrm{d}}{\mathrm{d}s} \end{bmatrix} \tag{18.88}$$

The stress resultant and couples–strain relations, Eqs. (16.13), can also be presented in the matrix form, as follows:

$$\{\sigma\} = [D]\{\varepsilon\}, \tag{18.89}$$

where

$$\{\sigma\}^T = [N_1, N_2, M_1, M_2] \tag{18.90}$$

is the stress resultants and couples vector and

$$[D] = \frac{Eh}{1-\nu^2}\begin{bmatrix} 1 & \nu & 0 & 0 \\ \nu & 1 & 0 & 0 \\ 0 & 0 & h^2/12 & \nu h^2/12 \\ 0 & 0 & \nu h^2/12 & h^2/12 \end{bmatrix} \tag{18.91}$$

is the elasticity matrix.

The strain energy, stored by an axisymmetrically loaded shell of revolution in bending, can be obtained from Eq. (12.53) by letting $S = H = 0$ and replacing $AB\mathrm{d}\alpha\mathrm{d}\beta$ with $\mathrm{d}A$. We have

$$U = \frac{1}{2}\int\int_A (N_1\varepsilon_1 + N_2\varepsilon_2 + M_1\chi_1 + M_2\chi_2)\mathrm{d}A. \tag{18.92}$$

Using the vector notations introduced above for the strains and stress resultants and couples, and noting that the area of the element $\mathrm{d}A = r\mathrm{d}s\mathrm{d}\theta$ and integrating (18.92) over θ from 0 to 2π, we can represent Eq. (18.92) for the one-dimensional finite element in Fig. 18.7, as follows:

$$U = 2\pi\int_{s_0}^{s_1} \{\varepsilon\}^T\{T\}r\mathrm{d}s, \tag{18.93}$$

where s_0 and s_1 are the end points of the s arc.

The vector of external forces can be represented in the form

$$\{P\}^T = [p_x, p_z], \tag{18.94}$$

where p_x and p_z are the horizontal (or radial) and vertical (or axial) components of an applied loading, respectively. If a shell is subjected to an external normal pressure q, then

$$p_z = q\cos\varphi, \quad p_x = q\sin\varphi. \tag{18.95}$$

The work done by external loads applied along the displacements given by the vector $\{f\}$ can be represented as follows:

$$W_e = 2\pi\int_{s_0}^{s_1} \{f\}^T\{P\}r\mathrm{d}s. \tag{18.96}$$

Next, let us introduce the two nodal displacement vectors that characterize the degrees of freedom of the finite element in the form of a frustum with a straight generator (see Fig. 18.7) and designated by e, as follows:

$$\{g\}_e = \begin{Bmatrix} \{g_i\} \\ \{g_j\} \end{Bmatrix}, \quad \{g_i\}^T = [u_i, w_i, \vartheta_i], \quad (i \to j), \tag{18.97}$$

$$\{\delta\}_e = \begin{Bmatrix} \{\delta_i\{ \\ \{\delta_j\} \end{Bmatrix}, \quad \{\delta_i\}^T = [\xi_i, \eta_i, \vartheta_i], \quad (i \to j), \tag{18.98}$$

where $\vartheta_i = (\mathrm{d}w/\mathrm{d}s)_i$ and $\xi_{i(j)}$ and $\eta_{i(j)}$ are the horizontal (or radial) and vertical (or axial) displacements at the nodal point $i(j)$. The nodal displacement vectors introduced above are related to one another, as follows (see Eq. (16.37)):

$$\{g_i\} = [\lambda]\{\delta_i\}, \quad (i \to j) \tag{18.99}$$

where

$$[\lambda] = \begin{bmatrix} -\cos\varphi & \sin\varphi & 0 \\ \sin\varphi & \cos\varphi & 0 \\ 0 & 0 & 1 \end{bmatrix}. \tag{18.100}$$

Let us approximate the displacement field across the given finite element by the following polynomials:

$$\begin{aligned} u &= \alpha_1 + \alpha_2 s, \\ w &= \alpha_3 + \alpha_4 s + \alpha_5 s^2 + \alpha_6 s^3. \end{aligned} \tag{18.101}$$

To determine the values of the coefficients α_k ($k = 1, 2, \ldots, 6$), the coordinate s of the nodal points is substituted in the displacement functions (18.101). This will generate six equations in which the only unknowns are the above coefficients. By so doing, we can solve for α_k in terms of the nodal displacements $u_i, w_i, \ldots, \vartheta_j$ and finally obtain the following:

$$\{f\} = \left[\hat{N}\right]\{g\}_e \tag{18.102}$$

where {f} is given by Eq. (18.86a)
and

$$\left[\hat{N}\right] = \begin{bmatrix} 1-l & 0 & 0 & l & 0 & 0 \\ 0 & 1-3l^2+2l^3 & L(l-2l+l^2) & 0 & 3l^2-2l^3 & L(-l+l^2) \end{bmatrix}; \tag{18.103}$$

here $l = s/L$, where L is the length of the frustum meridian for the given finite element (see Fig. 18.7).

Substituting for the vector $\{g\}$from Eq. (18.99) into Eq. (18.102), yields

$$\{f\} = \left[\hat{N}\right]\begin{bmatrix} [\lambda] & 0 \\ 0 & [\lambda] \end{bmatrix}\{\delta\}_e = \left[\left[\hat{N}_i\right][\lambda], \left[\hat{N}_j\right][\lambda]\right]\{\delta\}_e = [N]\{\delta\}_e. \tag{18.104}$$

Equation (18.87) then leads to

$$\{\varepsilon\} = [R][N]\{\delta\}_e = [B]\{\delta\}_e, \tag{18.105}$$

where

$$[B] = \left[[B_i][\lambda], [B_j][\lambda]\right] \tag{18.106}$$

and

$$[B_i] = [R]\left[\hat{N}_i\right] \quad (i \to j). \tag{18.107}$$

Substituting for $\{\sigma\}$ from Eq. (18.89) into Eq. (18.93) and taking into account Eq. (18.105), we obtain the expression of the strain energy stored by the finite element designated by e in the following form

$$U = \{\delta\}_e^T \left((\pi \int_{s_0}^{s_1} [B]^T [D][B] r \mathrm{d}s \right) \{\delta\}_e. \tag{18.108}$$

Using the notations adopted in Sec. 6.7, and letting $\mathrm{d}A = r\mathrm{d}s\mathrm{d}\theta = r\mathrm{d}\theta(L\mathrm{d}l)$ integrating over θ from 0 to 2π, we obtain from Eq. (6.63) the stiffness matrix for the finite element e, as follows:

$$[k]_e = 2\pi L \int_0^1 [B]^T [D][B] r \mathrm{d}l. \tag{18.109}$$

The explicit expressions for the matrices $[B]$ and $[k]_e$ are given in Ref. [14–16]. Prior to integration of the above expression, the radius of the parallel circle r must be expressed as a function of s.

Steps 1 to 5 of the general FEM procedure, described in Sec. 6.7, may now be applied to obtain the solution of the shell nodal displacements. Then, the strains, stress resultants and couples, and finally, the stress components can be determined from Eqs (18.87), (18.89), and (16.17).

In conclusion, note that the finite elements in the form of the frustum can be also applied to the analysis of asymmetrically loaded shells of revolution. If only the membrane solution is required, the quantities χ_1, χ_2, M_1, and M_2 are ignored and the expressions developed in this section are considerably reduced in complexity.

18.6.3 Analysis of shallow shells of double curvature by the FEM

The theory of thin shallow shells was presented in Sec. 17.4. Let us introduce the strain vector $\{\varepsilon\}$ and the vector of stress resultants and couples $\{\sigma\}$ for shallow shells, as follows:

$$\begin{aligned} \{\varepsilon\}^T &= [\varepsilon_1, \varepsilon_2, \gamma_{12}, \chi_1, \chi_2, \chi_{12}], \\ \{\sigma\}^T &= [N_1, N_2, S, M_1, M_2, H], \end{aligned} \tag{18.110}$$

where the strain components, internal forces, and moments are given by Eqs (17.43), (12.45), and (12.46), respectively.

The total potential energy of a shallow shell in bending, Π, can be defined as a sum of the strain energy U (Eq. 12.53) and the potential energy of the applied loads. Letting $\mathrm{d}A = AB\mathrm{d}\alpha\mathrm{d}\beta$, we obtain:

$$\begin{aligned} \Pi = \frac{1}{2} \int\int_A (N_1\varepsilon_1 + N_2\varepsilon_2 + S\gamma_{12} + M_1\chi_1 + M_2\chi_2 + 2H\chi_{12}) \mathrm{d}A \\ - \int\int_A (p_1 u + p_2 v + p_3 w) \mathrm{d}A. \end{aligned} \tag{18.111}$$

As mentioned previously, a midsurface of a shallow shell can be approximated by flat or by curved finite elements when applying the FEM technique. We consider below both two approximations of the shell geometry.

1. A curved finite element in the form of a shallow shell of double curvature

Let us consider a finite element in the form of a shallow shell of double curvature having a rectangular projection on the Oxy coordinate plane, as shown in Fig. 18.8. At each nodal (corner) point of this finite element, designated by 1, 2, 3, and 4, we consider the possible three displacement components u, v, and w in the directions of the coordinate axes x, y, and z, respectively; two angles of rotations, $\alpha \equiv \vartheta_1$ and $\beta \equiv \vartheta_2$, about the y and x axes, respectively; and the value ω modeling a twist at a nodal point of interest. Thus, the curved finite element of the shallow shell shown in Fig. 18.8, has 24 degrees of freedom.

To approximate the displacement fields in the above finite element, we make the following assumptions:

(a) The displacements $u(x, y)$ and $v(x, y)$ depend only on the in-plane displacements of the nodal points and they are distributed linearly across the finite element area. So, for example, all points of the finite element will receive only the horizontal (in the coordinate plane Oxy) displacements due to a unit displacement of the nodal point 4 along the x axis (i.e., $u_4 = 1$). The above horizontal displacements will be distributed along line 2–4, according to the relationship y/b, along line 3–4, according to x/a, and over the entire area of the finite element, according to the relationship $u(x, y) = \frac{x}{a}, \frac{y}{b}$.

(b) The deflections $w(x, y)$ do not depend on the in-plane (horizontal) displacements of the nodal points, and they can be approximated by a polynomial with 16 degrees of freedom.

These assumptions provide a way of presenting an approximation of displacements in the explicit form that avoids a very cumbersome operation of inverting the matrix $[C]$ (see Sec. 6.7.2).

The approximation of the displacements across the finite element can be given in the following compact form:

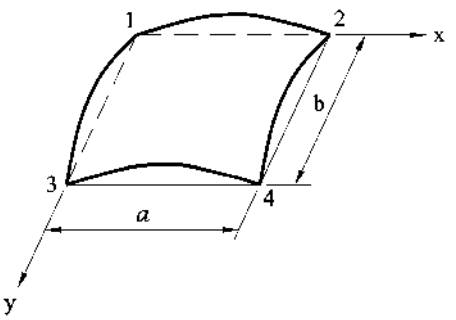

Fig. 18.8

$$
\begin{aligned}
u(x,y) &= X_1Y_1u_1 + X_2Y_1u_2 + X_1Y_2u_3 + X_2Y_2u_4,\\
v(x,y) &= X_1Y_1v_1 + X_2Y_1v_2 + X_1Y_2v_3 + X_2Y_2v_4,\\
w(x,y) &= X_3Y_3w_1 + X_4Y_3\alpha_1 - X_3Y_4\beta_1 + X_4Y_4\omega_1\\
&\quad + X_5Y_3w_2 + X_6Y_3\alpha_2 - X_5Y_4\beta_2 + X_6Y_4\omega_2 + X_3Y_5w_3\\
&\quad + X_4Y_5\alpha_3 + X_3Y_6\beta_3 + X_4Y_6\omega_3 + X_5Y_5w_4 + X_6Y_5\alpha_4\\
&\quad - X_5Y_6\beta_4 + X_6Y_6\omega_4,
\end{aligned}
\tag{18.112}
$$

where $u_i = u(x_i, y_i)$, $v_i = v(x_i, y_i)$, $w_i = w(x_i, y_i)$, $\alpha_i = \alpha(x_i, y_i)$, and $\beta_i = \beta(x_i, y_i)$, $i = 1, 2, 3, 4$; and

$$
X_1 = \frac{a-x}{a}, \quad X_2 = \frac{x}{a}, \quad X_3 = \frac{1}{a^3}(2x^3 - 3ax^2 + a^3), \quad X_4 = \frac{1}{a^2}(x^3 - 2ax^2 + a^2x),
$$
$$
X_5 = -\frac{1}{a^3}(2x^3 - 3ax^2), \quad X_6 = \frac{1}{a^2}(x^3 - ax^2).
\tag{18.113}
$$

The polynomials of the Y type are analogous to the X-type polynomials if one replaces x with y and a with b.

One can use other types of displacement approximations. For example, the deflections $w(x, y)$ can be approximated similar to the deflections for a rectangular bending finite element of a flat plate, introduced in Sec. 6.7 (see the polynomial (6.46)).

Applying the general procedure of the FEM described in Sec. 6.7, one can construct the stiffness matrix for the shallow shell element and then write the governing equations of the type (6.74) for the entire shell. Solving these equations, yields the nodal displacements in the shell field. Having determined these displacements, we can determine the in-plane strains, changes in curvature and in twist, the stress resultants and couples, and finally, the stress components.

The governing equation of the type (6.70) for the shell finite element relates the nodal displacements to the nodal forces. Recall that this equation was derived from the minimum potential energy principle. However, it may also be considered as a result of the direct application of the principle of virtual work. Since the degrees of freedom has a physical sense of displacements, the components of the stiffness matrix, $(k_{ij})_e$, can be treated as the nodal forces occurring in the direction of the ith degree of freedom due to the jth unit displacement if all other $(i \neq j)$ degrees of freedom $\delta_i = 0$ for a given finite element. Then, using the above, the coefficients of the stiffness matrix for the given shallow shell finite element can be represented in the following form:

$$
(k_{ij})_e = \int_0^a \int_0^b (N_{1i}\varepsilon_{1i} + N_{2i}\varepsilon_{2i} + S_i\gamma_{12i} + M_{1i}\chi_{1i} + M_{2i}\chi_{2i} + 2H\chi_{12i})\mathrm{d}x\mathrm{d}y.
\tag{18.114}
$$

As an example, determine the horizontal reaction of the node 1 in the y direction due to the deflection (w_1) of this node. We denote this component of the stiffness matrix by $k_{v_1w_1}$. First, determine the components of the deformation vector across the area of the finite element due to the deflection w_1. We have

$$\varepsilon^{(1)}_{1w_1} = -\frac{1}{R_1} X_3 Y_3 w_1, \quad \varepsilon^{(1)}_{2w_1} = \frac{1}{R_2} X_3 Y_3 w_1, \quad \gamma^{(1)}_{12w_1} = 0,$$
$$\chi^{(1)}_{1w_1} = -X_{3,XX} Y_3 w_1, \quad \chi^{(1)}_{2w_1} = -X_3 Y_{3,YY} w_1, \quad \chi^{(1)}_{12w_1} = -X_{3,X} Y_{3,Y} w_1, \tag{18.115}$$

where the superscript 1 denotes the number of the nodal point of interest. Then, we can find the components of the stress resultant vector due to v_1. We have

$$N^{(1)}_{1v_1} = \frac{Eh\nu}{1-\nu^2} X_1 Y_{1,Y} v_1, \quad N^{(1)}_{2v_1} = \frac{Eh}{1-\nu^2} X_1 Y_{1,Y} v_1, \quad S^{(1)}_{v_1} = \frac{Eh}{2(1+\nu)} X_{1,X} Y_1 v_1. \tag{18.116}$$

In Eqs (18.115) and (18.116), the comma notation denotes a partial differentiation of the polynomials X_i and Y_i, i.e.,

$$X_{3,XX} = \frac{\partial^2 X_3}{\partial x^2} = \frac{12x - 6a}{a^3}, \quad Y_{3,YY} = \frac{\partial^2 Y_3}{dy^2} = \frac{12y - 6b}{b^3},$$
$$X_{3,X} = \frac{\partial X_3}{\partial x} = \frac{6x^2 - 6ax}{a^3}, \quad Y_{3,Y} = \frac{\partial Y_3}{\partial y} = \frac{6y^2 - 6yb}{b^3},$$
$$X_{1,X} = \frac{\partial X_1}{\partial x} = -\frac{1}{a}, \quad Y_{1,Y} = \frac{\partial Y_1}{\partial y} = -\frac{1}{b}.$$

Substituting the components of vectors $\{\sigma\}_{v_1}$ and $\{\varepsilon\}_{w_1}$ into Eqs (18.115), (18.116), and (18.114) yields the following:

$$\begin{aligned} k_{v_1 w_1} &= \int_0^a \int_0^b \left(N^{(1)}_{1v_1} \varepsilon^{(1)}_{1w_1} + N^{(1)}_{2v_1} \varepsilon^{(1)}_{2w_1} + S^{(1)}_{v_1} \gamma^{(1)}_{12w_1} \right) \mathrm{d}x\mathrm{d}y, \\ &= \int_0^a \int_0^b \left[\frac{Eh\nu}{1-\nu^2} X_1 Y_{1,Y} \left(-\frac{1}{R_1} \right) X_3 Y_3 + \frac{Eh}{1-\nu^2} X_1 Y_{1,Y} \left(-\frac{1}{R_2} \right) X_3 Y_3 \right] \mathrm{d}x\mathrm{d}y, \\ &= \frac{7}{40} \frac{Eh}{1-\nu^2} \left[a \left(\frac{\nu}{R_1} + \frac{1}{R_2} \right) \right]. \end{aligned} \tag{18.117}$$

Similarly, the rest of the components of the stiffness matrix $(k_{ij})_e$ can be obtained. In this example, it was assumed that $\kappa_1 = \text{const}$ and $\kappa_2 = \text{const}$.

2. A flat finite element for the analysis of shallow shells

We considered above a curved shallow shell finite element whose surface is consistent to the surface of the entire shallow shell. However, the stiffness matrix constructed above has a serious drawback associated with the presence of rigid body motions. This means that if such a finite element is subjected to some displacement modeling its transfer in a space without straining (for example, $w_1 = w_2 = w_3 = w_4 = t$ while all the rest of the degrees of freedom are equal to zero), then some stresses occur in that element, resulting in an obvious contradiction. An appearance of such a phenomenon essentially decreases the accuracy of the analysis and sometimes can result in divergence of a solution. An elimination of this phenomenon can be carried out at the expense of a special treatment of the obtained stiffness matrix. However, this treatment may result in violation of the matrix symmetry, compatibility of its components,

and completeness of approximating functions. Therefore, the problem of the development of finite elements for shallow shells of double curvature is very complicated.

From a physical point of view, it is advantageous to employ flat finite elements for the analysis of shallow shells of double curvature. In this case, a shell element can be obtained as a simple combination of the corresponding elements for plane stress and for plate bending by satisfying all the necessary requirements. Geometric features of the shell are taken into account by the geometry of an inscribed polyhedron. Since the approximation accuracy of the shell surface is increased with a finer element mesh, it is possible to state that the FEM convergence will be achieved in this case.

When assigning an assemblage of flat finite elements for a shallow shell, one must inscribe the elements into the shell geometry. Therefore, one can use rectangular elements for developable surfaces on a plane (e.g., cylindrical surfaces) and triangular elements for undevelopable surfaces (e.g., spherical shells). The stiffness matrix of a rectangular (or triangular) flat shell finite element can be obtained as a simple superposition of the stiffness matrices of that element for plane stress and for plate bending. The stiffness matrix for a flat plate bending finite element was introduced in Sec. 6.7.

Consider the derivation of the stiffness matrix for the rectangular plane stress finite element 1–2–3–4 shown in Fig. 18.8 (the projection of a shallow shell curved element on the Oxy coordinate plane). Assume that the in-plane displacement pattern is defined by the following polynomials:

$$\begin{aligned} u(x, y) &= \alpha_1 + \alpha_2 x + \alpha_3 y + \alpha_4 xy, \\ v(x, y) &= \alpha_5 + \alpha_6 x + \alpha_7 y + \alpha_8 xy. \end{aligned} \tag{18.118}$$

Thus, the generalized displacements of a node of the flat rectangular finite element in a matrix form are the following

$$\begin{Bmatrix} u \\ v \end{Bmatrix} = \begin{bmatrix} 1 & x & y & xy & 0 & 0 & 0 & 0 \\ 0 & 0 & 0 & 0 & 1 & x & y & xy \end{bmatrix} \begin{Bmatrix} \alpha_1 \\ \alpha_2 \\ \dots \\ \alpha_8 \end{Bmatrix} = [N]\{\alpha\}. \tag{18.119}$$

Let us introduce the nodal displacement vector of the above-mentioned element, as follows:

$$\{\delta\}_e^T = [u_1, v_1, u_2, v_2, \dots, u_4, v_4]. \tag{18.120}$$

It is seen that the displacement functions (18.118) contain the same number of unknown parameters α_k $(k = 1, 2, \dots, 8)$ as the number of the nodal displacements u_i and $v_i (i = 1, \dots, 4)$ and yield the linear displacements along the element sides. If we express the above coefficients α_k via nodal displacements, i.e., via the components of the element displacement vector $\{\delta\}_e$, we obtain

$$\{\delta\}_e = [C]\{\alpha\}, \tag{18.121}$$

where $[C]$ is an 8×8 matrix whose terms depend on the x and y coordinates of the nodal points of the given finite element. From Eq. (18.121), the vector $\{\alpha\}$ can be expressed as a function of the finite element nodal displacement vector, as follows:

$$\{\alpha\} = [C]^{-1}\{\delta\}_e. \tag{18.122}$$

Since the displacement functions are now expressed in terms of the nodal displacements in the explicit form, we can follow the same procedure as described in Sec. 6.7 for evaluating the components of the stiffness matrix of the plane stress finite element.

Here, only the general information about the FEM analysis and its application to shell structures has been presented. It should be noted that many books have appeared during the last four decades and they contain extensive discussions of FEM approaches and the related numerical procedures, for example [Refs 12–17].

18.7 APPROXIMATE AND NUMERICAL METHODS FOR SOLUTION OF NONLINEAR EQUATIONS

Analysis of flexible plates and shells is reduced to a solution of nonlinear differential equations for the stress function and deflection, Eqs (7.87) and (18.31), respectively. The solution of these equations via the classical analytical route can be obtained in exceptional cases only. Therefore, approximate and numerical methods acquire a great importance for the nonlinear plate and shell analysis. These methods, based on some iterative procedures, are usually combined with other well-known variational and numerical methods, introduced in Chapter 6 and Sec. 18.6, to obtain the solution of Eqs (7.87) and (18.31) with a reasonable accuracy.

We introduce below some approximate methods specially adapted to the analysis of flexible plates and shells under external loads.

18.7.1 The method of successive approximations

Let us use the flexible plate problem to illustrate the method of successive approximations. We rewrite Eqs (7.87), as follows

$$\begin{aligned} \frac{1}{Eh}\nabla^2\nabla^2\Phi &= -\frac{1}{2}L(w,w), \\ D\nabla^2\nabla^2 w &= L(\Phi,w)+p, \end{aligned} \tag{18.123}$$

where the operator $L(\ldots)$ is given by Eq. (18.30).

In the first approximation, the above system of equations is taken in the form

$$\begin{aligned} \nabla^2\nabla^2\Phi_1 &= 0, \\ D\nabla^2\nabla^2 w_1 &= p. \end{aligned} \tag{18.124a}$$

In the second approximation, the functions Φ_1 and w_1 are substituted into the right-hand sides of Eqs (18.122). We obtain

$$\begin{aligned} \frac{1}{Eh}\nabla^2\nabla^2\Phi_2 &= -\frac{1}{2}L(w_1,w_1), \\ D\nabla^2\nabla^2 w_{21} &= L(\Phi_1,w_1)+p, \end{aligned} \tag{18.124b}$$

and equations of the $(n+1)$th approximation will have the form

$$\begin{aligned} \frac{1}{Eh}\nabla^2\nabla^2\Phi_{n+1} &= -\frac{1}{2}L(w_n,w_n), \\ D\nabla^2\nabla^2 w_{n+1} &= L(w_n,\Phi_n)+p, \end{aligned} \tag{18.124c}$$

The solutions of Eqs (18.124) must satisfy the prescribed boundary conditions. The above iterative procedure is continued as long as a difference between two successive approximations is in the limits of the required accuracy. Thus, the above method reduces the solution of the nonlinear system of equations to a successive solution of the system of linear equations. In doing so, a new total, more precise, solution is obtained on each step of the above approximations.

Investigations show that the method of successive approximations provides a slow convergence, especially in the field of critical values of load. However, for loads causing large deflections lying in the range $h \le w \le 2h$, the given method possesses a satisfactory convergence.

18.7.2 The small-parameter method

The small-parameter method was introduced in Sec. 3.8 for the linear analysis of stiff plates with a variable thickness. In this section, we employ this method for the nonlinear analysis of flexible plates and shells. As an example, let us consider a flexible plate under a transverse uniform load p.

Let w_0 be the deflection at some reference point of the middle surface with coordinates x_0 and y_0. The ratio of w_0 to the plate thickness (or to its span) can be chosen as a small parameter, f. The latter should be less than unity.

The unknown functions w, Φ, and load p are sought in the form of the following series in powers of the parameter f:

$$\Phi = \sum_{i=1}^{\infty} \varphi^i v_i(x, y), \quad w = \sum_{i=1}^{\infty} f^i v_i(x, y), \quad p = \sum_{i=1}^{\infty} p_i f^i, \tag{18.125}$$

where $\varphi_i(x, y)$ and $v_i(x, y)$ are unknown functions to be determined, and p_i are some constant coefficients. Let us insert the expressions (18.125) into Eqs (7.87) and select the terms containing equal powers of f. We obtain new differential equations involving the functions v_i and φ_i with sequentially increasing indexes. So, the following system of equations will correspond to index $i = 1$:

$$\begin{aligned} \frac{1}{Eh}\nabla^2\nabla^2\varphi_1 &= 0, \\ D\nabla^2\nabla^2 v_1 &= p_1. \end{aligned} \tag{18.126a}$$

For $i = 2$, the system of equations is of the form

$$\begin{aligned} \frac{1}{Eh}\nabla^2\nabla^2\varphi_2 &= -\frac{1}{2}L(v_1, v_1), \\ D\nabla^2\nabla^2 v_2 &= L(v_1, \varphi_1) + p_2. \end{aligned} \tag{18.126b}$$

For $i = 3$,we obtain the following system of equations:

$$\begin{aligned} \frac{1}{Eh}\nabla^2\nabla^2\varphi_3 &= -\frac{1}{2}L(v_1, v_2) - \frac{1}{2}L(v_2, v_1) = -L(v_1, v_2), \\ D\nabla^2\nabla^2 v_3 &= L(v_2, \varphi_1) + L(v_1, \varphi_2) + p_3. \end{aligned} \tag{18.126c}$$

The boundary conditions must be added to Eqs (18.126). Furthermore, some additional conditions for determining the constants $p_1, p_2, \ldots$, can be introduced. For example, one can use the relationship $(w)_{x_0,y_0} = f$. Then, we obtain

$$(v_1)_{x_0,y_0} = 1, \tag{18.127a}$$

$$(v_2)_{x_0,y_0} = (v_3)_{x_0,y_0.} = \ldots = 0. \tag{18.127b}$$

Equations (18.126a) are linear equations describing the bending problem of stiff plates. If there are no in-plane forces in the middle surface, then the stress function φ_1 can be taken identically equal to zero, i.e., $\varphi_1 \equiv 0$. From the second Eq. (18.126a) and the relations (18.127a), taking into account the boundary conditions, the constant p_1 and function $v_1(x, y)$ are determined. Further, the function $v_1(x, y)$ is substituted into the right-hand side of Eqs (18.126b); in this case, $L(v_1, \varphi_1) = 0$, so that the second Eq. (18.126b) will repeat the second Eq. (18.126a). The first Eq. (18.126b) will provide a way of determining $\varphi_2(x, y)$. At the third step, let us substitute v_1, v_2, and φ_2 into the right-hand sides of Eqs (18.126c). As a result, the constant p_3 and function $v_3(x, y)$ will be found. Once, the constants $p_1, p_2, p_3, \ldots$ have been found, the value of f is approximately determined from the last relation (18.125) for the given load p.

This method, like the method of successive approximations, allows one to reduce the given nonlinear problem to a subsequent solution of the system of linear equations. In so doing, one obtains on each step of approximations, a more precise – but not a new, more correct, as in the method of successive approximations – solution.

Apparently, the small-parameter method will converge rapidly for reasonably small deviations from linear solutions. However, confidence limits of the application of the method so far have not been defined.

18.7.3 The method of successive loadings [18]

According to this method, a given load p is applied to a shell (or plate) by small portions. It is assumed that each such a portion of loading causes insignificant changes in the state of stress and strain (in order to neglect the nonlinear terms in the corresponding governing equations), so that a flexible plate or shell, subjected to the above-mentioned portion loading, can be analyzed with the use of linear differential equations.

Following the outline of Ref. [19], let us illustrate the use of this method for the solution of the nonlinear equations of a flexible shallow shell. After application of the first portion of loading p_0, the shell deflections are assumed to be small, so they can be determined from the linear equations (17.36). The latter have the following form (in the zero approximation):

$$\begin{aligned} \frac{1}{Eh}\nabla^2\nabla^2\Phi_0 + \nabla^2_{\kappa 0} w_0 &= 0, \\ D\nabla^2\nabla^2 w_0 - \nabla^2_{\kappa 0}\Phi_0 &= p_0, \end{aligned} \tag{18.128}$$

where

$$\begin{aligned} \nabla^2_{\kappa 0} w_0 &= \kappa_1 \frac{\partial^2 w_0}{\partial y^2} + \kappa_2 \frac{\partial^2 w_0}{\partial x^2}, \\ \nabla^2_{\kappa 0}\Phi_0 &= \kappa_1 \frac{\partial^2 \Phi_0}{\partial y^2} + \kappa_2 \frac{\partial^2 \Phi_0}{\partial x^2}. \end{aligned} \tag{18.129}$$

Then, the next small portion of loading, Δp_1, is applied to the shell. The deflection and stress function will take the increments Δw_1 and $\Delta\Phi_1$, respectively; therefore, they can be represented in the form

$$w_1 = w_0 + \Delta w_1, \quad \Phi_1 = \Phi_0 + \Delta\Phi_1. \tag{18.130}$$

Substituting the expressions (18.130) into Eqs (17.36), one obtains

$$\begin{aligned}
&\frac{1}{Eh}\nabla^2\nabla^2(\Phi_0 + \Delta\Phi_1) + \nabla^2_{\kappa 0}(w_0 + \Delta w_1) = -L_1[(w_0 + \Delta w_1), (w_0 + \Delta w_1)],\\
&D\nabla^2\nabla^2(w_0 + \Delta w_1) - \nabla^2_{\kappa 0}(\Phi_0 + \Delta\Phi_1) = L_2[(\Phi_0 + \Delta\Phi_1), (w_0 + \Delta w_1)]\\
&\qquad\qquad + p_0 + \Delta p_1.
\end{aligned} \tag{18.131}$$

where the operators $L_1(\ldots)$ and $L_2(\ldots)$ are given by Eq. (18.30).

Subtracting Eqs (18.131) and (18.128) member by member, we obtain

$$\begin{aligned}
&\frac{1}{Eh}\nabla^2\nabla^2\Delta\Phi_1 + \nabla^2_{\kappa 1}\Delta w_1 = -L_1(\Delta w_1, \Delta w_1),\\
&D\nabla^2\nabla^2\Delta w_1 - \nabla^2_{\kappa 1}(\Delta\Phi_1) - \nabla^2_1(\Delta w_1) = L_2(\Delta\Phi_1, \Delta w_1) + \Delta p_1,
\end{aligned} \tag{18.132}$$

where

$$\begin{aligned}
\nabla^2_{\kappa 1}(\Delta w_1) &= \left(\kappa_1 + \frac{\partial^2 w_0}{\partial x^2}\right)\frac{\partial^2(\Delta w_1)}{\partial y^2} - 2\frac{\partial^2 w_0}{\partial x\partial y}\frac{\partial^2(\Delta w_1)}{\partial x\partial y} + \left(\kappa_2 + \frac{\partial^2 w_0}{\partial y^2}\right)\frac{\partial^2(\Delta w_1)}{\partial x^2},\\
\nabla^2_{\kappa 1}(\Delta\Phi_1) &= \left(\kappa_1 + \frac{\partial^2 w_0}{\partial x^2}\right)\frac{\partial^2(\Delta\Phi_1)}{\partial y^2} - 2\frac{\partial^2 w_0}{\partial x\partial y}\frac{\partial^2(\Delta\Phi_1)}{\partial x\partial y} + \left(\kappa_2 + \frac{\partial^2 w_0}{\partial y^2}\right)\frac{\partial^2(\Delta\Phi_1)}{\partial x^2},\\
\nabla^2_1(\Delta w_1) &= \frac{\partial^2\Phi_0}{\partial y^2}\frac{\partial^2(\Delta w_1)}{\partial x^2} - 2\frac{\partial^2\Phi_0}{\partial x\partial y}\frac{\partial^2(\Delta w_1)}{\partial x\partial y} + \frac{\partial^2\Phi_0}{\partial x^2}\frac{\partial^2(\Delta w_1)}{\partial y^2}.
\end{aligned} \tag{18.133}$$

Since the load portions are assumed to be small, it can be expected that the increments of the deflection and stress function will also be sufficiently small. Then, all the nonlinear terms, $L_1(\Delta w_1, \Delta w_1)$ and $L_2(\Delta\Phi_1, \Delta w_1)$ can be omitted on the right-hand sides of Eqs (18.132). As a result, Δw_1 and $\Delta\Phi_1$ can be found from the following system of linear differential equations:

$$\begin{aligned}
&\frac{1}{Eh}\nabla^2\nabla^2(\Delta\Phi_1) + \nabla^2_{\kappa 1}(\Delta w_1) = 0,\\
&D\nabla^2\nabla^2(\Delta w_1) - \nabla^2_{\kappa 1}(\Delta\Phi_1) - \nabla^2_1(\Delta w_1) = \Delta p_1.
\end{aligned} \tag{18.134}$$

Repeating this procedure for the consequent small load portions, Δp_i, one obtains the equations for the increments $\Delta w_2, \Delta\Phi_2, \Delta w_3, \Delta\Phi_3, \ldots$. For an arbitrary load portion Δp_i, one can write the following system of linear differential equations:

$$\frac{1}{Eh}\nabla^2\nabla^2(\Delta\Phi_i) + \nabla^2_{\kappa i}(\Delta w_i) = 0,$$
$$D\nabla^2\nabla^2(\Delta w_i) - \nabla^2_{\kappa i}(\Delta\Phi_i) - \nabla^2_i(\Delta w_i) = \Delta p_i, \tag{18.135}$$

where

$$\nabla^2_{\kappa i}(\Delta w_n) = \left(\kappa_1 + \frac{\partial^2 w_{i-1}}{\partial x^2}\right)\frac{\partial^2(\Delta w_i)}{\partial y^2} - 2\frac{\partial^2 w_{i-1}}{\partial x\partial y}\frac{\partial^2(\Delta w_i)}{\partial x\partial y} + \left(\kappa_2 + \frac{\partial^2 w_{i-1}}{\partial y^2}\right)\frac{\partial^2(\Delta w_i)}{\partial x^2},$$

$$\nabla^2_{\kappa i}(\Delta\Phi_i) = \left(\kappa_1 + \frac{\partial^2(\Delta w_{i-1})}{\partial x^2}\right)\frac{\partial^2(\Delta\Phi_i)}{\partial y^2} - 2\frac{\partial^2 w_{i-1}}{\partial x\partial y}\frac{\partial^2(\Delta\Phi_i)}{\partial x\partial y} + \left(\kappa_2 + \frac{\partial^2 w_{i-1}}{\partial y^2}\right)\frac{\partial^2(\Delta\Phi_i)}{\partial x^2}, \tag{18.136}$$

$$\nabla^2_i(\Delta w_i) = \frac{\partial^2\Phi_{i-1}}{\partial y^2}\frac{\partial^2(\Delta w_i)}{\partial x^2} - 2\frac{\partial^2\Phi_{i-1}}{\partial x\partial y}\frac{\partial^2(\Delta w_i)}{\partial x\partial y} + \frac{\partial^2\Phi_{i-1}}{\partial x^2}\frac{\partial^2(\Delta w_i)}{\partial y^2}.$$

The total values of the deflection and stress function are determined, after the ith iterative step, as follows:

$$w_n = w_0 + \sum_{i=1}^{n}\Delta w_i, \quad \Phi_n = \Phi_0 + \sum_{i=1}^{\infty}\Delta\Phi_i. \tag{18.137}$$

Note that the above iterative process assumes that some transformations that had been done with the differential equations (18.128), (18.132), and (18.135) should be performed with the corresponding boundary conditions, if that is necessary.

It should be noted that in the multiple repetition of the successive approximations, the error of determining the functions w and Φ, caused by omitting the nonlinear terms, can be accumulated. To increase the accuracy of determining the deflections and stress function, the method of successive loading can be combined with the Newton method, which is introduced next. The latter can correct a given solution obtained at each step of loading.

18.7.4 The Newton method

Using the variational methods, finite element or finite difference methods, etc., the nonlinear differential equations (7.87) and (18.31) are reduced to a system of nonlinear algebraic equations. An exact solution of these equations is practically impossible. We introduce below one more approximate method, the Newton method, which is highly efficient for the solution of nonlinear algebraic equations.

Consider the following system of nonlinear equations

$$
\begin{aligned}
&F_1(x_1, x_2, \ldots, x_n) = 0,\\
&F_2(x_1, x_2, \ldots, x_n) = 0,\\
&\ldots\ldots\ldots\ldots\ldots\ldots\\
&F_n(x_1, x_2, \ldots, x_n) = 0.
\end{aligned}
\tag{18.138}
$$

Assume that the functions $F_i(x)(i = 1, 2, \ldots, n)$ have continuous derivatives with respect to all variables $x_1, x_2, \ldots, x_k$. Let us represent the system of equations (18.138) in the following matrix form:

$$
\mathbf{F}(\mathbf{x}) = 0, \tag{18.139}
$$

where

$$
\mathbf{F} = [F_1, F_2, \ldots, F_n]^T, \quad \mathbf{x} = [x_1, x_2, \ldots, x_n]^T \tag{18.140}
$$

are the n-dimensional vectors of functions F_i and independent variables x_i.

Assume that the kth approximation of the solution of Eqs (18.139) has been found in the form

$$
\mathbf{x}^{(k)} = \left[x_1^{(k)}, x_2^{(k)}, \ldots, x_n^{(k)}\right].
$$

Then, the exact solution of Eqs (18.139) can be represented in the following form:

$$
\mathbf{x} = \mathbf{x}^{(x)} + \mathbf{e}^{(k)}, \tag{18.141}
$$

where $\mathbf{e}^{(k)} = [e_1^{(k)}, e_2^{(k)}, \ldots, e_n^{(k)}]$ are some corrections (the solution errors). Let us introduce the Jacobi matrix of the functions $F_1, F_2, \ldots, F_n$ with respect to the independent variables $x_1, x_2, \ldots, x_n$, as follows:

$$
\mathbf{W}(\mathbf{x}) = \begin{bmatrix}
\dfrac{\partial F_1}{\partial x_1} \dfrac{\partial F_1}{\partial x_2} \cdots \dfrac{\partial F_1}{\partial x_n}\\
\dfrac{\partial F_2}{\partial x_1} \dfrac{\partial F_2}{\partial x_2} \cdots \dfrac{\partial F_2}{\partial x_n}\\
\ldots\ldots\ldots\ldots\\
\dfrac{\partial F_n}{\partial x_1} \dfrac{\partial F_n}{\partial x_2} \cdots \dfrac{\partial F_n}{\partial x_n}
\end{bmatrix}. \tag{18.142}
$$

If this matrix is nonsingular, i.e., if $\det \mathbf{W}(x) \neq 0$, then the correction $\mathbf{e}^{(k)}$ can be expressed as follows:

$$
\mathbf{e}^{(k)} = -\mathbf{W}^{-1}(\mathbf{x}^{(k)}) \cdot \mathbf{F}(\mathbf{x}^{(k)}), \tag{18.143}
$$

where $\mathbf{W}^{-1}(\mathbf{x}^{(k)})$ is the inverse Jacobi matrix. Thus, the successive approximations of the solution of Eqs (18.139) are obtained according to the following numerical procedure:

$$
\mathbf{x}^{(k+1)} = \mathbf{x}^{(k)} - \mathbf{W}^{-1}(\mathbf{x}^{(k)}) \cdot \mathbf{F}(\mathbf{x}^{(k)}) \quad (k = 0, 1, 2, \ldots). \tag{18.144}
$$

As zero approximation of the solution, $\mathbf{x}^{(0)}$, any rough approximation (for example, a graphical approximation) may be taken. The numerical procedure, described by Eq. (18.144), will stop when the following inequality is satisfied:

$$
\left|\mathbf{x}^{(k+1)} - \mathbf{x}^{(k)}\right| \leq \varepsilon,
$$

where ε is the required level of a permissible level of calculations.

Example 18.4

Find an approximate positive solution of the system of equations by the Newton method.

$$x^2 + y^2 + z^2 - 1 = 0, \quad 2x^2 + y^2 - 4z = 0, \quad 3x^2 - 4y + z^2 = 0. \tag{a}$$

Solution

We have

$$\mathbf{F}(\mathbf{x}) = \begin{Bmatrix} x^2 + y^2 + z^2 - 1 \\ 2x^2 + y^2 - 4z \\ 3x^2 - 4y + z^2 \end{Bmatrix}. \tag{b}$$

Take the zero approximation of the solution as $x_0 = y_0 = z_0 = 0.5$. Then,

$$\mathbf{F}(\mathbf{x}^{(0)}) = \begin{Bmatrix} 0.25 + 0.25 + 0.25 - 1 \\ 0.50 + 0.25 - 2.0 \\ 0.75 - 2.0 + 0.25 \end{Bmatrix} = \begin{Bmatrix} -0.25 \\ -1.25 \\ -1.0 \end{Bmatrix}. \tag{c}$$

Let us make up the Jacobi matrix:

$$\mathbf{W}(x) = \begin{bmatrix} 2x & 2y & 2z \\ 4x & 2y & -4 \\ 6x & -4 & 2z \end{bmatrix}. \tag{d}$$

Substituting for $\mathbf{x}$ the zero approximation solution into the above, gives

$$\mathbf{W}(\mathbf{x}^{(0)}) = \begin{bmatrix} 1 & 1 & 1 \\ 2 & 1 & -4 \\ 3 & -4 & 1 \end{bmatrix}.$$

Calculate the determinant of the zero approximation Jacobi matrix. We obtain

$$\det \mathbf{W}(\mathbf{x}^{(0)}) = \begin{vmatrix} 1 & 1 & 1 \\ 2 & 1 & -4 \\ 3 & -4 & 1 \end{vmatrix} = -40.$$

Compute the inverse Jacobi matrix in the zero approximation. We obtain

$$\mathbf{W}^{-1}(\mathbf{x}^{(0)}) = -\frac{1}{40} \begin{bmatrix} -15 & -5 & -5 \\ -14 & -2 & 6 \\ -11 & 7 & -1 \end{bmatrix} = \begin{bmatrix} 0.375 & 0.125 & 0.125 \\ 0.35 & 0.05 & -0.15 \\ 0.275 & -0.175 & 0.025 \end{bmatrix}.$$

Applying Eq. (18.144), we obtain the first approximation of the solution of Eqs (a), as follows:

$$\mathbf{x}^{(1)} = \mathbf{x}^{(0)} - \mathbf{W}^{-1}(\mathbf{x}^{(0)}) \cdot \mathbf{F}(\mathbf{x}^{(0)})$$

$$= \begin{Bmatrix} 0.5 \\ 0.5 \\ 0.5 \end{Bmatrix} - \begin{bmatrix} 0.375 & 0.125 & 0.125 \\ 0.35 & 0.05 & -0.15 \\ 0.275 & -0.175 & 0.025 \end{bmatrix} \begin{Bmatrix} -0.25 \\ -1.25 \\ -1.00 \end{Bmatrix} = \begin{Bmatrix} 0.875 \\ 0.500 \\ 0.375 \end{Bmatrix}.$$

Then, the second approximation, $\mathbf{x}^{(2)}$ can be calculated. We have

$$\mathbf{F}(\mathbf{x}^{(1)}) = \begin{Bmatrix} (0.875)^2 + (0.500)^2 + (0.375)^2 - 1 \\ 2 \cdot (0.875)^2 + (0.500)^2 - 4 \cdot 0.375 \\ 3 \cdot (0.875)^2 - 4 \cdot 0.500 + 0.375 \\ 3 \cdot (0.875)^2 - 4 \cdot 0.500 + (0.375)^2 \end{Bmatrix} = \begin{Bmatrix} 0.15625 \\ 0.28125 \\ 0.43750 \end{Bmatrix}.$$

Find the first approximation Jacobi matrix. We have

$$\mathbf{W}(\mathbf{x}^{(1)}) = \begin{bmatrix} 2 \cdot 0.875 & 2 \cdot 0.500 & 2 \cdot 0.375 \\ 4 \cdot 0.875 & 2 \cdot 0.500 & -4 \\ 6 \cdot 0.875 & -4 & 2 \cdot 0.375 \end{bmatrix} = \begin{bmatrix} 1.750 & 1 & 0.750 \\ 3.500 & 1 & -4 \\ 5.250 & -4 & 0.750 \end{bmatrix}.$$

Computing the determinant of the above matrix gives

$$\det \mathbf{W}(\mathbf{x}^{(1)}) = \begin{vmatrix} 1.750 & 1 & 0.750 \\ 3.500 & 1 & -4 \\ 5.250 & -4 & 0.750 \end{vmatrix} = -64.750,$$

and the corresponding inverse matrix is given by

$$\mathbf{W}^{-1}(\mathbf{x}^{(1)}) = -\frac{1}{64.75} \begin{bmatrix} -15.25 & -3.75 & -4.75 \\ -23.625 & -2.625 & 9.625 \\ -19.25 & 12.25 & -1.75 \end{bmatrix}.$$

The second approximation of the solution is obtained from Eq. (18.144), as follows:

$$\mathbf{x}^{(2)} = \mathbf{x}^{(1)} - \mathbf{W}^{-1}(\mathbf{x}^{(1)}) \cdot \mathbf{F}(\mathbf{x}^{(1)})z$$

$$= \begin{Bmatrix} 0.875 \\ 0.500 \\ 0.375 \end{Bmatrix} + \frac{1}{64.75} \begin{bmatrix} -15.25 & -3.75 & -4.75 \\ -23.625 & -2.625 & 9.625 \\ -19.25 & 12.25 & -1.75 \end{bmatrix} \begin{Bmatrix} 0.15625 \\ 0.28125 \\ 0.43750 \end{Bmatrix}$$

$$= \begin{Bmatrix} 0.78981 \\ 0.49662 \\ 0.36993 \end{Bmatrix}.$$

Similarly, the consequent approximations can be found. In the third approximation we have

$$\mathbf{x}^{(3)} = \begin{Bmatrix} 0.78521 \\ 0.49662 \\ 0.36992 \end{Bmatrix}, \quad \mathbf{F}(\mathbf{x}^{(3)}) = \begin{Bmatrix} 0.00001 \\ 0.00004 \\ 0.00005 \end{Bmatrix}.$$

If we confine ourselves to the third approximation, then the solution of Eqs (a) is of the form

$$x = 0.7852, \quad y = 0.4966, \quad z = 0.3699.$$

Example 18.5

Find a solution of the differential equation

$$\frac{\mathrm{d}y}{\mathrm{d}x} = x^2 + y^2 \quad \text{for} \quad |\mathrm{x}| \le \frac{1}{\sqrt{2}}, \tag{a}$$

with the boundary conditions

$$y = 0\big|_{x=0}. \tag{b}$$

Use the method of successive approximations.

Solution

Equation (a) with the boundary conditions (b) represent the Cauchy problem. It is evident that the solution of the above problem is also in the interval $|y| \le \frac{1}{\sqrt{2}}$. Applying the method of successive approximations, let us take $y_0 = y(0) = 0$ as the zero approximation. Then, the iterative procedure of the method (See Sec. 18.7.1) can be represented, as follows

$$y_1(x) = \int_0^x t^2 \mathrm{d}t = \frac{1}{3}x^3,$$

$$y_2(x) = \int_0^x \left(t^2 + \frac{1}{9}t^6\right)\mathrm{d}t = \frac{1}{3}x^3 + \frac{1}{63}x^7,$$

$$y_3(x) = \int_0^x \left(t^2 + \frac{1}{9}t^6 + \frac{2}{189}t^{10} + \frac{1}{3969}t^{14}\right)\mathrm{d}t$$

$$= \frac{1}{3}x^3 + \frac{1}{63}x^7 + \frac{2}{2079}x^{11} + \frac{1}{59535}x^{15}.$$

For $|x| \le \frac{1}{\sqrt{2}}$ the difference between $y_2(x)$ and $y_3(x)$ does not exceed the value of

$$\frac{2}{2079}\left(\frac{1}{\sqrt{2}}\right)^{11} + \frac{1}{59535}\left(\frac{1}{\sqrt{2}}\right)^{15} \le 0.000022,$$

and one can approximately put

$$y(x) \approx y_2(x) = \frac{1}{3}x^3 + \frac{1}{63}x^7.$$

This example was taken from Ref. [20].

PROBLEMS

18.1 A long thin-walled steel tube is heated to 250°C above the room temperature 22°C. Assume that the ends of the tube are simply supported. Let the mean radius of the tube $R = 1.2\,\mathrm{m}$ and its thickness $h = 10\,\mathrm{mm}$. Determine the maximum thermal stresses in the tube if $E_s = 200\,\mathrm{GPa}$, $\nu_s = 0.3$, and $\alpha_s = 25.2 \times 10^{-6}/^{\circ}\mathrm{C}$.

18.2 A long thin-walled aluminum tube has free ends and is subjected to uniform temperatures $T_1 = 150^\circ\text{C}$ and $T_2 = 350^\circ\text{C}$ at the inner and outer surfaces, respectively. Let the mean radius of the tube be 0.8 m and its thickness $h = 10\,\text{mm}$. Calculate the maximum thermal stresses in the tube if $E_a = 70\,\text{GPa}$, $\alpha_a = 23 \times 10^{-6}/^\circ\text{C}$, and $\nu_a = 0.3$.

18.3 Compute the discontinuity stresses at the junction of the cylindrical shell and hemispherical head, as shown in Fig. 16.6, for the uniform temperature change $\Delta T = 120^\circ\text{C}$. Use the geometric and mechanical parameters of the compound shell structure given in Example 16.2 and $\alpha_s = 25 \times 10^{-6}/^\circ\text{C}$. Apply the approximate method of Sec. 16.4 for the problem solution.

18.4 Compute the stresses in the hemispherical shell stiffened on its edge by a flange, as shown in Fig. 16.5. Assume that the shell and flange are made of steel with $E_s = 210\,\text{GPa}$, $\nu_s = 0.3$, and $\alpha_s = 25 \times 10^{-6}/^\circ\text{C}$. Take the geometric parameters of the shell and flange from Example 16.1. Apply the approximate method of Sec. 16.4 for the problem solution.

18.5 Derive Eqs (18.17).

18.6 Verify Eqs (18.24) and (18.29).

18.7 Derive Eq. (18.54).

18.8 A closed, circular cylindrical shell of length L and radius R is stiffened by equally spaced collars, at a distance $L/10$, located inside the shell. The shell is simply supported at $x = 0$ and $x = L$ and is subjected to a uniform internal pressure p. Calculate the normal stresses in the stiffened shell in terms of p if the shell and collars are made of steel with $E_s = 210\,\text{GPa}$ and $\nu_s = 0.3$. Assume also that the collars have a form of the equal angle section $25 \times 25 \times 5$ mm and $R = 0.8\,\text{m}$, $L = 4\,\text{m}$, and $h = 1\,\text{mm}$. In your calculations, consider the stiffened shell as a structurally orthotropic homogeneous shell.

18.9 Verify Eqs (18.63) and (18.66).

18.10 Derive Eqs (18.82).

18.11 Consider two extreme cases for a sandwich shallow shell given by Eqs (18.82): (a) let $R_1 \to \infty$ and $R_2 \to \infty$ and (b) let $G_c \to \infty$. Transform the above governing equation for these two cases and explain their physical sense.

18.12 Based on the representations (18.106) and (18.107), write the matrices $[B_i]$ and $\left[B_j\right]$ in the explicit form.

18.13 Write a computer code for calculating the components of the stiffness matrix for the finite element in the form of a frustum (Fig. 18.7) for an axisymmetrically loaded shell of revolution. Use the relations introduced in Sec. 18.6.2. Assume reasonable values for any shell properties required.

18.14 Using the Newton method, find a solution of the equation

$$4x^3 - 2x^2 - 4x - 3 = 0.$$

18.15 Find a solution of the differential equation for the bending moments in a simply supported beam with a variable cross section:

$$\frac{\mathrm{d}^2 y}{\mathrm{d}x^2} + (1 + x^2)y = 0,$$

$$y = 0\big|_{x=-1} \quad \text{and} \quad y = 0\big|_{x=1}$$

Use the method of successive approximations.

REFERENCES

1. Carslaw, H.S. and Jaeger, J.C., *Conduction of Heat in Solids*, 2nd edn, Oxford University Press, London, 1959.

2. Von Karman, Th., *Encyklopadie der Mathematischen*, Wissenschaften, vol. IV, 1910.
3. Reissner, E., On the theory of thin elastic plates. In: *H. Reissner Anniversary Volume*, pp. 231–247 (1949). Ann Arbor, J. W. Edwards.
4. Sanders, L, Jr., Nonlinear Theories for Thin Shells, Contract NONR 1866(02), Office of Naval Research, Tech. Report No. 10, Harvard Press, Cambridge, Massachusetts, 1961.
5. Mushtari, Kh.M. and Galimov, K.Z., *Nonlinear Theory of Thin Elastic Shells*, Russian translational series, NASA TT-F-62, Washington, DC, US Department of Commerce, 1957.
6. Vlasov, V.Z., *General Theory of Shells and Its Application in Engineering*, NASA TTF-99, Washington, DC, 1964.
7. Alexandrov, A.V. and Potapov, V.D., *The Fundamentals of the Theory of Elasticity and Plasticity*, Izd-vo ''Vyshaya Shkola,'' Moscow, 1990 (in Russian).
8. Cook, R.D. and Young, W.C., *Advanced Mechanics of Materials*, 2nd edn, Prentice Hall, Englewood Cliffs, New Jersey, 1999.
9. Stein, M. and Mayers, J.A., *A Small Deflection Theory for Curved Sandwich Plates*, NACA, Washington, DC, 1950.
10. Plantema, F., *Sandwich Construction*, John Wiley and Sons, New York, 1966.
11. Baker, E.H., Cappelly, A.P., Lovalevsky, L., Risb, F.L., and Verette, R.M., *Shell Analysis Manual*, NASA CR-912, Washington, DC, April 1968.
12. Gallagher, R.H., Problems and progress in thin shell finite element analysis, In: *Finite Element for Thin Shells and Curved Members* (eds D.G. Ashwell and R.H. Gallagher), John Wiley and Sons, London, 1976.
13. Hughes, T.J.R., *The Finite Element Method*, Prentice-Hall, Englewood Cliffs, New Jersey, 1987.
14. Hughes, T.J.R. and Hinton, E., Finite element method for plate and shell structures, Vol 1: *Finite Element Technology*, Pineridge Press International, Swansea, UK, 1986.
15. Zienkiewitcz, D.C., *The Finite Element Method in Engineering Science*, McGraw-Hill, New York, 1969.
16. Gallagher, R.H., *Finite Element Analysis:Fundamentals*, Prentice-Hall, Englewood Cliffs, New Jersey, 1976.
17. Segerlind, L.J., *Applied Finite Element Analysis*, John Wiley, London, 1975.
18. Petrov, V.V., *The Method of Successive Loadings in the Nonlinear Theory of Plates and Shells,* Izd-vo Saratov University, Saratov, 1975 (in Russian).
19. Alexandrov, A.V. and Potapov, V.D., *The Fundamentals of the Theory of Elasticity and Plasticity*, Izd-vo ''Vyshaya Shkola,'' Moscow, 1990 (in Russian).
20. Krylov, A.N., *Lectures on Approximate Calculations*, Izd-vo Academy of Sciences of USSR, Moscow, 1949 (in Russian).

19

Buckling of Shells

19.1 INTRODUCTION

An efficiency of the membrane stress state, based on the strength conditions only, enables one to employ a very small shell thickness, as discussed in the preceding chapters of Part II. However, a possibility of the shell buckling impedes that, causing us either to increase the shell thickness or to reinforce the shell by stiffeners. It should be noted that the shell buckling is always disastrous, unlike, for example, a column or plate buckling. Therefore, the problem of the stability in designing shell structures is extremely vital. This problem is made worse because of some specific difficulties associated with determining correctly the critical values of loads applied to thin shells. Note that these difficulties are much greater than in the buckling analysis of columns, frames, and flat plates. They are associated with a complicated mathematical description of the deformed state of shells, and with a diversity of situations at which a shell can buckle.

General postulations, definitions, and fundamentals of the structural stability theory, introduced in Chapter 8 for the plate buckling problems, can be applied also to the shell buckling analysis. In this chapter, we present a systematic but simplified analysis of shell buckling, and obtain some useful relationships between the critical values of applied loads and shell parameters. We limit ourselves to the consideration of thin shells for which elastic buckling without plastic deformation is possible.

19.2 BASIC CONCEPTS OF THIN SHELLS STABILITY

Let us compare qualitatively the buckling behavior of columns, flat plates, and shells. For the sake of simplicity, we treat a column, plate, and shell as one degree of freedom systems and consider typical diagrams of the relationship between the applied load p and some deflection parameter f in the buckling problems. We assume

that the deflections are small compared with the overall dimensions of the structural member, but of the same order of magnitude as the depth of the column cross section, or the wall thickness of the plate or shell.

The representative "load–deflection" diagram for columns and plates of perfect geometric form and loaded by in-plane compressive forces p is shown in Fig. 19.1a. Each position plotted in this figure represents an equilibrium configuration of the member – stable, neutral, or unstable – depending upon whether the slope of the path at that point is positive, zero, or negative, respectively. Points not lying on this diagram, of course, correspond to nonequilibrium configurations. The equilibrium path consists of the three branches: (a) branch OA refers to an initial, unbuckled configuration of equilibrium that is assumed to be momentless; (b) two "rising" branches CA and AD refer to buckled configurations of equilibrium. Note that the curve CAD is symmetrical about the p axis. For the equilibrium path, shown in Fig. 19.1a, at the transition point A, a bifurcation of equilibrium is said to occur, since there are at least two possible states of equilibrium, $f = 0$ and $f \to \infty$. Such a

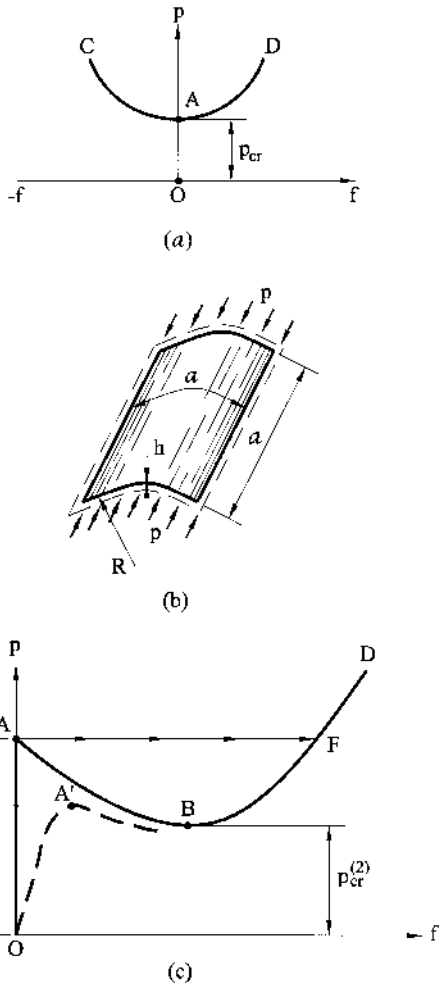

Fig. 19.1

transition point A, as mentioned in Sec. 8.2, is referred to as a *bifurcation point*, and the load at that point is called the *critical load*, p_{cr}. As shownin Fig. 19.1a, there are new and stable, buckled configurations of equilibrium in the immediate vicinity of the bifurcation point. Therefore, with the slight and smooth increase in the applied load above p_{cr}, the initial configuration of equilibrium of the structural member (column or plate) ceases to be stable, and smoothly, without any jumps, it goes over to an adjacent buckled, stable configuration of equilibrium. It follows from the above that the critical values of an applied load can be determined with the use of linear differential equations of the structural stability theory, introduced in Sec. 8.2. A geometrically nonlinear theory can be used only for describing the postbuckling behavior of the member.

Lets turn our attention to the analysis of a shell buckling process. The representative paths of equilibrium for a simply supported shallow cylindrical shell under a uniform axial loading p (Fig. 19.1b) are shown in Fig. 19.1c. The solid curve $OABD$ refers to the shell whose initial configuration is assumed to be perfect, i.e., without any geometric and other imperfections. The load p is applied statically such that the initial configuration of equilibrium of the shell is in the membrane state of stress, and thus, $f = 0$. The equilibrium path $OABD$ consists of the "rising" branches OA and BD, corresponding to stable equilibrium states, and the "descending" branch AB that corresponds to an unstable equilibrium configuration.

Point A on the curve $OABD$ can also be interpreted as a bifurcation point. However, unlike the equilibrium path, shown in Fig. 19.1a, for columns and flat plates, there are no new stable buckled configurations in the immediate vicinity of the bifurcation point A. The stable, buckled configurations of equilibrium are off from the initial ones at some finite distances (on the branch BD). Therefore, a transition from the initial configuration of equilibrium (branch OA) to a new, buckled and stable configuration of equilibrium (branch BD) occurs by a jump, i.e., the shell "jumps" from a stable state at A through the statically unstable state, given by the branch AB, to the stable state at F on the branch BD, as shown in Fig. 19.1c. This sudden transition from the initial configuration of equilibrium to the next, stable and buckled configuration of equilibrium, with the corresponding jump in f, is termed as *snap-through buckling*. As a result, the shell buckling analysis, in a general case, must be based on the geometrically nonlinear shell theory.

The curve $OABD$ has been analyzed above for the buckling model of some perfect shell. However, a real shell typically has some geometric and other imperfections due to manufacturing. Such irregularities of the shell geometric form are equivalent to prebuckling deformations imposed on the original shell configuration. Note, that experiments performed on columns and flat plates under in-plane compressive forces showed that they are relatively insensitive to slight geometric imperfections. This is not the case in a shell buckling process. Buckling experiments carried out on shells showed that some shells are very sensitive to geometric and loading imperfections. For instance, for the shallow cylindrical shell under consideration (Fig. 19.1b), such an elevated sensitivity to slight imperfections can be explained by the closeness of the unstable branch AB to the initial shell configuration of equilibrium given by straight line OA.

The path of shell instability for the given real shell with geometric and other imperfections is given by the dashed curve shown in Fig. 19.1c. It is seen that, due to the above-mentioned irregularities, the real shell begins to deviate from its

initial configuration at the beginning of loading, and thus, the latter cannot be assumed to be in a membrane state of stress. The branch OA' for increasing loading will no longer coincide with the p axis. A transition from one stable state to another will also occur by a jump at the level of the limit point A' (the snap-through buckling).

It follows from the above that there are three distinct values of the critical loads that characterize the buckling behavior of thin shells:

1. $p_{cr}^{(1)}$ is the "upper" critical load – it can be defined as the largest load up to which the initial configuration of equilibrium of the perfect shell remains stable with respect to infinitesimal disturbances;
2. $p_{cr}^{(2)}$is the "lower" critical load – it can be defined as the largest load up to which the initial configuration of equilibrium of the perfect shell remains stable with respect to both infinitesimal and finite disturbances;
3. $p_b$is the *critical load of a real shell,* also referred to as the *buckling load* – it can be defined as some load for which the jump (or snap-through buckling) of a real shell occurs, i.e., such a critical value of the load for which the initial state of equilibrium of a real shell ceases to be stable.

It will be shown later that the values of $p_{cr}^{(1)}$ are determined with the use of linear differential equations. In determining $p_{cr}^{(2)}$, it is necessary to solve extremely complicated problems of the geometrically nonlinear theory of shells. It is impossible to obtain an exact and analytical solution of the latter problems. Therefore, all available results are obtained by numerical methods.

For real shells, the critical load, p_b, is somewhere between the values of $p_{cr}^{(1)}$ and $p_{cr}^{(2)}$, obtained for perfect shells. The more precisely a shell is manufactured, the closer is value of p_b to $p_{cr}^{(1)}$. The value of p_b is extremely sensitive to geometric and loading imperfections and to small deviations in boundary conditions. On the one hand, it results in a large scatter of the experimental results of p_b. On the other hand, some conceptual difficulties occur in the theoretical determination of p_b because of the impossibility of taking into account, with a high degree of accuracy, all the imperfections and irregularities during the design stage. As a result, a severe discrepancy was noted between the theoretical and experimental results in determining the shell critical loads.

In summary, it should be noted that the linear stability theory is not sufficient to predict completely the buckling and postbuckling behavior of thin shells. The stability equations of shells can be derived successfully, based on the nonlinear equilibrium equations. The nonlinear theory can also be used to consider the influence of initial imperfections and other effects in the shell buckling analysis. It was believed that an accurate formulation of the buckling problem, in the framework of the nonlinear theory and exact solution of the corresponding equations, would result in a close agreement between the theoretical and numerical results in determining the critical loads. However, at present, in practice, this procedure has turned out to be prohibitively difficult and, so far, it has not lived up to the expectations placed on the geometrically nonlinear shell theory. The latter theory serves to broaden our knowledge of shell buckling analysis and to clarify the meaning and limitations of the linear stability theory. But, at present, it is not a design tool for directly determining the buckling load. Some details of the buckling design procedure for thin shells will be given in Sec. 19.8. At the same

time, the buckling analysis of thin shells by means of the linear theory yields some useful information about the buckling behavior of shells. Particularly, closed-form analytical expressions, obtained by the linear stability theory, demonstrate the interplay of various parameters that affect stability when combined with appropriate correction and statistical coefficients. One could complement those relations so that reliable design expressions would be obtained (see Sec. 19.8). In the next sections, we perform linear and nonlinear stability analyses of shells of various geometries, and compare the corresponding results.

The basic problem in the buckling analysis of shells, as for thin plates, is in determining the critical values of applied loads. Such a problem can be solved by using the equilibrium, energy, and dynamic methods introduced in Sec. 8.2 for the plate buckling problems. We discuss below some details of application of the equilibrium and energy methods to the elastic shell buckling analysis.

19.2.1 Equilibrium method

The equilibrium method is adequately applicable to only conservative systems (see Sec. 2.6). A perfect shell loaded by potential external forces is a particular case of a conservative system.

As mentioned in Sec. 8.2, the equilibrium method is based on the observation that at a critical load, a deformed state of a shell exists that is assumed to be an infinitesimally, close to its initial, unbuckled configuration of equilibrium. Thus, the appearance of a possible bifurcation in the solution corresponds to the critical load. This criterion for determining critical loads can be used to obtain the governing differential equations of the shell buckling analysis. As we have seen, the structure of the governing differential equations of the general, even linear, theory of thin shells is sufficiently complicated. Therefore, a solution of practical shell problems involves considerable difficulties. Fortunately, many shell stability problems, having great practical importance, can be simplified. For example, this is particularly true for such cases when a shell bucking is accompanied by an appearance of comparatively small-sized deformation waves (i.e., such waves whose dimensions are, at least in one direction, small compared with the radii of curvature of the middle surface or with the overall shell dimensions). In this case, a buckled shell in the neighborhood of the formed bulges can be treated as a shallow shell. In many cases that enables one to apply the theory of shallow shells, introduced in Sec. 17.4, for the shell buckling problems

Now, we derive the stability equations for shallow shells by the equilibrium method. Let w_0 and Φ_0 be the prebuckled values of the deflection and stress function, respectively. They correspond to the initial equilibrium position. The values of w and Φ, corresponding to the deformed adjacent position that occurs at buckling, would then be represented by the following:

$$w = w_0 + w_1, \quad \Phi = \Phi_0 + \Phi_1, \tag{19.1}$$

where w_1 and Φ_1 represent some increments in values of the deflection and stress function in transition from the initial position of equilibrium to an infinitesimally close adjacent configuration of equilibrium. Applying the governing differential equations of the geometrically nonlinear shallow shell theory, Eqs (18.31), to the

initial, prebuckled state of equilibrium, one obtains the following system of equations:

$$\begin{aligned}\nabla^2\nabla^2\Phi_0 &= -Eh\left[\frac{1}{2}L(w_0, w_0) + \nabla_k^2 w_0\right],\\ D\nabla^2\nabla^2 w_0 &- \left[\nabla_k^2\Phi_0 + L(\Phi_0, w_0)\right] = p_3.\end{aligned} \tag{19.2}$$

Now, let us apply Eqs (18.31) to the adjacent buckled configuration of equilibrium. Substituting for w and Φ from Eqs (19.1) into Eqs (18.31), we obtain the modified nonlinear differential equations of the shallow shell theory. Subtracting Eqs (19.2) from these modified equations gives the following equations that will be applied to the shell buckling problems:

$$\begin{aligned}\frac{1}{Eh}\nabla^2\nabla^2\Phi_1 &= -\nabla_k^2 w_1 - \frac{\partial^2 w_0}{\partial x^2}\frac{\partial^2 w_1}{\partial y^2} + 2\frac{\partial^2 w_0}{\partial x\partial y}\frac{\partial^2 w_1}{\partial x\partial y} - \frac{\partial^2 w_1}{\partial x^2}\frac{\partial^2 w_0}{\partial y^2},\\ D\nabla^2\nabla^2 w_1 &= \nabla_k^2\Phi_1 + \left(\frac{\partial^2\Phi_0}{\partial x^2}\frac{\partial^2 w_1}{\partial y^2} - 2\frac{\partial^2\Phi_0}{\partial x\partial y}\frac{\partial^2 w_1}{\partial x\partial y} + \frac{\partial^2\Phi_0}{\partial y^2}\frac{\partial^2 w_1}{\partial x^2}\right)\\ &+ \left(\frac{\partial^2\Phi_1}{\partial x^2}\frac{\partial^2 w_0}{\partial y^2} - 2\frac{\partial^2\Phi_1}{\partial x\partial y}\frac{\partial^2 w_0}{\partial x\partial y} + \frac{\partial^2\Phi_1}{\partial y^2}\frac{\partial^2 w_0}{\partial x^2}\right).\end{aligned} \tag{19.3}$$

In deriving these equations, the terms

$$\frac{\partial^2 w_1}{\partial x^2}\frac{\partial^2 w_1}{\partial y^2}, \quad \left(\frac{\partial^2 w_1}{\partial x\partial y}\right)^2, \quad \frac{\partial^2\Phi_1}{\partial x^2}\frac{\partial^2 w_1}{\partial y^2}, \quad 2\frac{\partial^2\Phi_1}{\partial x\partial y}\frac{\partial^2 w_1}{\partial x\partial y},$$

and

$$\frac{\partial^2\Phi_1}{\partial y^2}\frac{\partial^2 w_1}{\partial x^2}$$

were neglected, since they are small compared with the corresponding remaining terms. Equations (19.3) represent *a system of two linear differential equations in* w_1 and Φ_1 *with variable coefficients corresponding to* w_0 and Φ_0.

Thus, the procedure introduced above results in the replacement of nonlinear differential equations by the linear differential equations of shell stability. In so doing, the deflection w_0 and stress function Φ_0 can be determined from either linear or nonlinear equations, which are set up for the initial equilibrium path. The most common simplification is to apply the equations of the linear shell theory to the initial position of equilibrium, such that w_0 and Φ_0 are given by the solutions of the linear governing equations. A further simplification is usually introduced in the linear stability analysis. Since it is assumed that the classical linear shell theory is applicable to the prebuckled state, then, for consistency, all the terms containing prebuckled rotations can be omitted from Eqs (19.3). If these terms are neglected the stability equations (19.3) reduce to the form

$$\frac{1}{Eh}\nabla^2\nabla^2\Phi_1 = -\nabla_k^2 w_1,$$
$$D\nabla^2\nabla^2 w_1 = \nabla_k^2\Phi_1 + \frac{\partial^2\Phi_0}{\partial x^2}\frac{\partial^2 w_1}{\partial y^2} - 2\frac{\partial^2\Phi_0}{\partial x\partial y}\frac{\partial^2 w_1}{\partial x\partial y} + \frac{\partial^2\Phi_0}{\partial y^2}\frac{\partial^2 w_1}{\partial x^2}. \tag{19.4}$$

Using Eqs (17.31) and letting $\alpha = x$, $\beta = y$, and $A = B = 1$, we can express the prebuckled stress function Φ_0 in terms of the membrane internal forces acting in the middle surface of the shallow shell prior to buckling, N_{10}, N_{20}, and S_0. We have the following:

$$N_{10} = \frac{\partial^2\Phi_0}{\partial y^2}, \quad N_{20} = \frac{\partial^2\Phi_0}{\partial x^2}, \quad S_0 = -\frac{\partial^2\Phi_0}{\partial x\partial y} \tag{19.5}$$

Applying these relations to the second Eq. (19.4), we can rewrite the system of the stability equations (19.4) in the following alternative form:

$$\frac{1}{Eh}\nabla^2\nabla^2\Phi_1 = -\nabla_k^2 w_1, \tag{19.6a}$$
$$D\nabla^2\nabla^2 w_1 = \nabla_k^2\Phi_1 + \left(N_{10}\frac{\partial^2 w_1}{\partial x^2} + 2S_0\frac{\partial^2 w_1}{\partial x\partial y} + N_{20}\frac{\partial^2 w_1}{\partial y^2}\right). \tag{19.6b}$$

As for the plate buckling analysis (see Sec. 8.2), the terms in parentheses on the right-hand side of Eq. (19.6b) can be treated as some fictitious transverse surface load $p_3^{(f)}$. So, we can rewrite Eqs (19.6) in terms of this fictitious load, $p_3^{(f)}$, as follows:

$$\frac{1}{Eh}\nabla^2\nabla^2\Phi_1 = -\nabla_k^2 w_1,$$
$$D\nabla^2\nabla^2 w_1 = \nabla_k^2\Phi_1 + p_3^{(f)}, \tag{19.7}$$

where

$$p_3^{(f)} = N_{10}\frac{\partial^2 w_1}{\partial x^2} + 2S_0\frac{\partial^2 w_1}{\partial x\partial y} + N_{20}\frac{\partial^2 w_1}{\partial y^2}. \tag{19.8}$$

The coupled equations (19.4) or (19.6), or (19.7) are referred to as the *stability equations for shallow shells*. They are homogeneous partial differential equations in which the critical load appears as an unknown parameter. Equations (19.7) can be conveniently reduced to one uncoupled equation in w_1. Applying the operator ∇^4 to the second equation and the operator ∇_k^2 to the first equation of the above system, and adding these equations, one obtains the following governing stability equation:

$$D\nabla^4\nabla^4 w_1 + Eh\nabla_k^2\nabla_k^2 w_1 = \nabla^4(p_s^{(f)}). \tag{19.9}$$

The linear governing stability equations (19.7) or (19.9) can be applied to various stability problems of shallow and cylindrical shells. The general procedure of the equilibrium method, based on the above-mentioned governing equations, for determining the critical loads in shell buckling problems is quite similar to that of discussed in Sec. 8.2 for the plate bending problems. The application of this procedure will be illustrated in the next sections.

19.2.2 Energy method

The energy method of the buckling shell analysis is based on the observation that the total potential energy of a loaded shell is a relative minimum for a stable configuration along the equilibrium path, but is only stationary for unstable configurations.

We apply the energy criterion (8.5a) derived in Sec. 8.2 to the linear shell buckling problems. Applying this criterion, we assume that: (a) there is no bending prior to buckling, so that the initial shell is in the membrane state of stress only, and (b) at the onset of buckling, there are additional contributions to the strain energy due to the middle surface straining and bending.

We present the energy criterion (8.5a), as follows:

$$\Delta\Pi = \Delta U + \Delta\Omega = 0, \tag{19.10}$$

where

$$\Delta U = U - U_0 \tag{19.11}$$

is the change in the shell strain energy during buckling; U is the total strain energy of the shell after it has buckled; U_0 is the strain energy of the shell just before buckling; and $\Delta\Omega$ is the increment in the potential of the external loading owing to stretching of the middle surface and bending as the shell deflects due to the buckling action. The components of $\Delta\Pi$ in Eq. (19.10) can be obtained by using either Eqs (12.51)–(12.53) in the general case, or Eqs (17.50) if the shallow shell theory is of interest. We present below the expressions of the components U, U_0, and $\Delta\Omega$ for the shell buckling problems based on Eqs (12.51)–(12.53). We have the following:

$$U = \frac{Eh}{2(1-\nu^2)}\int\int_A \left\{(\varepsilon_1+\varepsilon_2)^2 + 2(1-\nu)\left[\frac{(\gamma_{12})^2}{4} - \varepsilon_1\varepsilon_2\right]\right\} AB\mathrm{d}\alpha\mathrm{d}\beta$$
$$+ \frac{D}{2}\int\int_A [(\chi_1+\chi_2)^2 + 2(1-\nu)(\chi_{12}^2 - \chi_1\chi_2)]AB\mathrm{d}\alpha\mathrm{d}\beta; \tag{19.12a}$$

$$U_0 = \frac{Eh}{2(1-\nu^2)}\int\int_A \left[(\varepsilon_{10}+\varepsilon_{20})^2 + 2(1-\nu)\left(\frac{(\gamma_{12}^0)^2}{4} - \varepsilon_{10}\varepsilon_{20}\right)\right] AB\mathrm{d}\alpha\mathrm{d}\beta, \tag{19.12b}$$

where

$$\varepsilon_1 = \varepsilon_{10} + \varepsilon_{11}; \quad \varepsilon_2 = \varepsilon_{20} + \varepsilon_{21}; \quad \gamma_{12} = \gamma_{12}^0 + \gamma_{12}^1. \tag{19.13}$$

Assuming that all loads applied to the shell remain unchanged during buckling, we obtain the following expression for $\Delta\Omega$:

$$\Delta\Omega = -\int\int_A (p_1u_1 + p_2v_1 + p_3w_1)AB\mathrm{d}\alpha\mathrm{d}\beta. \tag{19.14}$$

In the expressions (19.12)–(19.14), $\varepsilon_{10}, \varepsilon_{20}$, and γ_{12}^0 refer to prebuckled strain components corresponding to the initial position of equilibrium; u_1, v_1, w_1 are the incremental displacements due to the buckling, and $\varepsilon_{11}, \varepsilon_{21}, \gamma_{12}^1$, and $\chi_1, \chi_2, \chi_{12}$ represent the in-plane strain components, changes in curvature and twist corresponding to these incremental displacements, respectively; and p_1, p_2, and p_3 are in-plane compressive edge loads and normal surface load, respectively, applied to the shell. Since

the initial configuration of equilibrium is assumed to be momentless, the changes in curvature and twist may occur as a result of buckling only. Therefore, the index 1 for these components will be omitted from here on.

The general procedure of the energy method in the shell buckling analysis for determining the critical values of applied loading is analogous to that discussed in Sec. 8.4 for the plate bending problems.

19.3 LINEAR BUCKLING ANALYSIS OF CIRCULAR CYLINDRICAL SHELLS

19.3.1 General

Buckling of cylindrical shells can occur in those cases when they are subjected to the action of axial compression, transverse pressure, torsion, etc. These loads can be applied either separately or in various combinations. We present below the simplified linear buckling analysis of circular cylindrical shells based on the Donnel–Mushtari–Vlasov (DMV) theory, which is assumed to be applicable with reasonable accuracy to this analysis. It has been shown (see, for instance Ref. [1]) that the simplified linear equations of the DMV theory can be applicable to the local instability shell problems if the dimensions of bulging, formed in buckling, are small compared with the shell typical dimensions, at least in one direction.

19.3.2 Critical load for an axially compressed cylinder

Consider the stability problem of a closed cylindrical shell of radius R and of length L, simply supported on its edges and subjected to uniform compressive forces q_1. This case of loading is of a great practical importance. For example, an aircraft fuselage is subjected to compressive forces transmitted from the engine at the acceleration path. Some other problems including the buckling of shells in bending, can also be reduced to application of results obtained from the case of axially symmetrical compression. Along with that, the circular cylindrical shell compressed along its generator can serve as some standard for comparing the theoretical and experimental data to check various approaches in shell stability analysis.

The boundary conditions for the deflections, w, in buckling of the shell under consideration are of the following form:

$$w = 0|_{x=0,L}; \quad \left.\frac{\partial^2 w}{\partial x^2} = 0\right|_{x=0,L}. \tag{19.15}$$

The x and y coordinates can be chosen as coordinates that determine the location of a point on the middle surface. They define the position of a point along the shell generator and over the arc of its cross section, respectively, as shown in Fig. 19.2.

As a first variant of the solution of this buckling problem, let us assume that the *deflected surface of the shell after buckling is axisymmetric*, i.e., the shell cross section remains circular, as shown in Fig. 19.2. Assuming that the initial, prebuckled configuration of equilibrium of the cylindrical shell is momentless, take the equation for deflections w in buckling in the form

$$w = -f \sin\frac{m\pi x}{L}. \tag{19.16}$$

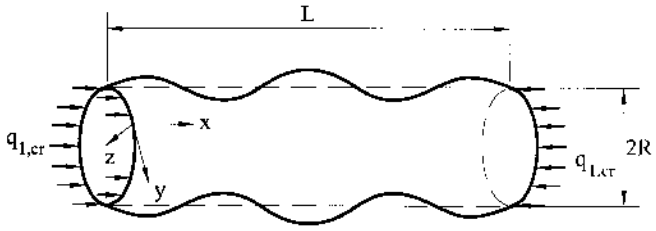

Fig. 19.2

The index 1 for w will be omitted since no confusion is possible when the initial state of equilibrium is momentless. It is evident that the deflections in the form of Eq. (19.16) satisfy the boundary conditions (Eqs (19.15)). We apply the *energy method* to determine the critical forces in the considered symmetrical buckling.

First, determine the strain components prior to buckling, i.e., in the pre-buckled, membrane state. Since there is no acting normal load, one obtains from Eq. (15.40) that $N_{20} = 0$. The applied compressive load is constant over the shell circumference, thus, we have $N_{10} = -q_1$. The axial strain, just before buckling, is found from Eq. (12.45), as follows:

$$\varepsilon_{10} = \frac{N_{10}}{Eh} = -\frac{q_1}{Eh}. \tag{19.17a}$$

The corresponding circumferential strain follows also from Eqs. (12.45), as shown below:

$$\varepsilon_{20} = -\nu\varepsilon_{10}. \tag{19.17b}$$

As a result of buckling, the deflection w occurs, producing the circumferential strain ε_{21}. Assuming that w is given by Eq. (19.16), we can determine ε_{21} from Eq. (15.38), as follows:

$$\varepsilon_{21} = -\frac{w}{R} = \frac{f}{R}\sin\frac{m\pi x}{a}. \tag{19.18}$$

Therefore, the total circumferential strain after the shell has buckled is

$$\varepsilon_2 = \varepsilon_{20} + \varepsilon_{21} = -\nu\varepsilon_{10} - \frac{w}{R} = -\nu\varepsilon_{10} + \frac{f}{R}\sin\frac{m\pi x}{L}. \tag{19.19}$$

To find the corresponding total meridional strain, ε_1, we now refer to the first Eq. (12.45), with $N_1 = N_{10} = -q_1$, as follows:

$$N_{10} = -q_1 = \frac{Eh}{1-\nu^2}(\varepsilon_1 + \nu\varepsilon_2),$$

from which,

$$\varepsilon_1 = -\frac{(1-\nu^2)}{Eh}q_1 - \nu\varepsilon_2.$$

Substituting for q_1/Eh from Eq. (19.17a) into the above yields

$$\varepsilon_1 = (1-\nu^2)\varepsilon_{10} + \nu\left(\frac{w}{R} + \nu\varepsilon_{10}\right) = \varepsilon_{10} + \nu\frac{w}{R} = \varepsilon_{10} - \frac{\nu}{R} f \sin\frac{m\pi x}{L}. \tag{19.20}$$

Note that, owing to the axisymmetric deformation, the shear strain is zero. Now we can analyze the buckled axisymmetric configuration of the shell equilibrium. Let us determine the changes in curvature. Due to axisymmetric bending deformation, we have the following:

$$\chi_1 = -\frac{\mathrm{d}^2 w}{\mathrm{d}x^2} = f\left(\frac{m\pi}{L}\right)^2 \sin\frac{m\pi x}{L}, \quad \chi_2 = \chi_{12} = 0 \tag{19.21}$$

The increase in strain energy during buckling, ΔU, can be determined. For this purpose, Eqs (19.19), (19.20), and (19.17) are introduced into Eqs (19.12a) and (19.12b), respectively. Then, subtracting U and U_0, we finally obtain ΔU, as follows:

$$\Delta U = 2\pi\upsilon q_1 \int_0^L f \sin\frac{m\pi x}{L}\mathrm{d}x + f^2\frac{\pi EhL}{2R} + f^2\frac{DR\pi^5 m^4}{2L^3}. \tag{19.22}$$

Let us determine the increment in the potential of the external loading, $\Delta\Omega$. In the case of axisymmetric loading, we have the following:

$$-N_{10} = q_1, N_2 = 0, \quad \text{and} \quad S = 0; \quad p_3^{(\mathrm{f})} = N_{10}\frac{\partial^2 w}{\partial x^2} = q_1 f\left(\frac{m\pi}{L}\right)^2 \sin\frac{m\pi x}{L}. \tag{19.23}$$

To evaluate $\Delta\Omega$, we use Eq. (19.14), setting $p_2 = p_3 = 0$. Determine the increment in the potential produced by the compressive forces q_1. As discussed in Sec. 2.5, $\Delta\Omega = -\Delta W_{\mathrm{e}}$, where, W_{e} is the work done by external loading. Let us first evaluate the elementary work done by the compressive forces during the buckling. We have (for dead load q_1) the following:

$$\Delta(\mathrm{d}W_e) = (q_1\mathrm{d}y)\mathrm{d}u_1 = (q_1\mathrm{d}y)\frac{\mathrm{d}u_1}{\mathrm{d}x}\mathrm{d}x = q_1\varepsilon_{11}\mathrm{d}x\mathrm{d}y.$$

Thus,

$$\Delta\Omega_1 = -\int\int_A q_1\varepsilon_{11}\mathrm{d}x\mathrm{d}y = -\int\int_A q_1(\varepsilon_1 - \varepsilon_{10})\mathrm{d}x\mathrm{d}y. \tag{19.24}$$

Substituting for ε_1 and ε_{10} from Eqs (19.20) and (19.17a) into the above integral, utilized for the circular cylindrical shell, yields the following:

$$\Delta\Omega_1 = 2\nu\pi q_1 \int_0^L w dx = -2\nu\pi q_1 f \int_0^L \sin\frac{m\pi x}{L}\mathrm{d}x. \tag{19.25a}$$

The increment in the potential of the normal component of the in-plane forces, $\Delta\Omega_2$ – refer to the loading $p_3^{(\mathrm{f})}$ given by Eq. (19.8) – can be evaluated from Eq. (19.14) by replacing p_3 with $p_3^{(f)}$ and letting $N_{10} = -q_1$, $N_{20} = S_0 = 0$. This integral, utilized for the given cylindrical shell, has the form

$$\Delta\Omega_2 = -\frac{1}{2}\int_0^L (p_3^{(\mathrm{f})} w)2\pi R\mathrm{d}x$$

or

$$\Delta\Omega_2 = -\frac{1}{2} q_1 (2\pi R) f^2 \int_0^L \left(\frac{m\pi}{L}\right)^2 \left(\sin\frac{m\pi x}{L}\right)^2 \mathrm{d}x. \tag{19.25b}$$

Finally, adding $\Delta\Omega_1$ and $\Delta\Omega_2$, we obtain the following:

$$\Delta\Omega = -2\pi q_1 \left(\nu \int_0^L f \sin\frac{m\pi x}{L}\,\mathrm{d}x + \frac{R}{4}\frac{m^2\pi^2}{L} f^2 \right). \tag{19.26}$$

Introducing the expressions for ΔU and $\Delta\Omega$ from Eqs (19.22) and (19.26), respectively, into the energy criterion (19.10), yields the following equation for determining the critical value of q_1:

$$\left(\frac{\pi E h L}{2R} + \frac{\pi^5 R m^4 D}{2L^3} - \frac{\pi^3 R m^2 q_1}{2L} \right) f^2 = 0.$$

For the above to be valid for any f, it is required that

$$q_1 = \frac{D\lambda^2}{R^2} + \frac{Eh}{\lambda^2}, \tag{19.27}$$

where

$$\lambda = \frac{m\pi R}{L}. \tag{19.28}$$

Determine the minimum value of q_1 by equating the first derivative of q_1 with respect to λ to zero. In so doing, we assume that $m \gg 1$. Then, we obtain the following:

$$\lambda_{\mathrm{cr}} = \sqrt[4]{\frac{EhR^2}{D}}. \tag{19.29}$$

Substituting for λ_{cr} from the above into Eq. (19.27) results in the critical value of the applied compressive load, $q_{1,\mathrm{cr}}$, corresponding to the bifurcation point in the framework of the linearized buckling analysis of the shell. We have the following expression:

$$q_{1,\mathrm{cr}} = \frac{1}{\sqrt{3(1-\nu^2)}} \frac{Eh^2}{R}. \tag{19.30}$$

For $\nu = 0.3$, we obtain

$$q_{1,\mathrm{cr}} = 0.605 \frac{Eh^2}{R}, \tag{19.31a}$$

and the corresponding critical stress is

$$\sigma_{1,\mathrm{cr}} = \frac{q_{1\mathrm{cr}}}{h} = 0.605 \frac{Eh}{R}. \tag{19.31b}$$

This formula is of fundamental importance in the structural theory of shell stability. It follows from Sec. 19.2 that Eqs (19.30) and (19.31) determine the upper value of the critical loads, i.e., $q^{(1)}_{1,\mathrm{cr}}$. However, hereafter, the superscript 1 is dropped because the linear buckling analysis of shells is of interest in this section. Determine the

length of half sine waves into which the shell buckles, $l_w = L/m$. It follows from Eqs (19.28) and (19.29) that one can show the following:

$$l_w = \frac{\pi\sqrt{Rh}}{\sqrt[4]{12(1-\nu^2)}}. \tag{19.32}$$

In the case of very short shells, if $(L/R)^2 \ll 1$, one should set $m = 1$ and the differentiation of Eq. (19.27) becomes invalid. However, in this case, λ will be so much larger that the second term in the above equation becomes negligible compared with the first term. As a result, we obtain the following:

$$q_{1,\mathrm{cr}} = \frac{\pi^2 D}{L^2} \quad \text{and} \quad \sigma_{1,\mathrm{cr}} = \frac{\pi^2 D}{hL^2}.$$

This is the well-known Euler's formula for a strip column [2] cut from the shell in the direction of its generator.

Now, let us turn our attention to a more general variant of the solution of the buckling problem under consideration and assume that the *shell buckled surface is asymmetric*. For this general case, we apply the *equilibrium method* introduced in Sec. 19.2. The stability equation (Eq. (19.9)) for an axially loaded, by uniform compressive forces q_1, cylindrical shell takes the form (assuming $N_{10} = -q_1$)

$$D\nabla^4\nabla^4 w + \frac{Eh}{R^2}\frac{\partial^4 w}{\partial x^4} + q_1\nabla^4\left(\frac{\partial^2 w}{\partial x^2}\right) = 0. \tag{19.33}$$

We solve this equation in the manner outlined by Batdorf [3]. The general solution satisfying the boundary conditions (19.15) will be sought in the following form:

$$w = f\sin\frac{m\pi x}{L}\sin\frac{ny}{R}, \tag{19.34}$$

where m and n are the numbers of half-waves in the longitudinal and circumferential directions, respectively. We also introduce the following dimensionless parameter β, where

$$\beta = \frac{nL}{\pi R}, \tag{19.35}$$

and rewrite Eq. (19.34) as follows:

$$w = f\sin\frac{m\pi x}{L}\sin\frac{\beta\pi y}{L}. \tag{19.36}$$

Substitution of Eq. (19.36) into Eq. (19.33), gives the following:

$$D\left(\frac{\pi}{L}\right)^8(m^2+\beta^2)^4 + \frac{Eh}{R^2}m^4\left(\frac{\pi}{L}\right)^4 - q_1\left(\frac{\pi}{L}\right)^6 m^2(m^2+\beta^2)^2 = 0. \tag{19.37}$$

Dividing Eq. (19.37) by $D(\pi/L)^8$, one obtains the following equation:

$$(m^2+\beta^2)^4 + \frac{12m^4Z^2}{\pi^4} - K_1 m^2(m^2+\beta^2)^2 = 0, \tag{19.38}$$

where

$$Z = \frac{L^2}{Rh}(1-\nu^2)^{1/2}$$

and

$$K_1 = \frac{q_1 L^2}{D\pi^2}. \tag{19.40}$$

The nondimensional parameter Z is a shape factor. It is a measure of the ratio of the shell length to its radius and is useful for distinguishing between short and long cylinders. The parameter K_1 is the buckling coefficient similar to the one that appears in the plate buckling analysis (see Eq. (8.8)). It is a measure of the ratio of the shell length to its radius and is useful for distinguishing between short and long cylinders. Solving Eq. (19.38) for K_1, one obtains

$$K_1 = \frac{(m^2 + \beta^2)^2}{m^2} + \frac{12Z^2 m^2}{\pi^4 (m^2 + \beta^2)^2}. \tag{19.41}$$

Differentiating the above expression with respect to $(m^2 + \beta^2)^2/m^2$ and setting the result equal to zero, shows that K_1 has a minimum value when

$$\frac{(m^2 + \beta^2)^2}{m^2} = \left(\frac{12Z^2}{\pi^4}\right)^{1/2}. \tag{19.42}$$

Substitution of (19.42) into (19.41), gives

$$K_1 = \frac{4\sqrt{3}}{\pi^2} Z, \tag{19.43}$$

from which

$$q_{1,\mathrm{cr}} = \frac{1}{\sqrt{3(1-\nu^2)}} \frac{Eh^2}{R}. \tag{19.44}$$

The corresponding critical stress is given by

$$\sigma_{1,\mathrm{cr}} = \frac{q_{1,\mathrm{cr}}}{h} = \frac{Eh}{R} \frac{1}{\sqrt{3(1-\nu^2)}}. \tag{19.45}$$

If $\nu = 0.3$, then

$$q_{1,\mathrm{cr}} = 0.605 \frac{Eh^2}{R} \quad \text{and} \quad \sigma_{1,\mathrm{cr}} = 0.605 \frac{Eh}{R}. \tag{19.46}$$

Comparing Eqs (19.44) or (19.46) and Eqs (19.30) and (19.31), it is seen that the critical loads for asymmetric and axisymmetric buckling modes coincide exactly. We return now to Eq. (19.42) to establish the range of validity of Eqs (19.43) and (19.46). Solving Eq. (1942) for β, we have

$$\beta = \left[\frac{(12Z^2)^{1/4}}{\pi} m - m^2\right]^{1/2}. \tag{19.47}$$

Since, as a minimum, $m = 1$, it is apparent that for real values of β one obtains the following:

$$Z \geq \frac{\pi^2}{12^{1/2}} \geq 2.85. \tag{19.48}$$

Thus, the expressions (19.43) and (19.46) can be applied to cylinders for which $Z \geq 2.85$ or whose length $L > 1.69\sqrt{Rh}/\sqrt[4]{1-\nu^2}$. Such cylinders are classified as *moderate-length cylinders*. For *short cylinders*, for Z less than 2.85, the values of $\beta = 0$ and $m = 1$ are to be substituted into Eq. (19.41). For a short and simply supported cylinder, we obtain

$$K_1 = 1 + \frac{12Z^2}{\pi^4}. \tag{19.49}$$

The critical stress for cylinders with $Z < 2.85$ is thus given by

$$\sigma_{1,\mathrm{cr}} = \frac{K_1 \pi^2 D}{hL^2}, \tag{19.50}$$

where K_1 is defined by Eq. (19.49). Expression (19.50) indicates that the critical stress of a short cylinder approaches that of a wide laterally unsupported plate as Z approaches zero or as a simply supported column.

In the foregoing analysis, it was assumed that failure would occur as a result of local surface buckling. This assumption is valid only as long as the cylinder is not extremely slender. Long narrow cylinders may become unstable as a result of Euler's column buckling (general or global instability) before the local instability stress is reached, and must therefore be checked for both modes of failure. It has thus been shown that the buckling mode of an axially loaded cylinder depends on the ratio of its length to its radius. The local instability occurs for short and moderate-length cylinders, whereas a long cylinder buckles as a column. There is a big difference between local and general bucklings of short and long cylinders. The buckling of a very long cylinder (Euler's buckling mode) does not involve surface distortion of the circular cross section at all. Instead, the member simply behaves like Euler's column. The local instability largely involves a surface distortion for short cylinders. Intermediate-length cylinders are to be found between these two extremes and represent the majority of actual cylinders. Cylinders of this type buckle by developing surface distortions in both the longitudinal and circumferential directions, and their critical stress is given by Eq. (19.46).

19.3.3 Buckling of cylindrical shells under external pressure

Consider the case when a shell is subjected to uniform external pressure of intensity p (Fig. 19.3). Such a type of loading is typical for submarine hulls and shell aircraft engine housings. Also tanks in chemical plants often experience an excessive external pressure.

The external uniform pressure causes the membrane longitudinal stress σ_1 and circumferential stress σ_2, as well as the bending stresses in a cylindrical shell. In analyzing the shell buckling, the circumferential compressive stresses are of great importance. If a shell is sufficiently long, then the critical values of the external pressure p only slightly affect the boundary conditions prescribed on the shell edges. This means that a distortion of the circular cross section will be identical throughout the length of the shell. Hence, the buckling analysis of long cylindrical shells can be replaced (for the sake of simplicity) by the analysis of the stability of a ring of unit length with the same radius and thickness as for the given shell. Such a

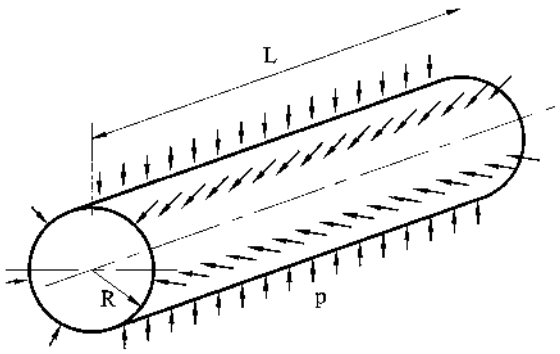

Fig. 19.3

buckling problem was analyzed, for example, in Ref. [2]. The critical value of the external pressure is given by

$$p_{\text{cr}} = \frac{(n^2 - 1)EI}{R^3}, \tag{19.51}$$

where n is the number of half-waves in the circumferential direction. The minimum value of p_{cr} is reached when $n = 2$, i.e.,

$$p_{\text{cr. min}} = \frac{3EI}{R^3}. \tag{19.52}$$

For long shells, p_{cr} is also given by Eq. (19.52), replacing EI by the flexural rigidity, $D = Eh^3/12(1 - \nu^2)$.

If a cylindrical shell subjected to a uniform external pressure is not too long, then its buckling analysis should be carried out with the use of equations of the structural stability theory, discussed in Sec. 19.2. Assume that the shell edges are simply supported and there is no bending of the shell. The circumferential stress is $\sigma_2 = -pR/h$. Hence, the action of the transverse pressure p is equivalent to the action of the compressive circumferential forces, equal to pR. Making use of the homogeneous equation (19.9) and setting $N_{10} = 0$, $N_{20} = -pr$, and $S = 0$ and dividing both sides by h, one obtains the following equation for the problem under consideration:

$$\frac{D}{h}\nabla^8 w + \frac{E}{R^2}\frac{\partial^4 w}{\partial x^4} + \frac{pR}{h}\nabla^4\left(\frac{\partial^2 w}{\partial y^2}\right) = 0. \tag{19.53}$$

where $\nabla^8 \equiv \nabla^4(\ldots)\nabla^4(\ldots)$.

One can take the solution of this equation in the form of Eq. (19.34) that satisfies the prescribed boundary conditions. Substituting the above expression for w into Eq. (19.53), one obtains the following:

$$\frac{D}{h}\left(\frac{m^2\pi^2}{L^2} + \frac{n^2}{R^2}\right)^4 + \frac{E}{R^2}\frac{m^4\pi^4}{L^4} - \frac{pR}{h}\left(\frac{m^2\pi^2}{L^2} + \frac{n^2}{R^2}\right)^2 \frac{n^2}{R^2} = 0, \tag{19.54}$$

from which

$$p_{mn} = DR\left(\frac{m^2\pi^2}{L^2 n} + \frac{n}{R^2}\right)^2 + \frac{Eh}{Rn^2}\frac{1}{\left(1 + \frac{n^2L^2}{R^2m^2\pi^2}\right)^2}. \tag{19.55}$$

It is evident that in determining the critical pressure we have to take $m = 1$. This means that the cylindrical shell subjected to external pressure has to buckle along the shell generator over one half-wave. Then we obtain the following from Eq. (19.55):

$$p_n = \frac{Dn^2}{R^3}\left[1 + \frac{1}{n^2}\left(\frac{\pi R}{L}\right)^2\right]^2 + \frac{Eh}{R}\frac{\left(\frac{\pi R}{L}\right)^4}{n^6\left[1 + \frac{1}{n^2}\left(\frac{\pi R}{L}\right)^2\right]^2}. \tag{19.56}$$

Determine from Eq. (19.56) the number of half-waves in the circumferential direction, n_{cr}, which provides a minimum value of p_n, i.e., the value of p_{cr}. In the general case, this problem can be solved only numerically; however, for some important practical cases, it may be simplified. For example, for intermediate-length shells when $0.3\sqrt{R/h} > L/R > \sqrt{h/R}$, the expression (19.56) is simplified significantly; it is possible to assume $n^2 \gg (\pi R/L)^2$. Then, instead of Eq. (19.56), one obtains

$$p_n = \frac{D}{R^3}n^2 + \frac{Eh}{R}\frac{(\pi R/L)^4}{n^6}.$$

Minimizing the above expression in n from the condition $\mathrm{d}p_n/\mathrm{d}n = 0$, we can find (for $\nu = 0.3$)

$$n_{\text{cr}}^2 = \frac{\pi R}{L}\sqrt[4]{36(1-\nu^2)}\sqrt{\frac{R}{h}} \approx 7.5\frac{R}{L}\sqrt{\frac{R}{h}} \tag{19.57}$$

and

$$p_{\text{cr}} = \frac{\pi\sqrt{6}}{9(1-\nu^2)^{3/4}}E\left(\frac{R}{L}\right)\left(\frac{h}{R}\right)^{5/2} = 0.92\frac{Eh^2}{RL}\sqrt{\frac{h}{R}}. \tag{19.58}$$

For short shells, when $L/R < \sqrt{h/R}$, the expression (19.56) can be also simplified. Investigations showed that buckling of such shells is accompanied by a large number of half-waves in the circumferential direction [4]. Consequently, the second term in the expression (19.56) can be neglected and we obtain

$$p_n = \frac{Dn^2}{R^3}\left[1 + \frac{1}{n^2}\left(\frac{\pi R}{L}\right)^2\right]^2.$$

The minimum value of p_n is reached for $n_{cr} = \pi R/L$. Thus, the critical value of the external pressure for the short shells is

$$p_{\text{cr}} = \frac{4D\pi^2}{RL^2}. \tag{19.59}$$

This value of the critical pressure corresponds to the following value of the circumferential force, $N_{2,\text{cr}}$

$$N_{2,\text{cr}} = p_{\text{cr}}R = \frac{4D\pi^2}{L^2}. \tag{19.60}$$

This expression is analogous to that obtained in Sec. 8.3 for the critical load of a simply supported rectangular plate compressed uniformly in one direction. Thus, a short cylindrical shell with simply supported edges under external pressure buckles as a simply supported plate, compressed in the longitudinal direction, whose width b is equal to L, and the number of half-waves is equal to $2n$.

It should be noted that expression (19.51) for long cylindrical shells cannot be obtained from Eq. (19.56) as a limiting case when $L/R \to \infty$. This can be explained as follows. Expression (19.56) was obtained on the basis of the simplified equations of the shallow shell theory, Eqs (19.53). It has been shown [4] that the assumptions of the shallow shell theory, introduced in Secs 17.3 and 17.4, are equivalent to the condition $n^2 \gg 1$ (assume that this inequality holds for $n \geq 4$) for the buckling problem under consideration. Thus, expression (19.56) is valid only if the above inequality holds. Cases $n = 2, 3$ that are typical for buckling of long cylindrical shells should be considered using a more refined shell theory: in particular, a more refined expression for a change of curvature of the deflected middle surface along the shell circumference. The latter can be obtained, for instance, by using the semi-membrane theory of the cylindrical shell, introduced in Sec. 17.2. Omitting the details of deriving the buckling governing equation based on this refined curvature expression, we present only the final result for the upper critical value of the external pressure for long shells, as follows [4]:

$$p_{\text{cr}} = \frac{DR}{n^2-1}\left\{\left(\frac{\pi^2}{L^2}+\frac{n^2}{R^2}\right)^2+\frac{1}{R^4}\left[1-2\left(\nu\frac{\pi^2R^2}{L^2}+n^2\right)\right]\right\} + \frac{Eh}{R}\frac{\pi^4}{L^4}\frac{1}{\left(\frac{\pi^2}{L^2}+\frac{n^2}{R^2}\right)^2(n^2-1)}; \quad n>1. \tag{19.61}$$

For a *very long cylindrical shell*, when $L \gg R$, this equation reduces to Eq. (19.51), i.e., the critical value of the external pressure for a ring of unit length.

19.3.4 Buckling of circular cylindrical shells under axial loads and external pressure

A combination of axial loads and external pressure is typical, for example, for elevated tower-shaped reservoirs or tanks used in chemical engineering. For these structures, the compressive stresses due to their self-weight occur at the bottom of tanks, whereas some vacuum may occur inside the tank.

Applying the linear buckling analysis, let us combine Eqs (19.33) (dividing it by h) and (19.53). As a result, we obtain the buckling governing equation for intermediate-length cylindrical shells subjected to axial compressive loads, q_1, and a uniform internal pressure, p, in the following form [4]:

$$\frac{D}{h}\nabla^4\nabla^4 w+\frac{E}{R^2}\frac{\partial^4 w}{\partial x^4}+\frac{q_1}{h}\nabla^4\left(\frac{\partial^2 w}{\partial x^2}\right)+\frac{pR}{h}\nabla^4\left(\frac{\partial^2 w}{\partial y^2}\right)=0. \tag{19.62}$$

Introducing the expression for w from Eq. (19.34) into the above, one obtains

$$\hat{q}_1+\frac{p}{\mu^2}=\frac{1}{12(1-\nu^2)}\frac{(1+\mu^2)^2}{\mu^2}\eta+\frac{\mu^2}{(1+\mu^2)\eta}, \tag{19.63}$$

where

$$\hat{q}_1 = \frac{q_1 R}{Eh}, \quad \hat{p} = \frac{p}{E}\left(\frac{R}{h}\right)^2, \quad \mu = \frac{m\pi R}{nL}, \quad \eta = \frac{n^2 h}{R}. \tag{19.64}$$

It is seen that the critical combinations of values $\hat{q}_1$ and $\hat{p}$ are related to one another by a linear relationship. The plot of $\hat{q}_1$ vs $\hat{p}$ represents some polygon $ACDB$, as shown in Fig. 19.4. This figure is taken from Ref. [4].

Note that points A and B in this figure correspond to the upper critical values of axial compressive load, $\hat{q}_{1cr}$, and external pressure, $\hat{p}_{cr}$, respectively, applied separately from one another. If we join these points by a straight line, we obtain some intermediate values of $\hat{q}_1$ and $\hat{p}$ corresponding to the following equation:

$$\frac{\hat{q}_1}{\hat{q}_{1cr}} + \frac{\hat{p}}{\hat{p}_{cr}} = 1$$

or

$$\frac{q_1}{q_{1cr}} + \frac{p}{p_{cr}} = 1 \tag{19.65}$$

(the superscript 1 that refers to the upper critical loads is omitted in the above and further equations, because in the linear buckling analysis only such a critical load can be obtained).

It is easily seen that Eq. (19.65) determines the critical combination of the axial loads and external pressure conservatively with respect to the polygon. Therefore, this equation can be used as a first approximation in a practical design.

Theoretical investigations and experiments showed that an axial compression decreases the value of the external critical pressure, compared with the case when this compression is absent. An axial tension increases the value of the external critical pressure. In turn, an internal pressure increases the value of the axial compressive critical force.

Also it should be noted that in the shell buckling problems introduced above, the solutions were obtained by assigning the boundary conditions for the deflections of the type of Eqs (19.15) on the shell edges, ignoring the in-plane displacements prescribed also on these edges. The investigations associated with the effect of the in-

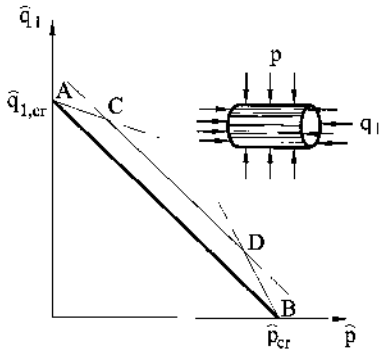

Fig. 19.4

plane boundary conditions on the values of the critical loads for simply supported shells showed that the critical stress is reduced drastically if the edges are permitted to move freely in the tangential direction [5,6].

19.3.5 Buckling analysis of cylindrical shells subjected to torsion

Let us consider a cylindrical shell of radius R and length L subjected to the twisting couples T applied to its ends. The unbuckled (initial) state of stress in such shells is determined by the shear stresses, τ. For thin cylindrical shells, such stresses are

$$\tau = \frac{T}{2\pi R^2 h}. \tag{19.66}$$

Buckling of cylindrical shells under twisting couples occurs when these couples reach some critical values T_{cr}. Such a type of buckling can take place under certain conditions in shells of aircraft structures and aircraft engines.

We consider here the linear buckling analysis only. Assume that the intermediate-length cylindrical shell, loaded by twisting couples T, is simply supported on its ends. Then, the stability equation (Eq. (19.9)) for this particular case of the shell geometry and loading will have the following form (after dividing both sides of the above equation by h):

$$\frac{D}{h}\nabla^4\nabla^4 w + \frac{E}{R^2}\frac{\partial^4 w}{\partial x^4} + 2\tau\nabla^4\left(\frac{\partial^2 w}{\partial x \partial y}\right) = 0. \tag{19.67}$$

By analogy with the stability problem of flat plates in shear, one can assume that the shell buckling in torsion will be followed by the formation of regularly located over a circumference waves, which are inclined under some angle to the shell generator.

A solution of Eq. (19.67) will be sought in the following form [4]:

$$w = f\cos\frac{\pi x}{L}\cos\frac{n}{R}(y + \gamma x), \tag{19.68}$$

where the origin of the x axis is taken at the shell midspan, n is the number of waves along a circumference, and γ is the slope of the crest of waves to the shell generator. Equation (19.68) satisfies the boundary conditions for $x = \pm L/2$.

After intermediate lengthy and cumbersome manipulation, we obtain some approximate expressions for the critical values of the twisting moment, T_{cr}. We have

$$T_{\text{cr}} = 2\pi\frac{E}{1-\nu^2}\frac{R^2h^3}{L^2}\left[2.8 + \sqrt{2.6 + 1.4\left(\frac{L^2}{2Rh}\sqrt{1-\nu^2}\right)^{1.5}}\right]. \tag{19.69a}$$

If the shell ends are fixed, then T_{cr} can be found from the following approximate equation:

$$T_{\text{cr}} = 2\pi\frac{E}{1-\nu^2}\frac{R^2h^3}{L^2}\left[4.6 + \sqrt{7.8 + 1.67\left(\frac{L^2}{2Rh}\sqrt{1-\nu^2}\right)^{1.5}}\right]. \tag{19.69b}$$

All the above equations were given for the intermediate-length cylindrical shells (the intermediate-length shell criterion was introduced in Sec. 19.3.4). For long-length shells when

$$\frac{L^2 h}{(2R)^3}\frac{1}{\sqrt{1-\nu^2}} > 7.8$$

for fixed shell ends, and

$$\frac{L^2 h}{(2R)^2}\frac{1}{\sqrt{1-\nu^2}} > 5.5$$

for simply supported shell ends, it had been established that T_{cr} does not depend on the shell boundary conditions and can be approximated by the following equation:

$$T_{cr} = \frac{1.5E}{\left(1-\nu^2\right)^{0.75}}\sqrt{Rh}. \tag{19.70}$$

The detailed buckling analysis of cylindrical shells in torsion is given in Ref. [4].

19.4 POSTBUCKLING ANALYSIS OF CIRCULAR CYLINDRICAL SHELLS

It was mentioned previously that the critical stress, given by the solution based on the linear buckling analysis, is not supported by test data. Experiments to validate the theoretical results inevitably indicated that the actual cylinders buckle at loads considerably below that those predicted by the linear stability theory. For instance, buckling loads for axially compressed cylinders were as low as 30% of the load given by the linear stability theory solution. Furthermore, the test results exhibited an unusually large degree of scatter.

Donnel [7,8] was the first to propose the use of the nonlinear or finite-deflection theory of cylindrical shells in an attempt to explain the existing discrepancy between the theoretical and experimental results. Then, von Karman and Tsien [9], using Donnel's large-deflection stability equations, obtained the first accurate description of the postbuckling behavior of an axially compressed cylinder. The next step in the study of the stability of cylindrical shells was made when Donnel and Wan [10] introduced in 1950 an initial imperfection into the buckling analysis. They showed that the initial imperfections can reduce appreciably the maximum load that an axially compressed cylinder can support. The next investigations supported the view that the discrepancy between the linear stability theory and test results was due mainly due to the presence of initial geometric and loading imperfections. For example, some investigators were be able to manufacture near-perfect shell specimens and thus minimize the effects of initial imperfections. For these near-perfect specimens, the observed buckling load was closer to the theoretically obtained critical load.

The governing equations of the large-deflection theory (Eqs (18.31)) are applicable for an initially perfect shallow shell. Several minor modifications must be introduced to make these equations valid also for a shallow shell with initial imperfections of shape. Assume that the lateral deflection consists of an initial deflection (comparable with the shell thickness), w_i, in addition to the deflection w produced by the

applied loads. Let us rewrite the strain–displacement relations (18.19) to include the effects of the initial imperfections. If in the derivation of these expressions given in Sec. 18.2.2 the lateral deflection w is replaced by $w + w_{\mathrm{i}}$, then Eqs (18.19) take the form

$$\begin{aligned}
\varepsilon_1 &= \frac{\partial u}{\partial x} - \kappa_1(w + w_i) + \frac{1}{2}\left(\frac{\partial w}{\partial x}\right)^2 + \frac{\partial w}{\partial x}\frac{\partial w_{\mathrm{i}}}{\partial x};\\
\varepsilon_2 &= \frac{\partial v}{\partial y} - \kappa_2(w + w_i) + \frac{1}{2}\left(\frac{\partial w}{\partial y}\right)^2 + \frac{\partial w}{\partial y}\frac{\partial w_{\mathrm{i}}}{\partial y};\\
\gamma_{xy} &= \frac{\partial u}{\partial y} + \frac{\partial v}{\partial x} + \frac{\partial w}{\partial x}\frac{\partial w}{\partial y} + \frac{\partial w_i}{\partial x}\frac{\partial w}{\partial y} + \frac{\partial w}{\partial x}\frac{\partial w_{\mathrm{i}}}{\partial y}.
\end{aligned} \tag{19.71}$$

Following the procedure for the derivation of the differential equations of the large-deflection theory, given in Sec. 18.2, we obtain the following

$$\begin{aligned}
\frac{D}{h}\nabla^2\nabla^2 w - L(w + w_{\mathrm{i}};\, \phi) - \nabla_k^2\phi &= \frac{p_3}{h},\\
\frac{1}{E}\nabla^2\nabla^2\phi &= -\frac{1}{2}L(w + 2w_{\mathrm{i}};\, w) - \nabla_k^2 w
\end{aligned} \tag{19.72}$$

where $\phi = \Phi/h$ and the operator $L(U, V)$ is given by Eqs. (18.30). The above equations are the *nonlinear governing equations of an initially imperfect shallow shells*.

We analyze below the postbuckling behavior of a shallow square cylindrical panel of side a, subjected to uniform compressive forces q_1 applied along the curvilinear edges of the panel, as shown in Fig. 19.5. The radius of curvature of the panel is R, and its thickness is h. The postbuckling behavior of such a panel is very similar to that of the entire cylinder, however, the calculation of the critical values of the compressive loads for this panel is less lengthy and less complicated than for the entire cylinder. The analysis presented here follows the general outline of that given by Volmir [4].

As far as the boundary conditions are concerned, it is assumed that (1) the edges are simply supported, (2) the shear force S vanishes along each edge, (3) the edges $y = 0$ and $y = a$ are free to move in the y direction, and (4) the panel retains its rectangular shape (in a plane) during buckling. These conditions are satisfied if we let

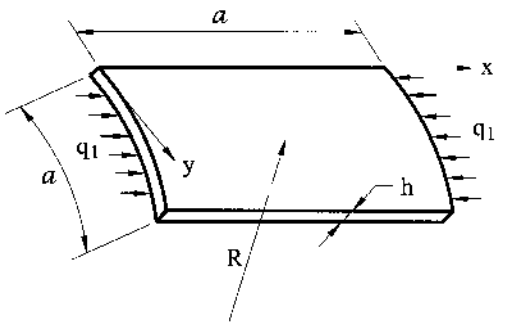

Fig. 19.5

$$w = f \sin\frac{\pi x}{a}\sin\frac{\pi y}{a}. \tag{19.73}$$

The panel is also assumed to have an initial deflection, given by

$$w_{\mathrm{i}} = f_{\mathrm{i}} \sin\frac{\pi x}{a}\sin\frac{\pi y}{a}. \tag{19.74}$$

It was shown [10] that the effect of initial imperfections is found to be stronger if their shape corresponds to the wave-like behavior of a perfect shell in buckling.

Let us substitute for w and w_{i} from Eqs (19.73) and (19.74) into the second Eq. (19.72). Making in the above equation $\kappa_2 = 1/R, \kappa_1 = 0$, one obtains the following:

$$\nabla^2\nabla^2\phi = E\left[(f^2 + 2f \cdot f_{\mathrm{i}})\frac{\pi^4}{2a^4}\left(\cos\frac{2\pi x}{a} + \cos\frac{2\pi y}{a}\right) + \frac{f\pi^2}{Ra^2}\sin\frac{\pi x}{a}\sin\frac{\pi y}{a}\right]. \tag{19.75}$$

A particular solution of this equation, obtained by the method of undetermined coefficients, is

$$\phi_{\mathrm{p}} = \frac{E(f^2 + 2f \cdot f_{\mathrm{i}})}{32}\left(\cos\frac{2\pi x}{a} + \cos\frac{2\pi y}{a}\right) + \frac{Efa^2}{4\pi^2 R}\sin\frac{\pi x}{a}\sin\frac{\pi y}{a}. \tag{19.76}$$

Determine the complementary solution of Eq. (19.75), ϕ_{h}. This solution should satisfy the homogeneous equation $\nabla^2\nabla^2\phi = 0$ and also has to correspond to the primary membrane forces that exist prior to buckling and are caused by the given loading q_1. We have that $N_1 = -q_1$,and $N_2 = S = 0$. Noting that

$$\frac{q_1}{h} = \frac{\partial^2\phi}{\partial y^2},$$

one obtains the following:

$$\phi_{\mathrm{h}} = -\frac{q_1 y^2}{2h}. \tag{19.77}$$

Thus, the general solution of the second Eq. (19.72) is obtained, as follows:

$$\phi = \frac{E(f^2 + 2f \cdot f_{\mathrm{i}})}{32}\left(\cos\frac{2\pi x}{a} + \cos\frac{2\pi y}{a}\right) + \frac{Efa^2}{4R\pi^2}\sin\frac{\pi x}{a}\sin\frac{\pi y}{a} - \frac{q_1 y^2}{2h}. \tag{19.78}$$

Now, let us return to the first Eq. (19.72). We satisfy this equation approximately only in Galerkin's procedure sense. So, setting $p_3 = 0, \kappa_1 = 0$, and $\kappa_2 = 1/R$, we obtain

$$\int^a \int_0^a \left[\frac{D}{h}\nabla^2\nabla^2 w - L(w, w_{\mathrm{i}}; \phi) - \frac{1}{R}\frac{\partial^2\phi}{\partial x^2}\right]\sin\frac{\pi x}{a}\sin\frac{\pi y}{a}\,\mathrm{d}x\mathrm{d}y = 0. \tag{19.79}$$

Substituting for w, w_{i}, and ϕ from Eqs (19.73), (19.74), and (19.78) into the above and integrating, we obtain, after some mathematics, the following equation:

$$\frac{Df\pi^4}{a^2} - \frac{q_1\pi^2}{4}(f + f_{\mathrm{i}}) + \frac{Efha^2}{16R^2} - \left(\frac{5}{6}f + f_{\mathrm{i}}\right)\frac{Eh}{R}f + \frac{Eh\pi^4}{32a^2}(f^2 + 3ff_{\mathrm{i}} + 2f_{\mathrm{i}}^2)f = 0, \tag{19.80}$$

from which

$$\hat{q}_1 = \left[\frac{\pi^2}{3(1-\nu^2)} + \frac{k^2}{4\pi^2} + \frac{\pi^2}{8}\left(\delta^2 + 3\delta\delta_i + 2\delta_i^2\right) - \frac{4k}{\pi^2}\left(\frac{5}{6}\delta + \delta_i\right)\right]\frac{\delta}{\delta + \delta_i}, \tag{19.81}$$

where

$$\hat{q}_1 = \frac{q_1 a^2}{Eh^3}, \quad k = \frac{a^2}{Rh}, \quad \delta = \frac{f}{h}, \quad \delta_i = \frac{f_i}{h}. \tag{19.82}$$

For $\nu = 0.3$, the relation (19.81) becomes

$$\hat{q}_1 = \left[3.6 + \frac{k^2}{39.5} + 1.23(\delta^2 + 3\delta\delta_i + 2\delta_i^2) - 0.405k(0.83\delta + \delta_i)\right]\frac{\delta}{\delta + \delta_i}. \tag{19.83}$$

Setting $\delta_i = 0$, we obtain the nonlinear load–deflection relationship for the perfect, axially compressed square shallow cylindrical shell, as follows:

$$\hat{q}_1 = \frac{\pi^2}{3(1-\nu^2)} + \frac{k^2}{4\pi^2} + \frac{\pi^2}{8}\delta^2 - \frac{10}{3\pi^2}k\delta. \tag{19.84}$$

If we set $k = 0$ (the curvature parameter), we derive the following nonlinear load–deflection relationship:

$$\hat{q}_1 = \frac{\pi^2}{3(1-\nu^2)} + \frac{\pi^2}{8}\delta^2, \tag{19.85}$$

which coincides with the corresponding nonlinear relationship for a square, simply supported flat plate.

Comparing Eqs (19.84) and (19.85), we can conclude that the presence of an additional linear term on the right-hand side of Eq. (19.84) indicates some peculiarities in the buckling behavior of a cylindrical panel compared with that of a flat plate. As buckling occurs, the applied compressive load drops, reaches a known minimum and only then is starting to increase. The minimum value of $\hat{q}_1$ can be obtained from the following:

$$\frac{d\hat{q}_1}{d\delta} = \frac{\pi^2}{4}\delta - \frac{10}{3\pi^2}k = 0, \tag{19.86}$$

from which

$$\delta = \frac{40k}{3\pi^4} \approx 0.14\text{k}. \tag{19.87}$$

The following critical load parameter corresponds to this definition:

$$\hat{q}_{1,cr}^{(2)} = \frac{\pi^2}{3(1-\nu^2)} + \frac{k^2}{4\pi^2} - \frac{200}{9\pi^6}k^2, \tag{19.88}$$

which represents the lower critical load parameter $\hat{q}_1$ for the perfect shallow cylindrical panel (see Sec. 19.2).

Approaching $\delta \to 0$ in Eq. (19.84), one obtains the following equation for the upper value of the critical load parameter $\hat{q}_1$ in a simply supported, axially compressed perfect square cylindrical panel by the linear buckling analysis:

$$\hat{q}_{1,\mathrm{cr}}^{(1)} = \frac{\pi^2}{3(1-\nu^2)} + \frac{k^2}{\pi^2}. \tag{19.89}$$

Thus, we can represent the nonlinear load–deflection relationship for the given perfect cylindrical panel as

$$\hat{q}_1 = \hat{q}_1^{(1)} + \frac{\pi^2}{8}\delta^2 - \frac{10}{3\pi^2}\mathrm{k}\delta. \tag{19.90}$$

Inserting Eq. (19.89) into Eq. (19.88) leads to the following:

$$\hat{q}_{1,\mathrm{cr}}^{(2)} = \hat{q}_{1,\mathrm{cr}}^{(1)} - \frac{200}{9\pi^6}k^2. \tag{19.91}$$

Let us turn to Eq. (19.83). As mentioned in Sec.19.2, there is a good reason to believe that the initial imperfections of a shell geometry have a great effect on the scatter of experimental data of the critical loads and on the discrepancies between the theoretical and experimental results. Figure 19.6 (taken from Ref. [11]) shows the load–deflection relationships for a flat plate with $k = 0$ (Fig. 19.6a) and for a cylindrical panel with $k = 24$ (Fig. 19.6b).

The curves in each figure depict the variation of the load parameter $\hat{q}_1$ with the total lateral deflection parameter $\delta + \delta_\mathrm{i}$. The curves for several different values of the initial imperfection δ_i are presented. It follows from Fig. 19.6a, that small initial deformations practically do not affect the buckling behavior of flat plates and the behavior of the flat plate is similar to that of a column. In fact, as in the case of the perfect plate ($\delta_\mathrm{i} = 0$), the critical load does not represent the maximum carrying capacity of the imperfect plate. Instead, as the deflection continues to grow, the imperfect plate is able to resist increasing loads. Furthermore, as the deflections increase, the curves of the initially imperfect plates approach that of the perfect plate.

The cylindrical panels demonstrate another behavior. A strong dependence of the maximum axial compressive load on the magnitude of the initial imperfection is seen from Fig. 19.6b. As long as the axial load is small, bending increases very gradually with an increase in the load. Then, suddenly, at a certain load whose magnitude appears to depend on the magnitude of the initial imperfection, the bending deflections begin to grow rapidly and the load drops. The important conclusion that can be drawn from this figure is that the maximum load, i.e., the buckling load, $q_{1\mathrm{b}}$ as introduced in Sec. 19.2, the initially imperfect panel can support, is considerably less that the upper critical load given by the linear stability theory. Even for very small imperfections, such as $\delta_\mathrm{i} = 0.05$, the maximum buckling load is only 75% of the upper critical load. Thus, small initial imperfections have a very significant effect on the buckling characteristics of cylindrical panels. The failure of the moderate-length cylinders in axial compression should be influenced profoundly by the magnitude of initial imperfections in the cylinder.

It should be noted that the general conclusions made above on the effect of the initial imperfections on the buckling characteristics of axially compressed panels are valid also for closed axially compressed cylinders. However, they are not typical for the buckling behavior of cylindrical shells under other loads.

Let us discuss briefly some important theoretical results available on the post-buckling behavior of cylinders subject to external pressure whose linear buckling analysis was presented in Sec. 19.3.3. It was shown [4,8] that the effect of nonlinear-

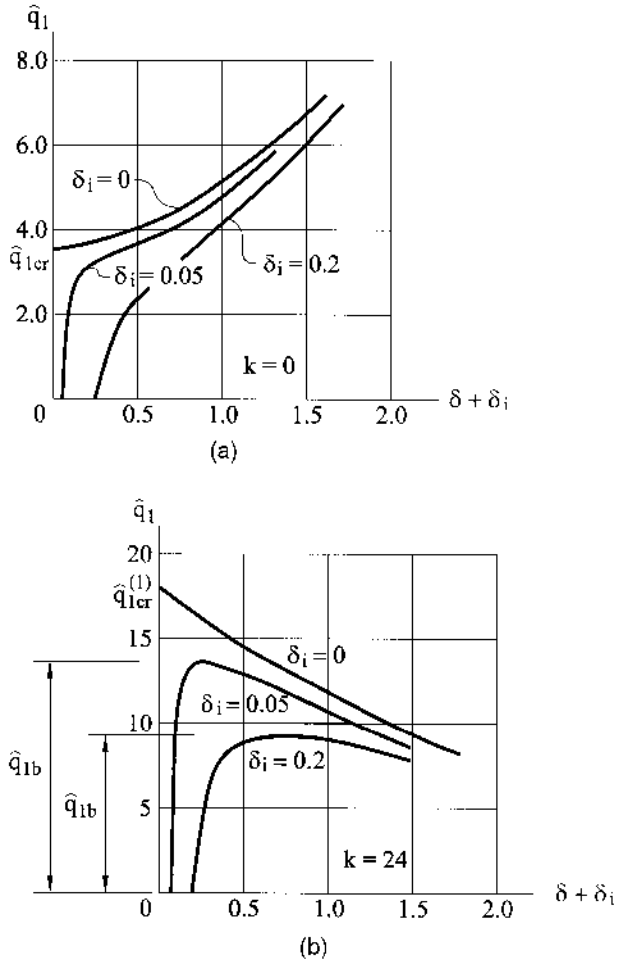

Fig. 19.6

ity in the case of the external pressure is significantly weaker than for the case of axial compression. The level of $\hat{q}^{(2)}_{1,cr}$ is about 70–75% of $\hat{q}^{(1)}_{1,cr}$, while for axial compression the above level lowered to 30–35%. Experimental data obtained by various investigators showed that the influence of the geometric imperfections on the critical value of applied loads depends essentially upon R/h. For instance, for very thin shells, the critical value of the transverse pressure drops significantly due to the presence of initial imperfections in the shell geometry.

19.5 BUCKLING OF ORTHOTROPIC AND STIFFENED CYLINDRICAL SHELLS

19.5.1 Orthotropic cylindrical shells under external pressure

Consider the stability problem for an orthotropic cylindrical shell of length L and radius R. The shell is simply supported on its ends and is subjected to an external

pressure p. Assume that the material of the shell is so arranged that at each point of the shell its mutual orthogonal directions of elastic symmetry coincide with the principal lines of curvature of the shell midsurface.

The differential equation of stability for orthotropic cylindrical shells under external pressure can be derived in much the same way as for isotropic shells (see Sec. 19.3.3). The solution of this equation can also be sought in the form of Eq. (19.34). Omitting the lengthy and cumbersome mathematics, we present below the following final expression for the critical value of external pressure, p_{cr}:

$$p_{cr} = \min\left\{\left[\frac{D_n}{R^3} + h\beta_n \frac{\alpha^2}{Rt_n}\right]\frac{1}{\gamma_n}\right\}, \tag{19.92}$$

where,

$$\begin{aligned}
D_n &= D_1\alpha^4 + 2D_3\alpha^2(n^2-1) + D_2(n^2-1)^2 + (D_3 - \nu_1 D_2)\alpha^2,\\
\beta_n &= \alpha^2 + (\alpha^2 - \nu_2 n^2)\left[D_3\alpha^2 + D_2(n^2-1)\right]\frac{1}{E_2R^2h},\\
t_n &= \alpha^4\delta_2 + 2\delta_3\alpha^2n^2 + \delta_1 n^4,\ \gamma_n = 0.5\alpha^2 + n^2 - 1,\\
\delta_1 &= \frac{1}{E_1},\quad \delta_2 = \frac{1}{E_2},\quad \delta_3 = \frac{1}{2G} - \frac{\nu_1}{E_1},\quad \alpha = \frac{\pi R}{L}.
\end{aligned} \tag{19.93}$$

The rigidities D_1, D_2, and D_G are given by Eqs (18.45b) and $D_3 = D_1\nu_2 + D_G$. It follows from Eq. (19.92), that the critical value of pressure, p_{cr}, is obtained by selecting the number of half-waves in the circumferential direction, n, so that it makes Eq. (19.92) a minimum.

19.5.2 Stability of stiffened cylindrical shells

As mentioned previously, cylinders are frequently manufactured with longitudinal (stringers) and circumferential (ribs or collars) stiffeners. An aircraft fuselage and a submarine hull are examples of stiffened shells. As a rule, stiffened shells are more efficient than unstiffened shells. In addition, they are less sensitive to initial imperfections. Therefore, the critical values of applied loads for such shells are closer to the theoretically determined values of the upper critical loads predicted by the linear stability theory.

The buckling analysis of stiffened shells, just as the corresponding analysis of stiffened plates, requires several steps. The first step in this analysis is to assess the overall or primary buckling response of the stiffened shell. The second step is to determine the local skin buckling response for skin segments located between stiffeners. The third step is to determine whether stiffener buckling has occurred at the given buckling load level. Our main concern in this book is with the primary buckling analysis of stiffened shells.

The primary buckling analysis of thin shells reinforced by closely spaced orthogonal stiffeners can be addressed conveniently with the use of the orthotropic shell theory, introduced in Sec. 18.3. In this case, the rigidities of the stiffeners are smearing along the shell middle surface, and a gird-stiffened shell is replaced by a structurally orthotropic unstiffened shell. We locate a point on the shell midsurface by the x and y coordinates (see Fig. 19.2). Following the simplified DMV theory of thin

shells, introduced in Sec. 17.3, let us derive the governing differential equations for the structurally orthotropic circular cylindrical shell. Assume that the stiffeners and shell skin are made of the same isotropic material having the modulus of elasticity E and Poisson's ratio ν, and that the stiffeners are symmetric with respect to the middle surface (i.e., $K_{11} = K_{22} = 0$). For this particular case, setting $R_1 \to \infty$ and $R_2 = R$, the governing equations of the stiffened cylindrical shells, Eqs (18.63) and (18.66), are reduced to the following form:

$$\begin{aligned} &D_{11}\frac{\partial^4 w}{\partial x^4} + 2(D_{21} + D_{33})\frac{\partial^4 w}{\partial x^2 \partial y^2} + D_{22}\frac{\partial^4 w}{\partial y^4} - \frac{1}{R}\frac{\partial^2 \Phi}{\partial x^2} = p_3, \\ &\frac{B_{11}}{B_s}\frac{\partial^4 \Phi}{\partial x^4} + \left(\frac{1}{B_{33}} - \frac{2B_{12}}{B_s}\right)\frac{\partial^4 \Phi}{\partial x^2 \partial y^2} + \frac{B_{22}}{B_s}\frac{\partial^4 \Phi}{\partial y^4} + \frac{1}{R}\frac{\partial^2 w}{\partial x^2} = 0. \end{aligned} \tag{19.94}$$

It can be shown that for an unstiffened circular cylindrical shell, $D_{11} = D_{22} = D$; $D_{12} = \nu D$; $D_{33} = D(1-\nu)$; $B_{11} = B_{22} = B$; $B_{12} = \nu B$; $B_{33} = B(1-\nu)/2$; $B_s = B^2(1-\nu^2)$, Eqs (19.94) are reduced to the governing equations of an isotropic circular cylindrical shells according to the DMV theory. If $R \to \infty$, the first Eq. of (19.94) transforms into Eq. (7.31), derived in Sec. 7.2 for the structurally orthotropic flat plates. Introducing the operators

$$\begin{aligned} \nabla_D^4(..) &\equiv D_{11}\frac{\partial^4(..)}{\partial x^4} + 2(D_{12} + D_{33})\frac{\partial^4(..)}{\partial x^2 \partial y^2} + D_{22}\frac{\partial^4(..)}{\partial y^4}, \\ \nabla_B^4(..) &\equiv \frac{B_{11}}{B_s}\frac{\partial^4(..)}{\partial x^4} + \left(\frac{1}{B_{33}} - \frac{2B_{12}}{B_s}\right)\frac{\partial^4(..)}{\partial x^2 \partial y^2} + \frac{B_{22}}{B_s}\frac{\partial^4(..)}{\partial y^4}, \end{aligned} \tag{19.95}$$

we can rewrite Eqs (19.94) as follows:

$$\nabla_D^4 w - \frac{1}{R}\frac{\partial^2 \Phi}{\partial x^2} = p_3; \quad \nabla_B^4 \Phi + \frac{1}{R}\frac{\partial^2 w}{\partial x^2} = 0. \tag{19.96}$$

In the buckling analysis problems, p_3 is replaced by $p_3^{(f)}$ from Eq. (19.8); then the first Eq. (19.96) becomes

$$\nabla_D^4 w - \frac{1}{R}\frac{\partial^2 \Phi}{\partial x^2} = N_{10}\frac{\partial^2 w}{\partial x^2} + N_{20}\frac{\partial^2 w}{\partial y^2} + 2S_0\frac{\partial^2 w}{\partial x \partial y}. \tag{19.97}$$

Consider a *structurally orthotropic circular cylindrical shell subjected to uniform axial compression forces* q_1. Using Eqs (19.96) and (19.97) and setting $N_{10} = -q_1$; $N_{20} = S_0 = 0$, one obtains the following:

$$\begin{aligned} &\nabla_D^4 w - \frac{1}{R}\frac{\partial^2 \Phi}{\partial x^2} + q_1\frac{\partial^2 w}{\partial x^2} = 0, \\ &\nabla_B^4 \Phi + \frac{1}{R}\frac{\partial^2 w}{\partial x^2} = 0. \end{aligned} \tag{19.98}$$

The Galerkin method can be applied to solving Eqs (19.98). Let us approximate the deflection w by the following series (the first-order approximation):

$$w = f \sin\frac{\pi x}{l_x}\sin\frac{\pi y}{l_y}, \tag{19.99}$$

where l_x and l_y are the lengths of the half-waves in the longitudinal and circumferential directions, respectively. Dropping intermediate and lengthy manipulations, we present below, following Volmir [4], the final result for the upper critical forces corresponding to the axisymmetric mode of buckling, when only circumferential axisymmetric bulges take place. In this particular case, $w = f \sin \pi x/l_x$ and the above-mentioned critical forces are

$$q_{1,\mathrm{cr}}^{(1)} = \frac{2}{R}\sqrt{\frac{D_{11}B_s}{B_{11}}}. \tag{19.100}$$

For an isotropic circular cylindrical shell subjected to compressive forces q_1 in the longitudinal direction, the above expression passes into Eq. (19.30).

Similarly, the stability problem for a *cylindrical shell simply supported on its ends and reinforced by closely spaced (at equal distances l_x stiffening rings under external pressure*, can be considered. Assume that the rings are symmetrically placed with respect to the shell midsurface and that the shell and rings are made of the same isotropic material, having the modulus of elasticity E and Poisson's ratio ν. For this particular case, Eqs (18.48) and (18.50) are simplified to the following form:

$$\begin{aligned}
&B_{11} = B = \frac{Eh}{1-\nu^2}, \quad B_{12} = B_{21} = B, \quad K_{11} = K_{22} = 0,\\
&B_{22} = B + \frac{EA_{\mathrm{c}}}{l_x}, \quad B_{33} = B\frac{1-\nu}{2},\\
&D_{11} = D = \frac{Eh^3}{12(1-\nu^2)}, \quad D_{12} = D_{21} = \nu D, \quad D_{22} = D + \frac{EI_{\mathrm{c}}}{l_x}, \quad D_{33} = D(1-\nu),
\end{aligned} \tag{19.101a}$$

where A_{c} and I_{c} are the cross-sectional area and moment of inertia of the rings about the tangent to the middle surface. Comparing the rigidities of the cylindrical shell reinforced by rings (Eqs (19.101a)) and the rigidities of the orthotropic cylindrical shell (Eqs (18.44) and (18.45b)), we can derive the following approximate relations for the elastic constants in the reduced structurally orthotropic shell:

$$\begin{aligned}
&E_1 = E, E_2 = E\left(1 + \frac{A_{\mathrm{c}}}{l_x h}\right), D_1 = D, D_2 = D + \frac{EI_{\mathrm{c}}}{l_x},\\
&\nu_2 = \nu, \nu_1 = \frac{\nu E}{E_2}, D_3 = D_G + \nu D_1 = D,\\
&\delta_1 = \frac{1}{E}, \quad \delta_2 = \frac{1}{E_2}, \quad \delta_3 = \frac{1 + \nu - \nu E/E_2}{E}.
\end{aligned} \tag{19.101b}$$

Substituting these values into Eqs (19.92) and (19.93) leads to the following expression for the critical value of external pressure:

$$p_{\text{cr}} = \min\left\{\frac{1}{0.5\alpha^2 + n^2 - 1}\left\{\frac{EI_c}{R^3 l_x}\left[(n^2-1)^2 + \frac{\alpha^2}{\Delta_n}(n^2-1)(\alpha^2 - \nu n^2)\right]\right.\right.$$
$$+ \frac{Eh}{R}\frac{(1+\mu)\alpha^4}{\Delta_n} + \frac{D}{R^3}\left[\frac{\alpha^2}{\Delta_n}(\alpha^2 - \nu n^2)(\alpha^2 + n^2 - 1) + (1-\nu)\alpha^2\right. \tag{19.102}$$
$$\left.\left.\left.+(\alpha^2 + n^2 - 1)^2\right]\right\}\right]$$

where

$$\mu = \frac{A_{\text{c}}}{l_x h}, \quad \Delta_n = (\alpha^2 + n^2)^2 + \mu n^2\left[2(1+\nu)\alpha^2 + n^2\right].$$

For thin stiffened shells of aircraft and marine structures, the value of μ is much less than unity and the flexural rigidity of rings, EI_{c}, is much larger than the stiffness of the shell between the rings, Dl_x. Therefore, with a small error, one can assume that $\mu = 0$ and $D = 0$. If, in addition, the small terms in the first brackets of Eq. (19.102) are omitted, then the above equation is simplified to the form

$$p_{\text{cr}} = \min\left\{\frac{E}{0.5\alpha^2 + n^2 - 1}\left[\frac{I_{\text{c}}}{R^3 l_x}(n^2-1)^2 + \frac{h}{R}\frac{\alpha^4}{(\alpha^2 + n^2)^2}\right]\right\}. \tag{19.103}$$

The critical value of the external pressure is obtained by selecting n so that it makes Eq. (19.102) or Eq. (19.103) a minimum. Conducted investigations have shown that a minimum is obtained, as a rule, if $n = 2, 3$.

If we take $\alpha = 0$ in Eq. (19.103), i.e., consider an infinitely long cylindrical shell reinforced by rings, one obtains, by setting $q = pl_x$, for $n = 2$, the expression for the critical value of external pressure in a closed circular ring in the form

$$q_{\text{cr}} = \frac{3EI_{\text{c}}}{R^3}.$$

As expected, the above equation coincides with Eq. (19.52).

For stiffened cylindrical shells subjected to axial compressive loads and external pressure, Eq. (19.65) is generalized to the following form [4]:

$$\left(\frac{q_1}{q_{1,\text{cr}}}\right)^{\alpha} + \frac{p}{p_{\text{cr}}} = 1, \tag{19.104}$$

where $\alpha > 0$ is some parameter. The recommended value of α is determined by the level of designed limiting state in combined loading. For example, for waffle shells, $\alpha = 1.7$. The values of this coefficient are given for some stiffened shells in Ref. [4].

Comprehensive theoretical and numerical investigations of stiffened shells subjected to global and local buckling, as well as the design strategy for optimal design of the above shells, are given in Refs [4,12,13]. In particular, it was shown that a waffle-type cylindrical shell with closely placed stringers and rings meets minimum weight requirements. Terebushko showed [14] that with typical geometric parameters for stiffeners and the distances between them, one can design a stiffened cylindrical shell that will be about 1.5 times lighter than the corresponding unstiffened isotropic cylindrical shell of the same overall geometry.

19.6 STABILITY OF CYLINDRICAL SANDWICH SHELLS

Consider a closed cylindrical sandwich shell loaded symmetrically about its middle surface. The buckling analysis of the sandwich shells includes two modes of buckling: a global (or general), associated with bending of the middle surface of the shell; and a local, which is manifested in bending of facing sheets without bending of the shell as a whole. The local bending of face sheets can be modeled by a shell resting on an elastic foundation. In this book, we consider only the global buckling of a sandwich shell.

The small-deflection theory of the shallow sandwich shells was introduced in Sec. 18.4. The governing differential equations (18.78), (7.129), and (18.81) derived for the shallow sandwich shells may also be applied to a circular cylindrical sandwich shell if its middle surface is referred to the coordinates x and y measured along the shell generator and arc of its cross section. To apply the above-mentioned equations for the stability problems, they should be modified. The value of the transverse surface load p_3 in the fifth equation of equilibrium (Eq. 18.78e)) has to be replaced by the value of $p_3^{(f)}$according to Eq. (19.8). Thus, Eqs (18.78a–d) remain unchanged, while Eq. (18.78e), for the buckling problems of the sandwich cylindrical shell, takes the form

$$\frac{\partial Q_1}{\partial x}+\frac{\partial Q_2}{\partial y}+N_{10}\frac{\partial^2 w}{\partial x^2}+N_{20}\left(\frac{1}{R}+\frac{\partial^2 w}{\partial y^2}\right)+2S_0\frac{\partial^2 w}{\partial x\partial y}=0. \tag{19.105}$$

The stress resultants–displacements relations have the form of Eqs (18.81). The constitutive equations in terms of the moments, shear forces, and deflections are, as follows (see Eqs. (7.129)):

$$\begin{aligned}
M_1 &= -D_1^*\left[\left(\frac{\partial^2 w}{\partial x^2}+\nu_2\frac{\partial^2 w}{\partial y^2}\right)-\left(\frac{1}{D_{Q_1}}\frac{\partial Q_1}{\partial x}+\frac{\nu_2}{D_{Q_2}}\frac{\partial Q_2}{\partial y}\right)\right],\\
M_2 &= -D_2^*\left[\left(\frac{\partial^2 w}{\partial y^2}+\nu_1\frac{\partial^2 w}{\partial x^2}\right)-\left(\frac{1}{D_{Q_2}}\frac{\partial Q_2}{\partial y}+\frac{\nu_1}{D_{Q_1}}\frac{\partial Q_1}{\partial x}\right)\right],\\
H &= -D_{12}\left[\frac{\partial^2 w}{\partial x\partial y}-\frac{1}{2}\left(\frac{1}{D_{Q_1}}\frac{\partial Q_1}{\partial y}+\frac{1}{D_{Q_2}}\frac{\partial Q_2}{\partial x}\right)\right],
\end{aligned} \tag{19.106}$$

where

$$D_1^*=\frac{D_1}{1-\nu_1\nu_2};\quad D_2^*=\frac{D_2}{1-\nu_1\nu_2}; \tag{19.107}$$

and ν_1, ν_2, D_1, D_2, and D_{12} are the flexural Poisson's ratios, flexural and twisting stiffness, respectively; D_{Q_1} and D_{Q_2} are the transverse shear stiffnesses (see Sec. 7.6).

Let us analyze the compressive buckling of an isotropic, sandwich circular cylindrical shell. For this special case, the above governing differential equations of the small-deflection sandwich shell theory can be reduced to a single eight-order differential equation in w in the form of Eq. (18.83). Modifying the above equations to the stability analysis of the sandwich circular plate, we obtain

$$D_s\nabla^4\nabla^4 w + \left(1 - \frac{D_s}{D_Q}\nabla^2\right)\left[\frac{2E_f t}{R^2}\left(\frac{\partial^4 w}{\partial x^4}\right) - \nabla^4\left(N_{10}\frac{\partial^2 w}{\partial x^2} + N_{20}\frac{\partial^2 w}{\partial y^2} + 2S_0\frac{\partial^2 w}{\partial x \partial y}\right)\right] = 0, \tag{19.108}$$

where D_s and D_Q are given by Eqs (18.82).

Following Plantema [17], consider the *axisymmetric buckling of an infinitely long, axially compressed isotropic sandwich cylinder*. Let the axial compressive load per unit run be q_1. Then, $N_{10} = -q_1$, $N_{20} = S_0 = 0$. For axisymmetric buckling, it is observed that all derivatives of the deflection w with respect to the y coordinate vanish. Thus, Eq. (19.108) is simplified to the following:

$$D_s\frac{\partial^8 w}{\partial x^8} + \left(1 - \frac{D_s}{D_Q}\frac{\partial^2}{\partial x^2}\right)\frac{\partial^4}{\partial x^4}\left(\frac{2E_f t}{R^2}w + q_1\frac{\partial^2 w}{\partial x^2}\right) = 0. \tag{19.109}$$

A solution of this equation may be represented in the form

$$w = A\sin\frac{\pi x}{l}, \tag{19.110}$$

where l is the half-wave length in the axial direction. Substituting the above into Eq. (19.109), we obtain, after some mathematics, the following:

$$q_1 = \frac{\pi^2 D_s}{l^2}\left(1 + \frac{\pi^2 D_s}{l^2 D_Q}\right)^{-1} + \frac{2E_f t l^2}{\pi^2 R^2}.$$

With

$$D_s = \frac{E_f t d^2}{2(1-\nu^2)}$$

this equation becomes

$$q_1 = D_s\left[\frac{\pi^2}{l^2}\left(1 + \frac{\pi^2 D_s}{l^2 D_Q}\right)^{-1} + \frac{4(1-\nu^2)l^2}{\pi^2 R^2 d^2}\right]. \tag{19.111}$$

Find the minimum value of q_1 as a function of the continuous variable l. The condition $\partial q_1/\partial l = 0$ leads to the following relationship:

$$\frac{l^2}{\pi^2} = \frac{Rd}{2\sqrt{1-\nu^2}} - \frac{D_s}{D_Q}. \tag{19.112}$$

Substitution of the above into Eq. (19.111) gives the following expression for the critical load:

$$q_{1,\mathrm{cr}} = \frac{4D_s\sqrt{1-\nu^2}}{Rd}\left(1 - \frac{D_s\sqrt{1-\nu^2}}{D_Q Rd}\right). \tag{19.113}$$

If the shear stiffness of the sandwich shell is infinite, then the corresponding critical load will be given by the following:

$$q_{1,\mathrm{cr}} = \frac{4D_s\sqrt{1-\nu^2}}{Rd} = \frac{2E_f td}{R\sqrt{1-\nu^2}}. \tag{19.114}$$

19.7 STABILITY OF SHALLOW SHELLS UNDER EXTERNAL NORMAL PRESSURE

Consider a shallow shell, rectangular in a plan, with the principal curvatures $\kappa_1 = 1/R_1 = \text{const}$ and $\kappa_2 = 1/R_2 = \text{const}$ (see Fig. 17.6). Assume that the shell edges are pin-connected with some diaphragms, which are absolutely stiff in bending in their own planes and have a small bending stiffness in planes tangent to the middle surface. In addition, we assume that points belonging to end sections of the shell are free to slide along the diaphragms. The following boundary conditions correspond to the these assumptions:

$$w = 0, \frac{\partial^2 w}{\partial x^2} = 0, \sigma_1 = 0, \quad \tau_{12} = 0 \Big|_{x=0, x=a} \tag{19.115}$$

Similar conditions are assigned to the shell edges $y = 0, b$. The external pressure p is uniformly distributed across the shell surface, and acts viewed from the shell convexity, i.e., $p_3 = p$. Assume that the shell is geometrically perfect.

The analysis presented here follows the general outline of that given by Volmir [4]. We use the nonlinear shell buckling analysis and the governing equations (18.31). The latter are represented in the form

$$\begin{aligned} X &\equiv \frac{D}{h}\nabla^2\nabla^2 w - L(\phi, w) - \nabla_k^2\phi - \frac{p_3}{h} = 0, \\ Y &\equiv \frac{1}{E}\nabla^2\nabla^2\phi + \frac{1}{2}L(w, w) + \nabla_k^2 w = 0, \end{aligned} \tag{19.116}$$

where $\phi = \Phi/h$.

The Galerkin method can be applied for integration of the above system of equations for the given boundary conditions (19.115). We seek the functions w and ϕ in the form of the following series:

$$\phi = \sum_m \sum_n A_{mn} \sin\frac{n\pi x}{a}\sin\frac{m\pi y}{b}; \quad w = \sum_m \sum_n B_{mn} \sin\frac{n\pi x}{a}\sin\frac{m\pi y}{b}. \tag{19.117}$$

Consider a solution of the problem based on the first approximation, retaining in the series (19.117) only the first terms. It can be shown that the first three boundary conditions (19.115) will be satisfied; the fourth condition is satisfied " on the average," for the shell edges $x = 0, a$ so this condition is satisfied in the following sense:

$$\frac{1}{a}\int_0^a \tau_{12}\mathrm{d}y = 0.$$

The Galerkin method equations (see Sec. 6.5) are the following:

$$\int_0^a \int_0^b X \sin\frac{\pi x}{a}\sin\frac{\pi y}{b}\mathrm{d}x\mathrm{d}y = 0; \quad \int_0^a \int_0^b Y \sin\frac{\pi x}{a}\sin\frac{\pi y}{b}\mathrm{d}x\mathrm{d}y = 0. \tag{19.118}$$

Substituting expressions (19.116) together with the approximations (19.117) into the above and integrating, one obtains

$$\begin{gathered}\frac{D}{h}B_1\frac{\pi^6}{16}\left(\frac{1}{a^2}+\frac{1}{b^2}\right)^2 - A_1B_1\frac{2}{3}\frac{\pi^4}{a^2b^2} + A\frac{\pi^4}{16}\left(\frac{k_1}{b^2}+\frac{k_2}{a^2}\right) - \frac{p}{h} = 0,\\ \frac{A_1}{E} + \frac{16B_1^2}{3\pi^2\left(\frac{b}{a}+\frac{a}{b}\right)^2} - \left(\frac{k_1}{b^2}+\frac{k_2}{a^2}\right)\frac{B_1}{\pi^2}\frac{1}{\left(\frac{1}{a^2}+\frac{1}{b^2}\right)^2} = 0.\end{gathered} \tag{19.119}$$

Introduce the following dimensionless parameters:

$$k_1^* = \frac{k_1a^2}{h}; \quad k_2^* = \frac{k_2b^2}{h}; \quad k^* = k_1^* + k_2^*; \quad \lambda = \frac{a}{b}; \quad \zeta = \frac{B_1}{h}; \quad \hat{p} = \frac{p}{E}\left(\frac{ab}{h^2}\right)^2. \tag{19.120}$$

Using the above-introduced parameters, we can represent a solution of Eqs (19.119), in the following load–deflection relationship:

$$\hat{p} = \frac{32\pi^2}{9}\frac{\zeta^3}{\left(1+\frac{1}{\lambda}\right)^2} - \frac{k^*\pi^2\zeta^2}{\left(1+\frac{1}{\lambda}\right)^2} + \left[\frac{(k^*)^2\pi^2}{16\left(1+\frac{1}{\lambda}\right)^2} + \frac{\pi^6\left(\frac{1}{\lambda}+\lambda\right)^2}{192(1-\nu^2)}\right]\zeta. \tag{19.121}$$

For a square shallow shell panel and $\nu = 0.3$, the above equation simplifies to the form

$$\hat{p} = 8.77\zeta^3 - 2.46k^*\zeta^2 + [0.154(k^*)^2 + 22]\zeta. \tag{19.122}$$

For a cylindrical shallow shell panel, $\kappa_1 = 0$ and $\kappa_2 = 1/R$, then $k^* = b^2/Rh$.

Figure 19.7 illustrates the diagrams of $\hat{p}$ vs $.\zeta$ for various values of k^* and for $\lambda = 1$. These diagrams are shown by dashed lines. The numerical data presented in the Fig. 19.7 are taken from Ref. [4]. It is seen that for small values of k^* the value of $\hat{p}$ increases continuously, just as for flat plates; for large values of k^*, the diagram $\hat{p}(\zeta)$ has a descending branch. To find the value of k^* at which jumping occurs from one stable configuration of equilibrium to another, it is necessary to analyze $\mathrm{d}\hat{p}/\mathrm{d}\zeta$. Equating it to zero, one finds the values of ζ corresponding to the upper and lower values of the critical pressure previously introduced in Sec. 19.2. We have the following:

$$\zeta = \frac{3}{32}k^* \mp \frac{1}{32}\sqrt{3(k^*)^2 - \frac{\pi^4\left(1+\frac{1}{\lambda}\right)^4}{2(1-\nu^2)}}. \tag{19.123}$$

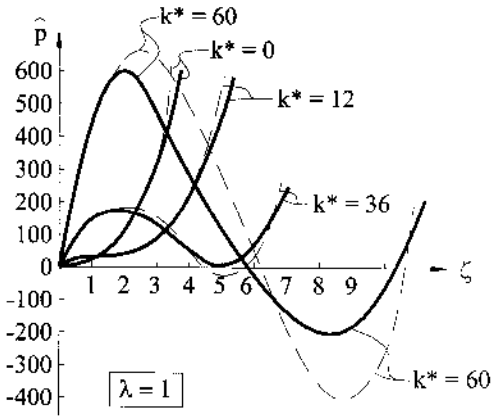

Fig. 19.7

The boundary of the domain of this jump corresponds to the case when the diagram $\hat{p}(\zeta)$ has a point of inflection with a horizontal tangent. In so doing, the expression under the radical sign must vanish. Thus, a limiting value of k^* will be of the form

$$\mathrm{k}^* = \frac{\pi^2\left(1+\frac{1}{\lambda}\right)^2}{\sqrt{6(1-\nu^2)}} \quad \text{for} \quad \zeta = \frac{3}{32}k^*. \tag{19.124}$$

If we retain four terms in series (19.177), the refined solutions will be obtained. They are shown by solid lines in Fig.19.7. It is seen from this figure that the distinctions of the refined diagrams from the first-approximation diagrams become perceptible only for "elevating" shells, starting with $k^* = 36$, and the refined diagrams give slightly lower upper critical values of pressure. However, the refined diagrams illustrate the changes in the lower critical loads: in some cases, the loads change sign.

19.8 BUCKLING OF CONICAL SHELLS

Thin conical shells find wide applications in the structures of jet engines, aircrafts, liquid storages, reservoirs, etc. Buckling analysis of conical shells is more complicated than the corresponding analysis of cylindrical shells, because of the complexity of the stability governing equations.

We consider below some final results of the linear buckling analysis of intermediate-length conical shells subjected to uniform external pressure p, as shown in Fig. 19.8. Assume that the shell ends cannot displace at their ends in the direction normal to the shell midsurface. The criterion of the "intermediate-length cylindrical shell" was introduced in Sec. 19.3. This criterion can be employed for conical shells, too, by replacing R with the mean radius of the parallel circle $r_m = (r_1 + r_2)/2$, and by setting L equal to the length of the longitudinal axis of the shell (Fig. 19.8). For the above-mentioned shells, $n^2 > \lambda^2$, where n is the number of half-waves in the circumferential direction of the shell and $\lambda = \pi r_m/L$. Then, the approximate relation for determining the critical value of the external pressure in a conical shell is

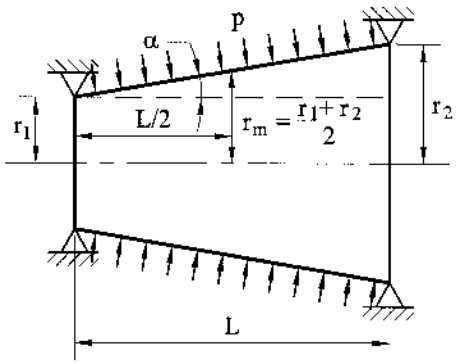

Fig. 19.8

$$p_{cr} = \frac{0.855}{(1-\nu^2)^{0.75}} \frac{Eh}{L} \left(\frac{h}{r_m}\right)^{1.5} (\cos\alpha)^{1.5}. \tag{19.125}$$

For $\nu = 0.3$, this relation appears in the form

$$p_{cr} = 0.92 \frac{Eh}{L} \left(\frac{h}{r_m}\right)^{1.5} (\cos\alpha)^{1.5}. \tag{19.126}$$

This expression differs from the corresponding value of critical pressure in cylindrical shells, Eq. (19.58), by the factor $(\cos\alpha)^{1.5}$. Hence, for angles of conicity of $2\alpha < 40^\circ$, p_{cr}, given by Eqs (19.125) or (19.126), will differ from the critical value of the external pressure, determined for a mean cylinder of length L and having $R = r_m$, not more than 10%.

The critical values of other loads (axial forces, twisting moments, etc.) applied to conical shells with an angle not more than 20°, can be approximately found from the corresponding relations for cylindrical shells by replacing R with r_m and setting the cylindrical shell length equal to the length of the longitudinal axis of the conical shell.

19.9 BUCKLING OF SPHERICAL SHELLS

The most important stability problem for thin spherical shells is referred to the case when they are loaded by external pressure. Such a type of problem is met in radar antenna caps in aircrafts, submarine bulkheads, bottoms of reservoirs, etc. We consider here the linear buckling analysis of spherical segments whose rise is comparable with their radius and closed spherical shells under external pressure. The stability analysis of shallow spherical shells under external pressure was considered in Sec. 19.7.

We determine the critical load for a closed spherical shell. It was shown that the critical stresses for the above shell and for elevated spherical segments under external pressure are identical [4]. We assume that within the limits of area of local initial bulging, the shell can be considered as a shallow one: therefore, Eqs (17.36) are applicable. For a spherical shell, the operator $\nabla_k^2(..) = \nabla^2(..)(1/R)$, where R is the radius of the middle surface. Thus, Eqs (17.36) for the spherical shell take the form

$$D\nabla^2\nabla^2 w = \frac{1}{R}\nabla^2\Phi + p_3,$$
$$\frac{1}{Eh}\nabla^2\nabla^2\Phi = -\frac{1}{R}\nabla^2 w. \tag{19.127}$$

Eliminating Φ from the above equations results in the following sixth-order differential equation for w:

$$D\nabla^6 w + \frac{Eh}{R^2}\nabla^2 w = \nabla^2 p_3, \tag{19.128}$$

where $\nabla^6(..) = \nabla^2\nabla^2\nabla^2(..)$. If an external pressure is applied to the spherical shell, then initial direct forces in all normal sections of the unbuckled shell are (see Sec. 14.3) the following:

$$N_1 = N_2 = -\frac{pR}{2}. \tag{19.129}$$

It should be noted that the uniform external pressure does not appear directly in Eq. (19.128) but indirectly only, in terms of the fictitious load $p_3^{(f)}$. The latter load is expressed through the direct internal forces (19.129) and can be found from Eq. (19.8). We have (setting $p_3 = p$)

$$p_3^{(f)} = -\frac{pR}{2}\nabla^2 w. \tag{19.130}$$

Therefore, Eq. (19.128) appears in the form

$$D\nabla^6 w + \frac{pR}{2}\nabla^4 w + \frac{Eh}{R^2}\nabla^2 w = 0. \tag{19.131}$$

Following the approach of Ref. [4], assume that the solution of Eq. (19.131) must satisfy the relation

$$\nabla^2 w = -\lambda^2 w, \tag{19.132}$$

where λ is some undetermined parameter. Substituting the above relation into Eq. (19.131) yields the following equation (for $\lambda \neq 0$):

$$\left(D\lambda^4 - \frac{pR}{2}\lambda^2 + \frac{Eh}{R^2}\right)\lambda^2 w = 0, \tag{19.133}$$

and solving this equation for p yields

$$p = \frac{2Eh}{R^3\lambda^2} + \frac{2D}{R}\lambda^2. \tag{19.134}$$

Taking the limit of p with respect to λ^2, one obtains

$$\lambda^2 = \sqrt{\frac{Eh}{DR^2}} = \frac{1}{Rh}\sqrt{12(1-\nu^2)}.$$

Substituting the above into Eq. (19.134) gives the following value of the critical pressure:

$$p_{cr} = \frac{2Eh^2}{R^2\sqrt{3(1-\nu^2)}} = \frac{2E}{\sqrt{3(1-\nu^2)}}\left(\frac{h}{R}\right)^2. \tag{19.135}$$

For $\nu = 0.3$, we obtain

$$p_{cr} \cong 1.21E\left(\frac{h}{R}\right)^2.$$

The corresponding value of the critical stress, σ_{cr}, is

$$\sigma_{cr} = \frac{N_{1,cr}}{h} = \frac{Eh}{R}\frac{1}{\sqrt{3(1-\nu^2)}}. \tag{19.136a}$$

or, for $\nu = 0.3$

$$\sigma_{cr} \cong 0.605\frac{Eh}{R}. \tag{19.136b}$$

Thus, the critical stress of a spherical shell under external pressure is the same as the critical stress of a closed cylindrical shell under axial uniform compression (see Eq. (19.31b)).

The critical stress given by Eqs (19.136) can be classified as the upper critical stress, $p_{cr}^{(1)}$, for the shell and loading under consideration (see Sec. 19.2). However, numerous experimental investigations showed that the actual critical stresses of spherical shells under external pressure are far below the values given by Eqs (19.136), obtained on the basis of the linear stability theory. It can be explained by the fact that the real spherical shells are found to be sensitive to the lightest initial imperfections, just as compressed cylindrical shells discussed in Sec. 19.3.2. Therefore, the buckling analysis of spherical shells should be performed in the framework of the nonlinear stability theory. Such a buckling analysis is more complicated from the mathematical and mechanical points of view (for details, see for example Ref. [4]). We present below only the final results of the nonlinear stability problem for the spherical shells under external pressure, associated with determining the lower value of the critical pressure, $p_{cr}^{(2)}$, which is [4]

$$p_{cr}^{(2)} = 0.31E\left(\frac{h}{R}\right)^2. \tag{19.137}$$

It is seen that this value is four times less than $p_{cr}^{(1)}$.

19.10 DESIGN STABILITY ANALYSIS

Let us summarize the basic theoretical and experimental results of buckling shell analysis, discussed in the preceding sections. As mentioned previously, there is a large discrepancy between the analytical predictions of the shell buckling behavior and the corresponding experimental results. In addition, the scatter of the test data may be quite large. The major reason for the above discrepancy is the sensitivity of shell buckling to the initial geometric and loading imperfections, and to deviation in boundary conditions. As a result of these imperfections, as well as the inelastic behavior of shells in buckling, the critical load of real shells, called the buckling load in Sec. 19.2, for some shell configurations and loads can be much less than $p_{cr}^{(1)}$, predicted by the linear buckling analysis. It should be noted that application of the geometrically nonlinear stability theory for determining $p_{cr}^{(2)}$, in order to eliminate the discrepancy between the theoretical and experimental data in the buckling of thin

shells, is associated with very cumbersome and difficult computations, and the results, obtained by this theory, did not justify such efforts [16].

Since the load-carrying capability of thin shells is mostly determined by the buckling load, it is very important to determine a reliable and accurate value of this load for design purposes. Because the effects of initial imperfections mentioned above are extremely difficult to determine at the design stage, many theoretical and experimental investigations have been directed toward the evaluation of an alternative to, or at least a modification of, the classical, linear stability theory. Now, the buckling design analysis of thin shells is based on the classical, linear stability theory applied to initially perfect elastic shell, provided one accounts for the reduction in critical load resulting from initial imperfections and inelastic behavior. On this basis, several approaches were developed for determining the allowable design buckling loads.

When sufficient experimental data exist for a given shell and loading, a statistical method of design curves may be useful in determining the allowable design buckling load. Each such design curve was obtained at a certain probability level. The load at which a shell may be expected to buckle is the load which corresponds to the curve best fit. This approach is described in Refs [12,13, 19, 22, 23, etc].

Whenever sufficient experimental data do not exist to obtain a statistical allowable design buckling load, design recommendations have been based on allowable behavior of a shell structure. In general, this involves empirical reduction factors to decrease the theoretical upper critical load [4,12,15, 24, etc.]. Due to the lack of test data for some types of shells and loads, the recommendations may be conservative for some cases. We consider here only the second approach and present below a small selection of the empirical equations for determining the allowable buckling loads for cylindrical shells that incorporate the above-mentioned correction factors.

19.10.1 Buckling of unstiffened cylindrical shells

(a) Axial compression

The classical critical stress formula (19.31b) can be used to predict buckling of initially imperfect cylindrical shells, provided it is written in the following form:

$$\sigma_{\text{cr}} = \mu \frac{Eh}{R}, \tag{19.138}$$

where μ is the so-called buckling coefficient that varies with R/h. For high-quality manufactured shells the above coefficient is determined from the following relationship, which agrees well with experimental data (for $R/h = 100 \ldots 1500$) [4]:

$$\mu = \frac{1}{\pi} \sqrt[8]{\left(\frac{100h}{R}\right)^3}. \tag{19.139}$$

If shells are manufactured under insufficient quality controls and the initial imperfections are comparable to the shell thickness, the design values of the buckling coefficient have to be divided by approximately two. Initial imperfections that exceed the shell thickness noticeably are absolutely inadmissible because they decrease the stiffness of shell structure appreciably.

The critical stress for a short and thin cylinder with length $L \leq 1.22\sqrt{Rh}$ for simply supported edges, and with $L \leq 2.5\sqrt{Rh}$ for fixed edges, can be determined from the buckling formula derived previously for a wide flat plate, as follows:

$$\sigma_{cr} = \mu \frac{Eh^2}{L^2}, \tag{19.140}$$

where $\mu = 0.9$ for simply supported and $\mu = 3.6$ for fixed shell edges.

The alternative buckling stress equations were derived by Donnel and Wan [10]. They are in good agreement with the relations (19.138) and (19.140).

The following approximate equation for the allowable axial compressive stress in cylindrical shells for elastic buckling was developed in the ASME Code [22] by using a factor of safety of 10 in Eq. (19.31b):

$$\sigma = \frac{0.0625Eh}{R}. \tag{19.141}$$

For structural steel cylinders, inelastic buckling cannot be readily dealt with using a plasticity reduction factor. Instead, it is customary to use some empirical formulas, such as those listed in Refs [22,23].

(b) External pressure

The critical value of external pressure for simply supported cylindrical shells (besides very short and very long shells) is given by [4]

$$p_{cr} = \alpha(0.855)\frac{Eh^2}{RL(1-\nu^2)^{0.75}}\sqrt{\frac{h}{R}}, \tag{19.142}$$

where the coefficient α depends on the ratio R/h, as follows:

R/h	250	500	1000	1500
α	0.7	0.6	0.5	0.4

In designing short $\left(L \leq 2.5\sqrt{Rh}\right)$, simply supported cylindrical shells under external pressure, the value of p_{cr} is given by [4]

$$p_{cr} = \alpha_1 \frac{Eh^2}{RL}, \tag{19.143}$$

where $\alpha_1 = 1.8$ for all-around pressure and $\alpha_1 = 3.6$ for side pressure.

For long, simply supported cylindrical shells ($L > 3.35R\sqrt{\frac{R}{h}}$), the critical value of the pressure can be determined from the following relationship:

$$p_{cr} = 0.275\frac{Eh^3}{R^3}. \tag{19.144}$$

The boundary conditions exert some effect on the critical value of the external pressure. For example, for a cylindrical shell having one pin-connected edge and the second one fixed, the critical value of external pressure, p^*_{cr}, is given by [4]

$$p^*_{cr} = 0.6p_{cr}, \tag{19.145}$$

where p_{cr} is the critical value of external pressure for the previously introduced simply supported cylindrical shell.

An empirical equation developed by the U.S. Navy [20] for the buckling of cylindrical shells under lateral and axial pressure in the elastic range is given by

$$p_{cr} = \frac{2.42E}{(1-\nu^2)^{3/4}} \frac{(h/2R)^{2.5}}{\left[L/2R - 0.45(h/2R)^{0.5}\right]}. \tag{19.146}$$

For cylindrical shells with large R/h ratios, the above equation can be simplified to

$$p_{cr} = \frac{2.42E}{(1-\nu^2)^{3/4}} \frac{(h/2R)^{2.5}}{L/2R}. \tag{19.147}$$

19.10.2 Buckling of unstiffened spherical shells under external pressure

The critical value of external pressure and critical stress is shown below [4]

$$p_{cr} = \alpha \frac{Eh^2}{R^2}, \quad \sigma_{cr} = \alpha \frac{Eh}{2R}, \tag{19.148}$$

where the coefficient α for high-quality manufactured shells and for $250 \leq R/h \leq 800$ is determined by the following formula:

$$\alpha = \frac{1}{2.36} \sqrt[8]{\left(\frac{100h}{R}\right)^3}. \tag{19.149}$$

For the range $R/h \leq 250$, according to the recommendations of Ref. [4], $\alpha = 0.3$. If a spherical shell is not manufactured with sufficient accuracy and initial imperfections are comparable with its thickness, the coefficient α is reduced by about 1.5–2 times.

The following empirical equations for determining the critical stress and the critical pressure were developed in Refs [17]:

$$\sigma_{cr} = 0.125 \frac{Eh}{R}, \quad p_{cr} = 0.25 \frac{Eh^2}{R^2}. \tag{19.150}$$

19.10.3 Buckling of unstiffened conical shells

Conical shells subjected to external pressure can be designed as cylindrical shells with the effective thickness, h_e, and efffective length, L_e, determined from the following relations [24]:

$$h_e = h \cos\alpha, \quad L_e = \frac{L}{2}\left(1 + \frac{r_1}{r_2}\right), \tag{19.151}$$

where h is thickness of the cone, L is the height of the conical shell, and r_1 and r_2 are the radii of parallel circles at the top and bottom sections of the truncated cone, respectively.

19.10.4 Stiffened shells

Experimental investigations showed that stiffened shells are less sensitive to overall and local imperfections [12]. Therefore, the critical values of applied loads for such shells are closer to the theoretically determined values of the upper critical loads

predicted by the linear stability theory. Some empirical equations were developed for determining the critical stresses and loads for stiffened shells of various configuration under axial compression, external pressure, torsion, shear, as well as various loading combinations [12,14,19,21]. For example, for the spherical shell with closely and equally spaced stiffeners in two mutually orthogonal directions under external pressure, the buckling value of the above pressure is given by [21]

$$p_{cr} = 0.366E\left(\frac{h_m}{R}\right)^2\left(\frac{h_b}{h_m}\right)^{3/2}, \tag{19.152}$$

where $h_m = h + A/s$ is the effective membrane thickness and $h_b = (12I/s)^{1/3}$is the effective bending thickness; A and I are the area and moment of inertia of the stiffener, s is the spacing between stiffeners.

Local buckling of the spherical shells between the stiffeners must also beconsidered for large-diameter shells. One such equation is given by

$$p_{cr} = 7.42\frac{Eh^3}{Rs^2}. \tag{19.153}$$

Only a small selection of the recommended design relations for determining the critical loads in thin shells has been introduced above. The interested reader is referred to Refs [4,12,13,14,19–24].

In conclusion, note that in practice one must tend to designing the shell structures whose stability would not depend on occasional and not easily controlled factors. The basic avenues of designing such shell structures is the use of stiffened shells, sandwich shells, corrugated shells, etc. In some, the most important cases, sharpened shells are applied.

PROBLEMS

19.1 It follows from Fig. 19.1a that the path of equilibrium for a flat plate is symmetric about the vertical, p axis, whereas the corresponding path for a shallow shell is nonsymmetrical. Explain the above difference in the buckling behavior of plates and shells.

19.2 Provide a detailed deviation of Eqs (19.3).

19.3 Derive Eqs (19.4) from (19.3) by neglecting all the terms containing prebuckled rotations.

19.4 Derive Eqs (19.9) from Eqs (19.7).

19.5 A water tower support constructed of a long steel piping of 1.0 m diameter is to carry an axial compression load of 520 kN. Assuming that the supports ends are pin-connected, determine the required thickness of the shell that will prevent this tower support from buckling. Use $L = 2.0\,\text{m}$, $E = 200\,\text{GPa}$, $\nu = 0.3$, and a factor of safety (FS) of 3.5.

19.6 Verify Eq. (19.22)

19.7 A thin steel pipe is subjected to a vacuum pressure of 150 psi. Assuming that the pipe edges are simply supported, determine the required thickness of the pipe, preventing the pipe from buckling. Given $E = 29{,}000$ psi, $\nu = 0.3$, $L = 10$ ft, $R = 2.5$ ft, and the factor of safety (FS) is 3.0.

19.8 Determine the critical stress in a simply supported circular cylindrical panel subjected to a uniformly distributed compressive forces q_1, as shown in Fig. P.19.1. Assume that the shell edges are simply supported.
Hint: take the deflection w in the form

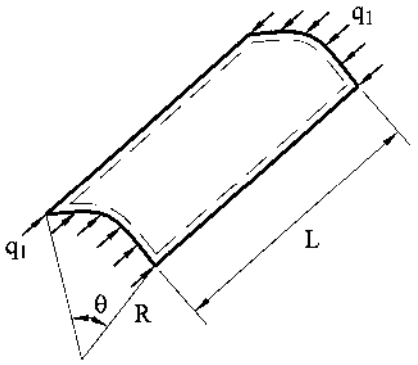

Fig. P19.1

$$w = f \sin\frac{m\pi x}{L} \cdot \sin\frac{m\pi\theta}{\theta_0}.$$

19.9 Determine the critical value of the external pressure p acting on a spherical shell of radius R.
Hint: eliminating Φ from Eqs (19.7) and letting $R_1 = R_2 = R$ and $p = \sigma h \nabla^2 w$, yields the following equation:

$$D\nabla^6 w + p\nabla^4 w + \frac{Eh}{R^2}\nabla^2 w = 0. \tag{a}$$

The solution of this equation satisfies the condition $\nabla^2 w = -\lambda^2 w$, where λ is some indeterminate parameter. Substituting $\nabla^2 w$ into Eq. (a) minimizing over λ^2, yields p_{cr}.

19.10 Determine the critical stress for an axially compressed unstiffened closed cylindrical shell of radius $R = 2.0\,\text{m}$ and of thickness $h = 0.01\,\text{m}$. The shell length is $L = 0.6\,\text{m}$. Assume that the shell manufactured is of insufficient quality. Use also $E = 220\,\text{GPa}$, and $\nu = 0.3$.

19.11 Determine the critical value of the external pressure p in an unstiffened cylinder having the radius $R = 2.5\,\text{m}$, thickness $h = 8\,\text{mm}$, and length $L = 0.5\,\text{m}$. Assume that one end of the cylinder is fixed and the other one is free. Take $E = 210\,\text{GPa}$, and $\nu = 0.3$.

19.12 A thin-walled cylinder is used to support a reactor of weight W. Find the maximum value of W that can be applied to the cylinder without causing it to buckle. Take $L =$ 10ft, $R = 2\,\text{ft}$, $E = 29{,}000\,\text{ksi}$, $h = 0.2\,\text{in.}$, $\nu = 0.25$, and the factor of safety (FS) is 2.5.

REFERENCES

1. Volmir, A.S. *Flexible Plates and Shells* (translated from Russian), Air Force Flight Dynamics Laboratory, Technical Report No. 66-216, Ohio, Wright-Patterson Air Force Base, 1967.
2. Brush, D.O. and Almroth, B.O., *Buckling of Bars, Plates, and Shells*, McGraw-Hill, New York, 1975.
3. Batdorf, S.B., *A Simplified Method of Elastic Stability Analysis for Thin Cylindrical Shells*, NACA, Technical Report, No. 874, Washington, DC, 1947.
4. Volmir, A.S., *Stability of Elastic Systems*, Gos. Izd-vo Fiz.-Mat. Lit., Moscow, 1963 (in Russian).

5. Hoff, N.J. and Rehfield, L.W., *Buckling of Axially Compressed Circular Cylindrical Shells at Stresses Smaller than the Classical Critical Value*, Stanford Univ., Department of Aeronautics and Astronautics, Report SUDAER No. 191, May 1964.
6. Almroth, B.O., Influence of edge conditions on the stability of axially compressed cylindrical shells, *Journal of the American Institute of Aeronautics and Astronautics*, vol. 4, No. 1 (1966).
7. Donnel, L.H., *Stability of Thin-Walled Tubes under Torsion*, NACA, Technical Report, No. 479, Washington, DC, 1933.
8. Donnel, L.H., A new theory for the buckling of thin cylinders under axial compression and bending, *Transactions ASME*, vol. 56, pp. 795–806 (1934).
9. von Karman, T. and Tsien, H.S., The buckling of thin cylindrical shells under axial compression, *Journal of the Aeronautical Sciences*, vol. 8, No. 8, pp. 302–312 (1941).
10. Donnel, L.H. and Wan, C.C., Effect of imperfections on buckling of thin cylinders, *J Appl. Mech*, pp. 75–83 (1950).
11. Chajes, A., *Principles of Structural Stability Theory*, Prentice-Hall, Englewood Cliffs, New Jersey, 1974.
12. Baker, E.H., Cappelli, A.P., Kovalevski, L., Rish, F.L., and Verette, R.M., *Shell Analysis Manual*, NACA 912, Washington, DC, 1968.
13. *Stability Analysis of Plates and Shells* (compiled by Knight, N.F., Jr, Nemeth, M.P). A collection of papers in honor of Dr. M. Stein, NASA/CR-1998-206280, Langly Research Center, Hampton, Virginia, January, 1998.
14. Terebushko, O.I., To the buckling analysis and design of stiffened cylindrical shells, *Analysis of Thin-Walled Structures*, vol. 7, pp. 119–133 (1962) (in Russian).
15. Plantema, F.J., *Sandwich Construction*, John Wiley and Sons, New York, 1966.
16. Hutchinson, J.W. and Koiter, W.T., Postbuckling theory, *Appl Mech Rev*, vol. 23, pp. 1353–1366 (1970).
17. Kollar, L. and Dulacska, E., *Buckling of Shells for Engineers*, John Wiley and Sons, New York, 1948.
18. Jonston, B.G., *Guide to Design Criteria for Metal Compression Members*, 3rd. edn, John Wiley and Sons, New York, 1973.
19. Gerard, G. and Becker, H., *Handbook of Structural Stability, Part III, Buckling of Curved Plates and Shells*, NACA TN 3783, Washington, DC, 1957.
20. Raetz, R.V., *An Experimental Investigation of the Strength of Small-Scale Conical Reducer Sections Between Cylindrical Shells Under External Hydrostatic Pressure*. U.S. Department of the NAVY, David Taylor Model Basin, Report 1187, Washington, D.C., US Navy, 1957.
21. Buchert, K.P., Stiffened thin shell domes, *AISC Engineering Journal*, Chicago, AISC, 1964.
22. *American Society of Mechanical Engineers. Pressure Vessel Code*, Section VIII, Division I, New York, ASME, 1992a. *American Society of Mechanical Engineers. Pressure Vessel Code-Alternate Rules*. Section VIII, Division 2, New York, ASME, 1992b.
23. American Petroleum Institute. Recommended Rules for Design and Construction of Large, Welded, Low-Pressure Storage Tanks-API 620, Washington, DC, API, 19.
24. Jawad, M.H., Design of conical shells under external pressure, *Journal of Pressure Vessel Technology*, vol. 102, New York, ASME (1980).

20

Vibrations of Shells

20.1 INTRODUCTION

The dynamic effects of time-dependent loads on shell structures are quite similar to those discussed in Chapter 9 for plates. Thus, the objectives of the vibration analysis of shells, as well the general approach for deriving the shell equations of motion, remain analogous to the plate vibration analysis introduced in Sec. 9.1.

Assume that the state of stress within a shell during vibrations has a character determined by the equations of equilibrium, and the shell middle surface deforms according to the same law during vibrations as in the static equilibrium state. Based on the above, the equations of motion of the vibrating shell can be obtained by applying the D'Alambert principle, just as it was done for vibrating plates – i.e., by adding the inertia forces to given external loads, assigned by components p_1, p_2, and p_3, namely (damping forces are not considered here):

$$p_1 \to p_1 - \rho h \frac{\partial^2 u}{\partial t^2}; \quad p_2 \to p_2 - \rho h \frac{\partial^2 v}{\partial t^2}; \quad p_3 \to p_3 - \rho h \frac{\partial^2 w}{\partial t^2}, \tag{20.1}$$

where p_1, p_2, p_3, and u, v, w are functions of the Cartesian coordinates of the middle surface and time, ρ is the mass density of the material, and h is the shell thickness. As for vibrating plates, we distinguish between *free vibrations* of shells, which occur in the absence of applied loads but are initiated by some initial conditions imposed on the shell, and *forced vibrations* of shells, which result from the application of time-dependent loads. We consider in this chapter both types of vibrations.

20.2 FREE VIBRATIONS OF CYLINDRICAL SHELLS

20.2.1 General

As mentioned in Sec. 9.1, free vibrations deal with some natural characteristics of shells. These natural vibrations occur at discrete frequencies, depending only on the geometry and material of the shell. A knowledge of the free-vibration characteristics of thin elastic shells is important both for our general understanding of the fundamentals of the shell behavior and for industrial applications of shell structures. In connection with the latter, the natural frequencies of shell structures must be known to avoid the destructive effect of resonance with adjacent rotating or oscillating equipment (such as jet and reciprocating aircraft engines, electrical machinery, marine turbines and propulsors, etc.).

Since the free vibrations occur in the absence of all external forces ($p_1 = p_2 = p_3 = 0$), we address the free-vibration analysis of shells with the solution of homogeneous partial differential equations with homogeneous boundary conditions. Let us derive the equations of the free vibrations of thin elastic cylindrical and shallow shells.

20.2.2 Axisymmetric free flexural vibrations of cylindrical shells

Consider the free flexural vibrations of a circular cylindrical shell when the radial w and longitudinal u displacements do not depend on the angular coordinate θ, and the circumferential displacement v is zero. Any cross section of such a shell will be a circular ring, and several half-waves can be placed throughout the shell length, as shown in Fig. 20.1.

The equation of axisymmetrical free vibrations can be obtained from the governing differential equation of the axisymmetrically loaded circular cylindrical shell, Eq. (15.44). One replaces, due to Eq. (20.1), the normal component of the external loading p_3 by the normal component of the inertia forces, and neglects the longitudinal component of the above forces. Thus, the differential equation of the axisymmetrically vibrating circular cylindrical shell is found to be

$$\frac{\partial^4 w}{\partial x^4} + 4\beta^4 w = -\frac{\rho h}{D}\frac{\partial^2 w}{\partial t^2}, \tag{20.2}$$

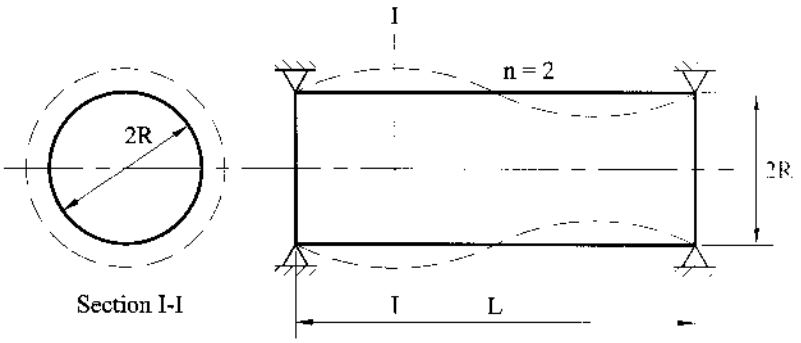

Fig. 20.1

where the deflection $w = w(x, t)$ is a function of the x coordinate and time t.

The solution of Eq. (20.2) for a simply supported shell of length L, assuming harmonic equations in time, is sought in the following form:

$$w(x, t) = \sum_{n=1}^{\infty} A_n \sin\frac{n\pi x}{L} \sin \omega t, \tag{20.3}$$

where ω is the *frequency of natural vibrations (or natural frequency)* of the given shell. It is related to the vibration period T by the relationship $\omega = 2\pi/T$. Substituting for w from Eq. (20.3) into Eq. (20.2), one obtains

$$D\left(\frac{n\pi}{L}\right)^4 + \frac{Eh}{R^2} = \rho h \omega^2,$$

and the natural frequency ω is given by

$$\omega^2 = \frac{E}{\rho R^2}(1 + \mu\lambda^4), \tag{20.4}$$

where

$$\mu = \frac{h^2}{12R^2(1 - \nu^2)}; \quad \lambda = \frac{n\pi R}{L}. \tag{20.5}$$

The value of μ for thin shells is small compared with unity. For shells that are not short, when $\lambda^4 < 1$, the product $\mu\lambda^4$ can be neglected. Then, the natural frequency of axisymmetrical vibrations for all numbers n will coincide with the natural frequency of axisymmetrical vibrations of a ring or an infinitely long shell. For other shells, not simply supported at their ends, a solution of Eq. (20.2) will be sought in the following general form:

$$w(x, t) = W(x) \sin \omega t. \tag{20.6}$$

Substituting the above into Eq. (20.2), we obtain an ordinary fourth-order differential equation in $W(x)$. Its solution will have an analogous form to that discussed in Sec. 15.3 if axisymmetrical deformations of a statically loaded circular cylindrical shell are of interest. Satisfying the given boundary conditions, one can obtain – from the condition of nontriviality of the above solution – the expression for the natural frequencies in axisymmetrically vibrating cylindrical shells. For example, for fixed shell edges, the natural frequency of the first mode of axisymmetrical vibrations (the fundamental natural frequency) is determined from the following equation:

$$\omega_1^2 = \frac{E}{\rho R^2}\left[1 + \mu\left(4.73\frac{R}{L}\right)^4\right]. \tag{20.7a}$$

The frequency of the second harmonics for the above shell is

$$\omega_2^2 = \frac{E}{\rho R^2}\left[1 + \mu\left(7.83\frac{R}{L}\right)^4\right]. \tag{20.7b}$$

Since the value of μ for thin shells is small, then, as follows from Eqs (20.7), the fixed edges of the shell have a low effect on the natural frequencies of vibrations as compared with the simply supported edges. Similar results will be obtained for other boundary conditions. Hence, the natural frequency of axisymmetrical (long-

itudinally-radial) vibrations of thin and not-short circular cylindrical shells depends a little on boundary conditions and on the mode of vibrations (for the first mode).

To determine the frequencies of axisymmetric vibrations, the energy method, based on the variational principles (see Sec. 2.6), can also be applied. As shown in Sec. 15.3, the axisymmetric bending of a circular cylindrical shell is quite similar to the bending of a strip-beam of unit width cut off the shell and resting on an elastic foundation with the foundation modulus $k = Eh/R^2$. The strain energy of such a strip-beam, deflecting by $w(x)$, will be of the form

$$U = \frac{EI}{2}\int_0^L \left(\frac{\mathrm{d}^2 w}{\mathrm{d}x^2}\right)^2 \mathrm{d}x + \frac{k}{2}\int_0^L w^2 \mathrm{d}x, \tag{20.8}$$

where L denotes the span of the strip-beam. It follows from the above that the strain energy consists of the strain energy of the strip-beam itself, which is proportional to h^3, and the energy of the elastic foundation, which is proportional to h (the shell thickness). If the small value of the strain bending energy (the first term in Eq. (20.8)) is neglected, then the maximum value of the strain energy will be equal to the following:

$$U_{\max} = \frac{Eh}{R^2}\int_0^L w^2 \mathrm{d}x. \tag{20.9}$$

The maximum value of the kinetic energy for any mode of free vibrations is given by

$$K_{\max} = \frac{\rho h \omega^2}{2}\int_0^L w^2 \mathrm{d}x.$$

Equating $U_{\max}$ and $K_{\max}$, we obtain the following expression for the frequency of free vibrations:

$$\omega^2 = \frac{E}{\rho R^2}. \tag{20.10}$$

Hence, under the assumption introduced above (neglecting the bending potential energy of a strip-beam in Eq. (20.8)), the frequency of natural radial vibrations does not depend on $w_{\max}$, i.e., on the vibration mode and boundary conditions. It is necessary only that a circular cross section is preserved on the shell ends.

In increasing the shell thickness and decreasing its length, the dependence of vibration frequencies on the mode and boundary conditions becomes more significant. For cylindrical shells, such a mode of axisymmetric vibrations is possible when $u = w = 0$. In this case, points of such shells are displaced in the circumferential direction only (i.e., $v \neq 0$); these are torsional vibrations.

20.2.3 Free asymmetric flexural vibrations of circular cylindrical shells

1. Closed cylindrical shells

The differential equations of equilibrium in terms of the displacement components for a circular cylindrical shell are given by Eqs (15.7)–(15.9). According to the Donnel–Mushtari–Vlasov (DMV) theory, they can be simplified by dropping the bending terms in the operators l_{23} and l_{32} that are proportional to h^2/R^2 (see Eqs

(15.9)). Taking into account the relations (20.1), we can write the differential equations of motion for a freely vibrating circular cylindrical shell in the framework of the DMV theory in terms of the x and θ coordinates, as follows:

$$\begin{aligned}
\frac{\partial^2 u}{\partial x^2}+\frac{1-\nu}{2R^2}\frac{\partial^2 u}{\partial \theta^2}+\frac{1+\nu}{2R}\frac{\partial^2 v}{\partial x\partial\theta}-\frac{\nu}{R}\frac{\partial w}{\partial x}&=\frac{1-\nu^2}{E}\rho\frac{\partial^2 u}{\partial t^2},\\
\frac{1+\nu}{2R}\frac{\partial^2 u}{\partial x\partial\theta}+\frac{1-\nu}{2}\frac{\partial^2 v}{\partial x^2}+\frac{1}{R^2}\frac{\partial^2 v}{\partial\theta^2}-\frac{1}{R^2}\frac{\partial w}{\partial\theta}&=\frac{1-\nu^2}{E}\rho\frac{\partial^2 v}{\partial t^2},\\
\frac{\nu}{R}\frac{\partial u}{\partial x}+\frac{1}{R^2}\frac{\partial v}{\partial\theta}-\frac{w}{R^2}-\frac{h^2}{12}\left(\frac{\partial^4 w}{\partial x^4}+\frac{2}{R^2}\frac{\partial^4 w}{\partial x^2\partial\theta^2}+\frac{1}{R^4}\frac{\partial^4 w}{\partial\theta^4}\right)&=\frac{1-\nu^2}{E}\rho\frac{\partial^2 w}{\partial t^2}.
\end{aligned}\tag{20.11}$$

Assume that the given closed cylindrical shell of length L is simply supported on its edges. Then, the solutions of Eqs (20.11) can be sought in the following form:

$$\begin{aligned}
u&=\sum_m\sum_n A_{mn}\cos m\theta\cos\frac{n\pi x}{L}\sin\omega t,\\
v&=\sum_m\sum_n B_{mn}\sin m\theta\sin\frac{n\pi x}{L}\sin\omega t,\\
w&=\sum_m\sum_n C_{mn}\cos m\theta\sin\frac{n\pi x}{L}\sin\omega t,
\end{aligned}\tag{20.12}$$

where A_{mn}, B_{mn}, and C_{mn} are some constants; m refers to the number of half-waves in the circumferential direction of the shell, whereas n characterizes the number of half-waves of displacements placed on the shell length L. The displacement components u, v, and w in the form of Eqs (20.12) satisfy the prescribed boundary conditions on the shell edges $x=0$ and $x=L$ and the periodicity conditions with respect to the variable θ.

Inserting Eqs (20.12) into Eqs (20.11), we obtain the following system of homogeneous algebraic equations in A_{mn}, B_{mn}, and C_{mn} :

$$\begin{aligned}
\left(-\lambda^2-\frac{1-\nu}{2}m^2+\Omega\right)A_{mn}+\frac{1+\nu}{2}m\lambda B_{mn}-\nu\lambda C_{mn}&=0,\\
\frac{1+\nu}{2}m\lambda A_{mn}+\left(-m^2-\frac{1-\nu}{2}\lambda^2+\Omega\right)B_{mn}+mC_{mn}&=0,\\
-\nu\lambda A_{mn}+mB_{mn}+\left[-1-a^2(\lambda^2+m^2)^2+\Omega\right]C_{mn}&=0,
\end{aligned}\tag{20.13}$$

where

$$\lambda=\frac{n\pi R}{L};\quad \Omega=\frac{(1-\nu^2)R^2}{E}\rho\omega^2;\quad a^2=\frac{h^2}{12R^2}.$$

The constants A_{mn}, B_{mn}, and C_{mn} cannot be simultaneously equal to zero. To determine nontrivial solutions of the above system of homogeneous equations, it is necessary to equate its determinant to zero. We have the following:

$$\begin{vmatrix}
-\lambda^2-\frac{1-\nu}{2}m^2+\Omega & \frac{1+\nu}{2}m\lambda & -\nu\lambda\\
\frac{1+\nu}{2}m\lambda & \left(-m^2-\frac{1-\nu}{2}\lambda^2+\Omega\right) & m\\
-\nu\lambda & m & -\left[1+a^2(\lambda^2+m^2)^2-\Omega\right]
\end{vmatrix}=0.$$

The resulting equation of the third power in Ω, or of the sixth power in ω determines the natural frequencies of vibrations of the given cylindrical shell corresponding to certain numbers of m and n. The above equation can also be written in the form

$$T_1\omega^6 + T_2\omega^4 + T_3\omega^2 + T_4 = 0, \tag{20.14}$$

where T_1, T_2, T_3, and T_4 are some coefficients depending on m and n, as well as geometric and mechanical parameters of the shell. It can be shown that all the roots of the characteristic equation (20.14) are always real, and three values of the natural frequencies ω correspond to each pair of numbers m and n. The negative values of ω, which are the roots of Eq. (20.14) but have no physical meaning, are dropped.

Having determined any of the three frequencies, the ratios between the amplitudes, for instance A_{mn}/C_{mn}, B_{mn}/C_{mn} can be calculated from the homogeneous equations (20.13). Each value of ω corresponds to a certain ratio between the amplitudes of the longitudinal, tangential, and normal displacements.

Conducted investigations showed that for mostly transverse (or normal) vibrations of circular cylindrical shells, the value ω^2 will be small and their degrees higher than second can be neglected. In this case, we obtain the following from Eq. (20.14):

$$\omega^2 = -\frac{T_4}{T_3} \quad \text{or} \quad \omega^2 = \frac{E}{\rho R^2(1-\nu^2)}\frac{(1-\nu^2)\lambda^4 + a^2(\lambda^2+m^2)^4}{m^2+(\lambda^2+m^2)^2}. \tag{20.15}$$

It is of great practical importance to determine the values of m and n for which the natural frequency of predominantly transverse vibrations, given by Eq. (20.15), will be the smallest. The analysis shows that the lowest natural frequency will be for $n = 1$, i.e., for one half-wave located over the shell length, and, hence, $\lambda = \pi R/L$. The natural frequency, as a function of m, has a minimum. It can be shown that for intermediate-length shells, the value of m^2, corresponding to the smallest frequency, can be neglected compared with $(\lambda^2 + m^2)^2$. Then, Eq. (20.15) can be rewritten for the above-mentioned shells, as follows:

$$\Omega = \frac{T_1}{(\lambda^2+m^2)^2} + a^2(\lambda^2+m^2)^2,$$

where $T_1 = (1-\nu^2)\lambda^4$. Denoting $X = (\lambda^2 + m^2)^2$, we can rewrite the above equation as follows:

$$\Omega = \frac{T_1}{X} + a^2X. \tag{20.16}$$

To determine the value of X (or m) corresponding to the minimum of Ω, we differentiate Eq. (20.16) with respect to X and equate this derivative to zero. We have the following:

$$\frac{\partial\Omega}{\partial X} = -\frac{T_1}{X^2} + a^2 = 0,$$

from which

$$X = \sqrt{\frac{T_1}{a^2}} = (\lambda^2+m^2)^2 \quad \text{or} \quad m^2 = \sqrt[4]{\frac{T_1}{a^2}} - \lambda^2. \tag{20.17}$$

Since the number of m may be an integer only, then, after determining m from Eq. (20.17), it should be taken to be equal to the nearest integer. The smallest natural frequency corresponds to this integer. The second derivative of Ω with respect to m will be positive; therefore, Eq. (20.17) defines a minimum.

Example 20.1

For a simply supported closed cylindrical shell of radius $R = 17$ cm and of length $L = 54$ cm, find the number of half-waves in the circumferential direction and the minimum natural frequency. Use the following geometric and mechanical parameters of the shell: $h = 0.08\,\text{cm}$, $\nu = 0.3$, $E = 200\,\text{GPa}$, and $\nu = 0.3$.

Solution

For the given geometric and mechanical shell parameters, we can find that $a^2 = 0.18 \times 10^{-5}$, $\lambda = 1$, and $T_1 = 0.9$. Substituting the above data into Eq. (20.17), gives $m = 5.1$. Hence, the minimum natural frequency of predominantly transverse vibrations, $\omega_{\min}$, takes place for five half-waves or for 10 nodal points placed over the circumference of the shell cross section. The value of ω is found from Eq. (20.15) for $m^* = 5$. The relationship between the frequency and m is shown in Fig. 20.2.

Figure 20.3 illustrates the relationship of the frequency for any fixed value of m from the shell length, L. It is seen that the frequency decreases as the length of the shell increases. However, starting from some length L^*, the frequency becomes a constant and practically coincides with the frequency determined for a shell having free edges or for a shell of an infinite length when the shell experiences only bending without stretching of the middle surface.

If a shell is not too short ($L > R$), then the natural frequency is virtually independent of the boundary conditions and it is possible to determine this frequency for a shell with any, say simply supported, boundary conditions.

The strain energy of a shell of any geometry is given by Eq. (12.51). The kinetic energy of a vibrating shell is of the following form:

$$K = \frac{\rho h}{2} \int\int_A \left[\left(\frac{\partial u}{\partial t}\right)^2 + \left(\frac{\partial v}{\partial t}\right)^2 + \left(\frac{\partial w}{\partial t}\right)^2 \right] AB\,\mathrm{d}\alpha\,\mathrm{d}\beta. \tag{20.18}$$

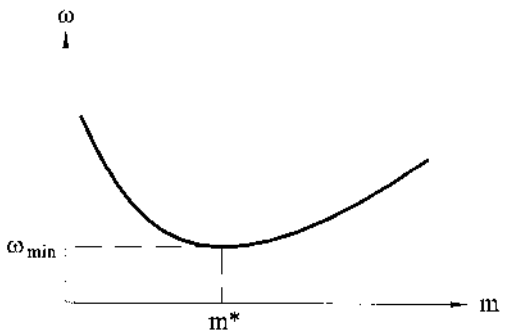

Fig. 20.2

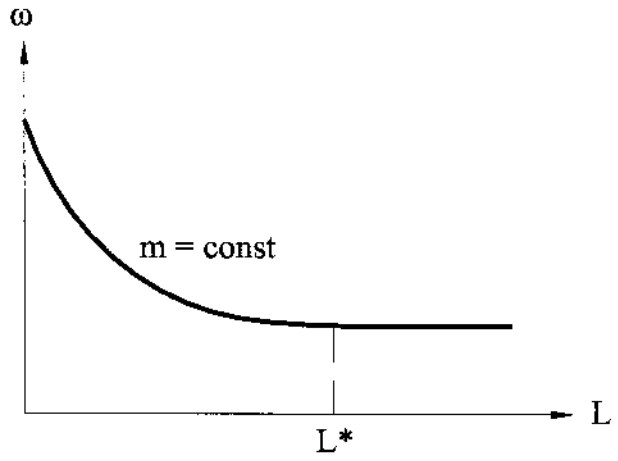

Fig. 20.3

Assuming, again, the harmonic vibrations in time, we can approximate the displacements of a cylindrical shell midsurface as follows:

$$u = u_0(x, \theta) \sin \omega t,$$

$$v = v_0(x, \theta) \sin \omega t,$$

$$w = w_0(x, \theta) \sin \omega t,$$

where u_0, w_0, and w_0 are the maximum displacements. Substituting the derivatives of u, v, and w with respect to time into Eq. (20.18), we can find the maximum value of the kinetic energy:

$$K_{\max} = \frac{\rho h}{2} \omega^2 \int\int_A \left[u_0^2 + v_0^2 + w_0^2\right] R \mathrm{d}x \mathrm{d}\theta. \tag{20.19}$$

Equating $K_{\max}$ and $U_{\max}$ and letting, $A = 1$, $B = R$, $\alpha = x$, and $\beta = \theta$, we obtain the following expression for the frequency of asymmetric flexural free vibrations of a cylindrical shell in terms of its strain and kinetic energies:

$$\omega^2 = 2 \frac{U_{\max}}{\rho h \int\int_A \left(u_0^2 + v_0^2 + w_0^2\right) R \mathrm{d}x \mathrm{d}\theta}. \tag{20.20}$$

2. Open cylindrical shells (panels)

The vibration analysis of cylindrical shells can be conveniently carried out with the use of Eqs (17.36) in terms of the stress function Φ and deflection w. Assuming that the stiffness of the shell in the middle surface is much greater than its stiffness in the normal direction with respect to the middle surface, we can use the following conditions according to Eqs (20.1):

$$p_1 = p_2 = 0 \quad \text{and} \quad p_3 = -\rho h \frac{\partial^2 w}{\partial t^2}.$$

Substituting the above into Eqs (17.36) and taking $\alpha = \xi = x/R$, $\beta = \theta = s/R$, $\kappa_1 = 0$, and $\kappa_2 = 1/R$, one obtains the following system of equations:

$$-\frac{\partial^2 \Phi}{\partial \xi^2} R + D\nabla^2\nabla^2 w + \rho h R^4 \frac{\partial^2 w}{\partial t^2} = 0,$$
$$\nabla^2\nabla^2 \Phi + REh \frac{\partial^2 w}{\partial \xi^2} = 0. \tag{20.21}$$

The above is a set of the *governing differential equations of the undamped, free linear, transverse vibrations of circular cylindrical shells*. The details of determining the natural frequencies of cylindrical shells is explained in the illustrative problem that follows.

Example 20.2

Determine the natural frequency of free vibrations of the circular cylindrical, simply supported shell shown in Fig. 20.4. Calculate the fundamental natural frequency for the shell made of reinforced concrete and having the following geometric and mechanical parameters: $L = 55\,\text{m}$, $l = 21\,\text{m}$, $f = 4.0\,\text{m}$, $R = 15.0\,\text{m}$, $h = 0.1\,\text{m}$, $\theta_0 = 1.6\,\text{rad}$, $E = 6\,\text{GPa}$, $\rho = 1.6 \times 10^3\,\text{kg/m}^3$, and $\nu = 0$.

Solution

The simply supported boundary conditions in the adapted coordinate system are of the form

$$w = v = M_1 = N_1 = 0\big|_{\xi=0,\xi=L/R},$$
$$w = u = M_2 = N_2 = 0\big|_{\theta=0.\theta=\theta_0}.$$

A solution of Eqs (20.15) is sought in the form of the following series:

$$\Phi = \sum_{m=1}^{\infty}\sum_{n=1}^{\infty} A_{mn} \sin \lambda_n \xi \sin \mu_m \theta \cdot \sin\, \omega t,$$
$$w = \sum_{m=1}^{\infty}\sum_{n=1}^{\infty} B_{mn} \sin \lambda_n \xi \sin \mu_m \theta \cdot \sin \omega t, \tag{a}$$

where

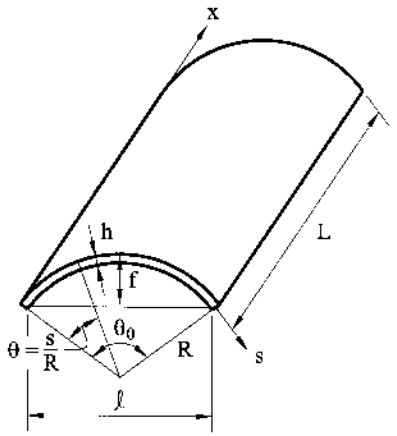

Fig. 20.4

$$\lambda_n = \frac{n\pi R}{L}, \quad \mu_m = \frac{m\pi}{\theta_0}.$$

Substituting the above into Eqs (20.21), one obtains the following:

$$A_{mn}R\lambda_n^2 + B_{mn}D(\lambda_n^2 + \mu_m^2)^2 - B_{mn}(\rho h)R^4\omega^2 = 0,$$

$$\frac{A_{mn}}{Eh}(\lambda_n^2 + \mu_m^2)^2 - B_{mn}R\lambda_n^2 = 0.$$

From the condition of nontriviality of the solution of the above system of the homogeneous algebraic equations, we obtain the following characteristic equation:

$$\omega^2 = \frac{1}{\rho h R^4}\left[\frac{EhR^2\lambda_n^4}{(\lambda_n^2 + \mu_m^2)^2} + D(\lambda_n^2 + \mu_m^2)^2\right]. \tag{b}$$

To determine the fundamental natural frequency of free vibrations, it is necessary to calculate the values of m and n (values of λ_n and μ_m) corresponding to the lowest frequency. Analysis of Eq. (b) shows that the fundamental mode of the vibrations corresponds to λ_1 (for $n = 1$, one half-wave in the longitudinal direction). Let us calculate the number m (the number of circumferential half-waves) that corresponds to the fundamental natural frequency of the given shell. For this purpose, take the first derivative of the expression (b) with respect to μ_m and equate it to zero for $\lambda_1 = \text{const}$. We have

$$\frac{\partial(\omega_{mn}^2)}{\partial\mu_m} = 0.$$

After some simple manipulations, one obtains

$$\mu_m = \sqrt{\lambda_1\left(\sqrt[4]{\frac{12R^2(1-\nu^2)}{h^2}} - \lambda_1\right)}.$$

It can be easily shown that for long and intermediate-length shells, the fundamental natural frequency occurs for $n = 1$ and $m = 2$ (one half-wave in the longitudinal and two half-waves in the circumferential directions, respectively). The shell under consideration, having $4 < L/l = 2.64 > 1$, can be classified as an intermediate-length shell. So, we obtain the following:

$$\lambda_1 = \frac{\pi(15.0)}{55.0} = 0.856, \quad \mu_2 = \frac{\pi(2)}{1.6} = 3.927.$$

Substituting the above data into Eq. (b), we obtain $\omega_{12} = 7.151/\text{s}$.

20.3 FREE VIBRATIONS OF CONICAL SHELLS

The governing equations of free vibrations of conical shells can be derived from Eqs (12.23), (12.24), and (12.41), (12.42), (12.45), (1246) of the general linear shell theory by introducing the curvilinear coordinates $\alpha = s$ and $\beta = \theta$ (where s is the distance of a point of the midsurface, measured from some reference point, e.g., from the shell vertex, and θ is the circumferential angle determining the location of the meridian), substituting the corresponding Lamé parameters, and replacing the distributed sur-

face loads p_1, p_2, and p_3 with the inertia forces according to Eqs (20.1). The governing equations of free vibrations in displacements obtained represent the partial differential equations with variable coefficients. Their solution represents a very complicated mathematical problem.

Conducted analyses and tests showed that for small angles of conicity 2α (about 30°–40°) (see Fig. 19.8), the frequency of axisymmetric, free radial vibrations can be approximately calculated by Eqs (20.4) and (20.7) by replacing R in these equations with $r_m = (r_1 + r_2)/2$ and setting the length of the longitudinal axis of the conical shell equal to L (cylindrical shell length). It should be noted that conical shells with these angles of conicity are met in nozzle structures of jet engines. The vibration shell analyses showed that the error introduced by the above approximate procedure was not more than 5–10%. For larger angles of conicity, refined solutions, based on the governing differential equations of free vibrations mentioned above, should be employed.

The dependence of the frequency of free radial vibrations on the number of waves along the shell cross section has a minimum, just as for a cylindrical shell (see Fig. 20.2). The above minimum is explained by relations between the strain energy due to elongation and the strain energy due to bending in various undulations.

A conical shell can have longitudinal and torsional vibrations but they are of less importance than the bending and normal axisymmetric vibrations.

20.4 FREE VIBRATIONS OF SHALLOW SHELLS

The governing differential equations of free vibrations of shallow shells can be obtained from Eqs (17.36) by using the relations (20.1), setting $p_1 = p_2 = p_3 = 0$, and assuming that stiffness of the shell in the middle surface is much greater than its stiffness in the direction normal to the middle surface. Therefore, putting $\alpha = x$ and $\beta = y$ and neglecting the in-plane inertia forces, we obtain the following *differential equations of free vibrations of shallow shells*:

$$\begin{aligned} D\nabla^2\nabla^2 w - \nabla_k^2 \Phi + \rho h \frac{\partial^2 w}{\partial t^2} &= 0, \\ \nabla^2\nabla^2 \Phi + Eh\nabla_k^2 w &= 0, \end{aligned} \tag{20.22}$$

where the operators ∇^2 and ∇_k^2 are given by Eqs (17.44), respectively.

To determine the natural frequencies of shallow shells having arbitrary boundary conditions, the approximate and numerical methods introduced in Chapter 6 may be used. Let us consider an application of some methods to the free-vibration problems of a shallow shell given by Eqs (20.22). Assume that the projection of the shell into the Oxy coordinate plane is a rectangle with sides a and b.

1. Galerkin method

The stress function Φ and deflection w are sought in the form of the following series:

$$\begin{aligned} \Phi &= \sum_m \sum_n A_{mn} \Phi_{mn}(x, y) \sin \omega t, \\ w &= \sum_m \sum_n B_{mn} W_{mn}(x, y) \sin \omega t. \end{aligned} \tag{20.23}$$

The functions Φ_{mn} and W_{mn} must satisfy the prescribed boundary conditions on shell edges $x = 0, a$ and $y = 0, b$. It is convenient to assign the above functions in the form of the product of two functions, each of which depends upon only one independent variable, i.e.,

$$\Phi_{mn} = X_n(x)Y_m(y), \quad W_{mn} = \Psi_n(x)\Lambda_m(y).$$

The functions X_n, Y_m, Ψ_n, and Λ_m are chosen such that they would satisfy the given boundary conditions on the corresponding shell edges. It is convenient to employ the so-called fundamental beam functions [1] as the above-mentioned approximating functions. The Galerkin equations (Eqs (6.39)) for free-vibration analysis of shallow shells can be represented in the following form:

$$\begin{aligned} \int\int_A \left(D\nabla^2\nabla^2 w - \nabla_k^2\Phi + \rho h \frac{\partial^2 w}{\partial t^2} \right) W_{ij} \mathrm{d}x\mathrm{d}y = 0, \\ \int\int_A \left(\nabla^2\nabla^2\Phi + Eh\nabla_k^2 w \right) \Phi_{ij} \mathrm{d}x\mathrm{d}y = 0. \end{aligned} \tag{20.24}$$

Substituting for w and Φ from Eqs (20.23) into the above and evaluating the integrals, we obtain a system of homogeneous algebraic equations in A_{mn} and B_{mn}. Equating the determinant of the above system of equations to zero results in the following characteristic equation for determining the natural frequencies:

$$\omega_{mn}^2 = \frac{1}{\rho h}\left[D\frac{J_4}{J_5} + Eh\frac{J_2 J_3}{J_1 J_5} \right], \tag{20.25}$$

where,

$$\begin{aligned} J_1 &= \int\int_A \left(X_n Y_m \nabla^2\nabla^2 (X_n Y_m) \right) \mathrm{d}x\mathrm{d}y; \\ J_2 &= \int\int_A X_n Y_m \left[\Lambda_m \frac{\partial}{\partial x}(\kappa_2 \Psi_n') + \Psi_n \frac{\partial}{\partial y}\left(\kappa_1 \Lambda_m'\right) \right] \mathrm{d}x\mathrm{d}y; \\ J_3 &= \int\int_A \Psi_n \Lambda_m \left[Y_m \frac{\partial}{\partial x}(\kappa_2 X_n') + X_n \frac{\partial}{\partial y}(\kappa_1 Y_m') \right] \mathrm{d}x\mathrm{d}y; \\ J_4 &= \int\int_A \Psi_n \Lambda_m \nabla^2\nabla^2 \Psi_n \Lambda_m \mathrm{d}x\mathrm{d}y; \quad J_5 = \int\int_A \Psi_n^2 \Lambda_m^2 \mathrm{d}x\mathrm{d}y. \end{aligned} \tag{20.26}$$

In choosing X_n, Y_m, Ψ_n, and Λ_m, it is important to assign orthogonal function, whose second and fourth derivatives also possess orthogonality properties. In this case, an infinite system of the homogeneous linear algebraic equations with an infinite number of equations is separated down into a system consisting of the pair of equations in A_{mn} and B_{mn} for each pair of the numbers m and n.

2. The Rayleigh–Ritz method

According to the Rayleigh–Ritz method, natural frequencies of free vibrations of shallow shells are determined from the condition of a minimum of the sum of the potential and kinetic energies of the shell. The strain energy of a shallow shell is given by Eq. (17.50) and the kinetic energy for the above shallow shell can be represented by Eq. (20.18), if we put $A = B = 1$, $\alpha = x$, and $\beta = y$. If the membrane inertia forces

are neglected compared with the transverse inertia forces, then we obtain, from Eq. (20.18), the following expression for the kinetic energy of a shallow shell:

$$K = \frac{\rho h}{2} \int\int_A \left(\frac{\partial w}{\partial t}\right)^2 \mathrm{d}x\mathrm{d}y. \tag{20.27}$$

If a shell is undergoing harmonic vibrations, then a maximum value of the kinetic energy is given by the following expression:

$$K_{\max} = \frac{\rho h \omega^2}{2} \int\int_A w^2 \mathrm{d}x\mathrm{d}y. \tag{20.28}$$

Assume that the stress function Φ and deflection w of the shell are approximated by the expressions (20.23). The conditions of the minimum of the Rayleigh's fraction gives

$$\frac{\partial}{\partial A_{mn}}\left(U_{\max} - \omega^2 K_{\max}\right) = 0; \quad \frac{\partial}{\partial B_{mn}}\left(U_{\max} - \omega^2 K_{\max}\right) = 0, \tag{20.29}$$

from which the characteristic equation for determining the natural frequencies is obtained.

Example 20.3

Determine the natural frequency of free vibrations of a shallow, simply supported shell of a double positive curvature. Assume that the shell is a rectangular in a plane, as shown in Fig. 17.6, and $\kappa_1 = 1/R_1 = \text{const}$, $\kappa_2 = 1/R_2 = \text{const}$.

Solution

The simply supported boundary conditions on the shell edges are of the form

$$w = v = M_1 = N_1 = 0\big|_{x=0,a}; \quad w = u = M_2 = N_2 = 0\big|_{y=0,b}. \tag{a}$$

Let us approximate the stress function Φ and deflection surface w by the following series:

$$\begin{aligned} \Phi &= \sum_{m=1}^{\infty}\sum_{n=1}^{\infty} A_{mn} \sin \lambda_n x \sin \mu_m y \sin \omega t, \\ w &= \sum_{m=1}^{\infty}\sum_{n=1}^{\infty} B_{mn} \sin \lambda_n x \sin \mu_m y \sin \omega t, \end{aligned} \tag{b}$$

where $\lambda_n = n\pi/a$; $\mu_m = m\pi/b$. It can be shown that the expressions for Φ and w in the form of Eqs (b) satisfy the boundary conditions (a). Substituting the expressions (b) into Eqs (20.22), we obtain the homogeneous system of linear algebraic equations in A_{mn} and B_{mn}. To obtain a nontrivial solution of this system, it is necessary to equate its denominator to zero. Expanding the above determinant, one obtains

$$\omega_{mn}^2 = \frac{1}{\rho h}\left[D(\lambda_n^2 + \mu_m^2)^2 + \frac{Eh\left(\frac{\lambda_n^2}{R_2} + \frac{\mu_m^2}{R_1}\right)^2}{(\lambda_n^2 + \mu_m^2)^2} \right]. \tag{c}$$

For a cylindrical, simply supported shallow shell, Eq. (c) takes the following form ($R_1 = \infty$, $R_2 = R = \text{const}$):

$$\omega_{mn}^2 = \frac{1}{\rho h}\left[D(\lambda_n^2 + \mu_m^2)^2 + \frac{Eh}{R^2}\frac{\lambda_n^4}{(\lambda_n^2 + \mu_m^2)^2}\right]. \tag{d}$$

Equations of a minimum $\partial\omega_{mn}^2/\partial\lambda_n = 0$ for a fixed value of μ_m and $\partial\omega_{mn}^2/\partial\mu_m = 0$ for a fixed value of λ_n have no real roots, which shows the monotonic character of the variation of ω_{mn}^2 as a function of λ_n and μ_{m}. Thus, the frequency of the fundamental mode, or the lowest natural frequency of free vibrations of a given shallow, simply supported shell, corresponds to one half-wave in the x and y directions, i.e., $m = n = 1$.

20.5 FREE VIBRATIONS OF STIFFENED SHELLS

The analytical solution of free-vibration problems of stiffened shells presents considerable difficulties. Consider the free vibrations of a cylindrical shell reinforced by transverse rings (collars). The method of an approximate analysis of flexural vibrations of such a shell depends on the ratio between the flexural stiffnesses of the ring (in its own plane) and the shell itself. If the shell stiffness D multiplied by the distance between the rings, l_x, is significantly less than the flexural stiffness of the ring, EI_{r}, then the natural frequencies can be found from Eqs (20.4) and (20.15), assuming $L = l_x$. If the value of $D \cdot l_x$ is significantly larger than EI_{r} then to determine the natural frequency of flexural vibrations of the stiffened shell, the stiffness of the rings can be uniformly distributed over the shell and the latter is considered as structurally orthotropic, i.e., having different flexural stiffnesses in the longitudinal and transverse directions (see Sec. 18.3.2). In the circumferential direction, such a shell will have the flexural stiffness equals to $D + EI_{\mathrm{r}}/l_x$, where I_{r} is the moment of inertia of the ring cross section with joined segment of the shell (of length l_x) about the common axis x of bending of this combined section.

Expression (20.15), for the structurally orthotropic cylindrical shell, can be written in the following form:

$$\omega^2 = \frac{1}{\rho h R^2}\frac{\lambda^4 Eh + \frac{(D + EI_{\mathrm{r}}/l_x)}{R^2}(\lambda^2 + m^2)^4}{(\lambda^2 + m^2)^2 + m^2}. \tag{20.30}$$

The relation (20.30) is valid if the modulus of elasticity of the shell material differs slightly from the modulus of elasticity of the ring material. If the moduli of elasticity of the shell and ring differ significantly, then the relation (20.15) must be transformed, as follows:

$$\omega^2 = \frac{B}{\hat{M}R^2}\frac{(1-\nu^2)\lambda^4 + \frac{(D + E_{\mathrm{r}}I_{\mathrm{r}}/l_x)}{BR^2}(\lambda^2 + m^2)^4}{m^2 + (\lambda^2 + m^2)^2}, \tag{20.31}$$

where

$B = \dfrac{E_{\mathrm{s}}h}{1-\nu_s^2}$ is the extensional stiffness of the shell at a section of unit length;

E_s and ν_s	are the modulus of elasticity and Poisson's ratio of the shell material;
$\hat{M} = \rho_s h + \dfrac{A_r \rho_r}{l_x}$	is a shell mass referred to an area of the shell middle surface;
A_r	is the ring's cross-sectional area;
ρ_s and ρ_r	are the mass densities of the shell and ring materials, respectively;
$D = \dfrac{E_s h^3}{12(1-\nu_s^2)} + \dfrac{E_r I_r}{l_x}$	is the flexural stiffness of the stiffened shell (see Eqs (18.50)); and
E_r	is the modulus of elasticity of the ring material.

All the above relations and equations of free vibrations have been derived for unloaded shells. However, it is known that the natural frequencies of free vibrations depend on the character and value of applied static loading, such as the normal surface pressure, axial force, torque, etc. Let us discuss first an influence of these static loads on the natural frequencies of closed unstiffened circular cylindrical shells. Assume that the shell is simply supported on its edges. The governing differential equations of free vibrations of such shells will be analogous to those of Eqs (20.11), with an addition of terms depending on the given static loading. Dropping the intermediate mathematics associated with deriving the above equations (these derivations are quite similar to those carried out in Sec. 20.2.3), we give only the final results. The natural frequency of free vibrations of a circular, simply supported cylindrical shell subjected to a combined static loading is

$$\Omega = \Omega_0 + \frac{(\lambda^2 + m^2)^2 \left[\psi_1 (m^2 - 1) + \psi_2 \lambda^2 - 2\psi_3 \lambda m\right]}{m^2 + (\lambda^2 + m^2)^2}, \tag{20.32}$$

where

$$\Omega_0 = \frac{(1-\nu^2)\rho R^2}{E}\omega_0^2 = \frac{(1-\nu^2)\lambda^4 + a^2(\lambda^2 + m^2)^4}{m^2 + (\lambda^2 + m^2)^2}, \tag{20.33}$$

ω_0 is the natural frequency of free vibrations of the unloaded shell, and

$$\psi_1 = \frac{pR(1-\nu^2)}{Eh}, \quad \psi_2 = \frac{N_1(1-\nu^2)}{Eh}, \quad \psi_3 = \frac{H(1-\nu^2)}{2\pi R^2 Eh}, \tag{20.34}$$

where p is the difference between the normal internal and external pressure, N_1 is an axial tension force, and H is a torque. Thus, it is seen from the expression (20.32) that the presence of the internal pressure and axial tensile force increases the natural frequencies of free vibrations in comparison with the corresponding natural frequencies of an unloaded shell. An application of the torque decreases the natural frequencies of free vibrations corresponding to certain wave numbers m and n.

If the value of m^2 in the denominator of Eq. (20.32) is neglected (which corresponds to neglecting the membrane internal forces in the vibration equations), then the expression for determining the natural frequencies in statically loaded shells is simplified to the following:

$$\Omega = \Omega_0 + \psi_1 (m^2 - 1) + \psi_2 \lambda^2 - 2\psi_3 \lambda m. \tag{20.35}$$

Such a simplification is absolutely coincident with the accuracy of the general shell theory for $m > 3$. If no torque and axial force are applied to the shell and only a normal internal pressure acts on the shell, then

$$\psi_3 = 0, \psi_2 = \frac{\psi_1}{2}.$$

Thus, in this case of loading, Eq. (20.32) becomes

$$\Omega = \frac{(1-\nu^2)\lambda^4 + a^2(\lambda^2+m^2)^4 + \psi_1(\lambda^2+m^2)^2(m^2-1)}{m^2+(\lambda^2+m^2)^2}. \tag{20.36}$$

This expression can be applied to the case of external pressure by replacing ψ_1 with $(-\psi_1)$. As seen from Eq. (20.32), for $m = 1$, i.e., for vibrations of a beam type when circumferences of the shell cross sections do not deform, the natural frequency of free vibrations does not depend on a normal pressure. The latter also does not influence the natural frequencies of axisymmetrical vibrations of cylindrical shells.

If a static load acts on the stiffened cylindrical shell reinforced by the transverse rings, then the natural frequency will also be determined by Eq. (20.32) in which Ω_0 is figured out for an unloaded structurally orthotropic shell, i.e.,

$$\Omega_0 = \frac{(1-\nu^2)\rho R^2}{E}\omega_{0s}^2, \tag{20.37}$$

where ω_{0s} is given by the expression (20.25).

20.6 FORCED VIBRATIONS OF SHELLS

In this section, we are concerned with determining the response of thin elastic shells to external time-dependent loads. Consider a problem of forced transverse vibrations of a simply supported shallow shell subjected to the action of an arbitrary load $p_3(x, y, t)$. Assume that the latter varies in time according to the harmonic law, i.e.,

$$p_3(x, y, t) = p_3(x, y)\sin\Omega t, \tag{20.38}$$

where Ω is the frequency of the applied load. The equations of forced transverse vibrations of a shallow shell can be represented in the form

$$\begin{aligned} \frac{1}{Eh}\nabla^2\nabla^2\Phi + \nabla_k^2 w &= 0, \\ D\nabla^2\nabla^2 w - \nabla_k^2\Phi + \rho h\frac{\partial^2 w}{\partial t^2} - p_3 &= 0. \end{aligned} \tag{20.39}$$

If the shallow shell projection on the xy-coordinate plane is a rectangle with sides a and b, then a solution of Eqs (20.39) is sought in the following form:

$$\begin{aligned} \Phi &= \sin\Omega t\sum_{m=1}^{\infty}\sum_{n=1}^{\infty} A_{mn}\sin\lambda_n x\sin\mu_m y, \\ w &= \sin\Omega t\sum_{m=1}^{\infty}\sum_{n=1}^{\infty} B_{mn}\sin\lambda_n x\sin\mu_m y. \end{aligned} \tag{20.40}$$

The external load applied to the shell is also extended into the following series:

$$p_3(x, y, t) = \sin \Omega t \sum_{m=1}^{\infty} \sum_{n=1}^{\infty} C_{mn} \sin \lambda_n x \sin \mu_m y, \tag{20.41}$$

where

$$C_{mn} = \frac{4}{ab} \int \int_A p_3(x, y) \sin \lambda_n x \sin \mu_m y \mathrm{d}x \mathrm{d}y$$

and

$$\lambda_n = \frac{n\pi}{a}, \quad \mu_m = \frac{m\pi}{b}. \tag{20.42}$$

Substituting Eqs (20.40) and (20.41) into Eqs (20.39), we obtain, after some mathematics, the following:

$$B_{mn} \left[\frac{Eh(k_2 \lambda_n^2 + k_1 \mu_m^2)^2}{(\lambda_n^2 + \mu_m^2)^2} + D(\lambda_n^2 + \mu_m^2)^2 - \rho h \theta^2 \right] = C_{mn}. \tag{20.43}$$

Taking into account expression (c) of Example 20.3 for determining the natural frequencies of free vibrations, Eq. (20.43) can be rewritten as follows:

$$B_{mn} = \frac{1}{\rho h} \frac{C_{mn}}{(\omega_{mn}^2 - \Omega^2)}. \tag{20.44}$$

Then, the amplitude of the forced vibrations is determined as follows:

$$w = \frac{1}{\rho h} \sum_{m=1}^{\infty} \sum_{n=1}^{\infty} \frac{C_{mn}}{\omega_{mn}^2 - \Omega^2}, \tag{20.45}$$

where ω_{mn}, the frequency of the natural vibrations of the shallow shell, is given by Eq. (c) of Example 20.3.

When the frequency of the forced vibrations, Ω, coincides with one of the natural frequencies, a resonance occurs ($w \to \infty$). If Ω is small compared with ω_{mn}, then the deflections will correspond to the case of static loading, i.e.,

$$\hat{B}_{mn} = \frac{1}{\rho h} \frac{C_{mn}}{\omega_{mn}^2}. \tag{20.46}$$

Let us introduce the *dynamic coefficient* μ, as the ratio of $B_{mn}/\hat{B}_{mn}$. Using the expressions (20.44) and (20.46) for the coefficients in the above ratio, we obtain

$$\mu = \frac{1}{1 - \Omega^2/\omega_{mn}^2}. \tag{20.47}$$

Let us now consider some special classes of dynamic loading applied to the shallow shell.

1. *Uniform surface loading* $p \sin \Omega t$

For this type of dynamic loading,

$$C_{mn} = \frac{16p}{\pi^2 mn}; \quad m = 1, 3, 5, \ldots, \infty; \quad n = 1, 3, 5, \ldots, \infty,$$

and the amplitude of the forced vibrations is given by

$$w = \frac{16p}{\pi^2 \rho h} \sum_{m=1,3,\ldots}^{\infty} \sum_{n=1,3,\ldots}^{\infty} \frac{\sin \lambda_n x \sin \mu_m y}{mn(\omega_{mn}^2 - \Omega^2)}. \tag{20.48}$$

2. *Concentrated force* $P \sin \Omega t$ *applied at a point* ξ, η

For this case of dynamic loading,

$$C_{mn} = \frac{4P}{ab} \sin \lambda_n \xi \sin \mu_m \eta; \quad m, n = 1.2, 3, \ldots, \infty,$$

and the amplitude of the forced vibrations is

$$w = \frac{4P}{\rho hab} \sum_{m=1}^{\infty} \sum_{n=1}^{\infty} \frac{\sin \lambda_n \xi \sin \mu_m \eta}{\omega_{mn}^2 - \Omega^2} \sin \lambda_n x \sin \mu_m y. \tag{20.49}$$

Example 20.4

Determine the amplitude of forced vibrations in a simply supported cylindrical shell having the dimensions of Example 20.2. The shell is subjected to a uniformly distributed surface loading varying with time as $p_3 = p \sin \Omega t$, where $p = 0.5\,\mathrm{kN/m^2}$ and $\Omega = 20/\mathrm{s}$.

Solution

We can use all the expressions derived in this section for cylindrical shells, replacing the coordinates x and y by $\alpha = x/R$ and $\theta = s/R$, respectively, where s is the arc of the circumference of the shell cross section. Expanding the load p into the trigonometric series in α and β, determine from Eq. (20.42) the coefficients C_{mn}. We have the following:

$$C_{mn} = \frac{4pR}{\theta_0 L} \int_0^{\theta_0} \int_0^{L/R} \sin \lambda_n \alpha \sin \mu_m \theta \mathrm{d}\alpha \mathrm{d}\theta = \frac{16p}{\pi^2 mn}; \quad m, n = 1, 3, 5, \ldots, \infty.$$

The amplitude of the forced vibrations is given by Eq. (20.49), where the natural frequencies can be calculated from Eq. (b) of Example 20.2. Calculating the first three natural frequencies from the above equations, corresponding to $m = 1$, $n = 1$; $m = 3$, $n = 1$; and $m = 5$, $n = 1$, we obtain

$$\omega_{11} = 18.841/s; \quad \omega_{31} = 9.6081/s; \quad \omega_{51} = 25.5911/s$$

(here only the frequencies for odd numbers of m and n are given). For these values of ω_{mn}, the value of w calculated from Eq. (20.49) is $w = 1.931 \times 10^{-2}$ m.

The case considered above of the transverse vibrations eliminating the deformations of the middle surface is approximate. It has been assumed that the extensional stiffness of a shell is infinitely large. Since a real shell has a finite stiffness in tension, the natural frequencies must be lower than those given above. It is important to note that, in some cases, vibrations without stretching of the middle surface are impossible (for instance, for closed spherical shells). However, the investigations of equations of motion of shells conducted show that stretching of the shell middle surface is significantly small for a larger part of the shell surface and it may play a significant role only near the shell edges.

This chapter contains only some general information about the dynamic response of thin shells. The interested reader is referred to Refs [2–5] for additional reading.

PROBLEMS

20.1 Determine the fundamental natural frequency of the axisymmetric radial free vibrations of a circular cylindrical shell of length L and radius R for the two types of boundary conditions at the shell ends $x = 0$ and $x = L$: (a) the fixed edges and (b) the simply supported edges. Let $R = 0.5\,\text{m}$, $h = 8\,\text{mm}$, $L = 4R$. The shell is made of steel.

20.2 Investigate the variation of frequency of free radial vibrations of a simply supported open circular cylindrical shell (see Fig. 20.4) from its length L. Take the geometric parameters of the shell in the transverse direction from Example 20.2. Let the shell length $L = 6.0, 10.0, \ldots, 54\,\text{m}$ with the step of 4.0 m.
Hint: Use Eq. (b) in Example 20.2 for your calculations and take $n = 1$; $m = 1, 2.3, 4, 5$.

20.3 Consider a shallow cylindrical shell having a square plan with sides $a \times a$. Investigate an influence of the shell shallowness f/a on the frequencies of free vibrations. Take in your calculations $n = 1$; $m = 1, 2$ in the series expansions. Use the following geometric and mechanical parameters of the shell: $a = 16\,\text{m}$, $h = 6\,\text{cm}$, $E = 15\,\text{GPa}$, $\nu = 0.15$, and $\rho = 2400\,\text{kg/m}^3$. Confine your analysis to the following range: $1/20 \leq f/a \leq 1/8$.

20.4 Calculate the lowest frequency of free vibrations of a spherical shallow shell on a square plan. Assume that the shell is simply supported on its edges. Let $a = 10\,\text{m}$, $f = 0.3\,\text{m}$, $E = 210\,\text{GPa}$, $\rho = 2300\,\text{kg/m}^3$, $\nu = 0.3$, $h = 0.1\,\text{m}$, and $R = 85\,\text{m}$.

20.5 Calculate the lowest frequency of free vibrations of a shallow shell of double curvature on a rectangular plane (Fig. 17.6). The shell is simply supported on its ends. Let $a = 20\,\text{m}$, $b = 20\,\text{m}$, $h = 10\,\text{cm}$, $f = 4\,\text{m}$, $R_1 = 25\,\text{m}$, $R_2 = 42\,\text{m}$, $E = 22\,\text{GPa}$, and $\nu = 0.15$.

20.6 Determine the amplitude of forced vibrations of a cylindrical shell loaded by a concentrated harmonic force $P \sin \Omega t$ applied at a point with the coordinates α_1 and β_1. Assume reasonable values for any additional properties and parameters required.
Hint: Replace the given concentrated force by a uniform load q distributed over a small portion of a cylindrical surface with sides ξ and η, so that $q = P/4R^2\xi\eta$.

20.7 Calculate the amplitude of the forced vibrations of a spherical shallow shell subjected to a uniformly distributed load $p = p_0 \sin \Omega t$. Take as the dimensions of the shell the frequencies of free vibrations from Problem 20.5. Use $p_0 = 0.8\,\text{kN/m}^2$ and $\Omega = 60\,s^{-1}$.

REFERENCES

1. Vlasov,V.Z., *General Theory of Shells and Its Application in Engineering* (English trans), NASA TT F-99, Washington, DC, April 1964.
2. Kraus, H., *Thin Elastic Shells*, John Wiley and Sons, New York, 1967.
3. Flügge, W., *Statik and Dynamik der Schalen*, Springer-Verlag, Berlin, 1962.
4. Nowacki, W., *Dynamics of Elastic Systems*, John Wiley and Sons, New York, 1963.
5. Leissa, A.W., *Vibration of Shells*, NASA SP-288, Washington, DC, 1973.

Appendix A

Some Reference Data

A.1 Typical properties of selected engineering materials at room temperatures[a] (U.S. Customary Units)

Material	Specific weight (lb/in^3)	Ultimate strength (ksi)		Yield strength[b] 0.2% offset tension (ksi)	Modulus of elasticity (10^6 psi)	Coefficient of thermal expansion $10^{-6}/°F$	Poisson's ratio
		Tensile	Compression[b]				
Steel:							
Structural, ASTM-A36	0.284	58	—	36	29	6.5	0.32
Tool L2	0.295	116	—	102	29	6.5	0.32
Stainless (304)	0.284	75	—	30	28	9.6	0.27
Cast iron:							
Gray, ASTM A-48	0.260	25	97	—	10	6.7	0.28
Malleable, ASTM A-47	0.264	40	83	33	24	6.7	0.28
Aluminum:							
Alloy 2014-T6	0.101	68	—	60	10.6	12.8	0.35
Alloy 6061-T6	0.098	42	—	38	10.0	13.1	0.35
Brass, yellow, cold-rolled	0.306	78	—	63	15	11.3	0.35
Bronze, cold-rolled	0.320	81	—	75	16	9.9	0.31
Magnesium alloys	0.065	40	—	22	6.5	14.3	0.30
Concrete:							
Medium strength	0.084	—	4	—	3.5	5.5	0.15
High strength	0.084	—	6	—	4.3	5.5	0.15
Timber (air dry):							
Douglas fir	0.017	0.30[c]	3.76[d]	—	1.9	—	0.29[c]
White spruce	0.130	0.36[c]	5.18[d]	—	1.4	—	0.31[c]
Glass, 98% silica	0.079	—	7	—	9.6	44	0.17
Plastic reinforced:							
Kevlar	0.0524	104	70	—	19	—	0.34
30% glass	0.0524	13	19		10.5		0.34
Rubber	0.033	2	—	—	—	90	0.5

[a] Properties may vary widely with changes in composition, heat treatment, and method of manufacture.
[b] The yield and ultimate strength for ductile metals are generally assumed to be equal for both tension and compression.
[c] Measured perpendicular to the grain.
[d] Measured parallel to the grain.

A.2 Typical properties of selected engineering materials at room temperature[a](International System (SI) Units)

Material	Density (mg/m^3)	Ultimate strength (MPa)		Yield strength[b] 0.2% Offset tension (MPa)	Modulus of elasticity (GPA)	Coefficient of thermal expansion $10^{-6}/^{\circ}C$	Poisson's ratio
		Tensile	Compression[b]				
Steel:							
Structural, ASTM-A36	7.86	400	—	250	200	11.7	0.32
Tool L2	8.16	800	—	703	200	11.7	0.32
Stainless (304), cold-rolled	7.86	517	—	207	193	17.3	0.27
Cast iron:							
Gray, ASTM A-48	7.2	179	689	—	67	12.1	0.28
Malleable, ASTM A-47	7.3	276	572	—	172	12.1	0.28
Aluminum:							
Alloy 2014-T6	2.8	469	—	414	73	23	0.35
Alloy 6061-T6	2.71	290	—	255	69	23.6	0.35
Brass, yellow, cold-rolled	8.47	540	—	435	105	20	0.35
Bronze, cold-rolled	8.86	560	—	520	110	17.8	0.31
Magnesium alloys	1.83	276	—	80–280	45	27	0.35
Concrete							
Medium strength	2.32	—	28	—	24	10	0.15
High strength	2.32	—	40	—	30	10	0.15
Timber (air dry):							
Douglas fir	0.47	2.1[c]	26[d]	—	13.1	4	0.29[c]
White spruce	3.60	2.5[c]	36[d]	—	9.65	4	0.31[c]
Glass, 98% silica	2.19	—	50	—	65	80	0.17
Plastic reinforced:							
Kevlar	1.45	717	483	—	131	—	0.34
30% glass	1.45	90	131		72.4	—	0.34
Rubber	0.91	14	—	—	—	162	0.5

[a] Properties may vary widely with changes in composition, heat treatment, and method of manufacture.
[b] The yield and ultimate strength for ductile metals are generally assumed to be equal for both tension and compression.
[c] Measured perpendicular to the grain.
[d] Measured parallel to the grain.

A.3 UNITS AND CONVERSION FACTORS

Quantity	International system (SI) units	Conversions of US customary units to SI units
Area	m^2	$1\,in.^2 = 645.2 \times 10^{-6}\,m^2$
Density	kg/m^3	$1\,slug/in.^3 = 890{,}600\,kg/m^3$
Force	N (newton)	$1\,lb = 4.448\,N$
Frequency	1/2 (Hz, hertz)	
Length	m (meter)	$1\,in. = 0.0254\,m$
Mass	kg (kilogram)	$1\,slug = 14.59\,kg$
Moment	$N \cdot m$	$1\,in \cdot lb = 0.1130\,N \cdot m$
Moment of inertia	m^4	$1\,in.^4 = 416.2 \times 10^{-9}\,m^4$
Power	$N \cdot m/s = J/s$ (W, watt)	$1\,in. \cdot lb/sec = 0.1130\,W$
Pressure, stress	N/m^2 (Pa, pascal)	$1\,psi = 6895\,Pa$
Time	s (second)	
Velocity	m/s	$1\,in./sec = 0.0254\,m/s$
Volume	m^3	$1\,in.^3 = 16.39 \times 10^{-6}\,m^3$
Work, energy	$N \cdot m$ (J, joule)	$1\,in. \cdot lb = 0.1130\,N \cdot m$

A.4 SOME USEFUL DATA

Atmospheric pressure	$p \approx 100\,kPa$
Acceleration of gravity	$g \approx 9.8\,ms/s/s$
Mass density of water	$\rho \approx 1000\,kg/m^3$
Weight density of water	$\gamma \approx 9800\,kN/m^3$
Mass to weight conversion	$w = mg$

A.5 TYPICAL VALUES OF ALLOWABLE LOADS

Quantity	US customary units	International system (SI) units
Soil:		
Ordinary clay and sand mixture	2–3 tons/ft^2	200–300 kPa
Hard clay and firm coarse sand	4–6 tons/ft^2	400–600 kPa
Bed rock	> 15 tons/ft^2	> 1400 kPa
Wood, yellow pine	1600 psi	11 MPa
Concrete	1000 psi	7 MPa
Steel	20,000 psi	140 MPa

A.6 FAILURE CRITERIA

Failure criteria are associated with failure of materials, not failure of structure. Commonly used failure criteria are employed to predict whether a given state of stress will cause (a) the material to yield (for ductile materials) or (b) the material to fracture (for brittle materials).

We consider briefly some failure criteria for isotropic materials. Let the algebraically largest and smallest principal stresses be designated σ_1 and σ_3, respectively.

A.6.1 Brittle failure criteria

1. Maximum normal stress criterion

This criterion predicts that a material fails when the maximum principal stress reaches or exceeds a limiting value. For the case in which this principal stress is the tensile stress, this criterion has the following form:

$$\text{failure predicted when } \sigma_1 \geq \sigma_{\text{tf}}, \tag{A.1}$$

where σ_{tf} is the limiting tensile stress for a given material determined from a failure test in uniaxial tension.

If the criterion is applied to a compressive state of stress, then the inequality (A.1) is of the form

$$\text{Failure predicted when } |\sigma_3| \geq \sigma_{\text{cf}}, \tag{A.2}$$

where $|\sigma_3|$ is the magnitude of the minimum principal stress ($\sigma_3 < 0$) and $\sigma_{\text{cf}}$is the strength determined by testing a specimen in uniaxial compression.

2. Mohr criterion

Failure is predicted when

$$\frac{\sigma_1}{\sigma_{\text{tf}}} - \frac{\sigma_3}{\sigma_{\text{cf}}} \geq 1. \tag{A.3}$$

A.6.2 Ductile failure criteria (yield criteria)

1. Maximum shear stress criterion (or Tresca criterion)

This criterion states that yielding will begin when the maximum shear stress reaches or exceeds limiting value τ_{y}, i.e.,

$$\text{yielding predicted when } \tau_{\max} \geq \tau_{\text{y}},$$

where τ_{y} is determined from a tension test. In terms of the principal stresses, the above inequality can be rewritten as follows ($\tau_{\max} = (\sigma_1 - \sigma_3/2)$, $\tau_y = \sigma_{\text{y}}/2$):

$$\sigma_1 - \sigma_3 \geq \sigma_{\text{y}}, \tag{A.4}$$

where σ_{y} is 0.2% tension offset yield strength. It is assumed here that a ductile material possesses the same yield strength σ_{y} in tension and compression.

2. Von Mises criterion (maximum distortion energy criterion)

This criterion postulates that failure by yielding occurs when the distortion energy per unit volume reaches or exceeds some limiting value associated with yielding in a simple tension test, i.e.,

$$\text{yielding predicted when } \sqrt{\frac{1}{2}\left[(\sigma_1 - \sigma_2)^2 + (\sigma_2 - \sigma_3)^2 + (\sigma_1 - \sigma_3)^2\right]} \geq \sigma_{\text{y}}. \tag{A.5}$$

Appendix B

Fourier Series Expansion

B.1 DIRICHLET'S CONDITIONS

A function $f(x)$ defined in the interval $-\pi \leq x \leq \pi$ can be expanded into a trigonometric series of the type

$$f(x) = \frac{a_0}{2} + \sum_{k=0}^{\infty} (a_k \cos kx + b_k \sin kx), \tag{B.1}$$

provided that:

(a) $f(x)$ has a finite number of jumps discontinuity points in the given interval and the limiting finite values of the function exist from the right, $f(x_1 + 0)$, and from the left, $f(x_1 - 0)$ at the above points;
(b) the finite limiting values of $f(x)$ exist at the interval ends, i.e., at points $f(\pi - 0)$ and $f(\pi + 0)$; and
(c) $f(x)$ has a finite number of maximum and minimum in the given interval $(-\pi, \pi)$.

B.2 THE SERIES SUM

If Dirichlet's conditions are satisfied and the coefficients a_0, a_k, and b_k are found (see below), then the Fourier series have a sum that is equal to

(a) the given function $f(x)$ at any point of continuity inside the interval $-\pi, +\pi$;
(b) the arithmetic mean of limiting values of $f(x)$ from the right and from the left from points of the discontinuity jump, i.e., $\frac{1}{2}[f(x_1 + 0) + f(x_1 - 0)]$ at discontinuity points; and
(c) the arithmetic mean of limiting values, i.e., $\frac{1}{2}[f(\pi - 0) + f(\pi + 0)]$ on both end points of the interval (i.e., at points $-\pi, +\pi$).

B.3 COEFFICIENTS OF THE FOURIER SERIES

These coefficients are evaluated by multiplying both parts of the equality (B.1) by $\cos kx\mathrm{d}x$ and $\sin kx\mathrm{d}x$ sequentially, and integrating in the limits $-\pi, +\pi$, i.e.,

$$a_0 = \frac{1}{\pi}\int_{-\pi}^{\pi} f(x)\mathrm{d}x; \quad a_k = \frac{1}{\pi}\int_{-\pi}^{\pi} f(x)\cos kx; \quad b_k = \frac{1}{\pi}\int_{-\pi}^{\pi} f(x)\sin kx\mathrm{d}x. \tag{B.2}$$

If $f(x)$ has discontinuity jumps for $x_1, x_2, \ldots, x_s$ then calculating the above coefficients,

$$a_k = \frac{1}{\pi}\int_{-\pi}^{x_1} f(x)\cos kx\mathrm{d}x + \frac{1}{\pi}\int_{x_1}^{x_2} f(x)\cos kx\mathrm{d}x + \ldots + \frac{1}{\pi}\int_{x_s}^{\pi} f(x)\cos kx\mathrm{d}x,$$

$$b_k = \frac{1}{\pi}\int_{-\pi}^{x_1} f(x)\sin kx\mathrm{d}x + \frac{1}{\pi}\int_{x_1}^{x_2} f(x)\sin kx\mathrm{d}x + \ldots + \frac{1}{\pi}\int_{x_s}^{\pi} f(x)\sin kx\mathrm{d}x.$$

B.4 MODIFICATION OF RELATIONS FOR THE COEFFICIENTS OF FOURIER'S SERIES

(a) A given function $f(x)$ is either even or odd

For even function $f(x)$, the Fourier expansion coefficients are

$$a_k = \frac{2}{\pi}\int_0^{\pi} f(x)\cos kx\mathrm{d}x, \; b_k = 0.$$

For odd function $f(x)$, the Fourier expansion coefficients are given by

$$a_k = 0, \quad b_k = \frac{2}{\pi}\int_0^{\pi} f(x)\sin kx\mathrm{d}x.$$

The Fourier expansions for the above two cases will be of the following form:

– for even function ($f(-x) = f(x)$):

$$\frac{a_0}{2} + \sum_{k=1}^{\infty} a_k \cos kx.$$

– for odd function ($f(-x) = -f(x)$)

$$\sum_{k=1}^{\infty} b_k \sin kx.$$

(b) A function $f(x)$ is defined in the interval $-l, +l$.

Then,

$$a_k = \frac{1}{l}\int_{-l}^{l} f(x)\cos\frac{k\pi x}{l}\mathrm{d}x, \quad b_k = \frac{1}{l}\int_{-l}^{l} f(x)\sin\frac{k\pi x}{l}\mathrm{d}x. \tag{B.3}$$

(c) A given function $f(x)$ is defined in the interval from 0 to 2π (half-range expansion)

Then, in this case, the Fourier expansion coefficients are given by:

$$a_0 = \frac{1}{2\pi}\int_0^{2\pi} f(x)\mathrm{d}x, \quad a_k = \frac{1}{\pi}\int_0^{2\pi} f(x)\cos kx\mathrm{d}x, \quad b_k = \frac{1}{\pi}\int_0^{2\pi} f(x)\sin kx\mathrm{d}x.$$

(d) A function $f(x)$ is defined in the interval $0, l$

Such a function can be expanded into the Fourier series either in sine or cosine. The expansions and their coefficients in these cases are:

– expansions in cosines (for even functions)

$$f(x) = \frac{a_0}{2} + \sum_{k=1}^{\infty} a_k \cos\frac{k\pi x}{l}; \quad a_k = \frac{2}{l}\int_0^l f(x)\cos\frac{k\pi x}{l}\mathrm{d}x. \tag{B.4a}$$

– expansions in sines (for odd functions)

$$f(x) = \sum_{k=1}^{\infty} b_k \sin\frac{k\pi x}{l}; \quad b_k = \frac{2}{l}\int_0^l f(x)\sin\frac{k\pi x}{l}\mathrm{d}x. \tag{B.4b}$$

B.5 THE ORDER OF THE FOURIER SERIES COEFFICIENTS

Let a function $f(x)$, defined on the interval $-\pi, +\pi$, have discontinuities at points $x_1^0, x_2^0, \ldots, x_s^0$. One of the end points, for instance π, should be referred to discontinuity points if the limiting values $f(\pi + 0)$ and $f(\pi - 0)$ are different. For the sake of notation symmetry, we designate that latter point by $x_{s+1}^0 = \pi$. Let δ_i^0 denote a jump of $f(x)$ at point x_i^0, so that

$$\delta_i^0 = f(x_i^0 + 0) - f(x_{i-0}^0).$$

The coefficients of the Fourier series will be of the form

$$a_n = \frac{1}{\pi}\int_{-\pi}^{x_i^0} f(x)\cos nx\mathrm{d}x + \frac{1}{\pi}\int_{x_1^0}^{x_2^0} f(x)\cos nx\mathrm{d}x + \ldots + \frac{1}{\pi}\int_{x_s^0}^{\pi} f(x)\cos nx\mathrm{d}x. \tag{B.5}$$

For example, let $f(x)$ be defined in the form (Fig. B.1)

$$f(x) = 0 \qquad -\pi \le x \le 0,$$
$$f(x) = 1 \qquad 0 \le x \le \pi.$$

In this case, we have two discontinuities, as follows:

$$x = 0 \qquad \delta_1^0 = 1$$
$$x = \pi \qquad \delta_2^0 = -1$$

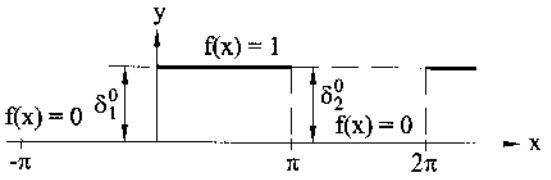

Fig. B.1

Integrating Eq. (B.5) by parts, yields the following:

$$a_n = -\frac{1}{n\pi}\sum_{i=1}^{i=s+1}\delta_i^0 \sin \pi x_i^0 - \frac{1}{n\pi}\int_{-\pi}^{\pi} f'(x)\sin nx\mathrm{d}x \tag{B.6}$$

where the prime notation indicates the first derivative of $f(x)$ with respect to x. Rewrite Eq. (B.6) as follows:

$$a_n = -\frac{B_0}{n} - \frac{b_n'}{n} \tag{B.7}$$

where

$$B_0 = \frac{1}{\pi}\sum_{i=1}^{i=s+1}\delta_i^0 \sin \pi x_i^0; \quad b_n' = \frac{1}{\pi}\int_{-\pi}^{\pi} f'(x)\sin nx\mathrm{d}x. \tag{B.8}$$

Similarly, the coefficient b_k is given by

$$b_n = \frac{A_0}{n} + \frac{a_n'}{n}, \tag{B.9}$$

where

$$A_0 = \frac{1}{\pi}\sum_{i=1}^{i=s+1}\delta_i^0 \cos \pi x_i^0, a_n' = \frac{1}{\pi}\int_{-\pi}^{\pi} f'(x)\cos nx\mathrm{d}x \tag{B.10}$$

Applying these relations for the derivative of the given function $f'(x)$, one obtains the following:

$$a_n' = -\frac{B_1}{n} - \frac{b_n''}{n}, b_n' = \frac{A_1}{n} + \frac{a_n''}{n},$$

where

$$A_1 = \frac{1}{\pi}\sum_{i=1}^{i=s_1+1}\delta_i' \cos kx_i'; B_1 = \frac{1}{\pi}\sum_{i=1}^{i=s_1+1}\delta_i' \sin kx;$$

x_i' are discontinuity points of $f'(x)$ and δ_i' are jumps of $f'(x)$ at those points. Extending this operation further and inserting the obtained values into the relations (B.7) and (B.9) gives the following:

$$\begin{aligned} a_n &= -\frac{B_0}{n} - \frac{A_1}{n^2} + \frac{B_2}{n^3} + \frac{A_3}{n^4} - \ldots, \\ b_n &= \frac{A_0}{n} - \frac{B_1}{n^2} - \frac{A_2}{n^3} + \frac{B_3}{n^4} + \ldots, \end{aligned} \tag{B.11}$$

where

$$A_j = \frac{1}{\pi}\sum_{i=1}^{i=s_j+1}\delta_i^{(j)} \cos nx_i^{(j)}; \quad B_j = \frac{1}{\pi}\sum_{i=1}^{i=s_j+1}\delta_i^{(j)} \sin nx_i^{(j)};$$

$x_i^{(j)}$ are discontinuity points of the jth derivative of the given function $f(x)$; $\delta_i^{(j)}$ are jumps of $f^{(j)}(x)$ at those points.

All the above relations will hold for the interval $-l, +l$ also, but in this case it is necessary to set

$$A_j = \left(\frac{l}{\pi}\right)^j \frac{1}{\pi} \sum_{i=1}^{i=s_j+1} \delta_i^{(j)} \cos\frac{\pi x_i^{(j)}}{l}; \quad B_j = \left(\frac{l}{\pi}\right)^j \frac{1}{\pi} \sum_{i=1}^{i=s_j+1} \delta_i^{(j)} \sin\frac{\pi x_i^{(j)}}{l}. \tag{B.12}$$

It follows from Eqs (B.11) that the order of the Fourier expansion coefficients is determined by the presence of discontinuities in a function itself and in its sequential derivatives. If $f(x)$ has at least one discontinuity, for instance, on the interval end, then Eqs (B.11) involve the terms A_0 and B_0 and, hence, the coefficients a_n and b_n will be of the order of $1/n$. If no discontinuities exist, then $A_0 = B_0 = 0$ and the order of the Fourier coefficients will be of $1/n^2$. If the first derivative of the given function has no discontinuity, then the order of the Fourier coefficients is increased by a unity $1/n^3$, etc.

It should be noted that the differentiation of the Fourier series makes worse its convergence, so that if for $f(x)$ the order of the coefficients is $1/n^2$, then for $f'(x)$ it becomes $1/n$, and for $f''(x)$ this series ceases to be the Fourier series because its coefficients will not approach zero as k increases; such a series fails for calculations.

B.6 DOUBLE FOURIER SERIES

The concept of a Fourier series expansion for a function of a single variable can be extended to the case of a function of two or more variables. For instance, we can expand $f(x, y)$ into a double Fourier series as follows:

$$f(x, y) = \sum_{m=1}^{\infty} \sum_{n=1}^{\infty} f_{mn} \sin\frac{m\pi x}{a} \sin\frac{n\pi y}{b}. \tag{B.13}$$

The above represents a half-range sine series in x multiplied by a half-range sine series in y, using for the period of expansions $2a$ and $2b$, respectively. That is

$$f(x, y) = \sum_{m=1}^{\infty} f_m(y) \sin\frac{m\pi x}{a}, \tag{B.14a}$$

with

$$f_m(y) = \sum_{n=1}^{\infty} f_{mn} \sin\frac{n\pi y}{b}. \tag{B.14b}$$

Treating Eq. (B.14a) as a Fourier series wherein y is kept constant, Eq. (B.14b) is applied to give

$$f_m(y) = \frac{2}{a} \int_0^a f(x, y) \sin\frac{m\pi x}{a} \mathrm{d}x. \tag{B.15}$$

Similarly, for Eq. (B.14b),

$$f_{mn} = \frac{2}{b} \int_0^b f_m(y) \sin\frac{n\pi y}{b} \mathrm{d}x. \tag{B.16}$$

Equation (B.16), together with Eq. (B.15), then leads to

$$f_{mn} = \frac{4}{ab}\int_0^a \int_0^b f(x, y) \sin\frac{m\pi x}{a} \sin\frac{n\pi y}{b} \mathrm{d}x\mathrm{d}y. \tag{B.17}$$

This agrees with Eq. (3.17) of Sec. 3.3, which was derived differently. Similarly, the results can be obtained for cosine series or for series having both cosines and sines.

B.7 SHARPENING OF CONVERGENCE OF THE FOURIER SERIES

The following efficient method for sharpening of the convergence of the Fourier series was proposed by Krylov [A.1].

Let a function $f(x)$ have some discontinuity points in a defined interval. We select such a function $F_0(x)$ that has the same discontinuity points and jumps as the given function. Then, the difference $f_1(x) = f(x) - F_0(x)$ will have no jumps and, hence, $f_1(x)$ will have the Fourier coefficients of the order of $1/n^2$. Similarly, a function $f'(x)$ (the prime notation indicates here the first derivative of the function with respect to x) can be treated by letting

$$f'(x) = f_1'(x) + F_0'(x) = f_2(x) + F_1(x)$$

where $F_1(x)$ is some linear function with the same jumps as $f'(x)$. Analogously,

$$f''(x) = f_2'(x) + F_1'(x) = f_3(x) + F_2(x).$$

Expanding this process as long as desired, one can obtain in remainder a Fourier series with coefficients of any order of smallness.

The present section contains only general information about the Fourier series. The interested reader is referred to Refs [A.2–A.4].

REFERENCES

A.1 Krylov, A.N., *Collected Works*, vol. 3, parts 1 and 2, Academy of Sciences of the USSR, Moscow, 1949 (in Russian).

A.2 Churchill, R.V., *Fourier Series and Boundary Value Problems*, McGraw-Hill, New York, 1960.

A.3 Wylie, C.R., *Advanced Engineering Mathematics*, McGraw-Hill, New York, 1960.

A.4 Kantorovich, L.V., and Krylov, V.I., *Approximate Methods of Higher Analysis*, John Wiley and Sons, New York, 1958.

Appendix C

Verification of Relations of the Theory of Surfaces

C.1 GEOMETRY OF SPACE CURVES

The equation of a three-dimensional curve l can be represented in the Cartesian coordinate system (X, Y, and Z) by the following one vector equation:

$$\mathbf{r}(\tau) = X(\tau)\mathbf{i} + Y(\tau)\mathbf{j} + Z(\tau)\mathbf{k}, \tag{C.1}$$

where $\mathbf{r}$ is a position vector from the origin of the coordinate system to a point of interest and τ is some parameter. If $X(\tau)$, $Y(\tau)$, and $Z(\tau)$ are single-valued and continuous functions of the parameter τ, then we will insure that a given value of that parameter defines only one point on the space curve. For example, an arc length s, measured along the space curve from some origin, can be chosen as such a parameter. In this case, the vectorial equation (C.1) can be written in the following form:

$$\mathbf{r} = \mathbf{r}(s). \tag{C.2}$$

Consider a typical point M and a neighboring point N on the curve l. The position vectors of those points are $\mathbf{r}$ and $\mathbf{r} + \Delta\mathbf{r}$, respectively (Fig. C.1). It is seen from this figure that the difference of the two vectors, $\Delta\mathbf{r}$, is depicted by a vector whose magnitude and direction coincide with the chord, joining the points M and N. When $N \to M$, the direction of $\Delta\mathbf{r}$ approaches the direction of the tangent to the curve at point M and its length to the arc length between the above points, Δs. Hence, in the limit (when $\Delta s \to 0$), we have

$$\mathrm{d}\mathbf{r} = \mathbf{t}\mathrm{d}s,$$

where $\mathbf{t}$ is the unit tangent vector directed along the tangent to the curve l at point M. Thus, the unit tangent vector to the curve at a point of interest is given by

$$\mathbf{t} = \frac{\mathrm{d}\mathbf{r}}{\mathrm{d}s}, \tag{C.3}$$

The definition of a curvature of a plane curve was given in Sec. 11.2. Now we rework this definition in a vector form for a space curve.

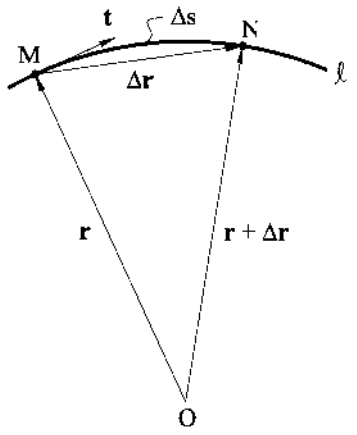

Fig. C.1

Let $\mathbf{t}_M$ and $\mathbf{t}_N$ be the two unit tangent vectors at neighboring points M and N, respectively. A change $\Delta\mathbf{t}$ in the vector $\mathbf{t}$ as we move from point M to point N on the surface is shown in Fig. C.2.

The vector $\Delta\mathbf{t}$ lies in a plane passing through point M and the vectors $\mathbf{t}_M$ and $\mathbf{t}_N$. This plane is called the *osculating plane*. The length of the vector $\Delta\mathbf{t}$ approaches the value

$$|\Delta\mathbf{t}| = \Delta\phi = \frac{\Delta s}{\rho}.$$

As one goes to the limit, for $\Delta s \to 0$, one obtains

$$\frac{\mathrm{d}\mathbf{t}}{\mathrm{d}s} = \frac{\mathbf{v}}{\rho} = \kappa\mathbf{v}, \tag{C.4}$$

where ρ is the radius of curvature and $\kappa\mathbf{v}$ ($\kappa = 1/\rho$) is the curvature vector at point M of the curve l. Differentiating the identity $\mathbf{t}^2 = 1$ with respect to s, one obtains

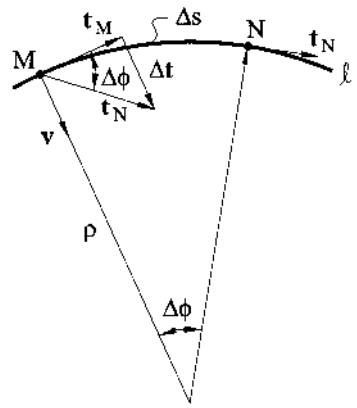

Fig. C.2

$$\frac{d\mathbf{t}}{ds} \cdot \mathbf{t} = 0.$$

Thus, $d\mathbf{t}/ds$, and hence, the unit vector $\mathbf{v}$, is perpendicular to the unit tangent vector $\mathbf{t}_M$. Let us introduce a *principal normal* to the curve l at a point M. It can be defined as that vector in the osculating plane at point M that is perpendicular to the tangent $\mathbf{t}_M$ to the curve at the point of interest. Thus, $\mathbf{v}$ represents the unit vector of the principal normal and it points in the direction of the curve convexity. Figure C.3 illustrates a curve l on the surface Ω, the osculating plane S passing through point M lying on this curve, and the principal normal given by the unit normal vector $\mathbf{v}$.

Taking into account the relation (C.3), we can represent (C.4) as follows:

$$\frac{d^2\mathbf{r}}{ds^2} = \frac{\mathbf{v}}{\rho} = \kappa\mathbf{v}. \tag{C.5}$$

The relationship (C.5) is referred to as the *Frenet formula*.

C.2 GEOMETRY OF A SURFACE

Assume that a surface Ω is assigned by the vector equation (11.1) and the parameters α and β are considered as the curvilinear coordinates of a point on the surface. Then, let the triad of the unit vectors, $\mathbf{e}_1, \mathbf{e}_2$, and $\mathbf{e}_3$, given by Eqs (11.24) form a local vectorial basis to which the displacements and internal forces are referred (see Fig. 11.7).

Consider an arbitrary curve l on the surface given by the following vectorial equation:

$$r = r(\alpha, \beta); \quad \alpha = \alpha(s), \quad \beta = \beta(s), \tag{C.6}$$

where s is the arc length of that curve, measured from some origin. We use the properties of the curvature vector $\kappa\mathbf{v}$ to derive the expression of the second quadratic

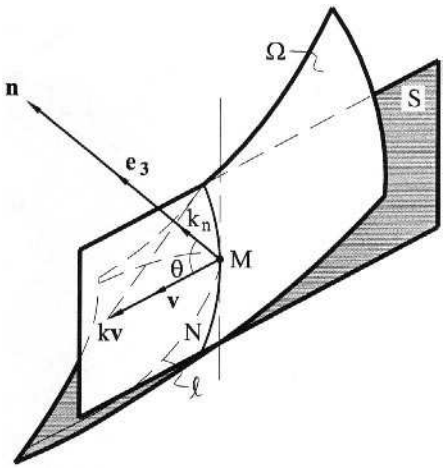

Fig. C.3

form of the surface. To do this, let us calculate the curvature of the curve l, assigned by Eq. (C.6). According to Eq. (C.5), we have

$$\frac{\mathbf{v}}{\rho}=\frac{\mathrm{d}^2\mathbf{r}}{\mathrm{d}s^2}=\frac{\mathrm{d}}{\mathrm{d}s}\left(\frac{\partial\mathbf{r}}{\partial\alpha}\frac{\mathrm{d}\alpha}{\mathrm{d}s}+\frac{\partial\mathbf{r}}{\partial\beta}\frac{\mathrm{d}\beta}{\mathrm{d}s}\right)=\frac{\partial\mathbf{r}}{\partial\alpha}\frac{\mathrm{d}^2\alpha}{\mathrm{d}s^2}+\frac{\partial\mathbf{r}}{\partial\beta}\frac{\partial^2\beta}{\partial s^2}+\frac{\partial^2\mathbf{r}}{\partial\alpha^2}\left(\frac{\mathrm{d}\alpha}{\mathrm{d}s}\right)^2 + 2\frac{\partial^2\mathbf{r}}{\partial\alpha\partial\beta}\frac{\partial\alpha}{\partial s}\frac{\mathrm{d}\beta}{\mathrm{d}s}+\frac{\partial^2\mathbf{r}}{\partial\beta^2}\left(\frac{\mathrm{d}\beta}{\mathrm{d}s}\right)^2. \tag{C.7}$$

As mentioned in Sec. C.1, the curvature vector $\kappa\mathbf{v}$ is directed along the principal normal to that curve l in the osculating plane S. Let us project that vector on the direction of the normal to the surface, given by the unit vector $\mathbf{e}_3$, at a point M. For this purpose, both sides of the expression (C.7) are multiplied by $\mathbf{e_3}$. In doing so, take into account that

$$\frac{\mathbf{v}}{\rho}\cdot\mathbf{e}_3=\cos\theta\frac{1}{\rho};\quad \frac{\partial\mathbf{r}}{\partial\alpha}\cdot\mathbf{e}_3=A\mathbf{e}_1\cdot\mathbf{e}_3=0;\quad \frac{\partial\mathbf{r}}{\partial\beta}\cdot\mathbf{e}_3=B\mathbf{e}_2\cdot\mathbf{e}_3=0,$$

where θ is an acute angle between the unit normal vectors to the surface, $\mathbf{e}_3$, and to the curve, $\mathbf{v}$ (see Fig. C.3), respectively. As a result of this scalar multiplication, we obtain

$$\frac{\cos\theta}{\rho}=\frac{1}{\mathrm{d}s^2}\left(b_{11}\mathrm{d}\alpha^2+2b_{12}\mathrm{d}\alpha\mathrm{d}\beta+b_{22}\mathrm{d}\beta^2\right). \tag{C.8}$$

The term in the parentheses on the right-hand side of Eq. (C.8) represents the second quadratic form of the surface introduced in Sec. 11.3 (see Eq. (11.18)) and the coefficients of that form, b_{ik} $(i,k=1,2)$ are given by Eqs (11.17).

It follows from Eq. (C.8) that, among all curves passing through a point of interest, a curve whose principal normal, defined by the unit vector $\mathbf{v}$, coincides with the normal to the surface, defined by the unit normal vector $\mathbf{e}_3$, has the smallest curvature (because in this case, $\cos\theta=1$). As mentioned in Sec. 11.2, such a curve is obtained at the intersection of the given surface by a plane passing through a normal to that surface and is referred to as a normal section. The curvature of such a normal section, κ_n, is defined by

$$\kappa_\mathrm{n}=\frac{1}{R}=b_{11}\left(\frac{\mathrm{d}\alpha}{\mathrm{d}s}\right)^2+2b_{12}\frac{\mathrm{d}\alpha}{\mathrm{d}s}\frac{\mathrm{d}\beta}{\mathrm{d}s}+b_{22}\left(\frac{\mathrm{d}\beta}{\mathrm{d}s}\right)^2. \tag{C.9}$$

According to Eq. (C.7), a curvature of any another plane section, κ, that makes an angle θ with the normal section and has the common tangent with the latter, is of the following form:

$$\kappa=\kappa_\mathrm{n}\frac{1}{\cos\theta}. \tag{C.10}$$

This expression relates the curvature κ of any inclined section of the surface to the normal curvature, κ_n.

The coefficients of the second quadratic form are given by the relations (11.17) in terms of the curvilinear coordinates α and β. Substituting the expressions (11.4) and (11.24) into Eqs (11.17), we obtain, after some mathematics, the expressions for the coefficients b_{ik} $(i,k=1,2)$ in terms of the Cartesian coordinates as follows:

$$b_{11} = \frac{1}{\omega}\begin{vmatrix} \frac{\partial^2 X}{\partial \alpha^2} & \frac{\partial^2 Y}{\partial \alpha^2} & \frac{\partial^2 Z}{\partial \alpha^2} \\ \frac{\partial X}{\partial \alpha} & \frac{\partial Y}{\partial \alpha} & \frac{\partial Z}{\partial \alpha} \\ \frac{\partial X}{\partial \beta} & \frac{\partial Y}{\partial \beta} & \frac{\partial Z}{\partial \beta} \end{vmatrix}; \quad b_{22} = \frac{1}{\omega}\begin{vmatrix} \frac{\partial^2 X}{\partial \beta^2} & \frac{\partial^2 Y}{\partial \beta^2} & \frac{\partial^2 Z}{\partial \beta^2} \\ \frac{\partial X}{\partial \alpha} & \frac{\partial Y}{\partial \alpha} & \frac{\partial Z}{\partial \alpha} \\ \frac{\partial X}{\partial \beta} & \frac{\partial Y}{\partial \beta} & \frac{\partial Z}{\partial \beta} \end{vmatrix};$$

$$b_{12} = \frac{1}{\omega}\begin{vmatrix} \frac{\partial^2 X}{\partial \alpha \partial \beta} & \frac{\partial^2 Y}{\partial \alpha \partial \beta} & \frac{\partial^2 Z}{\partial \alpha \partial \beta} \\ \frac{\partial X}{\partial \alpha} & \frac{\partial Y}{\partial \alpha} & \frac{\partial Z}{\partial \alpha} \\ \frac{\partial X}{\partial \beta} & \frac{\partial Y}{\partial \beta} & \frac{\partial Z}{\partial \beta} \end{vmatrix}, \tag{C.11}$$

where

$$\omega = \sqrt{a_{11}a_{22} - a_{12}^2}. \tag{C.12}$$

It was mentioned in Sec. 11.3 that the directions of principal curvatures are orthogonal. To prove this, it is sufficient to verify that an angle between the two principal directions is equal to $\pi/2$ at any point of the surface. Assume that these directions have been found and that they are characterized by the following quantities:

$$\lambda_1 = \frac{\mathrm{d}\beta}{\mathrm{d}\alpha} \quad \text{and} \quad \lambda_2 = \frac{\delta\beta}{\delta\alpha}.$$

The increments of the position vector $\mathbf{r}$ along each of these two directions can be written in the following form:

$$\mathrm{d}\mathbf{r} = \mathbf{r}_{,\alpha}\mathrm{d}\alpha + \mathbf{r}_{,\beta}\mathrm{d}\beta; \quad \delta\mathbf{r} = \mathbf{r}_{,\alpha}\delta\alpha + \mathbf{r}_{,\beta}\delta\beta.$$

If these two directions are orthogonal, then

$$(\mathrm{d}\mathbf{r}\cdot\delta\mathbf{r}) = (\mathbf{r}_{,\alpha}\cdot\mathbf{r}_{,\alpha})\mathrm{d}\alpha\delta\alpha + (\mathbf{r}_{,\beta}\cdot\mathbf{r}_{,\beta})\mathrm{d}\beta\delta\beta + (\mathbf{r}_{,\alpha}\cdot\mathbf{r}_{,\beta})(\mathrm{d}\alpha\delta\beta + \delta\alpha\mathrm{d}\beta) = 0, \tag{C.13}$$

or dividing the above equality by $\mathrm{d}\alpha\delta\alpha$, and taking into account the notations of Eqs (11.10),

$$a_{11} + a_{12}(\lambda_1 + \lambda_2) + a_{22}(\lambda\lambda_2) = 0. \tag{C.14}$$

Substituting for λ_1 and λ_2 from Eq. (11.20) into Eq. (C.14), we find that the orthogonality condition is identically satisfied. Thus, the directions of the principal curvatures are orthogonal.

C.3 DERIVATIVES OF UNIT COORDINATE VECTORS

Consider two neighboring points M and M_1 on the coordinate line α, separated by a small distance Δs_α. Let $\mathbf{e}_3$ and $\mathbf{e}_3 + \Delta\mathbf{e}_3$ be the inward normal unit vectors at those points, directed toward the center of curvature O, as shown in Fig. C.4. The corresponding principal radius of curvature of the surface is denoted by R_1.

It is seen from the above figure that an increment vector $\Delta\mathbf{e}_3$, obtained by moving $\mathbf{e}_3$ from point M to point M_1, is parallel to the chord MM_1, and in the limit

when $M \to M_1$; this increment becomes parallel to the tangent vector $\mathbf{e}_1$. Thus, $\Delta\mathbf{e}_3$ can be represented in the form

$$\Delta\mathbf{e}_3 = -\left|\Delta\mathbf{e}_3\right|\mathbf{e}_1. \tag{C.15}$$

The negative sign in the above equation indicates that the vector $\Delta\mathbf{e}_3$ points in the negative direction of the α-coordinate axis (see Fig. 11.7).

The magnitude of this increment can be found from similarity of the triangles (Fig. C.4), i.e.,

$$\frac{\left|\Delta\mathbf{e}_3\right|}{\left|\mathbf{e}_3\right|} = \frac{MM_1}{R_1}. \tag{C.16}$$

Substituting Eq. (C.15) into Eq. (C.16), and noting that $\left|\mathbf{e}_3\right| = 1$ and $MM_1 = \Delta s_\alpha = A\Delta\alpha$, yields

$$\frac{\Delta\mathbf{e}_3}{\Delta\alpha} = -\frac{A}{R_1}\mathbf{e}_1. \tag{C.17}$$

Taking the limit of both sides of the above relation as $\Delta\alpha \to 0$, one obtains

$$\frac{\mathrm{d}\mathbf{e}_3}{\mathrm{d}\alpha} = -\frac{A}{R_1}\mathbf{e}_1. \tag{C.18}$$

Similarly,

$$\frac{\mathrm{d}\mathbf{e}_3}{\mathrm{d}\beta} = -\frac{B}{R_2}\mathbf{e}_2. \tag{C.19}$$

Now we can proceed to determine the derivatives of the tangent unit vectors, $\mathbf{e}_1$ and $\mathbf{e}_2$, with respect to α and β. Obviously the following equality holds:

$$\frac{\partial\mathbf{r}_{,\alpha}}{\partial\beta} = \frac{\partial\mathbf{r}_{,\beta}}{\partial\alpha},$$

because it is equivalent to the following identity:

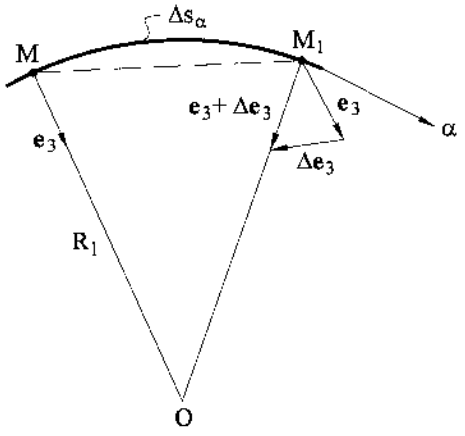

Fig. C.4

$$\frac{\partial^2 \mathbf{r}}{\partial\alpha\partial\beta} = \frac{\partial^2 \mathbf{r}}{\partial\beta\partial\alpha}.$$

From the above, and taking into account the relations (11.10) and (11.12), we obtain

$$\frac{\partial}{\partial\beta}(A\mathbf{e}_1) = \frac{\partial}{\partial\alpha}(B\mathbf{e}_2). \tag{C.20a}$$

The derivatives of the unit tangent vectors can be expressed in terms of their components along the triad of the unit vectors $\mathbf{e}_1$, $\mathbf{e}_2$, and $\mathbf{e}_3$. Notice that the derivative of any unit tangent vector is normal to the vector itself, so that there are no components in the direction of the vector being differentiated. Let us prove this statement. Consider the following scalar product of the two unit tangent vectors in the curvilinear coordinate system:

$$\mathbf{e}_i \cdot \mathbf{e}_j = \delta_{ij} \begin{cases} \delta_{ij} = 1 & \text{if} \quad i = j, \\ \delta_{ij} = 0 & \text{if} \quad i \neq j, \end{cases}$$

where $i, j = 1, 2,$ and 3. Differentiating the scalar product of the two unit vectors with respect to k ($k = 1$ or 2) yields

$$\left(\mathbf{e}_i \cdot \mathbf{e}_j\right)_{,k} = 0,$$

from which

$$\mathbf{e}_j \cdot \mathbf{e}_{i,k} + \mathbf{e}_i \cdot \mathbf{e}_{j,k} = 0.$$

Setting $i = j$ yields

$$2\left(\mathbf{e}_i \cdot \mathbf{e}_{i,k}\right) = 0,$$

as was to be shown.

First, determine the derivative $\partial\mathbf{e}_1/\partial\alpha$. As follows from the above, this derivative can be represented in terms of its components in the directions of $\mathbf{e}_2$ and $\mathbf{e}_3$ only. We have

$$\frac{\partial\mathbf{e}_1}{\partial\alpha} = q_\alpha\mathbf{e}_2 + t_\alpha\mathbf{e}_3, \tag{C.20b}$$

where unknown components q_α and t_α represent the projections of the vector $\partial\mathbf{e}_1/\partial\alpha$ on the directions of $\mathbf{e}_2$ and $\mathbf{e}_3$, respectively. It is known from the vector algebra that the projection of any vector $\mathbf{a}$ on the direction of a vector $\mathbf{b}$ is equal to the scalar product of $\mathbf{a} \cdot \mathbf{b}$. Therefore, the component q_α is given by

$$q_\alpha = \mathbf{e}_2 \cdot \left(\frac{\partial\mathbf{e}_1}{\partial\alpha}\right) = \frac{\partial}{\partial\alpha}(\mathbf{e_2} \cdot \mathbf{e}_1) - \left(\mathbf{e}_1 \cdot \frac{\partial\mathbf{e}_2}{\partial\alpha}\right) = -\mathbf{e}_1 \cdot \frac{\partial\mathbf{e}_2}{\partial\alpha} \tag{C.21}$$

$$\left(\frac{\partial}{\partial\alpha}(\mathbf{e_2} \cdot \mathbf{e}_1) = 0 \text{ because } \mathbf{e}_2 \text{ is normal to } \mathbf{e_1}\right).$$

It follows from Eq. (C.20a) that

$$\frac{\partial}{\partial\alpha}(B\mathbf{e}_2) = B\frac{\partial\mathbf{e}_2}{\partial\alpha} + \mathbf{e}_2\frac{\partial B}{\partial\alpha} = \frac{\partial}{\partial\beta}(A\mathbf{e}_1). \tag{C.22}$$

Thus,

$$\frac{\partial \mathbf{e}_2}{\partial \alpha} = \frac{1}{B}\frac{\partial (A\mathbf{e}_1)}{\partial \beta} - \frac{1}{B}\frac{\partial B}{\partial \alpha}\mathbf{e}_2. \tag{C.23}$$

From Eqs (C.21) and (C.22), one obtains the following:

$$q_\alpha = -\frac{A}{B}\left(\mathbf{e}_1 \cdot \frac{\partial \mathbf{e}_1}{\partial \beta}\right) - \frac{1}{B}\frac{\partial A}{\partial \beta}(\mathbf{e_1} \cdot \mathbf{e}_1).$$

Since $\mathbf{e_1} \cdot \mathbf{e}_1 = 1$ and $\mathbf{e}_1 \cdot \frac{\partial \mathbf{e_1}}{\partial \beta} = 0$, the above equation becomes

$$q_\alpha = -\frac{1}{B}\frac{\partial A}{\partial \beta}. \tag{C.24}$$

Let us proceed to determining the component t_α in Eq. (C.20b). We have

$$t_\alpha = \mathbf{e}_3 \cdot \frac{\partial \mathbf{e}_1}{\partial \alpha} = \frac{\partial}{\partial \alpha}(\mathbf{e_3} \cdot \mathbf{e}_1) - \left(\mathbf{e}_1 \cdot \frac{\partial \mathbf{e}_3}{\partial \alpha}\right) = -\mathbf{e}_1 \cdot \frac{\partial \mathbf{e}_3}{\partial \alpha} \tag{C.25}$$

(because $\mathbf{e_3} \cdot \mathbf{e}_1 = 0$). Using Eq. (C.18), we obtain

$$t_\alpha = -\mathbf{e}_1 \cdot \left(-\frac{A}{R_1}\mathbf{e}_1\right) = \frac{A}{R_1}. \tag{C.26}$$

Finally, substituting for q_α and t_α from Eqs (C.24) and (C.26), we obtain the following expression for the derivative $\partial e_1/\partial \alpha$:

$$\frac{\partial e_1}{\partial \alpha} = -\frac{1}{B}\frac{\partial A}{\partial \beta}\mathbf{e}_2 + \frac{A}{R_1}\mathbf{e}_3. \tag{C.27}$$

Determine the derivative $\partial e_1/\partial \beta$. Again, we can represent the above derivative in terms of its components along the unit vectors $\mathbf{e}_2$ and $\mathbf{e}_3$:

$$\frac{\partial e_1}{\partial \beta} = q_\beta \mathbf{e}_2 + t_\beta \mathbf{e_3}, \tag{C.28}$$

where q_β and t_β are the unknown projections of $\partial e_1/\partial \beta$ on the directions of the unit vectors $\mathbf{e}_2$ and $\mathbf{e}_3$, respectively (as mentioned previously, the projection of $\partial \mathbf{e}_1/\partial \beta$ on $\mathbf{e}_1$ is zero).

By analogy with Eq. (C.21), we can write

$$q_\beta = \mathbf{e}_2 \cdot \frac{\partial \mathbf{e}_1}{\partial \beta}.$$

Using the identity (C.20), the above relation appears as follows:

$$q_\beta = -\frac{1}{A}\frac{\partial A}{\partial \beta}(\mathbf{e_1} \cdot \mathbf{e}_2) + \frac{1}{A}\left[\mathbf{e}_2 \cdot \frac{\partial (B\mathbf{e}_2)}{\partial \alpha}\right] = \frac{1}{A}\frac{\partial B}{\partial \alpha}.$$

Thus

$$q_\beta = \frac{1}{A}\frac{\partial B}{\partial \alpha}. \tag{C.29}$$

Similarly,

$$t_\beta = \mathbf{e}_3 \cdot \left(\frac{\partial \mathbf{e}_1}{\partial \beta}\right) = \frac{\partial}{\partial \beta}(\mathbf{e_1} \cdot \mathbf{e}_3) - \mathbf{e}_1 \cdot \frac{\partial \mathbf{e}_3}{\partial \beta} = -\mathbf{e}_1 \cdot \frac{\partial \mathbf{e}_3}{\partial \beta}.$$

Using Eq. (C.19), we can rewrite the above relation as follows:

$$t_\beta = -\mathbf{e}_1 \cdot \left(-\frac{B}{R_1}\mathbf{e}_2\right) = \frac{B}{R_1}(\mathbf{e_1} \cdot \mathbf{e}_2) = 0.$$

Finally, substituting $t_\beta = 0$ and for q_β, from Eq. (C.29) into Eq. (C.28), we obtain the following expression for the derivative $\partial \mathbf{e}_1/\partial\beta$:

$$\frac{\partial \mathbf{e}_1}{\partial \beta} = \frac{1}{A}\frac{\partial B}{\partial \alpha}\mathbf{e}_2. \tag{C.30}$$

In a similar manner, one can determine the derivatives $\partial \mathbf{e}_2/\partial\alpha$ and $\partial \mathbf{e}_2/\partial\beta$. The final expressions for the derivatives of the unit vectors with respect to α and β are given by Eqs (11.26).

C.4 VERIFICATION OF CODAZZI AND GAUSS EQUATIONS

Using the evident identity

$$\frac{\partial^2 \mathbf{e}_3}{\partial\alpha\partial\beta} = \frac{\partial^2 \mathbf{e_3}}{\partial\beta\partial\alpha},$$

and substituting the expressions (11.26) for $\mathbf{e}_{3,\alpha}$ and $\mathbf{e}_{3,\beta}$ into the above, we obtain the following:

$$\begin{gathered}\frac{\partial}{\partial\beta}\left(\frac{A}{R_1}\mathbf{e_1}\right) = \frac{\partial}{\partial\alpha}\left(\frac{B}{R_2}\mathbf{e}_2\right) \quad \text{or} \\ \frac{\partial}{\partial\beta}\left(\frac{A}{R_1}\right)\mathbf{e}_1 + \frac{A}{R_1}\frac{\partial \mathbf{e}_1}{\partial\beta} = \frac{\partial}{\partial\alpha}\left(\frac{B}{R_2}\right)\mathbf{e}_2 + \frac{B}{R_2}\frac{\partial \mathbf{e}_2}{\partial\alpha}.\end{gathered} \tag{C.31}$$

Replacing $\partial \mathbf{e}_1/\partial\beta$ and $\partial \mathbf{e}_2/\partial\alpha$ in the above by their values from Eqs (11.26) and transferring all the terms in Eq. (C.31) to the left-hand side, one finds the following equation:

$$\left[\frac{\partial}{\partial\beta}\left(\frac{A}{R_1}\right) - \frac{1}{R_2}\left(\frac{\partial A}{\partial\beta}\right)\right]\mathbf{e}_1 - \left[\frac{\partial}{\partial\alpha}\left(\frac{B}{R_2}\right) - \frac{1}{R_1}\frac{\partial B}{\partial\alpha}\right]\mathbf{e}_2 = 0. \tag{C.32}$$

This vector equation is equivalent to the two scalar equations (11.27a), called the *conditions of Codazzi*.

Next, consider another identity

$$\frac{\partial^2 \mathbf{e}_1}{\partial\alpha\partial\beta} = \frac{\partial^2 \mathbf{e}_1}{\partial\beta\partial\alpha}.$$

This identity, using the relations (11.26), can be reduced to the following:

$$\left[\frac{\partial}{\partial\alpha}\left(\frac{1}{A}\frac{\partial B}{\partial\alpha}\right) + \frac{\partial}{\partial\beta}\left(\frac{1}{B}\frac{\partial A}{\partial\beta}\right) + \frac{AB}{R_1R_2}\right]\mathbf{e}_2 + \left[\frac{\partial}{\partial\beta}\left(\frac{A}{R_1}\right) - \frac{1}{R_2}\frac{\partial A}{\partial\beta}\right]\mathbf{e}_3 = 0. \tag{C.33}$$

The above vector equation may only be satisfied if the terms in the square brackets are equal to zero. This gives the two scalar equations, but only the first of these is new, while the second equation coincides with one of the relationships (Eq. (11.27a)). So, equating the first term in the square brackets to zero, one obtains Eq. (11.27b), known as the *condition of Gauss*.

Similarly, it is found that the identity

$$\frac{\partial^2 \mathbf{e}_2}{\partial\alpha\partial\beta} = \frac{\partial^2 \mathbf{e}_2}{\partial\beta\partial\alpha}$$

involves no new relationships between the parameters A, B, R_1, and R_2.

Appendix D

Derivation of the Strain–Displacement Relations

D.1 VARIATION OF THE DISPLACEMENTS ACROSS THE SHELL THICKNESS

Referring to Fig. 12.2, we can write the following vector equation:

$$\mathbf{D}^z + z\mathbf{e}_3 - z\mathbf{e}_3^* = \mathbf{D}, \tag{D.1}$$

where $\mathbf{D}$ and $\mathbf{D}^z$ are displacement vectors of points M and M^z, located on the middle and on the equidistant surfaces of the shell, separated by a distance z, respectively; e_3^* is the unit normal vector of a deformed middle surface at point M_1. From Eq. (D.1), it follows that

$$\mathbf{D}^z = \mathbf{D} + (\mathbf{e}_3^z - \mathbf{e}_3)z. \tag{D.2}$$

With the accuracy within the terms of the order of $(h/R)^2$ compared with unity, the unit normal vector $\mathbf{e}_3^*$ can be determined by the following equality:

$$\mathbf{e}_3^* = \mathbf{e}_1^* \times \mathbf{e}_2^*, \tag{D.3a}$$

where $\mathbf{e}_1^*$ and $\mathbf{e}_2^*$ are the unit vectors tangent to the α- and β-coordinate lines on the deformed middle surface. The equation of the deformed middle surface can be represented in the following vector form:

$$\mathbf{r}^*(\alpha, \beta) = \mathbf{r}(\alpha, \beta) + \mathbf{D} = \mathbf{r}(\alpha, \beta) + u\mathbf{e}_1 + v\mathbf{e}_2 + w\mathbf{e}_3, \tag{D.3b}$$

where $\mathbf{r}^*(\alpha, \beta)$ is a position vector of the deformed middle surface of the shell. Note that from here on, all functions and quantities associated with the deformed middle surface will be denoted by an asterisk.

Using Eq. (11.24), we can write

$$\mathbf{e}_1^* = \frac{\mathbf{r}_{,\alpha}^*}{\mathbf{A}^*}, \tag{D.4}$$

where

$$A^* = \sqrt{\mathbf{r}_{,\alpha}^* \cdot \mathbf{r}_{,\alpha}^*}. \tag{D.5}$$

Write out the vector $\mathbf{r}^*_{,\alpha}$ in the following expanded form:

$$\mathbf{r}^*_{,\alpha} = \frac{\partial \mathbf{r}^*}{\partial \alpha} = \frac{\partial}{\partial \alpha}(\mathbf{r} + u\mathbf{e}_1 + v\mathbf{e}_2 + w\mathbf{e}_3) = A\varepsilon_1 + u\frac{\partial \mathbf{e}_1}{\partial \alpha} + v\frac{\partial \mathbf{e}_2}{\partial \alpha} + w\frac{\partial \varepsilon_3}{\partial \alpha} + \frac{\partial u}{\partial \alpha}\mathbf{e}_1 + \frac{\partial v}{\partial \alpha}\mathbf{e}_2 + \frac{\partial w}{\partial \alpha}\mathbf{e}_3. \tag{D.6}$$

Substituting for the first derivative of the unit vectors from the relations (11.26) into the above, yields the following:

$$\mathbf{r}^*_{,\alpha} = A\left(1 + \frac{1}{A}\frac{\partial u}{\partial \alpha} + \frac{v}{AB}\frac{\partial A}{\partial \beta} - \frac{w}{R_1}\right)\mathbf{e}_1 + \left(-\frac{u}{B}\frac{\partial A}{\partial \beta} + \frac{\partial v}{\partial \alpha}\right)\mathbf{e}_2 + \left(\frac{A}{R_1}u + \frac{\partial w}{\partial \alpha}\right)\mathbf{e}_3. \tag{D.7}$$

Let us determine the Lamé parameter A^* of the deformed surface. It follows from Eqs (11.10) and (11.12) that $(A^*)^2 = r^*_{,\alpha} \cdot r^*_{,\alpha}$. Calculating the above scalar product, neglecting the products of displacements and their derivatives as small quantities of the second order, and retaining the terms depending linearly on the displacements and their derivatives only, we obtain

$$(A^*)^2 = A^2\left(1 + \frac{1}{A}\frac{\partial u}{\partial \alpha} + \frac{v}{AB}\frac{\partial A}{\partial \beta} - \frac{w}{R_1}\right)^2, \tag{D.8}$$

from which

$$A^* = A(1 + \varepsilon_1), \tag{D.9}$$

where

$$\varepsilon_1 = \frac{1}{A}\frac{\partial u}{\partial \alpha} + \frac{v}{AB}\frac{\partial A}{\partial \beta} - \frac{w}{R_1}. \tag{D.10}$$

Using Eqs (D.8)–(D.10), one can represent the unit tangent vector $\mathbf{e}^*_1$ as follows:

$$\mathbf{e}^*_1 = \frac{\mathbf{r}^*_{,\alpha}}{A^*} = \frac{1}{A(1+\varepsilon)}\left[A\left(1 + \frac{1}{A}\frac{\partial u}{\partial \alpha} + \frac{v}{AB}\frac{\partial A}{\partial \beta} - \frac{w}{R_1}\right)\mathbf{e}_1 + \left(\frac{\partial v}{\partial \alpha} - \frac{u}{B}\frac{\partial A}{\partial \beta}\right)\mathbf{e}_2 + \left(\frac{A}{R_1}u + \frac{\partial w}{\partial \alpha}\right)\mathbf{e}_3\right]. \tag{D.11}$$

Due to the small-displacement assumption, adopted in the linear theory of thin shells, all the strain components are negligible quantities in comparison with unity. Following this degree of accuracy, we can obtain from the above the following final expression for $\mathbf{e}^*_1$:

$$\mathbf{e}^*_1 \cong \mathbf{e}_1 + \omega_1\mathbf{e}_2 + \vartheta_1\mathbf{e}_3. \tag{D.12a}$$

Similarly, we can obtain

$$\mathbf{e}^*_2 \cong \mathbf{e}_2 + \omega_2\mathbf{e}_1 + \vartheta_2\mathbf{e}_3, \tag{D.12b}$$

where

$$\omega_1 = \frac{1}{A}\frac{\partial v}{\partial \alpha} - \frac{1}{AB}\frac{\partial A}{\partial \beta}u; \quad \omega_2 = \frac{1}{B}\frac{\partial u}{\partial \beta} - \frac{1}{AB}\frac{\partial B}{\partial \alpha}v;$$
$$\vartheta_1 = \frac{u}{R_1} + \frac{1}{A}\frac{\partial w}{\partial \alpha}; \quad \vartheta_2 = \frac{v}{R_2} + \frac{1}{B}\frac{\partial w}{\partial \beta}. \tag{D.13}$$

To clarify the geometric meaning of the parameters $\omega_1, \omega_2, \vartheta_1$, and ϑ_2 we set up the cross-products of the vectors $\mathbf{e_1}$ and $\mathbf{e}_1^*$ and the vectors $\mathbf{e}_2^*$ and $\mathbf{e}_2$. Using Eqs (D.12) and the properties of the cross-products of the unit vectors, we obtain the following:

$$\mathbf{e}_1 \times \mathbf{e}_1^* = \mathbf{e}_3\omega_1 - \mathbf{e}_2\vartheta_1; \quad \mathbf{e}_2^* \times \mathbf{e}_2 = \mathbf{e}_3\omega_2 - \mathbf{e}_1\vartheta_2.$$

The right-hand sides of the above relations represent the sines of angles by which the unit tangent vectors $\mathbf{e_1}$ and $\mathbf{e}_2$ rotate because of a deformation of the middle surface. Due to the small-displacement assumption, these sines are small quantities of the first order and they may be identified with the angles of rotations themselves. Thus, the rotation of the unit vector $\mathbf{e}_1$ consists of the rotation through the angle ω_1 about the direction $\mathbf{e}_3$ and of the rotation through the angle ϑ_1 about the direction $\mathbf{e}_2$. Correspondingly, the rotation of the vector $\mathbf{e}_2$ comprises the rotation through the angle ω_2 about $\mathbf{e}_3$ and through the angle ϑ_2 about $\mathbf{e}_1$.

Introducing the relations (D.12) into Eqs (D.3a) and neglecting the terms of second differential order, we obtain, after some mathematics, the following:

$$\mathbf{e}_3^* \cong \mathbf{e_3} - \vartheta_1\mathbf{e}_1 - \vartheta_2\mathbf{e}_2. \tag{D.14}$$

Inserting the above expression into the relation (D.2) yields the following:

$$\mathbf{D}^z = \mathbf{D} + (\mathbf{e}_3 - \vartheta_1\mathbf{e}_1 - \vartheta_2\mathbf{e}_2 - \mathbf{e}_3)z \quad \text{or}$$
$$\mathbf{D}^z = \mathbf{D} - (\vartheta_1\mathbf{e}_1 + \vartheta_2\mathbf{e}_2)z. \tag{D.15}$$

Projecting this vector on the directions of the unit vectors $\mathbf{e}_1, \mathbf{e}_2$, and $\mathbf{e}_3$, we obtain the three scalar equations (12.1).

D.2 STRAIN COMPONENTS OF THE SHELL

Consider two neighboring points $M(\alpha, \beta)$ and $M_1(\alpha + d\alpha, \beta)$ lying on the line $\alpha =$ const of the shell middle surface. The distance between these points is

$$- \text{ before deformation } - \mathrm{d}s_1 = A\mathrm{d}\alpha; \tag{D.16a}$$

$$- \text{ after deformation } - \mathrm{d}s_1^* = A^*\mathrm{d}\alpha \tag{D.16b}$$

The relative increase in length of a curvilinear linear element of the middle surface in the direction of the α-coordinate line is

$$\frac{\mathrm{d}s_1^* - \mathrm{d}s_1}{\mathrm{d}s_1}.$$

Substituting for $\mathrm{d}s_1^*$ and $\mathrm{d}s_1$ from Eqs (D.16) into the above and taking into account Eqs (D.9) and (D.10), we obtain the expression for the linear strain in the α direction, ε_1, in terms of the displacement components at a point of the middle surface in the α direction. Similarly, the expression for ε_2 can be obtained. The above strain–displacement components are given by Eqs (12.3) and (12.4).

Determine now the shear strain, γ_{12}, in the middle surface. By definition, the shear strain is equal to the change of an initially right angle between the tangent vectors $\mathbf{e}_1$ and $\mathbf{e}_2$, i.e.,

$$\gamma_{12} = \frac{\pi}{2} - \psi^*, \tag{D.17}$$

where ψ^* is the angle between the directions of $\mathbf{e}_1^*$ and $\mathbf{e}_2^*$. From the above relation,

$$\psi^* = \frac{\pi}{2} - \gamma_{12}$$

and $\cos\psi^* = \sin\gamma_{12} \approx \gamma_{12}$. Therefore, the shear strain can be determined as follows:

$$\gamma_{12} = \cos\psi^* = \mathbf{e}_1^* \cdot \mathbf{e}_2^*. \tag{D.18}$$

Substituting for $\mathbf{e}_1^*$ and $\mathbf{e}_2^*$ from Eqs (D.12) into the above, and neglecting the quantities of the second order of smallness, yields the following:

$$\begin{aligned}\gamma_{12} &= (\mathbf{e}_1 + \omega_1\mathbf{e}_2 + \vartheta_1\mathbf{e}_3)\cdot(\mathbf{e}_2 + \omega_2\mathbf{e}_1 + \vartheta_2\mathbf{e}_3)\\ &\approx \frac{1}{A}\frac{\partial v}{\partial\alpha} - \frac{1}{AB}\frac{\partial A}{\partial\beta}u + \frac{1}{B}\frac{\partial u}{\partial\beta} - \frac{1}{AB}\frac{\partial B}{\partial\alpha}v.\end{aligned} \tag{D.19}$$

Comparing Eq. (D.19) with the first two relations of (D.13), we can conclude that

$$\gamma_{12} = \omega_1 + \omega_2. \tag{D.20}$$

Equation (D.20) was given without proof in Sec. 12.2 (see Eq. (12.17)).

In deriving the equation describing a variation of the strain components across the shell thickness in Sec. 12.2, we assumed that the curvilinear coordinate lines were orthogonal on the equidistant surface, located at a distance z from the middle surface. Now we will verify the above assumption. The vector equation of the equidistant surface can be represented in the following form (see Fig. 12.3):

$$\mathbf{r}^z(\alpha, \beta, z) = \mathbf{r}(\alpha, \beta) - z\mathbf{e}_3, \tag{D.21}$$

where $\mathbf{r}^z(\alpha, \beta, z)$ and $\mathbf{r}(\alpha, \beta)$ are the position vectors of the equidistant and middle surface of the shell, respectively. Consider the following two vectors:

$$\mathbf{r}^z_{,\alpha} = \mathbf{r}_{,\alpha} - z\frac{\partial\mathbf{e}_3}{\partial\alpha} \quad \text{and} \quad \mathbf{r}^z_{,\beta} = \mathbf{r}_{,\beta} - z\frac{\partial\mathbf{e}_3}{\partial\beta}. \tag{D.22}$$

These vectors are tangents to the coordinate lines α and β, respectively, of the equidistant surface. We will prove that these vectors are orthogonal. The above requirement is equivalent to the following condition:

$$\mathbf{r}^z_{,\alpha} \cdot \mathbf{r}^z_{,\beta} = 0. \tag{D.23}$$

Substituting for $\mathbf{r}^z_{,\alpha}$ and $\mathbf{r}^z_{,\beta}$ from Eqs (D.22), we can write the left-hand side of the above equation as follows:

$$\mathbf{r}^z_{,\alpha} \cdot \mathbf{r}^z_{,\beta} = \mathbf{r}_{,\alpha} \cdot \mathbf{r}_{,\beta} - z\left[\mathbf{r}_{,\alpha} \cdot \frac{\partial\mathbf{e}_3}{\partial\beta} + \frac{\partial\mathbf{e}_3}{\partial\alpha} \cdot \mathbf{r}_{,\beta}\right] + z^2\left(\frac{\partial\mathbf{e}_3}{\partial\alpha} \cdot \frac{\partial\mathbf{e}_3}{\partial\beta}\right). \tag{D.24}$$

Using Eqs (11.26) for the differentiation of the unit vectors with respect to α and β, one obtains that each of the scalar products on the right-hand side of the equality is equal to zero. Equation (D.24) and, hence, Eq. (D.23), are identically satisfied and

Appendix E

Verification of Equilibrium Equations

Consider a differential element of the middle surface bounded by two pairs of the normal sections passing through the α- and β-coordinate lines and specify the equilibrium conditions of that element under external and internal forces and moments, as shown in Fig. 12.5.

We replace the internal forces and moments acting on the differential element by equivalent couple–force systems consisting of the resultant force $\mathbf{T}^{(i)}$ and resultant couple $\mathbf{M}^{(i)}$ $(i = 1.2)$, applied to every face of the element, as shown in Fig. E.1.

On the face $\alpha = 0$ the above resultant forces and resultant moments are

$$\begin{aligned} -\mathbf{T}^{(1)} &= -(N_1\mathbf{e}_1 + N_{12}\mathbf{e}_2 + Q_1\mathbf{e}_3)B\mathrm{d}\beta, \\ -\mathbf{M}^{(1)} &= -(M_1\mathbf{e}_2 - M_{12}\mathbf{e}_1)B\mathrm{d}\beta. \end{aligned} \tag{E.1}$$

On the face $\beta = 0$, the resultants $\mathbf{T}^{(2)}$ and $\mathbf{M}^{(2)}$ are

$$\begin{aligned} -\mathbf{T}^{(2)} &= -(N_{21}\mathbf{e}_1 + N_2\mathbf{e}_2 + Q_2\mathbf{e_3})A\mathrm{d}\alpha, \\ -\mathbf{M}^{(2)} &= -(M_{21}\mathbf{e}_2 - M_2\mathbf{e}_1)A\mathrm{d}\alpha. \end{aligned} \tag{E.2}$$

The signs preceding the internal forces and moments in the above equations have been chosen in accordance with Figs (12.5) and (E.1). The forces and moments of opposite signs act on the opposite faces of the differential element. The resultant forces and resultant moments acting on the faces α and $\alpha + \mathrm{d}\alpha$, as well as β and $\beta + \mathrm{d}\beta$, differ by increments and they have opposite signs, as shown in Fig. E.1. Thus, the resultant force $\mathbf{T}^{(1)}$ and resultant moment $\mathbf{M}^{(1)}$ are applied to the face 02; the resultants $\mathbf{T}^{(2)}$ and $\mathbf{M}^{(2)}$ act on the face 01; the resultants $\mathbf{T}^{(1)} + (\partial\mathbf{T}^{(1)}/\partial\alpha)\mathrm{d}\alpha$ and $\mathbf{M}^{(1)} + (\partial M^{(1)}/\partial\alpha)\mathrm{d}\alpha$ are applied to the face 13; while the resultants $\mathbf{T}^{(2)} + (\partial\mathbf{T}_2/\partial\beta)\mathrm{d}\beta$ and $\mathbf{M}^{(2)} + (\partial\mathbf{M}^{(2)}/\partial\beta)\mathrm{d}\beta$ act on the face 23. In addition, the differential element is acted upon by the external surface load $\mathbf{p}AB\mathrm{d}\alpha\mathrm{d}\beta$, where $\mathbf{p}$ is the vector of the intensity of the surface load, i.e.,

$$\mathbf{p} = p_1\mathbf{e}_1 + p_2\mathbf{e}_2 + p_3\mathbf{e}_3. \tag{E.3}$$

We now apply the equations of static equilibrium as follows:

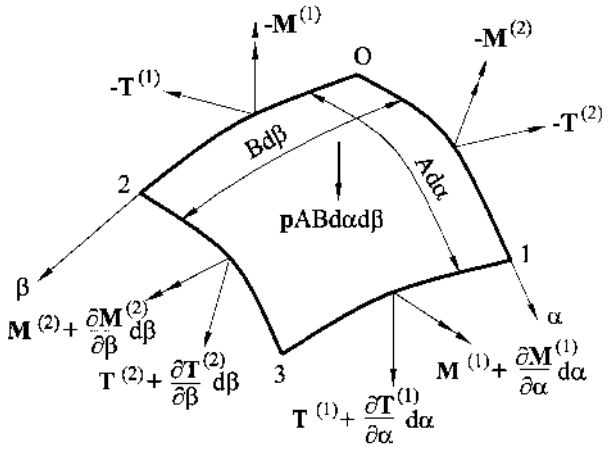

Fig. E.1

$$\sum \mathbf{T} = 0, \tag{E.4}$$

$$\sum \mathbf{M} = 0. \tag{E.5}$$

Referring to Fig. E.1, the force equilibrium equation (E.4) becomes

$$-\mathbf{T}^{(1)} + \mathbf{T}^{(1)} + \frac{\partial \mathbf{T}^{(1)}}{\partial \alpha} \mathrm{d}\alpha - \mathbf{T}^{(2)} + \mathbf{T}^{(2)} + \frac{\partial \mathbf{T}^{(2)}}{\partial \beta} \mathrm{d}\beta + \mathbf{p} AB \mathrm{d}\alpha \mathrm{d}\beta = 0,$$

from which

$$\frac{\partial \mathbf{T}^{(1)}}{\partial \alpha} \mathrm{d}\alpha + \frac{\partial \mathbf{T}^{(2)}}{\partial \beta} \mathrm{d}\beta + \mathbf{p} AB \mathrm{d}\alpha \mathrm{d}\beta = 0. \tag{E.6}$$

Substituting Eqs (E.1)–(E.3) for the resultants into Eq. (E.6), utilizing the rules for differentiating the unit vectors, Eqs (11.26), and canceling out the common term $\mathrm{d}\alpha\mathrm{d}\beta$, yields the following vector equation:

$$\begin{aligned} &\left[\frac{\partial}{\partial \alpha}(N_1 B) + \frac{\partial}{\partial \beta}(N_{21} A) + N_{12} \frac{\partial A}{\partial \beta} - N_2 \frac{\partial B}{\partial \alpha} - Q_1 \frac{AB}{R_1} + p_1 AB\right] \mathbf{e}_1 \\ &\quad + \left[\frac{\partial}{\partial \beta}(N_2 A) + \frac{\partial}{\partial \alpha}(N_{12} B) + N_{21} \frac{\partial B}{\partial \alpha} - N_1 \frac{\partial A}{\partial \beta} - Q_2 \frac{AB}{R_2} + p_2 AB\right] \mathbf{e}_2 \\ &\quad + \left[N_1 \frac{AB}{R_1} + N_2 \frac{AB}{R_2} + \frac{\partial}{\partial \alpha}(Q_1 B) + \frac{\partial}{\partial \beta}(Q_2 A) + p_3 AB\right] \mathbf{e}_3 = 0. \end{aligned} \tag{E.7}$$

Since the unit vectors are independent, Eq. (E.7) can only be satisfied if the terms in the square brackets are equal to zero, which gives the three scalar equations of the force equilibrium in the form of Eqs (12.41).

The moment equilibrium equation (E.5) is evaluated about the axes through point 0 in Fig. E.1. We obtain the following:

$$\mathbf{M}^{(1)} + \frac{\partial \mathbf{M}^{(1)}}{\partial \alpha} d\alpha - \mathbf{M}^{(1)} + \mathbf{M}^{(2)} + \frac{\partial \mathbf{M}^{(2)}}{\partial \beta} d\beta - \mathbf{M}^{(2)} + A d\alpha \left(\mathbf{e}_1 \times \mathbf{T}^{(1)} \right) + B d\beta \left(\mathbf{e}_2 \times \mathbf{T}^{(2)} \right) = 0,$$

from which

$$\frac{\partial \mathbf{M}^{(1)}}{\partial \alpha} d\alpha + \frac{\partial \mathbf{M}^{(2)}}{\partial \beta} d\beta + A d\alpha \left(\mathbf{e}_1 \times \mathbf{T}^{(1)} \right) + B d\beta \left(\mathbf{e}_2 \times \mathbf{T}^{(2)} \right) = 0. \tag{E.8}$$

The third and fourth terms in Eq. (E.8) represent the contribution of the resultant vectors $\mathbf{T}^{(i)}$ $(i = 1, 2)$ to the moment equilibrium equation (E.5). It is easy to verify that the in-plane shear forces N_{12} and N_{21} will contribute moments about the $\mathbf{e}_3$ axis, while the transverse shear forces Q_1 and Q_2 will contribute moments about the $\mathbf{e}_1$ and $\mathbf{e}_2$ axes.

In setting up Eq. (E.8), only terms of the second differential order were retained; terms of the third differential order were dropped out. Note that the moments due to the surface load $\mathbf{p}$ and due to the increments of the forces $\mathbf{T}^{(1)}$ and $\mathbf{T}^{(2)}$ also resulted in an appearance of the terms of the third differential order.

Substituting for $\mathbf{M}^{(1)}$, $\mathbf{M}^{(2)}$, $\mathbf{T}^{(1)}$, and $\mathbf{T}^{(2)}$ from Eqs (E.1) and (E.2) into Eq. (E.8), taking into account the relations (11.26) for the differentiation of the unit vectors, and canceling out the common factor $d\alpha d\beta$, we obtain the following vector equation:

$$\begin{aligned} &\left[M_1 \frac{\partial A}{\partial \beta} - \frac{\partial}{\partial \alpha}(M_{12} B) - M_{21} \frac{\partial B}{\partial \alpha} - \frac{\partial}{\partial \beta}(M_2 A) + Q_2 AB \right] \varepsilon_1 \\ &\quad + \left[\frac{\partial}{\partial \alpha}(M_1 B) + M_{12} \frac{\partial A}{\partial \beta} + \frac{\partial}{\partial \beta}(M_{21} A) - M_2 \frac{\partial B}{\partial \alpha} - Q_1 AB \right] \mathbf{e}_2 \\ &\quad + \left[-M_{12} \frac{AB}{R_1} + M_{21} \frac{AB}{R_2} + (N_{12} - N_{21}) AB \right] \mathbf{e}_3 = 0. \end{aligned} \tag{E.9}$$

This vector equation is equivalent to the three scalar equations (12.42).